ICES Journal of
Marine Science
Journal du Conseil
Volume 73 Number 3 February/March 2016
http://icesjms.oxfordjournals.org/

Towards a Broader Perspective on Ocean Acidification Research

A special issue of the ICES Journal of Marine Science

ICES CIEM
OXFORD UNIVERSITY PRESS

ICES Journal of Marine Science

Journal du Conseil

Volume 73 Number 3 February/March 2016

http://icesjms.oxfordjournals.org/

Contents

Published by Oxford University Press for
International Council for the Exploration of the Sea
Conseil International pour l'Exploration de la Mer
H. C. Andersens Boulevard 44-46, DK-1553 Copenhagen V, Denmark

ICES Journal of Marine Science

ICES Journal of Marine Science (2016), 73(3), 529–536. doi:10.1093/icesjms/fsw010

Introduction to Special Issue: 'Towards a Broader Perspective on Ocean Acidification Research'

Introduction

Applying organized scepticism to ocean acidification research

Howard I. Browman*

Institute of Marine Research, Marine Ecosystem Acoustics Disciplinary Group, Austevoll Research Station, 5392 Storebø, Norway

**Corresponding author: e-mail: howard.browman@imr.no*

Browman, H. I. Applying organized scepticism to ocean acidification research. – ICES Journal of Marine Science, 73: 529–536.

Received 18 January 2016; accepted 19 January 2016.

"Ocean acidification" (OA), a change in seawater chemistry driven by increased uptake of atmospheric CO_2 by the oceans, has probably been the most-studied single topic in marine science in recent times. The majority of the literature on OA report negative effects of CO_2 on organisms and conclude that OA will be detrimental to marine ecosystems. As is true across all of science, studies that report no effect of OA are typically more difficult to publish. Further, the mechanisms underlying the biological and ecological effects of OA have received little attention in most organismal groups, and some of the key mechanisms (e.g. calcification) are still incompletely understood. For these reasons, the *ICES Journal of Marine Science* solicited contributions to this special issue. In this introduction, I present a brief overview of the history of research on OA, call for a heightened level of organized (academic) scepticism to be applied to the body of work on OA, and briefly present the 44 contributions that appear in this theme issue. OA research has clearly matured, and is continuing to do so. We hope that our readership will find that, when taken together, the articles that appear herein do indeed move us "Towards a broader perspective on ocean acidification research".

Keywords: academic scepticism, calcification, climate change, high CO_2, multiple stressors, negative results, pH, publication bias, scientific method.

Background to this theme issue

"Ocean acidification" (OA), a change in seawater chemistry driven by increased uptake of atmospheric CO_2 by the oceans, has probably been the most-studied single topic in marine science in recent times (Figure 1). According to the Web of Science© (WOS), no articles used the term "OA" before 2000. Five articles responded to the search term "OA" in 2005, although only two of these deal with the topic in a manner consistent with contemporary research. From 2006 to 2015, >3100 articles on OA appeared—>300 per year! In 2015 alone, >600 articles were published on this topic. At the time of this writing, one of the first articles on OA, Orr *et al.* (2005), had been cited >1500 times according to the WOS and >2400 in Google Scholar. There have also been an extraordinary number of review articles, meta-analyses, special article theme sets, journal issues, and "white" (position) papers on OA produced by national and international agencies. The explosion of research on this topic is unprecedented in the marine sciences.

The majority of the literature on OA, particularly in the early days of research on the topic, report negative effects of CO_2 on organisms and conclude that OA will be detrimental to marine ecosystems. Some of these, typically published in "high impact" journals and covered by the mass media, predict an OA-generated ocean calamity (*sensu* Duarte *et al.*, 2014—see their Table 1). As is true across all of science, studies that report no effect of OA are typically more difficult to publish and, when published, seem to appear in lower-ranking journals (Browman, 1999). Further, the mechanisms underlying the biological and ecological effects of OA—via higher concentrations of CO_2, hydrogen ions (=lower pH), and/or carbonate chemistry (less carbonate ions)—have received little attention in most organismal groups (although see, for example, Pörtner, 2008; Kelly and Hoffmann, 2012; Bozinovic and Pörtner, 2015), and some of the key mechanisms (e.g. calcification) are still incompletely understood (see Roleda *et al.*, 2012; Cyronak *et al.*, 2016a, b; Waldbusser *et al.*, 2016). For these reasons, the *ICES Journal of Marine Science* (*IJMS*) solicited contributions to a special issue with the theme, "Towards a broader perspective on ocean acidification research".

Contributions were encouraged of studies showing no effect of OA; emphasizing the variability of responses to OA, including individuals that are not affected by the OA treatment, and how selection might act on that variability; multiple stressor experiments in which the effect of OA is assessed relative to and/or in combination with other drivers; assessments of the limits of using acute experiments to make inferences/conclusions about a chronic driver that will change slowly over decades; mechanisms of action of low pH

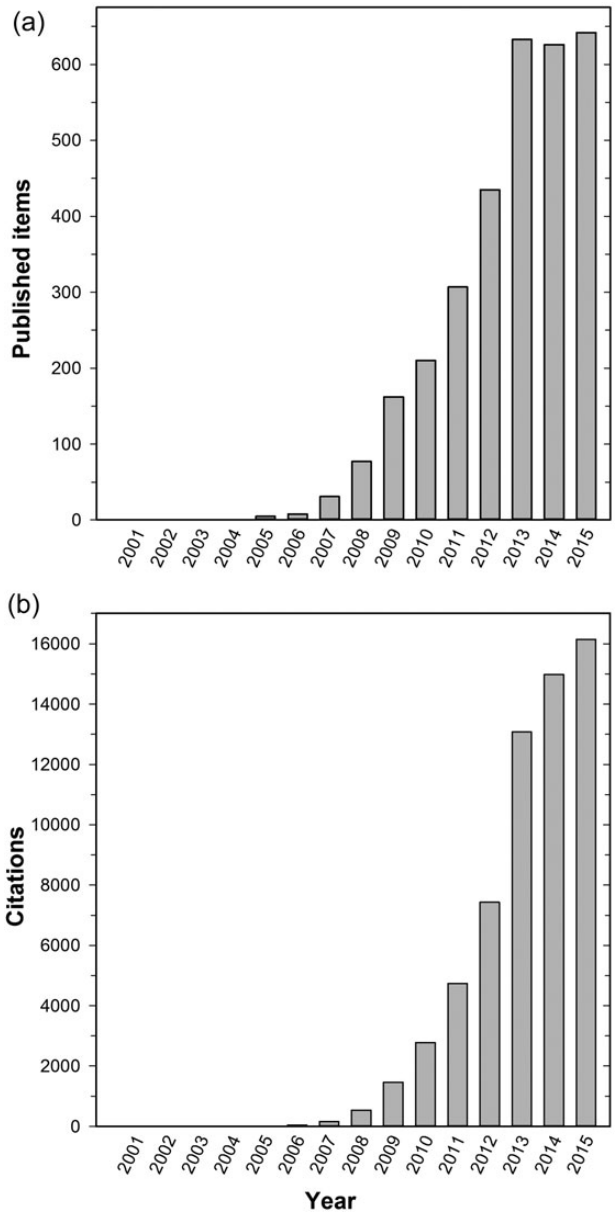

Figure 1. The number of articles per year (a) and the number of citations to those articles per year (b) returned in response to a topical search for "OA" conducted using the WOS© database on 16 January 2016.

and/or high CO_2 that consider realistic time-scales for changes in the driver; acclimation, carry-over, and epigenetic effects that consider realistic time-scales for changes in the driver; and evolutionary effects (e.g. development of resistance).

In the remainder of this introduction, I will (i) present a brief overview of the history of research on OA, (ii) call for a heightened level of organized (academic) scepticism to be applied to the body of work on OA (*sensu* Duarte *et al.*, 2014; Boonstra *et al.*, 2015), and (iii) briefly present the contributions that appear in this theme issue of the *IJMS*. Although I call for a more sceptical scrutiny and balanced interpretation of the body of research on OA, it must be emphasized that OA *is* happening and it *will* have effects on some marine organisms and ecosystem processes.

The progression of research on OA

The following qualitative and subjective overview is based on a perusal of the titles and abstracts of articles appearing in a WOS search for "ocean acidification" for each year (individually) from 2005 to 2015. Given the very large number of articles that could be used as examples of any of the study types referred to below, I have not cited any—the interested reader will not have any difficulty finding them.

The first articles on OA were descriptions of the process itself (CO_2-driven changes in the biogeochemistry of seawater and sediments) and its implications. This was followed by an explosion of work (mainly laboratory-based) on the possible effects of OA on various marine organisms, at first mainly calcifiers or the calcified hard parts of organisms without calcarious shells. These were mostly restricted to part of one generation (a limited number of life history stages), or at most a single complete life cycle, with one or a small number of biological endpoints measured as effect indicators. In early work, treatment exposure levels often greatly exceeded those predicted to occur hundreds of years into the future even without any reduction in CO_2 emissions. The majority of these early works reported significant negative effects of high CO_2, from which it was inferred that there would be a detrimental effect of OA over the coming decades–centuries. Thereafter, longer-term effect studies began to appear, which first included single-generation carry-overs and then multiple generations. By necessity, these have been on organisms with short generation times. As the approach to CO_2 exposures matured, very high treatment levels became less common. More studies that showed no effect of high CO_2 (predicted for the next century)—and even beneficial effects (e.g. for some phytoplankton and macrophytes)—appeared. Upwelling and vent systems were used as *in situ* case studies of natural future OA-like conditions. Some *in situ* work mimics such systems by injecting CO_2 and following the response of organisms/communities locally. Results of experiments that included multiple stressors in addition to CO_2 were published. The most common of these has been temperature, but salinity, oxygen, and a variety of others have also been included (in a global climate change context). Such studies typically report that the additional driver(s) has a stronger effect than CO_2, although it is difficult to isolate the effect of the individual variables. The reality that the functional response curve of each driver will likely differ, as will the organism's ability to adapt to them, further complicates interpretations of multiple driver experiments. Studies on the effect of CO_2 on trophic interactions (indirect effects) are sparse—such experiments are logistically complex and difficult to interpret. A small number of recent studies integrate the results of the preceding body of work into risk assessments and scenario modelling, typically on economically important species of fish and shellfish; most conclude that the prognosis is dire, although in the context of what follows, that conclusion might be premature.

The preceding describes how OA research has matured. The following describes how it still has a way to go.

Applying organized scepticism to research on the effects of OA

Scientific or academic scepticism calls for critical scrutiny of research outputs before they are accepted as new knowledge (Merton, 1973). Duarte *et al.* (2014) stated that "...there is a perception that scientific skepticism has been abandoned or relaxed in many areas..." of marine science. They argue that OA is one such

area, and conclude that there is, at best, weak evidence to support an OA-driven decline of calcifiers. Below, I raise some of the aspects of OA research to which I contend an insufficient level of organized scepticism has been applied (in some cases, also to the articles in this theme issue). I arrived at that conclusion after reading hundreds of articles on OA (including, to be fair, some that also raise these issues) and overseeing the peer-review process for the very large number of submissions to this themed issue. Importantly, and as Duarte *et al.* (2014) make clear, a retrospective application of scientific scepticism such as the one that follows could—and should—be applied to any piece of/body of research.

Exposure levels, water chemistry, and limits to making inferences about the effect of a long-term driver from a short-term experiment

Many early studies on OA applied treatment levels that greatly exceeded even worst-case climate change scenarios and did not report water chemistry in sufficient detail to determine if the treatment mimicked future OA-driven seawater conditions. Although most recent work has improved with respect to treatment levels, mimicking future water chemistry remains tricky.

A rationale commonly used to justify high CO_2/low pH treatments is the need to identify at what levels organisms are affected. However, the limits to making inferences about how an organism or ecosystem will respond to a climate-change scale variable (i.e. one that changes over decades–centuries) from their response during a short-term challenge experiment (i.e. hours–days–weeks) has not been adequately addressed—or even mentioned—in most studies. This is reflected in a confusion of terms common in OA studies—when describing the outcome of a short-term CO_2 challenge, authors often make the inferential leap and use "OA" when discussing their results, without any caveats. Oddly, incorporation of the extensive toxicology literature is almost entirely missing from OA studies, either when it comes to adopting established exposure protocols or to framing the inferences that can/cannot be drawn from short-term experiments. Also missing from most studies is anything more than a superficial statement about the possibility for acclimation, adaptation, or evolution, something that is necessary to extend the outcome of a short-term challenge experiment into an inference about the effect of a long-term driver (see below).

Spatio-temporal variability in CO_2 and pH

Biogeochemists are well aware of the spatio-temporal variability in CO_2 and pH—daily (high productivity areas), seasonal (blooms), interannual (higher temperatures), horizontal (coastal upwelling areas, high turbidity zones), and vertical (deep vs. surface waters) ranges in these can be extensive (e.g. Wootton *et al.*, 2008; Hofmann *et al.*, 2011; Waldbusser and Salisbury, 2014; Kapsenberg *et al.*, 2015). Biologists have struggled to incorporate this variability into experiments designed to test the effects of OA, and into their interpretations of the outcomes (Eriander *et al.*, 2016). Some researchers have pointed out that organisms that are exposed to large ranges in CO_2 and pH during their daily lives (e.g. vertical migrators), life cycles (e.g. organisms that reside offshore as larvae but move to the coast as juveniles or adults), or somewhere in their distributional ranges, should be more tolerant of OA (e.g. Lewis *et al.*, 2013).

Imbalanced focus on individuals that are affected and insufficient focus on inter-individual variability and within-experiment selection bias interpretations of ecological impacts

Almost all CO_2 challenge experiments produce a range of responses in the test organism—some individuals are badly affected, others less, and some not at all. There are several issues associated with all such experiments that it is important to be cognizant of and account for: (i) analyses and interpretations should not ignore or minimize individuals that are little affected or unaffected (after all, these are the ones whose genes will be passed on to the next generation); (ii) inter-individual variability should be highlighted; (iii) the longer that the experiment runs the more likely it is that an internal selection process for the tolerant individuals has occurred. All of these are important in the context of the next section.

Acclimation, generational carry-over effects, adaptation, epigenetics, and evolution

Almost all experiments conducted to assess OA are short-term toxicity challenges. Therefore, using them as the basis from which to make inferences about a process that will occur slowly over the next decades–centuries must be made with appropriate caution. That is, the experiments and the interpretations made from them must consider how populations might acclimatize, adapt, and evolve to climate change, including OA (e.g. Donelson *et al.*, 2011; Hoffmann and Sgrò, 2011; Sunday *et al.*, 2013; Harvey *et al.*, 2014). Recent studies indicate that even the effects of OA that are considered most worrisome—various behavioural impairments resulting from short-term exposure to high CO_2 (see Nagelkerken and Munday, 2016)—might be reduced or overcome through adaptation and evolution (Regan *et al.*, 2016). More knowledge of the mechanisms of direct action of OA-related drivers—higher concentrations of CO_2, hydrogen ions (=lower pH), and/or carbonate chemistry (less carbonate ions)—and of indirect drivers such as the effects of OA on food quality, are essential to understand what degree of adaption is possible. Readers should be duly sceptical of studies that completely ignore the possibility of adaptation when presenting their inferences about OA, particularly scenario modelling of socio-economic impacts.

We must also do better to incorporate analogous work in other fields, for example, rapid evolution of tolerance to envirotoxins (e.g. Whitehead *et al.*, 2012) and environmental change (e.g. Collins *et al.*, 2014; Stoks *et al.*, 2015; Thibodeau *et al.*, 2015) via a combination of genetic and epigenetic mechanisms (Yona *et al.*, 2015).

Publication bias

Negative results—those that do not support a research hypothesis (e.g. OA will have detrimental effects on marine organisms)—can provide more balance for a subject area for which most published research reports positive results. Negative results can indicate that a subject area is not mature or clearly enough defined, or that our current methods and approaches are insufficient to produce a definitive result. Gould (1993) asserted that positive results tell more interesting stories than negative results and are, therefore, easier to write about and more interesting to read. He calls this a privileging of the positive. This privileging leads to a bias that acts against the propagation of negative results in the scholarly literature (see also Browman, 1999). Further, it is also important to recognize that studies showing no effect of OA are less equivocal than those

that do, for all of the reasons noted above. Following from this, it is essential that authors writing about possible effects of OA present and discuss research that is inconsistent with their results and/or their interpretations—openly, honestly, and rigorously. Readers should be duly sceptical of articles that do not do this.

Despite all of the above, OA research has clearly matured and, as reflected in the contributions to this theme issue, is continuing to do so.

An overview of the contributions in this theme issue

Studies on the mechanisms of action of OA

Jokiel (2016) revisits four key simplifying assumptions that have been made to assess how OA will impact coral reefs and finds that there is currently insufficient evidence to support them and that they should be further evaluated. He presents the hypothesis that calcification in corals is limited by their ability to rid themselves of the protons generated by calcification rather than strictly by the aragonite saturation state of seawater. This is further developed by Cyronak *et al.* (2016a, b), although Waldbusser *et al.* (2016), in a comment on Cyronak *et al.*, discuss how a bicarbonate/proton flux and omega-based sensitivity model do not have to be mutually exclusive. These studies will hopefully serve to shift thinking towards a more synthetic view of the mechanisms through which OA will impact marine calcifiers.

Studies on methodological issues in OA research

Cornwall and Hurd (2016) assessed 465 OA studies published between 1993 and 2014, focusing on the methods used to replicate experimental units. They found that 95% of these studies had interdependent or non-randomly interspersed treatment replicates, or did not report sufficient methodological detail, and they provide guidelines on how to improve the design of such experiments. Reum *et al.* (2016) discuss the implications of co-variation among environmental variables (e.g. oxygen and temperature) for the interpretation of OA experimental results and suggest an approach for designing experiments with CO_2 levels that better reflect this co-variation. Eriander *et al.* (2016) (for the barnacle, *Balanus improvisus*) and Small *et al.* (2016) (for the sea urchins, *Paracentrotus lividus* and *Arbacia lixula*) report how introducing natural fluctuations in the pH/CO_2 levels to which organisms are exposed in experiments (vs. exposure to constant average levels) yields different responses. They conclude that these results support including fluctuating acidification treatments in experiments on species that live in variable environments.

Studies on the behavioural effects of OA

Kim *et al.* (2016) report that the metabolic rate of the deep-sea hermit crab (*Pagurus tanneri*) exposed to low pH increased transiently, and that olfactory behaviour was impaired. However, they also observed that crabs exposed to low pH exhibited higher individual variation in the speed of antennular flicking and prey detection than observed in the control pH treatment, and suggested that this phenotypic diversity could lead to adaptation to OA. Sundin and Jutfelt (2016) report that increased levels of CO_2 had no effect on behavioural lateralization, swimming activity, and prey olfactory preferences of goldsinny wrasse (*Ctenolabrus rupestris*), although there was an effect on predator olfactory cue avoidance—control fish initially avoided predator cue while the high CO_2 group was indifferent to it. Heinrich *et al.* (2016) report no effect of elevated CO_2 on the foraging or shelter seeking behaviour of the reef-dwelling epaulette shark (*Hemiscyllium ocellatum*). Munday *et al.* (2016), in a study on the early life stages of the yellowtail kingfish, *Seriola lalandi*, found no effect of elevated CO_2 on survival to hatching or to 3 d post-hatch, a decrease in oil globule diameter, but no effect on other morphometric traits nor on activity level, startle response, or phototaxis.

Studies on indirect effects of OA—via trophic interactions and competition

Isari *et al.* (2016) report that the nutritional characteristics of the autotrophic dinoflagellate *Heterocapsa* sp. were unaffected by exposure to high CO_2 and that feeding this dinoflagellate to the copepod *Acartia grani* had no effect on feeding, egg production rates, or egg hatching success. Brien *et al.* (2016) assessed whether elevated CO_2 influenced competitive interactions between the hard coral, *Porites cylindrica*, and soft corals. Elevated CO_2 impaired photosynthetic activity, but not growth, of *P. cylindrica* under competition with soft corals, while the soft corals themselves were tolerant. They propose that shifts in the species composition in coral communities in response to elevated CO_2 may be more strongly related to the individual tolerance of different species rather than a result of competitive interactions between species.

Studies on how nutritional conditions and an individual's physiological status affect responses to OA

Sala *et al.* (2016) investigated the effects of increased CO_2 on diatoms, dinoflagellates, nanoeukaryotes, picoeukaryotes, cyanobacteria, and heterotrophic bacteria and on bacterial activity, leucine incorporation, and extracellular enzyme activity, under low vs. high nutrient conditions. They conclude that microbial communities in oligotrophic waters are affected by high CO_2, while microbes in more productive waters are less affected. They further suggest that the observed beneficial effect of high CO_2 on eukaryotic pico- and nanophytoplankton, in contrast to the non-significant or negative response to nutrient-rich conditions of larger groups and autotrophic prokaryotes, may lead to a shift towards medium-sized producers under OA. Sugie and Yoshimura (2016) manipulated the availability of iron and carbonate chemistry, individually and simultaneously, to assess their effects on growth, cell size, and elemental stoichiometry of the diatom *Thalassiosira weissflogii*. They observed that the response of the diatom to CO_2 was related to iron availability.

Studies on the effects of OA in combination with other environmental drivers

Kram *et al.* (2016) investigated the independent and interactive effects of elevated CO_2 and warming on growth, carbonic anhydrase (CA) enzyme activity, pigment concentrations, and photosynthetic efficiency of six common species of calcified and fleshy macroalgae from southern California. They found no effect of elevated CO_2 on CA activity, pigment concentration, or photosynthetic efficiency in the macroalgal species studies, although the calcareous algae generally displayed reduced growth (species-specific). The combined effects of elevated CO_2 and warming had a significantly negative impact on growth for both fleshy and calcareous algae.

Vicente *et al.* (2016) report that rising CO_2 and temperature do not affect survival rates of the Hawai'ian sponge, *Mycale grandis*, but do cause them to biomineralize less silica.

Noonan and Fabricius (2016) investigated how elevated CO_2 and temperature, in combination, affected the bleaching susceptibility of tropical reef corals. Their field and laboratory data suggest that

levels of OA up to a pHT of 7.8 will have little effect on the sensitivity of tropical reef corals to thermal bleaching.

Collard *et al.* (2016) used laboratory experiments and collections of individuals from low pH intertidal pools and CO_2 seeps to study the impact of pH and temperature on the mechanical properties of the skeleton of the sea urchin, *P. lividus*. Decreases in pH to levels expected for 2100 did not alter the mechanical properties of the test of *P. lividus*, indicating that the decreasing seawater pH expected for the end of the century should not represent an immediate threat to this sea urchin.

Schram *et al.* (2016) investigated the effects of elevated temperature and decreased pH on growth, net calcification, and proximate body composition of select body tissues in the limpet *Nacella concinna* and the snail *Margarella antarctica*. Their findings suggest that both of these gastropod species are tolerant to near-future temperature and pH changes.

Belivermis *et al.* (2016) studied the combined effects of reduced pH and increased temperature on the bioconcentration of radionuclide and metals in the Pacific cupped oyster *Crassostrea gigas*. pH alone did not affect bioaccumulation in oyster. However, temperature, either alone or in combination with pH, altered bioaccumulation. Neither pH nor temperature affected the elemental distribution between shell and soft tissues.

Navarro *et al.* (2016) assessed the combined effect of increasing temperature and CO_2 on feeding, metabolism, and growth of the mussel, *Mytilus chilensis*. Their results suggest that temperature increases that are within the natural range experienced by *M. chilensis* increase feeding and nutrient absorption, while an increase in CO_2 to 1000 µatm, independent of temperature, significantly reduces energy allocated to growth.

Horn *et al.* (2016) studied the effects of warming and high CO_2 on abundance, biomass, and species composition of a Baltic Sea autumn microzooplankton (MZP) community. Warming led to a reduced time-lag between the phytoplankton bloom and the maximum MZP biomass. The growth rate of MZP was significantly higher and the biomass peak was earlier in the warm treatments while the biomass maximum was not affected. Increased CO_2 did not affect MZP biomass, growth rate, or species composition irrespective of the temperature, and there were no interactions between CO_2 and temperature. They attribute the high tolerance of this estuarine plankton community to natural fluctuations in CO_2 that are often greater than those predicted for the end of the century.

Graham *et al.* (2016) assessed sperm motility and fertilization success in the sea urchin *P. lividus* exposed to elevated CO_2 and a hypoxic event. Sperm swimming speed increased under elevated CO_2 and decreased under hypoxic conditions, such that the elevated CO_2 and hypoxic treatment were approximately equivalent to the control. There was also a combined negative effect of increased CO_2 and hypoxia on the percentage of motile sperm and a negative effect of elevated CO_2 on fertilization success—when this was combined with a simulated hypoxic event, there was an even greater effect.

Campanati *et al.* (2016) investigated the independent and interactive effect of low pH and low oxygen on the barnacle, *Balanus amphitrite*, with a focus on the critical transition between planktonic and benthic life history phases. Low oxygen significantly slowed naupliar development, although the interaction with low pH alleviated the negative effect. The percentage of larvae that became cyprids was unaffected by treatment. Overall, low oxygen was the major driver of the responses observed.

Dutra *et al.* (2016) examined the effects of elevated CO_2 on individual crustose coralline algae (CCA—*Peyssonnelia* sp.) and communities (using settling plates) at high and low irradiance. Their observations indicate that elevated CO_2 levels predicted for 2100 will not shift macroalgal communities under either high or low irradiance.

Zhang *et al.* (2016) investigated ingestion, absorption rate and efficiency, respiration, excretion, and scope for growth of the intertidal scavenging gastropod, *Nassarius festivus*, in response to the combined effects of elevated CO_2, salinity, and temperature. Low salinity reduced ingestion, absorption rate, respiration, excretion, and scope for growth in *N. festivus*. Low temperature had a similar effect on these parameters, except for scope for growth at the end of the 31 d exposure period. Elevated CO_2 in isolation had no effect on any of the variables measured and only weak interactions with temperature and/or salinity for excretion and scope for growth. These authors conclude that elevated CO_2 will not affect the energy budget of adult *N. festivus* at the levels predicted to occur by 2300.

Studies showing effects of OA and projecting economic impacts

Three related studies on Tanner crab (*Chionoecetes bairdi*) indicate that they will be negatively affected by ocean pH levels projected to occur over the next two centuries, unless they are able to adapt. Swiney *et al.* (2016) examined the effects of long-term exposure (2 years) to elevated CO_2 on embryonic development, hatching success, and calcification in *C. bairdi*. Oocyte development appeared to be sensitive to high CO_2 as was embryonic development and hatching success, with on average 71% fewer viable larvae hatched at pH 7.5 than in the other treatments. Per cent calcium was reduced in females exposed to pH 7.5 water and their carapaces were more pliable than the carapaces in the other treatments. Long *et al.* (2016) found that while the larval phase itself was tolerant of low pH, there was an effect when they were exposed as embryos or when egg-carrying females were exposed (i.e. there was a carryover effect). Punt *et al.* (2016) incorporated these and other results on the effects of CO_2 on Tanner crab early life stages into demographic models of pre- and post-recruitment population dynamics. These linked models indicated that catch and profits will decrease by more than 50% in 20 years if natural mortality is in fact affected by OA.

Studies showing no effect, little effect, and/or mixed effects of OA

Wang *et al.* (2016) applied phylogenetic molecular ecological networks to investigate the interactions of native bacterial communities in the Arctic Ocean in response to increased CO_2. Elevated CO_2 did not significantly affect microbial community structure and succession in the Arctic Ocean, suggesting tolerance of the bacterioplankton community to OA.

Takahashi *et al.* (2016) investigated the tropical subtidal seagrass communities at three shallow volcanic CO_2 vents in Papua New Guinea and conclude that OA may lead to higher cover and above- and below-ground biomass, but lower size-specific growth and altered species composition.

Nunes *et al.* (2016) report on two 1-month studies using two different non-calcifying macroalgae, the red alga, *Palmaria palmata*, and the kelp, *Saccharina latissima*, exposed to control and increased levels of CO_2. Although there were some effects on net primary production, respiration and growth (but not on dimethylsulphoniopropionate concentration), and algal growth, the overall conclusion was that these species are tolerant to elevated CO_2.

Strahl *et al.* (2016) investigated the mechanisms for shifts in coral communities observed at two natural volcanic seeps in Papua New Guinea. To accomplish this, biochemical parameters related to tissue biomass, energy storage, pigmentation, cell protection, and cell damage were compared between *Porites* spp. and *Acropora millepora* from control and elevated CO_2 seep sites. Their observations suggest that these biochemical measures are relatively unaffected in these two coral species in response to elevated CO_2 up to 800 μatm. In fact, most responses were smaller than the differences between species, locations, or in response to other environmental stressors such as temperature.

Enochs *et al.* (2016) tested the effect of elevated CO_2 on linear extension and on the morphology of calcified internal skeletal structures of the common Caribbean octocoral, *Eunicea flexuosa*. No differences were observed, suggesting a degree of tolerance to OA-stress in this species.

Cross *et al.* (2016) studied the response of the brachiopod, *Calloria inconspicua*, to elevated CO_2. Neither shell repair nor the growth rates of undamaged individuals >3 mm in length were affected by high CO_2, whereas undamaged individuals <3 mm grew faster than controls under high CO_2 conditions.

Hildebrandt *et al.* (2016) incubated *Calanus glacialis* and *Calanus finmarchicus* under different levels of CO_2 (up to 3000 μatm) and measured clearance and ingestion rates and body mass. Elevated CO_2 had no effect on these variables. Similarly, Runge *et al.* (2016) cultured *C. finmarchicus* from eggs to adult at control and elevated CO_2 concentrations and found no effect of elevated CO_2 on development time, lipid accumulation, feeding rate, or metabolic rate.

Chan *et al.* (2016) compared the developmental dynamics, survivorship, and swimming behaviour of plutei of the purple urchin, *Strongylocentrotus purpuratus*, and the infaunal brittlestar, *Amphiura filiformis*, exposed to elevated CO_2. Responses to elevated CO_2 differed between these two species and between maternal lineages. Larval brittlestars were generally more sensitive exhibiting, for example, reduced swimming speeds at elevated CO_2 while there was no negative effect on the swimming of larval urchins. The authors suggest that natural selection could act upon the significant variations observed between maternal lineages, resulting in populations that are more tolerant of OA.

Ross *et al.* (2016) present a short review of the small number of experiments that have measured the transgenerational response of mollusc and echinoderm species to elevated CO_2. They call for an increased focus on the impacts that carry-over effects have within and across generations as well as on understanding the mechanisms responsible for such adaptation.

Kelly *et al.* (2016) assessed the response of larvae of the California mussel, *Mytilus californianus,* to elevated CO_2. Larvae cultured under elevated CO_2 were smaller, but there was no consistent effect on gene expression. They conclude that the observed reduction in larval body size under high CO_2 was not mediated by changes in gene expression.

Sigwart *et al.* (2016) measured the growth, developmental time, oxygen consumption, yolk utilization, and morphology of the cuttlebone of the cuttlefish, *Sepia officinalis*, in response to elevated CO_2. Juvenile cuttlefish exhibited lower growth but increased calcification of their internal shell under high CO_2 conditions.

Finally, Hurst *et al.* (2016) report no effect of elevated CO_2 on egg survival, size at hatch, or growth until 28 d post-hatch in the northern rock sole (*Lepidopsetta polyxystra*).

The *IJMS* is grateful to the many authors who submitted their work for publication in this theme issue. We hope that our readership will find that, when taken together, the articles that appear herein do indeed move us "Towards a broader perspective on ocean acidification research".

Acknowledgements

Thanks to David Fields, Emory Anderson, Timothy Clark, Jeff Runge, and Anne Berit Skiftesvik for comments on earlier drafts. HIB's contribution to this special issue was supported by Projects # 83192-01 ("Ocean acidification"), 81529 ("Fine scale interactions in the plankton"), and 83741 ("Scientific publishing and editing") from the Institute of Marine Research, Norway.

References

Belivermis, M., Warnau, M., Metian, M., Oberhänsli, F., Teyssié, J., and Lacoue-Labarthe, T. 2016. Limited effects of increased CO_2 and temperature on metal and radionuclide bioaccumulation in a sessile invertebrate, the oyster *Crassostrea gigas*. ICES Journal of Marine Science, 73: 753–763.

Boonstra, W. J., Ottosen, K. M., Ferreira, A. S. A., Richter, A., Rogers, L. A., Pedersen, M. W., Kokkalis, A., *et al.* 2015. What are the major global threats and impacts in marine environments? Investigating the contours of a shared perception among marine scientists from the bottom-up. Marine Policy, 60: 197–201.

Bozinovic, F., and Pörtner, H-O. 2015. Physiological ecology meets climate change. Ecology and Evolution, 5: 1025–1030.

Brien, H. V., Watson, S-A., and Hoogenboom, M. O. 2016. Presence of competitors influences photosynthesis, but not growth, of the hard coral *Porites cylindrica* at elevated seawater CO_2. ICES Journal of Marine Science, 73: 659–669.

Browman, H. I. 1999. The uncertain position, status and impact of negative results in marine ecology: philosophical and practical considerations. Marine Ecology Progress Series, 191: 301–302.

Campanati, C., Yip, S., Lane, A., and Thiyagarajan, V. 2016. Combined effects of low pH and low oxygen on the early-life stages of the barnacle *Balanus amphitrite*. ICES Journal of Marine Science, 73: 791–802.

Chan, K. Y. K., Grünbaum, D., Arnberg, M., and Dupont, S. 2016. Impacts of ocean acidification on survival, growth, and swimming behaviours differ between larval urchins and brittlestars. ICES Journal of Marine Science, 73: 951–961.

Collard, M., Rastrick, S. P. S., Calosi, P., Demolder, Y., Dille, J., Findlay, H. S., Hall-Spencer, J. M., *et al.* 2016. The impact of ocean acidification and warming on the skeletal mechanical properties of the sea urchin *Paracentrotus lividus* from laboratory and field observations. ICES Journal of Marine Science, 73: 727–738.

Collins, S., Rost, B., and Rynearson, T. A. 2014. Evolutionary potential of marine phytoplankton under ocean acidification. Evolutionary Applications, 7: 140–155.

Cornwall, C. E., and Hurd, C. L. 2016. Experimental design in ocean acidification research: problems and solutions. ICES Journal of Marine Science, 73: 572–581.

Cross, E. L., Peck, L. S., Lamare, M. D., and Harper, E. M. 2016. No ocean acidification effects on shell growth and repair in the New Zealand brachiopod *Calloria inconspicua* (Sowerby, 1846). ICES Journal of Marine Science, 73: 920–926.

Cyronak, T., Schulz, K. G., and Jokiel, P. L. 2016a. Response to Waldbusser *et al.* 2016: "Calcium carbonate saturation state: on myths and this or that stories". ICES Journal of Marine Science, 73: 569–571.

Cyronak, T., Schulz, K. G., and Jokiel, P. L. 2016b. The Omega myth: what really drives lower calcification rates in an acidifying ocean. ICES Journal of Marine Science, 73: 558–562.

Donelson, J. M., Munday, P. L., McCormick, M. I., and Pitcher, C. R. 2011. Rapid transgenerational acclimation of a tropical reef fish to climate change. Nature Climate Change, 2: 30–32.

Duarte, C. M., Fulweiler, R. W., Lovelock, C. E., Martinetto, P., Saunders, M. I., Pandolfi, J. M., Stefan, G., *et al.* 2014. Reconsidering ocean calamities. Bioscience, 65: 130–139.

Dutra, E., Koch, M., Peach, K., and Manfrino, C. 2016. Tropical crustose coralline algal individual and community responses to elevated pCO_2 under high and low irradiance. ICES Journal of Marine Science, 73: 803–813.

Enochs, I. C., Manzello, D. P., Wirshing, H. H., Carlton, R., and Serafy, J. 2016. Micro-CT analysis of the Caribbean octocoral *Eunicea flexuosa* subjected to elevated pCO_2. ICES Journal of Marine Science, 73: 910–919.

Eriander, L., Wrange, A.-L., and Havenhand, J. N. 2016. Simulated diurnal pH fluctuations radically increase variance in—but not the *mean* of—growth in the barnacle *Balanus improvisus*. ICES Journal of Marine Science, 73: 596–603.

Gould, S. J. 1993. Cordelia's dilemma. Natural History, c102: 10–18.

Graham, H., Rastrick, S. P. S., Findlay, H. S., Bentley, M. G., Widdicombe, S., Clare, A. S., and Caldwell, G. S. 2016. Sperm motility and fertilisation success in an acidified and hypoxic environment. ICES Journal of Marine Science, 73: 783–790.

Harvey, B. P., Al-Janabi, B., Broszeit, S., Cioffi, R., Kumar, A., Aranguren-Gassis, M., Bailey, A., *et al.* 2014. Evolution of marine organisms under climate change at different levels of biological organisation. Water, 6: 3545–3574.

Heinrich, D. D. U., Watson, S-A., Rummer, J. L., Brandl, S. J., Simpfendorfer, C. A., Heupel, M. R., and Munday, P. L. 2016. Foraging behaviour of the epaulette shark *Hemiscyllium ocellatum* is not affected by elevated CO_2. ICES Journal of Marine Science, 73: 633–640.

Hildebrandt, N., Sartoris, F., Schulz, K., Riebesell, U., and Niehoff, B. 2016. Ocean acidification does not alter grazing in the calanoid copepods *Calanus finmarchicus* and *C. glacialis*. ICES Journal of Marine Science, 73: 927–936.

Hoffmann, A. A., and Sgrò. 2011. Climate change and evolutionary adaptation. Nature, 470: 479–485.

Hofmann, G. E., Smith, J. E., Johnson, K. S., Send, U., Levin, L. A., Micheli, F., Paytan, A., *et al.* 2011. High-frequency dynamics of ocean pH: a multi-ecosystem comparison. PLoS ONE, doi:10.1371/journal.pone.0028983.

Horn, H. G., Boersma, M., Garzke, J., Löder, M. G. J., Sommer, U., and Aberle, N. 2016. Effects of high CO_2 and warming on a Baltic Sea microzooplankton community. ICES Journal of Marine Science, 73: 772–782.

Hurst, T. P., Laurel, B. J., Mathis, J. T., and Tobosa, L. R. 2016. Effects of elevated CO_2 levels on eggs and larvae of a North Pacific flatfish. ICES Journal of Marine Science, 73: 981–990.

Isari, S., Zervoudaki, S., Peters, J., Papantoniou, G., Pelejero, C., and Saiz, E. 2016. Lack of evidence for elevated CO_2-induced bottom-up effects on marine copepods: a dinoflagellate–calanoid prey–predator pair. ICES Journal of Marine Science, 73: 650–658.

Jokiel, P. L. 2016. Predicting the impact of ocean acidification on coral reefs: evaluating the assumptions involved. ICES Journal of Marine Science, 73: 550–557.

Kapsenberg, L., Kelley, A. L., Shaw, E. C., Martz, T. R., and Hofmann, G. E. 2015. Near-shore Antarctic pH variability has implications for the design of ocean acidification experiments. Scientific Reports, 5: 9638.

Kelly, M. W., and Hoffmann, G. E. 2012. Adaptation and the physiology of ocean acidification. Functional Ecology, 27: 980–990.

Kelly, M. W., Padilla-Gamino, J. L., and Hofmann, G. E. 2016. High pCO_2 affects body size, but not gene expression in larvae of the California mussel (*Mytilus californianus*). ICES Journal of Marine Science, 73: 962–969.

Kim, T. W., Taylor, J., Lovera, C., and Barry, J. P. 2016. CO_2-driven decrease in pH disrupts olfactory behaviour and increases individual variation in deep-sea hermit crabs. ICES Journal of Marine Science, 73: 613–619.

Kram, S. L., Price, N. N., Donham, E. M., Johnson, M. D., Kelly, E. L. A., Hamilton, S. L., and Smith, J. E. 2016. Variable responses of temperate calcified and fleshy macroalgae to elevated pCO_2 and warming. ICES Journal of Marine Science, 73: 693–703.

Lewis, C. N., Brown, K. A., Edwards, L. A., Cooper, G., and Findlay, H. S. 2013. Sensitivity to ocean acidification parallels natural pCO_2 gradients experienced by Arctic copepods under winter sea ice. Proceedings of the National Academy of Sciences of the United States of America, 110: 4960–4967.

Long, W., Swiney, K. M., and Foy, R. 2016. Effects of high pCO_2 on Tanner crab reproduction and early life history, Part II: carryover effects on larvae from oogenesis and embryogenesis are stronger than direct effects. ICES Journal of Marine Science, 73: 836–848.

Merton, R. K. 1973. The Sociology of Science: Theoretical and Empirical Investigations. University of Chicago Press, Chicago, Illinois, USA. 636 pp.

Munday, P., Watson, S., Parsons, D., King, A., Barr, N., McLeod, I., Allan, B., *et al.* 2016. Effects of elevated CO_2 on early life history development of the yellowtail kingfish, *Seriola lalandi*, a large pelagic fish. ICES Journal of Marine Science, 73: 641–649.

Nagelkerken, I., and Munday, P. L. 2016. Animal behaviour shapes the ecological effects of ocean acidification and warming: moving from individual to community-level responses. Global Change Biology, doi:10.1111/gcb.13167.

Navarro, J., Duarte, C., Manríquez, P., Lardies, M., Torres, R., Acuña, K., Vargas, C., *et al.* 2016. Ocean warming and elevated carbon dioxide: multiple stressor impacts on the juvenile mussels from Southern Chile. ICES Journal of Marine Science, 73: 764–771.

Noonan, S. H. C., and Fabricius, K. E. 2016. Ocean acidification affects productivity but not the severity of thermal bleaching in some tropical corals. ICES Journal of Marine Science, 73: 715–726.

Nunes, J., McCoy, S. J., Findlay, H. S., Hopkins, F. E., Kitidis, V., Queirós, A. M., Rayner, L., *et al.* 2016. Two intertidal, non-calcifying macroalgae (*Palmaria palmata* and *Saccharina latissima*) show complex and variable responses to short-term CO_2 acidification. ICES Journal of Marine Science, 73: 887–896.

Orr, J. C., Fabry, V. J., Aumont, O., Bopp, L., Doney, S. C., Feely, R. A., Gnanadesikan, A., *et al.* 2005. Anthropogenic ocean acidification over the twenty-first century and its impact on calcifying organisms. Nature, 437: 681–686.

Pörtner, H-O. 2008. Ecosystem effects of ocean acidification in times of ocean warming: a physiologist's view. Marine Ecology Progress Series, 373: 203–217.

Punt, A. E., Foy, R. J., Dalton, M. G., Long, W. C., and Swiney, K. M. 2016. Effects of long term exposure to ocean acidification conditions on future southern Tanner crab (*Chionoecetes bairdi*) fisheries management. ICES Journal of Marine Science, 73: 849–864.

Regan, M. D., Turko, A. J., Heras, J., Kuhlmann Andersen, M., Lefevre, S., Wang, T., Bayley, M., *et al.* 2016. Ambient CO_2, fish behaviour and altered GABAergic neurotransmission: exploring the mechanism of CO_2-altered behaviour by taking a hypdercapnia dweller down to low CO_2 levels. Journal of Experimental Biology, 219: 109–118.

Reum, J. C. P., Alin, S. R., Harvey, C. J., Bednaršek, N., Evans, W., Feely, R. A., Hales, B., *et al.* 2016. Interpretation and design of ocean acidification experiments in upwelling systems in the context of carbonate chemistry co-variation with temperature and oxygen. ICES Journal of Marine Science, 73: 582–595.

Roleda, M. Y., Boyd, P. W., and Hurd, C. L. 2012. Before ocean acidification: calcifier chemistry lessons. Journal of Phycology, 48: 840–843.

Ross, P., Parker, L., and Byrne, M. 2016. Transgenerational responses of molluscs and echinoderms to changing ocean conditions. ICES Journal of Marine Science, 73: 537–549.

Runge, J. A., Fields, D. M., Thompson, C., Shema, S. D., Bjelland, R., Durif, C., Skiftesvik, A. B., *et al.* 2016. End of the century CO_2 concentrations do not have a negative effect on vital rates of Calanus

finmarchicus, an ecologically critical planktonic species in North Atlantic ecosystems. ICES Journal of Marine Science, 73: 937–950.

Sala, M. M., Aparicio-Bernat, F. L., Balagué, V., Boras, J. A., Borrull, E., Cardelús, C., Cros, L., *et al.* 2016. Contrasting effects of ocean acidification on the microbial food web under different trophic conditions. ICES Journal of Marine Science, 73: 670–679.

Schram, J., Schoenrock, K., McClintock, J., Amsler, C., and Angus, R. 2016. Testing Antarctic resilience: the effects of elevated seawater temperature and decreased pH on two gastropod species. ICES Journal of Marine Science, 73: 739–752.

Sigwart, J. D., Lyons, G., Fink, A., Gutowska, M. A., Murray, D., Melzner, F., Houghton, J. D. R., *et al.* 2016. Elevated pCO_2 drives lower growth and yet increased calcification in the early life history of the cuttlefish *Sepia officinalis* (Mollusca: Cephalopoda). ICES Journal of Marine Science, 73: 970–980.

Small, D., Milazzo, M., Bertolini, C., Graham, H., Hauton, C., Hall-Spencer, J., and Rastrick, S. 2016. Temporal fluctuations in seawater pCO_2 may be as important as mean differences when determining physiological sensitivity in natural systems. ICES Journal of Marine Science, 73: 604–612.

Stoks, R., Govaert, L., Pauwels, K., Jansen, B., and De Meester, L. 2015. Resurrecting complexity: the interplay of plasticity and rapid evolution in the multiple trait response to strong changes in predation pressure in the water flea *Daphnia magna*. Ecology Letters, 19: 180–190.

Strahl, J., Francis, D. S., Doyle, J., Humphrey, C., and Fabricius, K. E. 2016. Biochemical responses to ocean acidification contrast between tropical corals with high and low abundances at volcanic carbon dioxide seeps. ICES Journal of Marine Science, 73: 897–909.

Sugie, K., and Yoshimura, T. 2016. Effects of high CO_2 levels on the ecophysiology of the diatom *Thalassiosira weissflogii* differ depending on the iron nutritional status. ICES Journal of Marine Science, 73: 680–692.

Sunday, J. M., Calosi, P., Dupont, S., Munday, P. L., Stillman, J. H., and Reusch, T. B. H. 2013. Evolution in an acidifying ocean. Trends in Ecology and Evolution, 29: 117–125.

Sundin, J., and Jutfelt, F. 2016. 9–28 d of exposure to elevated pCO_2 reduces avoidance of predator odour but had no effect on behavioural lateralization or swimming activity in a temperate wrasse (*Ctenolabrus rupestris*). ICES Journal of Marine Science, 73: 620–632.

Swiney, K. M., Long, W., and Foy, R. 2016. Effects of high pCO_2 on Tanner crab reproduction and early life history, Part I: long-term exposure reduces hatching success and female calcification, and alters embryonic development. ICES Journal of Marine Science, 73: 849–864.

Takahashi, M., Noonan, S. H. C., Fabricius, K. E., and Collier, C. 2016. The effects of long-term *in situ* CO_2 enrichment on tropical seagrass communities at volcanic vents. ICES Journal of Marine Science, 73: 876–886.

Thibodeau, G., Walsh, D. A., and Beisner, B. E. 2015. Rapid eco-evolutionary responses in perturbed phytoplankton communities. Proceedings of the Royal Society B, 282: 20151215. doi: 10.1098/rspb.2015.1215.

Vicente, J., Silbiger, N. J., Beckley, B. A., Raczkowski, C. W., and Hill, R. T. 2016. Impact of high pCO_2 and warmer temperatures on the process of silica biomineralization in the sponge *Mycale grandis*. ICES Journal of Marine Science, 73: 704–714.

Waldbusser, G., Hales, B., and Haley, B. A. 2016. Calcium carbonate saturation state: on myths and this or that stories. ICES Journal of Marine Science, 73: 563–568.

Waldbusser, G. G., and Salisbury, J. E. 2014. Ocean acidification in the coastal zone from an organism's perspective: multiple system parameters, frequency domains, and habitats. Annual Reviews of Marine Science, 6: 221–247.

Wang, Y., Zhang, R., Zheng, Q., Deng, Y., Van Nostrand, J., Zhou, J., and Jiao, N. 2016. Bacterioplankton community resistance to ocean acidification: evidence from microbial network analysis. ICES Journal of Marine Science, 73: 865–875.

Whitehead, A., Pilcher, W., Champlin, D., and Nacci, D. 2012. Common mechanism underlies repeated evolution of extreme pollution tolerance. Proceedings of the Royal Society B, 279: 427–433.

Wootton, J. T., Pfister, C. A., and Forester, J. D. 2008. Dynamic patterns and ecological impacts of declining ocean pH in a high-resolution multi-year dataset. Proceeedings of the National Academy of Sciences of the United States of America, 105: 18848–18853.

Yona, A. H., Frumkin, I., and Pipel, Y. 2015. A relay race on the evolutionary adaptation spectrum. Cell, 163: 549–559.

Zhang, H., Shin, P. K. S., and Cheung, S. G. 2016. Physiological responses and scope for growth in a marine scavenging gastropod, *Nassarius festivus* (Powys, 1835), are affected by salinity and temperature but not by ocean acidification. ICES Journal of Marine Science, 73: 814–824.

ICES Journal of Marine Science

ICES Journal of Marine Science (2016), 73(3), 537–549. doi:10.1093/icesjms/fsv254

Contribution to Special Issue: 'Towards a Broader Perspective on Ocean Acidification Research'

Review

Transgenerational responses of molluscs and echinoderms to changing ocean conditions

Pauline M. Ross[1,2]*, Laura Parker[3], and Maria Byrne[3]

[1]*School of Science and Health, Western Sydney University, Hawkesbury Campus K12, Locked Bag 2751, Penrith South DC, NSW 2751, Australia*
[2]*School of Life and Environmental Sciences, University of Sydney, Carslaw Building, Level 5, Camperdown 2006, Australia*
[3]*Schools of Medical and Biological Sciences, F13, University of Sydney, Sydney, NSW 2006, Australia*

**Corresponding author: tel: +61 2 45 701306; fax: +61 2 45 701621; e-mail: pm.ross@westernsydney.edu.au*

Ross, P. M., Parker, L., and Byrne, M. Transgenerational responses of molluscs and echinoderms to changing ocean conditions. – ICES Journal of Marine Science, 73: 537–549.

Received 22 June 2015; revised 23 November 2015; accepted 1 December 2015; advance access publication 13 January 2016.

We are beginning to understand how the larvae of molluscs and echinoderms with complex life cycles will be affected by climate change. Early experiments using short-term exposures suggested that larvae in oceans predicted to increase in acidification and temperature will be smaller in size, take longer to develop, and have a greater incidence of abnormal development. More realistic experiments which factored in the complex life cycles of molluscs and echinoderms found impacts not as severe as predicted. This is because the performance of one life history stage led to a significant carryover effect on the subsequent life history stage. Carryover effects that arise within a generation, for example, embryonic and larval stages, can influence juvenile and adult success. Carryover effects can also arise across a generation, known as transgenerational plasticity (TGP). A transgenerational response or TGP can be defined as a phenotypic change in offspring in response to the environmental stress experienced by a parent before fertilization. In the small number of experiments which have measured the transgenerational response of molluscs and echinoderms to elevated CO_2, TGP has been observed in the larval offspring. If we are to safeguard ecological and economically significant mollusc and echinoderm species against climate change then we require more knowledge of the impacts that carryover effects have within and across generations as well as an understanding of the underlying mechanisms responsible for such adaptation.

Keywords: carryover effects, echinoderms, molluscs, ocean acidification, TPG, transgenerational effects.

Introduction

How will the larvae of molluscs and echinoderms with complex life cycles respond to climate change? The answer to this question, based on a growing body of evidence, suggests that mollusc and echinoderm larvae in acidified oceans will be smaller in size, take longer to develop, and be more abnormal. Subsequent juvenile and settler stages may also be affected. Recent reviews document a range of negative impacts from exposure to elevated CO_2 on molluscs and echinoderms larvae from intertidal and subtidal habitats (for reviews, see Byrne, 2010, 2011; Dupont *et al.*, 2010a; Ross *et al.*, 2011; Byrne, 2013; Byrne and Przeslawski, 2013; Gazeau *et al.*, 2013; Parker *et al.*, 2013).

Many of the studies in these reviews report on experiments where single life history stages of molluscs and echinoderms are exposed for short periods to elevated CO_2. The inferences that can be obtained from such short-term exposures are, however, potentially limited because they may over- or underestimate the impacts of climate change on marine larvae (Cripps *et al.*, 2014) as they do not simulate the real-world scenario, one where multiple stressors will interact and pH will decline slowly (Byrne and Przeslawski, 2013; Przeslawski *et al.*, 2015). Also in many experiments, the pH levels used often do not incorporate conditions in nature or natural pH variability (Hofmann *et al.*, 2011).

Further, molluscs, echinoderms, and other marine invertebrates have complex life cycles which include a series of free living larval stages as well as benthic juvenile and adult stages which go through ontogenic shifts in function and habitat. Although these stages differ dramatically in form and function and are often thought of as discrete and somewhat autonomous, they are nonetheless part of the continuum of life (Podolsky and Moran, 2006; Dupont *et al.*, 2013). Anywhere along this continuum, the performance at one life history stage may lead to significant positive or negative carryover

effects on subsequent life history stages, also known as the developmental domino phenomena (Byrne, 2011). These carryover effects can arise within a generation, for example, embryonic and larval experiences can influence juvenile and adult success; as well as across a generation, with the environment experienced by one generation directly influencing the success of the subsequent generation (Byrne, 2010; Kovalchuk, 2012; Munday, 2014).

A transgenerational response or transgenerational plasticity (TGP) is an across generational carryover effect which can be defined as a phenotypic change in offspring in response to the environmental stress experienced by one or both parents (Marshall, 2008; Kovalchuk, 2012; Shama and Wegner, 2014), especially during gamete development (Hamdoun and Epel, 2007; Byrne *et al.*, 2011). TGP occurs when the environment which is experienced by the parent influences phenotype of their offspring exposed to the same environment (Salinas *et al.*, 2013; Munday, 2014). For example, the optimum salinity and salinity range of embryos and larvae of the oyster *Crassostrea virginica* were influenced by the salinity at which the adults were held before spawning (Davis, 1958). Similarly, the offspring of the gastropod, *Crepidula convexa*, were found to be more tolerant of copper stress when adults were collected from a copper polluted site compared with offspring from adults collected in a control unpolluted site (Untersee and Pechenik, 2007). Similarly, the thermal environmental history of adult molluscs and echinoderms can determine the temperature tolerance limits of their offspring (Andronikov, 1975; Byrne *et al.*, 2011). More recently, a study on Antarctic marine echinoderm *Sterechinus neumayeri* found that contaminant-experienced mothers, which had higher baseline levels of antioxidants, transferred resilience against oxidative stress to their embryos (Lister *et al.*, 2015). This resilience, however, did not lead to less abnormal development and the benefit for overall fitness and survival was unclear.

As stated above, the impacts of climate change on molluscs, echinoderms, and other marine invertebrate life histories are comprehensively covered in many reviews (e.g. Dupont *et al.*, 2010a; Hofmann *et al.*, 2010; Albright, 2011; Byrne, 2011, 2012; Ross *et al.*, 2011; Byrne and Przeslawski, 2013; Parker *et al.*, 2013; Przeslawski *et al.*, 2015). In this review, we focus on the impacts of ocean acidification on the larvae of molluscs and echinoderms and within and across generation carryover effects to evaluate the evidence for TGP. To do this, we briefly discuss the results of studies which have measured responses of single larval life history stage of molluscs and echinoderms to short-term or acute exposures to elevated CO_2 .We then concentrate on studies which have measured responses of successive life history stages (i.e. larvae to juveniles, adults to larvae), to determine within and across transgenerational impacts. We need to understand the potential for carryover effects to determine the capacity of molluscs and echinoderms to acclimate and adapt to an ocean increasing in acidification and temperature due to climate change.

Acute effects: single larval life history stages

Larvae of molluscs and echinoderms have been found to be particularly sensitive to acidification and warming. Early on it was common to investigate impacts of elevated CO_2 on shell morphology and physiology of single life history stages of mollusc and echinoderm larvae using short-term or acute exposure experiments.

Such experiments found reduced larval size of molluscs (Kurihara *et al.*, 2007; Kurihara, 2008; Parker *et al.*, 2009, 2010, 2011; Talmage and Gobler, 2009, 2010, 2011, 2012; Watson *et al.*, 2009; Comeau *et al.*, 2010; Dupont *et al.*, 2010a,b; Gazeau *et al.* 2010; Lischka *et al.*, 2010) and echinoderms (Kurihara and Shirayama, 2004; Dupont *et al.*, 2008; Clark *et al.*, 2009; O'Donnell *et al.*, 2009a, b; Sheppard Brennand *et al.*, 2010; Stumpp *et al.*, 2011a, b, 2012; Byrne, 2013; Byrne *et al.*, 2013a, b; Gonzalez-Bernat *et al.*, 2013a, b; Uthicke *et al.*, 2013), hinge abnormalities, erosion and pitting of the Shell (Talmage and Gobler, 2010), reduced calcification (Comeau *et al.*, 2010; Range *et al.*, 2011), and decreased scope for growth (Stumpp *et al.*, 2011a, b, 2012). Overall, larvae were found to be more sensitive than adults to elevated CO_2 even in the most resilient classes of molluscs (i.e. cephalopods Gutowska *et al.*, 2008; Gutowska and Melzner, 2009; Sigwart *et al.*, 2016).

Larvae are thought to be particularly sensitive because of the high solubility of the amorphous calcium carbonate and aragonite that initiates skeleton development (O'Donnell *et al.*, 2009a, b). However, as this phase of calcium carbonate is intracellular in a highly regulated environment, it is unlikely to be directly vulnerable to environmental acidification (Stumpp *et al.*, 2012; Dubois, 2014).

Exposure to elevated CO_2 changes gene regulation (Zippay and Hofmann, 2010; Padilla-Gamino *et al.*, 2013), including skeletogenic pathways (Evans *et al.*, 2013; Thompson *et al.*, 2015), spicule matrix proteins (Evans and Watson-Wynn, 2014), ion-regulation (Stumpp *et al.*, 2012) ion transport (Evans and Watson-Wynn, 2014), and protein synthesis (Pan *et al.*, 2015; Thompson *et al.*, 2015).

Acute exposure to elevated CO_2 also delays development, increases abnormalities, and decreases larval survival in molluscs (Kurihara *et al.*, 2007; Ellis *et al.*, 2009; Kurihara *et al.*, 2009; Parker *et al.*, 2009, 2010, 2011; Talmage and Gobler 2009; Watson *et al.*, 2009) and echinoderms (Kurihara *et al.*, 2004a, b; Kurihara and Shirayama 2004; Dupont *et al.*, 2008; Clark *et al.*, 2009; Stumpp *et al.*, 2011a, b, 2012; Byrne, 2013; Gonzalez-Bernat *et al.*, 2013a, b; Uthicke *et al.*, 2013), perhaps because of changes in lipid reserves and energetics (molluscs Talmage and Gobler, 2010, 2011), but not always (echinoplutei, Matson *et al.*, 2012).

Studies also found physiological changes in mollusc and echinoderm larvae in response to short-term exposure to elevated CO_2 including changes in standard metabolic rate (SMR) in bivalves (Lannig *et al.*, 2010; Parker *et al.*, 2012, 2013) and echinoderms (Todgham and Hofmann, 2009; Beniash *et al.*, 2010; Stumpp *et al.*, 2012; Thomsen *et al.*, 2013).

Larvae which are smaller in size may have less energy reserves, spending longer in the plankton to reach metamorphosis, increasing their risk of predation and mortality (Byrne *et al.*, 2009; Ross *et al.*, 2011). Already, mortality of larvae in the plankton is thought to exceed 90% (Thorson, 1950; Gosselin and Qian, 1997), in an ocean altered by climate change, this may increase. Even if smaller larvae survive to settle, they may have a reduced competitive ability at settlement (Hobday and Tegner, 2002; Kurihara *et al.*, 2007; Byrne *et al.*, 2009, 2010) and increased post-settlement mortality (molluscs Kurihara *et al.*, 2007; Parker *et al.*, 2009, 2010; echinoderms Talmage and Gobler, 2009; echinoderms: Dupont *et al.*, 2008; Clark *et al.*, 2009).

Mollusc and echinoderm larvae also experience environmental stress from factors other than elevated CO_2 . Global sea surface temperatures are increasing and it is predicted that temperatures will continue to rise over this century up to 4°C by the 2100 (IPCC, 2013, 2014). Climate change will also alter salinity and turbidity regimes as a result of unpredictable rain events. Individually, each of these stressors has the potential to influence the growth and

survival of larvae. Together, how these stressors will interact to ameliorate or exacerbate conditions for larvae of molluscs and echinoderms remains unknown (Byrne, 2011; Byrne and Przeslawski, 2013; Przeslawski *et al.*, 2015).

Within-generation carryover effects: larvae to juveniles

Although studies on single life history stages using acute exposures to elevated CO_2 provide information on the vulnerabilities of embryos and larvae, they do not provide information on positive or negative carryover effects within generation from planktonic to juvenile stages. Studies have found that stressors present during early-life history stages can have carry-over effects within the generation (Hettinger *et al.*, 2012; White *et al.*, 2013). It is well known that early larval life may influence juvenile performance and adult fitness. Metamorphosis is not a new beginning, but dependent on the environmental experience of early-life history stages such as embryos and larvae (Pechenik *et al.*, 1998; Pechenik, 1999; Byrne *et al.*, 2008).

There are fewer studies which have measured the carryover effects of elevated CO_2 from larvae to juvenile stages of molluscs and echinoderms (Table 1). Those studies that have done so find negative impacts in larvae exposed to elevated CO_2 which typically continues until the juvenile stage after settlement (Byrne *et al.*, 2010; Hettinger *et al.*, 2012, 2013; Dupont *et al.*, 2013; Wangensteen *et al.*, 2013).

In echinoderms, Byrne *et al.* (2010) reported the first evidence of negative carryover effects from larvae to juveniles of the sea urchin *Heliocidaris erythrogramma* following a 5-d exposure to reduced pH (8.2_{NIST} *control*, 7.8_{NIST}, 7.6_{NIST}) and elevated temperature (22°C *control*, 24, 26°C). *Heliocidaris erythrogramma* gametes were fertilized at each pH and temperature treatments where they remained for the duration of larval development and settlement (4 d post-fertilization). Following settlement (5 d post-fertilization), the number of normal juveniles which developed and the number of spines per juvenile were significantly reduced in the low pH treatments relative to the ambient treatment. The negative effects on spine development were ameliorated at the moderately elevated temperature of +2°C, but not +4°C (Byrne *et al.*, 2010). Similar negative carryover effects from larvae to juveniles have also been observed in sea urchins following longer juvenile exposure periods (Dupont *et al.*, 2013). Larvae of the sea urchin, *Strongylocentrotus droebachiensis*, were exposed to present day (361 μatm) and elevated (941 μatm) CO_2 until settlement. Following this time, post-settled juveniles from each larval CO_2 treatment were transferred to present day (361 μatm) or elevated (941 μatm) CO_2 in a fully orthogonal design. After 3 months of juvenile exposure, pCO_2 had no direct negative impact on juvenile survival. Survival of juveniles was reduced only in treatments where both larvae and juveniles had been reared at elevated CO_2 (Dupont *et al.*, 2013). In contrast, within-generational carryover effects in the sea urchin, *Arbacia lixula*, were much less pronounced (Wangensteen *et al.*, 2013). Three-day-old juveniles of *A. lixula* reared from the beginning of larval development at elevated CO_2, pH of 7.7_T, had similar survival to juveniles reared at the control pH of 8.1_T. There was, however, a significant reduction in the diameter of juveniles (Wangensteen *et al.*, 2013).

In molluscs, exposure to elevated CO_2 during larval development has been shown to have negative carryover effects for juveniles even when the juvenile is reared at ambient CO_2 (Hettinger *et al.*, 2012, 2013). Hettinger *et al.* (2012) investigated whether the impacts of elevated CO_2 on larvae of Olympia oysters, *Ostrea lurida*, were transferred through metamorphosis to juveniles. Larvae were reared at control (8.0 pH units) and low (7.9 and 7.8) pH for the duration of larval development. At the time of settlement, larvae reared at low pH of 7.8 had a 15% decrease in growth rate and a 7% decrease in shell area. These effects were even more pronounced following settlement, with juveniles that had been reared at pH 7.8 during larval development having a 41% decrease in growth rate. The decrease in growth rate occurred regardless of the pH level that the juvenile was reared and persisted for 1.5 months after settlement (Hettinger *et al.*, 2012). Persistent negative carryover effects have also been found for larvae of *O. lurida* exposed to elevated CO_2 and returned to natural conditions in the field (Hettinger *et al.*, 2013). Larvae of *O. lurida* were reared at ambient (500 μatm) and elevated (1000 μatm) CO_2 until settlement. Following this, the newly settled juveniles were transferred into the field where they remained for a period of 4 months. Juveniles had reduced growth rates in the field when larval development had occurred at elevated compared with control CO_2. These negative carryover effects on juvenile growth persisted for 4 months post-settlement (Hettinger *et al.*, 2013).

Other studies on molluscs have found positive carryover effects. In contrast to *O. lurida*, juveniles of the bay scallop, *Argopecten irradians*, had positive specific growth rates when larvae were exposed to elevated CO_2 (Gobler and Talmage, 2013). Gobler and Talmage (2013) reared larvae *A. irradians* at ambient (390 μatm) and elevated (750 μatm) CO_2 in the laboratory through to early days of juvenile development. Juveniles were then transferred into the field where they remained for a period of 10 months. After 13–26 weeks post-fertilization, juveniles reared at elevated CO_2 during larval development had greater specific growth rates than the juveniles reared at ambient CO_2 (control juveniles). The authors suggested that the greater specific growth rate occurred because juveniles that survive CO_2 as larvae are those with greater "fitness" (Gobler and Talmage, 2013). By 10 months, the effects of larval exposure to elevated CO_2 on juvenile growth were no longer present; both juvenile lines had similar growth. Finally, in the hard clam, *Mercenaria mercenaria*, exposure of larvae to elevated CO_2 (1500 μatm) caused a significant reduction in the survival of post-set juveniles only when the juveniles were also reared at elevated CO_2 (Gobler and Talmage, 2013). Interestingly, there was an increase in the post-settlement survival of juveniles that were reared at elevated CO_2 as larvae and ambient CO_2 as juveniles. Once again, the authors suggested that high mortality during the larval stage in the elevated CO_2 treatment led to the survival of fitter individuals (Gobler and Talmage, 2013).

Collectively, these studies emphasize the importance of investigating the potential carryover effects that larval exposure to elevated CO_2 has for juvenile and adult stages. Indeed, studies on non-marine species suggest that experiences in early life can have direct consequences for later success (Burton and Metcalfe, 2014, and references therein). From the studies done to date, it is likely that responses of echinoderm and mollusc populations to elevated CO_2 need to be measured within generation to determine the potential carryover effects.

Transgeneration carryover effects: adults to larvae

Understanding whether marine invertebrates will have the capacity to acclimate and adapt to ocean acidification by the end of the century is an area of great uncertainty (Donelson *et al.*, 2011; Sunday *et al.*, 2014). Uncertainty exists because single-generation experiments are constrained by compressing 100 years of evolution

Table 1. Within-generational carryover effects: results of studies investigating the impacts of ocean acidification (pH/pCO_2, ppm) on the life history transition from larvae to juveniles in molluscs and echinoderms.

Species	Experiment duration	Measured	Larval, juvenile CO_2/pH exposure	Impact compared with control	Other stressors	Additional comments	Author
Molluscs							
Argopecten irradians (scallop)	10 months post-settlement	Growth rate	*390 µatm, field* 750 µatm, field	↑	Nil	Growth rate increased after 13 – 26 weeks but similar by 10 months	Gobler and Talmage (2013)
Mercenaria mercenaria (hard clam)	36 d post-fertilization	Survival	*390, 390 µatm* 390; 1500 µatm 1500; 390 µatm 1500; 1500 µatm	= ↑ ↓	Nil		Gobler and Talmage (2013)
Ostrea lurida (Olympia oyster)	1.5 months post-settlement	Growth rate	*8.0, 8.0$_{NIST}$* 8.0, 7.8$_{NIST}$ 7.8, 8.0$_{NIST}$ 7.8, 7.8$_{NIST}$	↓ (41%) ↓ (41%)	Nil	41% decrease in juvenile growth rate occurred when larvae were reared at elevated CO_2 regardless of juvenile treatment	Hettinger *et al.* (2012)
Ostrea lurida (Olympia oyster)	4 months post-settlement	Growth rate	*500 µatm, field* 1000 µatm, field	↓			Hettinger *et al.* (2013)
Echinoderms							
Heliocidaris erythrogramma (sea urchin)	1 d post-settlement	# normal juveniles, # spines	*8.2, 8.2$_{NIST}$* 7.8, 7.8$_{NIST}$ 7.6, 7.6$_{NIST}$	↓,↓ ↓,↓	22, 24, 26°C	−ive effects on spine development were ameliorated 24°C but not +26°C	Byrne *et al.* (2010)
Strongylocentrotus droebachiensis (sea urchin)	3 months post-settlement	Survival	*361, 361 µatm* 361, 941 µatm 941, 361 µatm 941, 941 µatm	= = ↓(95%)		Survival of juveniles was reduced when both larvae and juveniles reared at elevated CO_2	Dupont *et al.* (2013)
Arbacia lixula (Sea urchin)	3 d post-settlement	Survival, juvenile diameter	*8.1, 8.1$_T$* 7.7, 7.7$_T$	=, ↓			Wangensteen *et al.* (2013)

Molluscs: three studies, three species; echinoderms: three studies, three species. Control CO_2/pH listed in italics. For all studies, experimental exposure began during fertilization or early larval development.

into a period which is experimentally feasible and fundable (Fitzer *et al.,* 2012). Such a constraint, however, will underestimate the potential for marine organisms to cope with changing ocean conditions (Donelson *et al.,* 2011; Sunday *et al.,* 2014). Whether resilience to elevated CO_2 can occur over multiple generations has been investigated in marine invertebrates (Mayor *et al.,* 2007; Kurihara and Ishimatsu, 2008; Lohbeck *et al.,* 2012; Fitzer *et al.,* 2014; De Wit *et al.,* 2015), vertebrates (fish Donelson *et al.,* 2011), and algae (Collins and Bell, 2004) with short generation times (days to months; Table 2). For organisms with long generation times (months to years), such as molluscs and echinoderms, measuring the response of species across multiple generations is much more difficult (Sunday *et al.,* 2014). Studies on these species to date have focused on the transgenerational response to elevated CO_2.Transgenerational experiments allow parents to facilitate phenotypic acclimatory processes between generations in response to the environment, not solely due to genotype (Donelson *et al.,* 2011). Overall, these studies suggest that acclimation to elevated CO_2 may be possible for marine organisms over successive generations at time-scales which may be shorter than the rate of anticipated climate change in oceans. With so few studies, however, predictive capacity remains problematic. Parker *et al.* (2012) were the first to show that the negative effects of ocean acidification on marine invertebrate larvae could be reduced following transgenerational exposure to elevated CO_2. They exposed parents of the oyster *Saccostrea glomerata* to elevated CO_2 of 856 μatm for 5 weeks during reproductive conditioning and found that parental exposure had positive carryover effects for larval offspring. Larvae from parents exposed to elevated CO_2 were larger in size, developed faster, but had similar survival at elevated CO_2 compared with larvae from control parents (Parker *et al.,* 2012). These positive carryover effects persisted into adulthood and the next generation (Parker *et al.,* 2015). When offspring from CO_2-exposed parents reached adulthood, they had a greater capacity to regulate extracellular pH (pH_e) at elevated CO_2. Furthermore, subsequent exposure of these adults to elevated CO_2 led to similar positive carryover effects in their larval and juvenile offspring during exposure to elevated CO_2 (Parker *et al.,* 2015). Interestingly, offspring from CO_2-exposed parents also performed better at present-day CO_2, leading the authors to suggest that increased maternal provisioning into eggs may have been a key mechanism involved in the observed TGP.

Fitzer *et al.* (2014) similarly investigated the impacts of transgenerational exposure to elevated CO_2 on the composition of juvenile shells of the mussel, *Mytilus edulis*. They found that parental (6 months) and offspring exposure to elevated CO_2 at 1000 μatm resulted in juveniles that no longer produced aragonite in their shells and instead produced only calcite. Fitzer *et al.* (2014) suggested this was an acclamatory mechanism, aragonite being more vulnerable to calcium carbonate under-saturation than calcite. In this study, the response of larvae to the impacts of parental exposure to elevated CO_2 was not reported.

While there have been more studies on the TPG response of echinoderms, the small number of studies makes conclusions difficult. Whether transgenerational carryover effects are positive or negative for echinoderms (i.e. sea urchins) depends on the length of time that parents are exposed to elevated CO_2 and the stage of maturity of the gonads. For example, there were negative impacts on the reproductive output and success of the larvae from adult sea urchins, *St. droebachiensis*, exposed to elevated CO_2 of 1217 μatm for a period of 4 months. Fecundity was reduced by 4.5-fold and there were five to nine times fewer larvae reaching juvenile stages from parents exposed to elevated CO_2 (Dupont *et al.,* 2013).

Similar results were found for the larvae from adult Antarctic sea urchin, *S. neumayeri*. Larvae from parents exposed to the combined stressors of elevated CO_2 (928 and 1405 μatm) and temperature (+2°C) for either 6 or 17 months had different outcomes (Suckling *et al.,* 2015). After parents were exposed to 6 months of elevated CO_2 and temperature, egg size was smaller and hatching success was 63% lower compared with parents exposed to present-day control conditions. After parents were exposed to 17 months of elevated CO_2 and temperature, the egg size was larger and hatching success greater from parents reared at elevated CO_2 and temperature compared with ambient treatments (present-day control and elevated). Larval success (survival and development rate) was also greater from parents exposed to elevated CO_2 and temperature for 17 months. There was, however, an increase in abnormal development of larvae compared with the present-day controls (Suckling *et al.*, 2015). The authors suggested that the increase in abnormal development was because of the interactive effects of CO_2 and temperature rather than CO_2 alone.

Collectively for *St. droebachiensis* and *S. neumayeri*, it seems that parents require exposure to elevated CO_2 and/or temperature for a period more than 6 months before transgenerational carryover positive effects from parents to their larval offspring occur. This may reflect the time it takes for the adults to acclimate to the acidified conditions. For example, adult *S. neumayeri* exposed to elevated CO_2 and temperature for 6 months had an increase in SMR compared with adults exposed to present-day conditions. Following 17 months of exposure, however, SMR was restored to control levels, suggesting that adult acclimation had occurred (Suckling *et al.,* 2015). Time to acclimation may vary among sea urchin species. Suckling *et al.* (2014) exposed parents of *Psammechinus miliaris* to elevated CO_2 of 999 μatm for 28, 42, and 70 d and compared the response of larval offspring with those parents exposed to present-day CO_2 conditions. Their results showed positive carryover transgenerational effects after 42 and 70 d of parental exposure, but not after 28 d. Larvae from parents exposed to 42 and 70 d of elevated CO_2 were larger in size at the time of settlement compared with larvae from parents exposed to elevated CO_2 for 28 d or present-day conditions. Additionally, parental exposure to elevated CO_2 for 70 d ameliorated the impacts of elevated CO_2 on fertilization success.

In the only other transgenerational study on the tropical Pacific sea urchin, *Echinometra mathaei*, parents exposed to elevated CO_2 for 42 d were not long enough to facilitate positive carryover transgenerational effects in larvae (Uthicke *et al.,* 2013). There was no difference in the size of eggs from parents exposed to present-day or elevated CO_2. Irrespective of the parental exposure, the percentage and size of larvae decreased and arm asymmetry increased at elevated CO_2. Uthicke *et al.* (2013) suggested that acclimation of offspring did not occur following 42 d of adult exposure to elevated CO_2 because adults were not exposed from the onset of gonadal development. The time that the adults are introduced to ocean change stressors with respect to gametogenesis is likely to be a critical factor determining the outcomes of these experiments and identification of TGP to elevated CO_2 in echinoderm and other marine invertebrates, especially for species with seasonal reproduction and synchronous gametogenesis. The influence of maternal imprinting determined by the environment in which the eggs develop from the onset of oogenesis can have a major influence on offspring performance (Andronikov, 1975; Byrne, 2010; Byrne *et al.,* 2011).

Table 2. Transgenerational carryover effects: results of studies investigating the impacts of ocean acidification (pH/pCO_2, ppm) on the life history transition from adults to larvae in molluscs and echinoderms.

Species	Parental exposure	Measured	Adult, larval CO_2/pH exposure	Nature of carryover (+ive/−ive/=)	Response to transgenerational exposure	Author
Molluscs						
Saccostrea glomerata (oyster)	5 weeks	Survival, Shell length, % development	*385, 385 µatm* 385, 856 µatm 856, 385 µatm 856, 856 µatm	+ive	Larvae larger in size, developed faster but had similar survival at elevated CO_2 compared with larvae from control parents	Parker *et al.* (2012)
Mytilus edulis (mussel)	6 months	Juvenile shell composition	*380, 380 µatm* 550, 550 µatm 750, 750 µatm 1000; 1000 µatm	+ive	Juvenile shell no longer contained aragonite at 1000 µatm. Larval response not measured	Fitzer *et al.* (2014)
Echinoderms						
Strongylocentrotus droebachiensis (sea urchin)	4 and 16 months	Fecundity, # larvae to reach juvenile stage	*361, 361 µatm* 1217, 1217 µatm	−ive (4 months) +ive (16 months)	Adult exposure for 4 months had negative impacts reproductive output and larval offspring success. Fecundity reduced by 4.5-fold and 5–9 times fewer larvae reached the juvenile stage. After 16 months of adult exposure, negative effects on fecundity and larval survival no longer observed	Dupont *et al.* (2013)
Sterechinus neumayeri (sea urchin)	6 and 17 months	Egg size, hatching success, larval survival, development rate, % abnormal development	*361, 361 µatm;* 0̊C 928, 928 µatm; 2̊C 1405, 1405 µatm; 2̊C	−ive (6 months) +ive (17 months)	Adult exposure for 6 months caused reduced egg size and 63% lower hatching success compared with control adults. After 17 months of adult exposure, egg size was larger and hatching success was similar across all parental CO_2 and temperature treatments. Larval survival and development rate also improved following 17 months of adult exposure; however, abnormal development of larvae was increased compared with the present-day controls	Suckling *et al.* (2014)
Psammechinus miliaris (sea urchin)	28, 48, and 70 d	Fertilization success, size	*559, 559 µatm* 999, 999 µatm	+ive (42 and 70 d)	Positive transgenerational carryover effects were observed after 42 and 70 d of parental exposure, but not after 28 d. Adult exposure for 42 and 70 d led to larger larvae at the time of settlement compared with larvae from parents exposed to elevated CO_2 for 28 d or present-day conditions. Adult exposure for 70 d also ameliorated the impacts of elevated CO_2 on fertilization success	Sucking *et al.* (2014b)
Echinometra mathaei (sea urchin)	42 d	Egg size, % normal larvae, larval size, arm asymmetry	*485, 485 µatm* 1770, 1770 µatm	=	No difference in size of eggs from parents exposed to present-day or elevated CO_2. Percentage of normal larvae and size of larvae reduced and arm asymmetry increase at elevated CO_2, irrespective of the parental environment	Uthicke *et al.* (2013)

Strongylocentrotus purpuratus (sea urchin)	Field study	Larval size	Gravid adults collected from two different sites along Northeast Pacific. pH of both sites varied from 7.6 to 8.3_{NIST}, but there was a higher frequency of low pH at the northern site	+ive	Using a reciprocal breeding design the authors created 64 families with the aim of assessing the impact of maternal and paternal origin on larval offspring size when reared at elevated CO_2. There was a significant effect of maternal (but not paternal) origin on larval size at elevated CO_2. Overall, larval size was reduced in all family lines held at elevated compared with ambient CO_2 but the extent of reduction was significantly less for larvae whose mothers were collected from the northern site	Kelly *et al.* (2013)

Molluscs: two studies, two species; echinoderms: five studies, five species. Control CO_2/pH listed in italics.

There is also evidence of TGP in response to elevated CO_2 in an echinoderm species from field experiments (Kelly *et al.,* 2013). Kelly *et al.* (2013) collected adults of the purple sea urchin *Strongylocentrotus purpuratus* from two sites along the coast of the Northeast Pacific. The pH at both collection sites varied from 7.6 to 8.3_{NIST}, but there was a higher frequency of low pH at the northern compared with the southern site. Using a reciprocal breeding design, the authors created 64 families with the aim of assessing the impact of maternal and paternal origin on larval offspring size when reared at elevated CO_2. The results showed that there was a significant effect of maternal (but not paternal) origin on larval size at elevated CO_2. Overall, larval size was reduced in all family lines held at elevated compared with ambient CO_2, but the extent of this reduction was significantly less for larvae whose mothers were collected from the northern site with a higher frequency of low pH. Although the exact pH of the environment was not known, the authors reasonably concluded that high genetic variation within a population and the history of exposure to low pH will be critical determinants of the adaptation potential of echinoderms to elevated CO_2 over this century.

What are the mechanisms for transgenerational carryover effects/TGP?

TGP is non-genetic inheritance, whereby parents induce phenotypic changes in offspring traits without altering their DNA sequence (Salinas and Mulch, 2012). A transgenerational response or TGP can be defined as a phenotypic change in offspring in response to the environmental stress experienced by a parent(s) (Kovalchki 2012). TGP is acclamatory and can occur over rapid time-scales because of the absence of genetic modification. In contrast to TPG, evolutionary adaptation is a slower process which relies on heritable DNA genetic modification.

The two main non-genetic pathways which have been identified as mechanisms for transgenerational exposure to elevated CO_2 leading to carryover effects from parents to offspring are: (i) increased maternal provisioning and/or (ii) epigenetic modifications in gene expression, commonly referred to as epigenetic inheritance (Murray *et al.,* 2013; Burton and Metcalfe, 2014; Munday, 2014).

Increased maternal provisioning is an adaptive strategy employed by marine and other organisms to help offspring survive in suboptimal environmental conditions (Bernardo, 1996; Untersee and Pechenik, 2007; Allen *et al.,* 2008; Marshall, 2008; Marshall *et al.,* 2008; Sanford and Kelly, 2011; Allan *et al.,* 2014). Mothers which experience suboptimal environments can increase the energy which they invest per egg, often at the expense of fecundity, thereby increasing offspring fitness and survival in those same suboptimal conditions (Allen *et al.,* 2008). Elevated CO_2 is hypothesized to increase the energy demand of marine species (Pörtner and Farrell, 2008), particularly in larvae which have limited capacity to regulate acid–base status (Parker *et al.,* 2015). As such, increased energy reserves in eggs will be beneficial for mollusc and echinoderm larvae as our oceans continue to acidify. Evidence for increased maternal provisioning in the form of increased egg size was observed in the sea urchin, *S. neumayeri* following 17 months of parental exposure to elevated CO_2 (but not 6 months of exposure; Suckling *et al.,* 2014). Further in the oyster, *Sa. glomerata*, although egg size was not measured, 24 h larvae from parents exposed to elevated CO_2 were larger in size than larvae from parents exposed to present-day CO_2 (Parker *et al.,* 2012). This led the authors to suggest that increased maternal provisioning occurred.

For *St. droebachiensis* and *P. miliaris*, there was no significant increase in the size of eggs following transgenerational exposure of parents to elevated CO_2 (Dupont *et al.*, 2013; Suckling *et al.*, 2015). In fact, the egg size of *P. miliaris* significantly decreased. Despite this, TGP was still observed in the larval offspring following parental exposure to elevated CO_2, suggesting the involvement of mechanisms other than increased maternal energy provisioning (Dupont *et al.*, 2013). It is also possible that the nature of the energy reserves was altered in the eggs (Moran and McAlister, 2009). Moran and McAlister (2009) emphasized that although egg size is simple to measure, egg size can be altered by processes that do involve increased nutritive reserves.

Epigenetic inheritance is gaining considerable ground in the literature as a key mechanism of TGP in marine organisms during exposure to environmental stress (Vandegehuchte and Janssen, 2014). Poor environmental conditions trigger beneficial modifications in the gene expression pattern of parents which are passed to their offspring, influencing the offspring phenotype. These epigenetic changes are thought to occur predominantly through DNA methylation as well as histone modification and/or non-coding RNA (Riviere, 2014; Vandegehuchte and Janssen, 2014). These changes can be transmitted through generations, especially if environmentally reinforced or can eventually disappear over two to three generations (Flores *et al.*, 2013).

Direct correlations between TGP and differential gene expression are yet to be made in marine species following exposure to elevated CO_2. It has been hypothesized, however, that changes in the expression of key genes such as those relating to acid–base regulation and mitochondrial metabolism are likely to be involved (Miller *et al.*, 2012; Murray *et al.*, 2013). Evidence of acclimation to reduced pH through epigenetic changes has been shown within a generation in fish (Deigweiher *et al.*, 2008; Horng *et al.*, 2009; Tseng *et al.*, 2013). For example, acclimation to environmental hypercapnia of 10 000 ppm of adults of the eelpout *Zoarces viviparous* involved an initial down-regulation followed by an up-regulation of a key ion transporter (Na^+/HCO_3^-) pivotal for acid–base regulation, as well as, a twofold increase in Na^+–K^+–ATPase in gill tissue (Deigweiher *et al.*, 2008).

More recently, a study of the transgenerational effects of ocean warming on offspring of the marine stickleback, *Gasterostaus aculeatus*, found that acclimation of juvenile body size following transgenerational exposure to elevated temperature was closely linked to mitochondrial respiration rates (Shama *et al.*, 2014). Mitochondrial respiration rates in offspring were significantly lower at the elevated temperature of 21°C when mothers were reared at 21°C compared with 17°C. It is believed that mothers adjusted their mitochondria respiration capacities and that this adjustment was passed to their offspring to improve their performance at elevated temperature (Shama *et al.*, 2014). Adjustment of metabolic capacities may be an epigenetic mechanism employed by echinoderms following transgenerational exposure to elevated CO_2 as improvements in larval offspring traits in sea urchins were shown to occur only when gametes used to generate offspring were from parents that had adjusted their metabolism to that seen in control conditions (Dupont *et al.*, 2013; Suckling *et al.*, 2014). In contrast, in the oyster *Sa. glomerata*, transgenerational improvements in larval offspring traits during exposure to elevated CO_2 were still seen, despite parental metabolic rates remaining elevated (Parker *et al.*, 2012).

Understanding the mechanisms involved in the TGP in molluscs and echinoderms is a key area for future research. It is likely that the mechanisms of transfer are not mutually exclusive nor are limited to the mechanisms described above. In studies unrelated to ocean acidification, TGP has also been linked to the direct transfer of somatic factors such as protective chaperone proteins and hormones from parents to their offspring (Hamdoun and Epel, 2007). Meistertzheim *et al.* (2009) found that the concentration of heat shock proteins as well as other stress proteins in the adult gonad of the oyster *Crassostrea gigas* were threefold higher during gametogenesis compared with times of resting gonadal development. They hypothesized that high levels of stress proteins were provided to eggs via maternal transfer which is an effective strategy to overcome environmental stress (Meistertzheim *et al.*, 2009). De Wit *et al.* (2015) found that in the copepod *Pseudoclanus acuspes*, RNA transcription was down-regulated in populations with long-term exposure to elevated CO_2 even after transplantation back to control levels.

Another key question which remains unanswered is whether several mechanisms of TGP (i.e. maternal provisioning, epigenetic inheritance, somatic factors) will benefit species persistence in an ocean predicted to be increase in acidification and temperature. We do not know if one mechanism of TGP is better than another in terms of the acclimation or adaptation ability of a species? Will one mechanism benefit them more? Will one have greater negative implications for other life history stages? Will one persist longer than another? Answers to these questions remain unexplored in marine climate change research.

Are there limitations or repercussions of TGP?

From the handful of studies on mollusc and echinoderm larvae, we know that TGP may be an acclamatory mechanism that has the potential to reduce and ameliorate the impacts of elevated CO_2 over this century. Whether or not there are limitations of TGP or negative repercussions of TGP for later life history stages and future generations is unknown.

In nearly all marine species studied to date, the impacts of TGP have been considered only for larval and early juvenile development. There has been no consideration of how later stage juveniles and adult molluscs and echinoderms will respond (but see Thor and Dupont, 2015) who investigated TPG in a copepod. Each life history stage in the life cycle of marine invertebrates differs dramatically in form and function. As a result, phenotypic traits which benefit an organism during one life history stage may have negative repercussions for another (see Strauss *et al.*, 1996; Relyea, 2001, 2003 frogs; Marshall, 2008; fish Munday, 2014).

In addition, we have very limited understanding of the longevity of TGP. Are transgenerational carryover effects present only during the early-life history stages or do they persist into adulthood and possibly subsequent generations (Burton and Metcalfe, 2014; Munday, 2014; Shama and Wegner, 2014)? Early evidence in fish suggests that the persistence of transgenerational carryover effects may be trait-specific (Schade *et al.*, 2014). For example, juveniles of the three-spined stickleback *Gastrerosteus aculeatus*, from parents that were exposed to elevated CO_2, had otoliths that were larger in size and area from parents at elevated CO_2 but had reduced survival and growth at ambient CO_2. The transgenerational effects on otolith size and area were still present 100 d post-hatch; however, the effects on survival and growth were transient persisting for only 40 d post-hatch. Also in the oyster, *Sa. glomerata*, transgenerational carryover effects were still present in offspring 18 months after settlement (Parker *et al.*, 2015). Parker *et al.* (2015) reared offspring from CO_2-exposed parents of *Sa. glomerata* at elevated CO_2

throughout larval development, until settlement. Newly settled juveniles were then gradually weaned off the elevated CO_2 treatment before being transferred to the field, where they remained in ambient conditions. Following 18 months in the field, the offspring, now adults, were returned to the laboratory and exposed to elevated CO_2 for 5 weeks. The authors found that these adults had a greater capacity to regulate their pH_e than those with no previous history of CO_2 exposure.

Another important consideration for mollusc and echinoderm species is whether or not TGP can improve all phenotypic traits which are affected by ocean acidification. Evidence for TGP has been shown for vast number of traits (Salinas *et al.*, 2013). Nevertheless, recent studies on fish suggest that some phenotypic traits will not respond transgenerationally (Allan *et al.*, 2014; Welch *et al.*, 2014). For example, Welch *et al.* (2014) reported reduced levels of behavioural lateralization and abnormal responses to a chemical alarm cue in juvenile damselfish following exposure to elevated CO_2. These impairments in behaviour did not improve following transgenerational exposure of their parents to elevated CO_2. In a recent review by Munday (2014), it was suggested that some cognitive functions may have limited plasticity and will therefore not be shaped by the environment in which the parent was raised. Whether there are similar functions with limited plasticity in mollusc and echinoderm species and the role that this will play in species fitness over the next century requires prompt attention.

Finally, whether or not TGP will be limited by or even possible in the presence of multiple stressors is virtually unknown. The unfortunate truth for marine organisms is that ocean acidification will not occur as a sole stressor over this century (Byrne and Przeslawski, 2013; IPCC, 2013, 2014; Przeslawski *et al.*, 2015). Increasing ocean temperatures, fluctuations in salinity, increases in the presence and severity of hypoxic zones, and reductions in food availability, are just some of the stressors that marine organisms will face in addition to elevated CO_2 (Byrne and Przeslawski, 2013). We already know that living in a high-CO_2 world will cause an increase in the energy budget for many marine invertebrate species (Lannig *et al.*, 2010; Gazeau *et al.*, 2013; Parker *et al.*, 2013). This increase in energy budget arises because in the absence of acclimation or adaptation, the cost of routine maintenance is much higher at elevated CO_2 (Pedersen *et al.*, 2014). Pedersen *et al.* (2014) exposed adult copepod *Calanus finmarchicus* to elevated CO_2 in a multigenerational exposure and found that while a transgenerational exposure did not make offspring more vulnerable to other stressors, it did show that there was a negative effect on the offspring if they were reared at both CO_2 and reduced food. Whereas previous studies on this species found no effect of elevated CO_2.

For species which use increased maternal provisioning as a mechanism of TGP during exposure to elevated CO_2, added stressors such as elevated temperature and reduced food availability will put further constraints on the energy budget. These constraints may prevent TGP from occurring or reduce its effectiveness. For example (a) parents may no longer have the capacity to increase energy provisioning to their offspring or (b) the increased energy which is provisioned may not be adequate for larvae to overcome the energetic demands of a multiple stressor environment, and further (c) acclimatory processes benefiting larvae at elevated CO_2 could make them more vulnerable to other stressors. To date, there have been no studies which have measured the transgenerational response of a mollusc species to elevated CO_2 in the presence of other stressors and only a single study on an echinoderm species.

As mentioned previously, Suckling *et al.* (2015) exposed parents of the Antarctic sea urchin, *S. neumayeri*, to the combined stressors of elevated CO_2 (928 and 1405 μatm) and temperature (+2°C) and measured the response of their larvae at the same levels of CO_2 and temperature. After 17 months of parental exposure, adults were able to acclimate their SMRs, which were initially increased at elevated CO_2 and temperature, back to control levels. In addition to this, the adults produced eggs that were significantly larger at elevated CO_2 and temperature compared with eggs from the present-day controls. Thus, indicating that the ability of *S. neumayeri* adults to increase provisioning in their offspring was still maintained under the combined stress of elevated CO_2 and temperature. In contrast, while the survival and development of larvae was improved at elevated CO_2 and temperature following exposure of their parents, the number of abnormal larvae was significantly increased, suggesting that the energetic demands of their larvae may have been exceeded in the multiple stressor environment.

Evidence for exceeded energy budgets have also been shown in the copepod *C. finmarchicus* following multigenerational exposure to elevated CO_2 and reduced food availability (Pedersen *et al.*, 2014). Subadult copepods of the F1 generation had a reduced dry weight, body length, and were leaner in treatments with elevated CO_2 and reduced food availability compared to present-day controls. This was the first study to report negative effects of elevated CO_2 on morphometric characteristics in a *Calanus* species and highlights the importance of studying the impacts of elevated CO_2 in the presence of other stressors. Molluscs and echinoderms occupy a variety of intertidal and subtidal habitats from oceanic to estuarine locations over a large geographic range. As our oceans continue to acidify, the ability of these species to occupy such heterogeneous, multistressor habitats may be lost and species distribution may become more limited to areas where diel and seasonal fluctuations in other biotic and abiotic factors are minor. Indeed, one of the major impacts of climate change is poleward migrations of many species with predicted contractions and extinctions of species in their current range, resulting in an overall homogenization of global faunal diversity (García Molinos *et al.*, 2015).

Implications for marine larvae and future directions

Over 85% of marine invertebrates have a biphasic life history with planktonic larvae which metamorphose into benthic juveniles that grow into adults. In larval biology, it has long been recognized that dispersing larvae of all types face challenges; a time when "a huge waste takes place" (Thorson, 1950). If larval morality increases further because of ocean acidification, there will be far reaching consequences for adult individuals, population, and community dynamics (Ross *et al.*, 2011). Larvae which are smaller with thinner, weaker shells may have less energy reserves and require a longer (Pechenik, 1999) period in the plankton to obtain sufficient energy for metamorphosis. Longer larval life may increase the risk of predation and exposure to other environmental stressors, such as an increase in temperature or hypoxia, which may decrease survival and increase mortality, particularly in the absence of properly calcified shells and skeletons (Byrne, 2011). Reduced larval size can also decrease the feeding efficiency of larvae and smaller larvae are more susceptible to starvation because they encounter comparatively less food. Reduced energy reserves may influence the transition to benthic settlement, although there is some suggestion from recent studies that a positive maternal investment may provide larvae with sufficient energy and resilience to high CO_2 (Parker *et al.*, 2012). A reduction in the survival of larvae will reduce the number of individuals reaching

settlement (Ross, 2001). Even small sublethal perturbations have the potential to cause large alterations to recruitment and adult populations (Uthicke *et al.*, 2009).

Conclusion

Ultimately, we need a better understanding of the long-term consequences of elevated CO_2 for a wider range of marine species to improve predictive capacity. In addition, we require more knowledge on the mechanisms responsible for positive and negative carryover transgenerational effects, the impacts that carryover effects have for subsequent life history stages and future generations, and how these carryover effects impact performance in the presence of other climate and environmental stressors. Exposure to elevated CO_2 during early life history stage will have long-term carryover effects for subsequent life history stages and generations (Burton and Metcalfe, 2014). In six of the seven studies which have measured the transgenerational response of molluscs and echinoderms to elevated CO_2 to date, TGP has been observed in the larval offspring. This phenotypic response mechanism provided by parents may buffer mollusc and echinoderm populations over multiple generations, long enough for genetic adaptation to occur (Shama and Wegner, 2014).

References

Albright, R. 2011. Reviewing the effects of ocean acidification on sexual reproduction and early life history stages of reef-building corals. Journal of Marine Biology, ID 473615: 1–14.

Allan, B. J. M., Miller, G. M., McCormick, M. I., Domenici, P., and Munday, P. L. 2014. Parental effects improve escape performance of juvenile reef fish in a high-CO_2 world. Proceedings of the Royal Society B: Biological Sciences, 281: 1–7.

Allen, R. M., Buckley, Y. M., and Marshall, D. J. 2008. Offspring size plasticity in response to intraspecific competition: an adaptive maternal effect across life-history stages. American Naturalist, 171: 225–337.

Andronikov, V. 1975. Heat resistance of gametes of marine invertebrates in relation to temperature conditions under which the species exist. Marine Biology, 30: 1–11.

Beniash, E., Ivanina, A., Lieb, N. S., Kurochkin, I., and Sokolova, I. M. 2010. Elevated level of carbon dioxide affects metabolism and shell formation in oysters *Crassostrea virginica*. Marine Ecology Progress Series, 419: 95–108.

Bernardo, J. 1996. Maternal effects in animal ecology. American Zoologist, 36: 83–105.

Burton, T., and Metcalfe, N. B. 2014. Can environmental conditions experienced in early life influence future generations? Proceedings of the Royal Society B: Biological Sciences, 281: 20140311.

Byrne, M. 2010. Impact of climate change stressors on marine invertebrate life histories with a focus on the Mollusca and Echinodermata. *In* Climate Alert: Climate Change Monitoring and Strategy, pp. 142–185. Ed. by J. Yu, and A. Henderson-Sellers. University of Sydney Press, Sydney.

Byrne, M. 2011. Impact of ocean warming and ocean acidification on marine invertebrate life history stages: vulnerabilities and potential for persistence in a changing ocean. Annual Reviews, 49: 1–42.

Byrne, M. 2012. Global change ecotoxicology: identification of early life history bottlenecks in marine invertebrates, variable species responses and variable experimental approaches. Marine Environmental Research, 76: 3–15.

Byrne, M. 2013. Echinoderm ecotoxicology: application for assessing and monitoring vulnerabilities in a changing ocean. Echinoderms in a Changing World: 13th International Echinoderm Conference, CRC Press/Balkema, Leiden, The Netherlands.

Byrne, M., Foo, S., Soars, N., Wolfe, K., Nguyen, H., Hardy, N., and Dworjanyn, S. 2013b. Ocean warming will mitigate the effects of acidification on calcifying sea urchin larvae (*Heliocidaris tuberculata*) from the Australian global warming hot spot. Journal of Experimental Marine Biology and Ecology, 448: 250–257.

Byrne, M., Ho, M., Selvakumaraswamy, P., Nguyen, H., Dworjanyn, S., and Davis, A. 2009. Temperature, but not pH, compromises sea urchin fertilization and early development under near-future climate change scenarios. Proceedings of the Royal Society B: Biological Sciences, 276: 1883–1888.

Byrne, M., Ho, M., Wong, E., Soars, N. A., Selvakumaraswamy, P., Sheppard-Brennard, H., Dworjanyn, S. A., *et al.* 2010. Unshelled abalone and corrupted urchins: development of marine calcifiers in a changing ocean. Proceedings of the Royal Society B: Biological Sciences, 282: 1–8.

Byrne, M., Lamare, M., Winter, D., Dworjanyn, S. A., and Uthicke, S. 2013a. The stunting effect of a high CO_2 ocean on calcification and development in sea urchin larvae, a synthesis from the tropics to the poles. Philosophical Transactions of the Royal Society B. Biological Sciences, 368: 1–13.

Byrne, M., Prowse, T. A. A., Sewell, M. A., Dworjanyn, S., Williamson, J. E., and Vaïtilingon, D. 2008. Maternal provisioning for larvae and larval provisioning for juveniles in the sea urchin *Tripneustes gratilla*. Marine Biology, 155: 473–482.

Byrne, M., and Przeslawski, R. 2013. Multistressor impacts of warming and acidification of the ocean on marine invertebrates' life histories. Integrative and Comparative Biology, 53: 582–596.

Byrne, M., Selvakumaraswamy, P., Ho, M., Woolsey, E., and Nguyen, H. 2011. Sea urchin development in a global change hotspot, potential for southerly migration of thermotolerant propagules. Deep Sea Research II: Topical Studies in Oceanography, 58: 712–719.

Clark, D., Lamare, M., and Barker, M. 2009. Response of sea urchin pluteus larvae (Echinodermata: Echinoidea) to reduced seawater pH: a comparison among a tropical, temperate, and a polar species. Marine Biology, 156: 1125–1137.

Collins, S., and Bell, G. 2004. Phenotypic consequences of 1000 generations of selection at elevated CO_2 in a green alga. Nature, 431: 566–569.

Comeau, S., Gorsky, G., Alliouane, S., and Gattuso, J. P. 2010. Larvae of the pteropod *Cavolinia inflexa* exposed to aragonite undersaturation are viable but shell-less. Marine Biology, 157: 2341–2345.

Cripps, G., Lindeque, P., and Flynn, K. J. 2014. Have we been underestimating the effects of ocean acidification in zooplankton? Global Change Biology, 20: 3377–3385.

Davis, H. C. 1958. Survival and growth of clam and oyster larvae at different salinities. Biological Bulletin, 114: 296–307.

De Wit, P., Dupont, S., and Thor, P. 2015. Selection on oxidative phosphorylation and ribosomal structure as a multigenerational response to ocean acidification in the common copepod *Pseudocalanus acuspes*. Evolutionary Applications. doi: 10.1111/eva.12335.

Deigweiher, K., Koschnick, N., Pörtner, H-O., and Lucassen, M. 2008. Acclimation of ion regulatory capacities in gills of marine fish under environmental hypercapnia. The American Journal of Physiology—Regulatory, Integrative and Comparative Physiology, 295: R1660–R1670.

Donelson, J. M., Munday, P. L., McCormick, M. I., and Pitcher, C. R. 2011. Rapid transgenerational acclimation of a tropical reef fish to climate change. Nature Climate Change, 2: 30–32.

Dubois, P. 2014. The skeleton of postmetamorphic echinoderms in a changing world. Biological Bulletin, 226: 223–236.

Dupont, S., Dorey, N., Stumpp, M., Melzner, F., and Thorndyke, M. 2013. Long-term and trans-life-cycle effects of exposure to ocean acidification in the green sea urchin *Strongylocentrotus droebachiensis*. Marine Biology, 160: 1835–1843.

Dupont, S., Havenhand, J., Thorndyke, W., Peck, L., and Thorndyke, M. 2008. Near-future level of CO_2-driven ocean acidification radically affects larval survival and development in the brittlestar *Ophiothrix fragilis*. Marine Ecology Progress Series, 373: 285–294.

Dupont, S., Lundve, B., and Thorndyke, M. 2010b. Near future ocean acidification increases growth rate of the lecithotrophic larvae and juveniles of the sea star *Crossaster papposus*. Journal of Experimental Zoology B: Molecular and Developmental Evolution, 314B: 1–8.

Dupont, S., Ortega-Martínez, O., and Thorndyke, M. 2010a. Impact of near-future ocean acidification on echinoderms. Ecotoxicology, 19: 449–462.

Ellis, R. P., Bersey, J., Rundle, S. D., Hall-Spencer, J. M., and Spicer, J. I. 2009. Subtle but significant effects of CO_2 acidified seawater on embryos of the intertidal snail, *Littorina obtusata*. Aquatic Biology, 5: 41–48.

Evans, T. G., Chan, F., Menge, B. A., and Hofmann, G. E. 2013. Transcriptomic responses to ocean acidification in larval sea urchins from a naturally low pH environment. Molecular Ecology, 22: 1609–1625.

Evans, T. G., and Watson-Wynn, P. 2014. Effects of seawater acidification on gene expression: resolving broader-scale trends in sea urchins. Biological Bulletin, 226: 237–254.

Fitzer, S. C., Caldwell, G. S., Close, A. J., Clare, A. S., Upstill-Goddard, R. C., and Bently, M. G. 2012. Ocean acidification induces multigenerational decline in copepod naupliar production with possible conflict for reproductive resource allocation. Journal of Experimental Marine Biology and Ecology, 418–419: 30–36.

Fitzer, S. C., Cusack, M., Phoenix, V. R., and Kamenos, N. A. 2014. Ocean acidification reduces the crystallographic control in juvenile mussel shells. Journal of Structural Biology, 188: 39–45.

Flores, K. B., Wolschin, F., and Amdam, G. V. 2013. The role of methylation of DNA in environmental adaptation. Integrative and Comparative Biology, 53: 359–372.

García Molinos, J., Halpern, B. S., Schoeman, D. S., Brown, C. J., Kiessling, W., Moore, P. J., Pandolfi, J. M., *et al.* 2015. Climate velocity and the future global redistribution of marine biodiversity. Nature Climate Change. doi 10.1038/nclimate2769.

Gazeau, F., Gattuso, J. P., Dawber, C., Pronker, A. E., Peene, F., Peene, J., Heip, C. H. R., *et al.* 2010. Effect of ocean acidification on the early life stages of the blue mussel (*Mytilus edulis*). Biogeosciences Discussions, 7: 2927.

Gazeau, F., Parker, L. M., Comeau, S., Gattuso, J-P., O'Connor, W. A., Martin, S., P?rtner, H-O., *et al.* 2013. Impacts of ocean acidification on marine shelled molluscs. Marine Biology, 160: 2207–2245.

Gobler, C. J., and Talmage, S. C. 2013. Short- and long-term consequences of larval stage exposure to constantly and ephemerally elevated carbon dioxide for marine bivalve populations. Biogeosciences, 10: 2241–2253.

Gonzalez-Bernat, M. J., Lamare, M., and Barker, M. 2013a. Effects of reduced seawater pH on fertilisation, embryogenesis and larval development in the Antarctic seastar *Odontaster validus*. Polar Biology, 36: 235–247.

Gonzalez-Bernat, M. J., Lamare, M., and Barker, M. 2013b. Fertilisation, embryogenesis and larval development in the tropical intertidal sand dollar *Arachnoides placenta* in response to reduced seawater pH. Marine Biology, 160: 1927–1941.

Gosselin, L. A., and Qian, P. Y. 1997. Juvenile mortality in benthic marine invertebrates. Marine Ecology Progress Series, 146: 265–282.

Gutowska, M. A., and Melzner, F. 2009. Abiotic conditions in cephalopod (*Sepia officinalis*) eggs: embryonic development at low pH and high pCO_2. Marine Biology, 156: 515–519.

Gutowska, M. A., Pörtner, H. O., and Melzner, F. 2008. Growth and calcification in the cephalopod *Sepia officinalis* under elevated seawater pCO_2. Marine Ecology Progress Series, 373: 303–309.

Hamdoun, A., and Epel, D. 2007. Embryo stability and vulnerability in an always changing world. Proceedings of the National Academy of Sciences of the United States of America, 104: 1745–1750.

Hettinger, A., Sanford, E., Hill, T. M., Hosfelt, J. D., Russell, A. D., and Gaylord, B. 2013. The influence of food supply on the response of Olympia oyster larvae to ocean acidification. Biogeosciences, 10: 5781–5802.

Hettinger, A., Sanford, E., Hill, T. M., Russell, A. D., Sato, K. N. S., Hoey, J., Forsch, M., *et al.* 2012. Persistent carry-over effects of planktonic exposure to ocean acidification in the Olympia oyster. Ecology, 93: 2758–2768.

Hobday, A. J., and Tegner, M. J. 2002. The warm and the cold: influence of temperature and fishing on local populations dynamics of the red abalone. California Cooperative Oceanic Fisheries Investigations Reports, 43: 74–96.

Hofmann, G. E., Barry, J. P., Edmund, P. J., Gates, R. D., Hutchins, D. A., Klinger, T., and Sewell, M. A. 2010. The effects of ocean acidification on calcifying organisms in marine ecosystems: an organism to ecosystem perspective. Annual Review of Ecology, Evolution, and Systematics, 41: 127–147.

Hofmann, G. E., Smith, J. E., Johnson, K. S., Send, U., Levin, L. A., Micheli, F., Paytan, A., *et al.* 2011. High-frequency dynamics of ocean pH: a multi-ecosystem comparison. PLoS ONE. doi:10.1371/journal.pone.0028983.

Horng, J. L., Lin, L. Y., and Hwang, P. P. 2009. Functional regulation of H^+-ATPase-rich cells in zebrafish embryos acclimated to an acidic environment. American Journal of Physiology—Cell Physiology, 296: C682–C692.

IPCC. 2013. Climate Change 2013: the Physical Science Basis. Contribution of Working Group I to the Fifth Assessment Report of the Intergovernmental Panel on Climate Change, Cambridge, UK and New York, NY, USA.

IPCC. 2014. Summary for Policymakers. *In* Climate Change 2014: Impacts, Adaptation, and Vulnerability. Part A: Global and Sectoral Aspects. Contribution of Working Group II to the Fifth Assessment Report of the Intergovernmental Panel on Climate Change, pp. 1–32. Ed. by C. B. Field, V. R. Barros, D. J. Dokken, K. J. Mach, M. D. Mastrandrea, T. E. Bilir, M. Chatterjee, *et al.* Cambridge University Press, Cambridge,UK and New York, NY, USA.

Kelly, M. W., Padilla-Gamiño, J. L., and Hofmann, G. E. 2013. Natural variation and the capacity to adapt to ocean acidification in the keystone sea urchin *Strongylocentrotus purpuratas*. Global Change Biology, 19: 2536–2546.

Kovalchuk, I. 2012. Transgenerational epigenetic inheritance in animals. Frontiers of Genetics, 3: 76.

Kurihara, H. 2008. Effects of CO_2-driven ocean acidification on the early developmental stages of invertebrates. Marine Ecology Progress Series, 373: 275–284.

Kurihara, H., Asai, T., Kato, S., and Ishimatsu, A. 2009. Effects of elevated pCO_2 on early development in the mussel *Mytilus galloprovincialis*. Aquatic Biology, 4: 225–233.

Kurihara, H., and Ishimatsu, A. 2008. Effects of high CO_2 seawater on the copepod *(Acartia tsuensis)* through all life stages and subsequent generations. Marine Pollution Bulletin, 56: 1086–1090.

Kurihara, H., Kato, S., and Ishimatsu, A. 2007. Effects of increased seawater pCO_2 on early development of the oyster *Crassostrea gigas*. Aquatic Biology, 1: 91–98.

Kurihara, H., Shimode, S., and Shirayama, Y. 2004a. Effects of raised CO_2 concentration on the egg production rate and early development of two marine copepods (*Acartia steueri* and *Acartia erythraea*). Marine Pollution Bulletin, 49: 721–727.

Kurihara, H., Shimode, S., and Shirayama, Y. 2004b. Sub-lethal effects of elevated concentration of CO_2 on planktonic copepods and sea urchins. Journal of Oceanography, 60: 743–750.

Kurihara, H., and Shirayama, Y. 2004. Effects of increased atmospheric CO_2 on sea urchin early development. Marine Ecology Progress Series, 274: 161–169.

Lannig, G., Eilers, S., Pörtner, H-O., Sokolova, I. M., and Bock, C. 2010. Impact of ocean acidification on energy metabolism of oyster, *Crassostrea gigas*—changes in metabolic pathways and thermal response. Marine Drugs, 8: 2318–2339.

Lischka, S., Büdenbender, J., Boxhammer, T., and Riebesell, U. 2010. Impact of ocean acidification and elevated temperatures on early juveniles of the polar shelled pteropod *Limacina helicina*: mortality,

shell degradation, and shell growth. Biogeosciences Discussions, 7: 8177–8214.

Lister, K. N., Lamare, M. D., and Burritt, D. J. 2015. Pollutant resilience in embryos of the Antarctic sea urchin *Sterechinus neumayeri* reflects maternal antioxidant status. Aquatic Toxicology, 161: 61–72.

Lohbeck, K. T., Riebesell, U., and Reusch, T. B. H. 2012. Adaptive evolution of a key phytoplankton species to ocean acidification. Nature Geoscience, 5: 917–917.

Marshall, D. J. 2008. Transgenerational plasticity in the sea: context-dependent maternal effects across the life history. Ecology, 89: 418–427.

Marshall, D. J., Allen, R. M., and Crean, A. J. 2008. The ecological and evolutionary importance of maternal effects in the sea. *In* Oceanography and Marine Biology: an Annual Review, 46, pp. 203–250. Ed. by R. N. Gibson, R. J. A. Atkinson, and J. D. M. Gordon. CRC, Boca Raton, FL.

Matson, P. G., Pauline, C. Y., Sewell, M. A., and Hofmann, G. E. 2012. Development under elevated pCO_2conditions does not affect lipid utilization and protein content in early life-history stages of the purple sea Urchin, *Strongylocentrotus purpuratus*. The Biological Bulletin, 223: 312–317.

Mayor, D. J., Matthews, C., Cook, K., Zuur, A. F., and Hay, S. 2007. CO_2 induced acidification affects hatching success in *Calanus finmarchicus*. Marine Ecology Progress Series, 350: 91–97.

Meistertzheim, A. L., Lejart, M., LeGoïc, N., and Thébault, M. T. 2009. Sex, gametogenesis, and tidal height-related differences in levels of HSP70 and metallothioneins in the Pacific oyster *Crassostrea gigas*. Comparative Biochemistry and Physiology A: Molecular Integrative Physiology, 152: 234–239.

Miller, G. M., Watson, S-A., Donelson, J. M., McCormick, M., and Munday, P. L. 2012. Parental environment mediates impacts of increased carbon dioxide on a coral reef fish. Nature Climate Change, 2: 858–861.

Moran, A. I., and McAlister, J. S. 2009. Egg size as a life history character of marine invertebrates: is it all it's cracked up to be? Biological Bulletin, 216: 226–242.

Munday, P. L. 2014. Transgenerational acclimation of fishes to climate change and ocean acidification. F1000 Prime Reports, 6: 99.

Murray, C. S., Malvezzi, A., Gobler, C. J., and Baumann, H. 2013. Offspring sensitivity to ocean acidification changes seasonally in coastal marine fish. Marine Ecology Progress Series, 504: 1–11.

O'Donnell, M. J., Hammond, L. M., and Hofmann, G. E. 2009a. Predicted impact of ocean acidification on a marine invertebrate: elevated CO_2 alters response to thermal stress in sea urchin larvae. Marine Biology, 156: 439–446.

O'Donnell, M. J., Todgham, A. E., Sewell, M. A., Hammond, L. M., Ruggiero, K., Fangue, N. A., Zippay, M. L., *et al.* 2009b. Ocean acidification alters skeletogenesis and gene expression in larval sea urchins. Marine Ecology Progress Series, 398: 157–171.

Padilla-Gamino, J. L., Kelly, M. W., Evans, T. G., and Hofmann, G. E. 2013. Temperature and CO_2 additively regulate physiology, morphology and genomic responses of larval sea urchins, *Strongylocentrotus purpuratus*. Proceedings on the Biological Society Transactions Society B, 280: 20130155.

Pan, T. C. F., Applebaum, S. L., and Manahan, D. T. 2015. Experimental ocean acidification alters the allocation of metabolic energy. Proceedings of the National Academy of Sciences of the United States of America, 112: 4696–4701.

Parker, L. M., O'Connor, W. A., Raftos, D. A., Pörtner, H-O., and Ross, P. M. 2015. Persistence of positive carryover effects in oysters following transgenerational exposure to ocean. PLoS ONE, doi:10.1371/journal.pone.013227.

Parker, L. M., Ross, P. M., and O'Connor, W. A. 2009. The effect of ocean acidification and temperature on the fertilization and embryonic development of the Sydney rock oyster S*accostrea glomerata* (Gould 1850). Global Change Biology, 15: 2123–2136.

Parker, L. M., Ross, P. M., and O'Connor, W. A. 2010. Comparing the effect of elevated pCO_2 and temperature on the fertilization and early development of two species of oysters. Marine Biology, 157: 2435–2452.

Parker, L. M., Ross, P. M., and O'Connor, W. A. 2011. Populations of the Sydney rock oyster, *Saccostrea glomerata*, vary in response to ocean acidification. Marine Biology, 158: 689–697.

Parker, L. M., Ross, P. M., O'Connor, W. A., Borysko, L., Raftos, D. A., and Pörtner, H-O. 2012. Adult exposure influences offspring response to ocean acidification in oysters. Global Change Biology, 18: 82–92.

Parker, L. M., Ross, P. M., O'Connor, W. A., Pörtner, H-O., Scanes, E., and Wright, J. M. 2013. Predicting the response of molluscs to the impact of ocean acidification. Biology, 2: 651–692.

Pechenik, J. A. 1999. On the advantages and disadvantages of larval stages in benthic marine invertebrate life cycles. Marine Ecology Progress Series, 177: 269–297.

Pechenik, J. A., Wendt, D., and Jarrett, J. 1998. Metamorphosis is not a new beginning: larval experience reduces rates of postlarval growth, development, and survival in marine invertebrates. BioScience, 48: 901–910.

Pedersen, S. A., Ha?kedal, O. J., Salaberria, I., Tagliati, A., Gustavson, L. V., Jenssen, B. M., Olsen, A. J., *et al.* 2014. Multigenerational exposure to ocean acidification during food limitation reveals consequences for copepod scope for growth and vital rates. Environmental Science and Technology, 48: 12275–12284.

Podolsky, R. D., and Moran, A. L. 2006. Integrating function across marine life cycles. Integrative and Comparative Biology, 46: 577–586.

Pörtner, H. O., and Farrell, A. P. 2008. Physiology and climate change. Science, 322: 690–692.

Przeslawski, R., Byrne, M., and Mellin, C. 2015. A review and meta-analysis of the effects of multiple abiotic stressors on marine embryos and larvae. Global Change Biology, 21: 2122–2140.

Range, P., Chícharo, M. A., Ben-Hamadou, R., Piló, D., Matias, D., Joaquim, S., Oliveira, A. P., *et al.* 2011. Calcification, growth and mortality of juvenile clams *Ruditapes decussatus* under increased pCO_2 and reduced pH: variable responses to ocean acidification at local scales? Journal of Experimental Marine Biology and Ecology, 396: 177–184.

Relyea, R. A. 2001. The lasting effects of adaptive plasticity: predator-induced tadpoles become long-legged frogs. Ecology, 82: 1947–1955.

Relyea, R. A. 2003. Predators come and predators go: the reversibility of predator-induced traits. Ecology, 84: 1840–1848.

Riviere, G. 2014. Epigenetic features in the oyster *Crassostrea gigas* suggestive of functionally relevant promotor DNA methylation in invertebrates. Frontiers in Physiology, 5: 1–7.

Ross, P. M. 2001. Larval supply, settlement and survival of barnacles in a temperate mangrove forest. Marine Ecology Progress Series, 215: 237–249.

Ross, P. M., Parker, L., O'Connor, W. A., and Bailey, E. A. 2011. The impact of ocean acidification on reproduction, early development and settlement of marine organisms. Water, 3: 1005–1030.

Salinas, S., Brown, S. C., Mangel, M., and Munch, S. B. 2013. Non-genetic inheritance and changing environments. Non-Genetic Inheritance, 1: 38–50.

Salinas, S., and Mulch, S. B. 2012. Thermal legacies: transgenerational effects of temperature on growth in a vertebrate. Ecology Letters, 15: 159–163.

Sanford, E., and Kelly, M. W. 2011. Local adaptation in marine invertebrates. Annual Review of Marine Science, 3: 509–535

Schade, F. M., Clemmesen, C., and Wegner, K. M. 2014. Within- and transgenerational effects of ocean acidification on life history of marine three-spined stickleback *(Gasterosteus aculeatus)*. Marine Biology, 161: 1667–1676.

Shama, L. N. S., Strobel, A., Mark, F. C., and Wegner, K. M. 2014. Transgenerational plasticity in marine sticklebacks: maternal effects mediate impacts of a warming ocean. Functional Ecology, 15: 159–163.

Shama, L. N. S., and Wegner, K. M. 2014. Grandparental effects in marine sticklebacks: transgenerational plasticity across multiple generations. Journal of Evolutionary Biology, 27: 2297–2307.

Sheppard Brennand, H., Soars, N., Dworjanyn, S. A., Davis, A. R., and Byrne, M. 2010. Impact of ocean warming and ocean acidification on larval development and calcification in the sea urchin *Tripneustes gratilla*. PLoS ONE, 5: e11372.

Sigwart, J. D., Lyons, G., Fink, A., Gutowska, A., Murray, D., Melzner, F., Houghton, J. D. R., *et al.* 2016. Elevated pCO_2 drives lower growth and yet increased calcification in the early life history of the cuttlefish *Sepia officinalis* (Mollusca: Cephalopoda). ICES Journal of Marine Science, 73: 970–980.

Strauss, S. Y., Conner, J. K., and Rush, S. L. 1996. Foliar herbivory affects floral characters and pollinator attractiveness to pollinators: implications for male and female plant fitness. American Naturalist, 147: 1098–1107.

Stumpp, M., Dupont, S., Thorndyke, M. C., and Melzner, F. 2011b. CO_2 induced seawater acidification impacts sea urchin larval development II: gene expression patterns in pluteus larvae. Comparative Biochemistry and Physiology A: Molecular and Integrative Physiology, 160: 320–330.

Stumpp, M., Hu, M. Y., Melzner, F., Gutowska, M. A., and Dorey, N. 2012. Acidified seawater impacts sea urchin larvae pH regulatory systems relevant for calcification. Proceedings of the National Academy of Sciences of the United States of America, 109: 18192–18197.

Stumpp, M., Wren, J., Melzner, F., Thorndyke, M. C., and Dupont, S. T. 2011a. CO_2 induced seawater acidification impacts sea urchin larval development I: elevated metabolic rates decrease scope for growth and induce developmental delay. Comparative Biochemistry and Physiology A: Molecular and Integrative Physiology, 160: 331–340.

Suckling, C. C., Clark, M. S., Beveridge, C., Brunner, L., Hughes, A. D., Harper, E. M., Cook, E. J., *et al.* 2014. Experimental influence of pH on the early life-stages of sea urchins II: increasing parental exposure times gives rise to different responses. Invertebrate Reproduction and Development, 58: 161–175.

Suckling, C. C., Clark, M. S., Richard, J., Morley, S. A., Thorne, M. A. S., Harper, E. M., and Peck, L. S. 2015. Adult acclimation to combined temperature and pH stressors significantly enhances reproductive outcomes compared to short-term exposures. Journal of Animal Ecology, 84: 773–784.

Sunday, J. M., Calosi, P., Dupoint, S., Munday, P. L., Stillman, J. H., and Reusch, T. B. H. 2014. Evolution in an acidifying ocean. Trends in Ecology and Evolution, 29: 117–125.

Talmage, S. C., and Gobler, C. J. 2009. The effects of elevated carbon dioxide concentrations on the metamorphosis, size, and survival of larval hard clams (*Mercenaria mercenaria*), bay scallops (*Argopecten irradians*), and eastern oysters (*Crassostrea virginica*). Limnology and Oceanography, 54: 2072–2080.

Talmage, S. C., and Gobler, C. J. 2010. Effects of past, present, and future ocean carbon dioxide concentrations on the growth and survival of larval shellfish. Proceedings of the National Academy of Sciences of the United States of America, 107: 17246–17251.

Talmage, S. C., and Gobler, C. J. 2011. Effects of elevated temperature and carbon dioxide on the growth and survival of larvae and juveniles of three species of Northwest Atlantic bivalves. PLoS ONE, 6: e26941, doi:10.1371/journal.pone.0026941.

Talmage, S. C., and Gobler, C. J. 2012. Effects of carbon dioxide and a harmful alga (*Aureococcus anophagefferens*) on the growth and survival of larval oysters (*Crassostrea virginica*) and scallops (*Argopecten irradians*). Marine Ecology Progress Series, 464: 121–134.

Thomsen, J., Casties, I., Pansch, A., Kortzinger, A., and Melzner, F. 2013. Food availability outweighs ocean acidification effects in juvenile *Mytilus edulis*: laboratory and field experiments. Global Change Biology, 19: 1017–1027.

Thorson, G. 1950. Reproduction and larval ecology of marine bottom invertebrates. Biology Reviews, 25: 1–45.

Todgham, A. E., and Hofmann, G. E. 2009. Transcriptomic response of sea urchin larvae *Strongylocentrotus purpuratus* to CO_2-driven seawater acidification. Journal of Experimental Biology, 212: 2579–2594.

Thompson, E., O'Connor, W. A., Parker, L. M., Ross, P., and Raftos, D. A. 2015. Differential proteomic responses of two Sydney rock oyster populations exposed to elevated CO_2. Molecular Ecology Resources, 24, doi:10.1111/mec.13111.

Thor, P., and Dupont, S. 2015. Transgenerational effects alleviate severe fecundity loss during ocean acidification in a ubiquitous planktonic copepod. Global Change Biology, 21: 2261–2271.

Tseng, Y. C., Hu, M. Y., Stumpp, M., Lin, L. Y., Melzner, F., and Hwang, P. P. 2013. CO_2-driven seawater acidification differentially affects development and molecular plasticity along life history of fish (*Oryzias latipes*). Comparative Biochemistry and Physiology A: Molecular and Integrative Physiology, 165: 119–130.

Untersee, S., and Pechenik, J. A. 2007. Local adaptation and maternal effects in two species of marine gastropod (genus *Crepidula*) that differ in dispersal potential. Marine Ecology Progress Series, 347: 79–85.

Uthicke, S., Schaffelke, B., and Byrne, M. 2009. A boom-bust phylum? Ecological and evolutionary consequences of density variations in echinoderms. Ecological Monographs, 79: 3–24.

Uthicke, S., Soars, N., Foo, S., and Byrne, M. 2013. Effects of elevated pCO_2 and the effect of parent acclimation on development in the tropical Pacific sea urchin *Echinometra mathaei*. Marine Biology, 160: 1913–1926.

Vandegehuchte, M. B., and Janssen, C. R. 2014. Epigenetics in an ecotoxicological context. Mutation Research—Genetic Toxicology and Environmental Mutagenesis, 764–765: 36–45.

Wangensteen, O. S., Dupont, S., Castles, I., Turon, X., and Palacín, C. 2013. Some like it hot: temperature and pH modulate larval development and settlement of the sea urchin *Arbacia lixula*. Journal of Marine Biology and Ecology, 449: 304–311.

Watson, S. A., Southgate, P. C., Tyler, P. A., and Peck, L. S. 2009. Early larval development of the Sydney rock oyster *Saccostrea glomerata* under near-future predictions of CO_2-driven ocean acidification. Journal of Shellfish Research, 28: 431–437.

Welch, M. J., Watson, S-A., Welsh, J. Q., McCormick, M. I., and Munday, P. L. 2014. Effects of elevated CO_2 on fish behaviour is undiminished by transgenerational acclimation. Nature Climate Change, 4: 1086–1089.

White, M. M., McCorkle, D. C., Mullineaux, L. S., and Cohen, A. L. 2013. Early exposure of bay scallops (*Argopecten irradians*) to high CO_2 causes a decrease in larval shell growth. PLoS ONE, 8: e61065.

Zippay, M. K. L., and Hofmann, G. E. 2010. Effect of pH on gene expression and thermal tolerance of early life history stages of red abalone (*Haliotis rufescens*). Journal of Shellfish Research, 29: 429–439.

Handling editor: Joanna Norkko

ICES Journal of Marine Science

ICES Journal of Marine Science (2016), 73(3), 550–557. doi:10.1093/icesjms/fsv091

Contribution to Special Issue: 'Towards a Broader Perspective on Ocean Acidification Research'

Food for Thought

Predicting the impact of ocean acidification on coral reefs: evaluating the assumptions involved

Paul L. Jokiel*

Hawaii Institute of Marine Biology, PO Box 1346, Kaneohe, HI 96744, USA

**Corresponding author: e-mail: jokiel@hawaii.edu*

Jokiel, P. L. Predicting the impact of ocean acidification on coral reefs: evaluating the assumptions involved. – ICES Journal of Marine Science, 73: 550–557.

Received 7 March 2015; revised 21 April 2015; accepted 22 April 2015; advance access publication 21 May 2015.

Predictions of future impact of climate change on coral reefs indicate that bleaching mortality due to higher temperature will be the major factor in the decline of coral reefs. Ocean acidification (OA) is increasingly considered to be an important contributing factor, but estimates of its importance vary widely in the literature. Models of future reef decline due to OA generally involve four simplifying assumptions that can lead to contradictions. The assumptions are: (i) Oceanic conditions of Ω_{arag} control or are at least highly correlated with net calcification rate (G_{net}) on coral reefs. (ii) Calcification rate is driven by bulk water carbonate ion concentration [CO_3^{2-}] expressed as Ω_{arag}. (iii) Changes in coral calcification rate can be used to estimate future changes in coral reef calcification rate. (iv) The impact of OA is additive and not synergistic with other environmental factors such as increased temperature. The assumption that aragonite saturation state (Ω_{arag}) of seawater drives calcification is the most widely used and needs to be further evaluated. An alternate hypothesis is that calcification is limited by the ability of the system to rid itself of the protons generated by calcification. Recent studies allow further testing of the assumptions and point the way to resolving shortcomings in our understanding of how OA impacts coral reefs.

Keywords: climate change, corals, coral reefs, mathematical models, ocean acidification, proton flux.

Introduction

During 1999, three important publications established the potential seriousness of future anthropogenic global climate change and laid the basis for predictive modelling efforts. Kleypas *et al.* (1999) proposed that coral reef calcification rate depends on the aragonite saturation state (Ω_{arag}) of oceanic surface waters based on the correlation between current coral reef distribution and Ω_{arag} of the surrounding ocean waters. Gattuso *et al.* (1999) reviewed the potential effect of global climatic changes (pCO_2 and temperature) on the rate of calcification in marine organisms and showed that the rate of calcification in various calcifying photosynthetic organisms decreases as a function of increasing pCO_2 and decreasing Ω_{arag}. Their calculated decrease in $CaCO_3$ production due to ocean acidification (OA), estimated using the scenarios considered by the International Panel on Climate Change (IPCC), was 10% between 1880 and 1990, and 9–30% from 1990 to 2100. Hoegh-Guldberg (1999) presented a model of future coral reef demise based largely on modelled climate change temperature projections and coral mortality due to the higher temperature regimes, with additional decline resulting from projected changes in seawater Ω_{arag}.

The saturation state concept is widely used by physical chemists in describing seawater carbonate chemistry. The concept is especially attractive in relation to biological calcification on coral reefs because aragonite is the mineral form of $CaCO_3$ precipitated by reef corals. Aragonite saturation state (Ω_{arag}) is defined by the equation:

$$\Omega_{arag} = \frac{[Ca^{2+}][CO_3^{2-}]}{K_{sp}},$$

where K_{sp} is the solubility product of aragonite. The [Ca^{2+}] in present-day oceanic seawater is essentially constant at 10.3 mmol kg^{-1} SW, normalized to salinity. Likewise, K_{sp} is a constant (at a given temperature, pressure, and salinity), so Ω_{arag} is directly proportional to [CO_3^{2-}] in shallow oceanic waters. Therefore Ω_{arag} is essentially a function of the change in [CO_3^{2-}] on coral reefs. A correlation between Ω_{arag} and calcification rate does not establish cause and

effect because Ω_{arag} also correlates with various other components of the seawater carbonate system. Nevertheless, nearly all the literature on effects of past, present, and future impact of OA on coral growth present Ω_{arag} or $[CO_3^{2-}]$ as the independent variable and coral calcification rate as the dependent variable, leading to the widely held paradigm that $[CO_3^{2-}]$ drives calcification (Erez *et al.*, 2011). Therefore, the idea that $[CO_3^{2-}]$ drives coral and coral reef calcification is a central feature of most mathematical model projections of future climate change on coral reefs and calcification is frequently presented as a function of Ω_{arag}. Mathematical modelling is the process of applying mathematics to a real world problem as a means of gaining understanding of a process such as increasing global OA. The modelling process can shed light on the questions under investigation and thereby stimulate further inquiry, but assumptions used in developing models need to be evaluated whenever conflicting results arise.

Models describing impact of OA on corals and coral reefs

Two major types of modelling have been conducted on the question of global impact of OA on corals and coral reefs. The first is essentially a metadata analysis of published data showing response of calcification to changes in Ω_{arag}. The second category includes various numerical models based on coral or coral reef response to changes in Ω_{arag} as well as increased temperature.

Metadata models

Gattuso *et al.* (1999) was the first paper to model impact of OA on coral reefs. They compiled calcification vs. Ω_{arag} data on four datasets on temperate and tropical coralline algae, two datasets on scleractinian corals and one on a coral reef community. Six of 7 datasets clearly showed a linear or curvilinear decrease in the rate of calcification as a function of decreasing Ω_{arag} over the range 0–6.2. Using scenarios developed by the IPCC, the equations were used to describe historical and possible future changes in calcification due to climate change. Decreases in $CaCO_3$ production were calculated as 10% between 1880 and 1990, and 9–30% (mid-estimate: 22%) from 1990 to 2100. This model used the assumption that calcification is a function of Ω_{arag}. Also, changes in reef pCO_2 were assumed to be directly related to atmospheric pCO_2 as estimated by IPCC scenarios. The model addressed changes in calcification for organisms and did not consider net calcification rates for reefs, which is a more complex question.

Langdon and Atkinson (2005) expanded the work of Gattuso *et al.* (1999) to include results of 13 investigations on corals and coral reef systems. They proposed that calcification rate is controlled by a rate law with calcification being proportional to $(\Omega_{arag}-1)^n$. The experimental data from the various sources were too scattered to fit the model directly so they normalized the data. Rates of calcification were calculated from each experiment were calculated as a percentage of an extrapolated Ω_{arag} of 4.6, which is their estimated saturation state of the tropical ocean in 1880 when atmospheric pCO_2 was 280 ppm based on the report of Kleypas *et al.* (1999). The resulting plot still showed considerable scatter. The points fell between a line predicted by the linear first-order rate ($n = 1$) the second curvilinear second-order rate ($n = 2$). These points are said to predict a decrease of 60% in coral and coral reef calcification by the year 2065. Another set of points that show an insensitivity to Ω_{arag} fell outside of this region and was said to predict a decline of only 1–18% by 2065. These findings leave a great deal of uncertainty about the future of coral reefs as well as the basic assumptions and data manipulations involved in the analysis.

Pandolfi *et al.* (2011) further expanded the analysis of Langdon and Atkinson (2005) using similar techniques. This synthesis included results of seven CO_2 experiments at ambient temperature, three CO_2 experiments at elevated temperature, seven experiments using different combinations of acid and base to manipulate Ω_{arag}, along with two studies using field data. The response of calcification to decreasing Ω_{arag} was consistently negative among individual coral species, coral mesocosms, and *in situ* reef communities. Results were found to be highly variable and often non-linear. Calcification was strongly sensitive to Ω_{arag} in some experiments. In other experiments, calcification did not change significantly even where corals were exposed to CO_2 levels between two and three times greater than preindustrial concentrations. In some cases, calcification did not decline when held at below the aragonite saturation threshold ($\Omega_{arag} = 1$). In a few instances, calcification even increased under moderately reduced Ω_{arag}.

This series of three progressively larger metadata analyses based on the relationship between Ω_{arag} and calcification rate reinforced the idea that a linear equation can be used to describe the relationship between Ω_{arag} and calcification on a global basis. However, the resulting linear model parameters thus derived are of little predictive value on any given coral reef and are of dubious value in predicting global changes in corals and coral reefs in general. Nevertheless, this analysis does make the point that increasing OA is generally detrimental to coral and coral reef calcification rate.

Numerical models

Buddemeier *et al.* (2008) developed a spreadsheet-based numerical model that calculates the effects of climate change on coral reefs at local-to-regional scales using equations developed from data on coral growth and mortality rates. The model calculates the impacts to coral cover from changes in average sea surface temperature (*SST*) and Ω_{arag}, and from high-temperature mortality (bleaching) events. The model uses a probabilistic assessment of the frequency of high-temperature events under future climate scenarios to address scientific uncertainties about potential adverse effects. Further, the model demonstrates the relative importance of high-temperature events, increased average temperature, and increased CO_2 concentration on the future status of coral reefs. The Buddemeier *et al.* (2008) model allows comparisons of past environmental history with predictions. Coral growth in this model was controlled by Ω_{arag} and the focus was on coral coverage rather than net ecosystem calcification.

Silverman *et al.* (2009) made projections of global changes on coral reefs using a model parameterized by field studies of calcification's response to medium-term (~2-year) fluctuations in calcification and Ω_{arag} and concluded that most of the world's reefs will be compromised once atmospheric CO_2 reaches 560 ppm. This is based on an empirical rate law developed from field observations for gross community calcification as a function of (Ω_{arag}), *SST*, and live coral cover. Calcification rates were calculated for >9000 reef locations using model values of Ω_{arag} and *SST* at different concentrations of atmospheric CO_2. The model predicted that when the atmospheric partial pressure of CO_2 reaches 560 ppm all coral reefs will cease to grow and start to dissolve.

Evenhuis *et al.* (2015) developed a unified model that linked increased temperature and OA to coral reef condition. Changes were modelled by linking the rates of growth, recovery, and calcification to the rates of bleaching and temperature induced mortality

for corals. The model has novel aspects including use of is the Arrhenius equation, thermal specialization, resource allocation trade-offs, and adaption to local environments. The model was constructed using a range of experimental and observational data, but assumes that response of corals to Ω_{arag} can give a reasonable estimate for future impact of OA.

Major assumptions of the models

The models described above have employed simplifying assumptions. Recent findings have shown that in some cases OA model results do not agree with field and laboratory observations (e.g. Jury *et al.*, 2010; Pandolfi *et al.*, 2011; Shamberger *et al.*, 2011, 2014; Comeau *et al.*, 2012; Roleda *et al.*, 2012). Such contradictions give us new insight into the processes controlling response of coral reefs to OA and allow us to review some of the basic concepts. This is precisely the purpose of modelling, so it is appropriate to revisit and re-evaluate basic assumptions involved. Four major assumptions are listed and evaluated as follows:

Assumption 1: Oceanic conditions of Ω_{arag} control or are at least highly correlated with net calcification rate (G_{net}) on coral reefs.

The concept that open-ocean Ω_{arag} controls G_{net} and thus coral reef development was carried forward by many investigators as described above. More recently however, Duarte *et al.* (2013) pointed out that metabolism in inshore waters such as coral reefs results in strong diel to seasonal fluctuations in pH with characteristic ranges of 0.3 pH units or more over a diurnal cycle. Ohde and van Woesik (1999) in their Table 3 showed that pH varied 0.7 pH trough a diurnal cycle (1 d from 8.6 to 7.9; on another day from 8.4 to 7.8). Such extreme variability and presence of multiple, complex metabolic controls on coral reefs suggest that changes in the open-ocean Ω_{arag} cannot be transposed to coastal ecosystems directly. Hence, Duarte *et al.* (2013) contend that OA from anthropogenic CO_2 is largely an open-ocean syndrome. This concept has been further supported by the work of Cyronak *et al.* (2014) who showed biogeochemical processes can influence the pCO_2 and pH of coastal ecosystems on diel and seasonal time scales, potentially modifying the long-term predicted effects of increasing atmospheric CO_2. By compiling data from the literature and removing the effects of short-term variability, they showed that the average pCO_2 of coral reefs throughout the globe has increased ~3.5-fold faster than in the open ocean over the past 20 years. This rapid increase in coastal and reef pCO_2 has the potential to negate the results of models that calculate the predicted effects of OA on coral reef ecosystems based on oceanic Ω_{arag}. They constructed a model to demonstrate that potential drivers of elevated pCO_2 include additional anthropogenic disturbances such as enhanced nutrient and organic matter inputs.

Assumption 2: Calcification rate is driven by bulk water carbonate ion concentration [CO_3^{2-}] expressed as Ω_{arag}.

This assumption appears flawed. Carbonate ion concentration (and thus Ω_{arag}) of bulk water in laboratory incubations and in field flow metabolism experiments increases with increasing calcification rate, so carbonate ion concentration (or Ω_{arag}) cannot be limiting calcification (Jokiel *et al.* 2014). Aragonite saturation state lags behind calcification by 2 h over the diurnal cycle (Shamberger *et al.*, 2011; McMahon *et al.*, 2013; Jokiel *et al.*, 2014) and therefore cannot be driving calcification. However, there is a correlation between Ω_{arag} and G_{net}. The slope and intercept of the correlation varies from reef to reef depending on differences in the primary factors controlling both calcification and Ω_{arag}. The calcification rate of reefs is driven largely by photosynthetic rate of the calcifying component and limited by proton efflux from the corals (Jokiel *et al.*, 2014). Photosynthetic rate of a reef community changes with available irradiance and other factors such as community composition, nutrient, water motion, herbivore grazing, etc. If G_{net} is measured using the alkalinity depletion method (Kinsey 1978; Smith and Kinsey 1978) the result is greatly modified by dissolution rate of carbonates and changes in pH due to photosynthesis and other factors (Jokiel *et al.*, 2014; Murillo *et al.*, 2014). Thus, we find no consistent relationship between G_{net} and Ω_{arag} on different reefs. Figure 1 presents the results of four field investigations on coral reefs from different parts of the world. There is a lack of consistency in the relationship between Ω_{arag} and G_{net} for different reefs. The reef with lowest Ω_{arag} shows the highest G_{net}. Regression line slopes between Ω_{arag} and G_{net} are generally positive, but the positive slope observed that had been observed during summer at Ningaloo Reef did not occur in winter at the same location. Chan and Connolly (2013) pointed out that the number of experimental studies seeking to estimate the sensitivity of G_{net} to Ω_{arag} has increased dramatically in recent years, but the magnitude of the calcification response estimated in these studies has varied enormously, ranging from an increase in 25% to a decrease in 66%, per unit decrease in Ω_{arag}. Rodolfo-Metalpa *et al.* (2015) provide laboratory evidence that G_{net} of three common cold-water corals is not affected by pCO_2 levels expected for 2100 (pCO_2 1058 µatm, Ω_{arag} 1.29). A field transplant experiment with one of the species to 350 m depth (pH_T 8.02; pCO_2 448 µatm, Ω_{arag} 2.58) and to a 3 m depth CO_2 seep in oligotrophic waters (pH_T 7.35; pCO_2 2879 µatm, Ω_{arag} 0.76) showed that the transplants calcified at the same rates. The data suggest that OA will not disrupt cold-water coral calcification, although falling Ω_{arag} may affect other organismal physiological and/or reef community processes.

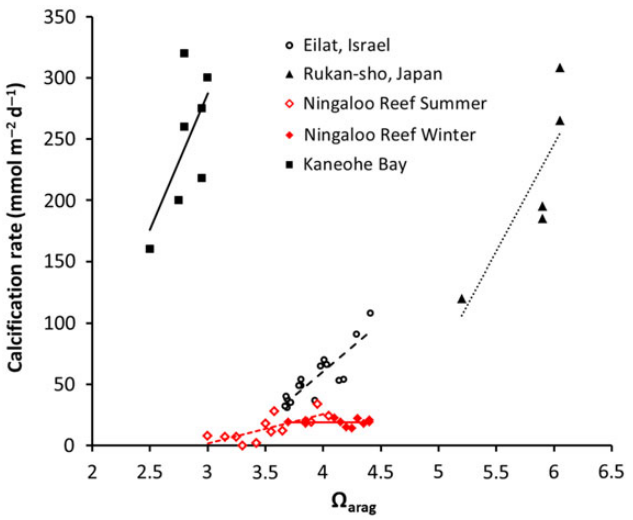

Figure 1. Plot of net calcification rate G_{net} vs. Ω_{arag} from four studies of calcification conducted in the field: Shamberger *et al.* (2011), Kaneohe Bay, Hawaii (solid squares); Ohde and van Woesik (1999), Rukan-sho, Japan (solid triangles); Silverman *et al.* (2007), Eilat Israel (open circles); Falter *et al.* (2012), Nigaloo Reef, Western Australia summer (open diamonds) and winter (solid diamonds).

Asumption 3: Changes in coral calcification rate can be used to estimate future changes in coral reef calcification rate.

This assumption is questionable because corals can continue to grow relatively well at levels of OA that result in net dissolution of a coral reef (Andersson *et al.*, 2009). A related issue is that growth of corals under various conditions of OA is generally measured directly by change in weight or linear extension (Jokiel *et al.*, 1978), whereas reef calcification is generally measured by the alkalinity depletion method (Kinsey, 1978, Smith and Kinsey, 1978). The alkalinity depletion method measures G_{net} and can include a substantial contribution of total alkalinity (A_T) from dissolving carbonate sediment and rocks (Murillo *et al.*, 2014) as well as contributions from other components such as macroalgae, crustose coralline algae, sediment diagenesis, etc. Important reef calcifiers such as crustose coralline algae (*CCA*) are far more sensitive to OA condition than corals and can be dissolving on a reef at OA levels that still allow substantial coral growth (Jokiel *et al.*, 2008; Kuffner *et al.*, 2008). There are many reefs in the world that are dominated by *CCA*, with a very small component of live coral.

Secondary calcification, bioerosion, and reef dissolution are integral to the structural complexity and long-term persistence of coral reefs, yet these processes have received less research attention than reef accretion by corals. Silbiger and Donahue (2015) found that secondary reef calcification and dissolution responded differently to possible future conditions of global warming and increasing OA. Calcification showed a non-linear response to the combined effect of increased pCO_2 and increased temperature while dissolution increased linearly, leading to the conclusion that dissolution may be more sensitive to climate change than calcification. Comeau *et al.* (2014) tested impact of OA on coral reef communities with associated sediments and sediments alone maintained in outdoor flumes under ambient pCO_2 vs. high pCO_2 at various flow rates. Calcification correlated positively with flow and negatively to increased pCO_2 with a substantial dissolution component due to the presence of sediment.

Assumption 4: The impact of ocean acidification is additive and not synergistic with other environmental factors.

Existing models assume that future reduction in reef coral cover due to elevated temperature (lower growth and high mortality) and OA (lower growth) are simply additive (Hoegh-Guldberg *et al.* (2007), but more recent reports have demonstrated antagonisms and synergisms. Reynaud *et al.* (2003) grew small colonies of the reef coral *Stylophora pistillata* in a matrix of two temperature treatments (25 vs. 28°C) and two pCO_2 treatments (460 vs. 750 μatm) and report no statistical difference between pCO_2 treatments at 25°C, but a large decline in calcification of ∼50% at 28°C under acidified conditions. Anlauf *et al.* (2011) studied the effects of a 1°C increase in temperature and a 0.2–0.25 unit decrease in pH on the growth of primary polyps in the coral *Porites panamensis*. The growth of polyps was reduced marginally by acidic seawater but the combined effect of higher temperature and lowered pH caused a significant growth reduction of ∼30%. A similar 30% decline at higher temperature—elevated pCO_2 was shown by Edmunds *et al.* (2012) for the rapidly growing branched coral *Porites rus*, but a slower growing massive *Porites* sp. did not show the effect. The temperature– pCO_2 interaction has been observed in other calcifying reef organisms. Martin and Gattuso (2009) observed an interaction effect between temperature and pCO_2 on the coralline alga *Lithophyllum cabiochae*. Algae were maintained in aquaria for 1 year at ambient or elevated temperature (+3°C) and at ambient pCO_2 (∼400 μatm) or elevated pCO_2 (∼700 μatm). During summer the net calcification of the algae decreased by 50% when both temperature and pCO_2 were elevated whereas no effect was found under elevated temperature or elevated pCO_2 alone.

Questioning the assumptions

The assumption that Ω_{arag} (or its surrogate $[CO_3^{2-}]$) drives G_{net} has been challenged by a series of publications (Jokiel, 2011a, b , 2013, Jokiel *et al.*, 2014; Cyronak *et al.*, 2016). These papers argue that calcification is not limited by $[CO_3^{2-}]$ but rather by the ability to dissipate excess protons generated by the calcification process. Various contradictions and inconsistencies in the calcification literature are resolved by the proposed proton flux model (Jokiel, 2011a, b). Recent observations have challenged paradigm that Ω_{arag} controls G_{net}. For example the presence of rich coral reefs in Kāneʻohe Bay, Hawaiʻi existing at low Ω_{arag} (high pCO_2 levels) as shown in Figure 1. The elevated pCO_2 is due to metabolism of terrigenous organic material transported into the bay by streams. Fagan and Mackenzie (2007) found that pCO_2 was averaging ∼500 μatm. Silverman *et al.* (2009) estimated that "by the time atmospheric partial pressure of CO_2 will reach 560 ppm all coral reefs will cease to grow and start to dissolve", yet these reefs are flourishing. Several reports have shown that Ω_{arag} lags behind G_{net} by 2 h over the diurnal cycle (Shamberger *et al.*, 2011; McMahon *et al.*, 2013; Jokiel *et al.*, 2014) which means that Ω_{arag} is not driving G_{net}.

Testing assumptions using exemplary data from the Rock Islands, Palau

Shamberger *et al.* (2014) reported the existence of highly diverse, coral-dominated reef communities under chronically low pH and low Ω_{arag} in the Rock Islands of Palau, affording an opportunity to test the validity of several of the above assumptions and provide additional explanations. Their comparison was made between sites located in the open ocean at (1–3 km offshore) with sites located in a shallow flow-restricted lagoon located at a distance of 7–9 km from open-ocean waters (Figure 2). The Rock Islands are located in the south lagoon of Palau between Koror and Peleliu. This area is an uplifted ancient coral reef that forms a complex carbonate labyrinth of shallow channels and lagoons containing 250–300 small islands, which are actually carbonate reef outcrops. Some of the islands display a mushroom shape with a narrow base created by rapid dissolution and bioerosion by sponges and bivalves and intense grazing by chitons, urchins, and fish in the intertidal (Lowenstam, 1974; Glynn, 1997). The extreme bioerosion and carbonate dissolution in the area coupled with very low rates of seawater exchange (Golbuu *et al.*, 2012) produces atypical conditions on the reef. Measurements made in the Rock Islands showed extremely low Ω_{arag} (∼2.4) and low pH (∼7.8) in this area of high coral coverage compared with high Ω_{arag} (∼3.8) and high pH (∼8.1) in the offshore area.

An analysis of the dynamic benthic processes involved in coral calcification on the Rock Island reefs can be made with the reported data for $[A_T]$, [DIC], and $[H^+]$. The analysis requires that we accept the assumptions implicit in the experimental design that horizontal mixing is uniform throughout the area of study and that $[A_T]$, [DIC], and $[H^+]$ are not greatly modified by pelagic processes in relation to benthic processes. The environmental gradient between the lagoon stations and offshore stations is shown for $[A_T]$ (Figure 2a),

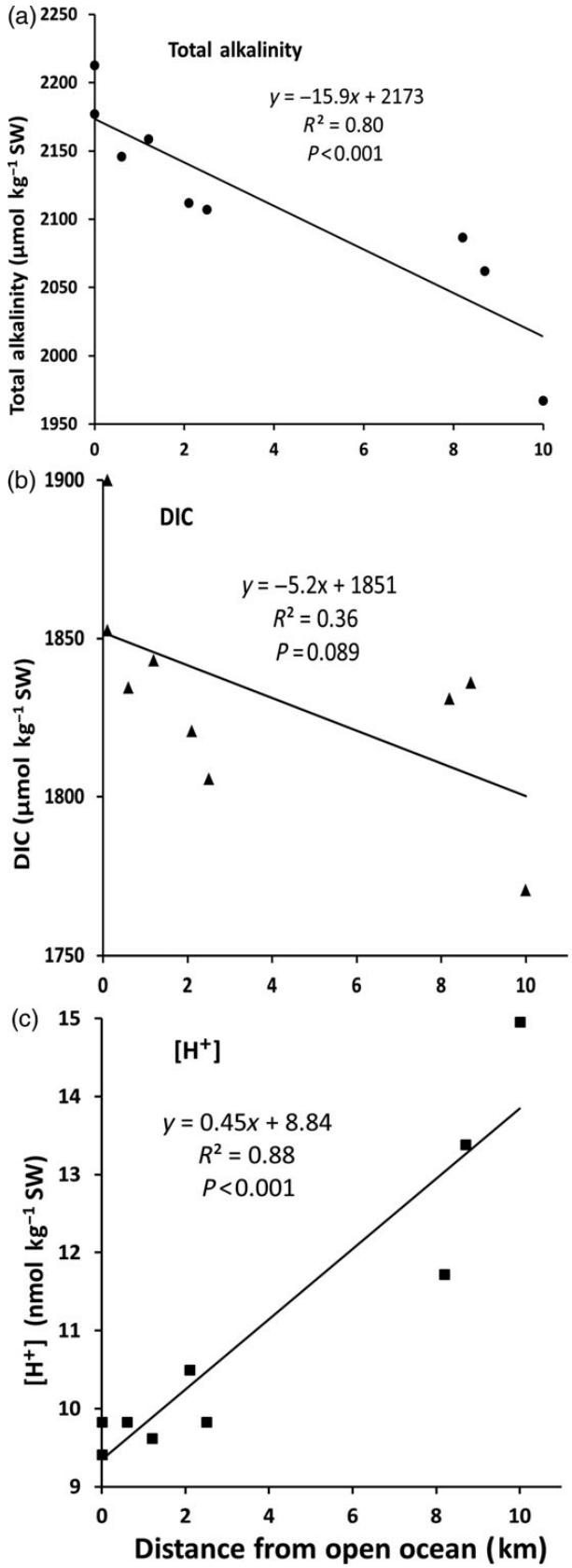

Figure 2. Change in water chemistry from open ocean to coral lagoon using data from Shamberger *et al.* (2014) for: (a) total alkalinity, (b) dissolved inorganic carbon, and (c) proton concentration.

[DIC] (Figure. 2b), and [H^+] (Figure 2c). The strongest gradient ($p < 0.001$, Figure 2c) is for net flux of protons out of the lagoon. Net flux of A_T into the lagoon also shows a strong gradient ($p < 0.001$, Figure 2a). Net DIC flux into the lagoon did not show a statistically significant correlation ($p = 0.089$, Figure 2b). This pattern is consistent with detailed observations made by Jokiel *et al.* (2014) showing the lag in proton flux in a rapidly calcifying system. Dissipation of the protons generated by the process of calcification is a major factor limiting coral growth. Flushing of the Rock Island system with oceanic waters removes H^+ and brings in water with higher [A_T]. DIC is abundant in seawater and is not limiting. Proton flux is the important parameter as shown by changes in [A_T] and [H^+] with distance from the open ocean.

An explanation for the presence of this rich coral reef growing under low Ω_{arag} can be developed based on the proton flux hypothesis (Jokiel, 2011a). Dissolution of carbonates increases A_T (Wisshak *et al.*, 2013), especially under low pH conditions at night. Such additional A_T will be retained in the system due to low water exchange and made available to the calcifying organisms during the day. High rainfall and tidal variation results in submarine groundwater discharge (*SGD*), which serves as another source of A_T to the calcifying organisms. Furthermore, rainfall in this area is high and varies from 200 to 450 mm $month^{-1}$ (Australian Bureau of Meteorology and CSIRO, 2011). Cyronak *et al.* (2013a, b) measured increased A_T flux due to *SGD* with the daily flux rate of up to 1080 mmol m^{-2} d^{-1}. Dissolution of the complex non-living carbonates supplemented with additional A_T from *SGD* in the low-flushing Rock Island reef system over the 24 h period would provide considerable A_T buffering of the protons being generated by calcification. Supplementary Figure S4 of the Shamberger *et al.* (2014) report shows a rich coral community at the Rock Islands lacking in macroalgae and turf algae, probably due to intense herbivore grazing pressure and low inorganic nutrient supply. Presence of a larger macroalgae component would have increased pH during daylight hours without altering A_T. The higher pH in such situations shifts the equilibria toward increased [CO_3^{2-}] and therefore higher Ω_{arag}. In this system, as in other systems, Ω_{arag} simply describes the portion of DIC that is being expressed as CO_3^{2-} under prevailing pH conditions (which can be modified to different degrees by algal photosynthesis without changing A_T) and thus is not of value as a universal metric driving coral calcification. There is a local correlation between Ω_{arag} and G_{net}, but Ω_{arag} is a dependent variable on several factors including P_{net} and local dissolution rate of carbonates (e.g. Murillo *et al.*, 2014). The relationship of G_{net} to Ω_{arag} relationship holds within a given system, but varies between systems due to differences in P_{net}, which drives G_{net}. Systems with a higher portion of P_{net} being provided by non-calcifying photosynthetic organisms will have a different relationship to Ω_{arag} than a system dominated by calcifying photosynthetic organisms.

Further evaluation of existing models and methodology

Jones *et al.* (2015) evaluated four published models of reef carbonate production in terms of their predictive power at local and global scales. The models are based on functions sensitive to combinations of light availability Ω_{arag} and temperature and were implemented within a specifically developed global framework, the Global Reef Accretion Model. None of the models reproduced the independent

rate estimates of whole-reef calcification. The output from the temperature-only based approach was the only model to significantly correlate with coral calcification rates. They pointed out that validation of reef carbonate budgets is severely hampered by limited and inconsistent methodology in reef-scale observations. Pandolfi *et al.* (2011) detected striking inconsistencies between experimental and field observations of the Ω_{arag} vs. calcification relationship and suggested that the role of dissolution could account for the differences. Tribollet *et al.* (2009) found that carbonate dissolution by microbial endoliths measured under elevated pCO_2 was 48% higher than under ambient pCO_2. Chan and Connolly (2013) tested whether the methodological and biological factors that have been hypothesized to drive variation in magnitude of response explain a significant proportion of the among-study variation. They found that the overall mean response of coral calcification is ~15% per unit decrease in Ω_{arag} over the range $2 < \Omega_{arag} < 4$. Among-study variation is large (standard deviation of 8% per unit decrease in Ω_{arag}). Neither differences in carbonate chemistry manipulation method, study duration, irradiance level nor study species growth rate explained a significant proportion of the among-study variation. Duarte *et al.* (2015) evaluated perceived ocean calamities and concluded that the issue of global decline of ocean calcifiers due to increasing OA is one of the areas with weak scientific support. Improved predictive models are needed, which means that we must sort out the mechanisms and strengthen the models.

Correlation between G_{net} and the factor $[CO_3^{2-}]$ which determines Ω_{arag} does not establish cause and effect (Jokiel, 2013). Experiments that documented correlations between G_{net}, P_{net}, and seawater chemistry have been conducted repeatedly since the development of the alkalinity depletion method to measure coral calcification. Initial experiments described calcification dynamics in static aquaria incubations (Smith and Kinsey, 1978) and reef field enclosures (Kinsey, 1978). More recently, these experiments have been expanded to include continuous flow measurements of proton flux in coral reef mesocosms (Jokiel *et al.*, 2014). There is a basic physiological explanation for the observed correlation between G_{net} and Ω_{arag} that must be understood. Daytime coral metabolism rapidly removes DIC (primarily in the form of HCO_3^-) from the seawater while photosynthesis provides the energy that drives G_{net} (Jokiel *et al.*, 2014). Higher pH resulting from photosynthesis pushes the seawater carbonate system equilibria toward higher $[CO_3^{2-}]$ (and therefore higher Ω_{arag}) although DIC is decreasing. This scenario results in a positive correlation between G_{net} and Ω_{arag}. Both Ω_{arag} and G_{net} are dependent variables on P_{net} and many other factors. The correlation between G_{net} and Ω_{arag} is modified by changes in pH. Changes in pH can be due to many processes (e.g. photosynthesis by macroalgae, addition of land-derived material, metabolism of organic materials). Changes in A_T occur due to bioerosion and dissolution of carbonate sediment and rocks. Other factors such as irradiance, temperature and water motion influence P_{net}, G_{net} and Ω_{arag}. Therefore, the slope and intercept of the regression line varies widely (Figure 1).

In conclusion, there are large inconsistencies in descriptions coral and coral reef response to OA. Part of this problem can be traced to assumptions used in these studies. Perhaps the major shortcoming of models lies in the belief that $[CO_3^{2-}]$ and thus Ω_{arag} controls calcification. The alternate explanation is the rate at which a calcifying system can rid itself of the excess protons produced as a waste product of calcification (Jokiel *et al.*, 2014). Results of Murillo *et al.* (2014) should also be considered. They found that corals growing in a mixed-community experience an environment that is more favourable to calcification (higher daytime pH and dissolved oxygen due to algae photosynthesis, additional input of A_T and inorganic carbon from sediments). They also showed that the widely used alkalinity depletion method yields a lower net calcification rate for a mixed-community vs. a coral-only community due to A_T recycling, although the corals may be calcifying at a higher rate under these conditions. Increased temperature will play the dominant role in the decline of reefs during future climate change with OA playing a lesser role, so the uncertainties on the effects of OA have less impact on the final estimates of reef decline. On the brighter side, the consequent expansion of OA research will eventually produce a better understanding of the processes that control coral calcification.

Acknowledgements

This work partially funded by the Pacific Island Climate Change Cooperative and by the United States Geological Survey, Coastal and Marine Geology Program cooperative agreement G13AC00130. N. Silbiger, M Donahue, and three anonymous reviewers provided comments that improved the original manuscript.

References

Andersson, A. J., Kuffner, I. B., Mackenzie, F. T., Jokiel, P. L., Rodgers, K. S., and Tan, A. 2009. Net loss of $CaCO_3$ from coral reef communities due to human induced seawater acidification. Biogeosciences, 6: 1811–1823.

Anlauf, H., D'Croz, L., and O'Dea, A. 2011. A corrosive concoction: the combined effects of ocean warming and acidification on the early growth of a stony coral are multiplicative. Journal of Experimental Marine Biology and Ecology, 397: 13–20.

Australian Bureau of Meteorology and CSIRO. 2011. Climate change in the Pacific: Scientific assessment and new research. Volume 1: Regional Overview (ISBN: 9781921826733 (pbk.) ISBN: 9781921826740 (ebook)).

Buddemeier, R. W., Jokiel, P. L., Zimmerman, K. M., Lane, D. R., Carey, J. M., Bohling, G. C., and Martinich, J. A. 2008. A modeling tool to evaluate regional coral reef responses to changes in climate and ocean chemistry. Limnology and Oceanography: Methods, 6: 395–411.

Chan, N. C. S., and Connolly, R. 2013. Sensitivity of coral calcification to ocean acidification: a meta-analysis. Global Change Biology, 19: 282–290.

Comeau, S., Carpenter, R. C., and Edmunds, P. J. 2012. Coral reef calcifiers buffer their response to ocean acidification using both bicarbonate and carbonate. Proceedings of the Royal Society of London B, 280: 20122374.

Comeau, S., Edmunds, P. J., Lantz, C. A., and Carpenter, R. C. 2014. Water flow modulates the response of coral reef communities to ocean acidification. Science Reports, 4: 6681.

Cyronak, T., Santos, I. R., Erler, D. V., and Eyre, B. D. 2013b. Groundwater and porewater as major sources of alkalinity to a fringing coral reef lagoon (Muri Lagoon, Cook Islands). Biogeosciences, 10: 2467–2480.

Cyronak, T., Santos, I. R., McMahon, A., and Eyre, B. D. 2013a. Carbon cycling hysteresis in permeable carbonate sands over a diel cycle: implications for ocean acidification. Limnology and Oceanography, 58: 131–143.

Cyronak, T., Schulz, K. G., and Jokiel, P. L. 2016. The Omega myth: what really drives lower calcification rates in an acidifying ocean. ICES Journal of Marine Science, 73: 558–562.

Cyronak, T., Schulz, K. G., Santos, I. R., and Eyre, B. D. 2014. Enhanced acidification of global coral reefs driven by regional biogeochemical feedbacks. Geophysics Research Letters, 41: 5538–5546.

Duarte, C. M., Fulweiler, R. W., Lovelock, C. E., Martinetto, P., Saunders, M. I., Pandolfi, J. M., Gelcich, S., *et al.* 2015. Reconsidering ocean calamities. BioScience, 65: 130–139.

Duarte, C. M., Hendriks, I. E., Moore, T. S., Olsen, Y. S., Steckbauer, A., Ramajo, L., Carstensen, J., *et al.* 2013. Is ocean acidification an open-ocean syndrome? Understanding anthropogenic impacts on seawater pH. Estuaries and Coasts, 36: 221–236.

Edmunds, P. J., Brown, D., and Moriarty, V. 2012. Interactive effects of ocean acidification and temperature on two scleractinian corals from Moorea, French Polynesia. Global Change Biology, 18: 2173–2183.

Erez, J., Reynaud, S., Silverman, J., Schneider, K., and Allemand, D. 2011. Coral calcification under ocean acidification and global change. *In* Coral Reefs: an Ecosystem in Transition, pp. 151–176. Ed. by Z. Dubinsky, and N. Stambler. Springer, New York. 371 pp.

Evenhuis, C., Lenton, A., Cantin, N. E., and Lough, J. M. 2015. Modeling coral calcification accounting for the impacts of coral bleaching and ocean acidification. Biogeosciences, 12: 2607–2630.

Fagan, K. E., and Mackenzie, F. T. 2007. Air–sea CO_2 exchange in a subtropical estuarine-coral reef system, Kaneohe Bay, Oahu, Hawaii. Marine Chemistry, 106: 174–191.

Falter, J. L., Lowe, R. J., Atkinson, M. J., and Cuet, P. 2012. Seasonal coupling and de-coupling of net calcification rates from coral reef metabolism and carbonate chemistry at Ningaloo Reef, Western Australia. Journal of Geophysical Research, 117: C05003.

Gattuso, J. P., Allemand, D., and Frankignoulle, M. 1999. Photosynthesis and calcification at cellular, organismal and community levels in coral reefs: a review on interactions and control by carbonate chemistry. American Zoologist, 39: 160–183.

Glynn, P. W. 1997. Bioerosion and coral reef growth: a dynamic balance. *In* Life and Death of Coral Reefs, pp. 68–95. Ed. by C. Birkeland. Chapman and Hall, New York. 536 pp.

Golbuu, Y., Wolanski, E., Idechong, J. W., Victor, S., Isechal, A. L., Oldiais, N. W., and Idip, D., Jr*et al.* 2012. Predicting coral recruitment in Palau's complex reef archipelago. PLoS ONE, 7: e50998.

Hoegh-Guldberg, O. 1999. Climate change, coral bleaching and the future of the world's coral reefs. Marine and Freshwater Research, 50: 839–866.

Hoegh-Guldberg, O., Mumby, P. J., Hooten, A. J., Steneck, R. S., Greenfield, P., Gomez, E., Harvell, C. D., *et al.* 2007. Coral reefs under rapid climate change and ocean acidification. Science, 318: 1737–1742.

Jokiel, P. L. 2011a. Ocean acidification and control of reef coral calcification by boundary layer limitation of proton flux. Bulletin of Marine Science, 87: 639–657.

Jokiel, P. L. 2011b. The reef coral two compartment proton flux model: a new approach relating tissue-level physiological processes to gross corallum morphology. Journal of Experimental Marine Biology and Ecology, 409: 1–12.

Jokiel, P. L. 2013. Coral reef calcification: carbonate, bicarbonate and proton flux under conditions of increasing ocean acidification. Proc R Soc Lond B. doi:10.1098/rspb.2013.0031.

Jokiel, P. L., Jury, C. P., and Rodgers, K. S. 2014. Coral-algae metabolism and diurnal changes in the CO_2-carbonate system of bulk sea water. PeerJ, 2: e378.

Jokiel, P. L., Maragos, J. E., and Franzisket, L. 1978. Coral growth: buoyant weight technique. *In* Coral Reefs: Research Methods, pp. 529–542. Ed. by D. R. Stoddart, and R. E. Johannes. UNESCO Monographs on Oceanographic Methodology, Paris. 581 pp.

Jokiel, P. L., Rodgers, K. S., Kuffner, I. B., Andersson, A. J., Cox, E. F., and Mackenzie, F. T. 2008. Ocean acidification and calcifying reef organisms: a mesocosm investigation. Coral Reefs, 27: 473–483.

Jones, N. S., Ridgwell, A., and Hendy, E. J. 2015. Evaluation of coral reef carbonate production models at a global scale. Biogeosciences, 12: 1339–1356.

Jury, C. P., Whitehead, R. F., and Szmant, A. 2010. Effects of variations in carbonate chemistry on the calcification rates of *Madracis auretenra* (= *Madracis mirabilis* sensu Wells, 1973): bicarbonate concentrations best predict calcification rates. Global Change Bioloy, 16: 1632–1644.

Kinsey, D. W. 1978. Productivity and calcification estimates using slack-water periods and field enclosures. *In* Coral Reefs: Research Methods, pp. 439–468. Ed. by D. R. Stoddart, and R. E. Johannes. UNESCO Monographs on Oceanographic Methodology, Paris. 581 pp.

Kleypas, J. A., Buddemeier, R. W., Archer, D., Gattuso, J-P., Langdon, C., and Opdyke, B. N. 1999. Geochemical consequences of increased atmospheric carbon dioxide on coral reefs. Science, 284: 118–120.

Kuffner, I. B., Andersson, A. J., Jokiel, P. L., Rodgers, K. S., and Mackenzie, F. T. 2008. Decreased abundance of crustose coralline algae due to ocean acidification. Nature Geoscience, 1: 114–117

Langdon, C., and Atkinson, M. J. 2005. Effect of elevated pCO_2 on photosynthesis and calcification of corals and interactions with seasonal change in temperature/irradiance and nutrient enrichment. Journal of Geophysical Research, 110: C09507.

Lowenstam, H. S. 1974. Impact of life on chemical and physical processes. *In* The Sea, Vol. 5, Marine Chemistry, pp. 725–796. Ed. by E. D. Goldberg, Wiley, New York. 914 pp.

Martin, S., and Gattuso, J-P. 2009. Response of Mediterranean coralline algae to ocean acidification and elevated temperature. Global Change Biology, 15: 2089–2100.

McMahon, A., Santos, I. R., Cyronak, T., and Eyre, B. D. 2013. Hysteresis between coral reef calcification and the seawater aragonite saturation state. Geophysical Research Letters, 40: 4675–4679.

Murillo, L. J., Jokiel, P. L., and Atkinson, M. J. 2014. Alkalinity to calcium flux ratios for corals and coral reef communities: variances between isolated and community conditions. PeerJ, 2: e249.

Ohde, S., and van Woesik, R. 1999. Carbon dioxide flux and metabolic processes of a coral reef, Okinawa. Bulletin of Marine Science, 65: 559–576.

Pandolfi, J. M., Connolly, R. M., Marshall, D. J., and Cohen, A. L. 2011. Projecting coral reef futures under global warming and ocean acidification. Science, 333: 418–422.

Reynaud, S., Leclercq, N., Romaine-Lioud, S., Ferrier-Pages, C., Jaubert, J., and Gattuso, J -P. 2003. Interacting effects of CO_2 partial pressure and temperature on photosynthesis and calcification in a scleractinian coral. Global Change Biology, 9: 1660–1668.

Rodolfo-Metalpa, R., Montagna, P., Aliani, S., Borghini, M., Canese, S., Hall-Spencer, J. M., Foggo, A., *et al.* 2015. Calcification is not the Achilles' heel of cold-water corals in an acidifying ocean. Global Change Biology, 21: 2238–2248.

Roleda, M., Boyd, P., and Hurd, C. 2012. Before ocean acidification: calcifier chemistry lessons. Journal of Phycology, 48: 840–843.

Shamberger, K. E. F., Cohen, A. L., Golbuu, Y., McCorkle, D. C., Lentz, S. J., and Barkley, H. C. 2014. Diverse coral communities in naturally acidified waters of a Western Pacific Reef. Geophysics Research Letters, 41: 499–501.

Shamberger, K. E. F., Feely, R. A., Sabine, C. L., Atkinson, M. J., DeCarlo, E. H., Mackenzie, F. T., Drupp, P. S., *et al.* 2011. Calcification and organic production on a Hawaiian coral reef. Marine Chemistry, 127: 64–75.

Silbiger, N. J., and Donahue, M. J. 2015. Secondary calcification and dissolution respond differently to future ocean conditions. Biogeosciences, 12: 567–578.

Silverman, J., Lazar, B., Cao, L., Caldeira, K., and Erez, J. 2009. Coral reefs may start dissolving when atmospheric CO_2 doubles. Geophysical Research Letters, 36: L05606.

Silverman, J., Lazar, B., and Erez, J. 2007. Effect of aragonite saturation, temperature, and nutrients on the community calcification rate of a coral reef. Journal of Geophysical Research Oceans, 112: C05004.

Smith, S. V., and Kinsey, D. W. 1978. Calcification and organic carbon metabolism as indicated by carbon dioxide. *In* Coral Reefs: Research Methods, pp. 469–484. Ed. by D. R. Stoddart, and R. E. Johannes. UNESCO Monographs on Oceanographic Methodology, Paris. 581 pp.

Tribollet, A., Godinot, C., Atkinson, M., and Langdon, C. 2009. Effects of elevated pCO_2 on dissolution of coral carbonates by microbial euendoliths. Global Biogeochemical Cycles, 23: GB3008.

Wisshak, M., Schönberg, C. H. L., Form, A., and Freiwald, A. 2013. Effects of ocean acidification and global warming on reef bioerosion—lessons from a clionaid sponge. Aquatic Biology, 19: 111–127.

Handling editor: Howard Browman

ICES Journal of Marine Science

ICES Journal of Marine Science (2016), 73(3), 558–562. doi:10.1093/icesjms/fsv075

Contribution to Special Issue: 'Towards a Broader Perspective on Ocean Acidification Research'

Food for Thought

The Omega myth: what really drives lower calcification rates in an acidifying ocean

Tyler Cyronak[1]*, Kai G. Schulz[2], and Paul L. Jokiel[3]

[1]*Scripps Institution of Oceanography, UC San Diego, 9500 Gilman Drive 0244, La Jolla, CA 92093-0244, USA*
[2]*Centre for Coastal Biogeochemistry, Southern Cross University, PO Box 157, Lismore 2480, NSW, Australia*
[3]*Hawaii Institute of Marine Biology, University of Hawaii, PO Box 1346, Kaneohe, HI 96744, USA*

**Corresponding author: e-mail: tcyronak@gmail.com*

Cyronak, T., Schulz, K. G., and Jokiel, P. L. The Omega myth: what really drives lower calcification rates in an acidifying ocean. – ICES Journal of Marine Science, 73: 558 – 562.

Received 2 February 2015; revised 7 April 2015; accepted 8 April 2015; advance access publication 21 May 2015.

The literature on ocean acidification (OA) contains a prevalent misconception that reduced organismal calcification rates in an acidifying ocean are driven by a reduction in carbonate ion (CO_3^{2-}) substrate availability (e.g. Omega or Ω). However, recent research in diverse organisms suggests that a reduction in seawater pH (i.e. increasing proton concentrations, $[H^+]$) is the most likely driver of reduced calcification rates in these organisms. OA leads to higher $[H^+]$ in seawater which alters the proton gradient between internal cellular reservoirs and external bulk seawater, making it difficult for organisms to maintain pH homeostasis. Biologically mediated calcification is a complex process, so it is unlikely that simple CO_3^{2-} substrate limitation is responsible for the observed decreases in calcification rates under OA conditions. Despite these inherent complexities, current predictions concerning the fate of calcifying organisms in an acidifying ocean have relied on the relationship between calcification rates and Ω. To more accurately predict how OA will affect the calcification of marine organisms, and consequently the global carbon cycle, we need to further elucidate the mechanisms driving observed decreases in calcification under acidified conditions.

Keywords: calcification, coral reef, ocean acidification, Omega, phytoplankton, saturation state.

Ocean acidification (OA) refers to the unprecedented reduction in seawater pH caused by anthropogenic CO_2 inputs (Hönisch *et al.*, 2012). OA is expected to reduce the ability of marine organisms such as corals, coccolithophores, foraminifera, and molluscs to secrete calcium carbonate ($CaCO_3$) skeletons, a process known as calcification (see Table 1) (Chan and Connolly, 2012; Kroeker *et al.*, 2013). As CO_2 dissolves into seawater, it lowers the pH and shifts the carbonate equilibria, decreasing the carbonate ion concentration ($[CO_3^{2-}]$). This lowers a chemical property of seawater known as the calcium carbonate saturation state or Ω. Seawater Ω is a function of CO_3^{2-} and calcium ion concentrations ($[Ca^{2+}]$) as follows

$$\Omega = \frac{[Ca^{2+}][CO_3^{2-}]}{K_{sp}}, \quad (1)$$

where K_{sp} is the solubility product of a specific $CaCO_3$ mineral phase (e.g. aragonite or calcite) at a specified temperature, salinity, and pressure (Zeebe and Wolf-Gladrow, 2001). Therefore, the thermodynamics of inorganic $CaCO_3$ precipitation and dissolution can largely be described by seawater Ω, with precipitation occurring at $\Omega > 1$ and dissolution at $\Omega < 1$ (Morse and Arvidson, 2002).

$$Ca^{2+} + CO_3^{2-} \leftrightarrow CaCO_3. \quad (2)$$

From an OA perspective, Ω is mainly controlled by changing $[CO_3^{2-}]$, which is lowered as anthropogenic CO_2 dissolves into seawater, while $[Ca^{2+}]$ remains unaffected.

Having the thermodynamic principles of inorganic $CaCO_3$ precipitation in mind, early OA work investigated the calcification rates of organisms such as corals in seawater of varying Ω by manipulating bulk seawater $[CO_3^{2-}]$ and $[Ca^{2+}]$ (e.g. Gattuso *et al.*, 1998; Langdon *et al.*, 2000). Experimental evidence showed a positive correlation between calcification and Ω, which led to the idea that seawater $[CO_3^{2-}]$ could drive calcification rates. However, to determine

Table 1. Definition of terms referring to calcification and inorganic $CaCO_3$ precipitation/dissolution in the OA literature.

Term	Definition
Calcification or gross calcification	Refers to the biologically controlled process of $CaCO_3$ production, often occurs isolated from bulk seawater in media called the calcifying fluid
$CaCO_3$ precipitation	Refers to the inorganic formation of $CaCO_3$ minerals from a super saturated solution
$CaCO_3$ dissolution	Refers to the inorganic dissolution of $CaCO_3$ minerals in an under saturated solution, sometimes decalcification is used synonymously
Net calcification	The net effect of gross calcification and dissolution, usually refers to individual organisms
Net community calcification or net ecosystem calcification	The net effect of gross calcification and dissolution in an entire ecosystem

how OA affects calcification it becomes critical to differentiate between the inorganic precipitation and dissolution of $CaCO_3$ (which is thermodynamically constrained by seawater Ω) and biologically mediated calcification (see Table 1). In fact, it has been suggested that inorganic $CaCO_3$ dissolution may be more of a threat to marine calcifying organisms and calcareous ecosystems than decreasing calcification rates under OA (Andersson *et al.*, 2009; Roleda *et al.*, 2012; Eyre *et al.*, 2014). However, many OA studies have not been able to isolate the effects of seawater Ω on organismal calcification rates in the absence of dissolution (i.e. gross calcification) because $CaCO_3$ is exposed to bulk seawater as either sediment or skeletal material. Therefore, any dissolution of exposed $CaCO_3$ could produce or enhance the observed relationships between Ω and net calcification. On the other hand, gross calcification is under biological control and mediated by organic tissue that separates the calcifying surface from overlying seawater. Therefore calcification occurs in a media (i.e. the calcifying fluid) that has significantly different $[CO_3^{2-}]$ than the bulk seawater. However, despite the complexities inherent to biological mediated calcification, much of the current OA literature presents the problem of reduced calcification under OA scenarios as an issue of simple CO_3^{2-} substrate availability [e.g. Equation (2)] (Hendriks *et al.*, 2015).

Recent work has demonstrated that corals can actively control carbonate chemistry at the site of calcification (Venn *et al.*, 2011; McCulloch *et al.*, 2012), which brings into question the mechanistic understanding of how external seawater Ω could influence organismal calcification rates. Currently, lines of research in different organisms and ecosystems are beginning to reach the same conclusion, that external seawater Ω (i.e. $[CO_3^{2-}]$) is not what drives changes in calcification rates. Here we show that these insights have been developed in two vastly different systems; scleractinian corals and open ocean phytoplankton known as coccolithophores.

The ability to modify carbonate chemistry at the site of calcification can produce internal conditions that are more thermodynamically favourable for inorganic $CaCO_3$ precipitation than in the surrounding seawater (i.e. a greater Ω). It has been shown that corals transport seawater to the site of calcification, however, once it is part of the calcifying fluid the chemistry of that seawater is actively modified (Gagnon *et al.*, 2012). Coccolithophores passively regulate cytosolic pH through voltage-gated H^+ channels; however, they actively regulate carbonate chemistry in their calcifying vesicles (Mackinder *et al.*, 2010). Marine organisms have also been shown to modulate calcification through the use of organic molecules that can both stimulate or inhibit specific crystal lattice structures (Marsh, 1994). Therefore, in order for the external seawater chemistry to affect calcification rates, it must somehow affect that organism's ability to modulate its internal carbonate chemistry or produce organic compounds that mediate precipitation. Two lines of physiological evidence suggest that bulk seawater Ω does not control the Ω in the calcifying fluid, and thus, is not the major factor controlling organismal calcification rates.

1. While CO_3^{2-} is the substrate for inorganic $CaCO_3$ precipitation, no CO_3^{2-} transporter has been described in corals (Goiran *et al.*, 1996) or coccolithophores (Mackinder *et al.*, 2010). However, there is ample evidence that bicarbonate (HCO_3^-) is actively transported into the calcifying fluid of corals (Goiran *et al.*, 1996; Moya *et al.*, 2008; Jury *et al.*, 2010) and coccolithophores (Berry *et al.*, 2002; Herfort *et al.*, 2002, Rost *et al.* 2003). Therefore, once HCO_3^- is transported into the calcifying fluid and CO_3^{2-} is combined with Ca^{2+} during calcification, H^+ ions build-up (Figure 1);

$$Ca^{2+} + HCO_3^- \rightarrow H^+ + CaCO_3 \quad (3)$$

   Since there is ~9 times the $[HCO_3^-]$ as $[CO_3^{2-}]$ in seawater, and OA increases $[HCO_3^-]$, it is unlikely that HCO_3^- substrate limitation under decreasing seawater pH is a problem for calcification. However, increasing seawater $[H^+]$ could be quite problematic.

2. As H^+ ions build-up in the calcifying fluid the pH is lowered and the carbonate system shifts away from CO_3^{2-}, thus lowering Ω. Therefore, to maintain conditions favourable to inorganic $CaCO_3$ precipitation within the calcifying fluid, the organism must passively or actively remove H^+ ions through membrane channels/transporters (Allemand *et al.*, 2011; Taylor *et al.*, 2012). As the oceans absorb CO_2 and seawater H^+ concentrations increase, the electrochemical gradient between coral tissue and cytosolic fluids will decrease, making it more difficult to maintain high Ω in the calcifying fluid. This is the underlying concept behind the proton flux limitation model of calcification.

The conceptual framework of the proton flux limitation model has been elucidated in both corals (Jokiel, 2011a, b) and coccolithophores (Suffrian *et al.*, 2011; Bach *et al.*, 2013) (Figure 1). Once protons are transported into the tissue or cytosolic fluid from the calcifying fluid they must be removed to the water column to maintain intracellular pH, which becomes more energetically demanding as the proton concentration of seawater increases. If proton flux limitation at the boundary layer between the organism and seawater is the limiting factor for calcification, then increased energy production should lead to higher calcification rates by allowing more H^+ ions to be actively pumped out of the calcifying fluid. This has been demonstrated in two distinct pathways in corals: (i) more light (and increases in photosynthesis) results in increased calcification rates (Marubini *et al.*, 2001; Al-Horani *et al.*, 2003) and (ii) feeding the coral with

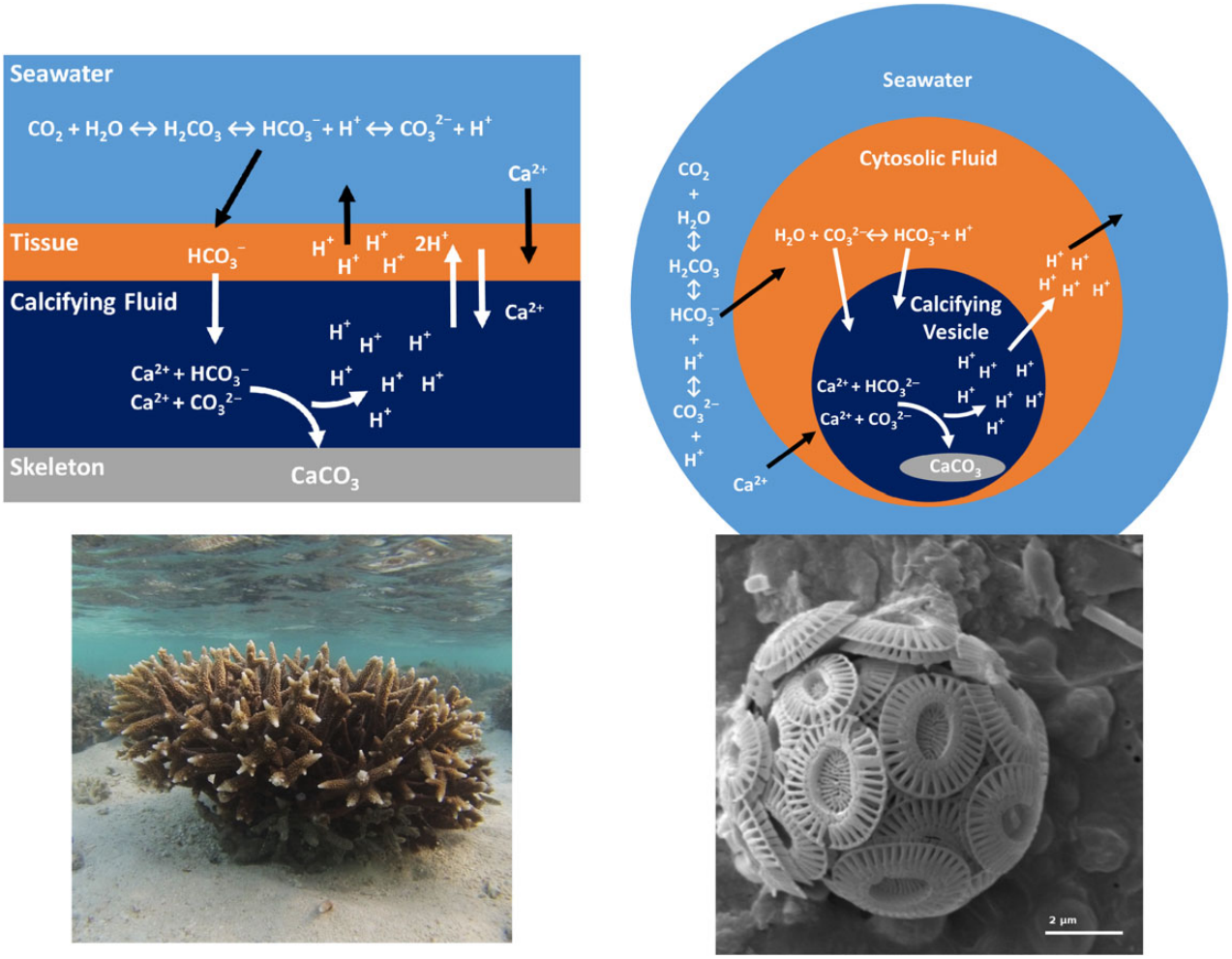

Figure 1. A simplified schematic demonstrating the internal build-up of protons during the calcification process in corals and coccolithophores. Corals (left panel) must dissipate excess protons produced by calcification through a boundary layer and into the water column as proposed by Jokiel (2011b). Internally, corals most likely actively pump HCO_3^- ions into the calcifying fluid where protons build-up as $CaCO_3$ is precipitated. To maintain favourable conditions for precipitation in the calcifying fluid, corals likely actively pump $2H^+$ out and Ca^{+2} in using a Ca^{+2}-ATPase (Allemand *et al.*, 2011). To maintain the pH inside their tissue corals must remove protons, which becomes more energetically demanding when the gradient between the tissue and seawater $[H^+]$ is less pronounced due to ocean acidification. Suffrian *et al.* (2011) demonstrated that internal cellular pH (pH_i) in coccolithophores like *Emiliania huxleyi* (right panel) is directly affected by the surrounding seawater pH. This is most likely because *E. huxleyi* uses passive gated H^+ channels to control cytosolic pH, which are forced to work against a less pronounced H^+ gradient in an acidifying ocean. Black arrows represent fluxes between the organism and external seawater while white arrows represent fluxes occurring within the organism.

plankton enhances calcification rates (Ferrier-Pages *et al.*, 2003; Houlbrèque *et al.*, 2004; Towle *et al.*, 2015). Another hypothesis explaining light enhanced coral calcification is in direct agreement with the proton flux limitation hypothesis. Moya *et al.* (2006) suggested that increased pH in the gut of coral polyps during the day (Furla *et al.*, 2000; Al-Horani *et al.*, 2003) decreases the gradient against which H^+ ions are pumped out of the calcifying fluid. It has also been suggested that the carbon concentrating mechanism (CCM) used by coral endosymbionts during daytime photosynthesis, which produces OH^- ions, can absorb excess H^+ (Furla *et al.*, 2000). In coccolithophores, the cytosolic pH is regulated by H^+ efflux via passive voltage-gated H^+ channels (Suffrian *et al.* 2011). However, under ocean acidification scenarios, the electrochemical gradient becomes less and less favourable, most likely affecting pH and Omega inside the calcifying vesicle.

Results from field and mesocosm studies of coral reef ecosystems are also consistent with the proton flux limitation model. Venti *et al.* (2014) recently demonstrated that light and temperature had much greater control than seawater Ω on changes in seasonal calcification rates of corals in the field. Also, a diel hysteretic pattern between external seawater Ω and calcification rates, with the highest rates of calcification occurring before the daily peak in bulk seawater Ω, has been observed in all levels of coral ecosystems from carbonate sediments (Cyronak *et al.*, 2013b), to corals and macroalgae (Jokiel *et al.*, 2014), and entire ecosystems (McMahon *et al.*, 2013; Shaw *et al.*, 2015). The hysteretic pattern observed in these studies is most likely due to the influence that benthic organisms have on seawater carbonate chemistry in coral reef ecosystems, with benthic production and calcification driving diel changes in seawater Ω, not the other way around. Importantly, these studies demonstrate the

complexity in extrapolating the effects of OA based on short term natural changes in Ω. There is also a strong correlation between primary production and calcification in a range of studies (e.g. Gattuso *et al.*, 1999), indicating that photosynthesis is a dominant control on coral calcification.

Field and laboratory evidence across organisms and ecosystems indicates that calcification in an acidifying ocean is not controlled by bulk seawater Ω, but most likely inhibited by an increase in the gradient of protons between the calcifying fluid and external seawater. Therefore, a much better indicator of the influence of seawater chemistry on calcification may be the ratio of the substrate (dissolved inorganic carbon; DIC or $[HCO_3^-]$) to the waste product ($[H^+]$) (Jokiel, 2011a, 2013). In fact, recent experimental evidence in mussels demonstrated that the seawater $[HCO_3^-]$ to $[H^+]$ ratio is important in controlling calcification rates (Thomsen *et al.*, 2015), indicating that pH homeostasis may be important in controlling biologically mediated calcification in a diverse range of organisms. In contrast, a recent study suggested that bivalve larvae were particularly sensitive to Ω (Waldbusser *et al.*, 2015). However, Waldbusser *et al.* (2015) did not distinguish between the effects of Ω on gross calcification and dissolution, and their results may be due to the dissolution of $CaCO_3$ shells exposed to under saturated seawater. Furthermore, an additional explanation for the lack of correlative power between changes in calcification rates and pH (instead of Ω) in some studies with un-coupled carbonate chemistry manipulations, such as in Langdon *et al.* (2000) or Waldbusser *et al.* (2015), is that increasing $[HCO_3^-]$ could partially compensate for unfavourable pH levels.

It is also important to remember that calcification is influenced by many other factors such as light availability and temperature, which may be more important in driving future changes in calcification rates (McNeil *et al.*, 2004). The coupling of seawater pH and Ω under ocean acidification scenarios (i.e. inputs of CO_2) can lead to positive correlations between calcification and both pH and Ω. However, pH and Ω can become decoupled or negatively correlated on geological time scales due to land-based weathering processes (Hönisch *et al.*, 2012), and on more modern timescales due to opposite effects of temperature on pH and Ω (Figure 2) (Gattuso *et al.*, 1999). While this decoupling is not likely on the timescale of modern OA in the open ocean, it could occur in some coastal areas with pronounced diel temperature variability.

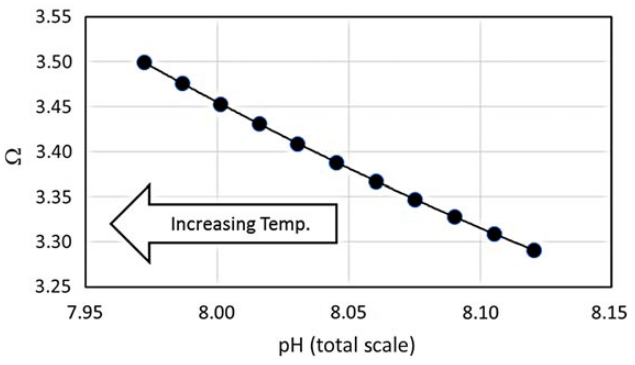

Figure 2. Correlation of pH and aragsonite saturation state (Ω) when temperature is increased from 20 to 30°C. pH and Ω were calculated at constant TA and DIC concentrations of 2300 and 2000 μmol kg^{-1}, respectively, while temperature was varied by 1°C from 20 to 30°C. It is important to note that global warming will not drive the uncoupling of pH and Ω due to ongoing CO_2 equilibration between the atmosphere and ocean.

Current predictions of the fate of coral reefs in an acidifying ocean which are reliant on the relationship between net ecosystem calcification and Ω (e.g. Figure 6 in Shamberger *et al.*, 2011 could be based on a basic misconception about the factors driving changes in coral physiology. With this in mind, it becomes vitally important to grasp the correct mechanistic understanding of how increasing CO_2 inhibits the calcification of marine organisms. We are not the first to stress this point. A recent perspective article noted a disconnect between the more recent OA literature and older studies on calcification physiology (Roleda *et al.*, 2012). Other recent work is beginning to highlight the sensitivity of $CaCO_3$ dissolution to OA, which may pose a more serious threat to coral reef ecosystems than changes in calcification (Andersson *et al.*, 2009; Cyronak *et al.*, 2013a; Eyre *et al.*, 2014). Multiple theories exist for the influence of OA on marine calcifiers (Allemand *et al.*, 2011). However, the prevailing notion in the OA literature that calcification is inhibited through a reduction in seawater $[CO_3^{2-}]$, and thus Ω, is most likely incorrect. Rather, as outlined above, it is most likely the decrease in seawater pH and associated problems of pH homeostasis within organisms that governs changes in calcification rates under OA conditions.

Acknowledgements

Many thanks to three anonymous reviewers, Howard Browman and Yui Takeshita for their thoughts and suggestions. KGS is the recipient of an Australian Research Council Future Fellowship (FT120100384).

References

Al-Horani, F. A., Al-Moghrabi, S. M., and de Beer, D. 2003. The mechanism of calcification and its relation to photosynthesis and respiration in the scleractinian coral *Galaxea fascicularis*. Marine Biology, 142: 419–426.

Allemand, D., Tambutté, É., Zoccola, D., and Tambutté, S. 2011. Coral calcification, cells to reefs. *In* Coral Reefs: An Ecosystem in Transition, pp. 119–150. Ed. by Z. Dubinsky, and N. Stambler. Springer, The Netherlands.

Andersson, A. J., Kuffner, I. B., Mackenzie, F. T., Jokiel, P. L., Rodgers, K. S., and Tan, A. 2009. Net Loss of $CaCO_3$ from a subtropical calcifying community due to seawater acidification: mesocosm-scale experimental evidence. Biogeosciences, 6: 1811–1823.

Bach, L. T., Mackinder, L. C. M., Schulz, K. G., Wheeler, G., Schroeder, D. C., Brownlee, C., and Riebesell, U. 2013. Dissecting the impact of CO2 and pH on the mechanisms of photosynthesis and calcification in the coccolithophore Emiliania huxleyi. New Phytologist, 199: 121–134.

Berry, L., Taylor, A. R., Lucken, U., Ryan, K. P., and Brownlee, C. 2002. Calcification and inorganic carbon acquisition in coccolithophores. Functional Plant Biology, 29: 289–299.

Chan, N. C. S., and Connolly, S. R. 2012. Sensitivity of coral calcification to ocean acidification: a meta-analysis. Global Change Biology, 19: 282–290.

Cyronak, T., Santos, I., and Eyre, B. 2013a. Permeable coral reef sediment dissolution driven by elevated pCO_2 and pore water advection. Geophysical Research Letters, 40: 4876–4881.

Cyronak, T., Santos, I., McMahon, A., and Eyre, B. D. 2013b. Carbon cycling hysteresis in permeable carbonate sands over a diel cycle: implications for ocean acidification. Limnology and Oceanography, 58: 131–143.

Eyre, B. D., Andersson, A. J., and Cyronak, T. 2014. Benthic coral reef calcium carbonate dissolution in an acidifying ocean. Nature Clim. Change, 4: 969–976.

Ferrier-Pages, C., Witting, J., Tambutté, E., and Sebens, K. 2003. Effect of natural zooplankton feeding on the tissue and skeletal growth of the scleractinian coral Stylophora pistillata. Coral Reefs, 22: 229–240.

Furla, P., Allemand, D., and Orsenigo, M. N. 2000. Involvement of H(+)-ATPase and carbonic anhydrase in inorganic carbon uptake for endosymbiont photosynthesis. American Journal of Physiology: Regulatory, Integrative and Comparative Physiology, 278: R870–R881.

Gagnon, A. C., Adkins, J. F., and Erez, J. 2012. Seawater transport during coral biomineralization. Earth and Planetary Science Letters, 329–330: 150–161.

Gattuso, J -P., Allemand, D., and Frankignoulle, M. 1999. Photosynthesis and calcification at cellular, organismal and community levels in coral reefs: A review on interactions and control by carbonate chemistry. American Zoologist, 39: 160–183.

Gattuso, J. P., Frankignoulle, M., Bourge, I., Romaine, S., and Buddemeier, R. W. 1998. Effect of calcium carbonate saturation of seawater on coral calcification. Global and Planetary Change, 18: 37–46.

Goiran, C., Al-Moghrabi, S., Allemand, D., and Jaubert, J. 1996. Inorganic carbon uptake for photosynthesis by the symbiotic coral/dinoflagellate association I. Photosynthetic performances of symbionts and dependence on sea water bicarbonate. Journal of Experimental Marine Biology and Ecology, 199: 207–225.

Hendriks, I. E., Duarte, C. M., Olsen, Y. S., Steckbauer, A., Ramajo, L., Moore, T. S., Trotter, J. A., *et al.* 2015. Biological mechanisms supporting adaptation to ocean acidification in coastal ecosystems. Estuarine, Coastal and Shelf Science, 152: A1–A8.

Herfort, L., Thake, B., and Roberts, J. 2002. Acquisition and use of bicarbonate by Emiliania huxleyi. New Phytologist, 156: 427–436.

Hönisch, B., Ridgwell, A., Schmidt, D. N., Thomas, E., Gibbs, S. J., Sluijs, A., Zeebe, R., *et al.* 2012. The geological record of ocean acidification. Science, 335: 1058–1063.

Houlbrèque, F., Tambutté, E., Allemand, D., and Ferrier-Pagès, C. 2004. Interactions between zooplankton feeding, photosynthesis and skeletal growth in the scleractinian coral Stylophora pistillata. Journal of Experimental Biology, 207: 1461–1469.

Jokiel, P. L. 2013. Coral reef calcification: carbonate, bicarbonate and proton flux under conditions of increasing ocean acidification. Proceedings of the Royal Society of London B, 20130031. [doi:10.1098/rspb.2013.0031].

Jokiel, P. L. 2011a. Ocean acidification and control of reef coral calcification by boundary layer limitation of proton flux. Bulletin of Marine Science, 87: 639–657.

Jokiel, P. L. 2011b. The reef coral two compartment proton flux model: A new approach relating tissue-level physiological processes to gross corallum morphology. Journal of Experimental Marine Biology and Ecology, 409: 1–12.

Jokiel, P. L., Jury, C. P., and Ku'ulei, S. R. 2014. Coral-algae metabolism and diurnal changes in the CO2-carbonate system of bulk sea water. PeerJ, 2: e378.

Jury, C. P., Whitehead, R. F., and Szmant, A. M. 2010. Effects of variations in carbonate chemistry on the calcification rates of *Madracis auretenra* (= *Madracis mirabilis* sensu Wells, 1973): bicarbonate concentrations best predict calcification rates. Global Change Biology, 16: 1632–1644.

Kroeker, K. J., Kordas, R. L., Crim, R., Hendriks, I. E., Ramajo, L., Singh, G. S., Duarte, C. M., *et al.* 2013. Impacts of ocean acidification on marine organisms: quantifying sensitivities and interaction with warming. Global Change Biology, 19: 1884–1896.

Langdon, C., Takahashi, T., Sweeney, C., Chipman, D., Goddard, J., Marubini, F., Aceves, H., *et al.* 2000. Effect of calcium carbonate saturation state on the calcification rate of an experimental coral reef. Global Biogeochemical Cycles, 14: 639–654.

Mackinder, L., Wheeler, G., Schroeder, D., Riebesell, U., and Brownlee, C. 2010. Molecular Mechanisms Underlying Calcification in Coccolithophores. Geomicrobiology Journal, 27: 585–595.

Marsh, M. E. 1994. Polyanion-mediated mineralization—assembly and reorganization of acidic polysaccharides in the Golgi system of a coccolithophorid alga during mineral deposition. Protoplasma, 177: 108–122.

Marubini, F., Barnett, H., Langdon, C., and Atkinson, M. 2001. Dependence of calcification on light and carbonate ion concentration for the hermatypic coral Porites compressa. Marine Ecology Progress Series, 220: 153–162.

McCulloch, M., Falter, J., Trotter, J., and Montagna, P. 2012. Coral resilience to ocean acidification and global warming through pH up-regulation. Nature Climate Change, 2: 623–627.

McMahon, A., Santos, I. R., Cyronak, T., and Eyre, B. D. 2013. Hysteresis between coral reef calcification and the seawater aragonite saturation state. Geophysical Research Letters, 40: 4675–4679.

McNeil, B. I., Matear, R. J., and Barnes, D. J. 2004. Coral reef calcification and climate change: The effect of ocean warming. Geophysical Research Letters, 31: L22309.

Morse, J. W., and Arvidson, R. S. 2002. The dissolution kinetics of major sedimentary carbonate minerals. Earth-Science Reviews, 58: 51–84.

Moya, A., Tambutté, S., Bertucci, A., Tambutté, E., Lotto, S., Vullo, D., Supuran, C. T., *et al.* 2008. Carbonic Anhydrase in the Scleractinian Coral *Stylophora pistillata*. Journal of Biological Chemistry, 283: 25475–25484.

Moya, A., Tambutte, S., Tambutte, E., Zoccola, D., Caminiti, N., and Allemand, D. 2006. Study of calcification during a daily cycle of the coral Stylophora pistillata: implications for 'light-enhanced calcification'. Journal of Experimental Biology, 209: 3413–3419.

Roleda, M. Y., Boyd, P. W., and Hurd, C. L. 2012. Before ocean acidification: Calcifier chemistry lessons. Journal of Phycology, 48: 840–843.

Rost, B., Riebesell, U., Burkhardt, S., and Sültemeyer, D. 2003. Carbon acquisition of bloom-forming marine phytoplankton. Limnology and Oceanography, 48: 55–67.

Shamberger, K. E. F., Feely, R. A., Sabine, C. L., Atkinson, M. J., DeCarlo, E. H., Mackenzie, F. T., Drupp, P. S., *et al.* 2011. Calcification and organic production on a Hawaiian coral reef. Marine Chemistry, 127: 64–75.

Shaw, E. C., Phinn, S. R., Tilbrook, B., and Steven, A. 2015. Natural in situ relationships suggest coral reef calcium carbonate production will decline with ocean acidification. Limnology and Oceanography. Doi:10.1002/lno.10048.

Suffrian, K., Schulz, K. G., Gutowska, M., Riebesell, U., and Bleich, M. 2011. Cellular pH measurements in Emiliania huxleyi reveal pronounced membrane proton permeability. New Phytologist, 190: 595–608.

Taylor, A. R., Brownlee, C., and Wheeler, G. L. 2012. Proton channels in algae: reasons to be excited. Trends in Plant Science, 17: 675–684.

Thomsen, J., Haynert, K., Wegner, K. M., and Melzner, F. 2015. Impact of seawater carbonate chemistry on the calcification of marine bivalves. Biogeosciences Discussion, 12: 1543–1571.

Towle, E. K., Enochs, I. C., and Langdon, C. 2015. Threatened Caribbean Coral Is Able to Mitigate the Adverse Effects of Ocean Acidification on Calcification by Increasing Feeding Rate. PLoS ONE, 10: e0123394.

Venn, A., Tambutté, E., Holcomb, M., Allemand, D., and Tambutté, S. 2011. Live tissue imaging shows reef corals elevate ph under their calcifying tissue relative to seawater. PLoS ONE, 6: e20013.

Venti, A., Andersson, A., and Langdon, C. 2014. Multiple driving factors explain spatial and temporal variability in coral calcification rates on the Bermuda platform. Coral Reefs, 33: 979–997.

Waldbusser, G. G., Hales, B., Langdon, C. J., Haley, B. A., Schrader, P., Brunner, E. L., Gray, M. W., *et al.* 2015. Saturation-state sensitivity of marine bivalve larvae to ocean acidification. Nature Climate Change, 5: 273–280.

Zeebe, R. E., and Wolf-Gladrow, D. 2001. CO_2 in Seawater: Equilibrium, Kinetics, Isotopes. Elsevier Oceanography Series, 65, Amsterdam.

Handling editor: Howard Browman

ICES Journal of Marine Science

ICES Journal of Marine Science (2016), 73(3), 563–568. doi:10.1093/icesjms/fsv174

Contribution to Special Issue: 'Towards a Broader Perspective on Ocean Acidification Research'

Comment

Calcium carbonate saturation state: on myths and this or that stories

George G. Waldbusser*, Burke Hales, and Brian A. Haley

College of Earth, Ocean, and Atmospheric Sciences, Oregon State University, Corvallis, OR 97331, USA

**Corresponding author: tel: + 1 541 737 8964; fax: + 1 541 737 2064; e-mail: waldbuss@coas.oregonstate.edu*

Waldbusser, G. G., Hales, B., and Haley, B. A. Calcium carbonate saturation state: on myths and this or that stories. – ICES Journal of Marine Science, 73: 563–568.

Received 14 July 2015; revised 1 September 2015; accepted 7 September 2015; advance access publication 13 December 2015.

In a recent opinion article titled "The Omega Myth", Cyronak *et al*. provide a series of arguments as to why saturation state should not matter to marine calcifiers. In sections of their article, they highlight several aspects of our published work, and unfortunately appear to misinterpret the foundation for the kinetic–energetic hypothesis we have laid out previously. While we are in full agreement that omega sensitivity is not a substrate limitation issue, we more clearly detail below what a kinetic limitation means and why it is different from a substrate limitation. The kinetic argument we have previously presented highlights how the energetic cost of calcification increases with a decreasing saturation state (or omega). We then highlight several issues with a bicarbonate/proton flux model applied to newly developing marine bivalve larvae, and discuss how a bicarbonate/proton flux and omega-based sensitivity model do not have to be mutually exclusive. Our intent with this comment is to clarify the points raised by Cyronak *et al*. about our work, and help to move the thinking past dialectic debate towards a more synthetic view on ocean acidification impacts on marine calcifiers.

Keywords: biocalcification, bivalve larvae, ocean acidification, proton flux, saturation state.

The recent opinion piece "The Omega Myth" by Cyronak *et al*. (2016) calls to mind one of the best lessons in graduate school: "the answer to any dialectic - 'this or that' - question in complex systems is almost always YES". George Wilhelm Frederick Hegel acknowledged the powerful utility of dialectic questioning to lead to greater understanding through "hypothesis, antithesis, synthesis". Elegant in its simplicity and its lyrical feel, one hopes applying this adage to the study of global change and marine organisms will eventually lead us to higher levels of synthesis, or more simply the "YES". Dialectic debates, however, have an unfortunate proclivity for oversimplification, misunderstanding, and dogmatism; the "Omega Myth" piece by Cyronak *et al*. (2016) unfortunately slips into this trap. Myths are often based on real-world observations, magnified and dramatized by story-telling. One needs to look no further than Moby Dick, Jaws, or the Kraken to see how real-world phenomena provide the foundation for some of the best told stories of our oceans. In this instance, it is the story-telling by Cyronak *et al*. (2016), and others, that is creating "the myth" surrounding omega; not the published work we are aware of, and most certainly not ours. Here, we hope to bring back to light the kernel of truth that others have fictionalized, a basic and mechanistic omega sensitivity in bivalve larvae.

We must first clarify the foundation for our kinetic perspective on larval bivalve sensitivity to calcium carbonate saturation, denoted by the Greek omega, and defined as

$$\Omega = \frac{[Ca^{2+}][CO_3{}^{2-}]}{K'_{sp}}, \quad (1)$$

where the numerator is the product of the concentrations of calcium ($[Ca^{2+}]$) and carbonate ($[CO_3{}^{2-}]$) ions, and the denominator, K'_{sp}, is the apparent thermodynamic solubility product of the $CaCO_3$ mineral in question (typically aragonite in the studies considered here).

Cyronak *et al*. (2016) mistakenly interpret omega sensitivity of biocalcification as substrate limitation, specifically the lack of carbonate ions limits biocalcification. While such an inference is

understandable from Equation (1), this is not our description of omega sensitivity. Indeed, we will present arguments subsequently directly against such a limitation-based argument. While an omega value below 1 (for the calcium carbonate mineral in question) indicates that dissolution is *thermodynamically* favoured over precipitation, Cyronak *et al.* (2016) aptly point out that calcifiers use all forms of dissolved inorganic carbon (DIC) in producing calcium carbonate [through the use of carbonic anhydrase, see Roleda *et al.* (2012)], and this has been well documented in the literature for decades [as reviewed in McConnaughey and Gillikin (2008)] and measured in bivalve larvae as well by us (Waldbusser *et al.*, 2013). Dissolution (driven by omega in fact) is not likely to be important in developing bivalve larvae given the relatively slow, abiotic nature of dissolution, relative to the very rapid calcification event of initial shell formation. We argue that omega matters, owing to the rapid rate of calcification during the formation of the initial larval shell; omega gains relevance as a *kinetic* constraint, not a *thermodynamic* constraint. At the foundation of our kinetic argument is the rate law for calcium carbonate formation:

$$r = k(\Omega - 1)^n, \tag{2}$$

where r is the rate of calcium carbonate formation, k is the rate constant, Ω is the saturation state with respect to the form of calcium carbonate (aragonite in bivalve larvae), and n is the reaction order (assume to be 1 here). A keen reader will note the ostensible problem of this relationship as omega goes to unity, or lower. Are we suggesting such conditions preclude biocalcification? It is well documented that bivalves calcify faster than predicted from abiotic rates, and at times when ambient waters are thermodynamically unfavourable, where $\Omega < 1$ (Gazeau *et al.*, 2007; Waldbusser *et al.*, 2010, 2011). Our reply is an importance nuance to our argument, which is that the actual calcification rate observed cannot be predicted from this equation; rather, the equation describes the magnitude of the physiochemical kinetic barrier that biology must overcome to precipitate shell.

The elegance of this simple relationship between r, k, and Ω becomes apparent if we solve the equation for k, at the shell formation rates we documented previously from the two larval shell stages in Pacific oyster, *Crassostrea gigas*, larvae (Waldbusser *et al.*, 2013), for a range of Ω (Figure 1). During the initial shell formation event (called prodissoconch I) in many bivalve larvae, rapid calcification is mandated to complete the shell and allow attachment of the velum for swimming and feeding, before exhausting endogenous energy reserves [detailed in Waldbusser *et al.* (2013, 2015a, b) and references therein]. Emphasizing the need to form a complete shell, our hypothesis posits that the larvae must somehow elevate k to support the accelerated calcification rates as omega decreases, or elevate omega at the calcification site; either approach demands a biological energy subsidy to manipulate the physical chemistry. The energetic cost of such manipulation has been documented under more acidified conditions; wherein calcification or growth is diminished in many marine calcifiers, consistent with the less energy available for growth and more spent on maintenance processes (Kroeker *et al.*, 2010; Gattuso *et al.*, 2015). Our hypothesis is that maintaining accelerated rates under decreasing omega requires more energy per unit of calcium carbonate formed. Additional energy or lack thereof seems to modulate the response either through changes through ontogeny (Waldbusser *et al.*, 2010, 2013) or if more food is available in otherwise food-limiting conditions (Melzner *et al.*, 2011). However, developing bivalve larvae in the PDI stage does not typically have the luxury of slowing growth, or access to exogenous energy sources, and thus, their sensitivity to omega is acute.

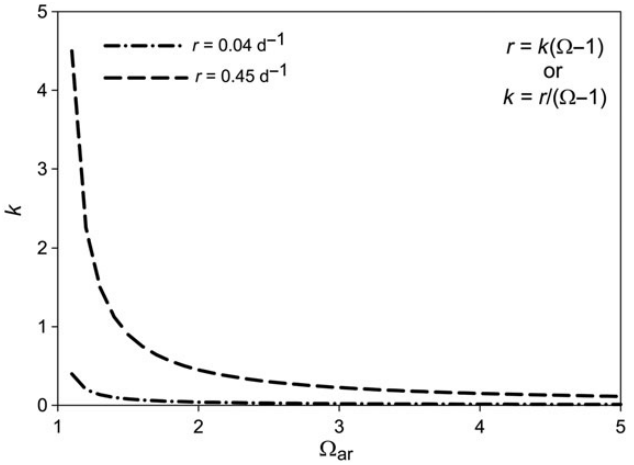

Figure 1. The computed rate constant (k) needed across a range of saturation states (Ω), at two representative calcification rates in Pacific oyster larvae, during the initial shell calcification known as prodissoconch I (PDI) (0.45 d^{-1}) and the rest of the larval shell known as prodissoconch II (0.04 d^{-1}). While this formulation does not permit calcification below the saturation horizon, it does describe the basic physical chemistry that organisms must contend with and overcome.

Where and how the organism spends energy to elevate k or omega at the calcification site is yet to be determined. We do, however, know the larger energetic cost for shell production is in protein synthesis, and not in pumping of the protons generated by calcium carbonate precipitation (Palmer, 1992; Cohen and Holcomb, 2009; Waldbusser *et al.*, 2013). Pan *et al.* (2015) recently provided more support to this argument by constraining the energetic expenses of acidification stress on sea urchin larvae and found that the greatest increase in energy spent under acidification stress was on protein synthesis, not on cross-membrane ion pumping. Alteration in the proteinaceous organic matrix that provides the framework for the calcium carbonate shell seems like one probable approach organisms can use to offset acidification stress. Additionally, the lower energetic investment in cross-membrane ion pumping, the exact mechanism for alleviating stress in a proton flux model, does not appear supported thus far by the energetic and growth relationships noted earlier. Ries (2011) proposed a physicochemical model of proton pumping in corals, and found in one species that a fixed proton gradient (between internal fluids and the external environment) model best explained the measured response. It is certainly possible that the limited up-regulation of cross-membrane ion pumps under acidification stress is due to the lack of capacity to do so, but more studies are needed along these lines to speak to the broader applicability. These observations and arguments do not preclude a proton flux stress/sensitivity in marine calcifiers; rather, they indicate that other physiological processes also appear at play to overcome this stress, and that the universal applicability/exclusivity of the proton flux model across taxa is uncertain.

Reiterating that while our omega sensitivity model is not framed in thermodynamics, but rather kinetics, we believe there is confusion arising from the fact that many of the chemical species in our kinetic model are defined in the oceans by the complex thermodynamics of carbonate chemistry. Specifically, here we refer to the

arguments centred on the $[HCO_3^-]/[H^+]$ construct. Efforts by our group and others (Jury *et al.*, 2010; Gazeau *et al.*, 2011; Waldbusser *et al.*, 2015a, b) to experimentally decouple carbonate system parameters in this debate are futile because the $[HCO_3^-]/[H^+]$ ratio is correlated with omega by the second dissociation constant of the carbonic acid system, which can be rearranged as

$$\frac{[HCO_3^-]}{H^+} = \frac{[CO_3^{2-}]}{K_2^*}, \quad (3)$$

where K_2^* is the second dissociation constant for the marine carbonate system. The rapid attainment of equilibrium for these acid–base reactions guarantees that carbonate ion concentration will always be simply proportional to the ratio of bicarbonate to proton concentrations, and it is easy to see from Equation (1) that this holds true for Ω as well in temperature- and salinity-controlled experimental systems. While it may seem like an academic argument, understanding what carbonate system parameter(s) matters most to various marine organisms is actually crucial to predicting ocean acidification (OA) impacts on marine ecosystems. In coastal zones, where many important calcium carbonate organisms reside, carbonate system parameters decouple because of changes in salinity, and thus alkalinity. For example, while the rapid global rise of atmospheric CO_2 has ensured a tight coupling of the present-day carbonate system parameters, in the geologic past, however, slower changes in CO_2 relative to ocean alkalinity resulted in a different response of carbonate system parameters to increasing CO_2 (Honisch *et al.*, 2012). Next, we will highlight five inductive lines of evidence of an omega-based sensitivity linked to a kinetic–energetic mechanism for marine calcifiers, and indicate the shortcomings of the competing proton flux/bicarbonate model where they appear. We present these arguments with the caveat that the relative importance of omega vs. $[HCO_3^-]/[H^+]$ may not always be mutually exclusive, nor does lack of applicability in one species invalidate its potential role in other species. Rather, ultimately we hope this discussion will lead to a more rational perspective across species, and to integrate these for a holistic organismal perspective within species.

First, in the formulation of the proton flux model (Jokiel, 2011), and subsequent arguments (Cyronak *et al.*, 2016; Thomsen *et al.* 2015), the authors correctly note that calcification lowers pH, as protons are generated when the basic carbonate ion is consumed into calcium carbonate. The subsequent removal of these protons from the calcification site is typically dependent on either active transport away from the calcification site (via proton pumps) or passive diffusion. In either case, mass balance requires those protons to be removed either from the fluids from which calcium carbonate is precipitate or the immediate surrounding water if pH is to be maintained or controlled at calcification surfaces. Diffusion is a generally slow process over larger time and space scales, which thus may seem to lead to proton accumulation in a larger organism. Developing bivalve (*C. gigas*) embryos are roughly 50–75 mm in diameter and have little ability to swim: they exist in low Reynolds number space, and thus, diffusion is the only way to exchange solutes. The diffusive boundary layer argument [as noted in Hurd *et al.* (2011)] has little applicability for most invertebrate larvae, as flow over a smooth surface is required to generate a diffusive boundary layer (DBL). Hurd *et al.* (2011), however, present DBL estimates for planktonic organisms, and these are all <1 mm in length, and at these spatial scales, diffusion is very rapid and effective in the transport of solutes. It is also critical to note that the original diffusion-based arguments were derived from oxygen fluxes in coral reefs and how these fluxes responded to changes in water flow over the reefs, thus altering diffusive boundary layers (Jokiel, 2011). What we stress is that the free diffusion coefficient for protons is roughly 10× greater than that of other solutes, including oxygen, in marine waters (Li and Gregory, 1974), such that for the same boundary layer and reaction rate, the gradient of protons will be 10 times less steep than for other solutes (and thus build-up of protons less severe). Moreover, regarding the $[HCO_3^-]/[H^+]$ model, bicarbonate is consumed by calcification at the same rate at which protons are released; therefore, the need for excess protons to be exported is much less of a theoretical hurdle than that posed by importing bicarbonate into the organism. While internal transport of protons away from calcification sites may be important, direct measurements and modelling exercises should help to determine the scenarios under which this phenomenon may or may not matter. Given the large proton diffusion coefficient relative to other solutes and sub-millimetre diffusive layers in planktonic organisms existing in low Reynolds number conditions, we would caution against assuming that protons cannot diffuse away before becoming a problem for bivalve larvae. If the exterior environment increases the proton concentration, then this should reduce the flux; however, it will still be rapid, until there is no longer a gradient. So whether or not the proton flux will affect marine calcifiers, the only reasonable answer seems to be YES!

Second, an important component of the $[HCO_3^-]/[H^+]$ model is the role of bicarbonate in offsetting or buffering the proton accumulation (Cyronak *et al.*, 2016). Adding bicarbonate to seawater solution will only improve pH if conditions are below pH of ~7.5 (or more exactly, the equivalence point of carbonic acid and carbonate ion concentration, achieved when $[H^+] = \sqrt{(K_1 \times K_2)}$, or when carbonate alkalinity and DIC are equivalent). While perhaps counterintuitive, increases in bicarbonate concentration when the system is at the alkalinity–DIC equivalence point noted above must be associated with an equivalent increase in both carbonic acid and carbonate ion concentrations, unless the solution is allowed to degas CO_2. Therefore, an increase in bicarbonate of a seawater-like fluid at pH ~7.5 would mean that both P_{CO_2} and omega increase, while pH is stable!

The measurements by Thomsen *et al.* (2010) indicate the pH of the extrapallial (calcifying) fluids in their adult mussels to be slightly higher than 7.5, and DIC levels near seawater values, so adding bicarbonate will not increase pH in this case. It will, however, improve saturation state [as noted in Equation (3)]. In a series of measurements on other bivalves (including a different mussel species), Crenshaw (1972) found DIC concentrations 1.5–2× seawater values, and pH between 7.3 and 7.4 in their calcifying fluids. Because of these high DIC concentrations, the resulting saturation states are above 2 in their calcifying fluids, even at these pH values. Bicarbonate accumulation in this case would *increase* pH, while omega is already in a favourable range. We have taken data from our experiments on mussel larvae (Waldbusser *et al.*, 2015a, b) to illustrate how, at least in this taxa and life history stage, a proton flux model linked to bicarbonate ion concentration is not very well supported. Again, acknowledging that Equation (3) thermodynamically binds the proton flux/bicarbonate ion model to saturation state, we show that if decomposed over a range of generally low pH (7.5–7.8), that omega explains ~25% more variance in shell length than does bicarbonate (Figure 2). This enhanced explanatory power of omega increases to roughly 50% if the full range of data is used, but we

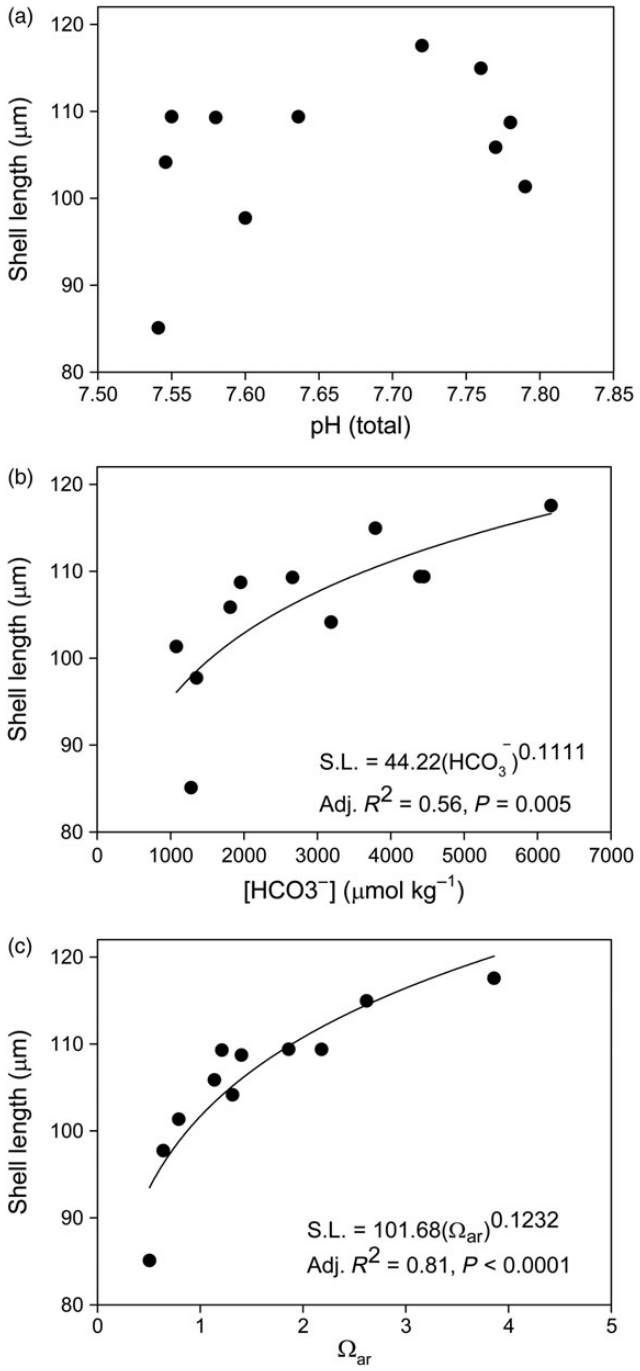

Figure 2. Data on shell length of 48-h-old *Mytilus galloprovincialis* and *Mytilus californianus* from Waldbusser *et al.* (2015a, b) plotted against (a) pH, (b) bicarbonate concentration, and (c) aragonite saturation state. Plotted are only data from pH conditions that fall between 7.5 and 7.8, pH conditions in which a proton flux-based sensitivity should be far more apparent. While bicarbonate concentration explains a significant amount of the variance in shell length across this range (supporting an increase in substrate benefit), omega explains roughly 25% more variance. Again, the thermodynamics prevents fully separating these variables. Our posit for an omega sensitivity does not preclude a bicarbonate accumulation mechanism by which omega would be increased.

chose to present the lower pH as this is when the greatest bicarbonate effect should manifest. So whether bicarbonate accumulation will be important or not to improving pH at calcification sites, we can answer YES, but only when the pH of calcifying fluids is below the critical values noted above.

Third, the previous arguments depend on the ability of marine calcifiers to isolate and control the chemistry in their calcifying fluid. Cyronak *et al.* (2016) point out that calcification occurs in isolated compartments within marine organisms, and thus environmental conditions are not identical with conditions within these calcification spaces (as has been well documented and reviewed elsewhere, and previously in our own work). The ability to isolate and control calcification fluid chemistry is not at all a generality across taxa or life stages within specific taxon. For instance, it appears that in adult bivalve mussels, there is little ability to regulate the calcifying fluids as P_{CO_2} levels increase in the surrounding waters (Thomsen *et al.*, 2010). The ability to isolate the calcifying fluids from the external environment also varies across bivalve taxa and life history stage (Crenshaw, 1972; Carriker, 1992; Waldbusser *et al.*, 2013). For bivalve larvae, it appears that the ability to isolate the calcification compartment from the external environment improves after the formation of the initial shell (Waldbusser *et al.*, 2013), but even adult bivalves are not always completely able to isolate these compartments [reviewed in Waldbusser *et al.* (2015b)]. Additionally, even in species thought to completely protect their calcified structures with soft tissue, such as corals, recent experimental work has highlighted that these calcification compartments may be more permeable to seawater than previously thought (Gagnon *et al.*, 2012; Tambutté *et al.*, 2012). So are calcification compartments in marine organisms exposed to, or isolated from, the external environment? We again answer a resounding YES!

Fourth, Cyronak *et al.* (2016) raise the spectre that perhaps shell dissolution is causing the responses we have recorded. We see clear sensitivity even when $\Omega > 1$, when dissolution would not be thermodynamically favoured. Dissolution does not explain the important observation of fully calcified, yet deformed larval shells recorded in our studies and others (Gazeau *et al.*, 2011; Thomsen *et al.*, 2015; Waldbusser *et al.*, 2015a, b). In fact, 2-d-old Pacific oyster larvae reared under corrosive conditions ($\Omega_{ar} \sim 0.5$) show severe deformities in a fully calcified shell (Waldbusser *et al.*, 2015a), rather than evidence of dissolution. Even after 4 d at saturation state of ~0.5, only very minor evidence of dissolution may be seen on the exterior of larval shells (Barton *et al.*, 2015, Figure 4). Furthermore, dissolution is typically abiotic and slow; Equation (2) can be rearranged to document dissolution as a function of saturation state by changing $(\Omega - 1)$ to $(1 - \Omega)$. Dissolution, in fact, is driven entirely by saturation state, so pH or bicarbonate concentrations will have no direct effect on dissolution; it is favoured or not in the definition of saturation state (Ω) and the rate is determined by Equation (2). Even still, would the predicted dissolution rate be able to explain the effects on the developing embryos of bivalve larvae we and others have noted? Over the course of 2 d, and during the course of the calcification event of the PDI shell, the mass balance simply cannot be satisfied by abiotic dissolution rates. It is well documented in slower calcifying organism that the interplay of dissolution and calcification will be far better balanced, and more easily tipped (and again saturation state is the driving variable for dissolution). We, therefore, contend that dissolution is likely trivial on the timescales of initial shell formation in many bivalve larvae, a day or less.

Finally, while we have used length as a proxy for calcification, the problem with shell length is that it assumes a constant relationship between shell extension, which results from organic matter addition to the shell (as periostracum), and shell thickening, which is, in fact,

the mineralization of the shell with calcium carbonate. Gaylord *et al.* (2011) found in California mussel larvae that shell area, shell thickness, and tissue mass did not all respond similarly to acidification after 8 d. Interestingly, shell thickness decreased under slightly elevated CO_2, but at higher levels did not change, whereas decreases in shell area were only significant at their highest CO_2 treatment. The largest effect they found was on tissue mass, and we would speculate that the increased demands of coping with the acidification stress are driving those responses, with dissolution likely only responsible for the differences in shell thickness. So does dissolution matter or not to marine calcifiers? We again answer YES, but it is very unlikely to be playing a major role on early shell development in bivalve larvae.

Finally, we note a striking pattern when looking at our data, or that of any other bivalve response to acidification experiments where enough data exist to document a pattern (Gazeau *et al.*, 2011; Thomsen *et al.*, 2015; Waldbusser *et al.*, 2015a, b): inflection points and threshold responses seen in measured variables almost always appear near the saturation horizon ($\Omega = 1$), and often above it. Importantly, we did just argue above that dissolution is probably of minor significance during the rapid calcification event of PDI shell formation, and we therefore believe, based on what would be predicted abiotic dissolution rates, that the omega sensitivity we see in developing bivalve larvae near (but not $=1$) is due to the energetic demand of rapid calcification in thermodynamically favourable, but kinetically challenging conditions. The ratio of $[HCO_3^-]/[H^+]$ is inextricably linked to omega, as noted above; we are, however, unaware of a mechanism that explains why the $[HCO_3^-]/[H^+]$ ratio would drive such an inflection point in larval bivalve responses. It is certainly worthy of further study to identify a mechanism that would force different species to share similar responses around a saturation state $= 1$, and perhaps these similar responses are for different reasons. So, we answer our final question whether omega or $[HCO_3^-]/[H^+]$ matters most to marine calcifiers with one final YES!

Our response to the "Omega Myth" may seem tongue in cheek; however, we believe Cyronak *et al.* (2016) fall squarely into the dialectic trap and in so doing miss the kinetic–energetic hypothesis for an omega sensitivity (Waldbusser *et al.*, 2013, 2015a, b). The vast diverse and beautiful array of marine calcifiers will likely prevent us from ever having a unified theory for calcification from ooids to otoliths, but some evident truths are present, and continued research will help further refine these and identify new hypotheses to test. To advance these truths, we must carefully define our questions; otherwise, we are left with the only rational answer to "this or that" questions, YES. The authors are correct in pointing out that an omega sensitivity linked to a substrate limitation is unfounded, and our work never laid claim to such a story. We want to be sure the omega myth based on dramatic licence is extinguished and our work is not misinterpreted. We also refrain from a naive approach to proclaim omega can explain the responses of all marine calcifiers, across all life history stages, as we have experimentally shown that ocean acidification can itself act as a multistressor on bivalve larvae (Waldbusser *et al.*, 2015b). We do strongly argue that the impact of omega (and not $[HCO_3^-]/[H^+]$) on the earliest life stages of marine bivalves is a major bottleneck for successful recruitment into adult populations, and that is one of the most imminent threats of ocean acidification to marine organisms. And therefore, as the Phoenix rises from the ashes for its rebirth, we argue the legend of (and mechanisms for) omega provides a greater understanding of how, in a more holistic sense, ocean acidification will impact marine calcifiers in an ever acidifying ocean.

Acknowledgements

The research supporting these views was supported by National Science Foundation OCE CRI-OA (#1041267 to GGW, BH, and BAH). GGW thanks A. Hettinger and K. Bernard for their thoughtful comments on previous versions of this manuscript.

References

Barton, A., Waldbusser, G. G., Feely, R. A., Weisberg, S. B., Newton, J. A., Hales, B., Cudd, S., *et al.* 2015. Impacts of coastal acidification on the Pacific Northwest Shellfish Industry and adaptation strategies implemented in response. Oceanography, 28: 146–159.

Carriker, M. R. 1992. Prismatic shell formation in continuously isolated (*Mytilus edulis*) and periodically exposed (*Crassostrea virginica*) extrapallial spaces—Explicable by the same concept. American Malacological Bulletin, 9: 193–197.

Cohen, A. L., and Holcomb, M. 2009. Why corals care about ocean acidification: Uncovering the mechanism. Oceanography, 22: 118–127.

Crenshaw, M. A. 1972. Inorganic composition of molluscan extrapallial fluid. Biological Bulletin, 143: 506–512.

Cyronak, T., Schulz, K. G., and Jokiel, P. L. 2016. The Omega myth: What really drives lower calcification rates in an acidifying ocean. ICES Journal of Marine Science, 73: 558–562.

Gagnon, A. C., Adkins, J. F., and Erez, J. 2012. Seawater transport during coral biomineralization. Earth and Planetary Science Letters, 329–330: 150–161.

Gattuso, J. P., Magnan, A., Billé, R., Cheung, W. W. L., Howes, E. L., Joos, F., Allemand, D., *et al.* 2015. Contrasting futures for ocean and society from different anthropogenic CO_2 emissions scenarios. Science, 349. doi: 10.1126/science.aac4722.

Gaylord, B., Hill, T. M., Sanford, E., Lenz, E. A., Jacobs, L. A., Sato, K. N., Russell, A. D., *et al.* 2011. Functional impacts of ocean acidification in an ecologically critical foundation species. Journal of Experimental Biology, 214: 2586–2594.

Gazeau, F., Gattuso, J-P., Greaves, M., Elderfield, H., Peene, J., Heip, C. H. R., and Middelburg, J. J. 2011. Effect of carbonate chemistry alteration on the early embryonic development of the Pacific Oyster (*Crassostrea gigas*). PLoS ONE, 6: 23011–23018.

Gazeau, F., Quiblier, C., Jansen, J. M., Gattuso, J. P., Middelburg, J. J., and Heip, C. H. R. 2007. Impact of elevated CO_2 on shellfish calcification. Geophysical Research Letters, 34: L07603.

Honisch, B., Ridgwell, A., Schmidt, D. N., Thomas, E., Gibbs, S. J., Sluijs, A., Zeebe, R., *et al.* 2012. The geological record of ocean acidification. Science, 335: 1058–1063.

Hurd, C. L., Cornwall, C. E., Currie, K., Hepburn, C. D., McGraw, C. M., Hunter, K. A., and Boyd, P. W. 2011. Metabolically induced pH fluctuations by some coastal calcifiers exceed projected 22nd century ocean acidification: A mechanism for differential susceptibility? Global Change Biology, 17: 3254–3262.

Jokiel, P. L. 2011. Ocean acidification and control of reef coral calcification by boundary layer limitation of proton flux. Bulletin of Marine Science, 87: 639–657.

Jury, C. P., Whitehead, R. F., and Szmant, A. M. 2010. Effects of variations in carbonate chemistry on the calcification rates of *Madracis auretenra* (Madracis mirabilis sensu Wells, 1973): Bicarbonate concentrations best predict calcification rates. Global Change Biology, 16: 1632–1644.

Kroeker, K. J., Kordas, R. L., Crim, R. N., and Singh, G. G. 2010. Meta-analysis reveals negative yet variable effects of ocean acidification on marine organisms. Ecology Letters, 13: 1419–1434.

Li, Y. H., and Gregory, S. 1974. Diffusion of ions in sea water and in deep-sea sediments. Geochimica et Cosmochimica Acta, 38: 703–714.

McConnaughey, T. A., and Gillikin, D. P. 2008. Carbon isotopes in mollusk shell carbonates. Geo-Marine Letters, 28: 287–299.

Melzner, F., Stange, P., Trubenbach, K., Thomsen, J., Casties, I., Panknin, U., Gorb, S. N., *et al.* 2011. Food supply and seawater pCO(2) impact calcification and internal shell dissolution in the Blue Mussel *Mytilus edulis*. PLoS ONE, 6: e24223.

Palmer, A. R. 1992. Calcification in marine mollusks—How costly is it. Proceedings of the National Academy of Sciences of the United States of America, 89: 1379–1382.

Pan, T. C. F., Applebaum, S. L., and Manahan, D. T. 2015. Experimental ocean acidification alters the allocation of metabolic energy. Proceedings of the National Academy of Sciences, 112: 4696–4701.

Ries, J. B. 2011. A physicochemical framework for interpreting the biological calcification response to CO_2-induced ocean acidification. Geochimica et Cosmochimica Acta, 75: 4053–4064.

Roleda, M. Y., Boyd, P. W., and Hurd, C. L. 2012. Before ocean acidification: Calcifier chemistry lessons. Journal of Phycology, 48: 840–843.

Tambutté, E., Tambutté, S., Segonds, N., Zoccola, D., Venn, A., Erez, J., and Allemand, D. 2012. Calcein labelling and electrophysiology: Insights on coral tissue permeability and calcification. Proceedings of the Royal Society B: Biological Sciences, 279: 19–27.

Thomsen, J., Gutowska, M. A., Saphorster, J., Heinemann, A., Trubenbach, K., Fietzke, J., Hiebenthal, C., *et al.* 2010. Calcifying invertebrates succeed in a naturally CO_2-rich coastal habitat but are threatened by high levels of future acidification. Biogeosciences, 7: 3879–3891.

Thomsen, J., Haynert, K., Wegner, K. M., and Melzner, F. 2015. Impact of seawater carbonate chemistry on the calcification of marine bivalves. Biogeosciences Discuss, 12: 1543–1571.

Waldbusser, G. G., Bergschneider, H., and Green, M. A. 2010. Size-dependent pH effect on calcification in post-larval hard clam *Mercenaria* spp. Marine Ecological Progress Series, 417: 171–182.

Waldbusser, G. G., Brunner, E. L., Haley, B. A., Hales, B., Langdon, C. J., and Prahl, F. G. 2013. A developmental and energetic basis linking larval oyster shell formation to acidification sensitivity. Geophysical Research Letters, 40: 2171–2176.

Waldbusser, G. G., Hales, B., Langdon, C. J., Haley, B. A., Schrader, P., Brunner, E. L., Gray, M. W., *et al.* 2015a. Saturation-state sensitivity of marine bivalve larvae to ocean acidification. Nature Climate Change, 5: 273–280.

Waldbusser, G. G., Hales, B., Langdon, C. J., Haley, B. A., Schrader, P., Brunner, E. L., Gray, M. W., *et al.* 2015b. Ocean acidification has multiple modes of action on bivalve larvae. PLoS ONE, 10: e0128376.

Waldbusser, G. G., Voigt, E. P., Bergschneider, H., Green, M. A., and Newell, R. I. E. 2011. Biocalcification in the Eastern Oyster (*Crassostrea virginica*) in relation to long-term trends in Chesapeake Bay pH. Estuaries and Coasts, 34: 221–231.

Handling editor: Howard Browman

ICES Journal of Marine Science

ICES Journal of Marine Science (2016), 73(3), 569–571. doi:10.1093/icesjms/fsv224

Contribution to Special Issue: 'Towards a Broader Perspective on Ocean Acidification Research'

Response

Response to Waldbusser *et al.* (2016): "Calcium carbonate saturation state: on myths and this or that stories"

Tyler Cyronak[1]*, Kai G. Schulz[2], and Paul L. Jokiel[3]

[1]*Scripps Institution of Oceanography, UC San Diego, 9500 Gilman Drive 0244, La Jolla, CA 92093-0244, USA*
[2]*Centre for Coastal Biogeochemistry, Southern Cross University, PO Box 157, Lismore, NSW 2480, Australia*
[3]*Hawaii Institute of Marine Biology, University of Hawaii, PO Box 1346, Kaneohe, HI 96744, USA*

**Corresponding author: tel: +1 610 701 1117; fax: +1 858 822 3310; e-mail: tcyronak@gmail.com*

Cyronak, T., Schulz, K. G., and Jokiel, P. L. Response to Waldbusser *et al.* (2016): "Calcium carbonate saturation state: on myths and this or that stories". – ICES Journal of Marine Science, 73: 569–571.

Received 23 October 2015; accepted 3 November 2015; advance access publication 13 December 2015.

Currently, almost any article searched with the keywords "calcification" and "ocean acidification" (OA) will inevitably bring up a link between calcification and bulk seawater carbonate saturation state (Ω) as a justification for the study. Therefore, it seems timely to highlight that from a physiological point of view, there are mechanisms that invoke control of calcification by seawater bicarbonate (HCO_3^-) and proton (H^+) concentrations rather than Ω in many marine organisms. While we agree with Waldbusser et al. (2016) that there is a vast diversity of marine calcifiers able to regulate carbonate chemistry internally at the site of calcification, it seems adequate to assume a similar underlying physiological response to OA unless shown otherwise.

We do not necessarily interpret the seeming Ω sensitivity of calcification as substrate limitation, as suggested by Waldbusser et al. (2016), we simply question the mechanisms that would invoke bulk seawater Ω as a driving force of calcification in the first place. Waldbusser et al. (2016) rightfully note the co-variability of seawater Ω with the ratio of $[HCO_3^-]$ to $[H^+]$. Recently, Bach (2015) demonstrated that a rearrangement of carbonate system equations results in an inevitable proportionality between Ω and the ratio of $[HCO_3^-]$ to $[H^+]$. Owing to this proportionality, calcification rates will always correlate as well with $[HCO_3^-]/[H^+]$ as they do with $[CO_3^{2-}]$ or Ω when temperature, salinity, and pressure are constant (Figure 1). Hence, the good correlations with bulk seawater $[CO_3^{2-}]$ or Ω that have previously been reported [examples given in Waldbusser et al. (2016)] can equally be interpreted as the influence of $[HCO_3^-]$ and $[H^+]$, which are physiologically more meaningful carbonate system parameters.

We acknowledge that Ω influences calcification rates in accordance with the kinetic mechanism invoked by Waldbusser et al. (2016), the difference being that it is the internal Ω (not bulk seawater Ω) that is important, which is most likely modulated by bulk seawater $[HCO_3^-]$ and $[H^+]$ and not bulk seawater Ω. The ratio of $[HCO_3^-]$ to $[H^+]$ incorporates both the substrate (needed to be supplied from bulk seawater to the site of calcification) and waste product (needed to be removed from the site of calcification to bulk seawater) during the biogenic production of $CaCO_3$. It must be emphasized that both parameters should be included when looking at the effects of seawater carbonate chemistry on calcification because increasing seawater HCO_3^- concentrations could compensate for unfavourable pH ($[H^+]$) conditions (see Bach, 2015). In essence, the more substrate (e.g. HCO_3^-) is available for uptake from bulk seawater the better a calcifying organisms is able to cope with lowered pH levels by keeping internal Ω at the site of calcification favourable for $CaCO_3$ precipitation. Low substrate availability together with low pH (high $[H^+]$) levels would make calcification more difficult. In general, high $[HCO_3^-]/[H^+]$ ratios would be favourable to calcification while low ones become detrimental. In this respect, it also does not matter how well an organism, or ontogenetic life stage, is able to separate the internal calcifying fluid from external seawater as suggested by Waldbusser et al. (2016), its sensitivity to external carbonate chemistry changes will simply scale with its ability to modulate internal carbonate chemistry. We also acknowledge that there are other processes involved in calcification such as protein synthesis, however, bulk seawater HCO_3^- and H^+ concentrations or its ratio ultimately influence the energetic demands of calcification.

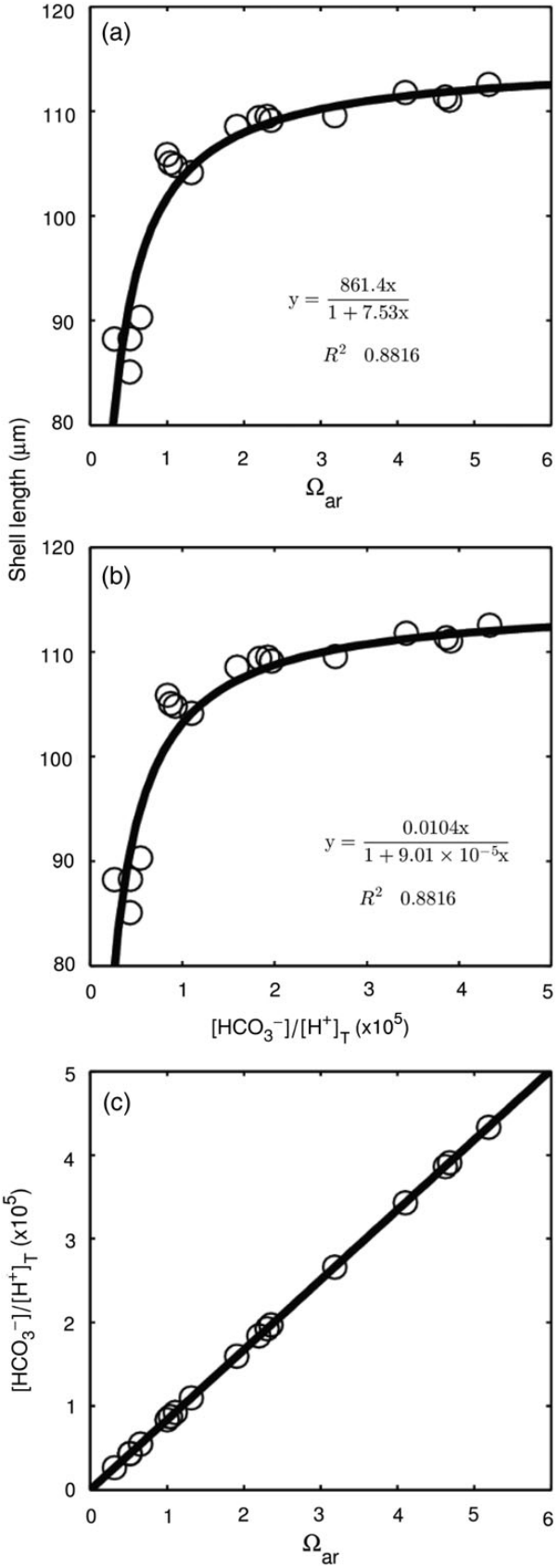

Figure 1. Mussel shell length vs. (a) aragonite saturation state (Ω_{ar}), (b) the ratio of bicarbonate (HCO_3^-) to proton (H^+) concentration in the total scale, and (c) Ω_{ar} vs. $[HCO_3^-]/[H^+]$. Data from Waldbusser *et al.* (2015b) were downloaded from the Biological and Chemical Oceanography Data Management website (http://www.bco-dmo.org/dataset/557253) and carbonate chemistry parameters were recalculated using the TA and DIC data at a salinity of 31 and temperature of 18°C.

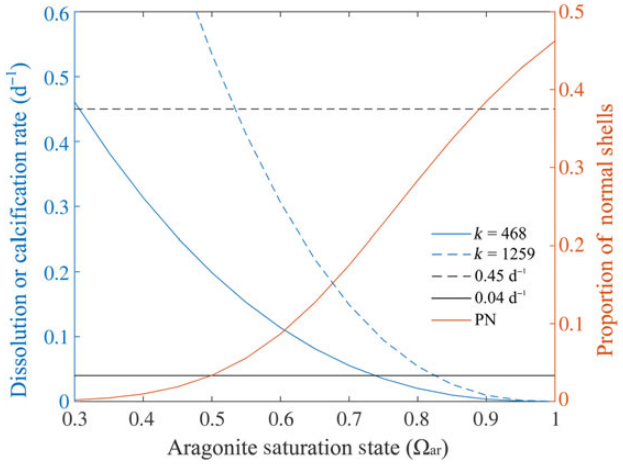

Figure 2. Plot showing the mass normalized dissolution rate (d^{-1}) of biogenic aragonites derived from $R = k \times (1 - \Omega)^{2.5}$ at the two extreme k values from Walter and Morse (1985). The black lines show the range of mass normalized calcification rates of larval mussels from Waldbusser *et al.* (2013). From this, it is obvious that dissolution rates can account for changes in bivalve net calcification once Ω drops below 1, which may happen in the calcifying fluid before in the external seawater (Thomsen *et al.*, 2010; Heinemann *et al.*, 2012). The proportion of normal (PN) mussel larvae (Waldbusser *et al.*, 2015b) is plotted to demonstrate how changes in mussel shell development could be related to dissolution rates.

Another potential issue concerning the influence of Ω on calcification rates is that $CaCO_3$ dissolution becomes thermodynamically favourable at $\Omega < 1$. If dissolution is not accounted for, it would enhance relationships between the biologically mediated process of calcification (gross calcification) and Ω $[HCO_3^-]/[H^+]$, Waldbusser et al. (2016) briefly discuss that $CaCO_3$ dissolution rates cannot account for changes in calcification under elevated CO_2 reported in several studies on bivalve larvae. However, they report no quantitative analysis of this except to say that dissolution follows the kinetic rate equation;

$$R = k \times (1 - \Omega)^n,$$

where R is the dissolution rate (µmol g^{-1} h^{-1}), k the rate constant (µmol g^{-1} h^{-1}), and n the reaction order. Using a reaction order of $n = 2.5$ and a range of k values (467.7–1258.9 µmol m^{-2} h^{-1}) for biogenic aragonites taken from Table 6 in Walter and Morse (1985) demonstrates that dissolution may in fact be very important in controlling a bivalve's response to increasing seawater CO_2 (Figure 2). At the highest k value, dissolution rates of aragonite exceed the mass normalized measured net calcification rates of larval mussels (0.45 d^{-1}) around an aragonite saturation state (Ω_{ar}) of 0.5, while at the lowest k value, dissolution exceeds measured net calcification around a seawater Ω_{ar} of 0.3. A bulk seawater Ω_{ar} of 0.3 also coincides with the point at which the proportion of

normal larval mussel shells approaches zero (Waldbusser *et al.*, 2015a, b, 2016). Therefore, this mass balance lends support to dissolution being a potential driver of changes in larval mussel shell development in high CO_2 seawater. In support of this, it has been demonstrated that internal (within the calcifying fluid) and external shell dissolution significantly affect the mortality of juvenile and adult bivalves at low Ω (Green *et al.*, 2004; Melzner *et al.*, 2011). As pointed out by Waldbusser et al. (2016), the response of larval mussels to Ω seems to have a threshold where shell development becomes severely compromised (Waldbusser *et al.*, 2015a, b). Considering the response of mussel larvae to seawater Ω occurs very close to a bulk seawater Ω of 1, and continues after $\Omega < 1$, perhaps the threshold is a response due to dissolution becoming thermodynamically favourable either inside or outside of the calcifying fluid. Therefore, the possibility that changes in $CaCO_3$ dissolution rates drive changes in larval mussel shell development when Ω of the calcifying fluid or external seawater <1 cannot be excluded.

We do not dispute the fact that Ω can, and does, affect the biogenic $CaCO_3$ budgets of marine organisms. However, it must be emphasized that, ultimately, it is the Ω of the calcifying fluid that controls precipitation kinetics, and not the bulk seawater. Furthermore, when Ω of either the calcifying fluid or bulk seawater is <1, dissolution of $CaCO_3$ could become important. Future studies should attempt to tease apart the influence of changes in bulk seawater chemistry on the chemistry of the calcifying fluid, and therefore, internal $CaCO_3$ precipitation kinetics, along with any changes in $CaCO_3$ dissolution. Organisms that are able to actively control carbonate chemistry at the site of calcification are most likely responding to changes in bulk seawater carbonate chemistry that affect their ability to maintain that physiological control. As outlined above and in the original paper, there is no clear physiological basis as to why seawater Ω should be one of these variables, but rather seawater $[HCO_3^-]$ and $[H^+]$.

References

Bach, L. T. 2015. Reconsidering the role of carbonate ion concentration in calcification by marine organisms. Biogeosciences, 12: 4939–4951.

Green, M. A., Jones, M. E., Boudreau, C. L., Moore, R. L., and Westman, B. A. 2004. Dissolution mortality of juvenile bivalves in coastal marine deposits. Limnology and Oceanography, 49: 727–734.

Heinemann, A., Fietzke, J., Melzner, F., Böhm, F., Thomsen, J., Garbe-Schönberg, D., and Eisenhauer, A. 2012. Conditions of *Mytilus edulis* extracellular body fluids and shell composition in a pH-treatment experiment: acid–base status, trace elements and $\delta^{11}B$. Geochemistry, Geophysics, Geosystems, 13: 1–17.

Melzner, F., Stange, P., Trübenbach, K., Thomsen, J., Casties, I., Panknin, U., Gorb, S. N., *et al.* 2011. Food supply and seawater pCO_2 impact calcification and internal shell dissolution in the blue mussel *Mytilus edulis*. PLoS ONE, 6: e24223.

Thomsen, J., Gutowska, M., Saphörster, J., Heinemann, A., Trübenbach, K., Fietzke, J., Hiebenthal, C., *et al.* 2010. Calcifying invertebrates succeed in a naturally CO_2-rich coastal habitat but are threatened by high levels of future acidification. Biogeosciences, 7: 3879–3891.

Waldbusser, G. G., Brunner, E. L., Haley, B. A., Hales, B., Langdon, C. J., and Prahl, F. G. 2013. A developmental and energetic basis linking larval oyster shell formation to acidification sensitivity. Geophysical Research Letters, 40: 2171–2176.

Waldbusser, G. G., Hales, B., Langdon, C. J., Haley, B. A., Schrader, P., Brunner, E. L., Gray, M. W., *et al.* 2015a. Saturation-state sensitivity of marine bivalve larvae to ocean acidification. Nature Climate Change, 5: 273–280.

Waldbusser, G. G., Hales, B., Langdon, C. J., Haley, B. A., Schrader, P., Brunner, E. L., Gray, M. W., *et al.* 2015b. Ocean acidification has multiple modes of action on bivalve larvae. PLoS ONE, 10: e0128376.

Walbusser, G. G., Hales, B., and Haley, B. 2016. Calcium carbonate saturation state: on myths and this or that stories. ICES Journal of Marine Science, 73: 563–568.

Walter, L. M., and Morse, J. W. 1985. The dissolution kinetics of shallow marine carbonates in seawater: a laboratory study. Geochimica et Cosmochimica Acta, 49: 1503–1513.

Handling editor: Howard Browman

ICES Journal of Marine Science

ICES Journal of Marine Science (2016), 73(3), 572–581. doi:10.1093/icesjms/fsv118

Contribution to Special Issue: 'Towards a Broader Perspective on Ocean Acidification Research'

Original Article

Experimental design in ocean acidification research: problems and solutions

Christopher E. Cornwall[1,2]* and Catriona L. Hurd[1]

[1]*Institute for Marine and Antarctic Studies, University of Tasmania, Private Bag 129, Hobart, TAS 7001, Australia*
[2]*School of Earth and Environment and ARC Centre of Excellence in Coral Reef Studies, The University of Western Australia, 35 Stirling Highway, Crawley, WA 6009, Australia*

**Corresponding author: tel: +61 8 6488 3644; fax: +61 3 62262973; e-mail: christopher.cornwall@uwa.edu.au*

Cornwall, C. E., and Hurd, C. L. Experimental design in ocean acidification research: problems and solutions. – ICES Journal of Marine Science, 73: 572–581.

Received 26 February 2015; revised 8 June 2015; accepted 10 June 2015; advance access publication 8 July 2015.

Ocean acidification has been identified as a risk to marine ecosystems, and substantial scientific effort has been expended on investigating its effects, mostly in laboratory manipulation experiments. However, performing these manipulations correctly can be logistically difficult, and correctly designing experiments is complex, in part because of the rigorous requirements for manipulating and monitoring seawater carbonate chemistry. To assess the use of appropriate experimental design in ocean acidification research, 465 studies published between 1993 and 2014 were surveyed, focusing on the methods used to replicate experimental units. The proportion of studies that had interdependent or non-randomly interspersed treatment replicates, or did not report sufficient methodological details was 95%. Furthermore, 21% of studies did not provide any details of experimental design, 17% of studies otherwise segregated all the replicates for one treatment in one space, 15% of studies replicated CO_2 treatments in a way that made replicates more interdependent within treatments than between treatments, and 13% of studies did not report if replicates of all treatments were randomly interspersed. As a consequence, the number of experimental units used per treatment in studies was low (mean = 2.0). In a comparable analysis, there was a significant decrease in the number of published studies that employed inappropriate chemical methods of manipulating seawater (i.e. acid–base only additions) from 21 to 3%, following the release of the "Guide to best practices for ocean acidification research and data reporting" in 2010; however, no such increase in the use of appropriate replication and experimental design was observed after 2010. We provide guidelines on how to design ocean acidification laboratory experiments that incorporate the rigorous requirements for monitoring and measuring carbonate chemistry with a level of replication that increases the chances of accurate detection of biological responses to ocean acidification.

Keywords: experimental design, manipulation experiments, ocean acidification, pseudoreplication, replication.

Introduction

Ocean acidification is a potential threat to marine ecosystems through its effect on the physiology and ecology of many marine species (e.g. Kroeker *et al.*, 2013b). As the research effort being invested into examining the effects of ocean acidification on marine systems increases, publications on the topic are increasing exponentially (Gattuso *et al.*, 2012; Riebesell and Gattuso, 2015). Experimental manipulations of CO_2 concentrations in the field are difficult, and the number of field studies are limited to a few locales where high CO_2 naturally occurs, or where large scale, costly, and labour intensive experiments have been employed (Barry *et al.*, 2010; Gattuso *et al.*, 2014). Consequently, the most studies are conducted in the laboratory (see reviews by Wernberg *et al.*, 2012; Kroeker *et al.*, 2013b), where CO_2 concentrations can potentially be controlled and reported accurately, and their effects isolated from those of other environmental variables. A multidisciplinary field of research such as ocean acidification brings together various research expertise including engineering sophisticated systems to manipulate and monitor seawater carbonate chemistry, building systems that can house organisms for long periods, and

expertise in measuring the appropriate physiological/biogeochemical/ecological responses to ocean acidification. Crucially, if the field of ocean acidification is to progress, these manipulation experiments need to be performed in such a way that clear conclusions can be drawn from the results.

One of the major challenges for ocean acidification research is that seawater carbonate chemistry must be manipulated correctly in order for experimental treatments to approximately simulate future high CO_2 oceans. Outwardly, this seems rather simple: seawater pH is manipulated using CO_2 gas or the chemically equivalent method of HCl and dissolved inorganic carbon (DIC; usually in the form of $NaHCO_3$ or Na_2CO_3), in a way that mimics changes in the future seawater, increasing in CO_2 concentrations and declines in pH. That is, total alkalinity (A_T) remains constant and DIC increases (Rost *et al.*, 2008; Hurd *et al.*, 2009; Gattuso *et al.*, 2010).

Other logistical constraints, however, make ocean acidification experiments more difficult than those in other related fields of biological research. Experimental tanks often need to be sealed because CO_2 can degas when exposed to the atmosphere, and the tanks require sufficient rates of seawater flow-through because the metabolic activity of organisms can modify seawater DIC and A_T (Rost *et al.*, 2008). The constant addition of chemicals (i.e. CO_2 or HCl/DIC) into experimental tanks over long periods of time, without directly exposing organisms to un-mixed chemicals and seawater, adds another aspect of logistic difficulty to ocean acidification research that is not present in many other manipulation experiments (Hurd *et al.*, 2009; Riebesell *et al.*, 2010b). Appropriate methods must also be employed to determine whether the seawater that organisms are exposed to represents the desired treatments required for ocean acidification research; at least two components of the seawater carbonate system must also be measured (pH, A_T, DIC, or pCO_2). If pH is used to parametrize the seawater carbonate system, then it must be measured using spectrophotometers or electrodes calibrated using TRIS buffers, not with electrodes calibrated using NBS buffers (Dickson *et al.*, 2007; Dickson, 2010). Also, to eliminate or reduce the chance of experimental artefacts or pre-existing gradients in other factors influencing treatments differently, treatments within manipulation experiments must all contain adequate numbers of randomly interspersed and independent treatment replicates (Hurlbert, 1984; Hurlbert and White, 1993; Hurd *et al.*, 2009; Hurlbert, 2009; Wernberg *et al.*, 2012). To complicate matters, ocean acidification will not be occurring in isolation, as other anthropogenic effects such as global warming and localized altered salinity, nutrients (nitrogen, phosphorous), light regimes, storm occurrence, and land-born pollutants will be occurring in synergy (Feely *et al.*, 2004; Boyd, 2011; Ciais *et al.*, 2013). Factorial designs where CO_2 is manipulated in combination with other factors therefore add further complexity and logistical challenges to experimental designs (Havenhand *et al.*, 2010; Wernberg *et al.*, 2012).

The inappropriate assignment of experimental units can be a problem in any form of research, and Hurlbert (1984) defines this inappropriate assignment of experimental units for a given treatment during statistical analyses as "pseudoreplication". Hurlbert defines the appropriate procedures for eliminating the risk of pseudoreplication by randomly interspersing replicates of different treatments with each other, and by removing any interdependence within replicates from the same treatment, i.e. experimental units are randomly interspersed replicates of a treatment. These procedures detailed by Hurlbert (1984) will not be repeated here in detail, but solutions to common problems in ocean acidification manipulation experiments will be mentioned in Discussion. Hurlbert (2013a) also defines experimental units as: "the smallest . . . unit of experimental material to which a single treatment (or treatment combination) is assigned by the experimenter and is dealt with independently . . . ", and defines independent experimental units as being units assigned to the same treatment that will not be subject to conditions that are more similar than conditions that are imposed on units from another treatment, other than the treatment under investigation (Cox, 1958; Kozlov and Hurlbert, 2006; Hurlbert, 2013a). The experimental unit can be constrained by two principles: (i) experimental units within one treatment must not influence each other more than they influence experimental units within another treatment and (ii) factors other than the treatment in question (e.g. seawater source, light, etc.) must, on average, be equal across all treatments (Hurlbert, 2013a). If these principles are adhered to, it will greatly reduce the risk of non-treatment effects differentially influencing one treatment and not others; these should be the basic tenets of experimental design. Regardless of the degree of precision that the treatment is applied and its effects measured, if treatment effects are confused with the effects of other factors not under investigation, then an accurate assessment of the effects of the treatment cannot be made. Hurlbert and White (1993) further define three types of pseudoreplication: (i) simple pseudoreplication, where there is one experimental unit per treatment and multiple individuals in one experimental unit whose responses to the treatment are measured (defined by Hurlbert, 2009 as the "evaluation unit") and treated as though they are independent experimental units; (ii) temporal pseudoreplication, where multiple measurements are made though time on the same experimental unit and treated as independent experimental units of a treatment; (iii) sacrificial pseudoreplication, where there are multiple experimental units per treatment and multiple individuals within each experimental unit, but the individuals are treated as the experimental units during statistical analysis. These three definitions demonstrate how a misinterpretation as to what constitutes an experimental unit vs. an "evaluation unit" could lead to inappropriate design and analysis.

The field of ocean acidification research is rapidly expanding, and so far the scientific community has revealed information crucial to understanding its future impacts at an impressive rate unprecedented in many other fields of research (Riebesell and Gattuso, 2015). However, if the field is to progress, then we need to maximize the information provided by each future study. The purpose of this study is not to exhaustively detail how to correctly replicate experiments of all types; these have already been fully explained previously (Cox, 1958; Hurlbert, 1984; Mead, 1988). Nor is it our goal to undermine previously conducted research, which has significantly advanced understanding of the potential effects of ocean acidification on biological systems (Riebesell and Gattuso, 2015). The objectives of this study is to highlight how well the basic principles for the design and analysis of experiments are followed (e.g. Cox, 1958; Hurlbert, 1984; Mead, 1988; Hurd *et al.*, 2009; Havenhand *et al.*, 2010; Wernberg *et al.*, 2012), and to highlight how the mistreatment of experimental units (not just during statistical analysis) hinders the ability to accurately predict the effects of ocean acidification in certain circumstances. Importantly, it was our goal to provide solutions to many commonly encountered problems in experimental design. The appropriate procedures to replicate experimental units in ocean acidification manipulation experiments are identified, and the prevalence of these appropriate methodological approaches is quantified. As well as presenting potential pitfalls in experimental design, a range of solutions to logistical limitations that are imposed by different CO_2-manipulation system designs

are provided, to increase the inference that can be drawn from future manipulation experiments.

Methods

To measure the prevalence of different designs in ocean acidification manipulation experiments, we searched the database Scopus http://www.scopus.com/ using the term "ocean acidification". We cross checked this search with the database used by Kroeker *et al.* (2013b) and the ocean acidification blog http://news-oceanacidification-icc.org/. Four hundred and sixty-five studies published between 1993 and February 2014 were examined, along with any others that came across our desk thereafter (Supplementary Table SI). Sixty-two of these studies were also analysed by Wernberg *et al.* (2012). Studies were only analysed if they met specific criteria. That is, the studies had to report: (i) the results of research containing the assessment of biological responses to experimental manipulations of seawater CO_2; (ii) state that their results were directly applicable to predicting the impacts of ocean acidification, increases in seawater CO_2 concentrations predicted for the future, or another analogous term. Studies that were investigating the impacts of carbon sequestration in the seabed, and made no mention of future high CO_2 seawater, ocean acidification, etc., were excluded. (iii) They needed to be conducted for longer than 24 h, in other words, we excluded short-term "response-assays". (iv) They had to be published in peer reviewed journals to be included. We excluded field-based correlative surveys due to the logistical limitations imposed on them by lack of availability of multiple "treatment" sites in some locations, and because treatments were not "manipulated" by the researchers usually. This is not to say that we viewed these studies as less worthy than laboratory studies.

After papers were identified that met the above criteria, their experimental design in respect to replication was examined. Specific designs were grouped as per the scheme outlined in Figure 1 in Hurlbert (1984) which we have re-constructed in the context of ocean acidification research (Figure 1), showing potential aquaria or "experimental tank" arrays. Hulbert considers designs whose letters start with an "A" are an appropriate design choice, while those with "B" are an inappropriate choice. They are A-1 completely randomized, A-2 randomized block, A-3 systematic, B-1 simple segregation, B-2 clumped segregation, B-3 isolative segregation, B-4 randomized but with interdependent treatment replicates, and B-5 no replication. In each study, the number of actual experimental units per treatment was also recorded, rather than those stated by the authors. In the context of ocean acidification research, we provide the following examples for each of the B type designs (Figure 1): (B-1) three different pCO_2 treatments are used and experimental tanks are lined up on a bench in order from lowest to highest pCO_2; (B-2) three different shaker tables are used next to each other, and each table contains the replicates of only one treatment; (B-3) three different experimental tanks are used, and each experimental tank contains all the individuals of one treatment only; (B-4) three different header tanks are used to supply seawater for an entire experiment, and one header tank provides seawater for all the replicates of one treatment only; (B-5) one individual per treatment is placed in one tank, and only one tank is used for each treatment of an experiment. In all these examples, pre-existing gradients in other factors or chance events could obscure the effects of the factor under investigation.

In our survey, we assumed that cylinders/containers of CO_2 gas, HCl, or a form of DIC is not likely to be a source of experimental artefact. In other words, we considered that using one source of chemicals to modify carbonate chemistry, and applying it to seawater in all elevated CO_2 treatments would not result in a lack of independence, as we considered that the likelihood of a contaminant such as a type of micro-organism (fungi, bacteria, diatoms, etc.)

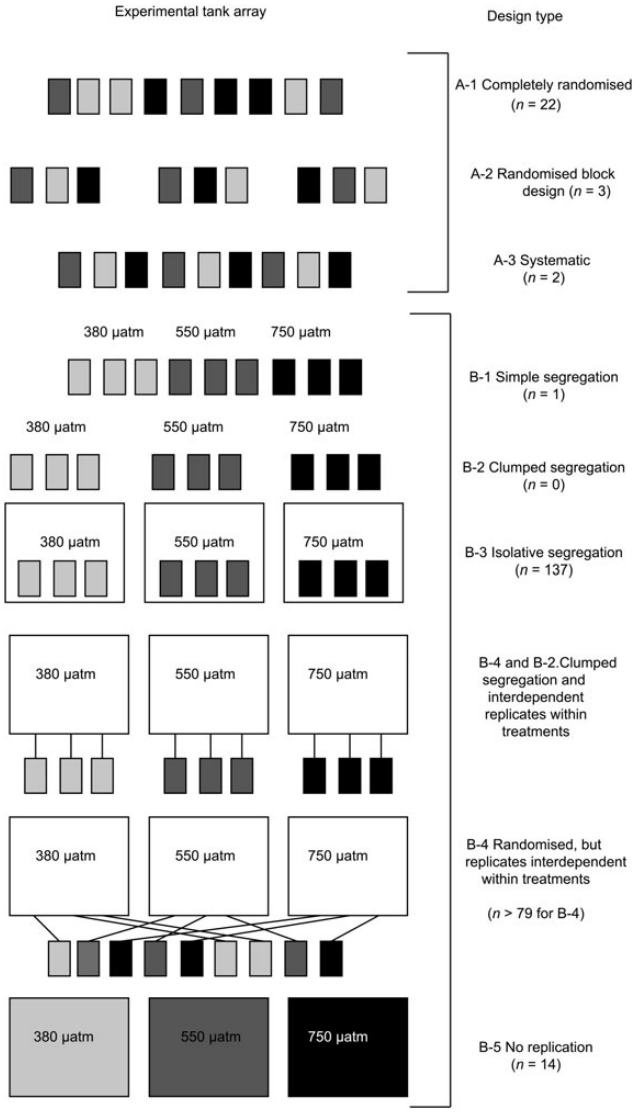

Figure 1. Different designs of tank arrays, modified and re-drawn from Hurlbert (1984) in the context of ocean acidification research. Different coloured tanks correspond to different CO_2 treatments. Design types preceded with an A are acceptable, while those preceded by a B are unacceptable ways to replicate experimental units of a treatment according to Hulbert. (A-1) Completely randomized. (A-2) Randomized block design. (A-3) Systematic. (B-1) Simple segregation. (B-2) Clumped segregation. (B-3) Isolative segregation. (B-4) Randomized but all replicates of one treatment interdependent with themselves more than other treatments (e.g. one header tank of seawater per treatment). (B-5) No replication. An example of replicates within treatments that are interdependent are treatment replicates that all share a common header tank that is not shared with replicates of other treatments large white boxes denote tanks of seawater that do not contain the organisms that are housed. Smaller boxes denote tanks that the organisms are housed in, with different colours representing different pCO_2 levels. n = number of studies using this design type in ocean acidification research. See results and methods for more details.

contaminating that container and changing the treatment was extremely low compared with the likelihood of micro-organisms living in tanks of seawater. This could be an issue, but was outside of the bounds of our analysis, as it is difficult to expect studies to report the number of containers of chemicals used.

The "Guide to Best Practices for Ocean Acidification Research and Data Reporting" (Dickson, 2010; Gattuso *et al.*, 2010; Riebesell *et al.*, 2010a) provided rationale and methods detailing how to manipulate seawater carbonate chemistry in a way that most accurately mimics the changes predicted for a future ocean, and guidelines on the appropriate methods to characterize seawater carbonate chemistry. To determine the impact of this publication on the frequency of studies that used appropriate methods to manipulate and monitor seawater carbonate chemistry, we examined the same 465 papers to determine if they altered seawater chemistry in a way that simulates future ocean acidification (using methods that should increase DIC and keep total alkalinity (A_T) constant) or not (methods resulting in constant DIC and decreased A_T). In other words, we examined whether HCl was used by itself to reduce seawater pH without the addition of DIC. Two components of the seawater carbonate system must be measured (pH, A_T, DIC, or pCO_2) along with temperature and salinity to appropriately measure seawater carbonate chemistry, and if pH is measured it should be measured on the total scale: involving using TRIS buffers to calibrate electrodes, or using spectrophotometric measurements (see Dickson *et al.*, 2007; Dickson, 2010 for complete guidelines). We also recorded the number of papers that measured two or more of seawater pH_T, A_T, DIC, or pCO_2.

Statistical analysis

We analysed whether or not there was a difference pre- and post-2010 (the year of the publication of The Guide to Best Practices in Ocean Acidification and Data Reporting) between the proportion of studies that possibly used inappropriate methods: (i) to manipulate seawater carbonate chemistry; (ii) to measure two or more of pH_T, A_T, DIC, or pCO_2; and (iii) to design/analyse experimental units. This was done using a z-test to examine differences between two proportions.

Definitions of tank types

In ocean acidification experiments, different containers (referred to here as tanks) have different purposes, and for clarity we assign names to each tank type. All manipulation experiments must have at least one of these tanks types, but not all laboratory manipulation experiments will use all types, and designs could incorporate tanks that have dual purposes. They are as follows: (i) storage tank: location where seawater is stored before being altered to create CO_2 treatments. (ii) Mixing tank: location where chemicals and seawater are mixed together to create CO_2 treatments before contact with the study species. (iii) Header tank: location where seawater is stored after mixing with chemicals, but before exposure to organisms. (iv) Experimental tank: the putative experimental unit, location where organisms are housed in the treatment seawater. Note that these "tanks" may not all be traditional aquaria, but can be any type of container that stores seawater for any length of time, and that in some designs storage "tanks" could technically be the ocean or pipes leading to tanks.

Results

The use of interdependent or non-randomly interspersed treatment replicates in experimental designs (i.e. B designs) was more common (173 studies) than the use of independent, randomly interspersed replicates of treatments (i.e. A designs, 28 studies) among ocean acidification manipulation studies (Figure 2). Note that 20 B-designed studies used random or nested factors in their analysis to attempt to deal with this type of data, and those without other design problems were therefore classified as A designs. A further 17 B studies initially also used this approach and dropped the random effect when it was not significant. The most common design type was B-3 (isolative segregation—Figure 1). Most studies that used designs that were classified as B type designs did so by using one of the following methods: (i) Multiple individuals were housed within one experimental tank but each individual was treated as an experimental unit (i.e. B-3 if only one tank per treatment existed); in this case, the tank itself is the experimental unit, giving $n = 1$ in this example. Often the subsampling of individuals from one replicate container was not mentioned, but then the degrees of freedom in the statistical analysis were higher than the number of experimental units per treatment (i.e. experimental tanks), which occurred in nine studies where the design and sampling procedures could not otherwise attribute it to another type of design. (ii) Utilizing one header tank per treatment, then having the header tank periodically or continuously deliver seawater to multiple experimental tanks, with no acknowledgment by the authors that the experimental tanks are interdependent (68 studies; design B-4). Note: it was deemed appropriate if all experimental units of all treatments are supplied with seawater from one header tank at the beginning of the experiment only. (iii) All replicates of one treatment were grown in one room or water bath, while the other treatments were housed in different room or water bath (B-3). There was no difference between the proportion of studies using appropriate designs before or after 2010 (94.3% in 2010 and before, 93.7% after 2010; $z = -0.25$, $P = 0.79$).

Around half (57%) of the studies did not present sufficient details on the design type to determine the precise design, and 34% of all studies total did not provide sufficient details to determine whether it was an "A" type or "B" type design. Using the limited information that was provided in these studies, it was determined that 28% of studies were either B-3 or B-4 designs (isolative segregation or interdependent replicates), while 24% were A-1 to B-2 designs. In the remainder of cases, insufficient information was provided to narrow down the design to any definitive type. For those studies, often there was no mention of replicate numbers,

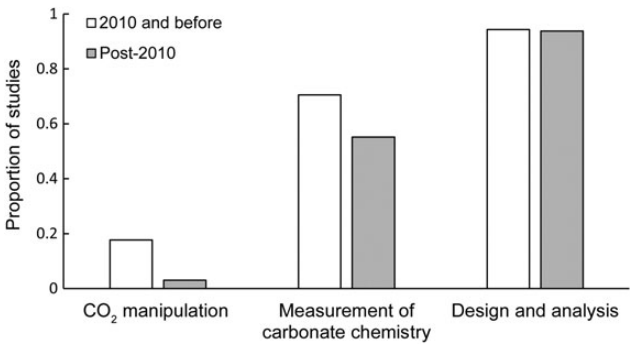

Figure 2. Proportion of studies that possibly use inappropriate methods to manipulate seawater CO_2 concentrations, to measure the carbonate chemistry of seawater, or to design their experiments/miss-assign the experimental unit during statistical analysis. See details in Introduction for descriptions/references to appropriate vs. inappropriate methods.

different tank type numbers, nor how the carbonate chemistry was modified—beyond mentioning the chemicals used—nor how seawater was introduced to the experimental organisms. In many instances the degrees of freedom were not provided, and in some cases it is impossible to derive the statistical differences that were reported by the authors when the true number of experimental units per treatment was so low (i.e. when $n \leq 2$). In other words, individuals were treated as treatment replicates rather than the experimental units being used as treatment replicates.

Among the 30% of studies (i.e. 180) where we could determine if treatment replicates were interspersed randomly or not, 36 studies employed a randomized design, whereas 130 were non-random and 13 employed no replication of treatments. We could not determine whether replicates of all treatments were randomly interspersed in 280 studies; this represented the sole problem in 13% of all studies examined.

Across all studies the number of true experimental units that were used per treatment was extremely low (mean = 2.00, s.e. = 0.12). A disparity between the numbers of actual and stated experimental units per treatment was often caused by studies in which individual organisms within the same tank were treated as independent replicates of that treatment, or where one room was used per treatment.

The proportion of studies that used recommended methods to simulate the carbonate chemistry of a future ocean (91%) was higher than the number of studies that used inappropriate methods (9%). The use of recommended chemical manipulations increased significantly over time, with a sharp increase after 2010 (97% correct after 2010, 78% in 2010 and earlier; Figure 2; $z = 6.5$, $P < 0.01$). The measurement of at least two of pH_T, A_T, DIC, or pCO_2 occurred in 39% of all studies, and there was an increase in this proportion after 2010 (29% pre-2010, 45% post-2010: Figure 2; $z = 3.27$, $P < 0.01$).

Discussion

This analysis identified that the most laboratory manipulation experiments in ocean acidification research used either an inappropriate experimental design and/or data analysis, or did not report these details effectively. Many studies did not report important methods, such as how treatments were created and the number of replicates of each treatment. The tendency for the use of inappropriate experimental design also undermines our confidence in accurately predicting the effects of ocean acidification on the biological responses of marine organisms. There are two contrasting philosophies of interpreting the validity of results with inappropriate design and analysis problems. These are that (i) any research adds to the body of literature, increasing our ability to predict the future effects of ocean acidification. (ii) No value can be taken from such studies, as potential artefacts could alter results, and there is no way of ruling such artefacts out often. As per Hulbert's statement in the seminal paper (1984), "despite errors of design or statics" these papers "nevertheless contain useful information". However, in cases where there is no way to distinguish the effects of potential experimental artefacts or gradients in other factors from the effects of the prescribed treatments (i.e. treatments are completely confounded with time, space, or another factor: i.e. one experimental unit per treatment) then caution should be applied in making conclusions from results. For studies where treatments are not completely confounded (i.e. there is more than one true experimental unit per treatment), but inappropriate analysis has occurred, any statistical significance of the results that are displayed (or estimates of effects sizes or something similar) could still overestimate the true effect size or level of significance. For some studies, re-analysis of the data using the correct statistical framework would facilitate a more accurate assessment of the exact magnitude of biological responses to ocean acidification. However, in some cases, there is no way to distinguish the effects of potential experimental artefacts, gradients in other factors, nor variation in time and space, from the effects of the prescribed treatments. Re-analysis of some of the current literature, potentially using the existing database on ocean acidification research (Nisumaa *et al.*, 2010), would greatly aid in assessing the real biological responses of ocean acidification on marine life and the extent to which ocean acidification research could be biased by non-significant trends.

Confusion regarding what constitutes an experimental unit is evident in ocean acidification research. This is demonstrated by a large proportion of studies that either treated the responses of individuals (i.e. the evaluation unit defined by Hurlbert and White, 1993; Hurlbert, 2009 in terms of statistical analysis) to treatments as experimental units, when multiple individuals were in each tank, or used tank designs where all experimental tanks of one treatment are more interconnected to each other than experimental tanks of other treatments (181 studies total). We consider that this information has not been adequately presented in the context of ocean acidification research previously, which lies at the core of the problem. Therefore, a series of potential solutions is presented to the problems highlighted above for ocean acidification research in the following section.

Advice for performing manipulation experiments: before the ocean acidification manipulation system is designed

In experimental systems that are designed to test the effects of ocean acidification on biological responses of any organism (from bacteria to fish), a number of independent experimental units are needed. It is best practice to have as many independent experimental units as possible to safeguard against confusing non-treatment effects with treatment effects. Not every experimental tank used needs its own storage, mixing, and header tank, as on average all experimental units in one treatment must be equally exposed to the same conditions as all experimental units in another treatment, barring the actual treatment under examination (Hurlbert, 2013a). However, not every experimental tank needs to be completely independent from each other, i.e. every tank does not need an independent source of seawater running from the sea through to individual storage tanks, then to individual mixing tanks, then to individual header tanks, then to the experimental tank. That is why it is equally valid to (i) mix the seawater of each individual experimental unit in one mixing tank per unit (Figure 3a and b), (ii) manipulate the seawater of all experimental units of multiple treatments in one mixing tank (Figure 3c and d), or (iii) mix the seawater for every treatment in multiple mixing tanks (Figure 3e) (i.e. in a randomized block design) as long as this can be taken into account during the statistical analysis (Hurlbert, 1984). The last example (Figure 3e) is a block design whereby an equal number of experimental units from each treatment (but not all experimental units within the experiment) would have their conditions manipulated in the same mixing tank, ensuring no interdependence replicates of the same treatment between blocks (Figures 1 and 3e). The same principals apply to seawater stored for each treatment, where it is equally valid to use individual storage tanks for each experimental unit (Figure 3b), to store seawater for every experimental unit in one storage tank (Figure 3c and d), or equal numbers of experimental units of every treatment in a block design (Figure 3e). However, it

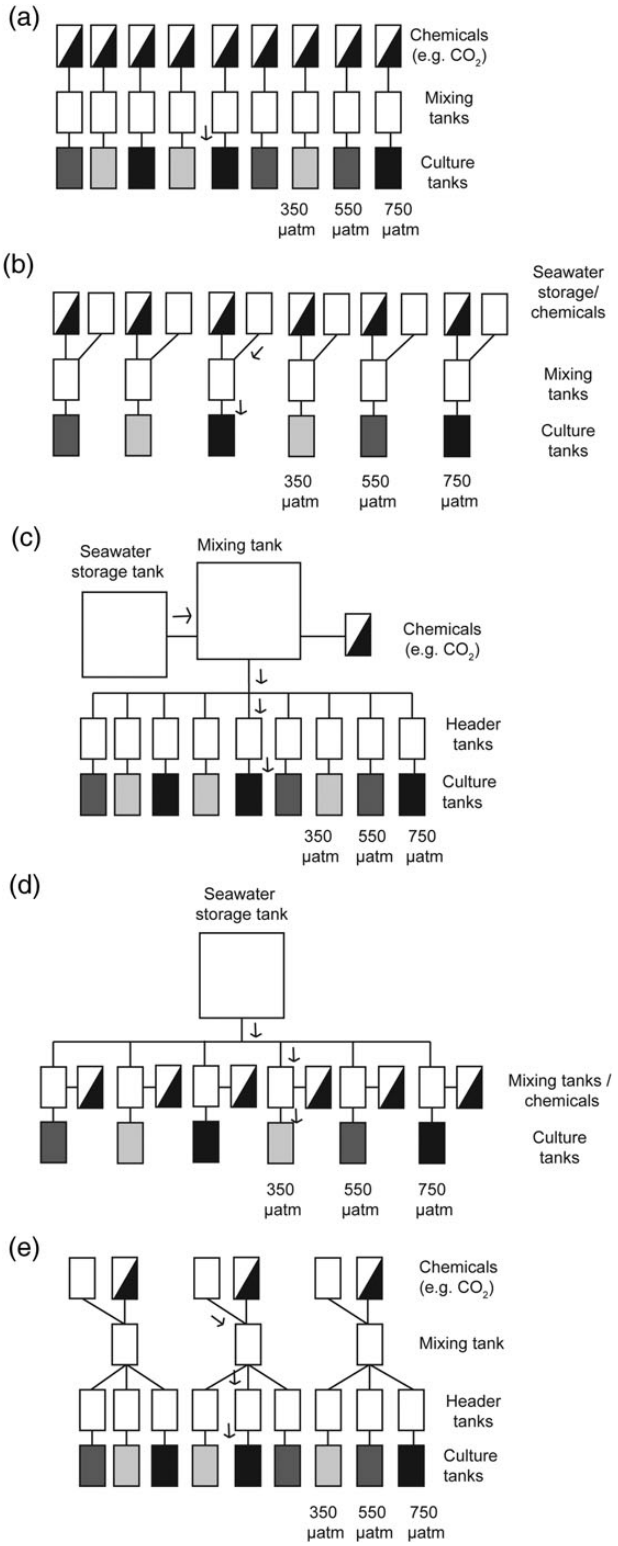

Figure 3. Five tank array types that could be used in ocean acidification research to create treatments with independent experimental units. White tanks indicate space where seawater could be stored other than in experimental tanks. Different coloured experimental tanks correspond to different CO_2 treatments. Half black and white boxes indicate sources of chemicals. See the text for a discussion.

is not valid to mix the seawater of all of one treatment's experimental units in one mixing tank and all of another treatment's experimental units in another mixing tank, and nor is it valid to segregate seawater of all of one treatment from another in one tank during the mixing or storage procedure (i.e. Figure 1, B-4).

The simplest way to manipulate seawater carbonate chemistry to create experimental units that are as independent from each other as they are from other treatment replicated involves at least two different systems of tanks. Several possible methods exist (Figure 3). For each example, a published CO_2-manipulation/housing system that can easily be replicated is referred to. Each of these designs either already fulfil these criteria or are so close to that they could be easily modified to do so by adding one tank or randomly interspersing tanks. The simplest method is to have one mixing tank for each experimental unit/experimental tank (i.e. multiple mixing tanks), so that chemicals are added at the beginning of the experiment from a mixing tank (Figure 3a). Alternatively, this mixing tank can be removed and chemicals added directly to the seawater before cultured organisms are added, or pre-mixed CO_2 at the appropriate level could be added in a way that does not interfere with the study organism. This design is appropriate for experiments that are short term in nature, wherein the organisms do not biologically modify seawater carbonate chemistry significantly over the duration of the experiment (e.g. as in Byrne *et al.*, 2009), or where their biological modification does not affect the study's hypotheses (Schulz *et al.*, 2013).

The second simplest method is to add one storage or header tank per experimental tank to the design (Figure 3b). This is appropriate for longer experiments that could incorporate flow-through seawater and controlled CO_2 conditions (e.g. Munday *et al.*, 2009; Russell *et al.*, 2009). Three more complex methods involve more complicated designs. A third method is to manipulate a source of seawater in one mixing tank for all the experimental units of all treatments (i.e. one mixing tank total) then, after manipulation, the seawater is transferred into separate experimental tanks for each experimental unit, or it is transferred into one header tank then subsequently down into the culture tank in a three-tiered system (Figure 3c). In this example, mixing takes place for one experimental unit at a time, not all of one treatment at a time, and it is important that the mixing order of treatments is randomly interspersed. This is appropriate for an experimental system that delivers seawater semi-continuously using an automated computer-controlled set-up to deliver seawater to the header tanks after measurement and modification (McGraw *et al.*, 2010; Cornwall *et al.*, 2013), such as when a spectrophotometer is used to measure pH and control pH, limiting the number of measurement devices. Another example is if seawater is manually mixed in one tank for all treatments (i.e. one tank total) then transferred into header or experimental tanks. Another modification of this practice is if seawater entering the CO_2-manipulation system is not chemically appropriate for use as controls (i.e. pH is too low or high) and chemicals need to be added before then going to another storage or mixing tank. The fourth design is similar to Figure 3c, where only one storage tank is used, but each culture tank has its own mixing tank (Figure 3d). This design could be used where CO_2 gas is programmed to flow-through the mixing tank at a set rate, or continuously using pre-mixed gases (Findlay *et al.*, 2008; Fangue *et al.*, 2010). The last and most complex design is a block design where one mixing tank manipulates the seawater for one experimental unit for all treatments, although data collected

using this approach needs to incorporate a blocking factor in the analysis (Figure 3e). This fifth design is appropriate if faster flow rates of seawater are used than the design of Figure 3c could permit, for example if multiple spectrophotometers are used in conjunction with a computer-controlled system to measure and control incoming seawater pH. In all these examples, the experimental tank may contain multiple individuals, and analyses can be done using either a simple ANOVA applied to tank means or with a nested ANOVA applied to values for the responses of individual organisms. The decision to include multiple or single individuals in one tank depends on the hypotheses of the study, logistic constraints, and ecological realism.

In addition to independent replication, there must also be a large enough number of experimental units for sufficient statistical power to accurately detect differences of interest between treatments, and these replicate experimental units must be randomly interspersed when appropriate. The magnitude of the biological response to OA treatments will be species-specific, and within a species the measured response metrics (e.g. growth, photosynthesis, respiration, or calcification rates) will vary among individuals, independent of any measurement error. It is beyond the scope of this review to recommend the use of statistics that employ hypothesis testing vs. other types of statistical approaches (for an excellent discussion, see Ellison *et al.*, 2014) nor to recommend the exact number of experimental units needed for every study; but regardless, the number of experimental units used per treatment should be >2.5, which was the mean in 2014.

Randomization is relatively simple to achieve, given that treatments must all equally on average experience the same conditions other than the treatment ascribed to them, and there are three choices according to Hurlbert (1984): completely randomized (A-1), randomized block (A-2), and systematic (A-3; which is not technically random but still pragmatically achieves an acceptable design). Regression style designs examining biological responses to large numbers of CO_2 treatments could reduce the need for a larger number of experimental units per treatment relative to traditional factorial analysis. Regression style analyses still, however, require a enough experimental units per treatment so that the variation due to differences among individual experimental units is lower than that required to observe any effects of CO_2 treatments. Regression designs also require randomization of treatments. To have spatial or temporal segregation will confound the effects of treatment and location/time. To use an extreme example for the sake of clarity, consider an experiment in which the experimental tanks are placed on a bench, with CO_2 treatments placed from left to right: 200, 400, 600, 800, 1000 ppm pCO_2. In this example, it is impossible to use statistics to differentiate the effects of bench location from the effects of CO_2 treatment. To correctly replicate in this experiment, the experimental tanks would be placed in a random order on the bench.

After the CO_2-manipulation system is designed as B-1 to B-4

In an experimental system where tanks from one treatment are either spatially segregated or are more interdependent with each other than with replicates of other treatments, the easiest way to control for artefacts is to repeat the experiment many times. Thereafter, the effect of tank identity can be incorporated as a random factor. This approach is difficult if there is only one experimental or header tank per treatment, as the effects of time will be difficult to separate from the effects of tank unless a large number of experimental runs are conducted. In some instances, these problems can be overcome during statistical analysis if the treatments are not completely confounded, i.e. if there are multiple header tanks per treatment and not just one, as was the case in 20 studies examined. Also, multiple experimental tanks per header tank could be employed if there are three or more independent header tanks per treatment, but only as long as header tank is treated as the experimental unit. Likewise, multiple individuals could be housed in the same experimental tank using the same principles, where tank is still treated as the experimental unit. This could be a desirable design where variation in individual responses to a treatment is known to be high, but logistical restraints prevent the use of more tanks.

After the experiment is conducted

An experimental culture system can be designed correctly but still result in an inappropriate manipulation experiment when: (i) measurements are interdependent through time (i.e. multiple measurements on one experimental unit over time are treated as independent measurements) and (ii) multiple measurements are made on the same experimental unit and are treated as independent measurements at the same time point. Similarly, treating the responses of multiple individuals within one experimental unit as multiple experimental units is inappropriate (classed as sacrificial pseudoreplication by Hurlbert, 1984; Hurlbert and White, 1993).

Conversely, an inappropriate design can be employed, but variation from non-treatment effects can be controlled for somewhat by treating these as random factors in the statistical analysis, not treating all experimental units at different time points as independent experimental units (classed as temporal pseudoreplication by Hurlbert, 1984; Hurlbert and White, 1993). Running an analysis that determines whether there is an effect of time or space (such as tank identity) on responses then removing this factor from the analysis if there is no effect is also inappropriate according to Hurlbert (1984), i.e. sacrificial pseudoreplication (Hurlbert, 1984; Hurlbert and White, 1993). For time or tank identity, we recommend that they could be incorporated in the analysis as a random factor, not a fixed factor, to incorporate some source of variance from tank identity or time, rather than to increase the degrees of freedom. Another approach is to determine what the mean change in a measured parameter is over time, and treat that mean as the experimental unit, or to take the mean of the evaluation unit's response over all repeated measures. Alternatively, repeated measures within one experimental unit can be removed by randomly removing data points until only one measurement per experimental unit remains.

During the review process

Fifty-seven per cent of studies examined did not report in the methods sufficient detail to assess the experimental design used. Details, such as the layout and numbers of tanks, are very important in allowing scientists to compare results of different studies and Table 1 provides a checklist of essential details that need to be reported in published ocean acidification studies with respect to replication and randomization. It is useful for publications to include a diagram of the experimental set-up, at least the first time an experimental facility is described (e.g. see Figure 1 in Asnaghi *et al.*, 2013).

Some studies did not report degrees of freedom adequately. If the degrees of freedom reported are larger than the total number of experimental units, then samples have been pooled in an inappropriate way. This could lead to reduced *P*-values (Hurlbert, 2013b). This could result in inaccurate findings, and because published experiments are rarely repeated, such spurious or inaccurate results and the conclusions drawn might direct future research

Table 1. A checklist of replication details that need to be included in published research investigating the effects of ocean acidification in a laboratory setting.

Can the following details be clearly determined from the manuscript?
The number of independent experimental units used
The randomization of treatments in space and time (when appropriate)
The configuration of mixing, header, and experimental tanks (when appropriate)
The model construction of the statistical analysis
The degrees of freedom in the statistical analysis
Location where the seawater was manipulated
Location where the measurements of seawater chemistry were taken
Chemicals used to manipulate seawater CO_2 concentrations
The measurement techniques used to characterize seawater carbonate chemistry ($\geq$2 of pH_T, A_T, DIC, and pCO_2; plus temperature and salinity)

erroneously. An accumulation of spurious results may counteract the ability to accurately predict the effects of ocean acidification or to detect any true trends in its potential impacts.

When assessing whether a study has used appropriate methods, it would be pragmatic to determine what was the likelihood that non-treatment effects could confound treatment effects, rather than grouping studies into "pseudoreplicated" vs. "non-pseudoreplicated" categories. Also, studies employing inappropriate statistical and design frameworks may still have important messages to convey. If inappropriate methods were inadvertently used, such that replicates of a treatment are not independent, then data can be reanalysed as described above. However, if this is not possible (i.e. if the resulting degrees of freedom are too small) then no discussion of differences should be made, and only trends can be described with strong caveats mentioned. It is equally important that studies are not miss-categorized by reviewers as using inappropriate methods; by applying the principles discussed here, and in the papers referenced herein, this could be easier for reviewers to achieve.

Conclusions

This study highlights the need for increased attention to the design, performance, analysis, and reporting of experimental procedures used during ocean acidification manipulation experiments. It is encouraging that most studies follow the "Guide to Best Practices for Ocean Acidification Research and Data Reporting (Gattuso *et al.*, 2010)" for manipulating seawater carbonate chemistry, and that this is also improving for measurements of seawater carbonate chemistry; we recommend the same rigour in the use of experimental units in experimental design is followed to avoid artefacts related to inappropriate replication and randomization. Ocean acidification is a relatively new research field, and if stricter guidelines are followed in future research, then greater inferences can be taken from studies, enhancing our ability to accurately predict how changes in ocean carbonate chemistry will affect species and ecosystems in the future. This paper deals specifically with designing manipulation experiments that minimize the effects of chance events or pre-existing gradients in other factors. However, other methodological considerations also need to be taken into account in ocean acidification research to improve the information that can be taken from such studies. Future research would also be improved if the duration of experiments increased, or if they incorporated gradual increases in CO_2 rather than rapid exposure (Kamenos *et al.*, 2013; Munday *et al.*, 2013; Munguia and Alenius, 2013; Gaylord *et al.*, 2015). Future studies should also focus on improving the environmental realism employed in laboratory experiments, for example by attempting to simulate environmentally realistic water motion, and diel cycles in light and pH (when appropriate). Ideally, this added realism would not be sacrificed in an attempt to increase the numbers of experimental units, which further highlights the complexities faced by future ocean acidification research.

A large number of studies have found that ocean acidification will likely negatively impact the calcification or growth of calcifying invertebrates, coccolithophores, calcifying macroalgae, and corals (Riebesell *et al.*, 2000; Gazeau *et al.*, 2007; Anthony *et al.*, 2008; Wood *et al.*, 2008; Byrne *et al.*, 2010), and influence the behavioural traits of invertebrates and fish (Munday *et al.*, 2009; Appelhans *et al.*, 2012; Nilsson *et al.*, 2012). Subsequent shifts in ecosystem structure and function are likely to occur due to the direct biological effects on many ecologically important species (Hall-Spencer *et al.*, 2008; Fabricius *et al.*, 2011; Kroeker *et al.*, 2013a). Yet, meta-analyses and reviews of published studies reveal that the effects of ocean acidification are variable, sometimes contrary to the expected outcome, and that they are species and context dependent, interacting with changes in other environmental stressors in both synergistic and additive ways (Fabry *et al.*, 2008; Pörtner, 2008; Hofmann *et al.*, 2010; Kroeker *et al.*, 2013b). Predicting accurate effects of ocean acidification on marine organisms will need new meta-analyses that can accurately re-analyse published results. Examining the extent to which the inappropriate assignment of experimental units has influenced our current knowledge base, and other potential sources of biases (such as the use of HCl without DIC additions), will involve meta-analyses that incorporate the true variance in responses of species to ocean acidification from all previously published studies. Completing that task then maintaining standards in the publication of ocean acidification research will enable stronger and more accurate predictions regarding the state of our future marine ecosystems. Without the maintenance of standards in ocean acidification research, there is a risk of collecting an ever increasing number of uninterpretable results (Moran, 2014) and misinterpreting likely future outcomes. However, caution must be applied when classifying research as having used inappropriate methods when details are incomplete (as in 34% of studies here), as they could be equally as sound as those with complete methods (Munday *et al.*, 2014). We strongly recommend that future research report sufficient details so that their methods are clear and repeatable. Our ability to more accurately predict the magnitude and context of the effects of ocean acidification rely on continuing to improve best practices in both experimental design, and the measurement and manipulation of seawater carbonate chemistry.

Supplementary material

Supplementary Material is available at *ICESJMS* online.

Acknowledgments

We acknowledge J.-P. Gattuso, S. Hurlbert, D. Moran, B. Russell, M. Wahl, and one anonymous reviewer for feedback on this manuscript, and C.D. Hepburn and C.M. McGraw for discussions over the years on associated topics.

References

Anthony, K. R. N., Kline, D. I., Diaz-Pulido, G., Dove, S., and Hoegh-Guldberg, O. 2008. Ocean acidification causes bleaching and productivity loss in coral reef builders. Proceedings of the National Academy of Sciences, 105: 17442–17446.

Appelhans, Y. S., Thomsen, J., Pansch, C., Melzner, F., and Wahl, M. 2012. Sour times: seawater acidification effects on growth, feeding behaviour and acid-base status of *Asterias rubens* and *Carcinus maenas*. Marine Ecology Progress Series, 459: 85–97.

Asnaghi, V., Chiantore, M., Mangialajo, L., Gazeau, F., Francour, P., Alliouane, S., and Gattuso, J. P. 2013. Cascading effects of ocean acidification in a rocky subtidal community. PLoS ONE, 8: e61978.

Barry, J. P., Hall-Spencer, J. M., and Tyrrell, T. 2010. In situ perturbation experiments: natural venting sites, spatial/temporal gradients in ocean pH, manipulative in situ $p(CO_2)$ perturbations. *In* Guide to Best Practices for Ocean Acidification Research and Data Reporting. Ed. by U. Riebesell, V. J. Fabry, L. Hansson, and J. P. Gattuso. Publications Office of the European Union, Luxembourg.

Boyd, P. W. 2011. Beyond ocean acidification. Nature Geoscience, 4: 273–274.

Byrne, M., Ho, M., Selvakumaraswamy, P., Nguyen, H. D., Dworjanyn, S. A., and Davis, A. R. 2009. Temperature, but not pH, compromises sea urchin fertilization and early development under near-future climate change scenarios. Proceedings of the Royal Society B: Biological Sciences, 276: 1883–1888.

Byrne, M., Ho, M., Wong, E., Soars, N. A., Selvakumaraswamy, P., Shepard-Brennand, H., Dworjanyn, S. A., *et al.* 2010. Unshelled abalone and corrupted urchins: development of marine calcifiers in a changing ocean. Proceedings of the Royal Society B: Biological Sciences, 276: 1883–1888.

Ciais, P., Sabine, C. L., Bala, G., Bopp, L., Brovkin, V., Canadell, J., Chhabra, A., *et al.* 2013. Carbon and other biogeochemical cycles. *In* Climate Change 2013: the Physical Science Basis. Contribution of Working Group I to the Fifth Assessment Report of the Intergovernmental Panel on Climate Change. Ed. by T. F. Stocker, D. Qin, G-K. Plattner, M. Tignor, S. K. Allen, J. Boschung, A. Nauels, Y. Xia, V. Bex, and P. M. Midgley. Cambridge University Press, Cambridge, UK and New York, NY, USA.

Cornwall, C. E., Hepburn, C. D., McGraw, C. M., Currie, K. I., Pilditch, C. A., Hunter, K. A., Boyd, P. W., *et al.* 2013. Diurnal fluctuations in seawater pH influence the response of a calcifying macroalga to ocean acidification. Proceedings of the Royal Society B: Biological Sciences, 280: doi:10.1098/rspb.2013.2201.

Cox, D. R. 1958. Planning of Experiments. Academic Press, New York, NY.

Dickson, A. G. 2010. The carbon dioxide system in seawater: equilibrium chemistry and measurements. *In* Guide to Best Practises for Ocean Acidification Research and Data Reporting. Ed. by U. Riebesell, V. J. Fabry, L. Hansson, and J. P. Gattuso. Publications Office of the European Union, Luxembourg.

Dickson, A. G., Sabine, C. L., and Christian, J. R. 2007. Guide to best practices for Ocean CO_2 measurements, North Pacific Marine Science Organization.

Ellison, A. M., Gotelli, N. J., Inouye, B. D., and Strong, D. R. 2014. *P* values, hypothesis testing, and model selection: it's déjà vu all over again. Ecology, 95: 609–610.

Fabricius, K., Langdon, C., Uthicke, S., Humphrey, C., Noonan, S., De'ath, G., Okazaki, R., *et al.* 2011. Losers and winners in coral reefs acclimatized to elevated carbon dioxide concentrations. Nature Climate Change, 1: 165–169.

Fabry, V. J., Seibel, B. A., Feely, R. A., and Orr, J. C. 2008. Impacts of ocean acidification on marine fauna and ecosystem processes. ICES Journal of Marine Science, 65: 414–432.

Fangue, N. A., O'Donnell, M. J., Sewell, M. A., Matson, P. G., MacPherson, A. C., and Hofmann, G. E. 2010. A laboratory-based, experimental system for the study of ocean acidification effects on marine invertebrate larvae. Limnology and Oceanography: Methods, 8: 441–452.

Feely, R. A., Sabine, C. L., Lee, K., Berelson, W., Kleypas, J. A., Fabry, V. J., and Millero, F. J. 2004. Impact of anthropogenic CO_2 on the $CaCO_3$ system in the oceans. Science, 305: 362–366.

Findlay, H. S., Kendall, K. A., Spicer, J. I., Turley, C., and Widdicombe, S. 2008. Novel microcosm system for investigating the effects of elevated carbon dioxide and temperature on intertidal organisms. Aquatic Biology, 3: 51–62.

Gattuso, J. P., Gao, K., Lee, K., Rost, B., and Schulz, K. G. 2010. Approaches and tools to manipulate the carbonate chemistry. *In* Guide to best practices for ocean acidification research and data reporting, pp. 41–51. Ed. by U. Riebesell, V. J. Fabry, L. Hansson, and J. P. Gattuso. Publications Office of the European Union, Luxembourg.

Gattuso, J -P., Kirkwood, W., Barry, J. P., Cox, E., Gazeau, F., Hansson, L., Hendriks, I., *et al.* 2014. Free-ocean CO_2 enrichment (FOCE) systems: present status and future developments. Biogeosciences, 11: 4057–4075.

Gattuso, J. P., Mach, K. J., and Morgan, G. 2012. Ocean acidification and its impacts: an expert survey. Climate Change, 117: 725–738.

Gaylord, B., Kroeker, K. J., Sunday, J. M., Anderson, K. M., Barry, J. P., Brown, N. E., Connell, S. D., *et al.* 2015. Ocean acidification through the lens of ecological theory. Ecology, 96: 3–15.

Gazeau, F., Quiblier, C., Jansen, J. M., Gattuso, J. P., Middelburg, J. J., and Heip, C. H. R. 2007. Impact of elevated CO_2 on shellfish calcification. Geophysical Research Letters, 34: doi: 10.1029/2006GL028554.

Hall-Spencer, J. M., Rodolfo-Metalpa, R., Martin, S., Ransome, E., Fine, M., Turner, S. M., Rowley, S. J., *et al.* 2008. Volcanic carbon dioxide vents show ecosystem effects of ocean acidification. Nature, 454: 96–99.

Havenhand, J., Dupont, S., and Quinn, G. P. 2010. Designing ocean acidification experiments to maximise inference. *In* Guide to best practices for ocean acidification research and data reporting, p. 260. Ed. by U. Riebesell, V. J. Fabry, L. Hansson, and J-P. Gattuso. Publications Office of the European Union, Luxembourg.

Hofmann, G. E., Barry, J. P., Edmunds, P. J., Gates, R. D., Hutchins, D. A., Klinger, T., and Sewell, M. A. 2010. The effect of ocean acidification on calcifying organisms in marine ecosystems: an organism-to-ecosystem perspective. Annual Reviews in Ecology, Evolution, and Systematics, 41: 127–147.

Hurd, C. L., Hepburn, C. D., Currie, K. I., Raven, J. A., and Hunter, K. A. 2009. Testing methods of ocean acidification on algal metabolism: consideration for experimental designs. Journal of Phycology, 45: 1236–1251.

Hurlbert, S. H. 1984. Pseudoreplication and the design of ecological field experiments. Ecological Monographs, 54: 187–211.

Hurlbert, S. H. 2009. The ancient black art and transdisciplinary extent of pseudoreplication. Journal of Comparative Psychology, 123: 434–443.

Hurlbert, S. H. 2013a. Affirmation of the classical terminology for experimental design via a critque of Casella's *Statistical Design*. Agronomony Journal, 105: 412–418.

Hurlbert, S. H. 2013b. Pseudofactorialism, response structures and collective responsibility. Austral Ecology, 38: 646–663.

Hurlbert, S. H., and White, M. D. 1993. Experiments with freshwater invertebrate zooplanktivores: quality of statistical analyses. Bulletin of Marine Science, 53: 128–153.

Kamenos, N. A., Burdett, H. L., Aloisio, E., Findlay, H. S., Martin, S., Longbone, C., Dunn, J., *et al.* 2013. Coralline algal structure is more sensitive to rate, rather than the magnitude, of ocean acidification. Global Change Biology, 19: 3621–3628.

Kozlov, M., and Hurlbert, S. H. 2006. Pseudoreplication, chatter, and the international nature of science. Journal of Fundamental Biology, 67: 128–135.

Kroeker, K. J., Gambi, M. C., and Micheli, F. 2013a. Community dynamics and ecosystem simplification in a high-CO_2 ocean. Proceedings of the National Academy of Sciences, 110: 12721–12726.

Kroeker, K. J., Kordas, R. L., Crim, R. N., Hendriks, I. E., Ramajo, L., Singh, G. G., Duarte, C. M., *et al.* 2013b. Impacts of ocean

acidification on marine organisms: quantifying sensitivities and interaction with warming. Global Change Biology, 19: 1884–1896.

McGraw, C. M., Cornwall, C. E., Reid, M. R., Currie, K. I., Hepburn, C. D., Boyd, P., Hurd, C. L., *et al.* 2010. An automated pH-controlled culture system for laboratory-based ocean acidification experiments. Limnology and Oceanography: Methods, 8: 686–694.

Mead, R. 1988. The Design of Experiments, Cambridge University Press, Cambridge. 620 pp.

Moran, D. 2014. The importance of accurate CO_2 dosing and measurement in ocean acidification studies. Journal of Experimental Biology, 217: 1827–1829.

Munday, P. L., Dixson, D. L., Donelson, J. M., Jones, G. P., Pratchett, M. S., Devitsina, G. V., and Døving, K. B. 2009. Ocean acidification impairs olfactory discrimination and homing ability of a marine fish. Proceedings of the National Academy of Sciences, 106: 1848–1852.

Munday, P. L., Warner, R. R., Monro, K., Pandolfi, J. M., and Marshall, D. J. 2013. Predicting evolutionary responses to climate change in the sea. Ecology Letters, 16: 1488–1500.

Munday, P. L., Watson, S -A., Chung, W -S., Marshall, N. J., and Nilsson, G. E. 2014. Response to 'The importance of accurate CO_2 dosing and measurement in ocean acidification studies'. Journal of Experimental Biology, 217: 1827–1829.

Munguia, P., and Alenius, B. 2013. The role of preconditoning in ocean acidification experiments: a test with the intertidal isopod *Paradella dianae*. Marine and Freshwater Behaviour and Physiology, 46: 33–44.

Nilsson, G. E., Dixson, D. L., Domenici, P., McCormick, M. I., Sørensen, C., Watson, S. A., and Munday, P. L. 2012. Near-future carbon dioxide levels alter fish behaviour by interfering with neurotransmitter function. Nature Climate Change, 2: 201–204.

Nisumaa, A -M., Gattuso, J -P., Bellerby, R. G. J., Delille, B., Geider, R. J., Middelburg, J. J., Orr, J. C., *et al.* 2010. EPOCA/EUR-OCEANS data compilation on the biological and biogeochemical responses to ocean acidification. Earth Systems Science Data, 2: 167–175.

Pörtner, H. O. 2008. Ecosystem effects of ocean acidification in times of ocean warming: a physiologist's view. Marine Ecology Progress Series, 373: 203–217.

Riebesell, U., and Gattuso, J -P. 2015. Lessons learned from ocean acidification research. Nature Climate Change, 5: 12–14.

Riebesell, U., Fabry, V. J., Hansson, L., and Gattuso, J. P. 2010a. Guide to Best Practices for Ocean Acidification Research and Data Reporting. Publications Office of the European Union, Luxembourg. 260 pp.

Riebesell, U., Lee, K., and Nejstgaard, J. C. 2010b. Pelagic mesocosms. *In* Guide to Best Practises for Ocean Acidification Research and Data Reporting, pp. 95–112. Ed. by U. Riebesell, V. J. Fabry, L. Hansson, and J. P. Gattuso. Publications Office of the European Union, Luxembourg.

Riebesell, U., Zondervan, I., Rost, B., Tortell, P. D., Zeebe, R. E., and Morel, F. M. M. 2000. Reduced calcification of marine phytoplakton in response to increased atmospheric CO_2. Nature, 407: 364–367.

Rost, B., Zondervan, I., and Wolf-Gladrow, D. 2008. Sensitivity of phytoplankton to future changes in ocean carbonate chemistry: current knowledge, contradictions and research directions. Marine Ecology Progress Series, 373: 227–237.

Russell, B. D., Thompson, J. I., Falkenberg, L. J., and Connell, S. D. 2009. Synergistic effects of climate change and local stressors: CO_2 and nutrient-driven change in subtidal rocky habitats. Global Change Biology, 15: 2153–2162.

Schulz, K. G., Bellerby, R. G. J., Brussaard, C. P. D., Büdenbender, J., Czerny, J., Engel, A., Fischer, M., *et al.* 2013. Temporal biomass dynamics of an Arctic plankton bloom in response to increasing levels of atmospheric carbon dioxide. Biogeosciences, 10: 161–180.

Wernberg, T., Smale, D. A., and Thomsen, M. S. 2012. A decade of climate change experiments on marine organisms: procedures, patterns and problems. Global Change Biology, 18: 1491–1498.

Wood, H. L., Spicer, J. I., and Widdicombe, S. 2008. Ocean acidification may increase calcification rates, but at a cost. Proceedings of the Royal Society B: Biological Sciences, 275: 1767–1773.

Handling editor: Howard Browman

ICES Journal of Marine Science

ICES Journal of Marine Science (2016), 73(3), 582–595. doi:10.1093/icesjms/fsu231

Contribution to Special Issue: 'Towards a Broader Perspective on Ocean Acidification Research'

Original Article

Interpretation and design of ocean acidification experiments in upwelling systems in the context of carbonate chemistry co-variation with temperature and oxygen

Jonathan C. P. Reum[1*‡], Simone R. Alin[2], Chris J. Harvey[1], Nina Bednaršek[2], Wiley Evans[2,3], Richard A. Feely[2], Burke Hales[4], Noelle Lucey[5], Jeremy T. Mathis[2,3], Paul McElhany[1], Jan Newton[6], and Christopher L. Sabine[2]

[1]*Conservation Biology Division, Northwest Fisheries Science Center, National Marine Fisheries Service, National Oceanic and Atmospheric Administration, 2725 Montlake Blvd. E, Seattle, WA 98112, USA*
[2]*Pacific Marine Environmental Laboratory, National Oceanic and Atmospheric Administration, 7600 Sand Point Way NE, Seattle, WA 98115, USA*
[3]*Ocean Acidification Research Center, School of Fisheries and Ocean Sciences, University of Alaska Fairbanks, 245 O'Neill Bldg, Fairbanks, AK 99775, USA*
[4]*College of Earth, Ocean and Atmospheric Sciences, Oregon State University, Corvallis, OR 97331, USA*
[5]*Marine Environment and Sustainable Development Unit ENEA, PO Box 224, La Spezia, Italy*
[6]*Applied Physics Laboratory, University of Washington, Box 355640, Seattle, WA 98105, USA*

**Corresponding author: tel: +1 206 860 3204; fax: +1 206 860 3217; e-mail: jonathan.reum@noaa.gov*
[‡]*Present address: Washington Sea Grant, University of Washington, Box 355640, Seattle, WA, USA*

Reum, J. C. P., Alin, S. R., Harvey, C. J., Bednaršek, N., Evans, W., Feely, R. A., Hales, B., Lucey, N., Mathis, J. T., McElhany, P., Newton, J., and Sabine, C. L. Interpretation and design of ocean acidification experiments in upwelling systems in the context of carbonate chemistry co-variation with temperature and oxygen. – ICES Journal of Marine Science, 73: 582 – 595.

Received 22 July 2014; revised 24 November 2014; accepted 26 November 2014; advance access publication 7 January 2015.

Coastal upwelling regimes are some of the most productive ecosystems in the ocean but are also among the most vulnerable to ocean acidification (OA) due to naturally high background concentrations of CO_2. Yet our ability to predict how these ecosystems will respond to additional CO_2 resulting from anthropogenic emissions is poor. To help address this uncertainty, researchers perform manipulative experiments where biological responses are evaluated across different CO_2 partial pressure (pCO_2) levels. In upwelling systems, however, contemporary carbonate chemistry variability remains only partly characterized and patterns of co-variation with other biologically important variables such as temperature and oxygen are just beginning to be explored in the context of OA experimental design. If co-variation among variables is prevalent, researchers risk performing OA experiments with control conditions that are not experienced by the focal species, potentially diminishing the ecological relevance of the experiment. Here, we synthesized a large carbonate chemistry dataset that consists of carbonate chemistry, temperature, and oxygen measurements from multiple moorings and ship-based sampling campaigns from the California Current Ecosystem (CCE), and includes fjord and tidal estuaries and open coastal waters. We evaluated patterns of pCO_2 variability and highlight important co-variation between pCO_2, temperature, and oxygen. We subsequently compared environmental pCO_2 – temperature measurements with conditions maintained in OA experiments that used organisms from the CCE. By drawing such comparisons, researchers can gain insight into the ecological relevance of previously published OA experiments, but also identify species or life history stages that may already be influenced by contemporary carbonate chemistry conditions. We illustrate the implications co-variation among environmental variables can have for the interpretation of OA experimental results and suggest an approach for designing experiments with pCO_2 levels that better reflect OA hypotheses while simultaneously recognizing natural co-variation with other biologically relevant variables.

Keywords: California Current, climate change, hypoxia, multistressor experiment, pH.

Introduction

Coastal upwelling systems located along the eastern boundary of ocean basins are some of the most productive ecosystems in the ocean but are also among the most vulnerable to OA (Feely *et al.*, 2008; Gruber *et al.*, 2012). The net transport of deep, nutrient-rich waters to the sunlit surface by upwelling-favourable winds promotes high rates of primary production which in turn supports productive foodwebs and major fisheries (Fréon *et al.*, 2009). However, subsurface and newly upwelled waters naturally exhibit low O_2 and high CO_2 concentrations due to the remineralization of organic material exported from surface layers. Consequently, they have a reduced capacity to buffer against changes in carbonate chemistry resulting from ocean uptake of anthropogenic CO_2 relative to open-ocean surface waters (Feely *et al.*, 2008; Fassbender *et al.*, 2011; Harris *et al.*, 2013). In eastern Pacific systems such as the California Current, the CO_2 burden and O_2 drawdown due to respiration are high because the source waters transported to upwelling centres along the coast have been isolated from the surface for a few decades (Feely *et al.*, 2008; Hauri *et al.*, 2009). In the California Current, anthropogenic CO_2 has already lowered pH by ~0.1, causing the depth of undersaturation with respect to aragonite to shoal and expanding the spatial extent of undersaturated surface waters (Feely *et al.*, 2008; Gruber *et al.*, 2012; Harris *et al.*, 2013). In only a few more decades, models suggest that the depth of undersaturation may shoal into the upper 75 m of the water column in some regions year-round (Gruber *et al.*, 2012; Hauri *et al.*, 2013). Given the economic, ecological, and biogeochemical importance of eastern boundary upwelling regions, understanding how species that compose these ecosystems will respond to OA has emerged as a high research priority (Fabry *et al.*, 2008; Gruber, 2011; Doney *et al.*, 2012).

To evaluate the sensitivity of species to OA, researchers commonly rely on manipulative experiments where organisms are exposed to different carbonate chemistry conditions. Typically, experiments include "control" conditions that attempt to simulate contemporary or preindustrial CO_2 concentrations and "acidified" treatments that correspond to potential future CO_2 uptake by the oceans. For studies focused on organisms from low productivity, open-ocean surface waters researchers can rely on IPCC scenarios of atmospheric pCO_2 concentrations to identify potential carbonate chemistry treatments because assumptions of air–sea pCO_2 equilibrium are often nearly met (Barry *et al.*, 2010; Orr, 2011). However, in upwelling systems, CO_2 levels are more variable relative to open ocean waters due to the outcropping of high-CO_2 subsurface waters and high rates of primary production and respiration that strongly modulate seawater carbonate chemistry (Hales *et al.*, 2005; Feely *et al.*, 2008; Borges and Abril, 2011; Fassbender *et al.*, 2011). Consequently, OA experiments that use organisms from these habitats and that rely on IPCC future atmospheric CO_2 scenarios to devise control and acidified seawater treatments may inadequately replicate contemporary carbonate chemistry or include treatments that fail to reflect realistic future OA hypotheses (Barry *et al.*, 2010; Andersson and Mackenzie, 2012; McElhany and Busch, 2012).

Recognition of the importance of including environmentally relevant pCO_2 levels in OA experiments has grown considerably, and has led to the use of seawater chemistry monitoring programmes to inform treatment design in several recent OA studies (Hofmann *et al.*, 2014). Less appreciated from an experimental perspective, however, is the possibility that carbonate chemistry conditions may also naturally co-vary with other biologically relevant variables including temperature and O_2 over multiple spatial and temporal scales (Reum *et al.*, 2014). This may have important implications for the design and interpretation of ocean acidification (OA) experiments because of the potential for non-additive interactions between carbonate chemistry, temperature, and O_2 on organismal performance and ecological interactions (Wernberg *et al.*, 2012, Harvey *et al.*, 2013; Koch *et al.*, 2013; Kroeker *et al.*, 2013). For many organisms, aerobic capacity and metabolic scope (the amount of energy that can be allocated to activities beyond those required for basic existence) may be influenced strongly by temperature, and adversely impacted by reductions in ambient oxygen availability or increases in CO_2 concentrations (Pörtner, 2010, 2012).

Given the combined effects that temperature and environmental O_2 and pCO_2 have on organismal physiology and experimental evidence indicating non-additive interactions on response variables related to fitness and ecosystem function (Pörtner and Farrell, 2008; Pörtner, 2010; Harvey *et al.*, 2013; Kroeker *et al.*, 2013), knowledge of their co-variability is essential for designing OA experiments that adequately characterize biological performance under contemporary relative to future acidified conditions. Yet for workers focused on laboratory OA experiments, these relationships are rarely incorporated into experimental designs. This poses important potential drawbacks. Foremost, if carbonate chemistry strongly covaries with temperature or O_2, researchers risk running experiments with control-water characteristics that are atypical of the habitat to which a focal organism/life stage may have acclimated or adapted to. Recently, pCO_2 was shown to range widely (~200–2500 μatm) and co-vary with temperature and O_2 in a fjord located in the northeast Pacific (Reum *et al.*, 2014). In that system, the strength and direction of the relationships changed with season, but also between subregions that differed in terms of vertical mixing. Consequently, within a given season and region, organisms occurring in low pCO_2 waters experience temperatures and O_2 levels that differed from those experienced by organisms that occupy high pCO_2 waters, and this has direct implications for how ecologically relevant OA experiments should be designed (Reum *et al.*, 2014).

Here, we expand on the topic and evaluate the potential importance of this issue for upwelling systems. To do so, we have assembled a large dataset of carbonate chemistry measurements from a variety of habitats throughout the California Current Ecosystem (CCE), a major eastern boundary upwelling system that supports highly productive foodwebs. Along the coast, equatorward winds during spring and summer drive surface flow offshore in an Ekman layer, leading to the upwelling of cold, salty, O_2-poor, and nutrient- and CO_2-rich subsurface water. In fall and winter, the wind direction reverses resulting in downwelling and shoreward advection of oceanic waters which are relatively warm, fresh, O_2-saturated, nutrient-deplete, and near air–sea CO_2 equilibrium (Evans *et al.*, 2011; Harris *et al.*, 2013). The dataset presented here consists of pCO_2 measurements from multiple moorings and ship-based sampling campaigns that collectively span 14° of latitude, and includes data from estuary and open coastal water habitats. Although the extent of data is constrained in either time or space for any single sampling campaign, the synthesis of many datasets offers an overview of the potential range of pCO_2, temperature, and O_2 conditions experienced by organisms from this region. Subsequently, we compared environmental pCO_2 and temperature measurements to conditions in OA experiments performed on organisms obtained from populations that reside within the CCE. In doing so, we place these

experiments in a larger environmental context and draw on observations that may help guide OA researchers in considering experimental designs that are more appropriate for organisms that occur in the CCE and similar coastal systems.

Material and methods

Carbonate chemistry data

Our analysis focused on coastal waters within the domain of the northern and central CCE (Figure 1). The region extends from northern Vancouver Island, British Columbia (50°N) to Point Conception, California (34°N), and is typified by distinct wind-driven upwelling (May–October) and downwelling (November–April) oceanographic seasons (Checkley and Barth, 2009). The region includes large expanses of open coastal habitat and many inlets and estuaries that range considerably in terms of surface area, depth, substrate, and connectivity with the open ocean (Hickey and Banas, 2003). To obtain an overview of the potential range of temperatures and carbonate chemistry conditions, we retrieved all publicly available records of measurements sampled within our region of interest from the Carbon Dioxide Information Analysis Center (CDIAC) and Surface Ocean CO_2 Atlas (SOCAT, Bakker *et al.*, 2013). The dataset includes carbonate chemistry measurements from discrete water samples collected at depth, shipboard measurements of surface water pCO_2, and mooring pCO_2 time-series of surface waters off the coast of California and Washington (Supplementary Table S1). In addition to CDIAC and SOCAT data, we also included unpublished carbonate chemistry data obtained from the 2011 and 2012 NOAA Ocean Acidification Programme West Coast Cruise survey, which sampled waters along the continental shelf of western North America; mooring pCO_2 time-series of surface waters from an open coast location (Newport, Oregon), and a shallow tidal estuary (Netarts Bay, Oregon); and published carbonate chemistry data from late summer and fall surveys in a large fjord estuary complex (Strait of Juan de Fuca and Puget Sound, Washington; Supplementary Table S1). Further details of the survey, sampling dates, sampling method, and habitats from which data were obtained are provided in Supplementary Table S1. Although the dataset does not include all habitat types that occur within the CCE, we believe these data are sufficiently representative enough to offer an overview of key patterns of carbonate chemistry, temperature, and O_2 covariation. For the purposes of the present study, we included all measurements extending up to 200 km from the coast.

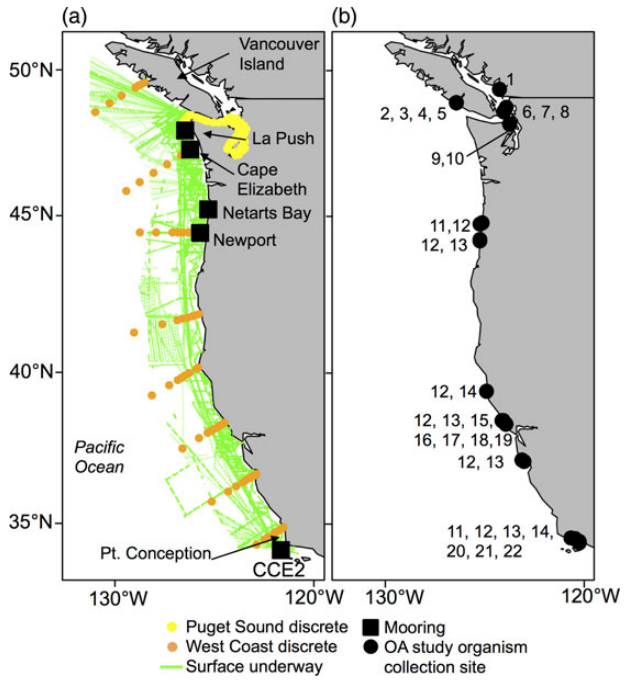

Figure 1. Map of coordinates where (a) environmental carbonate chemistry data were obtained from the northern and central CCE from moorings and ship-based underway and discrete samples, (b) the locations where organisms (or their broodstock) included in published OA experiments were collected. In (a), samples coded as Puget Sound also include measurements from the adjoining Strait of Juan de Fuca. For additional details on environmental carbonate chemistry datasets, see Supplementary Table S1.

For our analysis, we focused on pCO_2 rather than other parameters of the carbonate system because pCO_2 is directly changed by anthropogenic CO_2 emissions and is the most commonly used treatment variable in species-exposure OA experiments. Further, direct measurements of pCO_2 were more widely available than other parameters in the CDIAC and SOCAT databases, and when not available were readily estimated from other measured parameters of the carbonate system (see Supplementary Table S1 for details on estimation methods). We recognize that organisms may potentially be more sensitive to other variables of the carbonate system such as pH or to changes in the calcium carbonate saturation state of seawater (Barton *et al.*, 2012; Waldbusser and Salisbury, 2013) and that waters with similar pCO_2 values may differ with respect to aragonite or calcite saturation states if total alkalinities differ. However, pCO_2 is routinely reported in OA studies and is the parameter that allowed us to best standardize comparisons among experiments and between experiments and environmental carbonate chemistry measurements. Further, the focus on pCO_2 prevented the use of some carbonate chemistry datasets such as those including information only on pH (e.g. Hofmann *et al.*, 2011). We limited our analysis to pCO_2 measurements taken from the top 50 m of the water column because the species and life history stages for which OA experiments have been performed from the northern and central CCE typically occur in waters within this depth range, although individuals of some populations may occur for periods below this depth.

We evaluated separate relationships between pCO_2 and temperature and pCO_2 and O_2 within summer upwelling and winter downwelling periods. Co-variation patterns for pCO_2 and temperature were examined for data pooled from shipboard underway and discrete sample measurements collected along the West Coast continental shelf. In addition, we also examined co-variation patterns for Puget Sound and the Strait of Juan de Fuca discrete sample measurements (hereafter referred to as "Puget Sound"). A subset of these data were examined in an earlier study (Reum *et al.*, 2014), but we include them here for completeness and to facilitate comparisons among habitats represented within the CCE. We chose to present co-variation patterns for Puget Sound separately from the West Coast because Puget Sound exhibits slow exchange with open coastal waters and high rates of primary productivity and respiration (Feely *et al.*, 2010). The resulting pCO_2–temperature relationships therefore likely differ considerably from patterns observed in shelf waters. For the time-series data, we estimated pCO_2–temperature relationships for upwelling and downwelling seasons, but examined co-variation patterns separately for each mooring to evaluate site-level differences.

To evaluate pCO_2 and O_2 relationships and facilitate comparisons across survey types and seasons, we converted all O_2 concentration

measurements to micromole per kilogramme. As with the pCO_2 and temperature data, we examined co-variation within data pooled from shipboard West Coast measurements, Puget Sound, and each mooring and by season. To improve assumptions of normality in the residual error structure for the pCO_2–temperature and pCO_2–O_2 relationships, we $\log_{10}$-transformed pCO_2 values before estimating linear relationships using least-squares regression. For presentation purposes, the liner relationships were back-transformed to the original pCO_2 scale. Our goal was to estimate overall mean relationships within seasons and survey types to facilitate visual inspection and to evaluate co-variation patterns in an exploratory manner. We therefore did not test for significant differences between seasons or survey types. All linear relationships were fitted using the R version 2.11 statistical software package (R Development Core Team, 2011).

OA experimental studies

We searched the published literature for OA experiments that included organisms obtained directly from habitats within the northern and central CCE or that originated from broodstock collected from the region. To do so, we searched Google Scholar, ISI databases (Web of Science, Current Contents), and references included in recently published reviews and meta-analyses that address OA (Dupont *et al.*, 2010; Wernberg *et al.*, 2012; Harvey *et al.*, 2013; Kroeker *et al.*, 2013; Wittmann and Pörtner, 2013). We used the search terms "ocean acidification", "carbon dioxide", "experiment", and "manipulation". We included all studies published through 15 October 2013 that were found under these search criteria.

From each study, we retrieved information on the collection site of the organism (or their broodstock) and the temperatures and pCO_2 levels at which the experiment was performed. For nearly all studies, experimental O_2 concentrations were not reported nor could saturation conditions be safely assumed. We therefore focused our comparison of environmental and experimental conditions to pCO_2 and temperature. Following the authors' interpretation of the results, we recorded whether the dependent biological variables differed significantly in a positive or negative direction or showed no significant difference relative to the control pCO_2 level specified by the author. If authors did not explicitly designate a control pCO_2 level in their study, we considered treatments with pCO_2 levels closest to present-day air pCO_2 levels (~400 μatm) as the control to facilitate comparisons across studies. When more than one response variable was tested in an experiment, we coded the net outcome of the experiment at a given treatment level based on the result of the variable most sensitive to pCO_2.

From the outset, we recognized that the species and life history stages for which published OA experimental data were available held distributions that spanned large sections of the northern and central CCE or were planktonic with high dispersal potential. Further, the exact dispersal patterns of many of these species are not well understood. Although larvae of some species may be functionally limited to a subset of the CCE system (e.g. some species may occur primarily in bays or estuaries), "spillage" into adjoining habitats and waters through advective processes is also probable. We therefore used the full dataset of field pCO_2 and temperature measurements to demarcate the potential pCO_2–temperature space organisms may encounter. We acknowledge that the actual pCO_2 levels and temperatures experienced by organisms will differ for populations across locations, seasons, and due to possible interannual variation in upwelling and climate forcing. Our main intention, however, was to draw comparisons between the conditions maintained in OA experiments and the full range of environmental pCO_2 and temperature values based on empirical observations. In the absence of detailed information on the fine-scale distribution and movement patterns of most species and life history stages, and environmental pCO_2–temperature measurements of matching resolution, comparisons at finer spatio-temporal scales were not possible.

Results

pCO_2, temperature, and O_2 co-variation

Temperature and pCO_2 values in the upper 50 m of the CCE spanned 6–19°C and 100–1500 μatm, respectively, based on the pooled shipboard underway and discrete water sample measurements along the open coast. pCO_2 values tended to increase with decreasing water temperature during summer upwelling months (Figure 2a). In Puget Sound, a similar but steeper relationship was apparent relative to the open coastal waters, reflecting CO_2-enriched waters (Figure 2a). Along the open coast, the range of pCO_2 values was also wider at cool relative to warm temperatures. For instance, pCO_2 values at 9°C ranged from 320 to 1400 μatm, while at 16°C, the range extended from 130 to 420 μatm. In Puget Sound, the pCO_2 range was also wider at cooler temperatures (Figure 2a).

Although fewer measurements were available during winter in general (Supplementary Table S1), the data showed weak co-variation between pCO_2 and temperature in open coastal waters and the overall range of pCO_2 values and temperatures narrowed relative to summer (Figure 2b). This is due to the relative absence of the cold, high- pCO_2 upwelled source waters. In contrast, winter pCO_2 and temperature values in Puget Sound positively covaried, and the range of pCO_2 values and temperatures also narrowed relative to summer (Figure 2b).

Time-series data collected from moored platforms in open coastal waters from four locations also indicated co-variation between pCO_2 and temperature (Figure 3a–c). During summer upwelling months, pCO_2 again generally declined with increasing temperature (Figure 3a–c). The range of pCO_2 levels among stations, however, differed substantially. Time-series data collected at moorings in shelf waters off Washington and near Point Conception, CA. (Figure 3a and b) ranged in pCO_2 from 200 to 600 and 300 to 600 μatm, respectively, while off the coast of Oregon the range spanned 200–1100 μatm (Figure 3c). The differences among stations reflect considerable spatial variation in the supply of newly upwelled waters.

Time-series data collected from Netarts Bay, a shallow tidal estuary in northern Oregon, indicated summer range in pCO_2 values was also considerable, spanning 300–800 μatm and reflected high rates of primary production and respiration (Figure 3d). The overall relationship between pCO_2 and temperature, however, was also negative. In winter, co-variation between pCO_2 and temperature at all mooring stations was weaker relative to summer but variable across stations (Figure 3d). In addition, the range of temperatures and pCO_2 values were generally lower in winter relative to summer in two of the five stations (Figure 3c and d).

Measurements of O_2 were available for a subset of pCO_2 records included in the complete environmental pCO_2 and temperature dataset (Supplementary Table S1). For all survey types, mooring time-series, and seasons, pCO_2 levels decreased with increasing O_2 concentration (Figure 4). For most moorings on the shelf, O_2 ranged from 230 to 350 μmol kg^{-1} (both seasons combined). Summer O_2 levels at Newport Oregon, however, ranged from 120 to 350 μmol kg^{-1} (Figure 4). Summer O_2 measurements from discrete samples from

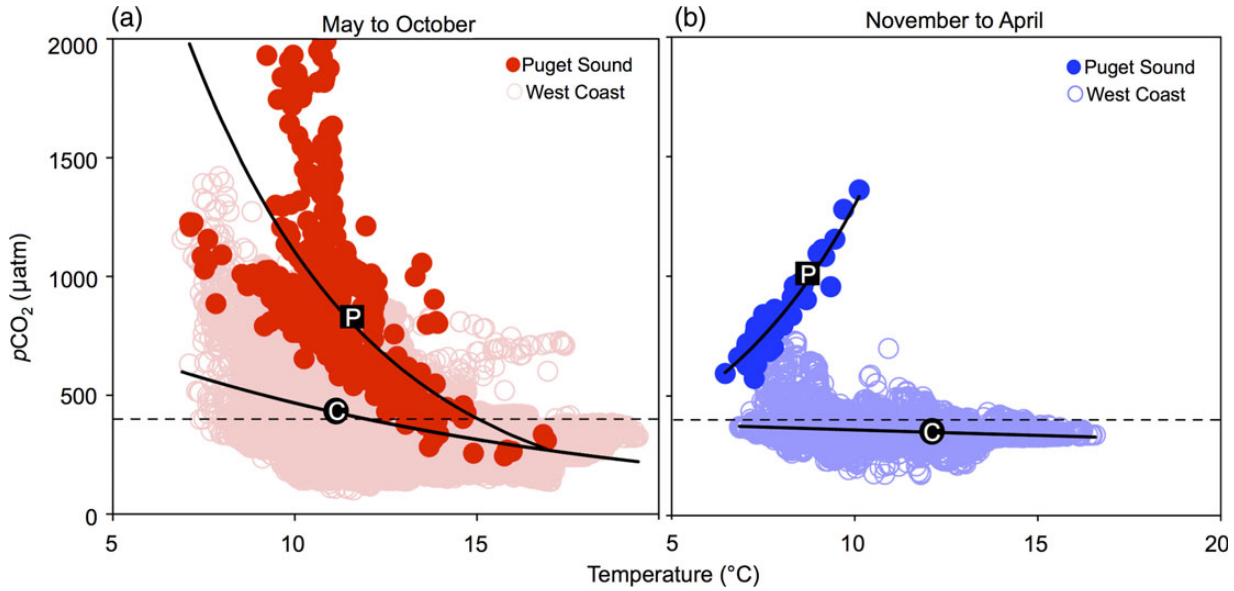

Figure 2. (a) Relationship between pCO_2 and temperature in the top 50 m of the water column in the northern and central CCE during summer upwelling season which approximately spans May through October and (b) winter (November through April) when downwelling-favourable winds predominate. All non-time-series data are displayed. Measurements of pCO_2 from cool waters in Puget Sound are elevated relative to other regions sampled in the CCE. Regression lines are overlaid to aid evaluation of patterns. Lines labelled P and C denote relationships for Puget Sound and open coastal locations, respectively. For reference, approximate present-day pCO_2 levels (~390 µatm) are indicated by the dashed horizontal line.

Puget Sound and the West Coast ranged more widely, from 40 to 400 µmol kg^{-1}, where concentrations below ~60 µmol kg^{-1} reflect hypoxic conditions (Figure 4). The general negative relationship between pCO_2 and O_2 corresponds to the well-understood effects of aerobic respiration and photosynthesis in marine ecosystems. When aerobic respiration dominates, CO_2 is remineralized and O_2 levels are drawn down, while the reverse occurs when photosynthesis dominates.

OA studies

In total, 26 experiments from 22 published OA studies included organisms (or broodstock) from the northern and central CCE (Figure 1b) and provided sufficient information on treatment water conditions to compare with the CCE pCO_2–temperature space defined by combining all environmental datasets (Table 1). In terms of taxonomic diversity, 50, 35, and 15% of experiments evaluated responses in echinoderms, molluscs, and teleosts, respectively. However, 35% of all experiments focused on responses in a single species, the echinoderm *Strongylocentrotus purpuratus* (Table 1). Of the experiments, 81% examined gamete, egg, or larval performance (survival, growth, calcification rates), while the remaining studies evaluated performance metrics (growth, development, or calcification rates) in juvenile or adult life history stages (Table 1). One study measured genetic diversity in echinoderm larvae after exposure to different pCO_2 treatments to evaluate evolutionary potential.

To facilitate visual inspection and comparison of experimental pCO_2 and temperature treatments with the pCO_2–temperature space defined by the complete set of environmental measurements in our dataset, we examined echinoderm and non-echinoderm studies separately (Figure 5). Overall, OA experiments included pCO_2 treatment levels that extended from 200 to 4000 µatm; 42% of experiments included a single elevated pCO_2 treatment in addition to a control at a given temperature, 38% considered two different elevated pCO_2 treatments, and 19% included three or more elevated treatments (Figure 5). In total, 72% of experiments included at least one control and one elevated pCO_2 treatment that occurred within the observed range of pCO_2 and temperature values in the CCE. Of those, 63% (10 out of 16) observed negative biological effects, 18% observed positive effects, and 18% observed no effect relative to control pCO_2 levels. Only two studies included pCO_2 treatments below approximate present-day atmospheric levels (~400 µatm; Figure 5).

Compared with the pCO_2–temperature space defined by the complete set of environmental measurements in our dataset, five experiments were performed at temperatures that matched or exceeded the warmest observed values (~19°C; Figure 5). These included three experiments on the early life history stages of the native Olympia oyster, an experiment on sand dollar larvae, and an experiment on the non-native Pacific oyster which is routinely reared at ~20°C to optimize survival under commercial hatchery conditions. One experiment included a 2.1°C treatment; though this temperature was meant to simulate cool conditions in Alaskan waters, the source stock was collected near Puget Sound (Table 1).

A review of each study indicated that Intergovernmental Panel on Climate Change (IPCC) estimates of future global surface ocean mean pCO_2 levels were used as the sole rationale for selecting OA treatments in 45% of studies, while 31% cited a combination of regional modelling studies, local field measurements, and IPCC estimates to support their choice of experimental pCO_2 treatment levels. Of the remaining studies, 13% provided no rationale for their choice of pCO_2 treatment levels, one based the high pCO_2 treatment level on observations of contemporary upwelling conditions, and one noted natural high carbonate chemistry variability in coastal upwelling systems which necessitated the need to test biological responses to a wide range of pCO_2 levels. In terms of temperature, 80% of studies did not provide a rationale for their choice of

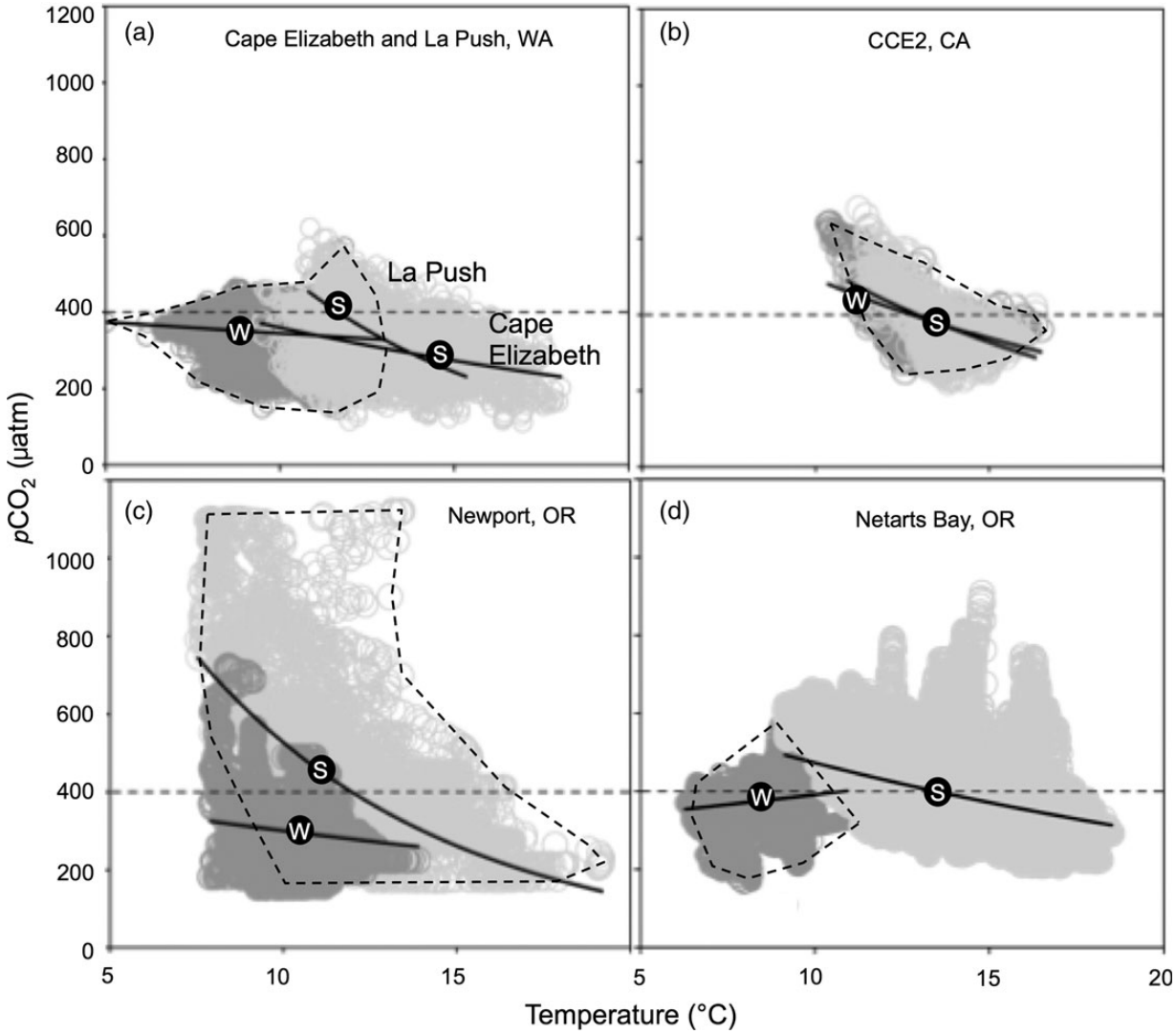

Figure 3. Relationship between pCO_2 and temperature of surface waters measured during summer (light grey open circle symbols) and winter (dark grey) at open coastal moorings in (a) Washington, (b) California, and (c) Oregon, and (d) a tidal estuary in Oregon. Regression lines are overlaid and labelled S and W to indicate summer or winter, respectively. Dashed line convex hulls demarcate data ranges where seasons overlap. For reference, approximate present-day pCO_2 levels (~390 µatm) are indicated by the dashed horizontal line.

experimental levels. The remaining studies cited similarity to local field conditions as a rationale for selecting temperatures. Of the two studies that performed experiments that included crossed temperature and pCO_2 treatments meant to correspond to conditions in the CCE, the warmer treatments were chosen in reference to IPCC global average temperature increase projections.

Discussion

Single-species response experiments have offered important initial evidence that some species and life history stages may be adversely impacted by OA (Kroeker *et al.*, 2013; Wittmann and Pörtner, 2013), but there is a pressing need for the development of experiments that include more appropriate reference treatments that reflect pCO_2 levels species have acclimated or adapted to and acidified treatments that more closely reflect natural heterogeneity in carbonate chemistry (Barry *et al.*, 2010; Andersson and Mackenzie, 2012; McElhany and Busch, 2012; Waldbusser and Salisbury, 2013). Our analysis shows that an additional source of concern is natural co-variation between carbonate chemistry and other biologically relevant variables including temperature and O_2. These findings have direct consequences for designing experiments that aim to include control treatments that are similar to natural water conditions and for selecting elevated pCO_2 treatment levels that more closely correspond to OA hypotheses. Further, by placing the findings of published OA experiments into a larger environmental context, we gain information on the ecological relevance of experimental water conditions and insight into the potential sensitivity of some species and life stages to carbonate chemistry conditions that already occur in the CCE.

Although researchers increasingly recognize the importance of basing experimental pCO_2 levels on *in situ* carbonate chemistry observations (Yu *et al.*, 2011; Evans *et al.*, 2013; Hofmann *et al.*, 2014), the implications of natural co-variation with temperature or O_2 to experimental design and inference are only beginning to be explored. Given experimental evidence and theoretical expectations of interactive or synergistic effects between pCO_2, temperature, and O_2 on organisms

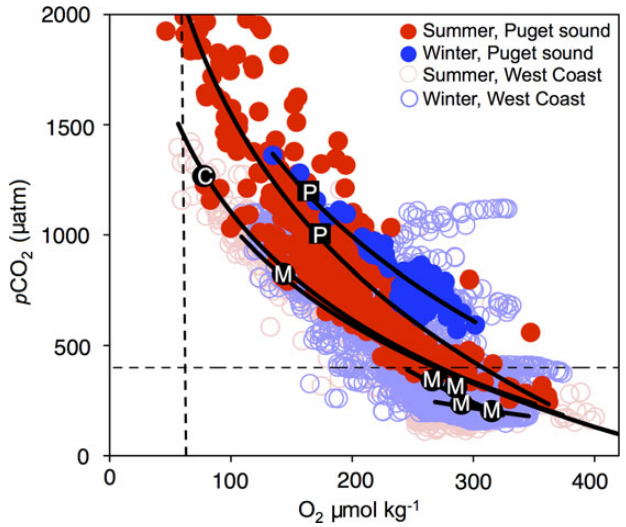

Figure 4. Relationships between pCO_2 and O_2 in the top 50 m of the water column during summer upwelling (May through October) and winter downwelling seasons (November through April). Regression lines are overlaid for summer and winter; lines labelled M, P, and C correspond to mooring, Puget Sound, and open coast datasets, respectively. For reference, approximate present-day pCO_2 levels (~390 µatm) are indicated by the dashed horizontal line, and the hypoxia threshold (60 µmol kg^{-1}) is indicated with a dashed vertical line.

(Pörtner, 2010, 2012; Harvey *et al.*, 2013), we suggest that failure to account for natural co-variation among these variables in habitats from the CCE may lead to results with diminished relevance for making predictions. To illustrate this point, we present an example multistressor experimental scheme typical of published OA experiments in which temperature (three levels at 8, 12, and 16°C) is crossed with two pCO_2 levels that correspond to approximate global surface ocean present-day (400 µatm) and future (800 µatm) conditions (Figure 6a). Under the conventional method, treatments are fully orthogonal which permits estimates of the effect sizes of the individual predictor variables and of their interaction on the response variable. The method holds merit as a tool for comparing the relative influence that each predictor has on the response variable, is widely applied in multistressor experiments, and facilitates the development of mechanistic models. However, if a goal of a study is to evaluate the potential sensitivity of organisms to future OA as is often the case, the design may be inadequate, given natural pCO_2–temperature co-variation within different habitats and water masses. For example, assuming an organism of interest occurs in shelf waters off Oregon during summer upwelling months (e.g. a pelagic larval invertebrate), the assumption that 800 µatm corresponds to a future OA prediction across all temperatures is not accurate. At the Newport, Oregon, mooring pCO_2 levels of 800 µatm already occur at 8°C under present-day conditions and "control" 400 µatm waters do not (Figure 6a). At temperatures above 13°C, the mean pCO_2 values approach air–sea equilibrium conditions. We do not doubt that simple crossed experimental designs will provide information on the interactive effects of pCO_2 and temperature, but we do question the efficacy of the design for testing OA hypotheses on future ecological response to OA, given naturally occurring pCO_2–temperature relationships and the wide range of both variables in the CCE.

In light of potential co-variation between carbonate chemistry and other important environmental variables, how should researchers select pCO_2 treatments that correspond to OA hypotheses? As a starting point, we recommend that OA experimental designs include multiple controls that reflect the span of pCO_2 levels and temperatures likely to be experienced by the organism under study (Figure 5b). To design pCO_2 treatments that represent future OA scenarios in productive coastal systems, we suggest that researchers focus on changes in the anthropogenic contribution to *in situ* dissolved inorganic carbon, DIC (e.g. Feely *et al.*, 2008, 2010; Barry *et al.*, 2010; Melzner *et al.*, 2012; Shaw *et al.*, 2013). At the Newport, Oregon, mooring, newly upwelled waters exhibit pCO_2 values that are elevated relative to air–sea equilibrium conditions due to the remineralization of organic material before surfacing (Evans *et al.*, 2011). However, after surfacing CO_2 concentrations can be drawn down rapidly by photosynthesis (Hales *et al.*, 2005; Hales *et al.*, 2006; Evans *et al.*, 2011), often at rates that typically far exceed CO_2 equilibration times across the air–sea interface (e.g. van Geen *et al.*, 2000; Fassbender *et al.*, 2011). Consequently, the anthropogenic CO_2 burden of upwelled waters is primarily acquired when they were last in contact with the atmosphere and before DIC changes due to biological processes post-surfacing. In our example, pCO_2 treatments reflecting future OA hypotheses could be obtained by increasing *in situ* DIC concentrations by an increment (ΔDIC) expected under a given CO_2 emissions scenario. The future DIC estimate (ΔDIC + *in situ* DIC), along with a second parameter from the carbonate system, could then be used to recalculate the carbonate system to estimate treatment pCO_2 levels.

Because the Newport, Oregon, time-series consists only of pCO_2, we first needed to estimate *in situ* DIC. To do so, we estimated total alkalinity (TA) from salinity measurements using a linear model parameterized with data from the CCE (Gray *et al.*, 2011). The relationship has relatively low residual error (approximately ± 20 µmol kg^{-1}) and was shown previously to adequately predict TA for the purposes of estimating the carbonate system when using pCO_2 as the second parameter (Harris *et al.*, 2013). We used the estimated TA and *in situ* pCO_2, salinity, and temperature measurements to solve the carbonate system and calculate *in situ* DIC. To estimate ΔDIC, we solved the carbonate system based on estimates of TA, and *in situ* temperature, and salinity, but assuming seawater equilibrium with average atmospheric pCO_2 levels during the period of the moored observations (~390 µatm; Harris *et al.*, 2013) and those predicted under an emissions scenario for the year 2100 (788 µatm; Intergovernmental Panel on Climate Change IS92a "continually increasing" emissions scenario). The present-day air–sea equilibrium DIC estimate was subtracted from the future equilibrium estimate to obtain ΔDIC. Although the same present day and future pCO_2 levels were used to calculate ΔDIC for all samples, ΔDIC values differ among samples because estimates of DIC at air–sea pCO_2 equilibrium vary based on the TA, temperature, and salinity of the sample. Across all water samples, ΔDIC spanned ~75–105 µmol kg^{-1} depending on the TA and temperature of samples. We then obtained future pCO_2 estimates by solving the carbonate system using the estimated TA and *in situ* DIC + ΔDIC values (Figure 6b). Versions of the method have been described previously (e.g. Barry *et al.*, 2010) and can be used to estimate preindustrial carbonate chemistry conditions (e.g. Feely *et al.*, 2008; Harris *et al.*, 2013).

Under this approach, and assuming the same number of treatments is used as depicted in Figure 6a, the effects of temperature and pCO_2 can no longer be separated because orthogonality in the design is lost (Figure 6b). However, a more realistic set of control treatments are included that offer a firmer basis for drawing

Table 1. Brief summary of experimental outcomes of reviewed OA studies that focus on organisms (or their broodstock) collected from the CCE.

Study number	Reference	Collection site	Species (common name)	Life stage	Duration (days, hours)	T (°C)	Control pCO_2 (μatm)	Treatment pCO_2 (μatm)	Outcome relative to control
1	Gooding *et al.* (2009)	Jaricho Beach, BC	*Pisaster ochraceus* (purple sea star)	Juvenile	70 d	12, 15	380	780	Increased growth rate, reduced calcified mass; feeding and growth increased with temperature
2	Reuter *et al.* (2011)	Barkley Sound, BC	*Strongylocentrotus franciscanus* (red sea urchin)	Sperm/eggs	1 h	10.2	400	800, 1800	Decreased range of sperm concentrations over which high fertilization success was likely
3	Nienhuis *et al.* (2010)	Barkley Sound, BC	*Nucella lamellose* (Frilled dogwinkle)	Adults	6 d	9.0	380	780, 1585	Enhanced shell dissolution
4	Sunday *et al.* (2011)	Barkley Sound, BC	*Strongylocentrotus franciscanus* (red sea urchin)	Larvae	1 d	12.0	400	1000	Reduced larval size, large variation among families
4	Sunday *et al.* (2011)	Barkley Sound, BC	*Mytilus trossulus* (bay mussel)	Larvae	1 d	12.0	400	1000	Reduced larval size, small variation among families
5	Crim *et al.* (2011)	Barkley Sound, BC	*Haliotis kamtschatkana* (northern abalone)	Larvae	8 d	12.0	400	800, 1800	Reduced survival, increased abnormalities in shell structure, reduced size in normal-shelled larvae
6	Chan *et al.* (2011)	Orcas Island, WA	*Dendraster excentricus* (Pacific sand dollar)	Larvae	10 d	20.0	380	1000	Reduced body size and stomachs; no effect on swimming speed
7	Timmins-Schiffman *et al.* (2012)	San Juan Island, WA	*Crassostrea gigas* (Pacific oyster)	Larvae	3 d	20.0	468	847, 1065	Increased calcification at day 1, but smaller average size on day 3
8	O'Donnell *et al.* (2013)	San Juan Island, WA	*Mytilus trossulus* (bay mussel)	Adults	20 d	10.4	432	299, 575, 736, 980, 1057, 1180, 1322, 1498	Weaker, less flexible byssal threads at treatments above 1200 μatm
9	Hurst *et al.* (2012)	Port Townsend, WA	*Theragra chalcogramma* (walleye pollock)	Yearlings	42 d	8.8	414	478, 815, 1805	No effect on growth but increase in otolith deposition rate, biological implication is unclear
9	Hurst *et al.* (2012)	Port Townsend, WA	*Theragra chalcogramma* (walleye pollock)	Sub-yearlings warm	196 d	8.3	596	828, 1285, 2894	Increase growth at pCO_2 higher than 900 μatm; no change in condition factor
9	Hurst *et al.* (2012)	Port Townsend, WA	*Theragra chalcogramma* (walleye pollock)	Sub-yearlings cool	196 d	2.4	386	225, 643, 1543	No difference in growth or condition factor across treatments
10	Hurst *et al.* (2013)	Port Townsend, WA	*Theragra chalcogramma* (walleye pollock)	Eggs/larvae	35 d	8.1	442	296, 871, 1844	No difference in egg hatch rate, size, or survival, but longer time till hatching; authors think elevated pCO_2 treatments have minor effect
11	Evans *et al.* (2013)	Fogarty Creek, OR	*Strongylocentrotus purpuratus* (purple sea urchin)	Larvae	96 h	12.8	435	813, 1255	Transcriptome up-regulation of genes related to calcification at intermediate pCO_2, no change at high level
12	Pespeni *et al.* (2013)	OR to CA., various locations	*Strongylocentrotus purpuratus* (purple sea urchin)	Larvae	17 d	14.1	428	897	Reduction in larval body length, change in allele frequency, no change in timing of settlement or competence to metamorphose

Continued

Table 1. *Continued*

Study number	Reference	Collection site	Species (common name)	Life stage	Duration (days, hours)	*T* (°C)	Control pCO_2 (μatm)	Treatment pCO_2 (μatm)	Outcome relative to control
13	LaVigne *et al.* (2012)	OR to CA, various locations	*Strongylocentrotus purpuratus* (purple sea urchin)	Larvae	50 d	14.1	490	1001	No change Sr/Mg composition in spines; though a difference was observed for a Santa Barbara population of urchins
14	Kelly *et al.* (2013)	Northern and southern CA, various locations	*Strongylocentrotus purpuratus* (purple sea urchin)	Larvae	5 d	13.0	424	1210	Reduced size in larvae from dams and sires taken from northern and southern locations; no difference in metabolism
15	Place and Smith (2012)	Bodega Bay, CA	*Strongylocentrotus purpuratus* (purple sea urchin)	Embryos	7 d	15.1	378	1486, 4110	No disruption to cell cycle in fertilized eggs
16	Hettinger *et al.* (2012)	Tomales Bay, CA	*Ostreola lurida* (Olympia oyster)	Larvae/ juveniles	45 d	20.0	739	933, 1355	Reduced larval and juvenile growth
17	Hettinger *et al.* (2013a)	Tomales Bay, CA	*Ostreola lurida* (Olympia oyster)	Larvae	22 d	19.4	520	1075	Reduced number of settlers; no difference in shell size or larval dry weight
18	Hettinger *et al.* (2013b)	Tomales Bay, CA	*Ostreola lurida* (Olympia oyster)	Larvae/ juveniles	127 d	20.0	485	1060	Reduced larval survival and growth; reduced growth in juveniles outplanted to an estuary
19	Gaylord *et al.* (2011)	Tomales Bay, CA	*Mytilus californianus* (California mussel)	Larvae	8 d	15.4	380	540, 970	Thinner, weaker shells
20	Padilla-Gamiño *et al.* (2013)	Santa Barbara, CA	*Strongylocentrotus purpuratus* (purple sea urchin)	Larvae	75 h	13, 18	400	1100	Reduced body size and respiration rate; difference in transcriptome observed
21	Matson *et al.* (2012)	Santa Barbara, CA	*Strongylocentrotus purpuratus* (purple sea urchin)	Larvae	6 d	15.6	365	1038, 1444	Reduced arm length; no difference in utilization of energy lipid reserves and protein content remained unchanged
22	Yu *et al.* (2011)	Santa Barbara, CA	*Strongylocentrotus purpuratus* (purple sea urchin)	Larvae	6 d	15.6	372	1057, 1469	Slight reduction in size
22	Yu *et al.* (2011)	Santa Barbara, CA	*Strongylocentrotus purpuratus* (purple sea urchin)	Larvae	6 d	15.6	432	1441	Slight reduction in size

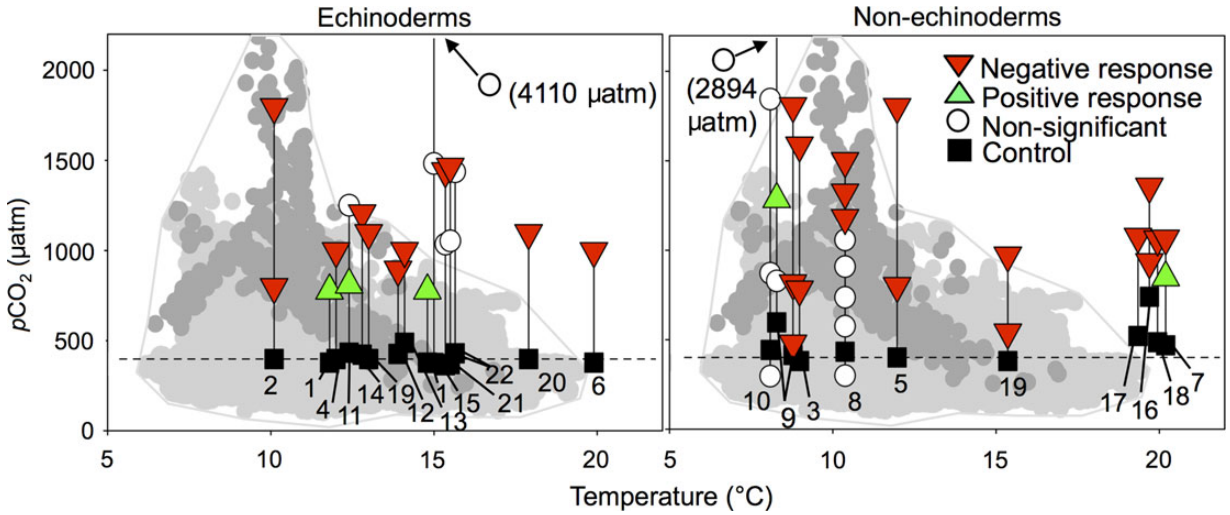

Figure 5. Environmental pCO_2 and temperature measurements (top 50 m) from the northern and central CCE and conditions maintained in OA experiments performed on organisms from the region. Dark grey circles correspond to environmental measurements from Puget Sound, Washington; light grey circles correspond to environmental measurements from all other regions. pCO_2 treatment levels included in an individual experiment at a given temperature are connected by solid black lines. Numbers denote study code (see Table 1). A convex hull (solid grey line) demarcating the extent of all environmental pCO_2 and temperature measurements is depicted to aid visual comparisons. For reference, approximate present-day atmospheric pCO_2 levels (~390 µatm) are indicated by the dashed horizontal line.

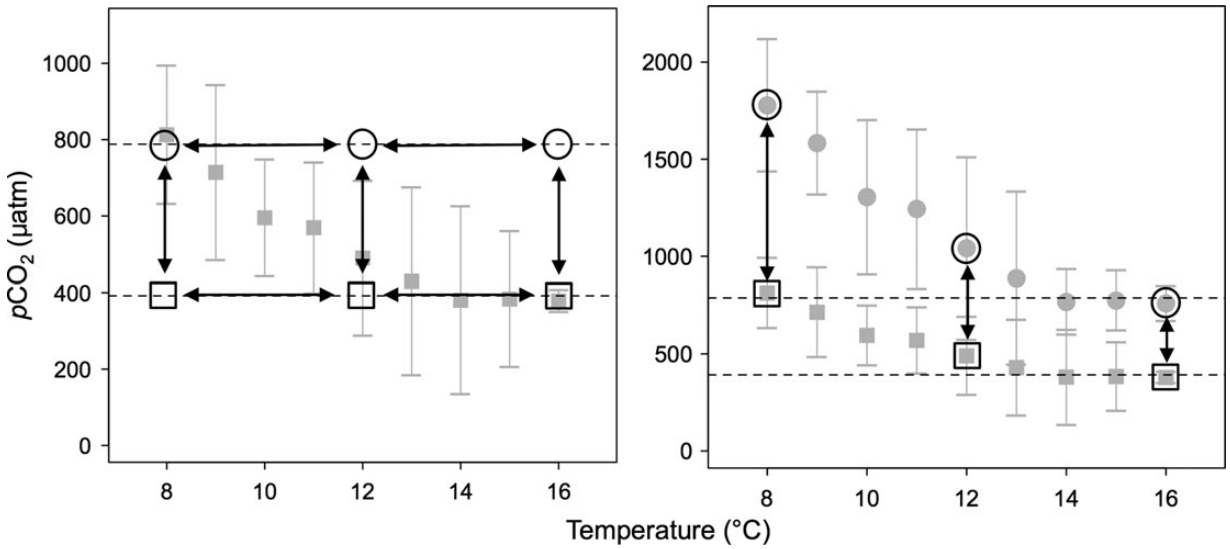

Figure 6. Schematic of potential experimental approaches to evaluate OA effects, given co-variation between pCO_2 and temperature. To illustrate the benefits and drawback of each approach, *in situ* pCO_2 and temperature measurements from the N10 mooring near Newport, Oregon, during summer upwelling season (2008) are depicted (grey, filled squares; bars indicate standard deviation). (a) A conventional temperature (three levels: 8, 12, and 16°C) by pCO_2 experimental design in which control pCO_2 values are based on approximate present-day global average surface ocean pCO_2 levels and the acidified treatments corresponding to IPCC emissions scenario IS92a projections for year 2100 (390 and 788 µatm; open square and circle symbols, respectively). Arrows indicate statistical comparisons permitted by the design. (b) Experimental design informed by *in situ* pCO_2 and temperature measurements. Under this design, three controls are included to account for natural co-variation in temperature and pCO_2. Treatment levels that more closely correspond to an OA hypothesis were obtained by specifying an increase in DIC attributed to anthropogenic CO_2 emissions (see Discussion for details). The future DIC estimate and estimates of TA were used to recalculate the carbonate system to obtain target pCO_2 treatment levels. We calculated pCO_2 using the R library "seacarb" (Lavigne and Gattuso, 2010) with dissociation constants from Lueker *et al.* (2000).

inferences about future OA impacts at a given temperature. The experimental design could be improved further by using O_2 concentrations that currently occur at the three different pCO_2–temperature controls.

The method we use to estimate future pCO_2 requires several important assumptions. First, the approach implicitly assumes that TA, salinity, and temperature will remain unchanged and that future difference in DIC between the observed *in situ* values and

those calculated assuming present-day air–sea equilibrium will remain the same. Further, to estimate ΔDIC, we assumed that all water properties measured at the time of sampling are the same as when the water mass last approached air–sea equilibrium. If waters were cooler at that time, this would result in a slight overestimate of ΔDIC of ~1.6 μmol kg^{-1} for each degree Celsius. Following earlier studies, we also assumed that waters upwelled at the mooring location possessed an anthropogenic CO_2 burden that approximated present-day atmospheric pCO_2 conditions (Harris *et al.*, 2013). In other locations within the CCE, such assumptions may not be justified because subsurface waters upwelled on to the shelf may last have had contact with the surface decades prior and therefore would contain less anthropogenic CO_2 (Feely *et al.*, 2008; Harris *et al.*, 2013).

The OA pCO_2–temperature relationship depicted in Figure 6b corresponds to one simple hypothesis for how present-day carbonate chemistry conditions might change with a simple augmentation of CO_2. However, marine organisms will be subjected to multiple stressors in the future, including warmer temperatures, lower ambient O_2 concentrations, cultural eutrophication, and pollution (Boyd, 2011; Gruber, 2011; Doney *et al.*, 2012). Treatments corresponding to an OA + warming hypothesis could be created by adding to *in situ* measurements of both temperature and DIC and recalculating the carbonate system to obtain appropriate estimates of pCO_2 (Melzner *et al.*, 2012). If a hypoxia + OA treatment is sought, any assumed reduction in O_2 owing to aerobic respiration necessarily corresponds to an increase in CO_2 (Melzner *et al.*, 2012; Sunda and Cai, 2012). The corresponding increase in DIC beyond that attributed to OA could be estimated based on the molar ratio of O_2 consumed to CO_2 released in the respiratory consumption of organic matter (Sunda and Cai, 2012). We caution, however, that the appropriateness of these simple methods for estimating treatment levels should be thoughtfully considered in the light of the physical and biological attributes of the system under study. Such simplifications do not take into account the indirect and cascading impacts that changes in individual properties such as temperature will have on ecosystem metabolism and thus the distribution and concentration of O_2 and CO_2 (e.g. Keeling *et al.*, 2010; Gruber, 2011; Doney *et al.*, 2012), nor would they reflect potential changes in large-scale circulation patterns or productivity regimes which might fundamentally alter relationships between pCO_2 and other variables (e.g. Rykaczewski and Dunne, 2010). Despite these uncertainties, developing experimental designs that include controls that reflect present-day pCO_2–temperature–O_2 relationships in upwelling systems should become the cornerstone of experiments that aim to quantify the potential response of organism to future predicted changes in their environment. The development of experimental systems that permit simultaneous control over pCO_2, temperature, and O_2 conditions remains a technical challenge, but a growing number of OA research facilities are acquiring the capacity to do so (Bockmon *et al.*, 2013).

Our compilation of environmental carbonate chemistry data is meant to offer an initial overview of the ranges of pCO_2, temperature, and O_2 in the CCE and the extent to which their relationships vary between seasons and regions. We examined patterns of co-variation between pCO_2 and temperature at coarse seasonal time-scales, but note that co-variation patterns may differ depending on temporal scale. On diel time-scales, solar heating and photosynthesis and respiration may drive strong cyclical patterns in temperature, pCO_2, and O_2 (Barton *et al.*, 2012; Frieder *et al.*, 2012; Waldbusser and Salisbury, 2013), while abrupt events such as storms or the advection of a different water mass into a region can result in rapid change in water characteristics that may persist for several days (Frieder *et al.*, 2012). Over interannual time-scales, large-scale climate phenomena like *El Niño*/Southern Oscillation can influence upwelling patterns, coastal productivity, carbonate chemistry (Chavez *et al.*, 1999; Friederich *et al.*, 2002), and thus potentially relationships among pCO_2 and temperature and O_2. To date, studies evaluating patterns of co-variation between pCO_2 and other biologically relevant variables over a range of temporal scales are sparse, but the topic is an area of research we are currently exploring. Incorporating both temporal dynamics and multiple stressors in experimental systems is technically challenging, but may be necessary for ecologically relevant predictions.

Conclusions

OA is expected to have far-reaching impacts on the structure and function of marine ecosystems by altering biogeochemical processes and the productivity and distribution of species (Fabry *et al.*, 2008; Doney *et al.*, 2009, 2012; Mora *et al.*, 2013; Waldbusser and Salisbury, 2013). Our ability to predict the response of complex ecological systems to OA, however, remains limited and is highly constrained by major uncertainties in the response of species to both direct (e.g. physiology, neurological impairment) and indirect (e.g. trophic interactions) processes that may be vulnerable to OA (Fabry *et al.*, 2008; Hofmann *et al.*, 2010). While authors have noted the need for OA researchers to use pCO_2 levels that correspond to ambient conditions a study species or life history stage is likely to experience (Andersson and Mackenzie, 2012; McElhany and Busch, 2012), patterns of co-variation with temperature and O_2 have yet to be incorporated into OA experimental designs (Reum *et al.*, 2014). As demonstrated here, this issue should be of concern to researchers in upwelling systems and other coastal environments where water conditions are highly dynamic over a range of spatial and temporal scales and where co-variation between pCO_2, temperature, and O_2 are generally expected. Because inferences on the potential response of organisms to future conditions are necessarily premised on the notion that experimental controls reflect present-day conditions, we strongly recommend researchers consider how pCO_2 naturally varies with other biologically important variables in their experimental designs. Importantly, the studies we reviewed for the CCE indicate that several species may be sensitive to carbonate chemistry conditions that already occur, and suggest that present-day variability in carbonate chemistry may be more important to contemporary ecological patterns than previously thought. With the continued collection of high-quality carbonate chemistry measurements and their archival on freely accessible databases, analyses like the one we present here for the CCE may yield further insight into the relevance of carbonate chemistry variability to contemporary ecological processes as well as guide OA experimental design in other marine systems.

Supplementary data

Supplementary material is available at the *ICESJMS* online version of the manuscript.

Acknowledgements

The authors wish to thank many research technical staff in the laboratories that contributed data used in this manuscript, particularly the scientific and engineering staff in NOAA's Pacific Marine Environmental Laboratory (PMEL) carbon, CTD-O_2, and engineering groups; UW's Applied Physics Laboratory (UW/APL) and

School of Oceanography; OSU's College of Earth, Ocean, and Atmospheric Sciences Ocean Ecology and Biogeochemistry division; and the Scripps Institution of Oceanography Ocean Time Series Group for the tremendous effort involved in making these datasets available. In addition, we thank the officers and crew on all spatial surveys, underway observing ships, and mooring deployments for their able assistance during field operations. Funding for JCPR was provided through a National Research Council Fellowship. Funding for NOAA/PMEL contributions to the mooring time-series, underway pCO_2, and spatial survey data used in these analyses were provided by NOAA's Climate Programme Office's Global Carbon Cycle Programme (grants GC05-288 and GC10-102), NOAA's Ocean Acidification Programme, and NOAA/PMEL. The Chá bă mooring off La Push, Washington, was also supported by the Murdock Charitable Trust, NANOOS (Northwest Association of Networked Ocean Observing Systems, a Regional Association of NOAA's US Integrated Ocean Observing System Programme), UW/APL, UW College of the Environment, and UW Provost's Office. The PRISM cruises were supported by the State of Washington through UW Oceanography and APL. The NH10 mooring is funded by NOAA through NANOOS, and by NSF through CMOP (Science and Technology Center for Coastal Margin Observation and Prediction OCE-0424602). Surface ocean pCO_2 data collected on the NH10 mooring were supported by NSF Chemical Oceanography OCE-0752576 awarded to BH and P.G. Strutton. I. Kaplan, T. Klinger, and three anonymous reviewers provided valuable comments on early versions of the manuscript. This is PMEL contribution number 4100.

References

Andersson, A. J., and Mackenzie, F. T. 2012. Revisiting four scientific debates in ocean acidification research. Biogeosciences, 9: 893–905.

Barry, J. P., Tyrrell, T., Hansson, L., Plattner, G., and Gattuso, J. 2010. Atmospheric CO_2 targets for ocean acidification perturbation experiments. *In* Guide to Best Practices for Ocean Acidification Research and Data Reporting, pp. 53–66. Ed. by U. Riebesell, V. J. Fabry, L. Hansson, and J-P. Gattuso. Publications Office of the European Union, Luxembourg.

Bakker, D. C. E., Pfeil, B., Smith, K., Hankin, S., Olsen, A, Alin, S. R., Cosca, C., *et al.* 2013. An update to the Surface Ocean CO2 Atlas (SOCAT version 2). Earth System Science Data, 6: 1–22, 6, doi:10.5194/essd-6-69-2014, 2014

Barton, A., Hales, B., Waldbusser, G. G., Langdon, C., and Feely, R. A. 2012. The Pacific oyster, *Crassostrea gigas*, shows negative correlation to naturally elevated carbon dioxide levels: implications for near-term ocean acidification effects. Limnology and Oceanography, 57: 698–710.

Bockmon, E., Frieder, C., Navarro, M., White-Kershek, L., and Dickson, A. 2013. Controlled experimental aquarium system for multi-stressor investigation: carbonate chemistry, oxygen saturation, and temperature. Biogeosciences, 10: 5967–5975.

Borges, A. V., and Abril, G. 2011. Carbon dioxide and methane dynamics in estuaries. *In* Treatise on Estuarine and Coastal Science, 5, pp. 119–161. Ed. by D. McClusky, and E. Wolanski. Academic Press, Waltham.

Boyd, P. W. 2011. Beyond ocean acidification. Nature Geoscience, 4: 273–274.

Chan, K. Y. K., Grünbaum, D., and O'Donnell, M. J. 2011. Effects of ocean-acidification-induced morphological changes on larval swimming and feeding. The Journal of Experimental Biology, 214: 3857–3867.

Chavez, F. P., Strutton, P. G., Friederich, C. E., Feely, R. A., Feldman, G. C., Foley, D. C., and McPhaden, M. J. 1999. Biological and chemical response of the equatorial Pacific Ocean to the 1997–98 El Niño. Science, 286: 2126–2131.

Checkley, D. M., and Barth, J. A. 2009. Patterns and processes in the California Current System. Progress in Oceanography, 83: 49–64.

Crim, R. N., Sunday, J. M., and Harley, C. D. 2011. Elevated seawater CO_2 concentrations impair larval development and reduce larval survival in endangered northern abalone (*Haliotis kamtschatkana*). Journal of Experimental Marine Biology and Ecology, 400: 272–277.

Doney, S. C., Fabry, V. J., Feely, R. A., and Kleypas, J. A. 2009. Ocean acidification: the other CO_2 problem. Annual Review of Marine Science, 1: 169–192.

Doney, S. C., Ruckelshaus, M., Emmett Duffy, J., Barry, J. P., Chan, F., English, C. A., Galindo, H. M., *et al.* 2012. Climate change impacts on marine ecosystems. Annual Review of Marine Science, 4: 11–37.

Dupont, S., Ortega-Martínez, O., and Thorndyke, M. 2010. Impact of near-future ocean acidification on echinoderms. Ecotoxicology, 19: 449–462.

Evans, T. G., Chan, F., Menge, B. A., and Hofmann, G. E. 2013. Transcriptomic responses to ocean acidification in larval sea urchins from a naturally variable pH environment. Molecular Ecology, 22: 1609–1625.

Evans, W., Hales, B., and Strutton, P. G. 2011. Seasonal cycle of surface ocean pCO_2 on the Oregon shelf. Journal of Geophysical Research, 116: C05012.

Fabry, V. J., Seibel, B. A., Feely, R. A., and Orr, J. C. 2008. Impacts of ocean acidification on marine fauna and ecosystem processes. ICES Journal of Marine Science, 65: 414–432.

Fassbender, A. J., Sabine, C. L., Feely, R. A., Langdon, C., and Mordy, C. W. 2011. Inorganic carbon dynamics during northern California coastal upwelling. Continental Shelf Research, 31: 1180–1192.

Feely, R. A., Alin, S. R., Newton, J., Sabine, C. L., Warner, M., Devol, A., Krembs, C., *et al.* 2010. The combined effects of ocean acidification, mixing, and respiration on pH and carbonate saturation in an urbanized estuary. Estuarine Coastal and Shelf Science, 88: 442–449.

Feely, R. A., Sabine, C. L., Hernandez-Ayon, J. M., Ianson, D., and Hales, B. 2008. Evidence for upwelling of corrosive "acidified" water onto the continental shelf. Science, 320: 1490–1492.

Fréon, P., Barange, M., and Arístegui, J. 2009. Eastern boundary upwelling ecosystems: integrative and comparative approaches. Progress in Oceanography, 83: 1–14.

Frieder, C. A., Nam, S. H., Martz, T. R., and Levin, L. A. 2012. High temporal and spatial variability of dissolved oxygen and pH in a nearshore California kelp forest. Biogeosciences, 9: 3917–3930.

Friederich, G., Walz, P., Burczynski, M., and Chavez, F. 2002. Inorganic carbon in the central California upwelling system during the 1997–1999 El Niño–La Niña event. Progress in Oceanography, 54: 185–203.

Gaylord, B., Hill, T. M., Sanford, E., Lenz, E. A., Jacobs, L. A., Sato, K. N., Russell, A. D., *et al.* 2011. Functional impacts of ocean acidification in an ecologically critical foundation species. The Journal of Experimental Biology, 214: 2586–2594.

Gooding, R. A., Harley, C. D., and Tang, E. 2009. Elevated water temperature and carbon dioxide concentration increase the growth of a keystone echinoderm. Proceedings of the National Academy of Sciences of the United States of America, 106: 9316–9321.

Gray, S. E., DeGrandpre, M. D., Moore, T. S., Martz, T. R., Friederich, G. E., and Johnson, K. S. 2011. Applications of in situ pH measurements for inorganic carbon calculations. Marine Chemistry, 125: 82–90.

Gruber, N. 2011. Warming up, turning sour, losing breath: ocean biogeochemistry under global change. Philosophical Transactions of the Royal Society A: Mathematical, Physical and Engineering Sciences, 369: 1980–1996.

Gruber, N., Hauri, C., Lachkar, Z., Loher, D., Frölicher, T. L., and Plattner, G-K. 2012. Rapid progression of ocean acidification in the California Current System. Science, 337: 220–223.

Hales, B., Karp-Boss, L., Perlin, A., and Wheeler, P. A. 2006. Oxygen production and carbon sequestration in an upwelling coastal margin. Global Biogeochemical Cycles, 20: GB002517.

Hales, B., Takahashi, T., and Bandstra, L. 2005. Atmospheric CO_2 uptake by a coastal upwelling system. Global Biogeochemical Cycles, 19: GB1009.

Harris, K. E., DeGrandpre, M. D., and Hales, B. 2013. Aragonite saturation state dynamics in a coastal upwelling zone. Geophysical Research Letters, 40: 2720–2725.

Harvey, B. P., Gwynn-Jones, D., and Moore, P. J. 2013. Meta-analysis reveals complex marine biological responses to the interactive effects of ocean acidification and warming. Ecology and Evolution, 3: 1016–1030.

Hauri, C., Gruber, N., Plattner, G.-K., Alin, S., Feely, R. A., Hales, B., and Wheeler, P. A. 2009. Ocean acidification in the California current system. Oceanography, 22: 60–77.

Hauri, C., Gruber, N., Vogt, M., Doney, S. C., Feely, R. A., Lachkar, Z., Leinweber, A., *et al.* 2013. Spatiotemporal variability and long-term trends of ocean acidification in the California Current System. Biogeosciences, 10: 193–216.

Hettinger, A., Sanford, E., Hill, T. M., Hosfelt, J. D., Russell, A. D., and Gaylord, B. 2013a. The influence of food supply on the response of Olympia oyster larvae to ocean acidification. Biogeosciences, 10: 6629–6638.

Hettinger, A., Sanford, E., Hill, T. M., Lenz, E. A., Russell, A. D., and Gaylord, B. 2013b. Larval carry-over effects from ocean acidification persist in the natural environment. Global Change Biology, 19: 3317–3326.

Hettinger, A., Sanford, E., Hill, T. M., Russell, A. D., Sato, K. N., Hoey, J., Forsch, M., *et al.* 2012. Persistent carry-over effects of planktonic exposure to ocean acidification in the Olympia oyster. Ecology, 93: 2758–2768.

Hickey, B. M., and Banas, N. S. 2003. Oceanography of the US Pacific Northwest Coastal Ocean and estuaries with application to coastal ecology. Estuaries, 26: 1010–1031.

Hofmann, G. E., Barry, J. P., Edmunds, P. J., Gates, R. D., Hutchins, D. A., Klinger, T., and Sewell, M. A. 2010. The effect of ocean acidification on calcifying organisms in marine ecosystems: an organism-to-ecosystem perspective. Annual Review of Ecology, Evolution, and Systematics, 41: 127–147.

Hofmann, G. E., Evans, T. G., Kelly, M. W., Padilla-Gamiño, J. L., Blanchette, C. A., Washburn, L., Chan, F., *et al.* 2014. Exploring local adaptation and the ocean acidification seascape—studies in the California Current Large Marine Ecosystem. Biogeosciences, 11: 1053–1064.

Hofmann, G. E., Smith, J. E., Johnson, K. S., Send, U., Levin, L. A., Micheli, F., Paytan, A., *et al.* 2011. High-frequency dynamics of ocean pH: a multi-ecosystem comparison. PLoS ONE, 6: e28983.

Hurst, T. P., Fernandez, E. R., and Mathis, J. T. 2013. Effects of ocean acidification on hatch size and larval growth of walleye pollock (*Theragra chalcogramma*). ICES Journal of Marine Science, 70: 812–822.

Hurst, T. P., Fernandez, E. R., Mathis, J. T., Miller, J. A., Stinson, C. M., and Ahgeak, E. F. 2012. Resiliency of juvenile walleye pollock to projected levels of ocean acidification. Aquatic Biology, 17: 247–259.

Keeling, R. F., Körtzinger, A., and Gruber, N. 2010. Ocean deoxygenation in a warming world. Annual Review of Marine Science, 2: 199–229.

Kelly, M. W., Padilla-Gamiño, J. L., and Hofmann, G. E. 2013. Natural variation and the capacity to adapt to ocean acidification in the keystone sea urchin *Strongylocentrotus purpuratus*. Global Change Biology, 19: 2536–2546.

Koch, M., Bowes, G., Ross, C., and Zhang, X. H. 2013. Climate change and ocean acidification effects on seagrasses and marine macroalgae. Global Change Biology, 19: 103–132.

Kroeker, K. J., Kordas, R. L., Crim, R., Hendriks, I. E., Ramajo, L., Singh, G. S., Duarte, C. M., *et al.* 2013. Impacts of ocean acidification on marine organisms: quantifying sensitivities and interaction with warming. Global Change Biology, 19: 1884–1896.

LaVigne, M., Hill, T. M., Sanford, E., Gaylord, B., Russell, A. D., Lenz, E. A., and Hosfelt, J. D. 2012. The elemental composition of purple sea urchin (*Strongylocentrotus purpuratus*) calcite and potential effects of pCO2 during early life stages. Biogeosciences, 10: 3465–3477.

Lavigne, H., and Gattuso, J. 2010. Seacarb: seawater carbonate chemistry with R. R package version 2.4.3.

Lueker, T. J., Dickson, A. G., and Keeling, C. D. 2000. Ocean pCO_2 calculated from dissolved inorganic carbon, alkalinity, and equations for K1 and K2: validation based on laboratory measurements of CO_2 in gas and seawater at equilibrium. Marine Chemistry, 70: 105–119.

Matson, P. G., Pauline, C. Y., Sewell, M. A., and Hofmann, G. E. 2012. Development under elevated pCO_2 conditions does not affect lipid utilization and protein content in early life-history stages of the purple sea urchin, *Strongylocentrotus purpuratus*. The Biological Bulletin, 223: 312–327.

McElhany, P., and Busch, D. S. 2012. Appropriate pCO_2 treatments in ocean acidification experiments. Marine Biology, 160: 1807–1812.

Melzner, F., Thomsen, J., Koeve, W., Oschlies, A., Gutowska, M. A., Bange, H. W., Hansen, H. P., *et al.* 2012. Future ocean acidification will be amplified by hypoxia in coastal habitats. Marine Biology, 160: 1875–1888.

Mora, C., Wei, C-L., Rollo, A., Amaro, T., Baco, A. R., Billett, D., Bopp, L., *et al.* 2013. Biotic and Human vulnerability to projected changes in ocean biogeochemistry over the 21st century. PLoS Biology, 11: e1001682.

Nienhuis, S., Palmer, A. R., and Harley, C. D. G. 2010. Elevated CO_2 affects shell dissolution rate but not calcification rate in a marine snail. Proceedings of the Royal Society B: Biological Sciences, 277: 2553–2558.

Orr, J. 2011. Recent and future changes in ocean carbonate chemistry. *In* Ocean Acidification. Ed. by J. Gattuso, and L. Hansson. Oxford University Press, New York, NY.

O'Donnell, M. J., George, M. N., and Carrington, E. 2013. Mussel byssus attachment weakened by ocean acidification. Nature Climate Change, 3: 587–590.

Padilla-Gamiño, J. L., Kelly, M. W., Evans, T. G., and Hofmann, G. E. 2013. Temperature and CO_2 additively regulate physiology, morphology and genomic responses of larval sea urchins, *Strongylocentrotus purpuratus*. Proceedings of the Royal Society B: Biological Sciences, 280: 20130155.

Pespeni, M. H., Sanford, E., Gaylord, B., Tessa, M. H., Hosfelt, J. D., Jaris, H. K., LaVigne, M., *et al.* 2013. Evolutionary change during experimental ocean acidification. Proceedings of the National Academy of Sciences of the United States of America, 110: 6937–6942.

Place, S. P., and Smith, B. W. 2012. Effects of seawater acidification on cell cycle control mechanisms in *Strongylocentrotus purpuratus* embryos. PLoS ONE, 7: e34068.

Pörtner, H. O. 2010. Oxygen- and capacity-limitation of thermal tolerance: a matrix for integrating climate-related stressor effects in marine ecosystems. The Journal of Experimental Biology, 213: 881–893.

Pörtner, H. O. 2012. Integrating climate-related stressor effects on marine organisms: unifying principles linking molecule to ecosystem-level changes. Marine Ecology Progress Series, 470: 273–290.

Pörtner, H. O., and Farrell, A. P. 2008. Physiology and climate change. Science, 322: 690–692.

R Development Core Team. 2011. R: a Language and Environment for Statistical Computing. R Foundation for Statistical Computing, Vienna, Austria.

Reum, J. C., Alin, S. R., Feely, R. A., Newton, J., Warner, M., and McElhany, P. 2014. Seasonal carbonate chemistry covariation with temperature, oxygen, and salinity in a fjord estuary: implications

for the design of ocean acidification experiments. PLoS ONE, 9: e89619.

Reuter, K. E., Lotterhos, K. E., Crim, R. N., Thompson, C. A., and Harley, C. D. 2011. Elevated pCO_2 increases sperm limitation and risk of polyspermy in the red sea urchin *Strongylocentrotus franciscanus*. Global Change Biology, 17: 163–171.

Rykaczewski, R. R., and Dunne, J. P. 2010. Enhanced nutrient supply to the California Current Ecosystem with global warming and increased stratification in an earth system model. Geophysical Research Letters, 37: GL045019.

Shaw, E. C., McNeil, B. I., Tilbrook, B., Matear, R., and Bates, M. L. 2013. Anthropogenic changes to seawater buffer capacity combined with natural reef metabolism induce extreme future coral reef CO_2 conditions. Global Change Biology, 19: 1632–1641.

Sunda, W. G., and Cai, W. J. 2012. Eutrophication induced CO_2-acidification of subsurface coastal waters: interactive effects of temperature, salinity, and atmospheric pCO_2. Environmental Science and Technology, 46: 10651–10659.

Sunday, J. M., Crim, R. N., Harley, C. D. G., and Hart, M. W. 2011. Quantifying rates of evolutionary adaptation in response to ocean acidification. PLoS ONE, 6: e22881. doi:10.1371/journal.pone.0022881.

Timmins-Schiffman, E., O'donnell, M. J., Friedman, C. S., and Roberts, S. B. 2012. Elevated pCO_2 causes developmental delay in early larval Pacific oysters, *Crassostrea gigas*. Marine Biology, 160: 1973–1982.

van Geen, A., Takesue, R. K., Goddard, J., Takahashi, T., Barth, J. A., and Smith, R. L. 2000. Carbon and nutrient dynamics during coastal upwelling off Cape Blanco, Oregon. Deep Sea Research, 47: 975–1002.

Waldbusser, G. G., and Salisbury, J. E. 2013. Ocean acidification in the coastal zone from an organism's perspective: multiple system parameters, frequency domains, and habitats. Annual Review of Marine Science, 6: 221–247.

Wernberg, T., Smale, D. A., and Thomsen, M. S. 2012. A decade of climate change experiments on marine organisms: procedures, patterns and problems. Global Change Biology, 18: 1491–1498.

Wittmann, A. C., and Pörtner, H-O. 2013. Sensitivities of extant animal taxa to ocean acidification. Nature Climate Change, 3: 995–1001.

Yu, P. C., Matson, P. G., Martz, T. R., and Hofmann, G. E. 2011. The ocean acidification seascape and its relationship to the performance of calcifying marine invertebrates: Laboratory experiments on the development of urchin larvae framed by environmentally-relevant pCO_2/pH. Journal of Experimental Marine Biology and Ecology, 400: 288–295.

Handling editor: Howard Browman

ICES Journal of Marine Science

ICES Journal of Marine Science (2016), 73(3), 596–603. doi:10.1093/icesjms/fsv214

Contribution to Special Issue: 'Towards a Broader Perspective on Ocean Acidification Research'

Original Article

Simulated diurnal pH fluctuations radically increase *variance* in—but not the *mean* of—growth in the barnacle *Balanus improvisus*

L. Eriander[1,2], A.-L. Wrange[1], and J. N. Havenhand[1]*

[1]*Department of Marine Sciences—Tjärnö, University of Gothenburg, Tjärnö, 45296 Strömstad, Sweden*
[2]*Department of Marine Sciences, University of Gothenburg, 40530 Gothenburg, Sweden*

**Corresponding author: tel: +46 31 786 9682; e-mail: jon.havenhand@marine.gu.se.*

Eriander, L., Wrange A.-L., and Havenhand, J.N. Simulated diurnal pH fluctuations radically increase *variance* in—but not the *mean* of—growth in the barnacle *Balanus improvisus*. – ICES Journal of Marine Science, 73: 596–603.

Received 30 June 2015; revised 23 October 2015; accepted 27 October 2015; advance access publication 27 November 2015.

Shallow coastal waters are characterized by substantial diurnal fluctuations in pH, especially in nearshore environments. The biological effects of ocean acidification in combination with these natural fluctuations have received relatively little attention to date. We exposed multiple batches (≈ different genotypes) of newly settled barnacles, *Balanus improvisus*, to constant pH under "control" (pH = 8.1) or "stable acidified" (pH = 7.7) conditions, as well as a treatment that simulated the maximum diurnal pH fluctuations seen in the nearshore habitats where this barnacle lives (± 0.2 pH units), superimposed on the stable acidified treatment ("fluctuating acidified"; 7.5 ≤ pH ≤ 7.9). We found that fluctuating acidification had no effect on *mean* response in growth and shell mineralogy, but caused an ~20-fold increase in *variance* of responses, compared with stable acidification. In contrast to these results, we found no effect of fluctuating acidification on variances of response ratios for barnacle survival and shell strength. Similarly, mean survival did not vary significantly with pH. However, we observed a strong negative effect of stable and fluctuating acidification on mean shell strength. Our finding that barnacles respond differently to fluctuating pH than to stable low pH indicate the importance of including fluctuating acidification treatments when studying species that live in variable environments. Importantly, because phenotypic variance is the raw material for natural selection, and thus lays at the heart of evolutionary responses to environmental variability and change, our findings also highlight the need to study changes in variance of—as well as mean—responses to changing ocean climates.

Keywords: crustacea, effect size, natural fluctuations, ocean acidification, penetrometry, response ratio.

Introduction

Shallow marine habitats experience substantial natural fluctuations in seawater chemistry that are typically far greater than those in the open oceans (Hofmann *et al.*, 2011; Duarte *et al.*, 2013). Seasonal changes in river run-off, upwelling, and shifts in primary and secondary production can cause pH fluctuations of up to—and sometimes more than—1 unit in these habitats (Blackford and Gilbert, 2007; Wootton *et al.*, 2008; Hofmann *et al.*, 2011; Pansch *et al.*, 2012). Even on much shorter diurnal time-scales, photosynthesis and respiration can cause very large pH excursions (Agnew and Taylor, 1986), although the effects of diurnal pH fluctuations are more typically 0.2–0.4 pH units in shallow habitats (Wootton *et al.*, 2008; Hofmann *et al.*, 2011; Cornwall *et al.*, 2013; Challener *et al.*, 2015).

The effects of diurnally fluctuating pH on organisms have been addressed in comparatively few studies to date; indeed, the great majority of published ocean acidification (OA) work has investigated the effects of constant levels of OA (which are well established to have generally, though not uniformly, negative effects across a variety of traits; Kroeker *et al.*, 2013). Clearly, the environmental relevance of using constant pH levels to determine the effects of OA on organisms that live in a fluctuating environment is limited, not only because future ocean pH is projected to vary at least as much as—and perhaps even more than—it does today (Takeshita *et al.*, 2015), but also because selection tends to be stronger under extreme, rather than average conditions (Darwin, 1859; Hoffmann and Parsons, 1997).

Recent reviews of the effects of environmental fluctuation on organisms have demonstrated that: (i) environmental variance

can lead to fluctuating selection pressures, which prevent species from tracking phenotypic optima (Kopp and Matuszewski, 2014); and (ii) changes in both the mean and variance of ecologically important environmental variables—such as might be expected under climate change—can have very different effects on organism growth rates (Lawson *et al.*, 2015). Experimental investigations of the effects of fluctuating environmental variables have tended to focus on factors other than OA (e.g. Stenseth *et al.*, 2002), and the few studies that have investigated organism responses to fluctuating acidification have found varying responses. Alenius and Munguia (2012) studied the effects of "low stable" (ΔpH $= -0.4$ units), "low variable" (ΔpH $= -0.4 \pm 0.1$ units) and "control" (ambient pH) treatments on the intertidal isopod *Paradella dianae*, and found the strongest negative effects in "low variable" treatments for the means of most (but not all) response variables (Alenius and Munguia, 2012). Stronger negative effects of fluctuating rather than stable acidification were also observed for mean growth and recruitment rates of coralline algae (Cornwall *et al.*, 2013). Other authors have found effects of fluctuating acidification (on calcification of coralline algae, Johnson *et al.*, 2014; or growth of salmon, Ou *et al.*, 2015), or even positive effects on calcification of corals (Dufault *et al.*, 2012; Comeau *et al.*, 2014) and recruitment of corals (Dufault *et al.*, 2012). Always, these publications have highlighted the need for more investigations of the effects of environmentally relevant pH fluctuations superimposed on projections of future OA. There is now a pressing need to determine whether the effects of diurnal naturally fluctuating acidification are similar to, or different from, the relatively well-documented responses of marine organisms to different levels of stable OA.

Importantly, although the aforementioned studies reported the effects of variable environment on mean organism response and its variance, the discussions focused on differences in *mean* response. This is a universal practice, perhaps precisely because comparison of mean responses is a core philosophy of almost all statistical testing in ecology. Yet changes in *variance* around the mean response can be at least as important as changes in mean response. Phenotypic variance—the product of genetic variation and phenotypic plasticity—is the raw material for differential selection, and thus lays at the heart of evolutionary responses to environmental variability and change. The importance of phenotypic variation both for bet-hedging and environmental buffering has been highlighted by many authors (see Jacobs and Podolsky, 2010, for a review in a marine context). Jacobs and Podolsky (2010) observe that although "studies of pattern in quantitative variation and its underlying causes have the potential to greatly expand our understanding of how selection works . . . quantitative comparisons of variation within and between populations are surprisingly rare" (pp. 639–640, Jacobs and Podolsky, 2010). Here, we address these issues by investigating the effects of control, stable OA, and fluctuating OA, on mean and variance of multiple response variables in the barnacle *Balanus improvisus*.

In barnacles, OA has been shown to decrease growth rate (*Elminius modestus*, Findlay *et al.*, 2010b), weaken shells (*Amphibalanus amphitrite*, McDonald *et al.*, 2009b; and *B. improvisus*, Pansch *et al.*, 2014), influence range-shifts (*Semibalanus balanoides*, Findlay *et al.*, 2010a, 2010c), and have no—or small—effects on larval development, survival, and settlement (several species; McDonald *et al.*, 2009a; Pansch *et al.*, 2012, 2013). Notably, the possibility that surplus energy can offset the negative effects of OA (Melzner *et al.*, 2011) has also been demonstrated for barnacles (Pansch *et al.*, 2014).

Balanus improvisus (Darwin) is eurythermal, euryhaline, and one of the most widespread barnacle species in the world (Foster, 1970; de Rivera *et al.*, 2011; Galil *et al.*, 2011). The species was introduced to Scandinavian waters around the mid-19th century (Blom, 1965; Foster, 1987) and is today found from 34 PSU in the Skagerrak down to 2 PSU in the Gulf of Bothnia (Leppakoski and Olenin, 2000). The population we studied, from Tjärnö on the Swedish west coast, typically experiences a salinity of 25 PSU and a maximum diurnal pH variation of ~0.3 units (Supplementary Figure S1). We used *B. improvisus* from this location to investigate the effects of medium-term (3 month) stable and fluctuating OA on a variety of traits, including growth, survival, mineral composition of the shell, and shell strength.

Material and methods

Experimental design

The experimental system comprised three header tanks (50 l each) with a constant flow-through of natural surface seawater (temperature $= 19^{\circ}C \pm 1$; salinity $= 26 \pm 6$; mean $\pm$ s.d.). Natural diurnal, and longer term, pH fluctuations in inflowing seawater were minimized by aerating the header tanks to pH ≈ 8.1 ($\approx$380 ppm CO_2, Table 1) before water treatment. Treatments comprised constant ambient "control" (target $pCO_2 = 380$ ppm), "stable OA" (target $pCO_2 = 970$ ppm), and "fluctuating OA" [target $pCO_2 = 1600$ ppm at night (18.00–06.00 h) and 610 ppm during the day (06.00–18.00 h)]. The stable OA treatment reproduced projections for the year 2100 (Orr *et al.*, 2005; IPCC, 2014) and standard practice in most OA experiments, whereas the fluctuating OA treatment was designed to mimic natural diurnal fluctuations in pH observed in the field (plus or minus ~0.2 pH units, Supplementary Figure S1) superimposed on the end of the century projections. Thus, by comparing results in "control" with "stable OA", we would mimic "typical" OA experiments, and by comparing "stable OA" with "fluctuating OA", we could determine the additional effects of fluctuating pH. Treatment levels were controlled with NBS-calibrated pH-computers (Aqua Medic GmbH, Germany) with a precision of ± 0.01 pH units ($\approx$12 ppm CO_2). Fluctuating treatments were obtained by using two such control

Table 1. Average pH, partial pressure of CO_2 (pCO_2), salinity, temperature, total alkalinity (A_T), dissolved inorganic carbon, and saturation state for calcite and aragonite (mean $\pm$ s.d.) in the control, stable OA, and fluctuating OA treatments during the 12-week experiment.

	pH_{NBS}	pCO_2 (µatm)	A_T (µmol kg^{-1})	Salinity (PSU)	T (°C)	C_T (µmol kg^{-1})	Ω_{Ca}	Ω_{Ar}
Control	8.10 ± 0.02	380	1567 ± 125	26 ± 4	19 ± 1	1498 ± 105	2.3 ± 0.5	1.4 ± 0.3
Stable OA	7.70 ± 0.03	970	1567 ± 125	26 ± 4	19 ± 1	1488 ± 92	0.9 ± 0.2	0.6 ± 0.1
Fluctuating OA								
Day	7.90 ± 0.02	625 ± 1	1567 ± 125	26 ± 4	19 ± 1	1499 ± 100	1.5 ± 0.3	0.9 ± 0.2
Night	7.50 ± 0.03	1665 ± 20	1567 ± 125	26 ± 4	19 ± 1	1586 ± 113	0.6 ± 0.1	0.4 ± 0.1

Salinity, temperature, and pCO_2 were measured or manipulated directly, A_T was estimated from salinity (see the Material and methods section), all other parameters were estimated with CO_2sys, using constants from Hansson and Merbach refit by Dickson and Millero (1987), Dickson (1990b), and Ho *et al.* (2006) as given by (Lewis and Wallace, 1998).

units with different set-points, the lower of which only operated between 18.00 and 06.00 h. pH_{NBS} set-points equivalent to desired pCO_2 levels in the treatments were determined by measuring pH_{NBS} in seawater equilibrated for 24 h with custom mixed gases at 380 or 970 μatmCO_2 (AGA, Sweden AB). To control for possible fluctuations in alkalinity (which would change the pH set-points required to achieve an equivalent pCO_2), calibrations were repeated every 2 weeks and the pH-computers adjusted accordingly. Total alkalinity was estimated from salinity using long-term salinity:alkalinity relationships for this location (SMHI, 2011; $r = 0.94$). Uncertainties arising from estimating alkalinity using this relationship were equivalent to ± 0.006 pH_{NBS} and 0.08 Ω_{Ar} (data for 99% CI around mean alkalinity estimated at 26 PSU, propagated through CO_2sys; Lewis and Wallace, 1998). Salinity (and hence alkalinity) fluctuations throughout the experimental period were relatively small (Table 1).

For each treatment, seven microcosms (5 l volume) were supplied with water from the respective header tank at 5 l h^{-1}. All tanks and microcosms were spatially interspersed to remove any artefacts arising from room effects, and all equipment was new to obviate any effects of prior history. Water and CO_2 flow rates into the header tanks, and microcosms, were manipulated, such that in the fluctuating acidification treatment, the transition from high to low pH in the microcosms took ~1 h. pH in each microcosm was monitored daily (NBS-calibrated Beckman Coulter pHi 460), and remained broadly consistent with target pCO_2s throughout the experiment (Table 1). Seawater salinity and temperature were recorded every 2–3 d using a YSI-30 conductivity meter. Carbonate system parameters were back-calculated from pH_{NBS} and A_T using the software CO_2sys using constants from Hansson and Merbach refitted by Dickson and Millero (1987), Dickson (1990b), and Ho *et al.* (2006) (Lewis and Wallace, 1998).

Balanus improvisus cyprid larvae were obtained from an established laboratory culture system (Berntsson *et al.*, 2000). Three separate collections of cyprid larvae were obtained from the barnacle culture that contained over 1000 adult broodstock. Collections (hereafter referred to as "batches") were made every third day within 1 week, and therefore, most likely represent output from different parents within the broodstock (mean frequency of larval release from individual *B. improvisus* is 5.81 ± 0.34 d, mean ± s.d.; JNH, pers. obs.). For each batch, cyprids were allowed to settle on acrylic panels in "control" seawater. After 48 h, panels bearing newly settled barnacles were distributed haphazardly among microcosms, so that each microcosm contained one panel from each larval batch (3 panels total). The mean barnacle density at the start of the experiment was 6.5 ± 2.9 per panel (mean ± s.d.). Panels were treated as replicates ($n = 7$ per batch). The experiment ran for 12 weeks (October–December 2010) under a 12:12 h light:dark cycle that coincided with the pH fluctuations (high pH during the day). In addition to natural food supplied from the inflowing seawater, every second day, barnacles were fed with a mixed microalgal diet at a final concentration of 20 000 cells ml^{-1} (Shellfish Diet 1800®). After 4 weeks, the barnacles had grown sufficiently to be able to capture and consume zooplankton, and therefore, their diet was supplemented with newly hatched *Artemia* nauplii.

Growth and survival

Barnacle growth and survival were recorded on each settlement panel every 2 weeks. Panels were temporarily removed from microcosms, cleaned gently and photographed in a standardized frame using an Olympus E-30 digital camera and 50 mm macro objective. A calibration scale was included in each image. Shell diameter (length and width) of all barnacles was measured from digital images using ImageJ (Abramoff *et al.*, 2004). Before photographing, any dead individuals were recorded and removed. Size was calculated only for barnacles that survived the entire experimental period (=3.95 ± 0.38 barnacles per panel, mean ± s.e.). Barnacle size throughout the experimental period was fitted against a Gompertz growth curve (Gompertz, 1825):

$$Y(t) = ae^{b\exp(ct)}$$

where Y is the diameter of the barnacle shell at time t, a the maximum diameter of the shell (asymptote), b represents the lag phase during early growth, and c is the maximum growth rate. Fitting this growth model facilitated a detailed understanding of the effects of the treatments on different components of growth (Wrange *et al.*, 2014).

Shell mineralogy

At the end of the experiment, shells from 14 individuals were haphazardly selected from each treatment. Mineral composition was determined using Inductively Coupled Plasma Mass Spectrometry (ICP-MS; Agilent 7500) calibrated with ICP multi-element standard solution (Merck, VI CertiPUR®). Samples comprised 10 mg of shell dissolved in 5% HNO_3, diluted ~50 000 times, with an internal standard containing 800 ppb indium. Drift and data quality were controlled using carbonate standards (Jls-1 and Jdo-1%). Accuracy was >97% and precision was >98.5% for both calcium and magnesium.

Shell strength

At the end of the experiment, shell strength was assessed in 16 individuals of similar size (shell length 5.7–6.7 mm), four from each treatment/batch. Crushing resistance of the rostral shell plate was measured using a Mark-10 force-gauge (ESM 3000). Shell plates were crushed with a blunt needle fixed to the force sensor (SSM10, accuracy ± 0.15 N) perpendicular to the centre of the plate at 0.25 m min^{-1}. Accumulated force required to crush the plate (to failure) was recorded.

Statistical analyses

Responses to pH treatments were visualized using log response ratios (LnRR; Nakagawa and Cuthill, 2007; Koricheva *et al.*, 2013). Survival, shell mineralogy, and shell strength were also analysed using two-way mixed-model ANOVA to test for effects of treatment (fixed) and batch (random). Growth data over time were compared between treatments and batches using repeated-measures ANOVA. Before statistical analysis, all data were tested for homogeneity of variance using Levene's test and for normality using Q–Q plots. Where necessary, data were transformed to meet assumptions (Quinn and Keough, 2002). Statistical analyses were performed using SPSS (IBM SPSS Statistics v. 20).

Results

Water chemistry

pH was relatively stable throughout the experimental period (Table 1) with a transition time from low pH to high pH (or *vice versa*) in the fluctuating treatment of ~60 min. Small fluctuations in carbonate chemistry parameters arose due to salinity variation in the natural seawater flowing through the system (Table 1). "Controls" were saturated with respect to calcite and aragonite

over the whole experimental period, whereas "stable OA" treatments were near saturation for calcite and under-saturated for aragonite, and "fluctuating OA" treatments were under-saturated for both calcite and aragonite at the lowest (night-time) pH levels (pH = 7.50; Table 1).

Growth and survival

By the end of the experiment (12 weeks after settlement), barnacles had reached adult size (shell diameter ~6.4 mm; Figure 1). In all treatments, maximum growth rate occurred after 4–6 weeks, at which time most individuals doubled in size within 2 weeks (Figure 1). Despite apparent trends for slower growth in stable OA and more rapid growth in fluctuating OA (Figure 1), log response ratios (LnRRs) showed that mean effect sizes were either very small or zero for all growth parameters (Figure 2). This result was corroborated by formal statistical analysis, which showed no significant effects of treatment on growth rate (Supplementary Table S2). Surprisingly, however, 95% confidence intervals (CIs) for LnRRs under fluctuating OA were almost 20-fold greater than for those under stable OA (Figure 2). This indicates that *variation* in growth responses was far greater under fluctuating acidification. This pattern of markedly increased variance in responses to fluctuating acidification was also seen in shell chemistry metrics (see below).

Growth rate varied significantly between barnacle batches (batch × time interaction; $F = 11.3$, $p < 0.001$; Supplementary Table S2), indicating that parentage may influence growth (replicate batches were likely produced by different subsets of the barnacle broodstock; see the Material and methods section). Importantly, however, there was no significant effect of treatment on this interaction (batch × time × treatment, $F = 0.47$, $p = 0.98$, Supplementary Table S2).

Both stable and fluctuating OA had only small effects on mean barnacle survival (Figures 2 and 3). Survival differed between batches (Figure 2) such that some batches showed no influence of pH treatment, whereas there were significant negative effects of both stable and fluctuating acidification for others (95% CIs do not overlap zero, Figure 2). This result was supported by formal analysis that showed a marginally significant effect of batch ($F = 3.09$, $p = 0.054$, Supplementary Table S3), and no significant effect of pH or pH × batch interaction (Supplementary Table S3). In contrast to the growth data, there were no apparent differences in the 95% CIs LnRRs for survival in stable and fluctuating treatments (Figure 2).

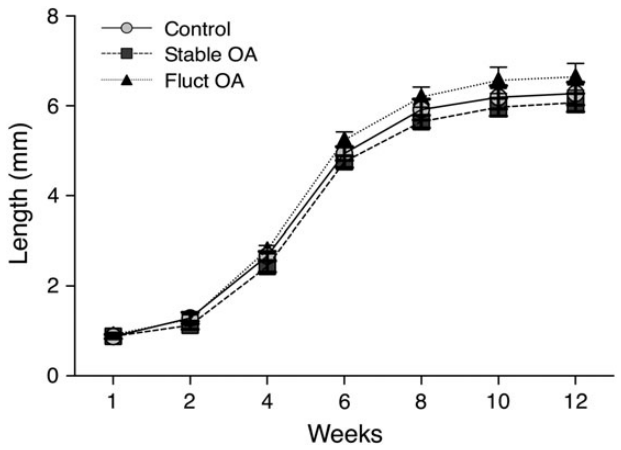

Figure 1. Mean shell diameter (± s.e.) of barnacles during the experimental period under different pH treatments (means of 3 batches per treatment, $n = 7$ replicate panels per batch).

Shell mineralogy

As for the growth data, the mean effect sizes for shell mineralogy in the different treatments were small, or zero (Figure 2), yet there were large differences in the magnitudes of the 95% CIs around these effect sizes for the different treatments (Figure 2). Once again, this indicates that variation in shell mineralogy was far greater under fluctuating acidification than under stable OA. ICP-MS indicated that both Ca and Mg content declined with acidification (control > stable OA > fluctuating OA; Supplementary Table S4), but these differences were small, and formal statistical analysis indicated no significant effects of treatment on either Ca content or Ca:Mg ratio (Supplementary Table S5). As was seen earlier for growth and survival, there was a significant effect of batch on Ca:Mg ratio (ANOVA, $F = 3.55$, $p = 0.038$; Supplementary Table S5).

Shell strength

Both stable and fluctuating acidification had a negative impact on the force (N) needed to penetrate the rostral shell plate of barnacles (Figure 4). The mean effect sizes for both OA treatments were similar

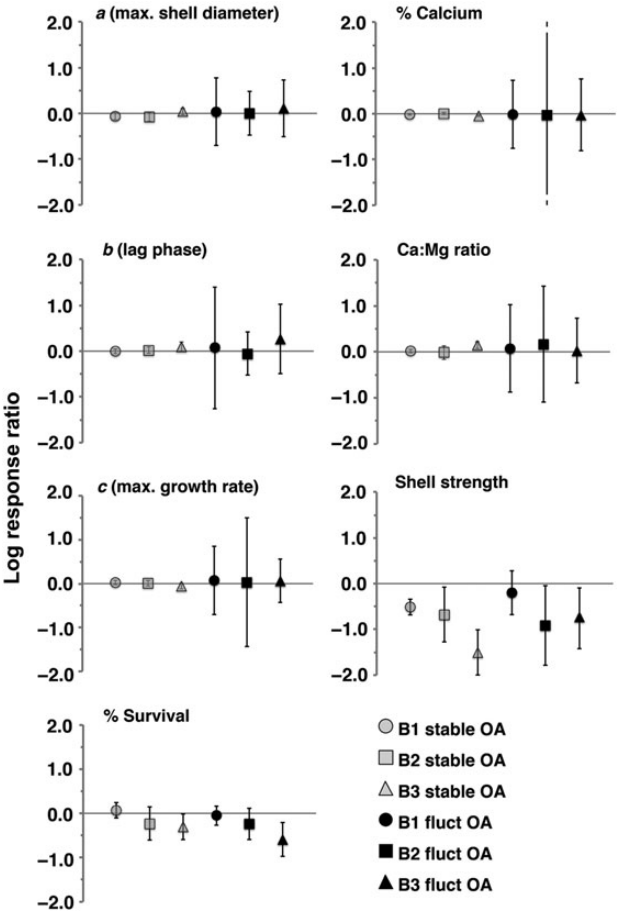

Figure 2. Log response ratios (mean ± 95% CI) for the effects of acidification (relative to controls) for Gompertz growth model parameters (*a*, *b*, and *c*; see text for details), % survival, % calcium content of shell, Ca:Mg ratio, and shell strength. Data are for "stable OA" (grey) and "fluctuating OA" treatments for each of the three batches (B1, B2, and B3; $n = 7$ replicate panels per batch).

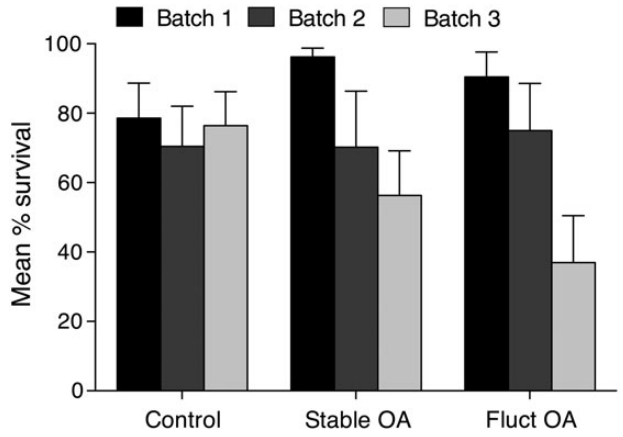

Figure 3. Percentage survival (mean ± s.e.) of barnacles for each pH treatment and batch over the experimental period ($n = 7$).

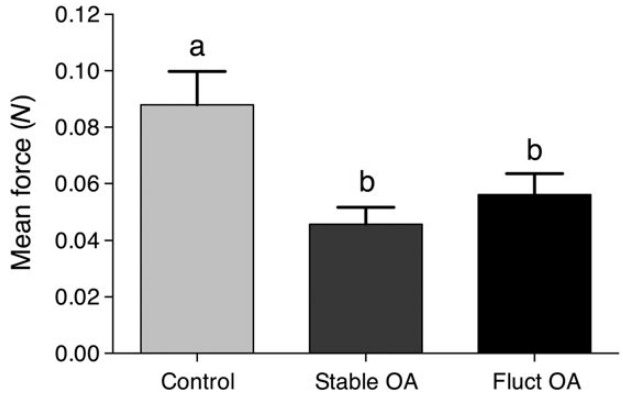

Figure 4. Force (mean ± s.e.) needed to penetrate the rostral shell plate of barnacles reared in three pH treatments, 12 weeks after cyprid settlement ($n = 14$). Letters indicate significantly different groups (Tukey's test, $p \leq 0.05$).

within batches and markedly negative, with 95% CIs that did not overlap zero for all but one of the batches (Figure 2; see also Supplementary Table S6). The variation in responses of different batches apparent in Figure 2 was not, however, reflected in formal statistical analysis (Supplementary Table S6). Shell strength was independent of shell thickness ($r = 0.183$, $p = 0.178$).

Discussion

Our finding that fluctuating OA had no effect on mean response, but caused an ~20-fold increase in *variance* of response (compared with stable OA; Figure 2) is unprecedented. The few published studies that have tested the effects of fluctuating OA (hereafter termed "fluctuating acidification") have found significant effects on mean responses (Alenius and Munguia, 2012; Dufault *et al.*, 2012; Cornwall *et al.*, 2013; Johnson *et al.*, 2014; Ou *et al.*, 2015), but none of these studies found the marked effects of fluctuating acidification on variance around mean responses that we report here.

In our experiments, greater variance in response ratios for fluctuating acidification was caused by some replicates showing markedly more positive responses, and some markedly more negative responses, than was seen under stable acidification. Without further investigation, the mechanisms by which this variation arose remain unclear; however, it is evident from Figure 2 that the growth and shell mineralogy of some individuals responded positively, and strongly, to fluctuating acidification (upper 95% CIs for fluctuating OA were typically ≈1.0 $\log_e$ unit, equivalent to nearly 3× greater growth, Ca content, or Ca:Mg ratio than was observed in the controls). Increased variance in mean response has previously been reported as indicative of "winners and losers" resulting from climate change (Loya *et al.*, 2001; Schlegel *et al.*, 2012). A key issue in this context is whether or not this variance reflects heritable genetic differences among barnacles or is rather the result of adult plasticity, acclimation, or environmental effects (Somero, 2010; Schlegel *et al.*, 2012). As our barnacle broodstock were collected simultaneously as newly settled juveniles from one location (Tjärnö, western Sweden), and raised together in the laboratory for 5 months at constant temperature and salinity before use in our experiments, we suggest that it is unlikely that the observed differences among replicates were due to parental acclimation to different environments and subsequent trans-generational inheritance of that plasticity (e.g. Miller *et al.*, 2012). Rather, it is far more plausible that the different responses we observed among replicates were the result of genetic differences among those replicates. It follows, therefore, that natural pH-fluctuations in present day—as well as acidified future—oceans may select for genetic variants that are not only tolerant of, but actually benefit from, future acidification. This is a biologically important finding that warrants further research.

In contrast to the results for growth and shell mineralogy, variances of response ratios for shell strength and survival did not differ between fluctuating and stable acidification treatments (Figure 2). This finding suggests a basic difference in the mechanisms by which growth and shell composition on the one hand, and survival and shell strength on the other, respond to fluctuating acidification. The mean shell strength was significantly, and negatively, influenced by acidification ($p = 0.013$, Supplementary Table S6), but the effects of fluctuating and stable acidification treatments did not differ (mean force to penetrate rostral plates was 0.089, 0.047, and 0.055 N for control, stable acidification, and fluctuating acidification treatments, respectively). Note that there were no predators in our microcosms and therefore no clear candidate mechanism for a causal link between shell strength and individual survival.

Previous studies have found that barnacles are generally tolerant of (stable) acidification. OA has been reported to only slightly decrease growth rates (*E. modestus*, Findlay *et al.*, 2010b), and have no—or small—effects on larval development rate, settlement, survival, and calcification rates (several species, McDonald *et al.*, 2009a; Pansch *et al.*, 2012, 2013). However, in keeping with our findings, other studies have reported that acidification resulted in weakened shells (*A. amphitrite*, McDonald *et al.*, 2009c; and *B. improvisus,* Pansch *et al.*, 2014), although McDonald *et al.* (2009b) also observed increased calcification in some parts of the shell (basal plate) under acidification. Acidification-induced changes in hardness of shells, such as those seen here (Figure 2, Supplementary Table S3), could have major implications for survival of barnacles. A weaker shell would leave them more susceptible to mortality by abrasion from ice and/or predation (e.g. from shore crabs, Buchsbaum, 2002).

Pansch *et al.* (2014) concluded that food limitation could enhance the negative effects of acidification on barnacles, but also mediate negative effects of OA when food was plentiful. We did not measure food supply in our study; however, we assumed this not to be limiting, as animals were fed every second day as well as receiving natural food through the flow-through seawater system.

The statistical strength of our experiments was aided by the use of three replicate batches of larvae from the same barnacle broodstock. Reproductively active pairs of *B. improvisus* in our cultures released batches of larvae on average every 5.81 d (range 5–62 d; JNH, pers. obs.), and our broodstock comprised over 1000 active individuals. Thus, by using three batches of larvae collected within 1 week, we maximized the likelihood that each batch derived from different parents and therefore represented a different genetic sample from the broodstock population (although we cannot exclude the possibility that a small number of parents may have contributed to both batch 1 and 3). Consistent with this aim, mean responses to shell strength and survival (the only two variables that showed a mean effect of treatment; Figure 2) were always greatest in batch 3, and weakest in batch 1 (Figure 2). As we noted earlier in our discussion of the consequences of increased variance in response ratios, this consistent difference between batches also constitutes evidence in support of the notion of "winners and losers"—although given the near-zero response ratios for batch 1 in both shell strength and survival (Figure 2), the distinction is perhaps better defined as being between "nonchalants and losers".

The differences we observed in the responses of different batches also emphasize the oft-repeated and oft-overlooked importance of using different genotypes (or populations) as replicates in experiments. Limiting the spatial and temporal extent of our samples—the "sampling universe"—limits the spatio-temporal extent of our conclusions, and can meaningfully constrain the validity and usefulness of our results (Havenhand *et al.*, 2010). Given this, we emphasize that the results we report here are for one population of *B. improvisus* from western Sweden, and that other populations of this same species—or indeed other species of barnacle—may well respond differently. Available evidence suggests that this is perhaps not likely in this case as phenotypic and genotypic differences among *B. improvisus* populations from Scandinavia and northern Germany are not great (Nasrolahi *et al.*, 2012; Wrange *et al.*, 2014; but see Pansch *et al.*, 2013), and consequently, we might expect other populations of this species to respond similarly to the patterns seen here. However, we stress the importance of testing for the effects of acidification—and other stressors—on multiple populations to ascertain the degree to which responses obtained from limited sampling universes can be generalized to whole species (e.g. Langer *et al.*, 2009; Walther *et al.*, 2010, 2011).

Although the field of OA research is still relatively new (Riebesell *et al.*, 2010), substantial advances have been made since Raven *et al.* (2005) brought this issue to a wider audience. The importance of fluctuating ocean pH is beginning to be recognized, as evidenced by the 200+ citations of Hofmann *et al.* (2011) in the 4 years since its publication. Yet few studies (to our knowledge, seven, including this one—see references above) have investigated experimentally the effects of simulated diurnal fluctuations in pH on organisms. Our finding that fluctuating pH has near-zero effects on mean responses of some, but not all, of the response variables we measured is perhaps not surprising: there is clear reporting bias against non-significant effects of OA (although this Special Issue takes an important step to address this bias). However, the increase in *variance* in responses that we observed under fluctuating acidification suggests that our previous focus on the effects of stable acidification has led us to miss environmentally and evolutionarily important responses of organisms. The challenge of investigating the combined effects of multiple simultaneously fluctuating environmental variables remains to be answered, but the results presented here and elsewhere (Alenius and Munguia, 2012; Dufault *et al.*, 2012; Cornwall *et al.*, 2013; Comeau *et al.*, 2014; Johnson *et al.*, 2014; Ou *et al.*, 2015) indicate that this is an important next step.

Supplementary data

Supplementary material is available at the *ICESJMS* online version of the manuscript.

Acknowledgements

This work was supported by a Linnaeus-grant from the Swedish Research Councils, VR and Formas (http://www.cemeb.science.gu.se). We are grateful to Martin Ogemark for maintaining the barnacle culturing barnacle facility from which we obtained the organisms used in this study.

References

Abramoff, M., Magalhaes, P., and Ram, S. 2004. Image processing with Image J. Biophotonics International, July: 1–7.

Agnew, D. J., and Taylor, A. C. 1986. Seasonal and diel variations of some physicochemical parameters of boulder shore habitats. Ophelia, 25: 83–95.

Alenius, B., and Munguia, P. 2012. Effects of pH variability on the intertidal isopod, *Paradella dianae*. Marine and Freshwater Behaviour and Physiology, 45: 245–259.

Berntsson, K. M., Jonsson, P. R., Lejhall, M., and Gatenholm, P. 2000. Analysis of behavioural rejection of micro-textured surfaces and implications for recruitment by the barnacle *Balanus improvisus*. Journal of Experimental Marine Biology and Ecology, 251: 59–83.

Blackford, J. C., and Gilbert, F. J. 2007. pH variability and CO_2 induced acidification in the North Sea. Journal of Marine Systems, 64: 229–241.

Blom, S. E. 1965. *Balanus improvisus* Darwin on the west coast of Sweden. Zoologiska bidrag från Uppsala, 37: 59–76.

Buchsbaum, C. 2002. Predation on barnacles on intertidal and subtidal mussel beds in the Wadden Sea. Helgoland Marine Research, 56: 37–43.

Challener, R. C., Robbins, L. L., and McClintock, J. B. 2015. Variability of the carbonate chemistry in a shallow, seagrass-dominated ecosystem: implications for ocean acidification experiments. Marine and Freshwater Research, http://dx.doi.org/10.1071/MF14219.

Comeau, S., Edmunds, P. J., Spindel, N. B., and Carpenter, R. C. 2014. Diel pCO_2 oscillations modulate the response of the coral *Acropora hyacinthus* to ocean acidification. Marine Ecology Progress Series, 501: 99–111.

Cornwall, C. E., Hepburn, C. D., McGraw, C. M., Currie, K. I., Pilditch, C. A., Hunter, K. A., Boyd, P. W., *et al.* 2013. Diurnal fluctuations in seawater pH influence the response of a calcifying macroalga to ocean acidification. Proceedings of the Royal Society B—Biological Sciences, 280: doi: 10.1098/rspb.2013.2201.

Darwin, C. 1859. On the Origin of Species by Means of Natural Selection. John Murray, London. 502 pp.

de Rivera, C. E., Steves, B. P., Fofonoff, P. W., Hines, A. H., and Ruiz, G. M. 2011. Potential for high-latitude marine invasions along western North America. Diversity and Distributions, 17: 1198–1209.

Duarte, C. M., Hendriks, I. E., Moore, T. S., Olsen, Y. S., Steckbauer, A., Ramajo, L., Carstensen, J., *et al.* 2013. Is ocean acidification an open-ocean syndrome? Understanding anthropogenic impacts on seawater pH. Estuaries and Coasts, 36: 221–236.

Dufault, A. M., Cumbo, V. R., Fan, T-Y., and Edmunds, P. J. 2012. Effects of diurnally oscillating pCO(2) on the calcification and survival of coral recruits. Proceedings of the Royal Society B—Biological Sciences, 279: 2951–2958.

Findlay, H. S., Burrows, M. T., Kendall, M. A., Spicer, J. I., and Widdicombe, S. 2010a. Can ocean acidification affect population

dynamics of the barnacle *Semibalanus balanoides* at its southern range edge? Ecology, 91: 2931–2940.

Findlay, H. S., Kendall, M. A., Spicer, J. I., and Widdicombe, S. 2010b. Post-larval development of two intertidal barnacles at elevated CO_2 and temperature. Marine Biology, 157: 725–735.

Findlay, H. S., Kendall, M. A., Spicer, J. I., and Widdicombe, S. 2010c. Relative influences of ocean acidification and temperature on intertidal barnacle post-larvae at the northern edge of their geographic distribution. Estuarine Coastal and Shelf Science, 86: 675–682.

Foster, B. A. 1970. Responses and acclimation to salinity in adults of some balanomorph barnacles. Philosophical Transactions of the Royal Society of London Series B—Biological Sciences, 256: 377–400.

Foster, B. A. 1987. Barnacle ecology & adaptation. In Crustacean Issue 5: Barnacle Biology. Ed. by A. J. Southward. A.A. Balkema, Rotterdam.

Galil, B. S., Clark, P. F., and Carlton, J. T. 2011. In the Wrong Place—Alien Marine Crustaceans: Distribution Biology and Impacts. 720 pp.

Gompertz, B. 1825. On the nature of the function expressive of the law of human mortality, and on a new mode of determining the value of life contingencies. Philosophical Transactions of the Royal Society, 115: 513–583.

Havenhand, J. N., Dupont, S., and Quinn, G. P. 2010. Designing ocean acidification experiments to maximise inference. *In* Guide to Best Practices for Ocean Acidification Research and Data Reporting, pp. 67–80. Ed. by U. Riebesell, V. J. Fabry, L. Hansson, and J-P. Gattuso. Pulications Office of the European Union, Luxembourg.

Hoffmann, A. A., and Parsons, P. A. 1997. Extreme Environmental Change and Evolution. Cambridge University Press, Melbourne. 272 pp.

Hofmann, G. E., Smith, J. E., Johnson, K. S., Send, U., Levin, L. A., Micheli, F., Paytan, A., *et al.* 2011. High-frequency dynamics of ocean pH: a multi-ecosystem comparison. PLoS ONE, 6: e28983.

IPCC. 2014. Climate Change 2014: the Physical Science Basis. Summary for Policymakers. 36 pp.

Jacobs, M. W., and Podolsky, R. D. 2010. Variety is the spice of life histories: comparison of intraspecific variability in marine invertebrates. Integrative and Comparative Biology, 50: 630–642.

Johnson, M. D., Moriarty, V. W., and Carpenter, R. C. 2014. Acclimatization of the crustose coralline alga *Porolithon onkodes* to variable pCO(2). PloS ONE, 9: e87678.

Kopp, M., and Matuszewski, S. 2014. Rapid evolution of quantitative traits: theoretical perspectives. Evolutionary Applications, 7: 169–191.

Koricheva, J., Gurevitch, J., and Mengersen, K. 2013. Handbook of Meta-analysis in Ecology & Evolution. Princeton University Press, Princeton. 498 pp.

Kroeker, K. J., Kordas, R. L., Crim, R., Hendriks, I. E., Ramajo, L., Singh, G. S., Duarte, C. M., *et al.* 2013. Impacts of ocean acidification on marine organisms: quantifying sensitivities and interaction with warming. Global Change Biology, 19: 1884–1896.

Langer, G., Nehrke, G., Probert, I., Ly, J., and Ziveri, P. 2009. Strain-specific responses of *Emiliania huxleyi* to changing seawater carbonate chemistry. Biogeosciences, 6: 2637–2646.

Lawson, C. R., Vindenes, Y., Baily, L., and van den Pol, M. 2015. Environmental variation and population responses to global change. Ecology Letters, 18: 724–736.

Leppakoski, E., and Olenin, S. 2000. Non-native species and rates of spread: lessons from the brackish Baltic Sea. Biological Invasions, 2: 151–163.

Lewis, E., and Wallace, D. 1998. Program developed for CO_2 system calculations. ICES Document 4735.

Loya, Y., Sakai, K., Yamazato, K., Nakano, Y., and Sambali, H. 2001. Coral bleaching: the winners and the losers. Ecology Letters, 4: 122–131.

McDonald, M. R., McClintock, J. B., Amsler, C. D., Rittschof, D., Angus, R. A., and Orihuela, B. 2009a. Effects of ocean acidification on larval development and settlement of the common intertidal barnacle *Amphibalanus amphitrite*. Integrative and Comparative Biology, 49: E270.

McDonald, M. R., McClintock, J. B., Amsler, C. D., Rittschof, D., Angus, R. A., Orihuela, B., and Lutostanski, K. 2009b. Effects of ocean acidification over the life history of the barnacle *Amphibalanus amphitrite*. Marine Ecology Progress Series, 385: 179–187.

Melzner, F., Stange, P., Trubenbach, K., Thomsen, J., Casties, I., Panknin, U., Gorb, S. N., *et al.* 2011. Food supply and seawater pCO(2) impact calcification and internal shell dissolution in the blue mussel *Mytilus edulis*. PloS ONE, 6: E24223.

Miller, G. M., Watson, S. A., Donelson, J. M., McCormick, M. I., and Munday, P. L. 2012. Parental environment mediates impacts of increased carbon dioxide on a coral reef fish. Nature Climate Change, 2: 858–861.

Nakagawa, S., and Cuthill, I. C. 2007. Effect size, confidence interval and statistical significance: a practical guide for biologists. Biological Reviews, 82: 591–605.

Nasrolahi, A., Pansch, C., Lenz, M., and Wahl, M. 2012. Being young in a changing world: how temperature and salinity changes interactively modify the performance of larval stages of the barnacle *Amphibalanus improvisus*. Marine Biology, 159: 331–340.

Orr, J. C., Fabry, V. J., Aumont, O., Bopp, L., Doney, S. C., Feely, R. A., Gnanadesikan, A., *et al.* 2005. Anthropogenic ocean acidification over the twenty-first century and its impact on calcifying organisms. Nature, 437: 681–686.

Ou, M., Hamilton, T., Eom, J., Lyall, E., Gallup, J., Jiang, A., Lee, J., *et al.* 2015. Responses of pink salmon to CO_2-induced aquatic acidification. Nature Climate Change, 5: 950–955.

Pansch, C., Nasrolahi, A., Appelhans, Y. S., and Wahl, M. 2012. Impacts of ocean warming and acidification on the larval development of the barnacle *Amphibalanus improvisus*. Journal of Experimental Marine Biology and Ecology, 420: 48–55.

Pansch, C., Schaub, I., Havenhand, J., and Wahl, M. 2014. Habitat traits and food availability determine the response of marine invertebrates to ocean acidification. Global Change Biology, 20: 765–777.

Pansch, C., Schlegel, P., and Havenhand, J. 2013. Larval development of the barnacle *Amphibalanus improvisus* responds variably but robustly to near-future ocean acidification. ICES Journal of Marine Science, 70: 805–811.

Quinn, G., and Keough, M. 2002. Experimental Design and Data Analysis for Biologists. Cambridge University Press, Cambridge, UK. 538 pp.

Raven, J., Caldeira, K., Elderfield, H., Hoegh-Guldberg, O., Liss, P., Riebesell, U., Shepherd, J., *et al.* 2005. Ocean Acidification due to Increasing Atmospheric Carbon Dioxide. Royal Society, London. 57 pp.

Riebesell, U., Fabry, V. J., Hansson, L., and Gattuso, J-P. 2010. Guide to best practices for ocean acidification research and reporting. Publications Office of the EU, Luxembourg. 260 pp.

Schlegel, P., Havenhand, J. N., Gillings, M. R., and Williamson, J. E. 2012. Individual variability in reproductive success determines winners and losers under ocean acidification: a case study with sea urchins. PloS ONE, 7: E5311.

SMHI. 2011. Swedish Oceanographic Data Centre. http://www.smhi.se/oceanografi/oce_info_data/SODC/download_en.htm.

Somero, G. N. 2010. The physiology of climate change: how potentials for acclimatization and genetic adaptation will determine "winners" and "losers". Journal of Experimental Biology, 213: 912–920.

Stenseth, N. C., Mysterud, A., Ottersen, G., Hurrell, J. W., Chan, K-S., and Lima, M. 2002. Ecological effects of climate fluctuations. Science, 297: 1292–1296.

Takeshita, Y., Frieder, C. A., Martz, T. R., Ballard, J. R., Feely, R. A., Kram, S., Nam, S., *et al.* 2015. Including high frequency variability in coastal ocean acidification projections. Biogeosciences Discussion, 12: 7125–7176.

Walther, K., Anger, K., and Portner, H. O. 2010. Effects of ocean acidification and warming on the larval development of the spider crab *Hyas araneus* from different latitudes (54 degrees vs. 79 degrees N). Marine Ecology Progress Series, 417: 159–170.

Walther, K., Sartoris, F. J., and Portner, H. 2011. Impacts of temperature and acidification on larval calcium incorporation of the spider crab *Hyas araneus* from different latitudes (54 degrees vs. 79 degrees N). Marine Biology, 158: 2043–2053.

Wootton, J. T., Pfister, C. A., and Forester, J. D. 2008. Dynamic patterns and ecological impacts of declining ocean pH in a high-resolution multi-year dataset. Proceedings of the National Academy of Sciences of the United States of America, 105: 18848–18853.

Wrange, A. L., Andre, C., Lundh, T., Lind, U., Blomberg, A., Jonsson, P., and Havenhand, J. 2014. The importance of plasticity and local adaptation for coping with changing salinity in coastal areas: a test case with barnacles in the Baltic Sea. BMC Evolutionary Biology, 14: 156–170.

Handling editor: Stéphane Plourde

ICES Journal of Marine Science

ICES Journal of Marine Science (2016), 73(3), 604–612. doi:10.1093/icesjms/fsv232

Contribution to Special Issue: 'Towards a Broader Perspective on Ocean Acidification Research'

Original Article

Temporal fluctuations in seawater pCO_2 may be as important as mean differences when determining physiological sensitivity in natural systems

Daniel P. Small[1]*, Marco Milazzo[2], Camilla Bertolini[3], Helen Graham[4,5], Chris Hauton[6], Jason M. Hall-Spencer[7], and Samuel P. S. Rastrick[6,8]

[1]*Biology Department, St Francis Xavier University, 2320 Notre Dame Avenue, Antigonish, NS, Canada B2G 2W5*
[2]*Department of Earth and Marine Science, Università degli studi di Palermo, CoNISMa, Via Archirafi 20, I-90123 Palermo, Italy*
[3]*School of Biological Sciences, Medical Biology Centre, Queen's University Belfast, 97 Lisburn Road, Belfast, Northern Ireland BT9 7BL, UK*
[4]*School of Marine Science and Technology, Ridley Building, Newcastle University, Newcastle upon Tyne, Tyne and Wear NE1 7RU, UK*
[5]*Uni Research Environment, Postboks 7810, 5020 Bergen, Norway*
[6]*Ocean and Earth Science, National Oceanography Centre Southampton, University of Southampton Waterfront Campus, European Way, Southampton SO14 3ZE, UK*
[7]*Marine Biology and Ecology Research Centre, School of Marine Science and Engineering, Plymouth University, Drake Circus, Plymouth, Devon PL4 8AA, UK*
[8]*Institute of Marine Research, PO Box 1870 Nordness, 5870 Bergen, Norway*

**Corresponding author: e-mail: dsmall@stfx.ca*

Small, D. P., Milazzo, M., Bertolini, C., Graham, H., Hauton, C., Hall-Spencer, J. M., and Rastrick, S. P. S. Temporal fluctuations in seawater pCO_2 may be as important as mean differences when determining physiological sensitivity in natural systems. – ICES Journal of Marine Science, 73: 604–612.

Received 13 June 2015; revised 9 November 2015; accepted 10 November 2015; advance access publication 8 December 2015.

Most studies assessing the impacts of ocean acidification (OA) on benthic marine invertebrates have used stable mean pH/pCO_2 levels to highlight variation in the physiological sensitivities in a range of taxa. However, many marine environments experience natural fluctuations in carbonate chemistry, and to date little attempt has been made to understand the effect of naturally fluctuating seawater pCO_2 (pCO_{2sw}) on the physiological capacity of organisms to maintain acid–base homeostasis. Here, for the first time, we exposed two species of sea urchin with different acid–base tolerances, *Paracentrotus lividus* and *Arbacia lixula*, to naturally fluctuating pCO_{2sw} conditions at shallow water CO_2 seep systems (Vulcano, Italy) and assessed their acid–base responses. Both sea urchin species experienced fluctuations in extracellular coelomic fluid pH, pCO_2, and $[HCO_3^-]$ (pH_e, pCO_{2e}, and $[HCO_3^-]_e$, respectively) in line with fluctuations in pCO_{2sw}. The less tolerant species, *P. lividus*, had the greatest capacity for $[HCO_3^-]_e$ buffering in response to acute pCO_{2sw} fluctuations, but it also experienced greater extracellular hypercapnia and acidification and was thus unable to fully compensate for acid–base disturbances. Conversely, the more tolerant *A. lixula* relied on non-bicarbonate protein buffering and greater respiratory control. In the light of these findings, we discuss the possible energetic consequences of increased reliance on bicarbonate buffering activity in *P. lividus* compared with *A. lixula* and how these differing physiological responses to acute fluctuations in pCO_{2sw} may be as important as chronic responses to mean changes in pCO_{2sw} when considering how CO_2 emissions will affect survival and success of marine organisms within naturally assembled systems.

Keywords: acid–base balance, natural variability, ocean acidification, sea urchin, volcanic vents.

Introduction

Most studies investigating the effects of elevated pCO_2 associated with ocean acidification (OA) on marine invertebrates have focused on stable mean differences in seawater pCO_2 (pCO_{2sw}). Such studies have indicated a range of variability in tolerances to elevated pCO_2 between species and phyla (e.g. Harvey *et al.*, 2013; Kroeker *et al.*, 2013), which drive shifts in species distributions along natural pCO_{2sw} gradients (e.g. Calosi *et al.*, 2013a, b). To understand species responses to elevated pCO_2, we need to know how organisms tolerate natural variations in carbonate conditions (Hofmann *et al.*, 2011). While large areas of Open Ocean vary little in seawater pCO_2 and pH, wide fluctuations occur in coastal marine habitats (e.g. Price *et al.*, 2012; Reum *et al.*, 2014). Upwelling systems, such as the eastern Pacific, have relatively high pCO_2 levels and aragonite under-saturation (Manzello, 2010; Harris *et al.*, 2013). Although nearshore carbonate chemistry has wide seasonal (Hauri *et al.*, 2012; Harris *et al.*, 2013) and daily fluctuations (Hofmann *et al.*, 2011), the underlying trend is for increasing CO_2 enrichment and aragonite under-saturation due mainly to burning fossil fuels (IPCC, 2013). In some instances, coastal systems, such as those in fjords and estuaries, can exceed mean atmospheric CO_2 due to high respiration rates in organic-rich conditions (Borges and Abril, 2011; Reum *et al.*, 2014). In addition to carbon flux from coastal respiration, photosynthesis and calcification can also drive short-term fluctuations in pO_2, pCO_2, pH, and total alkalinity (A_T) (e.g. Truchot and Duhamel-Jouve, 1980; Mucci *et al.*, 2011). As our understanding of nearshore carbonate chemistry increases, we must take this into account when selecting the appropriate pCO_2 levels in OA experiments (Andersson and Mackenzie, 2012; McElhany and Busch, 2013; Reum *et al.*, 2014). Understanding how organisms cope with their current environment can provide valuable insights into how species will respond to future OA. Specifically, the fluctuations in pCO_2 experienced by coastal species in many habitats are far greater in magnitude than the predicted long-term increase in mean CO_2 due to OA (Hofmann *et al.*, 2010; Joint *et al.*, 2011). Gaining a better understanding of the effect of fluctuating carbonate chemistry on marine organisms may provide basic insights into variations in OA tolerance found in physiological observations (Dupont and Pörtner, 2013).

The ability to maintain extracellular homeostasis is important in determining tolerance to elevated pCO_{2sw} (Whiteley, 2011). Most organisms are able to regulate their extracellular pH through acid–base buffering mechanisms, but this can be energetically costly (Pörtner *et al.*, 2004). Differences in extracellular pH regulatory capabilities and the ability to regulate metabolic rates between species indicate that certain taxa, e.g. teleost fish, brachyuran crustaceans, and cephalopod molluscs, will be more tolerant of elevated pCO_2 than others, including bivalve molluscs and echinoderms (Melzner *et al.*, 2009). Interspecies variability of acid–base regulation capabilities in closely related and/or co-habiting species may underpin comparative sensitivities to OA (e.g. Pane and Barry, 2007; Bressan *et al.*, 2014), which are important if we are to predict community and ecosystem responses to OA. It has been recognized that species living in distinctly different pCO_2 environments have differences in acid–base regulatory capabilities, for example, shallow water species are more able to compensate for acid–base disturbances than deep-water species (Pane and Barry, 2007). While such studies demonstrate variations in acid–base regulatory capabilities within phyla, they do not reveal the community or ecosystem effects of differing species sensitivities. It is these differences in sensitivities to elevated pCO_2 which drive decreases in species richness and increased dominance of tolerant species at naturally acidified vent sites (Kroeker *et al.*, 2011).

Understanding how closely related species living in the same habitat deal with natural pCO_2 conditions would form a basis to our understanding of how communities will be affected by future climate change. Differences in physiological regulatory capabilities have been suggested to drive differences in distribution patterns between closely related species across natural gradients in pCO_{2sw}, such as those found at volcanic CO_2 vent sites (e.g. Suggett *et al.*, 2012; Calosi *et al.*, 2013a, b). However, to date, all such studies on comparative growth and physiology have focused on chronic mean differences in pCO_{2sw} (e.g. Suggett *et al.*, 2012; Calosi *et al.*, 2013a, b), despite pCO_{2sw} at vent sites exhibiting considerable variation within the space of hours to days (Boatta *et al.*, 2013). To date, we have little understanding of how short-term natural fluctuations in pCO_{2sw} affect animal acid–base regulation and so distribution at vent sites. An example of this can be seen in the distributions of the sea urchin species used in the present study, *Arbacia lixula* and *Paracentrotus lividus*, at the CO_2 vent sites off Isola Vulcano (Sicily, Italy). Despite a greater capacity for bicarbonate buffering in response to stable elevated pCO_{2sw}, *P. lividus* decreases in population density at higher pCO_{2sw} closer to the vent sites compared with *A. lixula* (Calosi *et al.*, 2013a). This indicates that the ability to buffer stable increases in mean pCO_{2sw} via increased $[HCO_3^-]$ is not the primary physiological response driving distribution at the vent sites. The present study investigates the hypothesis that for species such as *P. lividus*, an increase in acute natural fluctuations in pCO_{2sw} may pose as great or a greater challenge to maintaining acid–base regulation as chronic mean elevations in pCO_{2sw} due to the constant need to up- or down-regulate possibly costly bicarbonate buffering responses. Changes in the distribution of related species across present natural pCO_{2sw} gradients at volcanic seep sites, or, in response to future climate change may have as much to do with physiological responses to increased acute fluctuations in pCO_{2sw} as with chronic mean elevations in pCO_{2sw}.

To test this hypothesis, *P. lividus* and *A. lixula* collected from control areas were exposed to acute natural fluctuations in pCO_{2sw} generated by the volcanic CO_2 vent. The coelomic fluid acid–base balance (pH_e, pCO_{2e}, and $[HCO_3^-]_e$) of *P. lividus* and *A. lixula* was measured every 6 h over the course of 4 d (90 h, total of 16 time points) in an attempt to understand the effect of fluctuating pCO_{2sw} conditions on the distribution of *A. lixula* compared with *P. lividus*. Individual responses in acid–base parameters to changes in pCO_{2sw} were determined along with differences in bicarbonate and non-bicarbonate buffering capacity between the two species. Bicarbonate and non-bicarbonate buffering capacity were determined by davenport models where bicarbonate buffering is indicated by increases in $[HCO_3^-]_e$ above the non-bicarbonate buffer line (NBL) and changes in non-bicarbonate buffering are indicated by changes in the slope of the NBL. Changes in non-bicarbonate buffering were also linked to changes coelomic fluid protein concentration.

Material and methods

Animal collection

On 18 May 2013, *A. lixula* and *P. lividus* ($n = 18$ *per* species) were collected from a 2–3 m depth in Ponente Bay, Vulcano well away from the effects of seabed CO_2 vents (coordinates = 38°25.185′N, 14°57.074′E). Sea urchins were immediately transported in fully

Table 1. Seawater chemistry throughout the exposure period, measured in the experimental tanks at each time point (means ± s.e.).

Seawater parameter	Control treatment	Fluctuating treatment
pH (NBS)	8.04 ± 0.01*	7.72 ± 0.07*
pH max	8.12	8.04
pH min	7.95	7.14
A_T (mEq kg^{-1})	2.53 ± 0.01	2.54 ± 0.01
Temperature (°C)	19.6 ± 0.2	19.5 ± 0.2
Salinity	38.2 ± 0.1	38.2 ± 0.1
pCO_2 (μatm)	608.8 ± 19.1*	1742.3 ± 352.7*
pCO_2 max	779.3	5497.4
pCO_2 min	492.5	599
Ω_{Cal}	3.97 ± 0.09*	2.34 ± 0.28*
Ω_{Ara}	2.59 ± 0.06*	1.52 ± 0.18*
HCO_3^- (μmol kg^{-1})	2102 ± 9*	2295 ± 28*
CO_3^{2-} (μmol kg^{-1})	170.1 ± 4.1*	100.2 ± 12.0*

*Significant differences between treatments ($p < 0.05$).

aerated aquaria (vol. = 15 l) to a volcanic CO_2 vent gradient in Levante Bay, Vulcano (coordinates = 38°25.189′ N, 14°57.711′E). The volume of each sea urchin was calculated by water displacement. Individuals were then blotted dry with a paper towel and wet body mass determined using a high-precision balance (SI-603, Denver Instrument, Bohemia, NY, USA). Individuals were then sealed in mesh containers (vol. = 1 l, mesh diameter = 1 cm, see Calosi *et al.*, 2013a) and placed into large aerated holding tanks (vol. = 60 l) containing control seawater collected from a control site in Levante Bay (salinity: 38, temperature: 19°C, coordinates = 38°25.215′N, 14°57.797′E, Table 1) for a recovery period of 6 h.

Experimental exposure

To investigate the effect of natural variations in pCO_{2sw} on sea urchin coelomic fluid acid–base balance, individuals were randomly assigned to one of two treatments; a stable control pCO_{2sw}, and naturally fluctuating pCO_{2sw} ($n = 9$ individuals *per* species *per* treatment). Exposure to naturally fluctuating pCO_{2sw} was achieved by pumping seawater into a holding tank from Levante Bay (coordinates = 38°25.176′N, 14°57.695′E) using a submersible water pump (FSP400DW, Adeo Services, Lille, France, max flow = 7500 l h^{-1}). The release of CO_2 from the vent site generated a natural pH and pCO_2 gradient (Hall-Spencer *et al.*, 2008; Johnson *et al.*, 2012; Boatta *et al.*, 2013; Milazzo *et al.*, 2014). The site from which fluctuating pCO_{2sw} was obtained was ca. 300 m from the main gas vents away from the influence of H_2S and heavy metals (Boatta *et al.*, 2013; Vizzini *et al.*, 2013). Exposure to stable pCO_{2sw} was achieved by pumping water directly from a site 390 m from the main CO_2 vent (Boatta *et al.*, 2013). Sea urchins were exposed to either fluctuating pCO_{2sw} or stable pCO_{2sw} for 90 h. Measurements of pH, temperature, and salinity in the tanks were taken at each experimental time point with a hand-held multiparameter instrument (Professional Plus YSI, YSI Inc., Yellow Springs, OH, USA). Water samples for total alkalinity (A_T) were collected daily from inflowing water from each site during the experiment. One-hundred-millilitre water sample was passed through 0.2 μm pore size filters, poisoned with 0.05 ml of 50% $HgCl_2$ to avoid biological alteration, and then stored in the dark at 4°C. Three replicate subsamples were analysed at 25°C using a titration system. The pH was measured at 0.02 ml increments of 0.1 N HCl. Total alkalinity was calculated from the Gran function applied to pH variations from 4.2 to 3.0, as mEq kg^{-1} from the slope of the curve HCl volume vs. pH. Total alkalinity measurements were corrected using standards provided by A.G. Dickson (batch 99 and 102). Parameters of the carbonate system (pCO_2, CO_3^{2-}, HCO_3^-) and saturation state of calcite and aragonite were calculated from pH, A_T, temperature and salinity using the free-access CO_2SYS (Lewis and Wallace, 1998) with constants provided by Mehrbach *et al.* (1973) refitted by Dickson and Millero (1987) and KSO_4 constants from Dickson (1990). Water chemistry throughout the exposure period is shown in Table 1.

Determination of coelomic fluid acid–base balance

The acid–base balance of sea urchin coelomic fluid was determined following the methods in Calosi *et al.* (2013a). Briefly, coelomic fluid (vol. = 100 μl) was extracted anaerobically from each individual using a gas-tight syringe (Gas-tight 1710 100 μl syringe with an RN 22S gauge needle, Hamilton Co., Bonaduz, Switzerland) inserted 1 cm into the coelomic cavity *via* the peristomial membrane at 6 h intervals for 90 h (4 d, 16 time points). Total bound and dissolved CO_2 (TCO_2) was analysed instantly in a subsample of coelomic fluid (vol. = 30 μl) using a TCO_2 analyser (956D TCO_2 Analyser, Corning Diagnostics, Cambridge, MA, USA). For determination of coelomic pH, the remaining coelomic fluid (vol. = 70 μl) was rapidly (within 5 s) injected into a 0.5 ml microcentrifuge tube (TUL-649-010L, Fisher Scientific, Loughborough, UK) and placed on a micro pH probe (Micro-Inlab pH combination electrode, Metter Toledo, Leicester, UK) connected to a pH meter (Seven Easy pH meter, Metter Toledo) forming a gas-tight seal between the air and sample (after, Rastrick *et al.*, 2014).

An additional 150 μl of coelomic fluid was extracted from nine freshly collected reference individuals from the collection site of *A. lixula* and *P. lividus*, and immediately frozen for later determination of coelomic fluid protein concentration ($[protein]_e$), NBL, and the first apparent dissociation constants of carbonic acid (pK_1) in urchin coelomic fluid. NBL were determined after Rastrick *et al.* (2014), modified from Spicer *et al.* (1988). Briefly, the 100 μl coelomic fluid sample from each reference individual was injected into a glass diffusion chamber and equilibrated to 0.1, 1.0, and 2.5% CO_2 (mixed with O_2-balanced N_2) in turn, using gas supplied by a gas mixing pump (Wösthoff pump, Wösthoff GmbH, Bochum, Germany). The sample was constantly measured for pH using a micro pH electrode connected to a pH meter. Samples were agitated with a magnetic stirrer and considered equilibrated when the pH value stopped decreasing (*circa* 15 min). At equilibration pH, the pH value was recorded and TCO_2 measured in a subsample (vol. = 30 μl) using a TCO_2 analyser. This was repeated for each pCO_2 level. NBLs were constructed using the Henderson–Hasselbalch equation in the following forms:

$$pCO_2 = \frac{TCO_2}{\alpha(10^{pH-pK'_1} + 1)}, \quad (1)$$

$$[HCO_3^-] = 10^{pH-pK'_1}\alpha pCO_2, \quad (2)$$

where α is the CO_2 solubility coefficient in seawater at 20°C (0.3293 mmol l^{-1} kPa^{-1}; Spicer *et al.*, 1988; after Harvey, 1955) and pK'_1 calculated as 6.03 for *P. lividus* and 5.91 for *A. lixula* at 20°C using Equation (3):

$$pK'_1 = pH\left(\frac{\mathrm{Log}_{10}(TCO_2 - \alpha pCO_2)}{\alpha pCO_2}\right), \quad (3)$$

$[HCO_3^-]_e$ and pCO_{2e} in experimental individuals were calculated from pH_e and TCO_{2e} determined above using Equations (4) and (5), respectively (Truchot, 1976);

$$pCO_2 = \frac{TCO_2}{\alpha(10^{pH-pK'_1}+1)}, \quad (4)$$

$$HCO_3^- = TCO_2 - \alpha pCO_2. \quad (5)$$

Determination of coelomic fluid protein concentration

$[Protein]_e$ concentration was determined by the Bradford coomassie blue assay; 10 µl of each coelomic fluid sample was diluted in to 90 µl of H_2O, 5 µl of each diluted sample was plated in to a 96 micro well plate with 250 µl of Coomassie reagent (23200, Thermo Scientific, Pierce Biotechnology, Rockford, IL, USA). After 10 min, the absorbance was read at 595 nm (iMark Microplate Absorbance Reader, Bio-Rad Laboratories, Hercules, CA, USA) and compared with albumin protein standards at nine concentrations from 0 to 2000 µg ml^{-1} (23209, Thermo Scientific) treated in the same way.

Statistical analysis

The pH_e, pCO_{2e}, $[HCO_3^-]_e$, and $[protein]_e$ of field collected control *A. lixula* and *P. lividus* were compared using a one-way ANOVA. To test if the possible relationship between pCO_{2e}, pH_e, or $[HCO_3^-]_e$ (dependant factors) and pCO_{2sw} (covariate) varied between site (control and fluctuating) and species (fixed factors), a repeated-measures, nested GLMM (with individual urchin as a random factor nested within site as a fixed factor) was performed, which considers the fact that the individuals sampled at the two sites are not true replicates (e.g. Collard *et al.*, 2016). To understand the species-specific differences in response to fluctuating pCO_{2sw}, linear regressions were also performed for each acid–base parameter vs. pCO_{2sw} on each individual. The slope of the individual regressions (B) was obtained, and the average for each species calculated. The average B for changes in *P. lividus* pH_e, pCO_{2e}, and $[HCO_3^-]_e$ with pCO_{2sw} was compared against that of *A. lixula* using a Student's t-test to determine any significant differences in coelomic fluid acid–base response with variations in pCO_{2sw}. The standard deviation of pH_e, pCO_{2e}, and $[HCO_3^-]_e$ for each individual were also compared using a Student's t-test to determine differences in acid–base variation between *A. lixula* and *P. lividus*. All statistical procedures were performed using SPSS software (V18, SPSS, Chicago, IL, USA); all values are presented as means ± standard error.

Results

Urchin coelomic fluid acid–base parameters before exposure

The acid–base balance of coelomic fluid from field collected (pH = 8.05) *A. lixula* was significantly different from that of *P. lividus* (Table 2). In summary, pH_e and $[HCO_3^-]_e$ were significantly lower in *A. lixula* than *P. lividus* ($F_{min1,17} = 101.692$, $p < 0.001$), while there was no significant difference in pCO_{2e} ($F_{1,17} = 0.628$, $p > 0.05$). The $[protein]_e$ of *A lixula* was almost threefold higher than in *P. lividus* ($F_{1,17} = 10.272$, $p < 0.01$), and the calculated NBL for *A. lixula* ($y = -1.504 \times +12.606$, $R^2 = 0.8254$) was significantly lower than that of *P. lividus* ($y = -0.493 \times +7.6358$, $R^2 = 0.7299$, $t_{10} = 8.925$, $p < 0.001$).

The effect of fluctuating pCO_{2sw} on urchin coelomic fluid acid–base balance

There was a significant three-way interaction between site, species, and pCO_{2sw} on pCO_{2e} ($F_{39.4,1} = 5.587$, $p < 0.05$, Figure 1). The relationship between pCO_{2sw} and pCO_{2e} in *P. lividus* was significantly different between the fluctuating and the control treatments ($F_{137.9,1} = 7.650$, $p < 0.01$, Figure 1). In contrast, *A. lixula* showed no significant difference between the two treatments ($F_{137.9,1} = 0.333$, $p = 0.565$, Figure 1).

There was also a significant three-way interaction between site, species, and pCO_{2sw} on pH_e ($F_{44.6,1} = 10.633$, $p < 0.01$, Figure 1). The relationship between pCO_{2sw} and pH_e in *P. lividus* was significantly different between the fluctuating and the control treatments ($F_{118.0,1} = 10.581$, $p < 0.01$, Figure 1), while *A. lixula* again showed no significant difference between the two treatments ($F_{118.0,1} = 0.106$, $p = 0.745$, Figure 1).

The relationship between pCO_{2sw} and $[HCO_3^-]_e$ also demonstrated a significant three-way interaction between site, species, and pCO_{2sw} ($F_{56.8,1} = 61.378$, $p < 0.001$, Figure 1). However, the relationship between pCO_{2sw} and $[HCO_3^-]_e$ is different between the fluctuating and the control treatments in both *P. lividus* ($F_{157.7,1} = 8.905$, $p < 0.01$, Figure 1) and *A. lixula* ($F_{157.9,1} = 7.719$, $p < 0.01$, Figure 1). This is because both species show some significant increase in $[HCO_3^-]_e$ as seawater pCO_2 increases; however, this response was significantly greater in *P. lividus* compared with *A. lixula* (where a bicarbonate response was extremely limited) when exposed to natural fluctuations in pCO_{2sw} ($F_{44,8,1} = 475.914$, $p < 0.001$, Figure 1).

While fluctuating pCO_{2sw} had a significant effect on the coelomic acid–base status of both species, the effect was greater on *P. lividus* than *A. lixula*, as demonstrated by comparing the average slopes of the regressions (B value) performed on the pH_e, pCO_{2e}, and $[HCO_3^-]_e$ of all individuals against pCO_{2sw} (Table 3). The pH_e of both *A. lixula* and *P. lividus* showed a negative relationship with pCO_{2sw}; however, the average B for the regression of pH_e against pCO_{2sw} of *P. lividus*, -0.091 ± 0.006 unit-pH_e unit-pCO_{2sw}^{-1}, was significantly greater than that of *A. lixula*, -0.055 ± 0.005 unit-pH_e unit-pCO_{2sw}^{-1} ($t_{16} = 4.645$, $p < 0.001$, Figure 2). This indicates that individual decreases in pH_e in response to fluctuations in pCO_{2sw} were greater (i.e. steeper response gradient) in *P. lividus* than in *A. lixula*. The pCO_{2e} and $[HCO_3^-]_e$ of both *P. lividus* and *A. lixula* had a positive relationship against pCO_{2sw}. The average B for pCO_{2e} against pCO_{2sw} of *P. lividus*, 0.174 ± 0.017 kPa pCO_{2sw}^{-1}, was significantly higher than that of *A. lixula*, 0.102 ± 0.014 kPa pCO_{2sw}^{-1} ($t_{16} = -3.193$, $p = 0.006$), as was the average B for $[HCO_3^-]_e$ against pCO_{2sw} (*P. lividus* $= 0.368 \pm 0.042$ mmol l^{-1} pCO_{2sw}^{-1}, *A. lixula* $= -0.065 \pm 0.025$ mmol l^{-1} pCO_{2sw}^{-1}, $t_{16} = -6.203$, $p < 0.001$). This indicates that individual increases in both pCO_{2e} and $[HCO_3^-]_e$ in response to increases in pCO_{2sw} were

Table 2. Acid–base balance of control field collected *A. lixula* and *P. lividus*.

	A. lixula	*P. lividus*
pH_e	7.31 ± 0.03*	7.73 ± 0.03*
pCO_{2e} (kPa)	0.28 ± 0.02	0.30 ± 0.02
$[HCO_3^-]_e$(mmol l^{-1})	2.29 ± 0.09*	5.07 ± 0.11*
$Protein_e$ (µg ml^{-1})	334.8 ± 66.2*	122.4 ± 19.8*
pK'_1	5.91	6.03

Data are means ± s.e.
*Significant differences between species ($p < 0.05$).

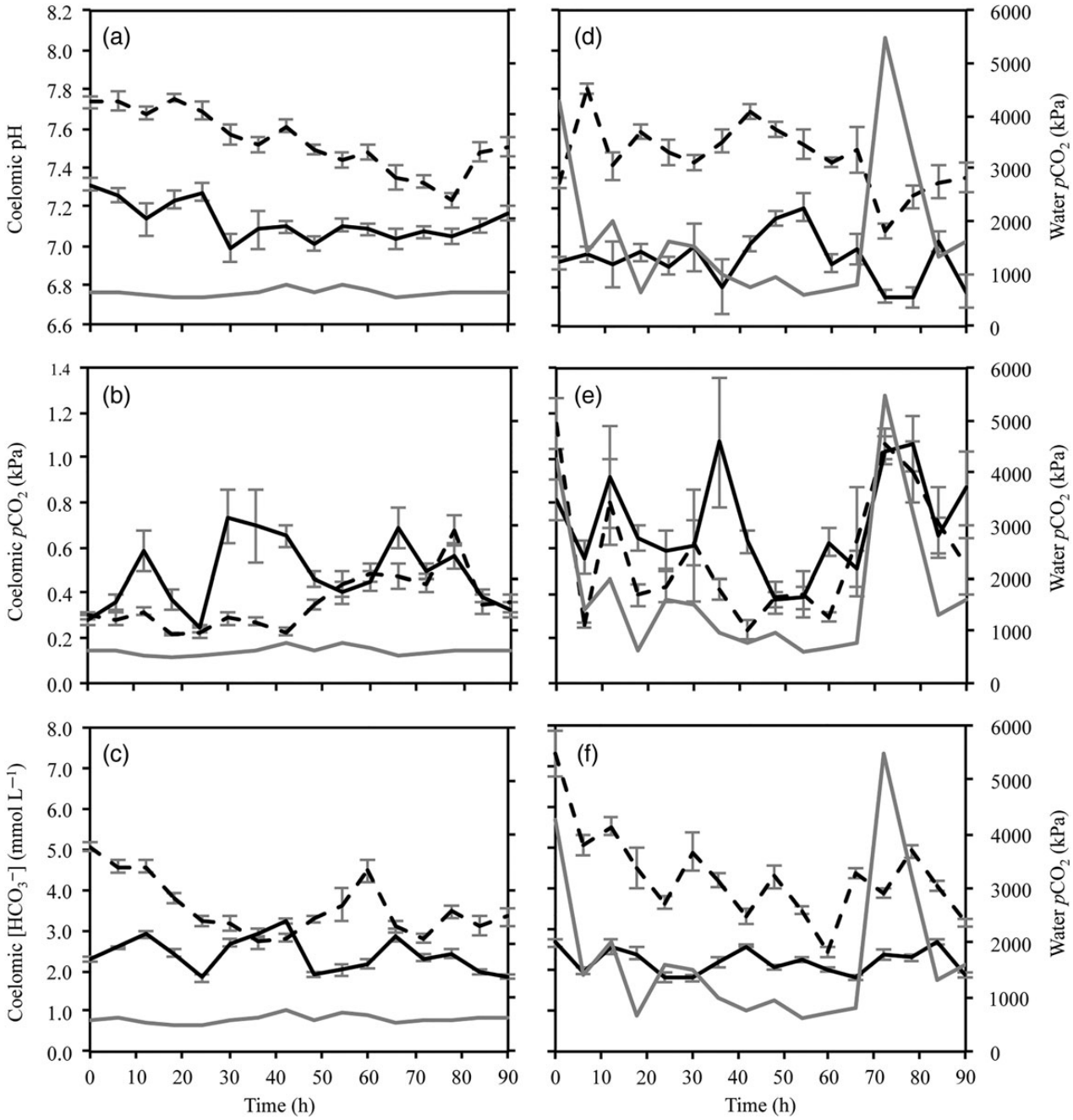

Figure 1. The coelomic fluid pH (a and d), pCO_2 (kPa, b and e), and $[HCO_3^-]$ (mmol l^{-1}, c and f) of *P. lividus* and *A. lixula* during 4 d exposure to stable control pCO_{2sw} conditions (a, b, and c) and fluctuating pCO_{2sw} conditions (d, e, and f). Each time point represents means ± s.e. Grey lines indicate seawater pCO_{2sw}. Black lines indicate *A. lixula*. Dashed lines indicate *P. lividus*.

greater in *P. lividus* than *A. lixula* (Figure 2). Finally, when exposed to fluctuating pCO_{2sw}, the standard deviation of $[HCO_3^-]_e$ in individual *P. lividus* was significantly higher than that in *A. lividus* ($t = 7.377$, $p < 0.001$).

No mortality was observed throughout the experimental period nor were there issues with urchin viability or infection encountered due to the repeated sampling of coelomic fluid (see Calosi *et al.*, 2013a); there was also no significant progressive acidosis throughout the experimental period showing that repeated sampling had no effect on acid–base balance.

Discussion

The present study demonstrates that naturally fluctuating pCO_{2sw} produced different magnitudes of bicarbonate acid–base responses in two species of sea urchin. The acid–base response of *P. lividus* in relation to fluctuating pCO_{2sw} was greater than that of *A. lixula* because *P. lividus* relies on limited bicarbonate buffering capabilities for acid–base regulation, whereas *A. lixula* relied on non-bicarbonate buffering capacity. The distributions of closely related species at CO_2 vents are driven by differences in acid–base regulatory capabilities (Calosi *et al.*, 2013a). However, despite variations

Table 3. Acid–base balance of *A. lixula* and *P. lividus* throughout the experimental period.

	Species			
	A. lixula		*P. lividus*	
Treatment	**Control**	**Fluctuating**	**Control**	**Fluctuating**
pH_e	7.12 ± 0.05	6.94 ± 0.05*	7.53 ± 0.04	7.45 ± 0.05*
Max	7.31	7.19	7.75	7.80
Min	6.99	6.74	7.23	7.08
pCO_{2e} (kPa)	0.48 ± 0.06	0.71 ± 0.11*	0.36 ± 0.03	0.58 ± 0.10*
Max	0.74	1.07	0.68	1.15
Min	0.24	0.37	0.22	0.24
$[HCO_3^-]_e$(mmol l^{-1})	2.40 ± 0.10	2.21 ± 0.09*	3.57 ± 0.17	4.37 ± 0.23*
Max	3.23	2.67	5.07	7.31
Min	1.83	1.81	2.70	2.44

Data are presented as means ± s.e., along with the minimum and maximum values observed.
*Significant effect of seawater pCO_2 on acid–base parameters ($p < 0.05$).

in carbonate chemistry being demonstrated in various ecosystems (Hofmann *et al.*, 2011) including volcanic vent sites (Boatta *et al.*, 2013), most studies pertaining to the comparative physiological responses between species to elevated pCO_2 and in naturally acidified environments have focused on stable mean differences in pCO_{2sw} conditions (e.g. Suggett *et al.*, 2012; Calosi *et al.*, 2013a, b). Understanding how species respond to natural pCO_{2sw} conditions will help explain some of the variation in physiological responses and may provide better predictions on how species will respond to future change (e.g. Kroeker *et al.*, 2011).

Echinoderm coelomic fluid acid–base parameters often conform according to the surrounding seawater (Farmanfarmaian, 1966; Miles *et al.*, 2007) and they have minimal acid–base regulatory capacity when exposed to elevated pCO_2 (Spicer *et al.*, 1988; Miles *et al.*, 2007; Appelhans *et al.*, 2012; Calosi *et al.*, 2013a). Despite the apparent poor acid–base and ion-regulatory mechanisms, when exposed to elevated pCO_2, some species of sea urchins have been shown to exhibit bicarbonate buffering to maintain acid–base homeostasis in response to stable elevated pCO_2 in laboratory (Miles *et al.*, 2007) and field conditions (Calosi *et al.*, 2013a). In the present study, there was no significant effect of stable pCO_{2sw} on the coelomic fluid acid–base balance of either *P. lividus* or *A. lixula* during control incubations.

The differences in acid–base responses to fluctuating pCO_{2sw} between the two species in the present study can be related to the differing mechanisms of acid–base regulation employed. *Paracentrotus lividus* relied on uncompensated bicarbonate acid–base buffering as while they exhibited a significant relationship between $[HCO_3^-]_e$ with pCO_{2sw}, there were also significant fluctuations in pH_e and pCO_{2e}. In contrast to *P. Lividus*, *A. lixula* exhibited comparatively lower fluctuations in $[HCO_3^-]_e$ and experienced no significant fluctuations in pCO_{2e} or pH_e in relation to fluctuating pCO_{2sw}. The bicarbonate buffering capacity of *A. lixula* was to the extent of being almost non-existent. The acid–base response of *A. lixula* to decreasing pCO_{2sw} closely follows the non-bicarbonate buffering line (Figure 3) and therefore is *due* to non-bicarbonate buffering rather that HCO_3^- regulation. This mechanism in *A. lixula* therefore appears to result in greater pH_e stability under fluctuating pCO_{2sw} conditions. The acid–base responses observed in the present study make an interesting comparison with those of stable mean elevations in pCO_{2sw} in the same species. When exposed to

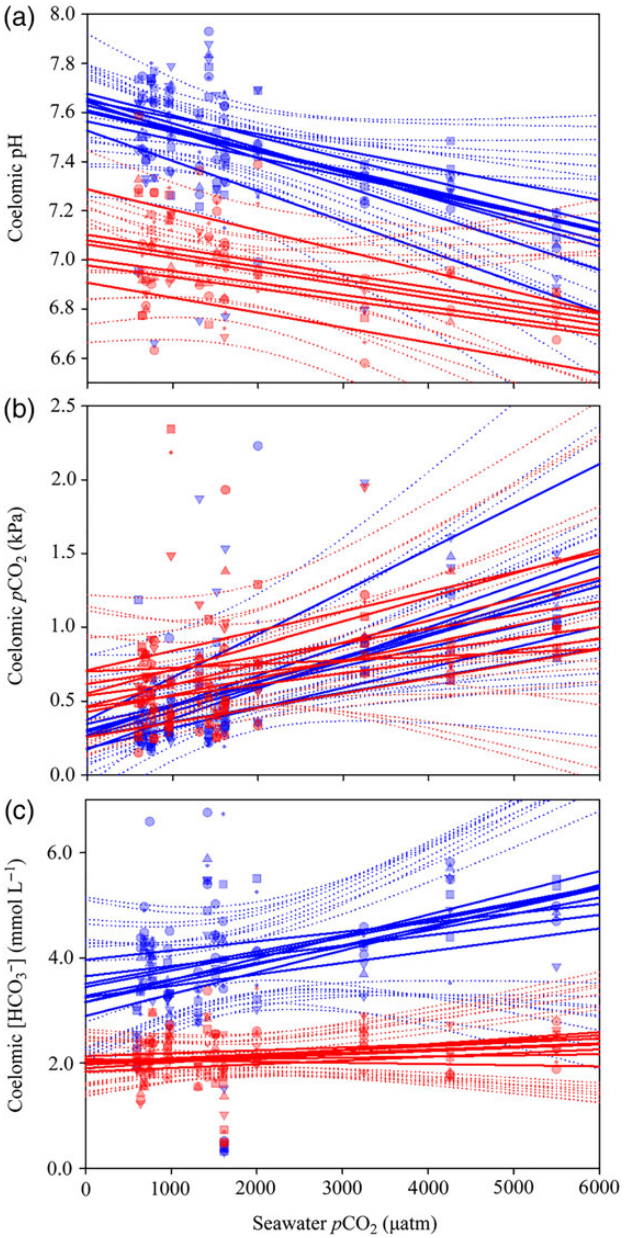

Figure 2. Individual regressions of acid–base parameters coelomic pH (a), coelomic pCO_2 (kPa, b), coelomic $[HCO_3^-]$ (mmol l^{-1}, c) vs. fluctuating pCO_{2sw} of *A. lixula* and *P. lividus*. Red indicates *A. lixula* and blue indicates *P. lividus*. Solid lines indicate individual regressions; dotted lines indicate 95% confidence limits of the regressions. Points indicate raw data from each individual at each pCO_{2sw}, represented by different symbols.

chronic exposure to high pCO_{2sw}, *A. lixula* also demonstrated a lower bicarbonate response than *P. lividus*; however, in both species, acid–base disturbances are fully compensated (Calosi *et al.*, 2013a). Conversely, the lack of full pH_e compensation by *P. lividus* in the present study indicates that this species is unable to respond efficiently to short-term fluctuations in pCO_{2sw}. It is therefore apparent that under fluctuating pCO_{2sw} conditions, the ability of *P. lividus* to compensate pH_e breaks down, while the non-bicarbonate buffering capacity of *A. lixula* allows the maintenance of pH_e homeostasis. The maintenance of pH_e homeostasis in *A. lixula*

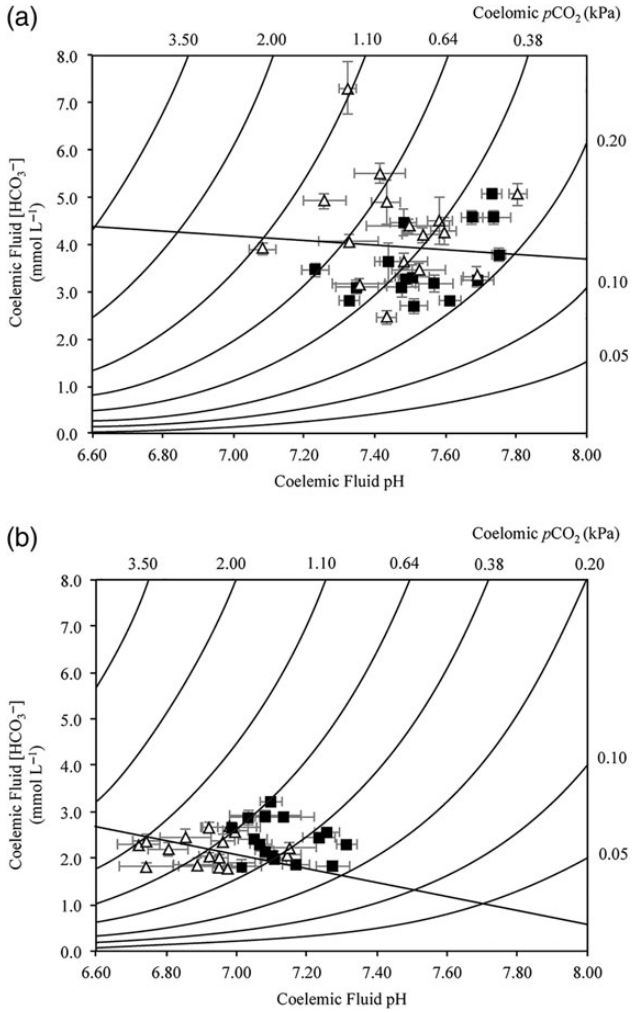

Figure 3. Davenport diagrams representing coelomic fluid acid–base balance of (a) *P. lividus* and (b) *A. lixula*. Each point represents mean ± s.e. of each species at each time point. Solid line indicates non-bicarbonate buffering line. Squares indicate stable control pH conditions; triangles indicate fluctuating pCO_{2sw} conditions.

may also, in part, be alleviated by comparatively low routine pH_e levels in this species. Throughout control incubations and in field collected individuals from the control site, *A. lixula* consistently had a lower pH_e (7.31 ± 0.03) than *P. lividus* (7.73 ± 0.03) with no difference in pCO_{2e}. Comparatively low pH_e under natural and control conditions have been reported previously for *A. lixula* (Calosi *et al.*, 2013a) and have been reported in other marine organisms (e.g. Gutowska *et al.*, 2010; Donohue *et al.*, 2012). Although the reasons for this, and possible physiological implications, are outside the scope of the present study, what is important is the ability of *A. lixula* to maintain pH_e homeostasis and avoid acidosis of the coelomic compartment (i.e. a decrease in pH_e away from its routine value) in response to fluctuations in than pCO_{2sw} with almost no change in $[HCO_3^-]$.

This greater capacity for non-bicarbonate buffering in *A. lixula* is reflected by the steeper NBL of *A. lixula* compared with *P. lividus*, and the acid–base responses in *A. lixula* being closely clustered around the NBL compared with the high variation in bicarbonate response show by *P. lividus* (Figure 3). *Paracentrotus lividus* has a significantly lower $[protein]_e$ than that of *A. lixula*, which while low compared with other species of marine invertebrates, is representative of the low protein concentrations seen in sea urchins (e.g. Spicer *et al.*, 1988; Miles *et al.*, 2007). Comparative differences in $[protein]_e$ between sea urchin species may be the main reason for differences in acid–base regulatory capacity, with species exhibiting higher $[protein]_e$ having greater capacity for pH_e regulation (Spicer *et al.*, 1988), as demonstrated in the present study.

Differences in $[HCO_3^-]_e$ response to fluctuating conditions may be related to routine rates of activity and metabolism, as seen in crustaceans where species with routinely higher rates of activity and metabolism have higher non-bicarbonate buffering capacities due to higher levels of extracellular protein (haemocyanin; Watt *et al.*, 1999; Whiteley, 2011). Whether the same conditions apply to urchins is currently unknown, but if true, may explain differences in pCO_2 sensitivity between the two species. The energetic consequences of relying on bicarbonate buffering in *P. lividus* may be greater than that of non-bicarbonate buffering in *A. lixula*. For example, Na^+/K^+-ATPase is one of a number of transport mechanisms utilized in invertebrate acid–base regulation (Reipschläger and Pörtner, 1996), the activity of which is energetically expensive accounting for up to 40% of the total energy demand in the sea urchin *Strongylocentrotus purporatus* (Leong and Manahan, 1997). While there are differences between acid–base regulatory mechanisms in the two species of urchins in the present study, it must also be noted that differences in energy acquisition and utilization between the two species under elevated pCO_2 may also be an important aspect of determining species distributions (Binyon, 1972; Stickle and Diehl, 1987) including across natural CO_2 gradients. *Arbacia lixula* is regarded as omnivorous, while *P. lividus* is an herbivorous grazer (Agnetta *et al.*, 2013) indicating higher protein acquisition in *A. lixula* compared with *P. lividus*. Non-bicarbonate buffering capacity, while perhaps initially expensive, may in the long term be less energetically expensive than constant HCO_3^- regulation. Therefore, species such as *A. lixula*, which demonstrate a higher capacity of non-bicarbonate buffering and therefore a reduced reliance on HCO_3^- regulation, may be more tolerant to not only chronic stable high pCO_{2sw} conditions but also acute fluctuations in pCO_{2sw} associated with natural coastal systems. This may be important in determining the resilience of a species as the ability to mobilize HCO_3^- in an attempt to compensate pH_e in response to OA may have energetic consequences that in the long term give an advantage to species that favour non-bicarbonate protein buffering and so exhibited smaller and presumable less costly fluctuations in acid–base statues. Given the ability of *P. lividus* to compensate stable increases in pCO_{2sw} (Calosi *et al.*, 2013a), it would be expected to maintain population density closer to the vent sites. However, this present study shows that it may be the inability of *P. lividus* to compensate for short-term fluctuations in pCO_{2sw} that ultimately controls its distribution at the vents. Importantly, the present study shows that natural acute fluctuations in pCO_{2sw} associated with natural costal systems and predicted to increases in the future are just as important in modulating this response as a chronic overall increase in pCO_{2sw} associated with OA.

In conclusion, this study shows that the differential sensitivity of closely related species to future climate change (i.e. the "winners" and "losers") may have as much to do with physiological compensatory responses to natural acute fluctuations in pCO_{2sw} as with chronic changes in mean pCO_{2sw}. Furthermore, many coastal marine habitats experience periodic and acute fluctuations in seawater carbonate chemistry, the level of variation within which is

predicted to increase. Understanding species physiological responses to variations in pCO_{2sw} in these habitats is essential in understanding the species and community responses to OA as closely related species, such as *P. lividus* and *A. lixula*, have trophic and ecological interactions which are important in characterizing the ecology of the systems in which they reside (Bulleri *et al.*, 1999; Privitera *et al.*, 2008).

Acknowledgements

Original concept and data collection by DPS, HG, and CB led by SPSR. First drafts of the paper and data analysis by DPS supported by SPSR. Repeated-measures nested GLMM was performed by SPSR. All authors contributed to the final draft of the paper. This work was funded by UK Ocean Acidification research programme (funded by NERC, Defra, and DECC; grant no. NE/H02543X/1) Added Value Award, awarded to SPSR supported by CH, MM, and JMH-S. The authors also thank Professor Stephen Widdicombe and Fred Staff at Plymouth Marine Laboratories for the use of equipment.

References

Agnetta, D., Bonaviri, C., Badalamenti, F., Scianna, C., Vizzini, S., and Gianguzza, P. 2013. Functional traits of two co-occurring sea urchins across a barren/forest patch system. Journal of Sea Research, 76: 170–177.

Andersson, A. J., and Mackenzie, F. T. 2012. Revisiting four scientific debates in ocean acidification research. Biogeosciences, 9: 893–905.

Appelhans, Y., Thomsen, J., Pansch, C., Melzner, F., and Wahl, M. 2012. Sour times: seawater acidification effects on growth, feeding behaviour and acid–base status of *Asterias rubens* and *Carcinus maenas*. Marine Ecology Progress Series, 459: 85–98.

Binyon, J. 1972. Physiology of Echinoderms. Pergamon Press, Oxford, UK.

Boatta, F., D'Alessandro, W., Gagliano, A. L., Liotta, M., Milazzo, M., Rodolfo-Metalpa, R., Hall-Spencer, J. M., *et al.* 2013. Geochemical survey of Levante Bay, Vulcano Island (Italy), a natural laboratory for the study of ocean acidification. Marine Pollution Bulletin, 73: 485–494.

Borges, A. V., and Abril, G. 2011. 5.04 - Carbon dioxide and methane dynamics in estuaries. In Treatise on Estuarine and Coastal Science, pp. 119–161. Ed. by R. Wolanski and D. McLusky. Academic Press, Waltham.

Bressan, M., Chinellato, A., Munari, M., Matozzo, V., Manci, A., Marčeta, T., Finos, L., *et al.* 2014. Does seawater acidification affect survival, growth and shell integrity in bivalve juveniles? Marine Environmental Research, 99: 136–148.

Bulleri, F., Benedetti-Cecchi, L., and Cinelli, F. 1999. Grazing by the sea urchins *Arbacia lixula* L. and *Paracentrotus lividus* Lam. in the Northwest Mediterranean. Journal of Experimental Marine Biology and Ecology, 241: 81–95.

Calosi, P., Rastrick, S. P. S., Graziano, M., Thomas, S. C., Baggini, C., Carter, H. A., Hall-Spencer, J. M., *et al.* 2013a. Distribution of sea urchins living near shallow water CO_2 vents is dependent upon species acid–base and ion-regulatory abilities. Marine Pollution Bulletin, 73: 470–484.

Calosi, P., Rastrick, S. P. S., Lombardi, C., de Guzman, H. J., Davidson, L., Jahnke, M., Giangrande, A., *et al.* 2013b. Adaptation and acclimatization to ocean acidification in marine ectotherms: an *in situ* transplant experiment with polychaetes at a shallow CO_2 vent system. Philosophical Transactions of the Royal Society B, 368: 20120444.

Collard, M., Rastrick, S. P. S., Calosi, P., Demolder, Y., Dille, J., Findlay, H. S., Hall-Spencer, J. M., *et al.* 2016. The impact of ocean acidification and warming on the skeletal mechanical properties of the sea urchin *Paracentrotus lividus* from laboratory and field observations. ICES Journal of Marine Science, 73: 727–738.

Dickson, A. G. 1990. Thermodynamics of the dissociation of boric-acid in synthetic seawater from 273.15 K to 318.15 K. Deep Sea Research, 37: 755–766.

Dickson, A. G., and Millero, F. J. 1987. A comparison of the equilibrium-constants for the dissociation of carbonic-acid in seawater media. Deep Sea Research, 34: 1733–1743.

Donohue, P. J. C., Calosi, P., Bates, A. H., Laverock, B., Rastrick, S., Mark, F. C., Strobel, A., *et al.* 2012. Impact of exposure to elevated pCO_2 on the physiology and behaviour of an important ecosystem engineer, the burrowing shrimp *Upogebia deltaura*. Aquatic Biology, 15: 73–86.

Dupont, S., and Pörtner, H-O. 2013. Get ready for ocean acidification. Nature, 498: 429.

Farmanfarmaian, A. 1966. The respiratory physiology of the echinoderms. *In* Physiology of Echinodermata, pp. 245–265. Ed. by R. A. Boolootian. John Wiley and Sons, New York.

Gutowska, M. A., Melzner, F., Langenbuch, M., Bock, C., Claireaux, G., and Pörtner, H-O. 2010. Acid–base regulatory ability of the cephalopod (*Sepia officinalis*) in response to environmental hypercapnia. Journal of Comparative Physiology B, 180: 323–335.

Hall-Spencer, J. M., Rodolfo-Metalpa, R., Martin, S., Ransome, E., Fine, M., Turner, S. M., Rowley, S. J., *et al.* 2008. Volcanic carbon dioxide vents show ecosystem effects of ocean acidification. Nature, 454: 96–99.

Harris, K. E., DeGrandpre, M. D., and Hales, B. 2013. Aragonite saturation state dynamics in a coastal upwelling zone. Geophysical Research Letters, 40: 2720–2725.

Harvey, B. P., Gwynn-Jones, D., and Moore, P. J. 2013. Meta-analysis reveals complex marine biological responses to the interactive effects of ocean acidification and warming. Ecology and Evolution, 3: 1016–1030.

Harvey, H. W. 1955. The Chemistry and Fertility of Sea Waters. Cambridge University Press, Cambridge.

Hauri, C., Gruber, N., Vogt, M., Doney, S. C., Feely, R. A., Lachkar, Z., Leinweber, A. M. P., *et al.* 2012. Spatiotemporal variability and long-term trends of ocean acidification in the California Current System. Biogeosciences Discussions, 9: 10371–10428.

Hofmann, G. E., Barry, J. P., Edmunds, P. J., Gates, R. D., Hutchins, D. A., Klinger, T., and Sewell, M. A. 2010. The effect of ocean acidification on calcifying organisms in marine ecosystems: an organism-to-ecosystem perspective. Annual Review of Ecology, Evolution, and Systematics, 41: 127–147.

Hofmann, G. E., Smith, J. E., Johnson, K. S., Send, U., Levin, L. A., Micheli, F., Paytan, A., *et al.* 2011. High-frequency dynamics of ocean pH: a multi-ecosystem comparison. PloS One, 6: e28983.

IPCC. 2013. Summary for policymakers. *In* Climate Change 2013: the Physical Science Basis. Contribution of Working Group 1 to the Fifth Assessment Report of the Intergovernmental Panel on Climate Change. Ed. by T. F. Stocker, D. Qin, G-K. Plattner, M. Tignor, S. K. Allen, J. Boschung, A. Nauels, *et al.* Cambridge University Press, UKandNew York, NY, USA.

Johnson, V. R., Russell, B. D., Fabricius, K. E., Brownlee, C., and Hall-Spencer, J. M. 2012. Temperate and tropical brown macroalgae thrive, despite decalcification, along natural CO_2 gradients. Global Change Biology, 18: 2792–2803.

Joint, I., Doney, S. C., and Karl, D. M. 2011. Will ocean acidification affect marine microbes? The ISME Journal, 5: 1–7.

Kroeker, K. J., Kordas, R. L., Crim, R., Hendriks, I. E., Ramajo, L., Singh, G. S., Duarte, C. M., *et al.* 2013. Impacts of ocean acidification on marine organisms: quantifying sensitivities and interaction with warming. Global Change Biology, 19: 1884–1896.

Kroeker, K. J., Micheli, F., Gambi, M. C., and Martz, T. R. 2011. Divergent ecosystem responses within a benthic marine community to ocean acidification. Proceedings of the National Academy of Sciences of the United States of America, 108: 14515–14520.

Leong, P. K. K., and Manahan, D. T. 1997. Metabolic importance of Na^+/K^+-ATPase activity during sea urchin development. Journal of Experimental Biology, 200: 2881–2892.

Lewis, E., and Wallace, D. W. R. 1998. CO_2SYS Dos Program Developed for CO_2 System Calculations. ORNL/CDIAC-105 Carbon Dioxide Information Analysis Center, Oak Ridge National Laboratory, US Department of Energy, Oak Ridge, TN.

Manzello, D. I. 2010. Ocean acidification hotspots: spatiotemporal dynamics of the seawater CO_2 system of eastern Pacific coral reefs. Limnology and Oceanography, 55: 239–248.

McElhany, P., and Busch, D. S. 2013. Appropriate pCO_2 treatments in ocean acidification experiments. Marine Biology, 160: 1807–1812.

Mehrbach, C., Culberso, C. H., Hawley, J. E., and Pytkowic, R. M. 1973. Measurement of apparent dissociation constants of carbonic acid in seawater at atmospheric pressure. Limnology and Oceanography, 18: 897–907.

Melzner, F., Gutowska, M. A., Langenbuch, M., Dupont, S., Lucassen, M., Thorndyke, M. C., Bleich, M., *et al.* 2009. Physiological basis for high CO_2 tolerance in marine ectothermic animals: pre-adaptation through lifestyle and ontogeny? Biogeosciences, 6: 2313–2331.

Milazzo, M., Rodolfo-Metalpa, R., Chan, V. B. S., Fine, M., Alessi, C., Thiyagarajan, V., Hall-Spencer, J. M., *et al.* 2014. Ocean acidification impairs vermetid reef recruitment. Scientific Reports, 4: 4189.

Miles, H., Widdicombe, S., Spicer, J. I., and Hall-Spencer, J. 2007. Effects of anthropogenic seawater acidification on acid–base balance in the sea urchin *Psammechinus miliaris*. Marine Pollution Bulletin, 54: 89–96.

Mucci, A., Starr, M., Gilbert, D., and Sundby, B. 2011. Acidification of lower St. Lawrence Estuary bottom waters. Atmosphere–Ocean, 49: 206–218.

Pane, E. F., and Barry, J. P. 2007. Extracellular acid–base regulation during short-term hypercapnia is effective in a shallow-water crab, but ineffective in a deep-sea crab. Marine Ecology Progress Series, 334: 1–9.

Pörtner, H. O., Langenbuch, M., and Reipschläger, A. 2004. Biological impact of elevated ocean CO_2 concentrations: lessons from animal physiology and earth history. Journal of Oceanography, 60: 705–718.

Price, N. N., Martz, T. R., Brainard, R. E., and Smith, J. E. 2012. Diel variability in seawater pH relates to calcification and benthic community structure on coral reefs. PLoS One, 7: e43843.

Privitera, D., Chiantore, M., Mangialajo, L., Glavic, N., Kozul, W., and Cattaneo-Vietti, R. 2008. Inter-and intra-specific competition between *Paracentrotus lividus* and *Arbacia lixula* in resource-limited barren areas. Journal of Deep Sea Research, 60: 184–192.

Rastrick, S. P. S., Calosi, P., Calder-Potts, R., Foggo, A., Nightingale, G., Widdicombe, S., and Spicer, J. I. 2014. Living in warmer, more acidic oceans retards physiological recovery from tidal emersion in the velvet swimming crab, *Necora puber*. Journal of Experimental Biology, 217: 2499–2508.

Reipschläger, A., and Pörtner, H. O. 1996. Metabolic depression during environmental stress: the role of extracellular versus intracellular pH in *Sipunculus nudus*. The Journal of Experimental Biology, 199: 1801–1807.

Reum, J. C. P., Alin, S. R., Feely, R. A., Newton, J., Warner, M., and McElhany, P. 2014. Seasonal carbonate chemistry covariation with temperature, oxygen, and salinity in a fjord estuary: implications for the design of ocean acidification experiments. PLoS One, 9: e89619.

Spicer, J. I., Taylor, A. C., and Hill, A. D. 1988. Acid–base status in the sea urchins *Psammechinus miliaris* and *Echinus esculentus* (Echinodermata: Echinoidea) during emersion. Marine Biology, 99: 527–534.

Stickle, W. B., and Diehl, W. J. 1987. Effects of salinity on echinoderms. *In* Echinoderm Studies, 2, pp. 235–285. Ed. by M. Jangoux, and J. M. Lawrence. Balkema, Rotterdam, The Netherlands.

Suggett, D. J., Hall-Spencer, J. M., Rodolfo-Metalpa, R., Boatman, T. G., Payton, R., Tye Pettay, D., Johnson, V. R., *et al.* 2012. Sea anemones may thrive in a high CO_2 world. Global Change Biology, 18: 3015–3025.

Truchot, J. P. 1976. Carbon dioxide combining properties of blood of shore crab *Carcinus maenas* (L)—carbon dioxide solubility coefficient and carbonic acid dissociation-constants. Journal of Experimental Biology, 64: 45–57.

Truchot, J. P., and Duhamel-Jouve, A. 1980. Oxygen and carbon dioxide in the marine intertidal environment: diurnal and tidal changes in rockpools. Respiration Physiology, 39: 241–254.

Vizzini, S., Di Leonardo, R., Costa, V., Tramati, C. D., Luzzu, F., and Mazzola, A. 2013. Trace element bias in the use of CO_2 vents as analogues for low pH environments: implications for contamination levels in acidified oceans. Estuarine, Coastal and Shelf Science, 134: 19–30.

Watt, A. J. S., Whiteley, N. M., and Taylor, E. W. 1999. An in situ study of respiratory variables in three British sublittoral crabs with different routine rates of activity. Journal of Experimental Marine Biology and Ecology, 239: 1–21.

Whiteley, N. M. 2011. Physiological and ecological responses of crustaceans to ocean acidification. Marine Ecology Progress Series, 430: 257–271.

Handling editor: C. Brock Woodson

ICES Journal of Marine Science

ICES Journal of Marine Science (2016), 73(3), 613–619. doi:10.1093/icesjms/fsv019

Contribution to Special Issue: 'Towards a Broader Perspective on Ocean Acidification Research'

Original Article

CO_2-driven decrease in pH disrupts olfactory behaviour and increases individual variation in deep-sea hermit crabs

Tae Won Kim[1,2]*, Josi Taylor[3], Chris Lovera[3], and James P. Barry[3]

[1]*Korea Institute of Ocean Science and Technology, 787 Haeanro, Sangnok, Ansan 426-744, Republic of Korea*
[2]*Korea University of Science and Technology, Daejeon 305-350, Republic of Korea*
[3]*Monterey Bay Aquarium Research Institute, 7700 Sandholdt Road, Moss Landing, CA 95039, USA*

**Corresponding author: tel: +82 31 400 7796; e-mail: ktwon@kiost.ac*

Kim, T. W., Taylor, J., Lovera, C., and Barry, J. P. CO_2-driven decrease in pH disrupts olfactory behaviour and increases individual variation in deep-sea hermit crabs. – ICES Journal of Marine Science, 73: 613–619.

Received 18 September 2014; revised 18 January 2015; accepted 20 January 2015; advance access publication 16 February 2015.

Deep-sea species are generally thought to be less tolerant of environmental variation than shallow-living species due to the relatively stable conditions in deep waters for most parameters (e.g. temperature, salinity, oxygen, and pH). To explore the potential for deep-sea hermit crabs (*Pagurus tanneri*) to acclimate to future ocean acidification, we compared their olfactory and metabolic performance under ambient (pH ~7.6) and expected future (pH ~7.1) conditions. After exposure to reduced pH waters, metabolic rates of hermit crabs increased transiently and olfactory behaviour was impaired, including antennular flicking and prey detection. Crabs exposed to low pH treatments exhibited higher individual variation for both the speed of antennular flicking and speed of prey detection, than observed in the control pH treatment, suggesting that phenotypic diversity could promote adaptation to future ocean acidification.

Keywords: hermit crabs, individual variation, ocean acidification, olfactory function, prey detection.

Introduction

Future ocean pH is projected to drop considerably at all depths as the rising inventory of atmospheric CO_2 is absorbed by surface waters and mixed to depth. This phenomenon of ocean acidification is a growing concern for the health of marine ecosystems (Orr *et al.*, 2005; Doney *et al.*, 2009). Owing to the accumulation of respiratory CO_2, the pH of deep ocean waters is generally lower than in surface waters (Feely *et al.*, 2008; Brewer and Hester, 2009). Under the SRES A1B scenario, the pH of deep-sea waters (ca. 1000 m) is expected to decrease by 0.2–0.4 units by the end of the 21st century (Ilyina *et al.*, 2010), and under the RCP 8.5 scenario, with larger CO_2 emissions, bathyal pH could decrease even more. Environmental hypercapnia and associated changes in deep-sea carbonate chemistry could affect physiological processes that contribute to the individual performance of deep-sea animals and ultimately to population survival. Though deep-sea animals are assumed to be physiologically adapted to the pH of their habitat depth (typically lower than surface waters), several studies indicate that further reduction in pH can be more stressful for deep-sea taxa than related upper ocean species (Seibel and Walsh, 2003; Pane and Barry, 2007; Pane *et al.*, 2008). Deep-sea animals are generally thought to be less tolerant of environmental changes (such as future ocean acidification) than shallow-living taxa because of the environmental stability (oxygen, temperature, pH, etc.) of deep-sea waters (Pane and Barry, 2007; Smith *et al.*, 2009).

Although some taxa may acclimatize to high environmental CO_2 levels (Ries *et al.*, 2009; Kroeker *et al.*, 2010), their physiology and behaviour may be affected, leading to potentially adverse impacts on their individual performance (Portner, 2008; Munday *et al.*, 2010; Briffa *et al.*, 2012; Sung *et al.*, 2014). Environmental hypercapnia can alter the metabolic rates of organisms (Bibby *et al.*, 2007; Wood *et al.*, 2008). It can also weaken olfactory functions of animals (de la Haye *et al.*, 2012; Nilsson *et al.*, 2012) and thus deter homing ability (Munday *et al.*, 2009), predator/prey detection (Munday *et al.*, 2009; Dixson *et al.*, 2010; Cripps *et al.*, 2011), resource assessment, and decision-making (de la Haye *et al.*, 2011). Exposure to low seawater pH can also affect the defensive abilities of prey species, perhaps rendering them more vulnerable

to potential predators (Bibby *et al.*, 2007). Such sensory and behavioural changes due to ocean acidification can alter the ecological function or role of some marine organisms and potentially affect the structure and function of marine communities (Briffa *et al.*, 2012).

Variation in responses to elevated environmental CO_2 within populations is another key factor concerning the response of marine species to ocean acidification. Although environmental change may cause significant negative impacts on most individuals' performance, tolerance by a subset of the population may promote adaptation for population persistence (Charmantier *et al.*, 2008; Sih *et al.*, 2012). Furthermore, behavioural differences among individuals (i.e. "personality") within populations (Sih *et al.*, 2004) can play an import role in determining the evolutionary and ecological consequences of human-induced rapid environmental changes (Sih *et al.*, 2011, 2012). High variation among individuals in response to elevated CO_2 has been shown to represent genetic diversity in some marine populations (Langer *et al.*, 2006; Pistevos *et al.*, 2011; Sunday *et al.*, 2011; Schlegel *et al.*, 2012; Kim *et al.*, 2013), but there was no evidence for individual variation in behavioural responses to high CO_2 (e.g. Munday *et al.*, 2009; Dixson *et al.*, 2010; Cripps *et al.*, 2011; de la Haye *et al.*, 2011).

The capacity for deep-sea organisms to adapt to lower pH conditions is largely unknown. Here, we investigate the influence of exposure to reduced pH waters on the behavioural and physiological function of the deep-sea hermit crab *Pagurus tanneri* (Benedict, 1892). *Pagurus tanneri* inhabits shells of *Neptunea* sp. or *Bathybembix bairdi*, and as benthic scavengers are a major consumer of organic debris on the continental slope (Ramsay *et al.*, 1997). In the dark, deep-sea environment, olfaction is likely their principal mode of food detection.

To determine if olfactory behaviour in *P. tanneri* is affected by ocean acidification, and to measure the range of variability in responses among individuals, experiments were conducted to evaluate several hypotheses. First, we tested whether the antennular flicking behaviour of *P. tanneri* is influenced by low pH. Antennular flicking is the equivalent of "sniffing" to detect chemical cues in a wide variety of decapod crustaceans including hermit crabs (de la Haye *et al.*, 2011). Therefore, this sensory behaviour was used as an indicator of olfactory ability. Second, we evaluated the hypothesis that exposure to low pH waters impairs the speed of prey detection by *P. tanneri*. We expect that the rate of antennular flicking is coupled to olfaction ability, such that a reduction in flicking rate will reduce or slow olfaction, consequently increasing the time required to detect and find prey. Finally, we measured rates of oxygen consumption to test the hypothesis that any behavioural changes in *P. tanneri* that are affected by pH are coupled to metabolic rate.

Methods

Collection and maintenance of *P. tanneri*

Hermit crabs were collected in October 2011 at 884 m depth in Monterey Bay (36.71°N 122.28°W) using a suction sampler on the Remotely Operated Vehicle (ROV) *Doc Ricketts* (Dive DR306), operated from the RV *Western Flyer* by the Monterey Bay Aquarium Research Institute (MBARI). A total of 32 individuals were collected and stored in a closed box on the ROV. Upon recovery of the ROV to the surface, specimens were transferred carefully to an ice cooler (57 l) with seawater at *in situ* temperature (5°C), pH 8.0, and 100% oxygen saturation in a thermally controlled (5°C) environmental chamber on the *Western Flyer* (5°C, pH 7.6, and DO 30 μM, were *in situ* seawater values at their depth of collection). Upon arrival at Moss Landing on the same day, the crabs were moved to an aquarium (60 × 30 × 35 cm) with replenishing seawater (5°C, 100% saturated with normal oxygen levels, and pH 8.0) flow in the dark wet seawater lab at MBARI.

Pagurus tanneri tolerated the holding conditions without any outward indication of stress. On 30 November, all crabs were fed to satiation with chopped frozen squid acquired from local fish market. Each crab was assigned to a 1 l transparent glass jar, coded, and assigned randomly to one of two pH treatment groups ("Control" or "Low-pH"). Chilled (5°C) ambient (100% saturated with normal oxygen levels, pH 8.0) seawater from a gas-controlled, flow-through aquarium system (see below) was delivered to each jar at 60 ml min^{-1}. Thirty-two jars (each housing 1 crab) were divided among 6 small (10 l) aquaria overflowing with treatment water. On the following day, claw size and shell length of each crab were measured using digital callipers. No differences were detected between pH treatment groups in either the larger claw length (Mann–Whitney *U*-test, $U = 111$, $p = 0.9504$) or shell length ($U = 108$, $p = 0.8519$). Crabs were maintained in a darkened room with only dim red light, from the time of crab placement in jars until the end of the experiment.

Seawater chemistry

Experimental conditions for seawater pH, dissolved oxygen, and temperature were maintained using a gas-controlled aquarium system, (Barry *et al.*, 2008). Oxygen (Aanderaa Inc., model 3835, www.aadi.no), pH (Honeywell DuraFET III), and temperature were logged continuously (1 Hz) using a LabVIEW (National Instruments Corp.) application. A PID-based feedback algorithm integrated with mass flow controllers (Sierra Instruments, Inc.) was used to regulate oxygen and pH in seawater reservoirs that supply experimental treatment waters.

From 1 to 5 December 2011, seawater pH delivered to both treatment groups was gradually adjusted from pH 8.0 to pH 7.6, and dissolved oxygen (DO) level was simultaneously changed from 300 to 30 μM. The pH of the Low-pH treatment group (16 jars) was then gradually adjusted from pH 7.6 to pH 7.1 between 19 and 21 December 2011. The pH of bathyal waters is expected to decrease by as much as 0.4 units by the end of the century. Therefore, pH 7.1 was regarded as a reasonable pH perturbation that the deep-sea hermit crab population may experience soon. A difference of 0.5 pH units was maintained between the Low-pH (pH 7.1) and Control (pH 7.6) treatments throughout the experiment (Table 1). Temperature and DO did not differ between treatments. Periodic measurements of pH using a spectrophotometric pH method (Byrne *et al.*, 1999; Low pH: 7.11 ± 0.01, Control pH: 7.58 ± 0.04) showed only negligible difference from measurements performed using the HoneyWell DuraFET pH sensors (Table 1). Seawater DO in each jar was also measured periodically during the experiment using Aanderraa® oxygen optodes (model 3835) to ensure the expected DO was maintained. To determine the calcite and aragonite saturation states of treatment waters, samples were collected from all treatments five times during the experiment, and dissolved inorganic carbon was measured by non-dispersive infrared analysis (LI-COR model 6262), as detailed by Friederich *et al.* (2002).

Olfaction behaviour (rate of antennular flicking)

Crabs naturally flick antennules to detect dissolved odours in seawater, and for this experiment, the rate of antennular flicking was

Table 1. Carbonate system and other physical parameters for experimental treatments measuring the response of hermit crabs (mean ± s.d.).

	Low pH	Control
pH	7.12 (± 0.02)	7.6 (± 0.01)
TCO_2	2365.57 ± 36.68	2677.67 ± 270.78
Salinity (ppt)	33.0 ± 0.1	33.0 ± 0.1
Temperature (°C)	6.0 ± 0.1	6.0 ± 0.1
PCO_2 (μatm)	3596.47 ± 159.18	1378.82 ± 111.55
Alkalinity (μEq kg^{-1})	2207.86 ± 36.19	2687.47 ± 274.02
Calcite saturation	0.36 ± 0.02	1.31 ± 0.18
Aragonite saturation	0.23 ± 0.01	0.83 ± 0.12
HCO_3^- (μmol· kg^{-1})	21 167.51 ± 35.09	2553.16 ± 258.80
CO_3^{2-} (μmol· kg^{-1})	15.00 ± 0.81	54.32 ± 7.60

The parameters were calculated with CO_2sys (Pierrot *et al.*, 2006) using the pH and TCO_2 values with dissociation constants from Dickson and Millero (1987) and KSO_4 using Dickson (1990).

recorded for each individual as the time taken for 10 flicks. No stimulus to elicit a flicking response was provided. To observe flicks clearly, a flashlight was used to illuminate the antennules. Crabs exhibited no apparent shrinking or withdrawal in response to the light, suggesting that it did not influence flicking rate. Flicking rates of each individual were measured using three separate trials from 7 to 8 December 2011, before adjusting the aquarium system to the respective treatment conditions. Once the Control and Low-pH treatment conditions were established, the rate of antennular flicking by each animal was measured once for each of 30 haphazardly selected days from 22 December 2011 to 9 May 2012 (see Figure 1 for dates of antennular flicking measurements).

Prey detection

The time required for crabs to detect and move to a food item nearby was measured under Control and Low-pH conditions during two periods: (i) 2 weeks into exposure, 5–9 January, and (ii) 4 weeks into exposure, 18–23 January 2012. Each crab from each treatment group was transferred from its jar to a 10 l test aquarium containing seawater of the appropriate treatment. The crab was then positioned in the centre of an acrylic tube (inner diameter 113 mm, outer diameter 126 mm, height 72.5 mm) standing vertically at one end of the aquarium. Using 30-cm long forceps, a portion of squid (0.2 g) was placed 3 cm from the opposite end of the aquarium, ~22 cm from the crab isolated in the acrylic tube. After 5 min, the tube was lifted from the aquarium using forceps. Each trial was then observed and recorded from outside the room using two wireless surveillance IR cameras (Foscam® model no. FI8904W). For each experimental trial, we measured the time required for the crab to locate and begin consuming the prey. If the crab failed to locate the prey within 30 min, the trial was terminated. After each trial, seawater in the test aquarium was replenished using the appropriate low- or high pH waters.

Respirometry

Oxygen consumption rates were measured for a subset (ca. 1/3) of the crabs in each group during three periods: (i) at *in situ* conditions immediately before exposure to the Control or Low-pH experimental treatments, 14–18 December; (ii) ~3 weeks into exposure, 11–15 January; and (iii) ~9 weeks into exposure, 13–16 February. For each respirometry period, five crabs were selected randomly from each treatment group. Before measurement, the shell surface of each individual was cleaned using a toothbrush. We also determined that the respiration rate of a single cleaned shell (i.e. no enclosed crab) was undetectable.

Crabs were held unfed for at least 72 h before being placed, in their shells, into one of five individual RC400 respiration chambers, each with a volume of ca. 730 ml. Each chamber was then submerged in an aquarium with seawater of the appropriate treatment chemistry, and water was allowed to circulate through the open ports of each chamber for 12–20 h before starting respiration measurements. Following this acclimation period, any small air bubbles were purged from each chamber, open ports were sealed with low surface area rubber bungs, and each was fitted with an oxygen electrode. The gas-tight chambers were then submerged inside an insulated, 5°C water bath (fresh). An oscillator (Thermolyne Bigger Bill Orbital Shaker) holding the water bath was then activated at a speed of ~25 rpm to ensure that chamber water was well mixed for accurate oxygen measurement. Oxygen was measured using microcathode oxygen electrodes and was recorded with a Strathkelvin 928 6-Channel Oxygen System (version 2.2).

Using this protocol, initial chamber O_2 levels were 60 (± 20) μM l^{-1}, and decreased due to crab respiration until O_2 in the static chamber reached 10 μM l^{-1} (3–12 h). As crabs individually reached this threshold or after 12 h (i.e. ~10% of trials), they were removed from the respirometer system and chamber, and returned to their treatment jar. Because these crabs inhabit an environment with ~30 μM O_2, we decided that respiration rates should be determined under conditions close to their environment. Therefore, the rate of oxygen consumption was calculated as a linear slope for the period when chamber O_2 levels ranged from 15 to 35 μM.

Respiration rates were scaled by the wet body mass of each crab at the end of the exposure period (determined to 0.01 g) so that O_2 consumption rates were comparable among individual as μmol O_2 g^{-1} h^{-1}. Body mass did not differ significantly between treatments (Mann–Whitney *U*-test, $U = 87.5$, $p = 0.6295$).

Ethical note

Collection of hermit crabs was approved by California Natural Resources Agency, Department of Fish and Game (Scientific Collecting Permit ID: SC-10696). There were no apparent adverse effects of bringing these crabs from the deep ocean to surface pressures—no mortality or loss of limbs during collection and transport were observed. During the experiment, a portion (~0.2 g) of chopped squid acquired at a local fishery market was given to each crab as food every 2 weeks. Some of the crabs released their larvae on February and March 2011. Therefore, we assumed the laboratory conditions were tolerable to these crabs. Six crabs (three in each treatment) died during the experiment, presumably due to asphyxiation related to failure of the water (oxygen) deliver system to their jars. At the end of the 6-month experiment, all remaining crabs were sacrificed for morphometric and body weight measurements.

Statistical analysis

The effect of pH on the rate of antennular flicking and time taken for prey detection was determined using repeated-measures analysis of variance (ANOVA). For antennular flicking rates (the number of antennular flicks min^{-1}), repeated-measures ANOVA was applied for three periods (7, 14, and 20 weeks) to determine if there was a cumulative effect of pH depending over the length of the experiment. If the assumption of equal between-group correlation and

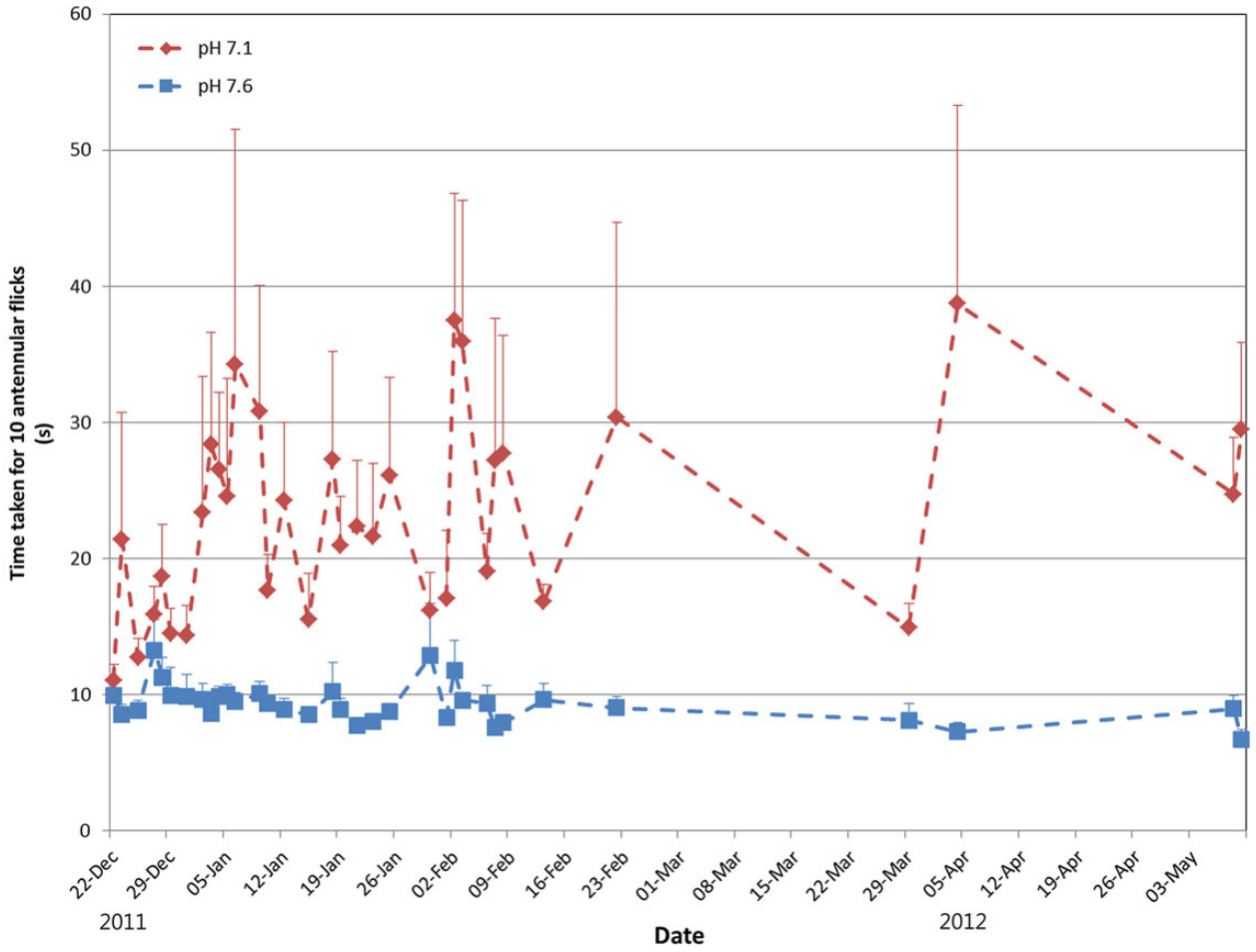

Figure 1. Time (mean ± s.e.) taken for ten antennular flicks of hermit crabs (*P. tanneri*) under Low-pH (red diamond) and Control (blue square) conditions. Crabs under Low-pH conditions required more time to flick antennules and exhibited much higher individual variation in time taken for antennular flicks than observed for crabs under Control conditions.

Table 2. Repeated-measures ANOVA results for the effect of low pH exposure on antennular flicking rates.

	7 weeks			15 weeks			20 weeks		
Source	***F***	**d.f.**	***p*-value**	***F***	**d.f.**	***p*-value**	***F***	**d.f.**	***p*-value**
Within-subject effect									
Day	1.488	25.6	0.06	1.485	29.1	0.057	1.436	33	0.058
Day × pH treatment	1.046	25.6	0.403	1.297	29.1	0.139	1.821	33	0.004
Error		487.2			552.9			495	
Between-subject effect									
pH treatment	19.323	1	<0.0001	21.137	1	<0.0001	30.219	1	<0.0001
Error		19			19			15	

variance ("sphericity") was violated (Mauchly's test, $p < 0.05$), a Huynh–Feldt correction was applied. To test for heteroscedasticity between treatments, we performed Levene's test on the average time taken for 10 antennular flicks per individual, on the time taken for prey detection 4 weeks after treatment exposure, and on respiration rates. Differences in respiration rates between treatment groups and exposure times were tested using a Mann–Whitney test because a subset (1/3) of the crabs in each groups were selected for respiration at three times and crabs were selected randomly for each treatment.

Results

Antennular flicks

The rate of antennular flicking for crabs in the Low-pH (7.1) treatment decreased through the experiment, and was significantly lower than for crabs under Control pH (7.6) after 7 days exposure to the low pH treatment (Table 2). There was a significant effect of pH treatment until the end of the experiment, whereas the effect of day or interaction between day and pH treatment was not significant until 15 weeks after exposure (Table 2).

Variation among individuals for the time required to complete ten antennular flicks was significantly higher for crabs in Low-pH seawater (pH 7.1) compared with those held in control conditions (Levine's test, $W_{1,28} = 46.028$, $p < 0.0001$, Figure 1). When we selected only one-third of all individuals from the Low-pH treatment with the shortest time for ten flicks, there was no significant difference in antennular flicking rates between treatments ($F_{1,13} = 4.468$, $p = 0.054$).

Prey detection

The time required for *P. tanneri* to detect prey did not differ between the two groups before treatment conditions (Control, Low-pH) were established (one-way ANOVA, $F_{1,18} = 0.058$, $p = 0.8128$). In contrast, crabs exposed to the Low-pH treatment for 4 weeks were slower to detect prey than those in the Control treatment (repeated-measures ANOVA, $F_{1,17} = 5.268$, $p = 0.034$, Figure 2). Variation in prey detection speed among individuals was also significantly greater for crabs exposed to Low-pH conditions for 4 weeks, compared with crabs in the Control treatment (Levene's test, $W_{1,19} = 17.079$, $p < 0.001$). Individual variation in response to Low-pH waters is evident in a subset of the population. For one-third of individuals ($n = 5$ each) in each treatment with the most rapid prey detection speeds, no difference in the mean speed was detectable (repeated-measures ANOVA, $F_{1,12} = 0.084$, $p = 0.7769$). There was a significant correlation between the average antennular flicking rate for each individual and its prey detection speed 4 weeks into the pH treatments ($R = 0.561$, $F_{1,17} = 8.720$, $p = 0.008$).

Respiration rates

Oxygen consumption rates were similar between groups for crabs exposed to *in situ* conditions before the experiment (Mann–Whitney $U = 25$, $n_1 = 8$, $n_2 = 7$, $p = 0.728$; Figure 3). After 3 weeks of exposure to treatment conditions, the mean O_2 consumption rates had increased in crabs exposed to Low-pH seawater, but the difference compared with their pretreatment rates was marginally significant (Mann–Whitney $U = 13$, $n_1 = 7$, $n_2 = 9$, $p = 0.050$). Rates in the Low-pH group were significantly greater than for Control animals after 3 weeks exposure (Mann–Whitney $U = 15$, $n_1 = 8$, $n_2 = 9$, $p = 0.043$). Furthermore, there was a significant negative correlation between O_2 consumption and antennular flicking rates ($R = 0.570$, $F_{1,17} = 7.218$, $p = 0.012$). The variance in O_2 consumption among individuals did not vary among pH treatments (Levene's test, $W_{1,15} = 0.958$, $p = 0.343$).

After 8 weeks of exposure, the mean rate of O_2 consumption in the Low-pH group had returned to pre-experiment levels (Mann–Whitney $U = 56$, $n_1 = 7$, $n_2 = 12$, $p = 0.237$) and did not differ from the Control group (Mann–Whitney $U = 61$, $n_1 = 12$, $n_2 = 11$, $p = 0.758$). Respiration rates of crabs in the Control group, however, gradually decreased during the 9-week exposure period (Mann–Whitney $U = 73$, $n_1 = 8$, $n_2 = 11$, $p = 0.017$; Figure 3).

Discussion

Our results indicate that seawater acidification impairs some behaviours in *P. tanneri* that are intimately coupled to their survival. Significant reduction in the rate of antennular flicking almost certainly disrupts olfactory function that may be essential for information gathering (e.g. detecting empty shells to change or prey to eat; de la Haye *et al.*, 2011). Antennule flicking is assumed to disrupt fluid boundary layers around antennule hairs and promote transport of odour molecules to sensory cells (Reidenbach and Koehl, 2011). A significant correlation between antennular flicking rate and prey detection time, and the significant increase in time required for detecting prey in crabs under low pH conditions supports this notion. These results indicate that a reduction in the pH of deep-sea waters expected in the future may impair olfactory functions of deep-sea hermit crabs and corresponding survival skills, unless *P. tanneri* can longer term acclimatization and adaptation to these conditions.

We expected metabolic rates to be positively correlated with antennular flicking rates. In contrast, we observed that after 3 weeks immersion in low pH waters, metabolic rates had increased, but antennular flicking rates were reduced. Higher metabolic activity may instead represent the energetic costs of up-regulating important homeostatic mechanisms (i.e. acid–base balance) related to exposure to high CO_2 conditions (Pane and Barry, 2007). Or, perhaps other physiological processes such as phasic contractions of short muscles, or stereotyped impulse bursts in motor neurons (Mellon, 1997) directly related to olfactory functions are inhibited by seawater acidification and reduce antennular flicking directly (Nilsson *et al.*, 2012). A return of respiration rates to pretreatment levels after 9 weeks exposure to low pH water suggests that this population has the capacity to acclimate to a lower pH, at least in relation to metabolic rate.

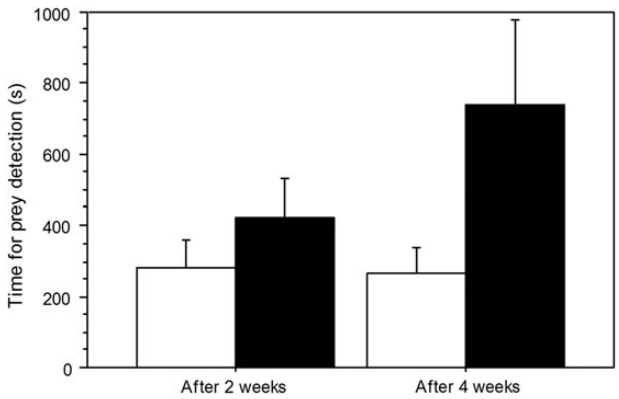

Figure 2. Time (mean ± s.e.) required for prey detection of hermit crabs (*P. tanneri*) under Low-pH (black bar) and Control (white bar) conditions. Crabs in the Low-pH treatment (pH 7.1) required more time for prey detection and had higher individual variation than crabs under Control conditions (pH 7.6) after 4-week exposure.

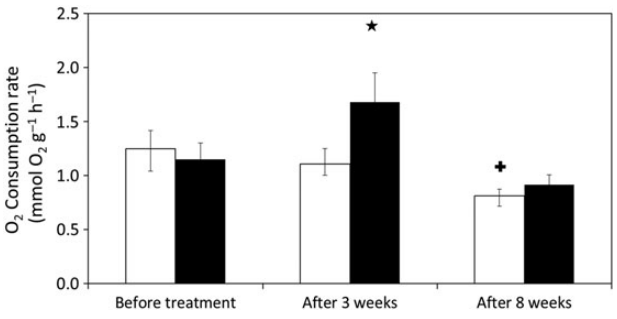

Figure 3. O_2 consumption (mean ± s.e.) of hermit crabs (*P. tanneri*) before and during exposure to Low-pH (black bar) and Control (white bar) conditions. Significant ($p < 0.05$) difference from pretreatment measurements is denoted by "plus symbol", while "asterisk" represents significant ($p < 0.05$) difference between the Low-pH and Control groups for the same period.

Hermit crabs use shells built by gastropods and are thus highly dependent on the availability of this resource (Williams and McDermott, 2004). Shells of most crabs in our experiment were considerably corroded by low pH seawater and even somewhat by control waters during the course of the experiment. The significant decrease in respiration rates of "control" crabs during the experimental time frame may be at least in part due to the observed deterioration of shell condition (Alcaraz and Kruesi, 2012). Shells become lighter due to the corrosion and so it may be easier to carry them. To this end, the ability of the snails providing shells to *P. tanneri* to survive and build carbonate shells must also be evaluated to predict the fate of deep-sea hermit crabs in future ocean chemistry.

Increased variation among individuals of *P. tanneri* in response to low pH conditions, for both antennular flicking rates and time taken for prey detection may represent a range of acclimation abilities among individuals and/or an epigenetic effect. Notably, the behaviour of the one-thirds of crabs in Low-pH treatment with the highest flicking rates did not differ from crabs in the Control group. This suggests that a large portion of the hermit crab population could acclimate to increased environmental CO_2 without a decrement in performance (i.e. survive without a fitness compromise) related to olfactory functions. Conversely, a portion of the population may be impaired to some degree, perhaps including a loss of fitness that would presumably promote adaptation favouring more tolerant genotypes. Indeed, recent reports suggest that various taxa may be able to adapt to human-induced rapid environmental changes through high individual variation in behavioural responses (Sih *et al.*, 2011, 2012; Tuomainen and Candolin, 2011). On the other hand, several studies documenting significant sensitivities of animals to ocean acidification have found no evidence for individual variation in behavioural responses to high CO_2 (e.g. Munday *et al.*, 2009; Dixson *et al.*, 2010; Cripps *et al.*, 2011; de la Haye *et al.*, 2011).

Our results showing evidence of high variation among individuals for behavioural and physiological responses to environmental hypercapnia have strong implications concerning the role of phenotypic (and presumably genetic) diversity within populations in promoting adaptation to ocean acidification. Several studies report that high individual variation in rates of development and growth in response to in low-pH exposure is linked to genetic variation (Parker *et al.*, 2011; Pistevos *et al.*, 2011; Sunday *et al.*, 2011; Kim *et al.*, 2013). We cannot confirm that tolerance or acclimation to low-pH conditions by a portion of adult hermit crabs examined is a heritable trait, as required for adaptation. Further studies on heritability of behavioural and physiological traits will shed light on understanding the adaptive capacity of deep-sea species to ocean acidification.

Acknowledgements

We thank Kurt Buck and Patrick Whaling for technical support, Peter Brewer for consultation on deep-sea carbonate chemistry, Kim Reisenbichler for technical assistance with respirometry, and Linda Kuhnz for identification of hermit crabs. This research was supported by the David and Lucile Packard Foundation, KIOST (PE99247 and PE99317), and MOF through KIMST (PM57991).

References

Alcaraz, C., and Kruesi, K. 2012. Exploring the phenotypic plasticity of standard metabolic rate and its inter-individual consistency in the hermit crab *Carcinus californiensis*. Journal of Experimental Marine Biology and Ecology, 412: 20–26.

Barry, J. P., Lovera, C., Okuda, C., Nelson, E., and Pane, E. F. 2008. A gas-controlled aquarium system for ocean acidification studies. IEEE Xplore, 978-4244-2126-4208/4208.

Bibby, R., Cleall-Harding, P., Rundle, S., Widdicombe, S., and Spicer, J. 2007. Ocean acidification disrupts induced defences in the intertidal gastropod *Littorina littorea*. Biology Letters, 3: 699–701.

Brewer, P., and Hester, K. 2009. Ocean acidification and the increasing transparency of the ocean to low-frequency sound. Oceanography, 22: 86–93.

Briffa, M., de la Haye, K., and Munday, P. 2012. High CO_2 and marine animal behaviour: potential mechanisms and ecological consequences. Marine Pollution Bulletin, 64: 1519–1528.

Byrne, R., McElligott, S., Feely, R., and Millero, F. 1999. The role of pH(T) measurements in marine CO_2-system characterizations. Deep Sea Research I: Oceanographic Research Papers, 46: 1985–1997.

Charmantier, A., McCleery, R., Cole, L., Perrins, C., Kruuk, L., and Sheldon, B. 2008. Adaptive phenotypic plasticity in response to climate change in a wild bird population. Science, 320: 800–803.

Cripps, I., Munday, P., and McCormick, M. 2011. Ocean acidification affects prey detection by a predatory reef fish. PLoS ONE, 6: e22736.

de la Haye, K., Spicer, J., Widdicombe, S., and Briffa, M. 2011. Reduced sea water pH disrupts resource assessment and decision making in the hermit crab *Pagurus bernhardus*. Animal Behaviour, 82: 495–501.

de la Haye, K., Spicer, J., Widdicombe, S., and Briffa, M. 2012. Reduced pH sea water disrupts chemo-responsive behaviour in an intertidal crustacean. Journal of Experimental Marine Biology and Ecology, 412: 134–140.

Dickson, A. G. 1990. Thermodynamics of the dissociation of boric-acid in synthetic seawater form 273.15 K to 318.15 K. Deep Sea Research, 37, 755–766.

Dickson, A. G., and Millero, F. J. 1987. A comparison of the equilibrium constants for the dissociation of carbonic-acid in seawater media. Deep Sea Research, 34: 1733–1743.

Dixson, D., Munday, P., and Jones, G. 2010. Ocean acidification disrupts the innate ability of fish to detect predator olfactory cues. Ecology Letters, 13: 68–75.

Doney, S., Fabry, V., Feely, R., and Kleypas, J. 2009. Ocean acidification: the other CO_2 problem. Annual Review of Marine Science, 1: 169–192.

Feely, R., Sabine, C., Hernandez-Ayon, J., Ianson, D., and Hales, B. 2008. Evidence for upwelling of corrosive "acidified" water onto the continental shelf. Science, 320: 1490–1492.

Friederich, G., Walz, P., Burczynski, M., and Chavez, F. 2002. Inorganic carbon in the central California upwelling system during the 1997–1999 El Nino–La Nina event. Progress in Oceanography, 54: 185–203.

Ilyina, T., Zeebe, R., and Brewer, P. 2010. Future ocean increasingly transparent to low-frequency sound owing to carbon dioxide emissions. Nature Geoscience, 3: 18–22.

Kim, T., Barry, J., and Micheli, F. 2013. The effects of intermittent exposure to low-pH and low-oxygen conditions on survival and growth of juvenile red abalone. Biogeosciences, 10: 7255–7262.

Kroeker, K., Kordas, R., Crim, R., and Singh, G. 2010. Meta-analysis reveals negative yet variable effects of ocean acidification on marine organisms. Ecology Letters, 13: 1419–1434.

Langer, G., Geisen, M., Baumann, K., Klas, J., Riebesell, U., Thoms, S., and Young, J. 2006. Species-specific responses of calcifying algae to changing seawater carbonate chemistry. Geochemistry Geophysics Geosystems, 7: Q09006.

Mellon, D. 1997. Physiological characterization of antennular flicking reflexes in the crayfish. Journal of Comparative Physiology A: Sensory Neural and Behavioral Physiology, 180: 553–565.

Munday, P., Dixson, D., Donelson, J., Jones, G., Pratchett, M., Devitsina, G., and Doving, K. 2009. Ocean acidification impairs olfactory discrimination and homing ability of a marine fish. Proceedings of

the National Academy of Sciences of the United States of America, 106: 1848–1852.

Munday, P., Dixson, D., McCormick, M., Meekan, M., Ferrari, M., and Chivers, D. 2010. Replenishment of fish populations is threatened by ocean acidification. Proceedings of the National Academy of Sciences of the United States of America, 107: 12930–12934.

Nilsson, G., Dixson, D., Domenici, P., McCormick, M., Sorensen, C., Watson, S., and Munday, P. 2012. Near-future carbon dioxide levels alter fish behaviour by interfering with neurotransmitter function. Nature Climate Change, 2: 201–204.

Orr, J., Fabry, V., Aumont, O., Bopp, L., Doney, S., Feely, R., Gnanadesikan, A., *et al.* 2005. Anthropogenic ocean acidification over the twenty-first century and its impact on calcifying organisms. Nature, 437: 681–686.

Pane, E., and Barry, J. 2007. Extracellular acid–base regulation during short-term hypercapnia is effective in a shallow-water crab, but ineffective in a deep-sea crab. Marine Ecology Progress Series, 334: 1–9.

Pane, E., Grosell, M., and Barry, J. 2008. Comparison of enzyme activities linked to acid–base regulation in a deep-sea and a sublittoral decapod crab species. Aquatic Biology, 4: 23–32.

Parker, L., Ross, P., and O'Connor, W. 2011. Populations of the Sydney rock oyster, *Saccostrea glomerata*, vary in response to ocean acidification. Marine Biology, 158: 689–697.

Pierrot, D., Lewis, E., and Wallace, D. W. R. 2006. CO2SYS DOS Program Developed for CO_2System Calculations. ORNL/CDIAC-105. Carbon Dioxide Information Analysis Center, Oak Ridge National Laboratory, US Department of Energy, Oak Ridge, CA.

Pistevos, J., Calosi, P., Widdicombe, S., and Bishop, J. 2011. Will variation among genetic individuals influence species responses to global climate change? Oikos, 120: 675–689.

Portner, H. 2008. Ecosystem effects of ocean acidification in times of ocean warming: a physiologist's view. Marine Ecology Progress Series, 373: 203–217.

Ramsay, K., Kaiser, M., Moore, P., and Hughes, R. 1997. Consumption of fisheries discards by benthic scavengers: utilization of energy subsidies in different marine habitats. Journal of Animal Ecology, 66: 884–896.

Reidenbach, M., and Koehl, M. 2011. The spatial and temporal patterns of odors sampled by lobsters and crabs in a turbulent plume. Journal of Experimental Biology, 214: 3138–3153.

Ries, J., Cohen, A., and McCorkle, D. 2009. Marine calcifiers exhibit mixed responses to CO_2-induced ocean acidification. Geology, 37: 1131–1134.

Schlegel, P., Havenhand, J. N., Gillings, M. R., and Williamson, J. E. 2012. Individual variability in reproductive success determines winners and losers under ocean acidification: a case study with sea urchins. PLoS ONE, 7: e53118.

Seibel, B., and Walsh, P. 2003. Biological impacts of deep-sea carbon dioxide injection inferred from indices of physiological performance. Journal of Experimental Biology, 206: 641–650.

Sih, A., Bell, A., and Johnson, J. 2004. Behavioral syndromes: an ecological and evolutionary overview. Trends in Ecology and Evolution, 19: 372–378.

Sih, A., Cote, J., Evans, M., Fogarty, S., and Pruitt, J. 2012. Ecological implications of behavioural syndromes. Ecology Letters, 15: 278–289.

Sih, A., Ferrari, M., and Harris, D. 2011. Evolution and behavioural responses to human-induced rapid environmental change. Evolutionary Applications, 4: 367–387.

Smith, K. L. J., Ruhl, H. A., Bett, B. J., Billett, D. S. M., Lampitt, R. S., and Kaufmann, R. S. 2009. Climate, carbon cycling, and deep-ocean ecosystems. Proceedings of the National Academy of Sciences of the United States of America, 106: 19211–19218.

Sunday, J., Crim, R., Harley, C., and Hart, M. 2011. Quantifying rates of evolutionary adaptation in response to ocean acidification. PLoS ONE, 6: e22881.

Sung, C., Kim, T., Park, Y., Kang, S., Inaba, K., Shiba, K., Choi, T., *et al.* 2014. Species and gamete-specific fertilization success of two sea urchins under near future levels of pCO_2. Journal of Marine Systems, 137: 67–73.

Tuomainen, U., and Candolin, U. 2011. Behavioural responses to human-induced environmental change. Biological Reviews, 86: 640–657.

Williams, J., and McDermott, J. 2004. Hermit crab biocoenoses: a worldwide review of the diversity and natural history of hermit crab associates. Journal of Experimental Marine Biology and Ecology, 305: 1–128.

Wood, H., Spicer, J., and Widdicombe, S. 2008. Ocean acidification may increase calcification rates, but at a cost. Proceedings of the Royal Society B: Biological Sciences, 275: 1767–1773.

Handling editor: Howard Browman

ICES Journal of Marine Science

ICES Journal of Marine Science (2016), 73(3), 620–632. doi:10.1093/icesjms/fsv101

Contribution to Special Issue: 'Towards a Broader Perspective on Ocean Acidification Research'

Original Article

9–28 d of exposure to elevated pCO_2 reduces avoidance of predator odour but had no effect on behavioural lateralization or swimming activity in a temperate wrasse (*Ctenolabrus rupestris*)

Josefin Sundin[1,2]* and Fredrik Jutfelt[1,2]

[1]*Department of Neuroscience, Uppsala University, Box 593, SE-751 24 Uppsala, Sweden*
[2]*Department of Biological and Environmental Sciences, University of Gothenburg, Gothenburg, Sweden*

**Corresponding author: tel: +46 730 302270; fax: +46 181 55140; e-mail: josefin@teamsundin.se*

Sundin, J., and Jutfelt, F. 9–28 d of exposure to elevated pCO_2 reduces avoidance of predator odour but had no effect on behavioural lateralization or swimming activity in a temperate wrasse (*Ctenolabrus rupestris*). – ICES Journal of Marine Science, 73: 620–632.

Received 1 March 2015; revised 9 May 2015; accepted 13 May 2015; advance access publication 1 June 2015.

Most studies on the impact of near-future levels of carbon dioxide on fish behaviour report behavioural alterations, wherefore abnormal behaviour has been suggested to be a potential consequence of future ocean acidification and therefore a threat to ocean ecosystems. However, an increasing number of studies show tolerance of fish to increased levels of carbon dioxide. This variation among studies in susceptibility highlights the importance of continued investigation of the possible effects of elevated pCO_2. Here, we investigated the impacts of increased levels of carbon dioxide on behaviour using the goldsinny wrasse (*Ctenolabrus rupestris*), which is a common species in European coastal waters and widely used as cleaner fish to control sea lice infestation in commercial fish farming in Europe. The wrasses were exposed to control water conditions (370 μatm) or elevated pCO_2 (995 μatm) for 1 month, during which time behavioural trials were performed. We investigated the possible effects of CO_2 on behavioural lateralization, swimming activity, and prey and predator olfactory preferences, all behaviours where disturbances have previously been reported in other fish species after exposure to elevated CO_2. Interestingly, we failed to detect effects of carbon dioxide for most behaviours investigated, excluding predator olfactory cue avoidance, where control fish initially avoided predator cue while the high CO_2 group was indifferent. The present study therefore shows behavioural tolerance to increased levels of carbon dioxide in the goldsinny wrasse. We also highlight that individual fish can show disturbance in specific behaviours while being apparently unaffected by elevated pCO_2 in other behavioural tests. However, using experiments with exposure times measured in weeks to predict possible effects of long-term drivers, such as ocean acidification, has limitations, and the behavioural effects from elevated pCO_2 in this experiment cannot be viewed as proof that these fish would show the same reaction after decades of evolution.

Keywords: chemoreception, choice flume, climate change, ecophysiology, predator avoidance, teleost.

Introduction

Animals may respond to rapid human-induced environmental change by adjusting their behaviour, which could improve an individual's chance of surviving the early stages of altered environmental conditions (Tuomainen and Candolin, 2010; Wong and Candolin, 2015). If the environment undergoes a drastic change, as can be the case with anthropogenic disturbance, behaviours may become dysfunctional under the new environmental conditions (Tuomainen and Candolin, 2010; Wong and Candolin, 2015). However, behavioural and/or phenotypic plasticity may allow animals to adjust and thereby mitigate the effects of the stressor (Endler, 1992; Wong and Candolin, 2015). As anthropogenic disturbance may alter the environment dramatically and/or rapidly, as well as in a way that the organisms have not encountered during their evolutionary history, maladaptive behavioural responses are quite likely (Ghalambor *et al.*, 2007; Tuomainen and Candolin, 2010; Wong and Candolin, 2015).

One potentially major anthropogenic disturbance is ocean acidification associated with global climate change, caused by increased

levels of carbon dioxide dissolving in the sea (Doney *et al.*, 2009; Hönisch *et al.*, 2012). Exposure to atmospheric CO_2 concentrations predicted by the end of the century for weeks to months may alter the behaviour of fish (reviewed in Heuer and Grosell, 2014). Among the reported behavioural effects in fish are changes in behavioural lateralization, activity level, and altered preferences towards olfactory cues (reviewed in Heuer and Grosell, 2014). Many experiments on ocean acidification and fish behaviour have used exposure times measured in days (reviewed in Heuer and Grosell, 2014). However, using such short exposure times to predict possible effects ocean acidification, which is a long-term driver, has limitations, and the behavioural effects from elevated pCO_2 in those experiments cannot be viewed as proof that these fish would show the same reaction after decades of evolution.

Behavioural lateralization refers to the preferential use of, for example, the left or the right eye and stems from the asymmetric control of cognitive functions in the brain (Vallortigara and Rogers, 2005; Bisazza and Brown, 2011). If an individual is lateralized, that is, shows a preference for using either the left or the right eye or a preference for turning left or right, this has been suggested to confer advantages in the form of enabling multiple stimuli to be processed simultaneously (Vallortigara and Rogers, 2005; Bisazza and Brown, 2011). When examining behavioural lateralization, both the preference to turn either left or right, termed relative lateralization, as well as the strength of a possible side bias, regardless of this bias being to the left or the right, termed absolute lateralization, is commonly tested (Vallortigara and Rogers, 2005). The impact of CO_2 on behavioural lateralization has been investigated in several CO_2 studies, with somewhat differing results. Domenici *et al.* (2012), Nilsson *et al.* (2012), and Jutfelt *et al.* (2013) report that exposure to CO_2 reduced absolute lateralization while relative lateralization was unaffected. One study, in contrast, reports a change in relative lateralization, with fish exposed to CO_2 being left lateralized while control fish were right lateralized, without any alteration in absolute lateralization, as in Domenici *et al.* (2014). Another study reports that CO_2 exposure reduced absolute lateralization, and in addition, there was a change in relative lateralization, this time from a left preference in control fish to no side preference in the CO_2 exposed fish (Welch *et al.*, 2014). However, there are also examples where no effect in either aspect of lateralized behaviour was found, such as in juvenile Atlantic cod (Jutfelt and Hedgärde, 2015).

Swimming activity is another behavioural measurement frequently used to investigate the effects of CO_2 exposure (reviewed in Heuer and Grosell, 2014). Many studies on fish report increased activity by CO_2 exposure (Munday *et al.*, 2010, 2013; Cripps *et al.*, 2011; Ferrari *et al.*, 2011, 2012; Devine *et al.*, 2012a; Forsgren *et al.*, 2013). The effect sizes are generally large, with some studies reporting doubled the activity level (Cripps *et al.*, 2011), and others up to 90 times more activity in CO_2 exposed fish compared with control fish (Munday *et al.*, 2013). On the contrary, a number of studies found no alterations in activity (Munday *et al.*, 2009; Nowicki *et al.*, 2012; Bignami *et al.*, 2013, 2014; Lönnstedt *et al.*, 2013; Sundin *et al.*, 2013; Jutfelt and Hedgärde, 2015; Maneja *et al.*, 2015), and differences in activity levels in opposite directions between different species have been reported for fish occurring at natural CO_2 seeps, with some species showing an increased activity in CO_2 and others a decrease (Munday *et al.*, 2014).

Olfaction is an important system for communication in aquatic environments as water can transfer olfactory cues over large distances, and chemical signals act as cues for a range of behaviours in fish (Magnhagen *et al.*, 2008). The impact of elevated pCO_2 on olfactory discrimination has been extensively investigated, and most studies report large effect sizes, particularly on predatory cue avoidance behaviour. For example, Dixson *et al.* (2010) report a shift from 100% avoidance of the predator odour by control fish to a 100% preference of predator olfactory cues over seawater in CO_2 exposed fish. CO_2 exposed fish also showed no preference for predatory fish or non-predatory fish cue (Dixson *et al.*, 2010). Similarly, other studies report that CO_2 exposed fish spent over 90% of the time in predator odour in a choice between predator cue and seawater (Munday *et al.*, 2010, 2013; Nilsson *et al.*, 2012), resulting in a 9-fold greater mortality rate in the wild (when placed on small reefs, made from live and dead coral, cleared of other fish and invertebrates) for CO_2 exposed fish compared with control (Munday *et al.*, 2010). Additional studies report an impaired ability to learn to recognize predator odour, again resulting in lower survival in the wild (Chivers *et al.*, 2014). Loss of antipredator responses for CO_2 exposed fish has also been reported for fish when exposed to conspecific chemical alarm cues (Lönnstedt *et al.*, 2013). It has also been reported that there is no transgenerational acclimation of olfactory behavioural responses, since juvenile coral reef fish still spent 75–80% of their time in water containing chemical alarm cues, regardless of the parental CO_2 treatment (Munday *et al.*, 2014). Hence, most studies found severe effects of CO_2 exposure on predator odour or conspecific chemical alarm cues avoidance behaviour, but differences between species exists, with some species, despite sharing the same ecology and life history, showing a less severe effect of CO_2 exposure on olfactory discrimination (Ferrari *et al.*, 2011).

Despite the large number of studies reporting detrimental effects on fish behaviour by near-future CO_2 levels, a growing number of studies are failing to find effects of CO_2 on a range of behaviours, including activity and predator avoidance (Bignami *et al.*, 2013, 2014; Jutfelt and Hedgärde, 2013, 2015; Lönnstedt *et al.*, 2013; Maneja *et al.*, 2013; Sundin *et al.*, 2013; Murray *et al.*, 2014; Näslund *et al.*, 2015). Further, as many experiments on ocean acidification and fish behaviour use short-term high pCO_2 exposures (reviewed in Heuer and Grosell, 2014), whereas ocean acidification occurs over evolutionary time, predictions about the possible impacts of future ocean acidification are highly speculative.

As the bulk of literature is growing, great variation between species is emerging, leaving us unable to predict the phylogenetic extent of behavioural disturbances at this point. Further experiments on phylogenetically diverse species are therefore desperately needed.

In this study, we examined the possible behavioural effects of increased levels of carbon dioxide using the abundant temperate goldsinny wrasse (*Ctenolabrus rupestris*). Wrasses (Labridae) are widely used as cleaner fish to control sea lice infestation in commercial farming of Atlantic salmon (*Salmo salar*) in northern Europe (e.g. Bjordal, 1991; Treasurer, 1994). Controlling salmon lice infestations is one of the greatest challenges to the sustainability of large-scale Atlantic salmon farming (Costello, 2009). However, despite the great economical value associated with wrasses, little is known about their behavioural ecology and general population ecology (but see Sayer, 1999; Skiftesvik *et al.*, 2014). We exposed goldsinny wrasse to elevated- and current-day levels of CO_2 for 1 month during which time we performed a series of behavioural tests, namely lateralization, activity, and prey and predator olfactory preference tests. Given the behavioural changes reported in the

majority of CO_2 research to date (reviewed in Heuer and Grosell, 2014), we hypothesized that exposure to CO_2 would alter lateralization, result in increased swimming activity, lead to indifference towards the prey cue and finally to attraction to predator odour.

Material and methods

The experiment was performed at Sven Lovén Centre for Marine Sciences, Kristineberg, at the west coast of Sweden during May to June 2014. Goldsinny wrasses were collected using fish trap cages in shallow water in the Gullmar fjord, near the marine station (58°15′N 11°28′E). The fish were caught in two bouts, 10–12 May (individuals used in lateralization tests) and 2–3 June (individuals used in activity and olfactory choice tests). The goldsinny wrasse is one of the most abundant fish species in coastal habitats in Europe (Hillden, 1981), but has been used surprisingly infrequent in experimental biology, despite the growing interest from the aquaculture industry (e.g. Bjordal, 1991; Treasurer, 1994). It readily acclimatizes to laboratory conditions, showing curiosity and feeding behaviour soon after entry into aquaria, and therefore according to Spooner (1937) "proves an excellent experimental animal". The total mortality over the duration of the experiment was 2 of 80 fish. Although the fish were collected at time of spawning (spawning period, May–June; Hillden, 1981), we were unable to sex the individuals, probably since only the smallest individuals caught were kept and those were most likely juveniles. In the laboratory, the fish were initially housed in flow-through holding aquaria (80 × 36 × 36 cm; length, width, height), brown algae (*Fucus vesiculosus*, *F. Serratus*, and *Laminaria sccarina*) collected at the site of capture were provided to all fish for shelter during the 2–3-d holding periods. Fish were fed shrimps and blue mussels (*Mytilus edulis*) daily. Water temperature and salinity followed natural conditions in the area during the holding periods [mean ± s.d., temperature 10–12 May: 10.8 ± 0.36°C; 2–3 June: 15.4 ± 0.34°C; salinity (PSU) 10–12 May: 24.2 ± 1.19; 2–3 June: 25.4 ± 0.28, data derived from the continuous monitoring of the flow-through system at the station (http://www.weather.loven.gu.se/kristineberg/en/data.shtml)]. The light cycle was set to L16 h: D8 h to mimic natural conditions.

CO_2 exposure

The CO_2 exposure was initiated on 13 May for the first batch of fish ($N = 24$ control, 24 CO_2, divided over 8 tanks) and on 3 June for the second batch (16 control, 16 CO_2, divided over 8 tanks). Fish were transferred to 38 × 36 × 35 cm aquaria where they were acclimated to the final CO_2 level. We gradually increased the CO_2 by gradually decreasing the set pH value on the pH stat computers, thereby slowly increasing the amount of CO_2 added to the header tanks (see below) over 48 h until the targeted concentration of 1000 μatm was reached. Half of the aquaria were randomly assigned to the CO_2 treatment, and the other half were kept as controls. The aquaria had a constant supply of flow-through seawater (rate of 2 l min^{-1}) from four header tanks (50 l; two per treatment). Each header tank had a flow of 5 l min^{-1} of flow-through seawater from the fjord, pumped from 5-m depth. All header tanks were aerated. The target value of 1000 μatm for the CO_2 treatment header tanks was maintained using pH stat Computers (Aqua Medic, Bissendorf, Germany) connected to solenoid valves regulating the administration of 100% CO_2 gas (AGA, Sweden). The pCO_2 of the experimental tanks was measured daily using direct pCO_2 measurements with an infrared CO_2 probe (GM 70, Vaisala, Finland) connected to a submerged gas-permeable PFTE probe (Qubit Systems, Kingston, Canada; following Hari *et al.*, 2008; Jutfelt and Hedgärde, 2013; Green and Jutfelt, 2014). The Vaisala CO_2 meter was factory calibrated (Vaisala) before the experiment and accuracy was validated weekly throughout the experiment by testing against a known gas mixture with 1010 μatm CO_2 in air (AGA), and no drift was detected. The water carbonate chemistry was calculated using the constants of Roy *et al.* (1993) and Dickson (1990) in CO2calc (Hansen, USGS, USA). Temperature and pCO_2 were measured daily, and alkalinity was measured weekly, data on salinity levels were derived from the continuous monitoring of the flow-through system at the station (Table 1).

Experimental design

The behavioural tests were carried out under the same environmental conditions (temperature, salinity, pCO_2) as the fish had experienced during the exposure, except for the last lateralization test where all fish were tested in control water. All tests were performed during daytime. The first batch of fish was used in the lateralization test, and the second batch of fish was used in the activity and prey and predator olfactory preference tests. Fish were carefully hand-netted from their home tank and individually introduced into the experimental arenas. The fish were weighed (g) and measured (total length, TL, in mm) after the behavioural trials (mean ± s.d., Control: length: 94.2 ± 8.46, weight: 10.1 ± 2.37; High CO_2: length: 93.7 ± 8.25, weight: 9.2 ± 2.43), where after they were returned to their home tank. The fish were released approximately at the site of capture when all experiments were completed.

The experiment was performed according to current national legislation on Animal Welfare, Swedish Board of Agriculture, and approved by the Ethical Committee on Animal Experiments, Gothenburg, under licence Dnr 151-2011 and 103-2014.

Lateralization

For the behavioural lateralization tests, we used a double T-chamber [dimensions: 50 cm long with a 9 cm wide double T-channel

Table 1. Water chemistry data during the exposure of the goldsinny wrasse (*C. rupestris*), measured daily (pCO_2, salinity, temperature) and weekly (alkalinity) for a four header tanks system (Control A and B; High CO_2 A and B).

Treatment	pCO_2 (μatm)	Temperature (°C)	Salinity	Alkalinity	pH_{tot} (calc.)
Control A	374.5 (65)	15.0 (2.5)	26.2 (4.6)	2 074.7 (158)	8.11 (0.07)
Control B	375.0 (76)	15.0 (2.5)	26.2 (4.6)	2 016.2 (168)	8.15 (0.09)
High CO_2 A	1 032.2 (127)	15.0 (2.5)	26.2 (4.6)	2 009.3 (178)	7.68 (0.02)
High CO_2 B	969.8 (76)	15.0 (2.5)	26.2 (4.6)	2 072.1 (148)	7.69 (0.04)
Mean Control	374.8 (70)	15.0 (2.5)	26.2 (4.6)	2 045.5 (154)	8.13 (0.08)
Mean High CO_2	994.5 (122)	15.0 (2.5)	26.2 (4.6)	2 036.2 (156)	7.68 (0.03)

The pCO_2, alkalinity, salinity, and temperature were measured, whereas the total pH was calculated with CO2calc (Hansen, USGS). The data are presented as the means with s.d. in parenthesis.

(PlastKapTek, Partille, Sweden)] as described in Jutfelt *et al.* (2013; Supplementary Figure S1). After being introduced to the experimental arena, the fish was gently encouraged (with a plastic rod) to swim to the central channel where after they swam towards the perpendicular channel and made a left or a right choice without further interference from the observer. Ten consecutive runs in alternating order of swimming direction in the double T-chamber was performed to account for any possible asymmetry in the set up (Bisazza *et al.*, 1998). Turning choices were recorded by direct visual observation by one observer (JS). The tests were performed on two occasions, on exposure day 9 ($N = 24$ per treatment group) and exposure day 19 to test for effects of exposure duration ($N = 23$ control, 17 CO_2, one high CO_2 tank was excluded for technical reasons). All replicates were tested within the same day. A final lateralization test was performed on exposure day 21 ($N = 18$ control, 17 high CO_2), where both treatment groups were tested in control water to investigate if a possible CO_2 effect in lateralization would be maintained despite an acute change in pCO_2. It has been reported previously that behavioural impairment caused by exposure to elevated CO_2 lasts for several days and is not affected by testing fish in CO_2-treated water vs. control water (Dixson *et al.*, 2010; Munday *et al.*, 2010). During the lateralization tests, the treatments were alternated, and the water changed for every 6th fish.

We calculated the relative lateralization index (L_R, the turning direction bias) and the absolute lateralization index (L_A, the strength of the side bias) using the formulae: $L_R = [(\text{turns to the right} - \text{turns to the left})/(\text{turns to the right} + \text{turns to the left})] \times 100$, with values ranging from -100 to $+100$ (positive values indicating a preference for turns to the right, negative values a preference for turns to the left), and $L_A = |L_R|$, with values ranging from 0 to 100 where higher values indicate a stronger side bias (Bisazza *et al.*, 1997).

Activity

For the activity tests, we used four vertical cylindrical arenas (diameter: 20 cm, water depth: 10 cm), made of white opaque Plexiglas, with flow-through water [two with control water and two with high CO_2 water (1000 μatm), in randomized order], placed on an infrared (IR) light board (Figure 1). After being

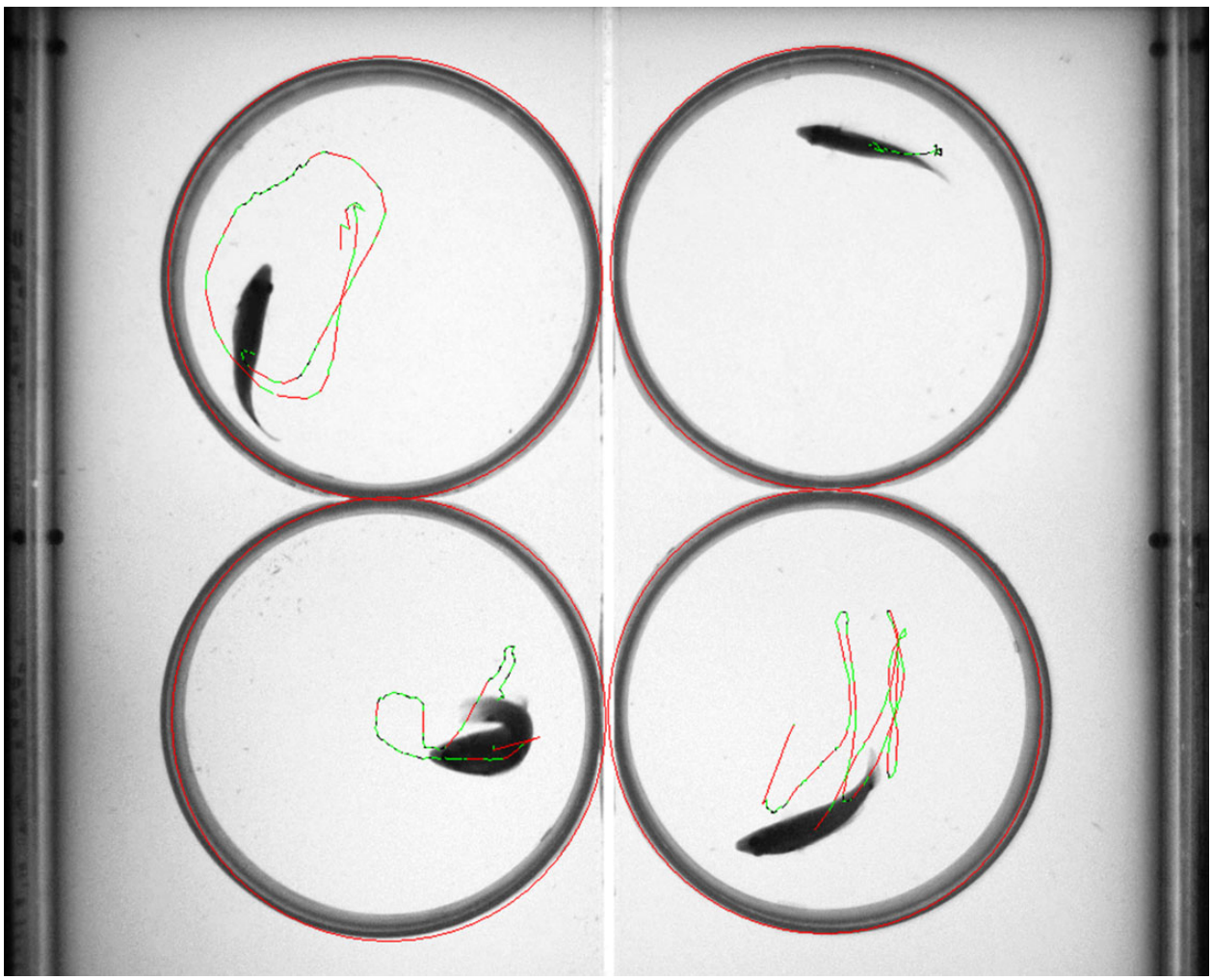

Figure 1. Experimental setup of the activity test with the four vertical cylindrical arenas made of white opaque Plexiglas, where activity was measured. The two sides of the vertical divider were independently supplied with flow-through water, one with control water and one with high CO_2 water. The cylinders were raised slightly from the bottom to ensure water replacement inside the arenas. The tracks show the movements covered during 1 min.

carefully introduced to the experimental arena, the fish were left undisturbed, in moderate ambient light, for 60 min during which time they were monitored using an IR sensitive firewire camera (Dragonfly 2, Pointgray, Richmond BC, Canada), mounted above the arenas. We used ViewPoint Zebralab (ViewPoint, Lyon, France), which is a commercial behaviour analysis system developed for zebrafish behaviour research. It automatically quantifies total activity (total swimming distance) and swimming duration (swimming was defined as all movements above 5 mm s^{-1}) in real time (Rihel *et al.*, 2010). Swimming duration as well as swimming distance for each animal was averaged for every minute of the experiment. We performed eight runs of the experiment using two fish from each treatment in each run, adding up to in all 16 fish from the control treatment and 15 from the high CO_2 treatment (one fish became lethargic during the exposure period and was not included in the behavioural tests). The runs were performed on exposure days 22 and 23 (i.e. all replicates were tested within 2 d). After the experiment, the fish were weighed, measured, and returned to their home tank.

Prey and predator olfactory preference

The olfactory preference tests were performed using the setup described in Atema *et al.* (2002), modified for larger fish as described in Jutfelt and Hedgärde (2013). The choice flume consisted of a two-choice flume channel (Choice Tank, Loligo Systems, Tjele, Denmark) containing a 32 by 40 cm choice arena with a water depth of 15 cm (Figure 2). The two water masses were continuously supplied, in a flow-through manner, by two 200 l header tanks, into which the olfactory cues were introduced. To create the prey cue, we placed one recently crushed blue mussel (*M. edulis*) into a net in one of the header tanks and exchanged the mussel every second run. Blue mussels are a known food source for goldsinny wrasse (Hillden, 1978). To create the predator cue, we placed one Atlantic cod (*Gadus morhua*; wild-caught, 1 kg), in one of the header tanks ~1 h before the start of the experiment, where it remained throughout the runs for each day. Wrasses are important prey for Atlantic cod (Salvanes and Nordeide, 1993). A main header tank upstream from the two side tanks (described further in Figure 3 in Jutfelt and Hedgärde, 2013) with a CO_2 manipulation system was used to supply the two downstream header tanks, making it possible to use the pCO_2 that the fish were acclimated to on both sides of the flume simultaneously (Jutfelt and Hedgärde, 2013). The two downstream header tanks supplied water to the two sides of the flume at a flow rate of 17 l min^{-1} each and 1 cm s^{-1} water speed in the arena. The flume inlets had a crossover switch, which allowed quick change of sides of the olfactory cue with no or minimal disturbance to the fish.

Fish behaviour was video recorded by a Dragonfly II camera (Pointgrey, Richmond, Canada) positioned above the flume. After 10 min, the flows were switched (the olfactory cue switched side of the flume within 1 min as confirmed by dye test before the experiment). After the switch, the flow was maintained for another 10 min (i.e. total trial time 20 min). We performed the prey cue preference experiment on exposure day 22–24 (i.e. all replicates were tested within 3 d), alternating the control and high CO_2 treatments, $N =$ 16 control and 15 high CO_2 (excluding one lethargic CO_2 fish). The predator cue avoidance experiment was performed on exposure day 27–28 (i.e. all replicates were tested within 2 d).

We used ViewPoint Zebralab to analyse the videos, analysing total duration for the left and the right side of the flume. For each run, we analysed 8 + 8 min, that is, excluding the first 2 min after trial start (regarded as acclimatization time) and the first 2 min after water switch.

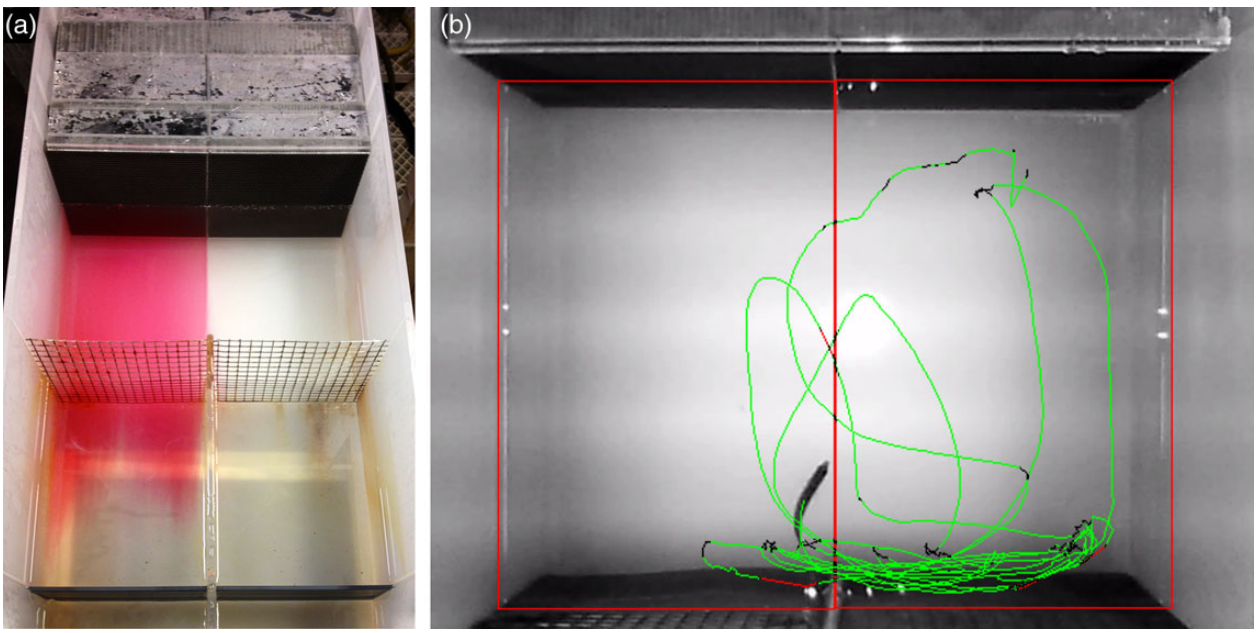

Figure 2. (a) Photo of the choice flume used for the olfactory cue tests from above, with the direction of water flow from the top of the picture and downwards. The flume has four layers of honeycomb structure (top) to create laminar flow, and the olfactory choice arena is the central rectangle, upstream from the mesh. Dye tests were regularly performed to ensure laminar water flow and minimal mixing of the two water flows; here, the left side receives water with red dye. (b) The central choice arena seen through the Viewpoint analysis software, with a wrasse centrally in the bottom of the picture. The two red boxes represent the two sides of the flume, one with and one without olfactory cue. The track shows the movement covered during 1 min.

Data analysis

We first tested for possible tank effects within each treatment for each behavioural test using nested ANOVAs. For the lateralization test, no such effects were found (all three runs, all tanks $p > 0.1$, Supplementary Table S1). However, for the activity tests (swimming duration and total distance), we found tank effects with decreased activity in one CO_2 tank (tank T3A, swimming duration: $t = -2.12$, $p = 0.045$; total distance: $t = -2.27$, $p = 0.033$, all remaining tanks $p > 0.1$, Supplementary Table S2), which was therefore excluded from further analysis (nested ANOVA excluding tank T3A, all remaining tanks $p > 0.1$, Supplementary Table S2). For the olfactory preference test, no tank effects were found (prey cue attraction and predator avoidance, all tanks $p > 0.1$, Supplementary Table S3). Statistical methods are described in brief, see Supplementary material for error distributions and link-functions.

For the lateralization experiment, we analysed test run 1 and 2 separately from test run 3, as the experimental setup differed between these runs, with all fish tested in control water in test run 3. For relative and absolute lateralization (used to allow for easier comparison to previous studies), test run 1 and 2, we performed Generalized Linear Models (GLMs) with appropriate error distribution and link-functions (Quinn and Keough, 2002), with the relative and absolute indexes as response variables and treatment, test run, and the interaction between them as fixed effects. For relative and absolute lateralization, test run 3, we used GLMs with treatment as fixed effect. Given the binomial error distribution, rather than Gaussian, of the detour test (choice of turning left or right), we also conducted two GLMs (with binomial error distribution), using the number of turns to the left as the response variable (corresponding to the relative index), and the maximum number of turns to the preferred side as the response variable (corresponding to the absolute index), both GLMs with the total number of left and right turns as the denominator, and treatment as the fixed factor.

For the activity test, we analysed proportion swimming duration (swimming duration out of total duration) and mean total distance using GLMs with treatment as fixed effect and fish length as covariate. To test whether there was any temporal change in activity across the testing period, we used a Generalized Linear Mixed Model, GLMM, with proportion inactive duration as the response variable, time, treatment, and the interaction between them as fixed effects, and the ID of each fish as random effect. All analyses on activity were performed excluding tank T3A, for which we found tank effects, including tank T3A, however, yielded similar results (Supplementary Table S4).

Table 2. The effect of treatment (high CO_2 and control) in the goldsinny wrasse (*C. rupestris*), for the behavioural tests lateralization, activity, and olfactory choice.

Test	Response variable	Explanatory variable	χ^2	*p*-value
Lateralization	Relative lat, run 1 and 2	Treatment (CO_2)	0.13	0.722
		Test run (1)	2.79	0.095
		Run (1) × Treatment (CO_2)	0.15	0.701
	Relative lat, run 3	**Treatment (CO_2)**	**4.33**	**0.037***
	Absolute lat, run 1 and 2	Treatment (CO_2)	0.63	0.428
		Test run (1)	**5.17**	**0.023***
		Run (1) × Treatment (CO_2)	**4.81**	**0.028***
	Absolute lat, run 3	Treatment (CO_2)	0.12	0.695
Activity	Swimming dur.	Treatment (CO_2)	0.17	0.684
		Length	0.68	0.408
	Accl. time removed	Treatment (CO_2)	0.17	0.680
		Length	0.97	0.324
	Total distance	Treatment (CO_2)	2.05	0.152
		Length	0.20	0.652
	Accl. time removed	Treatment (CO_2)	2.46	0.117
		Length	0.48	0.490
			Wald χ^2	*p*
	Temporal change	Treatment (CO_2)	0.01	0.940
	Swimming dur.	**Time**	**37.23**	**<0.001*****
		Time × Treatment (CO_2)	0.07	0.796
			χ^2	*P*
Olfactory choice				
	% time in prey cue	Treatment (CO_2)	0.00	0.989
		Length	0.69	0.407
	% time in predator cue	Treatment (CO_2)	3.18	0.075
		Length	0.02	0.893
			Wald χ^2	*P*
	Temporal change	Treatment (CO_2)	0.00	0.947
	% time in prey cue	Time	0.19	0.659
		Time × Treatment	0.62	0.430
	Temporal change	Treatment (CO_2)	2.70	0.100
	% time in predator cue	**Time**	**6.09**	**0.009****
		Time × Treatment (CO_2)	**21.57**	**<0.001*****

For the lateralization test, we included test run (1 and 2) and the interaction between test run and treatment as factors. Test run 3 was analysed separately due to differing experimental procedure. For the activity test, length was included as a covariate for all tests on swimming duration and total distance moved (with and without the removal of acclimation time). For swimming duration, we further analysed temporal change over time, with time and the interaction between time and treatment as factors. For the olfactory choice test, length was included as a covariate, analysing proportion of time spent in cue, as well as the temporal change over time of time spent in cue, with time and the interaction between time and treatment as factors. *$p < 0.05$, **$p < 0.01$, ***$p < 0.001$.

For the olfactory choice tests, we analysed the proportion of time spent in the odour cue using GLMs with treatment as the fixed effect and fish length as covariate. To test whether there was any temporal change in cue preference across the testing period, we used GLMMs with time spent in odour cue as the response variable, time, treatment, and the interaction between them as fixed effects, and the ID of each fish as random effect.

We used JMP 11 (SAS Institute Inc., Cary, NC, USA) for all statistical analyses, except for the GLMMs where GenStat 8 (VSN International Ltd, Hemel Hempstead, UK) was used.

Results

Lateralization

For the first two trials, performed day 9 and day 19, we found no effect of treatment in the relative lateralization index (non-significant effect of test run and non-significant interaction removed, Table 2, Figures 3 and 4). In the absolute lateralization index, the interaction between test run and treatment was significant (Table 2, Figures 3 and 4), showing that absolute lateralization was reversed between the treatments when tested the second time (with CO_2 exposed fish showing the strongest absolute lateralization on the first test run and Control

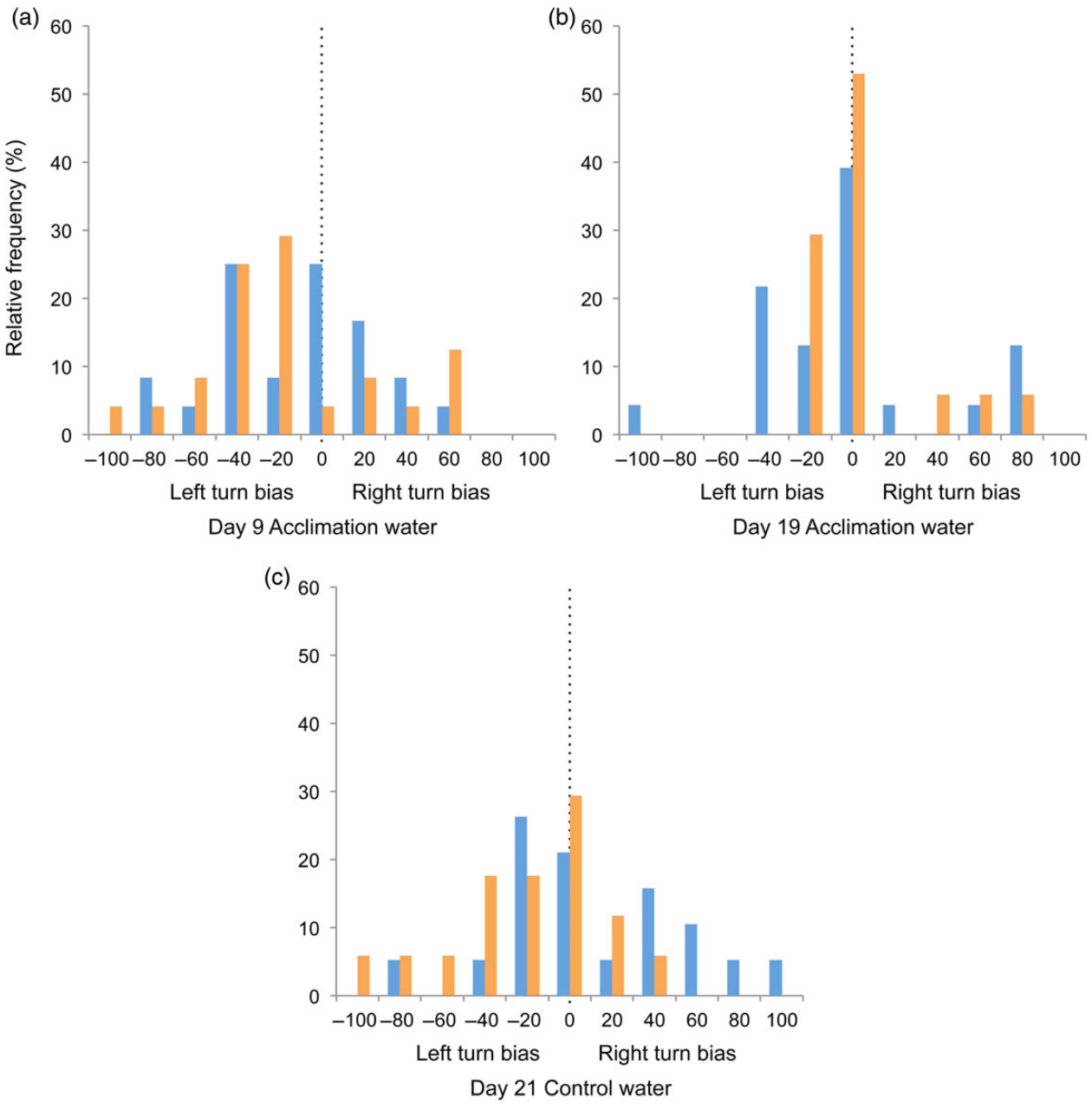

Figure 3. Frequency distribution of relative lateralization [blue/black bars: control (370 μatm), orange/grey bars: high CO_2 (995 μatm)] in the goldsinny wrasse (*C. rupestris*), after (a) 9 d of exposure, (b) 19 d of exposure (all fish tested in their respective acclimation water), and (c) 21 d of exposure (all fish tested in control water). Individuals with a negative score were behaviourally left biased, and individuals with a positive score were right biased (relative lateralization index: L_R = [(turns to the right − turns to the left)/(turns to the right + turns to the left)] × 100).

fish showing the strongest absolute lateralization on the second test run, Figures 3 and 4).

For the last trial, where both treatments were tested in control water (experiment performed day 21), there was a significant effect of treatment on relative, but not on absolute, lateralization (Table 2). In this trial, the control fish had a mean L_R index [8.9 ± 10.51 (± s.e.)] that did not deviate from 0 (one-sample *t*-test against an expected mean of 0: $t_{18} = 0.85$, $p = 0.409$), whereas the CO_2-exposed fish had the mean L_R index [−20.0 ± 8.91(± s.e.)] that did deviated from 0 (one-sample *t*-test against an expected mean of 0: $t_{17} = -2.24$, $p = 0.039$) indicating a turning preference towards the left (Figures 3 and 4). The binomial GLMs showed similar results (Supplementary Table S5).

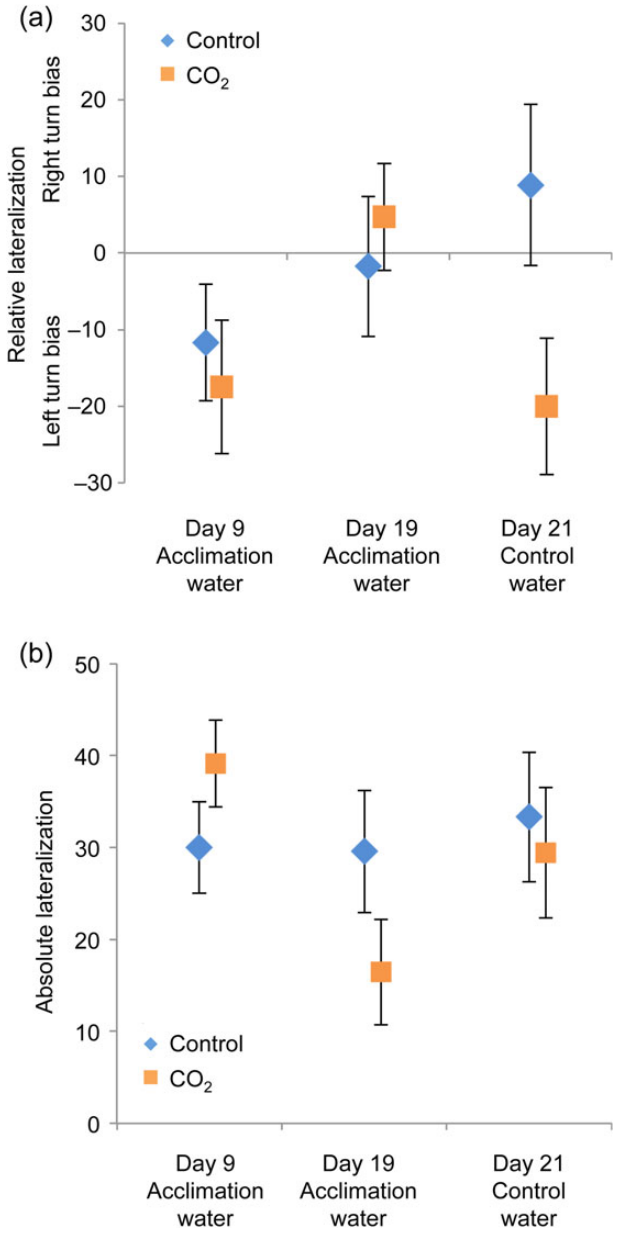

Figure 4. (a) Relative lateralization in the goldsinny wrasse (*C. rupestris*), showing the mean turning bias, positive scores indicate a right-turning bias, and negative scores indicate a left-turning bias. (b) Absolute lateralization, showing the strength of the bias, irrespective of side preference. The fish tested after exposed to control water (370 μatm; blue/black diamonds) or high CO_2 water (995 μatm; orange/grey squares) for 9 and 19 d. At 21 d, all fish were tested in control water (means ± s.e.m.).

Activity

We found no effect of CO_2 on either swimming duration or total distance moved (Table 2).

For the analysis of temporal change in activity (inactive duration) across the testing period, there was again no effect of treatment while time had a significant effect, showing that the fish became less active during the testing period (Table 2, Figure 5). However, with a mean proportion of time spent swimming for the first minutes of 0.95, compared with a mean for the last 10 min of 0.91, the effect is small and likely due to habituation to the novel arena. Excluding the first 10 min of each run, to allow for habituation, yielded similar results in swimming duration and total distance moved (Table 2).

Prey and predator olfactory preference

When testing the mean time spent in the cue for the total testing period, we found no effect of CO_2 in the choice of olfactory cue, neither on prey nor on predator cue (Table 2). For the analysis of temporal change in cue preference across the testing period, we found no effect of CO_2 treatment, time, or the interaction between treatment and time on time spent in the prey cue (Table 2). The wrasses actively avoided the prey cue, regardless of treatment and of what side the cue was presented on in the flume (Figure 6). For the predator cue, there was an interaction between time and treatment, showing that the control fish actively avoided the predator odour at the beginning of the experiment, whereas the CO_2 exposed fish showed indifference, and both control and CO_2 showed indifference towards the predator odour towards the end of the test run (Table 2, Figure 6).

Because previous studies on olfactory choice in general have been conducted by noting the position of the fish in the flume in a certain time interval (every fifth or every tenth second, e.g. Dixson *et al.*, 2010; Munday *et al.*, 2010; Devine *et al.*, 2012b; Munday *et al.*, 2012; Nilsson *et al.*, 2012; Jutfelt and Hedgärde, 2013) we, in addition to our high-precision automated flume analysis, used the same method here for the prey cue choice test, which allows cross validation of these two methods. We thus reanalysed the prey videos by noting what side the fish was on every 10th second and then analysed the proportion of times observed in the prey cue using similar statistics as described above. With this method, we obtained similar results to what was found when analysing the videos through ViewPoint (proportion of times observed in prey cue: effect of treatment: $\chi^2_{1,26} = 0.01$, $p = 0.924$, effect of length: $\chi^2_{1,26} = 0.15$, $p = 0.699$), suggesting that these two fish detection methods are comparable.

Discussion

In this study, on the goldsinny wrasse, we conducted a range of standard behavioural assays for behaviours in which adverse effects of CO_2 exposure have previously been reported in marine fish. We failed to detect any major effects of carbon dioxide in most behaviours investigated, except predator avoidance. This study thus adds to the growing literature where the effects of elevated CO_2 levels on behavioural responses were either minor or not observed (reviewed in Heuer and Grosell, 2014).

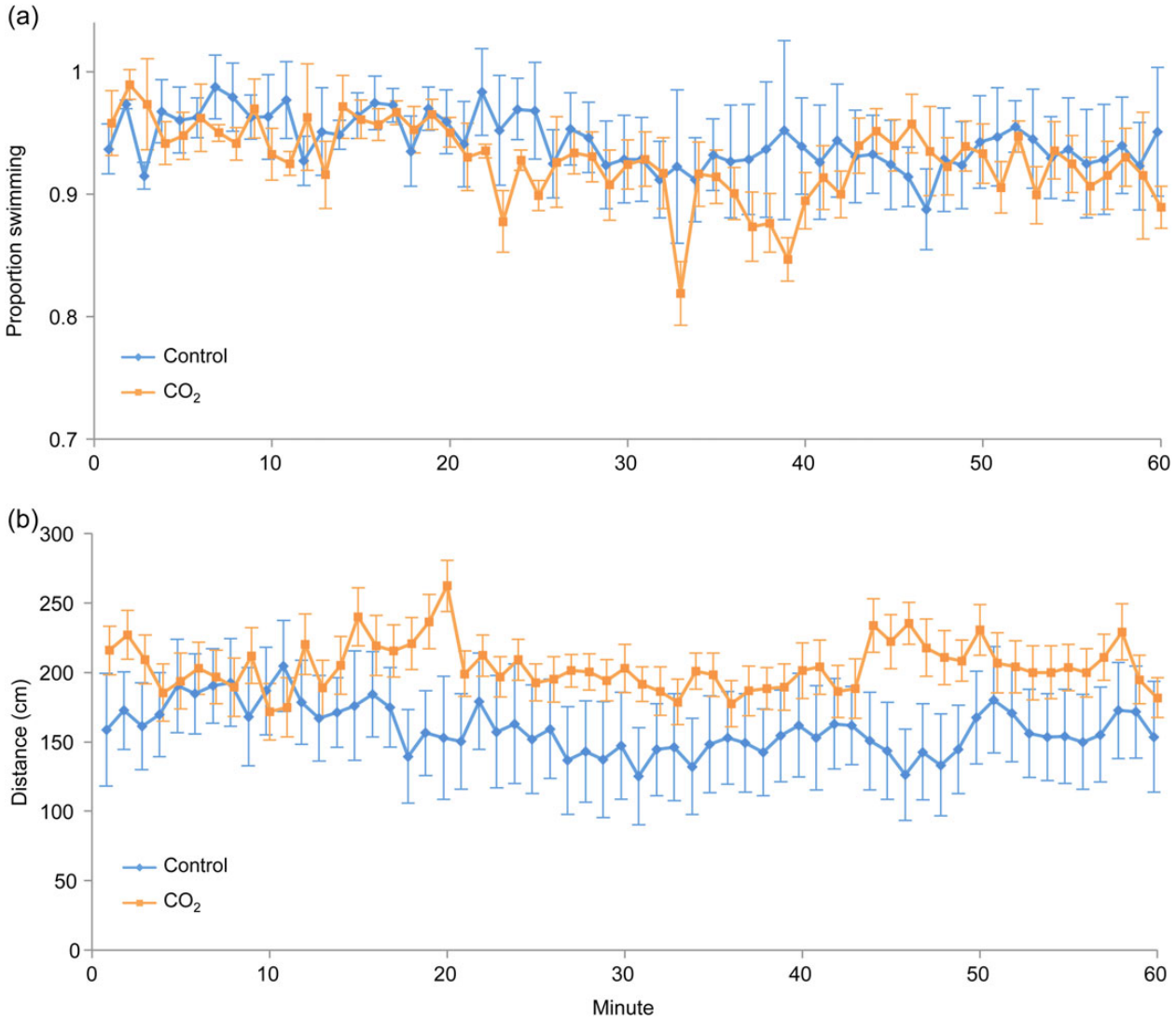

Figure 5. (a) The proportion of time spent moving in the goldsinny wrasse (*C. rupestris*), after 22 – 23 d of exposure to control water (blue/black) or elevated CO_2 levels (orange/grey). The value for each minute is the mean from continuous measurements of activity ($n_{control} = 16; n_{CO_2} = 11$) and the error bars show s.e.m. The two treatments are slightly offset on the *x*-axis to show the error bars. (b) Total distance moved each minute in the same experiment (mean ± s.e.m.).

Prey and predator olfactory preference

The impact of CO_2 exposure on olfactory discrimination is one of the most well studied areas in the ocean acidification literature, with most studies reporting that CO_2 exposed fish show a preference for predator cue (reviewed in Heuer and Grosell, 2014). We found reduced predator avoidance in CO_2 exposed fish, but the avoidance did not turn into attraction as reported for many coral reef fish (reviewed in Heuer and Grosell, 2014). Instead the CO_2 exposed fish showed indifference to the cue, staying in predator odour 50% of the time. If the effect of CO_2 reducing predator olfactory cue detection is repeatable and still present after longer exposures, it could be detrimental to fish in the wild under high CO_2 conditions. Transgenerational acclimation of CO_2-induced behavioural disturbance has been suggested to be limited in some species (Welch *et al.*, 2014), but not in others (Miller *et al.*, 2012; Allan *et al.*, 2014; Murray *et al.*, 2014), hence it should be investigated if the effect could persist in fish during multiple generations and therefore may cause maladaptive behaviour in a future ocean.

The control fish avoided the predator odour for the first part of the test run but showed indifference during the last part, a behaviour that could be explained by initial predator avoidance followed by sensory or neural habituation to the cue. However, habituation to cues has been suggested to be slow or non-existent in fish (Vilhunen, 2006; Jutfelt and Hedgärde, 2013). To answer why the control fish only showed predator avoidance during the first part of the run, detailed follow-up experiments are required.

Although the effect of CO_2 exposure on predator avoidance behaviour has been investigated in many studies, the possible effect of CO_2 on prey cue attraction is a largely neglected area with a few exceptions showing reduced prey detection (Cripps *et al.*, 2011) or no effect (Bignami *et al.*, 2013, 2014). In the present experiment, we failed to detect any effect of CO_2 on prey cue attraction and both treatments avoiding crushed mussel cues equally, spending 36% of the time in the mussel cue. In general, food odours elicit a strong stimulus action on the feeding behaviour and search behaviour in fish (Kasumyan and Döving, 2003), and our hypothesis was

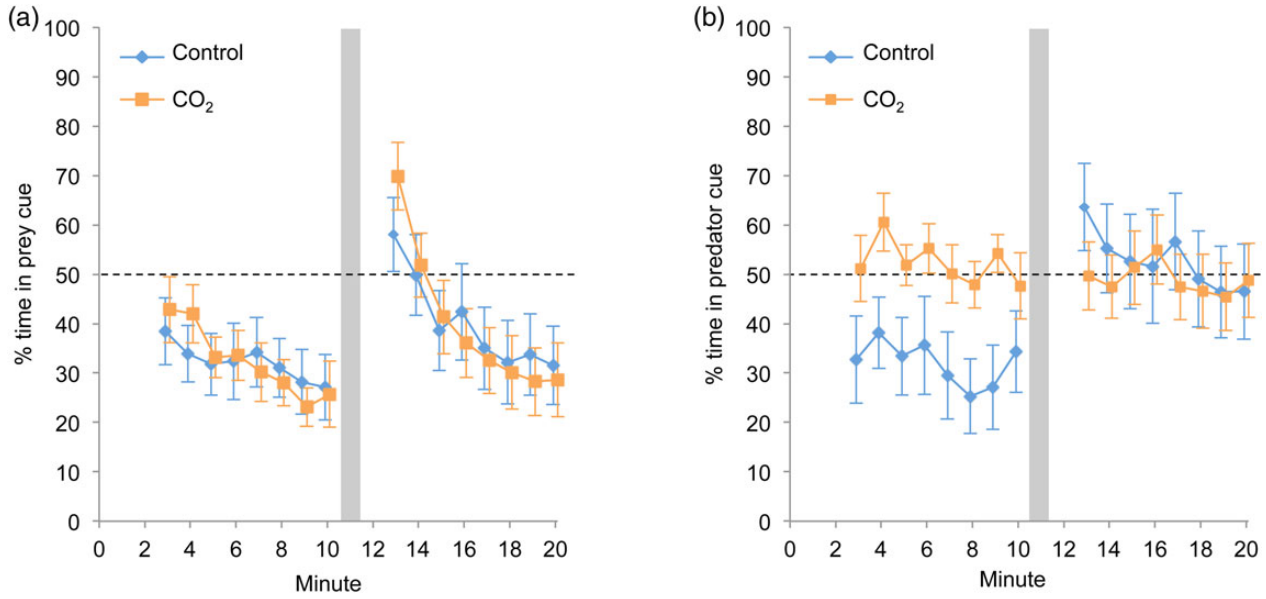

Figure 6. The mean % time the goldsinny wrasse (*C. rupestris*) spent in (a) prey odour and (b) in predator odour after 22 – 24 d of exposure to control water (blue/black) or elevated CO_2 levels (orange/grey). The value for each minute is the mean from continuous measurements of time spent on the side of the flume containing the odour ($n_{control} = 16$; $n_{CO_2} = 15$), with the first 2 min set as acclimation time (i.e. no data presented) and the first 2 min after the odour side was switched in the flume removed to ensure complete side switch of the odour (i.e. minute 11 and 12). The shaded area represents the time with mixed water after side switch, and the dashed line is the 50% mark representing no active side choice. Error bars show the s.e.m. The two treatments are slightly offset on the *x*-axis to show the error bars.

that crushed mussels would attract the fish and that CO_2 would alter this attraction. The fish readily fed on mussels in their exposure aquaria. It is therefore possible that the behavioural response to crushed mussel cues is highly context-dependent and that the transfer from the school in the familiar exposure aquaria to being alone in the flume arena caused a shift from considering the cue food to considering the cue a disturbance. It is also possible that olfactory cues from food items are not enough to elicit a feed search response in the goldsinny wrasse and that visual cues are needed in addition. As the fish were food deprived for only 24 h before olfactory choice experiments, it is possible that their feeding motivation was low. Similar results have been reported previously, where the introduction of food odour did not cause a noticeable search for food in the common carp (*Cyprinus carpio*; Kasumyan *et al.*, 2009). The prey cue avoidance behaviour, while surprising, was nonetheless strong and consistent between treatments, showing that the wrasses responded identically regardless of their pCO_2 exposure history as well as the pCO_2 in the flume during olfactory detection. This finding is in contrast to the strong effects of CO_2 exposure on many cues observed in several tropical species (reviewed in Briffa *et al.*, 2012).

The different effects of the CO_2 exposure on prey cue and predator cue avoidance behaviour is interesting, possibly suggesting that CO_2 can affect the olfactory detection at the olfactory-receptor level rather than at the central nervous system level via the $GABA_A$ receptor function as suggested previously (Nilsson *et al.*, 2012). Elevated CO_2 has been suggested to chemically reduce the olfactory receptor response in European sea bass (*Dicentrarchus labrax*; Porteus *et al.*, 2014), leading to higher detection thresholds for chemical cues and a reduction in maximum distance to the olfactory source wherefrom detection could occur by 48%. It is therefore possible that the observed discrepancy between control and CO_2 exposed fish in predator cue avoidance may be due to a higher detection threshold when CO_2 is present in the water. The potential for mitigation of this effect by acclimation or adaptation is unknown.

Activity

Activity is one of the behavioural traits where CO_2 exposure seems to elicit a broad range of responses. For fish occurring in naturally high CO_2, at CO_2 seeps, some species show an increase in activity while some species show a decrease, compared with control fish from otherwise comparable areas (Munday *et al.*, 2014). In this study, we found no effect of CO_2 on either swimming duration or total distance moved, matching a number of studies failing to detect effects of CO_2 on activity (Munday *et al.*, 2009; Nowicki *et al.*, 2012; Bignami *et al.*, 2013, 2014; Lönnstedt *et al.*, 2013; Sundin *et al.*, 2013; Jutfelt and Hedgärde, 2015; Maneja *et al.*, 2015). On the other hand, many studies report increased activity when exposing fish to CO_2 (Munday *et al.*, 2010, 2013; Cripps *et al.*, 2011; Ferrari *et al.*, 2011, 2012; Devine *et al.*, 2012a; Forsgren *et al.*, 2013). Thus, although some studies report great effects of CO_2 on activity, the results are not congruent, possibly suggesting that the response of increased levels of CO_2 varies between species and ecological settings.

Lateralization

When testing behavioural lateralization under the same environmental condition as the fish had experienced during the exposure (i.e. testing control fish in control water and CO_2 exposed fish in CO_2 water; test run 1 and 2), we found no difference between CO_2 and control fish in relative lateralization. However, for absolute lateralization, the significant interaction between test run and treatment indicated that the CO_2 exposed fish displayed the strongest side bias on the first test run, whereas the control fish showed the

strongest bias on the second test run. It appears the control fish showed a similar strength in lateralization throughout the test runs (also in the third test run), displaying a mean absolute lateralization around 30 for each run, whereas the CO_2 exposed fish had a mean absolute lateralization of 40 in the first run and 16 in the second run. This could be interpreted as the control fish persistently showing the same strength of the side bias while the CO_2 exposed fish exhibited alterations in the strength of side bias as the CO_2 exposure progressed. This inconsistency of behavioural lateralization in CO_2 exposed fish suggests that it may be necessary to monitor lateralization repeatedly during a treatment to describe the full effect on lateralization and that a snapshot at one time point may not tell the whole story. Hence, forthcoming studies should focus on assessing the impact CO_2 may have on lateralization over time, investigate the repeatability of the lateralization pattern, and further determine the adaptive significance of the observed effect (if any) in context of the specific species ecology. Since the relative and/or absolute lateralization can change within individuals depending on a range of factors, such as time in captivity (Bisazza *et al.*, 1997), sexual motivation (Bisazza *et al.*, 1998), and parasite prevalence (Roche *et al.*, 2013), this further suggests that laterality most likely is a context-dependent trait rather than fixed, which may be altered thorough individual experience (Bisazza *et al.*, 2000; Brown, 2005; Bisazza and Brown, 2011).

When the lateralization experiment was performed in control water for both treatment groups (i.e. testing control fish and CO_2 exposed fish in control water; test run 3), there was an effect of treatment on relative lateralization, suggesting that an acute change in pCO_2 could elicit a treatment effect not present when testing the fish under the same CO_2 conditions as what they were exposed to. Previous studies on other species report that behavioural impairment caused by exposure to elevated CO_2 lasts for several days and is not affected by testing fish in CO_2 exposed fish in control water (Dixson *et al.*, 2010; Munday *et al.*, 2010). This seemed not to be true for the goldsinny wrasse. Therefore, to avoid possible artefacts from acute water changes, it could be advisable that behavioural assays take place in water with the same pCO_2 as the fish were exposed to. As fish (Atlantic cod and the Japanese sea catfish) can detect the acute water pCO_2 (Jutfelt and Hedgärde, 2013; Caprio *et al.*, 2014), perhaps the water the fish were tested in could have immediate effects on behaviour through sensory pathways, which in the present experiment could explain why effects of CO_2 exposure on lateralization only appeared under an acute change in pCO_2.

Conclusions

We show that behavioural lateralization, activity, and olfactory preferences, all behaviours, where disadvantageous responses of fish exposed to near-future CO_2 levels have previously been reported, were largely unaffected by CO_2 in the goldsinny wrasse. The exception was predator smell avoidance behaviour, which was decreased by the CO_2 exposure. This study adds valuable balance in the reporting of the effects of CO_2 on fish, as the vast majority of studies on the impact of elevated pCO_2 report major detrimental behavioural responses (reviewed in Heuer and Grosell, 2014). In addition to the results found here, a growing number of studies report minor or no effects of CO_2 particularly studies using temperate species (Jutfelt and Hedgärde, 2013; Maneja *et al.*, 2013, 2015; Sundin *et al.*, 2013; Näslund *et al.*, 2015), but also in some coral reef fish experiments (Ferrari *et al.*, 2011; Nowicki *et al.*, 2012; Lönnstedt *et al.*, 2013). The interspecific variation in susceptibility demonstrates that we are far from able to predict possible future impacts of elevated pCO_2 on marine fish and ecosystems.

Supplementary data

Supplementary material is available at the *ICESJMS* online version of the manuscript.

Authors' contributions

JS and FJ designed the experiments, JS and FJ performed the experiments, JS analysed the data and wrote the manuscript draft. Both authors contributed to and approved the final manuscript.

Acknowledgements

We thank Johan Rudin, Laura Vossen, and Arianna Cocco for field assistance. The Sven Lovén Centre for Marine Sciences, Kristineberg, provided excellent laboratory facilities. Thanks to Bengt Lundve for technical assistance. This work was funded by the Swedish Research Council Formas (2013-947 to JS and 2009-596 to FJ), the Swedish Research Council VR (621-2012-4679 to FJ), and by the Royal Swedish Academy of Sciences (FOA14SLC027 to JS).

Conflict of interest

The authors declare no conflicts of interest.

References

Allan, B. J. M., Miller, G. M., McCormick, M. I., Domenici, P., and Munday, P. L. 2014. Parental effects improve escape performance of juvenile reef fish in a high-CO_2 world. Proceedings of the Royal Society of London, Series B: Biological Sciences, 281: 20132179.

Atema, J., Kingsford, M. J., and Gerlach, G. 2002. Larval reef fish could use odour for detection, retention and orientation to reefs. Marine Ecology Progress Series, 241: 151–160.

Bignami, S., Sponaugle, S., and Cowen, R. K. 2013. Response to ocean acidification in larvae of a large tropical marine fish, *Rachycentron canadum*. Global Change Biology, 19: 996–1006.

Bignami, S., Sponaugle, S., and Cowen, R. K. 2014. Effects of ocean acidification on the larvae of a high-value pelagic fisheries species, mahi-mahi *Coryphaena hippurus*. Aquatic Biology, 21: 249–260.

Bisazza, A., and Brown, C. 2011. Lateralization of cognitive functions in fish. *In* Fish Cognition and Behaviour, pp. 298–324. Ed. by C. Brown, K. Laland, and J. Krause. Blackwell Publishing, Cambridge.

Bisazza, A., Pignatti, R., and Vallortigara, G. 1997. Laterality in detour behaviour: interspecific variation in poeciliid fish. Animal Behaviour, 54: 1273–1281.

Bisazza, A., Facchin, L., Pignatti, R., and Vallortigara, G. 1998. Lateralization of detour behaviour in poeciliid fish: the effect of species, gender and sexual motivation. Behavioural Brain Research, 91: 157–164.

Bisazza, A., Cantalupo, C., Capocchiano, M., and Vallortigara, G. 2000. Population lateralisation and social behaviour: a study with 16 species of fish. Laterality, 5: 269–284.

Bjordal, A. 1991. Wrasse as cleaner-fish for farmed salmon. Progress in Underwater Science, 16: 17–28.

Briffa, M., de la Haye, K., and Munday, P. L. 2012. High CO_2 and marine animal behaviour: Potential mechanisms and ecological consequences. Marine Pollution Bulletin, 64: 1519–1528.

Brown, C. 2005. Cerebral lateralisation, "social constraints," and coordinated anti-predator responses. Behavioral and Brain Sciences, 28: 591–592.

Caprio, J., Shimohara, M., Marui, T., Harada, S., and Kiyohara, S. 2014. Marine teleost locates live prey through pH sensing. Science, 344: 1154–1156.

Chivers, D. P., McCormick, M. I., Nilsson, G. E., Munday, P. L., Watson, S.-A., Meekan, M. G., Mitchell, M. D., *et al.* 2014. Impaired learning

of predators and lower prey survival under elevated CO2: a consequence of neurotransmitter interference. Global Change Biology, 20: 515–522.

Costello, M. J. 2009. The global economic cost of sea lice to the salmonid farming industry. Journal of Fish Diseases, 32: 115–118.

Cripps, I. L., Munday, P. L., and McCormick, M. I. 2011. Ocean acidification affects prey detection by a predatory reef fish. PLoS One, 6:e22736.

Devine, B. M., Munday, P. L., and Jones, G. P. 2012a. Homing ability of adult cardinalfish is affected by elevated carbon dioxide. Oecologia, 168: 269–276.

Devine, B. M., Munday, P. L., and Jones, G. P. 2012b. Rising CO2 concentrations affect settlement behaviour of larval damselfishes. Coral Reefs, 31: 229–238.

Dickson, A. G. 1990. Standard potential of the reaction - AGCL(S)+1/2H-2(G)=AG(S)+HCL(AQ) and the standard acidity constant of the ion HSO4- in synthetic sea-water from 273.15-K to 318.15-K. Journal of Chemical Thermodynamics, 22: 113–127.

Dixson, D. L., Munday, P. L., and Jones, G. P. 2010. Ocean acidification disrupts the innate ability of fish to detect predator olfactory cues. Ecology Letters, 13: 68–75.

Domenici, P., Allan, B., McCormick, M. I., and Munday, P. L. 2012. Elevated carbon dioxide affects behavioural lateralization in a coral reef fish. Biology Letters, 8: 78–81.

Domenici, P., Allan, B. J. M., Watson, S-A., McCormick, M. I., and Munday, P. L. 2014. Shifting from right to left: the combined effect of elevated CO_2 and temperature on behavioural lateralization in a coral reef fish. PLoS One, 9:e87969.

Doney, S. C., Fabry, V. J., Feely, R. A., and Kleypas, J. A. 2009. Ocean acidification: the other CO_2 problem. *In* Annual Review of Marine Science, pp. 169–192. Annual Reviews, Palo Alto.

Endler, J. A. 1992. Signals, signal conditions, and the direction of evolution. American Naturalist, 139: S125–S153.

Ferrari, M. C. O., Dixson, D. L., Munday, P. L., McCormick, M. I., Meekan, M. G., Sih, A., and Chivers, D. P. 2011. Intrageneric variation in antipredator responses of coral reef fishes affected by ocean acidification: implications for climate change projections on marine communities. Global Change Biology, 17: 2980–2986.

Ferrari, M. C. O., McCormick, M. I., Munday, P. L., Meekan, M. G., Dixson, D. L., Lönnstedt, O., and Chivers, D. P. 2012. Effects of ocean acidification on visual risk assessment in coral reef fishes. Functional Ecology, 26: 553–558.

Forsgren, E., Dupont, S., Jutfelt, F., and Amundsen, T. 2013. Elevated CO_2 affects embryonic development and larval phototaxis in a temperate marine fish. Ecology and Evolution, 3: 3637–3646.

Ghalambor, C. K., McKay, J. K., Carroll, S. P., and Reznick, D. N. 2007. Adaptive versus non-adaptive phenotypic plasticity and the potential for contemporary adaptation in new environments. Functional Ecology, 21: 394–407.

Green, L., and Jutfelt, F. 2014. Elevated carbon dioxide alters the plasma composition and behaviour of a shark. Biology Letters, 10: 20140538.

Hari, P., Pumpanen, J., Huotari, J., Kolari, P., Grace, J., Vesala, T., and Ojala, A. 2008. High-frequency measurements of productivity of planktonic algae using rugged nondispersive infrared carbon dioxide probes. Limnology and Oceanography: Methods, 6: 347–354.

Heuer, R., and Grosell, M. 2014. Physiological impacts of elevated carbon dioxide and ocean acidification on fish. American Journal of Physiology: Regulatory Integrative and Comparative Physiology, 307: R1061–R1084.

Hillden, N. O. 1978. On the feeding of the gold sinny, *Ctenolabrus rupestris* L. (Pisces, Labridae). Ophelia, 17: 195–198.

Hillden, N. O. 1981. Territoriality and reproductive behavior in the Goldsinny, *Ctenolabrus rupestris* L. Behavioural Processes, 6: 207–221.

Hönisch, B., Ridgwell, A., Schmidt, D. N., Thomas, E., Gibbs, S. J., Sluijs, A., Zeebe, R., *et al.* 2012. The geological record of ocean acidification. Science, 335: 1058–1063.

Jutfelt, F., and Hedgärde, M. 2013. Atlantic cod actively avoid CO_2 and predator odour, even after long-term CO2 exposure. Frontiers in Zoology, 10: doi: 10.1186/1742-9994-10-81.

Jutfelt, F., and Hedgärde, M. 2015. Juvenile Atlantic cod behavior appears robust to near-future CO_2 levels. Frontiers in Zoology, 12: doi: 10.1186/s12983-015-0104-2.

Jutfelt, F., Bresolin de Souza, K., Vuylsteke, A., and Sturve, J. 2013. Behavioural disturbances in a temperate fish exposed to sustained high-CO_2 levels. PLoS One, 8: e65825.

Kasumyan, A. O., and Döving, K. B. 2003. Taste preferences in fishes. Fish and Fisheries, 4: 289–347.

Kasumyan, A. O., Marusov, E. A., and Sidorov, S. S. 2009. The effect of food odor background on gustatory preferences and gustatory behavior of carp *Cyprinus carpio* and cod *Gadus morhua*. Journal of Ichthyology, 49: 469–481.

Lönnstedt, O. M., Munday, P. L., McCormick, M. I., Ferrari, M. C. O., and Chivers, D. P. 2013. Ocean acidification and responses to predators: can sensory redundancy reduce the apparent impacts of elevated CO_2 on fish? Ecology and Evolution, 3: 3565–3575.

Magnhagen, M., Braithwaite, V. A., Forsgren, E., and Kapoor, B. G. 2008. Fish Behaviour. Science Publishers, Enfield.

Maneja, R. H., Frommel, A. Y., Browman, H. I., Clemmesen, C., Geffen, A. J., Folkvord, A., Piatkowski, U., *et al.* 2013. The swimming kinematics of larval Atlantic cod, *Gadus morhua* L., are resilient to elevated seawater pCO_2. Marine Biology, 160: 1963–1972.

Maneja, R. H., Frommel, A. Y., Browman, H. I., Geffen, A. J., Folkvord, A., Piatkowski, U., Durif, C. M. F., *et al.* 2015. The swimming kinematics and foraging behavior of larval Atlantic herring (*Clupea harengus* L.) are unaffected by elevated pCO_2. Journal of Experimental Marine Biology and Ecology, 466: 42–48.

Miller, G. M., Watson, S. A., Donelson, J. M., McCormick, M. I., and Munday, P. L. 2012. Parental environment mediates impacts of increased carbon dioxide on a coral reef fish. Nature Climate Change, 2: 858–861.

Munday, P. L., Dixson, D. L., Donelson, J. M., Jones, G. P., Pratchett, M. S., Devitsina, G. V., and Doving, K. B. 2009. Ocean acidification impairs olfactory discrimination and homing ability of a marine fish. Proceedings of the National Academy of Sciences of the USA, 106: 1848–1852.

Munday, P. L., Dixson, D. L., McCormick, M. I., Meekan, M., Ferrari, M. C. O., and Chivers, D. P. 2010. Replenishment of fish populations is threatened by ocean acidification. Proceedings of the National Academy of Sciences of the USA, 107: 12930–12934.

Munday, P. L., McCormick, M. I., Meekan, M., Dixon, D. L., Watson, S. A., Chivers, D. P., and Ferrari, M. C. O. 2012. Selective mortality associated with variation in CO_2 tolerance in a marine fish. Ocean Acidification, 1: 1–5.

Munday, P. L., Pratchett, M. S., Dixson, D. L., Donelson, J. M., Endo, G. G. K., Reynolds, A. D., and Knuckey, R. 2013. Elevated CO_2 affects the behavior of an ecologically and economically important coral reef fish. Marine Biology, 160: 2137–2144.

Munday, P. L., Cheal, A. J., Dixson, D. L., Rummer, J. L., and Fabricius, K. E. 2014. Behavioural impairment in reef fishes caused by ocean acidification at CO_2 seeps. Nature Climate Change, 4: 487–492.

Murray, C. S., Malvezzi, A., Gobler, C. J., and Baumann, H. 2014. Offspring sensitivity to ocean acidification changes seasonally in a coastal marine fish. Marine Ecology Progress Series, 504: 1–11.

Näslund, J., Lindström, E., Lai, F., and Jutfelt, F. 2015. Behavioural responses to simulated bird attacks in marine three-spined sticklebacks after exposure to high CO_2 levels. Marine and Freshwater Research, doi: 10.1071/MF14144.

Nilsson, G. E., Dixson, D. L., Domenici, P., McCormick, M. I., Sorensen, C., Watson, S. A., and Munday, P. L. 2012. Near-future carbon

dioxide levels alter fish behaviour by interfering with neurotransmitter function. Nature Climate Change, 2: 201–204.

Nowicki, J. P., Miller, G. M., and Munday, P. L. 2012. Interactive effects of elevated temperature and CO_2 on foraging behavior of juvenile coral reef fish. Journal of Experimental Marine Biology and Ecology, 412: 46–51.

Porteus, C., Hubbard, P., and Wilson, R. 2014. Ocean acidification directly impairs olfactory sensitivity in a marine teleost. Oral Presentation, American Physiological Society Comparative Physiology Conference, October 8, San Diego, USA.

Quinn, G. P., and Keough, M. J. 2002. Experimental Design and Data Analysis for Biologists. Cambridge University Press, New York.

Rihel, J., Prober, D. A., Arvanites, A., Lam, K., Zimmerman, S., Jang, S., Haggarty, S. J., *et al.* 2010. Zebrafish behavioral profiling links drugs to biological targets and rest/wake regulation. Science, 327: 348–351.

Roche, D. G., Binning, S. A., Strong, L. E., Davies, J. N., and Jennions, M. D. 2013. Increased behavioural lateralization in parasitized coral reef fish. Behavioral Ecology and Sociobiology, 67: 1339–1344.

Roy, R. N., Roy, L. N., Vogel, K. M., Portermoore, C., Pearson, T., Good, C. E., Millero, F. J., *et al.* 1993. The dissociation-constants of carbonic-acid in seawater at salinities 5 to 45 and temperatures 0-degrees-C to 45-degrees-C. Marine Chemistry, 44: 249–267.

Salvanes, A. G. V., and Nordeide, J. T. 1993. Dominating sublittoral fish species in a west Norwegian fjord and their trophic links to cod (*Gadus-morhua* L). Sarsia, 78: 221–234.

Sayer, M. D. J. 1999. Duration of refuge residence by goldsinny, *Ctenolabrus rupestris*. Journal of the Marine Biological Association of the UK, 79: 571–572.

Skiftesvik, A. B., Durif, C. M. F., Bjelland, R., and Browman, H. I. 2014. Distribution and habitat preferences of five species of wrasse (Family Labridae) in a Norwegian fjord. ICES Journal of Marine Science, 72: 890–899.

Spooner, G. M. 1937. The learning of detours by Wrassse (*Ctenolabrus rupestris*). Journal of the Marine Biological Association Plymouth NS, 21: 497–570.

Sundin, J., Rosenqvist, G., and Berglund, A. 2013. Altered oceanic pH impairs mating propensity in a pipefish. Ethology, 119: 86–93.

Treasurer, J. 1994. Prey selection and daily food-consumption by a cleaner fish, *Ctenolabrus rupestris* (L), on farmed Atlantic salmon, *Salmo salar* L. Aquaculture, 122: 269–277.

Tuomainen, U., and Candolin, U. 2010. Behavioural responses to human-induced environmental change. Biological Reviews, 86: 640–657.

Vallortigara, G., and Rogers, L. J. 2005. Survival with an asymmetrical brain: advantages and disadvantages of cerebral lateralization. Behavioral and Brain Sciences, 28:575–633.

Vilhunen, S. 2006. Repeated antipredator conditioning: a pathway to habituation or to better avoidance? Journal of Fish Biology, 68: 25–43.

Welch, M. J., Watson, S-A., Welsh, J. Q., McCormick, M. I., and Munday, P. L. 2014. Effects of elevated CO_2 on fish behaviour undiminished by transgenerational acclimation. Nature Climate Change, 4: 1086–1089.

Wong, B. B. M., and Candolin, U. 2015. Behavioral responses to changing environments. Behavioral Ecology, 26: 665–673.

Handling editor: Howard Browman

ICES Journal of Marine Science

ICES Journal of Marine Science (2016), 73(3), 633–640. doi:10.1093/icesjms/fsv085

Contribution to Special Issue: 'Towards a Broader Perspective on Ocean Acidification Research'

Original Article

Foraging behaviour of the epaulette shark *Hemiscyllium ocellatum* is not affected by elevated CO_2

Dennis D. U. Heinrich[1,2], Sue-Ann Watson[1,2], Jodie L. Rummer[2], Simon J. Brandl[1,2], Colin A. Simpfendorfer[1,3], Michelle R. Heupel[3,4], and Philip L. Munday[1,2]*

[1]*College of Marine and Environmental Sciences, James Cook University, Townsville, QLD 4811, Australia*
[2]*ARC Centre of Excellence for Coral Reef Studies, James Cook University, Townsville, QLD 4811, Australia*
[3]*Centre for Sustainable Tropical Fisheries and Aquaculture, James Cook University, Townsville, QLD 4811, Australia*
[4]*Australian Institute of Marine Science, Townsville, QLD 4810, Australia*

**Corresponding author: tel: +61 7 47815341; fax: +617 47816722; e-mail: philip.munday@jcu.edu.au*

Heinrich, D. D. U., Watson, S-A., Rummer, J. L., Brandl, S. J., Simpfendorfer, C. A., Heupel, M. R., and Munday, P. L. Foraging behaviour of the epaulette shark *Hemiscyllium ocellatum* is not affected by elevated CO_2. – ICES Journal of Marine Science, 73: 633–640.

Received 12 November 2014; revised 15 April 2015; accepted 16 April 2015; advance access publication 8 May 2015.

Increased oceanic uptake of atmospheric carbon dioxide (CO_2) is a threat to marine organisms and ecosystems. Among the most dramatic consequences predicted to date are behavioural impairments in marine fish which appear to be caused by the interference of elevated CO_2 with a key neurotransmitter receptor in the brain. In this study, we tested the effects of elevated CO_2 on the foraging and shelter-seeking behaviours of the reef-dwelling epaulette shark, *Hemiscyllium ocellatum*. Juvenile sharks were exposed for 30 d to control CO_2 (400 μatm) and two elevated CO_2 treatments (615 and 910 μatm), consistent with medium- and high-end projections for ocean pCO_2 by 2100. Contrary to the effects observed in teleosts and in some other sharks, behaviour of the epaulette shark was unaffected by elevated CO_2. A potential explanation is the remarkable adaptation of *H. ocellatum* to low environmental oxygen conditions (hypoxia) and diel fluctuations in CO_2 encountered in their shallow reef habitat. This ability translates into behavioural tolerance of near-future ocean acidification, suggesting that behavioural tolerance and subsequent adaptation to projected future CO_2 levels might be possible in some other fish, if adaptation can keep pace with the rate of rising CO_2 levels.

Keywords: carbon dioxide, climate change, elasmobranch, foraging behaviour, hypercapnia.

Introduction

Increased uptake of anthropogenic carbon dioxide (CO_2) at the ocean surface is a serious threat to marine organisms and ecosystems (Fabry *et al.*, 2008; Doney *et al.*, 2009). Approximately 30% of the CO_2 released by humans since the industrial revolution has been absorbed by the oceans, causing a 0.1-unit reduction in global ocean pH at a rate many times faster than any time over the past 800 000 years (Hoegh-Guldberg *et al.*, 2007; Lüthi *et al.*, 2008). If global CO_2 emissions continue on the current trajectory, atmospheric CO_2 is projected to exceed 900 ppm by 2100 (Meinshausen *et al.*, 2011) and ocean pH will decline by another 0.3–0.4 units (Caldeira and Wickett, 2005: Collins *et al.*, 2013). Elevated CO_2 levels can affect the behaviour of teleost fish (Briffa *et al.*, 2012; Branch *et al.*, 2013; Jutfelt *et al.*, 2013; Munday *et al.*, 2014). A range of sensory, cognitive, and behavioural abnormalities have been reported in reef fish that have been reared at CO_2 levels projected to occur by the end of this century (Munday *et al.*, 2009, 2012). For example, the innate response of juvenile reef fish to predator odours and conspecific alarm cues is impaired at higher CO_2 levels, causing them to become attracted to these odours rather than repelled from them (Dixson *et al.*, 2010; Welch *et al.*, 2014). Auditory preferences are altered (Simpson *et al.*, 2011), behavioural lateralization declines (Domenici *et al.*, 2011; Welch *et al.*, 2014), and the ability to learn is lost (Ferrari *et al.*, 2012; Chivers *et al.*, 2014). In addition, newly settled juveniles become more active and exhibit riskier behaviour, which increases mortality rates due to predation in natural coral reef habitat (Munday *et al.*, 2010). The effects of elevated CO_2 on reef fish behaviour are not

limited to larval and juvenile fish. Exposure to elevated CO_2 reduced homing success of adult cardinal fish (Devine *et al.*, 2012) and altered the attraction of a coral reef meso-predator (*Pseudochromis fuscus*) to the olfactory stimulus released by injured prey (Cripps *et al.*, 2011). Not all species or all behaviours are affected, but those behavioural changes that occur can affect the outcome of key ecological processes, such as predator–prey (Ferrari *et al.*, 2011) and competitive interactions (McCormick *et al.*, 2013), with implications for the structure and function of marine ecosystems in a high CO_2 world.

The behavioural changes observed in marine teleosts at high CO_2 appear to be caused by an interference with the GABA-A receptor, the primary inhibitory neurotransmitter receptor in the vertebrate brain (Nilsson *et al.*, 2012; Chivers *et al.*, 2014; Hamilton *et al.*, 2014). The GABA-A receptor is an ion-channel with conductance for Cl^- and HCO_3^-. Under normal conditions, ion gradients over the neuronal membrane result in an inflow of Cl^- and HCO_3^- upon binding of the GABA-A receptor, which then leads to hyperpolarization and inhibition of the neuron (Lambert and Grover, 1995; Nilsson *et al.*, 2012). However, when exposed to elevated CO_2, marine teleosts excrete Cl^- from their bodies to accumulate HCO_3^- from seawater to buffer the pH disturbance and prevent an acidosis (Brauner and Baker, 2009; Esbaugh *et al.*, 2012; Heuer and Grosell, 2014). The changes in the gradient of these ions over the neuronal membrane could alter the function of the receptor, leading to impaired behavioural responses. Depending on the magnitude of changes in HCO_3^- and Cl^- during acid-base regulation, the resultant alterations of ion gradients could either potentiate the GABA-A receptor function or reverse its action, making it excitatory rather than inhibitory (Nilsson *et al.*, 2012; Hamilton *et al.*, 2014; Heuer and Grosell, 2014).

In contrast to the many studies that have been conducted into the effects of near-future ocean acidification on the behaviour of teleost fish, especially on coral reefs, much less is known about the potential consequences of increasing levels of CO_2 on large predators, such as sharks (Rosa *et al.*, 2014). Elasmobranchs have the same GABA-A neurotransmitter receptor found in teleost brains (Lambert and Grover, 1995) and they also accumulate HCO_3^- from the seawater in exchange for Cl^- from the body to buffer an environmental pH disturbance (Heisler *et al.*, 1988; Claiborne *et al.*, 2002; Brauner and Baker, 2009). Elasmobranchs may also increase branchial ammonia excretion rates to further ameliorate an acidosis (King and Goldstein, 1983; Claiborne and Evans, 1992). We recently demonstrated that epaulette sharks, upon 90 d exposure to near-future CO_2 levels, exhibit an increase in plasma [HCO_3^-], and although this did not affect metabolic performance (Heinrich *et al.*, 2014), altered ion gradients might have affected neurotransmitter function and thus behaviour. Indeed, two recent studies have observed significant effects of elevated CO_2 on shark behaviours. Odour tracking of the smooth dogfish (*Mustelus canis*) declined following 5 d exposure to 1064 μatm CO_2 (Dixson *et al.*, 2014), and the nocturnal swimming pattern of the spotted catshark (*Scyliorhinus canicula*) changed from starts and stops to a more continuous swimming pattern after 28 d exposure to 990 μatm CO_2 (Green and Jutfelt, 2014). Furthermore, the catshark exhibited an accumulation of plasma HCO_3^-, which could be consistent with an effect of high CO_2 on neurotransmitter function, leading to behavioural changes.

The aim of this study was to test the effects of near-future CO_2 levels on the behaviour of a reef-dwelling shark that periodically experiences high CO_2 levels in its natural habitat. The epaulette shark (*Hemiscyllium ocellatum*) is a small, benthic, relatively sedentary species of shark that inhabits shallow coral reef flats and lagoons (Randall *et al.*, 1997). It frequently shelters in small caves and holes within the reef matrix. Due to this pattern of habitat use, epaulette sharks may experience episodes of short-term environmental hypoxia and hypercapnia, especially during nocturnal low tides (Kinsey and Kinsey, 1967; Routley *et al.*, 2002; Nilsson and Renshaw, 2004; Diaz and Breitburg, 2009). CO_2 levels in shallow coral reef habitat, such as in lagoons and on reef flats, can exceed 1000 μatm overnight during low tides (Shaw *et al.*, 2012) and may be further elevated within the reef matrix due to biological respiration. The epaulette shark is metabolically adapted to these conditions (Heinrich *et al.*, 2014), and we predicted that the behaviour of this small shark may be similarly tolerant of CO_2 levels that induce abnormal behaviour in reef fish and other sharks. We compared foraging and shelter-seeking behaviour of juvenile epaulette sharks acclimated to elevated CO_2 for over 30 d with individuals kept at current-day control conditions (~400 μatm) for the same period. Elevated CO_2 treatments were consistent with medium- (~615 μatm) and high-end projections (~910 μatm) for ocean pCO_2 by 2100 (Meinshausen *et al.*, 2011). Specifically, each shark's activity level and the time spent away from shelter over the course of 1 h in the presence of food were investigated. Furthermore, we determined activity levels while foraging and recorded the time required to locate and reach the food source. We then examined each individual's responses to a disturbance by recording activity and time required to find a new shelter upon disturbance.

Material and methods

Experimental animals

Hemiscyllium ocellatum is a small benthic elasmobranch common on reef flats and in lagoons on the Great Barrier Reef (GBR), Australia. Their relatively small size and benthic lifestyle make them well suited for laboratory experiments. Furthermore, they are not highly territorial and may shelter together in coral reef habitat, making them ideal to maintain in captivity (Michael, 2003). Animals were collected from the GBR under an A1 commercial harvest licence and were supplied by Northern Barrier and Cairns Marine (Cairns, Australia). Thirty sharks were shipped to James Cook University (JCU) where they were kept in groups of five individuals in six 700 l tanks (230 l × 105 W × 50 D cm) supplied with a continuous flow of seawater (Figure 1). Individuals were measured [standard length: 33.38 ± 7.29 cm (mean ± SD); weight: 232.47 ± 117.98 g] to ensure an equal distribution of sizes among tanks. *Hemiscyllium ocellatum* matures around 60 cm (Last and

Figure 1. Photograph of holding tank with PVC shelter at one end and food placed at the opposite end. Tank dimensions (internal): 230 l × 105 W × 50 D cm. Scale bar = 10 cm.

Stevens, 2009); therefore, all individuals were large juveniles. For identification, each individual was given a unique fin clip along the margins of pectoral, pelvic, and dorsal fins. Sharks were habituated to laboratory holding conditions (control CO_2) for at least 30 d before commencing CO_2 treatments. Sections of PVC pipe were placed in the tanks to provide shelter. Food was provided once every 24 h and consisted of raw prawn meat (4% of shark biomass). The epaulette shark is mostly a crepuscular feeder, but will readily feed throughout the day, especially in captivity.

Experimental conditions

The experimental system consisted of three 8000 l recirculating seawater systems each of which was set to simulate one of three CO_2 scenarios, current-day control (~400 μatm), medium (~615 μatm), and high (~910 μatm) CO_2. The experimental system supplied the 6 × 700-l rearing tanks containing sharks, plus an additional three experimental tanks, giving a total water volume of >10 000 l in each system. Although replicated treatment systems are preferable, this was not logistically or financially possible due to the large size of each system. Seawater in each system received constant particle filtration (50 μm), protein extraction, biological filtration (fluidised sand-bed), and ultraviolet filtration.

Two of the six tanks containing sharks were assigned to each CO_2 treatment and supplied with CO_2-equilibrated seawater at a rate of 25 l min^{-1}. A plastic cover was placed on each tank to reduce CO_2 loss. Target CO_2 levels, initial total alkalinity (TA), temperature, and salinity were entered in CO2SYS (Pierrot *et al.*, 2006) to generate pH set points for the experiment. Seawater pCO_2 was then established by adjusting and maintaining seawater pH within 0.05 units of the determined set-point using a pH computer (Aqua Medic AT-Control, Bissendorf, Germany). Electronic solenoids dosed CO_2 into a 3000-l sump on each system whenever the measured pH in the sump rose above the desired pH. This central approach of pH manipulation allowed for greater stability in seawater pH within the holding tanks. Temperature was maintained at 28.5°C with a heater/chiller unit attached to each system.

The pH_{TOTAL} of each tank was recorded daily by comparing the mV reading from a Hach HQ40d meter (Hach Company, Loveland, CO, USA) with the mV reading of Tris buffer (Dr A. G. Dickson, Scripps Institution of Oceanography) at the same temperature. Salinity and TA were measured weekly. TA was determined by Gran titration using certified reference materials (Dr A. G. Dickson, Scripps Institution of Oceanography). Measured pH_{TOTAL} and TA were used in CO2SYS (Pierrot *et al.*, 2006) to estimate seawater pCO_2 using the constants K1 and K2 from Mehrbach *et al.* (1973) refit by Dickson and Millero (1987), and Dickson (1990) for $KHSO_4$. Seawater carbonate chemistry parameters are shown in Table 1.

Experimental protocol

Sharks were maintained in CO_2 treatment for a minimum of 30 d before experimentation. Behavioural comparisons between treatment groups were made in two separate experiments, described below. Physiological traits measured in the same sharks are reported in Heinrich *et al.* (2014). This study was conducted under JCU animal ethics approval A1779 and all animal husbandry, and experimental procedures were consistent with Australian guidelines for animal care.

Foraging behaviour

Foraging behaviour was recorded within each of the six tanks on 10 consecutive days using high-resolution video cameras (GoPro II) installed centrally above the tanks with the lens parallel with the water surface. Video was recorded at a resolution of 1080 p for 60 min following the introduction of food by hand at the end of the tank opposite to the shelter location (Figure 1). Foraging behaviour was examined in groups within the treatment tanks, rather than individually, for several reasons. First, this eliminated handling stress that may have affected behaviour. Second, *H. ocellatum* exhibits highly social behaviour, and a reduced commitment to foraging when held in isolation (DDUH, pers. obs.); consequently, small groups provided a better representation of their natural behaviour.

Video files were viewed unconverted on a computer screen using Windows Media Player Version 12 (Microsoft, Redmond, WA, USA) in the slow playback mode. Information collected from the video included: (i) each individual's latency to the first bite, (ii) the activity level of each individual between leaving the shelter and reaching the food source, (iii) the total time spent outside of the shelters, and (iv) the total activity level over the course of 1 h. Individuals could be unambiguously tracked throughout the experimental period by the tags on their fins. The activity level was estimated by counting the number of times each animal crossed a line, using the animal's snout as a reference. To do this, a 10 × 10 cm grid was added to each video, post-recording. The number of line crossings was then converted into activity level, defined as the number of lines crossed per minute for foraging activity and the number of lines crossed in 1 h for total activity. Data on foraging behaviour were collected for 10 consecutive days for each individual.

Shelter-seeking behaviour

Following the last day of foraging behaviour trials, the response to a disturbance was tested. Individuals were transferred to a separate experimental tank (same dimensions as the holding tanks and filled with water from the same CO_2 treatment) containing a PVC shelter at one end. Following transfer and 10 min habituation to the new tanks and shelter, the shelter was removed and an alternative shelter was provided at the opposite end of the tank. The response of the animal was recorded using a high-definition video camera. The time the animal took to find and enter the new shelter, and each individual's activity during that time was determined from the video. Activity was determined in the same way as the foraging behaviour experiment described above. Following the behaviour trials, the length of each individual was measured to include in statistical analyses due to the potential for body size to influence behaviour.

Statistical analyses

Generalized linear mixed-effects models (GLMMs) were used to test for the effects of elevated CO_2 and standard length on foraging and shelter-seeking behaviours. For foraging behaviour, four separate models were performed on: (i) the time spent outside shelters, (ii) latency to the first bite, (iii) the number of line crossings between food introduction and the first bite, and (iv) the overall number of line crossings. As data were integer counts of events or seconds, the exponential family was used. In all models, the variance exceeded the mean in a Poisson model and, therefore, a negative binomial error distribution with a log-link function was used in all instances. In addition, due to the high prevalence of zero values in the time spent outside shelters and the total activity, models were specified with zero inflation as a single constant term across the model. For the variables describing latency to the first bite and line crossings before feeding, cases in which the shark did not feed during the observation period were omitted from the model. Zero-inflated models outperformed models lacking the specification for zero

Table 1. Mean (± s.d.) pCO_2, pH_T, temperature, salinity, and TA for experimental tanks.

Treatment	pCO_2 (μatm)	pH_T	Temperature (°C)	Salinity	TA (μmol kg^{-1} SW)
Control					
Tank 1	408 ± 46	8.01 ± 0.04	28.6 ± 0.33	35.6 ± 0.70	2154 ± 34
Tank 2	394 ± 52	8.02 ± 0.05	28.7 ± 0.42	35.6 ± 0.70	2154 ± 34
Medium					
Tank 1	621 ± 86	7.85 ± 0.05	28.8 ± 0.41	35.8 ± 0.64	2081 ± 30
Tank 2	613 ± 80	7.85 ± 0.05	28.6 ± 0.39	35.8 ± 0.64	2081 ± 30
High					
Tank 1	915 ± 73	7.70 ± 0.03	28.7 ± 0.20	36.0 ± 0.28	2083 ± 40
Tank 2	895 ± 83	7.71 ± 0.04	28.7 ± 0.26	36.0 ± 0.28	2083 ± 40

pCO_2 was estimated in CO2SYS from the other measured variables.

inflation. Given the non-independence of measurements made within tanks and length measurements on individuals, both tank ID and shark ID were included as a random factor, with individual sharks implicitly nested within tanks. In addition, we fitted a random intercept to the sequential days to account for potential systematic variation among days. Both activity variables (activity until the first bite and total activity) were modelled using the corresponding time measurements (latency to the first bite and time outside shelters) as offset on the log scale. Always, the inclusion of an interaction term between CO_2 treatment and standard length did not improve the model fit significantly (Supplementary Table S1).

For the two shelter-seeking variables, the time lapsed until a shelter was reached was again modelled using a GLMM with a negative binomial error distribution and a log-link function, whereas the number of line crossings per minute was approximately normally distributed and was therefore modelled using a Gaussian error distribution and an identity link function. As in the foraging models, the non-independence of measurements from the same tank was accounted for by including tank as a random factor. Likewise, performance of models with and without an interaction term between CO_2 treatment and standard length was assessed and no significant improvement was found when the interaction term was included. Model comparison was performed using Akaike's Information Criterion. Model validation was performed using residual plots. All analyses were performed in *R* (R Development Core Team, 2014) using the packages *lme4* (Bates *et al.*, 2012), *glmmadmb* (Skaug *et al.*, 2014), and *ggplot2* (Wickham, 2009). As behavioural variables associated with foraging and shelter-seeking behaviour are not fully independent, the results of this study require the contextual interpretation of the model outputs. The nature of the data rendered a multivariate approach impossible, making our statistical treatment the most robust extrapolation of the data.

Results

Foraging behaviour

Neither the time sharks spent outside of shelters (GLMM: $p = 0.98$ and 0.32 for medium and high CO_2, respectively) or the total activity level over the course of 1 h in the presence of food (GLMM: $p = 0.80$ and 0.51) were affected by CO_2 treatment (Figure 2a and b; Supplementary Table S1). There was a significant linear relationship between standard length of the sharks and the time spent outside of the shelters (GLMM: $p < 0.0001$), with larger individuals tending to spend more time away from shelters, but size had no effect on the overall activity (GLMM: $p = 0.08$).

When foraging, neither the time required to reach the food source (GLMM: $p = 0.99$ and 0. 19) or the level of activity during the search (GLMM: $p = 0.79$ and 0.13) were affected by CO_2 treatment. There was, however, a significant effect of standard length on the time and activity required to find food, with smaller individuals requiring more time and line-crossings to locate and reach the food source (GLMMs: $p < 0.0001$ and $p < 0.0001$, respectively; Figure 2c and d; Supplementary Table S1).

All models identified substantial individual variation among sharks, but the tank identity and the sequence of days during which observations were performed contributed little to the overall variation explained by the model (Supplementary Table S1).

Shelter-seeking behaviour

Shelter-seeking behaviour was not significantly affected by CO_2 treatment. Neither the time required to re-enter a shelter (GLMM: $p = 0.92$ and 0.99; Figure 3a; Supplementary Table S2) or activity before reaching the new shelter (GLMM: $p = 0.84$ and 0.42; Figure 3b; Supplementary Table S2) were affected by CO_2 treatment. In contrast to foraging behaviour, these traits were not influenced by body size (GLMMs: $p = 0.42$ and $p = 0.65$, respectively; Figure 3; Supplementary Table S2). The effect of tanks on the variance explained by the two models was negligible (Supplementary Table S2).

Discussion

In contrast to the behavioural effects of high CO_2 in some marine teleosts, projected near-future CO_2 levels did not affect foraging or shelter-seeking behaviours of epaulette sharks. *Hemiscyllium ocellatum* held under elevated CO_2 conditions for 30 d did not exhibit riskier behaviours by spending more time outside shelter than control counterparts, and likewise, the ability to successfully locate a familiar food source or shelter site when disturbed was unaffected. Our results suggest that the behaviour of the epaulette shark, and maybe other reef-dwelling benthic elasmobranchs, will be unaffected by elevated CO_2 and reduced seawater pH predicted for the end of this century. However, our results also contrast with two other recent studies that have observed significant effects of high CO_2 on response to olfactory cues (Dixson *et al.*, 2014) and swimming patterns (Green and Jutfelt, 2014) of small benthic or epibenthic sharks. The mechanistic basis underlying the behavioural effects of ocean acidification on marine teleosts and elasmobranchs appears to be associated with changes to ion concentrations across neuronal membranes. Specifically, changes in HCO_3^- and Cl^- gradients that occur when fish are exposed to elevated CO_2 can affect the function of GABA-A neurotransmitter receptors in the brain (Nilsson *et al.*, 2012; Chivers *et al.*, 2014; Hamilton *et al.*, 2014). Elasmobranchs are thought to use similar acid-base regulatory mechanisms to teleosts (Claiborne *et al.*, 2002; Brauner and Baker, 2009) and, consequently, could be sensitive to the effects of elevated

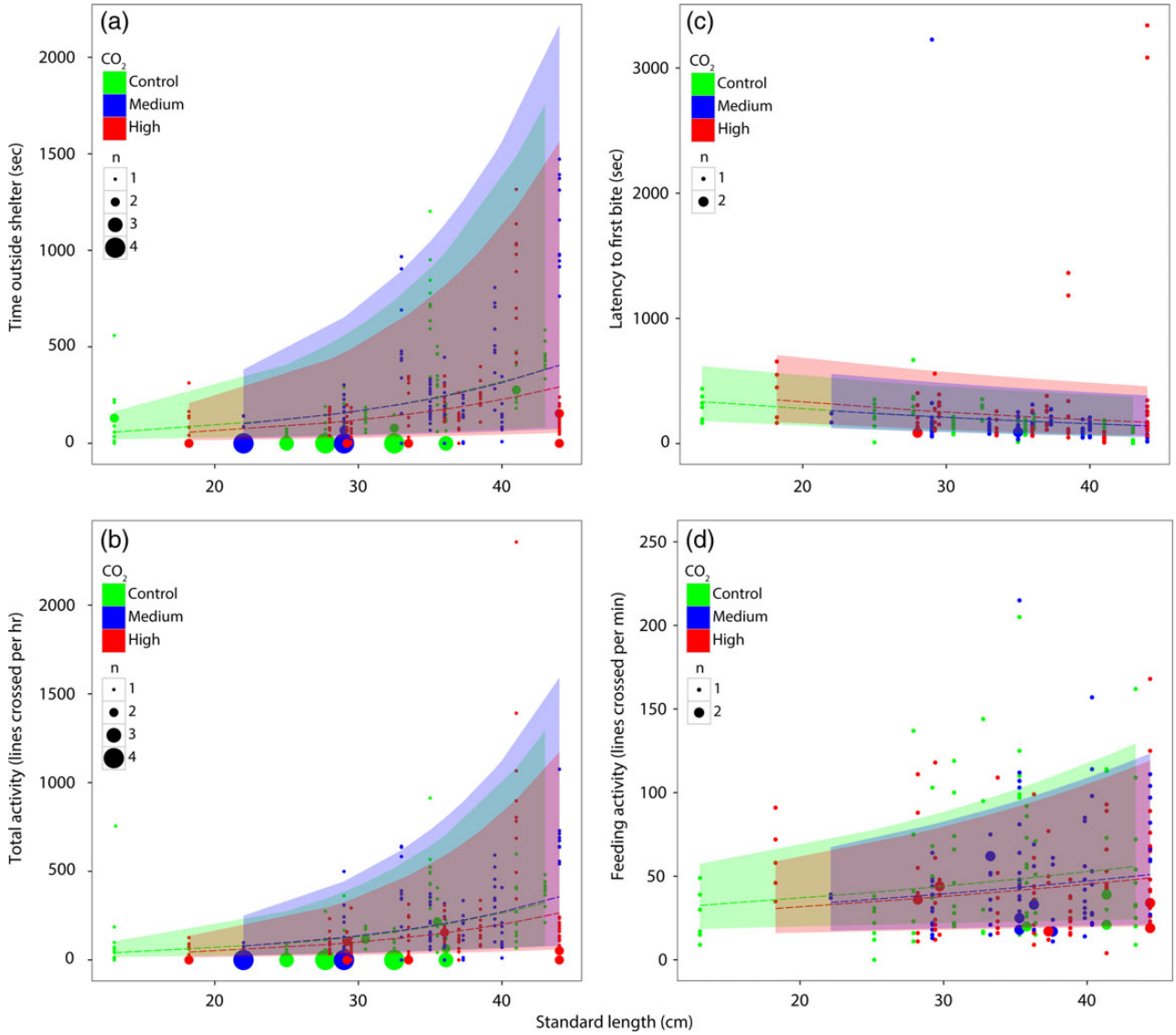

Figure 2. Individual foraging behaviour of epaulette sharks *H. ocellatum* with the predicted fit from GLMMs on the response scale superimposed (±95% confidence intervals). Time that individual sharks spent outside of shelters over the course of 1 h in the presence of food (a), total activity in the presence of food expressed as the number of line crossings per minute on a 10 × 10 cm grid during 1 h (b), time in minutes required by individuals to reach a food source and commence feeding (c), and foraging activity, calculated as the number of line crossings on a 10 × 10 cm grid, from when a shark left a shelter until it reached food (d). Behavioural traits are plotted against the standard length of each individual, with ten daily observations for each individual. Point size is adjusted based on the number of overlaying observations for each individual. Colours indicate the three CO_2 treatments: control =400 μatm, medium =615 μatm, high =910 μatm.

CO_2 on GABA-A receptor function. This raises the question of why behavioural effects were not detected in the epaulette shark. The most likely explanation as to why the behaviour of *H. ocellatum* was unaffected by higher CO_2 levels is that they are adapted to high CO_2 levels frequently encountered in their natural environment. This species is known for its exceptionally high tolerance to short-term hypoxia and possesses the lowest critical oxygen tension (an indicator of hypoxia tolerance) measured in any elasmobranch tested to date (Wise *et al.*, 1998; Routley *et al.*, 2002). Commonly found on shallow reef flats, epaulette sharks shelter within coral heads and other small crevices or holes (Last and Stevens, 2009). The oxygen concentration within these microhabitats can drop to very low levels, even nearing complete anoxia during low tides at night, due to the respiration of reef organisms (Kinsey and Kinsey, 1967; Diaz and Breitburg, 2009). This adaptation to hypoxic conditions allows *H. ocellatum* to reside in tide pools and on reef flats during nocturnal low tides, potentially providing protection from larger reef predators (Routley *et al.*, 2002; Nilsson and Renshaw, 2004; Last and Stevens, 2009). Seawater pCO_2 on shallow reef flats can exceed 1000 μatm for several hours overnight (Shaw *et al.*, 2012) and may be even higher in small caves, reef crevices, and other restricted habitats due to reef respiration (Gagliano *et al.*, 2010). Respiration by the shark itself is likely to further exacerbate local hypoxia and hypercapnia within the caves and holes where it shelters. The ability of *H. ocellatum* to routinely tolerate a very wide range of O_2 and CO_2 conditions, including very high CO_2 levels at night and in its shelter sites, suggests that this species may not engage acid-base regulation at the same pCO_2 threshold as fish from other habitats. *Hemiscyllium ocellatum* may

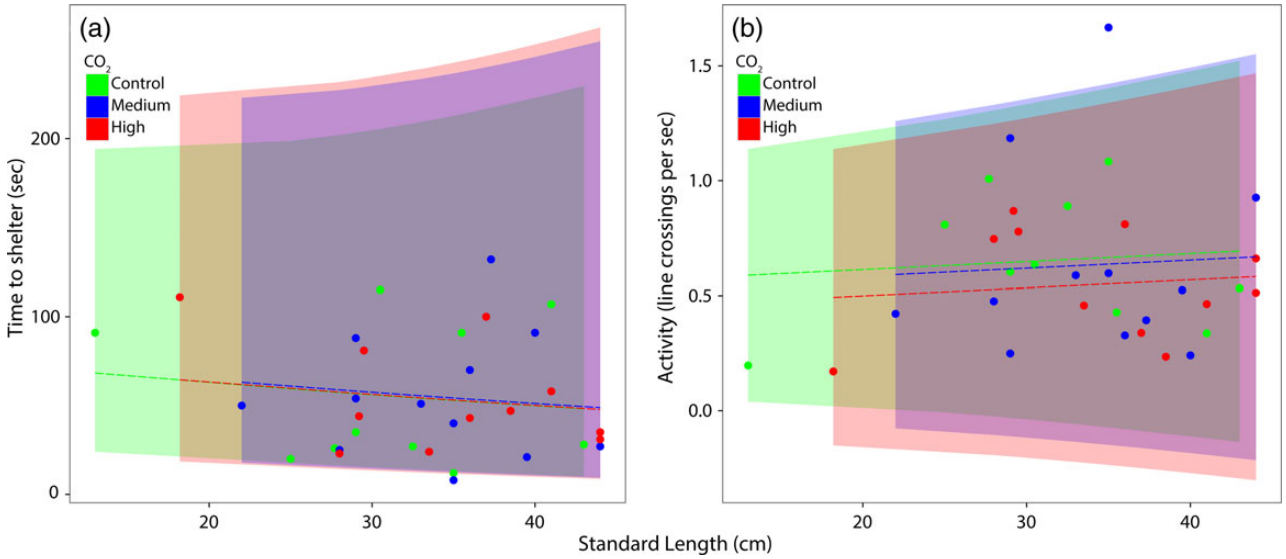

Figure 3. Individual shelter-seeking behaviour of epaulette sharks *H. ocellatum* with the predicted fit from the GLMM on the response scale ($\pm$95% confidence intervals) superimposed. Time in minutes required for sharks from control, medium, and high CO_2 treatments to reach an alternative shelter (a) and activity level expressed as number of line crossings on a 10 × 10 cm grid (b) after the removal of their original shelters. Both time and activity are plotted against the standard length of each individual. Each point represents a single individual. Colours indicate the three CO_2 treatments: control =400 μatm, medium =615 μatm, high =910 μatm.

simply allow inter- and intracellular pCO_2 and pH to fluctuate more broadly than in other reef fish. If so, there may be smaller changes to ion gradients that could interfere with the function of GABA-A receptors, and therefore, neural function and behaviour, at the relatively low pCO_2 levels studied here. Alternatively, *H. ocellatum* might regulate acid-base status to the same degree as other species, but may rely more heavily on alternative mechanisms, such as enhanced ammonia excretion or non-bicarbonate buffering (King and Goldstein, 1983; Claiborne and Evans, 1992). Either way, there would be smaller changes in HCO_3^- and Cl^- concentrations, which appear to be the underlying reason for behavioural disturbance of fish exposed to elevated CO_2.

Consistent with this hypothesis, HCO_3^- accumulation in the catshark, which exhibited altered nocturnal swimming behaviour at 990 μatm CO_2, was 0.5 mmol l^{-1} for every 100 μatm increase in CO_2 over the range 401–993 μatm (Green and Jutfelt, 2014). In contrast, the epaulette sharks in this study accumulated HCO_3^- at 0.39 mmol l^{-1} for every 100 μatm CO_2 over the range 390–870 μatm (Heinrich *et al.*, 2014). Furthermore, the average concentration of plasma HCO_3^- was 7.68 mmol l^{-1} in the catshark at 990 μatm CO_2, but is estimated to be 5.06 mmol l^{-1} in the epaulette shark at the same CO_2 level based on the observed rate of HCO_3^- accumulation. Although there were some differences in the sampling and analytical methods used in the two studies, these comparisons suggest that the epaulette shark may reach a lower final concentration of plasma HCO_3^- in an equivalent CO_2 environment than the catshark. This could influence the relative change in ion gradients at the neurotransmitter receptors, and thus the extent of behavioural changes (Heuer and Grosell, 2014).

In contrast to our findings for *H. ocellatum*, the benthic sharks *M. canis* and *S. canicula* exhibited significant changes in prey detection and swimming behaviour, respectively, when exposed to similar CO_2 levels used in this study. Although these two species of shark are benthic or epibenthic, they are more mobile than *H. ocellatum* and often rest on the open benthos rather than deep within small crevices and holes. Female *S. canicula* may shelter in shallow water caves when reproducing (Sims *et al.*, 2001), but they move to deep, well oxygenated water at night. Consequently, both these species are unlikely to routinely experience the same severe hypoxia and hypercapnia experienced by *H. ocellatum*. The reef-dwelling and shelter-seeking habits of the epaulette shark could be the reason its behaviour was unaffected by near-future CO_2 levels, whereas the two other species of small shark exhibit behavioural changes at similar CO_2 levels. Alternatively, our study could have come to different conclusions because of differences in the behaviours tested or differences in the experimental design. We focused on the foraging and shelter-seeking behaviour during the day, whereas Green and Jutfelt (2014) examined nocturnal swimming patterns. Dixson *et al.* (2014) investigated a more similar behaviour to our study, but their exposure period (5 d) was much less than ours (30 d). Perhaps, *H. ocellatum* might have exhibited altered behaviours after 5 d of exposure to elevated CO_2, but acclimated to a normal behaviour after 30 d. However, we consider this unlikely because reef fish exposed to high CO_2 for a month or more exhibit very similar changes in behaviour to those observed after just 4–5 d exposure (Munday *et al.*, 2013a, 2014). Furthermore, Green and Jutfelt (2014) observed significant effects on swimming behaviour in *S. canicula* after a similar exposure period to that used here.

Our results suggest that adaptation to shallow reef habitats could protect *H. ocellatum* from near-future ocean acidification, as observed in some other animals that occupy habitats that naturally experience episodes of high CO_2 (Melzner *et al.*, 2009). Maintaining vital behavioural traits under elevated CO_2 also suggests that there is potential for the adaptation of behaviours to a high CO_2 environment—but the rate of change in CO_2 will be a key. Epaulette sharks have adapted to their environment over millions of years, whereas the uptake of CO_2 into the ocean is occurring at a rate unprecedented in the recent geological record (Hoegh-Guldberg *et al.*, 2007). Whether marine organisms can adapt their acid-base

regulatory mechanisms or the sensitivity of neurotransmitter receptors at a rate that will keep pace with climate change must be determined. Since *H. ocellatum* is exceptionally tolerant of fluctuating environmental conditions, it may not be a general representation of how all elasmobranchs will respond to ocean acidification. Less-tolerant elasmobranchs may suffer physiological (Rosa *et al.*, 2014) or behavioural impacts (Dixson *et al.*, 2014; Green and Jutfelt, 2014) from rising CO_2 conditions, similar to those documented in teleosts. Earlier life stages in some elasmobranch may also be more sensitive to elevated CO_2 compared with adults (Rosa *et al.*, 2014). Future experiments on early life stages and pelagic elasmobranchs that may be less tolerant of elevated CO_2 are needed. Importantly, studies that use short-term experiments to predict the impacts of high CO_2 on fish and other marine organisms must consider the potential for acclimation and adaptation over the time frame that CO_2 levels will rise in the future (Munday *et al.*, 2013b; Sunday *et al.*, 2014; Welch *et al.*, 2014). Inferences about the impacts of future high CO_2 levels on animal populations, based on the results of studies that acutely expose animals to future conditions, must be made with the appropriate caution because they do not account for any adaptation that could occur as CO_2 levels rise over coming decades.

Supplementary data

Supplementary material is available at the *ICESJMS* online version of the manuscript.

Acknowledgements

Thanks to staff from JCU's Marine and Aquaculture Research Facility Unit (MARFU) for advice and assistance with maintenance of the experimental system. Shannon McMahon assisted with the preparation of the figures. This research was funded by the ARC Centre of Excellence for Coral Reef Studies and the JCU's Centre for Sustainable Tropical Fisheries and Aquaculture.

References

Bates, D., Maechler, M., and Bolker, B. 2012. lme4: linear mixed-effects models using S4 classes. R package version 1.1–7.

Branch, T. A., DeJoseph, B. M., Ray, L. J., and Wagner, C. A. 2013. Impacts of ocean acidification on marine seafood. Trends in Ecology and Evolution, 28: 178–186.

Brauner, C., and Baker, D. 2009. Patterns of acid-base regulation during exposure to hypercarbia in fishes. *In* Cardio-Respiratory Control in Vertebrates, pp. 43–63. Ed. by M. L. Glass, and S. C. Wood. Springer, Berlin. 546 pp.

Briffa, M., de la Haye, K., and Munday, P. L. 2012. High CO_2 and marine animal behaviour: potential mechanisms and ecological consequences. Marine Pollution Bulletin, 64: 1519–1528.

Caldeira, K., and Wickett, M. E. 2005. Ocean model predictions of chemistry changes from carbon dioxide emissions to the atmosphere and ocean. Journal of Geophysical Research, 110: C09S04.

Chivers, D. P., McCormick, M. I., Nilsson, G. E., Munday, P. L., Watson, S-A., Meekan, M. G., Mitchell, M. D., *et al.* 2014. Impaired learning of predators and lower prey survival under elevated CO_2: a consequence of neurotransmitter interference. Global Change Biology, 20: 512–522.

Claiborne, J. B., Edwards, S. L., and Morrison-Shetlar, A. I. 2002. Acid–base regulation in fishes: cellular and molecular mechanisms. Journal of Experimental Zoology, 293: 302–319.

Claiborne, J. B., and Evans, D. H. 1992. Acid-base balance and ion transfers in the spiny dogfish (*Squalus acanthias*) during hypercapnia: a role for ammonia excretion. Journal of Experimental Zoology, 261: 9–17.

Collins, M., Knutti, R., Arblaster, J., Dufresne, J -L., Fichefet, T., Friedlingstein, P., Gao, X., *et al.* 2013. Long-term Climate Change: Projections, Commitments and Irreversibility. *In* Climate Change 2013: the Physical Science Basis. Contribution of Working Group I to the Fifth Assessment Report of the Intergovernmental Panel on Climate Change. Ed. by Stocker, T. F., Qin, D., Plattner, G-K., Tignor, M., Allen, S. K., Boschung, J., Nauels, A., *et al.* Cambridge University Press, Cambridge, New York, NY, USA, UK.

Cripps, I. L., Munday, P. L., and McCormick, M. I. 2011. Ocean acidification affects prey detection by a predatory reef fish. PLoS One, 6: e22736.

Devine, B. M., Munday, P. L., and Jones, G. P. 2012. Homing ability of adult cardinalfish is affected by elevated carbon dioxide. Oecologia, 168: 269–276.

Diaz, R. J., and Breitburg, D. L. 2009. The hypoxic environment. Fish Physiology, 27: 1–23.

Dickson, A. G. 1990. Standard potential of the reaction: $AgCl(s) + \frac{1}{2}H_2(g) = Ag(s) + HCl(aq)$, and the standard acidity constant of the ion HSO_4^- in synthetic sea water from 273.15 to 318.15 K. Journal of Chemical Thermodynamics, 22: 113–127.

Dickson, A., and Millero, F. 1987. A comparison of the equilibrium constants for the dissociation of carbonic acid in seawater media. Deep Sea Research A: Oceanographic Research Papers, 34: 1733–1743.

Dixson, D. L., Jennings, A. R., Atema, J., and Munday, P. L. 2014. Odour tracking in sharks is reduced under future ocean acidification conditions. Global Change Biology. doi: 10.1111/gcb.12678.

Dixson, D. L., Munday, P. L., and Jones, G. P. 2010. Ocean acidification disrupts the innate ability of fish to detect predator olfactory cues. Ecology Letters, 13: 68–75.

Domenici, P., Allan, B., McCormick, M. I., and Munday, P. L. 2011. Elevated carbon dioxide affects behavioural lateralization in a coral reef fish. Biology Letters, 8: 78–81.

Doney, S. C., Fabry, V. J., Feely, R. A., and Kleypas, J. A. 2009. Ocean acidification: the other CO_2 problem. Annual Review of Marine Science, 1: 169–192.

Esbaugh, A. J., Heuer, R., and Grosell, M. 2012. Impacts of ocean acidification on respiratory gas exchange and acid–base balance in a marine teleost, *Opsanus beta*. Journal of Comparative Physiology B: Biochemical, Systemic, and Environmental Physiology, 182: 921–934.

Fabry, V. J., Seibel, B. A., Feely, R. A., and Orr, J. C. 2008. Impacts of ocean acidification on marine fauna and ecosystem processes. ICES Journal of Marine Science, 65: 414–432.

Ferrari, M. C., Manassa, R. P., Dixson, D. L., Munday, P. L., McCormick, M. I., Meekan, M. G., Sih, A., *et al.* 2012. Effects of ocean acidification on learning in coral reef fishes. PLoS One, 7: e31478.

Ferrari, M. C. O., McCormick, M. I., Munday, P. L., Meekan, M., Dixson, D. L., Lonnstedt, O., and Chivers, D. 2011. Putting prey and predator into the CO_2 equation: qualitative and quantitative effects of ocean acidification on predator-prey interactions. Ecology Letters, 14: 1143–1148.

Gagliano, M., McCormick, M. I., Moore, J. A., and Depczynski, M. 2010. The basics of acidification: baseline variability of pH on Australian coral reefs. Marine Biology, 157: 1849–1856.

Green, L., and Jutfelt, F. 2014. Elevated carbon dioxide alters the plasma composition and behaviour of a shark. Biology Letters, 10: 20140538.

Hamilton, T. J., Holcombe, A., and Tresguerres, M. 2014. CO_2-induced ocean acidification increases anxiety in Rockfish via alteration of $GABA_A$ receptor functioning. Proceedings of the Royal Society B: Biological Sciences, 281: 20132509. doi:10.1098/rspb.2013.2509.

Heinrich, D. D. U., Rummer, J. L., Morash, A. J., Watson, S. A., Simpfendorfer, C. A., Heupel, M. R., and Munday, P. L. 2014. A product of its environment: the epaulette shark (*Hemiscyllium ocellatum*) exhibits physiological tolerance to elevated environmental CO_2. Conservation Physiology, 2. doi:10.1093/conphys/cou047.

Heisler, N., Toews, D. P., and Holeton, G. F. 1988. Regulation of ventilation and acid-base status in the elasmobranch *Scyliorhinus stellaris* during hyperoxia-induced hypercapnia. Respiration Physiology, 71: 227–246.

Heuer, R. M., and Grosell, M. 2014. Physiological impacts of elevated carbon dioxide and ocean acidification on fish. American Journal of Regulatory, Integrative and Comparative Physiology, 307: R1061–R1084. doi:10.1152/ajpregu.00064.2014.

Hoegh-Guldberg, O., Mumby, P. J., Hooten, A. J., Steneck, R. S., Greenfield, P., Gomez, E., Harvell, C. D., *et al.* 2007. Coral reefs under rapid climate change and ocean acidification. Science, 318: 1737–1742.

Jutfelt, F., de Souza, K. B., Vuylsteke, A., and Sturve, J. 2013. Behavioural disturbances in a temperate fish exposed to sustained high-CO_2 levels. PLoS One, 8: e65825. doi:10.1371/journal.pone.0065825.

King, P. A., and Goldstein, L. 1983. Organic osmolytes and cell-volume regulation in fish. Molecular Physiology, 4: 53–66.

Kinsey, D., and Kinsey, E. 1967. Diurnal changes in oxygen content of the water over the coral reef platform at Heron I. Marine and Freshwater Research, 18: 23–34.

Lambert, N., and Grover, L. 1995. The mechanism of biphasic GABA responses. Science, 269: 928–929.

Last, P. R., and Stevens, J. D. 2009. Sharks and Rays of Australia. Harvard University Press, Cambridge.

Lüthi, D., Le Floch, M., Bereiter, B., Blunier, T., Barnola, J-M., Siegenthaler, U., Raynaud, D., *et al.* 2008. High-resolution carbon dioxide concentration record 650,000–800,000 years before present. Nature, 453: 379–382.

McCormick, M. I., Watson, S-A., and Munday, P. L. 2013. Ocean acidification reverses competition for space as habitats degrade. Scientific Reports, 3: 03280. doi:10.1038/srep03280.

Mehrbach, C., Culberson, C. H., Hawley, J. E., and Pytkowicz, R. N. 1973. Measurement of the apparent dissociation constants of carbonic acid in seawater at atmospheric pressure. Limnology and Oceanography, 18: 897–907.

Meinshausen, M., Smith, S., Calvin, K., Daniel, J., Kainuma, M., Lamarque, J. F., Matsumoto, K., *et al.* 2011. The RCP greenhouse gas concentrations and their extensions from 1765 to 2300. Climatic Change, 109: 213–241.

Melzner, F., Gutowska, M. A., Langenbuch, M., Dupont, S., Lucassen, M., Thorndyke, M. C., Bleich, M., *et al.* 2009. Physiological basis for high CO_2 tolerance in marine ectothermic animals: pre-adaptation through lifestyle and ontogeny? Biogeosciences, 6: 2313–2331.

Michael, S. W. 2003. Aquarium Sharks & Rays: an Essential Guide to Their Selection, Keeping, and Natural History. TFH Publications, Neptune City.

Munday, P. L., Cheal, A. J., Dixson, D. L., Rummer, J. L., and Fabricius, K. E. 2014. Behavioural impairment in reef fishes caused by ocean acidification at CO_2 seeps. Nature Climate Change, 4: 487–492.

Munday, P. L., Dixson, D. L., Donelson, J. M., Jones, G. P., Pratchett, M. S., Devitsina, G. V., and Døving, K. B. 2009. Ocean acidification impairs olfactory discrimination and homing ability of a marine fish. Proceedings of the National Academy of Sciences of the USA, 106: 1848–1852.

Munday, P. L., Dixson, D. L., McCormick, M. I., Meekan, M., Ferrari, M. C. O., and Chivers, D. P. 2010. Replenishment of fish populations is threatened by ocean acidification. Proceedings of the National Academy of Sciences of the USA, 107: 12930–12934.

Munday, P. L., McCormick, M. I., and Nilsson, G. E. 2012. Impact of global warming and rising CO2 levels on coral reef fishes: what hope for the future? Journal of Experimental Biology, 215: 3865–3873.

Munday, P. L., Pratchett, M. S., Dixson, D. L., Donelson, J. M., Endo, G. G. K., Reynolds, A. D., and Knuckey, R. 2013a. Elevated CO_2 affects the behaviour of an ecologically and economically important coral reef fish. Marine Biology, 160: 2137–2144.

Munday, P. L., Warner, R. R., Munro, K., Pandolfi, J. M., and Marshall, D. J. 2013b. Predicting evolutionary responses to climate change in the sea. Ecology Letters, 16: 1488–1500.

Nilsson, G. E., Dixson, D. L., Domenici, P., McCormick, M. I., Sorensen, C., Watson, S-A., and Munday, P. L. 2012. Near-future carbon dioxide levels alter fish behaviour by interfering with neurotransmitter function. Nature Climate Change, 2: 201–204.

Nilsson, G. E., and Renshaw, G. M. 2004. Hypoxic survival strategies in two fishes: extreme anoxia tolerance in the North European crucian carp and natural hypoxic preconditioning in a coral-reef shark. Journal of Experimental Biology, 207: 3131–3139.

Pierrot, D., Lewis, E., and Wallace, D. W. R. 2006. MS Excel Program Developed for CO2 System Calculations. Carbon Dioxide Information Analysis Center, Oak Ridge National Laboratory, U. S. Department of Energy, Oak Ridge, TN. http://cdiac.ornl.gov/ftp/co2sys/CO2SYS_calc_XLS_v2.1/.

R Core Team. 2014. R: a language and environment for statistical computing. R Foundation for Statistical Computing, Vienna, Austria. http://www.R-project.org/.

Randall, J. E., Allen, G. R., and Steene, R. C. 1997. Fishes of the Great Barrier Reef and Coral Sea. Crawford House Publishing, Bathhurst.

Rosa, R., Baptista, M., Lopes, V. M., Pegado, M. R., Ricardo Paula, J., Trübenbach, K., Leal, M. C., *et al.* 2014. Early-life exposure to climate change impairs tropical shark survival. Proceedings of the Royal Society B: Biological Sciences, 281: 20141738. doi:10.1098/rspb.2014.1738.

Routley, M. H., Nilsson, G. E., and Renshaw, G. M. C. 2002. Exposure to hypoxia primes the respiratory and metabolic responses of the epaulette shark to progressive hypoxia. Comparative Biochemistry and Physiology, Part A, 131: 313–321.

Shaw, E. C., McNeil, B. I., and Tilbrook, B. 2012. Impacts of ocean acidification in naturally variable coral reef flat ecosystems. Journal of Geophysical Research, 117: C03038. doi:10.1029/2011JC007655.

Simpson, S. D., Munday, P. L., Wittenrich, M. L., Manassa, R., Dixson, D. L., Gagliano, M., and Yan, H. Y. 2011. Ocean acidification erodes crucial auditory behaviour in a marine fish. Biology Letters, 7: 917–920.

Sims, D. W., Nash, J. P., and Morritt, D. 2001. Movements and activity of male and female dogfish in a tidal sea lough: alternative behavioural strategies and apparent sexual segregation. Marine Biology, 139: 1165–1175.

Skaug, H., Fournier, D., Bolker, B., Magnusson, A., and Nielsen, A. 2014. Generalized Linear Mixed Models using AD Model Builder. R package version 0.8.0.

Sunday, J. M., Calosi, P., Dupont, S., Munday, P. L., Stillman, J. H., and Reusch, T. B. H. 2014. Evolution in an acidifying ocean. Trends in Ecology and Evolution, 29: 117–125.

Welch, J. M., Watson, S. A., Welsh, J. Q., McCormick, M. I., and Munday, P. L. 2014. Effects of elevated CO_2 on fish behaviour undiminished by transgenerational acclimation. Nature Climate Change, 4: 1086–1089.

Wickham, H. 2009. ggplot2: Elegant Graphics for Data Analysis. Springer, New York.

Wise, G., Mulvey, J. M., and Renshaw, G. M. 1998. Hypoxia tolerance in the epaulette shark (*Hemiscyllium ocellatum*). Journal of Experimental Zoology, 281: 1–5.

Handling editor: Howard Browman

ICES Journal of Marine Science

ICES Journal of Marine Science (2016), 73(3), 641–649. doi:10.1093/icesjms/fsv210

Contribution to Special Issue: 'Towards a Broader Perspective on Ocean Acidification Research'

Original Article

Effects of elevated CO_2 on early life history development of the yellowtail kingfish, *Seriola lalandi*, a large pelagic fish

Philip L. Munday[1,2]*, Sue-Ann Watson[1], Darren M. Parsons[3], Alicia King[4], Neill G. Barr[5], Ian M. Mcleod[1,2,6], Bridie J. M. Allan[1,2], and Steve M. J. Pether[4]

[1]*ARC Centre of Excellence for Coral Reef Studies, James Cook University, Townsville, QLD 4811, Australia*
[2]*College of Marine and Environmental Sciences, James Cook University, Townsville, QLD 4811, Australia*
[3]*National Institute of Water and Atmospheric Research, Newmarket, Auckland 1149, New Zealand*
[4]*National Institute of Water and Atmospheric Research, Bream Bay, Ruakaka 0116, New Zealand*
[5]*National Institute of Water and Atmospheric Research, Greta Point, Kilbirnie, Wellington 6241, New Zealand*
[6]*TropWATER, James Cook University, Townsville, QLD 4811, Australia*

**Corresponding author: tel: + 61 7 47815341; fax: +61 7 47816722; e-mail: philip.munday@jcu.edu.au*

Munday, P. L., Watson, S-A., Parsons, D. M., King, A., Barr, N. G., Mcleod, Ian M., Allan, B. J. M., and Pether, S. M. J. Effects of elevated CO_2 on early life history development of the yellowtail kingfish, *Seriola lalandi*, a large pelagic fish. – ICES Journal of Marine Science, 73: 641–649.

Received 18 February 2015; revised 19 October 2015; accepted 21 October 2015; advance access publication 20 November 2015.

An increasing number of studies have examined the effects of elevated carbon dioxide (CO_2) and ocean acidification on marine fish, yet little is known about the effects on large pelagic fish. We tested the effects of elevated CO_2 on the early life history development and behaviour of yellowtail kingfish, *Seriola lalandi*. Eggs and larvae were reared in current day control (450 μatm) and two elevated CO_2 treatments for a total of 6 d, from 12 h post-fertilization until 3 d post-hatching (dph). Elevated CO_2 treatments matched projections for the open ocean by the year 2100 under RCP 8.5 (880 μatm CO_2) and a higher level (1700 μatm CO_2) relevant to upwelling zones where pelagic fish often spawn. There was no effect of elevated CO_2 on survival to hatching or 3 dph. Oil globule diameter decreased with an increasing CO_2 level, indicating potential effects of elevated CO_2 on energy utilization of newly hatched larvae, but other morphometric traits did not differ among treatments. Contrary to expectations, there were no effects of elevated CO_2 on larval behaviour. Activity level, startle response, and phototaxis did not differ among treatments. Our results contrast with findings for reef fish, where a wide range of sensory and behavioural effects have been reported. We hypothesize that the absence of behavioural effects in 3 dph yellowtail kingfish is due to the early developmental state of newly hatched pelagic fish. Behavioural effects of high CO_2 may not occur until larvae commence branchial acid–base regulation when the gills develop; however, further studies are required to test this hypothesis. Our results suggest that the early stages of kingfish development are tolerant to rising CO_2 levels in the ocean.

Keywords: behaviour, carbon dioxide, larval development, morphology, ocean acidification.

Introduction

Ocean acidification, caused by the uptake of anthropogenic carbon dioxide (CO_2) from the atmosphere, will affect the performance of many marine organisms, with implications for population dynamics, community structure, and ecosystem function (Doney *et al.*, 2009; Gaylord *et al.*, 2015). Atmospheric CO_2 concentrations were <300 ppm at the start of the 20th century, but have been rising steadily since then due to continued anthropogenic CO_2 emissions, reaching 400 ppm in 2014 (www.esrl.noaa.gov/gmd/ccgg/trends/) for the first time in at least 800 000 years (Luthi *et al.*, 2008). CO_2 levels in the surface ocean are rising at the same rate as the atmosphere (Doney *et al.*, 2009) and the continued uptake of additional CO_2 has caused ocean pH to decline by 0.1 units (Rhein *et al.*, 2013). If the current rate of anthropogenic CO_2 emissions is maintained, climate models project that CO_2 concentrations in the atmosphere and surface ocean will exceed 900 ppm by the end of this century and could reach 1900 ppm by 2250 (Meinshausen *et al.*, 2011).

Fish are generally considered to be relatively tolerant to rising CO_2 levels and declining seawater pH because of their well-developed mechanisms for acid–base regulation. Juvenile and adult fish actively regulate the concentrations of acid–base relevant ions in the blood and tissues to prevent acidosis in a high CO_2 environment (Heuer and Grosell, 2014) and this may help them cope with projected future CO_2 levels in the ocean (Melzner *et al.*, 2009). Early life stages, however, may be more susceptible to high CO_2, because they are still developing their physiological regulatory processes (Brauner, 2008). Consequently, much of the recent research into the effects of ocean acidification on fish has concentrated on embryos, larvae, and small juveniles. While some studies have found no effects, or only minor effects, of high CO_2 on growth, development, and survival of fish early life history stages (Munday *et al.*, 2009a, 2011; Franke and Clemmesen, 2011; Frommel *et al.*, 2013; Bignami *et al.*, 2013, 2014; Hurst *et al.*, 2013; Maneja *et al.*, 2013; Pope *et al.*, 2014), other studies have reported negative effects on embryonic development (Forsgren *et al.*, 2013), yolk provisioning (Chambers *et al.*, 2014), tissue and organ development (Frommel *et al.*, 2012; Chambers *et al.*, 2014), swimming duration (Pimentel *et al.*, 2014), and growth and survival (Baumann *et al.*, 2012). However, most of these negative effects have been observed at relatively high CO_2 levels ($\geq$1500 μatm CO_2), and sometimes only at very extreme levels (>4000 μatm CO_2). Nevertheless, these studies indicate that early life history stages of some species may be more susceptible to ocean acidification than others, especially in locations that may be exposed to periods of enhanced CO_2 from upwelling or eutrophication.

An increasing number of studies have also observed effects of elevated CO_2 on fish sensory systems and behaviours (Munday *et al.*, 2014). When exposed to high CO_2 for more than a few days, there are changes in olfactory (Munday *et al.*, 2009b), auditory (Simpson *et al.*, 2011), and visual function (Chung *et al.*, 2014). Activity levels (Munday *et al.*, 2010), phototaxis (Forsgren *et al.*, 2013), response to chemical cues (Dixson *et al.*, 2010; Ferrari *et al.*, 2011a), and startle behaviour (Allan *et al.*, 2013) are all affected in larval fish. These changes in behaviour can affect the outcome of predator–prey interactions (Ferrari *et al.*, 2011b; Allan *et al.*, 2013), leading to significantly increased rates of mortality (Munday *et al.*, 2010). Most research on behavioural effects of high CO_2 have been conducted on coral reef fish, but sticklebacks (Jutfelt *et al.*, 2013), sharks (Dixson *et al.*, 2014; Green and Jutfelt, 2014), and rockfish (Hamilton *et al.*, 2014) also exhibit altered behaviours when continuously exposed to elevated CO_2 for short periods of time. Importantly, many of the effects on fish sensory abilities and behaviour occur below 1000 μatm, well within the range of CO_2 levels projected to occur by 2100 as a result of anthropogenic CO_2 emissions. Therefore, behavioural effects of rising CO_2 levels may be a more immediate threat to marine fish than effects on life history traits.

The effects of high CO_2 on early life history stages of commercially important species have been examined in cod (Frommel *et al.*, 2012, 2013; Maneja *et al.*, 2013), herring (Franke and Clemmesen, 2011), walleye pollock (Hurst *et al.*, 2012), European sea bass (Pope *et al.*, 2014), and summer flounder (Chambers *et al.*, 2014). However, few studies have examined the potential effects of projected future CO_2 levels on large pelagic fish. In the few studies conducted to date, there were no consistent effects of $\leq$2100 μatm CO_2 on early life history traits of cobia (Bignami *et al.*, 2013) or dolphinfish (Bignami *et al.*, 2014), but oxygen consumption and swimming ability were reduced in dolphin fish at >1400 μatm CO_2 (Bignami *et al.*, 2014; Pimentel *et al.*, 2014). Consequently, there appear to be different sensitivities to elevated CO_2 among large pelagic species. Bromhead *et al.* (2014) recently reported negative effects of elevated CO_2 on growth and survival of yellowfin tuna, but the effects were predominantly observed above 2100 μatm and were strongest and most consistent above 8500 μatm. There is clearly a need to test the sensitivity of other large pelagic fish to high CO_2, especially at CO_2 levels that are consistent with climate change projections for this century.

The yellowtail kingfish, *Seriola lalandi*, is a large pelagic fish found throughout the subtropical and temperate western Pacific, including New Zealand and Australia. Adults are mostly found in open coastal waters where they form schools associated with areas of high water flow near rocky outcrops or pinnacles (Kailola *et al.*, 1993; Francis, 2012). Juveniles are generally found in offshore waters, often associated with drifting algae and debris (Kailola *et al.*, 1993). Kingfish are piscivorous, feeding mostly on small pelagic fish (Francis, 2012). In New Zealand, they are a revered sports fish and form an important recreational fishery (ca. 600 t annual catch), with a small (ca. 170 t annual catch), but high value, commercial fishery also in operation (Ministry for Primary Industries, 2014).

The aim of this study was to conduct an initial assessment of the sensitivity of early life history stages of the yellowtail kingfish to elevated CO_2. We focused on the embryonic and pre-feeding larval stages as they may be more sensitive to environmental stress than later life stages (Melzner *et al.*, 2009). Focusing on the earliest life stages also avoided problems associated with high and stochastic mortality of feeding-stage larvae in captivity. Eggs and larvae were reared for a total of 6 d, from 12 h post-fertilization to 3 dph. We used two elevated CO_2 treatments, one relevant to projections for the open ocean by year 2100 under emissions scenario RCP 8.5 (880 μatm CO_2) and a second, higher treatment (1700 μatm CO_2), relevant to CO_2 levels in high-productivity upwelling zones where pelagic fish often spawn (Bromhead *et al.*, 2014). The higher CO_2 treatment also enabled a comparison with previous studies on pelagic and commercially important fish that have been conducted at $\geq$1600 μatm CO_2 (e.g. Frommel *et al.*, 2012; Chambers *et al.*, 2014; Pimentel *et al.*, 2014). We investigated effects of elevated CO_2 on both life history traits and behaviour. For life history traits, we examined the effect of elevated CO_2 on hatching success, survival to 3 d post-hatch (dph), larval size, and yolk and oil globule development. For behavioural assays, we concentrated on three primary behavioural responses that can be affected by high CO_2 in small larval fish: activity level, startle response, and phototaxis.

Methods

Study location and fish husbandry

This study was conducted at the National Institute of Water and Atmospheric Research, Bream Bay Aquaculture Park, Ruakaka, Northland, New Zealand. Two sets of experiments were conducted in conjunction with mass spawning events that occurred during the nights of 26–27 January 2014 and 03–04 February 2014. The experiments from the two different spawning events are referred to as Trials 1 and 2. Larvae from each spawning were reared to 3 dph, which marks the end of the endogenous feeding stage (Moran *et al.* 2007; Martinez-Montano *et al.*, 2014). A subset of larvae in Trial 1 were also reared to 6 dph without feeding to further explore growth on residual energy stores.

Broodstock, eggs, and larval culture

Spawning stock of yellowtail kingfish were maintained outdoors in 20 m^3 circular tanks, each contained up to 10 locally sourced, wild-caught fish that had been domesticated in tanks for up to 6 years (approximately equal sex ratio in each tank). Each 20 m^3 tank was supplied with 130 l min^{-1} seawater filtered to 10 μm at ambient temperature (from 13°C in winter to 24°C in summer) and with an ambient photoperiod. Broodstock were fed a mixture of pilchard (*Sardinops sagax*) and squid (*Notodarus* spp.). Spawning was allowed to occur naturally and to maximize genetic variation, eggs were collected from multiple broodstock tanks in even proportions. For Trial 1, three broodstock tanks containing a total of nine females and eight males contributed to spawning. For Trial 2, a different combination of three broodstock tanks containing a total of nine females and seven males contributed to spawning. Time of spawning was consistent across all tanks, occurring within the last 2 h of daylight.

Kingfish eggs were collected using an external egg collector as described by Moran *et al.* (2007), with a 500-μm mesh net to retain eggs from the surface overflow of each tank. An equal proportion of floating eggs from all contributing tanks were mixed, rinsed with oxygenated water flow for 5 min, and disinfected with Tosylchloramide (chloramine-T) at 50 ppm for 15 min. Eggs were then rinsed with water and then evenly distributed to 15 conical rearing tanks. Each 400 l rearing tank received flow-through seawater at 20–21°C with a photoperiod of 14 h light and 10 h dark and at a flow rate of 4 l min^{-1}. Gentle aeration was maintained within each tank with a weighted 4 mm airline. Eggs hatched 3 d after stocking and larvae were reared for a further 3 d on their endogenous reserves. Dead eggs, larvae, and egg shells were removed daily by draining from an outlet at the bottom of the rearing tank.

Experimental system and water chemistry

Seawater pumped from the ocean was filtered through mixed-media (sand), bag filtered to 5 μm, UV light treated to 150 mW cm^{-2}, and delivered to large a header tank. Oxygen diffusers in the header tank maintained baseline minimum dissolved oxygen (100% saturation) and a foam fractionator removed any additional organics. Seawater from the header tank was gravity-fed into three separate 100 l sump tanks where CO_2 was maintained at ambient control (~450 μatm), mid (~880 μatm), and high (~1700 μatm) CO_2 (Table 1). Seawater from each of the three pH treatment sumps was pumped into five of the 400 l rearing tanks, so that there were five replicate rearing tanks at each CO_2 level. A Hailea HX-6540 aquarium pump in the pH treatment sump both mixed the experimental seawater and pumped water from each sump to the rearing tanks. The CO_2 level and pH, as described above, were controlled by direct diffusion of CO_2 into seawater using coils of thin walled silicone tubing immersed in the sump tanks. The supply of CO_2 to the diffusion coils was controlled by pinch valves, which in turn were controlled by Omega PHCN-37 pH controllers connected to Sensorex SE100 pH probes with precision PT100 probes for temperature compensation. The CO_2 levels in the treatment sump tanks and experimental tanks were switched between Trials 1 and 2 to randomize any potential tank effects.

The pH_{total} (SG8 SevenGo pro, Mettler Toledo, Switzerland) and temperature (C22, Comark, Norwich, UK) of each rearing tank was measured daily and seawater CO_2 confirmed with a portable CO_2 equilibrator and an infrared sensor (GMP343, Väisälä, Helsinki, Finland). Tris buffers were obtained from Professor A.G. Dickson (Scripps Institution of Oceanography). Water samples were taken from three random tanks at each CO_2 level at the start and end of each trial. Water samples were analysed for total alkalinity by Gran titration (888 Titrando, Metrohm, Switzerland) to within 0.4% of certified reference material (Professor A.G. Dickson, Scripps Institution of Oceanography). Carbonate chemistry parameters were calculated in CO2SYS (http://cdiac.ornl.gov/ftp/co2sys/CO2SYS_calc_XLS_v2.1) using the constants K1 and K2 from Mehrbach *et al.* (1973) refit by Dickson and Millero (1987), and Dickson for $KHSO_4$. Seawater carbonate chemistry parameters for each trial are summarized in Table 1.

Sampling protocols for life history traits

Eggs were sampled at collection (~12 h post-fertilization) and larvae were sampled at hatching (0 dph) and 3 dph to estimate survival and to compare growth and development among CO_2 treatments. This involved mixing the eggs or larvae within each rearing tank using aeration and mechanical mixing with a hand-held agitator. Five samples of 520 ml were then taken with a beaker and eggs/larvae counted on a 500-μm mesh flat screen. The average of the five counts was then used to calculate the total number of eggs or larvae in each rearing tank (using the sample volume to tank volume ratio).

Each rearing tank contained >50 000 larvae. Morphometric traits were measured in a random subset of 20 fish sampled from each tank. We measured seven morphometric traits that are indicators of growth and performance in larval fish: standard length (SL), muscle depth at vent (MDV), total depth at vent including fins (FDV), yolk length (YL) and yolk depth (YD), oil globule diameter (OG), and eye diameter (ED) (Figure 1; Jones and McCormick 2002; Holt 2011; Chambers *et al.*, 2014). Measurement landmarks followed Chambers *et al.* (2014). Each sampled larva was photographed with a Leica camera fitted to a Leica compound microscope. Morphometric traits were extracted from the photographs using ImageJ software with the image displayed on a high-resolution computer screen.

Table 1. Mean (± s.d.) temperature, salinity, pH_{total}, total alkalinity, and pCO_2 in experiments with yellowtail kingfish (*S. lalandi*) eggs and larvae.

Trial	Treatment CO_2	Temperature (°C)	Salinity	pH_{total}	Total alkalinity (μmol kg^{-1} SW)	pCO_2 (μatm)
1	Control	20.2 ± 0.1	34.6	7.99 ± 0.01	2330.3 ± 9.4	468.8 ± 9.9
1	Moderate	20.2 ± 0.1	34.6	7.75 ± 0.01	2331.9 ± 3.6	885.9 ± 23.3
1	High	20.3 ± 0.1	34.6	7.49 ± 0.01	2328.0 ± 8.5	1684.2 ± 64.2
2	Control	20.5 ± 0.2	34.6	8.03 ± 0.02	2326.6 ± 5.9	427.5 ± 29.0
2	Moderate	20.5 ± 0.2	34.6	7.76 ± 0.01	2328.1 ± 5.0	874.7 ± 17.8
2	High	20.5 ± 0.2	34.6	7.48 ± 0.02	2320.9 ± 4.3	1755.1 ± 73.6

Temperature, salinity, pH_{total}, and total alkalinity were measured directly. pCO_2 was estimated from these parameters in CO2SYS. Trial 1 used eggs from mass spawning on 26–27/01/2014 and Trial 2 used eggs from mass spawning on 03–04/02/2014.

In Trial 1, we also conducted a pilot study where a subset of larvae was reared to 6 dph without feeding to further examine growth on remaining exogenous energy reserves. Owing to logistical constraints, only one rearing tank from each CO_2 treatment could be continued to 6 dph. Thirty randomly selected larvae were sampled from each rearing tank as described for 3 dph. SL was the only morphometric trait measured in the 30 × 6 dph larvae sampled from each CO_2 treatment.

Behavioural assays

All behavioural assays were conducted on larvae at 3 dph. Rearing tanks were mixed by aeration and a random sample of well-mixed larvae removed with beakers. Activity level and startle response assays were videographed from above with a Canon Powershot G15 digital camera placed on a tripod directly above the experimental arena. Larval behaviour was quantified subsequently from video playback. All assays were conducted in seawater at the same CO_2 level as the experimental treatment of the individuals tested and seawater was changed after each assay.

Activity level: Activity levels were measured by gently transferring 10 individuals into a round plastic aquarium (14.5Ø × 9.2 H cm) with black sides and a clear base. Under the clear base, a white sheet of paper with thin black gridlines at 1 cm intervals provided a reference scale. The aquarium was filled with seawater to a depth of 2 cm (330 ml). The 10 larvae were videoed for 8 min. The first 5 min of the video recording provided a habituation period. Activity levels were assessed 5 min into the video recording for 2 min. The total number of line crosses on the 1-cm^2 grid made by the 10 individual larvae during this 2 min period was determined. Duplicate assays were conducted for each rearing tank.

Startle response: Groups of 10 larvae were treated exactly as described above except that a lead weight on a swinging pendulum was released after 8 min. The weight collided with the side of the aquarium and larval startle responses and behaviour were videoed for a further 1 min. Videos were calibrated with a gridline inside the tank. The fish closest to the pendulum impact and greater than two body lengths away from the wall was analysed for a number of escape response variables, defined as:

(i) Responsiveness: the proportion of animals that responded with a sudden acceleration after being startled.

(ii) Response distance (mm): the total distance covered by the fish from the onset of the startle response until the fish comes to a halt.

(iii) Response duration (s): the elapsed time from the start of the response until the fish came to a halt.

Escape speed was not quantified as a sufficiently high-speed camera was not available. Duplicate assays were conducted for each rearing tank. Different groups of larvae were used for testing activity level and startle response.

Phototaxis: Phototaxis assays were only conducted during Trial 2. Phototaxis assays were conducted in plastic aquaria (30L × 15W × 5 H cm), with all sides masked with black tape to exclude ambient light. Each aquarium was placed on a 1cm^2 grid and filled with water to 2 cm depth (∼300 ml). A habituation section was created by placing a plastic partition 5 cm from one end of the aquarium. On the opposite end of the aquarium, a down-facing LED light created a visible light gradient across the length of the tank. Ten larvae were gently transferred using a beaker into the 5 × 15 cm habituation section and given 5 min to habituate. The LED light was then turned on and the plastic partition removed. The number of larvae in each third of the aquarium (dark, mid, and light) was recorded after 2 and 10 min. The phototaxis assay was repeated six times with different larvae from each rearing tank.

Statistical analysis

Repeated-measures (RM) ANOVA was used to compare survival to hatching and 3 dph among CO_2 treatments. This analysis compared the estimated number of individuals in each rearing tank at the three developmental stages (fertilized eggs, hatched larvae, and 3 dph larvae) in Trials 1 and 2. CO_2 treatment and trial were the independent variables and survival at developmental stage was the repeated measure.

Morphometric traits (SL, MDV, FDV, YL, YD, OG, and ED) were analysed for each of the 20 randomly selected fish per rearing tank. Morphometric traits were not highly correlated with each other (correlation coefficients between pairs of measures varied from

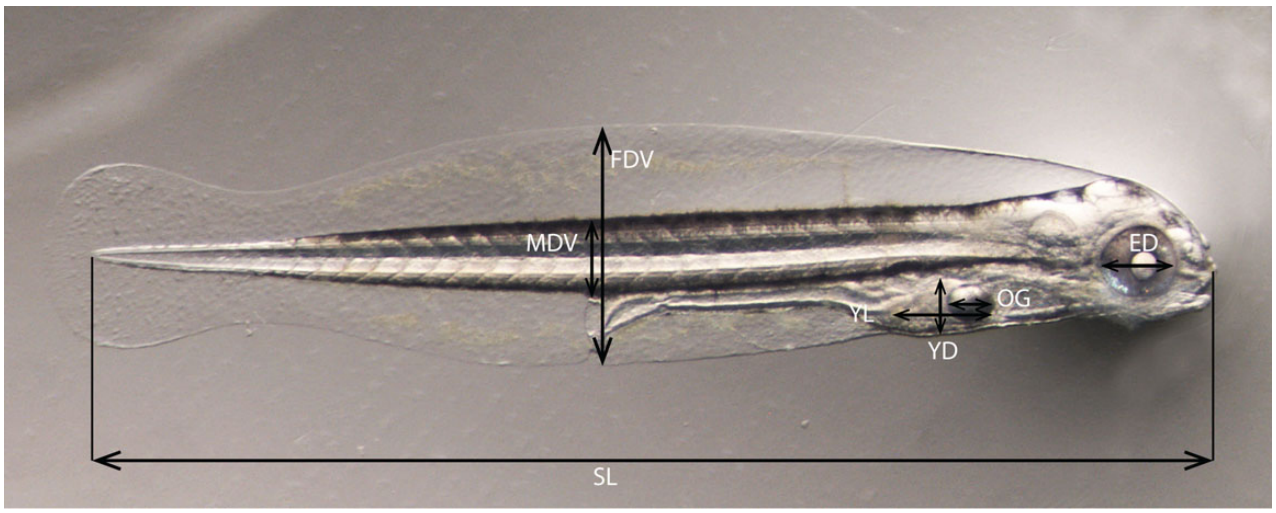

Figure 1. Photograph of 3 dph larval yellowtail kingfish (*S. lalandi*) showing morphometric traits measured. SL, standard length; MDV, muscle depth at vent; FDV, total depth at vent including fins; YL, yolk length; YD, yolk depth; OG, oil globule diameter; ED, eye diameter.

0.10 to 0.58). Linear mixed-effects models (LME), with CO_2 and trial as fixed effects, were used to determine any potential effect of elevated CO_2 on morphometric traits. Tank was included as a random effect to account for the subsampling of fish from replicate tanks within each CO_2 treatment. Individual fish were the level of replication ($n = 599$). One deformed fish was excluded from the final analysis.

One-way ANOVA was used to compare SL among CO_2 treatments in 6 dph larvae in the pilot study conducted in Trial 1. Individual fish were the level of replication ($n = 90$). As there was one rearing tank per CO_2 treatment in this analysis, the results must be interpreted with caution.

Factorial ANOVA was used to compare activity level among CO_2 treatments and trials. Activity level was determined by summing the total number of line crosses of the 10 individuals in each behavioural assay. The average of the duplicate assays per rearing tank was then used in the analysis. Tank was the level of replication in this analysis ($n = 30$).

Startle response was only tested in Trial 2. Logistic regression was used to compare the proportion of assays where the focal larva responded to the stimulus in the startle test vs. the proportion of assays where the focal larva did not respond to the stimulus. CO_2 treatment was the categorical variable in the logistic regression. Because the size of the focal larva and their distance from the stimulus strike-point may influence the likelihood of a reaction, these two factors were included as covariates in the model. The inclusion of tank did not improve the fit of the model, so it was not included in the final model. To maximize statistical power, the two assays per rearing tank were used in the analysis. Assay was the level of replication in this analysis ($n = 30$).

For fish that did respond to the stimulus ($n = 24$), LME was used to determine any potential effect of CO_2 on each of the three escape traits that were measured. CO_2 treatment, fish size, and distance of the fish from the stimulus were included as independent fixed effects in the models and tank was included as a random effect. Individual fish were the level of replication in this analysis ($n = 24$).

Phototaxis was only tested in Trial 2. LME was used to compare the proportion of larvae in the lit third of the chamber at 2 and 10 min among CO_2 treatments. CO_2 and time were the fixed effects, with rearing tank and assay container included in the model as random effects. Proportions were logit transformed before analysis. Assay was the level of replication in this analysis ($n = 90$).

LME analysis was performed in TIBCO Spotfire S+ 8.2. All other analyses were conducted in Statistica (version 12).

Results

As expected, the number of surviving individuals per tank declined from fertilized eggs to hatching and 3 dph (Figure 2; RM ANOVA $F_{2,52} = 81.89$, $P < 0.001$). There was also a significant interaction between developmental stage and trial ($F_{2,52} = 10.16$, $P < 0.001$), with fewer eggs surviving to hatching in Trial 2 compared with Trial 1 (Figure 2). However, there was no effect of CO_2 treatment on survival to hatching or survival to 3 dph.

Oil globule diameter was the only morphological trait that varied among CO_2 treatments in 3 dph larvae. Mean oil globule diameter exhibited a decline with increasing CO_2 level (Figure 3). Oil globule diameter was significantly smaller than the controls in the 1700-μatm treatment (LME $t_{26} = -2.14$, $P = 0.04$), but not in the 880-μatm CO_2 treatment (LME $t_{26} = -1.24$, $P = 0.23$). However, the magnitude of the effect was relatively small, with oil globule diameter ~5% smaller in the 1700-μatm treatment compared with the control. SL, MDV, FDV, YL, YD, and ED did not differ among CO_2 treatments for 3 dph fish. In the subset of fish that were reared to 6 dph in Trial 1, SL was ~2.5% smaller in the

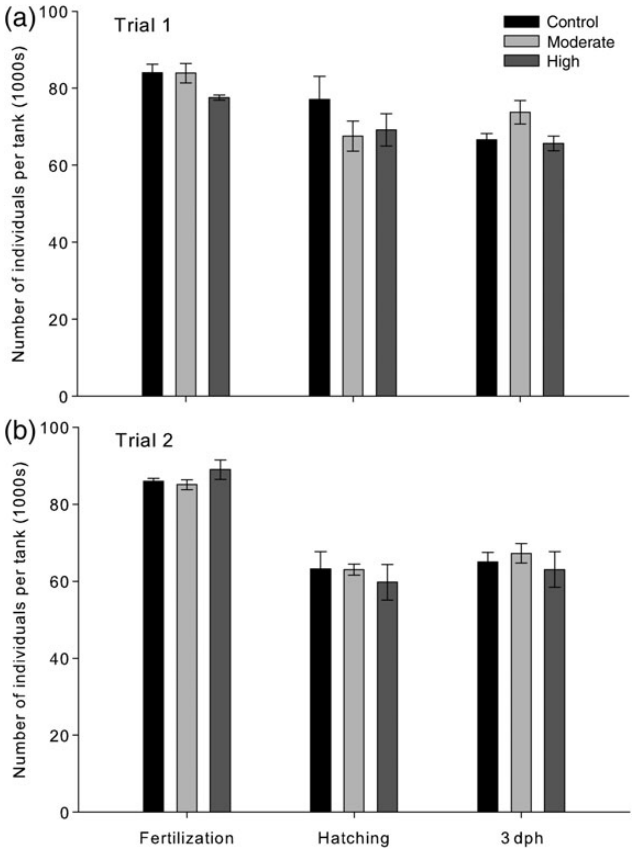

Figure 2. Mean (± SE) number of yellowtail kingfish (*S. lalandi*) individuals in control, moderate, and high CO_2 tanks at fertilization, hatching and 3 dph during Trial 1 (26–27/01/2014 spawning) and Trial 2 (03–04/02/2014 spawning). $n = 5$ tanks per treatment.

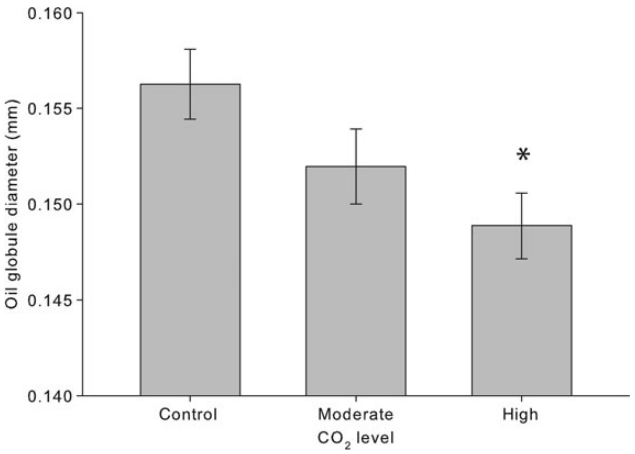

Figure 3. Mean (± SE) oil globule diameter of yellowtail kingfish (*S. lalandi*) larvae from control, moderate, and high CO_2 treatments at 3 dph. $n = 200$ larvae per treatment. Asterisk indicates statistically significant difference from control ($P < 0.05$). Note that the *y*-axis does not start at zero.

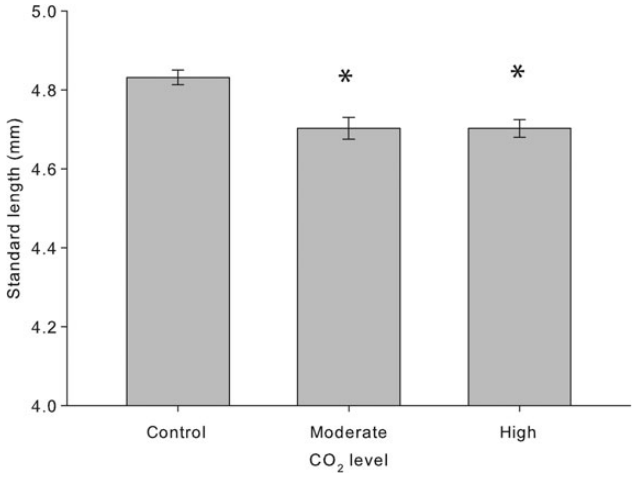

Figure 4. Mean (± SE) standard length of yellowtail kingfish (*S. lalandi*) larvae from control, moderate, and high CO_2 treatments at 6 dph in Trial 1. Other morphometric traits were not measured in 6 dph larvae. $n = 30$ larvae per treatment. Asterisk indicates statistically significant difference from control ($P < 0.05$). Note that the *y*-axis does not start at zero.

two elevated CO_2 treatments compared with the control (Figure 4; $F_{2,87} = 10.48$, $P < 0.001$), although this result must be interpreted with caution as there was no tank replication. Other morphological traits were not measured at 6 dph.

Activity level, measured as line crosses by 10 randomly selected individuals in a 2-min period, did not differ between CO_2 treatment or trial. Average line (± SE) crosses were 100 ± 7.8 in the control, 80 ± 9.8 in 880 μatm CO_2, and 116 ± 12.8 in the 1700 μatm CO_2.

Eighty per cent of individuals (24 of 30) responded to the stimulus in the startle test. Distance from the stimulus ($\chi^2 = 4.39$, $P = 0.036$), but not CO_2 treatment ($\chi^2 = 0.28$, $P = 0.869$), influenced the likelihood of responding to the stimulus. Among responders, there was no effect of CO_2 treatment, or the covariates (fish size and distance from stimulus) on escape distance or escape duration among the CO_2 treatments.

In the phototaxis experiment, more larvae were in the lit third of the chamber at 10 min compared with 2 min ($t_{87} = 5.07$, $P < 0.001$), but there was no effect of CO_2 treatment.

Discussion

While an increasing number of studies have examined the effects of projected future CO_2 levels and ocean acidification on marine fish, little is known about the effects on large pelagic fish. Here, we found that elevated CO_2 influenced the utilization of endogenous energy resources of newly hatched yellowtail kingfish, but not their survival or behaviour. Our results suggest that the earliest life stages of yellowtail kingfish are likely to be tolerant to projected future CO_2 levels in the ocean.

While some studies have reported negative effects of near-future CO_2 levels on the growth of larval fish (e.g. Baumann *et al.*, 2012), others have observed no effect (Bignami *et al.*, 2013; Frommel *et al.*, 2013; Hurst *et al.*, 2013), or even increased growth rates (Munday *et al.*, 2009a; Chambers *et al.*, 2014; Pope *et al.*, 2014). The reason for these contrasting findings is unknown, but they do indicate that the effects of elevated CO_2 on larval development may differ greatly among taxa. We found no effect of elevated CO_2 levels on growth or survival of larval kingfish to 3 dph. There was, however, a decline in oil globule size with an increasing CO_2 level, which indicates that larvae utilized a larger proportion of their endogenous energy reserves in reaching the same size in high CO_2 treatments. Oil globule diameter was 5% smaller in the 1700-μatm treatment, which would equate to an ~15% volume reduction in a spherical oil globule. While not a large effect, it could still have implications for individual performance. The oil globule of larval fish is a rich source of lipids that are catabolized during development (Heming and Buddington, 1988) and these lipids are the major sources of energy for growth and development after hatching (Rønnestad *et al.*, 1998). The oil globule is also an important energy buffer in larval fish and may enhance resistance to starvation once larvae commence exogenous feeding (Chambers *et al.*, 1989; Fisher *et al.*, 2007). The increased use of this key energy source in reaching a similar size at first feeding in yellowtail kingfish could have implications for the growth and survival of older age classes. In particular, older larvae may be more susceptible to mortality at times or places where food availability is suboptimal.

Consistent with greater energetic demands in the elevated CO_2 treatments, larvae reared for a further 3 d without feeding, to 6 dph, were slightly smaller (2.5% of SL) in the elevated CO_2 treatments compared with control fish. The mixed-feeding period, immediately after the capacity for exogenous feeding is reached but when endogenous energy reserves are still being used, is a critical period for larval fish (Kamler, 1992). In particular, they are especially vulnerable to starvation during this stage. The slower growth of feeding-stage larvae on residual energy reserves is consistent with increased energetic demand in a high CO_2 environment.

While we detected modest effects of high CO_2 on energy utilization by larval kingfish, there were no direct effects of 880 or 1700 μatm CO_2 on other morphometric traits or survival. This suggests that the development of embryos and newly hatched larvae of kingfish are tolerant to projected near-future CO_2 levels, but there are some energetic costs to this tolerance. A decline in yolk sac area in larval fish exposed to high CO_2, corresponding to an increase in body length, has been observed in larval clownfish (Munday *et al.*, 2009a) and summer flounder (Chambers *et al.*, 2014), indicating a different shift in energy utilization patterns in these species compared with the yellowtail kingfish studied here. In larval herring, yolk sac area was not affected by high CO_2 levels, but there was a drop in RNA/DNA ratios, potentially indicating an increased energetic cost to larvae at elevated CO_2 levels. Taken together, these studies suggest that there may be some energetic cost for larval fish to maintain growth and development in a high CO_2 environment, but how larvae fuel this cost, or the trade-offs made in energy allocation to different physiological processes, may differ among species.

There was no effect of either CO_2 treatment on swimming activity of the larvae, or the distance they travelled when startled. These results are consistent with the absence of any effect of 1800 μatm CO_2 on swimming kinematics of larval cod, but contrast with studies on dolphinfish, where reduced swimming activity (Pimentel *et al.*, 2014) and maximum velocity (Bignami *et al.*, 2014) were observed at 1600 and 1460 μatm CO_2, respectively. While it is possible that these different results could relate to differences in experimental design, they could also indicate that there are differences among pelagic fish in their sensitivity to high CO_2. Furthermore, Bignami *et al.* (2014) observed an effect on swimming velocity in one experiment, but not another,

therefore, the effects may be highly dependent on developmental stage or other environmental factors. More studies using identical experimental protocols in a range of species would be helpful in identifying if the variable results reported to date are indicative of differences in sensitivity to near-future CO_2 among species and/or developmental stages, or simply due to differences in experimental approaches.

Contrary to expectations, we did not detect significant effects of elevated CO_2 on the behaviour of 3 dph larval kingfish. Larval and juvenile reef fish are more active (Munday *et al.*, 2010) and have impaired responses to a threat stimulus (Allan *et al.*, 2013) when reared at CO_2 levels similar to those used here. Furthermore, newly hatched larval gobies are more positively phototactic if exposed to high CO_2 during embryonic development (Forsgren *et al.*, 2013). In contrast, there was no effect of high CO_2 on activity, startle responses, or phototaxis in 3 dph yellowtail kingfish. This raises the question; why didn't we detect behavioural effects in 3 dph larval kingfish when a wide range of behavioural and sensory impairments have been observed in reef fish? The behavioural changes observed in reef fish at high CO_2 appear to be caused by an interference with the GABA-A receptor, the primary inhibitory neurotransmitter receptor in the vertebrate brain (Nilsson *et al.*, 2012; Hamilton *et al.*, 2014). The GABA-A receptor is an ion-channel with conductance for Cl^- and HCO_3^-. Under normal conditions, ion gradients over the neuronal membrane result in an inflow of Cl^- and HCO_3^- upon opening of the GABA-A receptor, which then leads to hyperpolarization and inhibition of the neuron (Nilsson *et al.*, 2012). However, fish excrete Cl^- and accumulate HCO_3^- from seawater to prevent an acidosis when exposed to elevated CO_2 (Heuer and Grosell, 2014). Depending on the magnitude of changes in HCO_3^- and Cl^- during acid–base regulation, the resultant alterations of ion gradients could either potentiate the GABA-A receptor function, or reverse its action, making it excitatory rather than inhibitory (Nilsson *et al.*, 2012; Hamilton *et al.*, 2014). The absence of behavioural effects in 3 dph kingfish could indicate that HCO_3^- and/or Cl^- gradients have not changed sufficiently in these small preflexion fish to induce behavioural effects.

The mechanisms of acid–base regulation in embryonic and larval fish are very poorly understood (Brauner, 2008). That pH regulation occurs in these early life stages is clear, but the precise mechanisms and transporters involved are largely unknown. In juvenile and adult fish, the gills are the primary site of ion exchange for acid–base regulation. However, they cannot be involved in acid–base regulation of embryos or newly hatched larvae of pelagic fish, such as the *S. lalandi* larvae studied here, because they do not have gills. Instead, the skin and yolk epithelium are the primary site of ion exchange in the small larvae of broadcast spawned fish. Perhaps, kingfish larvae may be more reliant on Na^+/H^+ exchange during early development and then shift to Cl^-/HCO_3^- as the primary mechanism for acid–base regulation when the gills develop, which occurs between 2 and 15 dph (Martinez-Montano *et al.*, 2014). An increased dependence on Na^+/H^+ exchange across the skin and yolk sac before the development of gills could explain the absence of behavioural effects in 3 dph yellowtail kingfish. A greater reliance on Na^+/H^+ exchange during early ontogeny would mean that Cl^- concentrations may not decline as a result of acid–base regulation (Hayashi *et al.*, 2004). The maintenance of Cl^- concentrations may be sufficient to maintain normal function of the GABA-A receptors in a high CO_2 environment. Alternatively, the GABA-A neuroreceptors of early developmental stages may be far less sensitive to the change in ion gradients than they are in older and more developed fish. There is currently insufficient knowledge about the acid–base regulatory processes in the early developmental stages of marine fish, and the mechanism by which high CO_2 levels interfere with neurotransmitter function, to properly assess this hypothesis, but it would be an interesting avenue for future investigation.

Frommel *et al.* (2012) observed tissue damage in Atlantic cod larvae at 32 dph, which coincided with metamorphosis and gill development. However, tissue damage was not evident in older larvae. Similar patterns of tissue damage in early larval stages have been observed in anchovies (Frommel *et al.*, 2014) and summer flounder (Chambers *et al.*, 2014), both of which also hatch as very small larvae without functional gills and metamorphose after 3–4 weeks. Consequently, the shift from ion regulation across the skin and yolk sac to the gills may be a critical time in the development of broadcast spawned fish (Frommel *et al.*, 2012). In contrast, the larvae of demersally spawned reef fish are relatively large at hatching and develop quickly during the larval stage. Consequently, there could be very different effects of high CO_2 on the small and slowly developing larvae of temperate water broadcast spawning fish compared with the relatively large and fast developing larvae of tropical benthic spawning fish. Owing to the delayed development of gills, accompanied by branchial exchange of Cl^-/HCO_3^- for acid–base regulation, temperate water broadcast spawning fish may be more prone to morphological and energetic effects of high CO_2 during early life stages. In contrast, the large size and rapid development of gills may predispose tropical benthic spawned fish to behavioural effects of high CO_2. This hypothesis deserves further exploration and testing.

As with all ocean acidification research, any effects of high CO_2 observed in experimental studies must be considered in the context of the rate of environmental change and the potential for organisms to adapt (Sunday *et al.*, 2014). Perhaps the modest effects of high CO_2 on energy provisioning observed here in larval kingfish could be ameliorated by adaptation as CO_2 levels slowly rise in the ocean over coming decades. Furthermore, recent studies have shown that parental exposure to high CO_2 can reduce the effect of high CO_2 on larval and juvenile growth and survival (Miller *et al.*, 2012; Murray *et al.*, 2014). In this initial study of the effects of projected future CO_2 levels on the early developmental stages of larval kingfish, it was not possible to test for adaptive responses through evolution or plasticity; however, this should be a priority for future studies.

In conclusion, this study indicates that the pre-feeding larval stages of yellowtail kingfish are tolerant to projected near-future CO_2 levels, but there could be an energetic cost to this tolerance. Consequently, larvae may have lower energy reserves at the onset of feeding in a future high CO_2 world. Contrary to expectations, we observed no significant effects of high CO_2 on larval behaviour. We propose that behavioural effects of high CO_2 may not occur until larvae begin Cl^-/HCO_3^- acid–base regulation when the gills develop; however, further studies are required to test this hypothesis. A prediction from this hypothesis is that the small larvae of broadcast spawned fish, that do not have functional gills until flexion, may be less susceptible to behavioural effects of high CO_2 than the relatively large larvae of demersally spawned fish. Nevertheless, later ontogenetic stages may still suffer behavioural impairment. Future studies should test how spawning mode and developmental stage influences the sensitivity of larval fish to the effect of high CO_2 and ocean acidification.

Acknowledgements

We thank Alvin Setiawan, Steve Pope, Michael Bruce, Vonda Cummings, and Judi Hewitt for assistance with the experiments, Kim Curry for assistance with seawater chemistry, and Rhondda Jones and Simon Brandl for statistical advice. This project was supported by funding from the NIWA Coasts and Oceans Programme 3 (2013/14 SCI) and the Australian Research Council.

References

Allan, B. J. M., Domenici, P., McCormick, M. I., Watson, S. A., and Munday, P. L. 2013. Elevated CO_2 affects predator-prey interactions through altered performance. PLos ONE, 8: e58520.

Baumann, H., Talmage, S. C., and Gobler, C. J. 2012. Reduced early life growth and survival in a fish in direct response to increased carbon dioxide. Nature Climate Change, 2: 38–41.

Bignami, S., Sponaugle, S., and Cowen, R. K. 2013. Response to ocean acidification in larvae of a large tropical marine fish, *Rachycentron canadum*. Global Change Biology, 19: 996–1006.

Bignami, S., Sponaugle, S., and Cowen, R. K. 2014. Effects of ocean acidification on the larvae of a high-value pelagic fisheries species, mahimahi *Coryphaena hippurus*. Aquatic Biology, 21: 249–260.

Brauner, C. J. 2008. Acid-base balance. *In* Fish Larval physiology, pp. 185–198. Ed. by R. N. Finn, and B. G. Kapoor. Science Publishers, Enfield. 724 pp.

Bromhead, D., Scholey, V., Nicol, S., Margulies, D., Wexler, J., Stein, M., Hoyle, S., *et al.* 2014. The potential impact of ocean acidification upon eggs and larvae of yellowfin tuna (Thunnus albacares). Deep Sea Research Part II. doi:10.1016/j.dsr2.2014.03.019.

Chambers, R. C., Candelmo, A. C., Habeck, E. A., Poach, M. E., Wieczorek, D., Cooper, K. R., Greenfield, C. E., *et al.* 2014. Effects of elevated CO_2 in the early life stages of summer flounder, *Paralichthys dentatus*, and potential consequences of ocean acidification. Biogeosciences, 11: 1613–1626.

Chambers, R. C., Legget, W. C., and Brown, J. A. 1989. Egg size, female effects, and the correlation between early life history traits of capelin, *Mallotus villosus*: An appraisal at the individual level. Fisheries Bulletin, 87: 515–523.

Chung, W. S., Marshall, N. J., Watson, S. A., Munday, P. L., and Nilsson, G. E. 2014. Ocean acidification slows retinal function in a damselfish through interference with $GABA_A$ receptors. Journal of Experimental Biology, 217: 323–326.

Claiborne, J. B., Edwards, S. L., and Morrison-Shetlar, A. I. 2002. Acid-base regulation in fishes: Cellular and molecular mechanisms. Journal of Experimental Zoology, 293: 302–319.

Dickson, A., and Millero, F. 1987. A comparison of the equilibrium constants for the dissociation of carbonic acid in seawater media. Deep Sea Research Part A: Oceanographic Research Papers, 34: 1733–1743.

Dixson, D. L., Jennings, A. R., Atema, J., and Munday, P. L. 2014. Odour tracking in sharks is reduced under future ocean acidification conditions. Global Change Biology. doi:10.1111/gcb.12678.

Dixson, D. L., Munday, P. L., and Jones, G. P. 2010. Ocean acidification disrupts the innate ability of fish to detect predator olfactory cues. Ecology Letters, 13: 68–75.

Doney, S. C., Fabry, V. J., Feely, R. A., and Kleypas, J. A. 2009. Ocean acidification: The other CO_2 problem. Annual Review of Marine Science, 1: 169–192.

Ferrari, M. C. O., Dixson, D. L., Munday, P. L., McCormick, M. I., Meekan, M. G., Sih, A., and Chivers, D. P. 2011a. Intrageneric variation in antipredator responses of coral reef fishes affected by ocean acidification: Implications for climate change projections on marine communities. Global Change Biology, 17: 2980–2986.

Ferrari, M. C. O., McCormick, M. I., Munday, P. L., Meekan, M. G., Dixson, D. L., Lonnstedt, O., and Chivers, D. P. 2011b. Putting prey and predator into the CO_2 equation–Qualitative and quantitative effects of ocean acidification on predator-prey interactions. Ecology Letters, 14: 1143–1148.

Fisher, R., Sogard, S. M., and Berkeley, S. A. 2007. Trade-offs between size and energy reserves reflect alternative strategies for optimizing larval survival potential in rockfish. Marine Ecology Progress Series, 344: 257–270.

Forsgren, E., Dupont, S., Jutfelt, F., and Amundsen, T. 2013. Elevated CO_2 affects embryonic development and larval phototaxis in a temperate marine fish. Ecology and Evolution, 3: 3637–3646.

Francis, M. 2012. Coastal Fishes of New Zealand. 4th edn. Craig Potton Publishing, Nelson. 268 pp.

Franke, A., and Clemmesen, C. 2011. Effect of ocean acidification on early life stages of Atlantic herring (*Clupea harengus* L.). Biogeosciences, 8: 3697–3707.

Frommel, A. Y., Maneja, R., Lowe, D., Malzahn, A. M., Geffen, A. J., Folkvord, A., Piatkowski, U., *et al.* 2012. Severe tissue damage in Atlantic cod larvae under increasing ocean acidification. Nature Climate Change, 2: 42–46.

Frommel, A. Y., Maneja, R., Lowe, D., Pascoe, C. K., Geffen, A. J., Folkvord, A., Piatkowski, U., *et al.* 2014. Organ damage in Atlantic herring larvae as a result of ocean acidification. Ecological Applications, 24: 1131–1143.

Frommel, A. Y., Schubert, A., Piatkowski, U., and Clemmesen, C. 2013. Egg and early larval stages of Baltic cod, *Gadus morhua*, are robust to high levels of ocean acidification. Marine Biology, 160: 1825–1834.

Gaylord, B., Kroeker, K. J., Sunday, J. M., Anderson, K. M., Barry, J. P., Brown, N. E., Connell, S. D., *et al.* 2015. Ocean acidification through the lens of ecological theory. Ecology, 96: 3–15.

Green, L., and Jutfelt, F. 2014. Elevated carbon dioxide alters the plasma composition and behaviour of a shark. Biology Letters, 10: 20140538.

Hamilton, T. J., Holcombe, A., and Tresguerres, M. 2014. CO_2-induced ocean acidification increases anxiety in Rockfish via alteration of $GABA_A$ receptor functioning. Proceedings of the Royal Society London B, 281: 20132509.

Hayashi, M., Kita, J., and Ishimatus, A. 2004. Acid-base responses to lethal aquatic hypercapnia in three marine fishes. Marine Biology, 144: 153–160.

Heming, T. A., and Buddington, R. K. 1988. Yolk-absorption in embryonic and larval fishes. *In* Fish Physiology, 11A, pp. 407–446. Ed. by W. S. Hoar, and D. J. Randall. Academic Press, San Diego.

Heuer, R. M., and Grosell, M. 2014. Physiological impacts of elevated carbon dioxide and ocean acidification on fish. American Journal of Regulatory, Integrative and Comparative Physiology, 307: R1061–R1084.

Holt, G. P. 2011. Larval Fish Nutrition. Wiley-Blackwell, West Sussex.

Hurst, T. P., Fernandez, E. R., and Mathis, J. T. 2013. Effects of ocean acidification on hatch size and larval growth of walleye pollock (*Theragra chalcogramma*). ICES Journal of Marine Science, 70: 812–822.

Hurst, T. P., Fernandez, E. R., Mathis, J. T., Miller, J. A., Stinson, C. M., and Ahgeak, E. F. 2012. Resiliency of juvenile walleye pollock to projected levels of ocean acidification. Aquatic Biology, 17: 247–259.

Jones, J. P., and McCormick, M. I. 2002. Numerical and energetic processes in the ecology of coral reef fishes. *In* Coral Reef Fishes: Dynamics and Diversity in a Complex Ecosystem, pp. 221–238. Ed. by P. F. Sale. Academic Press, San Diego.

Jutfelt, F., de Souza, K. B., Vuylsteke, A., and Sturve, J. 2013. Behavioural disturbances in a temperate fish exposed to sustained high-CO_2 levels. PLoS ONE, 8: e65825.

Kailola, P. J., Williams, M. J., Stewart, P. C., Reichelt, R. E., McNee, A., and Grieve, C. 1993. Australian Fisheries Resources. Bureau of Resource Sciences and the Fisheries Research and Development Corporation, Canberra. 422 pp.

Kamler, E. 1992. Early Life History of Fish: An Energetic Approach. Chapman & Hall, London. 267 pp.

Luthi, D., Le Floch, M., Bereiter, B., Blunier, T., Barnola, J. M., Siegenthaler, U., Raynaud, D., *et al.* 2008. High-resolution carbon dioxide concentration record 650,000–800,000 years before present. Nature, 453: 379–382.

Maneja, R. H., Frommel, A. Y., Browman, H. I., Clemmesen, C., Geffen, A. J., Folkvord, A., Piatkowski, U., *et al.* 2013. The swimming kinematics of larval Atlantic cod, *Gadus morhua* L., are resilient to elevated seawater pCO_2. Marine Biology, 160: 1963–1972.

Martinez-Montano, E., Gonzalez-Alvarez, K., Lazo, J. P., Audelo-Naranjo, J. M., and Velez-Medel, A. 2014. Morphological development and allometric growth of yellowtail kingfish *Seriola lalandi* V. larvae under culture conditions. Aquaculture Research, doi:10.1111/are.12587.

Mehrbach, C., Culberson, C. H., Hawley, J. E., and Pytkowicz, R. N. 1973. Measurement of the apparent dissociation constants of carbonic acid in seawater at atmospheric pressure. Limnology and Oceanography, 18: 897–907.

Meinshausen, M., Smith, S. J., Calvin, K., Daniel, J. S., Kainuma, M. L. T., Lamarque, J. F., Matsumoto, K., *et al.* 2011. The RCP greenhouse gas concentrations and their extensions from 1765 to 2300. Climatic Change, 109: 213–241.

Melzner, F., Gutowska, M. A., Langenbuch, M., Dupont, S., Lucassen, M., Thorndyke, M. C., Bleich, M., *et al.* 2009. Physiological basis for high CO_2 tolerance in marine ectothermic animals: Pre-adaptation through lifestyle and ontogeny? Biogeosciences, 6: 2313–2331.

Miller, G. M., Watson, S. A., Donelson, J. M., McCormick, M. I., and Munday, P. L. 2012. Parental environment mediates impacts of increased carbon dioxide on a coral reef fish. Nature Climate Change, 2: 858–861.

Ministry for Primary Industries. 2014. Fisheries Assessment Plenary, May 2014: Stock Assessments and Stock Status. New Zealand Ministry for Primary Industries, Wellington. 1381 pp.

Moran, D., Smith, C. K., Gara, B., and Poortenaar, C. W. 2007. Reproductive behaviour and early development in yellowtail kingfish (*Seriola lalandi* Valenciennes 1833). Aquaculture, 262: 95–104.

Munday, P. L., Cheal, A. J., Dixson, D. L., Rummer, J. L., and Fabricius, K. E. 2014. Behavioural impairment in reef fishes caused by ocean acidification at CO_2 seeps. Nature Climate Change, 4: 487–492.

Munday, P. L., Dixson, D. L., Donelson, J. M., Jones, G. P., Pratchett, M. S., Devitsina, G. V., and Doving, K. B. 2009b. Ocean acidification impairs olfactory discrimination and homing ability of a marine fish. Proceedings of the National Academy of Sciences of the United States of America, 106: 1848–1852.

Munday, P. L., Dixson, D. L., McCormick, M. I., Meekan, M., Ferrari, M. C. O., and Chivers, D. P. 2010. Replenishment of fish populations is threatened by ocean acidification. Proceedings of the National Academy of Sciences of the United States of America, 107: 12930–12934.

Munday, P. L., Donelson, J. M., Dixson, D. L., and Endo, G. G. K. 2009a. Effects of ocean acidification on the early life history of a tropical marine fish. Proceedings of the Royal Society London B, 276: 3275–3283.

Munday, P. L., Gagliano, M., Donelson, J. M., Dixson, D. L., and Thorrold, S. R. 2011. Ocean acidification does not affect the early life history development of a tropical marine fish. Marine Ecology Progress Series, 423: 211–221.

Murray, C. S., Malvezzi, A., Gobler, C. J., and Baumann, H. 2014. Offspring sensitivity to ocean acidification changes seasonally in a coastal marine fish. Marine Ecology Progress Series, 504: 1–11.

Nilsson, G. E., Dixson, D. L., Domenici, P., McCormick, M. I., Sørensen, C., Watson, S-A., and Munday, P. L. 2012. Near-future CO_2 levels alter fish behaviour by interference with neurotransmitter function. Nature Climate Change, 2: 201–204.

Pimentel, M., Pegado, M., Repolho, T., and Rosa, R. 2014. Impact of ocean acidification in the metabolism and swimming behavior of the dolphinfish (*Coryphaena hippurus*) early larvae. Marine Biology, 161: 725–729.

Pope, E. C., Ellis, R. P., Scolamacchia, M., Scolding, J. W. S., Keay, A., Chingombe, P., Shields, R. J., *et al.* 2014. European sea bass, *Dicentrarchus labrax*, in a changing ocean. Biogeosciences, 11: 2519–2530.

Rhein, M., Rintoul, S. R., Aoki, S., Campos, E., Chambers, D., Feely, R. A., Gulev, S., *et al.* 2013. Observations: Ocean. *In* Climate Change 2013: The Physical Science Basis. Contribution of Working Group I to the Fifth Assessment Report of the Intergovernmental Panel on Climate Change, pp. 255–315. Ed. By T. F. Stocker, D. Qin, G-K. Plattner, M. Tignor, S. K. Allen, J. Boschung, A. Nauels, Y. Xia, V. Bex, and P. M. Midgley. Cambridge University Press, Cambridge. 65 pp.

Rønnestad, I., Koven, W., Tandler, A., Harel, M., and Fyhn, H. J. 1998. Utilisation of yolk fuels in developing eggs and larvae of European sea bass (*Dicentrarchus labrax*). Aquaculture, 162: 157–170.

Simpson, S. D., Munday, P. L., Wittenrich, M. L., Manassa, R., Dixson, D. L., Gagliano, M., and Yan, H. Y. 2011. Ocean acidification erodes crucial auditory behaviour in a marine fish. Biology Letters, 7: 917–920.

Sunday, J. M., Calosi, P., Dupont, S., Munday, P. L., Stillman, J. H., and Reusch, T. B. H. 2014. Evolution in an acidifying ocean. Trends in Ecology and Evolution, 29: 117–125.

Handling editor: Howard Browman

ICES Journal of Marine Science

ICES Journal of Marine Science (2016), 73(3), 650–658. doi:10.1093/icesjms/fsv078

Contribution to Special Issue: 'Towards a Broader Perspective on Ocean Acidification Research'

Original Article

Lack of evidence for elevated CO_2-induced bottom-up effects on marine copepods: a dinoflagellate – calanoid prey – predator pair

Stamatina Isari[1,2]*, Soultana Zervoudaki[1], Janna Peters[3], Georgia Papantoniou[4], Carles Pelejero[2,5], and Enric Saiz[2]

[1]*Institute of Oceanography, Hellenic Centre for Marine Research, PO 712, 46.7 km Avenue Athens-Sounio, 19013 Anavyssos, Athens, Greece*
[2]*Institut de Ciències del Mar (CSIC), Pg. Marítim de la Barceloneta 37-49, 08003 Barcelona, Catalonia, Spain*
[3]*Institute for Hydrobiology and Fisheries Science, Hamburg University, Grosse Elbstrasse 133, 22767 Hamburg, Germany*
[4]*Department of Biology, University of Athens, Panepistimioupoli, Ilisia, 15701 Athens, Greece*
[5]*Institució Catalana de Recerca i Estudis Avançats (ICREA), Pg. Lluís Companys 23, 08010 Barcelona, Catalonia, Spain*

**Corresponding author: tel: +30 2291076374; fax: +30 2291076347; e-mail: misari@hcmr.gr.*

Isari, S., Zervoudaki, S., Peters, J., Papantoniou, G., Pelejero, C., and Saiz, E. Lack of evidence for elevated CO_2-induced bottom-up effects on marine copepods: a dinoflagellate – calanoid prey – predator pair. – ICES Journal of Marine Science, 73: 650–658.

Received 16 January 2015; revised 8 April 2015; accepted 9 April 2015; advance access publication 6 May 2015.

Rising levels of atmospheric CO_2 are responsible for a change in the carbonate chemistry of seawater with associated pH drops (acidification) projected to reach 0.4 units from 1950 to 2100. We investigated possible indirect effects of seawater acidification on the feeding, fecundity, and hatching success of the calanoid copepod *Acartia grani*, mediated by potential CO_2-induced changes in the nutritional characteristics of their prey. We used as prey the autotrophic dinoflagellate *Heterocapsa* sp., cultured at three distinct pH levels (control: 8.17, medium: 7.96, and low: 7.75) by bubbling pure CO_2 via a computer automated system. *Acartia grani* adults collected from a laboratory culture were acclimatized for 3 d at food suspensions of *Heterocapsa* from each pH treatment (ca. 500 cells ml^{-1}; 300 μg C l^{-1}). Feeding and egg production rates of the preconditioned females did not differ significantly among the three *Heterocapsa* diets. Egg hatching success, monitored once per day for the 72 h, did not reveal significant difference among treatments. These results are in agreement with the lack of difference in the cellular stoichiometry (C : N, C : P, and N : P ratios) and fatty acid concentration and composition encountered between the three tested *Heterocapsa* treatments. Our findings disagree with those of other studies using distinct types of prey, suggesting that this kind of indirect influence of acidification on copepods may be largely associated with interspecific differences among prey items with regard to their sensitivity to elevated CO_2 levels.

Keywords: *Acartia grani*, bottom-up, copepods, dinoflagellates, food quality, *Heterocapsa*, ocean acidification, pH.

Introduction

Climate-driven changes in the marine environment have been largely associated with the anthropogenic rise of the atmospheric CO_2 concentration, projected to increase by a factor of 1.1–2.4 by the end of the century (IPCC, 2013; levels in 2011: 391 ppm). Elevated CO_2 in the atmosphere is driving, in addition to global warming, a concurrent change in the seawater carbonate chemistry and an associated pH drop that could reach up to 0.4 pH units from years 1950 to 2100 (IPCC, 2013), widely known as ocean acidification (OA).

A significant amount of data have been obtained in the last decade related to the OA impact on several groups of marine organisms [as reviewed by Fabry *et al.* (2008); Doney *et al.* (2009); Dupont *et al.* (2010); Hofmann *et al.* (2010); Koch *et al.* (2013)]. Among plankton, research interest has mainly focused on calcifying primary producers, given the anticipated impact of high CO_2/low pH on the processes of photosynthesis and calcification (e.g. Riebesell *et al.*, 2000; Van de Waal *et al.*, 2013). Copepods, comprising the major group of secondary producers in the planktonic foodweb, have been typically considered relatively tolerant of a

lowering in seawater pH due to the lack of calcite/aragonite formations in their exoskeleton. This has been verified in several occasions, in studies where the copepod physiological performance was tested at CO_2 levels projected at the end of the century (Zhang *et al.*, 2011; Mayor *et al.*, 2012; Weydmann *et al.*, 2012; McConville *et al.*, 2013; Zervoudaki *et al.*, 2014) or even in long-time exposures at CO_2 levels rising far beyond the near-future projections (Kurihara and Ishimatsu, 2008; Hildebrandt *et al.*, 2014). Sublethal effects may be of relevance under extreme acidification regimes related with deep ocean CO_2 sequestration (e.g. Kurihara *et al.*, 2004; Mayor *et al.*, 2007; Zhang *et al.*, 2011; Cripps *et al.*, 2014a). Some recent studies, however, report a high sensitivity of copepods even at near-future OA levels (Lewis *et al.*, 2013; Thor and Dupont, 2015), and others suggest that the most experimental works might have underestimated the actual direct effect of OA on copepods due to the inadequacy of the experimental approaches used (Cripps *et al.*, 2014a, b).

In addition to reconsidering potential biases in the estimation of the direct OA effects on copepods, future research should also take into deeper account the fact that CO_2-induced changes in seawater chemistry may influence copepod performance not only in a direct way (i.e. by changing the acid–base regulation of their physiological and metabolic functions), but also indirectly through foodweb "bottom-up" effects. Climate-related changes in the quantitative and qualitative properties of lower trophic level organisms may be transferred to upper trophic levels through the food chain, but this indirect OA effect has been only poorly investigated for copepods. Food quality is a determinant factor for copepod performance (e.g. Jónasdóttir, 1994; Koski *et al.*, 1998; Jones *et al.*, 2002; Klein Breteler *et al.*, 2005; Isari *et al.*, 2013) and interestingly, a couple of recent works have emphasized a negative indirect OA effect on copepods (e.g. a decrease in egg production or/and growth and development) through a deterioration of the nutritional quality of their prey when grown under high CO_2 (Rossoll *et al.*, 2012; Schoo *et al.*, 2013).

There are several evidences for CO_2-induced changes in algal quality (Burkhardt and Riebesell, 1997; Burkhardt *et al.*, 1999; Urabe *et al.*, 2003; Rossoll *et al.*, 2012; Schoo *et al.*, 2013), but the response patterns show a profound species/strain-dependence. The underlying physiological mechanisms and metabolic pathways for this variability are not yet well understood, but the exposure of algae to high CO_2 levels is often accompanied by a downregulation of the genes associated with cellular CO_2-concentrating mechanisms (CCMs; e.g. Ratti *et al.*, 2007; Crawfurd *et al.*, 2011; Van de Waal *et al.*, 2013, 2014); the CCMs are responsible for the increase of free CO_2 concentration near the RuBisCO (ribulose1,5-bisphosphate carboxylase/oxygenase) enzyme, involved in the carbon fixation (Giordano *et al.*, 2005; Hopkinson *et al.*, 2011). Such shifts in gene expression and protein production are assumed to save energy and elemental resources and can be further expressed through changes in algal physiology and elemental and biochemical properties (Giordano *et al.*, 2005). Ultimately, the final outcome will depend on the efficiency of RuBisCO and CCMs in each species (Reinfelder, 2011).

In this study, in contrast to the flagellate and diatom preys used by Schoo *et al.* (2013) and Rossoll *et al.* (2012), respectively, we assess the bottom-up effects of OA on copepods offering as a prey a dinoflagellate species. Dinoflagellates constitute a major prey for copepods in most of the oceans (Saiz and Calbet, 2011); in addition, this group is expected to particularly benefit under increased CO_2 levels, due to their less efficient RuBisCO (form II) and their high dependence on CCMs (Reinfelder, 2011). Our hypothesis is that a higher CO_2 supply under OA conditions could facilitate the growth and improve the nutritional quality of dinoflagellates, and therefore enhance copepod productivity. To test our hypothesis, we cultured the armored dinoflagellate *Heterocapsa* sp. at three pCO_2/pH levels representative of the projected values at the end of the century (IPCC, 2013), then examined the response of the copepod *Acartia grani* in terms of feeding on dinoflagellate and reproduction.

Methods

Target copepod species

Eggs from a culture of the calanoid copepod *A. grani* maintained at the Institut de Ciències del Mar (CSIC) were collected, hatched, and reared to adulthood at 18 ± 1°C and a salinity of 37.4. Throughout their development, the copepods were fed *ad libitum* a suspension of the Cryptophyte alga *Rhodomonas salina* grown exponentially in f/2 medium. Only adult female copepods that had matured within the previous week were used in the experiments.

Dinoflagellate culture conditions

The marine autotrophic dinoflagellate *Heterocapsa* sp. was grown in batch culture amended with nutrients (f/2 medium; Guillard, 1975), and 250-ml aliquots of exponentially growing cells (ca. 60 000 cells ml^{-1}) were inoculated into 13-l Nalgene polycarbonate bottles containing 5 l of autoclaved 0.2-μm filtered seawater (salinity 37.4). These algal cultures were exposed to three distinct pH_{NBS} (National Bureau of Standards pH scale) levels (control: 8.17, medium: 7.96, and low: 7.75 pH units), adjusted by injections of pure CO_2 through a solenoid valve controlled automatically by an Aqua-medic™ computer automated system with a plastic shafted pH electrode. During the night-time, CO_2-free air was bubbled in the cultures (using a home-made filter filled with soda lime, Sigma Aldrich) to compensate for the decrease of pH due to algal respiration. The small number and size of the bubbles produced by the gas/air injections precluded any harmful mechanical effect on the algae. Algal cultures were maintained for a period of 16 days under these conditions in a cold room (18 ± 1°C) with 18 : 6 h light : dark cycle (150 μmol m^{-2} s^{-1}), and cell number and volume were daily monitored *in vivo* with an Multisizer III Coulter Counter. Growth rate (μ, d^{-1}) was calculated as the slope of the least-squares linear regression of ln(*Ni*) vs. time, where *Ni* was the cell concentration at time *i*. The division rate (k, doublings d^{-1}) was calculated as $k = \mu/\ln 2$. For the first 6 d, the algal cultures were grown exponentially until reaching a concentration of 10 000 cells ml^{-1}, sufficient to provide enough algae for the experiments with copepods. Thereafter, and based on the estimated algal growth rate, the cultures were kept in a semi-continuous phase at a stable culture biomass of ca. 10 000 cells ml^{-1} by daily removing a certain volume of culture and its replacement with f/2 medium.

Seawater chemistry

Throughout the experiment, we took the seawater pH readings of our computer automated system in our experimental treatments every 30 min. The accuracy of the pH measurements performed by the electrodes connected to the automated system (which we never removed from the closed culture bottles to avoid contamination) was daily verified, immediately after culture sampling, with an Metrohm 826 pH meter fitted with a glass electrode (6.0257.600, Aquatrode plus, Metrohm), equipped with temperature sensor, and

previously calibrated with buffer solutions of pH_{NBS} 7 and 9. Salinity was measured daily using an YSI-30 M/10FT probe, and total alkalinity (TA) was analysed on day 13 by potentiometric titration (Perez and Fraga, 1987; Perez *et al.*, 2000). Calculations of the other parameters of the carbonate system were performed from TA and pH using the CO_2SYS program (Pierrot *et al.*, 2006), with dissociation constants for carbonate determined by Mehrbach *et al.* (1973) and refit by Dickson and Millero (1987), whereas the dissociation constants of sulphuric acid were taken from Dickson (1990) and total boron from Lee *et al.* (2010).

Algal elemental (C : N : P) and fatty acid compositions

We assessed the elemental (C, N, and P) and fatty acid (FA) compositions of the algae grown under the different CO_2/pH conditions on the 15th day of growth of the algal culture. Triplicate (30 ml for C–N analysis, 20 ml for P analysis) and tetraplicate (40 ml for FAs) aliquots of known cell concentration were filtered onto pre-combusted 25-mm Whatman GF/C filters (450°C, 6 h). Samples for C and N analysis were dried for 24 h at 60°C and kept in a desiccator until analysis (FLASH 2000 Thermo Scientific CHNS analyser). Filters for particulate phosphorus and FAs were frozen at −80°C immediately after filtration. For phosphorus determination, filters were subjected to orthophosphate acid persulphate oxidation and posterior analysis as inorganic phosphorus (Grasshoff *et al.*, 1999). For the FA analysis, lipid extraction and conversion of acyl groups into fatty acid methyl ester derivatives (FAMES) were performed after Peters *et al.* (2013) using modified protocols of Folch *et al.* (1957) and Kattner and Fricke (1986). Total lipids were extracted using ultrasonic disruption of the cells in dichloromethane : methanol (2 : 1, v/v) and a washing procedure with aqueous KCl solution (0.88%). For quantification of FAMES, tricosanoic acid was added as an internal standard before extraction. Acyl groups were converted into FAMEs using methanolic sulphuric acid (3%) at 80°C for 4 h. After adding Milli-Q water, FAMEs were extracted by washing the polar phase three times with hexane. FAMES and fatty alcohols were separated by gas chromatography (column DB-FFAP, programmable temperature vaporizer injector, and solvent vent mode), detected by flame ionization, and identified by comparing retention times with those derived from standards of known composition. Only compounds with >0.2% of total FAs and alcohols were included in the dataset. Statistical data analyses of FAs were performed with the 12 most important FAs (defined as those with values >1% of tFA), either as absolute or relative content (in the latter case, after arcsine square root transformation).

Copepod experiments

The impact of the three different diets (algae grown at the respective CO_2/pH treatments) on the feeding and reproductive output of the copepod *A. grani* was assessed after a 3-d preconditioning period at the specific diets. Food suspensions at 500 cells ml^{-1} (ca. 300 µg C l^{-1}) at each CO_2/pH level were prepared by diluting the respective algal stock cultures with filtered seawater (FSW) pre-equilibrated at the respective pH, either by bubbling CO_2 (medium and low pH treatments) or CO_2-free air (control treatment). Pyrex screw-cap bottles (2300 ml) were filled with the suspensions and groups of 20 females and 12 males (to ensure fertilization) were added for preconditioning. During this period, the copepods were daily transferred to fresh suspensions (discarding dead animals if present). After the conditioning period, four replicated groups (4 × Cop) of five females were placed in 625 ml Pyrex screw-cap bottles filled with the respective food suspensions; five additional bottles with food suspensions but without the addition of copepods served as initial (1 × Init) and control (4 × Contr) bottles. Initial bottles were sacrificed immediately at the beginning of the incubation, and subsamples withdrawn and preserved with 2% Lugol's acetic solution; the remaining bottles were incubated for 24 h at 18°C under the light conditions where the algae had been growing to determine the copepod feeding and egg production rates on each respective diet. After the incubation time, the pH of the bottle contents was first checked (no substantial change was observed), then they were carefully poured onto a 200- and 20-µm meshes to collect the females and the eggs, respectively. The number and condition of the copepods were checked (mortality was negligible), and subsamples of the food suspensions were preserved as described above. A proportion (40%) of the eggs laid in each bottle was transferred into Petri dishes filled with FSW equilibrated at the parental incubation pH, sealed with plastic covers (no bubbles left), and left undisturbed to determine hatching success; the rest of the eggs for each bottle were preserved in Lugol's acetic solution for posterior counting. The number of unhatched eggs was monitored daily for 3 d, and the hatching rate was calculated. To follow the pH throughout the hatching incubation, pH measurements were taken every 24 h in separate Petri dishes filled with pCO_2 equilibrated FSW (but no eggs), sealed similarly to the ones used for the hatching test.

Algal concentration in the feeding experiment samples was determined microscopically, and clearance and ingestion rates were computed according to Frost (1972). Assuming that C and N content of eggs were 0.046 and 0.0091 µg egg^{-1}, respectively (Kiørboe *et al.*, 1985), and calculating the egg phosphorus content applying the Redfield N : P ratio (16 : 1 similar to 16.5 : 1 of *A. grani* females from our culture), we estimated the respective elemental copepod gross-growth efficiencies (GGEs; %) for each treatment by dividing the egg production and ingestion rates expressed at the respective elemental units (carbon: GGE_C; nitrogen: GGE_N; phosphorus: GGE_P).

Results

Seawater carbonate chemistry

Overall, the level of pH in the algal cultures was maintained rather stable throughout the entire period (Figure 1), except for the medium pH treatment that exhibited larger deviations (control: 8.17 ± 0.02; medium pH: 7.93 ± 0.07; low pH: 7.75 ± 0.02; n = 16 d; NBS scale). Alkalinity, which was measured only on the 13th day of the experiment, was found similar between treatments (Table 1). The corresponding pCO_2 calculated from pH and

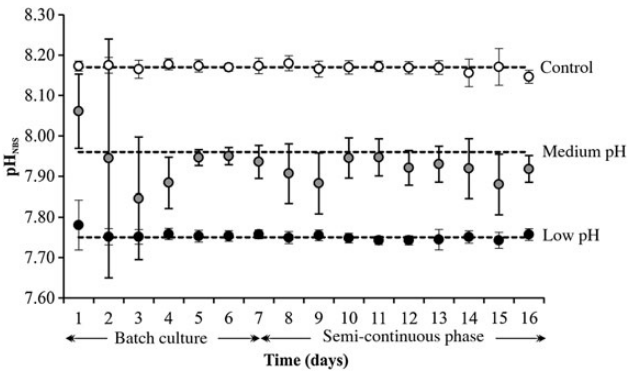

Figure 1. Daily average pH in the three *Heterocapsa* sp. cultures during the experimental period. The error bars indicate the *SD* in each 24 h period (n = 48 pH readings).

Table 1. Parameters of the seawater carbonate system in each pH treatment of the *Heterocapsa* sp. cultures on the 13th day of the experiment, the only day in which alkalinity was measured (averaged values with *SD* in parenthesis).

pH treatment	pH_{NBS}	pH_T	TA	pCO_2	χCO_2	DIC	HCO_3^-	CO_3^{2-}	Ω_A
Control	8.17 (0.02)	8.05 (0.02)	2454 (0.73)	414 (0.60)	423 (0.13)	2174 (0.67)	1962 (0.60)	199 (0.06)	3.025 (0.001)
Medium	7.93 (0.04)	7.81 (0.04)	2487 (0.80)	798 (0.26)	814 (0.27)	2328 (0.77)	2175 (0.72)	127 (0.04)	1.930 (0.001)
Low	7.74 (0.03)	7.62 (0.03)	2492 (0.19)	1296 (0.10)	1323 (0.11)	2410 (0.19)	2281 (0.18)	86 (0.01)	1.307 (0.000)

Total alkalinity (TA, μmol kg^{-1}-SW; $n = 3$), pH_{NBS} ($n = 48$), salinity (37.4), and temperature (18.5°C) were used to calculate the rest of the parameters using the CO_2SYS program (Pierrot *et al.*, 2006): pCO_2, partial pressure of CO_2 (μatm, $n = 3$); χCO_2, mole fraction of CO_2 in dry air (ppm, $n = 3$); DIC, dissolved inorganic carbon (μmol kg^{-1}-SW; $n = 3$); HCO_3^-, bicarbonate ion concentration (μmol kg^{-1}-SW; $n = 3$); CO_3^{2-}, carbonate ion concentration (μmol kg^{-1}-SW; $n = 3$), Ω_A, saturation state of seawater with respect to aragonite ($n = 3$). pH_T, pH in the total scale ($n = 48$) is also reported for better comparison with other studies, and it was calculated using the $SWCO_2$ package (Hunter, 2007).

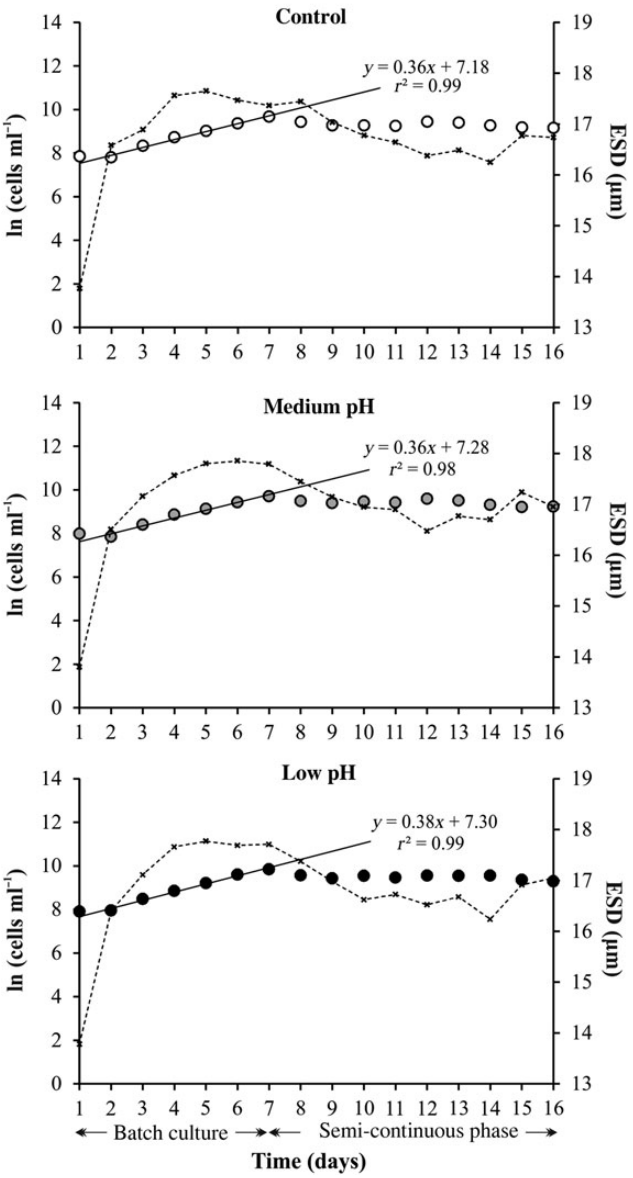

Figure 2. Cell concentration (circles) and ESD (crosses and dotted lines) of *Heterocapsa* sp. cultures grown at the three selected pCO_2/pH conditions. The slope of regression line corresponds to the growth rate for each treatment.

alkalinity reached 798 and 1296 μatm in the medium and low pH treatments, respectively, fitting well possible values projected for the end of the century (IPCC, 2013).

Algal growth, and elemental and FA composition

The growth rates (d^{-1}) of *Heterocapsa* sp. were similar among the pH treatments (control: 0.36, medium pH: 0.36, and low pH: 0.38; Figure 2), with no signs of cell damaging due to the CO_2/air bubbling. Given a ca. 2-d generation time, the total experimental period of 16 d corresponded to eight cell generations, which should be sufficient to condition the organisms to the experimental conditions. Throughout the algal growth period, the cell size varied similarly among the pH treatments (Figure 2). During the copepod incubation, which corresponded to the last 4 d of algal culture, the average equivalent spherical diameter (ESD, μm) of the cells was similar (control: 16.6 ± 0.24, medium pH: 16.9 ± 0.24, and low pH: 16.7 ± 0.36).

The elemental characteristics of the cells grown at the different pH treatments are summarized in Table 2. Cells cultured in the medium pH conditions had slightly higher biovolume (9%) and elemental content (carbon: 8%, nitrogen: 10%, and phosphorus: 3%) compared with the control treatment, whereas the molar elemental ratios (C : N, C : P, and N : P) did not differ significantly. Cells grown at the low pH conditions presented similar elemental composition characteristics to those of the control treatment. The comparison between the cells grown in medium and low pH conditions revealed that the former had slightly higher biovolume, nitrogen content, and lower C : N than the latter (Table 2). Regarding the FA composition of *Heterocapsa* sp., the saturated 16 : 0 and polyunsaturated FAs (PUFAs) were the main contributors, accounting for 18 and 63% of total FAs, respectively. Among PUFAs, the 18:4(n-3) (12% of total FA, 7–8 pg $cell^{-1}$), 18:5(n-3) (18–19% of total FA, 11–12 pg $cell^{-1}$), as well as 22:6(n-3) (20% of total FA, 12–13 pg $cell^{-1}$) isomers comprised together ca. 61–62% of the total FA (Table 3). The overall variation in FA composition between treatments was very small. Low but significant differences occurred in the relative amount as well as content of monounsaturated FAs (MUFAs) in the low pH treatment, caused by lower 16:1(n-7) and 18:1(n-9) isomer levels. The total FA content as well as the 18:3(n-3) and 22:6(n-3) isomer contents were significantly higher in the medium pH treatment, but the differences were, however, of low magnitude (~10% of the respective value).

Copepod feeding, reproduction, and egg hatching success

The average food concentration was ca. 500 cells ml^{-1} in all treatments ($F = 0.95$, $p > 0.05$; control: 512 ± 22, medium pH: 531 ± 18, and low pH: 532 ± 29). Neither feeding rates nor egg production rates of the copepod *A. grani* presented any significant differences among the three pH treatments (clearance rates 28–30 ml cop^{-1} d^{-1}: $F = 0.29$, $p = 0.76$; ingestion rates 15 895–15 812 cells cop^{-1} d^{-1}: $F = 0.31$, $p > 0.05$; egg production rates 49–54 eggs cop^{-1} d^{-1}: $F = 1.81$, $p > 0.05$; Figure 3). Although ingestion rates in terms of elemental

Table 2. Cell biovolume, elemental composition (C: carbon, N: nitrogen, and P: phosphorus), and molar elemental ratios of the distinct *Heterocapsa* sp. cultures grown at the three selected pH levels (control: 8.17, medium: 7.96, and low: 7.75).

					t-test		
	Control	**Medium**	**Low**	***F***	**Control vs. medium**	**Control vs. low**	**Medium vs. low**
Biovolume (μm^3)	2468.3^{a} (65.6)	2678.5^{b} (2.4)	2528.7^{a} (39.9)	19.2^{***}			
pg C $cell^{-1}$	581.7^{a} (24.7)	626.6^{b} (13.8)	$592.7^{a,b}$ (8.4)	5.6^{*}			
pg N $cell^{-1}$	82.1^{a} (2.5)	90.1^{b} (0.8)	80.2^{a} (1.3)	29.0^{**}			
pg P $cell^{-1}$	17.8^{a} (1.0)	18.4^{b} (0.9)	$16.2^{a,b}$ (0.7)	5.3^{ns}			
C : N (molar)	8.3 (0.2)	8.1 (0.1)	8.6 (0.1)		$0.99^{n.s.}$	$-2.24^{n.s.}$	-5.73^{**}
C : P (molar)	84.3 (5.0)	87.8 (4.6)	94.4 (4.0)		$-0.89^{n.s.}$	$-2.73^{n.s.}$	$-1.88^{n.s.}$
N : P (molar)	10.2 (0.6)	10.8 (0.6)	11.0 (0.5)		$-1.36^{n.s.}$	$-1.76^{n.s.}$	$-0.31^{n.s.}$

Differences among treatments were assessed with one-way ANOVA and Tukey *post hoc* tests (*F*: ANOVA statistics, $^{*}p < 0.05$, $^{**}p < 0.01$, $^{***}p < 0.001$, n.s.: not significant) as well as Student's *t*-test. Numbers in parentheses correspond to the *SD* and superscripts indicate the homogenous groups according to the Tukey *post hoc* test.

Table 3. FA content (pg $cell^{-1}$) and relative FA composition (% of total FA) for *Heterocapsa* sp. cultures grown at the three selected pH levels (control: 8.17, medium: 7.96, and low: 7.75).

pg $cell^{-1}$	**Control**	**Medium pH**	**Low pH**	***F***
14:0	2.5 (0.4)	3.1 (0.4)	3.1 (0.9)	$1.3^{n.s.}$
16:0	10.6 (0.8)	11.9 (0.5)	10.8 (0.9)	$3.7^{n.s.}$
18:0	1.3 (0.1)	1.4 (0.2)	1.2 (0.1)	$2.6^{n.s.}$
16:1(n-7)	$0.9^{a,b}$ (0.1)	1.1^{b} (0.3)	0.6^{a} (0.1)	8.4^{**}
16:1(n-9)	0.8 (0.1)	0.8 (0.0)	0.7 (0.1)	$1.4^{n.s.}$
18:1(n-7)	1.3^{a} (0.0)	1.4^{a} (0.1)	1.0^{b} (0.0)	146.6^{***}
18:1(n-9)	1.9^{a} (0.1)	2.0^{a} (0.1)	1.6^{b} (0.1)	35.8^{***}
18:2(n-6)	$4.0^{a,b}$ (0.2)	4.3^{b} (0.3)	3.8^{a} (0.1)	8.2^{**}
18:3(n-3)	2.2^{a} (0.1)	2.5^{b} (0.1)	2.1^{a} (0.1)	20.3^{***}
18:4(n-3)	7.2^{a} (0.3)	8.0^{b} (0.5)	7.2^{a} (0.4)	6.1^{*}
18:5(n-3)	11.1 (0.5)	12.3 (0.7)	11.1 (0.6)	$4.9^{n.s.}$
22:6(n-3)	11.6^{a} (0.3)	13.2^{b} (0.5)	11.9^{a} (0.6)	77.7^{**}
tFA	58.2^{a} (2.9)	64.9^{b} (2.6)	57.6^{a} (3.3)	7.6^{*}
MUFAs	4.9^{a} (0.3)	5.3^{a} (0.2)	3.9^{b} (0.2)	44.3^{***}
PUFAs	36.8^{a} (1.3)	41.0^{b} (2.1)	36.7^{a} (1.8)	7.9^{*}
% of total FA				
14:0	4.3 (0.5)	4.7 (0.5)	5.3 (1.2)	$1.8^{n.s.}$
16:0	18.2 (0.6)	18.4 (0.2)	18.8 (0.6)	$1.6^{n.s.}$
18:0	2.2 (0.1)	2.2 (0.2)	2.1 (0.2)	$0.1^{n.s.}$
16:1(n-7)	$1.5^{a,b}$ (0.1)	1.7^{a} (0.5)	1.1^{b} (0.1)	7.2^{*}
16:1(n-9)	1.3 (0.1)	1.2 (0.1)	1.2 (0.1)	$1.4^{n.s.}$
18:1(n-7)	2.3^{a} (0.1)	2.1^{b} (0.0)	1.7c (0.1)	79.1^{***}
18:1(n-9)	3.3^{a} (0.1)	3.1^{a} (0.1)	2.8^{b} (0.2)	13.3^{**}
18:2(n-6)	7.0^{a} (0.1)	6.6^{b} (0.2)	6.5^{b} (0.2)	7.9^{*}
18:3(n-3)	$3.7^{a,b}$ (0.1)	3.8^{a} (0.1)	3.6^{b} (0.1)	6.6^{*}
18:4(n-3)	12.4 (0.3)	12.3 (0.3)	12.4 (0.2)	$0.2^{n.s.}$
18:5(n-3)	19.1 (0.6)	18.9 (0.5)	19.3 (0.5)	$0.7^{n.s.}$
22:6(n-3)	19.9 (0.6)	20.3 (0.2)	20.6 (0.9)	$1.2^{n.s.}$
MUFAs	9.1^{a} (0.4)	8.7^{a} (0.7)	7.2^{b} (0.3)	17.2^{***}
PUFAs	63.3 (1.1)	63.1 (1.2)	63.6 (1.7)	$0.2^{n.s.}$

FA >1% of total FA (tFA) as well as values for tFA, total MUFAs, and total PUFAs are presented. Differences among treatments were assessed with one-way ANOVA and Tukey *post hoc* tests (*F*: ANOVA statistics, $^{*}p < 0.05$, $^{**}p < 0.01$, $^{***}p < 0.001$, n.s.: not significant). Numbers in parentheses correspond to the *SD* and superscripts indicate the homogenous groups according to the Tukey *post hoc* test.

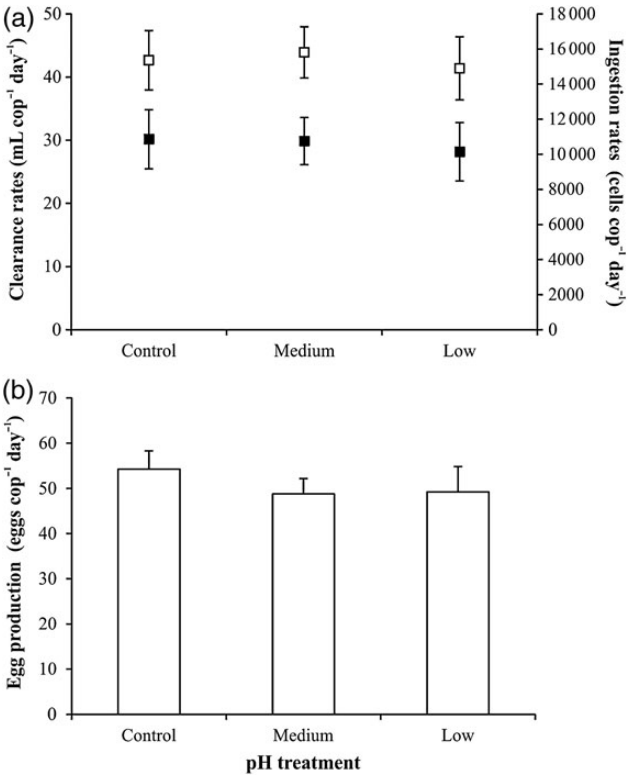

Figure 3. (a) Copepod feeding rates (clearance: black squares, ingestion: white squares) and egg production rates (b) in the different CO_2/pH treatments. Error bars indicate the *SD*.

units (C, N, and P) were slightly higher for the medium pH treatment (6–13%), those differences were not statistically significant neither in terms of carbon ($F = 1.48$, $p > 0.05$) and nitrogen ($F = 2.83$, $p > 0.05$) nor in terms of phosphorus ($F = 1.29$, $p > 0.05$; Figure 4). GGEs for each element were generally lower in the medium treatment (Figure 4). Those differences were more profound for GGE_N ($F = 5.72$, $p < 0.05$; 17–21% reduction compared with control and low pH treatments), whereas they were of marginal statistical significance for GGE_C and GGE_P ($F = 4.56$, $p = 0.043$ and $F = 4.44$, $p = 0.045$, respectively). Egg hatching increased with time in all treatments approaching ca. 95% of hatching success after 72 h. No significant differences among pH treatments were found in the cumulative hatching success percentage at the end of the incubation time ($F = 1.30$, $p > 0.05$).

Discussion

Until recently, the study of the impact of OA on planktonic copepods has mainly focused on assessing potential direct effects,

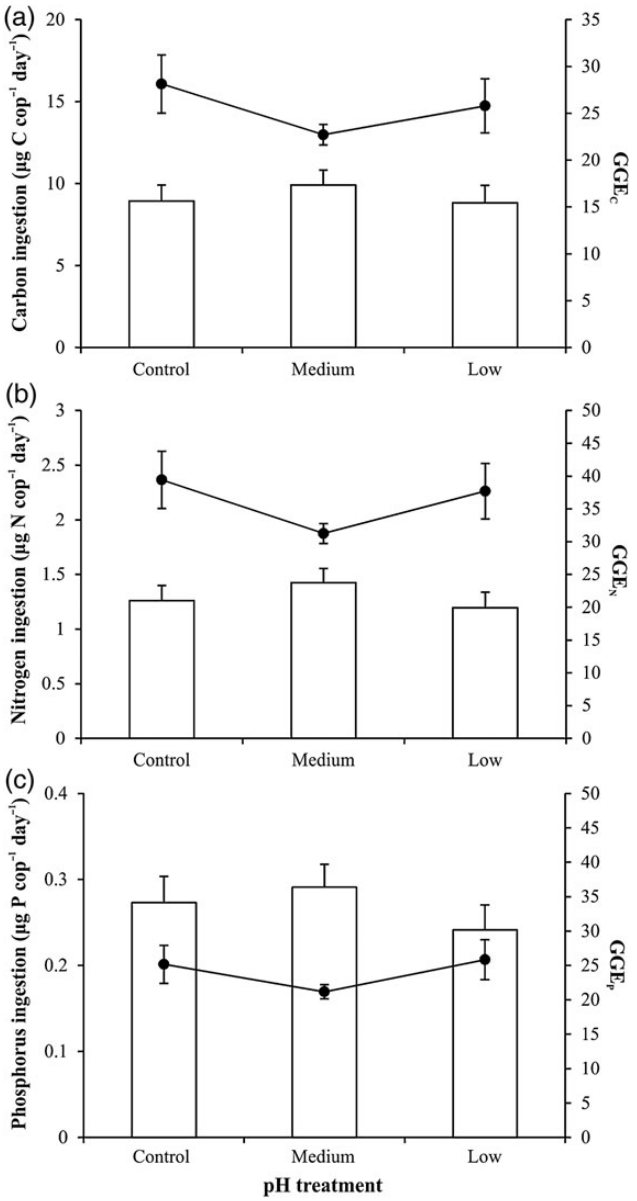

Figure 4. Ingestion rates (white bars) in the different CO_2/pH treatments in terms of (a) carbon, (b) nitrogen, and (c) phosphorus. Corresponding GGE for its element are given in black circles. Error bars indicate the *SD*.

often revealing the high tolerance of this group of organisms even under pCO_2 levels falling beyond near-future projections (e.g. Kurihara and Ishimatsu, 2008; Hildebrandt *et al.*, 2014). Interestingly, Rossoll *et al.* (2012) and Schoo *et al.* (2013) pointed out the possibility of "bottom-up" indirect effects on copepods at realistic acidification scenarios projected by the end of the century. On the one hand, Rossoll *et al.* (2012) observed a significant reduction in egg production and somatic growth of *Acartia tonsa* associated with a decrease in both the total FA concentration and the relative amount of PUFAs of the diatom *Thalassiosira pseudonana* grown under acidified conditions. On the other hand, and also for *A. tonsa*, Schoo *et al.* (2013) reported delayed development and a stage-dependent impact on respiration and excretion rates of the copepod associated with a decrease in the nutritional quality (expressed as higher C : N and C : P ratios) of its prey, the flagellate *R. salina*, grown under increased pCO_2 levels.

Although the algae used for the copepod experiments in our study were cultured at pCO_2 levels comparable or even higher to those of the two above-mentioned studies, we did not find any clear evidence of a change in the cell nutritional characteristics among experimental treatments (at least in terms of elemental and FA composition; other biochemical compounds, e.g. proteins and vitamins, have not been measured). In instances in which we detected statistically significant differences, the extent of such dissimilarity was very small, and most likely it would not affect substantially the nutritional quality of the copepod diet. In fact, drastic changes in the elemental ratios or FA content of prey seem to be required to detect considerable impacts in the reproductive output (Rossoll *et al.*, 2012; Isari *et al.*, 2013) and development (Rossoll *et al.*, 2012; Schoo *et al.*, 2013) of copepods.

Indeed, the slight and mostly insignificant variation in the elemental and biochemical properties of the prey offered in our experiments did not seem to have any statistically significant impact in the copepod feeding and egg production rates and hatching success. Nevertheless, the estimated GGEs for the distinct elements were generally lower (12–21%) in the medium pH treatment. However, those differences were most likely associated with the divergences in *Heterocapsa* sp. size among pH treatments and not with nutritionally mediated effects *per se*. During the copepod experiments, the biovolume of the cells grown at medium pH increased 10% compared with the others; given the similarity in copepod daily food consumptions on a cell basis (cells cop^{-1} d^{-1}) among treatments, this biovolume variation resulted in a higher elemental intake for the medium pH treatment (µg element cop^{-1} d^{-1}), which was not accompanied by an increase in the egg production output. The reason for such biovolume difference remains uncertain, but could be associated with the relatively higher pH variation observed in the medium pH culture. It has been documented that distinct environmental stressors may have an impact in the cell wall structure of algae and further impair their digestibility by predators (Van Donk and Hessen, 1995; Van Donk *et al.*, 1997). Cell material and related structures in algae have been also argued to constrain digestion and assimilation efficiency of copepods, decreasing their reproductive success (Dutz *et al.*, 2008). Therefore, it could be hypothesized that a larger variability in the pH growth conditions may induce changes in the morphological cell wall properties and affect digestibility and assimilation by copepods. And in fact, larger variability in pH is expected, in the future, not only in seawater from its decrease in buffering capacity but also at the exterior surface of marine organisms (Flynn *et al.*, 2012).

Since the exact elemental content of the eggs was not measured, a slightly higher C, N, and P content of the eggs produced in the medium pH treatment due to the higher copepod dietary elemental intake could be also possible. Although this may compensate for the calculated lower GGE in that treatment, the similarity observed in the egg hatching success among treatments can be most likely interpreted as indicating the lack of any quality difference (e.g. elemental difference) in the eggs laid.

Based on previous knowledge of the lack of direct OA effect on congeneric species even during multigenerational experiments (Kurihara and Ishimatsu, 2008), *a priori* our study assumed that no direct effect on the vital rates of *A. grani* would be imposed under our experimental pCO_2/pH levels. Some recent studies by Cripps *et al.* (2014a, b), however, have reported a reduction in the

reproductive output of *A. tonsa* at acidification levels and duration of exposure comparable to ours. Given the similarity in nutritional quality among the prey offered to *A. grani* in our experiments, the results we obtained (lack of any effects) can nevertheless be interpreted as further experimental evidence about the lack of direct impact of OA on our target copepod species, thus supporting our initial assumption. However, the observed absence of OA bottom-up effects on copepod performance under the dinoflagellate diet offered here did not lend support to our initial hypothesis.

Changes in seawater pCO_2 concentration may greatly impact several algal physiological processes and biochemical synthetic pathways; however, the final impact seems to be highly dependent on the algal group and may also vary even on a species basis (Riebesell, 2004). Dinoflagellate physiology is considered particularly sensitive, due to the low CO_2 affinity of their form II-RuBisCO and, therefore, the high dependence on the enzymatic machinery involved in maximizing CO_2 acquisition [the CCMs and also the carbonic anhydrases (CAs), which catalyse the interconversion of HCO_3^- and CO_2]. It could thus be argued that an increased CO_2 supply would lead to a beneficial downregulation in the expression of CCMs/CAs-related genes and might be positively reflected in the cellular physiology and biochemical composition of the dinoflagellate group (Giordano *et al.*, 2005), therefore ending up in positive bottom-up impact under OA conditions. Our findings, however, did not confirm this expectation since growth and cellular characteristics of *Heterocapsa* sp. under the pCO_2/pH scenarios tested were similar, although other dinoflagellate studies have indeed showed that elevated pCO_2 availability may result in a decreased activity of the CCM and CA activities (Ratti *et al.*, 2007; Van de Waal *et al.*, 2013; Van de Waal *et al.*, 2014) and an increase in the growth rates (Ratti *et al.*, 2007). Unfortunately, our planned experiment did not include the determination of CCM and CA activities of *Heterocapsa* sp., something that may have shed some light onto the physiological mechanisms behind the pattern found. It is noticeable, however, that a recent study by Van de Waal *et al.* (2014), carried out under elevated pCO_2 scenarios comparable to ours, indeed reported a downscaling of CCMs in the dinoflagellate *Alexandrium tamarense*, but such physiological change actually did not translate into changes in the algal growth and elemental composition, in line with the lack of effects found in our study. It seems likely that shifts in the gene expression and suppression of the enzymatic systems may be often associated with only subtle elemental and energy gain, insufficient to be reflected to growth, elemental, and biochemical composition.

An additional point to be considered regarding the effects of OA on algal physiology is that the sensitivity to changes in CO_2 supply may be also dependent in the ability for active uptake of bicarbonate (HCO_3^-) for a particular algal species. In this sense, Rost *et al.* (2006) reported a lesser dependence on CO_2 uptake for algae which were able to directly uptake bicarbonate. In that particular case, elemental ratios of algal cells might be less sensitive to changes in CO_2 supply, whereas a higher sensitivity would be expected for groups that predominantly use CO_2 (Burkhardt *et al.*, 1999; Fu *et al.*, 2008). Species-specific variability in CCM capabilities have been recorded in the genus *Heterocapsa*, with *H. oceanica* depicting a high dependence on free CO_2 and limited capacity for direct bicarbonate uptake (Dason *et al.*, 2004), whereas *H. triquetra* relies not only on diffusive CO_2 supply, but may also acquire HCO_3^- (Rost *et al.*, 2006). Therefore, it is uncertain if the lack of relevant effects of OA on *Heterocapsa* sp. in our experiments are the result of either the capability of this species to directly uptake bicarbonate (i.e. less dependence on CO_2 uptake) or that the pH levels in our experiments, within realistic predictions, were not sufficiently low to provide energy and elemental benefits that could influence other physiological processes.

The underlying algal physiological mechanisms and metabolic pathways that lead to the deterioration of the prey nutritional quality in the previous copepod studies (Rossoll *et al.*, 2012; Schoo *et al.*, 2013) seem unclear. The diatom cultured by Rossoll *et al.* (2012), *T. pseudonana*, showed a distinct FA profile when grown under elevated pCO_2 but, unfortunately, no further information was provided about the culture conditions (growth rates and cell size) and the elemental ratios under the different treatments. Remarkably, Crawfurd *et al.* (2011) found that the same diatom species, when subjected to a 3-month continuous culture at increased CO_2, showed a suppression of the genes involved with the CO_2 acquisition and had cellular C : N ratios closer to the Redfield ratio (i.e. better nutritional quality), which would be contradictory with the hypothesis of negative bottom-up effects. On the other hand, Schoo *et al.* (2013) reported that the cryptophyte *R. salina* maintained under elevated pCO_2 either in continuous chemostat or batch cultures had lower nutritional quality (higher molar ratios) that negatively affected copepod development. These authors, however, based on previous findings by Malzahn *et al.* (2007), made the assumption that algal cells with higher molar elemental ratios (high pCO_2 grown—*Rhodomonas*) would be a prey of better quality from a biochemical perspective (i.e. increased FA concentration and relative contribution of unsaturated FAs). Thus, one may wonder what would be the actual impact of a high pCO_2-*Rhodomonas* diet on other biological processes of copepods, i.e. reproductive success, and whether the stoichiometric characteristics or the FA properties of the prey would be the main nutritional drivers. It also remains unclear how the combined bottom-up effect on distinct copepod vital rates (e.g. development and reproduction) would ultimately influence copepod populations in nature.

The present study clearly points towards a lack of bottom-up effects mediated by OA in our particular predator–prey pair under realistic future scenarios, questioning the generalization of the results reported in previous copepod studies on this topic (Rossoll *et al.*, 2012; Schoo *et al.*, 2013). The physiological response of algae under OA conditions (combined with other climate change and human-related pressures, e.g. changes in inorganic nutrient supply) will not be uniform among taxa (Flynn *et al.*, 2015). Changes in phytoplankton competitive interactions and species succession are also anticipated (Flynn *et al.*, 2015), and it is thus evident that any potential indirect bottom-up effect on copepods in nature will be highly dependent on their prey-specific characteristics. To extrapolate laboratory results to nature and evaluate the OA foodweb implications, future research should integrate algal physiological approaches, describing the modes of carbon acquisition mechanisms of key algal species to better delimit their physiology, biochemistry, and their interactions.

Acknowledgements

The authors thank Kaiene Griffell and Àngel López-Sanz for assistance in the experimental work, Afrodite Adroni for the C–N analysis, Joachim Lütke for the support with the lipid analyses, and Xavier Leal for his technical help. Special thanks go to Jörg Dutz for his guidance on the experimental set-up and discussion on the topic as well as on three anonymous reviewers who helped in the improvement of the manuscript with their constructive

comments. The participation of ES and CP was helped from funding by the Spanish Ministry of Economy and Competitivity through projects CTM2011-23480 and CTM2012-32017, respectively. This work was supported by the project CROA (LS8-1893), implemented within the framework of the Action "Supporting Postdoctoral Researchers" of the Operational Program "Education and Lifelong Learning" (Action's Beneficiary: General Secretariat for Research and Technology), and is co-financed by the European Social Fund (ESF) and the Greek State.

References

Burkhardt, S., and Riebesell, U. 1997. CO_2 availability affects elemental composition (C:N:P) of the marine diatom *Skeletonema costatum*. Marine Ecology Progress Series, 155: 67–76.

Burkhardt, S., Zondervan, I., and Riebesell, U. 1999. Effect of CO_2 concentration on C:N:P ratio in marine phytoplankton: A species comparison. Limnology and Oceanography, 44: 683–690.

Crawfurd, K. J., Raven, J. A., Wheeler, G. L., Baxter, E. J., and Joint, I. 2011. The response of *Thalassiosira pseudonana* to long-term exposure to increased CO_2 and decreased pH. PLoS ONE, 6: e26695.

Cripps, G., Lindeque, P., and Flynn, K. 2014a. Have we been underestimating the effects of ocean acidification in zooplankton? Global Change Biology, 20: 3377–3385.

Cripps, G., Lindeque, P., and Flynn, K. 2014b. Parental exposure to elevated pCO_2 influences the reproductive success of copepods. Journal of Plankton Research, 36: 1165–1174.

Dason, J. S., Huertas, I. E., and Colman, B. 2004. Source of inorganic carbon for photosynthesis in two marine dinoflagellates. Journal of Phycology, 40: 285–292.

Dickson, A. G. 1990. Standard potential of the reaction: $AgCl(s) + 1/2\ H_2(g) = Ag(s) + HCl(aq)$, and the standard acidity constant of the ion HSO_4^- in synthetic seawater from 273.15 to 318.15 K. Journal of Chemical Thermodynamics, 22: 113–127.

Dickson, A. G., and Millero, F. J. 1987. A comparison of the equilibrium constants for the dissociation of carbonic acid in seawater media. Deep-Sea Research Part I-Oceanographic Research Papers, 34: 1733–1743.

Doney, S. C., Fabry, V. J., Feely, R. A., and Kleypas, J. A. 2009. Ocean acidification: The other CO_2 problem. Annual Review of Marine Science, 1: 169–192.

Dupont, S., Ortega-Martínez, O., and Thorndyke, M. 2010. Impact of near-future ocean acidification on echinoderms. Ecotoxicology, 19: 449–462.

Dutz, J., Koski, M., and Jónasdóttir, S. H. 2008. Copepod reproduction is unaffected by diatom aldehydes or lipid composition. Limnology and Oceanography, 53: 225–235.

Fabry, V. J., Seibel, B. A., Feely, R. A., and Orr, J. C. 2008. Impacts of ocean acidification on marine fauna and ecosystem processes. ICES Journal of Marine Science, 65: 414–432.

Flynn, K. J., Blackford, J. C., Baird, M. E., Raven, J. A., Clark, D. R., Beardall, J., Brownlee, C., *et al.* 2012. Changes in pH at the exterior surface of plankton with ocean acidification. Nature Climate Change, 2: 510–513.

Flynn, K. J., Clark, D. R., Mitra, A., Fabian, H., Hansen, P. J., Glibert, P. M., Wheeler, G. L., *et al.* 2015. Ocean acidification with (de)eutrophication will alter future phytoplankton growth and succession. Proceedings of the Royal Society B, 282: 20142604.

Folch, J., Lees, M., and Sloane-Stanley, G. H. 1957. A simple method for isolation and purification of total lipids from animal tissues. Journal of Biological Chemistry, 226: 497–509.

Frost, B. W. 1972. Effects of size and concentration of food particles on the feeding behavior of the marine planktonic copepod *Calanus pacificus*. Limnology and Oceanography, 17: 805–815.

Fu, F. X., Zhang, Y., Warner, M. E., Feng, Y., Sun, J., and Hutchins, D. A. 2008. A comparison of future increased CO_2 and temperature effects on sympatric *Heterosigma akashiwo* and *Prorocentrum minimum*. Harmful Algae, 7: 76–90.

Giordano, M., Beardall, J., and Raven, J. A. 2005. CO2 concentrating mechanisms in algae: Mechanisms, environmental modulation, and evolution. Annual Review of Plant Biology, 56: 99–131.

Grasshoff, K., Kremling, K., and Ehrhardt, M. 1999. Methods of seawater analysis. Wiley-VCH, Weinheim, New York, Chiester, Brisbane, Singopore, Toronto.

Guillard, R. 1975. Culture of phytoplankton for feeding marine invertebrates. *In* Culture of Phytoplankton for Feeding Marine Invertebrates, pp. 26–60. Ed. by W. L. Smith, and M. H. Chanley. Plenum Press, New York, USA.

Hildebrandt, N., Niehoff, B., and Sartoris, F. J. 2014. Long-term effects of elevated CO_2 and temperature on the Arctic calanoid copepods *Calanus glacialis* and *Calanus hyperboreus*. Marine Pollution Bulletin, 80: 59–70.

Hofmann, G. E., Barry, J. P., Edmunds, P. J., Gates, R. D., Hutchins, D. A., Klinger, T., and Sewell, M. A. 2010. The effect of ocean acidification on calcifying organisms in marine ecosystems: An organism-to-ecosystem perspective. Annual Review of Ecology, Evolution, and Systematics, 41: 127–147.

Hopkinson, B. M., Dupont, C. L., Allen, A. E., and Morela, F. M. M. 2011. Efficiency of the CO_2-concentrating mechanism of diatoms. Proceedings of the National Academy of Sciences of the United States of America, 108: 3830–3837.

Hunter, K. A. 2007. $XLCO_2$–Seawater CO_2 Equilibrium Calculations Using Excel Version 2. University of Otago, New Zealand. http://neon.otago.ac.nz/research/mfc/people/keith_hunter/software/swco2/.

IPCC 2013. Summary for policymakers. *In* Climate Change 2013: The Physical Science Basis. Contribution of Working Group I to the Fifth Assessment Report of the Intergovernmental Panel on Climate Change, pp. 3–29. Ed. by T. F. Stocker, D. Qin, G. K. Plattner, M. Tignor, S. K. Allen, J. Boschung, A. Nauels, Y. Xia, V. Bex, and P. M. Midgley. Cambridge University Press, Cambridge, United Kingdom; New York, NY, USA.

Isari, S., Antó, M., and Saiz, E. 2013. Copepod foraging on the basis of food nutritional quality: Can copepods really choose? PLoS ONE, 8: e84742.

Jónasdóttir, S. 1994. Effects of food quality on the reproductive success of *Acartia tonsa* and *Acartia hudsonica*: laboratory observations. Marine Biology, 121: 67–81.

Jones, R. H., Flynn, K. J., and Anderson, T. R. 2002. Effect of food quality on carbon and nitrogen growth efficiency in the copepod *Acartia tonsa*. Marine Ecology Progress Series, 235: 147–156.

Kattner, G., and Fricke, H. S. G. 1986. Simple gas-liquid chromatography method for simultaneous determination of fatty acids and alcohols in wax esters of marine organisms. Journal of Chromatography A, 361: 263–268.

Kiørboe, T., Mshlenberg, F., and Hamburgefl, K. 1985. Bioenergetics of the planktonic copepods *Acartia tonsa*: relation between feeding, egg production and respiration, and composition of specific dynamic action. Marine Ecology Progress Series, 26: 85–97.

Klein Breteler, W. C. M., Schogt, N., and Rampen, S. 2005. Effect of diatom nutrient limitation on copepod development: Role of essential lipids. Marine Ecology Progress Series, 291: 125–133.

Koch, M., Bowes, G., Ross, C., and Zhang, X. H. 2013. Climate change and ocean acidification effects on seagrasses and marine macroalgae. Global Change Biology, 19: 103–132.

Koski, M., Breteler, W. K., and Schogt, N. 1998. Effect of food quality on rate of growth and development of the pelagic copepod *Pseudocalanus elongatus* (Copepoda, Calanoida). Marine Ecology Progress Series, 170: 169–187.

Kurihara, H., and Ishimatsu, A. 2008. Effects of high CO_2 seawater on the copepod (*Acartia tsuensis*) through all life stages and subsequent generations. Marine Pollution Bulletin, 56: 1086–1090.

Kurihara, H., Shimode, S., and Shirayama, Y. 2004. Effects of raised CO_2 concentration on the egg production rate and early development of two marine copepods (*Acartia steueri* and *Acartia erythraea*). Marine Pollution Bulletin, 49: 721–727.

Lee, K., Kim, T. W., Byrne, R. H., Millero, F. J., Feely, R. A., and Liu, Y. M. 2010. The universal ratio of boron to chlorinity for the North Pacific and North Atlantic oceans. Geochimica et Cosmochimica Acta, 74: 1801–1811.

Lewis, C. N., Brown, K. A., Edwards, L. A., Cooper, G., and Findlay, H. S. 2013. Sensitivity to ocean acidification parallels natural pCO_2 gradients experienced by Arctic copepods under winter sea ice. Proceedings of the National Academy of Sciences of the United States of America, 110: E4960–E4967.

Malzahn, A. M., Aberle, N., Clemmesen, C., and Boersma, M. 2007. Nutrient limitation of primary producers affects planktivorous fish condition. Limnology and Oceanography, 52: 2062–2071.

Mayor, D. J., Everett, N. R., and Cook, K. B. 2012. End of century ocean warming and acidification effects on reproductive success in a temperate marine copepod. Journal of Plankton Research, 34: 258–262.

Mayor, D. J., Matthews, C., Cook, K., Zuur, A. F., and Hay, S. 2007. CO_2-induced acidification affects hatching success in *Calanus finmarchicus*. Marine Ecology Progress Series, 350: 91–97.

McConville, K., Halsband, C., Fileman, E. S., Somerfield, P. J., Findlay, H. S., and Spicer, J. I. 2013. Effects of elevated CO_2 on the reproduction of two calanoid copepods. Marine Pollution Bulletin, 73: 428–434.

Mehrbach, C., Culberson, C. H., Hawley, J. E., and Pytkowicz, R. M. 1973. Measurement of the apparent dissociation constants of carbonic acid in seawater at atmospheric pressure. Limnology and Oceanography, 18: 897–907.

Perez, F. F., and Fraga, F. 1987. A precise and analytical procedure for alkalinity determination. Marine Chemistry, 21: 169–182.

Perez, F. F., Rios, A. F., Rellan, T., and Alvarez, M. 2000. Improvements in a fast potentiometric seawater alkalinity determination. Ciencias Marinas, 26: 463–478.

Peters, J., Dutz, J., and Hagen, W. 2013. Trophodynamics and life-cycle strategies of the copepods *Temora longicornis* and *Acartia longiremis* in the Central Baltic Sea. Journal of Plankton Research, 35: 595–609.

Pierrot, D., Lewis, E., and Wallace, D. W. R. 2006. MS Excel Program Developed for CO_2 System Calculations. ORNL/CDIAC-105, Carbon Dioxide Information Analysis Center, Oak Ridge National Laboratory, US Department of Energy, Oak Ridge, TN.

Ratti, S., Giordano, M., and Morse, D. 2007. CO_2-concentrating mechanisms of the potentially toxic dinoflagellate *Protoceratium reticulatum* (Dinophyceae, Gonyaulacales). Journal of Phycology, 43: 693–701.

Reinfelder, J. R. 2011. Carbon concentrating mechanisms in eukaryotic marine phytoplankton. Annual Review of Marine Science, 3: 291–315.

Riebesell, U. 2004. Effects of CO_2 enrichment on marine phytoplankton. Journal of Oceanography, 60: 719–729.

Riebesell, U., Zondervan, I., Rost, B., Tortell, P. D., Zeebe, R. E., and Morel, F. M. M. 2000. Reduced calcification of marine plankton in response to increased atmospheric CO_2. Nature, 407: 364–366.

Rossoll, D., Bermúdez, R., Hauss, H., Schulz, K. G., Riebesell, U., Sommer, U., and Winder, M. 2012. Ocean acidification-induced food quality deterioration constrains trophic transfer. PLoS ONE, 7: e34737.

Rost, B., Riebesell, U., and Sültemeyer, D. 2006. Carbon acquisition of marine phytoplankton: Effect of photoperiod length. Limnology and Oceanography, 51: 12–20.

Saiz, E., and Calbet, A. 2011. Copepod feeding in the ocean: Scaling patterns, composition of their diet and the bias of estimates due to microzooplankton grazing during incubations. Hydrobiologia, 666: 181–196.

Schoo, K. L., Malzahn, A. M., Krause, E., and Boersma, M. 2013. Increased carbon dioxide availability alters phytoplankton stoichiometry and affects carbon cycling and growth of a marine planktonic herbivore. Marine Biology, 160: 2145–2155.

Thor, P., and Dupont, S. 2015. Transgenerational effects alleviate severe fecundity loss during ocean acidification in a ubiquitous planktonic copepod. Global Change Biology, in press; doi:10.1111/gcb.12815.

Urabe, J., Togari, J., and Elser, J. J. 2003. Stoichiometric impacts of increased carbon dioxide on a planktonic herbivore. Global Change Biology, 9: 818–825.

Van de Waal, D. B., Eberlein, T., John, U., Wohlrab, S., and Rost, B. 2014. Impact of elevated pCO_2 on paralytic shellfish poisoning toxin content and composition in *Alexandrium tamarense*. Toxicon, 78: 58–67.

Van de Waal, D. B., John, U., Ziveri, P., Reichart, G. J., Hoins, M., Sluijs, A., and Rost, B. 2013. Ocean acidification reduces growth and calcification in a marine dinoflagellate. PLoS ONE, 8: e65987.

Van Donk, E., and Hessen, D. O. 1995. Reduced digestibility of UV-B stressed and nutrient-limited algae by *Daphnia magna*. Hydrobiologia, 307: 147–151.

Van Donk, E., Lürling, M., Hessen, D. O., and Lokhorst, G. M. 1997. Altered cell wall morphology in nutrient-deficient phytoplankton and its impact on grazers. Limnology and Oceanography, 42: 357–364.

Weydmann, A., Søreide, J. E., Kwasniewski, S., and Widdicombe, S. 2012. Influence of CO_2-induced acidification on the reproduction of a key Arctic copepod *Calanus glacialis*. Journal of Experimental Marine Biology and Ecology, 428: 39–42.

Zervoudaki, S., Frangoulis, C., Giannoudi, L., and Krasakopoulou, E. 2014. Effects of low pH and raised temperature on egg production, hatching and metabolic rates of a Mediterranean copepod species (*Acartia clausi*) under oligotrophic conditions. Mediterranean Marine Science, 15: 74–83.

Zhang, D., Li, S., Wang, G., and Guo, D. 2011. Impacts of CO_2-driven seawater acidification on survival, egg production rate and hatching success of four marine copepods. Acta Oceanologica Sinica, 30: 86–94.

Handling editor: Stéphane Plourde

ICES Journal of Marine Science

ICES Journal of Marine Science (2016), 73(3), 659–669. doi:10.1093/icesjms/fsv162

Contribution to Special Issue: 'Towards a Broader Perspective on Ocean Acidification Research'

Original Article

Presence of competitors influences photosynthesis, but not growth, of the hard coral *Porites cylindrica* at elevated seawater CO_2

H. V. Brien[1†], S.-A. Watson[2*], and M. O. Hoogenboom[1,2†]

[1]*College of Marine and Environmental Science, James Cook University, Townsville, QLD 4811, Australia*
[2]*ARC Centre of Excellence for Coral Reef Studies, James Cook University, Townsville, QLD 4811, Australia*

**Corresponding author: tel: +61 (0)7 4781 5270; fax: +61 (0)7 4781 6722; e-mail: sueann.watson@jcu.edu.au*

Brien, H.V., Watson, S.-A., and Hoogenboom, M. O. Presence of competitors influences photosynthesis, but not growth, of the hard coral *Porites cylindrica* at elevated seawater CO_2. – ICES Journal of Marine Science, 73: 659–669.

Received 22 March 2015; revised 20 August 2015; accepted 25 August 2015; advance access publication 28 September 2015.

Changes in environmental conditions, such as those caused by elevated carbon dioxide (CO_2), potentially alter the outcome of competitive interactions between species. This study aimed to understand how elevated CO_2 could influence competitive interactions between hard and soft corals, by investigating growth and photosynthetic activity of *Porites cylindrica* (a hard coral) under elevated CO_2 and in the presence of another hard coral and two soft coral competitors. Corals were collected from reefs around Orpheus and Pelorus Islands on the Great Barrier Reef, Australia. They were then exposed to elevated pCO_2 for 4 weeks with two CO_2 treatments: intermediate (pCO_2 648) and high (pCO_2 1003) compared with a control (unmanipulated seawater) treatment (pCO_2 358). *Porites cylindrica* growth did not vary among pCO_2 treatments, regardless of the presence and type of competitors, nor was the growth of another hard coral species, *Acropora cerealis*, affected by pCO_2 treatment. Photosynthetic rates of *P. cylindrica* were sensitive to variations in pCO_2, and varied between the side of the fragment facing the competitors vs. the side facing away from the competitor. However, variation in photosynthetic rates depended on pCO_2 treatment, competitor identity, and whether the photosynthetic yields were measured as maximum or effective photosynthetic yield. This study suggests that elevated CO_2 may impair photosynthetic activity, but not growth, of a hard coral under competition and confirms the hypothesis that soft corals are generally resistant to elevated CO_2. Overall, our results indicate that shifts in the species composition in coral communities as a result of elevated CO_2 could be more strongly related to the individual tolerance of different species rather than a result of competitive interactions between species.

Keywords: climate change, coral growth, environmentally mediated competition, interspecific competition, photosynthetic efficiency.

Introduction

Competition plays a basic role in structuring coral reef communities as space is a limiting resource on shallow coral reefs. Hard corals of the order Scleractinia, soft corals of the family Alcyoniidae and algae (both macroalgae and coralline algae), are the major benthic space competitors on many Indo-Pacific coral reefs, including on the Great Barrier Reef (GBR) of Australia (e.g. Loya, 1972). Corals compete for space on the benthos using a variety of strategies. For example, tabular *Acropora* species often overgrow massive corals, resulting in reduced growth of the massive corals due to shading (Jackson, 1977). In contrast, soft corals, together with some algal species, can impede the growth and survival of hard corals and other competitors due to their production of toxic secondary metabolites (Sammarco *et al.*, 1983, 1985) that are released into surrounding waters. It has been shown that the outcomes of competitive interactions between corals and algae can vary with environmental conditions, such as water flow (Brown and Carpenter, 2015). Therefore, there is concern regarding a potential shift in the composition of coral communities, from hard coral-dominated to soft coral- or algal-dominated communities, under increasing temperatures or carbon dioxide (CO_2) scenarios.

Elevated CO_2 can influence rates of calcification, photosynthesis, and growth of corals (Dupont *et al.*, 2010; Harvey *et al.*, 2013). Elevated pCO_2 in seawater reduces the availability of carbonate ions (CO_3^{2-}) that are vital for corals to produce their calcium

†These two authors made an equal contribution to the manuscript.

carbonate ($CaCO_3$) skeletons. Corals, and other marine calcifying organisms, can precipitate two forms of $CaCO_3$, aragonite and calcite. Hard corals often precipitate external hard skeletons made from aragonite, whereas most soft corals precipitate internal sclerites made from the less soluble, low-magnesium calcite (Berner, 1975). The observed effects of elevated CO_2 are highly variable, and although there is a general decline in coral calcification in response to decreasing pH (Pandolfi *et al.*, 2011; Chan and Connolly, 2013), other studies have shown that elevated CO_2 can increase coral calcification rates (Ohki *et al.*, 2013; Takahashi and Kurihara, 2013). In addition to influencing calcification, the photosynthetic activity of symbiotic algae within coral tissue is potentially limited by CO_2 availability under high light and nutrient replete conditions and, as such, an increase in seawater pCO_2 concentrations could result in an increase in photosynthetic rates (Marubini *et al.*, 2008). There is some evidence that elevated CO_2 can increase productivity of corals by increasing zooxanthellae density and photosynthetic rates (Gattuso *et al.*, 1998; Schneider and Erez, 2006), although elevated pCO_2 can also cause expulsion of zooxanthellae from the coral host, or coral bleaching (Anthony *et al.*, 2008). Since corals deposit calcium carbonate skeletons, but also contain photosynthetic autotrophic symbionts, the potentially opposing effects of elevated CO_2 on calcification vs. photosynthesis mean that it is important to measure both response variables at elevated pCO_2 levels. Little is known about the possible effects of elevated CO_2 on soft corals. As soft corals are a key benthic component on coral reefs and can outcompete hard corals for space on reefs, it is important to understand their responses to elevated pCO_2. Similar to other Anthozoan species (e.g. sea anemones, Suggett *et al.*, 2012), it is generally considered that soft corals may be better able to tolerate elevated CO_2 because their fleshy tissues may act as a physical barrier to the ambient low pH seawater (Rodolfo-Metalpa *et al.*, 2011). Gabay *et al.* (2013) were the first to experimentally quantify the effects of elevated CO_2 on three Red Sea soft coral species, *Ovabunda macrospiculata* (Xeniidae), *Heteroxenia fuscescens* (Xeniidae), and *Sarcophyton* sp. (Alcyoniidae). Subsequently, Inoue *et al.* (2013) described a high soft coral cover of *Sarcophyton elegans* with elevated pCO_2 concentrations around a volcanic seep. Both studies found no mortality of colonies or primary polyps, and that photosynthesis, calcification, and growth of these soft corals remained unaffected after 5 months exposure to elevated pCO_2.

This study had two objectives. The first objective was to investigate the effects of elevated pCO_2 on the hard coral *Porites cylindirca* in the presence and absence of competitors. This was achieved by (i) quantifying growth and photosynthetic activity of *Porites cylindrica* under three contrasting pCO_2 levels in the presence or absence of competing corals either *Acropora cerealis* (another hard coral), *Sinularia* sp. or *Sacrophyton* sp. (both soft corals); and (ii) assessing whether and how effects of competitor presence or elevated pCO_2 were localized to specific areas of the coral tissue in proximity to competitors. The second objective was to assess the effects of elevated pCO_2 on the growth and photosynthetic activity of *A. cerealis* and on the tissue biomass, spicule mass, and photosynthetic activity of *Sinularia* sp. and *Sacrophyton* sp.

Material and methods

Coral species and collection

The hard coral, *P. cylindrica*, was chosen as the focal species of this experiment due to its local abundance and contrasting results from previous studies concerning the effect of elevated CO_2 on this species. To investigate the effects of competition with both hard and soft corals on *P. cylindrica* growth and photosynthesis under elevated CO_2, one hard coral from the order Scleractinia, *A. cerealis*, and two soft corals from the family Alcyonacea, *Sinularia* sp. and *Sarcophyton* sp., were chosen as competitors. Species selection was primarily based on high local abundance at the study site, and on the GBR more generally. Corals were collected from the leeward sides of Orpheus and Pelorus Islands in the Palm Group of Islands, ~18 km off the Australian mainland in the central region of the GBR. Corals were collected in February and March 2014 by cutting one 5–8 cm coral nubbin from randomly selected parental colonies using pliers (hard corals) or a scalpel (soft corals). Collection took place over a wide area (four different bays, 0.5–2 km apart) to ensure sampling of multiple coral genotypes. After collection, each hard coral fragment was mounted onto a terracotta tile using a water-resistant epoxy (Selleys "Knead it"). The soft corals were also mounted on tiles by inserting a small plastic toothpick through the coral fragment into a small PVC pipe that was attached to the tile, ensuring the fragment remained in an upright position. The experiment used aquarium facilities at Orpheus Island Research Station (OIRS) and all corals were allowed to recover and heal for >4 weeks before the experiment commenced. The experiment ran for 4 weeks.

Experimental set-up

The experiment was initially designed with fully factorial treatments (four levels of competition: none, *A. cerealis*, *Sinularia* sp., and *Sarcophyton* sp.; and three levels of pCO_2: control, intermediate, and high). However, soft corals are sensitive to handing (Ellis and Sharron, 1999) and, in the 2 weeks following initial collection, 49% of the *Sarcophyton* sp. and 29% of the *Sinularia* sp. died. In addition, 25% of collected *P. cylindrica* were consumed by a random infestation of coral-eating nudibranchs (*Phestilla* sp.) that naturally came into the flow-through aquarium system at OIRS and preferentially consume *Porites* (Faucci *et al.*, 2007). As a result of fragment mortality during the recovery period, the experimental design was modified by removing the intermediate pCO_2 treatment with *Sinularia*.

Corals were placed, either individually or in competition pairs, into one of the 60 small experimental aquaria (40 cm long, 10 cm wide, 8 cm deep, ~3.2 l volume) supplied with control or CO_2-treated seawater. Coral fragments were placed in the middle of each aquarium and, for the competition pairs, fragments were placed ~2 cm apart so that they were in proximity but not directly touching. This placement of colonies was chosen to avoid rapid digestion of tissue due to direct contact but to allow allellopathic competition effects (release of secondary metabolites into the water by soft corals). Each aquarium had an individual water supply (at 313 ± 2.3 ml min^{-1}) at one end and an outflow at the opposite end to generate approximately unidirectional flow through the aquarium. Consequently, in all competition pairs, *P. cylindrica* was placed downstream of its competitor to maximize potential exposure to allelochemicals excreted by competitors. As the competitors (*A. cerealis*, *Sarcophyton* sp., and *Sinularia* sp.) were always upstream of *P. cylindrica*, the flow was unidirectional, and the *P. cylindrica* were too small to shade the other colonies, we considered these corals to be unaffected by the presence of *P. cylindrica*. Hence, this positioning of fragments allowed us to identify the specific effect of elevated CO_2 on these species largely independently of competition, and we note that corals in the field are almost always in proximity to a competitor of some kind. All aquaria were cleaned weekly to remove algal growth. During the experiment, the corals did not receive supplemental feeding as the fresh seawater continually supplied to the system was considered to supply a sufficient food source. Aquaria were maintained outdoors under natural sunlight.

Description of the CO_2 dosing system

The CO_2 dosing system was designed as a semi-closed system, with water from 3 × 200 l sump tanks (treated or unmanipulated control) pumped into the individual treatment aquaria and the outflow of each aquarium returning to the appropriate sump tanks. Elevated pCO_2 seawater was achieved by dosing the sump tanks with pure CO_2, controlled and monitored based on pH. Seawater was pumped from the ocean through a 15-μm filter into sump tanks where it was treated with ambient air (control) or 100% CO_2 to achieve the desired pH before being pumped into the 60 replicate aquaria. A pH controller (pH Computer, Aqua Medic, Germany) was attached to the CO_2 treatment sump tanks to maintain the desired pH levels. Solenoid valves controlled the release of a slow stream of CO_2 into a small pump at the bottom of each sump tank whenever the seawater pH rose above the set point. To cover the broad range of pCO_2 conditions projected for the near future, experimental CO_2 dosing scenarios were set up to represent present day (control/unmanipulated seawater, pCO_2 358 ± 3 μatm, mean ± s.e.), intermediate (pCO_2 648 ± 6 μatm), and high (pCO_2 1003 ± 15 μatm). These values were based on the mean pCO_2 stabilization RCP 8.5 scenario for the year 2050 (intermediate) and 2100 (high) (Collins *et al.*, 2013). Sump tanks were also connected to a continual supply of new seawater (2.1 ± 0.34 l min^{-1}) to prevent any build-up of contaminants (including soft coral metabolites) in the systems. Seawater pH_T and temperature (HACH, PHC 30 103 pH probe) were recorded twice daily in each aquarium and in each sump tank. The pH probe was calibrated with Tris buffer (Scripps Institution of Oceanography). Salinity was measured daily in five random aquaria and all three sump tanks. Water samples taken from random aquaria were analysed for total alkalinity ($N = 8$) by Gran Titration (888 Titrando, Metrohm, Switzerland) to within 1% of certified reference material (Scripps Institution of Oceanography standards). Carbonate chemistry parameters for aquaria (Table 1) were calculated using CO2SYS (Pierrot *et al.*, 2006) using constants K1, K2 from Mehrbach *et al.* (1973) refit by Dickson and Millero (1987), and Dickson (1990) for $KHSO_4$. Seawater CO_2 levels were confirmed at the beginning of the experiment with a portable CO_2 equilibrator and an infrared sensor (GMP343, Vaisala, Helsinki, Finland).

Response variables

Photosynthetic efficiency

Photosynthetic efficiency of hard and soft corals was measured based on chlorophyll fluorescence using pulse amplitude modulated (PAM) fluorometry (Diving-PAM, Walz, Germany). We monitored both maximum photosynthetic yield (F_v/F_m, measured in darkness) and effective photosynthetic yield ($\Delta F/F_m$, measured under ambient light conditions). Maximum photosynthetic yield, measured when photosynthesis is inactive, indicates the maximum capacity of the photosynthetic machinery to utilize light for photosynthesis, whereas effective photosynthetic yield indicates the capacity of the photosynthetic machinery to processes additional light for photosynthesis when photosynthesis is already under way (Maxwell and Johnson, 2000). Effective photosynthetic yield is typically lower than maximum photosynthetic yield because additional non-photosynthetic biochemical pathways become active after exposure to light (e.g. Schreiber *et al.*, 1995).

Photosynthetic efficiency was measured for all fragments after 26 d of exposure to experimental conditions. Dark-adapted F_v/F_m was measured in darkness between 21:00–24:00 and $\Delta F/F_m$ was measured under ambient irradiance between 9:00–11:30. For the latter, light intensity was measured using an EasyView 33 light meter (Extech Instruments) directly above each aquarium immediately before measurements were taken so that we could statistically control for potential variation in photosynthetic efficiency due to changing light conditions. We anticipated that effects of competition on *P. cylindrica* might be highly localized to regions of coral tissue in proximity to competitors and, hence, that photosynthetic efficiency might vary between the side of the colony that faced the competitor compared with the opposite side that faced away from the competitor. Therefore, for each *P. cylindrica* colony, three replicate readings were taken on both sides of the colony. For *A. cerealis*, *Sarcophyton* sp. and *Sinularia* sp., which were assumed to be minimally affected by competitor presence given their upsteam positioning, three replicate measurements were taken from haphazardly selected positions close to the colony centre.

Skeletal growth: hard corals

The buoyant weight method (Davies, 1989) was used to measure growth rates of *P. cylindrica* and *A. cerealis* at the beginning and at the end of the experiment. Each fragment of *P. cylindrica* and *A. cerealis* was placed into 1 l of treatment seawater and weighed by attachment to a hook under a KERN-PCB 3-place balance. The salinity and temperature of this seawater was consistent over time and, hence, small changes in seawater density would not have affected the buoyant weight measurements. Growth rates were then expressed as the change in weight between the starting weight and the final weight (mg) standardized by the number of days between initial and final measurements (mg d^{-1}). Although many studies present buoyant weight data normalized to initial fragment size (i.e. proportional change in weight), we here present the raw change in buoyant weight because these values were not correlated with initial fragment size (Pearson's correlation, $t_{66} = -0.12$, $p = 0.9$).

Sclerite weight and tissue biomass: soft corals

Sinularia sp. and *Sarcophyton* sp. were evaluated based on sclerite weight and tissue biomass per unit tissue surface at the end of the experiment. Soft coral fragments were frozen at −80°C and transported frozen to laboratory facilities at James Cook University. Each fragment was divided into two subsamples, one of which was

Table 1. Water quality parameters (mean ± s.e.) for aquaria.

Treatment	Temperature (°C)	Salinity	pH_T	TA (μmol kg^{-1})	pCO_2 (μatm)	ΩArag.	HCO_3^- (μmol kg^{-1})	CO_3^{2-} (μmol kg^{-1})
Control	27.1 ± 0.04	35	8.09 ± 0.002	2294 ± 2.00	357.9 ± 2.58	3.80 ± 0.016	1702 ± 2.50	238 ± 1.01
Intermediate	27.1 ± 0.05	35	7.88 ± 0.004	2290 ± 1.73	648.1 ± 5.58	2.60 ± 0.020	1881 ± 3.05	163 ± 1.23
High	27.0 ± 0.05	35	7.73 ± 0.007	2290 ± 4.51	1003.0 ± 14.84	2.04 ± 0.030	1970 ± 4.68	128 ± 1.89

TA, total alkalinity. Intermediate and high pCO_2 treatments were chosen based on projections under the RCP 8.5 scenario for the year 2050 (intermediate treatment, 482–627 μatm) and 2100 (high treatment, 797–1142 μatm) (Collins *et al.*, 2013). Carbonate chemistry parameters were calculated using CO2SYS.

used to measure sclerite weight, and the other used to measure tissue biomass. Subsequently, tissue biomass and sclerite weights were standardized to tissue surface area. For *Sarcophyton*, two subsamples of fixed surface area (0.8 cm^2) were obtained by cutting the coral tissue using an apple corer. The branching morphology of *Sinularia* meant that the same approach could not be used so, to determine the surface area of each *Sinularia* subsample, the samples were defrosted and sliced longitudinally before being carefully flattened and photographed alongside a scale bar. The photographs were then analysed with ImageJ (NIH Image) to calculate the surface area (cm^2).

To calculate sclerite weight, subsamples were left in ~20 ml of a dilute sodium hydroxide solution (30% by volume) for up to 24 d to gradually dissolve the tissues and expose the sclerites. The solution was refreshed every 2–3 d by carefully pipetting off the solution and replacing with fresh 30% sodium hydroxide. After all tissue had been removed, and the solution was clear, sclerites were rinsed with distilled water before being dried to constant weight and weighed using a KERN-PCB 3-place balance ($\pm$0.001 g). To calculate tissue biomass, subsamples were crushed using a mortar and pestle, freeze-dried overnight, and weighed before being incinerated in a Muffle furnace (500°C for 4 h) to remove organic material. Samples were then cooled for 3 h and re-weighed using a KERN-PCB 3-place balance ($\pm$0.001 g), and biomass (ash-free dry weight) was determined from the difference between pre-incineration and post-incineration weights.

Data analysis

Results are presented as means $\pm$ s.e. and statistical analyses were conducted using R (R Foundation for Statistical Computing). Linear mixed-effects models (using "nlme" in R) were used to test whether position on the colony surface (i.e. facing towards or away from the competitor), pCO_2 treatment, or presence and identity of competitors influenced photosynthetic efficiency of *P. cylindrica*. In these analyses, colony identity was included as a random effect with position specified within colony to account for the repeated-measure of each colony (three replicate readings on the competitor-facing and opposite sides of each colony). All possible main effects and interactions were initially included in the analysis (see Supplementary Material for statistics from these initial analyses), and non-significant interactions and effects were sequentially removed by backwards deletion to identify the most parsimonious model which is reported in the Results section below. PAM data were arcsine-square-root transformed because photochemical efficiency is measured as a proportion. Due to the absence of colonies of *Sinularia* in the intermediate treatment, we analysed these data in two ways. First, we excluded the data for the intermediate treatment and used factorial mixed-effects ANOVA (as described above) to test effects of competitor (four levels: none, *Sarcophyton* sp., *Sinularia* sp., and *A. cerealis*), pCO_2 treatment (two levels: control and high), and colony position (two levels: facing and opposite) on photosynthetic efficiency of *P. cylindrica*. Second, we excluded the data for *Sinularia* sp. and tested effects of competitor (three levels: none, *Sarcophyton* sp., and *A. cerealis*), pCO_2 treatment (three levels: control, intermediate, and high), and position on colony (two levels: facing and opposite). The latter analysis was conducted primarily to confirm that our results were robust to small changes in sample sizes and treatments, and to test for variation between control, intermediate, and high pCO_2 treatments where possible. The effect of pCO_2 and competitor presence on calcification (buoyant weight) of *P. cylindrica* was tested using two-way ANOVA on square-root transformed data and one-way ANOVA on square-root transformed data was used to test the effect of pCO_2 on calcification of *Acropora*. Finally, two-way ANOVA on square-root transformed data was used assess effects of pCO_2 together with among-genus variation in sclerite density and tissue biomass of *Sarcophyton* and *Sinularia*. *Post hoc* multiple comparisons were implemented using "glht" in the R package "multcomp", with *p*-values adjusted to control for family-wise error rate using the single-step procedure.

Results

Carbonate chemistry and other water quality parameters during the experiment

The experimental CO_2 dosing system used here achieved three well-differentiated pCO_2 treatments (Table 1). Salinity and temperature were generally consistent across all treatments. Total alkalinity, pCO_2, and HCO_3^- had generally low variability within treatments.

General observations of coral health

Overall, based on visual inspection, the corals remained healthy throughout the experiment except for two *P. cylindrica* fragments under high pCO_2 and one *A. cerealis* fragment under intermediate pCO_2 that suffered partial mortality of ~10% of the tissue surface. Only one coral fragment, a *Sarcophyton* sp. in the high pCO_2 treatment, died during the 4-week experiment, indicating that the high fragment mortality immediately after collection was largely due to handling-stress rather than to conditions within the experimental aquaria. No visual signs of paling or bleaching of the coral tissue were observed, and all corals typically had their tentacles expanded at night exhibiting normal feeding behaviour. No visual signs of competition, such as tissue loss due to direct digestion by a competitor or paling of tissues, were observed, although the polyps of *Sarcophyton* sp. were occasionally in direct contact with *P. cylindrica*.

Effect of competitor presence on photosynthesis and growth of *P. cylindrica* under different pCO_2 levels

Maximum photosynthetic yield of symbionts with *P. cylindrica* was invariant to the presence and type of competitor (three-way mixed-effects ANOVA, competitor effect, $F_{3,39} = 1.5$, $p = 0.24$) and to the position on the colony surface (three-way mixed-effects ANOVA, position effect, $F_{1,43} = 0.23$, $p = 0.63$). The effect of position on the colony on photosynthetic yield did not depend on the presence and type of competitor, nor did it differ among pCO_2 treatments (three-way mixed-effects ANOVA, two- and three-way interactions, $p > 0.13$ in all cases, see Supplementary Table S1). In contrast, maximum photosynthetic yield was higher under control compared with high pCO_2 regardless of competitor type or position on the colony surface (Figure 1; three-way mixed-effects ANOVA, pCO_2 effect, $F_{1,42} = 5.9$, $p < 0.02$). These results were consistent whether the intermediate treatment was excluded from the analysis (as above) or whether all three pCO_2 treatments were included and data for *Sinularia* sp. were excluded. In the latter case, pCO_2 treatment was the only factor that significantly influenced maximum photosynthetic yield ($p > 0.38$ for all other main effects and interactions). *Post hoc* comparisons revealed that maximum photosynthetic yield was higher under control compared with high pCO_2 (Figure 1; three-way mixed-effects ANOVA, treatment contrasts: high vs. control, $t_{49} = -2.8$, $p < 0.01$) and mean yield under the intermediate treatment was closer to the mean

yield under high pCO_2 although not significantly different than measured under control conditions (control vs. intermediate, $t_{49} = -1.96$, $p = 0.06$; intermediate vs. high, $t_{49} = 0.72$, $p = 0.47$).

Effective photosynthetic yield of symbionts within *P. cylindrica* differed between different sides of the colony depending on pCO_2 treatment (Figure 2, three-way mixed-effects ANOVA, pCO_2 by Position interaction, $F_{1,39} = 6.5$, $p < 0.02$). These effects were not influenced by competitor identity (pCO_2 by Position by Competition treatment interaction, $F_{3,36} = 0.3$, $p = 0.81$, see Supplementary Table S2). *Post hoc* comparisons revealed that yield was higher on the facing compared with the opposite side within the control treatment (treatment contrasts, $z = -2.2$, $p < 0.05$) but not within the high pCO_2 treatment (treatment contrasts, $z = 1.1$, $p = 0.48$). Effective photosynthetic yield was also enhanced on the "upstream" side of the colony for *P. cylindrica* when in proximity to *Sarcophyton* sp. but not next to the other two competitors or when housed individually (Competition by Position interaction, $F_{3,39} = 3.02$, $p < 0.05$; treatment contrast facing vs. opposite within *Sarcophyton* sp. treatment, $z = -2.9$, $p < 0.02$). Ambient light intensity measured immediately before the measurement of effective quantum yield did not explain a significant amount of the variation in this parameter (three-way mixed-effects ANOVA, light intensity covariate, $F_{1,175} = 0.54$, $p = 0.46$).

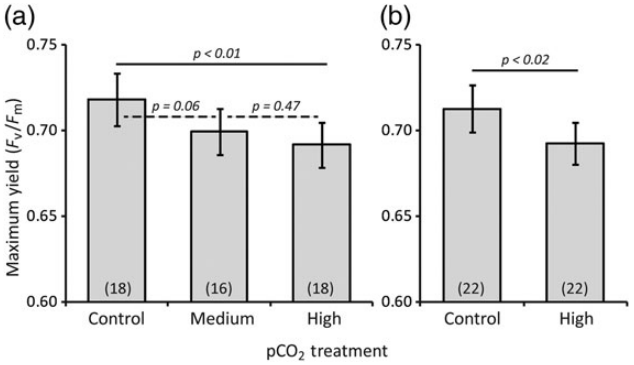

Figure 1. Maximum photosynthetic yield (dark-adapted F_v/F_m) for *P. cylindrica* (a) under three pCO_2 treatments and kept individually or in the presence of *Sarcophyton* sp. or *A. cerealis* or (b) under two pCO_2 treatments and kept individually or in the presence of *Sarcophyton* sp., *Sinularia* sp., or *A. cerealis*. Data are pooled across competition treatments because competitor identity did not influence F_v/F_m. Error bars show standard error and values in parentheses indicate sample sizes (*n* colonies). *p*-values indicate treatment comparisons from mixed-effects ANOVA.

Growth rates of *P. cylindrica* (measured as a change in buoyant weight) were highly variable among colonies within treatments, but did not vary in response to experimental pCO_2 levels (Figure 3; two-way ANOVA, pCO_2 effect $F_{1,30} = 1.1$, $p = 0.31$). Similarly, *P. cylindrica* growth was not influenced by the presence or type of competitor (two-way ANOVA, Competition effect $F_{3,30} = 0.44$, $p = 0.73$), and there was no evidence that pCO_2 had a different effect on *P. cylindrica* growth depending on competitor identity (Competition by pCO_2 interaction; $F_{3,30} = 2.2$, $p = 0.11$). Overall, growth of *P. cylindrica* fragments was slow and we recorded negative growth values for ~29% of the nubbins. These negative growth rates were primarily due to a methodological issue where many of the nubbins became detached from the tiles they were originally attached to and some of the epoxy (which was incorporated into the initial nubbin weight) flaked away from the nubbin base over time during routine cleaning. As this occurred for a large proportion of nubbins in all treatments, it does not confound our interpretation of effects of pCO_2 treatment on growth, but it does mean that the absolute values for the measured growth rates were lower than expected.

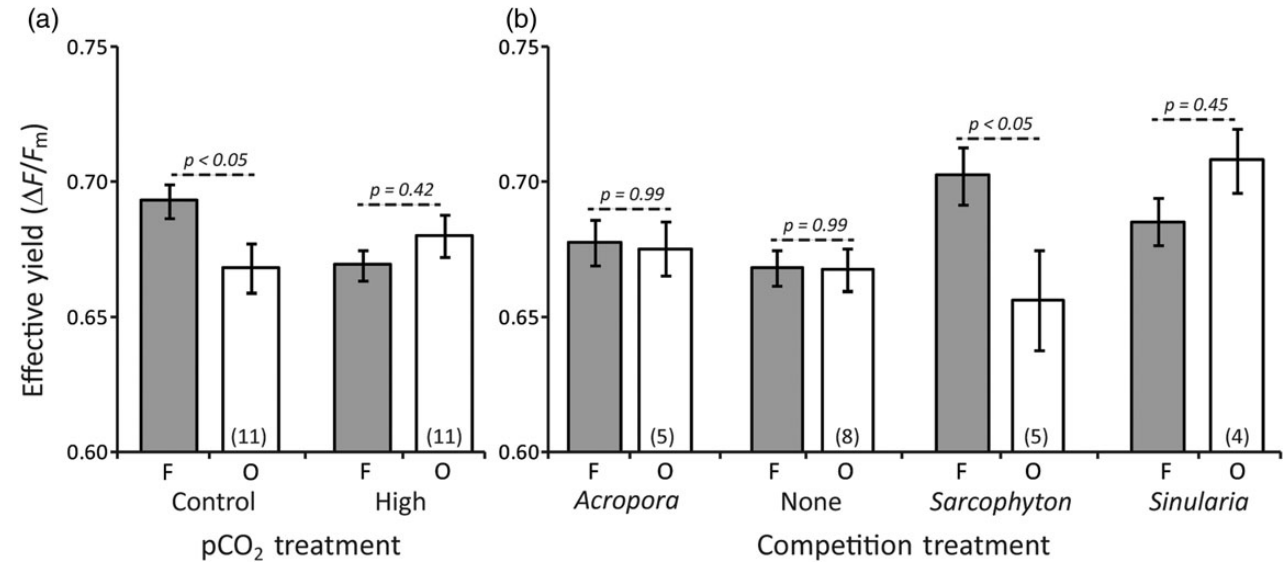

Figure 2. Variation in effective photosynthetic yield ($\Delta F/F_m$, measured under ambient irradiance) for *P. cylindrica* under competitive conditions between different sides of colonies (F, shaded bars, is the side directly facing competitors; O, open bars, is the opposite side of the colony) under (a) two pCO_2 treatments regardless of competitor type and (b) when kept either individually ("None") or in the presence of *Sarcophyton* sp., *Sinularia* sp., or *A. cerealis* regardless of pCO_2 treatment. Error bars show standard error and values in parentheses indicate sample sizes (*n* colonies). *p*-values indicate treatment comparisons from mixed-effects ANOVA.

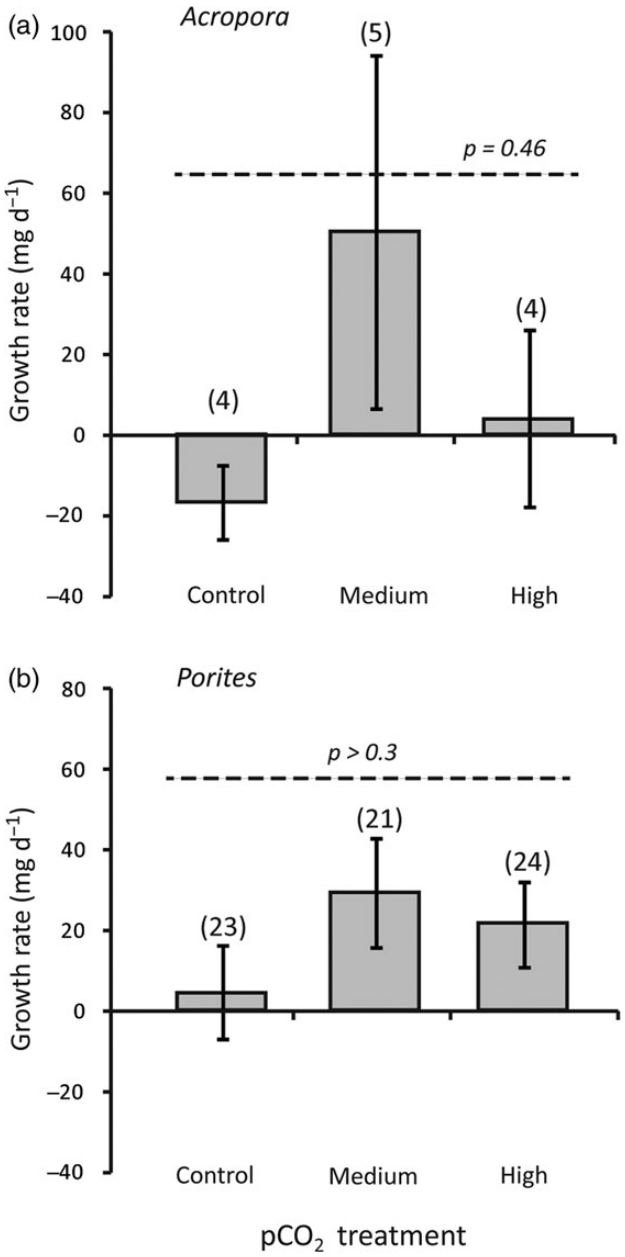

Figure 3. Effect of pCO_2 treatments on growth rates (measured as a change in buoyant weight) for two hard corals (a) *A. cerealis* (always upstream of *P. cylindrica*) and (b) *P. cylindrica* (all colonies both in the presence and absence of competitors). Error bars show standard error and values in parentheses indicate sample sizes. *p*-values indicate treatment effects from two-way factorial ANOVA. The presence and identity of competitors did not affect *Porites* growth, so data are here pooled across competition treatments.

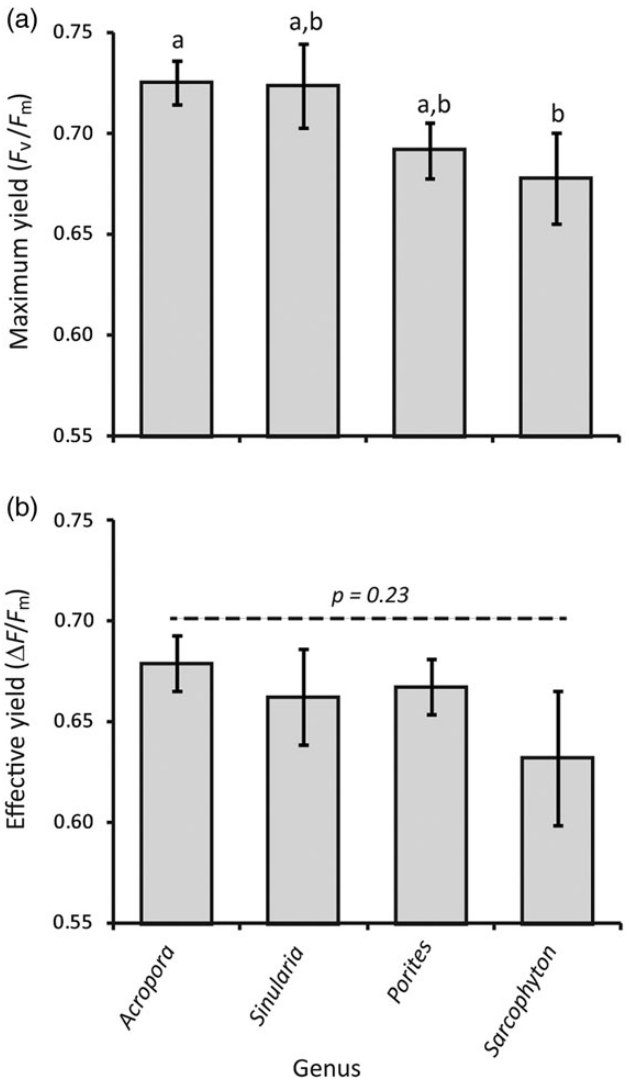

Figure 4. (a) Variation in maximum photosynthetic yield (dark-adapted F_v/F_m) and (b) effective photosynthetic yield ($\Delta F/F_m$, measured under ambient irradiance) among four coral genera; two hard corals (*A. cerealis* and *P. cylindrica*) and two soft corals (*Sarcophyton* sp. and *Sinularia* sp.). Species are plotted in order of decreasing F_v/F_m. Error bars show standard error for $n = 8–16$ colonies and letters in (a) indicate homogenous subsets based on *post hoc* multiple comparisons. Only colonies under high- and control-pCO_2 treatments were included and data for *P. cylindrica* include only measurements made on the opposite side of the colony (Figure 2) for colonies that were kept individually (no competitor present).

Effect of pCO_2 levels on *A. cerealis*, *Sarcophyton* sp., and *Sinularia* sp.

Growth rates of *A. cerealis* were consistent, on average, across all three pCO_2 treatments (Figure 3a; one-way ANOVA, pCO_2 effect $F_{2,10} = 0.8$, $p = 0.46$), but were also variable within treatments, and with some negative values recorded, due to the methodological issue noted previously. Maximum photosynthetic yield varied among the four coral genera included in this study (Figure 4, two-way mixed-effects ANOVA; genus effect $F_{3,39} = 4.0$, $p < 0.02$). Photosynthetic yield was significantly lower for *Sarcophyton* compared with *Acropora* (two-way mixed-effects ANOVA; among-genus contrasts *Acropora* vs. *Sarcophyton*, $z = 2.6$, $p < 0.05$) with *Porites* and *Sinularia* intermediate between the other two genera ($z > |2.4|$ and $p > 0.07$ for all other pairwise comparisons). Consistent with the results for *Porites* (Figure 1), there was a general trend towards lower maximum photosynthetic yield under high compared with control pCO_2 (mean 0.71 under control compared with 0.69 under high), although this difference was not statistically significant (two-way mixed-effects ANOVA; treatment effect $F_{1,39} = 3.7$, $p = 0.06$). This trend was generally consistent across the four genera (two-way

mixed-effects ANOVA; genus by treatment interaction $F_{3,36} = 0.39$, $p = 0.76$). In contrast, effective quantum yield did not vary among genera (two-way mixed-effects ANOVA; genus effect $F_{1,39} = 0.74$, $p = 0.39$), nor did it differ between colonies grown under control vs. high pCO_2 levels (two-way mixed-effects ANOVA; treatment effect $F_{3,39} = 1.4$, $p = 0.26$).

Consistent with differences in their overall colony morphology, *Sarcophyton* fragments had substantially higher tissue biomass per unit surface area ($\sim$1.6 g cm^{-2}) compared with *Sinularia* ($\sim$0.1 g cm^{-2}). Conversely, *Sinularia* had a much higher density of sclerites than *Sarcophyton* ($\sim$400 mg g^{-1} compared with $\sim$50 mg g^{-1}, respectively; Figure 5). This variation in sclerite density is likely

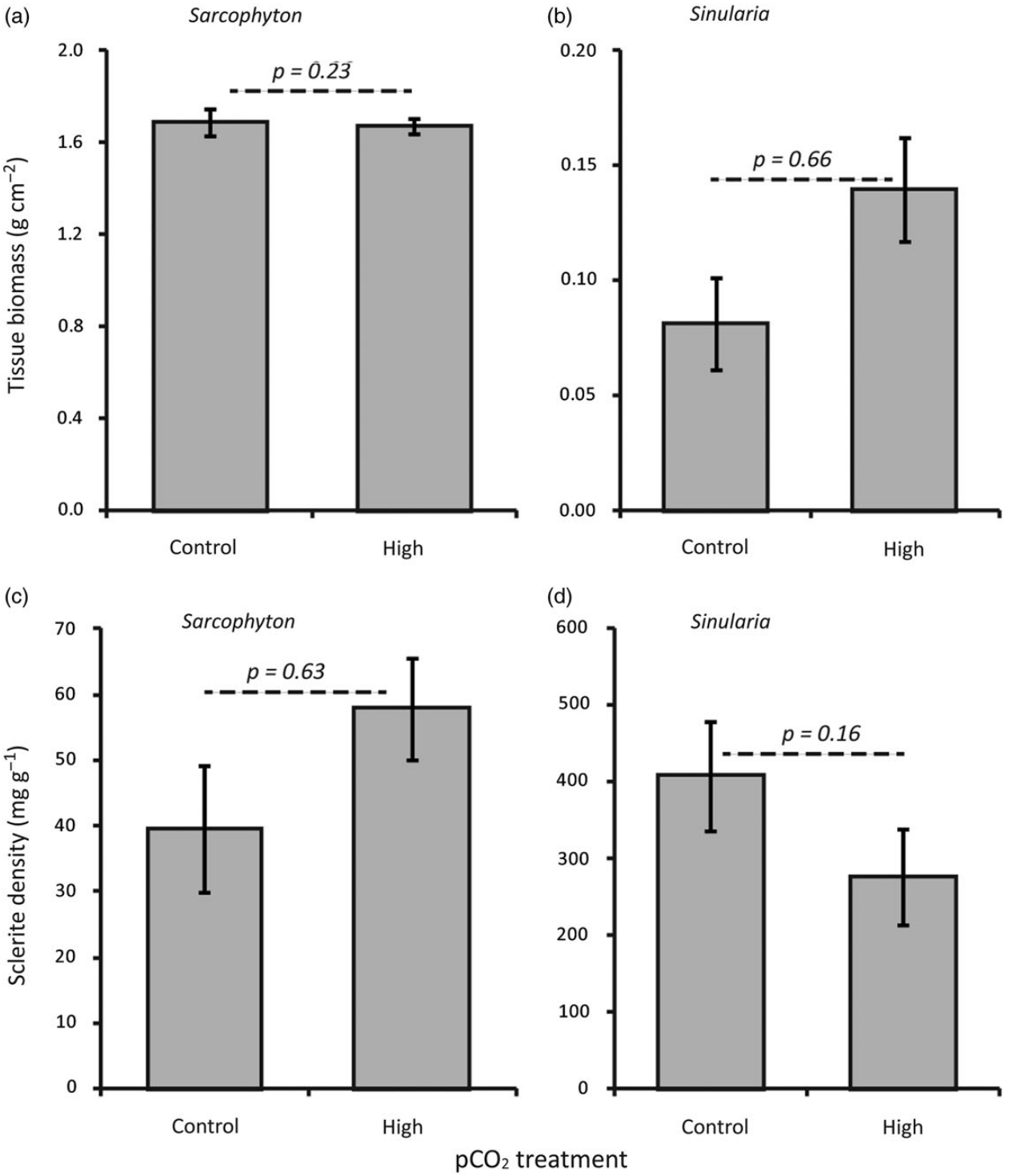

Figure 5. Effect of pCO_2 treatment on tissue biomass (a and b) and sclerite density (c and d) for the soft corals *Sarcophyton* sp. (a and c) and *Sinularia* sp. (b and d). Error bars show standard errors for $n = 3–6$ colonies and *p*-values indicate treatment effects from two-way factorial ANOVA. Data for *Sarcophyton* sp. under intermediate pCO_2 have been excluded from this analysis.

partly due to our sampling methods; samples of *Sarcophyton* were taken from the mantle of the colony, where sclerite density is likely to be lower compared with the stalk, whereas samples of *Sinularia* were obtained from vertically growing colony branches. There was no evidence that either sclerite density or tissue biomass differed among pCO_2 treatments for either genus (two-way ANOVA; treatment effect, $F_{1,14} = 0.07$, $p = 0.79$ for sclerite density and $F_{1,14} = 3.5$, $p = 0.08$ for tissue biomass; Figure 5).

Discussion

Using an experimental pCO_2 dosing system, this study has revealed when exposed to elevated pCO_2 growth rates and photosynthetic activity of *P. cylindrica* were not influenced by the presence of competing hard and soft corals (*A. cerealis*, *Sinularia* sp., and *Sarcophyton* sp.). Previous studies have shown that soft corals can impede hard coral fitness (Michalek and Bowen, 1997). For example, the production of alcyonacean diterpenes (secondary metabolites) can cause the loss of nematocysts and zooxanthellae of nearby scleractinian corals (Aceret *et al.*, 1995), including *P. cylindrica* and *A. cerealis*. Doing so disables the ability of scleractinian corals to feed and defend against other competitors for space and, hence, we hypothesized that proximity to soft corals would exacerbate the effects of high CO_2 on *Porites*. In contrast, our results indicate that elevated pCO_2 may impair the photosynthetic activity, but not the growth of *P. cylindrica*, regardless of the type or identity of nearby coral fragments.

Hard corals from the genus *Porites* are generally considered to be tolerant of various environmental stressors; for example, bleaching (Marshall and Baird, 2000; Loya *et al.*, 2001) and coral disease (Willis *et al.*, 2004). Yet, studies have shown that *Porites* corals may be sensitive to elevated CO_2 (e.g. Anthony *et al.*, 2008). In the present study, after 4 weeks of exposure to elevated CO_2, growth rates of *P. cylindrica* remained unaffected by elevated pCO_2. Consistent with previous data showing that *Porites* corals are generally slow growing [see Pratchett *et al.* (2015) for a review], we observed low, and highly variable, growth rates for the experimental nubbins. This variability, and the low average growth rate, was primarily due to methodological issues with buoyant weight measurement, and there was no visual evidence that the colonies decreased in tissue surface area over time. However, this highlights a potential constraint on the use of slow-growing corals in experiments because slow growth might necessitate a longer experimental exposure period before a difference in growth between experimental treatments is measureable. Nevertheless, one previous study, on the same species, found that photosynthetic and calcification rates were significantly reduced after 15 d of exposure to elevated pCO_2, to the point that there was dissolution of calcium carbonate from the coral fragments, and fragments were producing a substantial amount of mucus (Hii *et al.*, 2009), indicating that our 4-week experiment should have been long enough to detect differences in growth if, indeed, the experimental treatment affected growth rates. In that study, an elevated pCO_2 treatment was used with a pH_T of 7.9 that was similar to that of our intermediate CO_2 treatment (pH_T of 7.88). Although both this study and Hii *et al.* (2009) used CO_2 stimulation to alter pH, we note that the seawater carbonate chemistry used by Hii *et al.* (2009) was substantially different from this study (HCO_3 concentration of 1072 $\mu mol\ kg^{-1}$ compared with 1881 $\mu mol\ kg^{-1}$ in this study, and CO_3 concentration of 15.17 $\mu mol\ kg^{-1}$ compared with 163 $\mu mol\ kg^{-1}$ in this study for treatments with similar pH levels). In addition, Hii *et al.* (2009) used the alkalinity anomaly approach to detect treatment effects on calcification, and that method is more sensitive to small differences in calcification compared with the buoyant weight method. Such differences could explain the contrasting results between these studies.

Regardless of the presence or identity of nearby coral colonies, photosynthetic activity (maximum photosynthetic efficiency) of *P. cylindrica* significantly decreased with exposure to elevated pCO_2 over the 4-week experimental period. Maximum photosynthetic yields were also independent of the position on the colony surface. These results indicate that CO_2 availability in seawater is not the only factor that influences the photosynthetic rates of coral symbionts due to regulation of carbonate ions within the symbiosis (e.g. Muscatine *et al.*, 1989; Schneider and Erez, 2006). The decline in photosynthetic efficiency under elevated pCO_2 that we observed is consistent with the elevated CO_2 and temperature-related coral bleaching response observed in *Porites* and *Acropora* (Anthony *et al.*, 2008). A possible mechanism underlying this response could be a decrease in the expression of phosphoglycolate phosphatase (PGPase), as observed in *Acropora formosa* after acidification exposure (Crawley *et al.*, 2010). A decrease in PGPase can lead to an increase of the production of reactive oxygen species during photosynthesis and this could, in turn, cause oxidative stress of zooxanthellae (Iguchi *et al.*, 2012) that reduces photosynthetic activity. Collectively, these results indicate that elevated pCO_2 destabilizes symbiont photosynthetic activity, and that such effects outweigh any release of CO_2 limitation of photosynthesis.

Contrary to our expectations, we found that maximum photosynthetic yields (measured in darkness) were more sensitive to variations in pCO_2 than effective photosynthetic yields (measured under mid-day irradiance). These findings support that release of CO_2 limitation of photosynthesis has a minimal effect on photosynthesis of *P. cylindrica*: elevated pCO_2 had a greater effect on photosynthetic yield when photosynthetic rate was light-limited rather than when photosynthesis was limited by gas diffusion and/or enzyme processing at saturating light levels. We also found that effects of competitor presence and pCO_2 on effective photosynthetic yields were localized on coral nubbins. The increased effective photosynthetic yield on the upstream sides of the *P. cylindrica* colonies in the control treatment is consistent with many previous studies, demonstrating that photosynthesis rates increase with increasing water flow (e.g. Hoogenboom and Connolly, 2009). A similar mechanism potentially underlies the decreased photosynthetic yield on the downstream side of *P. cylindrica* nubbins in proximity to *Sarcophyton* sp. because, when fully expanded, the *Sarcophyton* sp. nubbins were considerably larger than the nubbins of the other coral species and, thus, are likely to have had a much greater influence on the flow regime within the experimental aquaria. Furthermore, having a coral upstream has been shown to elevate pCO_2 and reduce aragonite saturation state to an extent that downstream corals may have more compounding effects of elevated CO_2 (Anthony *et al.*, 2011). However, our dataset does not explain why effective photosynthetic yield was not enhanced on the upstream side of nubbins in the high pCO_2 treatment. The effects of water flow on photosynthesis rates are driven by differences in the rates of diffusion of gases between seawater and coral tissue (Hoogenboom and Connolly, 2009). Such diffusion processes are influenced by actual concentrations of gases in seawater and, hence, altering seawater pCO_2 levels could influence gas exchange. Nevertheless, further research is required to test these hypotheses.

Unlike other hard corals, *P. cylindrica* has no apparent aggressive competitive strategy: it does not digest the tissue of neighbouring

colonies nor does it grow rapidly to overtop or overgrow neighbouring colonies (e.g. Dai, 1990). Instead, it persists on the reef through fragmentation (Seebauer, 2001) and relatively high stress tolerance and resistance to damage (e.g. Marshall and Baird, 2000 for *Porites*). Our results showing no effects of elevated pCO_2 on growth are generally consistent with these studies. Massive *Porites* have been shown to be resistant to elevated CO_2 around a volcanic seep (Fabricius *et al.*, 2011) and elevated CO_2 from a manipulated dosing system in a laboratory. In contrast, using elevated CO_2 from a manipulated dosing system in a laboratory, other studies have shown decreases in the calcification and photosynthesis of *Porites* spp., both in mound-shaped species of *Porites* (e.g. Anthony *et al.*, 2008 for *P. lobata* and Iguchi *et al.*, 2012 for *P. australiensis*) and in branching species (Hii *et al.*, 2009 for *P. cylindrica* and Edmunds *et al.*, 2012 for *P. rus*). Similar to *P. cylindrica*, growth of *A. cerealis* (the other hard coral in the current experiment) remained unaffected by elevated CO_2, with no significant difference in fragment growth (measured as a change in buoyant weight) across the experiment among treatments. Other studies have found significant declines in growth of Acroporids as a result of elevated pCO_2. For example, using the same method as this study (change in buoyant weights), Anthony *et al.* (2008) found growth (percentage weight increase per month) of *A. intermedia* declined under elevated CO_2. The absence of a consistent response to elevated pCO_2 for corals of the same genus and/or species across multiple studies indicates that such effects may be dependent on specific combinations of environmental and laboratory conditions (including temperature, Schoepf *et al.*, 2013). Alternatively, among-species (and potentially, among-environment) differences in the type of symbiont (*Symbiodinium* spp.) present within coral tissues could affect growth and photosynthetic activity and thus influence susceptibility to elevated pCO_2. For instance, Brading *et al.* (2011) found that *Symbiodinium* phylotypes A1 and B1 were largely unaffected by elevated pCO_2, whereas types A13 and A2 performed better under elevated pCO_2.

The condition of both soft coral species investigated in this study, based on total tissue biomass and sclerite density, was also unaffected by elevated pCO_2. This is consistent with previous studies, showing that external tissue layers can help protect shells and coral skeletons from acidic seawater (Rodolfo-Metalpa *et al.*, 2011). Although there are relatively few previous studies on soft corals, our results regarding soft coral photosynthesis are consistent with Gabay *et al.* (2013); zooxanthellae density, chlorophyll content per symbiont cell, and photosynthesis rates of *Sarcophyton* sp. collected at Eilat did not decline under elevated pCO_2. A field study of Iwotorishima Island in Japan where volcanic activity has naturally elevated pCO_2 (831 atm) found that the soft coral *S. elegans* dominated areas with elevated pCO_2 (Inoue *et al.*, 2013). Thus, under the levels of elevated CO_2 anticipated over the coming century (as considered in this study), soft corals could become more abundant on coral reefs. To our knowledge, there is, as yet, no direct evidence that the relative abundance of soft vs. hard corals in reef benthic communities has changed over the past few decades. However, a long-term study in Taiwan indicated changes in benthic community composition between 1992 and 2003, with some replacement of branching *Acropora* by the anemone *Condylactis* (Chen and Dai, 2004).

A 4-week exposure experiment is adequate to investigate immediate physiological responses to elevated CO_2 as studies have observed such effects after shorter experimental periods [e.g. 15 d in Hii *et al.* (2009); 3.5 weeks in Schoepf *et al.* (2013)]. The three pCO_2 treatments in this study covered a realistic range of conditions and were well differentiated based on carbonate chemistry and, hence, insufficient difference in pCO_2 among treatments is unlikely to explain the lack of variation in coral growth. Nevertheless, extrapolating the results of a 4-week acute exposure to understand changes in coral competition dynamics over the coming decades of gradual changes in seawater chemistry must be done with caution. Although few studies have assessed the capacity of corals to acclimatize or adapt to increased pCO_2, such acclimation is likely to decrease the effects of elevated pCO_2 on coral growth. However, pre-experiment mortality was pronounced in the soft corals used here leading to the possibility that sublethal effects of handling-stress reduced the metabolite production by the soft coral fragments and, hence, could have reduced any effects of soft coral presence on *Porites*. Future studies should consider a different collection technique for soft corals; for example, finding small size whole colonies on reefs rather than removing small fragments from large colonies. It is also possible that the small soft coral colonies used here did not excrete sufficient quantities of metabolites to affect hard corals. No study as yet has determined whether colony size affects the outcome of competitive interactions between hard and soft corals; however, larger individuals are generally competitively dominant (Connell, 1961). Having a smaller distance or contact between *P. cylindrica* and its competitors may result in more obvious competition tissue scars. Furthermore, having an open wound exposed to surrounding elevated CO_2 may exacerbate the effects of elevated CO_2 on growth and photosynthetic rates. However, these soft corals favour the use of alleochemicals to compete against neighbouring colonies, a strategy that does not rely on contact.

This study shows that photosynthetic rates of *P. cylindrica* may be compromised under elevated pCO_2, whereas growth rates remained unchanged, and these effects were not sensitive to the presence or identity of nearby corals. Furthermore, this study has further strengthened the hypothesis that soft corals are not strongly influenced by near-future elevated CO_2, as growth and of *Sinularia* sp. and *Sarcophyton* sp. remained unaffected. Overall, our results indicate that shifts in the species composition of coral communities under elevated CO_2 will most likely be related to the individual tolerances of different species rather than to changes in the outcomes of competitive interactions.

Acknowledgements

This study was supported by the Australian Research Council Centre of Excellence for Coral Reef Studies and James Cook University. We thank the staff of Orpheus Island Research Station, a facility of James Cook University, and P.L. Munday.

Supplementary material

Supplementary material is available at the *ICESJMS* online version of the manuscript.

References

Aceret, T. L., Sammarco, P. W., and Coll, J. C. 1995. Toxic effects of alcyonacean diterpenes on scleractinian corals. Journal of Experimental Marine Biology and Ecology, 188: 63–78.

Anthony, K., Kleypas, J. A., and Gattuso, J. P. 2011. Coral reefs modify their seawater carbon chemistry–implications for impacts of ocean acidification. Global Change Biology, 17: 3655–3666.

Anthony, K. R., Kline, D. I., Diaz-Pulido, G., Dove, S., and Hoegh-Guldberg, O. 2008. Ocean acidification causes bleaching

and productivity loss in coral reef builders. Proceedings of the National Academy of Sciences USA, 105: 17442–17446.

Berner, R. A. 1975. The role of magnesium in the crystal growth of calcite and aragonite from sea water. Geochimica et Cosmochimica Acta, 39:489–504.

Brading, P., Warner, M. E., Davey, P., Smith, D. J., Achterberg, E. P., and Suggett, D. J. 2011. Differential effects of ocean acidification on growth and photosynthesis among phylotypes of *Symbiodinium* (Dinophyceae). Limnology and Oceanography, 56: 927.

Brown, A. L., and Carpenter, R. C. 2015. Water flow influences the mechanisms and outcomes of interactions between massive *Porites* and coral reef algae. Marine Biology, 162:459–468.

Chan, N., and Connolly, S. R. 2013. Sensitivity of coral calcification to ocean acidification: A meta-analysis. Global Change Biology, 19:282–290.

Chen, C. A., and Dai, C-F. 2004. Local phase shift from *Acropora*-dominant to *Condylactis*-dominant community in the Tiao-Shi reef, Kenting National Park, southern Taiwan. Coral Reefs, 23: 508.

Collins, M., Knutti, R., Arblaster, J., Dufresne, J. -L., Fichefet, T., Friedlingstein, P., Gao, X., *et al.* 2013. Long-term Climate Change: Projections, Commitments and Irreversibility. *In* Climate Change 2013: The Physical Science Basis Contribution of Working Group I to the Fifth Assessment Report of the Intergovernmental Panel on Climate Change, pp. 1029–1136. Ed. by T. F. Stocker, D. Qin, G. -K. Plattner, M. Tignor, S. K. Allen, J. Boschung, *et al.* Cambridge University Press, Cambridge, United Kingdom and New York, NY.

Connell, J. H. 1961. Effects of competition, predation by *Thais lapillus*, and other factors on natural populations of the barnacle *Balanus balanoides*. Ecological Monographs, 31: 61–104.

Crawley, A., Kline, D. I., Dunn, S., Anthony, K. E. N., and Dove, S. 2010. The effect of ocean acidification on symbiont photorespiration and productivity in *Acropora formosa*. Global Change Biology, 16: 851–863.

Dai, C. F. 1990. Interspecific competition in Taiwanese corals with special reference to interactions between alcyonaceans and scleractinians. Marine Ecology Progress Series, 60: 291–297.

Davies, P. S. 1989. Short-term growth measurements of corals using an accurate buoyant weighing technique. Marine Biology, 101: 389–395.

Dickson, A. G. 1990. Standard potential of the reaction: $AgCl(s)+1/2\ H_2(g)=Ag(s)+HCl(aq)$, and the standard acidity constant of the ion HSO_4^- in synthetic seawater from 273.15 to 318.15 K. Journal of Chemical Thermodynamics, 22: 113–127.

Dickson, A. G., and Millero, F. J. 1987. A comparison of the equilibrium constants for the dissociation of carbonic acid in seawater media. Deep Sea Research, 34: 1733–1743.

Dupont, S., Dorey, N., and Thorndyke, M. 2010. What meta-analysis can tell us about vulnerability of marine biodiversity to ocean acidification? Estuarine, Coastal and Shelf Science, 89: 182–185.

Edmunds, P. J., Brown, D., and Moriarty, V. 2012. Interactive effects of ocean acidification and temperature on two scleractinian corals from Moorea, French Polynesia. Global Change Biology, 18: 2173–2183.

Ellis, S., and Sharron, L. 1999. The culture of soft corals (Order: Alcyonacea) for the marine aquarium trade. CTSA, 137: 26.

Fabricius, K. E., Langdon, C., Uthicke, S., Humphrey, S., Noonan, S., De'ath, G., Okazaki, R., *et al.* 2011. Losers and winners in coral reefs acclimatized to elevated carbon dioxide concentrations. Nature Climate Change, 1: 165–169.

Faucci, A., Toonen, R. J., and Hadfield, M. G. 2007. Host shift and speciation in a coral-feeding nudibranch. Proceedings of the Royal Society B: Biological Sciences, 274: 111–119.

Gabay, Y., Benayahu, Y., and Fine, M. 2013. Does elevated pCO_2 affect reef octocorals? Ecology and Evolution, 3: 465–473.

Gattuso, J. P., Frankignoulle, M., Bourge, I., Romaine, S., and Buddemeier, R. W. 1998. Effect of calcium carbonate saturation of seawater on coral calcification. Global and Planetary Change, 18: 37–46.

Harvey, B. P., Gwynn-Jones, D., and Moore, P. J. 2013. Meta-analysis reveals complex marine biological responses to the interactive effects of ocean acidification and warming. Ecology and Evolution, 3: 1016–1030.

Hii, Y. -S., Ambok Bolong, A. M., Yang, T. -T., and Liew, H. C. 2009. Effect of elevated carbon dioxide on two scleractinian corals: *Porites cylindrica* (Dana, 1846) and *Galaxea fascicularis* (Linnaeus, 1767). Journal of Marine Biology. doi:10.1155/2009/215196.

Hoogenboom, M. O., and Connolly, S. R. 2009. Defining fundamental niche dimensions of corals: Synergistic effects of colony size, light, and flow. Ecology, 90: 767–780.

Iguchi, A., Ozaki, S., Nakamura, T., Inoue, M., Tanaka, Y., Suzuki, A., Kawahata, H., *et al.* 2012. Effects of acidified seawater on coral calcification and symbiotic algae on the massive coral. Marine Environmental Research, 73:32–36.

Inoue, S., Kayanne, H., Yamamoto, S., and Kurihara, H. 2013. Spatial community shift from hard to soft corals in acidified water. Nature Climate Change, 3: 683–687.

Jackson, J. B. C. 1977. Competition on marine hard substrata: The adaptive significance of solitary and colonial strategies. American Naturalist, 111: 743–767.

Loya, Y. 1972. Community structure and species diversity of hermatypic corals at Eilat, Red Sea. Marine Biology, 13:100–123.

Loya, Y., Sakai, K., Yamazato, K., Nakano, Y., Sambali, H., and van Woesik, R. 2001. Coral bleaching: The winners and the losers. Ecology Letters, 4: 122–131.

Marshall, P. A., and Baird, A. H. 2000. Bleaching of corals on the Great Barrier Reef: Differential susceptibilities among taxa. Coral Reefs, 19: 155–163.

Marubini, F., Ferrier-Pages, C., Furla, P., and Allemand, D. 2008. Coral calcification responds to seawater acidification: A working hypothesis towards a physiological mechanism. Coral Reefs, 27: 491–499.

Maxwell, K., and Johnson, G. N. 2000. Chlorophyll fluorescence—A practical guide. Journal of Experimental Botany, 51: 659–668.

Mehrbach, C., Culberson, C. H., Hawley, J. E., and Pytkowicz, R. N. 1973. Measurement of the apparent dissociation constants of carbonic acid in seawater at atmospheric pressure. Limnology and Oceanography, 18: 897–907.

Michalek, K., and Bowden, B. F. 1997. A natural algacide from soft coral *Sinularia flexibilis* (Coelenterata, Octocorallia, Alcyonacea). Journal of Chemical Ecology, 23: 259–273.

Muscatine, L., Porter, J. W., and Kaplan, I. R. 1989. Resource partitioning by reef corals as determined from stable isotope composition. I. $\delta^{13}C$ of zooxanthellae and animal tissue versus depth. Marine Biology, 100: 185–193.

Ohki, S., Irie, T., Inoue, M., Shinmen, K., Kawahata, H., Nakamura, T., and Woesik, R. V. 2013. Calcification responses of symbiotic and aposymbiotic corals to near-future levels of ocean acidification. Biogeosciences, 10: 6807–6814.

Pandolfi, J. M., Connolly, S. R., Marshall, D. J., and Cohen, A. L. 2011. Projecting coral reef futures under global warming and ocean acidification. Science, 333: 418–422.

Pierrot, D., Lewis, E., and Wallace, D. W. R. 2006. MS Excel Program Developed for CO2 System Calculations. ORNL/CDIAC-105a. Carbon Dioxide Information Analysis Center, Oak Ridge National Laboratory, U.S. Department of Energy, Oak Ridge, Tennessee, U.S.A.

Pratchett, M. S., Anderson, K. D., Hoogenboom, M. O., Widman, E., Baird, A. H., Pandolfi, J. M., Edmunds, P. J., *et al.* 2015. Spatial, temporal and taxonomic variation in coral growth—implications for the structure and function of coral reef ecosystems. OMBAR, 53: 215–295.

Rodolfo-Metalpa, R., Houlbrèque, F., Tambutté, É., Boisson, F., Baggini, C., Patti, F. P., Jeffree, R., *et al.* 2011. Coral and mollusc resistance to

ocean acidification adversely affected by warming. Nature Climate Change, 1: 308–312.

Sammarco, P. W., Coll, J. C., and La Barre, S. 1985. Competitive strategies of soft corals (Coelenterata: Octocorallia). II. Variable defense responses and susceptibility to scleractinian corals. Journal of Experimental Marine Biology and Ecology, 91: 199–215.

Sammarco, P. W., Coll, J. C., La Barre, S., and Willis, B. L. 1983. Competitive strategies of soft corals (Coelenterata: Octocorallia): Allellopathic effects on selected scleractinian corals. Coral Reefs, 1: 173–178.

Schneider, K., and Erez, J. 2006. The effect of carbonate chemistry on calcification and photosynthesis in the hermatypic coral *Acropora eurystoma*. Limnology Oceanography, 51:1284–1293.

Schoepf, V., Grottoli, A. G., Warner, M. E., Cai, W-J., Melman, T. F., Hoadley, K. D., Pettay, D. T., *et al.* 2013. Coral energy reserves and calcification in a high-CO_2 world at two temperatures. PLoS ONE, 8: e75049.

Schreiber, U., Bilger, W., and Neubaur, C. 1995. Chlorophyll fluorescence as a nonintrusive indicator for rapid assessment of in vivo photosynthesis. Ecophysiology of Photosynthesis, 100: 49–70.

Seebauer, J. 2001. Zoology of *Porites cylindrica*: Potential for use in reef rehabilitation transplantation efforts. SUNY Geneseo Journal of Science and Mathematics, 2: 26–34.

Suggett, D. J., Hall-Spencer, J. M., Rodolfo-Metalpa, R., Boatman, T. G., Payton, R., Pettay, D. T., Johnson, V. R., *et al.* 2012. Sea anemones may thrive in a high CO_2 world. Global Change Biology, 18: 3015–3025.

Takahashi, A., and Kurihara, H. 2013. Ocean acidification does not affect the physiology of the tropical coral *Acropora digitifera* during a 5-week experiment. Coral Reefs, 32: 305–314.

Willis, B. L., Page, C. A., and Dinsdale, E. A. 2004. Coral disease on the Great Barrier Reef. *In* Coral Health and Disease, pp. 69–104. Springer, Berlin, Heidelberg.

Handling editor: Howard Browman

ICES Journal of Marine Science

ICES Journal of Marine Science (2016), 73(3), 670–679. doi:10.1093/icesjms/fsv130

Contribution to Special Issue: 'Towards a Broader Perspective on Ocean Acidification Research'

Original Article

Contrasting effects of ocean acidification on the microbial food web under different trophic conditions

M. M. Sala[1]*, F. L. Aparicio[1], V. Balagué[1], J. A. Boras[1], E. Borrull[1], C. Cardelús[1], L. Cros[1], A. Gomes[1], A. López-Sanz[1], A. Malits[1†], R. A. Martínez[1], M. Mestre[1], J. Movilla[1], H. Sarmento[1‡], E. Vázquez-Domínguez[1], D. Vaqué[1], J. Pinhassi[2], A. Calbet[1], E. Calvo[1], J. M. Gasol[1], C. Pelejero[1,3], and C. Marrasé[1]

[1]*Institut de Ciències del Mar (CSIC), Passeig Marítim de la Barceloneta 37-49, Barcelona, Catalunya 08003, Spain*
[2]*Centre for Ecology and Evolution in Microbial Model Systems, Linnaeus University, Kalmar SE-39182, Sweden*
[3]*Institució Catalana de Recerca i Estudis Avançats (ICREA), Pg. Lluís Companys 23, Barcelona, Catalunya 08010, Spain*

**Corresponding author: tel: +34 93 2309500; fax: +34 93 2309555; e-mail: msala@icm.csic.es*
[†]*Present address: Centro Austral de Investigaciones Científicas (CONICET), Ushuaia, Argentina.*
[‡]*Present address: Department of Hydrobiology, Federal University of São Carlos, Sao Paulo, Brazil.*

Sala, M. M., Aparicio, F. L., Balagué, V., Boras, J. A., Borrull, E., Cardelús, C., Cros, L., Gomes, A., López-Sanz, A., Malits, A., Martínez, R. A., Mestre, M., Movilla, J., Sarmento, H., Vázquez-Domínguez, E., Vaqué, D., Pinhassi, J., Calbet, A., Calvo, E., Gasol, J. M., Pelejero, C., and Marrasé, C. Contrasting effects of ocean acidification on the microbial food web under different trophic conditions. – ICES Journal of Marine Science, 73: 670–679.

Received 24 December 2014; revised 30 June 2015; accepted 1 July 2015; advance access publication 7 August 2015.

We investigated the effects of an increase in dissolved CO_2 on the microbial communities of the Mediterranean Sea during two mesocosm experiments in two contrasting seasons: winter, at the peak of the annual phytoplankton bloom, and summer, under low nutrient conditions. The experiments included treatments with acidification and nutrient addition, and combinations of the two. We followed the effects of ocean acidification (OA) on the abundance of the main groups of microorganisms (diatoms, dinoflagellates, nanoeukaryotes, picoeukaryotes, cyanobacteria, and heterotrophic bacteria) and on bacterial activity, leucine incorporation, and extracellular enzyme activity. Our results showed a clear stimulation effect of OA on the abundance of small phytoplankton (pico- and nanoeukaryotes), independently of the season and nutrient availability. A large number of the measured variables showed significant positive effects of acidification in summer compared with winter, when the effects were sometimes negative. Effects of OA were more conspicuous when nutrient concentrations were low. Our results therefore suggest that microbial communities in oligotrophic waters are considerably affected by OA, whereas microbes in more productive waters are less affected. The overall enhancing effect of acidification on eukaryotic pico- and nanophytoplankton, in comparison with the non-significant or even negative response to nutrient-rich conditions of larger groups and autotrophic prokaryotes, suggests a shift towards medium-sized producers in a future acidified ocean.

Keywords: acidification, eutrophication, Mediterranean sea, mesocosm, microorganisms.

Introduction

Human activity is currently emitting ~10 Pg C in the form of CO_2 into the atmosphere every year (Peters *et al.*, 2012). About 30% of this CO_2 dissolves in the upper layers of the oceans, leading to a lowering of pH and, consequently, to fundamental changes in the chemistry of seawater (Doney *et al.*, 2009; Pelejero *et al.*, 2010). Marine organisms show a wide range of responses to this ocean acidification (OA) (e.g. Kroeker *et al.*, 2010; Harvey *et al.*, 2013).

Many of the studies performed to understand OA effects on picoplankton have used cultures (see Liu *et al.*, 2010 for a review). However, culture-based experiments, which are necessary to understand important physiological aspects, might not reflect the indirect effects that occur through biological interactions. Assays with natural communities in containers that are as large as possible would be an appropriate tool, and mesocosm experiments have been identified as a good approach to ecosystem studies (Lawton, 1995; Duarte *et al.*, 2000; Thingstad *et al.*, 2007).

Table 1. Selection of representative published mesocosm experiments testing the effect of OA on microbes.

Site	Season	pCO_2 or pH levels assayed	Nutrients added	pH manipulation	References
Coastal, North Sea	June 2011	Decrease of 0.4 pH units	NO_3+PO_4+Si	CO_2	Calbet *et al.* (2014)
Coastal, Greenland Sea	May 2010	145–1050 ppm	NO_3+PO_4+Si	CO_2	Motegi *et al.* (2013), Roy *et al.* (2013), Piontek *et al.* (2013), Schulz *et al.* (2013), Brussaard *et al.* (2013)
Open ocean, Greenland Sea	June 2009	250–400 ppm	NO_3+PO_4+Si	Acid	Ray *et al.* (2012)
Coastal, East China Sea	Jan. 2009	800 and 1200 ppm	NO_3+PO_4+Si	CO_2	Hama *et al.* (2012)
Coastal, East China Sea	Nov. 2008	400 and 900 ppm	$NO_3+NO_2+PO_4+Si$	CO_2	Kim *et al.* (2013)
Coastal, Baltic Sea	Mar. 2008	Decrease of 0.4 pH units	None	CO_2	Lindh *et al.* (2013)
Coastal, North Sea	May 2006	750 ppm	NO_3+PO_4	CO_2	Newbold *et al.* (2012), Meakin and Wyman (2011)
Coastal, North Sea	May 2005	350–1050 ppm	NO_3+PO_4	CO_2	Allgaier *et al.* (2008), Paulino *et al.* (2008)
Coastal, North Sea	Spring 2003	190–750 ppm	NO_3+PO_4+Si	CO_2	Grossart *et al.* (2006), Engel *et al.* (2008), Arnosti *et al.* (2011)
Coastal, NW Mediterranean	Feb. 2010 & July 2011	7.5–8.3 units in pH, variable pH, see Figure 1	None/ NO_3+PO_4+Si	CO_2	This study

Until now, few such mesocosm experiments have addressed OA effects on picoplankton (Table 1). Although comparative analyses are difficult because of differences between experimental set-ups, in general these experiments show a stimulatory effect of OA on photosynthetic picoeukaryotes and nanoeukaryotes (Paulino *et al.*, 2008, Newbold *et al.*, 2012, Brussaard *et al.*, 2013) and complex responses of heterotrophic prokaryotes, which often follow the dynamics of large phytoplankton (Grossart *et al.*, 2006, Allgaier *et al.*, 2008, Arnosti *et al.*, 2011). However, most of these experiments were conducted under high nutrient concentrations, either because they were high in the initial water (Lindh *et al.*, 2013) or because nutrient was added to produce a phytoplankton bloom (e.g. Riebesell *et al.*, 2013). Therefore, these experiments have provided important information on the effects of OA under eutrophic conditions, but not under oligotrophic conditions, which are those that prevail throughout the year in most open-ocean surface waters. Furthermore, mesocosm experiments to test the effects of OA on natural microbial planktonic communities have mostly been conducted at high latitudes [e.g. in the Arctic (Ray *et al.*, 2012) and in the Baltic Sea (Lindh *et al.*, 2013)], while at lower latitudes only two experiments have been published (Hama *et al.*, 2012; Kim *et al.*, 2013) (Table 1). Our knowledge of the responses of microbes to acidification in medium- or low-latitude oligotrophic oceans is still very poor (Maugendre *et al.*, 2015).

The NW Mediterranean is an oligotrophic temperate sea that exhibits contrasting seasonal nutrient and phytoplankton levels in winter vs. summer (e.g. Gasol *et al.*, 2012). The planktonic phytoplankton communities also show contrasting composition, while in winter microphytoplankton are dominant, in summer nano- and picoplankton phototrophs are dominant. The high alkalinity and active overturning circulation of this area compared with the global oceans must involve higher absorption and penetration of anthropogenic CO_2, although it is not clear whether this high penetration translates into a pH decrease (Palmiéri *et al.*, 2014). These characteristics (oligotrophy, seasonality, and high alkalinity) might very well be fundamental in determining the effects of acidification on microbes, but no results have been presented on the variability of the response of the Mediterranean microbial communities to OA in different seasons.

To gain insight into the consequences of acidification of marine ecosystems, we evaluated the effects of OA on microbial dynamics experimentally in NW Mediterranean waters, and determined the importance of contrasting community composition (i.e. winter vs. summer communities) and different levels of nutrient concentrations on the observed responses. We will use the term OA throughout the manuscript to refer to a high pCO_2 level.

Material and methods

Experimental setup

We conducted two experiments: one in winter 2010, during the period of maximum chlorophyll *a* concentration in the area, and one in summer 2011, when chlorophyll *a* is at its annual low in the area (Gasol *et al.*, 2012). Common features of the two experiments were the following: Eight 200-L polyethylene tanks were filled with coastal surface water from the Blanes Bay Microbial Observatory (BBMO), NW Mediterranean, 1 km offshore (41°40′N 2°48′E). The experiments were conducted in a temperature-controlled chamber, set at *in situ* temperature and with a light : dark cycle of 12:12 h. The light conditions were set by a combination of cool-white and GRO-LUX lamps, which mimic the quality of natural light. The pH manipulation was performed by bubbling very small amounts of CO_2 (99.9% purity) directly into the mesocosms. This addition was performed manually every morning, in order to maintain the levels of pH in the acidified tanks ~0.25–0.30 pH units lower than the controls. This pH lowering is equivalent to that expected by the end of the century with atmospheric CO_2 concentrations of 750–800 ppm (Joos *et al.*, 2011). The lowering of pH was closely monitored using glass electrodes (LL Ecotrode plus—Metrohm), which were calibrated on a daily basis with a Tris buffer, following standard procedures (SOP6a of Dickson *et al.*, 2007). The pH in the tanks was continuously recorded by a D130 data logger (Consort, Belgium). In order to mimic the physical perturbation associated with CO_2 bubbling, the control tanks were also bubbled with similar small amounts of compressed air at current atmospheric CO_2 concentrations.

Four experimental conditions were randomly assigned to duplicated tanks: KB_1 and KB_2 (controls), KA_1 and KA_2 (pH-modified), NB_1 and NB_2 (nutrient amended), and NA_1 and NA_2 (nutrient

Table 2. Summary of the *in situ* and experimental conditions.

	Winter		Summer	
In situ conditions				
Temperature (°C)	13		22	
Light intensity (μmol m^{-2} s^{-1})	110		1001	
pH	8.045		8.069	
Salinity	37.92		37.83	
Total alkalinity (μmol kg^{-1})	2533		2540	
Chlorophyll *a* (μg l^{-1})	0.96		0.20	
Experimental conditions				
Temperature (°C)	14		22	
Light intensity (μmol m^{-2} s^{-1})	121		217–261	
	K	*N*	*K*	*N*
Average pH lowering	0.18	0.13	0.28	0.28
NO_3+NO_2 concentration (μM)	3.11	16.8	0.39	4.69
PO_4 concentration (μM)	0.14	1.14	0.02	0.24
SiO_4 concentration (μM)	2.01	31.0	0.34	6.51

Initial conditions are variables measured in Blanes Bay at the time of sampling on the dates of the experiments: winter (17 February 2010) and summer (6 July 2011). Experimental conditions are the temperature of the incubation chamber, the light intensity measured inside the microcosms, nutrient concentrations added in the *N* treatments, and the average lowering of pH in the acidified treatments vs. controls (days 2–9).

amended and pH modified). We gradually modified the pH (in the A treatments) starting immediately after mesocosm filling, and the following day we added inorganic nutrients (to the N treatments) to reach a final molar ratio of 1 : 16 : 30 and 0.25 : 4 : 8 (P : N : Si) in the winter and summer experiments, respectively (Table 2). In both cases, the nitrogen enrichment was close to 8× the monthly average concentration measured in the BBMO during the last 10 years. Nitrogen and phosphorus were added at the Redfield ratio, whereas silicate was added in excess to assure no limitation for diatoms.

In the winter experiment (see initial conditions of the experiments in Table 2), the temperature of the chamber was set to 14 ± 1°C, and the measured light intensity inside of the containers was 121.3 ± 3.5 μmol m^{-2} s^{-1}. In the summer experiment, temperature was set to 22 ± 1°C, and the actual light intensity in the tanks ranged from 217 to 261 μmol m^{-2} s^{-1}.

The pH in the acidified treatments was lowered initially to values ~7.81 units in the winter experiment, which were achieved in the third day, and later they were manipulated to mimic the evolution of the corresponding control (with and without nutrients), but ~0.2 pH units lower. In the summer experiment, pH was progressively lowered in the acidified treatments with the aim of maintaining a relatively constant offset of ~0.2–0.3 units in pH in comparison with the controls.

Chemical parameters

Prior to each morning's controlled addition of CO_2, we measured pH and alkalinity precisely in all the mesocosms. pH was measured by spectrophotometry after the addition of m-cresol purple (Clayton and Byrne, 1993) and alkalinity was determined with a fast, single-point potentiometric titration (Perez *et al.*, 2000). Samples for inorganic nutrients were kept frozen at −20°C until analysis, which was performed using a CFA Bran + Luebbe autoanalyser following the methods described by Hansen and Koroleff (1999).

Chlorophyll *a* was measured according to the procedure of Yentsch and Menzel (1963). Briefly, 50 ml were filtered through Whatman GF/F glass fibre filters. The filters were placed in 90% acetone at 4°C for 24 h and the fluorescence of the extract was measured using a Turner Designs fluorometer.

Microbial abundances

Pico- and nanophytoplankton and bacterial abundance were determined by flow cytometry (Gasol and del Giorgio, 2000). For pico- and nanophytoplankton, the samples were analysed without addition of fixative and run at high speed (ca. 100 μl min^{-1}). Phototrophic populations (*Prochlorococcus*, *Synechococcus*, two groups of picoeukaryotes [small and large] and nanoeukaryotes) were discriminated according to their scatter and fluorescence signals. For heterotrophic bacteria, abundances were estimated after fixing 1.2-ml samples with a 1% paraformaldehyde + 0.05% glutaraldehyde solution, and deep-freezing in liquid N_2. Afterwards, the samples were unfrozen, stained with SybrGreen at a 10× dilution and run at low speed (ca. 15 μl min^{-1}). Cells were identified in plots of side scatter vs. green fluorescence and green vs. red fluorescence.

Microphytoplankton counts were performed after fixing the sample with formalin–hexamine (0.4% final concentration). Afterwards, 50 ml of each sample was placed in sedimentation columns for 24 h. The sedimentation chamber was then scanned in an inverted microscope at ×100 and ×400 magnification.

Bacterial activity

Bacterial heterotrophic activity was estimated using the ^{3}H-leucine incorporation method (Kirchman *et al.*, 1985). Quadruplicate aliquots of 1.2 ml and two trichloroacetic acid (TCA)-killed controls were taken immediately after sample collection. The samples were incubated with 40 nM ^{3}H-leucine (final concentration) for ~1.5 h in the dark in a temperature-regulated room. The incorporation was stopped with the addition of 120 μl of cold TCA 50% to each replicate and the samples were kept frozen at −20°C until processing, which was carried out by the centrifugation method described by Smith and Azam (1992).

Extracellular enzyme activities

The activity of four hydrolytic extracellular enzymes was assayed using fluorogenic substrates that are molecules linked to 4-methylumbelliferone (MUF) or 4-methylcoumarinyl-7-amide, following the method described in Sala and Gude (1999) and adapted to the use of microplates. The enzymes studied were α-glucosidase, β-glucosidase, chitobiase, and leu-aminopeptidase; and the substrates used were 4-methylumbelliferyl α-D-glucopyranoside, 4-methylumbelliferyl β-D-glucopyranoside, 4-methylumbelliferyl *N*-acetyl-β-D-glucosaminide, and L-leucine-7-amido-4-methyl coumarin. The assays were arrayed in black, 96-well microplates using a protocol similar to that in Sala *et al.* (2010). For each enzyme, 350 μl of the sample was added to a well together with 50 μl of substrate solution. Each assay was replicated in four wells. The substrate solutions were prepared in sterile deionized water and methanol 1% at a final concentration of 1 mM, yielding a final substrate concentration of 125 μM in the assay wells. Fluorescence was measured regularly at different times for 5 h using a Modulus microplate reader set to an excitation wavelength of 365 nm and an emission wavelength of 450 nm. Fluorescence units were transformed into activity using a standard curve prepared with the end product of the reactions: 7-amido-4-methylcoumarin for leu-aminopeptidase and MUF for the rest of the enzymes.

Statistical analysis

We used STATISTICA version 8.0 (StatSoft, Inc., 2007) for the statistical analyses. To test the hypothesis that there were no effects of acidification within treatments of the same experiment and nutrient addition, we used independent two-tailed *t*-tests. The overall differences between acidified and control treatments were tested with sign tests (Figure 2). Data from day 3 to 9 were chosen for both analyses because it was during this period that the effects of acidification were more conspicuous.

Results

A difference in pH in the range of 0.1–0.5 was maintained between the acidified and control mesocosms in both experiments (Figure 1a and b). In summer, pH varied only slightly between the nutrient-enriched and non-enriched conditions. However, in winter, the intense phytoplankton bloom in the nutrient-enriched treatments (up to 29.6 μg chlorophyll *a* l^{-1}, Figure 1) induced an increase of pH on day 5, reaching levels of up to 8.3 pH units in the non-acidified enriched treatment.

We examined the effects of pH in our set of measured parameters with independent *t*-tests (Table 3). Chlorophyll *a* concentration was positively affected by acidification (Figure 1c and d) except in the nutrient-enriched treatment of the winter experiment, in which no effects were observed (Table 3). The composition of the winter and summer blooms also differed considerably: diatoms of the genus *Thalasssiosira*, *Chaetoceros*, and *Pseudo-nitzschia* dominated the winter bloom (80% of the abundance of the phytoplankton community), whereas the summer community was mostly composed of small pico- and nanoflagellates. No effect of acidification on diatoms was observed, and both positive and negative effects on dinoflagellates were observed (Table 3). The abundances of phototrophic nanoeukaryotes and of large picoeukaryotes were consistently positively affected by acidification (Table 3), with significant differences in both experiments.

Although the initial abundances of heterotrophic bacteria were similar in both seasons ($5–8 \times 10^5$ cells ml^{-1}), their concentration during the experiment increased more in winter than in summer, to maximum values of 4.5×10^6 cells ml^{-1} (Figure 1). The abundance of the different groups of prokaryotes (heterotrophic bacteria, *Synecchococcus*, and *Prochlorococcus*) and leucine incorporation showed a stimulation effect in non-enriched conditions in summer. However, we also found a negative effect of acidification in winter with the nutrient-enriched treatment for *Synechococcus* (Table 3).

Among the four bacterial extracellular enzyme activities tested, α- and β-glucosidase were affected by acidification in summer (Table 3). The other enzyme activities, leu-aminopeptidase, and chitobiase were not affected by acidification under any of the conditions tested.

To summarize the main results obtained, Figure 2 shows a comparison of the abundances of the main groups of organisms between the control and acidified pairs of mesocosms in the two experiments (filled circle, winter; empty circle, summer). To compare the general trends of the effects of acidification on the measured variables, we performed a sign test, i.e. a non-parametric test aimed at comparing pairs of data of acidified vs. non-acidified treatments. The sign test revealed no significant global differences between treatments for heterotrophic bacteria and *Synechococcus* (a negative sign of acidification effect in winter neutralized the positive sign in summer). In contrast, significantly higher concentrations were found in acidified treatments for nanoeukaryotes ($n = 56$; $p < 0.001$), large picoeukaryotes ($n = 56$; $p < 0.001$), and chlorophyll *a* concentrations ($n = 54$; $p < 0.001$) (Figure 2).

Discussion

We assessed the response of the microbial community to a decrease in pH in the Mediterranean. Because in the likely future ocean the response of the microbial planktonic community to OA will interact with other stressors linked to global change, such as eutrophication and increased temperature, we tried to deepen our understanding of possible OA-eutrophication interactions. The major findings of this study are (i) phototrophic pico- and nanoeukaryotes were consistently stimulated by acidification; (ii) prokaryotic picoplankton and phototrophic microplankton exhibited different responses to acidification in winter and summer; and (iii) overall, the magnitude of the acidification effects was lower under nutrient-rich conditions.

Effects of acidification on phototrophic pico- and nanoeukaryotes

We observed a consistent stimulation of the large pico- and nanoeukaryotic phototrophic communities in both winter and summer and in conditions with high and low nutrient levels (i.e. treatments). Stimulation of pico- or nanoeukaryotes by acidification has previously been reported in some mesocosm studies (Engel *et al.*, 2008, Newbold *et al.*, 2012, Brussaard *et al.*, 2013, Calbet *et al.*, 2014), although no effect or a negative effect has also been observed (Paulino *et al.*, 2008, Calbet *et al.*, 2014). Here, the positive effect found in most of the experimental conditions contrasts with the negative effect observed in dinoflagellates in the winter, nutrient-enriched conditions. These divergent results might be due to differences in the species-specific sensitivities to CO_2, in accordance with different carbon concentration mechanisms (CCMs; Rost *et al.*, 2003). Eutrophication and pH decreases are predicted in coastal waters for the near future (IPCC, 2013). In such scenarios, our results suggest that small phototrophic organisms will show a relative increase in comparison with large ones. Temperature rises will also promote small-sized organisms (Morán *et al.*, 2009). These changes in size distribution will affect food web interactions and sedimentation processes (Legendre and Le Fèvre, 1991), which should be considered when it is attempted to predict the likely communities of a future ocean.

Effects of acidification in winter vs. summer

The number of variables affected by acidification in the controls was lower in winter than in summer, and the sign of the responses was always positive in summer, whereas in winter it was negative for *Synechococcus* and dinoflagellates (Table 3). This differential response to acidification in the two experiments suggests a clear role of the initial community composition and environmental trophic conditions. Blanes Bay surface waters exhibit a temperate seasonal cycle with a winter phytoplankton bloom driven in part by elevated nutrient concentrations, typically with diatom dominance, and a summer period dominated by picophytoplankton, microheterotrophs, and low inorganic nutrient concentrations (Alonso-Sáez *et al.*, 2008; Gasol *et al.*, 2012). Contrasting with phototrophic pico- and nanoeukaryotes, which showed a similar number of positive responses in both seasons, all prokaryotes were affected positively in summer and no effects, or negative effects, were detected in winter (Table 3). The only study that evaluated the planktonic community response to OA in different seasons, conducted in 1-l bottles in the Baltic Sea, showed no clear differences in acidification effects on bacterial abundance and diversity during

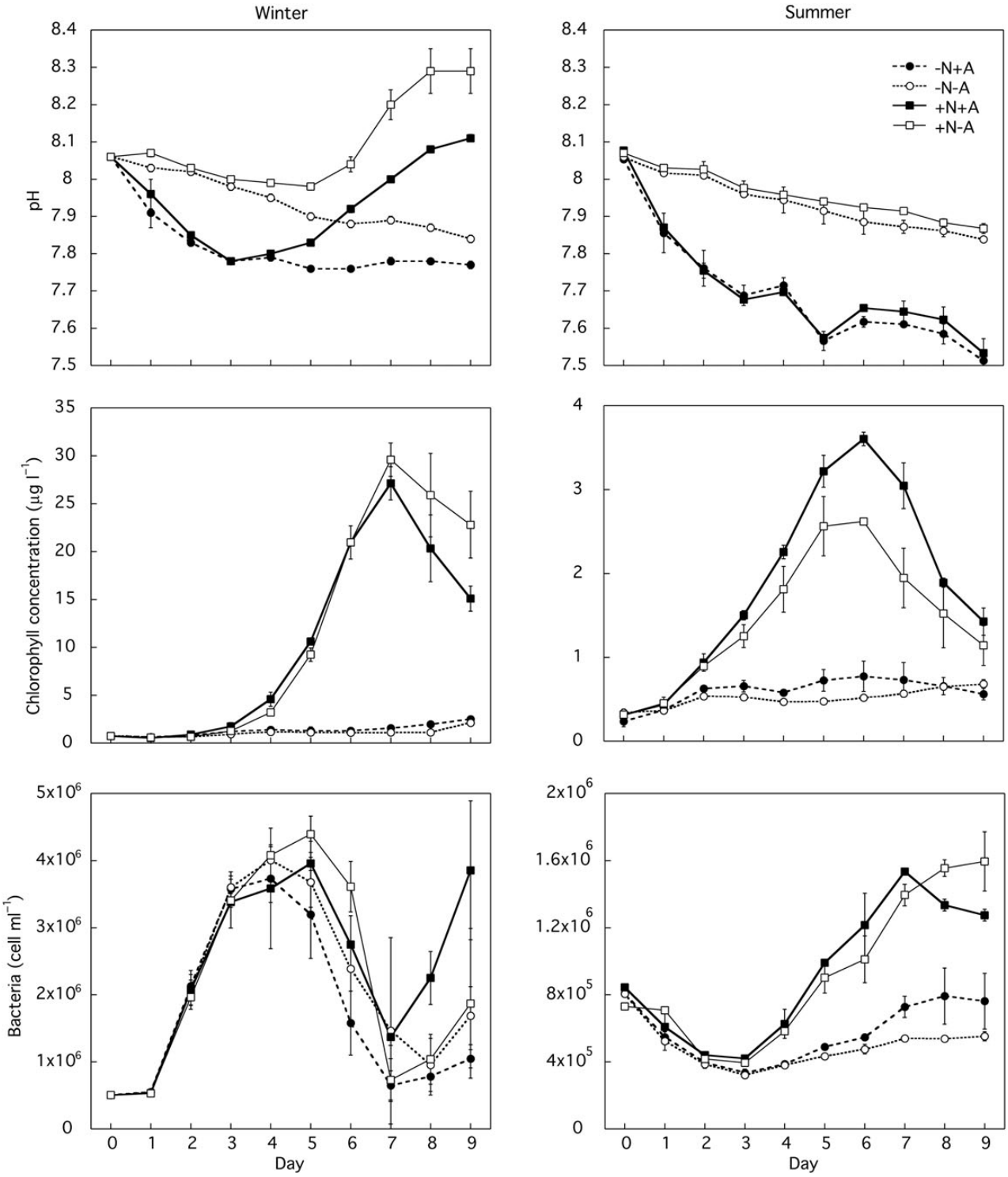

Figure 1. Evolution of pH, chlorophyll concentration, and bacterial abundance in the winter (left panels) and summer (right panels) experiments. Squares, nutrient-amended treatments; circles, controls without nutrient additions; full symbols, acidified treatments; empty symbols, and non-acidified treatments. Error bars denote standard deviations for duplicate treatments.

the year (Krause *et al.*, 2012). Ours is the first study to show differences between winter and summer in the prokaryote response to OA. The higher number of effects of acidification in summer than in winter may be related to differences in initial species composition, but also to the different nutrient levels or to a combination of both factors (see next section).

Cyanobacteria are known to use CCMs to actively transport inorganic C species and maintain their growth even at low external dissolved inorganic carbon concentrations (Badger and Price, 2003). Therefore, it is reasonable to assume that, at increased CO_2, the need for CCMs would decrease, and this would result in energy savings that could be allocated to growth. Indeed, several

Table 3. Results of independent *t*-tests for various abundance and microbial activity data.

	Winter		Summer	
	−Nutrients	+Nutrients	−Nutrients	+Nutrients
Parameter				
Chlorophyll *a* (μg l^{-1})	0.041		0.007	0.046
Chlorophyll *a* < 3 μm (μg l^{-1})				
Microplankton (cell l^{-1})				
Diatoms				
Dinoflagellates		0.031	0.004	
Picoplankton (cell ml^{-1})				
Nanoeukaryotes	<0.001	0.014		
Large picoeukaryotes			0.002	0.049
Small picoeukaryotes				
Prokaryotes (cell ml^{-1})				
Synechococcus		<0.001	<0.001	
Prochlorococcus			0.020	
Heterotrophic bacteria			0.050	
Prokaryotic activity				
Leucine incorporation			0.001	
Leu-aminopeptidase				
Chitobiase				
α-Glucosidase			0.050	
β-Glucosidase			0.010	<0.000

Comparison between acidified and control duplicate treatments after day 3. Numbers correspond to *p*-values and only those <0.05 are shown. Light grey denotes the positive effect and dark grey denotes the negative effect of acidification.

culture-based studies have found a stimulation of the growth rate or CO_2 fixation in cyanobacteria with acidification (Fu *et al.*, 2007; Hutchins *et al.*, 2009). However, negative responses to acidification were found in our winter experiment and also in some previous mesocosm studies (e.g. Paulino *et al.*, 2008).

The recent literature tends to suggest that the impact of OA on bacterioplankton community composition is negligible (Ray *et al.*, 2012, , 2013), but compositional shifts (Lindh *et al.*, 2013; Krause *et al.*, 2012) and strain-dependent effects (Teira *et al.*, 2012) have also been encountered. Studies in nutrient-enriched mesocosms have reported decreases (Rochelle-Newall *et al.*, 2004; Grossart *et al.*, 2006) or lack of effects (Allgaier *et al.*, 2008) in bacterial abundance in acidified conditions. In addition, contrasting results were also found in the magnitude and direction of the effect of OA on bacterial activity (Grossart *et al.*, 2006; Allgaier *et al.*, 2008; Motegi *et al.*, 2013).

We also looked at specific functions mediated by heterotrophic bacteria, such as the extracellular enzymatic activities which mediate important biogeochemical processes such as the decomposition and transformation of organic carbon and the release of nutrients (Hoppe, 1983). Still very little is known about the direct effects of OA on extracellular enzyme activities, but effects could be expected since changes in pH have direct effects on the functioning of enzymes in bacterial cultures (Page *et al.*, 1988). However, the results to date have been controversial (see Cunha *et al.*, 2010, for a review). Some authors have found that OA stimulated the activity of a set of extracellular enzymes in different environments (Grossart *et al.*, 2006; Piontek *et al.*, 2010, 2013; Maas *et al.*, 2013), but others reported a lack of stimulation (Arnosti *et al.*, 2011; Engel *et al.*, 2014). In our study, the only enzyme activities for which we found some effect were α- and β-glucosidases, which mediate the final step of the hydrolysis of polysaccharides. Similar to the bulk heterotrophic activity, both glucosidase activities were higher in summer under acidified treatments; Piontek *et al.* (2010) and Maas *et al.* (2013) similarly observed increased β-glucosidase activities under OA. These results suggest higher hydrolysis of carbohydrates. Since carbohydrates represent a large fraction in the composition of organic aggregates of marine ecosystems, an increase in glucosidase activities might contribute to changes in the degradation patterns of different types of organic matter, which could eventually lead to a reduction of the strength of the biological pump in the future ocean.

Effects of nutrient addition on OA

In general, effects of OA on plankton communities have been studied under high nutrient concentrations, either induced or natural (Table 1), and the combined effects of extra inorganic carbon and nutrients promoted phytoplankton growth on most occasions. It is noteworthy that in our experiments the effects of acidification on bacterial abundance and production were more evident in the treatments with the lowest nutrient concentrations. Moreover, the amendment with nutrients altered the responses of phototrophic picoeukaryotes and microplankton. Overall, the compilation of variables that were significantly affected by acidification in our experiment (Table 3) shows that the treatment with the clearly lowest nutrient concentrations (summer non-enriched, see Table 2) had a higher number of variables with significant responses to acidification ($n = 9$) than the other treatments ($n = 2–3$).

The most similar approximation to our study in terms of nutrient dynamics is the EPOCA mesocosm experiment, in which a set of very large enclosures manipulated with CO_2 were enriched in nutrients only after day 14 (Riebesell *et al.*, 2013). In that study, unlike in ours, no significant effects on the abundance of any of the analysed planktonic groups were observed before nutrient addition. However, contrasting responses of phytoplankton abundance and activity to OA (from positive to negative) were observed between the first and the second bloom phases of their study. In the EPOCA experiment, nutrients were added at a point when treatments might have evolved differently during the first few days of the experiment. Although their results cannot be directly compared

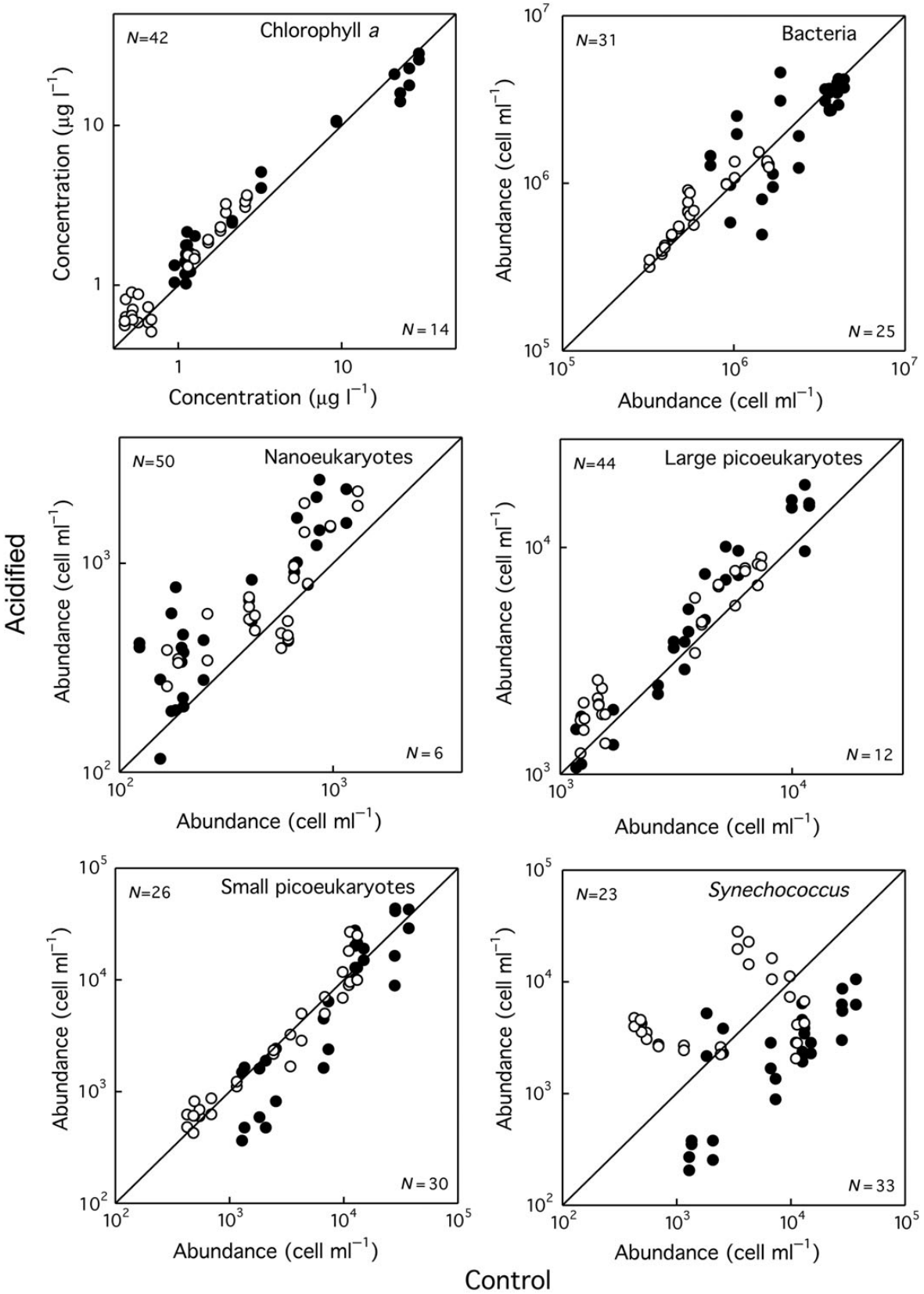

Figure 2. Concentration of chlorophyll *a*, heterotrophic bacteria, and photosynthetic picoplankton groups in acidified vs. non-acidified treatments. Empty symbols, summer experiment; full symbols, winter experiment. The *N* in the upper left corner corresponds to the number of cases in which the value of the acidified treatment is higher than that of the non-acidified treatment. The *N* in the lower right corner is the number of cases with values lower in the non-acidified than in the acidified treatment.

with ours, the present findings corroborate their conclusions about the importance of examining the effect of acidification in contrasting stages of plankton community succession. They evaluated different phases of succession by conducting longer experiments than ours (1 month), whereas we collected natural water in two different seasons with divergent community structures. The initial percentage of diatoms with respect to the total phytoplankton cells was 22% in winter and 2% in summer, a finding that could explain the clear positive response of chlorophyll in summer in contrast with the low response in winter. This result agrees with those of Riebesell *et al.* (2013), in which diatoms responded negatively to acidification. Different photosynthetic groups reacting in opposite ways and indirect effects mediated by changes in prey biochemical composition (i.e. changing the food quality of prey; Schoo *et al.*, 2012) would induce changes in the community structure of grazers, which in turn would feed back on their prey. For instance, if different predators are favoured, then a different nutrient competition could be established between prokaryotes and microphytoplankton, etc. The existence of these complex interdependences requires further research on multiple trophic interactions when ecosystem responses to acidification are evaluated.

At a smaller scale (4-l bottles), a recent study in the Mediterranean reported a very limited impact of OA on the planktonic communities of nutrient-depleted waters (Maugendre *et al.*, 2015). This experiment could be closely related to our work because of the area of study, although the original community may have been different. The species-specific responses to nutrient additions and acidification, usually veiled by bulk analyses (chlorophyll, cytometry, etc.), may be the key to explaining the discrepancies between that study and ours. As seen above, many groups benefit from nutrient additions and OA. Others, however, may be outcompeted by faster-growing species with better capabilities of incorporating and accumulating CO_2.

The fact that we observed a larger number of effects of acidification under low nutrient concentrations emphasizes the importance of running experiments under natural conditions. When the effects of OA on very productive communities need to be investigated, it would be advisable to conduct the experiments during natural bloom situations, rather than generating an artificial one. In addition, to better represent the natural environmental conditions, we advise that research should focus on communities of areas of great importance that remain mostly unexplored so far, such as the oligotrophic ocean.

The duration of the mesocosm experiment is an additional important variable to consider. Normally, mesocosm studies on planktonic communities have been conducted over timescales ranging from days to one month. Experimentation over longer periods of time would be interesting to address issues related to acclimation and adaptation. However, prolonging mesocosm experiments for too long is not trivial, and there is an inherent danger of driving the community away from the real world over time (i.e. due to wall effects, unreal water mixing, etc.). In our case, though the 9-d experiment is too short to be meaningful for assessing potential acclimation/adaptation, it is set up over a temporal pH variability that parallels the real world, particularly in the coastal areas. These environments often exhibit natural short-term changes in seawater at scales of days or even hours of similar magnitude to that induced in our experiments. Furthermore, progressive OA due to anthropogenic CO_2 emissions superimposed on these short-term pH changes will induce similar changes to those experienced by our mesocosm communities.

Further understanding of OA effects on plankton communities will come from the integration of single-species studies, short mesocosm experiments such as the present one, field observations in naturally or artificially acidified environments and ecosystem modelling, together with data on potential acclimation and adaptation through multi-generational studies.

As a general trend, in our study we observed a stimulatory effect of OA on the abundance of small phytoplankton (pico- and nanoeukaryotes) independently of the nutrients added. Considering the effects of combining acidification and eutrophication, our observations point towards a lower sensitivity of the microbial community to OA under eutrophic conditions, which may have implications on the interpretation of the effects of OA in coastal and more nutrient-rich systems compared with oligotrophic open-ocean environments. They also highlight the need for comparative experimental studies during different periods of the year and with different levels of nutrient concentrations to provide a broader assessment of the effects of acidification on marine ecosystems

Supplementary data

Supplementary material is available at the *ICESJMS* online version of the manuscript.

Acknowledgements

The authors thank Despoina Sousoni, Berta de la Vega and Anderson Cabral for research assistance. Financial support from the Spanish Ministry of Economy and Competitiveness is acknowledged, specifically through the projects STORM (CTM2009–09352), DOREMI (CTM2012-34294), MANIFEST (CTM2012-32017), and PROTOS (CTM2009-08783) of the Spanish Ministry of Economy and Competitiveness. We are also grateful for the financial support of the Generalitat de Catalunya to the "Grup de Diversitat Microbiana en Ecosistemes Acuàtics" (2014SGR/1591) and the "Grup d'Estructura i Funció de Xarxes Tròfiques Microbianes Planctòniques" (2014SGR/1179).

References

Allgaier, M., Riebesell, U., Vogt, M., Thyrhaug, R., and Grossart, H. P. 2008. Coupling of heterotrophic bacteria to phytoplankton bloom development at different pCO_2 levels: a mesocosm study. Biogeosciences, 5: 1007–1022.

Alonso-Sáez, L., Vazquez-Domínguez, E., Cardelus, C., Pinhassi, J., Sala, M. M., Lekunberri, I., Balagué, V., *et al.* 2008. Factors controlling the year-round variability in carbon flux through bacteria in a coastal marine system. Ecosystems, 11: 397–409.

Arnosti, C., Grossart, H. P., Muehling, M., Joint, I., and Passow, U. 2011. Dynamics of extracellular enzyme activities in seawater under changed atmospheric pCO_2: a mesocosm investigation. Aquatic Microbial Ecology, 64: 285–298.

Badger, M. R., and Price, G. D. 2003. CO_2 concentrating mechanisms in cyanobacteria: molecular components, their diversity and evolution. Journal of Experimental Botany, 54: 609–622.

Brussaard, C. P. D., Noordeloos, A. A. M., Witte, H., Collenteur, M. C. J., Schulz, K. G., Ludwig, A., and Riebesell, U. 2013. Arctic microbial community dynamics influenced by elevated CO^2 levels. Biogeosciences, 10: 719–731.

Calbet, A., Sazhin, A. F., Nejstgaard, J. C., Berger, S. A., Tait, Z. S., Olmos, L., Sousoni, D., *et al.* 2014. Future climate scenarios for a coastal productive planktonic food web resulting in microplankton phenology changes and decreased trophic transfer efficiency. PLoS ONE, 9/journal.pone.0094388.

Clayton, T. D., and Byrne, R. H. 1993. Spectrophotometric seawater pH measurements – total hydrogen-ion concentration scale calibration of m-cresol purple and at-sea results. Deep-Sea Research Part I-Oceanographic Research Papers, 40: 2115–2129.

Cunha, A., Almeida, F. J. R. C., Coelho, N. C. M., Gomes, V., Oliveira, V., and Santos, A. L. 2010. Bacterial extracellular enzymatic activity in globally changing aquatic ecosystems. *In* Current research, Technology and Education Topics in Applied Microbiology and Microbial Biotechnology, pp. 124–135. Ed. by A. Méndez-Vilas. Formatex Research Center.

Dickson, A. G., Sabine, C. L., and Christian, J. R. 2007. Guide to Best Practices for Ocean CO_2 measurements. North Pacific Marine Science Organization, Sidney, BC. 191 pp.

Doney, S. C., Balch, W. M., Fabry, V. J., and Feely, R. A. 2009. Ocean acidification: a critical emerging problem for the ocean sciences. Oceanography, 22: 16–25.

Duarte, C. M., Agustí, S., Gasol, J. M., Vaqué, D., and Vázquez-Domínguez, E. 2000. Effect of nutrient supply on the biomass structure of planktonic communities: an experimental test on a Mediterranean coastal community. Marine Ecology Progress Series, 206: 87–95.

Engel, A., Piontek, J., Grossart, H. P., Riebesell, U., Schulz, K. G., and Sperling, M. 2014. Impact of CO_2 enrichment on organic matter dynamics during nutrient induced coastal phytoplankton blooms. Journal of Plankton Research, 36: 641–657.

Engel, A., Schulz, K. G., Riebesell, U., Bellerby, R., Delille, B., and Schartau, M. 2008. Effects of CO_2 on particle size distribution and phytoplankton abundance during a mesocosm bloom experiment (PeECE II). Biogeosciences, 5: 509–521.

Fu, F - X., Warner, M. E., Zhang, Y., Feng, Y., and Hutchins, D. A. 2007. Effects of increased temperature and CO_2 on photosynthesis, growth, and elemental ratios in marine *Synechococcus* and *Prochlorococcus* (Cyanobacteria). Journal of Phycology, 43: 485–496.

Gasol, J. M., and Del Giorgio, P. A. 2000. Using flow cytometry for counting natural planktonic bacteria and understanding the structure of planktonic bacterial communities. Scientia Marina, 64: 197–224.

Gasol, J. M., Massana, R., Simó, R., Marrasé, C., Acinas, S. G., Pedrós-Alió, C., Pelejero, C., *et al.* 2012. Blanes Bay (site 55). *In* ICES Phytoplankton and Microbial Plankton Status Report 2009/2010. ICES Cooperative Research Report No. 313, pp. 138–141. Ed by T. D. O'Brien, W. K. W. Li, and X. A. G. Morán.

Grossart, H. P., Allgaier, M., Passow, U., and Riebesell, U. 2006. Testing the effect of CO_2 concentration on the dynamics of marine heterotrophic bacterioplankton. Limnology and Oceanography, 51: 1–11.

Hama, T., Kawashima, S., Shimotori, K., Satoh, Y., Omori, Y., Wada, S., Adachi, T., *et al.* 2012. Effect of ocean acidification on coastal phytoplankton composition and accompanying organic nitrogen production. Journal of Oceanography, 68: 183–194.

Hansen, H. P., and Koroleff, F. 1999. Determination of nutrients. *In* Methods of Seawater Analysis, pp. 159–228. Ed. by K. Grasshoff, K. Kremling, and M. Ehrhardt. Wiley-VCH, Weinheim, Germany.

Harvey, B. P., Gwynn-Jones, D., and Moore, P. J. 2013. Meta-analysis reveals complex marine biological responses to the interactive effects of ocean acidification and warming. Ecology and Evolution, 3: 1016–1030.

Hoppe, H. G. 1983. Significance of exoenzymatic activities in the ecology of brackish water: measurements by means of methylumbelliferyl-substrates. Marine Ecology Progress Series, 11: 299–308.

IPCC. 2013. Climate change 2013: the physical science basis. Contribution of Working Group I to the Fifth Assessment Report of the Intergovernmental Panel on Climate Change. Cambridge University Press, Cambridge, New York. 1535 pp.

Joos, F., Frölicher, T. L., Steinarcher, M., and Plattner, G -K. 2011. Impact of climate change mitigation on ocean acidification projections. *In* Ocean Acidification, pp. 272–290. Ed. by J. P. Gattuso, and L. Hanson. Oxford University Press, Oxford.

Kim, J. H., Kim, K. Y., Kang, E. J., Lee, K., Kim, J. M., Park, K. T., Shin, K., *et al.* 2013. Enhancement of photosynthetic carbon assimilation efficiency by phytoplankton in the future coastal ocean. Biogeosciences, 10: 7525–7535.

Kirchman, D., Knees, E., and Hodson, R. 1985. Leucine incorporation and its potential as a measure of protein-synthesis by bacteria in natural aquatic systems. Applied and Environmental Microbiology, 49: 599–607.

Krause, E., Wichels, A., Gimenez, L., Lunau, M., Schilhabel, M. B., and Gerdts, G. 2012. Small changes in pH have direct effects on marine bacterial community composition: a microcosm approach. PLoS ONE, 7/journal.pone.0047035.

Kroeker, K. J., Kordas, R. L., Crim, R. N., and Singh, G. G. 2010. Meta-analysis reveals negative yet variable effects of ocean acidification on marine organisms. Ecology Letters, 13: 1419–1434.

Lawton, J. H. 1995. Ecological experiments with model systems. Science, 269: 328–331.

Legendre, L., and Le Fèvre, J. 1991. From individual plankton cells to pelagic marine ecosystems and to global biogeochemical cycles. *In* Particle Analysis in Oceanography, pp. 261–300. Ed. by S. Demers. NATO ASI Series, Springer-Verlag, Berlin.

Lindh, M. V., Riemann, L., Baltar, F., Romero-Oliva, C., Salomon, P. S., Graneli, E., and Pinhassi, J. 2013. Consequences of increased temperature and acidification on bacterioplankton community composition during a mesocosm spring bloom in the Baltic Sea. Environmental Microbiology Reports, 5: 252–262.

Liu, J. W., Weinbauer, M. G., Maier, C., Dai, M. H., and Gattuso, J -P. 2010. Effect of ocean acidification on microbial diversity and on microbe-driven biogeochemistry and ecosystem functioning. Aquatic Microbial Ecology, 61: 291–305.

Maas, E. W., Law, C. S., Hall, J. A., Pickmere, S., Currie, K. I., Chang, F. H., Voyles, K. M., *et al.* 2013. Effect of ocean acidification on bacterial abundance, activity and diversity in the Ross Sea, Antarctica. Aquatic Microbial Ecology, 70: 1–15.

Maugendre, L., Gattuso, J -P., Louis, J., de Kluijver, A., Marro, S., Soetaert, K., and Gazeau, F. 2015. Effect of ocean warming and acidification on a plankton community in the NW Mediterranean Sea. ICES Journal of Marine Science, 72: 1744–1755.

Meakin, N. G., and Wyman, M. 2011. Rapid shifts in picoeukaryote community structure in response to ocean acidification. The ISME Journal, 5: 1397–1405.

Morán, X. A. G., López-Urrutia, A., Calvo-Díaz, A., and Li, W. K. W. 2009. Increasing importance of small phytoplankton in a warmer ocean. Global Change Biology, 16: 1137–1144.

Motegi, C., Tanaka, T., Piontek, J., Brussaard, C. P. D., Gattuso, J -P., and Weinbauer, M. G. 2013. Effect of CO_2 enrichment on bacterial metabolism in an Arctic fjord. Biogeosciences, 10: 3285–3296.

Newbold, L. K., Oliver, A. E., Booth, T., Tiwari, B., DeSantis, T., Maguire, M., Andersen, G., *et al.* 2012. The response of marine picoplankton to ocean acidification. Environmental Microbiology, 14: 2293–2307.

Page, M. G. P., Rosenbusch, J. P., and Yamato, I. 1988. The effects of pH on proton sugar symport activity of the lactose permease purified from Escherichia coli. Journal of Biological Chemistry, 263: 15897–15905.

Palmiéri, J., Orr, J. C., Dutay, J -C., Beranger, K., Schneider, A., Beuvier, J., and Somot, S. 2014. Simulated anthropogenic CO_2 uptake and acidification of the Mediterranean Sea. Biogeosciences Discussions, 11: 6461–6517.

Paulino, A. I., Egge, J. K., and Larsen, A. 2008. Effects of increased atmospheric CO_2 on small and intermediate sized osmotrophs during a nutrient induced phytoplankton bloom. Biogeosciences, 5: 739–748.

Pelejero, C., Calvo, E., and Hoegh-Guldberg, O. 2010. Paleo-perspectives on ocean acidification. Trends in Ecology and Evolution, 25: 332–344.

Perez, F. F., Rios, A. F., Rellan, T., and Alvarez, M. 2000. Improvements in a fast potentiometric seawater alkalinity determination. Ciencias Marinas, 26: 463–478.

Peters, G. P., Marland, G., Le Quere, C., Boden, T., Canadell, J. G., and Raupach, M. R. 2012. Rapid growth in CO_2 emissions after the 2008–2009 global financial crisis. Nature Climate Change, 2: 2–4.

Piontek, J., Borchard, C., Sperling, M., Schulz, K. G., Riebesell, U., and Engel, A. 2013. Response of bacterioplankton activity in an Arctic fjord system to elevated pCO_2: results from a mesocosm perturbation study. Biogeosciences, 10: 297–314.

Piontek, J., Lunau, M., Haendel, N., Borchard, C., Wurst, M., and Engel, A. 2010. Acidification increases microbial polysaccharide degradation in the ocean. Biogeosciences, 7: 1615–1624.

Ray, J. L., Topper, B., An, S., Silyakova, A., Spindelbock, J., Thyrhaug, R., DuBow, M. S., *et al.* 2012. Effect of increased pCO_2 on bacterial assemblage shifts in response to glucose addition in Fram Strait seawater mesocosms. FEMS Microbiology Ecology, 82: 713–723.

Riebesell, U., Gattuso, J. P., Thingstad, T. F., and Middelburg, J. J. 2013. Arctic Ocean acidification: pelagic ecosystem and biogeochemical responses during a mesocosm study. Preface. Biogeosciences, 10: 5619–5626.

Rochelle-Newall, E., Delille, B., Frankignoulle, M., Gattuso, J -P., Jacquet, S., Riebesell, U., Terbruggen, A., *et al.* 2004. Chromophoric dissolved organic matter in experimental mesocosms maintained under different pCO_2 levels. Marine Ecology Progress Series, 272: 25–31.

Rost, B., Riebesell, U., Burkhardt, S., and Sultemeyer, D. 2003. Carbon acquisition of bloom-forming marine phytoplankton. Limnology and Oceanography, 48: 55–67.

Roy, A. S., Gibbons, S. M., Schunck, H., Owens, S., Caporaso, J. G., Sperling, M., Nissimov, J. I., *et al.* 2013. Ocean acidification shows negligible impacts on high-latitude bacterial community structure in coastal pelagic mesocosms. Biogeosciences, 10: 555–566.

Sala, M. M., Arrieta, J. M., Boras, J. A., Duarte, C. M., and Vaque, D. 2010. The impact of ice melting on bacterioplankton in the Arctic Ocean. Polar Biology, 33: 1683–1694.

Sala, M. M., and Gude, H. 1999. Role of protozoans on the microbial ectoenzymatic activity during the degradation of macrophytes. Aquatic Microbial Ecology, 20: 75–82.

Schoo, K. L., Malzahn, A. M., Krause, E., and Boersma, M. 2012. Increased carbon dioxide availability alters phytoplankton stoichiometry and affects carbon cycling and growth of a marine planktonic herbivore. Marine Biology, 160: 2145–2155.

Schulz, K. G., Bellerby, R. G. J., Brussaard, C. P. D., Budenbender, J., Czerny, J., Engel, A., Fischer, M., *et al.* 2013. Temporal biomass dynamics of an Arctic plankton bloom in response to increasing levels of atmospheric carbon dioxide. Biogeosciences, 10: 161–180.

Smith, D. C., and Azam, F. 1992. A simple, economical method for measuring bacterial protein synthesis rates in seawater using ^{3}H-leucine. Marine Microbial Food Webs, 6: 107–114.

Teira, E., Fernandez, A., Álvarez-Salgado, X. A., Garcia-Martin, E., Serret, P., and Sobrino, C. 2012. Response of two marine bacterial isolates to high CO_2 concentration. Marine Ecology Progress Series, 453: 27–36.

Thingstad, T. F., Havskum, H., Zweifel, U. L., Berdalet, E., Sala, M. M., Peters, F., Alcaraz, M., *et al.* 2007. Ability of a "minimum" microbial food web model to reproduce response patterns observed in mesocosms manipulated with N and P, glucose, and Si. Journal of Marine Systems, 64: 15–34.

Yentsch, C. S., and Menzel, D. W. 1963. A method for the determination of phytoplankton chlorophyll and phaeophytin by fluorescence. Deep-Sea Research, 10: 221–231.

Handling editor: Howard Browman

ICES Journal of Marine Science

ICES Journal of Marine Science (2016), 73(3), 680–692. doi:10.1093/icesjms/fsv259

Contribution to Special Issue: 'Towards a Broader Perspective on Ocean Acidification Research'

Original Article

Effects of high CO_2 levels on the ecophysiology of the diatom *Thalassiosira weissflogii* differ depending on the iron nutritional status

Koji Sugie*‡ and Takeshi Yoshimura

Central Research Institute of Electric Power Industry, 1646 Abiko, Abiko, Chiba 270-1194, Japan

*Corresponding author. tel: +81 46 867 9449; fax: +81 46 867 9455; e-mail: sugie@jamstec.go.jp

‡Present address: Research and Development Center for Global Change, Japan Agency for Marine-Earth Science and Technology, 2-15, Natsushima-cho, Yokosuka, Kanagawa 233-0061, Japan.

Sugie, K., and Yoshimura, T. Effects of high CO_2 levels on the ecophysiology of the diatom *Thalassiosira weissflogii* differ depending on the iron nutritional status. – ICES Journal of Marine Science, 73: 680–692.

Received 23 April 2015; revised 7 December 2015; accepted 8 December 2015; advance access publication 6 January 2016.

Iron availability in seawater, namely the concentration of dissolved inorganic iron ([Fe′]), is affected by changes in pH. Such changes in the availability of iron should be taken into account when investigating the effects of ocean acidification on phytoplankton ecophysiology because iron plays a key role in phytoplankton metabolism. However, changes in iron availability in response to changes in ocean acidity are difficult to quantify specifically using natural seawater because these factors change simultaneously. In the present study, the availability of iron and carbonate chemistry were manipulated individually and simultaneously in the laboratory to examine the effect of each factor on phytoplankton ecophysiology. The effects of various pCO_2 conditions (~390, ~600, and ~800 μatm) on the growth, cell size, and elemental stoichiometry (carbon [C], nitrogen [N], phosphorus [P], and silicon [Si]) of the diatom *Thalassiosira weissflogii* under high iron ([Fe′] = ~240 pmol l^{-1}) and low iron ([Fe′] = ~24 pmol l^{-1}) conditions were investigated. Cell volume decreased with increasing pCO_2, whereas intracellular C, N, and P concentrations increased with increasing pCO_2 only under high iron conditions. Si:C, Si:N, and Si:P ratios decreased with increasing pCO_2. It reflects higher production of net C, N, and P with no corresponding change in net Si production under high pCO_2 and high iron conditions. In contrast, significant linear relationships between measured parameters and pCO_2 were rarely detected under low iron conditions. We conclude that the increasing CO_2 levels could affect on the biogeochemical cycling of bioelements selectively under the iron-replete conditions in the coastal ecosystems.

Keywords: diatoms, elemental composition, iron availability, nutrients, ocean acidification, *Thalassiosira weissflogii*.

Introduction

Ongoing increases in CO_2 in seawater resulting from anthropogenic activities affect carbonate chemistry and result in a decrease in pH and an increase in the partial pressure of CO_2 (pCO_2; i.e. ocean acidification; Doney *et al.*, 2009). The effect of changing carbonate chemistry on phytoplankton has attracted much research attention over the last decade. Because phytoplankton is a crucial component of the marine ecosystem, understanding the effects of ocean acidification on phytoplankton processes is important to predict the future health of the marine ecosystem (Doney *et al.*, 2009; IGBP, IOC, and SCOR, 2013).

The bioavailability of trace metals is affected by changing carbonate chemistry, which in turn affects the relationship between trace metals and pH-sensitive inorganic/organic coordination chemistry (Millero *et al.*, 2009). Shi *et al.* (2010) reported that the conditional stability constant of iron–organic ligand complexes increased as pH decreased when the ligand was an acidic binding group. Previous CO_2 perturbation studies have indicated that iron availability can decrease in low pH–high CO_2 conditions (Shi *et al.*, 2010; Sugie *et al.*, 2013), but the results may largely depend on the sensitivity of each phytoplankton community to changes in iron availability

(Sugie *et al.*, 2013; Yoshimura *et al.*, 2013, 2014). In addition, the chemical nature of iron-binding ligands in natural seawater is largely uncertain. Such uncertainty implies that simultaneous changes in carbonate chemistry and iron availability in natural seawater make it difficult to discriminate the effect of each factor on phytoplankton ecophysiology. To properly interpret the results of ocean acidification studies in the natural environment, it is necessary to understand the individual effects of changes in carbonate chemistry and iron availability on phytoplankton ecophysiology.

Iron has important roles in the metabolism of phytoplankton such as photosynthesis, nitrogen (N) assimilations, and respiration (Raven *et al.*, 1999). One of the most bioavailable form of iron for eukaryotic phytoplankton is dissolved inorganic iron (Fe′) species mainly composed of $Fe(OH)_2^+$, $Fe(OH)_4^-$, and $Fe(OH)_3^0$ in seawater (Morel *et al.*, 2008). In contrast, iron uptake from iron–organic ligand complex is often a very slow process for eukaryotes, indicating that such complex shows low iron bioavailability. Therefore, to investigate the effect of iron availability on phytoplankton processes, Fe′ rather than total iron in seawater must be considered. The binding affinities of iron with ethylene diamine tetraacetic acid (EDTA) and with bacterial hydroxamate siderophore desferrioxamine B are sensitive to changes in seawater pH (Shi *et al.*, 2010). For example, 100 μmol l^{-1} EDTA bound with 100 nmol l^{-1} ferric iron under 20°C and 100 μmol photon m^{-2} s^{-1}, 12:12 h light:dark conditions was used to demonstrate that a decrease in pH from 8.0 to 7.8 potentially decreased the concentration of Fe′ ([Fe′]) from 90 to 26 pmol l^{-1} (Sunda and Huntsman, 2003). Recently, Sugie and Yoshimura (2013) demonstrated that a combination of iron, EDTA, and CO_2 concentration-controlled air can be used to manipulate [Fe′] and carbonate chemistry separately and simultaneously. However, most previous studies did not discriminate the effects of changes in iron availability from changes in carbonate chemistry.

Dissolved iron (<0.2 μm) concentrations in coastal waters (>~1 nmol l^{-1}) are generally higher and more spatio-temporally dynamic than that of oceanic waters (<~0.5 nmol l^{-1}; Kuma *et al.*, 2000; Nishioka *et al.*, 2013). The dynamic nature of dissolved iron concentrations in coastal environment reflects the iron sources, and physical and chemical properties of seawater. For example, riverine inputs and vertical mixing involving sediments could increase iron concentrations, whereas intrusion of oceanic waters and the low solubility of Fe′ in seawater could decrease the concentrations (Kuma *et al.*, 2000). Furthermore, one of the most important factors determining dissolved iron concentrations is the concentration and binding affinity (Log $K^{Cond}_{FeL,Fe'}$) of organic ligands (Kuma *et al.*, 2000; Bundy *et al.*, 2015). Therefore, iron bioavailability, namely the [Fe′], could dynamically change depending on the organic and inorganic chemistry of seawater.

Iron requirement is generally higher in coastal phytoplankton species than in oceanic species, probably reflecting the environmental conditions of their habitats (e.g. Sunda and Huntsman, 1995). As a result, the effects of changes in iron availability with changes in CO_2 conditions could differ depending on the nature of the iron requirement of each phytoplankton species. One of the notable effects of iron availability on phytoplankton is change in the elemental composition of diatoms (e.g. Takeda, 1998). Changes in CO_2 concentrations can also alter the cellular elemental composition of diatoms (e.g. Sun *et al.*, 2011; Sugie and Yoshimura, 2013), indicating that changes in either iron availability or CO_2 concentration could affect marine biogeochemical cycling of bioelements. However, other than the study by Sugie and Yoshimura (2013), no studies have demonstrated the individual effects of iron availability and CO_2 conditions on the elemental composition of phytoplankton. Because the response to the changes in iron availability and CO_2 variations differ among species (Burkhardt *et al.*, 1999; Doney *et al.*, 2009; Bucciarelli *et al.*, 2010), more studies on the elemental composition of phytoplankton are needed to better understand the biogeochemistry of the ocean.

To date, prediction of future environments has relied on *in silico* simulations. One of the major problems in estimating biogeochemical cycling of bioelements in modelling studies is the behaviour of the elemental composition of phytoplankton, which is usually fixed as the canonical Redfield ratio (Passow and Carlson, 2012). In forecasts on global and long-time-scales, Redfield ratio-based simulation is assumed to be representative of the nutrient budget in the ocean. However, models simulating changes on regional, and short-time-scales should consider the flexible elemental composition of phytoplankton to represent the ecological stoichiometry in dynamic environments (Smith *et al.*, 2011; Passow and Carlson, 2012). Quigg *et al.* (2003) reported that individual phytoplankton taxa have unique elemental stoichiometry. The regional characteristics of elemental composition of marine particulate matter therefore reflect the elemental stoichiometry of dominant phytoplankton taxa (Weber and Deutsch, 2010). Similarly, changes in the elemental composition of phytoplankton communities in response to environmental changes differ among reports, probably as a result of differences in the community composition (Sugie *et al.*, 2013; Eggers *et al.*, 2014; Richier *et al.*, 2014; Yoshimura *et al.*, 2014). Therefore, more information is needed on species-specific differences in the effects of environmental disturbances on the ecophysiology of phytoplankton.

Here, we examine the individual effects of carbonate chemistry and iron availability on the elemental composition (carbon [C], [N], phosphorus [P], and silicon [Si]) of estuarine and coastal diatom *Thalassiosira weissflogii*. In addition to the dynamics of iron, coastal and estuarine systems are also more dynamic in terms of carbonate chemistry than oceanic systems (Wootton *et al.*, 2008; Dore *et al.*, 2009). This study can provide useful information about first-order biogeochemical processes of nutrients in neritic ecosystems.

Material and methods

Experimental set-up

Seawater used for the experiment (salinity 34.2) was collected from a coastal region in the North Pacific, near Onjuku, Chiba, Japan (35°18′N, 140°38′E). About 50 l of seawater was filtered through a 0.22-μm cartridge filter (Advantech Co. Ltd, Tokyo, Japan). Stock solutions of macronutrients were passed through a Chelex 100 resin (Bio-Rad, CA, USA) to eliminate trace metals (Price *et al.*, 1988/1989), and then added to the filtered seawater to make final concentrations of ~100 μmol l^{-1} NO_3^-, ~6 μmol l^{-1} PO_4^-, and ~150 μmol l^{-1} $Si(OH)_4$. The seawater with added nutrients was aged for more than 1 month in an acid-washed 50-l polypropylene carboy, to precipitate dissolved iron excess to its solubility (Sugie *et al.*, 2010; Sugie and Yoshimura, 2013). The aged seawater was passed through a 0.1-μm cartridge filter (Merck Millipore, MA, USA) to sterilize it and to eliminate particulate iron before use. The background iron concentration of the filtered seawater was 0.4 nmol l^{-1}, as measured by flow-injection with chemiluminescence detection (Obata *et al.*, 1993). The culture medium used in this study was modified Aquil medium (Price *et al.*, 1988/1989), which was composed of nutrient-enhanced 0.1 μm filtered seawater and Aquil metals chelated with 100 μmol l^{-1} of EDTA. Only iron

concentrations were modified during the culture experiment. An algal strain of *T. weissflogii* (Grunow) G. Fryxell and Hasle [currently accepted as *Conticribra weissflogii* (Grunow) K. Stachura-Suchoples and D.M. Williams; CCMP1336] was maintained in modified Aquil medium at 20°C under cool fluorescent light at 150 μmol photons m^{-2} s^{-1} (measured using QSL radiometer; Biospherical Instrument Inc., CA, USA), and a 12:12 h light:dark cycle. All equipment used in the culture experiment was acid-washed (soaked for at least 24 h in either 1 or 4 mol l^{-1} HCl solution) followed by thorough rinsing with Milli-Q water (>18.0 MΩ cm^{-1}, Merck KGaA, Darmstadt, Germany). Preparation and sampling were conducted in a class 1000 clean room and at a class 100 clean bench, respectively, to avoid inadvertent trace metal contamination.

Culture design

Iron, other trace metals, and EDTA stock solutions were mixed and left for ~1 h in 4-l polycarbonate culture bottles before pouring 3-l of nutrient-enhanced 0.1-μm filtered seawater. Next, CO_2 concentration (xCO_2)-controlled air (Nissan Tanaka Corp., Saitama, Japan) was injected to manipulate the carbonate chemistry of the culture medium. The xCO_2 of the injected air was set at 386, 614, or 795 ppm, corresponding to the present and two possible future CO_2 conditions, respectively, and these high CO_2 conditions could also be found in the present coastal region during winter (Wootton *et al.*, 2008). The injected air was humidified by passing through Milli-Q water and it was also passed through a 0.2 μm inline filter to avoid contaminations from the gas cylinder or lines. The flow rate of xCO_2-controlled air was set at 40 ml min^{-1} for 4 d before the start of the experiment to ensure steady state of carbonate chemistry and to equilibrate [iron–EDTA], [EDTA], and [Fe′] conditions. The [Fe′] was set at 30 or 250 pmol l^{-1} for low iron (LFe) and high iron (HFe) treatments, respectively. The values for [Fe′] were determined based on a presurvey of the relationship between specific growth rates and [Fe′] (Figure 1). Non-linear fitting of the growth rate and [Fe′] data to the Monod equation, resulted in a maximum specific growth rate (μ_{max}) = 1.24 ± 0.04 (d^{-1}) and a half saturation constant for growth (k_μ) = 28.1 ± 3.2 (pmol l^{-1}) ($R^2 = 0.98$, $p < 0.001$). The [Fe′] of 30 and 250 pmol l^{-1} were selected to produce ~50 and >90% of the μ_{max} of *T. weissflogii*, respectively. In coastal seawater, given the dissolved iron and iron-binding ligand concentrations of 1–150 and 10–500 nmol l^{-1}, respectively, with (Log $K^{Cond}_{FeL,Fe'}$) of ligands ranging 8.7–12 (Kuma *et al.*, 2000; Laglera and van den Berg, 2009; Hassler *et al.*, 2011; Bundy *et al.*, 2015), the [Fe′] could range from 0.1 to 297 pmol l^{-1}. Given these iron conditions and the dynamics of carbonate chemistry in the coastal region, this study could partially simulates the present coastal environment as well as future high CO_2 conditions. Six treatments based on different xCO_2 and [Fe′] were established as follows: LFe386, LFe614, LFe795, HFe386, HFe614, and HFe795. When estimating [Fe′] according to the method of Sunda and Huntsman (2003), the background concentration of iron was included in the added iron concentrations. Defined [Fe′] were obtained using total iron and EDTA concentrations, pH, light intensity and duration, and temperature. The pH values were calculated from measurements of total alkalinity (TA) and dissolved inorganic C (DIC) concentrations (Table 1). Cultures were set in duplicate bottles for each treatment.

The dilute batch culture technique was used in this study (LaRoche *et al.*, 2011); the diatom cells were harvested <20% of the carrying capacity of the culture medium to avoid large changes in carbonate chemistry and iron availability. To acclimate

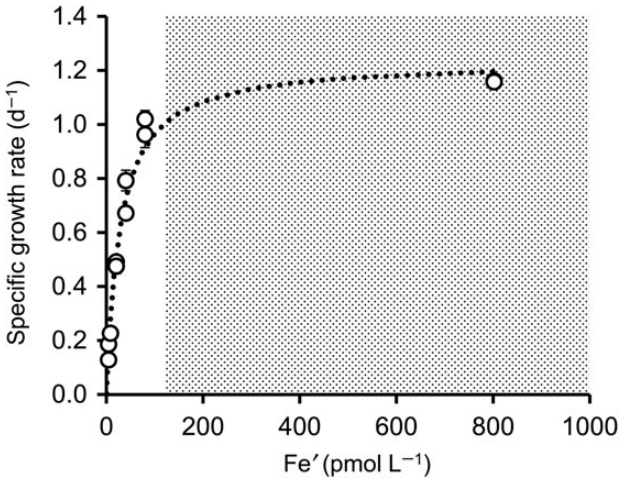

Figure 1. Change in the specific growth rate of *T. weissflogii* against the change in dissolved inorganic iron (Fe′) concentration. The hatched area represents where solid iron hydroxides are precipitating (e.g. Stumm and Morgan, 1996), and therefore [Fe′] may not be correct. The dotted hyperbolic line was obtained by non-linear fitting of the data on the relationship between the specific growth rate of *T. weissflogii* and [Fe′] to the Monod equation.

and to reduce intracellularly stored iron of the *T. weissflogii* cells to experimental conditions, cells in stock culture (exponential growth phase) were transferred to each xCO_2 with 1/100 Aquil trace metals medium and grown in the exponential growth phase corresponding to ~10 cell divisions. The xCO_2-acclimated cells were then transferred to the experimental media to give an initial cell density of 100 and 50 cells ml^{-1} in the LFe- and HFe-treated bottles, respectively. Cultures were continued for 10 and 6 d in the LFe and HFe treatments, respectively, representing 6–7 cell divisions under the experimental conditions. Geider *et al.* (1993) reported that iron-limited diatom cell could acclimate under high-iron conditions within 24 h, and thus, *T. weissflogii* should acclimate each iron conditions during the experiment. After inoculation of the diatoms into the experimental media, the flow rate of xCO_2-controlled air was reduced to 10 ml min^{-1}.

Measurements

Growth was monitored daily at a fixed time (mid of the light phase) using a Multisizer 4 Coulter Counter (Beckman Coulter Inc., CA, USA) to calculate specific growth rates and to measure cell volume and surface area (SA). Specific growth rates (μ, d^{-1}) were determined from the slope of a plot of the natural log density of biovolume (i.e. abundance × cell volume) against time during the exponential growth phase. At the end of the experiment, cells were harvested on precombusted GF/F filters for particulate organic C (POC), particulate N (PN), and particulate P (PP) analysis. For biogenic Si (BSi) analysis, samples were collected on a 0.8-μm polycarbonate filter. The methods for POC, PN, PP, and BSi measurements have been described elsewhere (Sugie and Yoshimura, 2013). In brief, for POC and PN analysis, filters were freeze-dried, and the concentrations were measured using a CHN analyser. Filters for PP analysis were combusted in high temperature followed by acid hydrolysis and measured using a spectrophotometer as described by Solórzano and Sharp (1980). For BSi analysis, the filter was digested in 0.5% Na_2CO_3 solution (Paasche, 1980) and measured with a QuAAtro-2 continuous flow analyser. For chlorophyll *a*

Table 1. Measured TA (in μmol kg^{-1}) and DIC (in μmol kg^{-1}), and calculated dissolved inorganic iron species (Fe′ in pmol l^{-1}) conditions during the experiment.

	Initial			Day 2 (HFe) or day 3 (LFe)			Day 6 (HFe) or day 9 (LFe)		
Treatment	**TA**	**DIC**	**Fe′**	**TA**	**DIC**	**Fe′**	**TA**	**DIC**	**Fe′**
LFe-386	2344	2087	23.0	2349	2076	26.1	2356	2063	30.7
LFe-614	2353	2161	24.6	2359	2160	25.9	2364	2162	26.8
LFe-795	2350	2196	24.9	2359	2197	26.8	2368	2199	28.5
HFe-386	2351	2113	168*	2352	2081	220*	2365	2047	322*
HFe-614	2357	2164	222*	2355	2157	233*	2364	2145	280*
HFe-795	2353	2200	220*	2354	2193	237*	2363	2185	276*

Data represents mean of the duplicate bottles. Note that the Fe′ concentrations in the HFe treatments with asterisks show an approximate values because the concentrations were over-saturated with respect to the solubility of dissolved inorganic Fe(III) hydroxide (e.g. Stumm and Morgan, 1996).

(Chl *a*) measurements, seawater samples were filtered on GF/F filters, soaked in *N*,*N*-dimethylformamide (Suzuki and Ishimaru, 1990) and quantified by fluorometry (Welschmeyer, 1994). All data for POC, PN, PP, BSi, and Chl *a* concentrations were corrected by subtracting values obtained from filter blanks. The cell quota of each element (Q_E) was calculated by dividing the concentration of each element by abundance. To estimate intracellular concentrations of each element ($In_{cell}[E]$), POC, PN, PP, and Chl *a* concentrations were divided by abundance and cell volume, to obtain $In_{cell}[C]$, $In_{cell}[N]$, $In_{cell}[P]$, and $In_{cell}[Chl\ a]$, respectively. The BSi concentration was normalized by abundance and SA ([Si]/SA) because most BSi localizes outwards as siliceous frustules. Net elemental production (NEP) was calculated as follows: $NEP = Q_E \times \mu$.

The DIC and TA samples were collected and measured at days 0, 2, and 6 for HFe conditions and days 0, 3, and 10 for LFe conditions. Both parameters were measured using a potentiometric Gran plot method with 0.1 mol l^{-1} HCl (Wako Co. Ltd, Osaka, Japan) and a TA analyser (Kimoto Electric Co. Ltd, Osaka, Japan), according to the method of Edmond (1970). Titration data below pH 4 were eliminated because EDTA began absorbing protons below pH ∼4. The stability of the DIC and TA analyses was checked using DIC reference material (KANSO Co. Ltd, Osaka, Japan) and the analytical errors in this study were <0.1% for both DIC (∼1.1 μmol kg^{-1}) and TA (∼1.4 μmol kg^{-1}). The DIC and TA values of the reference material were traceable to the certified reference materials supplied by Professor Andrew Dickson, University of California, San Diego, USA. Carbonate chemistry was calculated using the CO2SYS program and DIC and TA data (Lewis and Wallance, 1998). Samples for macronutrient analysis were collected at the end of the experiment and measured using a QuAAtro-2 continuous flow analyser.

Statistics

Linear regression was used to test the relationship between measured parameters and pCO_2. When significant linearity was found ($p < 0.05$), the regression line was described in the figure. When the hypothesis of linearity was rejected, differences among the different xCO_2 treatments were tested with Tukey's HSD ANOVA test. To test the effect of the different [Fe′] of each of three xCO_2 treatments, two-tailed, paired-sample *t*-tests were performed. All statistics were carried out using PASW statistical software (version 17.0 SPSS Inc., Chicago, IL, USA). Significant differences are reported at the 95% confidence level.

Results

The pH and pCO_2 were clearly different among the xCO_2 tested throughout the experiment with a slight increase in pH and a decrease in pCO_2 during incubations (Figure 2, Table 1). The [Fe′] was not statistically different among the three xCO_2 treatments under both LFe and HFe conditions (Figure 3, Table 1). The specific growth rate differed significantly between the HFe614 and HFe795 treatments, but there was no significant difference in specific growth rate between the HFe386 and HFe614 treatment or between the HFe386 and HFe795 treatment (Figure 4a). Under LFe conditions, the specific growth rate was slightly increased by the change in carbonate chemistry, but the difference was not statistically significant ($p = 0.13$, ANOVA; Figure 4a, Table 2). The cell volume decreased linearly with increasing pCO_2 under HFe conditions (Table 2), whereas no linearity was found under LFe conditions (Figure 4b). Under LFe conditions, there was a significant decrease in the cell volume for the LFe614 treatment compared with the LFe386 and LFe795 treatments (Figure 4b).

A significant increase in the N cell quota under HFe conditions and a significant decrease in the P cell quota under LFe conditions were measured with increasing pCO_2 (Figure 5). The cell quota of C, Si, and Chl *a* did not differ significantly with changes in pCO_2 under LFe or HFe conditions (Figure 5). The $In_{cell}[C]$, $In_{cell}[N]$, $In_{cell}[P]$, and $In_{cell}[Chl\ a]$ under HFe conditions increased significantly with increasing pCO_2 (Supplementary Figure S1a–c and e, Table 2). Only $In_{cell}[P]$ decreased significantly with increasing pCO_2 under LFe conditions (Supplementary Figure S1c, Table 2). The [Si]/SA did not differ significantly because of a difference in carbonate chemistry under both LFe and HFe conditions (Supplementary Figure S1d). The NCP, NSiP, and NChl*a*P did not differ significantly among the three xCO_2 treatment in both iron conditions (Supplementary Figure S2a, d, and e). The NNP and NPP under HFe conditions increased significantly with increasing pCO_2 (Table 2), but those trends were not seen under LFe conditions (Supplementary Figure S2b and c). The C:N, C:P, and N:P ratios did not show any significant trends or differences among the three xCO_2 conditions under HFe and LFe conditions (Figure 6a–c). The Si:N, Si:C, and Si:P ratios under HFe conditions decreased significantly with increasing pCO_2, but the ratios did not differ significantly under LFe conditions (Figure 6d–f, Table 2).

Different Fe′ conditions produced significant differences in most of the parameters measured in this study, except for $In_{cell}[P]$, C:N, and Si:P ratios (Table 3). Lower iron availability decreases the cell quota of C and N synchronously. The different iron conditions affected the Si cell quota and Si/SA, but the degree of the change was small compared with the change for C and N, resulting in increasing Si:C and Si:N ratios with increasing iron availability (Table 3). The Chl *a* cell quota, $In_{cell}[Chl\ a]$, and NChl*a*P decreased dramatically with a decrease in iron availability (Supplementary Figure S2, Table 3).

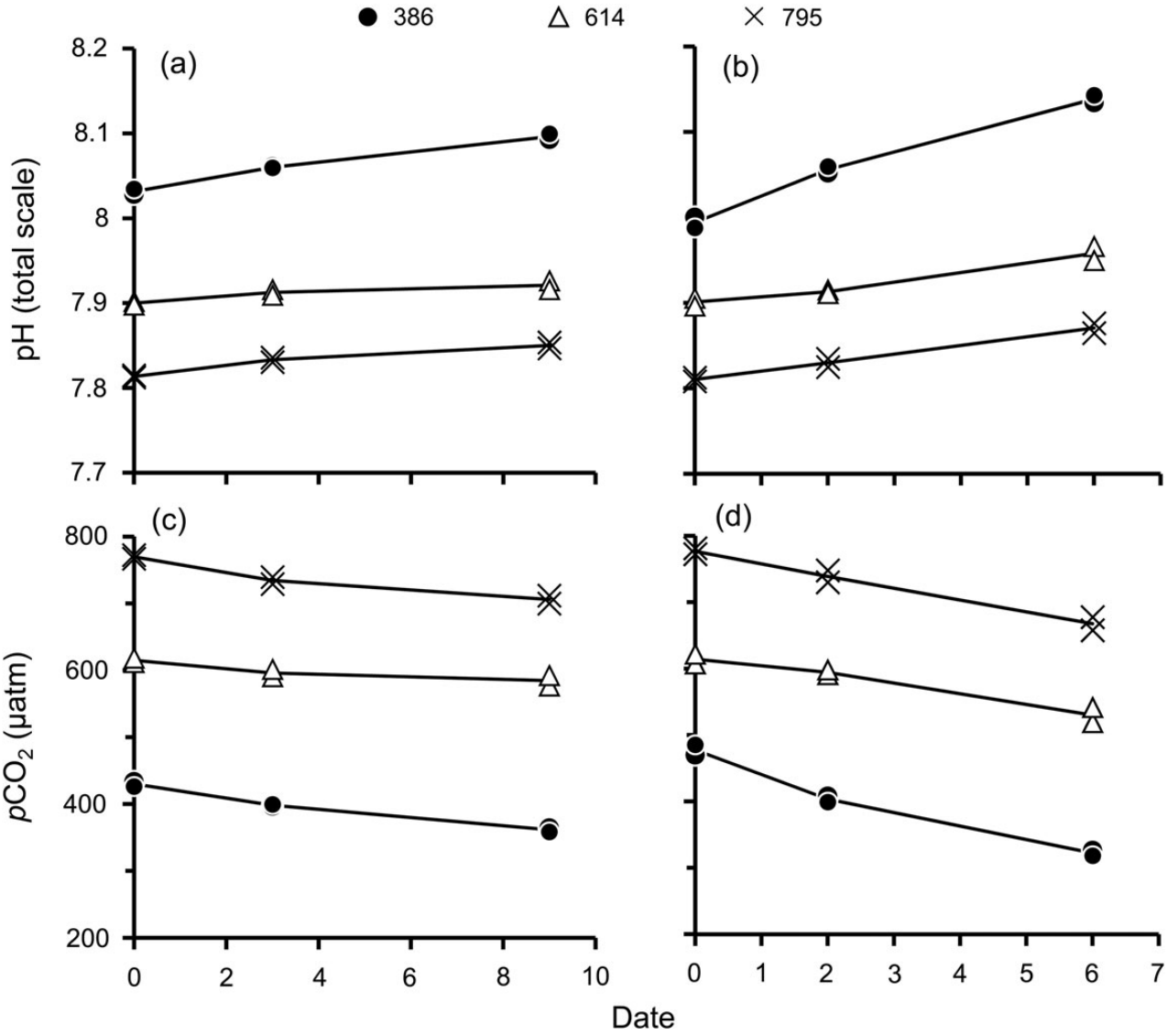

Figure 2. Temporal changes in (a and b) pH (total scale), and (c and d) pCO_2 under LFe (a and c) and HFe (b and d) conditions.

Discussion

This study shows that the cell size and elemental composition of the diatom *T. weissflogii* changed with both separate and simultaneous changes in iron availability and carbonate chemistry. The proper control of bioavailable [Fe′] in seawater under different pCO_2 conditions enables the investigation of individual effects of iron availability and carbonate chemistry on the cellular elemental dynamics of phytoplankton species (Sugie and Yoshimura, 2013). The present study demonstrates that the ecophysiological properties of the coastal and estuary diatom *T. weissflogii* changed in response to the change in CO_2 levels, mainly under iron-replete condition.

Effects of different CO_2 levels on cellular elemental dynamics

Under HFe conditions, $In_{cell}[C]$, $In_{cell}[N]$, $In_{cell}[P]$, and $In_{cell}[Chl\,a]$ increased significantly with increasing pCO_2 (Supplementary Figure S1), suggesting the increasing concentration of intracellular constituents. However, the cell quota of C, P, and Chl *a* did not change (Table 2), because cell size decreased with increasing pCO_2 under HFe conditions. A decrease in cell size in response to high pCO_2 conditions has been reported for micro- and nano-sized phytoplankton such as the diatom *Pseudo-nitzschia pseudodelicatissima* (Sugie and Yoshimura, 2013) and the coccolithophore *Emiliania huxleyi* (Lohbeck *et al.*, 2012). Previous studies have demonstrated that the increase in temperature also decrease cell size of marine phytoplankton ~2.5–4% $°C^{-1}$ (Montagnes and Franklin, 2001; Atkinson *et al.*, 2003). According to the IPCC AR5 (IPCC, 2013), temperature increase in the range 1–3°C (RCP2.6) or 3–10°C (RCP8.5) has been predicted with atmospheric CO_2 concentrations ranging from 421 to 936 ppm by 2100. Such temperature rises could decrease phytoplankton cell size by 2.5 to >40%. Our study estimated the decrease in cell volume to be 1.4×10^{-2}% per pCO_2 increases (Table 2), suggesting that the increase in CO_2 levels in 2100 from the present conditions (~400 µatm) could decrease cell volume by 0.3–7.5% under RCP2.6 and RCP8.6 scenarios, respectively. These estimations suggest that the effect of temperature on cell volume is stronger

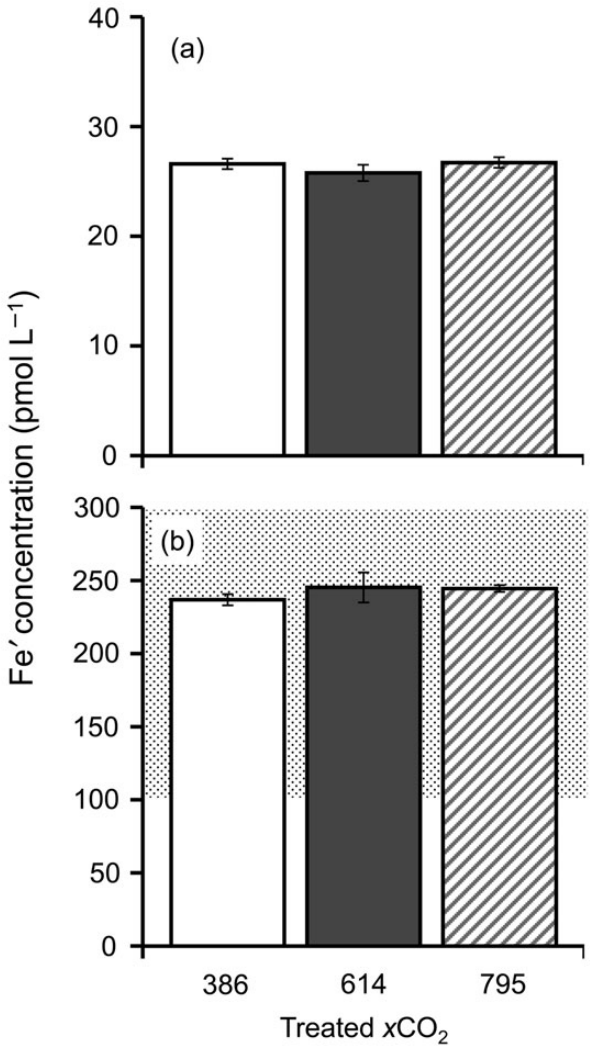

Figure 3. The mean Fe′ concentration under (a) LFe and (b) HFe conditions during the course of the experiment. Error bars represent the range of the values in duplicate incubation bottles. The hatched area indicates where solid iron hydroxides are precipitating.

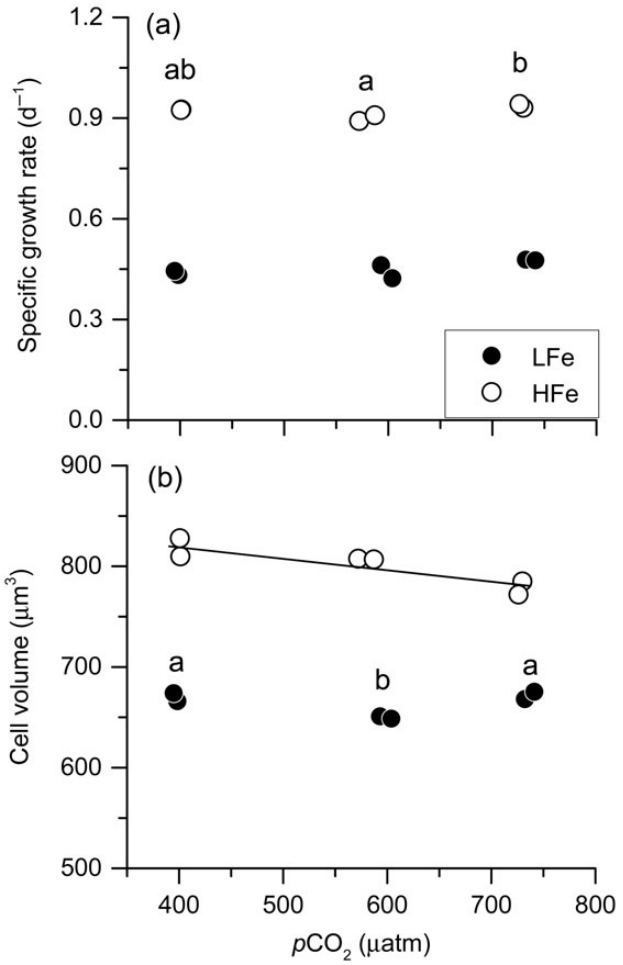

Figure 4. Change in (a) specific growth rate and (b) cell volume of *T. weissflogii* grown under different pCO_2 and iron conditions. The solid line in (b) represents the regression between pCO_2 and cell volume. Statistics are shown in Tables 2 and 3. Labels above the symbols represent the results of Tukey's group test ($p < 0.05$), which did not show a linear trend.

than pCO_2, but pCO_2 increase could contribute substantially (12–19% under RCP2.6 and RCP8.6 scenarios, respectively) to the decrease in cell volume of *T. weissflogii* in the forecasted future conditions, given the decrease in cell size emerge due to the additive effects of hightemperature and pCO_2 under iron-replete conditions. Seebah *et al.* (2014) reported that the aggregate size and sinking velocity of *T. weissflogii* decreased under high pCO_2, which can increase the remineralization of organic matters in the water column. The reduction in cell size found in the present study may partly explain the sinking behaviour of *T. weissflogii* reported by Seebah *et al.* (2014). In addition to the slower sinking rate of *T. weissflogii* under high CO_2 conditions (Seebah *et al.*, 2014), the relatively stable cell quota of C, N, P, and Chl *a* suggest that increasing pCO_2 could have negative impact on the export flux of these bioelements in the high CO_2 conditions.

In contrast, the [Si]/SA and NSiP were not affected significantly by changes in pCO_2 (Table 2). Sugie and Yoshimura (2013) reported that the [Si]/SA and NSiP of *P. pseudodelicatissima* decreased with increasing pCO_2 under various [Fe′] conditions, suggesting that the effect of increasing CO_2 levels is species-specific or differs between centric and pennate diatoms. Milligan *et al.* (2004) examined the Si metabolism of *T. weissflogii* under iron-replete conditions and found that the rates of intracellular Si efflux and frustule dissolution increased in 750 ppm CO_2 compared with 100 ppm CO_2. During that experiment, the Si cell quota did not differ significantly between 380 and 750 ppm CO_2 because of the high Si uptake rate under the high CO_2 conditions. The small but insignificant decrease in [Si]/SA with increasing pCO_2 under LFe conditions may result from the pH-dependent change in Si metabolism as previously reported (Milligan *et al.*, 2004; Hervé *et al.*, 2012). Muggli *et al.* (1996) found that phytoplankton cells suffered from energy limitation under iron-limited conditions. Because Si uptake and mineralization are associated with energy from respiration (Martin-Jézéquel *et al.*, 2000), the [Si]/SA may be slightly affected by changing pCO_2 under conditions of low iron availability.

Effects of different CO_2 levels on elemental compositions

The present study confirms that the cellular C:N, C:P, and N:P ratios do not change with changes in pCO_2 under iron-replete or iron-limited conditions (Figure 6). Previous studies also observed

Table 2. Statistical results of the relationships between partial pressure of CO_2 (pCO_2, μatm) and specific growth rate (μ, d^{-1}), cell volume (CV, μm^3), intracellular organic carbon (In_{cell} [C], mol l^{-1}), intracellular nitrogen (In_{cell} [N], mol l^{-1}), intracellular phosphorus (In_{cell} [P], mol l^{-1}), silicon concentration per unit surface area ([Si]/SA, mmol m^{-2}), intracellular chlorophyll *a* (In_{cell}[Chl-*a*], mg l^{-1}), Net C, N, P, Si, and chlorophyll *a* productions (NCP, NNP, NPP, NSiP, and NChl-*a*P; pmol cell^{-1} d^{-1} for C, N, and Si, and fmol cell^{-1} d^{-1} for P, pg cell^{-1} d^{-1} for chlorophyll *a*), and elemental compositions.

	LFe			HFe		
	a	***b***	**Significance**	***a***	***b***	**Significance**
μ	n.s.	n.s.	n.s.	n.s.	n.s.	n.s.
Cell volume	n.s.	n.s.	n.s.	871**	−0.12*	$F_{1,4} = 15.8$, $p = 0.016$, $R^2 = 0.75$
C quota	n.s.	n.s.	n.s.	n.s.	n.s.	n.s.
N quota	n.s.	n.s.	n.s.	1.2**	2.4×10^{-5}*	$F_{1,4} = 10.4$, $p = 0.032$, $R^2 = 0.65$
P quota	75**	−0.22**	$F_{1,4} = 52.9$, $p = 0.002$, $R^2 = 0.91$	n.s.	n.s.	n.s.
Si quota	n.s.	n.s.	n.s.	n.s.	n.s.	n.s.
Chl *a* quota	n.s.	n.s.	n.s.	n.s.	n.s.	n.s.
In_{cell}[C]	n.s.	n.s.	n.s.	7.8**	2.1×10^{-3}*	$F_{1,4} = 15.7$, $p = 0.017$, $R^2 = 0.75$
In_{cell}[N]	n.s.	n.s.	n.s.	1.3**	5.5×10^{-4}**	$F_{1,4} = 23.4$, $p = 0.008$, $R^2 = 0.82$
In_{cell}[P]	0.12	-3.7×10^{-5}**	$F_{1,4} = 47.8$, $p = 0.002$, $R^2 = 0.90$	0.072**	4.7×10^{-5}*	$F_{1,4} = 12.8$, $p = 0.023$, $R^2 = 0.70$
[Si]/SA	n.s.	n.s.	n.s.	n.s.	n.s.	n.s.
In_{cell}[Chl-*a*]	n.s.	n.s.	n.s.	6.0**	9.5×10^{-4}**	$F_{1,4} = 8.9$, $p = 0.040$, $R^2 = 0.61$
NCP	n.s.	n.s.	n.s.	n.s.	n.s.	n.s.
NNP	n.s.	n.s.	n.s.	1.0**	2.7×10^{-4}*	$F_{1,4} = 12.7$, $p = 0.024$, $R^2 = 0.70$
NPP	n.s.	n.s.	n.s.	58**	0.026*	$F_{1,4} = 8.9$, $p = 0.041$, $R^2 = 0.61$
NSiP	n.s.	n.s.	n.s.	n.s.	n.s.	n.s.
NChl *a*P	n.s.	n.s.	n.s.	n.s.	n.s.	n.s.
C:N	n.s.	n.s.	n.s.	n.s.	n.s.	n.s.
C:P	n.s.	n.s.	n.s.	n.s.	n.s.	n.s.
N:P	n.s.	n.s.	n.s.	n.s.	n.s.	n.s.
Si:N	n.s.	n.s.	n.s.	0.62**	-1.2×10^{-4}**	$F_{1,4} = 29.7$, $p = 0.006$, $R^2 = 0.85$
Si:C	n.s.	n.s.	n.s.	0.11**	-1.1×10^{-5}*	$F_{1,4} = 11.0$, $p = 0.030$, $R^2 = 0.66$
Si:P	n.s.	n.s.	n.s.	11.0**	-3.3×10^{-3}*	$F_{1,4} = 14.0$, $p = 0.020$, $R^2 = 0.72$
C:Chl *a*	n.s.	n.s.	n.s.	n.s.	n.s.	n.s.

Listed are the constant (*a*) and the coefficients (*b*) of regression equation of $y = a + b \times pCO_2$. Asterisks represent the significance level of the constant and coefficients (*$p < 0.05$; **$p < 0.01$; *t*-test, d.f. = 5). n.s., not significant.

that these ratios of *T. weissflogii* were not affected by changes in pCO_2 under both macronutrient-replete and -depleted conditions (Burkhardt *et al.*, 1999; Clark *et al.*, 2014). In the studies by Burkhardt *et al.* (1999) and Clark *et al.* (2014), carbonate chemistry was manipulated by adding acid or base, whereas in the present study, it was manipulated by injecting xCO_2-controlled air. The method of carbonate chemistry manipulation is reported to be one of the most important factors affecting biological responses to ocean acidification (Shi *et al.*, 2009; Hoppe *et al.*, 2011). The major difference between these manipulation methods is DIC concentrations: the bubbling of high CO_2 air increases DIC, whereas the acid/base addition did not change DIC (Burkhardt *et al.*, 2001; Shi *et al.*, 2009). Taken together, the present and previous findings indicate that increasing CO_2 levels have no effect on the C:N, C:P, and N:P ratios of *T. weissflogii*, irrespective of the different manipulation methods.

However, some previous studies have reported that cellular C:P and N:P ratios of phytoplankton are affected by increases in pCO_2 under iron-replete conditions. Many centric and pennate diatom species showed an increase in C:P ratio in response to increases in pCO_2 (Burkhardt *et al.*, 1999; King *et al.*, 2011; Sun *et al.*, 2011; Sugie and Yoshimura, 2013). An increase in the C:P ratio with increasing pCO_2 has also been found in Dinophyceae, Raphidophyceae, and Prymnesiophyceae (Feng *et al.*, 2008; Fu *et al.*, 2008). Some diatom species such as *Asteionellopsis glacialis* and *Phaeodactylum tricornutum* did not show changes in the C:P ratio with changing pCO_2 (Burkhardt *et al.*, 1999), similar to the finding for *T. weissflogii* in the present study. Sugie and Yoshimura (2013) demonstrated using *P. pseudodelicatissima* that a steeper decline in In_{cell}[P] and NPP compared with those of C and N with increasing pCO_2 is a key mechanism underlying increasing C:P and N:P ratios in high CO_2 conditions. They suggested that increases in C:P and N:P ratios with increasing CO_2 availability were derived from decreases in the expenditure of P-rich cellular constituents such as ATP, which is used to maintain/operate carbon concentration mechanisms (CCMs; Hopkinson *et al.*, 2011). A notable characteristic of C assimilation in *T. weissflogii* is the presence of both C_3 and C_4 photosynthetic pathways, where the latter functions as a biochemical CCM. In contrast, other diatoms are mainly C_3 photosynthesizers (Roberts *et al.*, 2007). The initial products of DIC uptake are glycerate-P and hexose-P in C_3 diatoms, and malate in C_4 diatoms of *T. weissflogii* (Roberts *et al.*, 2007). If C_4 pathway-mediated CCMs decrease with increasing CO_2 availability, the contribution of sugar-P compounds such as glycerate-P mediated from C_3 photosynthesis can increase with increasing CO_2 availability. Such adaptive photosynthetic strategies result in an increase in NPP (Supplementary Figure S2), which could offset increases in C:P and N:P ratios of *T. weissflogii* with increasing pCO_2.

In contrast to the relatively stable C:N, C:P, and N:P ratios in the present study, we found that the ratios of Si to C, N, and P changed in response to changes in carbonate chemistry (Figure 6). This discrepancy reflected different trends in the effect of pCO_2 on the rates of NEP between Si and C, N, and P (Supplementary Figure S2). Under HFe conditions, the decrease in Si:N and Si:P with increasing pCO_2 was derived from the significant increases in NNP and NPP with increasing pCO_2. The decreasing trend of Si:C with increasing pCO_2 resulted from the small but insignificant ($p = 0.16$, ANOVA)

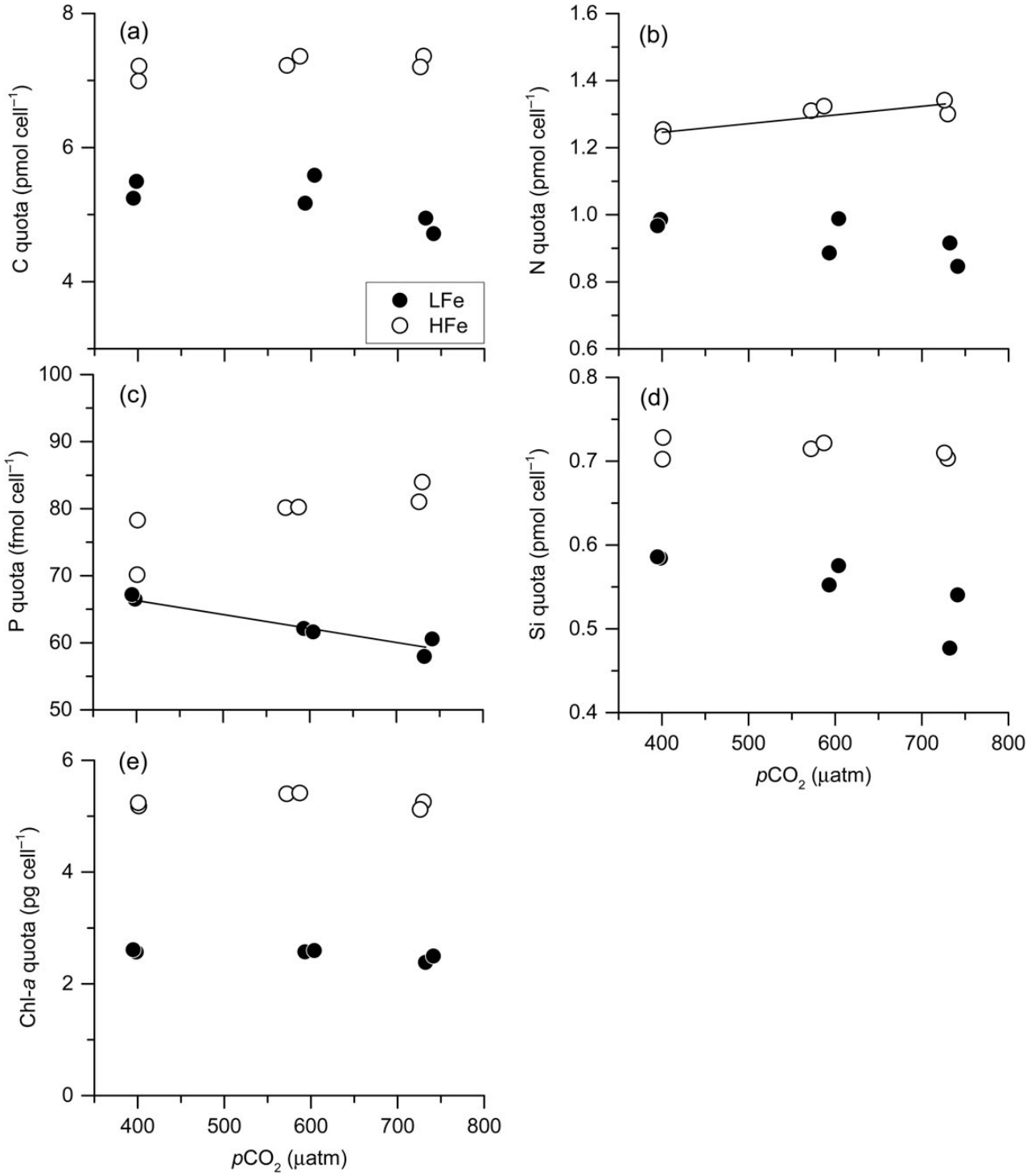

Figure 5. Changes in the cell quota of (a) carbon, (b) nitrogen, (c) phosphorus, (d) silicon, and (e) chlorophyll *a* of *T. weissflogii* grown under different pCO_2 and iron conditions. Solid lines in (b) and (c) represent the regression between pCO_2 and N and P cell quota, respectively. Statistics are shown in Tables 2 and 3.

increase in NCP and constant NSiP with increasing pCO_2. Decreasing Si relative to C, N, and P in response to increasing pCO_2 has been previously reported for diatoms (*Pseudo-nitzschia multiseries*, Sun *et al.*, 2011; *P. pseudodelicatissima*, Sugie and Yoshimura, 2013). It has also been reported that cell cycle-dependent uptake of Si and C, N, and P were uncoupled (Claquin *et al.*, 2002). The present results further support such uncoupling and indicate that ratios of Si to other nutrients in diatoms can change in response to changes in environmental conditions including carbonate chemistry.

Under LFe conditions, elemental compositions did not differ significantly among the three pCO_2 conditions because of constant

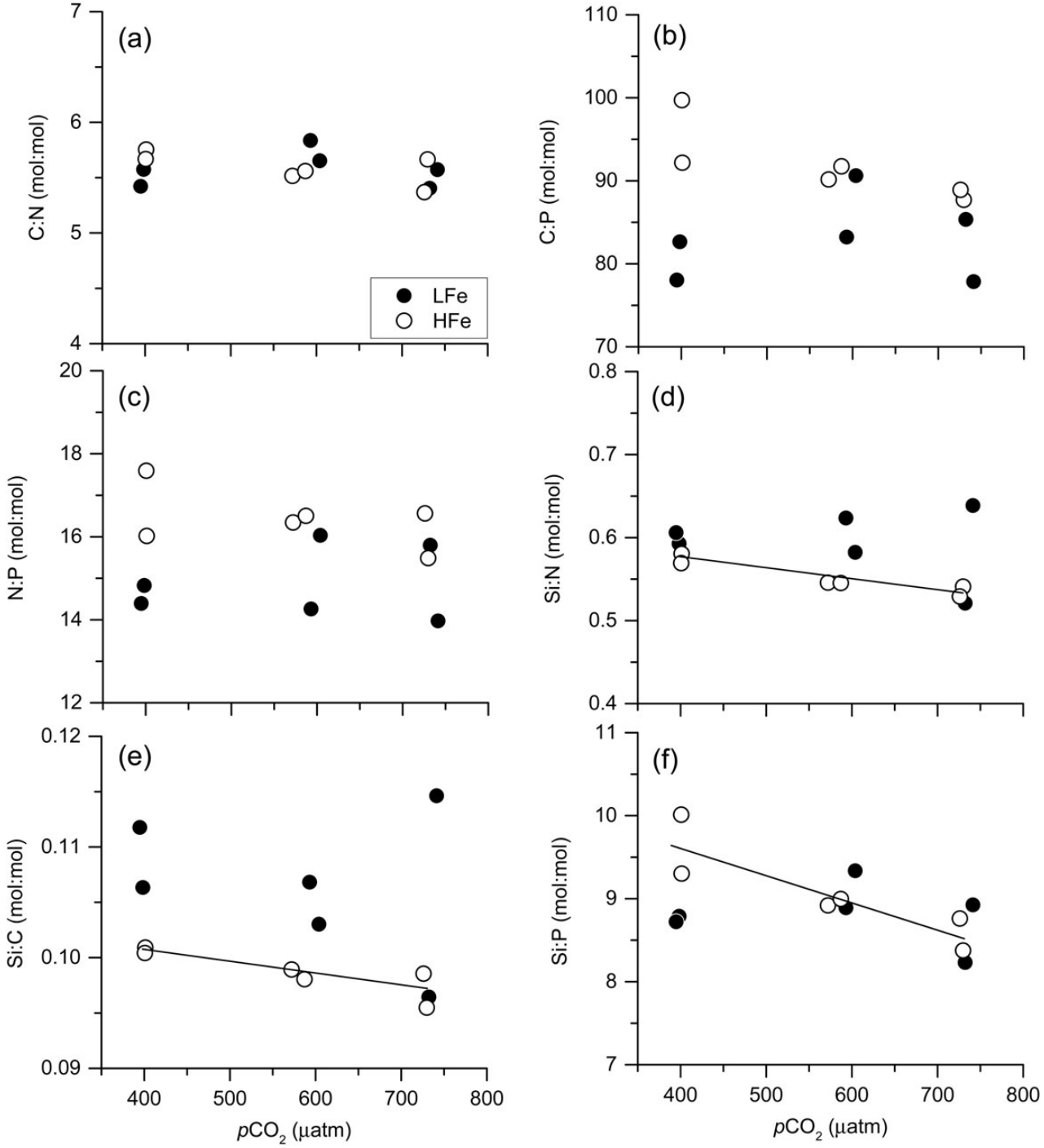

Figure 6. Change in (a) C:N, (b) C:P, (c) N:P, (d) Si:N, (e) Si:C, and (f) Si:P ratios of *T. weissflogii* grown under different pCO_2 and iron conditions. Solid lines in (d–f) represent the significant regressions between pCO_2 and Si:N, Si:C, and Si:P ratios, respectively. Statistics are shown in Tables 2 and 3.

NCP, NNP, NPP, and NSiP (Supplementary Figure S2), which are clearly different from the results obtained in the HFe conditions (Figure 6). This discrepancy may be caused by unexplored physiological mechanisms. We assume that the processes responsible for the increase in NEP with increasing pCO_2 as was found in the HFe conditions require additional energy for nutrient uptake. Under the energy-limited LFe conditions (Muggli *et al.*, 1996), the CO_2-related change in NEP was regulated by the iron-limitation. Hoppe *et al.* (2013) also observed that the effects of high CO_2 conditions on natural phytoplankton communities in the Southern Ocean were minimal under iron-depleted (siderophore desferrioxamine B added) conditions compared with iron-replete conditions. However, the rates of change in NEP of the diatom *P. pseudodelicatissima* were affected by changes in pCO_2 under conditions of low iron availability (Sugie and Yoshimura, 2013). The notable difference between *T. weissflogii* and *P. pseudodelicatissima* is k_μ value that *T. weissflogii* and *P. pseudodelicatissima* showed $k_\mu = 28$ and 1.5–5.0 pmol [Fe′] l^{-1}, respectively. These results

Table 3. Results of two-tailed, paired-sample *t*-test ($n = 12$) to test the effect of iron availability on the measured parameters, comparing the LFe ($Fe' = \sim 26$ pmol l^{-1}) and the HFe treatments ($Fe' = \sim 240$ pmol l^{-1}).

	Effect of decreasing Fe′	*p*-value
μ	Decrease	<0.001
Cell volume	Decrease	<0.001
C quota	Decrease	<0.001
N quota	Decrease	<0.001
P quota	Decrease	<0.001
Si quota	Decrease	<0.001
Chl *a* quota	Decrease	<0.001
In_{cell}[C]	Decrease	0.009
In_{cell}[N]	Decrease	0.018
In_{cell}[P]	n.s.c.	0.526
In_{cell}[Chl *a*]	Decrease	<0.001
Si/SA	Decrease	0.010
NCP	Decrease	<0.001
NNP	Decrease	<0.001
NPP	Decrease	<0.001
NSiP	Decrease	<0.001
NChl *a*P	Decrease	<0.001
C:N	n.s.c.	0.914
C:P	Decrease	0.034
N:P	Decrease	0.037
Si:N	Increase	0.045
Si:C	Increase	0.016
Si:P	n.s.c.	0.354
C:Chl *a*	Increase	<0.001

Three CO_2 treatments were pooled in LFe and HFe treatments, respectively. n.s.c., not significant change.

indicate that responses to the interaction between changes in pCO_2 and changes in iron availability vary among species depending on the affinity for uptake of [Fe′]. Previous studies have reported that the elemental composition of diatoms is not always related linearly to iron availability (Price, 2005; Bucciarelli *et al.*, 2010). More experiments manipulating various Fe′ and pCO_2 conditions using more phytoplankton species are required to better understand the effect of different CO_2 conditions on biogeochemical cycling of bioelements.

Effect of different iron availability on ecophysiology of *T. weissflogii*

Decreasing iron availability affected most of the measured parameters of *T. weissflogii*, indicating that iron availability is more important to determine ecophysiological processes of diatoms than variations in carbonate chemistry. Yoshimura *et al.* (2014) also suggested that changes in pCO_2 do not play a major role in the dynamics of particulate and dissolved organic matter produced by subarctic plankton communities during the exponential growth phase. Price (2005) reported that the C:N:Si:P ratio of *T. weissflogii* changed from 97:14:4.7:1 to 70:10:5.9:1 under iron-replete and iron-limited conditions, respectively. In the present study, we obtained similar results under HFe (96:17:9.7:1) and LFe (80:15:8.8:1) conditions in the 386 ppm xCO_2 treatments. By calculating Q_E ratios (RQ_E) between LFe386 and HFe386 ($RQ_E = Q_{E\text{-}LFe}/Q_{E\text{-}HFe}$, where $Q_{E\text{-}LFe}$ and $Q_{E\text{-}HFe}$ represent cell quota of each element in LFe386 and HFe386 treatment, respectively), we obtained 0.76, 0.78, 0.90, and 0.82 for RQ_C, RQ_N, RQ_P, and RQ_{Si}, respectively (Supplementary Figure S3). This estimate suggests that Q_C, Q_N, and Q_{Si} are highly variable compared with Q_P in response to the different iron conditions. In addition, the changes in carbonate chemistry modulated the elemental composition of *T. weissflogii* possibly via uncoupling of the cell cycle-dependent uptake of each bioelement (Claquin *et al.*, 2002). Specifically, the difference in the Si:N ratio between HFe and LFe conditions increased with increasing pCO_2 (Figure 6d). Such unexplored flexible nutrient stoichiometry may be a consequence of optimality of nutrient uptake or assimilations (Milligan *et al.*, 2004; Smith *et al.*, 2011), the mechanisms of which should be incorporated into the model simulations to better predict the biogeochemical cycling of nutrients.

Relevance of this study for ocean acidification study

Results of our short-term experiment contribute to better understanding of first-order biogeochemical processes of nutrients in dynamic coastal environment, but the progress of ocean acidification in nature is a slower process compared with our short-term experiment. Extrapolating our results to the future acidified environment require attention because long-term adaptive responses often differ from short-term phenotypic plasticity (Lohbeck *et al.*, 2012; Collins *et al.*, 2014). Crawfurd *et al.* (2011) and Tatters *et al.* (2013) reported that there was no clear difference in the effect of high CO_2 conditions on the ecophysiology of diatoms, when comparing the results of short-term plastic response with acclimation/adaptation responses for >100 cell divisions. On the other hand, Torstensson *et al.* (2015) reported that the specific growth rate decreased in the high CO_2 conditions only after the acclimation of ~60 cell divisions. Because phenotypic plasticity may be important for the subsequent adaptation or evolution of organisms (Collins *et al.*, 2014), plastic response found in this study could provide relevant information for the future acidified ocean ecosystem. However, there is very limited information available to date concerning adaptation of diatoms, and no reports are available on the adaptive response of cell size and cellular elemental content of diatoms. We need more information on the long-term effect of CO_2 on phytoplankton ecophysiology.

Conclusions

Our study demonstrated that some ecophysiological properties of coastal diatom *T. weissflogii* changed in response to changing CO_2 levels under iron-replete conditions. In coastal environment, iron concentration is generally higher than the oceanic region (Kuma *et al.*, 2000; Nishioka *et al.*, 2013; Bundy *et al.*, 2015), suggesting the change in the ecophysiological properties of *T. weissflogii* could occur with increasing CO_2 levels in the modern coastal seas (Wootton *et al.*, 2008). These changes may affect the food availability of higher trophic levels, sinking behaviour of *T. weissflogii*, and nutrient availability for other phytoplankton in the coastal regions. However, in addition to the differences in the response of individual phytoplankton species to changes in CO_2 levels (e.g. Doney *et al.*, 2009; Collins *et al.*, 2014), previous studies of the impacts of increasing CO_2 levels on the elemental composition of natural plankton communities have produced conflicting results, including no effect (Martin and Tortell, 2006; Feng *et al.*, 2010; Tortell *et al.*, 2010), increased particulate Si:N and Si:C ratios (Sugie *et al.*, 2013), and inconsistent changes in the production of dissolved and particulate organic matters (Yoshimura *et al.*, 2010, 2013, 2014). To interpret these results, it is necessary to improve knowledge of the effects of carbonate chemistry and iron availability on phytoplankton processes using both natural phytoplankton communities and laboratory-based unialgal cultures.

Supplementary data

Supplementary material is available at the *ICESJMS* online version of the manuscript.

Acknowledgements

We acknowledge three anonymous reviewers for providing valuable comments, which significantly improved the paper. The iron data in the medium were kindly provided by Dr J. Nishioka of Hokkaido University. We also thank K. Sugita, A. Tsuzuku, and N. Kageyama for their help on maintaining our culture collection of marine phytoplankton. This work was conducted in the framework of the Plankton Ecosystem Response to CO_2 Manipulation Study (PERCOM) project and supported by the grants from CRIEPI (#060215) and Grants-in-Aid for Scientific Research (#22681004) and by the Japan Agency for Marine-Earth Science and Technology (JAMSTEC).

References

Atkinson, D., Ciotti, B. J., and Montagnes, D. J. S. 2003. Protists decrease in size linearly with temperature: *ca*. 2.5% $^{\circ}C^{-1}$. Proceedings of Royal Society London, Series B, 270: 2605–2611.

Bucciarelli, E., Pondaven, P., and Sarthou, G. 2010. Effects of an iron-light co-limitation on the elemental composition (Si, C, N) of the marine diatoms *Thalassiosira oceanica* and *Ditylum brightwellii*. Biogeosciences, 7: 657–669.

Bundy, R. M., Abdulla, H. A. N., Hatcher, P. G., Biller, D. V., Buck, K. N., and Barbeau, K. A. 2015. Iron-binding ligands and humic substances in the San Francisco Bay estuary and estuarine-influenced shelf regions of coastal California. Marine Chemistry, 173: 183–194.

Burkhardt, S., Amoroso, G., Riebesell, U., and Sültemeyer, D. 2001. CO_2 and HCO_3^- uptake in marine diatoms acclimated to different CO_2 concentrations. Limnology and Oceanography, 46: 1378–1391.

Burkhardt, S., Zondervan, I., and Riebesell, U. 1999. Effect of CO_2 concentration on C:N:P ratio in marine phytoplankton: a species comparison. Limnology and Oceanography, 44: 683–690.

Claquin, P., Martin-Jézéquel, V., Kromkamp, J. C., Veldhuis, M. J. W., and Kraay, G. W. 2002. Uncoupling of silicon compared with carbon and nitrogen metabolisms and the role of the cell cycle in continuous culture of *Thalassiosira pseudonana* (Bacillariophyceae) under light, nitrogen, and phosphorus control. Journal of Phycology, 38: 922–930.

Clark, D. R., Flynn, K. J., and Fabian, H. 2014. Variation in elemental stoichiometry of the marine diatom *Thalassiosira weissflogii* (Bacillariophyceae) in response to combined nutrient stress and changes in carbonate chemistry. Journal of Phycology, 50: 640–651.

Collins, S., Rost, B., and Rynearson, T. A. 2014. Evolutionary potential of marine phytoplankton under ocean acidification. Evolutionary Applications, 7: 140–155.

Crawfurd, K. J., Raven, J. A., Wheeler, G. L., Baxter, E. J., and Joint, I. 2011. The response of *Thalassiosira pseudonana* to long-term exposure to increased CO_2 and decreased pH. PLoS ONE, 6: e26695.

Doney, S. C., Fabry, V. J., Feely, R. A., and Kleypas, J. A. 2009. Ocean acidification: the other CO_2 problem. Annual Review of Marine Science, 1: 169–192.

Dore, J. E., Lukas, R., Sadler, D. W., Church, M. J., and Karl, D. M. 2009. Physical and biogeochemical modulation of ocean acidification in the central North Pacific. Proceedings of the National Academy of Sciences of the United States of America, 106: 12235–12240.

Edmond, J. W. 1970. High precision determination of titration alkalinity and total carbon dioxide content of seawater by potentiometric titration. Deep-Sea Research, 17: 737–750.

Eggers, S. L., Lewandowska, A. M., Barcelos e Ramos, J., Blanco-Ameijeiras, S., Gallo, F., and Matthiessen, B. 2014. Community composition has greater impact on the functioning of marine phytoplankton communities than ocean acidification. Global Change Biology, 20: 713–723.

Feng, Y., Hare, C. E., Rose, J. M., Handy, S. M., DiTullio, G. R., Lee, P. A., Smith, W. O., Jr., *et al.* 2010. Interactive effects of iron, irradiance and CO_2 on Ross Sea phytoplankton. Deep Sea Research I, 57: 368–383.

Feng, Y., Warner, M. E., Zhang, Y., Sun, J., Fu, F. X., Rose, J. M., and Hutchins, D. A. 2008. Interactive effects of increased pCO_2, temperature and irradiance on the marine coccolithophore *Emiliania huxleyi* (Prymnesiophyceae). European Journal of Phycology, 43: 87–98.

Fu, F. X., Zhang, Y., Warner, M. E., Feng, Y., Sun, J., and Hutchins, D. A. 2008. A comparison of future increased CO_2 and temperature effects on sympatric *Heterosigma akashiwo* and *Prorocentrum minimum*. Harmful Algae, 7: 76–90.

Geider, R. J., La Roche, J., Greene, R. M., and Olaizola, M. 1993. Response of the photosynthetic apparatus of *Phaeodactylum tricornutum* (Bacillariophyceae) to nitrate, phosphate, or iron starvation. Journal of Phycology, 29: 755–766.

Hassler, C. S., Schoemann, V., Nichols, C. M., Butler, E. C. V., and Boyd, P. W. 2011. Saccharides enhance iron bioavailability to Southern Ocean phytoplankton. Proceedings of the National Academy of Sciences of the United States of America, 108: 1076–1081.

Hervé, V., Derr, J., Douady, S., Quinet, M., Moisan, L., and Lopez, P. L. 2012. Multiparametric analysis reveal the pH-dependence of silicon biomineralization in diatoms. PLoS ONE, 7: e46722.

Hopkinson, B. M., Dupont, C. L., Allen, A. E., and Morel, F. M. M. 2011. Efficiency of the CO_2-concentrating mechanism of diatoms. Proceedings of the National Academy of Sciences of the United States of America, 108: 3830–3837.

Hoppe, C. J. M., Hassler, C. S., Payne, C. D., Tortell, P. D., Rost, B., and Trimborn, S. 2013. Iron limitation modulates ocean acidification effects on Southern Ocean phytoplankton communities. PLoS ONE, 8: e79890.

Hoppe, C. J. M., Langer, G., and Rost, B. 2011. *Emiliania huxleyi* shows identical response to elevated pCO_2 in TA and DIC manipulations. Journal of Experimental Marine Biology and Ecology, 406: 54–62.

IGBP, IOC, and SCOR. 2013. Ocean acidification summary for policymakers—Third Symposium on the Ocean in a High-CO_2 World. International Geosphere-Biospere Programme, Stockholm, Sweden.

IPCC. 2013. Summary for policymakers. *In* Climate Change 2013: the Physical Science Basis. Contribution of Working Group I to the Fifth Assessment Report of the Intergovernmental Panel on Climate Change. Ed. by T. F. Stocker, D. Qin, G-K. Plattner, M. Tignor, S. K. Allen, J. Boschung, A. Nauels, *et al.* Cambridge University Press, Cambridge, UK and New York, USA.

King, A. L., Sañudo-Wilhelmy, S. A., Leblanc, K., Hutchins, D. A., and Fu, F. 2011. CO_2 and vitamin B_{12} interactions determine bioactive trace metal requirements of a subarctic Pacific diatom. The ISME Journal, 5: 1388–1396.

Kuma, K., Katsumoto, A., Shiga, N., Sawabe, T., and Matsunaga, K. 2000. Variation of size-fractionated Fe concentrations and Fe(III) hydroxide solubilities during a spring phytoplankton bloom in Funka Bay (Japan). Marine Chemistry, 71: 111–123.

Laglera, L. M., and van den Berg, C. M. G. 2009. Evidence for geochemical control of iron by humic substances in seawater. Limnology and Oceanography, 54: 610–619.

LaRoche, J., Rost, B., and Engel, A. 2011. Bioassays, batch culture and chemostat experimentation. *In* Guide to Best Practices for Ocean Acidification Research and Data Reporting, pp. 81–94. Ed. by U. Rievesell, V. J. Fabry, L. Hansson, and J. P. Gattuso. Publications Office of the European Union, Luxembourg. 260 pp.

Lewis, E., and Wallance, D. W. R. 1998. Program developed for CO_2 system calculations. ORNL/CDIAC-105. Carbon Dioxide Information Analysis Center, Oak Ridge National Laboratory, US Department of Energy, Oak Ridge, TN.

Lohbeck, K. T., Riebesell, U., and Reusch, T. B. H. 2012. Adaptive evolution of a key phytoplankton species to ocean acidification. Nature Geoscience, 5: 346–351.

Martin, C. L., and Tortell, P. D. 2006. Bicarbonate transport and extracellular carbonic anhydrase activity in Bering Sea phytoplankton assemblages: results from isotope disequilibrium experiments. Limnology and Oceanography, 51: 2111–2121.

Martin-Jézéquel, V., Hildebrand, M., and Brzezinski, M. A. 2000. Silicon metabolism in diatom: implications for growth. Journal of Phycology, 36: 821–840.

Millero, F. J., Woosley, R., DiTrolio, B., and Waters, J. 2009. Effect of ocean acidification on the speciation of metals in seawater. Oceanography, 22: 72–85.

Milligan, A. J., Varela, D. E., Brzezinski, M. A., and Morel, F. M. M. 2004. Dynamics of silicon metabolism and silicon isotopic discrimination in a marine diatom as a function of pCO_2. Limnology and Oceanography, 49: 322–329.

Montagnes, D. J. S., and Franklin, D. J. 2001. Effect of temperature on diatom volume, growth rate, and carbon and nitrogen content: reconsidering some paradigms. Limnology and Oceanography, 46: 2008–2018.

Morel, F. M. M., Kustka, A. B., and Shaked, Y. 2008. The role of unchelated Fe in the iron nutrition of phytoplankton. Limnology and Oceanography, 53: 400–403.

Muggli, D. L., Lecourt, M., and Harrison, P. J. 1996. Effects of iron and nitrogen source on the sinking rate, physiology and metal composition of an oceanic diatom from the subarctic Pacific. Marine Ecology Progress Series, 132: 215–227.

Nishioka, J., Nakatsuka, T., Watanabe, Y. W., Yasuda, I., Kuma, K., Ogawa, H., Ebuchi, N., *et al.* 2013. Intensive mixing along an island chain controls oceanic biogeochemical cycles. Global Biogeochemical Cycles, 27: 1–10.

Obata, H., Karatani, H., and Nakayama, E. 1993. Automated determination of iron in seawater by chelating resin concentration and chemiluminescence detection. Analitycal Chemistry, 65: 1524–1528.

Paasche, E. 1980. Silicon content of five marine plankton diatom species measured with a rapid filter method. Limnology and Oceanography, 25: 474–480.

Passow, U., and Carlson, C. A. 2012. The biological pump in a high CO_2 world. Marine Ecology Progress Series, 249: 249–271.

Price, N. M. 2005. The elemental stoichiometry and composition of an iron-limited diatom. Limnology and Oceanography, 50: 1159–1171.

Price, N. M., Harrison, G. I., Hering, J. G., Hudson, R. J. M., Nirel, P. M. V., Palenik, B. P., and Morel, F. M. M. 1988/1989. Preparation and chemistry of the artificial algal culture medium Aquil. Biological Oceanography, 6: 443–461.

Quigg, A., Finkel, Z. V., Irwwin, A. J., Rosenthal, Y., Ho, T. Y., Reinfelder, J. R., Schofield, O., *et al.* 2003. The evolutionary inherence of elemental stoichiometry in marine phytoplankton. Nature, 425: 291–293.

Raven, J. A., Evans, M. C. W., and Korb, R. E. 1999. The role of trace metals in photosynthetic electron transport in O_2-evolving organisms. Photosynthesis Research, 60: 111–149.

Richier, S., Achterberg, E. P., Dumousseaud, C., Poulton, A. J., Suggett, D. J., Tyrrell, T., Zubkov, M. V., *et al.* 2014. Phytoplankton responses and associated carbon cycling during shipboard carbonate chemistry manipulation experiments conducted around Northwest European shelf seas. Biogeosciences, 11: 4733–4752.

Roberts, K., Granum, E., Leegood, R. C., and Raven, J. A. 2007. C3 and C4 pathways of photosynthetic carbon assimilation in marine diatoms are under genetic, not environmental, control. Plant Physiology, 145: 230–235.

Seebah, S., Fairfield, C., Ullrich, M. S., and Passow, U. 2014. Aggregation and sedimentation of *Thalassiosira weissflogii* (diatom) in a warmer and more acidified future ocean. PLoS ONE, 9: e112379.

Shi, D., Xu, Y., Hopkinson, B. M., and Morel, F. M. M. 2010. Effect of ocean acidification on iron availability to marine phytoplankton. Science, 327: 676–679.

Shi, D., Xu, Y., and Morel, F. M. M. 2009. Effects of the pH/pCO_2 control method on medium chemistry and phytoplankton growth. Biogeosciences, 6: 1199–1207.

Smith, S. L., Pahlow, M., Merico, A., and Wirtz, K. W. 2011. Optimality-based modeling of planktonic organisms. Limnology and Oceanography, 56: 2080–2094.

Solórzano, L., and Sharp, J. H. 1980. Determination of total dissolved phosphorus and particulate phosphorus in natural waters. Limnology and Oceanography, 25: 754–758.

Stumm, W., and Morgan, J. J. 1996. Aquatic Chemistry, 3rd edn. Wiley Interscience, New York.

Sugie, K., Endo, H., Suzuki, K., Nishioka, J., Kiyosawa, H., and Yoshimura, T. 2013. Synergistic effects of pCO_2 and iron availability on nutrient consumption ratio of the Bering Sea phytoplankton community. Biogeosciences, 10: 6309–6321.

Sugie, K., Kuma, K., Fujita, S., and Ikeda, T. 2010. Increase in Si:N drawdown ratio due to resting spore formation by spring bloom-forming diatoms under Fe- and N-limited conditions in the Oyashio region. Journal of Experimental Marine Biology and Ecology, 382: 108–116.

Sugie, K., and Yoshimura, T. 2013. Effects of pCO_2 and iron on the elemental composition and cell geometry of the marine diatom *Pseudo-nitzschia pseudodelicatissima*. Journal of Phycology, 49: 475–488.

Sun, J., Hutchins, D. A., Feng, Y., Seubert, E. L., Caron, D. A., and Fu, F. X. 2011. Effects of changing pCO_2 and phosphate availability on domoic acid production and physiology of the marine harmful bloom diatom *Pseudo-nitzschia multiseries*. Limnology and Oceanography, 56: 829–840.

Sunda, W., and Huntsman, S. 2003. Effect of pH, light, and temperature on Fe-EDTA chelation and Fe hydrolysis in seawater. Marine Chemistry, 84: 35–47.

Sunda, W. G., and Huntsman, S. A. 1995. Iron uptake and growth limitation in oceanic and coastal phytoplankton. Marine Chemistry, 50: 189–206.

Suzuki, R., and Ishimaru, T. 1990. An improved method for the determination of phytoplankton chlorophyll using N, N-dimethylformamide. Journal of Oceanographic Society of Japan, 46: 190–194.

Takeda, S. 1998. Influence of iron availability on nutrient consumption ratio of diatoms in oceanic waters. Nature, 393: 774–777.

Tatters, A. O., Roleda, M. Y., Schnetzer, A., Fu, F., Hurd, C. L., Boyd, P. W., and Caron, D. A., et al. 2013. Short- and long-term conditioning of a temperate marine diatom community to acidification and warming. Philosophical Transactions of the Royal Society B, 368: 20120437.

Torstensson, A., Hedblom, M., Björk, M. M., Chierici, M., and Wulff, A. 2015. Long-term acclimation to elevated pCO_2 alters carbon metabolism and reduces growth in the Antarctic diatom *Nitzschia lecointei*. Proceedings of the Royal Society B, 282: 20151513.

Tortell, P. D., Trimborn, S., Li, Y., Rost, B., and Payne, C. D. 2010. Inorganic carbon utilization by Ross Sea phytoplankton across natural and experimental CO_2 gradients. Journal of Phycology, 46: 433–443.

Weber, T. S., and Deutsch, C. 2010. Ocean nutrient ratios governed by phytoplankton biogeography. Nature, 467: 550–554.

Welschmeyer, N. A. 1994. Fluorometric analysis of chlorophyll *a* in the present of chlorophyll *b* and pheopigments. Limnology and Oceanography, 39: 1985–1992.

Wootton, J. T., Pfister, C. A., and Forester, J. D. 2008. Dynamic patterns and ecological impacts of declining ocean pH in a high-resolution multi-year dataset. Proceedings of the National Academy of Sciences of the United States of America, 105: 18848–18853.

Yoshimura, T., Nishioka, J., Suzuki, K., Hattori, H., Kiyosawa, H., and Watanabe, W. Y. 2010. Impacts of elevated CO_2 on organic carbon dynamics in nutrient depleted Okhotsk Sea surface waters. Journal of Experimental Marine Biology and Ecology, 395: 191–198.

Yoshimura, T., Sugie, K., Endo, H., Suzuki, K., Nishioka, J., and Ono, T. 2014. Organic matter production response to CO_2 increase in open subarctic plankton communities: comparison of six microcosm experiments under iron-limited and -enriched conditions. Deep Sea Research I, 94: 1–14.

Yoshimura, T., Suzuki, K., Kiyosawa, H., Ono, T., Hattori, H., Kuma, K., and Nishioka, J. 2013. Impacts of elevated CO_2 on particulate and dissolved organic matter production: microcosm experiments using iron deficient plankton communities in open subarctic waters. Journal of Oceanography, 69: 601–618.

Handling editor: Shubha Sathyendranath

ICES Journal of Marine Science

ICES Journal of Marine Science (2016), 73(3), 693–703. doi:10.1093/icesjms/fsv168

Contribution to Special Issue: 'Towards a Broader Perspective on Ocean Acidification Research'

Original Article

Variable responses of temperate calcified and fleshy macroalgae to elevated pCO_2 and warming

S. L. Kram[1]*, N. N. Price[1†], E. M. Donham[2], M. D. Johnson[1], E. L. A. Kelly[1], S. L. Hamilton[2], and J. E. Smith[1]

[1]*Center for Marine Biodiversity and Conservation, Marine Biology Research Division, Scripps Institution of Oceanography, La Jolla, CA 92093-0202, USA*
[2]*Moss Landing Marine Laboratories, 8272 Moss Landing Road, Moss Landing, CA 95039, USA*

**Corresponding author: tel: +415 497 5811; fax: +858 822 2167; e-mail: skram@ucsd.edu*
[†]*Present address: Bigelow Laboratory for Ocean Sciences, 60 Bigelow Drive, East Boothbay, ME 04544, USA.*

Kram, S. L., Price, N. N., Donham, E. M., Johnson, M. D., Kelly, E. L. A., Hamilton, S. L., and Smith, J. E. Variable responses of temperate calcified and fleshy macroalgae to elevated pCO_2 and warming. – ICES Journal of Marine Science, 73: 693–703.

Received 29 April 2015; revised 24 August 2015; accepted 31 August 2015; advance access publication 25 September 2015.

Anthropogenic carbon dioxide (CO_2) emissions simultaneously increase ocean temperatures and reduce ocean surface pH, a process termed ocean acidification (OA). OA is expected to negatively affect the growth and physiology of many calcified organisms, but the response of non-calcified (fleshy) organisms is less well understood. Rising temperatures and pCO_2 can enhance photosynthetic rates (within tolerance limits). Therefore, warming may interact with OA to alter biological responses of macroalgae in complicated ways. Beyond thresholds of physiological tolerance, however, rising temperatures could further exacerbate negative responses to OA. Many studies have investigated the effects of OA or warming independently of each other, but few studies have quantified the interactive effects of OA and warming on marine organisms. We conducted four short-term independent factorial CO_2 enrichment and warming experiments on six common species of calcified and fleshy macroalgae from southern California to investigate the independent and interactive effects of CO_2 and warming on growth, carbonic anhydrase (CA) enzyme activity, pigment concentrations, and photosynthetic efficiency. There was no effect of elevated pCO_2 on CA activity, pigment concentration, and photosynthetic efficiency in the macroalgal species studies. However, we found that calcareous algae suffered reduced growth rates under high pCO_2 conditions alone, although the magnitude of the effect varied by species. Fleshy algae had mixed responses of growth rates to high pCO_2, indicating that the effects of pCO_2 enrichment are inconsistent across species. The combined effects of elevated pCO_2 and warming had a significantly negative impact on growth for both fleshy and calcareous algae; calcareous algae experienced five times more weight loss than specimens in ambient control conditions and fleshy growth was reduced by 76%. Our results demonstrate the need to study the interactive effects of multiple stressors associated with global change on marine communities.

Keywords: carbon-concentrating mechanisms, carbon dioxide, carbonic anhydrase, global warming, multiple stressors, photosynthesis, seawater pH.

Introduction

The continued release of anthropogenic carbon dioxide (CO_2) from the burning of fossil fuels is a major driver of climate change, and is predicted to result in an increase in sea surface temperature and decreased pH in open ocean surface waters (IPCC, 2013). The oceanic uptake or absorption of anthropogenic CO_2 has already resulted in a drop of 0.1 pH units (and, consequently, a 16% decrease in aragonite and calcite saturation state) in open ocean surface water (Caldeira and Wickett, 2003; Feely *et al.*, 2012), a process termed ocean acidification (OA). Continued absorption of CO_2 by the ocean is predicted to further reduce open ocean surface pH by 0.06–0.32 units by the end of the 21st century, through associated changes in carbonate chemistry, whereas atmospheric warming is predicted to result in an increase in sea surface temperature by 0.6–2.0°C (IPCC, 2013). Both OA and warming have the potential to negatively impact organisms' success and survival. Many OA studies to date have tested the effects of increased CO_2 in isolation (often with constant and stable carbonate chemistry parameters), reporting negative effects on survival, growth, calcification, and reproduction for many marine organisms (Hendriks *et al.*, 2010;

Kroeker *et al.*, 2010, 2013; McCoy and Kamenos, 2015). However, these studies have not necessarily been representative of the environmental conditions organisms experience *in situ*. Recent evidence indicates that natural variation in the carbonate system near shore is much more complex and difficult to predict than in the open ocean (Hoffmann *et al.*, 2011; Frieder *et al.*, 2012); this variation has only recently been incorporated into experimental designs (Cornwall *et al.*, 2013). Additionally, studies thus far predominantly test only a single stressor, and are therefore unable to capture synergistic effects of warming and elevated CO_2 [but see Anthony *et al.* (2008), Martin and Gattuso (2009), Byrne (2011), Diaz-Pulido *et al.* (2012), Johnson and Carpenter (2012), and Williams *et al.* (2014)], which may exacerbate or mitigate the effects of changing carbonate chemistry on species' performances. We addressed these issues by investigating the combined effects of increased CO_2 and warming on ecologically important temperate, fleshy, and calcified macroalgae.

Because of the necessary and diverse ecosystem services that different species of macroalgae provide, such as food, habitat, refugia, and settlement cues for invertebrate larvae, it is vital to understand their physiological tolerances and responses to environmental stressors (i.e. warming and OA), which in turn will determine population abundance and distribution. Calcified and fleshy algae may exhibit opposing responses to OA due to different physiological demands for particular carbon species. CO_2 enrichment has been shown to negatively affect the growth, calcification, and reproductive rates of at least some species of calcareous algae, as well as their physiological performance and competitive abilities (Gao *et al.*, 1993; Kleypas and Langdon, 2006; Diaz-Pulido *et al.*, 2007; Anthony *et al.*, 2008; Fabry *et al.*, 2008; Kuffner *et al.*, 2008; Martin and Gattuso, 2009; Price *et al.*, 2011; Johnson *et al.*, 2014a; Williams *et al.*, 2014). Fleshy macroalgae, in contrast, exhibit more variable responses to increased CO_2 (Beardall *et al.*, 1998; Cornwall *et al.*, 2012; Johnson *et al.*, 2014a), yet the physiological mechanisms underlying these responses are still largely unknown.

The lack of consistent responses among fleshy algae to CO_2 enriched seawater could be due, in part, to the capacity of different taxa to utilize different species of dissolved inorganic carbon, such as bicarbonate (HCO_3^-), for photosynthesis. Macroalgae are able to uptake CO_2 directly via passive diffusion, but many species are unable to achieve maximum rates of photosynthesis using only CO_2 (Kübler *et al.*, 1999; Morison *et al.*, 2005). CO_2 is the least abundant species of inorganic carbon in seawater, it is highly diffusive, and it is thus difficult to concentrate at the site of photosynthesis. Some algae have evolved the use of carbon-concentrating mechanisms (CCMs), such as the enzyme carbonic anhydrase (CA), to convert bicarbonate (more easily concentrated in cellular tissue) to CO_2 (Sültemeyer, 1998). CA activity can be used as a proxy to assess whether marine algae employ internal and/or external CA as a CCM for photosynthesis. CA is energetically costly (Hepburn *et al.*, 2011), but pelagic phytoplankton have been shown to downregulate CA production under CO_2 enrichment because dissolved CO_2 is no longer limiting (Hopkinson *et al.*, 2011). Benthic algae may respond similarly, but this hypothesis has been tested on only a limited number of species (García-Sánchez *et al.*, 1994; Hofmann *et al.*, 2012a). Macroalgae that are able to downregulate CA activity may then be able to divert further energy into somatic or reproductive growth and/or photosynthetic machinery such as photosynthetic pigments.

In addition to CO_2, temperature-adaptive physiological variation and ecological interactions are instrumental in structuring the biogeography and distribution of many marine species (Stillman, 2002; Compton *et al.*, 2007). Increases in temperature elevate the metabolic rates of many organisms living well within optimal temperature envelopes. In primary producers, photosynthetic rates gradually increase with temperature until an optimum is reached; if temperatures continue to rise and exceed thermal tolerance limits, photosynthetic rates will decline precipitously (Davison, 1991). Photosynthetic rates increase through the production of more photosynthetic pigments, or by increasing photosynthetic efficiency (Schreiber, 2004). Therefore, overall growth, productivity, and pigmentation of macroalgae are expected to be positively affected by temperature increases (Pereira *et al.*, 2006), within an optimal temperature envelope.

While the impacts of elevated CO_2 and increased temperatures have been investigated individually, little is known about the potential interaction between CO_2 and rising ocean temperatures on the physiology of marine algae. Due to the potential positive effects of warming on photosynthesis, it has been suggested that increased temperatures may allow organisms to compensate for the negative effects of OA. However, the limited research available suggests these two stressors result in synergistic antagonistic impacts on calcifiers, such that warming exacerbates the effect of CO_2 enrichment (Anthony *et al.*, 2008; Gao *et al.*, 2012; Diaz-Pulido *et al.*, 2012). Relatively few multistressor studies exist to date for fleshy species [but see Connell and Russell, (2009)], but we predict that increased CO_2 and temperature would have a synergistic positive effect because both CO_2 and temperature have the potential to increase photosynthetic rates.

The response of organisms to environmental stressors, such as OA and warming, may be influenced by the extent of habitat specialization. Some species are ecological generalists and have wider tolerances for fluctuating temperature and/or pCO_2, and may be better equipped to tolerate and/or acclimate, and ultimately to survive, future global change (Zerebecki and Sorte, 2011). Most OA experiments have been conducted in recirculating or flow-through aquaria experiencing constant ambient control or elevated CO_2 conditions. However, recent studies have documented that pH and pCO_2 in the natural environment are highly dynamic, especially in shallow coastal systems. The variability in pCO_2 that exists over a diel or tidal cycle or during an upwelling event includes conditions equivalent to or surpassing those expected to occur by the turn of the century under OA (Hoffmann *et al.*, 2011). Therefore, some taxa, such as ecological generalists, may already have the potential to acclimate and cope with changing ocean chemistry. For example, Johnson *et al.* (2014b) found that *Porolithon onkodes*, a crustose coralline alga collected from a habitat experiencing more variable pCO_2, was able to calcify 42% more than individuals from habitats experiencing more constant conditions. This disparity indicates that organisms already existing in dynamic pCO_2 habitats may be acclimated to future OA. Given this variability in environmental conditions and species' response, it must be emphasized to capture natural variation in temperature and pCO_2 in experiments to enable more realistic predictions of ecosystem-level responses in the future.

In this study, we assessed the responses of six functionally different, common southern California macroalgae to increased pCO_2 and warming, by elevating temperature and pCO_2 above the existing natural variability of local coastal conditions. The species chosen were representative of potential varied vulnerabilities to OA and/or warming based on ecological habitat specialization, species origin (native vs. invasive species), and functional morphology

(calcified vs. fleshy, and articulated vs. encrusting). We measured several biological responses including growth rate, calcification rate, photosynthetic efficiency, pigment concentration, and CA activity. Two types of experiments were conducted: single manipulation (elevated pCO_2 only) and factorial design (elevated pCO_2 crossed with elevated temperature). In the pCO_2-only experiments, we hypothesized that calcareous algae would experience decreased growth and calcification rates under naturally fluctuating, high pCO_2 conditions. If the fleshy algae downregulated CA activity, we predicted that they would be positively affected (increased growth, pigmentation, and photosynthetic efficiency) by the pCO_2 treatment. However, if CA enzyme activity was not downregulated, or was not present, we predicted that fleshy algae would not be affected by elevated pCO_2. We also predicted that the invasive species, or ecological generalist, would respond more positively to pCO_2 than the native counterpart. Calcified articulated species were predicted to respond more negatively to increased pCO_2 than encrusting species, due to higher surface area exposure to reduced carbonate saturation state seawater. In the factorial experiments, we expected all algae to have increased growth, production, photosynthetic efficiency, and higher pigment content under the warming treatment. We predicted that only the fleshy algae would have a synergistic positive effect with the combination of high pCO_2 and temperature, and that calcified algae would have mixed responses.

Material and methods

Study species and study system

All experiments were conducted in an experimental flow-through seawater system at the Scripps Institution of Oceanography (SIO) in La Jolla, California, from July 2012 to March 2013. Six commonly occurring calcified and fleshy macroalgae were chosen for four independent elevated pCO_2 or elevated pCO_2 × warming experiments that ranged in length from 17 to 31 d (Table 1). Two elevated pCO_2 experiments were conducted with paired species of algae comparing the effects of increased CO_2 on (i) native and non-native brown fleshy algae (*Dictyopteris undulata* and *Sargassum horneri*) and (ii) articulated and encrusting calcareous red algae (*Jania adhaerens* and *Lithothamnion californicum*). Elevated pCO_2 and warming experiments examined responses of single algal species to multiple stressors, including the fleshy red alga, *Plocamium cartilagineum*, and the calcified articulated red alga, *Corallina vancouveriensis*. Specimens were collected subtidally by snorkel (within 12 km of SIO) or from the low intertidal zone (<3.2 km from SIO), and were acclimated to laboratory conditions for a least 1 week in aerated, flow-through tanks. Water was sourced from the SIO pier, ~300 m offshore at 3–4 m depth. Algal epiphytes were removed by hand using tweezers and specimens were dipped in insecticide (Garden Tech *Sevin* Concentrate Bug Killer: 4 l seawater: 20 ml *Sevin*) 2 d before the initiation of the experiment to remove herbivorous invertebrates that were found to have significant effects on biomass in preliminary trials. Carpenter (1986) showed that *Sevin* has no negative effects on algal biomass or productivity. Algal specimens were loosely attached to mesh stands and each placed in 1 l experimental aquaria.

Experimental conditions

The two single-manipulation pCO_2 experiments were conducted, with two levels of pCO_2 targeted at 400 and 900 μatm, with $n = 10$ replicates per treatment and species. For the two combined pCO_2 and warming experiments, factorial manipulations of pCO_2 and temperature were used, with target values for temperature (ambient = 15–17°C and elevated = +2°C above ambient) and pCO_2 at 400 and 900 μatm, with $n = 10$ replicates per treatment (Figure 1). All treatment levels were selected based on the IPCC (2013) Representative Concentration Pathway (RCP) 8.5 for conditions projected in 2100.

Aquaria were maintained under four full-spectrum 54 W Giesemann T-5 fluorescent bulbs (Supplementary Figure S1). The lights mimicked sunrise and sunset by gradually increasing or decreasing light levels over the course of an hour and were set to 10 h of daylight for experiments conducted in winter and 14 h of daylight in experiments conducted in summer (Table 1). Ambient and treatment aquaria alternated positions along the bench and their locations were rotated weekly to prevent lighting dissipation effects.

Each aquarium contained an individual algal specimen and was continuously supplied with flow-through filtered seawater (0.25 l filtered seawater min^{-1}). Constant seawater flow rates within each aquarium were maintained using Rain Bird pressure compensator modules placed within Rain Bird Xeri-Bird 8-Outlet Manifolds. This flow-through design prevented nutrient limitation or total alkalinity draw-down due to calcification in the long-term experimental setting, and allowed for natural temporal pH variability and high replication per treatment level.

pCO_2 treatments

Mass flow controllers (Omega FMA 5400/5500) were used to blend ambient air with pure CO_2 before bubbling gases into each aquarium to create experimental conditions. Filtered ambient air, originating in a non-oil-based Ingersoll air compressor, was sent

Table 1. Details of each of the four experiments performed in this study (two elevated pCO_2 only and two elevated pCO_2 and warming experiments on southern CA macroalgae).

Exp #	Experiment type	Dates	# Days	Species 1	Cal/non-cal	Native/invasive	Species 2	Cal/non-cal	Native/invasive	Collection depth
1	OA	3 July 2012 – 19 July 2012	17	*Dictyopteris undulata*	Non-cal	Native	*Sargassum horneri*	Non-cal	Invasive	2 – 3 meters
2	OA	26 July 2012 – 22 August 2012	27	*Jania adhaerens*	Cal	Native	*Lithothamnion californicum*	Cal	Native	Intertidal
3	OA + warming	28 November 2012 – 19 December 2012	21	*Plocamium cartilagineum*	Non-cal	Native	–	–	–	Intertidal
4	OA + warming	5 February 2013 – 8 March 2013	31	*Corallina vancouveriensis*	Cal	Native	–	–	–	Intertidal

Cal, calcified; Non-cal, non-calcified/fleshy.

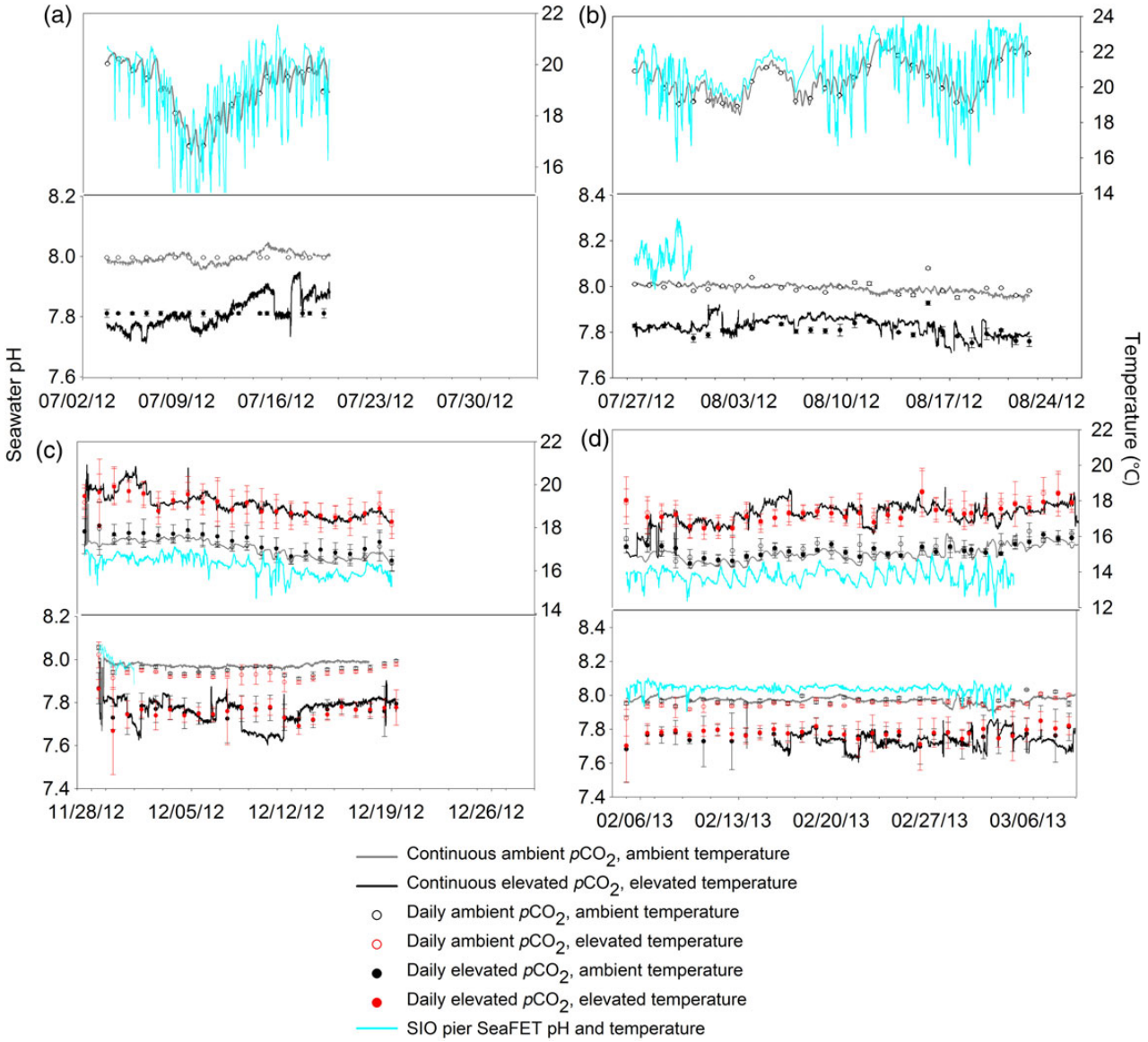

Figure 1. [colour version] Daily mean (± SE) and continuous (logged every 15 min) temperature and pH for all experiments. Solid grey lines are ambient CO_2, ambient temperature treatments, and solid black lines are elevated CO_2, elevated temperature collected continuously from Honeywell Non-Glass pH Electrode Durafets that were kept in control (without alga sample) aquaria. The solid blue lines are continuous *in situ* pH measurements collected by a SeaFET off the SIO pier. The points are daily means (± SE) from a HACH (HQ40d meter and PCH201 glass electrode pH probe) that were calibrated daily with certified Tris buffer from the Dickson laboratory at the SIO. (a) pCO_2 only (exp. 1, Table 1); average ambient pH: 8.02 ± 0.006; average elevated CO_2 pH: 7.80 ± 0.011; average ambient temperature: 18.92 ± 0.172°C. (b) pCO_2 only (exp. 2, Table 1); average ambient pH: 8.00 ± 0.014; average elevated CO_2 pH: 7.81 ± 0.009; average ambient temperature: 20.20 ± 0.137°C. (c) pCO_2 and warming (exp. 3, Table 1); average ambient pH: 7.96 ± 0.007; average elevated CO_2 pH: 7.75 ± 0.025; average ambient temperature: 17.21 ± 0.072°C, average elevated temperature: 19.02 ± 0.069°C. (d) pCO_2 and warming (exp. 4, Table 1); average ambient pH: 7.97 ± 0.017; average elevated CO_2 pH: 7.81 ± 0.032; average ambient temperature: 15.27 ± 0.049°C; average elevated temperature: 17.35 ± 0.064°C.

directly to the ambient treatment aquaria or through a desiccant (DRIERITE Laboratory Air and Gas Drying) unit before being blended with pure CO_2. A CO_2 gas analyser (LI-COR 820) was used to manually set and log the concentration of CO_2 in the CO_2–air blend that entered aquaria. Blank control aquaria ($n = 3$ per treatment), which did not contain living samples, were maintained to quantify potential impacts the organisms may have had on seawater carbonate chemistry, though unlikely given the flow-through nature of the system. Ambient pH conditions were set to represent field conditions at the site of seawater intake. The desired decreased pH levels and saturation states were created by constantly bubbling a CO_2–air blend into individual treatment aquaria (1-l glass aquaria) at a rate sufficient to lower the seawater pH (pH_{SW}) by 0.2 ± 0.05 (Figure 1) from ambient given that the aquaria water residence time was ~4 min.

Temperature treatments

Ambient temperatures were set according to field conditions at the site of seawater intake. Elevated temperatures of 2 ± 0.5°C in the experimental aquaria (Figure 1) were created by placing the aquaria

inside a large water bath that was heated using aquarium heaters (Hydro Thermal Submersible 400 W). Six water baths were used with three ambient and three with the elevated temperature treatment. The position of aquaria bubbled with high CO_2 ($n = 4$ per water bath) and that of aquaria bubbled with ambient air ($n = 4$ per water bath) were alternated within each bath.

In situ pH and temperature data acquisition

An autonomous Ion Sensitive Field Effect Transistor (ISFET) Honeywell Durafet pH sensor (hereafter called SeaFET; Martz *et al.*, 2010) was deployed next to the SIO seawater intake pipe, allowing for continued monitoring of ambient field conditions (Figure 1). Measurements were taken every 15 min, and discrete samples for total alkalinity (A_T) and dissolved inorganic carbon (DIC) were collected weekly from alongside the sensors for calibration and quality control. The water samples were analysed in the Dickson laboratory at SIO according to standard operating procedures (SOPs; Dickson *et al.*, 2007). The sensor was serviced monthly to remove biofouling organisms that may have affected sensor measurements.

Monitoring experimental conditions

Temperature and pH_{sw} were measured daily at midday (13:00 PST $\pm$ 2 h) in all aquaria using a hand-held pH meter (HACH HQ40d Portable pH, Conductivity, Dissolved Oxygen, ORP and ISE Multi-Parameter meter). The glass electrode pH probes (HACH, PCH201) were calibrated daily against certified Tris buffer from the Dickson laboratory at SIO to account for probe error and drift. Minor adjustments were made to bubbling rates in individual aquaria if the experimental pH did not lie within the desired window of 0.2 $\pm$ 0.05 pH units below ambient. Temperature and pH_{sw} were also continuously logged (Honeywell Durafet Non-Glass pH Electrodes) every 15 min in one blank control ambient air, ambient temperature, and one CO_2 enriched, elevated temperature aquaria (if a warming treatment was used; Figure 1).

In addition to temperature, light intensities were continuously logged every 15 min (Onset HOBO® Pendant UA-002-64) in the control aquaria without algae. Light intensities, measured in lux, were converted to available photosynthetically active radiation (PAR) using the following conversion: 1 μmol photon m^{-2} s^{-1} = 51.2 lux (Valiela, 1984; Supplementary Figure S1). These conversions were validated by additional PAR measurements made in the water baths, using a LICOR 4π quantum sensor.

To quantify the effects of treatments on water chemistry, water samples were collected from all control aquaria (without algae; $n = 6$ for pCO_2-only experiments and $n = 4$ for factorial pCO_2 and warming experiments) and one aquaria per treatment per species at two time points or more during each experiment. The samples were collected and analysed in the Dickson laboratory at the SIO according to the SOP (Dickson *et al.*, 2007). Total DIC was determined using a Single Operator Multi-parameter Metabolic Analyser (SOMMA) and an UIC Model 5011 CO_2 coulometer (SOP 2). A_T was determined by open cell acid titration using a Metrohm Dosimat Model 665 and Thermo Scientific Ross potentiometric pH probe and meter (SOP 3b). Salinity was determined using a Metler Toledo Model DE45 density meter. Seawater DIC parameters (HCO_3^-, CO_3^{2-}, CO_2, and pCO_2), pH_{SW}, and saturation state of carbonate minerals (Ω-calcite and Ω-aragonite) were calculated based on measured DIC and A_T using the computer program CO2SYS (version 14; Pierrot *et al.*, 2006) and stoichiometric dissociation constants defined by Mehrbach *et al.* (1973) and refit by Dickson and Millero (1987) (Table 2).

Table 2. Mean seawater chemistry for experimental aquaria ± SE, including both blank control aquaria and aquaria with macroalgae; discrete samples were averaged across treatments.

Exp.	Treatment	Daily mean temperatures	# Discrete samples	Salinity	A_T (μmol kg^{-1})	DIC_T (μmol kg^{-1})	pH_{sw}	HCO_3^- (μmol kg^{-1})	CO_3^{2-} (μmol kg^{-1})	CO_2 (μmol kg^{-1})	pCO_2 (μatm)	Calcite	Aragonite
1	Ambient air	18.91 ± 0.24	10	33.54 ± 0.002	2239 ± 3.115	2012 ± 1.024	8.02 ± 0.006	1834 ± 2.350	164 ± 2.100	13.8 ± 0.193	408 ± 5.786	4.0 ± 0.051	2.6 ± 0.033
1	High CO_2	18.94 ± 0.24	10	33.55 ± 0.002	2234 ± 0.525	2105 ± 4.434	7.80 ± 0.012	1975 ± 6.144	105 ± 2.467	25.2 ± 0.753	744 ± 22.831	2.5 ± 0.060	1.6 ± 0.039
2	Ambient air	20.20 ± 0.19	14	33.57 ± 0.005	2241 ± 6.820	2010 ± 3.649	8.00 ± 0.014	1828 ± 7.357	168 ± 5.375	14.1 ± 0.513	444 ± 16.975	4.1 ± 0.131	2.6 ± 0.085
2	High CO_2	20.22 ± 0.19	14	33.57 ± 0.006	2235 ± 0.904	2090 ± 3.513	7.81 ± 0.009	1952 ± 5.044	115 ± 2.081	23.2 ± 0.505	731 ± 17.104	2.8 ± 0.050	1.8 ± 0.033
3	Ambient air	17.09 ± 0.10	4	33.49 ± 0.016	2237 ± 3.921	2049 ± 1.567	7.96 ± 0.002	1893 ± 0.706	139 ± 1.683	16.9 ± 0.154	479 ± 1.785	3.4 ± 0.041	2.2 ± 0.027
3	Ambient air high temperature	19.03 ± 0.09	3	33.52 ± 0.009	2238 ± 4.254	2048 ± 2.045	7.93 ± 0.004	1889 ± 2.307	141 ± 2.174	17.2 ± 0.230	519 ± 4.550	3.4 ± 0.053	2.2 ± 0.036
3	High CO_2	17.34 ± 0.09	4	33.51 ± 0.012	2236 ± 3.577	2143 ± 8.204	7.72 ± 0.019	2026 ± 9.597	85 ± 3.113	31.8 ± 1.513	901 ± 45.261	2.1 ± 0.075	1.3 ± 0.048
3	High CO_2 high temperature	19.01 ± 0.10	5	33.51 ± 0.007	2235 ± 2.778	2130 ± 5.451	7.72 ± 0.013	2008 ± 6.534	92 ± 2.237	29.8 ± 0.916	896 ± 29.997	2.2 ± 0.054	1.4 ± 0.035
4	Ambient air	15.32 ± 0.07	3	33.47 ± 0.014	2230 ± 2.395	2041 ± 7.033	8.00 ± 0.008	1886 ± 9.472	139 ± 2.894	16.3 ± 0.444	436 ± 9.255	3.3 ± 0.070	2.1 ± 0.046
4	Ambient air high temperature	17.41 ± 0.09	4	33.43 ± 0.043	2228 ± 3.407	2036 ± 6.424	7.97 ± 0.002	1878 ± 8.182	141 ± 4.183	16.4 ± 0.285	466 ± 71.366	3.4 ± 0.052	2.2 ± 0.036
4	High CO_2	15.22 ± 0.06	5	33.46 ± 0.008	2227 ± 2.372	2095 ± 19.414	7.85 ± 0.046	1964 ± 27.370	106 ± 10.683	24.3 ± 2.722	650 ± 71.366	2.6 ± 0.258	1.6 ± 0.165
4	High CO_2 high temperature	17.29 ± 0.08	4	33.47 ± 0.013	2222 ± 4.508	2114 ± 9.289	7.76 ± 0.030	1993 ± 12.994	93 ± 6.206	28.7 ± 2.371	817 ± 62.913	2.2 ± 6.206	1.4 ± 2.371

Seawater pH (pH_{sw}) and DIC parameters (pCO_2, CO_2, HCO_3^-, and CO_3^{2-}) were calculated from measured values of total DIC (DIC_T) and A_T with the computer program CO2SYS (version 14; Pierrot *et al.*, 2006). Mean temperatures calculated from daily means across all aquaria within a treatment.

Response variables

Algal growth rates were calculated as a change in wet weight for fleshy algae and a change in buoyant weight (Davies, 1989) for calcareous algae. The fleshy algae were spun in a salad spinner, then gently blotted dry with paper towels before being weighed. Samples were weighed immediately before and after the experiments, and growth rates were calculated as the difference between final and initial, standardized by initial weight and by the duration of the experiment ($g\ g^{-1}\ d^{-1}$).

Dark-adapted yield, a proxy for photosynthetic efficiency, was measured using a submersible pulse amplitude modulation (PAM) fluorometer (DIVING-PAM, Walz, Germany). The ratio of variable to maximal fluorescence in a darkened sample is correlated with the quantum yield of photosynthesis and is a convenient measure of the maximum potential quantum yield (Björkman and Demmig, 1987; Jones *et al.*, 1999). The maximum quantum yield was determined by dark adapting the algae for 1 h at the end of each experiment. After dark adaption, F_v/F_m was measured using a saturating pulse with the diving PAM.

Photosynthetic pigments were assessed by collecting a wet weight tissue sample (<0.1 g) from each specimen at the end of each experiment. Samples were submerged in 1.0 ml of dimethylformamide and stored in the dark at 0°C for at least 24 h. The resulting liquid was transferred to glass cuvettes and absorbance at wavelengths: 480, 510, 630, 643, 664 and 750 nm was measured using a spectrophotometer (HP 8453) to quantify chlorophyll *a* and carotenoid content. Pigment concentrations were calculated based on Jeffrey and Humphrey (1975) and normalized to each subsample's wet weight. Phycobilin pigment content was assessed for red algae from two experiments (Supplementary Table S3) following the protocol developed by Rosenberg and Ramus (1982) in phosphate buffer and was normalized to subsample wet weight.

CA activity was assessed for all samples from two experiments using the potentiometric technique described by Giordano and Maberly (1989). Immediately following the end of each experiment, 1.0 g tissue (wet weight) was removed from each algal specimen; *P. cartilagineum* samples were flash frozen in liquid nitrogen before being placed in −80°C freezer, and *D. undulata* and *S. horneri* samples were placed directly in a −80°C freezer, until they could be processed. Preliminary trials demonstrated no difference in CA activity expression between the two freezing methods (data not shown). Total CA was extracted on ice (at 5°C) by grinding the algal samples with acid-washed sand and 5 ml of Tris-borate buffer. Extracted enzymes were separated from ground algal contents by centrifuge [as per Giordano and Maberly (1989)]. The supernatant was aliquoted into two portions: one to measure enzymatic activity and one as a control (boiled at 100°C for 10 min to denature the enzyme). The reaction was initiated by adding 1.5 ml of distilled deionized water, saturated with CO_2 using dry ice, to 0.1 ml of the supernatant stirred in a glass reaction chamber kept at 5°C with 15 ml of phosphate buffer (pH 8.36 ± 0.02). Hand-held pH meters (HQ40d HACH) with glass electrode pH probes (PHC201 HACH) were used to record the time taken for the pH to fall from 8.2 to 7.8. Probes were three-point calibrated daily to NBS buffers. The relative rate of pH decline, which was assumed to be linear, was compared between treatment samples and boiled controls. CA activity units were standardized by the fresh weight of the alga.

Statistical analysis

Mean values (± standard error) were calculated for growth rates, F_v/F_m, pigment analysis, and CA activity for each species and treatment combination. All statistical analyses were completed with the program JMP (version 10). The assumption of normality was validated using the Shapiro–Wilk test and Normal Quantile Plots of residuals. For the elevated pCO_2-only experiments where data were normal, a two-tailed *t*-test was used to test the null hypothesis that elevated pCO_2 had no effect on the response variables. For the factorial experiments of CO_2 addition and warming (both fixed factors with two-levels), a two-way analysis of variance (ANOVA) was used to examine differences among treatments. *Post hoc* contrasts were used to compare relative responses among subsets of treatments.

Results

By bubbling a CO_2 blend into treatment aquaria, we successfully maintained the two distinct treatments, ambient and elevated pCO_2, while simultaneously incorporating natural pH variability (Figure 1 and Table 2).

Response of native vs. invasive fleshy species to increased pCO_2

The invasive fleshy brown alga *S. horneri* was not affected by the high CO_2 treatment relative to the controls ($t_{18} = 0.57$, $p = 0.57$; Figure 2a); however, the native fleshy brown alga species *D. undulata* experienced elevated growth rates when exposed to high CO_2 ($t_{18} = 2.22$, $p = 0.03$; Figure 2a). Photosynthetic performance as measured by CA (Figure 3 and Supplementary Table S1), pigment concentrations (chl *a*, carotenoids, and phycobilins) (Supplementary Tables S3 and S4), and F_v/F_m (Figure 4 and Table 2) were not affected by the pCO_2 treatments (Supplementary Tables S1–S4). CA activity, irrespective of the CO_2 treatment, was detected in *D. undulata* and *S. horneri* relative to controls containing the denatured enzyme suggesting the use of CA as a CCM (Figure 3 and Supplementary Table S1).

Response of articulated vs. encrusting calcified algae to increased pCO_2

Both of the coralline algae, *J. adhaerens* (articulated) and *L. californicum* (encrusting), showed a negative growth response to elevated pCO_2, but these trends were not statistically significant (*J. adhaerens:* $t_{18} = 1.58$, $p = 0.13$; *L. californicum:* $t_{18} = 0.37$, $p = 0.71$; Figure 2b). F_v/F_m (Figure 4) for both species and pigment concentrations for *J. adhaerens* (chl *a* and phycobilins) were not affected by the pCO_2 treatments (Supplementary Tables S2, S3, and S5).

Response of fleshy and calcified macroalgae to increased pCO_2 and warming

Plocamium cartilagineum grew over the course of the factorial experiment in all treatments, aside from the warming-only treatment where it lost biomass. However, exposure to elevated pCO_2 mitigated the negative temperature effect so that, on average, the warmed specimens gained 170% more mass when simultaneously exposed to elevated pCO_2 (Figure 2c). Thus, there was a significant interaction between the increased pCO_2 and warming treatments on the growth rates of *P. cartilagineum* (two-way ANOVA, $pCO_2 \times$ Temp: $F_{1,36} = 6.96$, $p = 0.012$; Figure 2C). Elevated pCO_2 significantly affected overall growth rates, but to different magnitudes and in opposing directions depending on temperature exposure. In ambient temperature conditions, elevated pCO_2 depressed growth of *P. cartilagineum* by 45% on average compared with the untreated specimens; however, this difference was not significant due to high variability between replicates. CA (Figure 3 and Supplementary Table S1),

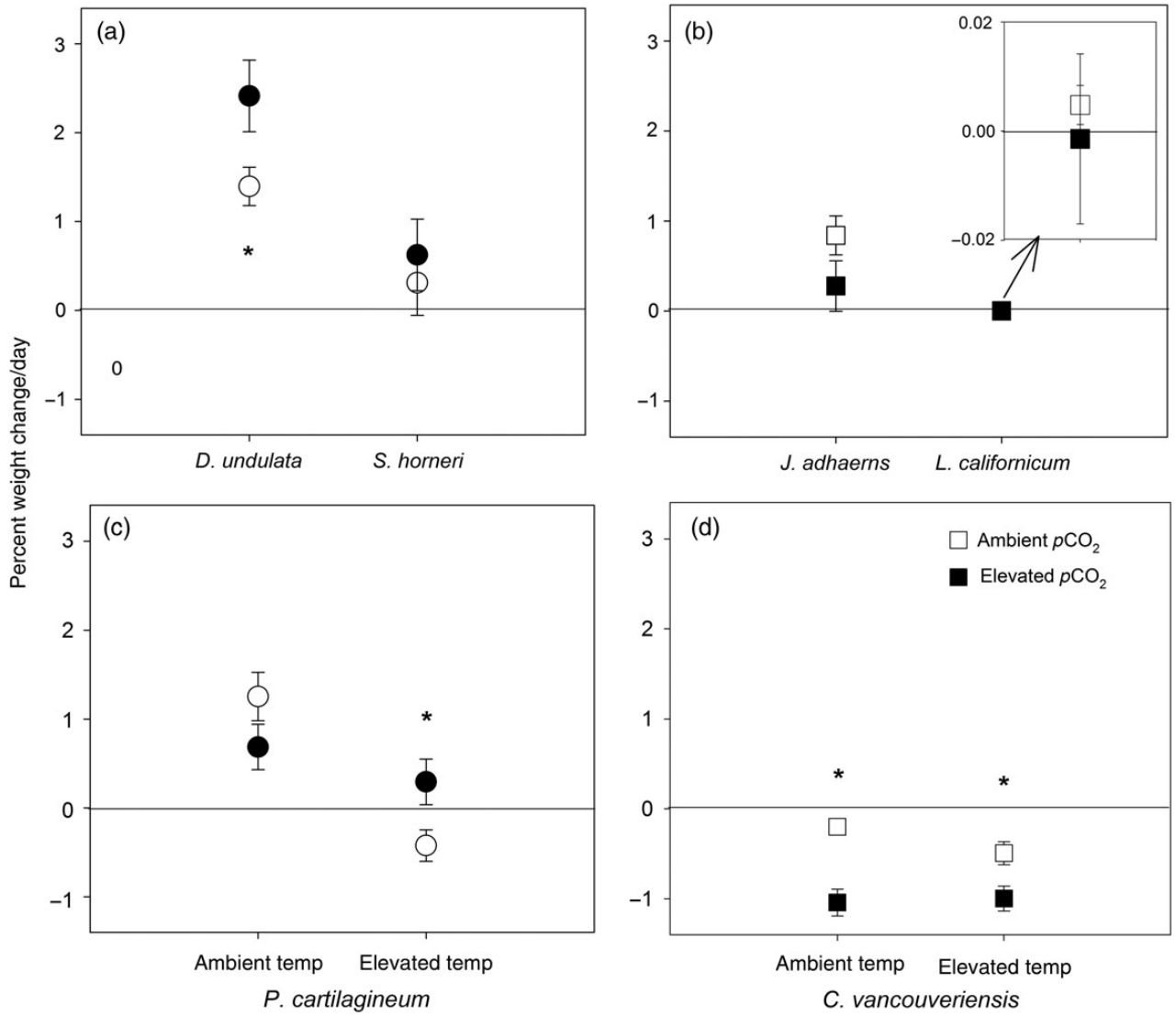

Figure 2. Results from increased pCO_2 experiments showing mean percent weight change/d ($\pm$ SE) on (a) the brown, fleshy invasive *S. horneri* vs. the brown, native species *D. undulata* and (b) the red, calcified articulated *J. adhaerens* vs. non-articulated *L. californicum*. pCO_2 × warming experiments on (c) the red, fleshy *P. cartilagineum* and (d) the red, calcified *C. vancouveriensis*. Circles designate fleshy species and squares designate calcified species. Open shapes indicate ambient air treatment and closed shapes indicate elevated pCO_2 treatment. A significant difference between treatments is denoted by $^*p < 0.05$.

pigment concentrations (chl *a* and phycobilins; Supplementary Tables S3 and S6), and F_v/F_m (Figure 4 and Supplementary Table S2) were not affected by any treatment, or combination thereof. Activity levels of CA were found to be positive for *P. cartilagineum*, relative to denatured enzyme controls, suggesting that the enzyme is active and used as a CCM by this alga (Figure 3 and Supplementary Table S1).

Corallina vancouveriensis, an articulated coralline alga, experienced negative growth rates due to bleaching and tissue fragmentation across all treatments (Figure 2d). Despite this overall loss, there were detectable significant effects of pCO_2 on growth and calcification (two-way ANOVA, pCO_2: $F_{1,36} = 30.42$, $p < 0.01$; Temp: $F_{1,36} = 1.03$, $p = 0.31$; $pCO_2 \times$ Temp: $F_{1,36} = 1.91$, $p = 0.17$). Growth rates for *C. vancouveriensis* were significantly reduced by 420% when exposed to increased CO_2. The combination of increased CO_2 and temperature relative to control ambient conditions also had a negative effect on growth, although those two treatments did not differ significantly from each other. *Corallina vancouveriensis* was not affected by increased temperature alone. F_v/F_m (Figure 4 and Supplementary Table S2) and pigment concentrations (chl *a*; Supplementary Tables S3 and S7) were not affected by any treatment, or combination thereof.

Discussion

We investigated the effects of CO_2 enrichment alone and the independent and combined effects of CO_2 enrichment and warming on common species of temperate marine algae. We expected the fleshy algae to respond positively or not at all to increases in CO_2 depending on their ability to use CA as a CCM. Our results showed that while one of three fleshy taxa did in fact respond positively to CO_2 elevation, we were not able to correlate these responses to CA activity (or lack thereof). One of three calcareous algae species was negatively affected by elevated CO_2, as hypothesized, whereas the other two

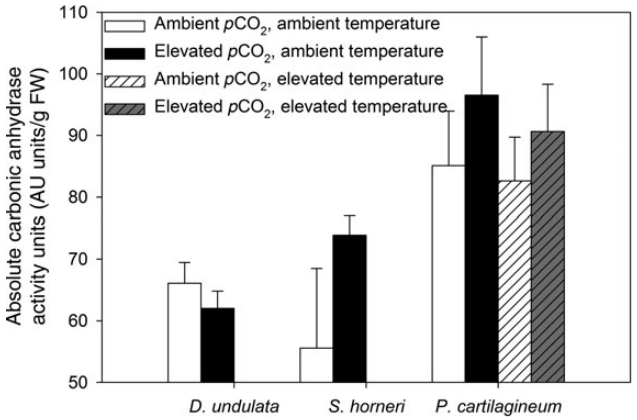

Figure 3. Mean (± SE) CA activity units for three non-calcified species of macroalgae (*D. undulata, S. horneri,* and *P. cartilagineum*). See Supplementary Table S1 for statistical results.

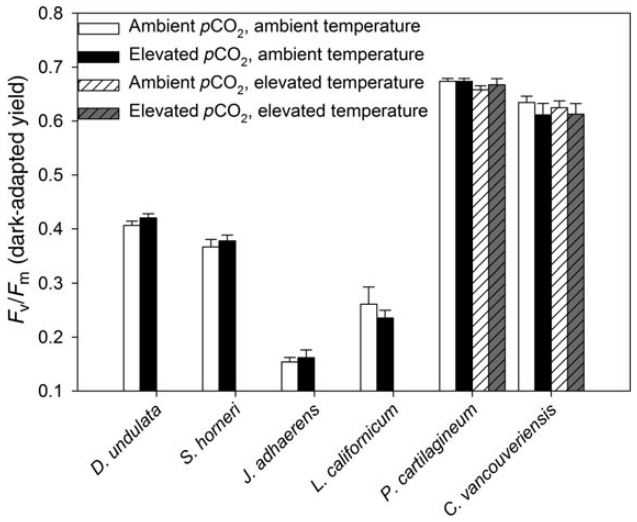

Figure 4. Mean (± SE) F_v/F_m (dark-adapted yield) for six common southern California fleshy and calcified macroalgae. Chlorophyll fluorescence, a proxy for photosynthetic efficiency, was measured using a pulse amplitude-modulated fluorometer. See Supplementary Table S2 for statistical results.

calcareous taxa showed no response. Both fleshy and calcified macroalgae were expected to be positively affected by increased temperature; however, we found negative effects on fleshy *P. cartilagineum* and no effect on calcareous *C. vancouveriensis*. For *P. cartilagineum*, we found a significant interaction between elevated pCO_2 and temperature while a significant interaction was absent from the *C. vancouveriensis* experiment, suggesting that the responses of benthic marine communities to global change are likely to be complex.

The increase of CO_2 and/or temperature did not affect F_v/F_m or pigment concentrations for any of the calcified and fleshy macroalgae examined (Supplementary Tables S2–S7). Similar studies have likewise found no effect of elevated CO_2 on these physiological response variables. Cornwall *et al.* (2013) exposed a temperate calcifying coralline, *Arthrocadia corymbosa*, to elevated CO_2 conditions for 40 d, and found that while algal growth rates were significantly reduced, there was no effect of increased CO_2 on F_v/F_m or pigment concentrations. Hofmann *et al.* (2012b) also found that F_v/F_m was not affected by increased CO_2 in the temperate calcified macroalga *Corallina officinalis*, although it also exhibited significantly reduced growth rates. Despite these results, one would still expect to see some form of enrichment of photosynthesis as more CO_2 is made available; perhaps measuring photosynthesis directly via oxygen evolution would be more appropriate in future studies. Given the diversity in algal taxonomy, morphology, and physiology, it is not surprising that the responses of different species to elevated CO_2 and/or warming are largely species-specific (Price *et al.*, 2011; Comeau *et al.*, 2014, Johnson *et al.*, 2014a).

Increased pCO_2 impacts on invasive vs. native species

We compared the response of a native and an invasive brown alga to elevated pCO_2 conditions, and found that the native *D. undulata* may grow faster under future pCO_2 conditions than the non-indigenous *S. horneri*. This suggests that *D. undulata* may be more successful than *S. horneri* under future OA conditions. Though *S. horneri* can invade new habitats under current conditions (Miller *et al.*, 2007), its competitive ability under future OA conditions may be reduced. Many studies have shown that elevated pCO_2 positively affects terrestrial invasive species; however, few marine examples exist. Nagel *et al.* (2004) found that an invasive desert grass had a significant reduction in the energetic cost of above-ground biomass construction under CO_2 enrichment, which its native counterpart did not exhibit. Mateos-Naranjo *et al.* (2010) reported that an invasive *Spartina* (saltmarsh grass) exhibited increased growth under elevated atmospheric CO_2. While individual species growth rates differ in our study, the invasive, brown fleshy alga *S. horneri* was not significantly affected by elevated pCO_2, whereas the native, brown fleshy *D. undulata* was significantly positively affected, suggesting differential effects on competitive interactions with future OA.

Increased pCO_2 impacts on encrusting vs. articulated coralline algae

Calcareous algae face a paradox under elevated pCO_2 conditions. While there is increased CO_2 available for photosynthesis, the corresponding decrease in carbonate saturation state may limit their ability to calcify. Here, CO_2 enrichment consistently had a negative effect on growth, although the magnitude of the response was species-specific and differed greatly between the articulated and crustose coralline algal species. McCoy and Ragazzola (2014) argued that increased pCO_2 may be more stressful for species of calcified algae with thicker cell walls and crusts, because they contain larger quantities of skeletal calcium carbonate ($CaCO_3$) per unit biomass of photosynthetic tissue. Our results indicated that *C. vancouverensis*, a densely branched species with a high surface area to biomass ratio, exhibited the largest negative response, suggesting that the amount of tissue exposed to reduced carbonate saturation state water may contribute to the strong negative responses observed. Furthermore, the effects of OA may not be as negative to coralline algae photosynthesis as early research indicated. While it is widely accepted that net calcification rates are expected to decline, our study and others (Hofmann *et al.*, 2012b; Cornwall *et al.*, 2013) have yet to find a relationship between declining net calcification and photosystem functions, such as F_v/F_m and pigment concentration.

Increased pCO_2 impacts on fleshy vs. calcareous algae

Overall, fleshy algae responded more positively to elevated CO_2 than calcareous algae. One of the three fleshy species used in experiments had a significantly positive response to increased CO_2, whereas one

of the three calcified species had a significantly negative response; no calcified algae were positively affected, and no fleshy algae were negatively affected by increased CO_2. This is in agreement with the most findings thus far in the literature [reviewed in Kroeker *et al.* (2010, 2013), Hendriks *et al.* (2010), and Johnson *et al.* (2014a)]. CO_2 enrichment resulted in significantly increased growth rates for the fleshy *D. undulata*, while the other two fleshy species were not affected. Other studies have found that other species of fleshy algae exhibited increased growth rates under elevated CO_2 (Zou, 2005; Connell and Russell, 2009; Russell *et al.*, 2009). However, until we understand the physiological mechanisms behind these responses to increased CO_2, predicting species' responses to OA will be challenging.

Synergistic interactions of increased pCO_2 and warming

We hypothesized that increased temperature would positively affect both fleshy and calcareous algae, but that fleshy algae would have a synergistically positive response to increased temperature and CO_2. Interestingly, for the fleshy red alga *P. cartilagineum*, the effects of CO_2 on growth rate were only positive under increased temperatures, suggesting that the increase in temperature offsets the negative effects of increased CO_2. Growth rates were negative overall in response to increased temperature, despite the antagonistic interaction with exposure to elevated pCO_2. During the course of the experiment (November–December 2012), the average ambient seawater temperature was $17.21 \pm 0.07^{\circ}C$ ($\pm$SE), whereas the average elevated temperature treatment was $19 \pm 0.06^{\circ}C$ (Figure. 1). However, for 2011 and 2012, the maximum temperature recorded off the SIO Pier in the summer (June–September) was 22.48 and 23.94°C, respectively (SCCOOS, publically available data). The resulting loss of biomass is surprising, therefore, since the experimentally elevated temperature was well within the natural temperature range. The negative response may have been in part a result of the shock from the rapid introduction of algal specimens into warm experimental conditions, rather than gradual acclimation as they would experience seasonally. These algae were collected from the intertidal however, where they likely experience large daily fluctuations in temperature and pH. The loss in biomass therefore may not have been a negative reaction after all, but could have been a result of increased reproductive fragmentation. A study completed in Stillwater Cove, Carmel Bay, California, found that *P. cartilagineum* produces spores throughout the entire year, with slight peaks in spring and summer (Downing, 1995), and that *P. cartilagineum* utilizes vegetative fragmentation as a form of reproduction. Since the experimental temperature increases simulated summer conditions, the alga may have increased vegetative fragmentation, causing the high temperature treatment to lose biomass. All algal fragments found during the experiment were collected; however, because of the flow-through nature of the experimental design, it was not always possible to identify the fragments' origin.

The calcareous species *C. vancouverensis* was significantly negatively affected by elevated CO_2, regardless of temperature. Similar negative effects were found by Hofmann *et al.* (2012a, b) who exposed *C. officinalis* to elevated CO_2 levels. In each study, they found *C. officinalis* to have decreased growth rates and hypothesized that it may become less competitive under future CO_2 levels. Diaz-Pulido *et al.* (2012) also found similar negative results of elevated CO_2 on a tropical coralline alga, with rates of advanced partial mortality (% dead white, and green areas colonized by endolithic algae) increasing from <1 to 9% under high CO_2. Unlike the results presented here, they found that a 3°C increase in temperature exacerbated the effects of CO_2 and partial mortality increased to 15%. The temperature treatment did not affect *C. vancouverensis* in this study.

CCMs as a CO_2 relief mechanism for fleshy species

We did not find significant effects of elevated pCO_2 on CA activity; however, this may be an artifact of the methods used to measure the enzymatic activity. It may also be that, given the differential response of fleshy algal growth to CO_2 relative to calcifier growth, CCMs such as CA may be mechanisms underlying different responses. CCM activity levels may be responsive to other environmental factors not tested in these experiments. For example, Cornwall *et al.* (2015) suggests that the activity levels of CCMs of some species may be more flexible to light levels, rather than CO_2. Additionally, downregulation of any active CCM component, which uptakes bicarbonate, directly may explain changes in growth rates, pigmentation, etc., as CA enzymes are just one example of a CCM.

Although the treatment effects were not significant, CA activity was found in the fleshy algae, *D. undulata* and *S. horneri*. There have been no other studies investigating CA activity in either of these species. Thomas and Tregunna (1968), however, reported that *Sargassum muticum* does not directly use CO_2 for photosynthesis, thus concluding that it must use bicarbonate ions for photosynthesis. If *S. horneri* also relies on bicarbonate, as opposed to CO_2 for photosynthesis, this species may not downregulate CA activity, preventing it from taking advantage of the more readily available CO_2 for growth. If this is the case, then future OA conditions may limit the success of invasive *S. horneri* when compared with native species in similar subtidal habitat such as *D. undulata*.

Although *P. cartilagineum* growth rates were not affected by an increase in CO_2 alone, high levels of CA were found. While isotopic evidence from Raven *et al.* (2005) suggested that *P. cartilagineum* relies on diffusive uptake of CO_2 rather than CCMs, Mercado *et al.* (2009) show that in fact several of these algal species may actually have higher CA activity than species where evidence generally points towards the presence of CCMs. The lack of response to increased CO_2, but the detectable CA enzyme activity units, suggests that *P. cartilagineum* may not have been carbon-limited in our experimental setting. If so, then *P. cartilagineum* may be less competitive against other fleshy species in the future, such as *D. undulata*, which was able to utilize increased CO_2 in our experiments.

Conclusions and implications

The data presented here provide additional support for the hypothesis that the responses of marine algae to increased pCO_2 will be species-specific, but in general more negative for calcifying vs. fleshy taxa. We provide data on a small subset of the diverse assemblage of macroalgae common on temperate shores that contribute to the growing body of information on the likely future effects of OA. More information is still needed on the responses of species to more gradual and thus more realistic increases in pCO_2 to allow for acclimatization or adaptation. Additionally, more long-term experiments [multiple months; as in Martin and Gattuso (2009) and Form and Riebesell (2012)] are needed as lengthened experiments may reveal impacts on organisms that are missed in shorter duration experiments (Dupont *et al.*, 2010). Finally, the interactive effects of multiple stressors, including additional local and global impacts, are needed to improve our predictive capacity of future change. It must be emphasized that a variety of response variables be examined to identify additional effects of OA, warming, and their interaction to be able to extrapolate these effects to an ecosystem level.

Macroalgae are ecosystem engineers, providing habitat, refugia, and energy as a food source to countless organisms in coastal habitats. Understanding how climate change will affect them will give researchers a better idea of how coastal ecosystems may change in the coming centuries.

Acknowledgements

We thank Molly Gleason, Samantha Clements, and Alex Neu for their help collecting specimens and maintaining experiments in the laboratory. Funding was provided by NOAA (NA10OAR4170060), California Sea Grant (R/CC-05), and the CSU Council for Ocean Affairs, Science, and Technology (COAST).

Supplementary data

Supplementary material is available at the *ICESJMS* online version of the manuscript.

References

Anthony, K. R. N., Kline, D. I., Diaz-Pulido, G., Dove, S., and Hoegh-Guldberg, O. 2008. Ocean acidification causes bleaching and productivity loss in coral reef builders. Proceedings of the National Academy of Sciences of the United States of America, 105: 17442–17446.

Beardall, J., Beer, S., and Raven, J. A. 1998. Biodiversity of marine plants in an arc of climate change; some predictions based on physiological performance. Botanica Marina, 41: 113–123.

Björkman, O., and Demmig, B. 1987. Photon yield of O_2 evolution and chlorophyll fluorescence characteristics at 77 K among vascular plants of diverse origins. Planta, 170: 489–504.

Byrne, M. 2011. Impact of ocean warming and ocean acidification on marine invertebrate life history stages: Vulnerabilities and potential for persistence in a changing ocean. Oceanography and Marine Biology: An Annual Review, 49: 1–42.

Caldeira, K., and Wickett, M. E. 2003. Anthropogenic carbon and ocean pH. Nature, 425: 3–65.

Carpenter, R. C. 1986. Partitioning herbivory and its effects on coral reed algal communities. Ecological Monographs, 56: 345–364.

Comeau, S., Edmunds, P. J., Spindel, N. B., and Carpenter, R. C. 2014. Fast coral reef calcifiers are more sensitive to ocean acidification in short-term laboratory incubations. Limnology Oceanography, 59: 1081–1091.

Compton, T. J., Rijkenberg, M. J. A., Drent, J., and Piersma, T. 2007. Thermal tolerance ranges and climate variability: A comparison between bivalves from differing climates. Journal of Experimental Marine Biology and Ecology, 0352: 200–211.

Connell, S. D., and Russell, B. D. 2009. The direct effects of increasing CO_2 and temperature on non-calcifying organisms: Increasing the potential for phase shifts in kelp forests. Proceedings of the Royal Society B. doi:10.1098/rspb.2009.2069.

Cornwall, C. E., Hepburn, C. D., McGraw, C. M., Currie, K. I., Pilditch, C. A., Hunter, K. A., Boyd, P. W., *et al.* 2013. Diurnal fluctuations in seawater pH influence the response of a calcifying macroalga to ocean acidification. Proceedings of the Royal Society B, 280: 20132201.

Cornwall, C. E., Hepburn, C. D., Pritchard, D., Currie, K. I., McGraw, C. M., Hunter, K. A., and Hurd, C. L. 2012. Carbon-use strategies in macroalgae: Differential responses to lowered pH and implications for ocean acidification. Journal of Phycology, 48: 137–144.

Cornwall, C. E., Revill, A. T., and Hurd, C. L. 2015. High prevalence of diffusive uptake of CO_2 by macroalgae in a temperate subtidal ecosystem. Photosynthesis Research, 124: 181–190.

Davies, S. P. 1989. Short-term growth measurements of corals using an accurate buoyant weighting technique. Marine Biology, 101: 389–395.

Davison, I. R. 1991. Environmental effects on algal photosynthesis: Temperature. Journal of Phycology, 27: 2–8.

Diaz-Pulido, G., Anthony, K. R. N., Kline, D. I., Dove, S., and Hoegh-Guldberg, O. 2012. Interactions between ocean acidification and warming on the mortality and dissolution of coralline algae. Journal of Phycology, 48: 32–39.

Diaz-Pulido, G., McCook, L. J., Larkum, A. W. D., Lotze, H. K., Raven, J. A., Schaffelke, B., Smith, J. E., *et al.* 2007. Vulnerability of macroalgae of the Great Barrier Reef to climate change. *In* Climate change and the Great Barrier Reef, pp. 153–192. Ed. by J. E. Johnson, and P. A. Marshall. Great Barrier Reef Marine Park Authority, The Australian Greenhouse Office, and the Department of Environment Water and Natural Resources, Townsville.

Dickson, A. G., and Millero, F. J. 1987. A comparison of the equilibrium constants for the dissociation of carbonic acid in seawater media. Deep Sea Research Part A, 34: 1733–1743.

Dickson, A. G., Sabine, C. L., and Christian, J. R. (Ed.) 2007. Guide to Best Practices for Ocean CO_2 Measurements. North Pacific Marine Science Organization, Sidney, BC. PICES Special Publication 3, 191 pp.

Downing, J. W. 1995. The effects of vegetative reproduction on the recruitment and small scale distribution of the red alga *Plocamium cartiagnieum*. Master's theses. San Jose State University, SJSU ScholarWorks. Paper 1137.

Dupont, S., Ortega-Martinez, O., and Thorndyke, M. 2010. Impact of near-future ocean acidification on echinoderms. Ecotoxicology, 19: 449–462.

Fabry, V. J., Seibel, B. A., Feely, R. A., and Orr, J. C. 2008. Impacts of ocean acidification on marine fauna and ecosystem processes. ICES Journal of Marine Science, 65: 414–432.

Feely, R. A., Sabine, C. L., Bryne, R. H., Millero, F. J., Dickson, A. G., Wanninkhof, R., Murata, A., *et al.* 2012. Decadal changes in the aragonite and calcite saturation state of the Pacific Ocean. Global Biogeochemical Cycles, 26: GB3001.

Form, A. U., and Riebesell, U. 2012. Acclimation to ocean acidification during long-term CO_2 exposure in the cold-water coral *Lophelia pertusa*. Global Change Biology, 18: 843–853.

Frieder, C. A., Nam, S. H., Martz, T. R., and Levin, L. A. 2012. High temporal and spatial variability of dissolved oxygen and pH in a nearshore California kelp forest. Biogeosciences Discuss, 9: 4099–4132.

Gao, K., Aruga, Y., Asada, K., Ishihara, T., Akano, T., and Kiyohara, M. 1993. Calcification in the articulated coralline alga *Corallina pilulifera*, with special reference to the effect of elevated CO_2 concentration. Marine Biology, 117: 129–132.

Gao, K., Helbling, W. E., Hader, D. P., and Hutchins, D. A. 2012. Responses of marine primary producers to interactions between ocean acidification, solar radiation, and warming. Marine Ecology Press Series, 470: 167–189.

García-Sánchez, M. J., Fernández, J. A., and Niell, X. 1994. Effect of inorganic carbon supply on the photosynthetic physiology of *Gracilaria tenuistipitata*. Planta, 194: 55–61.

Giordano, M., and Maberly, S. C. 1989. Distribution of carbonic anhydrase in British marine macroalgae. Oecologia, 81: 534–539.

Hendriks, I. E., Duarte, C. M., and Alvarez, M. 2010. Vulnerability of marine biodiversity to ocean acidification: A meta-analysis. Estuarine Coastal and Shelf Science, 86: 157–164.

Hepburn, C. D., Pritchard, D. W., Cornwall, C. E., McLeod, R. J., Beardall, J., Raven, J. A., and Hurd, C. L. 2011. Diversity of carbon use strategies in a kelp forest community: Implications for a high CO_2 ocean. Global Change Biology, 17: 2488–2497.

Hofmann, G. E., Smith, J. E., Johnson, K. S., Send, U., Levin, L. A., Micheli, F., Paytan, A., *et al.* 2011. High-frequency dynamics of ocean pH: A multi-ecosystem comparison. PLoS ONE, 6: e28983.

Hofmann, L. C., Straub, S., and Bischof, K. 2012b. Competition between calcifying and noncalcifying temperate marine macroalgae under elevated CO_2 levels. Marine Ecology Progress Series, 464: 89–105.

Hofmann, L. C., Yildiz, G., Hanelt, D., and Bischof, K. 2012a. Physiological responses of the calcifying rhodophyte, *Corallina officinalis*, (L.), to future CO_2 levels. Marine Biology, 159: 783–792.

Hopkinson, B. M., Dupont, C. L., Allen, A. E., and Morel, F. M. M. 2011. Efficiency of the CO_2-concentrating mechanism of diatoms. Proceedings of the National Academy of Sciences of the United States of America, 108: 3830–3837.

IPCC. 2013. Climate Change 2013 The Physical Science Basis: Working Group I Contribution to the Fifth Assessment Report of the Intergovernmental Panel on Climate Change.

Jeffrey, S. W., and Humphrey, G. F. 1975. New spectrophotometric equations for determining chlorophylls *a*, *b*, *c1* and *c2* in higher plants, algae and natural phyoplankton. Biochemie und Physiologie der Pflanzen, 167: 191–194.

Johnson, M. D., and Carpenter, R. C. 2012. Ocean acidification and warming decrease calcification in the crustose coralline alga *Hydrolithon onkodes* and increase susceptibility to grazing. Journal of Experimental Marine Biology and Ecology, 434: 94–101.

Johnson, M. D., Moriarty, V. W., and Carpenter, R. C. 2014b. Acclimatization of the crustose coralline alga *Porolithon onkodes* to variable pCO_2. PLoS ONE, 9: e87678.

Johnson, M. D., Price, N. N., and Smith, J. E. 2014a. Contrasting effects of ocean acidification on tropical fleshy and calcareous algae. PeerJ, doi:10.7717/peerj.411.

Jones, R. J., Kildea, T., and Hoegh-Guldberg, O. 1999. PAM chlorophyll fluorometry: A new *in situ* technique for stress assessment in scleractinian corals, used to examine the effects of cyanide from cyanide fishing. Marine Pollutions Bulletin, 38: 864–874.

Kleypas, J. A., and Langdon, C. 2006. Coral reefs and changing seawater carbonate chemistry. *In* Coral Reefs and Climate Change: Science and Management, pp. 73–110. Ed. by J. T. Phinney, O. Hoegh-Guldberg, J. Kleypas, W. Skirving, and A. Strong. American Geophysical Union, Washington, DC. 244 pp.

Kroeker, K. J., Kordas, R. L., Crim, R., Hendriks, I. E., Ramajo, L., Singh, G. S., Duarte, C. M., *et al.* 2013. Impacts of ocean acidification on marine organisms: Quantifying sensitivities and interaction with warming. Global Change Biology, 19: 1884–1896.

Kroeker, K. J., Kordas, R. L., Crim, R. N., and Singh, G. G. 2010. Meta-analysis reveals negative yet variable effects of ocean acidification on marine organisms. Ecology Letters, 13: 1419–1434.

Kübler, J. E., Johnston, A. M., and Raven, J. A. 1999. The effects of reduced and elevated CO_2 and O_2 on the seaweed *Lomentaria articulate*. Plant Cell Environment, 22: 1303–1310.

Kuffner, I. B., Andersson, A. J., Jokiel, P. L., Rodgers, K. S., and Mackenzie, F. T. 2008. Decreased abundance of crustose coralline algae due to ocean acidification. Nature Geoscience, 1: 114–118.

Martin, S., and Gattuso, J. 2009. Response of Medetaranian coralline algae to ocean acidification and elevated temperature. Global Change Biology, 15: 2089–2100.

Mateos-Naranjo, E., Redondo-Gómez, S., Andrades-Moreno, L., and Davy, A. J. 2010. Growth and photosynthetic responses of the cordgrass *Spartina maritime* to CO_2 enrichment and salinity. Chemosphere, 81: 725–731.

Martz, T. R., Connery, J. G., and Johnson, K. S. 2010. Testing the Honeywell Durafet® for seawater pH applications. Limnology and Oceanography: Methods, 8: 172–184.

McCoy, S. J., and Kamenos, N. A. 2015. Coralline algae (Rhodophyta) in a changing world: Integrating ecological, physiological, and geochemical responses to global change. Journal of Phycology, 51: 6–24.

McCoy, S. J., and Ragazzola, F. 2014. Skeletal trade-offs in coralline algae in response to ocean acidification. Nature Climate Change, 4: 719–723.

Mehrbach, C., Culberso, C. H., Hawley, J. E., and Pytkowic, R. M. 1973. Measurement of apparent dissociation constants of carbonic acid in seawater at atmospheric pressure. Limnology and Oceanography, 18: 897–907.

Mercado, J. M., de los Santos, C. B., Pérez-Lloréns, J. L., and Vergara, J. J. 2009. Carbon isotope fractionation in macroalgae from Cádiz Bay (Southern Spain): Comparison with other bio-geographic regions. Estuarine, Coastal and Shelf Science, 85: 449–458.

Miller, K. A., Engle, J. M., Uwai, S., and Kawai, H. 2007. First report of the Asian seaweed *Sargassum filicinum* Harvey (Fucales) in California, USA. Biological Invasions, 9: 609–613.

Morison, J. I. L., Gallouët, E., Lawson, T., Cornic, G., Herbin, R., and Baker, N. R. 2005. Lateral Diffusion of CO_2 in leaves is not sufficient to support photosynthesis. American Society of Plant Biologists, 139: 254–266.

Nagel, J. M., Huxman, T. E., Griffin, K. L., and Smith, S. D. 2004. CO_2 enrichment reduces the energetic costs of biomass construction in an invasive desert grass. Ecology, 85:100–106.

Pereira, R., Yarish, C., and Sousa-Pinto, I. 2006. The influence of stocking density, light and temperature on the growth, production and nutrient removal capacity of *Porphyra dioica* (Bangiales, Rhodophyta). Aquaculture, 252: 66–78.

Pierrot, D., Lewis, E., and Wallace, D. W. R. 2006. MS Excel Program Developed for CO_2 System Calculations. ORNL/CDIAC-105a. Carbon Dioxide Information Analysis Center, Oak Ridge National Laboratory, U.S. Department of Energy, Oak Ridge, TN.

Price, N. N., Hamilton, S. L., Tootell, J. S., and Smith, J. E. 2011. Species-specific consequences of ocean acidification for the calcareous tropical green algae *Halimeda*. Marine Ecology Progress Series, 440: 67–78.

Raven, J. A., Ball, L. A., Beardall, J., Giordano, M., and Maberly, S. C. 2005. Algae lacking carbon-concentrating mechanisms. Canadian Journal or Botany, 83: 879–890.

Rosenberg, G., and Ramus, J. 1982. Ecological growth strategies in the seaweeds *Gracilaria-foliifera* (Rhodophyceae) and *Ulva* sp (Chlorophyceae)—Photosynthesis and antenna composition. Marine Ecology Progress Series, 8: 233–241.

Russell, B. D., Thompson, J. O., Falkenberg, L. J., and Connell, S. D. 2009. Synergistic effects of climate change and local stressors: CO_2 and nutrient-driven change in subtidal rocky habitats. Global Change Biology, 15: 2153–2162.

Schreiber, U. 2004. Chlorophyll fluorescence: A signature of photosynthesis. *In* Advances in Photosynthesis and Respiration, 19, pp. 1–42. Ed. by G. C. Papageorgiou, and G. C. Govindjee. Kluwer Academic Publishers, The Netherlands. 823 pp.

SCCOOS (Southern California Coastal Ocean Observing System). http://sccoos.org/query/> (last accessed 5 June 2013).

Stillman, J. H. 2002. Causes and consequences of thermal tolerance limits in rocky intertidal porcelain crabs, genus *Petrolisthes*. Integrative and Comparative Biology, 42: 790–796.

Sültemeyer, D. 1998. Carbonic anhydrase in eukaryotic algae: Characterization, regulation, and possible function during photosynthesis. Canadian Journal of Botany, 76: 962–972.

Thomas, A. E., and Tregunna, E. B. 1968. Bicarbonate ion assimilation in photosynthesis by *Sargassum muticum*. Canadian Journal of Botany, 46: 411–415.

Valiela, I. 1984. Marine Ecological Processes, 2nd edn. Springer-Verlag, New York. 686 pp.

Williams, G. J., Price, N. N., Ushijima, B., Aeby, G. S., Callahan, S., Davy, S. K., Gove, J. M., *et al.* 2014. Ocean warming and acidification have complex interactive effects on the dynamics of a marine fungal disease. Proceedings of the Royal Society B, 281: 20133069.

Zerebecki, R. A., and Sorte, C. J. B. 2011. Temperature tolerance and stress proteins as mechnanisms of invasive species success. PLoS ONE. doi:10.1371/journal.pone.0014806.

Zou, D. 2005. Effects of elevated atmospheric CO_2 on growth, photosynthesis and nitrogen metabolism in the economic brown seaweed, *Hizikia fusiforme*, (Sargassaceae, Phaeophyta). Aquaculture, 250: 726–735.

Handling editor: Joanna Norkko

ICES Journal of Marine Science

ICES Journal of Marine Science (2016), 73(3), 704–714. doi:10.1093/icesjms/fsv235

Contribution to Special Issue: 'Towards a Broader Perspective on Ocean Acidification Research'

Original Article

Impact of high pCO_2 and warmer temperatures on the process of silica biomineralization in the sponge *Mycale grandis*

Jan Vicente[1], Nyssa J. Silbiger[2], Billie A. Beckley[1], Charles W. Raczkowski[3], and Russell T. Hill[1]*

[1]*Institute of Marine and Environmental Technology, University of Maryland Center for Environmental Science, 701 E Pratt St Suite 236, Baltimore, MD 21202, USA*
[2]*Hawai'i Institute of Marine Biology, University of Hawai'i at Mānoa, PO Box 1346, Kāne'ohe, HI 96744, USA*
[3]*Department of Natural Resources, North Carolina A&T State University, Greensboro, NC 27411, USA*

**Corresponding author: tel: +1 410 234 8802; fax: +1 410 234 8818; e-mail: hill@umces.edu*

Vicente, J., Silbiger, N. J., Beckley, B. A., Raczkowski, C. W., and Hill, R. T. Impact of high pCO_2 and warmer temperatures on the process of silica biomineralization in the sponge *Mycale grandis*. – ICES Journal of Marine Science, 73: 704–714.

Received 23 April 2015; revised 10 November 2015; accepted 13 November 2015; advance access publication 18 December 2015.

Siliceous sponges have survived pre-historical mass extinction events caused by ocean acidification and recent studies suggest that siliceous sponges will continue to resist predicted increases in ocean acidity. In this study, we monitored silica biomineralization in the Hawaiian sponge *Mycale grandis* under predicted pCO_2 and sea surface temperature scenarios for 2100. Our goal was to determine if spicule biomineralization was enhanced or repressed by ocean acidification and thermal stress by monitoring silica uptake rates during short-term (48 h) experiments and comparing biomineralized tissue ratios before and after a long-term (26 d) experiment. In the short-term experiment, we found that silica uptake rates were not impacted by high pCO_2 (1050 µatm), warmer temperatures (27°C), or combined high pCO_2 with warmer temperature (1119 µatm; 27°C) treatments. The long-term exposure experiments revealed no effect on survival or growth rates of *M. grandis* to high pCO_2 (1198 µatm), warmer temperatures (25.6°C), or combined high pCO_2 with warmer temperature (1225 µatm, 25.7°C) treatments, indicating that *M. grandis* will continue to prosper under predicted increases in pCO_2 and sea surface temperature. However, ash-free dry weight to dry weight ratios, subtylostyle lengths, and silicified weight to dry weight ratios decreased under conditions of high pCO_2 and combined pCO_2 warmer temperature treatments. Our results show that rising ocean acidity and temperature have marginal negative effects on spicule biomineralization and will not affect sponge survival rates of *M. grandis*.

Keywords: marine sponges, *Mycale grandis*, ocean acidification, silica biomineralization, silica uptake, spicules.

Introduction

Skeleton mineralogy plays an important role in the sensitivity of marine invertebrates to ocean acidification and warming. Calcifying organisms are particularly vulnerable to rising ocean acidity and temperatures (Hoegh-Guldberg *et al.*, 2007; Fabry *et al.*, 2008; Hofmann *et al.*, 2010), but non-calcifying organisms such as siliceous sponges are thought to be less affected (Bell *et al.*, 2013). Studies testing the physiological response of calcifying and non-calcifying organisms to ocean acidification have led to predictions about which invertebrates will dominate in tropical, benthic ecosystems in a more acidified ocean. For example, small-scale benthic community shifts have been reported in pH gradients caused by natural volcanic CO_2 seeps of Papua New Guinea (Morrow *et al.*, 2014), where a transition from coral to sponge dominance was observed with closer proximity to the seep (higher pCO_2). Large-scale shifts of coral to sponge-dominated reefs are already being observed in coral reefs of the Caribbean (Diaz and Rützler, 2001; Pawlik, 2011; Loh *et al.*, 2015; McMurray *et al.*, 2015). Transitions from coral to sponge-dominated reefs may cause carbon release rates to increase (de Goeij *et al.*, 2013) which could play an important role in structuring higher trophic levels of the ecosystem (Silveira *et al.*, 2015). Because of results from these studies and others, predicting the impact of ocean acidification and warming on sponges is gaining considerable attention (Duckworth *et al.*, 2012; Webster *et al.*, 2013; Goodwin *et al.*, 2014; Stubler *et al.*, 2014).

Sponge skeletons can be composed of calcium carbonate, silica, or collagen fibres (Hooper and Van Soest, 2002). Like corals,

calcifying sponges are vulnerable to dissolution when exposed to lower pH levels (Smith *et al.*, 2013), but siliceous and collagenous sponges are believed to resist dissolution in more acidified ocean conditions (Bell *et al.*, 2013). For example, growth and survival rates in six Caribbean sponges with skeletons composed of silica and collagen fibre were not affected by a 24-d exposure period to increased ocean acidity and temperatures relative to ambient conditions (Duckworth *et al.*, 2012). In fact, studies have shown that some sponges may even benefit from predicted ocean acidification conditions; bioerosion rates from clionid boring sponges increased in low pH treatments relative to controls (Wisshak *et al.*, 2012, 2013; Stubler *et al.*, 2014; Enochs *et al.*, 2015). Despite the number of studies showing an increase in bioerosion by marine sponges and no detrimental impacts on sponges under high CO_2 scenarios, little is known about the response of sponge morphology or skeleton synthesis to warmer and more acidic conditions.

Like ocean acidification, thermal tolerance may vary across sponge species with different skeletal compositions. In the Caribbean and in the Mediterranean Sea, warmer seawater temperatures have caused local extinction events in keratose (aspiculated) sponges (Vicente, 1989; Cebrian *et al.*, 2011). In mesocosm studies, thermal stress caused necrosis and eliminated key bacterial symbionts from the keratose sponge *Rhopaloeides odorabile* at 33°C (Webster *et al.*, 2008). While several species of keratose sponges are sensitive to warmer temperatures, spiculated sponges are able to tolerate these conditions and actually accelerate their attachment rates to substrates (Duckworth *et al.*, 2012). However, studies that measure thermal tolerance of sponges have not considered whether resistance to thermal stress by sponges correlates with a particular skeleton type. Looking at the process of siliceous skeleton synthesis under high pCO_2 and warmer temperatures will help us understand whether sponges with a siliceous skeleton could be at an advantage under different pCO_2 and temperature regimes.

Many studies support the hypothesis that siliceous sponges will adapt to ocean acidification (Duckworth and Peterson, 2012; Duckworth *et al.*, 2012; Wisshak *et al.*, 2012; Stubler *et al.*, 2014); however, it is not clear whether having a siliceous skeleton is actually an advantageous trait for sponges under these conditions. Silica uptakes rates for sponges with a siliceous skeleton are believed to follow a Michaelis–Menten kinetic model and are also heavily dependent on silica concentrations—silica uptake rates increase exponentially when exposed to higher silica concentrations (Maldonado *et al.*, 2012b). Other environmental factors such as high nutrients in upwelling habitats influence the shape and size of spicules (Uriz *et al.*, 2003). Although the process by which silica is taken up remains speculative, there is a preliminary model that suggests that silicate assimilated by the sponge *Suberites domuncula* for spicule synthesis is co-transported through sclerocyte cells with a Na^+- HCO_3^- symporter protein (Schröder *et al.*, 2004). Polycondensation of silica in *S. domuncula* primmorph cells occurs within vesicles by silicatein proteins in the intracellular space of sclerocytes where the axial filament of a spicule is formed (Wang *et al.*, 2012). Fibrils then associate with one end of the spicule and extrude it out of the cell where silicate continues to deposit in layers around the axial filament. *Mycale grandis* may have a similar mechanism of silica uptake to *S. domuncula* because these two sponges belong to the same class and both have densely spiculated skeletons. If all siliceous Demosponges use a Na^+- HCO_3^- symporter mechanism to take up $Si(OH)_4$ through the cell membrane, we speculate that siliceous sponges may benefit from high pCO_2 during spicule synthesis. In addition, the chemical equilibrium shift of dissolved silica (DSi) caused by high pCO_2 will favour the speciation of $Si(OH)_4$ and HCO_3^- which could make $Si(OH)_4$ and HCO_3^- substrates more available for the Na^+- HCO_3^- symporter protein to transport and facilitate uptake of silica through the cell membrane (Zeebe and Wolf-Gladrow, 2001).

In this study, we used end of the century pCO_2 (1100 ppm) and temperature (+3°C) values from the Representative Concentration Pathway (RCP) 8.5 climate scenario (Riahi *et al.*, 2011) to test the impact of rising ocean acidity and temperature on spicule biomineralization in the Hawaiian invasive sponge *M. grandis* (Gray, 1867). *Mycale grandis* was introduced in Kāneʻohe Bay in the mid-1990s and was found aggressively overgrowing the hermatypic coral species *Montipora capitata* and *Porites compressa* by 2005 (Coles and Bolick, 2007). Studies have shown that *M. grandis* per cent cover doubled in some reefs of Kāneʻohe Bay between 2005 and 2006 (Coles *et al.*, 2006). *Mycale grandis* is a fast-growing sponge with a densely spiculated siliceous skeleton, making it a fitting model organism to measure silica uptake and spicule biomineralization in short periods.

We measured DSi uptake rates using closed system 48-h incubation experiments, exposing individuals of *M. grandis* to increased temperature (+3°C), increased pCO_2 (1100 µatm), combined increased pCO_2 and temperature (+3°C; 1100 µatm), and ambient temperature and pCO_2 from Kāneʻohe Bay (24°C, 580 µatm). Sponges were also exposed to similar conditions during a 26-d flow-through experiment to test the impact of high pCO_2 and temperature on spicule synthesis.

Based on the silica uptake models proposed for other siliceous sponges, like *S. domuncula*, we hypothesize that: (i) treatments with pCO_2 enrichment will accelerate silica uptake rates of *M. grandis* resulting in enhanced spicule production and denser skeletons (more silicification) and (ii) temperature increments of 3°C will increase silica uptake rates through increased metabolism (Nwewll and Northcroft, 1967), although there are currently no published studies on the impacts of temperature on sponge spicule production and morphology. This is the first study that addresses the impact of high pCO_2 and thermal stress on the process of spicule biomineralization in marine sponges.

Methods

Silica uptake closed system experiment

Sponge collection

One sponge piece from each of 72 individuals of *M. grandis* (wet weight: 4–56 g) was collected with a sterile scalpel around Moku o Loʻe (Coconut Island) in Kāneʻohe Bay at a depth of 3–9 m. We confirmed that the sponge individuals used for our experiments were *M. grandis* by comparing partial sequences of the 18S and 28S rRNA genes with those in GenBank. For a full description of the phylogenetic analysis, see Supplementary Figure S1.

Mycale grandis grows as thickly encrusting cushions in between coral colonies making it difficult to collect without causing a large area of injury (injury area size: 1–35 cm^2). Brittlestars found living on the surface of the sponge tissue were removed to avoid interference with ash-free dry weight/dry weight (AFDW/DW) ratio calculations. Brittlestars that were embedded deep inside the sponge tissue were left and removed after the experiment to avoid further injury to the sponge. To stabilize the sponges in incubation chambers, we gently tied fishing weights (85 g) with small (6 cm) tie wraps around each sponge. Sponge individuals were acclimated to their intended pH and temperature treatment conditions in

flow-through tanks and were allowed to heal for 36 h at background silica concentrations (6–7 μM).

Silica uptake rates

To test the impact of high pCO_2 and temperature on silica uptake in sponges, we used a closed system experimental set-up at the Hawai'i Institute of Marine Biology (HIMB) mesocosm facility. This facility was well suited for our experimental conditions (Putnam, 2012; Silbiger and Donahue, 2015). All experiments were performed between March and May 2014.

Incubation chambers (plastic buckets) were prepared with 4 l of filtered seawater (3 μm pore size Pentair bag filter) and a water pump to ensure a well-mixed system. Chambers were sealed with Saran® wrap with clips to prevent evaporation and off-gassing. In each incubation chamber, pCO_2 was maintained by bubbling in CO_2 or CO_2-free air with airlines equipped with air-stones. A gas blending system was used to manipulate pCO_2 by mixing pure CO_2 -free atmospheric air with pure CO_2 using mass flow controllers (C100L Sierra Instruments). pCO_2 conditions were controlled using a calibrated CO_2 analyzer (A151, Qubit System) that measured the output CO_2 going into each chamber. pCO_2 conditions were monitored and adjusted every 8 h. Temperature was controlled with dual-stage temperature controllers (Aqualogic TR115DN) and aquarium heaters. An LED system (AI Sol, 72 W 100–240 VAC/50–60 Hz, C2 Development Inc., Ames, IA, USA) was used to control lighting. Lights were set over each tank and were switched on at sunrise (06:15), and ramped up for 4 h until 600 μmol photons m^{-2} s^{-1} irradiance was reached which resembled similar conditions to the reefs in Kāneʻohe Bay. Irradiance was held at maximum for 4 h before ramping down to zero by sunset (18:15; Gibbin *et al.*, 2015). All buckets, air-stones, air lines, and water pumps were pre-cleaned with 5% hydrochloric acid (HCl) and rinsed with DI water before every experiment.

We had four experimental treatments: control (C; 24°C, 593 μatm), high temperature (*T*; +3°C), high pCO_2 ($pCO2$; 1050 μatm), and high temperature and pCO_2 (pCO_2T; +3°C, 1119 μatm; Table 1, Supplementary Table S1 and Supplementary Figure S2). The conditions closely simulated ambient Kāneʻohe Bay conditions (Silbiger and Donahue, 2015) and future temperature and pCO_2 values predicted by 2100 (+3°C, 1100 ppm; Riahi *et al.*, 2011). A +3°C temperature increase also closely resembles sea surface temperature values for summer in Kāneʻohe Bay. Treatments were randomly assigned to incubation chambers. Incubation chambers were preconditioned for 12 h without sponges until the desired pCO_2 and temperature conditions were achieved: experiments began only when parameters were consistent across all incubation chambers. Sponges were rinsed with filtered seawater to remove any diatom contamination and transferred from their flow-through acclimation tank to the incubation chamber. Sponges were acclimated to incubation chamber conditions for 12 h before each experimental run. Background silica concentrations (6–7 μM) were calculated for each bucket before the start of each experiment. After incubation chambers were at the desired pCO_2 and temperature conditions, they were enriched with 45–50 mg of sodium hexafluorosilicate to bring the DSi concentration to 60–70 μM in each bucket. We chose to increase the silica concentration rather than using background concentrations to increase the likelihood of finding detectable differences in silica uptake over the short period of the experiment. The experiment was run four times. On the first run, we used three incubation chambers (replicates) per treatment. On runs two, three, and four, we used four incubation chambers (replicates) per treatment in each run resulting in a total of 15 replicates per treatment. A 48-h period was chosen to assure that the absorbed silica was biomineralized into spicules and that sponges did not starve (Weissenfels, 1981; Maldonado *et al.*, 2011). We added an additional no-sponge control to test for silica uptake from diatoms in the filtered seawater (Supplementary Figure S3). We analysed silica concentration in empty incubation chambers for each treatment (3 per treatment) during each experimental run. To examine silica uptake rates of *M. grandis* at normal silica concentrations (6 μM DSi), we ran eight uptake experiments with sponges held at control temperature and pCO_2 concentrations. Salinity, temperature, pH_t, and DSi were monitored every 8 for 48 h. Total alkalinity (A_T) samples (250 ml) were collected from the pre-filtered seawater before the start of each experiment and subsequent samples were taken from individual incubation chamber after the 48-h period.

After each experiment, we recorded the sponge wet weight on an analytical scale and sponge volume via volume displacement. To calculate size of injury (cm^2) per individual, we took photographs of each individual and analysed them in ImageJ® (Abràmoff *et al.*, 2004; http://imagej.nih.gov/ij/). Samples were then combusted (500°C) for 12 h to determine the AFDW.

Silica uptake rates were normalized to sponge volume (ml), AFDW (g), and injury area (cm^2) caused by the incision produced at the time of collection. Sponge volume and AFDW have previously been used to determine uptake rates from sponges (Maldonado *et al.*, 2011, 2012a). The size of injury was considered an additional variable as sponge silica uptake rates are shown to increase when sponges are injured (Ayling, 1983; Maldonado *et al.*, 2011). Sponges that showed signs of necrosis or incubation chambers that showed signs of diatoms (dramatic DSi uptake) at the end of the experiment were discarded and were not used in the statistical analysis. Uptake rates were calculated at each 8 h interval [$\text{Uptake} = (\text{DSi}_{t2,i} - \text{DSi}_{t1,i})/(\text{time} \times V_i)$], where DSi is the concentration of dissolved Si in μmol from sponge *i*, t_1 the first time point, t_2 the second time point, time the time between collections in hours, and *V* the volume of water in the bucket for sponge *i*. Total uptake rates across 48 h were also calculated for sponges exposed to each treatment by calculating the difference in silica concentrations between 0 and 48 h.

Flow-through system experiment

Sponge collection

Sponge pieces from individuals ($n = 72$) of *M. grandis* (wet weight: 29–263 g) were collected around Moku o Loʻe (Coconut Island) in Kāneʻohe Bay at a depth of 3–9 m. Sponge samples were acclimated to aquaria facilities with ambient Kāneʻohe Bay seawater for 3 weeks before the experiment. Sponges were tagged with pigeon tags using a small tie wrap. The morphological characteristics used to determine spicule biomineralization were spicule size dimensions ($L \times W$), ash-free dry weight to dry weight (AFDW/DW) ratios, and silicified weight to dry weight (SIW/DW) ratios. One thick section (~500 μm) from the surface of each sponge was cut by hand and collected to compare spicule sizes, and six, smaller, 1 cm^3 (1–2 g) sections were cut from each individual to calculate AFDW/DW and SIW/DW ratios in triplicate. To determine SIW/DW, we exposed sponge tissues to 5% hydrofluoric acid (HF). All incisions were performed next to each other to reduce potential variance of spicule types or silica densities in the irregular sponge body.

All samples for spicule measurements, AFDW/DW, and SIW/DW ratio analyses were collected again using the same methods at the end of the experiment (day 26) to compare morphological

Table 1. Mean and standard error of chemical parameters measured from all incubations for each treatment during 48-h sponge incubations.

Treatment	Hour	Temp (°C)	Salinity (ppt)	A_T (μmol kg^{-1})	pH_T (t)	pCO_2 (μatm)	HCO_3^- (μmol kg^{-1})	CO_3^- (μmol kg^{-1})	Ω_{arag}
Control	0	24.1 ± 0.04	34.82 ± 0.1	2 174 ± 3.0	7.82 ± 0.01	672 ± 7.3	1849 ± 3.1	131.3 ± 1.2	2.08 ± 0.02
$n_{bucket} = 17$	8	24.2 ± 0.06	34.92 ± 0.08	–	7.83 ± 0.02	–	–	–	–
	16	24.1 ± 0.04	35.06 ± 0.09	–	7.85 ± 0.02	–	–	–	–
	24	24.1 ± 0.04	35.12 ± 0.09	–	7.88 ± 0.02	–	–	–	–
	32	24.3 ± 0.06	35.12 ± 0.1	–	7.84 ± 0.02	–	–	–	–
	40	24.0 ± 0.04	35.22 ± 0.1	–	7.88 ± 0.02	–	–	–	–
	48	24.0 ± 0.04	35.23 ± 0.1	1 942 ± 18.2	7.89 ± 0.09	515 ± 34.0	1595 ± 23.8	136.1 ± 5.5	2.15 ± 0.09
T	0	27.3 ± 0.10	35.04 ± 0.1	2173.5 ± 3.3	7.85 ± 0.03	630 ± 10.7	1794 ± 7.9	153.6 ± 3.1	2.47 ± 0.03
$n_{bucket} = 14$	8	27.2 ± 0.08	35.1 ± 0.08	–	7.81 ± 0.04	–	–	–	–
	16	27.1 ± 0.09	35.24 ± 0.08	–	7.84 ± 0.04	–	–	–	–
	24	27.1 ± 0.08	35.31 ± 0.09	–	7.86 ± 0.05	–	–	–	–
	32	27.1 ± 0.09	35.34 ± 0.09	–	7.82 ± 0.04	–	–	–	–
	40	27.2 ± 0.08	35.44 ± 0.1	–	7.85 ± 0.04	–	–	–	–
	48	27.1 ± 0.07	35.47 ± 0.1	1953.2 ± 17.7	7.87 ± 0.05	570 ± 50.9	1594 ± 25.2	145.9 ± 6.2	2.33 ± 0.15
pCO_2	0	23.8 ± 0.07	34.97 ± 0.1	2175 ± 3.7	7.61 ± 0.01	1121 ± 18.4	1962 ± 3.3	85.2 ± 1.3	1.34 ± 0.02
$n_{bucket} = 13$	8	24.0 ± 0.05	35.02 ± 0.1	–	7.62 ± 0.01	–	–	–	–
	16	23.9 ± 0.06	35.21 ± 0.09	–	7.61 ± 0.02	–	–	–	–
	24	23.9 ± 0.05	35.26 ± 0.09	–	7.62 ± 0.02	–	–	–	–
	32	23.9 ± 0.05	35.33 ± 0.1	–	7.62 ± 0.02	–	–	–	–
	40	23.9 ± 0.06	35.42 ± 0.1	–	7.61 ± 0.02	–	–	–	–
	48	24.0 ± 0.07	35.44 ± 0.1	1964 ± 15.8	7.63 ± 0.02	978 ± 50.8	1745 ± 1676	82.1 ± 4.0	1.29 ± 0.06
pCO_2 T	0	27.0 ± 0.08	35.12 ± 0.07	2175.8 ± 2.8	7.60 ± 0.01	1190 ± 18.1	1945 ± 3.9	93.3 ± 1.2	1.49 ± 0.02
$n_{bucket} = 14$	8	27.1 ± 0.10	35.18 ± 0.07	–	7.62 ± 0.01	–	–	–	–
	16	27.0 ± 0.07	35.36 ± 0.07	–	7.62 ± 0.02	–	–	–	–
	24	27.1 ± 0.05	35.45 ± 0.08	–	7.61 ± 0.02	–	–	–	–
	32	27.2 ± 0.07	35.42 ± 0.07	–	7.62 ± 0.01	–	–	–	–
	40	27.0 ± 0.09	35.46 ± 0.07	–	7.61 ± 0.01	–	–	–	–
	48	26.8 ± 0.08	35.47 ± 0.07	1978.8 ± 12.8	7.61 ± 0.01	1048 ± 35.2	1762 ± 11.2	85.9 ± 2.8	1.37 ± 0.04
6 μM DSi	0	24.0 ± 0.07	34.14 ± 0.08	2158.5	7.86 ± 0.02	618 ± 19.1	1819 ± 7.6	137.0 ± 3.0	2.18 ± 0.05
$n_{bucket} = 8$	8	24.0 ± 0.08	34.29 ± 0.06	–	7.86 ± 0.01	–	–	–	–
	16	23.8 ± 0.09	34.69 ± 0.06	–	7.90 ± 0.02	–	–	–	–
	24	24.0 ± 0.05	34.68 ± 0.06	–	7.87 ± 0.01	–	–	–	–
	32	24.1 ± 0.04	34.76 ± 0.03	–	7.86 ± 0.01	–	–	–	–
	40	23.9 ± 0.04	34.63 ± 0.07	–	7.86 ± 0.01	–	–	–	–
	48	23.8 ± 0.04	34.84 ± 0.06	2189.7 ± 9.9	7.87 ± 0.01	605 ± 13.6	1836 ± 9.5	142.7 ± 2.0	2.25 ± 0.03

differences before and after exposure to treatments. Thin sections for spicule analysis were made on healed tissue from the first sampling incision to ensure that the spicules collected were biomineralized during the time of the experiment.

Morphological response of M. grandis

To measure morphological differences in silica biomineralization, we used a 26-d, flow-through experimental set-up with similar pCO_2 and temperature conditions to the silica uptake experiment. The control conditions were changed to mimic ambient Kāne'ohe seawater temperature which cooled by 1°C at the time of the experiment (NOAA.NOS.CO-OPS Moku o Lo'e station 1612480). The four treatments were: control (C; 23°C, 692 μatm), high temperature (T; +3°C), high pCO_2 (pCO_2; 1100 μatm), and a combination of high temperature and pCO_2 (pCO_2T; +3°C, 1100 μatm; Table 2, Supplementary Table S1 and Supplementary Figure S4). Ambient water from Kāne'ohe Bay passed through a water chiller (Aqualogic Multi Temp MT-1 model no. 2TTB3024A1000AA) and was fed into one of two 150 l header tanks. pCO_2 was manipulated in each header with gas-lines pumping in pre-mixed pCO_2 and then water from each header tank was fed into six 50 l experimental tanks (a total of six high CO_2 and six control CO_2 tanks). Temperature was controlled in each tank with aquarium heaters and dual-stage temperature controllers (Aqualogic TR115DN) similarly to the silica uptake experiment. There were three tank replicates per treatment in a completely randomized design; six sponges were placed in each tank for a total of 18 individuals per experimental treatment. The flow rate in each tank was maintained at 200 ml min^{-1} with a turnover every 4.2 h. Each incubation chamber was equipped with a submersible power head pump (Sedra KSP-7000 power head) to keep seawater well mixed. The same light parameters described in the silica uptake experiment were used. Temperature, pH_T, salinity, and dissolved oxygen of each tank were measured daily in each aquarium and seawater flow was monitored and adjusted twice a day to ensure consistency for all tanks. A_T and silica concentrations were measured every 3 d (Table 2).

Sponges were weighed with an analytical scale before and after the experiment by placing them in a 500 ml beaker with seawater; sponges were briefly exposed to air during the transfer from the tank to the beaker (Pawlik *et al.*, 2013). To determine differences in spicule size across treatments, the mean spicule dimensions ($L \times W$) were compared before and after exposure to treatments. To measure spicule sizes, sponge sections ($n = 18$ per treatment) were submerged in 1 ml of 65% nitric acid using a 2 ml Eppendorf tube. Tubes were hand shaken and incubated at room temperature for 24 h. Samples were then centrifuged (110g) and supernatant discarded. Pellets were rinsed with distilled water and a few drops of liquid containing spicules were mounted on a microscope slide. Photographic images of 20 subtylostyle spicules per sponge (a total of 360 spicules per treatment) were photographed and measured ($L \times W$) using ImageJ. Subtylostyles were chosen as the response variable because they made up >90% of spicule content.

Triplicate samples collected for AFDW measurements were dried (60°C) and weighed until a consistent weight was reached. Dry weights of samples were recorded and samples were then combusted (500°C) for 8–12 h, following the protocol of Maldonado *et al.* (2012a). To measure desilicification of sponge samples, triplicates of each individual were dried at 60°C until a consistent weight was reached. Samples were then submerged in HFA (5%) in 15 ml Falcon tubes and incubated at room temperature for 48 h. Samples were centrifuged (2700g) and the supernatant was discarded. The pellets were rinsed with distilled water and centrifuged again. The supernatant was discarded and pellets were dried (60°C) for 3 d or until a consistent weight was reached. To obtain silicified weight, we subtracted the desilicified weight (DSI) and divided by DW to obtain the DSI/DW ratio. To determine treatment differences between AFDW/DW and SIW/DW ratios, the average of each triplicate sample for each individual was taken. All averages showed a precision within ±0.02 S.E. (standard error). Differences in ADFW/DW and SIW/DW ratios were used to examine biomineralized silica in proportion to the whole mass of the sponge.

Measuring seawater chemistry parameters

All sample vials and stoppers were prewashed with 10% HCl for 24 h and rinsed three times with MilliQ water. Containers for all water samples collected to measure chemical parameters were rinsed three times with sampled water before a final sample was taken.

Samples (250 ml) for A_T analysis were collected and processed within 4 h using open cell potentiometric titrations on a Mettler T50 autotitrator (Dickson *et al.*, 2007). A certified reference material (CRM- Reference Material for Oceanic CO_2 Measurements, A. Dickson, Scripps Institution of Oceanography) was run at the beginning of each sample set. Titrator accuracy was within ±0.8% from the CRM standard and A_T measurements were corrected for this error. The precision was 4.75 μEq (measured as the standard deviation of the duplicate water samples).

Seawater pH was measured on the total scale. For the open-system experiment, borosilicate glass vials (20 ml) were used to take duplicate pH_T samples. Samples were immediately processed

Table 2. Mean and standard error for chemical parameters in all experimental tanks for each treatment during the flow-through system experiment.

Parameter	Control	*T*	pCO_2	pCO_2T	Header T2[a]	Header T3[a]
Temp (°C)	23.1 ± 0.03	25.6 ± 0.03	23.0 ± 0.03	25.7 ± 0.04	24.09 ± 0.14	24.04 ± 0.14
Salinity (ppt)	33.82 ± 0.07	33.99 ± 0.07	33.79 ± 0.07	33.87 ± 0.08	34.31 ± 0.09	34.16 ± 0.10
A_T (μmol kg^{-1})	2167.9 ± 3.1	2165.4 ± 3.2	2168.4 ± 3.3	2171.2 ± 2.8	2177.2 ± 9.2	2170.0 ± 5.3
pH_T	7.82 ± 0.004	7.82 ± 0.004	7.60 ± 0.004	7.60 ± 0.004	7.54 ± 0.006	7.90 ± 0.006
pCO_2(μatm)	693 ± 13.9	692 ± 11.3	1198 ± 22.5	1225 ± 21.4	1442 ± 37.6	569 ± 24.1
HCO_3^-(μmol kg^{-1})	1863 ± 4.9	1836 ± 4.7	1972 ± 4.1	1960 ± 3.5	2000 ± 26.9	1807 ± 14.1
CO_3^-(μmol kg^{-1})	122.9 ± 1.6	132.9 ± 1.5	79.3 ± 1.3	85.7 ± 1.2	71.6 ± 1.5	147.9 ± 1.9
Ω_{arag}	1.94 ± .03	2.13 ± .02	1.26 ± .02	1.37 ± 0.02	1.14 ± 0.02	2.35 ± 0.03
$Si(OH)_4$ (μmol l^{-1})	4.16 ± 0.28	3.98 ± 0.27	3.91 ± 0.23	4.49 ± 0.22	6.1 ± 0.41	6.04 ± 0.43
O_2 (mg l^{-1})	6.11 ± 0.35	6.02 ± 0.41	5.97 ± 0.36	5.86 ± 0.37	5.94 ± 0.07	5.99 ± 0.04

[a]Header T2 supplies seawater for incubations with treatments pCO_2, pCO_2T and Header T3 supplies seawater for incubations with treatments Control, *T*.

and brought to a constant temperature of 25°C in a water bath. An *m*-cresol dye was added to each sample and analysed using a spectrophotometric technique (Dickson *et al.*, 2007). The precision for pH_T measurements was 0.003 pH_t units (measured as the standard deviation of the duplicate water samples). During the closed system experiments, pH_T was measured using a Tris calibrated Mettler Toledo DG 115-SC pH probe with an Orion 3star pH portable meter. Calibrations for the pH probe were performed each week following the SOP 6a protocol from Dickson *et al.* (2007). Other carbon parameters (pCO_2, HCO_3^-, CO_3^-, Ω_{arag}) were calculated using the CO_2SYS_V2.1 (Lewis *et al.*, 1998) with known pH_T, A_T, temperature, and salinity values. The K1K2 equilibrium constants were taken from Mehrbach *et al.* (1973) and refitted according to Dickson and Millero (1987). The HSO_4^- dissociation constants from Uppström (1974) and Dickson (1990) were used. Dissolved oxygen measurements in open system experiments were taken using a ROX^{TM} Optical Dissolved Oxygen mg l^{-1} 6150 Sensor integrated in a YSI 6920 V2 sonde that was calibrated using the one-point saturated water following standard calibration protocols. Salinity measurements were taken with a YSI conductivity, salinity, temperature meter (model # 30–50), and calibrated using a 50 mS cm^{-1} conductivity standard (YSI Catalogue# 3169) following standard calibration protocols.

Triplicate samples were taken with 15 ml sterile falcon tubes to measure DSi concentrations. A Hach ultra low range (0–6 μM) silica reagent set was used to measure DSi for flow-through experiments and a Hach low range (20–120 μM) silica test kit was used for closed system experiments. These two silica test kits with different detection limits were used because the open and closed system experiments had different silica concentrations. Both of these methods follow a molybdate-reactive standard colorimetric method for measuring silicate (Grasshoff *et al.*, 2009). Standard curves were generated before each run using a wavelength of 820 nm. Only dilutions that generated a standard curve with an $R^2 > 0.99$ were used to calculate DSi concentrations. Chemical reagents were added at 24°C following the Hach protocol guidelines. Precision for silica samples was >0.4 μM l^{-1} (measured as the standard deviation of the triplicate water samples).

Statistical analysis

We used two-way repeated-measures ANOVA to test for differences in silica uptake rates normalized to three different variables (AFDW, sponge volume, and injury size) across the treatments. Time (each 8-h interval over the 48 h experiment), treatment, and the interaction between time and treatment were included in the analysis. ANOVAs were also done by period for all variables with partitioning of the treatment effect into the pCO_2 and temperature main effects and the interaction between these two factors. Because we had an unbalanced design (i.e. there were missing data points), we used a general linear model procedure (Proc GLM). pH, temperature, pCO_2, and A_T for each 8-h period was also analysed with a two-way repeated-measures ANOVA to ensure that treatments were kept at the intended pH and temperature values. *F*-tests were performed to test the homogeneity of the error variances obtained in the ANOVAs for the six periods for both analysis. We removed 12 sponges (Control = 1, pCO_2 = 4, T = 3, pCO_2T = 1, 6 μMDSi = 3) from the analysis that showed signs of necrosis, which caused silica concentrations to increase inside the incubation chamber. A total of 54 sponge individuals (Control = 14, pCO_2 = 11, T = 10, pCO_2T = 11, 6 μMDSi = 8) remained healthy throughout the 48-h incubations and were used in the analysis.

In the flow-through experiment, sponge weight loss, spicule sizes, AFDW/DW, and SIW/DW ratio differences were log-transformed to meet assumptions of normality. We used an ANOVA to assess differences in spicule size, AFDW/DW, SIW/DW ratios, pH, temperature, pCO_2, and A_T across treatments (Control, T, pCO_2, and pCO_2T) during the 26-d flow-through experiment. A two-way ANOVA was run for carbonate chemistry and temperature variables (pH, temperature, pCO_2, and A_T) using factors treatment, time, and treatment by time. Time refers to the number of days of the experiment. ANOVAs were also done by period for all variables with partitioning of the treatment effect into the pCO_2 and temperature main effects and the interaction between these two factors. All data were analysed using Statistical Analysis Systems (SAS; Statistical Analysis Systems Institute, 2001). Duncan's multiple range tests was used to test for significant differences between treatment means. All statistical test interpretations were made at the 5% level of significance.

Results

Silica uptake experiments

Uptake rates

Results from the ANOVA for silica uptake rate showed no significant treatment or treatment × time interaction effects when normalized to any of the variables (AFDW, injury area, sponge volume; Figure 1, Table 3). The factorial ANOVAs conducted by time of sampling showed no significant pCO_2 and temperature main effects nor a

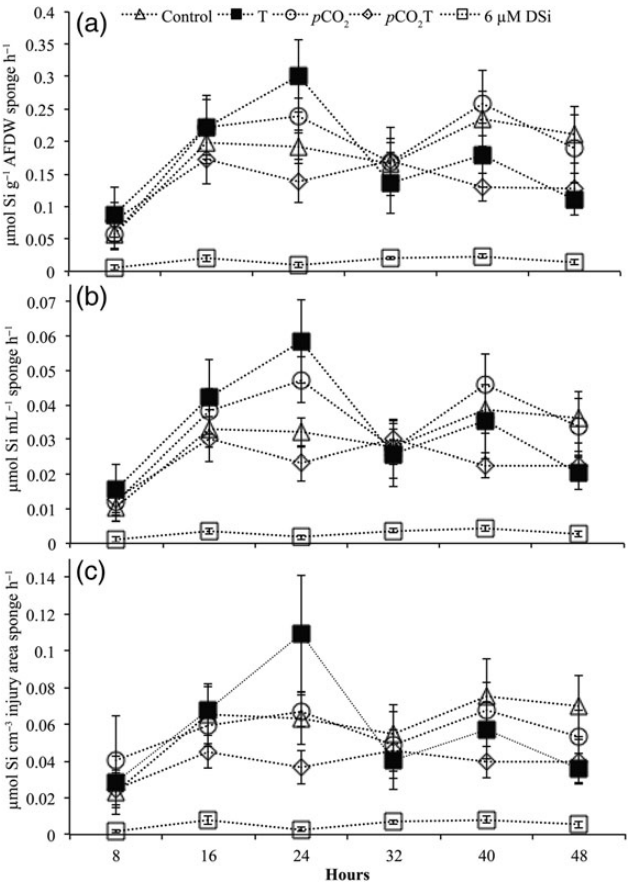

Figure 1. Mean and standard error of DSi uptake rates by the sponge *M. grandis*. Uptake rates were determined by (a) AFDW (g), (b) sponge volume (ml), and (c) area of injury (cm^2).

Table 3. *p*-values from a two-way ANOVA for *M. grandis* silica uptake rates normalized by AFDW, volume, and injury size.

		Source of variation			
Experiment	**Variable**	**Treatment (TMT)**	**Time (*T*)[a]**	**TMT × *T***	***CV* (%)**
Silica uptake	AFDW	0.7339	**<0.0001**	0.2898	46.0
	Volume	0.4843	**<0.0001**	0.2017	50.8
	Injury	0.3976	**0.0011**	0.3195	52.9
Flow-through	Weight loss	0.7020	–	–	21.1
	Spicule length	0.4324	–	–	238.9
	Spicule width	0.7696	–	–	309.1
	AFDW/DW ratio	**0.0001**	–	–	21.3
	SIW/DW ratio	0.0673	–	–	596.0

[a]Time for silica uptake experiment was for every 8 h and for the flow through and days for the flow-through experiment.
CV, coefficient of variation.
p-values from an ANOVA for the changes in *M. grandis* weight loss, spicule size, AFDW/DW, and SIW/DW ratios across treatments during the flow-through experiment. Bold values are significant. Significant differences were only observed in changes of AFDW/DW ratios.

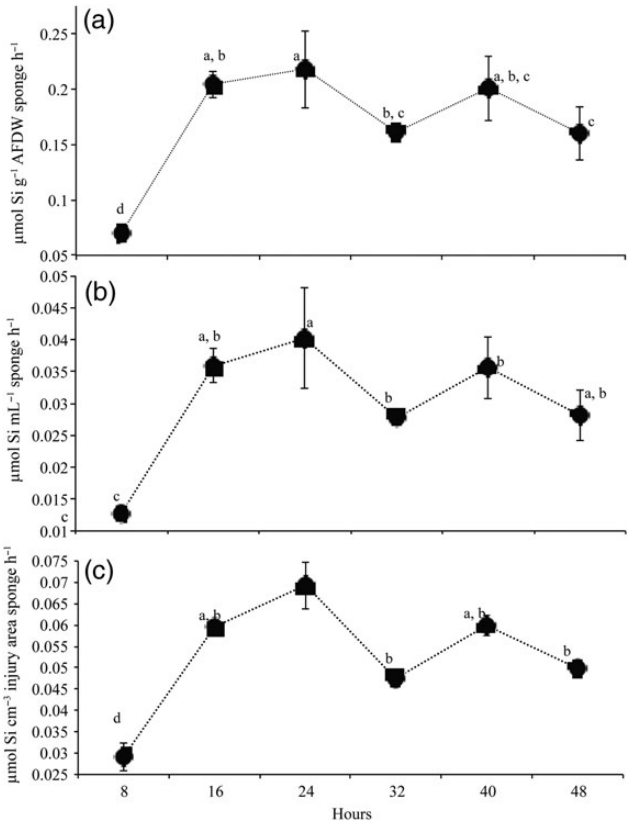

Figure 2. Silica uptake rates with time averaged ($n = 46$) across treatments determined by (a) AFDW, (b) sponge volume (ml), and (c) area of injury (cm^2). Within each subplot, means with the same letters in common are not significantly different as indicated by Duncan's multiple range test.

pCO_2 × temperature interaction. However, there was a significant difference by time ($p < 0.001$ for AFDW and volume, $p = 0.0011$ for injury; Table 3) and coefficients of variation for the ANOVAs ranged from 0.6 to 52.9%.

In general, each silica uptake rate across all treatments followed a curvilinear pattern. Rates for all three variables were lowest during the 0–8 h period, while maximum uptake rate was at the 16–24 h period with 0.20 μmol Si g^{-1} AFDW sponge h^{-1}, 0.06 μmol Si cm^{-2} injury area of sponge h^{-1}, and 0.04 μmol Si ml^{-1} of sponge h^{-1} (Figure 2). A decrease in uptake rate was observed for all three variables from the 24 to the 40-h period, a slight increase between 32 and 40 h period, and a slight decrease between the 40 and 48 h period. There was no detectable DSi uptake in incubation chambers without sponges with values remaining between 60 and 65 μM of DSi throughout 48 h, indicating that filtered seawater was free of diatoms (Supplementary Figure S2).

Total silica uptake rates showed no significant differences across treatments. However, the total silica uptake rate of the enrichment condition applied to all treatments and was substantially higher than the background silica (6 μM DSi) treatment. The 6 μM DSi was run only one time with six replicates as a control and therefore could not be included in the ANOVA. Average uptake rates across the 48 h of *M. grandis* for background levels of silica (6 μM DSi) were 0.016 ± 0.003 (mean ± s.e.) μmol Si g^{-1} AFDW h^{-1} (Table 4). Total silica uptake rates in the Control with enriched DSi (70 μM) conditions accelerated to 0.155 ± 0.029 μmol Si g^{-1} AFDW h^{-1}, an almost tenfold increase in uptake rates compared with background DSi levels (Table 4).

Flow-through system experiment

Morphological response of M. grandis

All sponge individuals used for the flow-through system experiments survived the 26-d experiment. A weight loss of 28.4% was observed for all treatments, but no significant differences were observed between treatments. The coefficient of variation for weight loss was 21.1% (Table 3; Figure 3a). There were no significant differences across treatments for spicule length, width, or SIW/DW (Table 1; Figure 3b and c). The factorial ANOVA with partitioning of the treatment effect into main effects (pCO_2 and temperature) and interaction (pCO_2 × temperature) showed no significant differences.

There was a significant difference across treatments for AFDW/DW ratios ($p = 0.0001$, Table 3; Figure 3d). The factorial ANOVA showed a non-significant $pCO_2 \times T$ interaction ($p = 0.99$) and a non-significant temperature main effect ($p = 0.12$). The pCO_2 main effect was significant ($p = 0.0013$). In general, increasing pCO_2 from background levels to 1100 μatm decreased AFDW/DW ratio by 0.03 mg units regardless of the temperature level. The coefficient of variations for AFDW/DW and SIW/DW ratios were 21.3 and 596.0%, respectively (Table 3).

Average differences between spicule lengths ranged between 2 and 6 ± 2.0 μm and widths ranged between 0.1 and 0.6 ± 0.2 μm for all treatments. Although no differences between treatments

Table 4. Mean DSi uptake rate with standard error of *M. grandis* silica concentrations taken at time 0 and at 48 h.

Treatment	μmol Si ml^{-1} sponge h^{-1}	μmol Si g^{-1} AFDW h^{-1}	μmol Si cm^{-3} injury h^{-1}
Control	0.025 ± 0.004	0.155 ± 0.029	0.051 ± 0.015
pCO_2	0.028 ± 0.006	0.164 ± 0.033	0.045 ± 0.011
T	0.030 ± 0.005	0.158 ± 0.031	0.051 ± 0.010
pCO_2T	0.021 ± 0.003	0.123 ± 0.023	0.035 ± 0.006
6 μM DSi[a]	0.003 ± 0.001	0.016 ± 0.003	0.006 ± 0.001

[a]6 μM DSi treatment was only ran once using six replicates.

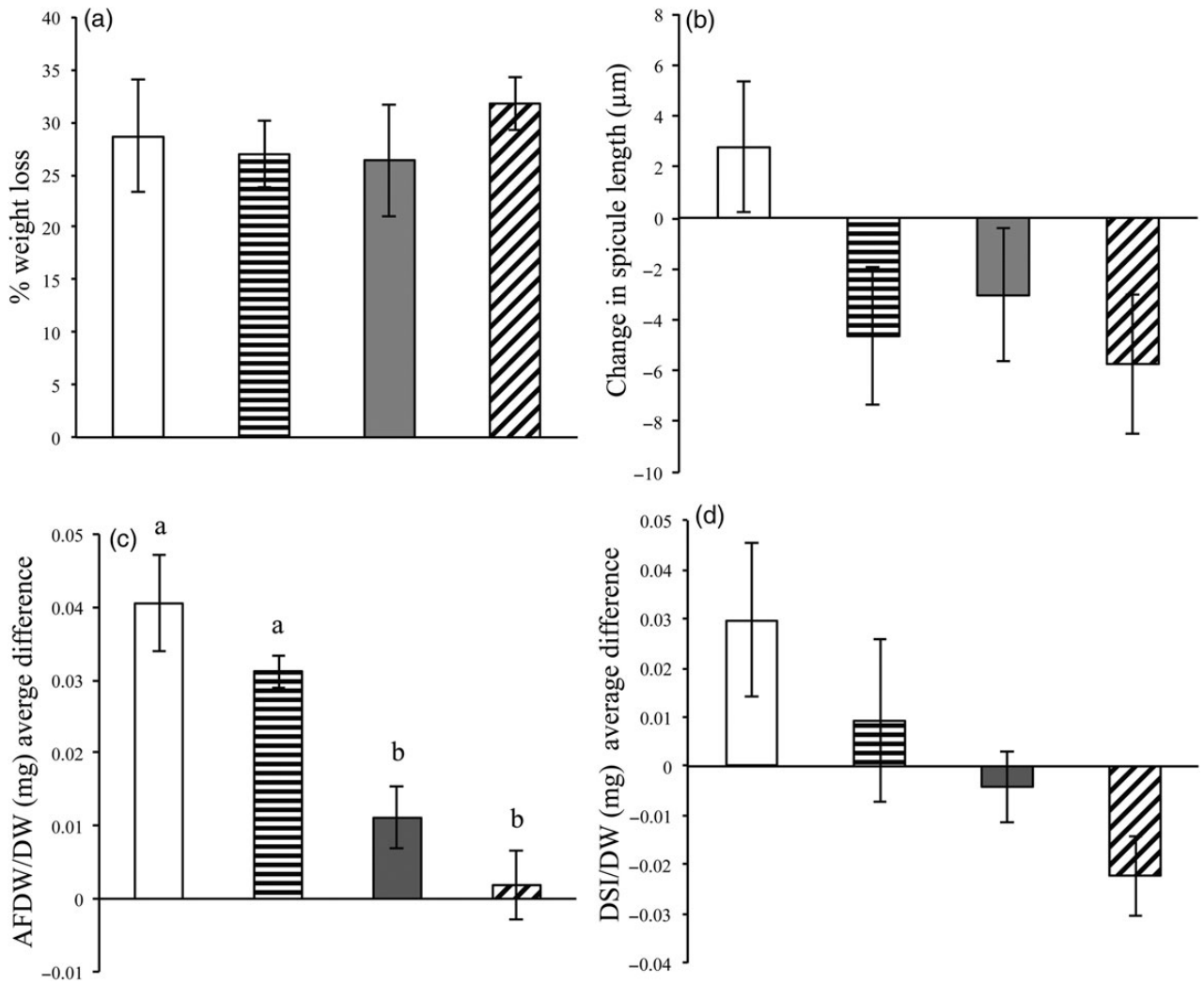

Figure 3. Mean and standard error of (a) % biomass loss for sponges in each treatment. Morphological differences between (b) subtylostyle length, (c) AFDW/DW ratio, and (d) DSI/DW ratio of sponges in the 26-d flow-through experiment. Within each subplot, means with the same letters in common are not significantly different as indicated by Duncan's multiple range test. The factorial ANOVA for AFDW/DW ratio showed a non-significant $pCO_2 \times T$ interaction ($p = 0.99$) and a non-significant temperature main effect ($p = 0.12$). The pCO_2 main effect was significant ($p = 0.0013$). Treatments are indicated as follows: control (white bars), *T* (bars with horizontal lines), pCO_2 (grey bars), pCO_2T (bars with diagonal lines).

were found for spicule length, the control treatment means increased slightly, while all other treatments showed a net decrease (Figure 3b). An average decrease of 0.21 ± 0.1 μm spicule width was observed for all four treatments. The coefficient of variations for spicule length and width were 93.3 and 309.1%, respectively (Table 3).

The average AFDW/DW ratio differences of sponge samples ranged from 0.67 to 0.81 and averaged 0.74 ± 0.006 before exposure. Differences in AFDW/DW ratios throughout the 26 d resulted in net ratios that were significantly lower in treatments pCO_2 and pCO_2T than Control and *T* treatments ($p = 0.0001$, Table 3). AFDW/DW ratios had the highest increase in the Control treatment (0.04 ± 0.01) followed by *T* (0.03 ± 0.002), pCO_2 (0.01 ± 0.004), and pCO_2T (0.002 ± 0.004; Figure 3c).

SIW/DW ratio differences of sponge samples ranged from 0.71 to 0.99 and averaged 0.88 ± 0.006 before exposure. There were no

significant differences in SIW/DW ratios throughout the 26 d (Table 3). However, similar to AFDW/DW ratios, net average SIW/DW ratio differences followed a similar trend with the highest net increase observed in the Control (0.03 ± 0.02) followed by T (0.01 ± 0.02). A net decrease was observed for pCO_2 (-0.004 ± 0.01) and a greater decrease in pCO_2T (-0.02 ± 0.01; Figure 3d).

Discussion

Neither higher pCO_2 nor warmer temperature treatments affected silica uptake rates in the sponge *M. grandis* over 48 h (Figure 1). The availability of HCO_3^- and $Si(OH)_4$ did not facilitate up-regulation of silica uptake. Perhaps sponges are using the membrane symporter mechanism described for *S. domuncula* by Schröder *et al.* (2004), but that neither pCO_2 nor temperature affect the rate of silica transport by this process. The 26-d exposure to end-of-century pCO_2 (1198 μatm) revealed a decrease in the proportion of mineralized tissue (AFDW/DW) that appears to be aggravated when combined with a temperature increase (pCO_2T; 1225 μatm, +3°C μatm; Figure 3c). However, the factorial analysis revealed that the negative effect of pCO_2 on AFDW/DW ratio happened regardless of the temperature value, indicating that temperature had no effect. A decreasing trend was also observed in SIW/DW ratios and spicule lengths (Figure 3d).

Our results show that although no differences in silica uptake nor growth rates were detected as a result of high pCO_2 or warmer temperatures, these factors did have a marginal effect on the process of silica biomineralization in *M. grandis*. Previous studies have found that sponge growth rates of six Caribbean species were not affected by pH or warmer temperatures (Duckworth *et al.*, 2012), although other morphological characteristics such as spicule composition or biomineralization were not assessed. Other studies that have monitored sponge biodiversity and spicule composition along a natural pH gradient found that acidification caused a decrease in sponge cover but no differences in spicule morphology (Goodwin *et al.*, 2014). Particular interest has been paid to understanding how ocean acidification will affect sponge boring rates, where some species are found to accelerate their boring rates when exposed to acidification (Duckworth and Peterson, 2012; Wisshak *et al.*, 2013; Stubler *et al.*, 2014). Future ocean acidification studies on sponge boring rates should observe the morphological response of the sponge to see if faster boring rates correlate with a decrease in silica biomineralization. Under acidification scenarios, sponges might allocate their metabolic requirements less towards skeleton synthesis and more towards other processes that help fulfil the biochemical requirement for acid–base regulation (Pörtner, 2008).

Silica uptake rates for *M. grandis* increased proportionally with silica concentrations. A tenfold increase was observed when concentrations were spiked from 6–7 to 60–70 μM during closed system experiments (Table 4). These results suggest that *M. grandis* is potentially limited by silica and follows a similar uptake rate pattern to *Halichondria panicea* (Reincke and Barthel, 1997), *Axinella* sp., and *Hymeniacidon perlevis* (Maldonado *et al.*, 2011, 2012a). However, uptake rates for *M. grandis* (0.016 ± 0.003 μmol Si g^{-1} AFDW h^{-1}/ 0.003 ± 0.001 μmol Si ml^{-1} sponge h^{-1}) at background silica concentrations were the lowest when compared with *H. panicea* (3.42 μmol Si g^{-1} AFDW h^{-1}), *H. perlevis* (1.16 ± 0.50 μmol Si g^{-1} AFDW h^{-1}), and *Axinella* sp. (0.016 μmol Si ml^{-1} sponge h^{-1}), suggesting that silica biomineralization is a slow process in *M. grandis*. These observations agree with the hypothesis stated by Maldonado *et al.* (2012a, b) that uptake rates might be species dependent based on the proportion of their biomineralized silica to dry weight ratios. For example, the proportion of biomineralized silica in *M. grandis* averaged up to 74% (AFDW/DW), and 88% (SIW/DW) of biomineralized tissue in proportion to dry weight, which is the highest of any sponge previously studied for silica uptake kinetics.

Although silica uptake rates were not impacted by temperature or high pCO_2, there was a significant effect of time on average silica uptake rates across all treatments. Uptake rates for *M. grandis* (at 60–70 μM) resulted in a non-circadian oscillation with time reaching a maximum after 24 h (08:00) and a second maximum at 40 h (00:00) after incubation. Similar oscillations have been observed by Maldonado *et al.* (2012a, b) where *H. perlevis* had a maximum uptake rate between 0 and 6 h and a second maximum between 12 and 18 h under silica enrichments of 70 μM. These results support the hypothesis by Maldonado *et al.* (2012a, b) that silica transport is likely an active mechanism.

Sponge biomass decreased (25–35%) for all individuals in the 26-d experiment, an overall response probably due to our inability to fully simulate natural conditions of the reef environment. One possible explanation is that silica concentrations in experimental tanks were difficult to keep at natural incoming silica concentrations likely due to the presence of diatoms inside the tanks. For example, silica concentrations of incoming water from Kāneʻohe Bay into two of the header tanks averaged between 5 and 6 μM, but dropped to 3–4 μM in the experimental tanks (Table 2). A lack of food availability resulting from the slow flow rate might have also caused sponges to lose biomass. Despite observing an overall decrease in sponge biomass during our experiments, this effect did not prevent sponges from increasing biomineralization in the control treatment. It is also unlikely that spicules deposited in tanks from necrotic sponge tissue would affect spicule biomineralization as spicule dissolution happens at a very slow rate (Maldonado *et al.*, 2005).

Addressing the molecular response of genes involved in spicule synthesis of *M. grandis* would allow us to understand if the decrease in silica biomineralization caused by high pCO_2 in this study is inhibiting gene expression of proteins involved in spicule synthesis. Specifically, monitoring silicatein gene expression would provide us with helpful information as silicatein proteins are known to be directly linked with spicule synthesis (Cha *et al.*, 1999; Müller *et al.*, 2003, 2005). A transcriptomic assessment of genes involved in spicule synthesis would allow us to gain a comprehensive understanding of how ocean acidification and thermal stress might affect *M. grandis*.

Predicting how *M. grandis* will respond to warmer and high pCO_2 conditions is important as this sponge has already been known to aggressively spread through coral reefs of Kāneʻohe since its introduction (Coles *et al.*, 2006). Despite showing resilience under acute warmer temperatures and high pCO_2, it is very difficult to assess whether these short experimental windows are suggestive of a potential phase shift from coral to sponge by the end of the century, as suggested by Bell *et al.* (2013). Our findings highlight the exceptional ability of *M. grandis* to withstand pCO_2 and temperature conditions that are stressful to many organisms, suggesting that this invasive species will continue to be a competitor in the reefs of Kāneʻohe Bay in a warmer and more acidic ocean.

Supplementary data

Supplementary material is available at the *ICESJMS* online version of the manuscript.

Acknowledgements

We thank Hollie Putnam for her logistical support and Megan Donahue for advice on experimental design for this study. Funding for this project was supported by NOAA's Nancy Foster Scholarship award NA12NOS4290142 to JV and NJS. Support for sequencing of sponge samples was provided by the NSF BIO/IOS Programme (IOS-0919728) grant to RTH. We thank reviewers for constructive suggestions and in particular thank one reviewer for recommendations that greatly improved our statistical analyses. All samples were collected under collection permit No. 2014-52.

References

Abràmoff, M. D., Magalhães, P. J., and Ram, S. J. 2004. Image processing with ImageJ. Biophotonics International, 11: 36–42.

Ayling, A. L. 1983. Growth and regeneration rates in thinly encrusting demospongiae from temperate waters. The Biological Bulletin, 165: 343–352.

Bell, J. J., Davy, S. K., Jones, T., Taylor, M. W., and Webster, N. S. 2013. Could some coral reefs become sponge reefs as our climate changes? Global Change Biology, 19: 2613–2624.

Cebrian, E., Uriz, M. J., Garrabou, J., and Ballesteros, E. 2011. Sponge mass mortalities in a warming Mediterranean Sea: are cyanobacteria-harboring species worse off? PLoS One, 6: e20211.

Cha, J. N., Shimizu, K., Zhou, Y., Christiansen, S. C., Chmelka, B. F., Stucky, G. D., and Morse, D. E. 1999. Silicatein filaments and subunits from a marine sponge direct the polymerization of silica and silicones in vitro. Proceedings of the National Academy of Sciences of the United States of America, 96: 361–365.

Coles, S., and Bolick, H. 2007. Invasive introduced sponge *Mycale grandis* overgrows reef corals in Kāne ʻohe Bay, O ʻahu, Hawai ʻi. Coral Reefs, 26: 911.

Coles, S. L., Bolick, H., and Longenecker, K. 2006. Assessment of Invasiveness of the Orange Keyhole Sponge *Mycale armata* in Kāne ʻohe Bay, O ʻahu, Hawai ʻi. Final Report Year, 1: 2006-2002.

de Goeij, J. M., van Oevelen, D., Vermeij, M. J., Osinga, R., Middelburg, J. J., de Goeij, A. F., and Admiraal, W. 2013. Surviving in a marine desert: the sponge loop retains resources within coral reefs. Science, 342: 108–110.

Diaz, M. C., and Rützler, K. 2001. Sponges: an essential component of Caribbean coral reefs. Bulletin of Marine Science, 69: 535–546.

Dickson, A., and Millero, F. 1987. A comparison of the equilibrium constants for the dissociation of carbonic acid in seawater media. Deep Sea Research Part A. Oceanographic Research Papers, 34: 1733–1743.

Dickson, A. G. 1990. Standard potential of the reaction: $AgCl\,(s) + 12H_2\,(g) = Ag\,(s) + HCl\,(aq)$, and the standard acidity constant of the ion HSO_4^- in synthetic sea water from 273.15 to 318.15 K. Journal of Chemical Thermodynamics, 22: 113–127.

Dickson, A. G., Sabine, C. L., and Christian, J. R. (Eds) 2007. Guide to best practices for ocean CO_2 measurements. PICES Special Publication 3, 191 pp.

Duckworth, A. R., and Peterson, B. J. 2012. Effects of seawater temperature and pH on the boring rates of the sponge *Cliona celata* in scallop shells. Marine Biology, 160: 27–35.

Duckworth, A. R., West, L., Vansach, T., Stubler, A., and Hardt, M. 2012. Effects of water temperature and pH on growth and metabolite biosynthesis of coral reef sponges. Marine Ecology Progress Series, 462: 67–77.

Enochs, I. C., Manzello, D. P., Carlton, R. D., Graham, D. M., Ruzicka, R., and Colella, M. A. 2015. Ocean acidification enhances the bioerosion of a common coral reef sponge: implications for the persistence of the Florida Reef Tract. Bulletin of Marine Science, 91: 271–290.

Fabry, V. J., Seibel, B. A., Feely, R. A., and Orr, J. C. 2008. Impacts of ocean acidification on marine fauna and ecosystem processes. ICES Journal of Marine Science, 65: 414–432.

Gibbin, E. M., Putnam, H. M., Gates, R. D., Nitschke, M. R., and Davy, S. K. 2015. Species-specific differences in thermal tolerance may define susceptibility to intracellular acidosis in reef corals. Marine Biology, 162: 717–723.

Goodwin, C., Rodolfo-Metalpa, R., Picton, B., and Hall-Spencer, J. M. 2014. Effects of ocean acidification on sponge communities. Marine Ecology, 35: 41–49.

Grasshoff, K., Kremling, K., and Ehrhardt, M. 2009. Methods of Seawater Analysis. John Wiley & Sons, Federal Republic of Germany.

Gray, J. 1867. Notes on the arrangement of sponges, with the description of some new genera. *In* Proceedings of the Zoological Society of London, pp. 492–558.

Hoegh-Guldberg, O., Mumby, P., Hooten, A., Steneck, R., Greenfield, P., Gomez, E., Harvell, C., *et al.* 2007. Coral reefs under rapid climate change and ocean acidification. Science, 318: 1737–1742.

Hofmann, G. E., Barry, J. P., Edmunds, P. J., Gates, R. D., Hutchins, D. A., Klinger, T., and Sewell, M. A. 2010. The effect of ocean acidification on calcifying organisms in marine ecosystems: an organism-to-ecosystem perspective. Annual Review of Ecology, Evolution, and Systematics, 41: 127–147.

Hooper, J. N., and Van Soest, R. W. 2002. Systema Porifera. A Guide to the Classification of Sponges. Springer.

Lewis, E., Wallace, D., and Allison, L. J. 1998. Program developed for CO_2 system calculations. Carbon Dioxide Information Analysis Center. Managed by Lockheed Martin. Energy Research Corporation for the US Department of Energy Tennessee.

Loh, T-L., McMurray, S. E., Henkel, T. P., Vicente, J., and Pawlik, J. R. 2015. Indirect effects of overfishing on Caribbean reefs: sponges overgrow reef-building corals. PeerJ, 3: e901.

Maldonado, M., Carmona, M. C., Velásquez, Z., Puig, A., Cruzado, A., López, A., and Young, C. M. 2005. Siliceous sponges as a silicon sink: an overlooked aspect of benthopelagic coupling in the marine silicon cycle. Limnology and Oceanography, 50: 799–809.

Maldonado, M., Cao, H., Cao, X., Song, Y., Qu, Y., and Zhang, W. 2012a. Experimental silicon demand by the sponge *Hymeniacidon perlevis* reveals chronic limitation in field populations. Hydrobiologia, 687: 251–257.

Maldonado, M., Navarro, L., Grasa, A., Gonzalez, A., and Vaquerizo, I. 2011. Silicon uptake by sponges: a twist to understanding nutrient cycling on continental margins. Scientific Reports, 1: 30.

Maldonado, M., Ribes, M., and van Duyl, F. C. 2012b. 3 Nutrient fluxes through sponges: biology, budgets, and ecological implications. Advances in Marine Biology, 62: 113.

McMurray, S. E., Finelli, C. M., and Pawlik, J. R. 2015. Population dynamics of giant barrel sponges on Florida coral reefs. Journal of Experimental Marine Biology and Ecology, 473: 73–80.

Mehrbach, C., Culberson, C., Hawley, J., and Pytkowicx, R. 1973. Measurement of the apparent dissociation constants of carbonic acid in seawater at atmospheric pressure. Limnology and Oceanography, 18: 897–907.

Morrow, K. M., Bourne, D. G., Humphrey, C., Botte, E. S., Laffy, P., Zaneveld, J., Uthicke, S., *et al.* 2014. Natural volcanic CO_2 seeps reveal future trajectories for host-microbial associations in corals and sponges. ISME Journal, 9: 894–908.

Müller, W. E., Krasko, A., Le Pennec, G., Steffen, R., Wiens, M., Ammar, M. S. A., Müller, I. M., *et al.* 2003. Molecular mechanism of spicule formation in the demosponge *Suberites domuncula*: silicatein-collagen-myotrophin. *In* Silicon Biomineralization, pp. 195–221. Springer, Berlin Heidelberg.

Müller, W. E., Rothenberger, M., Boreiko, A., Tremel, W., Reiber, A., and Schröder, H. C. 2005. Formation of siliceous spicules in the marine demosponge *Suberites domuncula*. Cell and Tissue Research, 321: 285–297.

Nwewll, R., and Northcroft, H. 1967. A re-interpretation of the effect of temperature on the metabolism of certain marine invertebrates. Journal of Zoology, 151: 277–298.

Pawlik, J. R. 2011. The chemical ecology of sponges on Caribbean reefs: natural products shape natural systems. Bioscience, 61: 888–898.

Pawlik, J. R., Loh, T-L., McMurray, S. E., and Finelli, C. M. 2013. Sponge communities on Caribbean coral reefs are structured by factors that are top-down, not bottom-up. PLoS One, 8: e62573.

Pörtner, H. 2008. Ecosystem effects of ocean acidification in times of ocean warming: a physiologist's view. Marine Ecology Progress Series, 373: 203–217.

Putnam, H. M. 2012. Resilience and acclimatization potential of reef corals under predicted climate change stressors. PhD thesis. University of Hawai'i Mānoa.

Reincke, T., and Barthel, D. 1997. Silica uptake kinetics of *Halichondria panicea* in Kiel Bight. Marine Biology, 129: 591–593.

Riahi, K., Rao, S., Krey, V., Cho, C., Chirkov, V., Fischer, G., Kindermann, G., *et al.* 2011. RCP 8.5—a scenario of comparatively high greenhouse gas emissions. Climatic Change, 109: 33–57.

Schröder, H-C., Perović-Ottstadt, S., Rothenberger, M., Wiens, M., Schwertner, H., Batel, R., Korzhev, M., *et al.* 2004. Silica transport in the demosponge *Suberites domuncula*: fluorescence emission analysis using the PDMPO probe and cloning of a potential transporter. Biochemistry Journal, 381: 665–673.

Silbiger, N., and Donahue, M. 2015. Secondary calcification and dissolution respond differently to future ocean conditions. Biogeosciences, 12: 567–578.

Silveira, C. B., SilvaLima, A. W., FranciniFilho, R. B., Marques, J. S., Almeida, M. G., Thompson, C. C., Rezende, C. E., *et al.* 2015. Microbial and sponge loops modify fish production in phase-shifting coral reefs. Environmental Microbiology, 17: 3832–3846.

Smith, A. M., Berman, J., Key, M. M., and Winter, D. J. 2013. Not all sponges will thrive in a high-CO_2 ocean: review of the mineralogy of calcifying sponges. Palaeogeography, Palaeoclimatology, Palaeoecology, 392: 463–472.

Stubler, A. D., Furman, B. T., and Peterson, B. J. 2014. Effects of pCO_2 on the interaction between an excavating sponge, *Cliona varians*, and a hermatypic coral, *Porites furcata*. Marine Biology, 161: 1851–1859.

Uppström, L. R. 1974. The boron/chlorinity ratio of deep-sea water from the Pacific Ocean. Deep Sea Research and Oceanographic Abstracts, 21: 161–162.

Uriz, M. J., Turon, X., and Becerro, M. A. 2003. Silica deposition in demosponges. *In* Silicon Biomineralization, pp. 163–193. Springer, Berlin Heidelberg.

Vicente, V. P. 1989. Regional commercial sponge extinctions in the West Indies: are recent climatic changes responsible? Marine Ecology, 10: 179–191.

Wang, X., Schröder, H. C., Wiens, M., Schloβmacher, U., and Müller, W. E. 2012. 5 Biosilica: molecular biology, biochemistry and function in Demosponges as well as its applied aspects for tissue engineering. Advances in Marine Biology, 62: 231.

Webster, N., Pantile, R., Botte, E., Abdo, D., Andreakis, N., and Whalan, S. 2013. A complex life cycle in a warming planet: gene expression in thermally stressed sponges. Molecular Ecology, 22: 1854–1868.

Webster, N. S., Cobb, R. E., and Negri, A. P. 2008. Temperature thresholds for bacterial symbiosis with a sponge. ISME Journal, 2: 830–842.

Weissenfels, N. 1981. Bau und Funktion des Süßwasserschwamms *Ephydatia fluviatilis* L.(Porifera). Zoomorphology, 98: 35–45.

Wisshak, M., Schönberg, C. H., Form, A., and Freiwald, A. 2012. Ocean acidification accelerates reef bioerosion. PLoS One, 7: e45124.

Wisshak, M., Schönberg, C. H. L., Form, A., and Freiwald, A. 2013. Effects of ocean acidification and global warming on reef bioerosion—lessons from a clionaid sponge. Aquatic Biology, 19: 111–127.

Zeebe, R. E., and Wolf-Gladrow, D. A. 2001. CO_2 in seawater: equilibrium, kinetics, isotopes. Vol. 65. Gulf Professional Publishing.

Handling editor: Howard Browman

ICES Journal of Marine Science

ICES Journal of Marine Science (2016), 73(3), 715–726. doi:10.1093/icesjms/fsv127

Contribution to Special Issue: 'Towards a Broader Perspective on Ocean Acidification Research'

Original Article

Ocean acidification affects productivity but not the severity of thermal bleaching in some tropical corals

Sam H. C. Noonan* and Katharina E. Fabricius

Australian Institute of Marine Science, PMB 3, Townsville MC, QLD 4810, Australia

**Corresponding author: tel: + 61 7 4753 4131; fax: + 61 7 4772 5852; e-mail: s.noonan@aims.gov.au*

Noonan, S. H. C., and Fabricius, K. E. Ocean acidification affects productivity but not the severity of thermal bleaching in some tropical corals. – ICES Journal of Marine Science, 73: 715–726.

Received 25 March 2015; revised 22 June 2015; accepted 26 June 2015; advance access publication 22 July 2015.

Increasing carbon dioxide (CO_2) emissions are raising sea surface temperature (SST) and causing ocean acidification (OA). While higher SST increases the frequency of mass coral bleaching events, it is unclear how OA will interact to affect this process. In this study, we combine *in situ* bleaching surveys around three tropical CO_2 seeps with a 2-month two-factor (CO_2 and temperature) tank experiment to investigate how OA and SST in combination will affect the bleaching susceptibility of tropical reef corals. Surveys at CO_2 seep and control sites during a minor regional bleaching event gave little indication that elevated pCO_2 influenced the bleaching susceptibility of the wider coral community, the four most common coral families (Acroporidae, Faviidae, Pocilloporidae, or Poritidae), or the thermally sensitive coral species *Seriatopora hystrix*. In the tank experiment, sublethal bleaching was observed at 31°C after 5 d in *S. hystrix* and 12 d in *Acropora millepora*, whereas controls (28°C) did not bleach. None of the measured proxies for coral bleaching was negatively affected by elevated pCO_2 at pH_T 7.79 (vs. 7.95 pH_T in controls), equivalent to ~780 µatm pCO_2 and an aragonite saturation state of 2.5. On the contrary, high pCO_2 benefitted some photophysiological measures (although temperature effects were much stronger than CO_2 effects): maximum photosystem II quantum yields and light-limited electron transport rates increased in both species at high pCO_2, whereas gross photosynthesis and pigment concentrations increased in *S. hystrix* at high pCO_2. The field and laboratory data in combination suggest that OA levels up to a pH_T of 7.8 will have little effect on the sensitivity of tropical corals to thermal bleaching. Indeed, some species appear to be able to utilize the more abundant dissolved inorganic carbon to increase productivity; however, these gains offset only a small proportion of the massive bleaching-related energy losses during thermal stress.

Keywords: carbon dioxide, carbon limitation, coral reef, global climate change, interactive effects, photophysiology.

Introduction

The continual anthropogenic pollution of Earth's atmosphere with carbon dioxide (CO_2) is causing planetary warming and ocean acidification (OA). These global changes are ongoing and projected to be exacerbated into the future as atmospheric CO_2 levels continue to rise (IPCC, 2013). In the marine environment, climate change is raising sea surface temperature (SST), while the oceanic uptake of CO_2 is causing a suite of chemical changes, increasing dissolved inorganic carbon (C_T), and reducing carbonate saturation states and pH (Langdon and Atkinson, 2005). The warming and OA stressors are occurring simultaneously and are considered among the greatest threats to marine biodiversity (Kleypas, 1999; Hoegh-Guldberg *et al.*, 2007). It is thus necessary to consider the effects of these global stressors in conjunction with each other as their effects may differ in combination and isolation (Harvey *et al.*, 2013).

Coral reefs are among the most vulnerable ecosystems to the changes associated with CO_2 emissions (Hoegh-Guldberg, 1999; Anthony *et al.*, 2011). The primary concern under increasing SST is the breakdown of the symbiosis between scleractinian corals and dinoflagellate algae of the genus *Symbiodinium* (zooxanthellae) in a process known as bleaching (e.g. Brown, 1997; Lesser, 2011). During thermal bleaching, damage to the photosynthetic machinery in *Symbiodinium*, including photosystem II (PSII), reduces their photosynthetic capacity and may eventually lead to their expulsion from the coral host (Lesser, 2011). Loss of autotrophy can starve the coral, and large-scale coral mortality has been observed when conditions that induce bleaching persist for some time (e.g. Brown, 1997; Berkelmans *et al.*, 2004). Periodic heat stress events, where temperatures exceed the long-term summer maximum for weeks at a time, are superimposed upon the gradual warming trend and

often prompt bleaching (Brown, 1997; Berkelmans *et al.*, 2004). The frequency of extreme weather conditions and subsequent heat stress events are projected to increase with rising atmospheric CO_2 (IPCC, 2013). However, it remains unclear how the thermal bleaching susceptibility of corals will be influenced by OA.

The issue of OA has received less attention than global warming; however, recent years have seen a surge in research effort. To date, coral reef research has primarily focused on the effects of OA on rates of calcification (e.g. Anthony *et al.*, 2008; Uthicke and Fabricius, 2012) and the metabolic demands that potentially increase to maintain high calcification rates (Cohen and Holcomb, 2009; Cyronak *et al.*, 2016). However, other effects of increasing pCO_2 remain less clear, especially on the corals' *Symbiodinium* partners, and many results are contradictory. Some authors report that pCO_2 increases can enhance primary production in *Symbiodinium* in a range of host taxa and suggest that carbon is the limiting substrate for photosynthesis (Crawley *et al.*, 2010; Brading *et al.*, 2011; Uthicke and Fabricius, 2012), while other studies have seen negligible (Wall *et al.*, 2013) and even negative effects of increased pCO_2 on photophysiology (Anthony *et al.*, 2008).

Studies examining the interactive effects of elevated SST and dissolved inorganic carbon on the bleaching susceptibility and photobiology of corals are few, and often have contradictory results. Some investigators have found increases in pigment content and the number of *Symbiodinium* per coral cell under elevated temperatures and CO_2 (Reynaud *et al.*, 2003), whereas others have found null (Schoepf *et al.*, 2013; Wall *et al.*, 2013) or opposite results. Anthony *et al.* (2008) observed declining pigmentation and oxygen production in two species of coral exposed to OA and temperature, suggesting that elevated CO_2 may increase thermal bleaching severity in corals. On the other hand, pCO_2 increases may boost primary production and could reduce the severity of thermally induced bleaching (Hoogenboom *et al.*, 2012).

An important factor determining responses to rising SST and OA is acclimatization through prolonged or repeated prior exposure to the stressor. While short-term experimental studies are certainly informative, in isolation they are unable to account for potential acclimatization. Longer term tank experiments provide more robust results as study organisms become acclimatized with the experimental environment (Krief *et al.*, 2010). Some evidence is emerging which suggests corals from reefs with a history of heat stress tend to bleach less severely during subsequent heat stress events (Berkelmans *et al.*, 2004; Maynard *et al.*, 2008). Tropical CO_2 seeps also allow studies to be conducted on organisms that have been acclimatized to higher levels of pCO_2 throughout their lifetime (Fabricius *et al.*, 2011). More longer term experiments and *in situ* studies around CO_2 seeps are needed to more confidently predict how chronic OA will interact with warming SST to shape coral reefs into the future.

This two-part study combines field observations and an experiment to investigate the effects of increased pCO_2 on coral thermal bleaching susceptibility. Part 1 reports on field data collected during a mild bleaching event in Milne Bay Province, Papua New Guinea in April 2011, including at coral reefs surrounding three CO_2 seeps. To determine if zooxanthellate corals are more or less susceptible to thermal bleaching if they had been exposed to elevated levels of pCO_2 since settlement, surveys were used to quantify coral pigmentation near and away from the seeps. This represents the first set of direct measurements of *in situ* coral thermal bleaching susceptibility in the face of OA [but see Manzello (2010)]. The field data were complemented by a 2-month crossed two-factor laboratory experiment to investigate the interactive effects of elevated pCO_2 and temperature on the bleaching susceptibility, photobiology, photosynthetic production, and *Symbiodinium* pigment dynamics in two common coral species, namely *Seriatopora hystrix and Acropora millepora*.

Material and methods

Bleaching surveys of reefs with elevated and ambient pCO_2

Bleaching surveys were conducted at three locations with volcanic CO_2 seeps and adjacent control sites (namely Upa Upasina, Esa'Ala, and Dobu, in Milne Bay Province, Papua New Guinea) over a 1-week period in April 2011. Seep and control sites are described in detail by Fabricius *et al.* (2011). The emerging gas is >98% CO_2, and the seep and control sites are very similar in their geomorphology, flow, light, wave exposure, and nutrients (Tables S1 and S2 of Fabricius *et al.*, 2011). Three years of continuous benthic temperature logging since April 2011 (Reef net, Census Ultra, Canada) has shown that temperatures are similar between seep and control sites (Supplementary Figure S2 and Table S1). Spatial maps of mean seawater carbonate chemistry (Fabricius *et al.*, 2011) were used to confine surveys to seep areas with mean seawater pH_T ~7.8 ± 0.2 to 7.9 ± 0.2 *SD*. We observed mild bleaching (i.e. a proportion of colonies were pale and a very small number was almost white) at all visited reefs (Supplementary Figure S1).

The first set of surveys was a series of 20 × 0.5 m belt transects at the six seep and control sites, at 3–4 m depth ($n = 4$ each at the seep and control sites of Upa Upasina and Dobu, and $n = 2$ per site at the smaller Esa'Ala reef). A single observer recorded the taxonomic identity (mainly genus but family for less common taxa) and pigmentation of any zooxanthellate hard coral and octocoral colonies within the belts ($n = 874$ colonies). Pigmentation was estimated on the upper surface of the colony to the nearest 0.25 colour chart units of the Coral Watch Coral Health Chart (http://www.coralwatch.org) on a scale of 1 (severely bleached) to 6 (dark pigmentation), which correlates well with symbiont density and chlorophyll *a* content (Siebeck *et al.*, 2006) (Supplementary Figure S1d). Of the 874 colonies surveyed, 780 came from the families Acroporidae, Faviidae, Pocilloporidae, or Poritidae.

During the surveys, the coral *S. hystrix* was noted to be particularly bleached. As the belt transects failed to capture enough of these colonies for statistical analyses, a second set of surveys was conducted at the Upa Upasina between 2 and 6 m depth, recording the depth and pigmentation on the upper surface of the first 14–15 colonies of *S. hystrix* encountered each at the control and seep site.

Laboratory experiment

A 2-month, two-factor aquarium experiment (two temperatures: 28 and 31°C, and two pH_T levels: 7.8 and 8.0, Table 1) was conducted at the Australian Institute of Marine Science in September to December 2011 to investigate coral bleaching susceptibility to pCO_2 and temperature exposures at levels projected to occur before the end of the century (atmospheric CO_2 ~750 ppm in the representative concentration pathway 8.5; Moss *et al.*, 2010; IPCC, 2013). The elevated temperature treatment of 31°C is considered the 10-d summer bleaching threshold for corals from the study area (long-term summer mean ~28°C; Berkelmans *et al.*, 2004). The two common and widely distributed coral species used, *S. hystrix* and *A. millepora*, are both highly susceptible to thermal bleaching.

Eighteen partial colonies of *S. hystrix* and *A. millepora* were collected from two reefs in the central Great Barrier Reef (Orpheus

Table 1. Treatment conditions in the 54-d flow-through experiment: pH_T and temperature (measured daily), and seawater carbonate parameters (measured weekly).

	Measured parameters				Calculated parameters		
Treatment	**pH_T**	**Temperature (°C)**	**A_T (μmol kg^{-1} SW)**	**C_T (μmol kg^{-1} SW)**	**pCO_2 (μatm)**	**HCO_3^- (μmol kg^{-1} SW)**	**Ω_{ar}**
TL.CL	7.97 (0.05)	28.07 (0.17)	2318 (22)	2026 (13)	479 (38)	1819 (45)	3.27 (0.31)
TL.CH	7.79 (0.05)	27.85 (0.25)	2325 (24)	2116 (35)	738 (65)	1950 (47)	2.44 (0.21)
TH.CL	7.99 (0.05)	30.81 (0.33)	2328 (23)	2019 (9)	500 (32)	1789 (15)	3.57 (0.30)
TH.CH	7.79 (0.03)	30.83 (0.36)	2326 (23)	2119 (35)	835 (85)	1940 (41)	2.56 (0.26)

The four experimental treatments are a combination of low and high temperature (TL and TH) and low and high pCO_2 (CL and CH). Measured values of temperature, salinity (35 ppt), total alkalinity (A_T) and dissolved inorganic carbon (C_T) were used to calculate the seawater carbonate parameters ($n = 9$ per treatment) including the saturation state of aragonite (Ω_{ar}). Standard deviations are shown in brackets.

Island and Davies Reef), Australia, between 3 and 5 m of depth. Each colony was divided into four ~5 cm nubbins ($n = 72$ nubbins per species) and one nubbin per colony was assigned to one of the four experimental treatments to remove any effects of parental colony identity. Initial measurements of net oxygen production and PAM fluorometer parameters, taken after the acclimation period (outlined below), did not differ between corals collected from the two sites (ANOVA, all $p > 0.05$).

Nubbins were allowed 7 d of acclimation in partially shaded (maximum irradiance ~500 μmol photons m^{-2} s^{-1}), outdoor holding tanks with flow through seawater (~28°C) before being distributed across 12 glass aquaria (17 l volume) in a temperature-controlled room (25 ± 1°C), supplied (400 ml min^{-1}) with filtered (5 μm) seawater at 28°C and ambient atmospheric pCO_2 for a further 17-d acclimation. There were three aquaria per treatment, each containing six nubbins per species. Illumination was delivered in 12 h cycles by white fluorescent light (10 000 K), and was consistent between aquaria (180 μmol photons m^{-2} s^{-1}, 15.6 mol photons d^{-1}, meter LI205A, sensor LI201SA, LICOR, USA). Each aquarium had an individual power head for circulation.

After acclimation, the elevated pCO_2 treatment was applied directly for 21 d before the onset of heat stress by controlling pH in header tanks through a diffused feedback control CO_2 gas injection system (Aquamedic, Germany). Daily pH_{NBS} measurements were conducted in each experimental aquarium (meter: Oakton pH 1100, USA; electrode: Eutech, USA), with measurements being compared with the Dickson seawater TRIS pH standard (Table 1) and converted to pH_T (Dickson, 2007).

A heat stress event was then simulated by ramping the temperature in heated treatments at 0.5°C per 12 h with a separate feedback control system (Neptune Apex aqua controller, USA), then maintained in the header tanks with a computer-controlled data logger (CR 1000, Campbell Scientific, Australia). Treatments were alternated to eliminate any potential environmental effects within the room. Aquarium water temperatures were monitored daily and remained constant (Table 1). Water samples were taken weekly throughout the experiment for C_T and A_T analyses (Marianda VINDTA 3C, Germany), which were used to calculate carbonate system parameters with the program CO2SYS (Lewis and Wallace, 1998; Table 1).

Coral nubbins were inspected for survivorship and visual signs of bleaching nearly daily. To ensure there would be living samples for final analyses, the experiment was terminated once ~60% of nubbins per species within the heated treatments showed visual signs of bleaching. Nubbins were immediately snap-frozen in liquid nitrogen and stored at −80°C for later analyses. We used photosynthetically active radiance (PAR) absorptivity and F_v/F_m measurements (outlined below) as bleaching indices throughout the experiment and further examined the content of different pigments at the experiment's end.

Pulse amplitude-modulated fluorometry

Pulse amplitude-modulated (PAM) fluorometry measurements of dark adapted (>30 min) maximum quantum yields (F_v/F_m) and PAR absorptivity were taken with an Imaging PAM fluorometer (IPAM, Walz, Germany; Unit IMAG-CM fitted with a Maxi head). Measurements of all 144 nubbins were recorded weekly from the start of the acclimation period, then every 4 d once the heat treatment began. F_v/F_m provides a measure of the maximum proportion of available light that can be photochemically quenched through PSII. PAR absorptivity is the fraction of incident red light that is absorbed by photosynthetically active pigments (Ralph *et al.*, 2005).

Rapid light curve (RLC) measurements were taken with the IPAM (Ralph *et al.*, 2005) on the day before each species was removed from the aquaria ($n \geq 15$ per species per treatment), applying 10 s exposures to increasing irradiances (38, 88, 160, 264, 309, 369, 504, 658, 861 and 995 μmol photons m^{-2} s^{-1}). Measured RLCs were fitted with an exponential function to derive light-limited electron transport rate (α) and the maximum electron transport rate (ETR_{max}) following standard procedures (Ralph and Gademann, 2005).

Oxygen flux

Gross photosynthesis and respiration were measured after the acclimation period, after 21 d of CO_2 treatment, and in the closing days of the experiment ($n > 6$ per species per treatment per time point). Real time changes in oxygen concentration were measured in stirred and temperature-controlled 210 ml clear Perspex incubation chambers fitted with oxygen sensor spots ("optodes", Ø 0.5 cm, Presens, Germany), and an Oxy-4 fibre-optic oxygen meter [Presens; for details see Uthicke *et al.* (2012)]. The same lights and intensities used in the aquaria were used in the gross photosynthesis runs. Treatment water was obtained from the header tanks of the experiment and further filtered to 0.5 μm. Measurements lasted ~30 min and each run included a blank chamber. Respiration and gross photosynthesis rates were normalized to nubbin surface area. Net production was calculated by subtracting hourly respiration from hourly gross photosynthesis.

Protein and pigment content

Three nubbins per species per tank were water-picked to remove coral tissue in 10 ml of ultra-filtered seawater (0.05 μm). This slurry was homogenized and a supernatant of coral tissue was prepared for spectrophotometric protein quantification following Dove *et al.* (2006) using the DC protein assay kit (Bio-Rad Laboratories, Australia). Protein content was standardized to

nubbin surface area, determined using the single wax dipping technique (Veal *et al.*, 2010).

Pigments from the *Symbiodinium* pellet obtained after centrifuging the water-picked coral nubbins were sonicated and extracted on ice in the dark in two 1-h extractions in 1 ml of chilled (4°C) buffered methanol (98% MeOH/2% 0.5 M tetrabutylammonium acetate [TBAA] pH 6.5). Extracts were prepared for analysis with an ultra-performance liquid chromatography (UPLC) system (Waters Acquity UPLC) following Uthicke *et al.* (2012) and were standardized to nubbin surface area for analysis.

Statistical analyses

In the wider bleaching surveys, two-factor analysis of variance (ANOVA) was used to compare mean pigmentation between locations and CO_2 exposures for all taxa combined, and separately for the four common families. Tukey's HSD was used for *post hoc* examinations. ANOVA was used in the *S. hystrix* bleaching surveys to compare the mean pigmentation of colonies between the seep and control site, with colony depth as a covariate.

In the experiment, data were averaged across nubbins for each species within aquaria. Unless otherwise stated, all reported statistics satisfied the assumptions of homoscedasticity, Gaussian distributions, and independence. Generalized additive mixed models (GAMMs) were fitted to assess trends in PAR absorptivity and quantum yields across treatments over time. One-way and two-factor ANOVA were used to compare quantum yields and PAR absorptivity between the treatments at specific dates, as well as RLC parameters, protein and pigment contents, pigment ratios, and oxygen flux at three time points (after the acclimation period, after 21 d CO_2 treatment, and in the last days of the experiment). The statistical program R (version 3.0.2) was used including the packages mgcv and nlme (R Development Core Team, 2014).

Results

Bleaching surveys

Mild bleaching was observed at all six sites. Coral pigmentation data from all 874 colonies combined displayed a significant interaction between location and CO_2 exposure (two-factor ANOVA, Location × CO_2: $F_{(2,868)} = 5.616$, $p = 0.004$), as the mean pigmentation at the Dobu control site was ~0.2 colour chart units darker than that of the Upa-Upasina control and Esa'Ala and Dobu seep sites (Figure 1, Tukey's HSD: $p < 0.05$, Supplementary Table S2). No differences were detected between any of the other CO_2 and site combinations for mean pigmentation across all coral taxa (Figure 1).

The pigmentation values for the Acroporidae and Faviidae differed between some specific sites (Location × CO_2 interaction), but no differences were attributable to CO_2 exposure as a main effect (Figure 1 and Supplementary Table S2). Pigmentation values in the Poritidae ($n = 466$ colonies) displayed a significant main effect of CO_2 exposure, with colonies at the seep sites being ~4% paler (3.59 ± 0.55 *SD* colour chart units) than the control sites (3.76 ± 0.74). No differences in pigmentation were detected in the Pocilloporidae.

In *S. hystrix*, most colonies were obviously pale (mean 1.81 ± 0.47), indicating moderate bleaching in this species, and 57 and 33% of colonies had a pigmentation value of ≤1.5 at the high CO_2 and control site, respectively (i.e. were almost completely

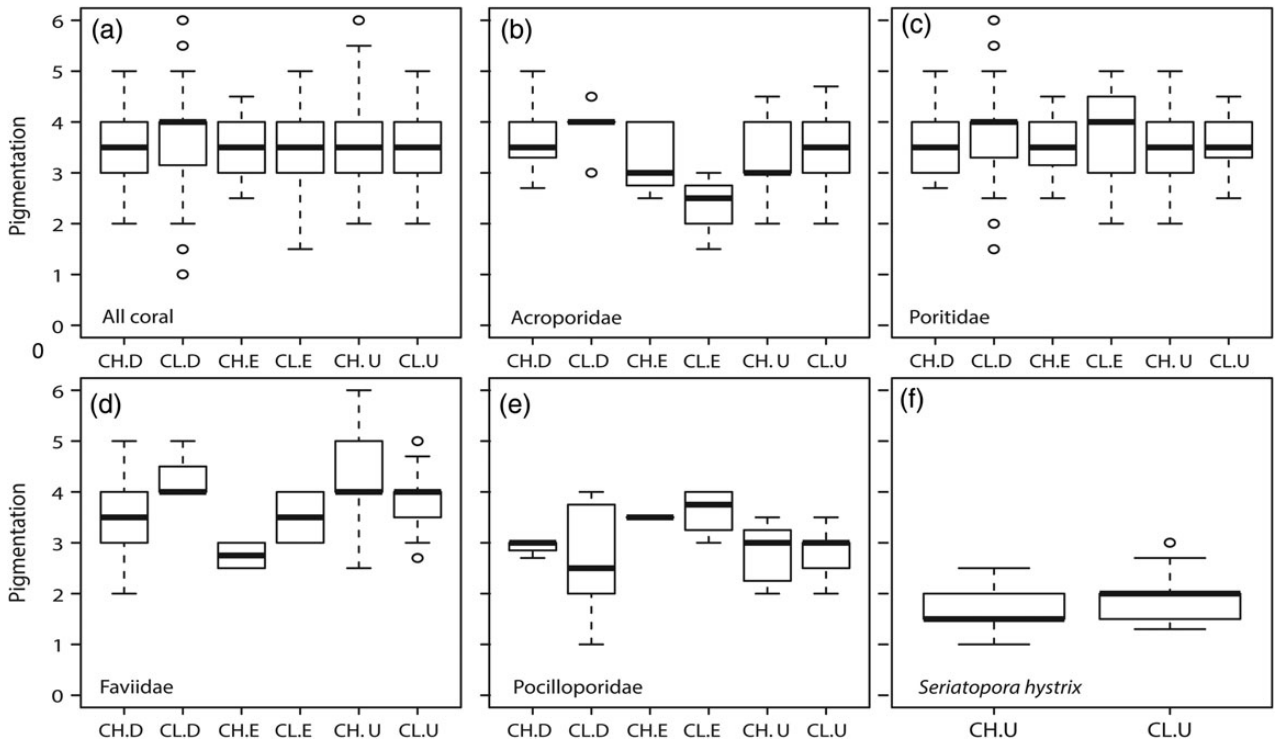

Figure 1. Field surveys of coral pigmentation during a mild bleaching event. Coral colour chart scores (6 = darkest and 1 = lightest) for all coral taxa combined (a: $n = 874$), the Acroporidae (b: $n = 128$), Poritidae (c: $n = 466$), Faviidae (d: $n = 145$), Pocilloporidae (e: $n = 41$), and *S. hystrix* (f: $n = 29$) at seep and control sites (pCO_2 high and low: CH and CL) at the three reefs Dobu (D), Esa'Ala (E), and Upa Upasina (U). Plots are standard boxplots, with the top and bottom of the box enclosing the first to third quartiles (horizontal bar: median; the whiskers: 1.5 interquartile ranges; and the circles: outliers).

white, Figure 1f). There was no difference in the mean pigmentation of the upper surfaces of *S. hystrix* between the seep and control site ($F_{(1,26)} = 2.073$, $p = 0.16$), nor was depth a significant covariate ($F_{(1,26)} = 0.753$, $p = 0.39$).

Laboratory experiment

Mortality and visual signs of bleaching

In the laboratory experiment, none of the nubbins displayed visual loss in pigmentation at control temperatures (28°C). In *S. hystrix*, the first visual signs of bleaching were recorded at 31°C five days after the temperature ramp finished, 60% of *S. hystrix* appeared visually bleached 4 d later, and the final measurements were taken before removing the surviving nubbins from the experiment. All bleached and dead nubbins ($n = 3$ total) were confined to, and evenly distributed across, the two heated treatments. In *A. millepora*, visual signs of bleaching were first observed 12 d after the temperature ramp finished, and ~60% of nubbins in the heated treatments appeared visually bleached and the experiment ended on the 16th d after the temperature ramp. No mortality was recorded in *A. millepora*.

The PAR absorptivity initially increased in both species during the acclimation period, and all but plateaued by the time the pCO_2 treatments began and remained relatively constant throughout the pCO_2 exposure period (Supplementary Figures S3 and S4). Absorptivity values did not differ in either species at the end of the acclimation period between tanks that would later become treatments, or after 3 weeks of CO_2 treatment (ANOVA: all $p > 0.05$). However, absorptivity values declined once temperatures were ramped (Supplementary Figures S3 and S4), and final values were significantly lower in the heated treatments compared with the control temperature (Table 2). Absorptivity values from both species changed significantly over the course of the experiment (GAMM smooth term: *S. hystrix*: $F_{(5.984)} = 14.05$, $p < 0.001$; *A. millepora*: $F_{(5,27)} = 8.75$, $p < 0.001$); however, pCO_2 did not affect absorptivity ($p > 0.1$), while the heated treatments had significant reductions in both species (GAMM: *S. hystrix*: $T = 14.05$, $p < 0.05$; *A. millepora*: $T = 2.97$, $p < 0.01$). The models explained 42 and 35% of the variation in PAR absorptivity for *S. hystrix* and *A. millepora*, respectively (Supplementary Figures S3 and S4).

Quantum yields and rapid light curves

After acclimation, the F_v/F_m for both species did not differ between tanks that would later become treatments (two-factor ANOVA, all $p > 0.05$). F_v/F_m was 0.65 ± 0.03 (*SD*) and 0.67 ± 0.03 for *S. hystrix* and *A. millepora*, respectively. After 3 weeks of pCO_2 exposure, F_v/F_m in *S. hystrix* was significantly higher at elevated compared with ambient pCO_2 (0.53 ± 0.03 vs. 0.63 ± 0.04, one-way ANOVA: $F_{(1,10)} = 22.43$, $p < 0.001$). In contrast, F_v/F_m in *A. millepora* remained similar between pCO_2 treatments (0.61 ± 0.05 vs. 0.64 ± 0.04, one-way ANOVA, $p > 0.05$). While declines in F_v/F_m were observed in all treatments, values in the final days after heat stress, for both species, were influenced significantly by both pCO_2 and temperature in an additive fashion (Figure 2c and d, and Table 2). In both species, the highest mean F_v/F_m values were recorded in the high pCO_2 + low temperature treatment, whereas the lowest values were observed in the low pCO_2 + high temperature treatment. This decline was ~20% in both species (*S. hystrix*: 0.64 ± 0.03 vs. 0.50 ± 0.03; *A. millepora* 0.62 ± 0.02 vs. 0.53 ± 0.09). The changes over time in F_v/F_m were significant in both species (GAMM smooth term: *S. hystrix*: $F_{(6.18)} = 14.43$, $p < 0.001$; *A. millepora*: $F_{(4.58)} = 16.94$, $p < 0.001$), with CO_2 addition significantly increasing F_v/F_m in *S. hystrix* (GAMM: $T = 2.66$, $p < 0.01$) and elevated temperature significantly reducing it in *A. millepora* (GAMM: $T = 2.67$, $p < 0.01$). The models explained 62 and 52% of the variation in F_v/F_m for *S. hystrix* and *A. millepora*, respectively (Supplementary Figures S5 and S6).

At the end of the experiment, RLCs in *S. hystrix* indicated that light-limited electron transport rates (α) were influenced by both pCO_2 and temperature, and that their effects were additive (Figure 2e and f, and Table 2). Elevated pCO_2 increased α, while increasing temperature lowered them. Mean values of α were lowest in the low pCO_2 + high temperature treatment (0.07 ± 0.01), being 43% of those observed in the high pCO_2 + low temperature treatment (0.16 ± 0.01, Table 2). Maximum electron transport rate (ETR_{max}) in *S. hystrix* was influenced by temperature alone

Table 2. ANOVA results comparing photophysiological parameters for *S. hystrix* and *A. millepora* between the experimental treatments of CO_2 (C), temperature (T), and their interaction (C : T): mean absorptivity and maximum quantum yield (F_v/F_m, both averaged over the final two measurements); alpha and ETR_{max} values derived from rapid light curves, and final net oxygen flux and chlorophyll *a* concentration at the end of the 54-d experiment.

	S. hystrix			***A. millepora***	
	d.f.	***F***	***p***	***F***	***p***
Absorptivity					
C	1	0.34	0.54	0.93	0.35
T	1	15.17	<0.01	11.18	<0.01
C : T	1	0.50	0.49	0.92	0.35
Res	20				
F_v/F_m					
C	1	64.14	<0.01	5.78	0.03
T	1	11.68	<0.01	11.27	<0.01
C : T	1	0.72	0.41	1.19	0.29
Res	20				
Alpha (α)					
C	1	17.28	<0.01	17.44	<0.01
T	1	32.98	<0.01	11.72	<0.01
C : T	1	0.13	0.73	0.10	0.76
Res	8				
ETR_{max}					
C	1	2.92	0.13	2.31	0.17
T	1	24.72	<0.01	0.81	0.39
C : T	1	0.36	0.57	0.80	0.40
Res	8				
Respiration					
C	1	1.00	0.33	0.60	0.45
T	1	1.55	0.23	0.22	0.64
C : T	1	0.56	0.46	0.97	0.34
Res	20				
Production					
C	1	4.99	0.04	0.01	0.93
T	1	31.36	<0.01	38.40	<0.01
C : T	1	0.7	0.41	0.81	0.38
Res	20				
Net O_2 production					
C	1	6.52	0.02	0.01	0.93
T	1	28.51	<0.01	38.40	<0.01
C : T	1	1.13	0.30	0.81	0.38
Res	20				
Chlorophyll *a*					
C	1	12.62	<0.01	0.34	0.58
T	1	51.80	<0.01	67.28	<0.01
C : T	1	1.72	0.23	1.57	0.24
Res	8				

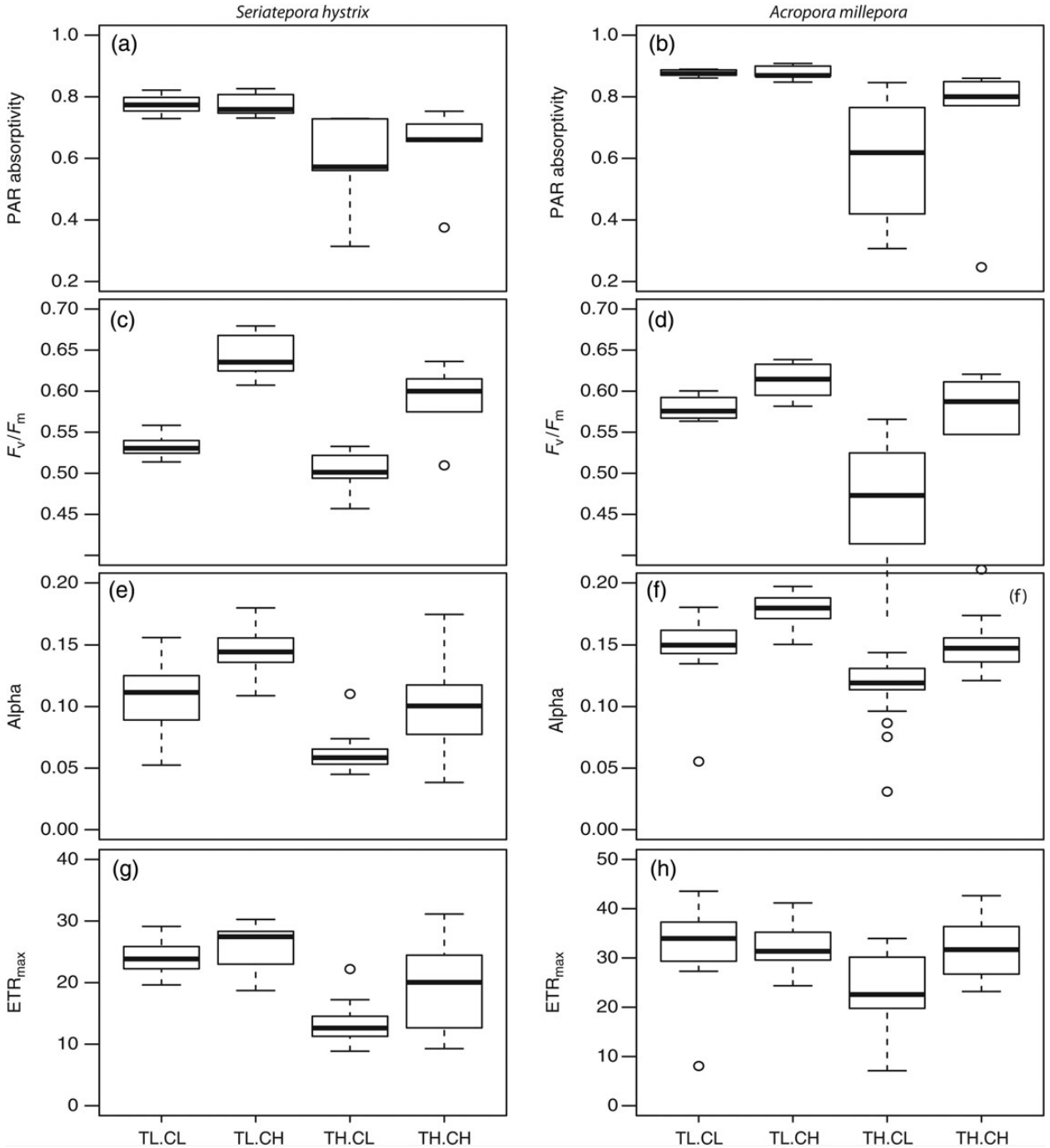

Figure 2. Photophysiological responses in corals in the laboratory to the treatments of low and high temperature (TL and TH) and low and high pCO_2 (CL and CH). Shown are PAR absorptivity (a and b) and maximum PSII quantum yield (F_v/F_m, c and d) in the last 5 d of heat stress, and light-limited electron transport rate (photosynthetic efficiency, α; e and f), and the maximum electron transport rate (ETR_{max}; g and h) at the end of the experiment. $n = 3$ tanks per treatment (averaging 6 colonies per species) for F_v/F_m and absorptivity; $n \geq 15$ per treatment for α and ETR_{max}. See Figure 1 legend for boxplot description.

(Figure 2f and h, and Table 2). ETR_{max} values in the higher temperature treatment (0.09 ± 0.02) were 63% of those observed in the lower temperature treatment (0.14 ± 0.02, Figure 3). The α values in *A. millepora* were also significantly affected by both CO_2 and temperature in an additive fashion (Table 2). As per *S. hystrix*, they were lowest in the low CO_2 + high temperature treatment (0.11 ± 0.03), being 64% of the values observed in the high CO_2 + low temperature treatment (0.18 ± 0.01). No significant differences in ETR_{max} values were detected between the experimental treatments in *A. millepora* (Table 2).

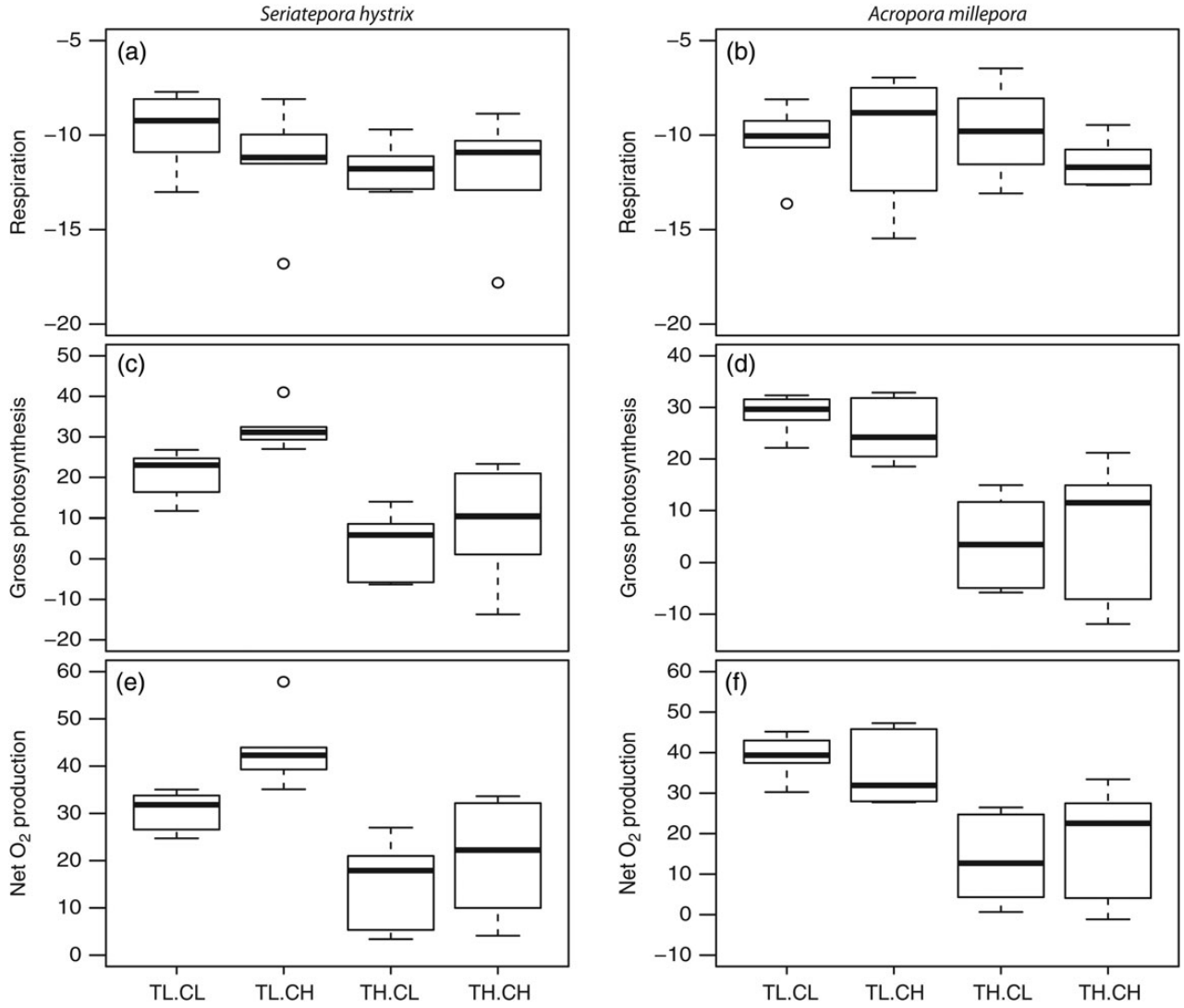

Figure 3. Respiration (a and b), gross photosynthesis (c and d), and average hourly net production (e and f) (all in μg O_2 cm^{-2} h^{-1}) in *S. hystrix* and *A. millepora* at the end of the experiment. Values are standardized per unit surface area of the coral nubbins ($n = 6$ per treatment). Legends as in Figure 2.

Oxygen flux

Rates of respiration and photosynthesis did not differ after 3 weeks of differential pCO_2 exposure (before heat treatment) in either species (one-way ANOVA: $p > 0.05$), and final rates in the control treatments closely matched initial rates. Respiration rates after 3 weeks of pCO_2 treatment were -9.65 ± 0.90 and -9.90 ± 2.61 μg O_2 cm^{-2} h^{-1} for *S. hystrix* and *A. millepora*, respectively, whereas gross photosynthesis rates were 29.64 ± 5.35 and 36.80 ± 10.79 μg O_2 cm^{-2} h^{-1}. In *S. hystrix*, the final net oxygen production rates were influenced by both pCO_2 and temperature in an additive fashion (Table 2), with CO_2 addition increasing and increased temperature reducing net production (Figure 3e). This was driven by changes in gross photosynthesis, as respiration remained unchanged between treatments (Figure 3a and c). Net production was highest in the high pCO_2+ low temperature treatment (43.47 ± 7.75 μg O_2 cm^{-2} h^{-1}) and lowest in the low pCO_2 + high temperature treatment (15.42 ± 9.29), i.e. a 2.5-fold difference (Figure 3e). In *A. millepora*, net O_2 production measurements at the end of the experiment were influenced by temperature alone (Table 2). Corals in the two heated treatments produced ~2.5 times less O_2 than in low temperature treatments (15.88 ± 12.10 vs. 37.30 ± 7.19 μg O_2 cm^{-2} h^{-1}; Figure 3f). This difference was driven by changes in gross photosynthesis, as respiration rates remained unaffected (Table 2). Analyses of O_2 flux and pigment contents (see below), standardized by units of protein, gave no further insights compared with the values standardized by surface area.

Coral protein content

Protein content per unit surface area at the end of the experiment showed no difference between treatments in either species (two-factor ANOVA: all $p > 0.1$). *Seriatopora hystrix* nubbins had 3.43 ± 0.65 mg cm^{-2} protein (mean of all treatments), whereas in *A. millepora* this value was 5.10 ± 0.92 mg cm^{-2} and was significantly higher than in *S. hystrix* (one-way ANOVA: $F_{(1,22)} = 26.36$, $p < 0.001$).

Symbiodinium *pigment content*

At the end of the experiment, many of the *Symbiodinium* pigment concentrations in *S. hystrix* were influenced by both pCO_2 exposure and temperature, without major interactions between these treatments (Supplementary Table S3). Temperature and pCO_2 changes had an additive effect on concentrations of chlorophyll *a* and *c*2 and peridinin, which increased with elevated pCO_2 and declined at high temperature (Figure 4a–d and f). Pigment concentrations in the high pCO_2 + low temperature treatment were ~5-fold higher than at low pCO_2 + high temperature. β-Carotene and the combination of diadinoxanthin (Ddx) and dinoxanthin (Dnx) were significantly reduced at high temperatures (Supplementary Table S3). Conversely, the concentration of diatoxanthin (Dtx), the relative proportion of Dtx to the total xanthophyll pool, and

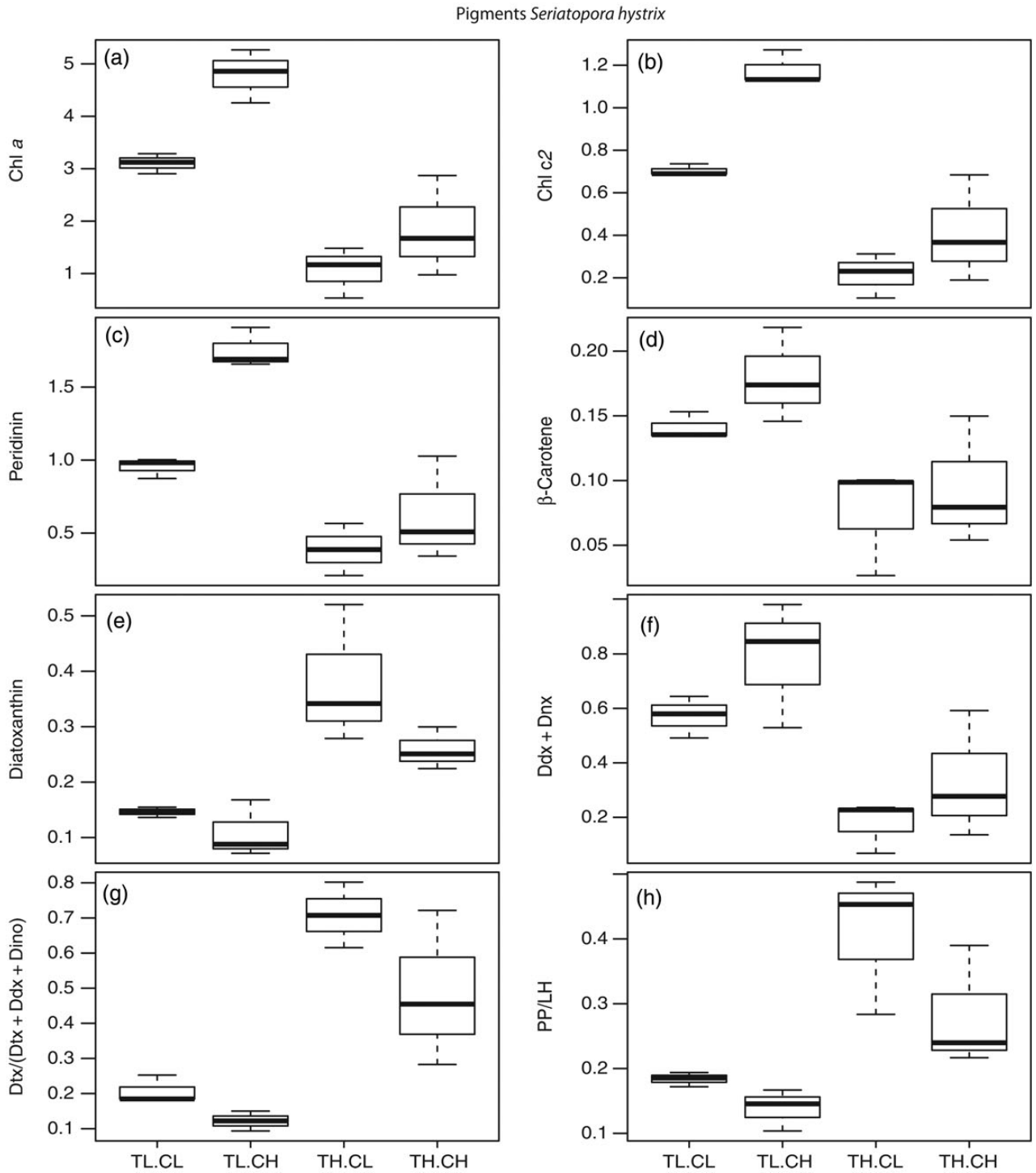

Figure 4. Molar concentrations of pigments (nmol cm^{-2} coral surface area) and pigment ratios from the *Symbiodinium* of *S. hystrix* at the end of the experiment ($n = 9$ per treatment). Legend as in Figure 2.

the ratio of photoprotective (PP: Ddx, Dnx, Dtx, and β-carotene) to light harvesting (LH: chlorophyll *a*, chlorophyll *c*2, and peridinin) pigments showed the opposite patterns, increasing with temperature and declining with elevated pCO_2.

In *A. millepora*, the *Symbiodinium* pigment concentrations and ratios were influenced by temperature only (Figure 5 and Supplementary Table S3). Concentrations of chlorophyll *a* and *c*2, peridinin, β-carotene, and the combination of Ddx and Dnx all declined in the heated treatments (Figure 5a–d and f), whereas Dtx, the relative proportion of Dtx to the total xanthophyll pool, and the ratio of PP to LH pigments increased (Figure 5e, g, and h). Chlorophyll *a* and *c*2, peridinin, and β-carotene showed a fivefold reduction in heated compared with control temperatures, whereas Ddx + Dnx was reduced approximately threefold. Concentrations

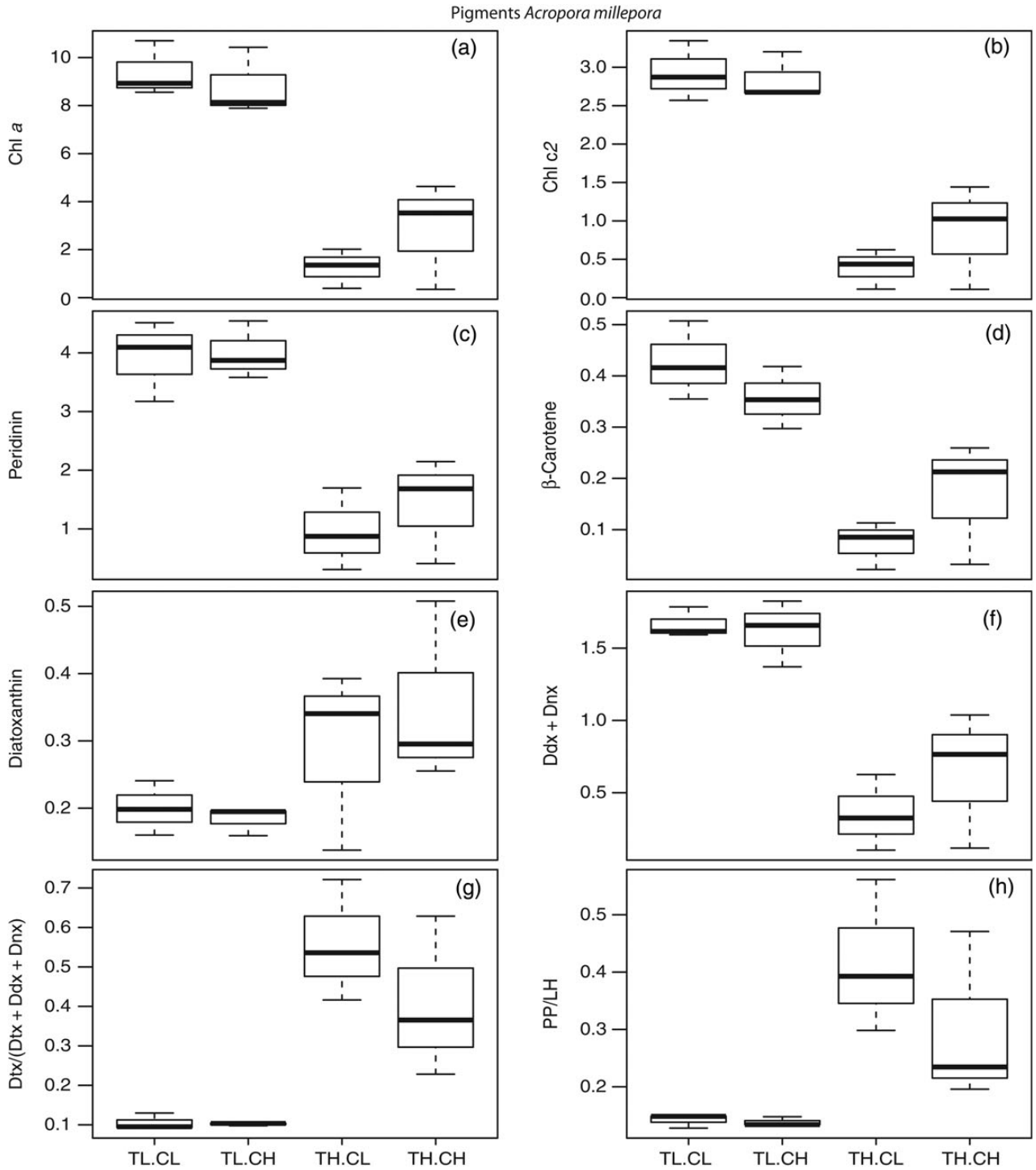

Figure 5. Molar concentrations of pigments (nmol cm^{-2} coral surface area) and pigment ratios from the *Symbiodinium* of *A. millepora* at the end of the experiment ($n = 9$ per treatment). Legend as in Figure 2.

of Dtx were approximately twice as high in the heated compared with the control treatments, while xanthophyll cycling and PP : LH increased five- to sixfold (Figure 5).

Discussion

Despite rapidly progressing global climate change and OA, which is irreversible on a time-scale of thousands of years, science is still largely uncertain about the interactive effects of these changes on marine organisms. The present study investigated whether the thermal bleaching tolerance of tropical reef corals would be influenced by elevated pCO_2 at levels predicted for later this century under OA. Contrary to some earlier observations and predictions (e.g. Anthony *et al.*, 2008), our field and experimental data showed minimal negative effects of CO_2 exposure on the bleaching susceptibility of symbiotic corals. Furthermore, we found that pCO_2 increases can provide some benefits to the symbionts' photosystem, enhancing maximum PSII quantum yields and light-limited electron transport rates in both species, and additionally promoting photosynthetic productivity and pigment concentrations in *S. hystrix*. This study shows that although OA may provide an avenue to improve photosynthetic carbon gains for some corals, even during heat stress, the detrimental effects of warming temperatures remained disproportionately stronger, and did not fully offset bleaching-related losses in productivity.

The bleaching surveys at the three CO_2 seep and control sites represent the first *in situ* data that specifically investigate coral thermal bleaching susceptibility under elevated pCO_2. They gave little indication that the thermal bleaching susceptibility of the major components of the coral community was influenced by elevated pCO_2. Slight CO_2 effects were detected in the Poritidae at all sites, and in the Faviidae at Dobu; however, differences were very minor (~4% change in pigmentation in the Poritidae). Pervious work in the same study area also detected reduced colour chart scores in massive *Porites* at the seep compared with the control sites during winter when bleaching was not observed (Fabricius *et al.*, 2011). We therefore conclude that the observed minor reductions in *Porites* pigmentation at the seeps cannot be unequivocally attributed to a significant increase in bleaching sensitivity.

Thermal bleaching in corals can be co-determined by natural dynamics in food supply, water flow, and light regimes (Fabricius, 2006; Anthony *et al.*, 2009; Hoogenboom *et al.*, 2012), the combined effects of which cannot be effectively replicated in the laboratory. Furthermore, experiments are relatively short term by nature and hence unable to fully account for potential acclimatization. Seep sites are not perfect representations of future reefs, as temperatures remain at ambient levels and CO_2 regimes are more temporarily variable. However, organism acclimatization and ecological interactions between taxa can be examined. The use of seep sites as natural laboratories, in conjunction with controlled experiments, provide the best available information to predict how OA will impact marine ecosystems.

In the laboratory experiment, heat stress induced a bleaching response in both coral species. *Seriatopora hystrix* was more sensitive to thermal stress than *A. millepora*, but heat stress was not exacerbated by increased CO_2 in either species as shown in the field. While CO_2 addition reduced the severity of temperature effects on some photophysiological parameters, thermal bleaching (as quantified by commonly used photophysiological measures) was still observed in both coral species in both pCO_2 treatments, and the temperature effects were much stronger than the pCO_2 effects. It remains to be seen whether this finding will hold for other species and other experimental conditions. For example, corals in the present study were relative sensitive species, were not fed, and were kept under moderate light levels, and previous studies have shown that all these factors co-determine thermal tolerance (Marshall and Baird, 2000; Anthony *et al.*, 2009; Hoogenboom *et al.*, 2012). The fact that our field study resulted in similar findings for both highly sensitive and more thermally tolerant taxa (e.g. *S. hystrix* vs. *Faviidae*), under natural levels of light, flow, and food supply, confirms that the findings from the laboratory study are likely to apply to other species and other study conditions.

The extent of coral thermal bleaching is influenced by factors within the host coral and their *Symbiodinium*. While different *Symbiodinium* types have been shown to vary in their temperature tolerance (Berkelmans and van Oppen, 2006), previous work at the same CO_2 seep locations did not detect any difference in *Symbiodinium* types due to CO_2 exposure in six common corals (Noonan *et al.*, 2013). In our laboratory experiment, the parental corals were divided evenly across all experimental treatments to prevent differences in genotypes or symbiont identity from confounding our results.

The results of previous works that have examined the effects of elevated pCO_2 or the interactive effect of elevated pCO_2 and increased temperature on coral bleaching and photobiology have been highly inconsistent. Anlauf *et al.* (2011) showed that *Porites panamensis* bleached at increased temperature under ambient pH, but not under reduced pH (the number of *Symbiodinium* per coral polyp remained unaffected). Schoepf *et al.* (2013) documented a range of responses to OA and increased temperature across four species of corals, with no clear pattern emerging. Reynaud *et al.* (2003) showed an increase in chlorophyll *a* and the number of *Symbiodinium* per coral cell in *Stylophora pistillata* with increased temperature and CO_2, respectively, whereas Anthony *et al.* (2008) found pigmentation (measured by luminance) decreased in two species of coral under similar treatments. Moreover, Wall *et al.* (2013) concluded that changes in CO_2 had no influence on the bleaching susceptibility of *Seriatopora caliendrum*. Anthony *et al.* (2008) attributed the differences between their results and that of Reynaud *et al.* (2003) to the higher light levels used in their study; however, the null effects observed by Wall *et al.* (2013) were in corals exposed to saturating light levels. The use of different species, methodologies, and metrics of bleaching may be contributing to the disparities seen between works to date.

The present study confirmed that increases in pCO_2 can stimulate photosynthesis in corals, suggesting that carbon supply may limit their photosynthesis. A greater proportion of quanta were funnelled through PSII for use in photosynthesis under higher pCO_2, and light-limited electron transport rate and maximum quantum yields in both *S. hystrix* and *A. millepora* increased. In *S. hystrix*, this further manifested in greater oxygen production. Carbon limitation has been reported in *Symbiodinium* in many taxa including corals and in culture (Brading *et al.*, 2011; Uthicke and Fabricius, 2012), with photosynthesis being stimulated by the addition of CO_2 (Crawley *et al.*, 2010) or bicarbonate (Herfort *et al.*, 2008). These results are not universal however, with some authors reporting either null or negative effects of elevated pCO_2 on photosynthesis (Langdon and Atkinson, 2005; Anthony *et al.*, 2008; Edmunds, 2012; Wall *et al.*, 2013). Carbon may only become limiting in high light, as well as in relatively nutrient-rich waters (Chauvin *et al.*, 2011) such as those of the inshore GBR lagoon used in the present experiment and that conducted by Crawley *et al.* (2010). In contrast, experiments conducted using relatively

oligotrophic waters (Langdon and Atkinson, 2005; Anthony *et al.*, 2008; Edmunds, 2012) may experience limitation in other substrates required for photosynthesis before carbon supply becomes limiting. Moreover, other carbonate system changes associated with OA, such as pH declines, may contribute to increased productivity and warrant further investigation.

In the present study, the effects of increased pCO_2 were more evident in *S. hystrix* than in *A. millepora*. In *S. hystrix*, pigment dynamics, including the xanthophyll cycle which non-photochemically quenches excess light energy, net photosynthetic oxygen production, maximum PSII quantum yields, and ETRs, were all up-regulated at high pCO_2 and reduced with temperature stress. In contrast, pigments and net photosynthetic oxygen production responded only to temperature stress in *A. millepora*. Such species-specific responses may help explain the disparities seen between different experimental works conducted to date and may be due to differences in the efficiency of their carbon concentrating mechanism (Comeau *et al.*, 2012). Furthermore, many of the negative effects of elevated pCO_2 on coral photophysiology and photosynthetic production documented in previous studies have occurred in treatments where CO_2 values were experimentally increased to very high levels (Krief *et al.*, 2010). For example, Anthony *et al.* (2008) found that net productivity in *Acropora intermedia* and *Porites lobata* did not change with moderately increased pCO_2 (similar to those in the present study); however, productivity dramatically declined once pCO_2 was further increased. Similarly, Crawley *et al.* (2010) documented a 38% increase in photosynthetic capacity in *Acropora formosa* under conservative but not under high emission scenarios. Such non-linear (Gil, 2013; Schoepf *et al.*, 2013), species-specific (Marshall and Baird, 2000; Schoepf *et al.*, 2013) responses to environmental pressures are not uncommon. It may be that groups of closely related species have separate non-linear responses to CO_2 where minor increases have negligible effects or are beneficial for net photosynthesis, while additional increases in CO_2 may result in negative effects.

Maintaining rates of calcification in corals potentially becomes increasingly energy demanding with increasing seawater pCO_2 (Cohen and Holcomb, 2009; Comeau *et al.*, 2013; Cyronak *et al.*, 2016; Jokiel, 2016). During times of thermal stress, energetic demands are also placed on corals to maintain the symbiosis with their *Symbiodinium* partners (Lesser, 2011). With OA progressing and SST anomaly frequencies increasing, the opportunity cost for corals to maintain the *status quo* may include declines in calcification, bleaching resistance, fecundity, or other energetically demanding processes. As carbon emissions continue to increase, we are likely to see the gradual deterioration of coral species that are more susceptible to OA effects on calcification (Comeau *et al.*, 2013) and temperature stress (Marshall and Baird, 2000) and decline in those species that are unable to utilize the more abundant CO_2 for photosynthesis in eutrophic waters (Crawley *et al.*, 2010; Brading *et al.*, 2011). Unfortunately for the most reef associated taxa, it appears that the most competitive species of coral, in the face of OA and increasing SST, are massive varieties that support a low diversity of associates (Marshall and Baird, 2000; Fabricius *et al.*, 2011, 2014). While it is difficult to be sanguine in the face of projected trajectories for coral reefs, the only feasible option to prevent the exacerbation of these effects is to reduce anthropogenic CO_2 emissions.

Supplementary data

Supplementary material is available at the *ICESJMS* online version of the manuscript.

Acknowledgements

We thank the communities at Upa Upasina, Esa'Ala, and Dobu for their ongoing support of this project. Thanks also go to S. Uthicke, F. Flores, C. Schmidt, and J. Doyle for assistance in running the laboratory experiment, to J. Strahl for comments on the manuscript, and to Qantas and Qantas Link for continued support. This project was funded by the National Environmental Research Program (NERP 5.2) of the Australian Commonwealth Government's Department of the Environment, and AIMS.

References

Anlauf, H., D'Croz, L., and O'Dea, A. 2011. A corrosive concoction: The combined effects of ocean warming and acidification on the early growth of a stony coral are multiplicative. Journal of Experimental Marine Biology and Ecology, 397: 13–20.

Anthony, K. R. N., Hoogenboom, M. O., Maynard, J. A., Grottoli, A. G., and Middlebrook, R. 2009. Energetics approach to predicting mortality risk from environmental stress: A case study of coral bleaching. Functional Ecology, 23: 539–550.

Anthony, K. R. N., Kline, D. I., Diaz-Pulido, G., Dove, S., and Hoegh-Guldberg, O. 2008. Ocean acidification causes bleaching and productivity loss in coral reef builders. Proceedings of the National Academy of Sciences of the United States of America, 105: 17442–17446.

Anthony, K. R. N., Maynard, J. A., Diaz-Pulido, G., Mumby, P. J., Marshall, P. A., Cao, L., and Hoegh-Guldberg, O. 2011. Ocean acidification and warming will lower coral reef resilience. Global Change Biology, 17: 1798–1808.

Berkelmans, R., De'ath, G., Kininmonth, S., and Skirving, W. J. 2004. A comparison of the 1998 and 2002 coral bleaching events on the Great Barrier Reef: Spatial correlation, patterns, and predictions. Coral Reefs, 23: 74–83.

Berkelmans, R., and van Oppen, M. J. H. 2006. The role of zooxanthellae in the thermal tolerance of corals: A "nugget of hope" for coral reefs in an era of climate change. Proceedings of the Royal Society of London, Series B: Biological Sciences, 273: 2305–2312.

Brading, P., Warner, M. E., Davey, P., Smith, D. J., Achterberg, E. P., and Suggett, D. J. 2011. Differential effects of ocean acidification on growth and photosynthesis among phylotypes of *Symbiodinium* (Dinophyceae). Limnology and Oceanography, 56: 927–938.

Brown, B. E. 1997. Coral bleaching: Causes and consequences. Coral Reefs, 16: 129–138.

Chauvin, A., Denis, V., and Cuet, P. 2011. Is the response of coral calcification to seawater acidification related to nutrient loading? Coral Reefs, 30: 911–923.

Cohen, A., and Holcomb, M. 2009. Why corals care about ocean acidification: Uncovering the mechanism. Oceanography, 22: 118–127.

Comeau, S., Carpenter, R. C., and Edmunds, P. J. 2012. Coral reef calcifiers buffer their response to ocean acidification using both bicarbonate and carbonate. Proceedings of the Royal Society of London B: Biological Sciences, 280: 20130031.

Comeau, S., Edmunds, P. J., Spindel, N. B., and Carpenter, R. C. 2013. The responses of eight coral reef calcifiers to increasing partial pressure of CO_2 do not exhibit a tipping point. Limnology and Oceanography, 58: 388–398.

Crawley, A., Kline, D. I., Dunn, S., Anthony, K. R. N., and Dove, S. 2010. The effect of ocean acidification on symbiont photorespiration and productivity in *Acropora formosa*. Global Change Biology, 16: 851–863.

Cyronak, T., Schulz, K. G., and Jokiel, P. L. 2016. The Omega myth: What really drives lower calcification rates in an acidifying ocean. ICES Journal of Marine Science, 73: 558–562.

Dickson, A. G. 2007. Guide to Best Practices for Ocean CO_2 Measurements. PICES Special Publication 3. North Pacific Marine Science Organization, British Columbia, in press.

Dove, S., Ortiz, J. C., Enrı, S., Fine, M., Fisher, P., Iglesias-Prieto, R., Thornhill, D., *et al.* 2006. Response of holosymbiont pigments from the scleractinian coral *Montipora monasteriata* to short-term heat stress. Limnology and Oceanography, 51: 1149–1158.

Edmunds, P. J. 2012. Effect of pCO_2 on the growth, respiration, and photophysiology of massive *Porites* spp. in Moorea, French Polynesia. Marine Biology, 159: 2149–2160.

Fabricius, K. E. 2006. Effects of irradiance, flow, and colony pigmentation on the temperature microenvironment around corals: Implications for coral bleaching? Limnology and Oceanography, 51: 30–37.

Fabricius, K. E., De'ath, G., Noonan, S. H. C., and Uthicke, S. 2014. Ecological effects of ocean acidification and habitat complexity on reef-associated macroinvertebrate communities. Proceedings of the Royal Society of London B: Biological Sciences, 281: 20132.

Fabricius, K. E., Langdon, C., Uthicke, S., Humphrey, C., Noonan, S., De'ath, G., Okazaki, R., *et al.* 2011. Losers and winners in coral reefs acclimatized to elevated carbon dioxide concentrations. Nature Climate Change, 1: 165–169.

Gil, M. A. 2013. Unity through nonlinearity: A unimodal coral–nutrient interaction. Ecology, 94: 1871–1877.

Harvey, B. P., Gwynn-Jones, D., and Moore, P. J. 2013. Meta-analysis reveals complex marine biological responses to the interactive effects of ocean acidification and warming. Ecology and Evolution, 3: 1016–1030.

Herfort, L., Thake, B., and Taubner, I. 2008. Bicarbonate stimulation of calcification and photosynthesis in two hermatypic corals. Journal of Phycology, 44: 91–98.

Hoegh-Guldberg, O. 1999. Climate change, coral bleaching and the future of the world's coral reefs. Marine and Freshwater Research, 50: 839–866.

Hoegh-Guldberg, O., Mumby, P. J., Hooten, A. J., Steneck, R. S., Greenfield, P., Gomez, E., Harvell, C. D., *et al.* 2007. Coral reefs under rapid climate change and ocean acidification. Science, 318: 1737–1742.

Hoogenboom, M. O., Campbell, D. A., Beraud, E., Dezeeuw, K., and Ferrier-Pagès, C. 2012. Effects of light, food availability and temperature stress on the function of photosystem II and photosystem I of coral symbionts. PLoS ONE, 7: e30167.

IPCC. 2013. Climate Change 2013: The Physical Science Basis. Contribution of Working Group I to the Fifth Assessment Report of the Intergovernmental Panel on Climate Change. Cambridge University Press, Cambridge, UK; New York.

Jokiel, P. L. 2016. Predicting the impact of ocean acidification on coral reefs: Evaluating the assumptions involved. ICES Journal of Marine Science, 73: 550–557.

Kleypas, J. A. 1999. Geochemical consequences of increased atmospheric carbon dioxide on coral reefs. Science, 284: 118–120.

Krief, S., Hendy, E. J., Fine, M., Yam, R., Meibom, A., Foster, G. L., and Shemesh, A. 2010. Physiological and isotopic responses of scleractinian corals to ocean acidification. Geochimica et Cosmochimica Acta, 74: 4988–5001.

Langdon, C., and Atkinson, M. J. 2005. Effect of elevated pCO_2 on photosynthesis and calcification of corals and interactions with seasonal change in temperature/irradiance and nutrient enrichment. Journal of Geophysical Research, 110: C09S07.

Lesser, M. P. 2011. Coral bleaching: causes and mechanisms. *In* Coral Reefs: An Ecosystem in Transition, pp. 405–419. Ed. by Z. Dubinsky, and N. Stambler Springer, Netherlands.

Lewis, E., and Wallace, D. 1998. Program Developed for CO_2 system calculations. Carbon Dioxide Information Analysis Center, Oak Ridge National Laboratory, Oak Ridge, Tenn.

Manzello, D. 2010. Ocean acidification hot spots: Spatiotemporal dynamics of the seawater CO_2 system of eastern Pacific coral reefs. Limnology and Oceanography, 55: 239–248.

Marshall, P. A., and Baird, A. H. 2000. Bleaching of corals on the Great Barrier Reef: Differential susceptibilities among taxa. Coral Reefs, 19: 155–163.

Maynard, J. A., Anthony, K. R. N., Marshall, P. A., and Masiri, I. 2008. Major bleaching events can lead to increased thermal tolerance in corals. Marine Biology, 155: 173–182.

Moss, R. H., Edmonds, J. A., Hibbard, K. A., Manning, M. R., Rose, S. K., van Vuuren, D. P., Carter, T. R., *et al.* 2010. The next generation of scenarios for climate change research and assessment. Nature, 463: 747–756.

Noonan, S. H. C., Fabricius, K. E., and Humphrey, C. 2013. Symbiodinium community composition in Scleractinian corals is not affected by life-long exposure to elevated carbon dioxide. PLoS ONE, 8: e63985.

R Development Core Team. 2014. A Language and Environment for Statistical Computing. R Foundation for Statistical Computing, Vienna; http://www.R-project.org.

Ralph, P. J., and Gademann, R. 2005. Rapid light curves: A powerful tool to assess photosynthetic activity. Aquatic Botany, 82: 222–237.

Ralph, P. J., Schreiber, U., Gademann, R., Kühl, M., and Larkum, A. W. D. 2005. Coral photobiology studied with a new imaging pulse amplitude modulated fluorometer 1. Journal of Phycology, 41: 335–342.

Reynaud, S., Leclercq, N., Romaine-Lioud, S., Ferrier-Pages, C., Jaubert, J., and Gattuso, J.-P. 2003. Interacting effects of CO_2 partial pressure and temperature on photosynthesis and calcification in a scleractinian coral. Global Change Biology, 9: 1660–1668.

Schoepf, V., Grottoli, A. G., Warner, M. E., Cai, W. J., Melman, T. F., Hoadley, K. D., Pettay, D. T., *et al.* 2013. Coral energy reserves and calcification in a high-CO_2 world at two temperatures. PLoS ONE, 8: e75049.

Siebeck, U. E., Marshall, N. J., Klüter, A., and Hoegh-Guldberg, O. 2006. Monitoring coral bleaching using a colour reference card. Coral Reefs, 25: 453–460.

Uthicke, S., and Fabricius, K. E. 2012. Productivity gains do not compensate for reduced calcification under near-future ocean acidification in the photosynthetic benthic foraminifer species *Marginopora vertebralis*. Global Change Biology, 18: 2781–2791.

Uthicke, S., Vogel, N., Doyle, J., Schmidt, C., and Humphrey, C. 2012. Interactive effects of climate change and eutrophication on the dinoflagellate-bearing benthic foraminifer *Marginopora vertebralis*. Coral Reefs, 31: 401–414.

Veal, C. J., Carmi, M., Fine, M., and Hoegh-Guldberg, O. 2010. Increasing the accuracy of surface area estimation using single wax dipping of coral fragments. Coral Reefs, 29: 893–897.

Wall, C. B., Fan, T.-Y., and Edmunds, P. J. 2013. Ocean acidification has no effect on thermal bleaching in the coral *Seriatopora caliendrum*. Coral Reefs, 33: 119–130.

Handling editor: Howard Browman

ICES Journal of Marine Science

ICES Journal of Marine Science (2016), 73(3), 727–738. doi:10.1093/icesjms/fsv018

Contribution to Special Issue: 'Towards a Broader Perspective on Ocean Acidification Research'

Original Article

The impact of ocean acidification and warming on the skeletal mechanical properties of the sea urchin *Paracentrotus lividus* from laboratory and field observations

Marie Collard[1,2]*, Samuel P. S. Rastrick[3,4], Piero Calosi[3,5], Yoann Demolder[1], Jean Dille[6], Helen S. Findlay[7], Jason Michael Hall-Spencer[3], Marco Milazzo[8], Laure Moulin[1,9], Steve Widdicombe[3], Frank Dehairs[2], and Philippe Dubois[1]

[1]*Laboratoire de Biologie Marine, Université Libre de Bruxelles, 50 Avenue F.D. Roosevelt, Brussels B-1050, Belgium*
[2]*Laboratory for Analytical, Environmental and Geo-Chemistry, Earth Systems Science Research Group, Vrije Universiteit Brussel, Pleinlaan 2, Brussels 1050, Belgium*
[3]*Marine Biology and Ecology Research Centre, Plymouth University, Plymouth PL4 8AA, UK*
[4]*Marine Invertebrate Physiology and Immunology Ocean and Earth Science, National Oceanography Centre Southampton, University of Southampton Waterfront Campus, European Way, Southampton SO14 3ZE, UK*
[5]*Département de Biologie, Chimie et Géographie, Université du Québec à Rimouski, 300 Allée des Ursulines, Rimouski, QC, Canada G5L 3A1*
[6]*4MAT Department, Université Libre de Bruxelles, 50 Avenue F.D. Roosevelt, Brussels B-1050, Belgium*
[7]*Plymouth Marine Laboratory, Prospect Place, West Hoe, Plymouth PL1 3 DH, UK*
[8]*Dipartimento di Scienze della Terra e del Mare, Università di Palermo, Via Archirafi, 28, Palermo, Italy*
[9]*Laboratoire d'Ecologie Numérique des Milieux Aquatiques, Université de Mons-Hainaut, 23 Place du Parc, Mons B-7000, Belgium*

**Corresponding author: tel: +32 2 650 29 70; fax: +32 2 650 27 96; e-mail: marie.collard9@gmail.com*

Collard, M., Rastrick, S. P. S., Calosi, P., Demolder, Y., Dille, J., Findlay, H. S., Hall-Spencer, J. M., Milazzo, M., Moulin, L., Widdicombe, S., Dehairs, F., and Dubois, P. The impact of ocean acidification and warming on the skeletal mechanical properties of the sea urchin *Paracentrotus lividus* from laboratory and field observations. – ICES Journal of Marine Science, 73: 727–738.

Received 20 August 2014; revised 15 January 2015; accepted 17 January 2015; advance access publication 16 February 2015.

Increased atmospheric CO_2 concentration is leading to changes in the carbonate chemistry and the temperature of the ocean. The impact of these processes on marine organisms will depend on their ability to cope with those changes, particularly the maintenance of calcium carbonate structures. Both a laboratory experiment (long-term exposure to decreased pH and increased temperature) and collections of individuals from natural environments characterized by low pH levels (individuals from intertidal pools and around a CO_2 seep) were here coupled to comprehensively study the impact of near-future conditions of pH and temperature on the mechanical properties of the skeleton of the euechinoid sea urchin *Paracentrotus lividus*. To assess skeletal mechanical properties, we characterized the fracture force, Young's modulus, second moment of area, material nanohardness, and specific Young's modulus of sea urchin test plates. None of these parameters were significantly affected by low pH and/or increased temperature in the laboratory experiment and by low pH only in the individuals chronically exposed to lowered pH from the CO_2 seeps. In tidal pools, the fracture force was higher and the Young's modulus lower in ambital plates of individuals from the rock pool characterized by the largest pH variations but also a dominance of calcifying algae, which might explain some of the variation. Thus, decreases of pH to levels expected for 2100 did not directly alter the mechanical properties of the test of *P. lividus*. Since the maintenance of test integrity is a question of survival for sea urchins and since weakened tests would increase the sea urchins' risk of predation, our findings indicate that the decreasing seawater pH and increasing seawater temperature expected for the end of the century should not represent an immediate threat to sea urchins vulnerability.

Keywords: CO_2 seep, intertidal pools, long-term exposure, mechanical properties, ocean acidification, *Paracentrotus lividus*, sea urchin, skeleton.

Introduction

The atmospheric carbon dioxide (CO_2) concentration has increased from 280 to 400 ppm due to anthropogenic activities such as fossil fuel burning (IPCC, 2013). The continually increasing concentration of atmospheric CO_2 is leading to an increase in the mean global seawater temperature, which is expected to be 2°C warmer by the end of this century, and is changing seawater carbonate chemistry as CO_2 dissolves into the surface waters (decreasing pH and carbonate ions concentration; Caldeira and Wickett, 2003; Sokolov *et al.*, 2009; Orr, 2011). A reduction in carbonate ions results in a decreased saturation state (Ω) of seawater for carbonate calcium minerals. Such minerals are built by several marine organisms, including echinoderms which produce high-magnesium calcite, one of the most soluble forms of calcium carbonate (Morse *et al.*, 2006).

Changes in the ocean carbonate chemistry have been indicated to have potential negative effects on the integrity of calcifying marine organisms' skeleton. As previously shown for crustaceans, coccolithophores, and molluscs, calcification may be impaired and calcium carbonate skeletons may dissolve (e.g. McDonald *et al.*, 2009; Welladsen *et al.*, 2010; Ziveri *et al.*, 2014). Although some organisms upregulate calcification rates as carbonate saturation states fall, unprotected skeletons and shells dissolve once Ω falls below 1 (Rodolfo-Metalpa *et al.*, 2011). Thus, in general, the mechanical properties of skeletons could be affected as Ω falls (McDonald *et al.*, 2009; Welladsen *et al.*, 2010). Sea urchin skeletons are of basic importance in defining the organism structure, providing protection against hydrodynamic forces and predators, and enabling locomotion and food gathering. Consequently, any deterioration of the skeleton would have considerable consequences on the sea urchin fitness. However, sea urchins thrive in naturally undersaturated waters such as upwelling zones where pH may reach values of 7.75, tidal pools where during nocturnal low tide pH can decrease to 7.4, around CO_2 seep in areas with pH 7.4, in deep ocean, and in Antarctic waters where the $CaCO_3$ saturation state is below 1 (e.g. David *et al.*, 2005; Hall-Spencer *et al.*, 2008; Moulin *et al.*, 2011; LaVigne *et al.*, 2013; Collard *et al.*, 2014a; Dery *et al.*, 2014).

In adult sea urchins, the skeleton is embedded within the dermis which is itself covered by the epidermis (except for the particular case of the cidaroid sea urchins' spines which lack a covering epidermis; Dery *et al.*, 2014). The skeleton is principally composed of the test, encompassing the body, the spines (Figure 1), and the chewing apparatus, called Aristotle's lantern. The different ossicles of the skeleton are made of a three-dimensional network of calcium carbonate trabeculae called the stereom which has pores filled with connective tissue, the stroma (Dubois and Chen, 1989). The test plates are almost never fused but are tightly held against each other by ligaments rolled around the outermost trabeculae and the trabeculae from one plate are inserted within the pores of the adjacent plates (Ellers *et al.*, 1998). The main calcium carbonate mineral formed by adult sea urchins is high-magnesium calcite, one of the most soluble forms of calcite (Morse *et al.*, 2006). However, calcification takes place intracellularly, within closed syncytia, and therefore the skeleton is almost never in contact with seawater (Dubois and Chen, 1989). Indirectly, calcification could be impacted by the cost of maintaining acid–base balance, i.e. removing protons and CO_2 that are produced during the calcification process. Indeed, the cost of maintaining homeostasis across a natural pH gradient can affect the distribution of marine invertebrates (Calosi *et al.*, 2013a). The elimination of protons into the extracellular fluids will have an increased energetic cost if the concentration of protons within these fluids is also elevated by acidosis due to lower pH seawater, as shown in the gastropod *Littorina littorea* (Melatunan *et al.*, 2013). Some sea urchin species appear able to partly or fully compensate extracellular pH (Stumpp *et al.*, 2012; Collard *et al.*, 2013, 2014b; Moulin *et al.*, 2014) including across natural pH gradients (Calosi *et al.*, 2013a). Others appear unable to do so (Kurihara *et al.*, 2013) and some species show naturally a low coelomic fluid pH, and an undersaturation towards high-magnesium calcite (pH 7.1, $\Omega_{Ar} < 1$; Calosi *et al.*, 2013b; Collard *et al.*, 2013, 2014a, b).

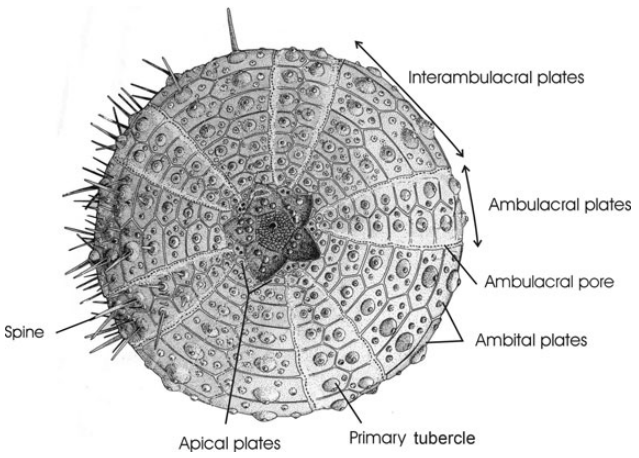

Figure 1. Aboral view of the test of an euechinoid and illustration of the plates sampled for the mechanical tests (adapted from Trousset, 1885).

Mechanical properties can be affected through different processes. Changes in the growth rate may affect the three-dimensional morphology or density of the stereom (Smith, 1980), which will result in modified mechanical properties (e.g. Moureaux *et al.*, 2010). Alternatively, the structural properties of the material itself may be affected by the formation of imperfections during the $CaCO_3$ precipitation (e.g. Moureaux *et al.*, 2011). For these reasons, different mechanical tests should be applied to fully describe the mechanical properties. Bending and compression tests measure the structural properties and how a change in the shape and/or the repartition of the material within the skeletal piece may affect its overall strength. Complementarily, nanoindentation measures the strength of the material itself as it is applied to a very small surface. Using both types of measurements may disentangle the question of knowing if it is the shape that is affected or the material.

Most studies carried out on ocean acidification impacts on sea urchin skeletons concern growth (for a review, see Dubois, 2014). Several studies reported reduced growth rates of the test and/or spines, especially in juveniles; while other studies showed no effect of the same conditions on these rates (Dubois, 2014). The studies investigating the impact of temperature on sea urchin skeleton have also focused on growth rates showing either no impact or enhanced growth when temperature is increased (e.g. Hermans *et al.*, 2010; Wolfe *et al.*, 2013). Very few studies have addressed the impact of seawater acidification on mechanical properties of the skeleton, and none investigated the impact of temperature (e.g. Asnaghi *et al.*, 2013; Holtmann *et al.*, 2013). However, the methods used in those studies presented bias resulting in difficultly interpretable data (Ellers *et al.*, 1998; Dubois, 2014). More importantly, all the aforementioned studies have investigated the effects of ocean acidification after short-term exposures (<6 months), but recent studies have shown that long-term exposures (≥1 year) may allow

for the acclimatization of sea urchins to acidified conditions. In particular, Dupont *et al.* (2013) showed that after 12 months of exposure the negative effects of reduced seawater pH observed during short-term exposure do not apply anymore. Furthermore, previous studies have used analogue open systems for future ocean conditions such as CO_2 seeps or intertidal pools to study the impact of reduced pH exposure on sea urchins (e.g. Hall-Spencer *et al.*, 2008; Calosi *et al.*, 2013b) but none of them focused on skeletal mechanical properties of sea urchins.

The goal of the present study was to comprehensively assess the impact of changes in seawater pH and temperature on the skeletal mechanical properties of the sea urchin *Paracentrotus lividus* (Lamarck, 1816), in both a laboratory experiment and in the field. First, we investigated the effect of long-term (12 months) laboratory exposure to decreased pH (8.0 as control, 7.9 and 7.8) and increased temperature (+2°C). Second, we investigated the effect of natural acclimatization/adaptation in intertidal pools where individuals are intermittently exposed to pH changes (of up to 0.5 pH units during a single tide) and chronically exposed to natural pH levels along a gradient (pH 8.2–7.7) at CO_2 seeps off Vulcano Island, Italy. We applied several mechanical tests including compression, three-point bending, and nanoindentation tests (Ellers *et al.*, 1998; Moureaux *et al.*, 2011) to evaluate the effect of ocean acidification on whole-organism structural strength and individual plate (ambital and apical) properties.

Material and methods

Plate sampling

All measurements were carried out on skeletons of adult individuals of the sea urchin *P. lividus*. The sea urchin test is composed of individual plates held together by tissue. On those plates, the spines are articulated on the tubercles. The plates are arranged in five interambulacral and five ambulacral double rows (Figure 1). We used interambulacral plates for all mechanical tests rather than the ambulacral plates, since the latter result from the fusion of 2–3 platelets and are pierced with pores for the extrusion of the tube feet, rendering calculations of mechanical properties particularly complex (Smith, 1980). We used two types of interambulacral plates: the apical plates, i.e. the uppermost plates which are the most recently added and the smallest plates, and the ambital plates, i.e. middle plates which are the largest and are located along the ambitus (the largest diameter) of the sea urchin (Deutler, 1926; Figure 1). Samples were collected by dissecting along an ambulacral row from the peristomial membrane to ~1 cm from the apical disc, from there, they were cut horizontally across two interambulacral rows and down to the peristomial membrane again along an ambulacral row. This avoided any damage to the interambulacral ambital and apical plates.

Twelve-month laboratory acclimation

The effects of long-term exposure to elevated temperature and reduced pH conditions predicted to occur by the end of this century (Caldeira and Wickett, 2003; Sokolov *et al.*, 2009; Orr, 2011) on skeletal structures of adult *P. lividus* (supplied by Dunmanus Seafoods Ltd, Durrus, Bantry, Co. Cork, Ireland) were assessed by conducting a 49 weeks long mesocosm experiment at the Plymouth Marine Laboratory (PML, Plymouth, UK) from March 2011 to February 2012 (same system as Findlay *et al.*, 2013, and Queiros *et al.*, 2014). Five nominal treatments were used: "present" [380 μatm (pH 8.0) and seasonal temperature cycle, 380A]; "elevated pCO_2" [750 μatm (pH 7.9) and seasonal temperature cycle, 750A]; "extreme elevated pCO_2" [1000 μatm (pH 7.8) and seasonal temperature cycle, 1000A]; "elevated temperature" [380 μatm (pH 8.0) and 2°C added to the seasonal temperature cycle, 380A+2]; and "combined" [750 μatm (pH 7.9) and 2°C added to the seasonal temperature cycle, 750A+2]. Present day pCO_2 conditions of 380 μatm were maintained by bubbling untreated air, whereas higher pCO_2 treatments were bubbled with enriched-CO_2 air (after, Findlay *et al.*, 2008). Temperature was maintained by the use of heaters and chillers and monthly adjustments were made to reproduce the natural seasonal variations. pCO_2 and temperature were maintained separately in each aquarium. The photoperiod was also adjusted monthly to that of the natural conditions (winter L:D period 8.5 h:15.5 h, summer L:D period 16.5 h:7.5 h). Each nominal treatment was replicated four times and sea urchins randomly assigned to the four aquaria (1 m^3). Within each aquarium, the sea urchins were further divided into individual boxes pierced with holes for water circulation. Water quality was assessed by weekly measurements of nitrate levels (Bran+Luebbe Ltd AAIII, Seal Analytical, Mecquon, WI, USA), and when the concentration reached 25 mg l^{-1}, a third of the seawater volume was changed (in addition to the standard 1/3 volume change done every 3 weeks for all aquaria). The mean (± s.d.) nitrate concentration was 3.7 ± 11.1 (range: 0.02–78.85 μmol l^{-1}). Sea urchins were fed with macroalgae (*Ulva lactuca* and *Laminaria* sp.) collected from Plymouth Sound once a week for 48 h. Excessive food and faecal pellets were removed after feeding.

Seawater used for our experimental system was collected from PML's long-term monitoring site "L4" in the Western English Channel (50°15.00′N 4°13.02′W; L4, Western Channel Observatory; for seasonal data on carbon cycle, see Kitidis *et al.*, 2012). Seawater physicochemical parameters were measured three times a week. All methods and data are available online from Findlay *et al.* (2013). Carbonate system parameters that were not directly measured were calculated from temperature, salinity, pH, and A_T as described in Findlay *et al.* (2013). Water chemistry parameters are presented in Table 1.

Sea urchins employed for mechanical tests were sampled from all four replicate aquaria for each treatment after 12 months of exposure, dissected, cleaned of internal organs, and dried for 48 h at 50°C: $n = 10$ for 380A, 11 for 750A+2, and 12 for 750A, 1000A, and 380A+2. The mean diameter at the ambitus (mean ± s.d.) was 39.9 ± 5.4, 41.4 ± 3.7, 38.8 ± 4.5, 40.6 ± 3.2, and 41.9 ± 6.4 mm for treatments 380A, 750A, 1000A, 380A+2, and 750A+2, respectively. Three ambital interambulacral plates and three apical interambulacral plates per sea urchin were used for mechanical tests. Also, three plates of each type were taken from three individuals per treatment (from different aquaria) for nanoindentation measurements.

Intertidal pools

The effect of intermittent exposure to low pH was investigated by collecting sea urchins in intertidal pools in Crozon (Brittany, France) in February 2013. They were taken from three intertidal rock pools previously characterized (Moulin *et al.*, 2011) and showing different pH regimes during low tide. Seawater in tide pool A was characterized by moderate pH variation during a night tide (−0.2 pH units), tide pool C showed the largest pH changes (−0.5 pH units), and tide pool B was intermediate (−0.4 pH

Table 1. Mean water and carbonate system parameters (mean ± s.d.) for the different treatments of the laboratory experiment per 3-month periods.

	Time point (months)	A_T (μmol kg_{SW}^{-1})	pH_{NBS}	Temp (°C)	Salinity	DIC (μmol kg_{SW}^{-1})	pCO_2 (μatm)	Ω Ca	Ω Ar
380 A	0–3	2131.0 ± 0.0	8.02 ± 0.09	10.49 ± 0.71	34.3 ± 0.1	2003.3 ± 30.8	531.8 ± 142.5	2.32 ± 0.39	1.48 ± 0.25
750 A	0–3	2097.9 ± 0.0	7.93 ± 0.09	10.53 ± 0.73	34.5 ± 0.2	2002.9 ± 28.4	663.0 ± 146.5	1.89 ± 0.34	1.20 ± 0.21
1000 A	0–3	2355.1 ± 25.7	7.81 ± 0.10	9.66 ± 0.91	34.5 ± 0.2	2297.9 ± 39.7	1003.1 ± 244.7	1.61 ± 0.33	1.02 ± 0.21
380 A+2	0–3	2357.2 ± 3.7	7.97 ± 0.09	11.84 ± 0.85	34.9 ± 0.2	2233.2 ± 31.6	679.2 ± 170.3	2.43 ± 0.39	1.55 ± 0.25
750 A+2	0–3	2402.7 ± 7.1	7.90 ± 0.09	12.04 ± 0.95	35.0 ± 0.2	2299.8 ± 30.6	815.8 ± 184.6	2.18 ± 0.37	1.39 ± 0.24
380 A	3–6	2171.7 ± 84.4	7.94 ± 0.12	11.37 ± 1.17	35.2 ± 0.2	2060.2 ± 55.2	664.7 ± 167.2	2.16 ± 0.70	1.38 ± 0.45
750 A	3–6	2090.8 ± 17.5	7.86 ± 0.10	11.60 ± 1.21	35.2 ± 0.2	2010.5 ± 48.7	790.9 ± 183.7	1.72 ± 0.42	1.10 ± 0.27
1000 A	3–6	2351.4 ± 13.3	7.75 ± 0.09	11.03 ± 0.36	35.3 ± 0.2	2302.8 ± 44.6	1136.6 ± 230.5	1.53 ± 0.35	0.98 ± 0.22
380 A+2	3–6	2361.2 ± 75.4	7.92 ± 0.09	12.85 ± 1.42	35.3 ± 0.1	2248.2 ± 96.6	771.3 ± 167.6	2.29 ± 0.46	1.47 ± 0.30
750 A+2	3–6	2238.8 ± 89.8	7.80 ± 0.10	12.84 ± 1.38	35.4 ± 0.2	2168.8 ± 107.2	990.8 ± 258.3	1.71 ± 0.41	1.09 ± 0.26
380 A	6–9	2255.2 ± 133.1	8.08 ± 0.03	15.04 ± 0.90	35.0 ± 0.1	2073.9 ± 122.9	483.0 ± 24.6	3.18 ± 0.25	2.04 ± 0.15
750 A	6–9	2183.2 ± 101.6	7.93 ± 0.09	15.66 ± 0.65	34.9 ± 0.2	2062.9 ± 131.3	722.4 ± 198.2	2.31 ± 0.32	1.49 ± 0.21
1000 A	6–9	2251.0 ± 81.7	7.79 ± 0.05	15.63 ± 0.37	34.9 ± 0.1	2176.5 ± 1.7	1028.6 ± 118.1	1.79 ± 0.19	1.15 ± 0.12
380 A+2	6–9	2111.9 ± 96.0	8.01 ± 0.07	17.93 ± 0.38	35.2 ± 0.2	1950.1 ± 109.1	568.1 ± 129.9	2.83 ± 0.38	1.83 ± 0.25
750 A+2	6–9	2170.4 ± 110.6	7.86 ± 0.11	17.90 ± 0.16	35.1 ± 0.2	2061.7 ± 140.6	871.9 ± 252.6	2.17 ± 0.47	1.40 ± 0.30
380 A	9–12	2238.0 ± 52.7	8.06 ± 0.04	13.06 ± 1.55	34.9 ± 0.1	2079.4 ± 59.8	508.3 ± 54.8	2.83 ± 0.20	1.81 ± 0.13
750 A	9–12	2228.7 ± 66.7	7.94 ± 0.07	12.89 ± 1.60	34.8 ± 0.1	2116.6 ± 69.5	694.4 ± 139.5	2.21 ± 0.29	1.41 ± 0.18
1000 A	9–12	2218.5 ± 90.6	7.78 ± 0.09	12.73 ± 1.74	34.9 ± 0.1	2157.4 ± 85.9	1015.9 ± 225.2	1.60 ± 0.29	1.02 ± 0.18
380 A+2	9–12	2165.5 ± 47.0	8.03 ± 0.06	15.55 ± 1.96	34.9 ± 0.2	2005.9 ± 38.9	536.6 ± 93.9	2.81 ± 0.30	1.81 ± 0.19
750 A+2	9–12	2164.6 ± 57.2	7.93 ± 0.08	15.63 ± 1.75	35.1 ± 0.1	2041.1 ± 62.6	694.7 ± 134.1	2.32 ± 0.33	1.50 ± 0.21

A_T, total alkalinity; Temp, temperature; DIC, dissolved inorganic carbon; Ω Ca, saturation state of calcite; Ω *Ar*, saturation state of aragonite.

Table 2. Characteristics and physicochemical conditions of the intertidal pools sampled for *P. lividus* sea urchins.

Tide pool	Size (m × m)	Depth (cm)	Urchins in crevices	Prevailing alga type	pH_{NBS} start of the night tide	pH_{NBS} end of the night tide	Mean pH_{NBS} over the time course (± s.d.)	Salinity	Temperature (°C)
October 2008									
A	15 × 16	50–100	No	Erected macroalgae	8.13	7.95	8.05 ± 0.06	35.3	14.6
B	5 × 1.5	30–50	Yes	Erected macroalgae	8.10	7.70	7.89 ± 0.14	35.3	14.3
C	2.4 × 0.6	<30	Yes	Encrusting calcified algae	8.04	7.54	7.71 ± 0.18	35.4	13.9
April 2009									
A	15 × 16	50–100	No	Erected macroalgae	8.14	7.80	7.99 ± 0.12	34.7	12.8
B	5 × 1.5	30–50	Yes	Erected macroalgae	8.07	7.59	7.84 ± 0.17	34.6	12.1
C	2.4 × 0.6	<30	Yes	Encrusting calcified algae	7.84	7.40	7.59 ± 0.14	34.7	11.9

units) (Table 2). Temperature and salinity were similar in the different tide pools.

From each pool, ten individuals were collected and brought back in aerated water to the laboratory in Brussels for mechanical tests on live individuals. The mean diameter at the ambitus (mean ± s.d.) was 33.2 ± 2.7, 37.8 ± 3.4, and 34.7 ± 4.0 mm for tide pools A, B, and C, respectively. These individuals were then maintained in aquarium (recirculating system, pH_{NBS} 8.34 ± 0.01, salinity 32.2 ± 0.1, temperature 10.0 ± 0.1°C; mean ± s.d. and $n = 3$ for all parameters) for a maximum of 4 d before the mechanical tests were run.

A further ten individuals were sampled from each pool and immediately dissected, cleaned of internal organs, and dried for 48 h at 50°C for mechanical tests on individual plates. The diameter at the ambitus (mean ± s.d.) was 35.2 ± 2.7, 35.9 ± 3.3, and 33.5 ± 2.4 mm for tide pools A, B, and C, respectively. For each of these individuals, three ambital interambulacral plates and three apical interambulacral plates were analysed. Three plates of each type were also taken from three individuals per tide pool for nanoindentation measurements.

CO_2 seep site

To investigate the skeletal effects of natural acclimatization to a reduced pH system, adult *P. lividus* were collected from a volcanic seep gradient at Levante Bay off the island of Vulcano, Italy, in June 2013 (Calosi *et al.*, 2013b). The continuous release of CO_2 generates a natural pH and pCO_2 gradient along the north side of the bay (Boatta *et al.*, 2013; Vizzini *et al.*, 2013). Two sites were chosen: the site used as "control condition" was located 380 m away from the main CO_2 seeps and had a mean pH of 8.1, same as that measured for sites outside the gradients (Boatta *et al.*, 2013); the second site used as "low pH condition" was situated 300 m away from the seeps and had a mean pH of 7.8, close to predicted end-of-century values (Boatta *et al.*, 2013). This distance from the CO_2 seeps limited the influence of contaminants produced by the seeps, such as H_2SO_4 (Boatta *et al.*, 2013). Vizzini *et al.* (2013) showed that these sites were in "good condition" and only "moderately impacted" according to widely used pollution indices. Seawater chemistry parameters measured at the time of sea urchin collection are shown in Table 3. These are similar to results reported earlier for this location (e.g. Boatta *et al.*, 2013; Calosi *et al.*, 2013b; Vizzini *et al.*, 2013).

Table 3. Characteristics of the CO_2 seep sites sampled for *P. lividus* sea urchin (midday, 12/06/2013).

	Control site	Low pH site
pH_{NBS}	8.21	7.78
Salinity	38.2	38.1
Temperature (°C)	20.0	20.1
Total alkalinity (mmol kg_{SW}^{-1})	2.545	2.506

At both the control and low pH sites, three adult *P. lividus* were collected by snorkelling at a depth of 1–2 m. Urchins were then dissected, cleaned of internal organs, and dried for 48 h at 50°C. Three ambital interambulacral plates and three apical interambulacral plates from each urchin were then used for nanoindentation measurements.

Mechanical tests

To measure the fracture force of whole live individuals, a simple compression test was applied to the sea urchins. After measuring the diameter of the live sea urchins using a calliper (precision: ± 0.1 mm), the spines at the ambitus were manually removed to avoid any interference of the spines on the measurement of the test strength. The whole sea urchins were tested in a home-made device (Figure 2a) designed to mimic the jaws of a predatory fish (Guidetti and Mori, 2005). They were placed in a first container which has a perforation in the bottom part and in which acrylic plates could be inserted according to the size of the sea urchin to hold it firmly in place. This first container was placed in a second larger container filled with seawater from the aquarium at a temperature of ca. 10°C and in which was anchored a metal spike. The sea urchin was adjusted on the metal spike (which fitted through the perforation in the bottom part of the first container)

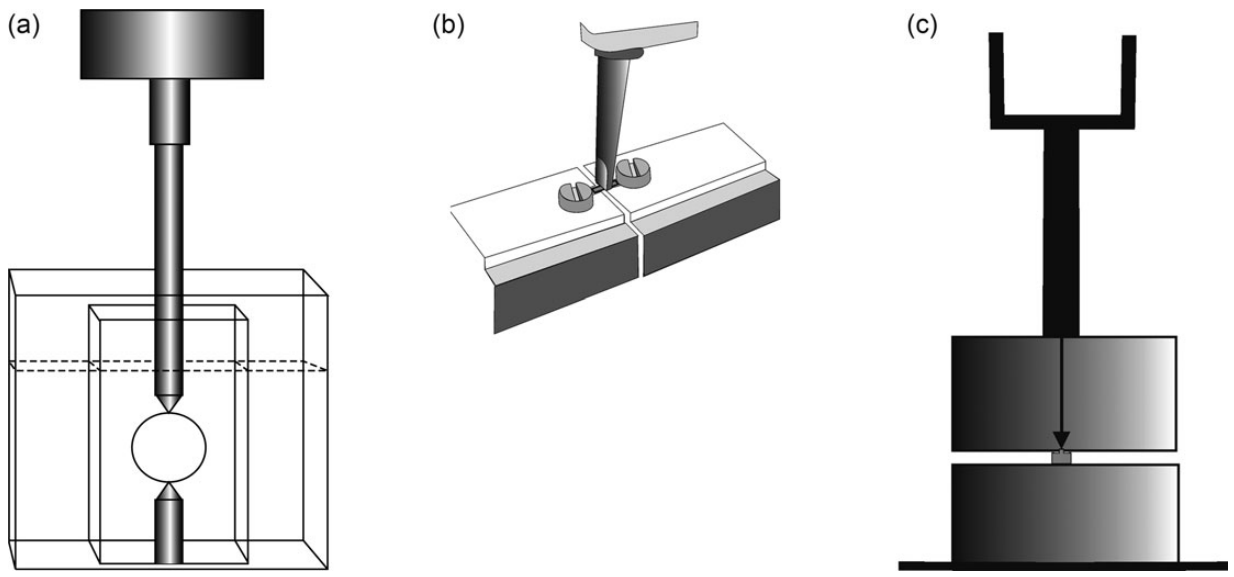

Figure 2. Schematic representation of the devices used for the mechanical tests. (a) "Jaw" device to test the strength of whole live sea urchins, (b) three-point bending stand and non-cutting blade for ambital plates, and (c) simple compression device for apical plates.

in such a way that the ambitus was balanced upon it. The mechanical test was performed using a second metal spike fixed on the load frame of a force stand (Instron 5543, Instron, Norwood, MA, USA) which was lowered at a speed of 0.35 mm min^{-1} until perforation of the test. A slow compression speed was used to avoid the rupture of the test sutures instead of the plates (Byrne *et al.*, 2014). Displacement and force were recorded continuously at a frequency of 10 Hz. Each sea urchin was tested three times, turning the sea urchin 60° each time.

All mechanical tests performed on the individual plates were carried out at room temperature (21 to 23°C). The individualized plates were cleaned of soft tissues by soaking in NaOCl 2.5% for 1.5 h and then in NaOCl 5.25% for 2.5 h; this was monitored using a dissecting microscope. In both cases, the solution was mixed frequently to immediately neutralize the lactic acid forming naturally at the surface of the skeleton during tissue digestion.

To measure the fracture force of the ambital plates, a three-point bending test was performed. The largest, and so oldest, plates were chosen. Each ambital plate was first photographed sideways in front of millimetre paper to measure the effective length (length in-between the two supporting points; see Moureaux *et al.*, 2011) and the thickness of the plates using the Image J software (Rasband, W.S., U.S. National Institutes of Health, Bethesda, MD, USA). They were then placed on a metal stand and the mechanical test was performed using a non-cutting blade fixed on the load frame of the force stand (Instron 5543) which was lowered on the primary tubercle of the plate at a speed of 0.1 mm min^{-1} (three-point bending test) until fracture (Figure 2b). Displacement and force were recorded continuously at a frequency of 10 Hz. The two halves of the plates were recovered and one was mounted on an aluminium stub, coated with gold for 4 min (JFC-1100 E ion sputter), and observed in a scanning electron microscope (JEOL JSM-6100). Digital pictures of the cross sections were recorded and subsequently used in ImageJ with the macro MomentMacro developed for the calculation of the second moment of area (I_2) (Ruff C., Johns Hopkins University School of Medicine, MD, USA) and for the measure of the plate density. I_2 is a measure of the distribution of the stereom within the plate. The density reflects the proportion of stereom in the plate fracture surface (vs. pores). The apparent Young's modulus (E_1), characterizing the material's stiffness, was calculated according to the linear-elastic beam theory:

$$I_2 = \int y^2 \mathrm{d}A(\mathrm{m}^4),$$
$$E_1 = \frac{F_{\max} {L_e}^3}{48 \Delta L I_2}$$

where F_{max} is the force at fracture (N), A the area (in transverse section) (m^2), ΔL the displacement (m), L_e the effective length (m), and y the distance from the neutral plane (m) (Moureaux *et al.*, 2011).

The fracture force of the apical plates was tested using a simple compression method. The plates chosen were the smallest ones available, as they are the youngest. Each apical plate was first photographed sideways in front of millimetre paper to measure the effective length of the plates as well as the diameter of the tubercle for subsequent estimation of the area of contact using the ImageJ software. They were then placed on a metal block and the mechanical test was carried out using a second metal block fixed on the load frame of the force stand (Instron 5543) which was lowered on the tubercle of the plate at a speed of 0.3 mm min^{-1} (simple compression test) until fracture (Figure 2c). Displacement and force were recorded continuously at a frequency of 10 Hz. All apical plates were fractured into two pieces and not crushed. To determine the Young's modulus for the apical plates, the force–displacement curves were transformed into stress–strain curves using the following equations:

$$\text{Stress}: \quad \varepsilon = \frac{\Delta L}{L_e},$$
$$\text{Strain}: \quad \sigma = \frac{F}{A}.$$

where F is the force at a time point (N), A the area of the tubercle calculated from the picture using ImageJ software (m^2), ΔL the displacement (m), and L_e the effective length (m). The E_1 is calculated as the slope between two points of the final linear part of the curve, in this case the maximum force and the 100th point before that.

$$E_1 = \frac{\sigma_{\max} - \sigma_{100\text{th point}}}{\varepsilon_{\max} - \varepsilon_{100\text{thpoint}}}(\mathrm{Pa}).$$

Finally, nanoindentation measurements were realized to test the strength of the calcium carbonate itself. For nanoindentation analysis, the samples were embedded in epoxy resin and polished until the calcium carbonate of the skeleton was exposed at the surface. Thereafter, they were ultra-polished using sandpapers of increasing grain size (from 180 to 2400), and then with aluminium oxide. Each plate was measured once and three plates from each type from three individuals were analysed for each treatment. The nanoindentation measurements were done using a nanoindenter (TriboIndenter, Hysitron, Minneapolis, MN, USA) with a charge of 3000 μN and a Berkovich tip (a low charge was chosen to avoid any confounding effect of the resin; Presser *et al.*, 2010). The sample elastic modulus (Young's modulus; E_2) and hardness values were automatically determined from the unloading curve of the indentation test (Oliver and Pharr, 1992).

Statistical analysis

All ANOVA models were built according to the recommendations of Doncaster and Davey (2007). Data obtained from the samples of intertidal pools and CO_2 seeps were tested using a two-factor nested ANOVA (tide pool or site, fixed factor; sea urchin, random factor nested within tide pool or site) followed by Tukey tests for multiple comparisons. For the laboratory experiment measures, the data were regrouped under a variable named "condition" which figured the different treatments (380A, 750A, 1000A, 380A+2, and 750A+2) as using a fully crossed model was not possible due to the lack of a 1000-μatm treatment with increased temperature. Data other than nanoindentation measurements obtained from the samples of the laboratory experiment were tested using a nested cross-factored model ANOVA (condition, fixed factor; aquarium, random factor nested within condition; sea urchin, random factor nested within aquarium). The nested ANOVAs are model III ANOVAs which consider that the individuals sampled in the same tanks are not true replicates (MS of the seawater pH effect/MS of the tanks nested in seawater pH to calculate the F-ratio instead of using the MS of the model error) (Doncaster and Davey, 2007). Nanohardness measurements for the laboratory experiment were analysed using a two-factor nested ANOVA (condition, fixed factor; sea urchin, random factor nested within condition) as only one sea urchin per aquarium was used. When fracture force was significantly

correlated with length, ANCOVAs were used with size as a covariate (whole sea urchins for the tide pools, apical plates for the tide pools and the laboratory experiment, ambital plates for the laboratory experiment). All correlation analyses were carried out using simple correlations of Spearman with associated Bonferroni probabilities. All tests were realized using the software Systat 12 (Systat Software Inc., USA). Among treatment responses were also assessed using logarithmic response ratios according to the equations from Hedges *et al.* (1999) for L and the 95% confidence interval (CI). Results of the analysis are reported in Supplementary Figure S1.

Results

Twelve-month laboratory acclimation

A summary of the values measured and the results of the statistical analyses are presented in Table 4. There was no significant difference in the length of the ambital plates from the different treatments (condition ANOVA, $p = 0.998$) or of the apical plates (condition ANOVA, $p = 0.934$). The fracture force of the ambital plates was significantly correlated with the effective length of the plate (L_e range: 4.5–12.0 mm; $n = 171$; $r = 0.263$, $p = 0.001$) and also to the size at the ambitus of the sea urchin (ambitus range: 29.4–54.7 mm; $n = 171$; $r = 0.329$, $p < 10^{-3}$). For the apical plates, the fracture force was correlated with the effective length of the plates (L_e range: 1.0–3.6 mm; $n = 171$; $r = 0.221$, $p = 0.004$) and to the size at the ambitus of the sea urchin (ambitus range: 29.4–54.7 mm; $n = 171$; $r = 0.210$, $p = 0.006$). The mechanical properties measured on the ambital plates and the apical plates for individuals from the five different treatments did not show any significant differences according to treatment [condition AN(C)OVA, $p \geq 0.315$]. This was confirmed by the log response ratio analysis (Supplementary Figure S1a).

Intertidal pools

A summary of the values measured and the results of the statistical analyses are presented in Table 5. There was no significant difference in the length of the ambital plates from the different tide pools (tide pool ANOVA, $p = 0.090$) or of the apical plates (tide pool ANOVA, $p = 0.400$). The fracture force of whole sea urchins was significantly correlated with size at the ambitus of the sea urchin (ambitus range: 27.2–42.7 mm; $n = 30$; $r = 0.416$, $p = 0.022$). The force needed to break whole sea urchins did not differ significantly between the individuals from the different tide pools (tide pool ANCOVA, $p = 0.543$). This was confirmed by the log response ratio analysis (Supplementary Figure S1b).

The fracture force for the ambital plates was neither correlated with the effective length of the plate (L_e range: 4.1–7.9 mm; $n = 90$; $r = -0.018$, $p = 0.867$) nor correlated with the size at the ambitus of the sea urchin (ambitus range: 29.4–40.2 mm; $n = 90$; $r = -0.180$, $p = 0.089$). The fracture force needed to break the ambital plates differed significantly according to the tide pool of origin of the sea urchins (tide pool ANOVA, $p = 0.041$), with the plates from individuals of tide pool A breaking at a lower force

Table 4. Results of the different mechanical tests (mean ± s.d.) and of the statistical analyses performed on the samples from *P. lividus* sea urchins from the laboratory experiment.

Mechanical test	Mechanical property	380 A	750 A	1000 A	380 A+2	750 A+2	AN(C)OVA *F*	AN(C)OVA *p*	*n*
Ambital plates	*F* (N)	11.5 ± 3.7	12.7 ± 4.2	13.4 ± 4.3	12.4 ± 5.1	13.5 ± 4.1	0.077	0.971	10, 11, or 12
	E_1 (GPa)	11.2 ± 4.8	9.2 ± 4.3	10.9 ± 5.1	10.7 ± 6.6	8.3 ± 4.7	$<10^{-3}$	1.000	10, 11, or 12
	I_2 ($\times 10^{-13}$ m^4)	1.7 ± 1.2	1.9 ± 1.1	1.6 ± 1.1	1.6 ± 0.9	2.1 ± 1.7	1.069	0.315	10, 11, or 12
	H (GPa)	4.3 ± 0.7	4.3 ± 0.5	4.4 ± 0.7	4.1 ± 0.6	4.4 ± 0.7	0.222	0.920	3
	E_2 (GPa)	57.1 ± 10.9	57.4 ± 9.3	59.5 ± 12.1	53.4 ± 13.6	48.1 ± 20.0	0.542	0.709	3
Apical plates	*F* (N)	25.5 ± 9.8	26.5 ± 10.6	23.3 ± 8.4	23.9 ± 12.0	22.9 ± 9.3	$<10^{-3}$	0.994	10, 11, or 12
	E_1 (GPa)	1.3 ± 0.7	1.6 ± 1.0	1.5 ± 0.8	1.3 ± 0.7	1.6 ± 0.9	0.020	0.980	10, 11, or 12
	H (GPa)	4.6 ± 0.3	4.2 ± 0.5	4.3 ± 0.5	4.5 ± 0.6	4.3 ± 0.8	0.805	0.549	3
	E_2 (GPa)	61.7 ± 11.9	46.0 ± 16.3	54.1 ± 15.0	56.5 ± 7.2	50.1 ± 11.2	0.718	0.599	3

F, force at fracture; E_1, Young's modulus calculated from the mechanical test (three-point bending for ambital plates or simple compression for apical plates); E_2, Young's modulus obtained from nanoindentation measurements; I_2: second moment of area; *H*, hardness from nanoindentation measurements.

Table 5. Results of the different mechanical tests (mean ± s.d.) and of the statistical analyses performed on the samples from *P. lividus* sea urchins from the intertidal pools.

Mechanical test	Mechanical property	Tide pool A (low variation)	Tide pool B (intermediate)	Tide pool C (high variation)	AN(C)OVA *F*	AN(C)OVA *p*	*n*
Whole sea urchin	*F* (N)	58.1 ± 10.6	61.2 ± 14.5	51.8 ± 9.4	0.625	0.543	10
Ambital plates	*F* (N)	9.6 ± 3.8^a	10.5 ± 3.0^{a,b}	12.6 ± 3.1^b	3.616	**0.041**	10
	E_1 (GPa)	9.1 ± 6.1	9.3 ± 6.7	6.7 ± 4.6	1.267	0.298	10
	I_2 ($\times 10^{-13}$ m^4)	1.3 ± 0.6	1.4 ± 0.9	1.4 ± 0.7	1.196	0.318	10
	H (GPa)	4.6 ± 1.3	3.7 ± 0.9	3.8 ± 0.7	3.919	0.082	3
	E_2 (GPa)	62.0 ± 8.1^a	44.6 ± 10.7^b	46.7 ± 10.4^b	11.048	**0.010**	3
Apical plates	*F* (N)	24.8 ± 6.9	27.5 ± 7.2	26.4 ± 7.7	0.981	0.388	10
	E_1 (GPa)	1.2 ± 0.6	1.5 ± 0.8	1.2 ± 0.7	1.378	0.269	10
	H (GPa)	4.8 ± 1.2	4.1 ± 0.8	4.3 ± 1.4	0.419	0.676	3
	E_2 (GPa)	56.1 ± 12.7	55.1 ± 12.0	58.3 ± 12.3	0.109	0.899	3

Probabilities in bold highlight a significant difference ($p < 0.05$). Means sharing the same superscript are not significantly different ($p > 0.05$). *F*, force at fracture; E_1, Young's modulus calculated from the mechanical test (three-point bending for ambital plates or simple compression for apical plates); E_2, Young's modulus obtained from nanoindentation measurements; I_2, second moment of area; *H*, hardness from nanoindentation measurements.

Table 6. Results of the different mechanical tests (mean ± s.d.) and of the statistical analyses performed on the samples from *P. lividus* sea urchins from the CO_2 seep sites.

Mechanical test	Mechanical property	Control site	Low pH site	ANOVA *F*	ANOVA *p*	*n*
Ambital plates	*H* (GPa)	3.7 ± 0.9	4.1 ± 1.0	0.535	0.505	3
	E (GPa)	44.7 ± 3.7	50.4 ± 22.4	0.195	0.682	3
Apical plates	*H* (GPa)	3.8 ± 0.6	3.7 ± 1.0	0.058	0.822	3
	E (GPa)	43.3 ± 8.9	38.4 ± 19.4	0.167	0.704	3

E, Young's modulus obtained from nanoindentation measurements; *H*, hardness from nanoindentation measurements.

than those from the tide pool C ($p_{Tukey} = 0.036$), whereas the forces measured for individuals of tide pool B were not different from that of any of the two other tide pools ($p_{Tukey} \geq 0.189$). The log response ratio analysis did not find any significant effect, although the force needed to break the ambital plates of sea urchins from tide pool C was on the margin of being significantly different from that of sea urchins from tide pool A ($L = 0.27$; 95% CI between −0.02 and 0.56). The Young's modulus measured via nanoindentation (E_2) showed significant differences according to the tide pool from which the sea urchins originated (tide pool ANOVA, $p = 0.010$), with those from tide pool A having significantly greater E_2 values than those from the two other tide pools ($p_{Tukey} \leq 0.012$). Those from tide pools B and C had E_2 that did not differ from each other ($p_{Tukey} = 0.856$). The difference in E_2 between sea urchins from tide pools A and B was confirmed by the log response ratio analysis ($L = -0.33$; 95% CI between −0.020 and −0.639). With this analysis, the difference in E_2 between the sea urchins of tide pools A and C was on the margin of significance ($L = -0.28$; 95% CI between 0.009 and −0.576; Supplementary Figure S1b). The modulus measured via the three-point bending method (E_1) did not show any significant difference in between the individuals from the different tide pools (tide pool ANOVA, $p = 0.298$). No other parameter measured differed significantly (tide pool ANOVA, $p \geq 0.082$). There were no significant differences in thickness of the plates (tide pool ANOVA, $p = 0.158$), which was of 0.6 ± 0.1, 0.7 ± 0.1, and 0.7 ± 0.1 mm for tide pools A, B, and C, respectively. Also, there was no significant difference in the density of the skeleton within the plates (tide pool ANOVA, $p = 0.496$), which was of 81 ± 18, 79 ± 18, and 75 ± 24% for tide pools A, B, and C, respectively.

The fracture force of the apical plates was significantly correlated with the effective length of the plate (L_e range: 1.3–2.9 mm; $n = 88$; $r = 0.460$, $p < 10^{-3}$) but not with the size at the ambitus of the sea urchin (ambitus range: 29.4–40.2 mm; $n = 88$; $r = 0.019$, $p = 0.857$). Apical plates from the sea urchins originating from the three tide pools showed no significant differences for any of the parameters measured [tide pool AN(C)OVA, $p \geq 0.269$]. This was confirmed by the log response ratio analysis (Supplementary Figure S1b).

CO_2 seep site

A summary of the values measured and the results of the statistical analyses are presented in Table 6. None of the nanoindentation parameters measured on the ambital and apical plates differed significantly between the individuals from the control site and those from the low pH site (site ANOVA, $p \geq 0.505$). This was confirmed by the log response ratio analysis (Supplementary Figure S1c).

Discussion

The results of this study showed that long-term (12-month) laboratory exposure to reduced pH (8.0 as control, 7.9, and 7.8) and increased temperature (+2°C) had no statistically significant effect on the skeletal mechanical properties of the sea urchin *P. lividus*. Similar conclusions are drawn from the observations for sea urchins exposed to naturally constant low pH conditions at the CO_2 seep site.

However, tide pool sea urchins exposed to the most variable pH (ΔpH: −0.4 to −0.5) showed ambital plates with a significantly (although marginally) higher fracture force and a lower Young's modulus, i.e. a lower stiffness, than those from sea urchins in tide pools characterized by smaller pH fluctuations (ΔpH: −0.2). Sea urchins growing in tide pools with large pH fluctuations may experience reduced growth rates and show a modified allocation of resources. This leads to increased maintenance of the skeleton and thickening, as was shown for sea urchins living in wave exposed environments compared with those living in protected areas (Ebert, 1975). However, thickness of the plates was not significantly different for individuals from the different tide pools (0.6–0.7 mm). Reduced growth may also result in a density increase of the test (Smith, 1980). However, there were no significant differences in the density of the plates in-between the individuals from the different tide pools. In fact, the material properties themselves were modified, resulting in a higher flexibility. Changes in material properties according to subpopulations of *P. lividus* from the same region were also found for the spines and were correlated with differences in wave exposure (Moureaux *et al.*, 2010). This change in flexibility is probably the reason the fracture force increases: as the material composing the plate increases in flexibility, the bending tension that the plate can withstand before it breaks also increases. Depending on the energetic cost of these changes, this may lead to changes in growth rates and gonad development (e.g. Stumpp *et al.*, 2012). The sea urchins from the tide pool with the largest pH variability and showing changes of mechanical properties are on average much smaller in size than those from the other tide pools (although for this study specimens of the same size were purposely collected in each tide pool) (MC, pers. obs.). Interestingly, the tide pools harbouring sea urchins with a higher fracture force mainly contained encrusting calcifying algae, whereas the two other pools contained erected non-calcifying macroalgae (Table 2). This is reminiscent of results by Asnaghi *et al.* (2013) who showed that acidification effects on growth and skeleton strength were increased when juvenile *P. lividus* were fed non-calcifying algae compared with those fed coralline algae. This result is particularly interesting as it has been shown recently that fleshy algae are usually favoured by reduced seawater pH over crustose algae, including in rock pools (Olischläger *et al.*, 2013).

The results from the laboratory experiment and from field exposed sea urchins at the CO_2 seeps in Vulcano showed that long-term exposure to moderate seawater acidification and warming, in the range expected by 2100, did not affect the mechanical properties of the skeleton plates of *P. lividus*. This observation holds for ambital

plates but also for the apical plates which were entirely or mostly formed during the long-term experiment. This supports the short-term (6 weeks) results of Holtmann *et al.* (2013) on *Strongylocentrotus droebachiensis*. Our results also agree with observations showing that some sea urchins do survive well and calcify in waters undersaturated for aragonite and/or calcite, such as deep waters or upwelling regions, but also when their coelomic fluid is undersaturated for $CaCO_3$ (David *et al.*, 2005; Calosi *et al.*, 2013b; Collard *et al.*, 2014a, b). The lack of any temperature effect in our study may be due to the small temperature increment applied. Indeed, except for summer period (months 6–9), the sea urchins were exposed to temperatures which were within their natural seasonal range, although it should be noted that in the field such increases temperature are transitory and not chronic as in the present study. *Paracentrotus lividus* is also a eurythermal species as its distribution limits correspond more or less to the 8°C winter and 28°C summer isotherms (Boudouresque and Verlaque, 2013). Hermans *et al.* (2010) also showed that *P. lividus* juveniles maintained at temperatures ranging from 13 to 24°C did not show differences in growth rates after 6 months of exposure. This lack of a significant pH and/or temperature effect on skeletal mechanical properties might appear contradictory to the decrease in the abundance of *P. lividus* observed near CO_2 seeps (Hall-Spencer *et al.*, 2008; Calosi *et al.*, 2013b). However, the ability of the sea urchins to build their skeleton under low pH conditions does not preclude other problems such as energetic costs linked to the need of eliminating protons from the calcification site, making the seep sites not unbearable but less favourable compared with surrounding sites where the main food source, non-calcified macroalgae, is less abundant but the pH not so low (Calosi *et al.*, 2013b).

Similar mechanical results were found for the serpulid tubeworm *Hydroides elegans* for which Chan *et al.* (2013) showed no significant impact of pH on hardness (H) or the Young's modulus (E_2) of the worm tubes exposed to a pH of 7.8 for 17 d, the tubes were completely formed in reduced pH conditions. However, they did find a significant increase in H and E_2 under strongly increased temperature conditions ($\Delta T = 6$°C). For the bivalve *Arctica islandica* exposed to pH down to 7.8 for 90 d, no modifications of the shell growth rate or the shell microstructure were reported (Stemmer *et al.*, 2013). Finally, the same was observed for the barnacle *Amphibalanus improvisus* with shells exhibiting no difference in strength after exposure to a pH of 7.5 for 12 and 20 weeks and of 7.3 for 86 d (Pansch *et al.*, 2013, 2014). However, in the latter case, food availability increased the strength of the shells (Pansch *et al.*, 2014).

E_1 values measured for *P. lividus* ambital test plates ranged between 7 and 11 GPa. These values are lower than those measured previously for the spines of the same species which averaged 22 GPa (Moureaux *et al.*, 2010). This is due to differences in the shape (rectangular cuboid vs. cone) and structure (unorganized mesh structure vs. highly organized structure formed of radial septa linked by stereomic bridges) of the plates and spines (Smith, 1980; Moureaux *et al.*, 2010). Alternatively, values obtained via nanoindentation (E_2) were of 38–60 GPa and are of the same order of magnitude than those for sea urchin spines and for other marine invertebrates, analysed with the same method (Table 7). These values are much higher than E_1 values obtained via the bending test. Such a difference between E_1 and E_2 was reported previously for sea urchins (Moureaux *et al.*, 2010; Presser *et al.*, 2010) and may be explained by the method of calculation of I_2 and the anisotropic nature of the material. On the contrary, the E values obtained through nanoindentation (at very small indentation loads) are measured directly within the material (Presser *et al.*, 2010). This could suggest that nanoindentation is more appropriate and should be favoured when investigating the material properties. However, bending tests are more relevant on the ecological point of view as they provide the fracture forces and stiffness characteristics directly in relation to forces to which the sea urchin is submitted.

The values obtained for E_1, E_2, and H were all in the same range, no matter the origin of the sea urchins. The processes regulating the structure and composition of the calcite mineral are thus similar in all the different populations studied here. The values measured for both nanoindentation parameters are similar, or sometimes higher for H, to those measured in other sea urchins and some marine invertebrates (Table 7). As reported previously, the biogenic calcite produced by the sea urchins shows mechanical properties different from that of pure calcite with hardness increased by ~1 GPa, and stiffness reduced by ~20 GPa. This implies a more flexible material which is more resistant when hit for instance by pebbles displaced by waves or when facing predator attacks (Guidetti and Mori, 2005). The strength of the test of whole live sea urchins submitted to a perforation stress is on average 57 ± 5 N. Considering that the force developed by the jaw of a great barracuda (the only fish for which jaw force is available) may reach 93 N (Habegger *et al.*, 2011), the device we used in this study is well suited to replicate a fracture test in the same order of magnitude as what could be induced by the jaw of a fish: for example, that of *Diplodus sargus* or *Diplodus vulgaris*, two species of fish which turn the sea urchins upside down and attack the skeleton until it fractures (Guidetti and Mori, 2005). The fracture forces for the ambital and apical plates averaged 12 and 25 N, respectively; the difference is probably due to the different methodologies used (see the "Material and methods" section). The obtained values for the ambital plates correspond to those reported by Ellers *et al.* (1998) for the sea urchin *S. droebachiensis*, using the same method of three-point bending, which were of 12–20 N. Fracture force of apical and ambital plates was correlated with the effective length and/or to the ambital size of the sea urchin. This is probably due to changes in plate length/width during the growth of the sea urchin (Deutler, 1926). The effect of the ambital plates size was only evidenced in the laboratory experiment because of a narrower size range in the tide pool urchins, as previously reported by Ellers *et al.* (1998).

The results indicate that *P. lividus* can building a skeleton mechanically efficient when exposed to pH values close to that predicted for 2100 in laboratory and field conditions. Significant differences were only recorded between sea urchins from tide pools with different natural levels of pH fluctuation. As factors other than pH differ between these tide pools (Table 2), the observed differences cannot be attributed without ambiguity to pH alone. In fact, differences in mechanical properties of the sea urchin spines were previously reported and linked to factors such as wave exposure or food availability (Moureaux and Dubois, 2012). The effect of food availability on the capacity of organisms to build a skeleton as shown in barnacles by Pansch *et al.* (2014) and that of a calcified diet would deserve further investigation as emphasized by Asnaghi *et al.* (2013, 2014) and Moulin *et al.* (2014). Also, individuals living in very variable environments did not cope better with changes predicted to occur by the end of this century. Sea urchins studied here were sampled from very different environments and still all showed similar skeleton mechanical properties, thus confirming the validity of our general results. This is in accordance with the results of LaVigne *et al.* (2013) who found no variation in skeletal composition

Table 7. Values (mean ± s.d.) of nanohardness (*H*) and Young's modulus (*E*) measured via nanoidentation using a Berkovitch tip reported for organisms producing calcium carbonate minerals.

Group	Species	Structure	Load (μN)	*H* (GPa)	*E* (GPa)	Reference
Pure calcite			5×10^{-3}	2.4 ± 0.1	74.4 ± 2.9	Raman and Kumar (2011)
				2.7 ± 0.2	73.5 ± 2.9	Ma *et al.* (2008)
			15×10^{3}	1.9 ± 0.1	76.6 ± 1.9	Presser *et al.* (2010)
Pure dolomite				6.5 ± 0.9	117 ± 7.8	Ma *et al.* (2008)
Euechinoid	*Paracentrotus*	Spines—septa	50×10^{3}	3.8 ± 0.3	58.6 ± 3.8	Moureaux *et al.* (2010)
Sea urchin	*lividus*	Spines—central stereom	50×10^{3}	1.8 ± 0.7	32.2 ± 3.3	Moureaux *et al.* (2010)
		Ambital plates—tidal pools	3×10^{3}	4.0 ± 1.0	51.1 ± 13.7	This study
		Ambital plates—laboratory experiment	3×10^{3}	4.3 ± 0.6	55.1 ± 13.7	This study
		Ambital plates—CO_2 seeps	3×10^{3}	3.9 ± 0.9	47.6 ± 17.4	This study
		Apical plates—tidal pools	3×10^{3}	4.4 ± 1.2	56.5 ± 11.9	This study
		Apical plates—laboratory experiment	3×10^{3}	4.4 ± 0.6	53.7 ± 13.3	This study
		Apical plates—CO_2 seeps	3×10^{3}	3.8 ± 0.8	40.8 ± 14.9	This study
	Heterocentrotus	Spine—Growth ring 1	15×10^{3}	3.7 ± 0.3	61.9 ± 2.7	Presser *et al.* (2010)
	mamillatus	Spine—Growth ring 2	15×10^{3}	3.4 ± 0.4	62.6 ± 3.7	Presser *et al.* (2010)
		Spine—Growth ring 3	15×10^{3}	3.5 ± 0.3	60.9 ± 4.0	Presser *et al.* (2010)
		Spine—Growth ring 4	15×10^{3}	3.4 ± 0.4	61.5 ± 3.9	Presser *et al.* (2010)
		Spine—Outer porous area	15×10^{3}	3.3 ± 0.3	50.5 ± 3.0	Presser *et al.* (2010)
		Spine—Inner porous area	15×10^{3}	3.1 ± 0.4	39.8 ± 6.1	Presser *et al.* (2010)
Cidaroid	*Phyllacanthus*	Spine—Outer porous area	15×10^{3}	4.0 ± 0.3	48.4 ± 4.2	Presser *et al.* (2010)
Sea urchin	*imperialis*	Spine—Middle porous area	15×10^{3}	4.0 ± 0.5	46.9 ± 5.1	Presser *et al.* (2010)
		Spine—Inner porous area	15×10^{3}	2.8 ± 0.8	28.9 ± 5.8	Presser *et al.* (2010)
	Prinocidaris	Spine—Porous outer part	15×10^{3}	3.9 ± 0.4	59.1 ± 5.0	Presser *et al.* (2010)
	baculos	Spine—Massive outer part (cortex)	15×10^{3}	3.5 ± 0.2	71.7 ± 3.8	Presser *et al.* (2010)
		Spine—Outer porous area	15×10^{3}	3.7 ± 0.5	52.8 ± 7.8	Presser *et al.* (2010)
		Spine—Inner porous area	15×10^{3}	3.5 ± 0.5	48.5 ± 5.7	Presser *et al.* (2010)
Serpulid tubeworm	*Hydroides elegans*	Tube	$1.5–7 \times 10^{3}$	1.5–3	20–50	Chan *et al.* (2013) (from Figure 3a)
Barnacle	*Amphibalanus reticulatus*	Pariete outer lamina	5×10^{-3}	3.3 ± 0.2	66.3 ± 2.7	Raman and Kumar (2011)
Oyster	*Crassostrea gigas*	Folia	5×10^{-3}	3.2 ± 0.1	73 ± 1.2	Lee *et al.* (2008)
Pteropod	*Limacina helicina antarctica*	Piece of shell	5×10^{3}	2.3 ± 0.1	45.3 ± 0.9	Teniswood *et al.* (2013)
	Cavolinia uncinata	Shell—transverse cross section	$1.2–1.3 \times 10^{3}$	5.2 ± 0.4	85.9 ± 2.7	Zhang *et al.* (2011)
		Shell—parallel section	$1.2–1.3 \times 10^{3}$	5.6 ± 0.3	51.5 ± 1.6	Zhang *et al.* (2011)

Values from this study are averages of the data from all treatments.

according to environmental conditions in adult *Strongylocentrotus purpuratus*. Because test integrity defines individual predation risk, and thus survival (unlike spines which are easily regenerated in *P. lividus*), the fact that neither the calcification nor some aspects of physiology of *P. lividus* are highly affected by ocean acidification, at least over short-term exposure (Calosi *et al.*, 2013b; Collard *et al.*, 2013, 2014b), points out that this species structural integrity, activity and survival at the adult stage should not be significantly compromised by near-future changes in ocean chemistry. However, reduced seawater pH can affect some of their primary food item (e.g. algae; Asnaghi *et al.*, 2013; Borell *et al.*, 2013; Burnell *et al.*, 2013). In fact, Asnaghi *et al.* (2013) showed that calcifying algae lose weight with an increased pCO_2 and that sea urchin grazing increased this phenomenon, whereas non-calcifying algae did not seem affected by reduced seawater pH. Similarly, Burnell *et al.* (2013) showed that ocean acidification and warming accentuated sea urchin grazing. The results of our study combined to those of previously published research indicate a good resistance of sea urchin skeleton to reduced seawater pH, contrarily to what was suggested. As the calcification process is intracellular in sea urchins, this is not so surprising as the calcification fluid composition may be biologically controlled.

Authors' contributions

MC was responsible for the original concept and was supported in the development of the concept by PD, SPSR, and FD. MC also analysed all the data and wrote the manuscript. Test samples from the lab experiment were collected and prepared by MC and SPSR, with the water chemistry analysed by HSF, supported by PC and SW. Test samples from the tide pools were collected and prepared by MC and YD, supported by LM. Test samples from the CO_2 seep site were collected and prepared by SPSR supported by MM and JMH-S. The analysis of the mechanical properties of the test samples was carried out by MC and YD supported by PD and JD. All the authors contributed to the final manuscript.

Supplementary data

Supplementary material is available at the *ICESJMS* online version of the manuscript.

Acknowledgements

MC and LM are the holders of a Belgian FRIA grant. PD is a Research Director of the National Fund for Scientific Research (FRS-FNRS; Belgium). SPSR and the laboratory experiment were supported by

UKOA NERC Consortium Grant "Impacts of ocean acidification on key benthic ecosystems, communities, habitats, species and life cycles" (grant NE/H017127/1) awarded to SW and PC. The collection/analysis of samples was also supported by FRFC contract 2.4532.07 (Belgium). All the work at the CO_2 seep site was supported by a NERC AVA grant awarded to SPSR. The authors also acknowledge the support of the EU FP7 MedSeA Project awarded to PC, MM and JH-S. We would also like to thank members of the Plymouth Marine Laboratory for their help with system design and maintenance, including J. Nunes and A. Beesley. We would also like to thank M. Bauwens, P. Postiau, and S. De Kegel for their technical help; in addition to Helen Graham, Daniel Small, and Camilla Bertolini for assisting in the field. Also thank you to Dr Chris Hauton, whose comments helped improve an early version of this manuscript.

References

Asnaghi, V., Chiantore, M., Mangialajo, L., Gazeau, F., Francour, P., Alliouane, S., and Gattuso, J. P. 2013. Cascading effects of ocean acidification in a rocky subtidal community. PLoS One, 8: e61978.

Asnaghi, V., Mangialajo, L., Gattuso, J. P., Francour, P., Privitera, D., and Chiantore, M. 2014. Effects of ocean acidification and diet on thickness and carbonate elemental composition of the test of juvenile sea urchins. Marine Environmental Research, 93: 78–84.

Boatta, F., D'Alessandro, W., Gagliano, A. L., Liotta, M., Milazzo, M., Rodolfo-Metalpa, R., Hall-Spencer, J. M., *et al.* 2013. Geochemical survey of Levante Bay, Vulcano Island (Italy), a natural laboratory for the study of ocean acidification. Marine Pollution Bulletin, 73: 485–494.

Boudouresque, C. F., and Verlaque, M. 2013. *Paracentrotus lividus*. *In* Sea Urchins: Biology and Ecology. Developments in Aquaculture and Fisheries Science, 3rd edn, 38, pp. 297–327. Ed. by J. M. Lawrence. Elsevier, London, UK. 531 pp.

Borell, E. M., Steinke, M., and Fine, M. 2013. Direct and indirect effects of high pCO_2 on algal grazing by coral reef herbivores from the Gulf of Aqaba (Red Sea). Coral Reefs, 32: 937–947.

Burnell, O. W., Russell, B. D., Irving, A. D., and Connell, S. D. 2013. Eutrophication offsets increased sea urchin grazing on seagrass caused by ocean warming and acidification. Marine Ecology Progress Series, 485: 37–46.

Byrne, M., Smith, A., West, S., Collard, M., Dubois, P., Graba-landry, A., and Dworjanyn, S. 2014. Warming influences Mg^{2+} content, while warming and acidification influence calcification and test strength of a sea urchin. Environmental Science and Technology, 48: 12620–12627.

Caldeira, K., and Wickett, M. 2003. Anthropogenic carbon and ocean pH. Nature, 425: 365.

Calosi, P., Rastrick, S. P. S., Graziano, M., Thomas, S. C., Baggini, C., Carter, H. A., Hall-Spencer, J. M., *et al.* 2013b. Distribution of sea urchins living near shallow water CO_2 vents is dependent upon species acid-base and ion-regulatory abilities. Marine Pollution Bulletin, 73: 470–484.

Calosi, P., Rastrick, S. P. S., Lombardi, C., de Guzman, H. J., Davidson, L., Jahnke, M., Giangrande, A., *et al.* 2013a. Adaptation and acclimatization to ocean acidification in marine ectotherms: an *in situ* transplant experiment with polychaetes at a shallow CO_2 vent system. Philosophical Transactions of the Royal Society, Series B, 368: 20120444.

Chan, V. B., Thiyagarajan, V., Lu, X. W., Zhang, T., and Shich, K. 2013. Temperature dependent effects of elevated CO_2 on shell composition and mechanical properties of *Hydroides elegans*: insights from a multiple stressor experiment. PLoS One, 8: e78945.

Collard, M., De Ridder, C., David, B., Dehairs, F., and Dubois, P. 2014a. Could the acid-base status of Antarctic sea urchins indicate a better-than-expected resilience to near-future ocean acidification? Global Change Biology, doi:10.1111/gcb.12735.

Collard, M., Dery, A., Dehairs, F., and Dubois, P. 2014b. Euechinoidea and Cidaroidea respond differently to ocean acidification. Comparative Biochemistry and Physiology Part A, 174: 45–55.

Collard, M., Laitat, K., Moulin, L., Catarino, A., Grosjean, P., and Dubois, P. 2013. Buffer capacity of the coelomic fluid in echinoderms. Comparative Biochemistry and Physiology Part A, 166: 199–206.

David, B., Choné, T., Mooi, R., and De Ridder, C. 2005. Antarctic Echinoidea. Synopses of the Antarctic Benthos, 10. Koeltz Scientific Books, Königstein, 274 pp.

Dery, A., Guibourt, V., Catarino, A. I., Compère, P., and Dubois, P. 2014. Properties, morphogenesis, and effect of acidification on spines of the cidaroid sea urchin *Phyllacanthus imperialis*. Invertebrate Biology, 133: 188–199.

Deutler, F. 1926. Uber das wachstum des seeigelskeletts. Zoologische Jahrbuecher Abteilung fuer Anatomie und Ontogenie der Tiere, 48: 119–200.

Doncaster, C. P., and Davey, A. J. 2007. Analysis of Variance and Covariance. Cambridge University Press, Cambridge, UK, 287 pp.

Dubois, P. 2014. The skeleton of postmetamorphic echinoderms in a changing world. Biological Bulletin, 226: 223–236.

Dubois, P., and Chen, C. P. 1989. Calcification in echinoderms. *In* Echinoderm Studies, 3, pp. 55–136. Ed. by M. Jangoux, and J. M. Lawrence. Balkema, Rotterdam, The Netherlands, 383 pp.

Dupont, S., Dorey, N., Stumpp, M., Melzner, F., and Thorndyke, M. 2013. Long-term and trans-life-cycle effects of exposure to ocean acidification in the green sea urchin *Strongylocentrotus droebachiensis*. Marine Biology, 160: 1835–1843.

Ebert, T. A. 1975. Growth and mortality of post-larval echinoids. The American Society of Zoologists, 15: 755–775.

Ellers, O., Johnson, A. S., and Moberg, P. E. 1998. Structural strengthening of urchin skeletons by collagenous sutural ligaments. Biological Bulletin, 195: 135–144.

Findlay, H. S., Beesley, A., Dashfield, S., McNeill, C. L., Nunes, J., Queirós, A. M., and Woodward, E. M. S. 2013. UKOA Benthic Consortium, PML intertidal mesocosm experimental environment dataset. British Oceanographic Data Centre - Natural Environment Research Council, UK.

Findlay, H. S., Kendall, M. A., Spicer, J. I., Turley, C., and Widdicombe, S. 2008. Novel microcosm system for investigating the effects of elevated carbon dioxide and temperature on intertidal organisms. Aquatic Biology, 3: 51–62.

Guidetti, P., and Mori, M. 2005. Morpho-functional defences of Mediterranean sea urchins, *Paracentrotus lividus* and *Arbacia lixula*, against fish predators. Marine Biology, 147: 797–802.

Habegger, M. L., Motta, P. J., Huber, D. R., and Deban, S. M. 2011. Feeding biomechanics in the great barracuda during ontogeny. Journal of Zoology, 283: 63–72.

Hall-Spencer, J. M., Rodolfo-Metalpo, R., Martin, S., Ransome, E., Fine, M., Turner, S. M., Rowley, S. J., *et al.* 2008. Volcanic carbon dioxide vents show ecosystem effects of ocean acidification. Nature, 454: 96–99.

Hedges, L. V., Gurevitch, J., and Curtis, P. S. 1999. The meta-analysis of response ratios in experimental ecology. Ecology, 80: 1150–1156.

Hermans, J., Borremans, C., Willenz, P., André, L., and Dubois, P. 2010. Temperature, salinity and growth rate dependences of Mg/Ca and Sr/Ca ratios of the skeleton of the sea urchin *Paracentrotus lividus* (Lamarck): an experimental approach. Marine Biology, 157: 1293–1300.

Holtmann, W. C., Stumpp, M., Gutowska, M., Syré, S., Himmerkus, N., Melzner, F., and Bleich, M. 2013. Maintenance of coelomic fluid pH in sea urchins exposed to elevated CO_2: the role of body cavity epithelia and stereom dissolution. Marine Biology, 160: 2631–2645.

IPCC. 2013. Climate Change 2013: The physical science basis. *In* Contribution of Working Group I to the Fifth Assessment Report of the Intergovernmental Panel on Climate Change. Ed. by T. F. Stocker, D. Qin, G. K. Plattner, M. Tignor, S. K. Allen, J.

Boschung, A. Nauels, Y. Xia, V. Bex, and P. M. Midgley. Cambridge University Press, Cambridge, New York, NY, USA, UK.

Kitidis, V., Hardman-Mountford, N. J., Litt, E., Brown, I., Cummings, D., Hartman, S., Hydes, D., *et al.* 2012. Seasonal dynamics of the carbonate system in the Western English Channel. Continental Shelf Research, 42: 30–40.

Kurihara, H., Yin, R., Nishihara, G. N., Soyano, K., and Ishimatsu, A. 2013. Effect of ocean acidification on growth, gonad development and physiology of the sea urchin *Hemicentrotus pulcherrimus*. Aquatic Biology, 18: 281–292.

LaVigne, M., Hill, T. M., Sanford, E., Gaylord, B., Russell, A. D., Lenz, E. A., Hosfelt, J. D., *et al.* 2013. The elemental composition of purple sea urchin (*Strongylocentrotus purpuratus*) calcite and potential effects of pCO_2 during early life stages. Biogeosciences, 10: 3465–3477.

Lee, S. W., Kim, G. H., and Shoi, C. S. 2008. Characteristic crystal orientation of folia in oyster shell, *Crassostrea gigas*. Materials Science and Engineering C, 28: 258–263.

Ma, Y., Cohen, S. R., Addadi, L., and Weiner, S. 2008. Sea urchin tooth design: an "all-calcite" polycrystalline reinforced fiber composite for grinding rocks. Advanced Materials, 20: 1555–1559.

McDonald, M. R., McClintock, J. B., Amsler, C. D., Rittschof, D., Angus, R. A., Orihuela, B., and Lutostanki, K. 2009. Effects of ocean acidification over the life history of the barnacle *Amphibalanus amphitrite*. Marine Ecology Progress Series, 385: 179–187.

Melatunan, S., Calosi, P., Rundle, S. D., Widdicombe, S., and Moody, A. J. 2013. Effects of ocean acidification and elevated temperature on shell plasticity and its energetic basis in an intertidal gastropod. Marine Ecology Progress Series, 472: 155–168.

Morse, J. W., Andersson, A. J., and Mackenzie, F. T. 2006. Initial response of carbonate-rich shelf sediments to rising atmospheric pCO_2 and "ocean acidification": role of high Mg-calcites. Geochimica and Cosmochimica Acta, 70: 5814–5830.

Moulin, L., Catarino, A., Claessens, T., and Dubois, P. 2011. Effects of seawater acidification on early development of the intertidal sea urchin *Paracentrotus lividus* (Lamarck 1816). Marine Pollution Bulletin, 62: 48–54.

Moulin, L., Grosjean, P., Leblud, J., Batigny, A., and Dubois, P. 2014. Impact of elevated pCO_2 on acid-base regulation of the sea urchin *Echinometra mathaei* and its relation to resistance to ocean acidification: a study in mesocosms. Journal of Experimental Marine Biology and Ecology, 457: 97–104.

Moureaux, C., and Dubois, P. 2012. Plasticity of biometrical and mechanical properties of *Echinocardium cordatum* spines according to environment. Marine Biology, 159: 471–479.

Moureaux, C., Pérez-Huerta, A., Compère, P., Zhu, W., Leloup, T., Cusack, M., and Dubois, P. 2010. Structure, composition and mechanical relations to function in sea urchin spine. Journal of Structural Biology, 170: 41–49.

Moureaux, C., Simon, J., Mannaerts, G., Catarino, A., Pernet, P., and Dubois, P. 2011. Effects of field contamination by metals (Cd, Cu, Pb, Zn) on biometry and mechanics of echinoderm ossicles. Aquatic Toxicology, 105: 698–707.

Olischläger, M., Bartsch, I., Gutow, L., and Wiencke, C. 2013. Effects of ocean acidification on growth and physiology of *Ulva lactuca* (Chlorophyta) in a rockpool-scenario. Phycological Research, 61: 180–190.

Oliver, W. C., and Pharr, G. M. 1992. An improved technique for determining hardness and elastic modulus using load and displacement sensing indentation experiments. Journal of Materials Research, 7: 1564–1583.

Orr, J. C. 2011. Recent and future changes in ocean carbonate chemistry. *In* Ocean Acidification, pp. 41–66. Ed. by J. P. Gattuso, and L. Hansson. Oxford University Press, NY, USA. 326 pp.

Pansch, C., Nasrolahi, A., Appelhans, Y., and Whal, M. 2013. Tolerance of juvenile barnacles (*Amphibalanus improvisus*) to warming and elevated pCO_2. Marine Biology, 160: 2023–2035.

Pansch, C., Schaub, I., Havenhand, J., and Wahl, M. 2014. Habitat traits and food availability determine the response of marine invertebrates to ocean acidification. Global Change Biology, 20: 765–777.

Presser, V., Gerlach, K., Vohrer, A., Nickel, K. G., and Dreher, W. F. 2010. Determination of the elastic modulus of highly porous samples by nanoindentation: a case study on sea urchin spines. Journal of Materials Science, 45: 2408–2418.

Queiros, A. M., Fernandes, J. A., Faulwetter, S., Nunes, J., Rastrick, S. P. S., Mieszkowska, N., Artioli, Y., *et al.* 2014. Scaling up experimental ocean acidification and warming research: from individuals to the ecosystem. Global Change Biology, 21: 130–143.

Raman, S., and Kumar, R. 2011. Construction and nanomechanical properties of the exoskeleton of the barnacle *Amphibalanus reticulatus*. Journal of Structural Biology, 176: 360–369.

Rodolfo-Metalpa, R., Houlbrèque, F., Tambutté, E., Boisson, F., Baggini, C., Patti, F. P., Jeffree, R., *et al.* 2011. Coral and mollusc resistance to ocean acidification adversely affected by warming. Nature Climate Change, 1: 308–312.

Smith, A. 1980. Stereom microstructure of the echinoid test. Palaeontology, 25: 1–81.

Sokolov, A. P., Stone, P. H., Forest, C. E., Prinn, R., Sarofim, M. C., Webster, M., Paltsev, S., *et al.* 2009. Probabilistic forecast for twenty-first-century climate based on uncertainties in emissions (without policy) and climate parameters. Journal of Climate, 22: 5175–5204.

Stemmer, K., Nehrke, G., and Brey, T. 2013. Elevated CO_2 levels do not affect the shell structure of the bivalve *Arctica islandica* from the Western Baltic. PLoS One, 8: e70103.

Stumpp, M., Trübenbach, K., Brennecke, D., Hu, M. Y., and Melzner, F. 2012. Resource allocation and extracellular acid-base status in the sea urchin *Strongylocentrotus droebachiensis*. Aquatic Toxicology, 110–111: 194–207.

Teniswood, C. M., Roberts, D., Howard, W. R., and Bradby, J. E. 2013. A quantitative assessment of the mechanical strength of the polar pteropod *Limacina helicina antarctica* shell. ICES Journal of Marine Science, 70: 1499–1505.

Trousset, J. 1885. Nouveau dictionnaire encyclopédique universel illustré: répertoire des connaissances humaines. Volume 4, p. 372.

Vizzini, S., Di Leonardo, R., Costa, V., Tramati, C. D., Luzzu, F., and Mazzola, A. 2013. Trace element bias in the use of CO_2 vents as analogues for low pH environments: Implications for contamination levels in acidified oceans. Estuarine, Coastal and Shelf Science, 134: 19–30.

Welladsen, H. M., Southgate, P. C., and Heimann, K. 2010. The effects of exposure to near-future levels of ocean acidification on shell characteristics of *Pinctada fucata* (Bivalvia: Pteriidae). Molluscan Research, 30: 125–130.

Wolfe, K., Dworjanyn, S. A., and Byrne, M. 2013. Effects of ocean warming and acidification on survival, growth and skeletal development in the early benthic juvenile sea urchin (*Heliocidaris erythrogramma*). Global Change Biology, 19: 2698–2707.

Zhang, T., Ma, Y., Chen, K., Kunz, M., Tamura, N., Qiang, M., Xu, J., *et al.* 2011. Structure and mechanical properties of a pteropod shell consisting of interlocked helical aragonite nanofibers. Angewandte Chemie International Edition, 50: 10361–10365.

Ziveri, P., Passaro, M., Incarbona, A., Milazzo, M., Rodolfo-Metalpa, R., and Hall-Spencer, J. M. 2014. Decline in coccolithophore diversity and impact on coccolith morphogenesis along a natural CO_2 gradient. Biological Bulletin, 226: 282–290.

Handling editor: Howard Browman

ICES Journal of Marine Science

ICES Journal of Marine Science (2016), 73(3), 739–752. doi:10.1093/icesjms/fsv233

Contribution to Special Issue: 'Towards a Broader Perspective on Ocean Acidification Research'

Original Article

Testing Antarctic resilience: the effects of elevated seawater temperature and decreased pH on two gastropod species

Julie B. Schram*, Kathryn M. Schoenrock, James B. McClintock, Charles D. Amsler, and Robert A. Angus

Department of Biology, University of Alabama at Birmingham, 1300 University Boulevard, CH 464, Birmingham, AL 35294-1170, USA

**Corresponding author: tel: +1 205 975 6097; e-mail: jbschram@uab.edu*

Schram, J. B., Schoenrock, K. M., McClintock, J. B., Amsler, C. D., and Angus, R. A. Testing Antarctic resilience: the effects of elevated seawater temperature and decreased pH on two gastropod species. – ICES Journal of Marine Science, 73: 739–752.

Received 29 June 2015; revised 4 November 2015; accepted 11 November 2015; advance access publication 17 December 2015.

Ocean acidification has been hypothesized to increase stress and decrease shell calcification in gastropods, particularly in cold water habitats like the western Antarctic Peninsula (WAP). There is limited information on how calcified marine benthic invertebrates in this region will respond to these rapidly changing conditions. The present study investigated the effects of elevated seawater temperature and decreased pH on growth (wet mass and shell morphometrics), net calcification, and proximate body composition (protein and lipid) of body tissues in two common benthic gastropods. Individuals of the limpet *Nacella concinna* and the snail *Margarella antarctica* collected from the WAP were exposed to seawater in one of four treatment combinations: current ambient conditions (1.5°C, pH 8.0), near-future decreased pH (1.5°C, pH 7.8), near-future elevated temperature (3.5°C, pH 8.0), or combination of decreased pH and elevated temperature (3.5°C, pH 7.8). Following a 6-week exposure, limpets showed no temperature or pH effects on whole body mass or net calcification. Despite no significant differences in whole body mass, the shell length and width of limpets at elevated temperature tended to grow less than those at ambient temperature. There was a significant interaction between the sex of limpets and pH. There were no significant temperature or pH effects on growth, net calcification, shell morphologies, or proximate body composition of snails. Our findings suggest that both gastropod species demonstrate resilience to initial exposure to temperature and pH changes predicted to occur over the next several hundred years globally and perhaps sooner along the WAP. Despite few significant impacts of elevated temperature or decreased pH, any response to either abiotic variable in species with relatively slow growth and long lifespan is of note. In particular, we detected modest impacts of reduced pH on lipid allocation in the reproductive organs of the limpet *N. concinna* that warrants further study.

Keywords: climate change, growth, *Margarella antarctica*, *Nacella concinna*, net calcification, shell morphology, western Antarctic Peninsula.

Introduction

Phenotypic plasticity is a mechanism by which an organism can adjust an expressed phenotype, such as morphology or behaviour, without any genetic modification in response to an environmental shift, potentially increasing survival potential when exposed to climate-change conditions (Harvey *et al.*, 2014). Phenotypic plasticity can play a role in an organism's acclimation potential, making it possible for long-lived or slow-growing individuals to survive rapid environmental changes (Peck, 2005). Decreased seawater pH is one such environmental shift that has been demonstrated to induce phenotypic responses in marine shelled gastropods. These responses include disruptions in shell growth, specifically slower growth and smaller increases in shell thickness at decreased pH as well as shifts in overall shell morphology (Melatunan *et al.*, 2013). Ocean acidification (OA), defined as decreased seawater pH resulting from surface water absorption of atmospheric CO_2, has driven a global average decline of 0.1 pH units in the world's oceans since the onset of the industrial revolution (IPCC, 2007). Polar regions such as the Southern Ocean are particularly vulnerable to OA because of the increased atmospheric CO_2 solubility in cold water. The increased solubility of CO_2 is primarily due to the naturally higher Revelle factor (lower buffer capacity) associated with high latitude waters (Sabine *et al.*, 2004). Additionally, regional decreases in annual sea ice cover along the western Antarctic Peninsula (WAP) contribute to an increase in surface seawater absorption of atmospheric CO_2. Increased variability in sea ice cover has been linked

to rapidly rising atmospheric and sea surface temperatures (SST) along the WAP (reviewed by Turner *et al.*, 2014). For example, over the past half century, the mean annual air temperature has risen ~3°C while summer SST have risen ~1°C (Meredith and King, 2005).

As a result of the inverse correlation between temperature and the solubility of atmospheric CO_2 becomes more soluble in cold water, leading to reductions in the saturation state of the $CaCO_3$ polymorphs aragonite and calcite. This shift can make it more difficult for shelled organisms to produce and maintain calcified body elements. The increased cost of shell maintenance at cold temperatures and lack of shell crushing predators (reviewed by Aronson *et al.*, 2007), has resulted in thin-shelled organisms in the Southern Ocean (Orr *et al.*, 2005). The maintenance of calcite or aragonite can be more energetically costly when saturation states are low ($\Omega \leq 1$) and this is an important consideration because models predict that aragonite saturation states will reach undersaturation in the Southern Ocean within 25 years (McNeil and Matear, 2008). Species living in marine environments that experience a higher degree of temperature or pH variability may be more tolerant of predicted changes (Pespeni *et al.*, 2013). However, some benthic Antarctic invertebrates have exhibited a decreased potential for effective acclimation to rapidly changing abiotic conditions through phenotypic plasticity, adaptation to new conditions, or migration to more hospitable regions (Peck, 2005).

Studies of the effects of climate change on Antarctic marine invertebrates have to date largely focused on the effects of single factors, such as temperature or pH (reviewed by Ingels *et al.*, 2012). However, a growing number of studies worldwide are investigating the simultaneous effects of multiple climate-change-induced stressors, building on previous work demonstrating a wide range of interactive effects (reviewed by Crain *et al.*, 2008; Ingels *et al.*, 2012; Kroeker *et al.*, 2013). Multi-stressor studies have demonstrated that factors such as elevated temperature and reduced pH can have additive, synergistic, or antagonistic effects, underscoring the importance of these stressor studies for the development predictive models and conservation strategies (reviewed by Crain *et al.*, 2008).

The majority of Antarctic multi-stressor studies performed to date have focused on physiological, metabolic, or developmental aspects of the Antarctic sea urchin *Sterechinus neumayeri* (e.g. Ericson *et al.*, 2011; Ho *et al.*, 2013; Kapsenberg and Hofmann, 2014; Suckling *et al.*, 2014). Other studies have evaluated the effects of decreased pH as a single stressor. These studies included evaluations of shell dissolution in a pelagic pteropod (Bednaršek *et al.*, 2012, 2014a, b), energetic plasticity of pteropods (Seibel *et al.*, 2012) or the physiology and metabolism benthic bivalves (Cummings *et al.*, 2011). Alternately, two additional studies investigated the combined the effects of elevated temperature and decreased pH, on growth and photosynthetic capacity in marine algae (Schoenrock *et al.*, 2015, 2016) and on escape and righting responses in gastropods (Schram *et al.*, 2014).

Benthic gastropods comprise a significant component of the benthic megafauna found along the WAP and are conspicuous members of mesograzer assemblages associated with macroalgae (Amsler *et al.*, 2015). The herbivorous limpet and snail species in the present study occupy somewhat overlapping niches in the intertidal–subtidal zones of shallow coastlines of the WAP (Linse *et al.*, 2006; Waller, 2013). The limpet *Nacella concinna* is one of the most prominent invertebrates found in the littoral zone of the Antarctic Peninsula and adjacent islands (Picken, 1980). This common limpet can also be found in subtidal regions associated with macroalgae and often living directly on rocks and boulders (Linse *et al.*, 2006; González-Wevar *et al.*, 2010). At least one subpopulation has been documented to complete a seasonally vertical migration (Brêthes *et al.*, 1994; Peck and Veal, 2001). They depend on coordinated synchronized spawning events in the austral summer from November to early December, relying on pelagic development (Picken and Allan, 1983), and are thought to be prominent generalist consumers of the benthic microalgae (Shabica, 1976; Brêthes *et al.*, 1994; Kim, 2001; Peck and Veal, 2001). The shells of *N. concinna* are primarily made up of magnesium calcite while the shells of the Antarctic topshell snail *Margarella antarctica* are purely aragonite (J.B. Schram, unpublished X-ray diffraction data). The snail *M. antarctica* is widely distributed along the WAP and frequently found associated with macroalgae such as *Gigartina skottsbergii* and *Desmarestia anceps* (Amsler *et al.*, 2015) as well as rock substrates (Linse *et al.*, 2006). The *M. antarctica* can also be a dominant species in soft bottom habitats (Liu *et al.*, 2015). This gastropod species relies on non-pelagic development in the austral autumn and winter (Picken, 1980) and feeds on microepibiota from substrates such as sponges (Gutt and Schickan, 1998) and macroalgae (Amsler *et al.*, 2015).

In Antarctic foodwebs, gastropods provide important trophic links between benthic microalgae and top predators, including sea stars (McClintock, 1994) and kelp gulls (Favero *et al.*, 1997). Biotic pressures, such as predation (Cotton *et al.*, 2004), and abiotic pressures, such as sea ice scour or temperature (Linse *et al.*, 2006; Watson *et al.*, 2012), can influence gastropod shell morphology. Increased predation pressure can induce the production of thicker shells (Palmer, 1990) as well as shifts in overall shell morphology (Cotton *et al.*, 2004). Abiotic pressures such as ice scour have been demonstrated to influence shell height and strength in *N. concinna* across their depth distribution (Morley *et al.*, 2010). Previous work investigating the impacts of elevated temperature and decreased pH found that both stressors can induce shifts in the shell morphology of the temperate intertidal gastropod *Littorina littorea* (Melatunan *et al.*, 2013). Such changes in shell morphology or the proximate body composition (protein and lipid content of body tissues) of these gastropods could alter trophic transfer. For example, shifts in shell morphology could increase handling time by shifting overall shell morphology to a more globose shape (Melatunan *et al.*, 2013; Chen *et al.*, 2015). Decreases in nutritional quality, due to changes in the proximate composition (standard measures of macronutrients; herein protein and lipid) of tissues of prey species could reduce the efficiency of trophic transfer (Cebrian *et al.*, 2009).

The primary goal of the present study was to investigate the prospective effects of elevated temperature and decreased pH on two ecologically prominent Antarctic benthic gastropods that occupy coastal communities along the WAP. Due to their common occurrence *N. concinna* has been more extensively studied than other benthic gastropods. These studies have investigated genetic diversity and subtidal distribution (e.g. Beaumont and Wei, 1991; González-Wevar *et al.*, 2010; Hoffman *et al.*, 2010; Fuenzalida *et al.*, 2014), physiology (e.g. Picken, 1980; Abele *et al.*, 1998; Peck and Veal, 2001; Clark *et al.*, 2008; Weihe and Abele, 2008), temperature tolerance (e.g. Peck, 1989; Clark *et al.*, 2008; Morley *et al.*, 2012), and shell maintenance (e.g. Nolan, 1991; Peck *et al.*, 1996; Cadée, 1999). This wealth of knowledge makes *N. concinna* ideal for study of the impacts of elevated temperature and decreased pH.

Due to a similar high abundance of the sympatric *M. antarctica* and its contrasting reproductive mode, previous studies of Antarctic benthic gastropods have coupled these two species in comparative studies (e.g. Linse *et al.*, 2006; Hoffman *et al.*, 2011). We quantified gastropod growth (change in total wet mass), net calcification (change in buoyant weight), shell morphology (shell length, width, height, etc.), and proximate body composition (soluble protein, nonpolar lipids) of body tissues of the limpet *N. concinna* and snail *M. antarctica*. We hypothesized that (i) both thin-shelled gastropod species would be impacted by near-future elevated seawater temperature and decreased pH, and that these factors might exhibit interactive effects, (ii) the limpet *N. concinna*, which relies on pelagic development and is more widely distributed across depth, would be more tolerant of elevated temperature and decreased pH than the topshell snail *M. antarctica*, and (iii) that both gastropod species would maintain shell mass at the expense of maintaining tissue protein and lipid levels due to the potential importance of shells for protection.

Materials and methods

Animal collection

Adult individuals of the limpet *N. concinna* and the topshell snail *M. antarctica* were collected in February 2012 by hand using scuba from depths between 1 and 30 m within a 3.5 km radius of the US Antarctic Program's Palmer Station (64°46′ S, 64°03′ W). Individuals were collected from the rocky substrate or from the surfaces of large macroalgae and placed in fine mesh bags. Collection bags were subsequently immersed in 19 l buckets containing seawater from the collection site, and transported to Palmer Station. Limpets and snails were maintained in seawater tables with untreated, ambient flow-through seawater sourced directly from the benthos of Arthur Harbour, next to Palmer Station. Individuals were acclimatized for 3 weeks before experiments to equalize nutritive condition and avoid potential artefacts due to differential nutritional condition of individuals at the time of collection. During this acclimation period and for the subsequent experimental period limpets and snails remained active and were allowed to feed *ad libitum* on naturally occurring diatom assemblages that colonized the surfaces of the flow-through seawater tables as well as fresh thalli of the red alga *Palmaria decipiens*. Algal thalli and diatom growth was maintained in excess of what the gastropods could consume over the 3-week holding period. This holding period coincided with the late austral summer/early austral autumn following a concentrated period of rich phytoplankton and macroalgal productivity. Seawater temperature and carbonate chemistry for this region over the period of the present study is reported in Table 1 and in Schram *et al.* (2015). The righting behaviour and escape responses for the same limpets and snails investigated in the present study have previously been reported (Schram *et al.*, 2014).

Experimental setup and procedure

The experimental setup and procedures used in the present study have been described by Schram *et al.* (2014) and are briefly summarized below. Adult limpets (mean shell length = 41 ± 2 mm; $n = 72$) and snails (mean shell width = 9 ± 2 mm; $n = 360$) were haphazardly assigned to one of 18 replicates per treatment (square opaque plastic containers; 15 × 15 × 13 cm). Each replicate was independent of all other replicates with no flow-through water and was divided by fine plastic screen into four equally sized compartments to prevent contact between organisms in each compartment. One compartment housed a single limpet while another housed five snails. The smaller snail size made it necessary to house multiple individuals in each replicate to ensure sufficient tissue mass for tissue protein and lipid analysis. The five snails within each replicate were pooled and represented a single sample for all statistical analyses. The two remaining compartments within each replicate contained rocks with encrusting macroalgae for a separate, complementary study (Schoenrock *et al.*, 2016). Benthic macroalgal coverage in the region surrounding Palmer Station is not uniform with macroalgal biomass ranging between 3.3 and 6.3 kg m^2 benthos at depths between 2 and 15 m (Amsler *et al.*, 1995). The macroalgal biomass maintained in each replicate was consistent with these previously observed levels in the region (Amsler *et al.*, 1995; Schoenrock *et al.*, 2016). Limpets and snails were maintained on an *ad libitum* diet of the generally palatable red alga *P. decipiens* (Iken, 1999; Amsler *et al.*, 2005) for the duration of the 6-week exposure period. Every day, if one half of the 5 g piece of *P. decipiens* placed in each compartment had been consumed, it was removed and replaced with fresh thallus tissue. Otherwise, thallus tissue and associated diatom assemblages were exchanged twice weekly. The housing for the present experiment was maintained on a 12L: 12D photoperiod throughout the experiment. The photoperiod for this experiment was primarily set to ensure sufficient light availability for the macroalgae and was consistent with the photoperiod experienced by all organisms at collection. We do not anticipate that there were alterations in gastropod behaviour over the exposure period as a result of this standardized photoperiod.

A 2 × 2 factorial design was utilized to expose limpets and snails to combinations of current seawater temperature and pH conditions, based on recent documentation of annual seawater

Table 1. Seawater chemistry observations (± s.d.) performed for *in situ* and experimental microcosms.

		1.5°C		3.5°C	
	In situ	**pH 8.0**	**pH 7.8**	**pH 8.0**	**pH 7.8**
pH	8.06 ± 0.03	8.11 ± 0.18	7.81 ± 0.30	8.03 ± 0.17	7.79 ± 0.24
TA	2342 ± 100	2358 ± 67	2379 ± 78	2339 ± 174	2358 ± 71
Temp	0.83 ± 0.40	1.36 ± 0.21	1.34 ± 0.23	3.42 ± 0.45	3.41 ± 0.42
Salinity	34.0 ± 0.22	34.2 ± 0.29	34.2 ± 0.33	34.2 ± 0.34	34.2 ± 0.22
pCO_2	383 ± 39	371 ± 160	944 ± 888	455 ± 204	922 ± 817
Ω_{arg}	1.51 ± 0.07	1.82 ± 0.71	1.10 ± 0.77	1.67 ± 0.66	1.10 ± 0.60
Ω_{cal}	2.41 ± 0.11	2.90 ± 1.13	1.76 ± 1.23	2.66 ± 1.05	1.74 ± 0.95

Here we report spectrophotometric pH (total scale, pH_T), TA (μmol kg^{-1} SW), salinity (ppt), and temperature (°C) recorded every 3 days for water quality throughout the 6-week exposure period. Carbonate chemistry parameters (± s.d.) of pCO_2 (μatm) and saturation states of aragonite (Ω_{arg}) and calcite (Ω_{cal}) were calculated using CO2calc software and recorded data.

temperature and carbonate chemistry (Schram *et al.*, 2015) and those predicted to occur in the Palmer Station region based on global models by 2100 (IPCC, 2007). The four treatments consisted of a control, representing current mean austral summer ambient conditions (1.5°C, pH 8.0, Schram *et al.*, 2015, Table 1, an elevated temperature treatment (3.5°C, pH 8.0; Vaughn *et al.*, 2003), a high pCO_2-low pH treatment (1.5°C, pH 7.8; IPCC, 2007) and an elevated temperature and high pCO_2-low pH treatment (3.5°C, pH 7.8; IPCC, 2007). Stocks of pre-adjusted seawater were prepared and maintained in two separate 50-l carboys at each pH level, resulting in a total of four "header" tanks, for use in each of the experimental seawater treatments. To create seawater stocks, natural seawater was bubbled with an ambient air/CO_2 mixture to maintain an appropriate level of CO_2 to adjust seawater to the appropriate pH. Ambient air was obtained from the immediate external vicinity of the Palmer Station aquarium with a Super Luft (SL-65, Coralife, USA) high-pressure aquarium air pump. Decreased pH treatments were maintained by bubbling a combination of ambient air and CO_2 gas. By adjusting the level of CO_2 bubbled, it was possible to adjust seawater to the appropriate pCO_2-pH level. The seawater stocks were continuously monitored with an automated AT-Control System (Aqua Medic, USA) pH monitoring system, which modulated the delivery of CO_2 as appropriate. Seawater in each replicate was exchanged with the appropriate pre-adjusted stock seawater daily to ensure pH levels remained at target levels. Seawater temperature was maintained by recirculating distilled water-glycol (70−30% solution) around replicates in each of four acrylic rectangular water baths (113 cm × 58 cm × 13 cm) plumbed to one of four Digital Water Bath Recirculators (temperature control precision ± 0.01°C; 1186D, VWR Scientific, Radnor, PA, USA). Replicates from each of the temperature treatments were assigned randomly to one of the two acrylic water baths dedicated to each temperature (1.5 or 3.5°C). Replicates in each water bath were randomly arranged with respect to pH treatment (pH 8.0 or 7.8). The water-glycol solution was necessary for maintaining seawater temperatures close to zero to prevent freezing in the recirculators and was available in sufficient volume for the present experiment.

Seawater was subsampled every 3 days in each replicate for spectrophotometric pH (total hydrogen scale, pH_T) and total alkalinity (TA) determinations. Spectrophotometer measurements of pH were made with an ultraviolet-visible spectrophotometry Spectrometer Lambda 40P (Perkin Elmer, Waltham, MA, USA) equipped with a temperature controlled cell plumbed to an external water bath (Digital One RTE 17 Chiller Recirculating Water Bath, Neslab, Thermo Scientific, USA). Replicate spectrophotometric pH measurements of seawater subsamples indicated instrument and technician precision of 0.03 pH_T units (mean s.d., $N = 11$). We used a manual alkalinity titrator (T50, Mettler-Toledo Inc., Columbus, OH, USA) plumbed to a jacketed 250 ml beaker to determine TA (Dickson *et al.*, 2007). Titration temperatures in the jacketed beaker were maintained with a small water bath (Digital One RTE 17 Chiller Recirculating Water Bath, Neslab). We confirmed TA calibration by titrating certified reference materials provided by A. Dickson at UCSD Scripps Institute of Oceanography. An instrument and technician precision of 4.02 μmol kg^{-1} SW (mean s.d., $n = 17$) was established through replicate analysis of individual seawater samples.

Temperatures in replicates were measured with a Cole-Parmer Digi-Sense® ThermoLogR Thermister on the same interval as utilized for pH and TA measurements. Seawater salinity values in replicates were measured using a YSI Conductivity Instrument (Model 3200) equipped with a conductivity cell (YSI 3253 Model B) accurate to a salinity of 0.1 ppt, was used to determine seawater salinity. Carbonate chemistry (calcite (Ω_{cal}), aragonite saturation states (Ω_{arg}), and pCO_2 was calculated from pH_T, TA, temperature, and salinity measurements (Table 1). We used CO2calc software (Robbins *et al.*, 2010) with predetermined CO_2 constants (Millero, 2010) and $KHSO_4$ acidity constant (Dickson, 1990) for carbonate chemistry determinations.

Net body growth and net calcification

To assess net changes in net growth (wet body mass) and net calcification (change in shell weight) over the course of the 6-week experimental period, we recorded wet and buoyant weights for each limpet and snail immediately before and immediately following the 6-week exposure period. Wet weights (ww) were recorded using a top-loading balance (PM4600, Mettler-Toledo, Columbus, OH, USA) after gently placing each individual onto a dry piece of paper towel for 30 s to blot excess seawater from oral and aboral surfaces. Gastropods were then weighed on the top-loading balance and ww was measured to the nearest 0.01 g. The per cent change (% Δ) in ww was determined using Equation (1):

$$\%\ \text{change}\ (\Delta) = \frac{\text{Final}_{ww} - \text{Initial}_{ww}}{\text{Initial}_{ww}} \times 100. \quad (1)$$

The % Δ in ww represents net whole body growth over the experimental period, including changes in both whole body tissue and shell mass. Buoyant weight (bw) was measured based on the technique described by Davies (1989) by suspending a small glass platform in seawater from the bottom-loading accessory of a balance (PM4600, Mettler-Toledo, Columbus, OH, USA). The glass platform was completely submerged under ~10 cm of seawater (ambient conditions mean ± s.d., temperature = 1.82 ± 0.94, salinity = 35 ± 0.5, $n = 432$). Before weighing, each limpet or snail was submerged in ambient seawater for 5 min to ensure there were no air bubbles trapped inside their shells. Once submerged, individuals remained submerged until after their bw was recorded. The per cent weight difference of an individual's bw was calculated from as the difference in the bw recorded at the beginning and end of the experimental period (as in Equation 1). The % Δ in bw reflected the net shell calcification over the course of the experimental period. It must be emphasized that measurements of whole body ww and bw are not completely independent measures. Nonetheless, these measures are well suited to relative comparisons of net changes in whole body mass and shell mass between treatments (Davies, 1989).

Shell morphometric measurements

Limpets were digitally imaged with a Canon Mark II 5D EOS DLSR camera with a scale bar for determination of shell length, width, and height (Figure 1). Snails were similarly digitally imaged for shell length and width measurements as well as for aperture length and width (Figure 1). Snail images were collected with Nikon DS-Fi1c camera mounted on a Zeiss dissecting scope with a Nikon Digital Sight at ×0.8 magnification. The dissecting scope was lit by a Fiber-Lite high Intensity Illuminator Series 180 (Dolan-Jenner Industries, Inc.). We quantified gastropod shell morphology using ImageJ programme software (Rasband, 1997-2012), using measurements calibrated to 1 mm. Measurements for all parameters (e.g. shell height, width, etc.) were made in triplicate to ensure repeatability and the average of the three measurements was used for

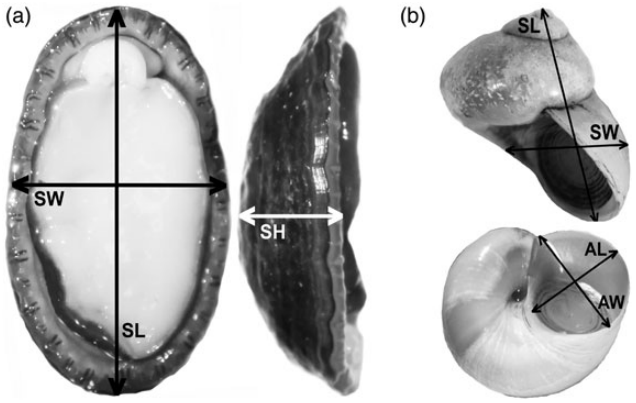

Figure 1. Measured shell morphometric dimensions for (a) the limpet *N. concinna* and (b) the snail *M. antarctica*. SW, shell width; SL, shell length; SH, shell height; AL, aperture length; AW, aperture width.

subsequent calculations for each parameter. The measured morphometrics were subsequently used to calculate the aspect and aperture ratios for gastropods [Equations (2) and (3)].

$$\text{aspect ratio} = \frac{SL}{SW}, \tag{2}$$

$$\text{aperture ratio} = \frac{AL}{AW}. \tag{3}$$

These ratios are related to shell shape and are determined based on the shell length (*SL*) and width (*SW*) as well as the aperture length (*AL*) and width (*AW*; Figure 1a and b). We recorded images of every limpet and snail before placement in and following exposure to experimental treatments for the calculation of the % Δ [Equation (1)] for each measurement.

Proximate composition of body components

Whole body tissue for measures of protein and lipid was collected following exposure to experimental conditions. Whole tissue samples were immediately frozen at −80°C in small plastic Whirl-Pak® bags (Nasco, Modesto, CA, USA) and kept frozen until dissection. We dissected whole body limpet tissues into two body components—foot muscle and gonads (either ovary or testes—readily discerned by colour). For snails, insufficient tissue remained for analysis if gonads were separated from muscle tissue, so a single body component (made up of muscle and gonad tissue) was used. This "whole body" component represented the eviscerated whole body (gut removed). Snail tissues within a given temperature and pH replicate were combined due to their small individual mass. Gut and viscera tissues were not included in any of the tissue analyses to ensure protein and lipid measurements were representative of organismal tissue and not recently ingested material. Dissected body tissues were lyophilized and ground to a fine homogenous powder using a ceramic mortar and pestle. Powdered tissues were weighed to the nearest 0.1 mg on a microbalance (Mettler AM 100, Mettler-Toledo International Inc., Heights Town, NJ, USA).

For soluble protein analysis, limpet and snail tissues were weighed and extracted in 5 ml of 1 M NaOH, and after which 5 µl of each protein extract was added to 250 µl of Bradford Dye Reagent (Bio-Rad). Following dye addition, protein extracts were analysed in triplicate on a microplate spectrophotometer (BioTek® Instruments, Inc., Winooski, Vermont, USA; Bradford, 1976). The absorbance was measured (595 nm) and plotted against a standard curve, created using bovine serum albumin. Protein concentrations were standardized to dry weights of each individual tissue sample to calculate µg protein mg^{-1} dry tissue. Levels of nonpolar lipids were determined by a modification of the technique given in Folch *et al.* (1957). We graphed resultant nonpolar lipid content (% dry wt) as a function of soluble protein content (% dry wt) to visualize how changes in lipid and protein contribute to net composition of limpet and snail body components in the four temperature-pH treatments.

Statistical analyses

Data were all tested for normality using the Shapiro-Wilks test. In cases where data were not normally distributed, we performed an additional Grubb's test to determine the presence of potential outliers, which if present were eliminated from subsequent analyses. If data remained not normally distributed, they were rank transformed. Data for net growth (ww) and calcification (bw), shell morphometrics (% Δ), and tissue composition of tissues (% dry weight) were analysed with a two-way analysis of variance (two-way ANOVA) for limpets and snails maintained in each of the four temperature-pH treatments at the completion of the 6-week exposure period. The mean % Δ in limpet and snail shell morphometric measurements were analysed with a two-way ANOVA. We used a three-way ANOVA to analyse the lipid levels of limpet muscle and gonad tissues due the significant difference in lipid allocation between female and male gonadal tissue. Significance was set at the 0.05 level for each statistical test. All ANOVA statistical analyses were conducted using JMP®, Version 12.0.1 (SAS Institute Inc., Cary, NC 1989–2007). Results for snails were pooled by replicate for all statistical analyses. In addition to ANOVA analyses, we performed a Pearson's correlation analysis for all possible combinations of measured response variables to identify significant relationships between measurement variables using SPSS Statistics software (IBM, Armonk, New York, USA). Figures for significant correlations were subsequently graphed (Supplementary Figures S1 and S2).

Results

Net body growth and net calcification

Despite a small net decrease in adult body (mean < 10%) and shell mass (mean < 3%), there were no significant temperature, pH, or interactive temperature-pH effects on whole body mass (ww) or shell mass (bw) in limpets (Table 2). There was a net decrease in body growth (ww) and net calcification (bw) for adult limpets maintained in all four temperature-pH treatments (Figure 2). The non significant trend for loss in body mass (ww) was not entirely due to a reduction in net calcification (loss in shell mass as inferred by bw). We observed different trends for mean % Δ in ww and bw of individual limpets maintained in the four temperature-pH treatments (Figure 2). This is most evident in the ambient/control treatment group (1.5°C, pH 8.0), where limpets experienced the greatest decrease in ww (mean ± s.e.; −10.1 ± 2.4%) but the smallest decrease in bw (mean ± s.e.; −1.8 ± 1.2%; Figure 2). There was a significant correlation between limpet ww and bw (Pearson's correlation, $r = 0.31$, $p = 0.01$) but no significant correlations between ww and bw with any other measured response variables (Supplementary Table S1 and Figure S1).

In contrast to the limpets, the snails in experimental treatments, except the pH 7.8, 3.5°C group, experienced a net increase (positive % Δ) in whole body growth and net calcification over the course of

Table 2. Results of two-way ANOVAs investigating the effects of elevated temperature and decreased pH on growth (wet weight: ww) and net calcification (buoyant weight: bw) for the limpet *N. concinna* and snail *M. antarctica*.

Trait	Source	d.f.	MS	*F*	*p*
Limpet growth (% Δ ww)	temp	1	1.75	0.02	0.88
	pH	1	158.31	1.95	0.17
	temp × pH	1	158.58	1.95	0.17
Limpet net calcification (% Δ bw)	temp	1	0.66	0.05	0.83
	pH	1	14.23	0.99	0.32
	temp × pH	1	0.09	0.01	0.94
Snail growth (% Δ ww)	temp	1	51.38	2.05	0.16
	pH	1	0.39	0.02	0.90
	temp × pH	1	49.57	1.98	0.16
Snail net calcification (% Δ bw)	temp	1	33.16	0.34	0.56
	pH	1	116.79	1.19	0.28
	temp × pH	1	22.07	0.22	0.64

d.f., degrees of freedom; MS, mean square; *F*, *F*-ratio.

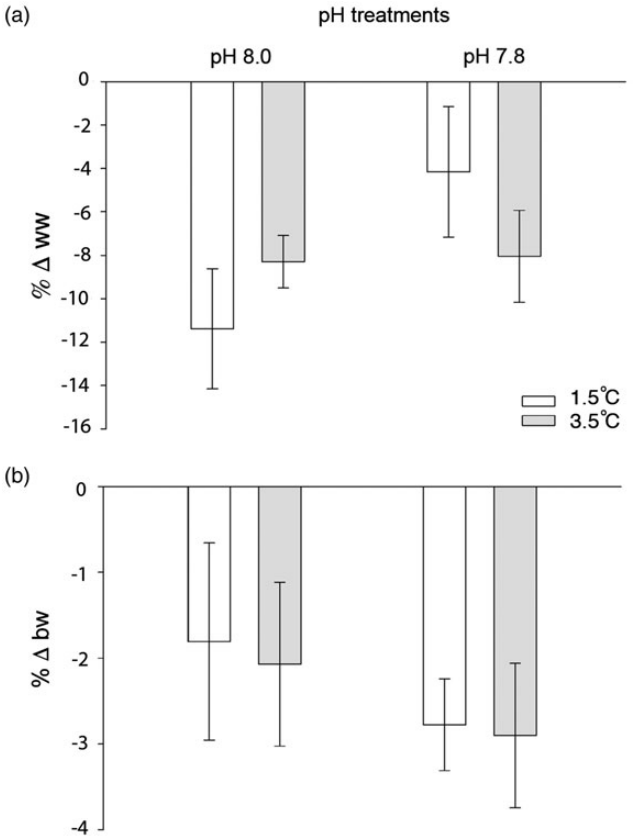

Figure 2. Per cent change (% Δ) in body and shell mass in the limpet *N. concinna* following the 6-week exposure to experimental treatments. (a) Mean (± s.e.) per cent change in wet weight (ww) and (b) mean (± s.e.) per cent change in buoyant weight (bw).

the experiment. Yet, similar to the limpets there was no significant temperature, pH, or interactive temperature-pH effects following the 6-week exposure period (Figure 3; Table 2). Unlike the limpet results, ww and bw trend together in each treatment. The ambient pH treatment groups at both temperatures exhibited very similar mean ww (mean ± s.e.; 1.5°C: 4.3 ± 1.5%; 3.5°C: 4.2 ± 0.8%)

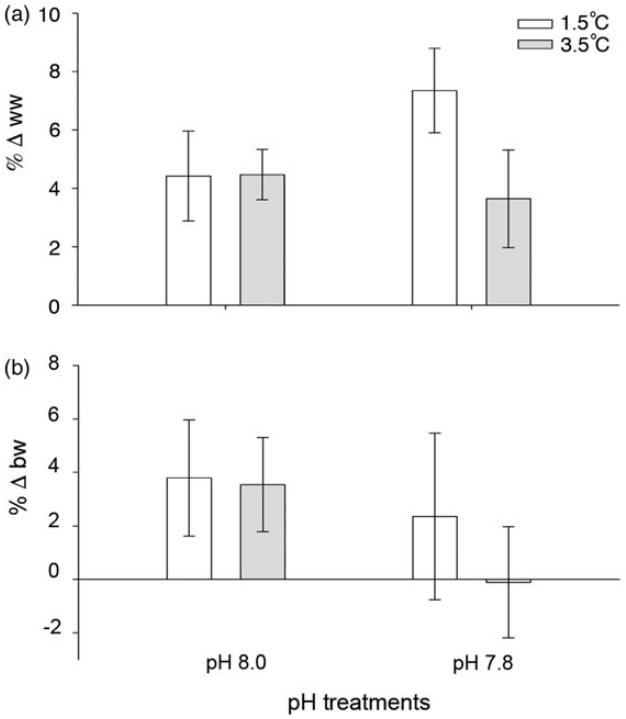

Figure 3. Per cent change (% Δ) in body and shell mass in the snail *M. antarctica* following the 6-week exposure to experimental treatments. (a) Mean (± s.e.) per cent change in wet weight (ww) and (b) mean (± s.e.) per cent change in buoyant weight (bw).

and bw (mean ± s.e.; 1.5°C: 3.8 ± 2.2%; 3.5°C: 3.5 ± 1.8%, Figure 3a and b). In contrast, in the decreased pH treatments the mean % Δ in ww and bw was more variable in combination with elevated temperature (Figure 3a and b). However, there was greater overall variability in snail growth and net calcification results for individuals in the decreased pH treatments (Figure 3). There was a significant correlation between snail ww and bw (Pearson's correlation, $r = 0.35$, $p = 0.03$) and between ww and % Δ lipid (Pearson's correlation, $r = 0.29$, $p = 0.05$) but no significant correlations between ww and bw with any other measured response variables (Supplementary Table S2 and Figure S2).

Shell morphometric measurements

Limpets exposed to the two elevated temperature (3.5°C) treatments had significantly smaller increases in both shell length and shell width when compared with the two ambient temperature (1.5°C) treatments (Table 3, Figure 4a and b). There was no significant temperature-pH interactive effect on limpet shell length or width (Table 3). The mean % Δ in shell length and width displayed similar patterns across treatments. For instance, the ambient/control (1.5°C, pH 8.0) treatment shell length changed by 7.4 ± 1.1% (mean ± s.e.) and shell width changed by 7.7 ± 1.1% (mean ± s.e.; Figure 4a and b). There was no significant change in shell height due to temperature, pH, or the interaction between temperature and pH (Table 3). However, the shell height results displayed a similar trend with the length and width results (somewhat increased % Δ in 1.5°C than in the 3.5°C temperature treatments) but with greater variability (Figure 4c). There were several significant correlations between snail morphometric measures (Pearson correlation, $p < 0.05$; Supplementary Table S1 and Figure S1).

Table 3. Results of two-way ANOVAs investigating the effects of elevated temperature and decreased pH on the per cent change in biometric shell traits for limpet *N. concinna* and snail *M. antarctica*.

Trait	Source	d.f.	MS	*F*	*p*
Limpet shell length (% Δ)	temp	1	0.87	11.84	**0.001**
	pH	1	0.02	0.24	0.63
	temp × pH	1	0.12	1.69	0.20
Limpet shell width (% Δ)	temp	1	0.45	9.07	**0.004**
	pH	1	2.01E−05	4.00E−04	0.98
	temp × pH	1	0.05	1.03	0.31
Limpet shell height (% Δ)	temp	1	0.02	0.25	0.62
	pH	1	0.01	0.15	0.70
	temp × pH	1	0.02	0.18	0.68
Snail shell length (% Δ)	temp	1	544.44	1.42	0.24
	pH	1	728.36	1.89	0.17
	temp × pH	1	43.44	0.11	0.74
Snail shell width (% Δ)	temp	1	342.50	0.89	0.35
	pH	1	19.27	19.27	0.82
	temp × pH	1	1108.94	2.89	0.09
Snail aspect ratio (% Δ)	temp	1	47.03	1.97	0.17
	pH	1	19.12	0.80	0.37
	temp × pH	1	11.96	0.50	0.48
Snail aperture length (% Δ)	temp	1	351.13	0.79	0.38
	pH	1	1.13	0.003	0.96
	temp × pH	1	325.13	0.73	0.40
Snail aperture width (% Δ)	temp	1	63.28	0.14	0.71
	pH	1	188.50	0.42	0.52
	temp × pH	1	49.17	0.11	0.74
Snail aperture ratio (% Δ)	temp	1	882.00	204	0.16
	pH	1	264.50	0.61	0.44
	temp × pH	1	329.39	0.76	0.39

d.f., degrees of freedom; MS, mean square; *F*, *F*-ratio. Bold letter indicates tests showing significant treatment effects.

Additionally, there was a significant correlation between the % Δ in shell width with the per cent muscle protein (Pearson's correlation, $r = 0.31$, $p = 0.001$; Supplementary Table S1).

For snails, there were no significant differences in shell length, width, or aspect ratio due to temperature, pH, or the interaction between temperature and pH (Table 3, Figure 5a–c). Snails exposed to each of the four temperature-pH treatments exhibited small but measurable increases in shell length and width over the 6-week exposure period (Figure 5a–c). The snail shell length generally increased less than the shell width and the % Δ in the aspect ratios decreased (Figure 5a–c). In contrast to the shell length and width, the aperture length and width for the snails exhibited slight, non-significant decreases over the exposure period (Figure 5d–f). There were significant correlations between all snail morphometric measures (Pearson correlation, $p < 0.05$; Supplementary Table S2 and Figure S2).

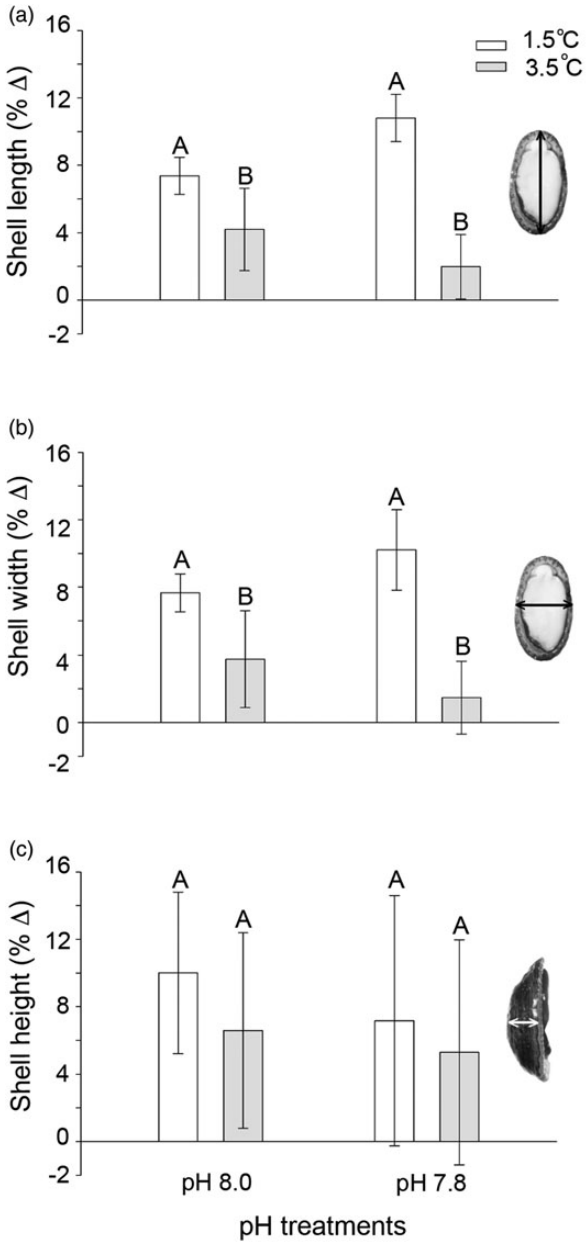

Figure 4. Limpet *N. concinna* shell morphometric measurements. (a) Mean shell responses (per cent change, % Δ, ± s.e.) in limpet shell length, (b) width, and (c) height. Bars with different capital letters differ significantly.

Proximate composition of body components

There was a significant pH-sex interactive effect on the lipid content of the limpet gonadal tissue (Table 4). This interactive effect translated to significantly different lipid content of the female and male gonad tissues and how these parameters responded to changes in pH (8.0 and 7.8). For instance, female limpet gonad tissue exhibited a slight not significant decrease in lipid content in the 3.5°C, pH 7.8, treatment and marginal not significant increase in lipid in the 1.5°C, pH 8.0, treatment (Table 4; Figure 6a). In contrast, the % Δ in male gonad lipid tissue was slightly elevated at decreased pH (pH 7.8; Table 4; Figure 6a). Despite this interactive effect, there were no single effects of temperature or pH on the lipid content of male or female gonadal tissue, resulting in greater % Δ in male lipid stores at decreased pH (Table 4; Figure 6a).

There was no significant difference in protein of limpet gonad or muscle tissue content due to sex or any interaction between these factors (Table 4; Figure 6a). Additionally, there were no significant differences in the lipid or protein levels of limpet muscle, despite a general decrease in lipid content in the 3.5°C, pH 7.8, treatment (Table 4; Figure 6b). Aside from a significant correlation between protein content and the %Δ in shell width (see above), there were no significant correlations between proximate body composition and other response variables (Supplementary Table S1). Similar to

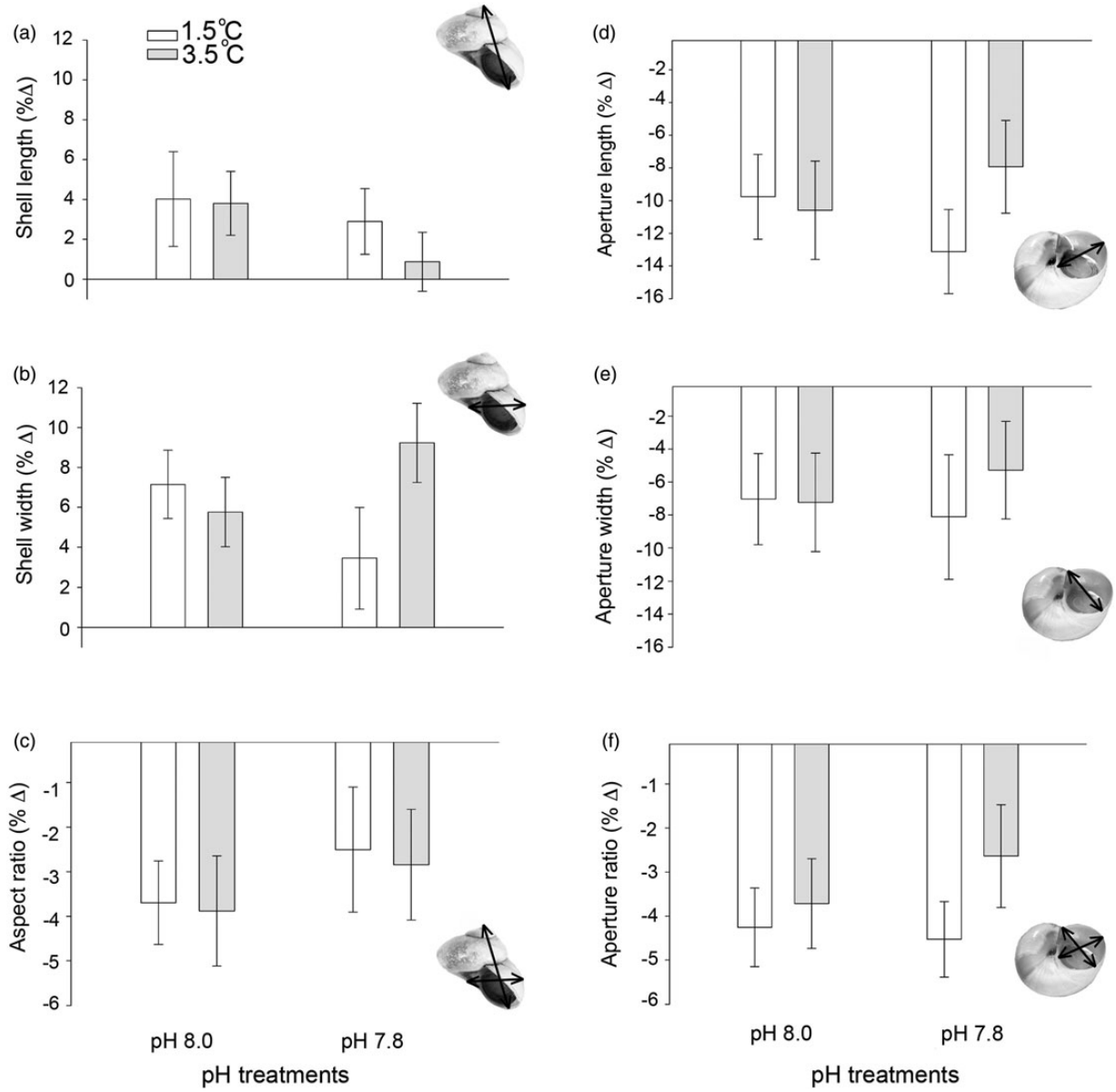

Figure 5. Snail *M. antarctica* shell morphometric measurements. Mean shell responses per cent change (% Δ) in snail shell morphology represented by the mean (± s.e.) (a) the shell length, (b) shell width, and (c) aspect ratio (shell length: shell width). Mean (± s.e.) (d) aperture length, (e) aperture width, and (f) aperture ratio (aperture length: aperture width) are also illustrated. Picture insets demonstrate shell measurements represented in each panel.

the limpet muscle tissue, there were no significant differences in snail whole body lipid or protein content between treatments based on temperature, pH, or interaction between temperature-pH (Table 4; Figure 7). There was a significant correlation between the % Δ lipid and protein in snails (Pearson's correlation, $r = 0.48$, $p < 0.001$; Supplementary Table S2 and Figure S2).

Discussion

The phenotypic response of Antarctic marine gastropods in the present study exhibits species-specific acclimation responses to increased seawater temperature and CO_2-induced reductions in seawater pH. We detected significant differences for the % Δ in limpet shell length and width at elevated temperature and a significant interactive effect between pH and sex in the per cent lipid content observed in limpet gonad tissue. Perhaps due to the relatively short experimental period relative to the lengthy lifespan of both gastropods, the adult limpet *N. concinna* and snail *M. antarctica* exhibited no significant differences in body or shell mass due to temperature or pH following a 6-week exposure period. Additionally, the small observed changes in ww and bw measures for both gastropods were correlated due to the overlapping nature of these measures. We anticipated only small changes in adult whole body and shell mass to be induced by temperature or pH due to the longevity of the species investigated. The limpet weights (in all temperature-pH treatments) had a tendency to decrease and the snail weights had a tendency to increase slightly.

Table 4. Results of two-and three-way ANOVAs investigating the effects of elevated temperature and decreased pH on proximate tissue composition (% dry weight protein and lipid) for limpet gonad and muscle tissue and all snail tissues.

Trait	Source	d.f.	MS	*F*	*p*
Limpet gonad lipid (% dry wt)	temp	1	2.78	0.77	0.39
	pH	1	0.18	0.05	0.82
	temp × pH	1	7.89	2.17	0.15
	sex	1	2675.57	737.68	**<0.001**
	temp × sex	1	0.67	0.19	0.67
	pH × sex	1	19.86	5.47	**0.03**
	temp × pH × sex	1	7.12	1.96	0.17
Limpet gonad protein (% dry wt)	temp	1	14.49	1.02	0.32
	pH	1	10.14	0.71	0.40
	temp × pH	1	22.91	1.61	0.21
	sex	1	0.42	0.03	0.86
	temp × sex	1	1.01	0.07	0.79
	pH × sex	1	4.91	0.35	0.56
	temp × pH × sex	1	3.71	0.26	0.61
Limpet muscle lipid (% dry wt)	temp	1	0.91	1.12	0.30
	pH	1	2.38	2.93	0.09
	temp × pH	1	2.07	2.54	0.12
	sex	1	0.001	0.001	0.97
	temp × sex	1	0.43	0.53	0.47
	pH × sex	1	0.34	0.41	0.52
	temp × pH × sex	1	0.02	0.03	0.87
Limpet muscle protein (% dry wt)	temp	1	2.95	0.24	0.63
	pH	1	2.62	0.21	0.65
	temp × pH	1	0.00	0.00	0.99
	sex	1	9.60	0.79	0.38
	temp × sex	1	9.06	0.74	0.39
	pH × sex	1	8.39	0.69	0.41
	temp × pH × sex	1	2.44	0.20	0.66
Snail lipid (% dry wt)	temp	1	5.39	2.26	0.14
	pH	1	0.88	0.37	0.55
	temp × pH	1	1.73	0.72	0.40
Snail protein (% dry wt)	temp	1	1105.70	1.69	0.20
	pH	1	2.03	0.003	0.96
	temp × pH	1	1.57	0.002	0.96

d.f., degrees of freedom; MS, mean square; *F*, *F*-ratio. Bold letter indicates tests showing significant treatment effects.

This trend in the bw, representing the net calcification, may have been influenced by the $CaCO_3$ polymorph comprising the shells of the limpets (magnesium calcite) and snails (aragonite). Perhaps these small changes in whole body mass may be a species-specific seasonal response (the experiment was performed during the austral autumn), or simply a differential species level response to being maintained in the laboratory. However, it is unlikely that this differential response between species is due to food availability. At the termination of the experimental period, diatoms were present on all replicate surfaces and macroalgal tissue remained available in each replicate compartment throughout the duration of the experimental exposure period. Additionally, upon dissection, all limpet and snail guts were full of diatoms (author's personal observation), indicating sufficient food availability to maintain body mass.

In a study carried out in a temperate region, Nienhuis *et al.* (2010) showed that over an exposure period to reduced pH of just six days, the benthic gastropod *Nucella lamellosa* displayed decreased calcification and increased shell dissolution. The authors of this study suggest that dissolution is influenced more by increased levels of seawater CO_2 (decreased pH) than shell deposition. One previous Antarctic study has demonstrated that shells removed from the limpet *N. concinna* suffer significant dissolution in as few as 14 days when exposed to pH 7. 4 seawater (McClintock *et al.*, 2009). Although the reduced pH level in the present study was less aggressive (pH 7.8), the absence of any observable effects of reduced pH on shells of living *N. concinna* suggests that this species is actively maintaining calcium carbonate structures.

Additionally, the increases in shell length, width, and height observed in the present study suggest that limpets increased their shell size over the experimental period despite a tendency towards a decrease in shell weight (bw). Maintenance and growth of body tissue and overall shell length under warmer and hypercapnic conditions has been previously documented with *Mytilus galloprovincialis* despite steady or decreased net calcification rates over a 10-month exposure period (Gazeau *et al.*, 2014). In another temperate species, chronic exposure for 6 months to decreased seawater pH associated with only a 200 ppm increase in seawater pCO_2 resulted in decreased in shell growth and body weight in the snail *Strombus lubuanus* (Shirayama and Thornton, 2005). These results suggest that some gastropod species are sensitive to shifts in seawater pCO_2 at levels lower than IPCC predictions for 2100, and even so despite a 6-month acclimation period. Perhaps the small changes in net calcification observed in the present study could be exacerbated over a longer exposure period as demonstrated by Shirayama and Thornton (2005).

Despite the absence of temperature or pH effects on the growth or net calcification of the gastropods investigated, we observed a significant influence of temperature on shell morphometric measurements in limpets, with individuals exhibiting shell plasticity in

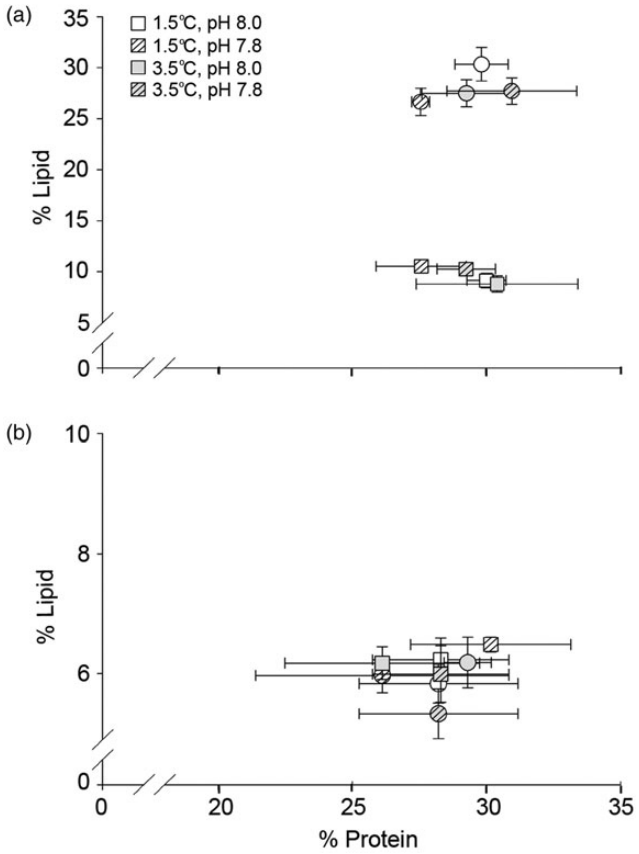

Figure 6. Limpet *N. concinna* proximate tissue composition represented as a percentage of dry weight in the tissues of limpets maintained in experimental treatments for 6 weeks. Each symbol represents the mean percentages of protein and lipid (± s.e.), respectively. (a) Represents mean protein and lipid in gonad tissue; (b) represents mean protein and lipid in muscle tissue. Circles represent females and squares represent males.

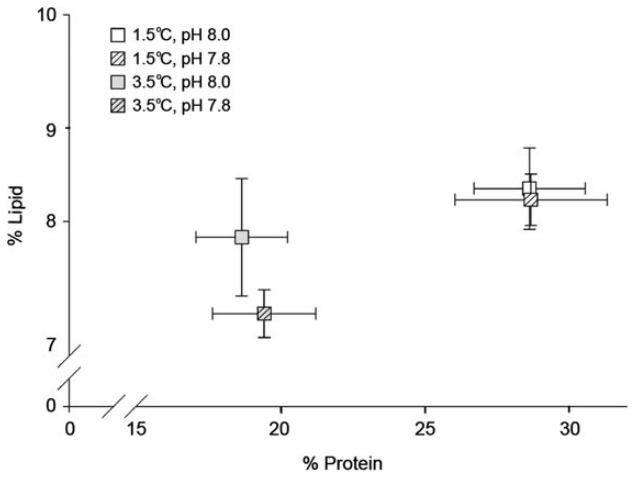

Figure 7. Pooled (by replicate) snail *M. antarctica* proximate tissue composition represented as a percentage of dry weight in whole body tissues of snails maintained in experimental treatments for 6 weeks. Each symbol represents the mean percentages of protein and lipid (± s.e.), respectively.

response to elevated temperature. Following exposure to elevated temperature treatments, the limpets exhibited significantly less shell growth resulting in shorter, and narrower shell morphology. The correlations between all aspects of shell morphology measured for this limpet species suggests that temperature acts as a general stressor, resulting in no alteration in net shell morphology. This suggests that the decreased growth is likely the consequence of reallocation of resources, away from shell growth, and potentially to the maintenance of another body component. This is in contradiction to our original hypothesis that energy would be preferentially allocated to maintenance of shell rather than tissue material. We did observe a significant correlation between the per cent protein content of muscle tissue and % Δ shell width. Higher protein content correlated with small changes or decreases in shell width suggested that limpets may have maintained the integrity of their muscle tissue rather than increasing shell width, which may have interesting downstream implications over longer exposure periods.

Shifts in shell morphology following exposure to decreased pH and elevated seawater temperature have previously been observed in the temperate intertidal periwinkle *Littorina littorea* following a 30-d exposure period (Melatunan *et al.*, 2013). Depending on the morphological shell trait considered, elevated temperature and decreased pH had a range of single factor, additive, synergistic, or null effects in *L. littorea*. However, one conclusion of this study was that *L. littorea* maintained a more globular-shaped shells in decreased pH treatments (Melatunan *et al.*, 2013). Previous work has suggested that gastropods whose body shapes have larger aspect ratios, resulting in a more elongate body form, are more vulnerable to predation, possibly due to increased predator handling efficiency (Cotton *et al.*, 2004). In the present study, in contrast to limpets, we observed no significant differences in aspects of shell morphology measured or correlations between shell morphology and response variables other than morphology measures for the topshell snail due to elevated temperature or reduced pH exposure. Significant correlations between all measured aspects of snail shell morphology measurements provide further support for the conclusion that the snails in the present study did not exhibit shifts in overall shell morphology.

In the present study, we did not observe significant changes in overall aspect and aperture ratios of snails in any of the temperature-pH treatments. The slight decreases in measured shell morphologies across all treatment combinations may have been the result of analysing the average measurements for each aperture parameter. Overall, it is unclear whether a smaller, more globose body morphology in response to predicted future ocean conditions, like that observed in temperate gastropods, would aid in predator avoidance because the shallow marine benthos of Antarctica lacks crushing predators (Aronson *et al.*, 2009). However, Antarctic benthic gastropods commonly fall prey to larger fauna such as kelp gulls (Favero *et al.*, 1997) and sea stars (Mahon *et al.*, 2002). In addition to being influenced by biotic factors such as predator avoidance, shell morphology has been linked to latitudinal shifts in seawater carbonate chemistry (Watson *et al.*, 2012). An investigation of the latitudinal influence on body size in molluscs found that temperature was correlated with body size, food availability, and ice scour (Linse *et al.*, 2006). The present study addressed only the results of exposure of single species to elevated temperature and decreased pH. To address the role of biotic factors such as predation and additional regional abiotic interactions (e.g. ice scour) on gastropod shell morphology, future research is needed.

To investigate the potential that elevated temperature and decreased pH have to alter Antarctic gastropod proximate body

composition as a phenotypically flexible response, we evaluated the protein and lipid levels of limpet and snail tissues. Overall, the composition of body tissues for the limpet *N. concinna* and snail *M. antarctica* did not change dramatically over the 6-week exposure period, in large part because of a high degree of individual variation in all temperature-pH treatments. Regardless of the high variation, as expected, female *N. concinna* limpets had significantly greater lipid levels in their gonadal tissue than males. Despite sex-related differences in lipid concentrations in limpets (ovaries generally higher than testes), a significant pH–sex interaction effect resulted in a relatively greater increase in the lipid content of ovaries of individuals maintained in the elevated temperature, reduced pH treatment (3.5°C, pH 7.8) when compared with lipid levels in testes. This intriguing response to future environmental conditions of temperature and pH could influence reproductive success and survival of offspring and should be further investigated. These findings are particularly relevant because several studies have indicated that sea urchin larval stages may demonstrate relative resilience to elevated seawater temperature and decreased pH (Ho *et al.*, 2013; Kapsenberg and Hofmann, 2014). To date, there has been limited research in polar regions on the effect of parental exposure to elevated temperature and decreased pH on offspring (Suckling *et al.*, 2014).

The lack of significant differences in protein and lipid levels in limpet and snail tissues suggests an ability to acclimate to temporarily shifted abiotic conditions by maintaining relative tissue lipid and protein levels, at least over a 6-week exposure period. The absence of environmental stress-induced changes in lipid and protein levels in organismal tissues has been observed in a temperate sea urchin species (Matson *et al.*, 2012). Following exposure to elevated pCO_2, Matson *et al.* (2012) did not find significant impacts on the total protein and lipid levels in the eggs and early developmental stages of the sea urchin *Strogylocentrotus purpuratus*. When we consider the results of the present study in conjunction with the change in tissue mass and shell morphology measurements, it appears that both limpets and snails maintain tissue protein and lipid levels in lieu of whole body growth. In contrast to the negligible growth in all treatments in the present study, Cross *et al.* (2015) followed growth of the brachiopod *Liothyrella uva* held at reduced pH over a 7-month period and did not observe a reduction in growth. The present study did not identify significant temperature or pH effects on growth or tissue maintenance using broad techniques targeted at detecting large changes in body condition. Perhaps use of multiple physiological measurements such as a condition index, RNA content (as a measure of protein synthesis potential), or scope for growth measures following exposure to combinations of elevated temperature and decreased pH would produce a more nuanced representation of growth of long-lived, cold water species like those investigate in the present study under environmental stress (Norkko *et al.*, 2005).

In contrast to Antarctic pelagic gastropods such as the shelled pteropods (Bednaršek *et al.*, 2014a), the benthic gastropods investigated in the present study were generally resilient to the elevated temperature and decreased pH conditions predicted by the IPCC to occur by 2100. There was a small but measurable change in net growth and calcification over the 6-week exposure period, which was expected for long-lived, cold-adapted species, but there was no negative impact of elevated temperature or decreased pH. The small changes in size did not result in significant shifts in shell morphology or tissue composition. Moreover, a previous study with the same gastropods found no significant impact of elevated temperature or decreased pH on escape responses to a predator (Schram *et al.*, 2014).

Perhaps the two gastropod species investigated in the present study were still acclimating to experimental conditions. Previous research estimates that the Antarctic limpet *N. concinna* can take anywhere from 2 to 4 months to acclimate to elevated temperature (Peck *et al.*, 2014). Additionally, spawning behaviour has been linked to increases in seawater temperature in the same species (Picken, 1980). Both gastropod species investigated in the present study either spawn or deposit eggs during the austral spring (September—November) (Shabica, 1976; Picken, 1979) and the present study was performed during the austral autumn. More significant differences in the provisioning and development of gonad tissue might be detected following a longer exposure period or immediately before or after spawning. The individuals used in the present experiment were adults. Perhaps more marked differences in growth and calcification may be more easily detected in juveniles than in adults, which tend to grow more slowly (Shabica, 1976; Picken, 1979). Ultimately, further research integrating the acclimation capacity at multiple levels of biological organization over more than one generation are needed to better address this possibility (Harvey *et al.*, 2014). Nonetheless, the results of the present study, documenting few species-specific responses to seawater warming and acidification, are timely in the rapidly changing WAP environment, which hosts a wide variety of ecological and economically important organisms, many of which are not well understood.

Supplementary data

Supplementary material is available at the *ICESJMS* online version of the manuscript.

Acknowledgements

The authors gratefully acknowledge the outstanding science and logistical support staff of Raytheon Polar Services Company and Antarctic Support Contract for their invaluable help and support of the United States Antarctic Program. In particular, we recognize the field and dive support provided by Nell Herrmann, Jeff Otten, Lily Glass, Paul Queior, Steve Sweet, and Neil Schiebe. Margaret Amsler and Jerry Sewell of the UAB Departments of Biology and Physics provided valuable assistance. Winfried Engl helped us to identify the Antarctic topshell snail included in the present experiment. Casey Philips provided invaluable help in the lab at UAB analysing gastropod shell morphometrics. Thanks are due to Kenan Matterson for his assistance with protein analyses. Comments provided by Jennifer Greer and Samantha Giordano helped improve this manuscript. The present study was supported by NSF award ANT-1041022 (JBM, CDA, RAA) from the Antarctic Organisms and Ecosystems programme. The UAB Department of Biology and an Endowed Professorship in Polar and Marine Biology provided additional support to JBM.

References

Abele, D., Burlando, B., Viarengo, A., and Pörtner, H.-O. 1998. Exposure to elevated temperatures and hydrogen peroxide elicits oxidative stress and antioxidant response in the Antarctic intertidal limpet *Nacella concinna*. Comparative Biochemistry and Physiology Part B: Biochemistry and Molecular Biology, 120: 425–435.

Amsler, C. D., Iken, K., McClintock, J. B., Amsler, M. O., Peters, K. J., Hubbard, J. M., Furrow, F. B., *et al.* 2005. Comprehensive evaluation of the palatability and chemical defenses of subtidal macroalgae from the Antarctic Peninsula. Marine Ecology Progress Series, 294: 141–159.

Amsler, C. D., Rowley, R. J., Laur, D. R., Quetin, L. B., and Ross, R. M. 1995. Vertical distribution of Antarctic peninsular macroalgae: cover, biomass and species composition. Phycologia, 34: 424–430.

Amsler, M. O., Huang, Y. M., Engl, W., McClintock, J. B., and Amsler, C. D. 2015. Abundance and diversity of gastropods associated with dominant macroalgae from the Western Antarctic Peninsula. Polar Biology, 38: 1171–1181.

Aronson, R. B., Moody, R. M., Ivany, L. C., Blake, D. B., Werner, J. E., and Glass, A. 2009. Climate change and trophic response of the Antarctic bottom fauna. PLoS ONE, 4: e4385.

Aronson, R. B., Thatje, S., Clarke, A., Peck, L. S., Blake, D. B., Wilga, C. D., and Seibel, B. A. 2007. Climate change and invasibility of the Antarctic Benthos. Annual Review of Ecology, Evolution, and Systematics, 38: 129–154.

Beaumont, A. R., and Wei, J. H. C. 1991. Morphological and genetic variation in the Antarctic limpet *Nacella concinna* (Strebel, 1908). Journal of Molluscan Studies, 57: 443–450.

Bednaršek, N., Feely, R., Reum, J., Peterson, B., Menkel, J., Alin, S., and Hales, B. 2014a. *Limacina helicina* shell dissolution as an indicator of declining habitat suitability owing to ocean acidification in the California Current Ecosystem. Proceedings of the Royal Society B: Biological Sciences, 281: 20140123.

Bednaršek, N., Tarling, G., Bakker, D., Fielding, S., Jones, E., Venables, H., Ward, P., *et al.* 2012. Extensive dissolution of live pteropods in the Southern Ocean. Nature Geoscience, 5: 881–885.

Bednaršek, N., Tarling, G. A., Bakker, D. C. E., Fielding, S., and Feely, R. A. 2014b. Dissolution dominating calcification process in polar pteropods close to the point of aragonite undersaturation. PLoS ONE, 9: e109183.

Bradford, M. M. 1976. A rapid and sensitive method for the quantitation of microgram quantities of protein utilizing the principle of protein-dye binding. Analytical Biochemistry, 72: 248–254.

Brêthes, J.-C., Ferreyra, G., and De La Vega, S. 1994. Distribution, growth and reproduction of the limpet *Nacella* (*Patinigera*) *concinna* (Strebel 1908) in relation to potential food availability, in Esperanza Bay (Antarctic Peninsula). Polar Biology, 14: 161–170.

Cadée, G. C. 1999. Shell damage and shell repair in the Antarctic limpet *Nacella concinna* from King George Island. Journal of Sea Research, 41: 149–161.

Cebrian, J., Shurin, J. B., Borer, E. T., Cardinale, B. J., Ngai, J. T., Smith, M. D., and Fagan, W. F. 2009. Producer nutritional quality controls ecosystem trophic structure. PLoS ONE, 4: e4929.

Chen, Y. J., Wu, J. Y., Chen, C. T. A., and Liu, L. L. 2015. Effects of low-pH stress on shell traits of the dove snail, *Anachis misera*, inhabiting shallow-vent environments off Kueishan Islet, Taiwan. Biogeosciences, 12: 2631–2639.

Clark, M. S., Geissler, P., Waller, C., Fraser, K. P. P., Barnes, D. K. A., and Peck, L. S. 2008. Low heat shock thresholds in wild Antarctic intertidal limpets (*Nacella concinna*). Cell Stress and Chaperones, 13: 51–58.

Cotton, P. A., Rundle, S. D., and Smith, K. E. 2004. Trait compensation in marine gastropods: shell shape, avoidance behavior, and susceptibility to predation. Ecology, 85: 1581–1584.

Crain, C. M., Kroeker, K., and Halpern, B. S. 2008. Interactive and cumulative effects of multiple human stressors in marine systems. Ecology Letters, 11: 1304–1315.

Cross, E. L., Peck, L. S., and Harper, E. M. 2015. Ocean acidification does not impact shell growth or repair of the Antarctic brachiopod *Liothyrella uva* (Broderip, 1833). Journal of Experimental Marine Biology and Ecology, 462: 29–35.

Cummings, V., Hewitt, J., Van Rooyen, A., Currie, K., Beard, S., Thrush, S., Norkko, J., *et al.* 2011. Ocean acidification at high latitudes: Potential effects on functioning of the Antarctic bivalve *Laternula elliptica*. PLoS ONE, 6: e16069.

Davies, P. S. 1989. Short-term growth measurements of corals using an accurate buoyant weighing technique. Marine Biology, 101: 389–395.

Dickson, A. G. 1990. Standard potential of the reaction: AgCl(s) + 1/2 H_2(g)and the standard acidity constant of the ion HSO_4 in synthetic sea water from 273.15 to 318.15 K. Journal of Chemical Thermodynamics, 22: 113–127.

Dickson, A. G., Sabine, C. L., and Christen, J. R. 2007. Guide to best practice for ocean CO_2 measurements. Pices Special Publication, 3: 1–175.

Ericson, J. A., Ho, M. A., Miskelly, A., King, C. K., Virtue, P., Tilbrook, B., and Byrne, M. 2011. Combined effects of two ocean change stressors, warming and acidification, on fertilization and early development of the Antarctic echinoid *Sterechinus neumayeri*. Polar Biology, 35: 1027–1034.

Favero, M., Silva, P., and Ferreyra, G. 1997. Trophic relationships between the kelp gull and the Antarctic limpet at King George Island (South Shetland Islands, Antarctica) during the breeding season. Polar Biology, 17: 431–436.

Folch, J., Lees, M., and Stanley, G. H. S. 1957. A simple method for the isolation and purification of total lipides from animal tissues. Journal of Biological Chemistry, 226: 497–509.

Fuenzalida, G., Poulin, E., Gonzalez-Wevar, C., Molina, C., and Cardenas, L. 2014. Next-generation transcriptome characterization in three *Nacella* species (Patellogastropoda: Nacellidae) from South America and Antarctica. Marine Genomics, 18: 89–91.

Gazeau, F., Alliouane, S., Bock, C., Bramanti, L., López Correa, M., Gentile, M., Hirse, T., *et al.* 2014. Impact of ocean acidification and warming on the Mediterranean mussel (*Mytilus galloprovincialis*). Frontiers in Marine Science, 1: 99.

González-Wevar, C. A., Nakano, T., Cañete, J. I., and Poulin, E. 2010. Molecular phylogeny and historical biogeography of *Nacella* (Patellogastropoda: Nacellidae) in the Southern Ocean. Molecular Phylogenetics and Evolution, 56: 115–124.

Gutt, J., and Schickan, T. 1998. Epibiotic relationships in the Antarctic benthos. Antarctic Science, 10: 398–405.

Harvey, B. P., Al-Janabi, B., Broszeit, S., Cioffi, R., Kumar, A., Aranguren-Gassis, M., Bailey, A., *et al.* 2014. Evolution of marine organisms under climate change at different levels of biological organisation. Water, 6: 3545–3574.

Ho, M., Price, C., King, C., Virtue, P., and Byrne, M. 2013. Effects of ocean warming and acidification on fertilization in the Antarctic echinoid *Sterechinus neumayeri* across a range of sperm concentrations. Marine Environmental Research, 90: 136–141.

Hoffman, J., Clarke, A., Linse, K., and Peck, L. 2011. Effects of brooding and broadcasting reproductive modes on the population genetic structure of two Antarctic gastropod molluscs. Marine Biology, 158: 287–296.

Hoffman, J. I., Peck, L. S., Hillyard, G., Zieritz, A., and Clark, M. S. 2010. No evidence for genetic differentiation between Antarctic limpet *Nacella concinna* morphotypes. Marine Biology, 157: 765–778.

Iken, K. 1999. Feeding ecology of the Antarctic herbivorous gastropod *Laevilacunaria antarctica* Martens. Journal of Experimental Marine Biology and Ecology, 236: 133–148.

Ingels, J., Vanreusel, A., Brandt, A., Catarino, A. I., David, B., De Ridder, C., Dubois, P., *et al.* 2012. Possible effects of global environmental changes on Antarctic benthos: a synthesis across five major taxa. Ecology and Evolution, 2: 453–485.

IPCC. 2007. Climate change 2007: The physical science basis. 996 pp.

Kapsenberg, L., and Hofmann, G. E. 2014. Signals of resilience to ocean change: high thermal tolerance of early stage Antarctic sea urchins (*Sterechinus neumayeri*) reared under present-day and future pCO_2 and temperature. Polar Biology, 37: 967–980.

Kim, D. 2001. Seasonality of marine algae and grazers of an Antarctic rocky intertidal, with emphasis on the role of the limpet *Nacella concinna* Strebel (Gastropoda: Patellidae). Berichte zur Polar-und Meeresforschung (Reports on Polar and Marine Research). 397 pp.

Kroeker, K. J., Kordas, R. L., Crim, R., Hendriks, I. E., Ramajo, L., Singh, G. S., Duarte, C. M., *et al.* 2013. Impacts of ocean acidification on

marine organisms: quantifying sensitivities and interaction with warming. Global Change Biology, 19: 1884–1896.

Linse, K., Barnes, D. K. A., and Enderlein, P. 2006. Body size and growth of benthic invertebrates along an Antarctic latitudinal gradient. Deep Sea Research Part II: Topical Studies in Oceanography, 53: 921–931.

Liu, X., Wang, L., Li, S., Huo, Y., He, P., and Zhang, Z. 2015. Quantitative distribution and functional groups of intertidal macrofaunal assemblages in Fildes Peninsula, King George Island, South Shetland Islands, Southern Ocean. Marine Pollution Bulletin, 99: 284–291.

Mahon, A. R., Amsler, C. D., McClintock, J. B., and Baker, B. J. 2002. Chemo-tactile predator avoidance responses of the common Antarctic limpet *Nacella concinna*. Polar Biology, 25: 469–473.

Matson, P. G., Yu, P. C., Sewell, M. A., and Hofmann, G. E. 2012. Development under elevated pCO_2 conditions does not affect lipid utilization and protein content in early life-history stages of the purple sea urchin, *Strongylocentrotus purpuratus*. The Biological Bulletin, 223: 312–327.

McClintock, J. B. 1994. Trophic biology of Antarctic shallow-water echinoderms. Marine Ecology Progress Series, 111: 191–202.

McClintock, J. B., Angus, R. A., McDonald, M. R., Amsler, C. D., Catledge, S. A., and Vohra, Y. K. 2009. Rapid dissolution of shells of weakly calcified Antarctic benthic macroorganisms indicates high vulnerability to ocean acidification. Antarctic Science, 21: 449–456.

McNeil, B. I., and Matear, R. J. 2008. Southern Ocean acidification: a tipping point at 450-ppm atmospheric CO_2. Proceedings of the National Academy of Sciences of the United States of America, 105: 18860–18864.

Melatunan, S., Calosi, P., Rundle, S. D., Widdicombe, S., and Moody, A. J. 2013. Effects of ocean acidification and elevated temperature on shell plasticity and its energetic basis in an intertidal gastropod. Marine Ecology Progress Series, 472: 155–168.

Meredith, M. P., and King, J. C. 2005. Rapid climate change in the ocean west of the Antarctic Peninsula during the second half of the 20th century. Geophysical Research Letters, 32: L19604.

Millero, F. J. 2010. Carbonate constants for estuarine waters. Marine and Freshwater Research, 61: 139–142.

Morley, S. A., Clark, M. S., and Peck, L. S. 2010. Depth gradients in shell morphology correlate with thermal limits for activity and ice disturbance in Antarctic limpets. Journal of Experimental Marine Biology and Ecology, 390: 1–5.

Morley, S. A., Martin, S. M., Day, R. W., Ericson, J., Lai, C.-H., Lamare, M., Tan, K.-S., *et al.* 2012. Thermal reaction norms and the scale of temperature variation: Latitudinal vulnerability of intertidal Nacellid limpets to climate change. PLoS ONE, 7: e52818.

Nienhuis, S., Palmer, A. R., and Harley, C. D. G. 2010. Elevated CO_2 affects shell dissolution rate but not calcification rate in a marine snail. Proceedings of the Royal Society B: Biological Sciences, 277: 2553–2558.

Nolan, C. P. 1991. Size, shape and shell morphology in the Antarctic limpet *Nacella concinna* at Signy Island, South Orkney Islands. Journal of Molluscan Studies, 57: 225–238.

Norkko, J., Pilditch, C. A., Thrush, S. F., and Wells, R. M. G. 2005. Effects of food availability and hypoxia on bivalves: the value of using multiple parameters to measure bivalve condition in environmental studies. Marine Ecology Progress Series, 298: 205–218.

Orr, J. C., Fabry, V. J., Aumont, O., Bopp, L., Doney, S. C., Feely, R. A., Gnanadesikan, A., *et al.* 2005. Anthropogenic ocean acidification over the twenty-first century and its impact on calcifying organisms. Nature, 437: 681–686.

Palmer, A. R. 1990. Effect of crab effluent and scent of damaged conspecifics on feeding, growth, and shell morphology of the Atlantic dogwhelk *Nucella lapillus* (L.). *In* Progress in Littorinid and Muricid Biology, pp. 155–182. Ed. by K. Johannesson, D. G. Raffaelli, and C. J. Hannaford Ellis. Springer, The Netherlands.

Peck, L. S. 1989. Temperature and basal metabolism in two Antarctic marine herbivores. Journal of Experimental Marine Biology and Ecology, 127: 1–12.

Peck, L. S. 2005. Prospects for survival in the Southern Ocean: vulnerability of benthic species to temperature change. Antarctic Science, 17: 497–507.

Peck, L. S., Baker, A. C., and Conway, L. Z. 1996. Strondium labelling of the shell of the Antarctic limpet *Nacella concinna* (Strebel, 1908). Journal of Molluscan Studies, 62: 315–325.

Peck, L. S., Morley, S. A., Richard, J., and Clark, M. S. 2014. Acclimation and thermal tolerance in Antarctic marine ectotherms. The Journal of Experimental Biology, 217: 16–22.

Peck, L. S., and Veal, R. 2001. Feeding, metabolism and growth in the Antarctic limpet, *Nacella concinna* (Strebel 1908). Marine Biology, 138: 553–560.

Pespeni, M. H., Chan, F., Menge, B. A., and Palumbi, S. R. 2013. Signs of adaptation to local pH conditions across an environmental mosaic in the California Current ecosystem. Integrative and Comparative Biology, 53: 857–870.

Picken, G. B. 1979. Growth, production and biomass of the Antarctic gastropod *Laevilacunaria antarctica* Martens 1885. Journal of Experimental Marine Biology and Ecology, 40: 71–79.

Picken, G. B. 1980. The distribution, growth, and reproduction of the Antarctic limpet *Nacella (Patinigera) concinna* (Strebel, 1908). Journal of Experimental Marine Biology and Ecology, 42: 71–85.

Picken, G. B., and Allan, D. 1983. Unique spawning behavior by the Antarctic limpet *Nacella (Patinigera) concinna* (Strebel, 1980). Journal of Experimental Marine Biology and Ecology, 71: 283–287.

Rasband, W. S. 1997-2012. ImageJ, U. S. National Institutes of Health, Bethesda, Maryland, USA. http://imagej.nih.gov/ij/, Java 1.6.0_51 (32-bit) (last accessed 2 August 2012).

Robbins, L. L., Hansen, M. E., Kleypas, J. A., and Meylan, S. C. 2010. CO2calc: A user-friendly seawater carbon calculator for Windows, Max OS S, and iOS (iPhone). U.S. Geological Survey Open-File report 2010-1280: 1–17.

Sabine, C. L., Feely, R. A., Gruber, N., Key, R. M., Lee, K., Bullister, J. L., Wanninkhof, R., *et al.* 2004. The oceanic sink for anthropogenic CO_2. Science, 305: 367–371.

Schoenrock, K. M., Schram, J. B., Amsler, C. D., McClintock, J. B., and Angus, R. A. 2015. Climate change impacts on overstory *Desmarestia* spp. from the western Antarctic Peninsula. Marine Biology, 162: 377–389.

Schoenrock, K. M., Schram, J. B., Amsler, C. D., McClintock, J. B., and Angus, R. A. 2016. Climate change confers a potential advantage to fleshy Antarctic crustose macroalgae over calcified species. Journal of Experimental Marine Biology and Ecology, 474: 58–66.

Schram, J. B., Schoenrock, K. M., McClintock, J. B., Amsler, C. D., and Angus, R. A. 2014. Multiple stressor effects of near-future elevated seawater temperature and decreased pH on righting and escape behaviors of two common Antarctic gastropods. Journal of Experimental Marine Biology and Ecology, 457: 90–96.

Schram, J. B., Schoenrock, K. M., McClintock, J. B., Amsler, C. D., and Angus, R. A. 2015. Multi-frequency observations of seawater carbonate chemistry on the central coast of the western Antarctic Peninsula. Polar Research, 34: 25582.

Seibel, B. A., Maas, A. E., and Dierssen, H. M. 2012. Energetic plasticity underlies a variable response to ocean acidification in the pteropod, *Limacina helicina antarctica*. PLoS ONE, 7: e30464.

Shabica, S. V. 1976. The natural history of the Antarctic limpet *Patinigera polaris* (Hombron and Jacquinot). *In* Oceanography, p. 317. Oregon State University.

Shirayama, Y., and Thornton, H. 2005. Effect of increased atmospheric CO_2 on shallow water marine benthos. Journal of Geophysical Research: Oceans, 110: C09S08.

Suckling, C. C., Clark, M. S., Richard, J., Morley, S. A., Thorne, M. A., Harper, E. M., and Peck, L. S. 2014. Adult acclimation to combined

temperature and pH stressors significantly enhances reproductive outcomes compared to short-term exposures. Journal of Animal Ecology, 84: 773–784.

Turner, J., Barrand, N. E., Bracegirdle, T. J., Convey, P., Hodgson, D. A., Jarvis, M., Jenkins, A., *et al.* 2014. Antarctic climate change and the environment: an update. Polar Record, 50: 237–259.

Vaughn, D. G., Marshall, G. J., Connolley, W. M., Parkinson, C., Mulvaney, R., Hodgson, D. A., King, J. C., *et al.* 2003. Recent rapid regional climate warming on the Antarctic Peninsula. Climate Change, 60: 243–274.

Waller, C. L. 2013. Zonation in a cryptic Antarctic intertidal macrofaunal community. Antarctic Science, 25: 62–68.

Watson, S. A., Peck, L. S., Tyler, P. A., Southgate, P. C., Tan, K. S., Day, R. W., and Morley, S. A. 2012. Marine invertebrate skeleton size varies with latitude, temperature and carbonate saturation: implications for global change and ocean acidification. Global Change Biology, 18: 3026–3038.

Weihe, E., and Abele, D. 2008. Differences in the physiological response of inter- and subtidal Antarctic limpets *Nacella concinna* to aerial exposure. Aquatic Biology, 4: 155–166.

Handling editor: Joanna Norkko

ICES Journal of Marine Science

ICES Journal of Marine Science (2016), 73(3), 753–763. doi:10.1093/icesjms/fsv236

Contribution to Special Issue: 'Towards a Broader Perspective on Ocean Acidification Research'

Original Article

Limited effects of increased CO_2 and temperature on metal and radionuclide bioaccumulation in a sessile invertebrate, the oyster *Crassostrea gigas*

Murat Belivermiş[1], Michel Warnau[2], Marc Metian[2], François Oberhänsli[2], Jean-Louis Teyssié[2], and Thomas Lacoue-Labarthe[2,3]*

[1]*Department of Biology, Faculty of Science, Istanbul University, 34134 Vezneciler, Istanbul, Turkey*
[2]*International Atomic Energy Agency-Environment Laboratories, 4 Quai Antoine Ier, MC 98000 Monaco, Monaco*
[3]*Littoral Environnement et Sociétés, UMR 7266 CNRS—Université de La Rochelle, 2 rue Olympe de Gouges, 17000 La Rochelle, France*

*Corresponding author: tel: +33 5 46 45 83 88; e-mail: tlacouel@univ-lr.fr

Belivermiş, M., Warnau, M., Metian, M., Oberhänsli, F., Teyssié, J-L., and Lacoue-Labarthe, T. Limited effects of increased CO_2 and temperature on metal and radionuclide bioaccumulation in a sessile invertebrate, the oyster *Crassostrea gigas*. – ICES Journal of Marine Science, 73: 753–763.

Received 29 June 2015; revised 11 November 2015; accepted 13 November 2015; advance access publication 19 December 2015.

This study investigated the combined effects of reduced pH and increased temperature on the capacities of the Pacific cupped oyster *Crassostrea gigas* to bioconcentrate radionuclide and metals. Oysters were exposed to dissolved radiotracers (^{110m}Ag, ^{241}Am, ^{109}Cd, ^{57}Co, ^{54}Mn, and ^{65}Zn) at three pH (7.5, 7.8, 8.1) and two temperatures (21 and 24°C) under controlled laboratory conditions. Although calcifying organisms are recognized as particularly vulnerable to ocean acidification, the oyster did not accumulate differently the studied metals when exposed under the different pH conditions. However, temperature alone or in combination with pH somewhat altered the bioaccumulation of the studied elements. At pH 7.5, Cd was accumulated with an uptake rate constant twofold higher at 24°C than 21°C. Bioaccumulation of Mn was significantly affected by an interactive effect between seawater pH and temperature, with a decreased uptake rate at pH 7.5 when temperature increased (27 ± 1 vs. 17 ± 1 d^{-1} at 21 and 24°C, respectively). Retention of Co and Mn tended also to decrease at the same pH with decreasing temperature. Neither pH nor temperature affected strongly the elements distribution between shell and soft tissues. Significant effects of pH were found on the bioaccessibility of Mn, Zn, and ^{241}Am during experimental *in vitro* simulation of human digestion.

Keywords: bioaccumulation, *in vitro* digestion, metal, ocean acidification, Pacific oyster, radiotracer.

Introduction

The increase in partial pressure of CO_2 (pCO_2) in the atmosphere due to anthropogenic activities is well recognized as a driver of major global changes such as the elevation of atmospheric temperature. The global mean surface air temperature is projected to increase by 1–3.7°C by the end of the century (IPCC, 2013). Therefore, the temperature of ocean will increase by 0.6–2.0°C for the top 100 m (IPCC, 2013). Additionally, the ocean is a major sink for atmospheric CO_2 (it absorbs ~25% of the anthropogenic emissions) and thus the increase in pCO_2 in the atmosphere implies an increase in pCO_2 in surface ocean waters, that causes the "other" CO_2 problem (Doney *et al.*, 2009), better known as "ocean acidification".

Marine organisms can be affected by ocean acidification through (i) limitation of available carbonates, mainly affecting calcifying organisms, (ii) the increase in H^+ ions in the water resulting in decreasing pH, i.e. acidification of the surrounding environment, and (3) an increase in pCO_2 within their body (hypercapnia). In this context, attention should be paid to vulnerable species, which have key role(s) in the food chains, or are of high economic interest for aquaculture or fisheries.

The Pacific cupped oyster *Crassostrea gigas* is the most farmed oyster species in the world (FAO, 2014), with an annual production of 0.609 million t for ca. US$ 1.3 billion (2012 data). Consequently, many researchers focused on this marine resource and recently investigated, among others, the responses of the Pacific cupped

oyster to ocean acidification. Several studies assessed growth, calcification, development, and survival of oysters under realistic low pH and low carbonate concentrations conditions (for a review, see Gazeau *et al.*, 2013). A particular attention has been paid to the early life stages of the oyster, which are considered as the most vulnerable and thereby as a bottleneck for population dynamics (Dupont *et al.*, 2010). Overall, reduced shell size and thickness, developmental retardation, and increased mortality are the most common effects of elevated pCO_2 on *C. gigas* (e.g. Parker *et al.*, 2010; Gazeau *et al.*, 2011; Barton *et al.*, 2012). Intraspecific variations have been highlighted, and it has been suggested that some populations could be pre-adapted to ocean acidification (Parker *et al.*, 2010, 2011; Timmins-Schiffman *et al.*, 2013).

The elevated pCO_2 in seawater is expected to affect the metabolism through disturbances of acid–base regulation and respiration (Pörtner *et al.*, 2004). It is admitted that active organisms, such as fish, cephalopods, and crustaceans, have naturally the required physiological machinery to deal with elevated extracellular pCO_2 (Melzner *et al.*, 2009). In contrast, sessile organisms, such as oysters, are weak acid–base regulators and, in the light of the current knowledge, tend to increase their energy demand to poorly compensate the body acidosis (Parker *et al.*, 2013). This energy budget change is exacerbated when seawater temperature increases (Lannig *et al.*, 2010) and could affect other performances such as somatic growth and survival (Beniash *et al.*, 2010).

Mining, fossil fuel combustion, industrial activities, and uncontrolled discharges are common sources of trace element and radionuclide releases in the environment and are major contributors to the contamination of coastal marine ecosystems over the last century. Widespread in the environment, these contaminants are accumulated in organisms, and potentially bio-magnified along the food chains (Zhou *et al.*, 2008). Excessive accumulation of essential (e.g. Co, Mn or Zn) or non-essential (e.g. Ag, ^{241}Am, Cd) elements in organisms can induce toxic effects (Rainbow, 2002). Since bioaccumulation of metals in biota depends on (i) the bioavailability of the element determined by physicochemical conditions of the environment, (ii) the biological traits of organisms (e.g. metabolism, feeding strategy), and (iii) the element properties with respect to biological tissues (e.g. ligand affinities, biological function), it appears pertinent to investigate the effect of ocean acidification on metal bioaccumulation capacities. Indeed, pH and seawater chemistry changes caused by increased pCO_2 affect chemical speciation of metals and therefore their bioavailability to organisms (Millero *et al.*, 2009), especially for elements that form strong complexes with carbonates (e.g. Am—Choppin, 2006). Furthermore, increased temperature or hypercapnia (as discussed above) can influence the bioaccumulation of metals (White and Rainbow, 1984; Houlbrèque *et al.*, 2011), and can thus enhance their toxicity (e.g. Pascal *et al.*, 2010; Roberts *et al.*, 2013).

This study aims at assessing the bioaccumulation behaviours of radionuclides/metals in a sessile species of economic importance, the Pacific cupped oyster, *C. gigas*, usually cultured in coastal areas subjected to metal contamination and high pCO_2 variations (e.g. Green *et al.*, 2009). Radiotracer techniques were used to determine uptake and depuration parameters of six elements during experimental exposures of oysters to dissolved radiotracers (^{110m}Ag, ^{241}Am, ^{109}Cd, ^{57}Co, ^{54}Mn, and ^{65}Zn) at three pH (7.5, 7.8, 8.1) and two temperatures (21 and 24°C) under controlled laboratory conditions (Warnau and Bustamante, 2007). *In vitro* human digestion simulations (Versantvoort *et al.*, 2005) were also carried out to determine the bioaccessible fraction of metals and radionuclides in oysters that would be ingested by humans (Metian *et al.*, 2009a).

Material and methods

Organisms, acclimation, and experimental conditions

One hundred and sixty-two adult oysters *C. gigas* (17.71 ± 3.36 g wet wt) were purchased at the "Satmar" farm in Oleron Island, Charentes-Maritimes, France, in January 2013. At the IAEA-EL premises, the oysters were randomly distributed among six 70 l glass aquaria and acclimated for 2 weeks in 0.45 μm filtered, UV-sterilized natural seawater (aerated open circuit 70 l aquarium; seawater flux: 70 l h^{-1}; salinity: 38 p.s.u.; light/dark cycle: 12/12 h). Then, the pH and the temperature were progressively modified over 1 week until targeted values (see experimental procedure below) and acclimation to these targeted conditions was allowed for at least 15 d before the radiotracers exposure. During the whole acclimation period, oysters were fed daily with a mixed algal diet composed of *Isochrysis galbana* and *Skeletonema costatum*.

The oysters were maintained under controlled temperature and pH in a crossed experimental design (temperatures × 3 pH levels). Owing to technical constraints (mainly in terms of radiotracer cost and wastewater management), only one 70 l tank could be dedicated per pCO_2–temperature condition. To avoid other variation in other factors (e.g. light), the tanks were randomly interspersed on the bench. In addition, seawater was very frequently renewed (every 1–2 d) and tanks were cleaned at each seawater renewal to prevent any "tank" effect due to the development of different biomasses or to the accumulation of detritus such as pseudo faeces, or bacterial proliferation, which might affect the metabolism of oysters or the bioavailability of the chemicals. The three selected pH values were 8.10 (~400 μatm), 7.80 (~800 μatm), and 7.50 (~1800 μatm) and the two temperatures were 21 and 24°C in accordance with the projected values over the next two centuries (Orr *et al.*, 2005; Solomon *et al.*, 2007; current condition: pH 8.1–21°C; estimated conditions by 2100: pH 7.8–24°C; estimated conditions by 2200: pH 7.5–24°C). The pH was controlled in each aquarium to within ± 0.05 pH unit with a continuous pH-stat system (IKS, Aquastar©) that bubbled pure CO_2 into the tanks that were continuously aerated with CO_2-free air (see Lacoue-Labarthe *et al.*, 2012). The pH values of the pH-stat system were calibrated every week from measurements of pH on the total scale, using Tris/HCl buffer solution with a salinity of 38 p.s.u. and prepared according to Dickson *et al.* (2007). The pCO_2 was determined from pH and total alkalinity using the R package seacarb (Gattuso *et al.*, 2015).

Radiotracer exposures

The oysters were exposed for 21 d to dissolved radiotracers: ^{110m}Ag [as $^{110m}AgNO_3$; $T_{\frac{1}{2}} = 250$ d], ^{241}Am [as $^{241}AmNO_3$; $T_{\frac{1}{2}} = 432$ year], ^{109}Cd [as $^{109}CdCl_2$; $T_{\frac{1}{2}} = 464$ d], ^{57}Co [as $^{57}CoCl_2$; $T_{\frac{1}{2}} = 272$ d], ^{54}Mn [as $^{54}MnCl_2$; $T_{\frac{1}{2}} = 312$ d], and ^{65}Zn [as $^{65}ZnCl_2$; $T_{\frac{1}{2}} = 244$ d]. Uptake kinetics were followed during that period, after which seawater was no longer spiked to assess the metal retention capacities of the oysters.

During the exposure period, the seawater of each 70 l tank was spiked with typically 5 μl of radioactive stock solution (^{110m}Ag, dissolved in 0.1 M HCl, ^{241}Am in 1 M HCl, ^{109}Cd in 0.5 M HCl, ^{57}Co 0.1 M in HCl, ^{54}Mn in 0.5 M HCl, and ^{65}Zn in 0.5 M HCl). Seawater and spikes were renewed daily during the first week and then every second day to maintain good water quality and radiotracer concentrations as constant as possible (Metian *et al.*, 2008) as metal could

be removed from seawater medium through absorption (in organisms) or adsorption on surface (e.g. aquarium glasses). For water renewal, each tank was emptied and then, immediately slowly refilled (30 min for ~60 l) with new seawater at the required temperature. The slow refill allowed for immediate regulation of the targeted pCO_2 level by the IKS system. Before renewal of the seawater, the oysters were fed with the algal diet for 30 min, after which time, the new seawater was spiked with the required volumes of the radioactive stock solutions.

Activity of the radiotracers in seawater was checked before and after each spike renewal, yielding for the time-integrated activities in seawater for the six radiotracers shown in Table 1.

Five oysters from each aquarium were identified (tagged), weighted, and whole-body radioanalysed alive (same individuals each time) daily during the first week, and then every second day to follow the radiotracers uptake kinetics. During the counting sessions, oysters were held out of the seawater as briefly as possible (typically 10–20 min). At the end of the 21-d exposure period, three individuals (not belonging to the tag-identified batch) from each tank were collected and dissected. Shell and all soft tissues were separated and radio-analysed to assess the distribution of radiotracers between these two compartments.

The remaining exposed oysters were placed in non-contaminated conditions (open-circuit 70 l tank with same salinity, temperature, pH, and light:dark conditions as previously indicated) for 38 d. Flowing seawater was adjusted to maintain pH values as constant as possible (seawater flux: 70 l h^{-1}). The five tag-identified oysters in each tank were radioanalysed every day during the first week and then every second day to follow the depuration kinetics of the radiotracers. Three individuals from each tank were collected at the end of the depuration period and dissected for radio-analysis as described above.

In vitro digestion simulation

At the end of the exposure and depuration periods, three oysters were collected in each tank to perform *in vitro* simulated digestion (Versantvoort *et al.*, 2005) to assess the bioaccessible fraction of elements for human consumers of oysters. The method consists of a three-step procedure simulating quiet closely the human digestion processes. Homogenized oyster tissues were step by step exposed to artificial saliva, gastric juice and mixture of duodenal juice, bile, and $NaHCO_3$ (chemicals and enzymes were purchased from Sigma®). Following the *in vitro* digestion, the resulting chyme was centrifuged and the radiotracers activities in supernatant, considered as the bioaccessible element fraction, were counted. The detailed procedure has been previously described by Metian *et al.* (2009a).

Radioanalyses and data treatments

The radiotracers were counted using a high-resolution γ-spectrometry system consisting of five coaxial Germanium (N- or P-type) detectors (EGNC 33-195-R, Canberra® and Eurysis®) connected to a multi-channel analyser and a computer equipped with a spectra analysis software (Interwinner® 6). The radioactivity of the samples (whole-body oysters, seawater, soft tissues, and supernatant and pellets) was determined by comparison with standards of known activities and appropriate geometries and was corrected for background and physical decay of the radiotracers. The counting time was adjusted to obtain a propagated counting error of <5% (Rodriguez *y* Baena *et al.*, 2006).

The uptake of radiotracer was expressed as change in concentration factors (*CF*), which is the ratio between radiotracer activity in the whole-body oyster (Bq g^{-1}) and the time-integrated radiotracer activity in seawater (Bq g^{-1}) over time. Uptake kinetics were fitted using either a linear equation [Equation (1)] or a saturation exponential equation [Equation (2)]:

$$CF_t = k_u t, \tag{1}$$

$$CF_t = CF_{ss}(1 - e^{-k_e t}), \tag{2}$$

where CF_t and CF_{ss} ($CF_{ss} = k_u/k_e$) are the concentration factors at time t (d) and at steady state, respectively, and k_e and k_u are the biological depuration and uptake rate constants (d^{-1}), respectively (Whicker and Schultz, 1982).

Radiotracer depuration kinetics were expressed in terms of change in percentage of remaining activity (i.e. radioactivity at time t divided by the initial radioactivity measured in the individual at the beginning of the depuration period × 100) with time. The depuration kinetics were fitted by a simple exponential model [Equation (3)]:

$$A_t = A_0 e^{-k_e t}, \tag{3}$$

Table 1. Carbonate system parameters during the uptake and depuration phase of the experiment on the bioaccumulation of metal and radionuclide in oyster exposed.

Experiment phase	Temperature (°C)	pH_T	pCO_2 (μatm)	^{110m}Ag (Bq ml^{-1})	^{241}Am (Bq ml^{-1})	^{109}Cd (Bq ml^{-1})	^{57}Co (Bq ml^{-1})	^{54}Mn (Bq ml^{-1})	^{65}Zn (Bq ml^{-1})
Uptake	20.9 ± 0.9	7.43 ± 0.03	2161 ± 177	0.06 ± 0.05	0.15 ± 0.08	0.28 ± 0.05	0.44 ± 0.09	0.25 ± 0.08	0.38 ± 0.12
	20.8 ± 0.9	7.79 ± 0.03	854 ± 54	0.06 ± 0.05	0.14 ± 0.07	0.25 ± 0.02	0.43 ± 0.09	0.21 ± 0.10	0.37 ± 0.13
	20.8 ± 0.8	8.03 ± 0.02	451 ± 27	0.06 ± 0.04	0.13 ± 0.07	0.26 ± 0.03	0.44 ± 0.09	0.19 ± 0.11	0.36 ± 0.12
	23.7 ± 0.2	7.52 ± 0.03	1732 ± 125	0.07 ± 0.03	0.14 ± 0.07	0.27 ± 0.03	0.44 ± 0.08	0.23 ± 0.09	0.39 ± 0.11
	24.0 ± 0.1	7.88 ± 0.08	699 ± 157	0.07 ± 0.04	0.14 ± 0.08	0.25 ± 0.03	0.42 ± 0.11	0.18 ± 0.12	0.38 ± 0.11
	24.0 ± 0.1	8.08 ± 0.05	396 ± 63	0.07 ± 0.04	0.15 ± 0.08	0.28 ± 0.05	0.45 ± 0.09	0.19 ± 0.12	0.38 ± 0.12
Loss	21.6 ± 0.1	7.45 ± 0.04	2023 ± 180	–	–	–	–	–	–
	21.6 ± 0.1	7.85 ± 0.03	742 ± 61	–	–	–	–	–	–
	21.2 ± 0.2	8.03 ± 0.01	444 ± 16	–	–	–	–	–	–
	24.0 ± 0.2	7.54 ± 0.11	1689 ± 355	–	–	–	–	–	–
	23.8 ± 0.1	7.79 ± 0.07	867 ± 149	–	–	–	–	–	–
	24.0 ± 0.1	8.06 ± 0.04	413 ± 50	–	–	–	–	–	–

The indicative average partial pressure of CO_2 (pCO_2) were calculated for a seawater salinity of 38 and a total alkalinity of 2540 μmol kg^{-1} average.

where A_t and A_0 are the remaining activities at time t (d) and 0, respectively, and k_e is the biological depuration rate constant (d^{-1}) (Warnau *et al.*, 1996). The biological half-life (d) of the radiotracer can then be calculated according to the relation [Equation (4)]:

$$T_{b1/2} = \frac{\ln 2}{k_e}. \quad (4)$$

All statistics and graphics were performed using R freeware (R Core Team, 2014). Model constants and their statistics were estimated by iterative adjustment of the models using linear and non-linear mixed effect models (*lme* and *nlme* functions from the package "nlme"; Pinheiro *et al.*, 2014), in which individual oyster identity had been considered a random factor. Marginal R^2 representing the variance explained by the fixed factor (i.e. time) has been applied to linear models using the *r.squaredGLMM* function (package "MuMIn"; Bartoń, 2014). Comparison of uptake and elimination constant rates among the different pH/temperature conditions was performed using two-way ANOVA on k_u and k_e calculated for each individual oyster (the best fitting model obtained for the entire set of oysters was applied to individuals). A χ^2 test was used to compare bioaccessible fractions of metals among the different oyster groups. The level of significance for statistical analyses was always set at $\alpha = 0.05$.

Results

During the whole experimental period (i.e. 3 and 5 weeks of uptake and depuration phase, respectively) where the oysters were exposed to six different conditions (combinations of two temperatures and three pH; see the Material and methods section), limited growth of individual (<1%) was measured, and mortality was relatively high (18.5–29.6% according to tank), although no connection between mortality and specific exposure condition could be detected. Specific mortality of oysters with condition of exposure were the following: 18.5% for 7.5 (pH)–21°C (temperature), 26% for 7.8–21°C, 26% for 8.1–21°C, 29.6% for 7.5–24°C, 18.5% for 7.8–24°C, and 26% for 8.1–24°C.

The whole-body bioaccumulation kinetics of ^{110m}Ag, ^{241}Am, ^{109}Cd, ^{57}Co, ^{54}Mn, and ^{65}Zn in oysters and their respective model parameters are shown in Figure 1 and Table 2. The uptake of all elements except ^{241}Am were best fitted by linear models. The actinide displayed an exponential uptake pattern, tending to reach a steady-state value ranging between 360 and 470 according to pH–temperature conditions (Table 2) after 3 weeks of exposure. At the end of the exposure period and whatever the pH/temperature conditions, the estimated uptake rate constant (k_u) allowed ranking radiotracers taken up linearly according to their bioaccumulation capacities: ^{110m}Ag > ^{65}Zn > ^{54}Mn > ^{109}Cd ~ ^{57}Co.

At the end of the exposure period, oysters were placed in non-contaminating conditions and depuration of radiotracers was followed for 37 d (Supplementary Figure S1). The whole-body depuration kinetics of all elements were best fitted by a one-compartment exponential model (Table 3). However, it was not possible to determine accurately the depuration kinetic parameters for ^{109}Cd as the activity rapidly dropped below the detection limits of gamma spectrometers. All radiotracers were efficiently retained by *C. gigas* ($T_{b\frac{1}{2}}$ between 50 and >600 d).

Statistical analyses carried out on individual uptake rate constants (k_u; two-way ANOVA; Table 4) revealed that neither pH nor temperature significantly affected the bioaccumulation of metals in oysters (uptake and depuration biokinetics) except ^{109}Cd and ^{54}Mn. The highest temperature affected Cd accumulation (Figure 1, Table 4), which displayed an uptake rate constant at pH 7.5 twofold higher at 24°C than at 20°C (23 ± 1 vs. 11 ± 1 d^{-1}, respectively; Table 4, interactive effect pH × temperature: $p < 0.1$). For Mn, k_u was significantly affected by an interactive effect between seawater pH and temperature, with a decreased uptake rate constant at pH 7.5 when temperature increased (27 ± 1 vs. 17 ± 1 d^{-1} at 21 and 24°C, respectively; see Figure 1 and Table 4). Regarding the depuration rate constant of ^{241}Am, a significant interactive effect was observed at pH 7.8 where $T_{b\frac{1}{2}}$ was twofold lower at 24°C than at 21°C (Tukey's test; $p = 0.049$; Table 4). Retention of Co and Mn tended also to decrease at the same pH when comparing warmer with colder temperatures (Table 4; pH × temperature; $p < 0.1$).

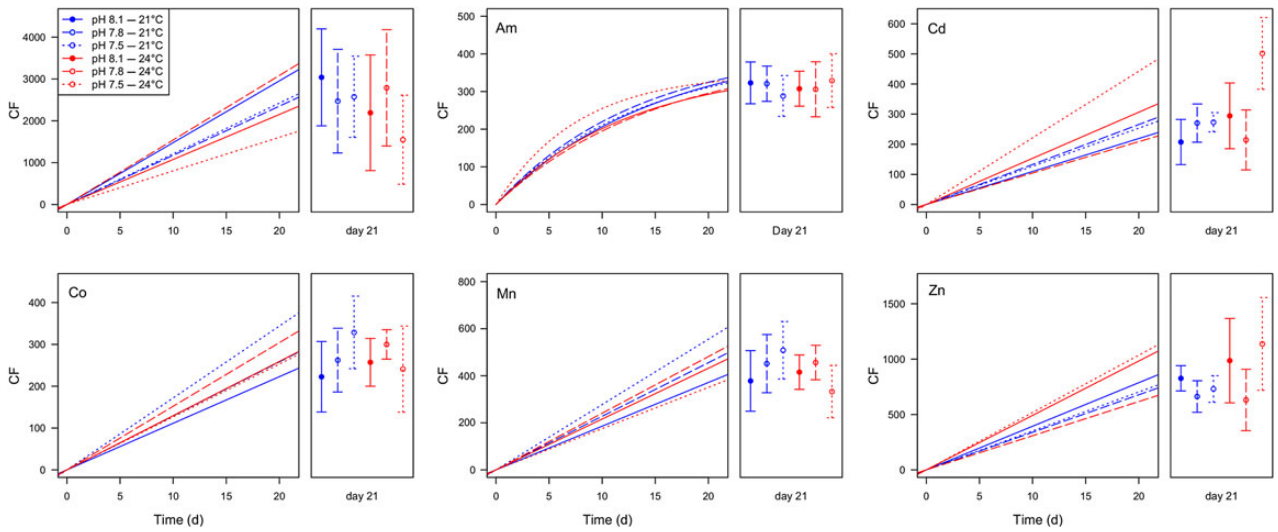

Figure 1. *Crassostrea gigas*. Uptake kinetics of ^{110m}Ag, ^{241}Am, ^{109}Cd, ^{57}Co, ^{54}Mn, ^{65}Zn (*CF*) in the oysters exposed to dissolved radiotracers at three different pHs—pH 8.1, pH 7.8, and pH 7.5, and two temperatures (21°C in blue and 24°C in red). Points are omitted for clarity and only kinetics models are delineated along the uptake phase. Mean ± s.d. of *CF* are plotted for the day 24 at the end of the uptake. Parameters of models and statistics are reported in Tables 2 and 4, respectively.

Table 2. Parameters of the uptake kinetics of ^{110m}Ag, ^{241}Am, ^{109}Cd, ^{57}Co, ^{54}Mn, ^{65}Zn in oysters exposed for 21 d to dissolved radiotracers under three pHs and two temperatures conditions.

Element	Temp (°C)	pH	Model	$k_u \pm$ s.e.	$k_e \pm$ s.e.	$CF_{ss} \pm$ s.e.	Marginal R^2	CF_{21d}
^{110m}Ag	21	7.5	L	123.0 ± 6.4	–	–	0.755	2661 ± 1003
		7.8	L	118.2 ± 7.9	–	–	0.644	2549 ± 1278
		8.1	L	146.5 ± 8.2	–	–	0.719	3141 ± 1198
	24	7.5	L	68.2 ± 6.2	–	–	0.443	1587 ± 1092
		7.8	L	146.1 ± 11.0	–	–	0.610	2844 ± 1419
		8.1	L	110.5 ± 9.2	–	–	0.556	2236 ± 1409
^{241}Am	21	7.5	E	30.4 ± 5.3	0.078 ± 0.011	390 ± 39	–	281 ± 53
		7.8	E	31.9 ± 5.5	0.078 ± 0.011	407 ± 39	–	330 ± 48
		8.1	E	30.2 ± 4.7	0.074 ± 0.008	408 ± 48	–	329 ± 56
	24	7.5	E	45.7 ± 8.0	0.127 ± 0.019	362 ± 32	–	311 ± 102
		7.8	E	24.8 ± 5.3	0.052 ± 0.010	474 ± 33	–	314 ± 75
		8.1	E	30.3 ± 4.1	0.085 ± 0.008	357 ± 33	–	315 ± 48
^{109}Cd	21	7.5	L	12.5 ± 0.5	–	–	0.887	272 ± 32
		7.8	L	13.2 ± 0.8	–	–	0.726	272 ± 64
		8.1	L	10.5 ± 0.8	–	–	0.642	209 ± 76
	24	7.5	L	22.8 ± 1.0	–	–	0.852	504 ± 120
		7.8	L	10.2 ± 1.1	–	–	0.502	216 ± 100
		8.1	L	14.7 ± 1.2	–	–	0.545	295 ± 109
^{57}Co	21	7.5	L	16.9 ± 0.6	–	–	0.895	332 ± 88
		7.8	L	12.6 ± 0.6	–	–	0.827	266 ± 77
		8.1	L	10.7 ± 0.6	–	–	0.753	226 ± 86
	24	7.5	L	12.0 ± 0.7	–	–	0.725	244 ± 104
		7.8	L	14.9 ± 0.3	–	–	0.966	305 ± 36
		8.1	L	12.4 ± 0.4	–	–	0.882	261 ± 58
^{54}Mn	21	7.5	L	26.8 ± 0.9	–	–	0.900	518 ± 124
		7.8	L	22.5 ± 0.9	–	–	0.829	468 ± 128
		8.1	L	18.1 ± 0.8	–	–	0.792	391 ± 133
	24	7.5	L	16.7 ± 0.8	–	–	0.796	341 ± 114
		7.8	L	22.8 ± 0.7	–	–	0.917	473 ± 76
		8.1	L	20.1 ± 0.6	–	–	0.900	430 ± 76
^{65}Zn	21	7.5	L	34.7 ± 1.0	–	–	0.921	740 ± 122
		7.8	L	32.8 ± 1.2	–	–	0.876	671 ± 144
		8.1	L	39.2 ± 1.1	–	–	0.922	842 ± 116
	24	7.5	L	52.1 ± 3.0	–	–	0.763	1160 ± 426
		7.8	L	30.5 ± 2.0	–	–	0.665	641 ± 282
		8.1	L	48.3 ± 2.9	–	–	0.657	996 ± 385

E, exponential model; L, Linear model; k_u, uptake rate d^{-1}; k_e, elimination rate d^{-1}; s.e., standard error; CF_{ss}, steady-state concentration factor; Marginal R^2, marginal coefficient of determination.

When looking at the distribution of the radiotracers between shells and soft tissues (Table 5), ^{241}Am, ^{57}Co, and ^{54}Mn were mainly associated with the shells (>94%), whereas ^{109}Cd was equally distributed between the two compartments and ^{110m}Ag and ^{65}Zn were mainly found in soft tissues (76–98 and 67–92%, respectively). It is also noteworthy that ^{65}Zn fraction in soft tissues increased between the end of uptake period and the end of depuration period, at all pH and temperature conditions, suggesting a faster depuration of Zn associated with shells than that with soft tissues when non-contaminating conditions were restored. Neither pH nor temperature affected strongly distribution of metals and radionuclide between shells and soft tissues, except that the fraction of ^{110m}Ag associated with soft tissues at the end of the uptake phase were lower in oysters maintained at 24°C when compared with those kept at 21°C ($p < 0.05$, Mann–Whitney *U*-test; Table 5). Finally, the radiotracer CFs reached in the oyster shells at the end of the uptake phase were not affected significantly by pCO_2 conditions (Supplementary Table S1).

The *in vitro* digestion simulations revealed that the bioaccessible fraction of metals and radionuclide varied from 30% (^{241}Am in oyster maintained at 24°C and pH 7.8) to more than 90% (^{57}Co in all oysters; Figure 2). Significant effects of pH were highlighted for ^{241}Am, ^{109}Cd, ^{54}Mn, and ^{65}Zn (Table 6). For these elements, the bioaccessible fraction at the end of the uptake phase tended to increase with decreasing pH except at pH 8.1–24°C. At the end of the depuration phase, a similar trend was observed in oysters maintained at 24°C, whereas a decrease in bioacessibility with decreasing pH was noted for the 21°C-maintained oysters. Nevertheless, these results must be considered with caution due to the small number of oysters analysed per condition ($n = 3$).

Discussion

Contamination of coastal waters is a worldwide concern. Ocean acidification and thus modified chemistry of seawater may change the way contaminants will interact with marine biota. For example, it affects the chemical speciation of cations, especially those that form complexes with carbonates and potentially increases their bioavailability for biota (e.g. Byrne *et al.*, 1988) by increasing the free-ion form in acidified conditions. Among the elements considered in the present study, only ^{241}Am is known as being able to

bind to carbonates but with limited change in speciation in the tested pH range, largely dominated by hydroxyl-Am form (Choppin, 2006). According to previous work and metal speciation model as a function of seawater pH, metals that are mainly bound to chloride (such as Ag and Cd) or those that are predominantly found in the free-ion form (e.g. Co, Mn, Zn) are not strongly affected by decreasing pH. Indeed, the free metal ion concentrations of these elements increased from only few per cent when pH decreased from 8.1 to 7.5 (Lacoue-Labarthe *et al.*, 2009; Millero *et al.*, 2009). We thus assume that, for the seawater pH range tested in the context of ocean acidification, bioaccumulation would be less affected by change in metal speciation itself than by resulting change in the biological mechanisms of metal uptake and/or elimination.

Table 3. Parameters of the depuration kinetics of ^{110m}Ag, ^{241}Am, ^{57}Co, ^{54}Mn, and ^{65}Zn in oysters previously exposed for 21 d to dissolved radiotracers under three pHs and two temperatures conditions and maintained for 37 d in non-contaminated conditions.

Element	Temp (°C)	pH	A_{0l} ± s.e. (%)	k_{el}	$T_{b\frac{1}{2}}$ ± s.e. (d)
^{54}Mn	21	7.5	98.2 ± 1.4	0.007 ± 0.001**	97 ± 13
		7.8	101.0 ± 1.4	0.006 ± 0.001**	119 ± 19
		8.1	99.3 ± 1.2	0.006 ± 0.001**	118 ± 16
	24	7.5	96.3 ± 2.5	0.003 ± 0.002	217 ± 121
		7.8	99.9 ± 0.9	0.013 ± 0.001**	56 ± 3
		8.1	97.8 ± 1.3	0.005 ± 0.001**	110 ± 18
^{57}Co	21	7.5	99.7 ± 1.7	0.006 ± 0.001**	120 ± 24
		7.8	99.0 ± 1.6	0.005 ± 0.001**	132 ± 26
		8.1	99.0 ± 1.7	0.007 ± 0.001**	95 ± 15
	24	7.5	98.9 ± 2.6	0.003 ± 0.002	236 ± 143
		7.8	100.4 ± 1.3	0.013 ± 0.001**	55 ± 4
		8.1	97.3 ± 1.6	0.006 ± 0.001**	115 ± 21
^{65}Zn	21	7.5	97.2 ± 1.5	0.007 ± 0.001**	100 ± 16
		7.8	99.6 ± 2.5	0.008 ± 0.002**	92 ± 21
		8.1	99.6 ± 1.2	0.005 ± 0.001**	153 ± 26
	24	7.5	97.4 ± 3.7	0.006 ± 0.003*	125 ± 59
		7.8	95.8 ± 1.5	0.005 ± 0.001**	149 ± 34
		8.1	98.8 ± 1.3	0.005 ± 0.001**	134 ± 22
^{110m}Ag	21	7.5	99.9 ± 1.7	0.005 ± 0.001**	137 ± 31
		7.8	102.1 ± 2.0	0.006 ± 0.001**	110 ± 22
		8.1	101.8 ± 1.2	0.003 ± 0.001**	260 ± 72
	24	7.5	92.3 ± 4.6	0.001 ± 0.003	613 ± 1173
		7.8	98.9 ± 1.5	0.003 ± 0.001	273 ± 102
		8.1	100.9 ± 1.1	0.004 ± 0.001**	185 ± 33
^{241}Am	21	7.5	95.1 ± 1.5	0.012 ± 0.001**	56 ± 5
		7.8	97.8 ± 1.9	0.009 ± 0.001**	77 ± 11
		8.1	96.7 ± 1.6	0.011 ± 0.001**	61 ± 6
	24	7.5	98.0 ± 2.5	0.006 ± 0.001**	107 ± 30
		7.8	97.1 ± 2.0	0.016 ± 0.002**	42 ± 4
		8.1	92.8 ± 3.3	0.007 ± 0.002**	88 ± 27

All kinetics were best fitted by a one-compartment exponential model: A_0, assimilation efficiency; s.e., standard error; $T_{b\frac{1}{2}}$, biological half-life (d), k_e, depuration rate constant; R^2, regression coefficient. Significant differences of k_e are indicated by *($p < 0.05$), **($p < 0.005$).

In the current study, we examined the bioaccumulation patterns of six metals and one actinide in the Pacific cupped oyster *C. gigas* under elevated conditions of temperature and pCO_2, using the levels projected for the end of the current century. Like other sessile invertebrates living in estuarine, intertidal, and subtidal zones, *C. gigas* uses to be exposed to broad ranges of pH and temperatures in their habitats, potentially leading to an adaptation to a wide range of abiotic conditions (Lannig *et al.*, 2010). For example, metabolic depression is an adaptive mechanism used by shelled intertidal molluscs to preserve energy during low tides. This physiological plasticity is time-limited and might not be adapted to long-term, continuous exposure to hypercapnic conditions. In the present study, the greater mortality observed at the lowest pH and highest temperature may suggest that energetic balance were pushed to the edge when both stressors were combined (Lannig *et al.*, 2010).

The distribution of radiotracers between soft tissues and shells was in accordance with previous studies: ^{241}Am, Co, Mn were mainly adsorbed on the calcareous structures, whereas Cd, Zn, and Ag fraction associated with soft tissues was gradually increasing during the depuration period (Metian *et al.*, 2009b, 2011; Hédouin *et al.*, 2010). *CF*s of ^{241}Am, Co, and Mn in shells at the end of the uptake phase were not significantly affected by seawater pCO_2 conditions, implying that the adsorption capacity of shells is not strongly affected by decreasing pH for these metals. This might be explained by the fact that (i) increasing protons concentration resulting from decreasing pH does not significantly compete with metallic cations for shell binding sites and/or (ii) the binding sites are not affected by hypercapnia in the conditions tested (shells of *C. gigas*—mainly made of calcite—are considered less vulnerable to calcareous dissolution than aragonitic shells; Gazeau *et al.*, 2007).

The main result of our study is that no effect of increasing pCO_2 and temperature has been detected on Ag, Cd, and Zn bioaccumulation capacities in *C. gigas* soft tissues. Only few

Table 4. Two-way ANOVA parameters testing the effects of three pH (7.5, 7.8, and 8.1) and two temperatures (21 and 24°C) on the uptake kinetic parameters, i.e. k_u (see Figure 1 and Table 1), and on the loss kinetics parameters, i.e. k_e (see Supplementary Figure S1 and Table 2) for all elements.

	pH			Temperature			pH × temperature		
Parameter	d.f.	MS	*F*	d.f.	MS	*F*	d.f.	MS	*F*
^{110m}Ag—k_u	2	3042	0.816	1	2018	0.541	2	8735	1.172
^{241}Am—k_u	2	235	2.144	1	303	2.772	2	199	1.817
^{109}Cd—k_u	2	64	2.713°	1	143	6.061*	2	65	2.735°
^{57}Co—k_u	2	22	1.682	1	0.05	0.004	2	38	2.860°
^{54}Mn—k_u	2	32	1.192	1	26	0.969	2	132	4.835*
^{65}Zn—k_u	2	380	1.847	1	522	2.537	2	207	1.006
^{110m}Ag—k_{el}	2	1.6×10^{-3}	1.787	1	1.1×10^{-3}	1.282	2	1.4×10^{-3}	1.551
^{241}Am—k_{el}	2	2.8×10^{-5}	2.070	1	1.1e−6	0.081	2	9.9×10^{-5}	7.367**
^{57}Co—k_{el}	2	1.4×10^{-5}	0.785	1	8.3×10^{-5}	4.620*	2	4.8×10^{-5}	2.714°
^{54}Mn—k_{el}	2	4.2×10^{-5}	2.215	1	6.7×10^{-5}	3.529	2	3.3×10^{-5}	1.762°
^{65}Zn—k_{el}	2	1.1×10^{-4}	1.848	1	2.0×10^{-5}	0.344	2	5.7×10^{-5}	0.972

d.f., degree of freedom; MS, mean squares. Probability levels for significant effects: $p < 0.01$**, $p < 0.05$*, $p < 0.1$°.

Table 5. ^{54}Mn, ^{57}Co, ^{65}Zn, ^{110m}Ag, ^{109}Cd, and ^{241}Am distribution (%; mean ± s.d.) among soft tissue and shell of oysters exposed for 21 d of the uptake ($n = 3$) and 37 d of depuration phase ($n = 5$) to dissolved radiotracers at three different pH and two temperatures.

Parameters	Compartments	Weight	^{54}Mn	^{57}Co	^{65}Zn	^{110m}Ag	^{109}Cd	^{241}Am
21°C × pH 7.5								
End of uptake	Soft tissue	1.4 ± 0.3	0.8 ± 0.2	2.1 ± 0.7	82.9 ± 1.7	95.7 ± 1.9	50.0 ± 13.0	5.7 ± 1.5
	Shell	9.7 ± 2.2	99.2 ± 0.2	97.9 ± 0.7	17.1 ± 1.7	4.3 ± 1.9	50.0 ± 13.0	94.3 ± 1.5
End of depuration	Soft tissue	1.9 ± 0.5	0.4 ± 0.1	0.8 ± 0.4	91.5 ± 3.6	97.8 ± 1.8	–	2.9 ± 1.2
	Shell	11.2 ± 2.3	99.6 ± 0.1	99.2 ± 0.4	8.5 ± 3.6	2.2 ± 1.8	–	97.1 ± 1.2
21°C × pH 7.8								
End of uptake	Soft tissue	1.3 ± 0.2	0.4 ± 0.1	1.5 ± 0.5	84.6 ± 4.9	97.5 ± 0.4	48.0 ± 19.4	3.1 ± 1.4
	Shell	8.9 ± 0.9	99.6 ± 0.1	98.5 ± 0.5	15.4 ± 4.9	2.5 ± 0.4	52.0 ± 19.4	96.9 ± 1.4
End of depuration	Soft tissue	1.9 ± 0.9	0.4 ± 0.1	1.0 ± 0.3	89.2 ± 7.6	96.1 ± 3.4	–	2.1 ± 0.7
	Shell	9.7 ± 3.0	99.6 ± 0.1	99.0 ± 0.3	10.8 ± 7.6	3.9 ± 3.4	–	97.9 ± 0.7
21°C × pH 8.1								
End of uptake	Soft tissue	1.8 ± 0.4	0.8 ± 0.4	1.8 ± 0.7	78.4 ± 9.2	97.3 ± 1.5	43.3 ± 15.3	3.5 ± 1.2
	Shell	11.5 ± 1.1	99.2 ± 0.4	98.2 ± 0.7	21.6 ± 9.2	2.7 ± 1.5	56.7 ± 15.3	96.5 ± 1.2
End of depuration	Soft tissue	2.0 ± 0.8	0.5 ± 0.3	1.0 ± 0.7	91.1 ± 6.3	96.9 ± 1.9	–	1.5 ± 0.4
	Shell	10.8 ± 3.4	99.5 ± 0.3	99.0 ± 0.7	8.9 ± 6.3	3.1 ± 1.9	–	98.5 ± 0.4
24°C × pH 7.5								
End of uptake	Soft tissue	1.7 ± 0.2	0.9 ± 0.2	1.8 ± 0.2	76.3 ± 9.2	90.7 ± 5.4	68.8 ± 15.8	4.2 ± 0.7
	Shell	10.7 ± 2.7	99.1 ± 0.2	98.2 ± 0.2	23.7 ± 9.2	9.3 ± 5.4	31.2 ± 15.8	95.8 ± 0.7
End of depuration	Soft tissue	1.6 ± 0.6	0.7 ± 0.4	1.4 ± 0.6	86.5 ± 11.5	94.7 ± 5.1	–	5.1 ± 2.3
	Shell	11.9 ± 2.0	99.3 ± 0.4	98.6 ± 0.6	13.5 ± 11.5	5.3 ± 5.1	–	94.9 ± 2.3
24°C × pH 7.8								
End of uptake	Soft tissue	1.2 ± 0.1	0.4 ± 0.1	0.9 ± 0.2	73.2 ± 3.5	90.8 ± 0.7	52.7 ± 2.2	1.4 ± 0.4
	Shell	8.9 ± 1.2	99.6 ± 0.1	99.1 ± 0.2	26.8 ± 3.5	9.2 ± 0.7	47.3 ± 2.2	98.6 ± 0.4
End of depuration	Soft tissue	1.1 ± 0.2	0.7 ± 0.3	1.7 ± 0.9	84.2 ± 13.6	92.8 ± 9.2	–	2.7 ± 1.4
	Shell	9.0 ± 1.6	99.3 ± 0.3	98.3 ± 0.9	15.8 ± 13.6	7.2 ± 9.2	–	97.3 ± 1.4
24°C × pH 8.1								
End of uptake	Soft tissue	1.4 ± 0.7	0.9 ± 0.7	1.7 ± 1.3	66.6 ± 16.5	75.8 ± 16.5	63.9 ± 10.2	8.4 ± 10.6
	Shell	9.1 ± 0.3	99.1 ± 0.1	98.3 ± 1.3	33.4 ± 16.5	24.2 ± 16.5	36.1 ± 10.2	91.6 ± 10.6
End of depuration	Soft tissue	1.3 ± 0.5	0.7 ± 0.4	1.2 ± 0.5	89.7 ± 6.7	96.8 ± 1.9	–	2.4 ± 1.5
	Shell	9.9 ± 1.3	99.3 ± 0.4	98.8 ± 0.5	10.3 ± 6.7	3.2 ± 1.9	–	97.6 ± 1.5

studies have investigated so far the impact of warming and hypercapnia on metal accumulation and/or their effects on marine organisms (Lacoue-Labarthe *et al.*, 2009, 2011, 2012; Pascal *et al.*, 2010; Ivanina *et al.*, 2013, 2014; Roberts *et al.*, 2013) and contrasting responses (metal- or species-dependent) were observed. For instance, Cd accumulation was lowered in cuttlefish embryos and Cd toxicity decreased in benthic copepod with decreasing pCO_2 (Lacoue-Labarthe *et al.*, 2009; Pascal *et al.*, 2010) presumably due to increasing competition between metallic cations and protons for biological binding sites. Similarly, a lower Cd uptake was observed in mantle cells of clams *Mercenaria mercenaria*, supposedly due to a decrease in transmembrane channel activities with metabolic depression of clams in short-term hypercapnic conditions (Ivanina *et al.*, 2013). In contrast, we noted in this study a higher Cd uptake in *C. gigas* when oysters were exposed to pH 7.5 (~1700 µatm) and 24°C for 3 weeks. Similar observation of enhanced Cd bioaccumulation in *Crassostrea virginica* maintained at pH 7.8 (~800 µatm) during 4–5 weeks were reported by Götze *et al.* (2014). The mechanistic explanation of this Cd bioaccumulation modulation remains unclear. However, it is noteworthy that, in contrast to other bivalves that maintain a comparatively constant internal pH by decreasing their metabolic rates and/or dissolving their shell (Berge *et al.*, 2006), *C. gigas* was shown to have elevated standard metabolic rate under hypercapnia when exposed to temperature stress (Lannig *et al.*, 2010). This is turn could increase Cd ion uptake in oyster tissues.

Interestingly, it has been previously shown that the non-essential element Ag is more efficiently accumulated, up to 2.5-fold, in embryos and larvae of cuttlefish and squid when exposed to elevated pCO_2 ranged from 600 to 1500 µatm (Lacoue-Labarthe *et al.*, 2009, 2011). This higher Ag uptake might be due to the Na mimetic properties of this element and caused by the enhanced acid–base regulation combined to the ionic regulation machinery. Indeed, the Na^+/H^+-exchanger, an ionic channel, is expected involved in Ag uptake (Webb and Wood, 2000; Grosell and Wood, 2001) in mobile organisms when they are exposed to environmental hypercapnia (Melzner *et al.*, 2009; Hu *et al.*, 2011, 2014). In oysters, no significant change of Ag uptake was observed in soft tissues as a consequence of change in seawater pCO_2. This is congruent with the less-developed ion-exchange machinery in sessile invertebrates, and their subsequent limited ion regulation capacities (Lannig *et al.*, 2010; Gazeau *et al.*, 2013). This limited physiological capacity to compensate environmental acidosis might also explain the absence of modulation of the Zn bioaccumulation in soft tissues according to pCO_2 conditions. Indeed, Zn is a co-factor of the carbonic anhydrase (CA) that catalyses the conversion of CO_2 to bicarbonate and *vice versa*, and that is involved in the acid–base regulation and calcification in shelled mollusc (Gazeau *et al.*, 2013). Beniash *et al.* (2010) have reported an increase in CA expression levels in the mantle of *C. virginica* exposed to 3500 µatm, but the latter partial pressure was much higher than those tested in the present study.

Oysters are a very important marine resource and constitute a major source of animal protein for humans. They are also rich in essential elements such as Fe and Zn (Tacon and Metian, 2013). Preliminary experiments were carried out to determine whether

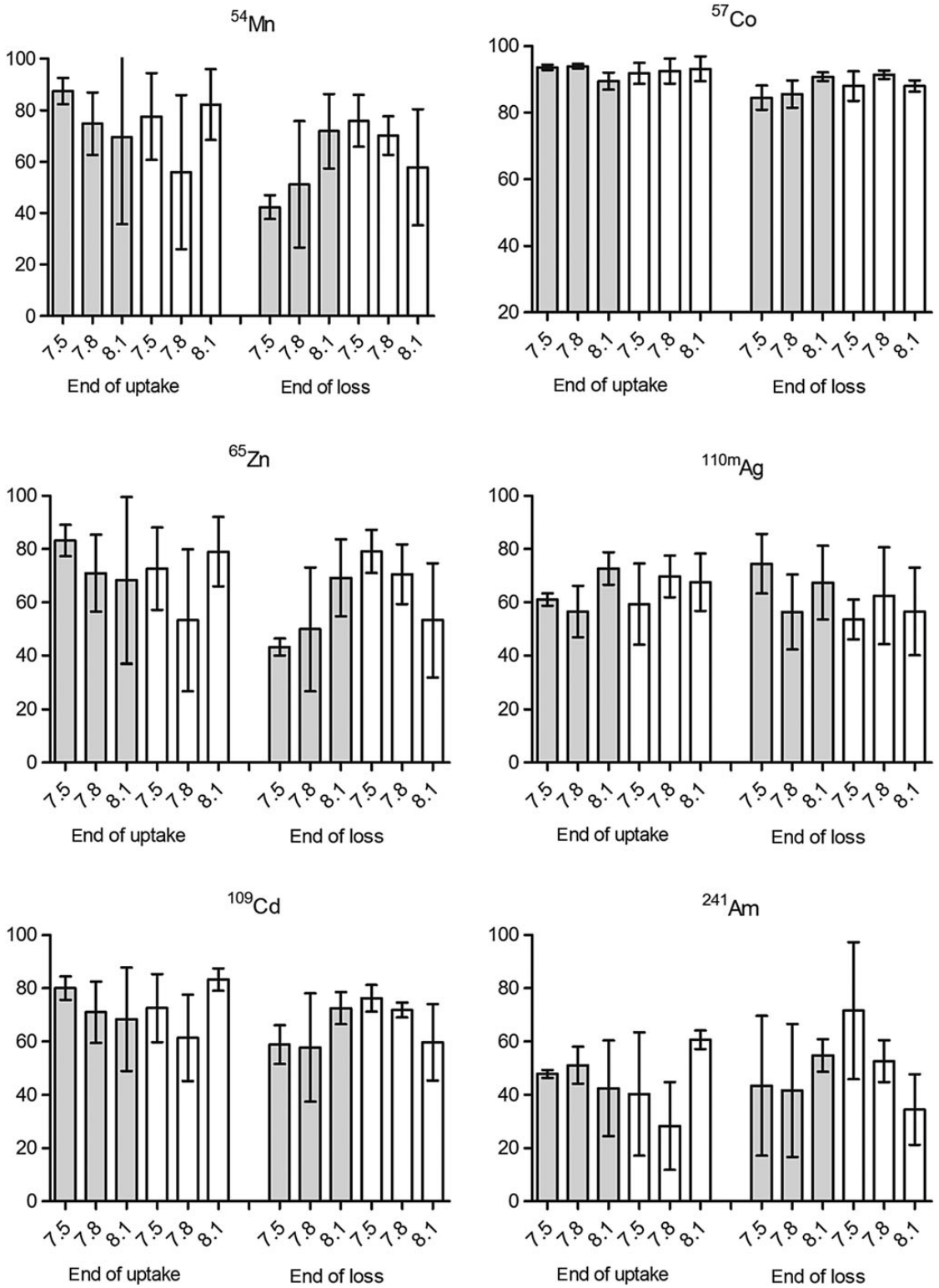

Figure 2. Radiotracer bioaccessibility (%, mean ± s.d., $n = 3$) from oyster soft tissues to human consumers assessed using the simulated *in vitro* digestion method (grey: 21°C, white: 24°C).

lower pH and higher temperatures may affect metal and radionuclide bioaccessibilty to human consumers. Results indicated that ^{241}Am, Mn, and Zn bioaccessibility tended to be enhanced when oysters were exposed to high temperature and lower pH. Although these results have to be considered with caution, they raise the question of the possible impact of environmental hypercapnia on metal detoxification mechanisms in oysters and subsequent subcellular storage of elements. Oysters are well known to

Table 6. χ^2 test on the effects of three pH levels on bioaccessible fraction of metals in oyster tissue following *in vitro* digestion.

Digestion time	Temperature	^{54}Mn	^{57}Co	^{65}Zn	^{110m}Ag	^{109}Cd	^{241}Am
End of the uptake	21°C	8.71*	2.35	6.55*	0.78	3.96	1.69
	24°C	19.44***	0.10	17.13***	0.30	12.13**	22.77***
End of the loss	21°C	19.15***	1.87	14.57***	1.78	–	3.12
	24°C	7.72*	0.74	16.21***	0.28	–	27.51***

d.f. (degree of freedom): 2.
*$p < 0.05$, **$p < 0.01$, ***$p < 0.001$.

accumulate efficiently trace elements such as Zn in soft tissues in the form of metabolically inert, metal-rich granules (e.g. Wallace and Luoma, 2003). These Mg/Ca carbonate granules are known to have the physiological role of buffering the extracellular pH (Viarengo and Nott, 1993) and might thus be easily dissolved when oysters are experiencing hypercapnia. In this context, the increased seawater pCO_2 is susceptible to affect the metal detoxification strategies and thus the trophically available fraction (Wallace and Luoma, 2003) that drives the bioaccessibility and transfer of metals to higher trophic levels.

Finally, the present study brought new data on the potential impact of ocean acidification on metal accumulation in a marine resource of high economic importance and raised the question of the seafood safety that could be worsen by future ocean conditions. Despite the limited number of oysters, the experimentaldesign offered enough statistical power (with power =90%, $n = 5$, standard deviation = s.d. max in Table 2) to detect a putative twofold Ag uptake increase and a threefold Cd uptake decrease and corroborate previous observations made in active (mobile) organisms (Lacoue-labarthe *et al.*, 2009, 2011). We therefore assume that our results bring a new insight on the potential effect of environmental factors such as combined pCO_2 and temperature on the transfer and integration of metals in coastal organisms.

However, our experimental approach (oysters were acclimated to temperature and pCO_2 conditions for 2 weeks before the experiments) implies that the responses observed with respect to metal accumulation efficiency reflected oyster physiological acclimation performances. They are therefore relevant to a coastal or estuarine context where high and short-term variations of these factors do occur (Melzner *et al.*, 2013). Hence, our results do not allow figuring out what could be the impact of ocean acidification and warming over longer time-scale, during which adaptation processes will set up. Further studies should be carried out to highlight finer modulations of metal uptake at tissue and subcellular levels, taking into account the high variability of responses between oyster populations (Parker *et al.*, 2011), and the adaptive capacities of organisms facing long-term major changes.

Supplementary data

Supplementary material is available at the *ICESJMS* online version of the manuscript.

Acknowledgements

The IAEA is grateful to the Government of the Principality of Monaco for the support provided to its Environment Laboratories. MB was supported by a post-doctoral scholarship provided by Council of Higher Education of Turkish Republic. MW is an Honorary Senior Research Associate of the National Fund for Scientific Research (NFSR, Belgium). Authors are grateful to Florian Rivello, Kevin Calabro, and Marie-Yasmine Dechraoui for their technical assistance in the laboratory.

References

Barton, A., Hales, B., Waldbusser, G. G., Langdon, C., and Feely, R. A. 2012. The Pacific oyster, *Crassostrea gigas*, shows negative correlation to naturally elevated carbon dioxide levels: implications for near-term ocean acidification effects. Limnology and Oceanography, 57: 698–710.

Bartoń, K. 2014. MuMIn: Multi-Model Inference. R package version 1.12.1.

Beniash, E., Ivanina, A., Lieb, N. S., Kurochkin, I., and Sokolova, I. M. 2010. Elevated level of carbon dioxide affects metabolism and shell formation in oysters *Crassostrea virginica*. Marine Ecology Progress Series, 419: 95–108.

Berge, J. A., Bjerkeng, B., Pettersen, O., Schaanning, M. T., and Øxnevad, S. 2006. Effects of increased sea water concentrations of CO_2 on growth of the bivalve *Mytilus edulis* L. Chemosphere, 62: 681–687.

Byrne, R. H., Kump, L. R., and Cantrell, K. J. 1988. The influence of temperature and pH on trace metal speciation in seawater. Marine Chemistry, 25: 163–181.

Choppin, G. R. 2006. Actinide speciation in aquatic systems. Marine Chemistry, 99: 83–92.

Dickson, A. G., Sabine, C. L., and Christian, J. R. 2007. Determination of the pH of sea water using a glass/reference electrode cell. *In* Guide to Best Practices for Ocean CO_2 Measurements, pp. 1–7. Ed. by A. G. Dickson, C. L. Sabine, and J. R. Christian. PICES Special Publication 3.

Doney, S. C., Fabry, V. J., Feely, R. A., and Kleypas, J. 2009. Ocean acidification: the other CO_2 problem. Annual Review of Marine Science, 1: 169–192.

Dupont, S., Dorey, N., and Thorndyke, M. 2010. What meta-analysis can tell us about vulnerability of marine biodiversity to ocean acidification? Estuarine Coastal and Shelf Science, 89: 182–185.

FAO. 2014. Global Aquaculture Production 1950–2012. http://www.fao.org/fishery/statistics/global-aquaculture-production/en.

Gattuso, J-P., Epitalon, J-M., and Lavigne, H. 2015. seacarb: Seawater Carbonate Chemistry. R package version 3.0.5.

Gazeau, F., Gattuso, J-P., Greaves, M., Elderfield, H., Peeene, J., Heip, C. H. R., and Middelburg, J. J. 2011. Effect of carbonate chemistry alteration on the early embryonic development of the pacific oyster (*Crassostrea gigas*). PLos ONE, 6: e23010.

Gazeau, F., Parker, L. M., Comeau, S., Gattuso, J-P., O'Connor, W. A., Martin, S., Pörtner, H-O., *et al.* 2013. Impacts of ocean acidification on marine shelled molluscs. Marine Biology, 160: 2207–2245.

Gazeau, F., Quiblier, C., Jansen, J. M., Gattuso, J. P., Middelburg, J. J., and Heip, C. H. R. 2007. Impact of elevated CO_2 on shellfish calcification. Geophysical Research Letters, 34: L07603.

Götze, S., Matoo, O. B., Beniash, E., Saborowski, R., and Sokolova, I. M. 2014. Interactive effects of CO_2 and trace metals on the proteasome activity and cellular stress response of marine bivalves *Crassostrea*

virginica and *Mercenaria mercenaria*. Aquatic Toxicology, 149: 65–82.

Green, M. A., Waldbusser, G. G., Reilly, S. L., Emerson, K., and O'Donnella, S. 2009. Death by dissolution: sediment saturation state as a mortality factor for juvenile bivalves. Limnology and Oceanography, 54: 1037–1047.

Grosell, M., and Wood, C. M. 2001. Branchial versus intestinal silver toxicity and uptake in the marine teleost *Parophrys vetulus*. Journal of Comparative Physiology, 171B: 585–594.

Hédouin, L., Metian, M., Teyssié, J-L., Fichez, R., and Warnau, M. 2010. Delineation of heavy metal contamination pathways (seawater, food and sediment) in tropical oysters from New Caledonia using radiotracer techniques. Marine Pollution Bulletin, 61: 542–553.

Houlbrèque, F., Rodolfo-Metalpa, R., Jeffree, R., Oberhänsli, F., Teyssié, J-L., Boisson, F., Al-Trabeen, K., *et al.* 2011. Effects of increased pCO_2 on zinc uptake and calcification in the tropical coral *Stylophora pistillata*. Coral Reefs, 31: 101–109.

Hu, M. Y., Guh, Y-J., Stumpp, M., Lee, J-R., Chen, R-D., Sung, P-H., Chen, Y-C., *et al.* 2014. Branchial NH_4^+-dependent acid–base transport mechanisms and energy metabolism of squid (*Sepioteuthis lessoniana*) affected by seawater acidification. Frontiers in Zoology, 11: 55.

Hu, M. Y., Tseng, Y-C., Stumpp, M., Gutowska, M. A., Kiko, R., Lucassen, M., and Melzner, F. 2011. Elevated seawater PCO_2 differentially affects branchial acid–base transporters over the course of development in the cephalopod *Sepia officinalis*. American Journal of Physiology—Regulatory, Integrative and Comparative Physiology, 300: R1100–R1114.

IPCC. 2013. Climate Change 2013: the Physical Science Basis. *In* Contribution of Working Group I to the Fifth Assessment Report of the Intergovernmental Panel on Climate Change. Cambridge University Press, Cambridge, UK.

Ivanina, A. V., Beniash, E., Etzkorn, M., Meyers, T. B., Ringwood, A. H., and Sokolova, I. M. 2013. Short-term acute hypercapnia affects cellular responses to trace metals in the hard clams *Mercenaria mercenaria*. Aquatic Toxicology, 140–141: 123–133.

Ivanina, A. V., Hawkins, C., and Sokolova, I. M. 2014. Immunomodulation by the interactive effects of cadmium and hypercapnia in marine bivalves *Crassostrea virginica* and *Mercenaria mercenaria*. Fish and Shellfish Immunology, 37: 299–312.

Lacoue-Labarthe, T., Martin, S., Oberhänsli, F., Teyssié, J-L., Jeffree, R., Gattuso, J-P., and Bustamante, P. 2012. Temperature and pCO_2 effect on the bioaccumulation of radionuclides and trace elements in the eggs of the common cuttlefish *Sepia officinalis*. Journal of Experimental Marine Biology and Ecology, 413: 45–49.

Lacoue-Labarthe, T., Martin, S., Oberhänsli, F., Teyssie, J. L., Markich, S. J., Jeffree, R., and Bustamante, P. 2009. Effects of increased pCO_2 and temperature on trace element (Ag, Cd and Zn) bioaccumulation in the eggs of the common cuttlefish, *Sepia officinalis*. Biogeosciences, 6: 2561–2573.

Lacoue-Labarthe, T., Réveillac, E., Oberhänsli, F., Teyssié, J-L., Jeffree, R., and Gattuso, J-P. 2011. Effects of ocean acidification on trace element accumulation in the early-life stages of squid *Loligo vulgaris*. Aquatic Toxicology, 105: 166–176.

Lannig, G., Eilers, S., Pörtner, H. O., Sokolova, I. M., and Bock, C. 2010. Impact of ocean acidification on energy metabolism of oyster, *Crassostrea gigas*—changes in metabolic pathways and thermal response. Marine Drugs, 8: 2318–2339.

Melzner, F., Gutowska, M. A., Langenbuch, M., Dupont, S., Lucassen, M., Thorndyke, M. C., Bleich, M., *et al.* 2009. Physiological basis for high CO_2 tolerance in marine ectothermic animals: pre-adaptation through lifestyle and ontogeny? Biogeosciences, 6: 2313–2331.

Melzner, F., Thomsen, J., Koeve, W., Oschlies, A., Gutowska, M. A., Bange, H. W., Hansen, H. P., *et al.* 2013. Future ocean acidification will be amplified by hypoxia in coastal habitats. Marine Biology, 160: 1875–1888.

Metian, M., Bustamante, P., Cosson, R. P., Hédouin, L., and Warnau, M. 2008. Investigation of Ag in the king scallop *Pecten maximus* using field and laboratory approaches. Journal of Experimental Marine Biology and Ecology, 367: 53–60.

Metian, M., Charbonnier, L., Oberhänsli, F., Bustamante, P., Jeffree, R., Amiard, J. C., and Warnau, M. 2009a. Assessment of metal, metalloid, and radionuclide bioaccessibility from mussels to human consumers, using centrifugation and simulated digestion methods coupled with radiotracer techniques. Ecotoxicology and Environmental Safety, 72: 1499–1502.

Metian, M., Warnau, M., Hédouin, L., and Bustamante, P. 2009b. Bioaccumulation of essential metals (Co, Mn and Zn) in the king scallop *Pecten maximus*: seawater, food and sediment exposures. Marine Biology, 156: 2063–2075.

Metian, M., Warnau, M., Teyssié, J-L., and Bustamante, P. 2011. Characterization of ^{241}Am and ^{134}Cs bioaccumulation in the king scallop *Pecten maximus*: investigation via three exposure pathways. Journal of Environmental Radioactivity, 102: 543–550.

Millero, F. J., Woosley, R., Ditrolo, B., and Waters, J. 2009. Effect of ocean acidification on the speciation of metals in seawater. Oceanography, 22: 72–85.

Orr, J. C., Fabry, V. J., Aumont, O., Bopp, L., Doney, S. C., Feely, R. A., Gnanadesikan, A., *et al.* 2005. Anthropogenic ocean acidification over the twenty-first century and its impact on calcifying organisms. Nature, 437: 681–686.

Parker, L. M., Ross, P. M., and O'Connor, W. A. 2010. Comparing the effect of elevated pCO_2 and temperature on the fertilization and early development of two species of oysters. Marine Biology, 157: 2435–2452.

Parker, L. M., Ross, P. M., and O'Connor, W. A. 2011. Populations of the Sydney rock oyster, *Saccostrea glomerata*, vary in response to ocean acidification. Marine Biology, 158: 689–697.

Parker, L. M., Ross, P. M., O'Connor, W. A., Pörtner, H-O., Scanes, E., and Wright, J. M. 2013. Predicting the response of molluscs to the impact of ocean acidification. Biology, 2: 651–692.

Pascal, P-Y., Fleeger, J. W., Galvez, F., and Carman, K. R. 2010. The toxicological interaction between ocean acidity and metals in coastal meiobenthic copepods. Marine Pollution Bulletin, 60: 2201–2208.

Pinheiro, J., Bates, D., DebRoy, S., Sarkar, D., R Core Team. 2014. {nlme}: Linear and Nonlinear Mixed Effects Models. R package version 3.1-118.

Pörtner, H. O., Langenbuch, M., and Reipschläger, A. 2004. Biological impact of elevated ocean CO_2 concentrations: lessons from animal physiology and earth history. Journal of Oceanography, 60: 705–718.

R Core Team. 2014. R: a Language and Environment for Statistical Computing. R Foundation for Statistical Computing, Vienna, Austria.

Rainbow, P. S. 2002. Trace metal concentrations in aquatic invertebrates: why and so what? Environmental Pollution, 120: 497–507.

Roberts, D. A., Birchenough, S. R., Lewis, C., Sanders, M., Bolam, T., and Sheahan, D. 2013. Ocean acidification increases the toxicity of contaminated sediments. Global Change Biology, 19: 340–351.

Rodriguez y Baena, A. M., Metian, M., Teyssie, J. L., De Broyer, C., and Warnau, M. 2006. Experimental evidence for ^{234}Th bioaccumulation in three Antarctic crustaceans: potential implications for particle flux studies. Marine Chemistry, 100: 354–365.

Solomon, S., Qin, D., Manning, M., Chen, Z., Marquis, M., Averyt, K. B., Tignor, M., *et al.* 2007. IPCC, 2007: Climate Change 2007: the physical science basis. *In* Contribution of Working Group I to the Fourth Assessment Report of the Intergovernmental Panel on Climate Change. Cambridge University Press, New York.

Tacon, A. G. J., and Metian, M. 2013. Fish matters: importance of aquatic foods in human nutrition and global food supply. Reviews in Fisheries Science, 21: 22–38.

Timmins-Schiffman, E., O'Donnell, M. J., Friedman, C. S., and Roberts, S. B. 2013. Elevated pCO_2 causes developmental delay in early larval Pacific oysters, *Crassostrea gigas*. Marine Biology, 160: 1973–1982.

Versantvoort, C. H. M., Oomen, A. G., Van de Kamp, E., Rompelberg, C. J. M., and Sips, A. J. A. M. 2005. Applicability of an in vitro digestion model in assessing the bioaccessibility of mycotoxins from food. Food and Chemical Toxicology, 43: 31–40.

Viarengo, A., and Nott, J. A. 1993. Mechanisms of heavy metal cation homeostasis in marine invertebrates. Comparative Biochemistry and Physiology, 104C: 355–372.

Wallace, W. G., and Luoma, S. N. 2003. Subcellular compartmentalization of Cd and Zn in two bivalves. II. Significance of trophically available metal (TAM). Marine Ecology Progress Series, 257: 125–137.

Warnau, M., and Bustamante, P. 2007. Radiotracer techniques: a unique tool in marine ecotoxicological studies. Environmental Bioindicators, 2: 217–218.

Warnau, M., Teyssié, J-L., and Fowler, S. W. 1996. Biokinetics of selected heavy metals and radionuclides in the common Mediterranean echinoid *Paracentrotus lividus*: sea water and food exposures. Marine Ecology Progress Series, 141: 83–94.

Webb, N. A., and Wood, C. M. 2000. Bioaccumulation and distribution of silver in four marine teleosts and two marine elasmobranchs: influence of exposure duration, concentration, and salinity. Aquatic Toxicology, 49: 111–129.

Whicker, F. W., and Schultz, V. 1982. Radioecology: Nuclear Energy and the Environment. CRC Press, Boca Raton, FL.

White, S. L., and Rainbow, P. S. 1984. Regulation of zinc concentration by *Palaemon elegans* (Crustacea:Decapoda): zinc flux and effects of temperature, zinc concentration and moulting. Marine Ecology Progress Series, 16: 135–147.

Zhou, Q., Zhang, J., Fu, J., Shi, J., and Jiang, G. 2008. Biomonitoring: an appealing tool for assessment of metal pollution in the aquatic ecosystem. Analytica Chimica Acta, 606: 135–150.

Handling editor: Joanna Norkko

ICES Journal of Marine Science

ICES Journal of Marine Science (2016), 73(3), 764–771. doi:10.1093/icesjms/fsv249

Contribution to Special Issue: 'Towards a Broader Perspective on Ocean Acidification Research'

Original Article

Ocean warming and elevated carbon dioxide: multiple stressor impacts on juvenile mussels from southern Chile

Jorge M. Navarro[1,2]*, Cristian Duarte[3,4], Patricio H. Manríquez[5], Marco A. Lardies[6], Rodrigo Torres[7], Karin Acuña[1], Cristian A. Vargas[8], and Nelson A. Lagos[9]

[1]*Instituto de Ciencias Marinas y Limnológicas, Laboratorio Costero de Calfuco, Facultad de Ciencias, Universidad Austral de Chile, Valdivia, Chile*
[2]*Centro Fondap de Investigación de Ecosistemas Marinos de Altas Latitudes (IDEAL), Valdivia, Chile*
[3]*Departamento de Ecología y Biodiversidad, Facultad de Ecología y Recursos Naturales, Universidad Andres Bello, Santiago, Chile*
[4]*Center for the Study of Multiple-drivers on Marine Socio-Ecological System (MUSELS), Universidad de Concepción, Concepción, Chile*
[5]*Laboratorio de Ecología y Conducta de la Ontogenia Temprana (LECOT), Centro de Estudios Avanzados en Zonas Áridas (CEAZA), Av. Ossandón 877, Coquimbo, Chile*
[6]*Facultad de Artes Liberales and Facultad de Ingeniería y Ciencias, Universidad Adolfo Ibáñez, Santiago, Chile*
[7]*Centro de Investigación en Ecosistemas de la Patagonia (CIEP), Coyhaique, Chile*
[8]*Laboratorio de Funcionamiento de Ecosistemas Acuáticos (LAFE), Departamento de Sistemas Acuáticos, Facultad de Ciencias Ambientales, Universidad de Concepción, Concepción, Chile*
[9]*Centro de Investigación e Innovación para el Cambio Climático, Universidad Santo Tomás, Santiago, Chile*

**Corresponding author: tel: + 56 63 2221556; fax: + 56 63 2221455; e-mail: jnavarro@uach.cl*

Navarro, J. M., Duarte, C., Manríquez, P. H., Lardies, M. A., Torres, R., Acuña, K., Vargas, C. A., and Lagos, N. A. Ocean warming and elevated carbon dioxide: multiple stressor impacts on juvenile mussels from southern Chile. – ICES Journal of Marine Science, 73: 764 – 771.

Received 17 June 2015; revised 24 November 2015; accepted 25 November 2015; advance access publication 4 January 2016.

The combined effect of increased ocean warming and elevated carbon dioxide in seawater is expected to have significant physiological and ecological consequences at many organizational levels of the marine ecosystem. In the present study, juvenile mussels *Mytilus chilensis* were reared for 80 d in a factorial combination of two temperatures (12 and 16°C) and three pCO_2 levels (380, 700, and 1000 μatm). We investigated the combined effects of increasing seawater temperature and pCO_2 on the physiological performance (i.e. feeding, metabolism, and growth). Lower clearance rate (CR) occurred at the highest pCO_2 concentration (1000 μatm) compared with the control (380 μatm) and with the intermediate concentration of pCO_2 (700 μatm). Conversely, CR was significantly higher at 16°C than at 12°C. Significant lower values of oxygen uptake were observed in mussels exposed to 1000 μatm pCO_2 level compared with those exposed to 380 μatm pCO_2. Scope for growth (SFG) was significantly lower at the highest pCO_2 concentration compared with the control. Mussels exposed to 700 μatm pCO_2 did not show significantly different SFG from the other two pCO_2 treatments. SFG was significantly higher at 16°C than at 12°C. This might be explained because the experimental mussels were exposed to temperatures experienced in their natural environment, which are within the range of thermal tolerance of the species. Our results suggest that the temperature rise within the natural range experienced by *M. chilensis* generates a positive effect on the processes related with energy gain (i.e. feeding and absorption) to be allocated to growth. In turn, the increase in the pCO_2 level of 1000 μatm, independent of temperature, adversely affects this species, with significantly reduced energy allocated to growth (SFG) compared with the control treatment.

Keywords: high CO_2, multiple stressors, mussels, ocean warming, scope for growth, thermal window.

Introduction

Fossil fuel burning and land use change are the dominant causes of the increase in atmospheric CO_2 concentration from pre-industrial levels (ca. 280 μatm) reaching current values of ca. 400 μatm (IPCC, 2013). Atmospheric CO_2 concentration increased at an average rate of 2.0 ± 0.1 μatm $year^{-1}$ during 2002–2011, being higher than any

previous decade since direct atmospheric concentration measurements began in 1958 (IPCC, 2013). According to the current tendency, it is expected that by the end of this century atmospheric CO_2 concentration could reach 700 μatm and will exceed 1500 μatm between the years 2100 and 2200 (Caldeira and Wickett, 2003; Pörtner *et al.*, 2004; IPCC, 2013). Approximately 30% of atmospheric CO_2 dissolves in the ocean, resulting in reduction of pH and the availability of carbonate ions, which are essential to calcium carbonate deposition in calcifier organisms. According to the current trend of increasing CO_2 concentration, ocean acidification (OA) will decrease from 0.2 to 0.4 pH units by 2100, together with a reduction of 50% of carbonate ions (Caldeira and Wickett, 2003; Feely *et al.*, 2004). OA is not an isolated stressor, yet acts together with other environmental shifts such as ocean warming (Meier, 2006; IPCC, 2013). Sea surface temperature has increased by ~0.6°C during the last 50 years (Walther *et al.*, 2002), and it is expected that it will continue to rise between 1 and 4°C by the end of the century (IPCC, 2013).

Growing evidence shows that many environmental stressors can act synergistically, affecting many physiological processes of marine organisms (Schiedek *et al.*, 2007; Gooding *et al.*, 2009). Increased CO_2 concentration in seawater has significant physiological and ecological consequences at many organizational levels of the marine ecosystem (Fabry *et al.*, 2008). A wide range of sensitivities to projected rates of OA exist within and across groups of marine organisms (e.g. corals, oysters, mussels, crabs, and sea urchins), with a trend for greater sensitivity in early life stages (Vargas *et al.*, 2013; Gobler and Talmage, 2014). However, key uncertainties remain in our understanding of the impacts on organisms, life histories, and ecosystems. Most results describe that marine organisms are affected by high pCO_2 levels by disturbances in acid–base regulation, respiration, metabolism, growth rates, reproduction, and calcification (Pörtner, 2008; Widdicombe and Spicer, 2008; Navarro *et al.*, 2013; Duarte *et al.*, 2014; Gazeau *et al.*, 2014).

Because many marine organisms live close to their thermal compensatory capacity (Somero, 2002), the increase in temperature associated with global climate change is expected to impact all physiological processes, survival, and many ecological interactions (Godbold and Solan, 2013). Biological response to rising temperature may vary within and among species, and even across ontogenetic stages (Harley *et al.*, 2006). Seawater temperature is shown to have strong effects on the physiological performance (Pörtner, 2010; Hiebenthal *et al.*, 2013) and reproduction (Navarro *et al.*, 2000; Philippart *et al.*, 2003) of benthic organisms. Recent studies show that the effects of increased CO_2 could be modified by a rise in temperature (Gooding *et al.*, 2009; Findlay *et al.*, 2010). The interaction of elevated seawater CO_2 and extreme temperatures is described to narrow the thermal tolerance window of an organism exposed to high CO_2 levels (Pörtner, 2008; Pörtner and Farrel, 2008). Metzger *et al.* (2007) found that at elevated seawater CO_2 concentrations, the upper thermal tolerance limits were reduced by several Celsius degrees in crustaceans. High temperature and elevated CO_2 lead to a significant decrease in shell hardness in the oyster *Crassostrea virginica* and the clam *Mercenaria mercenaria*, suggesting major changes in their biomineralization processes (Ivanina *et al.*, 2013). However, early juveniles and adults may be vulnerable to skeletal dissolution, although warming may diminish the negative impact of acidification on calcification (Byrne, 2011). In a recent study, we found that the net rate of calcium deposition in juveniles of *Mytilus chilensis* was not significantly affected by temperature, but was negatively affected by high levels of CO_2 (Duarte *et al.*, 2014).

In high-latitude coastal areas of South America, the edible mussel *M. chilensis* forms extensive subtidal and intertidal beds that play an important ecological role, affecting the community structure of the associated macrofauna (Duarte *et al.*, 2006). *Mytilus chilensis* is an important species in Chile for aquaculture activities, with a landing of ca. 300 000 tons per year. These facts make this bivalve species a key group of marine invertebrates for studying the biological impacts of the interaction of elevated pCO_2 levels and global warming on their physiology and growth. In a previous study, Navarro *et al.* (2013) described the effects of high levels of pCO_2 for another population of *M. chilensis* of southern Chile, concluding that growth rate might be significantly reduced under medium-term exposure to elevated pCO_2 levels.

In the present study, juvenile individuals of the mussel *M. chilensis* were reared in a factorial combination of two temperatures (12 and 16°C) and three pCO_2 levels (380, 700, and 1000 μatm). We analysed the combined effects of increasing seawater temperature and pCO_2 on the physiological performance (i.e. feeding, metabolism, and growth) of *M. chilensis*. We hypothesized that the sensitivity of juvenile mussel *M. chilensis* exposed to elevated levels of pCO_2 increases with rising temperature.

Material and methods

Juvenile individuals of *M. chilensis* were collected from suspended cultures (permanently submerged) at Huelmo Bay, Puerto Montt (41°67′S, 73°03′W), during the 2011 winter season (sea surface temperature = 11.5°C; pH 8.09 at the day of collection) and transported to the laboratory under chilled conditions. Mussels of approximately equal length (24.2 ± 0.4 mm SE) and dry tissue weight (33.4 ± 1.6 mg SE) were selected. Before the experiments, mussels were acclimated for 2 weeks in aquaria with circulating seawater (temperature = 12–13°C and salinity 32–33 psu) and fed daily with the microalgae *Isochrysis galbana*.

Experimental set-up

Following the acclimation period, experimental mussels were transferred to the aquaria and exposed to six different treatments at the combination of two temperatures (12 and 16°C) and three pCO_2 levels (380, 700, and 1000 μatm), for a period of 80 d. Each treatment was replicated four times, and each replicate contained five experimental animals, which were identified using bee tags. The experimental temperatures were within the range of thermal tolerance of the species; 12°C represents the average and 16°C the extreme highest value for the area although this was last recorded in a narrow temporal window during summer (Navarro and Jaramillo, 1994). Experimental pCO_2 concentrations were selected to match current day and expected near-future levels according to the predicted values by the IPCC (2013), based on the extreme scenario (RCP8.5) of atmospheric CO_2. Two thermo-regulated baths were prepared for each experimental temperature (12 and 16°C) consisting each of 12 plastic 3.5 l tanks (four replicates for each pCO_2 treatment). The different pCO_2 concentrations were obtained using a mesocosm system, following Navarro *et al.* (2013) and Torres *et al.* (2013). Briefly, for 380 μatm, pure atmospheric air was bubbled into experimental containers. For 700 and 1000 μatm, dry air was blended with pure CO_2 to each CO_2 concentration using mass flow controllers (MFCs, www.aalborg.com) for air and CO_2. During the experiments, water pH and total alkalinity were monitored every 3 d in equilibration tanks. pH measurements were done in closed 25 ml cells thermostated at 25°C using a Metrohm 713 pH meter, calibrated with 8.089 Tris-buffer at 25°C. Temperature and salinity

were measured in the equilibration tanks using a small CTD (Ocean Seven 305 Plus CTD, www.Idronaut.it). Total alkalinity was measured using the method of Haraldsson *et al.* (1997). Resulting hydrographic data were used to calculate the rest of the carbonate system parameters and the saturation stage of Omega Aragonite and Calcite using CO_2SYS software (Lewis and Wallace, 1998) set with Mehrbach solubility constants (Mehrbach *et al.*, 1973) refitted by Dickson and Millero (1987). All experimental individuals were fed with a daily amount of food (*I. galbana*) equal to 5% of the body weight. An open system, consisting of a stock suspension of the microalgae and a multichannel peristaltic pump (Masterflex 7524), was used to deliver the suspension directly to each experimental aquarium. Food concentration was maintained within a range similar to that found in the natural southern Chilean environment throughout the year (ca. 0.8–1.5 mg l^{-1} dry weight). Seawater was gently changed every day, with the corresponding pCO_2 level from the seawater acidification system.

Physiological parameters

Physiological measurements (below) were done on 120 individual mussels taken randomly from each experimental aquarium of the six treatments (two temperatures and three pCO_2 concentrations), starting on day 0 (initial exposure) and continuing every 20 d along a period of 80 d.

Feeding experiments

Clearance rate (CR) of mussels exposed to the experimental temperature and CO_2 combinations (six treatments) was estimated in a static system homogenized by aeration using a food concentration of 25×10^6 cells *I. galbana* l^{-1}. One juvenile mussel was taken randomly from the replicates of each treatment and placed in an experimental chamber (0.4 l). Subsequently, the decrease in the number of particles was monitored every 30 min over a period of 3 h, using an Elzone 180XY particle counter, equipped with a tube of 120-μm aperture. A control aquarium without mussels was used to discard the sedimentation of particles and the CR (l h^{-1} $mussel^{-1}$) was calculated according to Coughlan (1969). Organic ingestion rate was calculated as the product of the CR and the organic material contained in the diet.

After CR measurements were completed, absorption efficiency (AE) was estimated by determining the organic and inorganic content of the food and the faeces following the ratio method of Conover (1966). Samples of food and faeces were filtered through pre-washed, preweighed, 25-mm glassfibre filters. Filters were rinsed with isotonic ammonium formate, dried to a constant weight at 100°C, weighed, combusted at 450°C for 3 h, and weighed again to estimate the organic and inorganic fraction contained in the food and faeces. Absorption rate was calculated as the product of the organic ingestion rate and AE.

Ammonia excretion and oxygen uptake

Ammonia excretion and oxygen uptake were determined immediately after the CR measurements were made. Individual mussels were placed in sealed glass beakers (0.14 l) containing filtered (0.45 μm) seawater. One additional beaker containing filtered seawater but without mussels was used as a control. All beakers were filled with the corresponding experimental pCO_2 levels (380, 700, and 1000 μatm) and maintained at 12 and 16°C by submerging them in two thermostatic water baths. After 2 h, water samples (5 ml) from each beaker were taken and analysed for ammonia–nitrogen by the phenol-hypochlorite colorimetric method of Solórzano (1969). Values for excretion rate were expressed in microgram of NH_4-N. The oxygen uptake by each mussel was estimated by the difference between the oxygen contained in the control and that contained in the experimental beaker over the period of 2 h and analysed by the micro-Winkler method, modified by Ohle (1953), which uses titration to determine dissolved oxygen in the water.

Scope for growth

Scope for growth (SFG) was calculated after converting all the physiological rates to energy equivalents (J h^{-1}): 1 ml O_2 = 19.9 J; 1 μg NH_4-N = 0.0249 J (Elliot and Davison, 1975), and 1 mg of organic material of *I. galbana* = 18.75 J (Whyte, 1987).

Statistical analyses

To avoid pseudo-replication problems, the measured physiological processes were averaged for five mussels of each replicate. A two-way ANOVA was used to estimate the effects of temperature and pCO_2 concentrations on different physiological measurements. When the analyses did not show significant interactions, multiple comparisons were carried out using Tukey's *a posteriori* HSD test on each factor that showed significant differences (Underwood, 1997). Before analyses, normality and homoscedasticity of the data were tested using Kolmogorov–Smirnov and Bartlett tests, respectively. All the analyses were performed using the program Statgraphics Plus 5.1.

Results

Experimental seawater system

The physical and chemical characteristics of the experimental seawater are summarized in Table 1, and were previously described by Duarte *et al.* (2014) in a parallel study on the calcification rate of mussels. The experimental seawater showed very similar values for salinity at all the temperature/pCO_2 combinations. There was a constant decreasing trend of pH, carbonate contents, and aragonite with the increase in the pCO_2 concentrations at both experimental temperatures.

Physiological parameters

CR of *M. chilensis* (Figure. 1a) was significantly affected by pCO_2 and temperature (two-way ANOVA; pCO_2: $F_{1,12} = 7.72$, $p < 0.01$; temperature: $F_{1,12} = 30.17$, $p < 0.001$). Lower values of CR occurred at the highest pCO_2 concentration (1000 μatm) compared with the control (380 μatm) and with the intermediate concentration of pCO_2 (700 μatm). Conversely, CR was significantly higher at 16°C. The interaction between both factors did not have a significant effect ($p > 0.05$) on the CR (temperature * pCO_2: $F_{1,12} = 0.13$, $p > 0.05$). A similar pattern was found for the organic ingestion rate, where the highest level of pCO_2 had a negative effect on this physiological process, while a rise in temperature produced an increase in the organic ingestion rate (Figure. 1b).

AE was not affected by temperature; while under the higher concentration of pCO_2 (1000 μatm), it was significantly lower than in the control treatment (380 μatm CO_2). Individuals maintained at 700 μatm CO_2 exhibited intermediate values, without stating significant differences with the two other treatments (two-way ANOVA; temperature: $F_{1,12} = 3.00$, $p > 0.05$; pCO_2: $F_{2,12} = 4.10$, $p < 0.05$; temperature * pCO_2: $F_{2,12} = 0.77$, $p > 0.05$; Figure. 2a). The absorption rate was affected significantly both by pCO_2 and by temperature, but not for the interaction of both factors. It was significantly lower at the highest pCO_2 concentration compared with the other two treatments; while between 380 and 700 μatm pCO_2, there were no

Table 1. Seawater characteristics (mean ± SD) used to maintain *M. chilensis* during the experimental period [see Material and methods for details on the temperature and CO_2 values used in the study; from Duarte *et al.* (2014)].

	Experimental treatments: temperature and CO_2 concentrations					
	12°C	**16°C**	**12°C**	**16°C**	**12°C**	**16°C**
CO_2 system parameters	**380 µatm (current)**		**700 µatm (2050 year)**		**1000 µatm (2100 year)**	
pH *in situ* (pH units)	8.057 ± 0.026	7.996 ± 0.026	7.835 ± 0.035	7.776 ± 0.034	7.673 ± 0.030	7.618 ± 0.030
Salinity (psu)	31.79 ± 1.88	31.80 ± 1.66	31.81 ± 1.90	31.83 ± 1.72	31.87 ± 1.87	31.88 ± 1.66
TA (µmol kg^{-1})	2156.44 ± 86.24		2148.63 ± 90.76		2142.19 ± 93.23	
pCO_2 *in situ* (µatm)	371.35 ± 23.52	439.54 ± 27.63	656.91 ± 50.44	772.64 ± 58.46	977.56 ± 60.52	1141.90 ± 69.19
$[CO_3^{2-}]$ *in situ* (µmol kg^{-1})	129.48 ± 14.65	131.08 ± 14.74	82.45 ± 11.24	83.97 ± 11.32	58.47 ± 7.92	59.95 ± 8.00
Ω_{ca}	3.14 ± 0.33	3.19 ± 0.33	1.99 ± 0.25	2.04 ± 0.25	1.42 ± 0.18	1.46 ± 0.18
Ω_{ar}	1.99 ± 0.22	2.04 ± 0.22	1.27 ± 0.17	1.31 ± 0.17	0.90 ± 0.12	0.93 ± 0.12

TA, total alkalinity; $[CO_3^{2-}]$, carbonate ion concentration; Ω_{ca}, omega calcite; Ω_{ar}, omega aragonite.

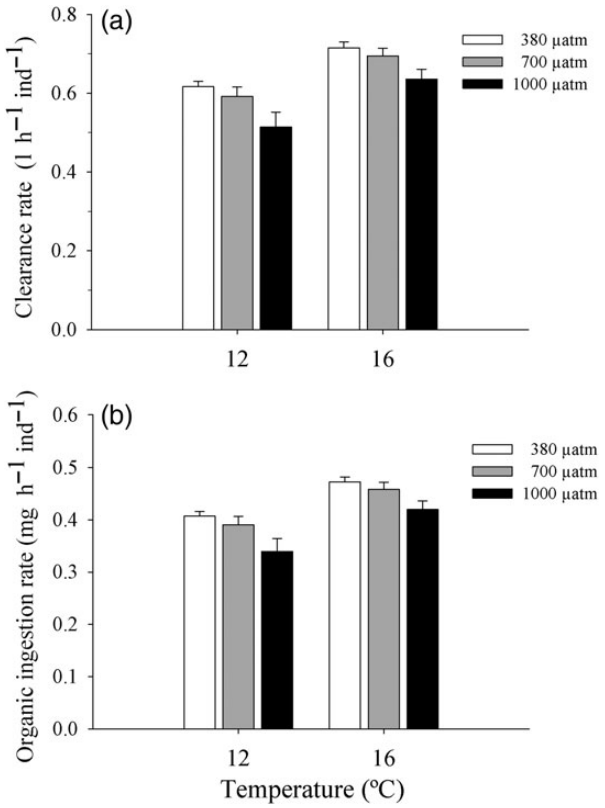

Figure 1. CR (a) and organic ingestion rate (b) of juvenile individuals of the mussel *M. chilensis* exposed to different combinations of temperature and pCO_2 for 80 d. Values are means ± standard error.

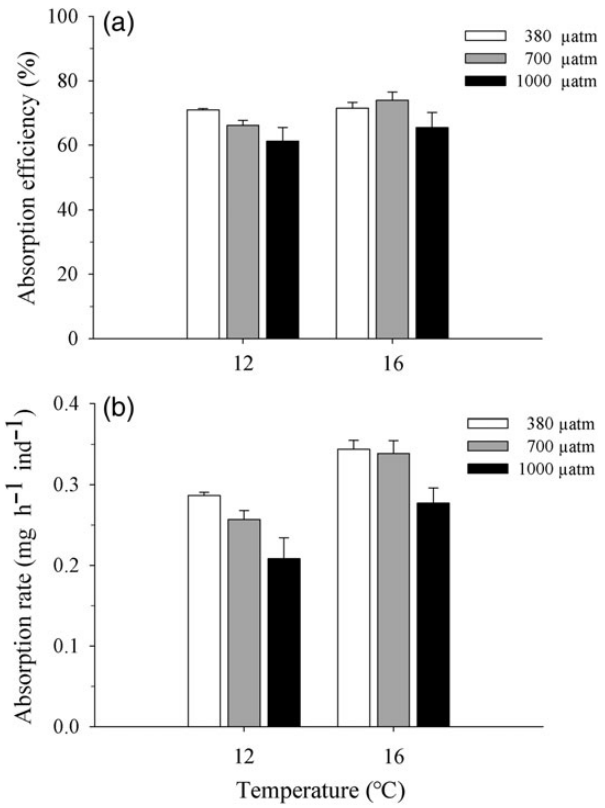

Figure 2. AE (a) and absorption rate (b) of juvenile individuals of the mussel *M. chilensis* exposed to different combinations of temperature and pCO_2 for 80 d. Values are means ± standard error.

significant difference. The absorption rate was significantly higher in mussels exposed to 16°C. (two-way ANOVA; pCO_2: $F_{2,12} = 11.20$, $p < 0.05$; temperature: $F_{1,12} = 28.00$, $p < 0.01$; temperature * pCO_2: $F_{2,12} = 0.28$, $p > 0.05$; Figure. 2b).

The excretion rate of *M. chilensis* was not affected by pCO_2 concentration; however, it was affected significantly by temperature, with higher values at 16°C (two-way ANOVA; pCO_2: $F_{2,12} = 0.77$, $p > 0.05$; temperature: $F_{1,12} = 5.32$, $p < 0.05$; temperature * pCO_2: $F_{2,12} = 0.84$, $p > 0.05$; Figure. 3a).

Oxygen consumption was significantly affected by pCO_2, but not by temperature or by the temperature * pCO_2 interaction (two-way ANOVA; pCO_2: $F_{2,12} = 6.10$, $p < 0.01$; temperature: $F_{1,12} = 0.031$, $p > 0.05$; temperature * pCO_2: $F_{2,12} = 0.26$, $p > 0.05$). Significantly lower values of oxygen uptake were observed in mussels exposed to 1000 µatm pCO_2 compared with those exposed to 380 µatm pCO_2. Individuals maintained at 700 µatm pCO_2 exhibited intermediate values of oxygen uptake, without stating significant differences with the two other treatments (Figure. 3b).

Two-way ANOVA showed a significant effect of the factors pCO_2 ($F_{1,12} = 4.38, p < 0.05$) and temperature ($F_{1,12} = 15.58, p < 0.001$) on the SFG of *M. chilensis*. However, the interaction between both factors did not have a significant effect ($F_{1,12} = 0.59$, $p > 0.05$).

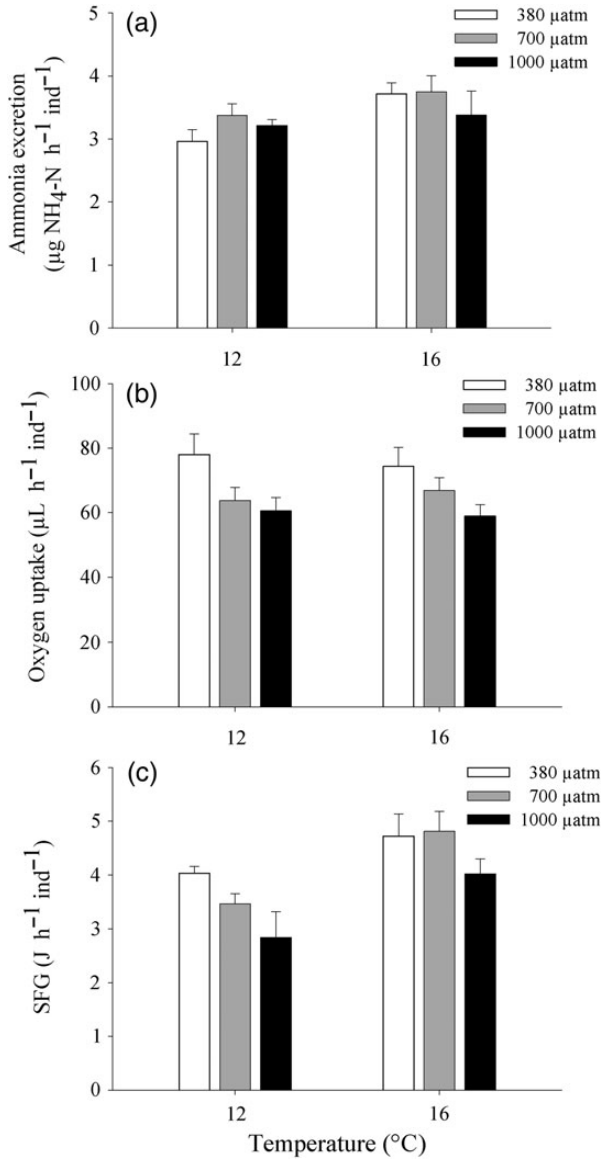

Figure 3. Ammonia excretion (a), oxygen uptake (b) and SFG (c) of juvenile individuals of the mussel *M. chilensis* exposed to different combinations of temperature and pCO_2 for 80 days. Values are means ± standard error.

SFG was significantly lower at the highest pCO_2 concentration (1000 µatm) compared with the control (380 µatm). Mussels exposed to 700 µatm pCO_2 did not show significantly different values of SFG from the other two pCO_2 treatments. SFG was significantly higher at 16°C than at 12°C (Figure. 3c).

Discussion

Our results showed that the rise in temperature from 12 to 16°C in a scenario of elevated pCO_2 (1000 µatm pCO_2) did not increase the sensitivity of the physiological processes measured in *M. chilensis*. On the contrary, it was observed that the increase in temperature induced a positive effect on the physiological processes associated with increased energy. In turn, the increase of pCO_2 adversely affected this species by reducing the energy intake, which resulted in significantly lower values of SFG at 1000 µatm pCO_2 at both temperatures, compared with 380 µatm pCO_2.

Contrasting results have been described in previous studies on the combined effects of warming and elevated pCO_2 levels on different groups of marine invertebrates. Catarino *et al.* (2012) demonstrated that ocean warming and acidification antagonistically interacted on oxygen uptake of the sea urchin *Paracentrotus lividus*. Byrne and Przeslawski (2013) reviewed the combined effect of ocean warming and high pCO_2 levels in >20 species of invertebrates. Their results showed that antagonistic effects were common, where ocean warming reduces the negative effects of pCO_2, unlike synergies, which were less common. Previous studies have shown that feeding activity in molluscs can increase within the thermal window of each species and drastically reduced when the temperature exceeds the limit of thermal tolerance (Navarro *et al.*, 2002; Peck *et al.*, 2009). Wang *et al.* (2015) found that increasing temperature significantly reduced CR of the mussel *Mytilus coruscus*, but elevated levels of pCO_2 did not show an additive or antagonistic effect with temperature. In our study, temperature positively affected CR, increasing from 12 to 16°C at all experimental pCO_2 levels. This can be explained by the experimental temperature range used, which is within the thermal window (9–16°C) of the studied population of *M. chilensis* (Navarro and Jaramillo, 1994). The negative effect of elevated concentrations of pCO_2 on the feeding rate of *M. chilensis* observed in our study has been also described for other species of bivalves. Fernandez-Reiriz *et al.* (2011) observed a reduction in the feeding rate in the clam *Ruditapes decussatus* at the highest experimental pCO_2 concentration (pH 7.48). Navarro *et al.* (2013) also described negative effects of elevated levels of pCO_2 (pH 7.57) on the feeding rate of the mussel *M. chilensis*.

There are few studies on the combined effects of ocean warming and high pCO_2 levels on AE of marine organisms. Zhang *et al.* (2015) found that AE of the gastropod *Nassarius conoidalis* was not significantly affected at the beginning of the experimental period (day 2) by temperature, pCO_2 level, nor the interaction between temperature and pCO_2 levels. However, on day 30, the temperature negatively affected AE when this gastropod was exposed at the highest pCO_2 concentration. Wang *et al.* (2015) described low values for AE (20–45%) on the mussel *M. coruscus* with no significant differences between three different pH levels (8.1, 7.7, and 7.3). Our results showed that pCO_2 levels significantly affected the AE of *M. chilensis*, but this effect was not registered for neither temperature nor the interaction between temperature and pCO_2. In a previous study, Navarro *et al.* (2013) reported that elevated pCO_2 levels (pH 7.57) reduced significantly the AE of *M. chilensis*, indicating possible deficiencies in the functioning of the digestive system under conditions of seawater acidification.

Similar to other studies on marine bivalves (Bayne and Newell, 1983; Velasco and Navarro, 2005), ammonia excretion of *M. chilensis* represented a low amount of the energy absorbed, with a minimal impact on the energy balance. Ammonia excretion was only affected by temperature, and the increase observed in mussels exposed to the highest temperature (16°C) could be explained by the larger amount of food ingested and absorbed under these conditions. Navarro *et al.* (2013) found similar values for ammonia excretion in juveniles of *M. chilensis* exposed to a wide range of pCO_2 levels (7.91–7.57).

There is evidence of the capability of marine organisms to acclimate the metabolic rate within certain range of temperature (thermal window), being a species-specific response (Pörtner *et al.*, 2005, Pörtner, 2008, 2010; Ezgeta-Balic *et al.*, 2011). However, at high temperatures, beyond the range of thermal tolerance of a species, a

drastic decline occurs in oxygen consumption and an increase in the anaerobic metabolic pathways (Jansen *et al.*, 2007). In our study, oxygen consumption was not affected by temperature. This can be explained because the mussels were exposed to a temperature range that the animals experience in their natural environment. However, temperatures over the thermal window naturally could have a negative impact on oxygen consumption of *M. chilensis*. Several studies have described metabolic depression in different species of marine organisms at elevated pCO_2 concentrations, caused by the low capacity to compensate for disturbances in extracellular ion and acid–base status (Michaelidis *et al.*, 2005; Pörtner, 2008). Our study showed a depletion of oxygen consumption when mussels were exposed to the highest pCO_2 level, suggesting that *M. chilensis* also is not able to cope with high pCO_2 levels in the seawater.

Different physiological processes related with gain and expenditure of energy largely depend on an organism's environmental temperature (Bayne and Newell, 1983). Populations that can maintain their aerobic capacity at warmer temperatures have a higher thermal tolerance, and are thereby predicted to persist longer as the temperature increases (Pörtner, 2001; Gardiner *et al.*, 2010). SFG represents the integration of all these processes varying as a function of temperature (Ezgeta-Balic *et al.*, 2011). Wang *et al.* (2015), studying the combined effects of seawater temperature and pH on the mussel *M. coruscus*, described positive values of SFG for all treatments, with no significant effects of pH. However, temperature showed a significant effect on the SFG, being reduced from 25 to 30°C. Ezgeta-Balic *et al.* (2011) recorded negative values of SFG for the mussel *Modiolus barbatus* when temperature rises from 26 to 28°C. Anestis *et al.* (2010), when studying the response of the mussel *Mytilus galloprovincialis* to increasing seawater temperature, found that the SFG values became negative at temperatures higher than 24°C, associated with a reduction in CR. Contrary to these authors, the present study showed a significant positive effect of temperature on SFG at all pCO_2 levels. This might be explained because the experimental mussels were exposed to temperatures experienced in their natural environment, which are within the range of thermal tolerance of the species although the highest temperature (16°C) is recorded in a narrow temporal window during summer (Navarro and Jaramillo, 1994). The increase of the SFG observed in the present study matches well with the significant increase of CR and absorption rate from 12 to 16°C. Oxygen uptake was not affected by increasing temperature, suggesting that metabolic activity is maintained constant within the thermal window of *M. chilensis*. Similar conclusions were reported by Findlay *et al.* (2010) to explain the lack of differences between the growth rates of *Semibalanus balanoides* exposed to a range of temperatures experienced in their natural environment. The zone of the Reloncaví Sound, located 50 km east from the place where the experimental mussels were collected (Bay of Huelmo), has been described as an environment with a low calcium carbonate saturation and even "corrosive" when occurring in waters with low salinity and alkalinity (Alarcón *et al.*, 2015). This can explain the lack of significant differences in some of the physiological responses between the 380 and 700 pCO_2 levels, suggesting that mussels from this area might be pre-adapted to natural pH variability.

There are still few studies on the combined effect of pCO_2 with other environmental stressors. Gazeau *et al.* (2014) found that somatic and shell growth of *M. galloprovincialis* did not appear very sensitive to OA and warming during most of the experiment. However, growth was significantly reduced after summer in the lowered pH treatment. According to these authors, there is a progressive insufficiency in acid–base regulation capacity, which was also consistent with shell net dissolution observed in the mussels (Gazeau *et al.*, 2014). Other studies described that growth might be significantly reduced under medium- and long-term exposure to elevated pCO_2 levels (Beniash *et al.*, 2010; Navarro *et al.*, 2013; Duarte *et al.*, 2014). Both shell and soft tissue growth of the oyster *C. virginica* were reduced when exposed to high pCO_2 levels (pH 7.5; Beniash *et al.*, 2010). Similarly, Duarte *et al.* (2014) found that net rate of calcium deposition and total weight of the mussel *M. chilensis* were not significantly affected by temperature, but were negatively affected by high pCO_2 levels. Our results suggest that a rise in temperature within the natural range experienced by juveniles *M. chilensis* generates a positive effect on the processes related with energy gain from the environment (i.e. feeding and absorption) to be allocated for growth. In turn, the increase in 1000 μatm pCO_2, independent of temperature, adversely affects this species, with significantly reduced energy allocated to growth (SFG) compared with the control treatment (380 μatm pCO_2). Our results are interpreted as answers to short-term toxicity challenges with temperature and CO_2 as environmental factors. On the basis of these, inferences about environmental changes that would slowly occur over the next 100–200 years must be made with appropriate caution. This is because animals used for testing would vary in geno- and phenotypes.

The effect of elevated pCO_2 on marine organisms can be negative (Gazeau *et al*, 2014), reduced, or absent in the presence of high temperature (Pörtner and Farrel, 2008; Duarte *et al.*, 2014). This is because the effect of warming will depend on the experimental temperature range and thermal window of the species under study. Thus, the studies related to the combined effect of ocean warming and elevated concentrations of pCO_2 must consider the thermal windows of each species to avoid contradictory interpretations. Future experiments with different levels of temperatures should be designed in a way that will allow greater predictive power, selecting temperature treatments that will be physiologically realistic to the animal's thermal windows and to future climate scenarios.

Acknowledgements

The authors are grateful to Elizabeth Encalada and Alejandro Ortíz for their assistance during the laboratory and fieldwork. Special thanks are due to the reviewers for very constructive comments on the manuscript. This study was mainly funded by the Programa de Investigación Asociativa, PIA CONICYT-CHILE (Grant Anillos ACT-132). Additional support came from FONDECYT Grant 1120470 to JMN and from Center FONDAP-CONICYT IDEAL 15150003. CAV is supported by Red Doctoral (REDOC.CTA) MINEDUC project UCO1202 at Universidad de Concepción.

References

Alarcón, E., Valdés, N., and Torres, R. 2015. Saturación del carbonato de calcio en un área de cultivo de mitílidos en el Seno Reloncaví, Patagonia norte, Chile. Revista Chilena de Historia Natural, 43: 277–281.

Anestis, A., Pörtner, H. O., Karagiannis, D., Angelidis, P., Staikou, A., and Michaelidis, B. 2010. Response of *Mytilus galloprovincialis* (L.) to increasing seawater temperature and to marteliosis: Metabolic and physiological parameters. Comparative Biochemistry and Physiology Part A: Molecular and Integrative Physiology, 156(1): 57–66.

Bayne, B. L., and Newell, R. C. 1983. Physiological energetics of marine molluscs. In The Mollusca Vol. 4. Physiology. Part 1, pp. 407–515. Ed. by K. M. Wilbur. Academic Press, New York.

Beniash, E., Ivanina, A., Lieb, N. S., Kurochkin, I., and Sokolova, I. M. 2010. Elevated level of carbon dioxide affects metabolism and shell formation in oysters *Crassostrea virginica*. Marine Ecology Progress Series, 419: 95–108.

Byrne, M. 2011. Impact of ocean warming and ocean acidification on marine invertebrate life history stages: Vulnerabilities and potential for persistence in a changing ocean. Oceanography and Marine Biology: An Annual Review, 49: 1–42.

Byrne, M., and Przeslawski, R. 2013. Multistressor impacts of warming and acidification of the ocean on marine invertebrates' life histories. Integrative and Comparative Biology, 53: 582–596.

Caldeira, K., and Wickett, M. E. 2003. Oceanography: Anthropogenic carbon and ocean pH. Nature, 425: 365.

Catarino, A. I., Bauwens, M., and Dubois, P. 2012. Acid-base balance and metabolic response of the sea urchin *Paracentrotus lividus* to different seawater pH and temperatures. Environmental Science and Pollution Research International, 19: 2344–2353.

Conover, R. J. 1966. Assimilation of organic matter by zooplankton. Limnology and Oceanography, 11: 338–345.

Coughlan, J. 1969. The estimation of filtering rate from the clearance of suspensions. Marine Biology, 2: 356–358.

Dickson, A. G., and Millero, F. J. 1987. A comparison of the equilibrium constants for the dissociation of carbonic acid in seawater media. Deep-Sea Research Part A: Oceanographic Research Papers, 34: 1733–1743.

Duarte, C., Jaramillo, E., Contreras, H., and Figueroa, L. 2006. Community structure of the macroinfauna in the sediments below and intertidal mussel bed (*Mytilus chilensis*) (Hupe) of southern Chile. Revista Chilena de Historia Natural, 79: 353–368.

Duarte, C., Navarro, J. M., Acuña, K., Torres, R., Manriquez, P. H., Lardies, M. A., Vargas, C. A., *et al.* 2014. Combined effects of temperature and ocean acidification on the juvenile individuals of the mussel *Mytilius chilensis*. Journal of Sea Research, 85: 308–314.

Elliot, J. M., and Davison, W. 1975. Energy equivalents of oxygen consumption in animal energetics. Oecologia, 19: 195–201.

Ezgeta-Balic, D., Rinaldi, A., Peharda, M., Prusina, I., Montalto, V., Niceta, N., and Sarà, G. 2011. An energy budget for the subtidal bivalve *Modiolus barbatus* (Mollusca) at different temperatures. Marine Environmental Research, 71: 79–85.

Fabry, V. J., Seibel, B. A., Feely, R. A., and Orr, J. C. 2008. Impacts of ocean acidification on marine fauna and ecosystem processes. ICES Journal of Marine Science, 65: 414–432.

Feely, R. A., Sabine, C. L., Lee, K., Berelson, W., Kleypas, J., Fabry, V. J., and Millero, F. J. 2004. Impact of anthropogenic CO_2 on the $CaCO_3$ system in the oceans. Science, 305: 362–366.

Fernandez-Reiriz, M. J., Range, P., Álvarez-Salgado, X. A., and Labarta, U. 2011. Physiological energetics of juvenile clams *Ruditapes decussatus* in a high CO_2 coastal ocean. Marine Ecology Progress Series, 433: 97–105.

Findlay, H. S., Kendall, M. A., Spicer, J. I., and Widdicombe, S. 2010. Post-larval development of two intertidal barnacles at elevates CO_2 and temperature. Marine Biology, 157: 725–735.

Gardiner, N. M., Munday, P. L., and Nilsson, G. E. 2010. Counter-gradient variation in respiratory performance of coral reef fishes at elevated temperatures. PLoS ONE, 5: e13299.

Gazeau, F., Alliounane, S., Bock, C., Bramanti, L., Lopez Correa, M., Gentile, M., Hirse, T., *et al.* 2014. Impact of ocean acidification and warming on the Mediterranean mussel (*Mytilus galloprovincialis*). Frontiers Marine Science, 1: 62.

Gobler, C. J., and Talmage, S. C. 2014. Physiological response and resilience of early life-stage Eastern oysters (*Crassostrea virginica*) to past, present and future ocean acidification. Conservation Physiology, 2. doi:10.1093/conphys/cou004.

Godbold, J. A., and Solan, M. 2013. Long-term effects of warming and ocean acidification are modified by seasonal variation in species responses and environmental conditions. Philosophical Transactions of the Royal Society of London Series B-Biological Sciences, 368: 20130186.

Gooding, R. A., Harley, C. D. G., and Tang, E. 2009. Elevated water temperature and carbon dioxide concentration increase the growth of a keystone echinoderm. Proceedings of the National Academy of Sciences, 106: 9316–9321.

Haraldsson, C., Anderson, L. G., Hassellöv, M., Hulth, S., and Olsson, K. 1997. Rapid, high-precision potentiometric titration of alkalinity in ocean and sediment pore waters. Deep-Sea Research Part 1: Oceanographic Research Papers, 44: 2031–2044.

Harley, C. D., Randall Hughes, A., Hultgren, K. M., Miner, B. G., Sorte, C. J., Thornber, C. S., Rodriguez, L. F., *et al.* 2006. The impacts of climate change in coastal marine systems. Ecology Letters, 9: 228–241.

Hiebenthal, C., Philipp, E. E. R., Eisenhauer, A., and Wahl, M. 2013. Effects of seawater pCO_2 and temperature on shell growth, shell stability, condition and cellular stress of Western Baltic Sea *Mytilus edulis* (L.) and *Arctica islandica* (L.). Marin Biology, 160: 2073–2087.

IPCC. 2013. The Physical Science Basis. Working Group I Contribution to the Fifth Assessment Report of the Intergovernmental Panel on Climate Change, Cambridge University Press, Cambridge.

Ivanina, A. V., Dickinson, G. H., Matoo, O. B., Bagwe, R., Dickinson, A., Beniash, E., and Sokolova, I. M. 2013. Interactive effect of elevated temperature and CO_2 levels on energy metabolism and biomineralization of marine bivalves *Crassostrea virginica* and *Mercenaria mercenaria*. Comparative Biochemistry and Physiology Part A: Molecular and Integrative Physiology, 166: 101–111.

Jansen, J. M., Pronker, A. E., Kube, S., Sokolowski, A., Sola, J. C., Marquiegui, M. A., Shiedek, D., *et al.* 2007. Geographic and seasonal patterns and limits on the adaptive response to temperature of European *Mytilus* spp. and *Macoma balthica* populations. Oecologia, 154: 23–34.

Lewis, E., and Wallace, D. 1998. Program Developed for CO_2 System Calculations. Carbon Dioxide Information Analysis Center, Oak Ridge, TN, USA.

Mehrbach, C., Culberson, C. H., Hawley, J. E., and Pytkowicz, R. M. 1973. Measurement of the apparent dissociation constants of carbonic acid in seawater at atmospheric pressure. Limnology and Oceanography, 18: 897–907.

Meier, H. E. M. 2006. Baltic Sea climate in the late twenty-first century: A dynamical downscaling approach using two global models and two emission scenarios. Climate Dynamics, 27: 39–68.

Metzger, R., Sartoris, F. J., Langenbuch, M., and Pörtner, H. O. 2007. Influence of elevated CO_2 concentrations on thermal tolerance of the edible crab *Cancer pagurus*. Journal of Thermal Biology, 32: 144–151.

Michaelidis, B., Ouzounis, C., Paleras, A., and Pörtner, H. O. 2005. Effects of long-term moderate hipercapnia on acid-base balance and growth rate in marine mussels *Mytilus galloprovincialis*. Marine Ecology Progress Series, 293: 109–118.

Navarro, J. M., and Jaramillo, R. 1994. Evaluación de la oferta alimentaria natural disponible a organismos filtradores en la Bahía de Yaldad (43–08; 73–44′), sur de Chile. Revista de Biología Marina, 29: 57–75.

Navarro, J. M., Leiva, G. E., Gallardo, C. S., and Varela, C. 2002. Influence of diet and temperature on physiological energetics of *Chorus giganteus* (Gastropoda:Muricidae) during reproductive conditioning. New Zealand Journal of Marine and Freshwater Research, 36: 321–332.

Navarro, J. M., Leiva, G. E., Martínez, G., and Aguilera, C. 2000. Interactive effects of diet and temperature on the scope for growth of the scallops *Argopecten purpuratus* during reproductive conditioning. Journal of Experimental Marine Biology and Ecology, 247: 67–83.

Navarro, J. M., Torres, R., Acuña, K., Duarte, C., Manriquez, P. H., Lardies, M., Lagos, N. A., *et al.* 2013. Impact of medium-term

exposure to elevated pCO_2 levels on the physiological energetic of the mussel *Mytilus chilensis.* Chemosphere, 90: 1242–1248.

Ohle, W. 1953. Die chemische und elektrochemische Bestimmung des molekular gelösten Sauerstoffs der Binnengewäser. Mitteilungen Internationale Vereinigung der Limnologie, 3: 1–44.

Peck, L. S., Massey, A., Thorne, M. A., and Clark, M. S. 2009. Lack of acclimation in *Ophionotus victoriae*: Brittle stars are not fish. Polar Biology, 32: 399–402.

Philippart, C. J. M., Van Aken, H. M., Beukema, J. J., Bos, O. G., Cadée, G. C., and Dekker, R. 2003. Climate-related changes in recruitment of the bivalve *Macoma balthica*. Limnology and Oceanography, 48: 2171–2185.

Pörtner, H. O. 2001. Climate change and temperature-dependent biogeography: Oxygen limitation of thermal tolerance in animals. Naturwissenschaften, 88: 137–146.

Pörtner, H. O. 2008. Ecosystem effects of ocean acidification in times of ocean warming: A physiologist's view. Marine Ecology Progress Series, 373: 203–217.

Pörtner, H. O. 2010. Oxygen-and capacity-limitation of thermal tolerance: A matrix for integrating climate-related stressor effects in marine ecosystems. The Journal of Experiment Biology, 213: 881–893.

Pörtner, H. O., and Farrel, A. P. 2008. Physiology and climate change. Science, 322: 690–692.

Pörtner, H. O., Langenbuch, M., and Michaelidis, B. 2005. Synergistic effects of temperature extremes, hypoxia, and increases in CO_2 on marine animals: From Earth history to global change. Journal of Geophysical Research, 110: 1–15.

Pörtner, H. O., Langenbuch, M., and Reipschläger, A. 2004. Biological impact of elevated ocean CO_2 concentrations: Lessons from animal physiology and Earth history. Journal of Oceanography, 60: 705–718.

Schiedek, D., Sundelin, B., Readman, J. W., and Macdonald, R. W. 2007. Interactions between climate change and contaminants. Marine Pollution Bulletin, 54: 1845–1856.

Solórzano, L. 1969. Determination of ammonia in natural waters by the phenolhypochlorite method. Limnology and Oceanography, 14: 799–801.

Somero, G. N. 2002. Thermal physiology and vertical zonation of intertidal animals: Optima, limits and costs of living. Integrative and Comparative Biology, 42: 780–789.

Torres, R., Manriquez, P. H., Duarte, C., Navarro, J. M., Lagos, N. A., Vargas, C. A., and Lardies, M. A. 2013. Evaluation of a semi-automatic system for long-term seawater carbonate chemistry manipulation. Revista Chilena de Historia Natural, 86: 443–451.

Underwood, A. J. 1997. Experiments in Ecology: Their Logical Design and Interpretation Using Analysis of Variance. Cambridge University Press, Cambridge.

Vargas, C. A., De la Hoz, M., Aguilera, V., San Martín, V., Manriquez, P. H., Navarro, J. M., Torres, R., *et al.* 2013. CO_2-driven ocean acidification reduces larval feeding efficiency and change food selectivity in the mollusk *Concholepas concholepas*. Journal of Plankton Research, 35: 1059–1068.

Velasco, L. A., and Navarro, J. M. 2005. Feeding physiology of two bivalves under laboratory and field conditions in response to variable food concentrations. Marine Ecology Progress Series, 291: 115–124.

Walther, G. R., Post, E., Convey, P., Menzel, A., Parmesan, C., Beebee, T., Fromentin, J-M., *et al.* 2002. Ecological responses to recent climate change. Nature, 416: 389–395.

Wang, Y., Li, L., Hu, M., and Lu, W. 2015. Physiological energetic of the thick shell mussel *Mytilus coruscus* exposed to seawater acidification and thermal stress. Science of the Total Environment, 1: 261–272.

Whyte, J. 1987. Biochemical composition and energy content of six species of phytoplankton used in mariculture of bivalves. Aquaculture, 60: 231–241.

Widdicombe, S., and Spicer, J. I. 2008. Predicting the impact of ocean acidification on benthic biodiversity: What can animal physiology tell us? Journal of Experimental Marine Biology and Ecology, 366: 187–197.

Zhang, H., Shin, P. K. S., and Cheung, S. G. 2015. Physiological responses and scope for growth upon medium-term exposure to the combined effects of ocean acidification and temperature in a subtidal scavenger *Nassarius conoidalis*. Marine Environmental Research, 106: 51–60.

Handling editor: Howard Browman

ICES Journal of Marine Science

ICES Journal of Marine Science (2016), 73(3), 772–782. doi:10.1093/icesjms/fsv198

Contribution to Special Issue: 'Towards a Broader Perspective on Ocean Acidification Research'

Original Article

Effects of high CO_2 and warming on a Baltic Sea microzooplankton community

Henriette G. Horn[1]*, Maarten Boersma[1,2], Jessica Garzke[3], Martin G. J. Löder[1‡], Ulrich Sommer[3], and Nicole Aberle[1]

[1]*Biologische Anstalt Helgoland, Alfred-Wegener-Institut Helmholtz-Zentrum für Polar- und Meeresforschung, Postfach 180, 27483 Helgoland, Germany*
[2]*University of Bremen, Bremen, Germany*
[3]*GEOMAR Helmholtz Centre for Ocean Research Kiel, Düsternbrooker Weg 20, 24105 Kiel, Germany*

**Corresponding author: tel: + 49 4725 819 3372; fax: + 49 4725 819 3369; e-mail: henriette.horn@awi.de*
‡*Present address: University of Bayreuth, Animal Ecology I, Universitätsstraße 30, 95440 Bayreuth, Germany.*

Horn, H. G., Boersma, M., Garzke, J., Löder, M. G. J., Sommer, U., and Aberle, N. Effects of high CO_2 and warming on a Baltic Sea microzooplankton community. – ICES Journal of Marine Science, 73: 772–782.

Received 10 April 2015; revised 4 October 2015; accepted 8 October 2015; advance access publication 2 November 2015.

Global warming and ocean acidification are among the most important stressors for aquatic ecosystems in the future. To investigate their direct and indirect effects on a near-natural plankton community, a multiple-stressor approach is needed. Hence, we set up mesocosms in a full-factorial design to study the effects of both warming and high CO_2 on a Baltic Sea autumn plankton community, concentrating on the impacts on microzooplankton (MZP). MZP abundance, biomass, and species composition were analysed over the course of the experiment. We observed that warming led to a reduced time-lag between the phytoplankton bloom and an MZP biomass maximum. MZP showed a significantly higher growth rate and an earlier biomass peak in the warm treatments while the biomass maximum was not affected. Increased pCO_2 did not result in any significant effects on MZP biomass, growth rate, or species composition irrespective of the temperature, nor did we observe any significant interactions between CO_2 and temperature. We attribute this to the high tolerance of this estuarine plankton community to fluctuations in pCO_2, often resulting in CO_2 concentrations higher than the predicted end-of-century concentration for open oceans. In contrast, warming can be expected to directly affect MZP and strengthen its coupling with phytoplankton by enhancing its grazing pressure.

Keywords: CO_2, global warming, heterotrophic protists, mesocosm experiment, ocean acidification, protozooplankton.

Introduction

The concentration of CO_2 in the atmosphere has increased considerably in the last decades, from 280 ppm in pre-industrial times to currently ~400 ppm (Le Quéré *et al.*, 2013). By the end of this century, atmospheric concentrations are predicted to reach 1000 ppm (Collins *et al.*, 2013). Apart from the well-known greenhouse effect, a rise in CO_2 has a direct effect on the surface oceans. Acting as major sinks for CO_2, the increase in dissolved CO_2 in the surface waters results in a change in carbonate chemistry and a decrease in pH, termed ocean acidification (OA; Sabine *et al.*, 2004). On a global scale, pH values have already decreased by 0.1 units in the last 100 years (Hoegh-Guldberg and Bruno, 2010), but there are differences in the amount of CO_2 taken up by the oceans depending on the region (Sabine *et al.*, 2004). Linked to the predicted increase in CO_2, a further decrease in pH by up to 0.32 units by the end of the 21st century is likely (Ciais *et al.*, 2013).

OA is most problematic for organisms with skeletal calcium carbonate structures, especially molluscs, corals, and calcifying algae (Kroeker *et al.*, 2013). On the other hand, there are non-calcifying phytoplankton species that benefit from a higher availability of carbon enhancing their growth (Rost *et al.*, 2008; Low-Decarie *et al.*, 2014). Although a direct effect of a lowered pH on phytoplankton (Riebesell *et al.*, 2000a; Kim *et al.*, 2006) and zooplankton (Pedersen and Hansen, 2003; Mayor *et al.*, 2007; Cripps *et al.*, 2014) has been reported for some species, other studies point at only the indirect effects of OA, e.g. by changes in phytoplankton availability, quality, or changes in C : N : P ratios affecting higher levels (Iglesias-Rodriguez *et al.*, 2008; Suffrian *et al.*, 2008; Nielsen

et al., 2010; Aberle *et al.*, 2013). Therefore, several authors have argued for the necessity of community level experiments to understand whether and how biotic interactions dampen or amplify single-species responses (Joint *et al.*, 2011; Kroeker *et al.*, 2013; Rossoll *et al.*, 2013).

Microzooplankton (MZP) in the size range of 20–200 μm is a major phytoplankton consumer in planktonic foodwebs where it plays a vital role as intermediary between the microbial loop and higher trophic levels (Calbet and Landry, 2004; Calbet *et al.*, 2008). Owing to its high specific growth and grazing rates, MZP can have a strong impact on the biomass and species composition of phytoplankton communities, which can lead to dietary overlap and competition between MZP and mesozooplankton (Löder *et al.*, 2011). At the same time, higher trophic levels use MZP as a food source and can benefit from its ability to buffer nutritional imbalances especially at times when food quality of phytoplankton is low (Malzahn *et al.*, 2010).

On top of changes in ocean carbonate chemistry, warming will have a strong impact on the oceans: according to the IPCC report (Collins *et al.*, 2013), sea surface temperature will increase between 1 and 5°C within this century. This is predicted to cause a decrease in phytoplankton biomass and productivity (Boyce *et al.*, 2010; Hoegh-Guldberg and Bruno, 2010; Sommer *et al.*, 2012). Such a decline in phytoplankton biomass has been attributed to a strengthened top-down control on phytoplankton (Rose and Caron, 2007), because growth and grazing rates of heterotrophic protists as well as copepods show a stronger temperature dependence than autotrophic protists (Aberle *et al.*, 2007, 2012; Lewandowska *et al.*, 2014). As grazing of both MZP and copepods is species- or size-selective, certain species are preferably grazed upon thus leading to changes in the phytoplankton community structure (Riegman *et al.*, 1993; Lewandowska and Sommer, 2010).

While investigations of single factors are of importance, there is a strong need to consider interactive effects of multiple stressors in future analyses (Caron and Hutchins, 2012). In one of the few experiments on the joint effects of OA and warming, Rose *et al.* (2009) found significant differences in MZP abundance and community composition for a combination of factors in a North Atlantic spring bloom plankton community. Their study suggests that indirect effects due to changes in the phytoplankton community could be more important in changing MZP community structure than direct effects of OA or warming. In contrast, Calbet *et al.* (2014) performed a multiple-stressor mesocosm experiment in a Norwegian fjord and added eutrophication as a third stressor. Contrasting effects of warming and acidification for different plankton groups were observed, pointing at the importance of indirect effects due to changes in phytoplankton food quality leading to a lower ciliate biomass maximum and a shift of the plankton community in the combined treatment (Calbet *et al.*, 2014).

Generally, pCO_2 in highly productive estuarine areas such as the Kiel Fjord is much more variable than in the open ocean (Feely *et al.*, 2010; Melzner *et al.*, 2013). Thus, the responses of plankton communities to warming and OA highly depend on the community composition and the ecosystem characteristics. Currently, seawater pCO_2 in the Kiel Fjord is often as high as 700 ppm, with peaks in summer and autumn reaching values of up to 2300 ppm (Thomsen *et al.*, 2010). While the community in the Fjord is thus expected to be resilient to a high pCO_2 (Melzner *et al.*, 2013; Rossoll *et al.*, 2013), there is evidence that Baltic Sea plankton communities are strongly affected by warming (Sommer and Lewandowska, 2011; Aberle *et al.*, 2012, 2015; Winder *et al.*, 2012; Lewandowska *et al.*, 2014).

Here, we present an indoor mesocosm study on the combined effects of enhanced CO_2 and warming on natural autumn plankton communities from Kiel Fjord, characterized by a diatom-dominated phytoplankton bloom in autumn (Wasmund *et al.*, 2008). Our working hypotheses considering the combined effects of warming and CO_2 were as follows:

(i) Warming will enhance MZP growth (timing and biomass), thus leading to a strong top-down control of phytoplankton and a strong copepod predation on MZP.

(ii) Based on the high pH tolerance of coastal MZP communities, only indirect effects on MZP due to an altered phytoplankton quality and community composition are likely.

(iii) Due to positive effects on photosynthesis, high pCO_2 will cause an increase in phytoplankton biomass leading to a higher MZP biomass.

(iv) The combined effects of warming and pCO_2 will lead to a dampening of the effects of high pCO_2. The increase in MZP biomass and growth rate with warming is expected to compensate for indirect effects on MZP due to changes in phytoplankton community composition and quality.

Material and methods

Experimental design

Twelve mesocosms with a volume of 1400 l each and a depth of 1 m were installed in four temperature-controlled culture rooms at GEOMAR, Kiel, Germany, for an experiment in autumn 2012. The setup is described in more detail by Sommer *et al.* (2007); however, mesocosm lids were added for the CO_2 manipulation. Two temperatures (9 and 15°C, hereafter called "cold" and "warm") and two CO_2 levels (target levels 560 and 1400 ppm, hereafter called "low" and "high") were crossed in a full-factorial design with each treatment in triplicate. The temperatures reflect a difference of 3°C from the ambient temperature of ~12°C. The symmetric design was chosen to avoid confounding the effects of the direction of temperature change (warming or cooling) with the effects of temperature change as such. The low target CO_2 concentration of 560 ppm was chosen to represent actual values measured in Kiel Fjord the day before filling the mesocosms, which is well below the average concentration of 700 ppm expected for the Kiel Fjord in autumn (Thomsen *et al.*, 2010). The high CO_2 level of 1400 ppm represents the value predicted for the end of the century for surface waters of the Baltic Sea (Collins *et al.*, 2013).

Light was provided by computer-controlled light units (GHL Groß Hard- und Softwarelösungen, Lampunit HL3700 and ProfiluxII). The light units consisted of five HIBay-LED spotlights (purpose built units by Econlux, each 100 W), illuminating each mesocosm from above. Light supply and daylength were calculated after Brock (1981), resembling the solar irradiance of a cloudless 21st October in Kiel and reduced by 50% to account for under water light attenuation. The light : dark cycle was 11 h50 min : 12 h10 min. The daily maximum light intensity in the middle of the water column was 252.3 μmol m^{-2} s^{-1}.

The mesocosms were filled with unfiltered seawater from Kiel Fjord on 19 October 2012, containing a natural autumn community of phytoplankton, bacteria, and protozoa. To ensure the same starting conditions in all mesocosms, the water was pumped from ~2 m

depth in a collecting tank using a rotary pump before distributing it into the mesocosms with a 12-way valve. Mesozooplankton was added from net catches with a target copepod concentration of 10 individuals l^{-1} to resemble natural densities and species composition for that time of the year (Javidpour *et al.*, 2009). The mesocosms were gently stirred by a propeller to minimize sedimentation and to ensure a homogenous distribution of plankton throughout the water column. Previous experiments with the same design have shown that this treatment does not lead to an increase in mesozooplankton mortality (Sommer *et al.*, 2007).

A PVC lid covered each mesocosm with only a small sampling port being opened for daily samplings. CO_2 levels were achieved by a flow-through of CO_2-enriched air with 560 and 1400 ppm CO_2 through the headspace between the water surface and the mesocosm lid with a rate of 30–60 l h^{-1}. The headspace was used to simulate a more natural CO_2 addition compared with the addition of CO_2-saturated water. However, the biological drawdown of CO_2 due to photosynthetic CO_2 consumption in combination with an incomplete equilibration between headspace and mesocosm water led to CO_2 concentrations below the target level. This was compensated by the addition of sterile-filtered, CO_2-saturated mesocosm water three times during the experiment; the necessary volumes were calculated based on dissolved inorganic carbon and alkalinity.

Target temperatures and divergence of CO_2 levels were reached 3 d after filling in all treatments on 22 October (hereafter called day 0) and the experiment ran until 12 November 2012 (day 21) with constant light and temperature conditions.

Sampling and measurements

Daily measurements included water temperature, salinity, and pH. Three times per week, samples for *in situ* fluorescence, heterotrophic nanoflagellates, phytoplankton, and MZP were taken by siphoning seawater from the middle of the water column using a silicone tube. Similarly, particulate organic carbon, phosphorus, and nitrogen as well as inorganic nutrients were sampled three times per week. Mesozooplankton was sampled once per week by three vertical hauls with a plankton net (64 μm mesh size), resulting in a sampled volume of 5.1 l.

In situ fluorescence was measured directly after sampling with a 10 AU fluorometer (Turner Design). For the MZP samples, 250 ml of mesocosm water was transferred into brown glass bottles, fixed with acid Lugol's solution, and stored dark. Counting and taxonomic identification of MZP was carried out using the Utermöhl method (Utermöhl, 1958). Depending on the plankton density, either 50 or 100 ml of each sample was transferred to a sedimentation cylinder and allowed to settle for 24 h before counting with an inverted microscope (Zeiss Axiovert 135). To reduce the counting bias against rare species and to assure comparability of the counts both at high and low MZP abundances, the whole surface of the sedimentation chamber was counted at 200-fold magnification.

MZP was identified to the lowest possible taxonomic level (species or genus level) according to Carey (1992), Montagnes *et al.* (2001), and Kraberg *et al.* (2010) and otherwise grouped into size classes (small: <30 μm, medium: 30–55 μm, and large: >55 μm). Biovolumes of ciliates were calculated according to geometric proxies by Hillebrand *et al.* (1999). For each group, the dimensions of 20 random cells were measured digitally (AxioVision 4.9 and AxioCam, Carl Zeiss Microscopy GmbH). Ciliate carbon biomass was estimated from the biovolumes using the conversion factors provided by Putt and Stoecker (1989).

Details on phytoplankton, nutrients, and carbonate chemistry and copepod sampling and analysis are given by Paul *et al.* (2015) and Garzke *et al.* (2015), respectively. Copepod biomass was calculated from abundances of adults and copepodites using standard conversion factors (Lengfellner, 2008).

Data analysis

First, we identified the day (D_{max}) when biomass reached its peak in each mesocosm. Growth rates μ (d^{-1}) of total ciliates and single species of ciliates were calculated as the slope of a regression of biomass over time (ln transformed) from day 0 until D_{max}. This day was defined as the bloom timing (D_{max}) for the respective mesocosm. The biomass maximum was the highest measured value from each single mesocosm, independent of the experimental day. The species diversity index (H', $\log_e$) was calculated after Shannon and Weaver (1963) on a sample day basis.

For the statistical analysis, all data were tested for normality and homogeneity of variance and transformed (ln) if necessary. To investigate the interactions between the factors temperature, CO_2 level, and time, repeated-measures ANOVAs were calculated with ciliate biomass, total copepod biomass, ciliate diversity, or chlorophyll fluorescence as a dependent variable. Two-way ANOVAs were performed to test for significant effects of temperature and CO_2 level (independent variables) as well as the interactions of these two factors on biomass maximum, D_{max}, and growth rates for total ciliates and single species of ciliates (dependent variables). Likewise, chlorophyll fluorescence maximum and bloom timing were tested with two-way ANOVAs.

Statistica 12 (StatSoft, Inc.) was used for ANOVAs and SigmaPlot 12.5 (Systat Software, Inc.) for regressions and graphs.

Results

Owing to a technical problem with the light control units of mesocosm 9 at the beginning of the experiment, the plankton community of this specific mesocosm showed a strongly reduced plankton development and was thus excluded from further analysis (thus, the cold low CO_2 treatment only had two replicates instead of three).

Temperatures in the mesocosms were 9.44°C (±0.39) and 14.78°C (±0.31) and remained stable over the course of the experiment (Figure 1a). The pCO_2 values decreased over time, but this was compensated by the addition of CO_2-enriched water on days 7, 12, and 19 (Figure 1b). Overall, the average value was 439 ppm (±180) for the low and 1040 ppm (±228) for the high CO_2 treatments.

Biomass and growth rate

There was an immediate numerical response in terms of ciliate biomass to the increasing phytoplankton biomass in the warm mesocosms in contrast to a delayed response in the cold ones (Figure 2a and b). Ciliate biomass was significantly different between the temperature treatments, although it depended on the time of the experiment (significant interaction time × temperature, $p < 0.001$; Table 1). Neither CO_2 nor the interaction of CO_2 and temperature had a significant effect on ciliate biomass. The peak of ciliate biomass was reached on day 11 in the warm treatments, followed by a sharp decline to initial levels (Table 2 and Figure 2b). In the cold treatments, peak densities of ciliates were observed on day 18 or 21 (Table 2). The ciliate biomass maximum was not affected by warming or CO_2 or interactions of these factors (Table 3). However, the timing of the biomass maximum was significantly affected by the temperature ($p < 0.001$), and this was also the case

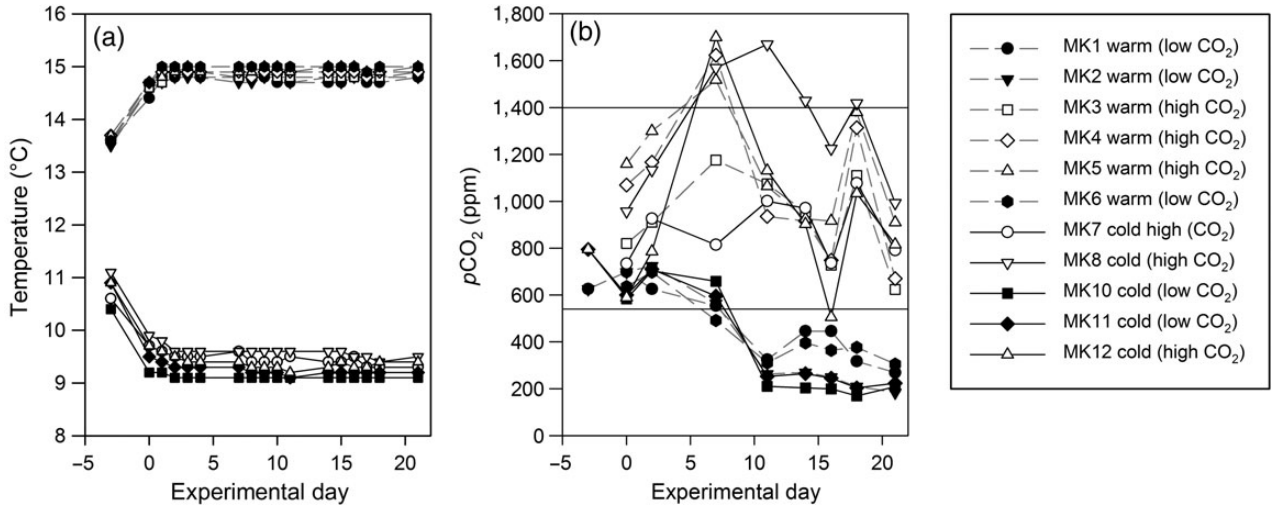

Figure 1. Actual temperatures and pCO_2 levels in the 12 mesocosms with the treatments of 9°C (black lines) and 15°C (dashed grey lines) at low (540 ppm; filled symbols) and high (1400 ppm; open symbols) CO_2 levels. Horizontal black lines denote target pCO_2 levels.

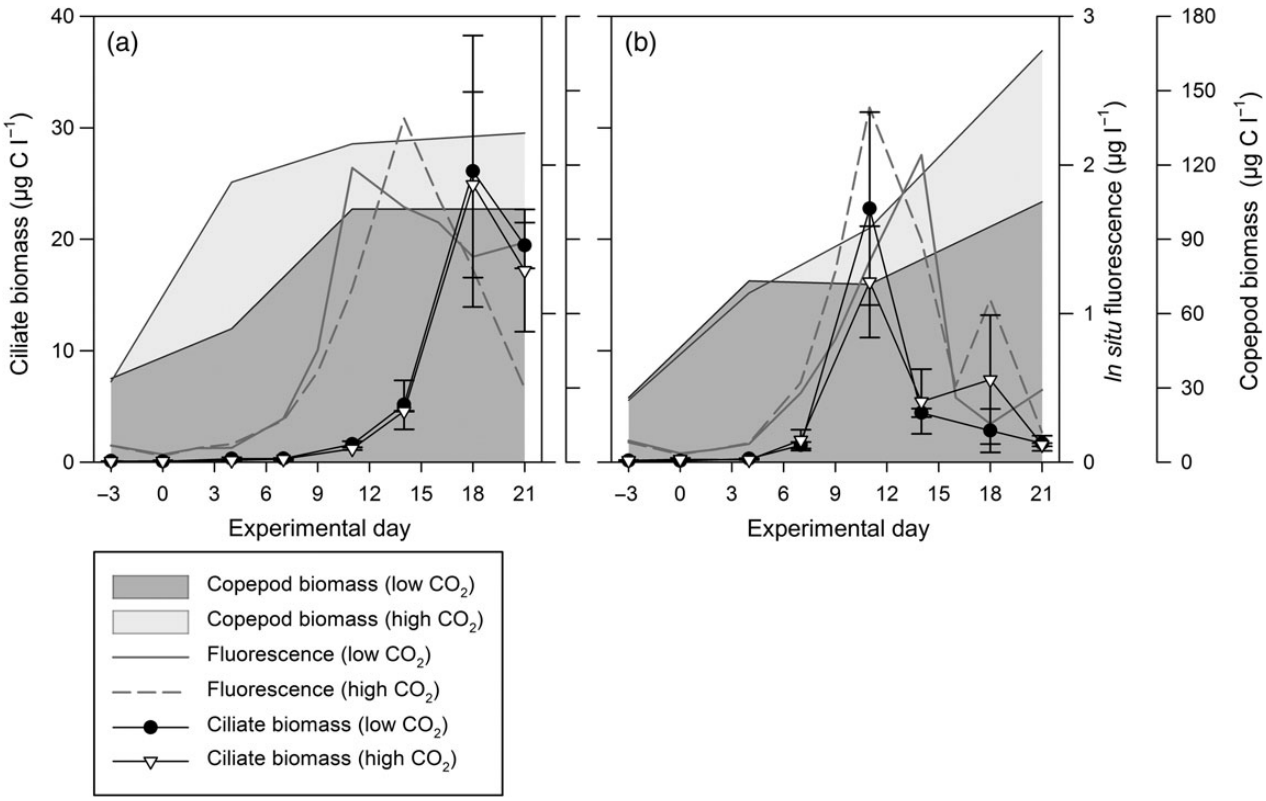

Figure 2. Ciliate biomass (mean ± SD) in µg C l^{-1} at low (filled symbols) and high CO_2 levels (open symbols) and total copepod biomass (adult copepods and copepodites) in µg C l^{-1} at low (dark grey fields) and high CO_2 levels (light grey fields) as well as *in situ* fluorescence (µg l^{-1}) at low (grey lines) and high CO_2 levels (dashed grey lines) in the (a) cold and (b) warm treatments over the course of the experiment.

for the ciliate growth rate µ ($p < 0.017$). It was higher in the warm treatments (mean 0.45 ± 0.08 d^{-1}) than in the cold ones (mean 0.31 ± 0.03 d^{-1}). An effect of the interactions of temperature and CO_2 could not be found.

Chlorophyll fluorescence was significantly affected by temperature and the interactions of temperature and time (Table 1). Maximum fluorescence was not different between any of the treatments; however, its timing was marginally affected by temperature ($p < 0.097$), leading to a slightly earlier bloom in the warm mesocosms (Table 3). Total copepod biomass was significantly higher in the high CO_2 treatments, but not affected by temperature or the interaction of both factors (Table 1).

Table 1. Results of the repeated-measures ANOVA for the effects of time, CO_2, temperature, and their interactions on ciliate biomass, total copepod biomass, chlorophyll fluorescence, and ciliate species diversity H' over the duration of the experiment.

Variable	Effect	d.f.	MS	*F*	*p*-values
ln total ciliate biomass ($\mu g\ C\ l^{-1}$)	CO_2	1	0.000	0.000	0.994
	Temperature	1	0.402	1.707	0.233
	CO_2 × temperature	1	0.441	1.870	0.214
	Time	6	33.873	123.448	<0.001***
	Time × CO_2	6	0.307	1.120	0.367
	Time × temperature	6	8.755	31.905	<0.001***
	Time × CO_2 × temperature	6	0.067	0.243	0.960
ln total copepod biomass ($\mu g\ C\ l^{-1}$)	CO_2	1	1.023	5.683	0.044*
	Temperature	1	0.034	0.187	0.677
	CO_2 × temperature	1	0.186	1.031	0.340
	Time	2	0.658	7.038	0.006**
	Time × CO_2	2	0.051	0.544	0.591
	Time × temperature	2	0.274	2.931	0.082
	Time × CO_2 × temperature	2	0.155	1.660	0.221
ln fluorescence ($\mu g\ l^{-1}$)	CO_2	1	0.116	0.278	0.614
	Temperature	1	2.764	6.653	0.037*
	CO_2 × temperature	1	1.167	2.808	0.138
	Time	9	15.569	58.539	<0.001***
	Time × CO_2	9	0.190	0.716	0.692
	Time × temperature	9	0.893	3.359	0.002**
	Time × CO_2 × temperature	9	0.242	0.909	0.523
Species diversity H'	CO_2	1	0.010	0.425	0.535
	Temperature	1	0.799	34.436	<0.001***
	CO_2 × temperature	1	0.024	1.055	0.339
	Time	6	0.319	5.240	<0.001***
	Time × CO_2	6	0.082	1.352	0.256
	Time × temperature	6	0.190	3.113	0.013*
	Time × CO_2 × temperature	6	0.092	1.516	0.197

Significant results are marked by $*p < 0.05$, $**p < 0.01$, and $***p < 0.001$.

Table 2. Ciliate biomass maximum values (max.), bloom timing D_{max}, and ciliate growth rate μ for all treatments.

Temperature (°C)	CO_2 (ppm)	Biomass max. ($\mu g\ C\ l^{-1}$)	D_{max} (d)	μ (d^{-1})
15°C	439	34.52	11	0.55
	439	19.78	11	0.44
	439	13.95	11	0.46
	1040	20.93	11	0.53
	1040	9.27	11	0.30
	1040	18.33	11	0.41
9°C	439	21.49	21	0.29
	439	38.27	18	0.29
	1040	28.47	18	0.29
	1040	23.82	21	0.30
	1040	32.82	18	0.38

Species composition

Ciliate species diversity H' was significantly higher in the warm treatments, but not affected by CO_2 or the interactions of both factors (Table 1). The taxonomic composition of ciliates over the course of the experiment is given in Figure 3. Although present at very low initial densities, the small oligotrich *Strobilidium* sp. rapidly increased in density in all treatments and contributed up to 80% of the total ciliate community at D_{max} (day 11 for the warm mesocosms and day 18 for the cold ones) irrespective of the temperature or CO_2 level. While the growth rate of *Strobilidium* sp. was not significantly different in any of the treatments, the timing of the peak was significantly earlier in the warm treatments independent of the CO_2 level (Table 3). The biomass maximum of *Strobilidium* sp. was marginally affected by temperature ($p < 0.075$). In the warm treatments, they declined after the peak to almost initial levels which was not the case in the cold ones where they still made up >50% of the biomass on day 21.

The opposite trend was observed for the cyclotrich *Myrionecta rubrum* which made up the main proportion (40–80%) of the biomass in the cold treatments until day 7, followed by a rapid decline thereafter until day 21. In the warm mesocosms, density increased again after D_{max}. The hypotrich *Euplotes* sp. was present in all mesocosms but more abundant in the warm ones, especially towards the end of the experiment. A significant effect of the manipulated factors on the biomass maxima of *M. rubrum* and *Euplotes* sp. was not found (data not shown). There was also no clear trend for the succession of *Strombidium* sp. (Oligotrichids), *Balanion comatum* (Prorodontids), *Lohmaniella oviformis* (Choreotrichids), and thecate tintinnids which were found in small numbers only. However, *B. comatum* and *L. oviformis* were absent from the warm treatments after day 14. An increase in tintinnids was only observed in the cold treatments for the last day. Owing to a high variability between mesocosms, no significant effect on the biomass maxima of different taxa over time in response to warming or high CO_2 could be observed.

At the beginning of the experiment, some dinoflagellates were observed in the mesocosms: *Ceratium* sp. was present in all mesocosms until day 7 and *Prorocentrum micans* was present at very small numbers in some of the treatments. Since these species are considered as mainly autotroph (*Ceratium* sp.) or mixotroph (*P. micans*), they were not included in the analyses and are presented by Sommer *et al.* (2015) instead.

Table 3. Results of the two-way ANOVA for the effects of temperature, CO_2, and their interactions on total ciliate biomass, *Strobilidium* sp. biomass, and chlorophyll fluorescence regarding maximum (max.), bloom timing D_{max}, and growth rate μ.

Response variable	Factor	d.f.	MS	*F*	*p*-values
Biomass max. total ciliates (μg C l^{-1})	CO_2	1	43.568	0.634	0.452
	Temperature	1	248.998	3.623	0.099
	CO_2 × temperature	1	17.091	0.249	0.633
Biomass max. *Strobilidium* sp. (μg C l^{-1})	CO_2	1	0.146	1.145	0.320
	Temperature	1	0.553	4.350	0.075
	CO_2 × temperature	1	0.149	1.173	0.315
Fluorescence max. (μg l^{-1})	CO_2	1	0.079	0.214	0.658
	Temperature	1	0.173	0.472	0.514
	CO_2 × temperature	1	0.362	0.987	0.354
ln D_{max} total (d)	CO_2	1	0.001	0.110	0.749
	Temperature	1	0.826	208.680	<0.001**
	CO_2 × temperature	1	0.001	0.110	0.749
ln D_{max} *Strobilidium* sp. (d)	CO_2	1	0.001	0.110	0.075
	Temperature	1	0.826	208.680	<0.001**
	CO_2 × temperature	1	0.001	0.110	0.075
ln D_{max} fluorescence (d)	CO_2	1	0.001	0.015	0.907
	Temperature	1	0.141	3.663	0.097
	CO_2 × temperature	1	0.057	1.481	0.263
ln μ total ciliates (d^{-1})	CO_2	1	0.001	0.164	0.697
	Temperature	1	0.052	9.784	0.017*
	CO_2 × temperature	1	0.007	1.287	0.294
ln μ *Strobilidium* sp. (d^{-1})	CO_2	1	0.160	1.229	0.304
	Temperature	1	0.110	0.848	0.388
	CO_2 × temperature	1	0.126	0.965	0.359

Significant results are marked by *$p < 0.05$, and **$p < 0.001$.

Discussion

Although mesocosm approaches show some limitations when mimicking natural conditions such as diurnal variations in abiotic conditions (e.g. light and temperature) or vertical migration of zooplankton, mesocosms are a useful tool to simulate changes in abiotic conditions (e.g. warming and OA) and investigate their effects on plankton communities under near-natural conditions. While biases in species composition and foodweb complexity cannot be ruled out, the given experimental setup allowed the combined manipulation of temperature and CO_2, thus enabling an analysis on short-term reactions of a near-natural plankton community to future ocean conditions.

This indoor mesocosm facility has already been successfully used during a series of previous experiments investigating the effects of ocean warming on Baltic Sea plankton communities (Sommer *et al.*, 2007; Lewandowska and Sommer, 2010; Sommer and Lewandowska, 2011). As shown by Sommer *et al.* (2007), the mesocosms allowed the simulation of *in situ* species composition and plankton succession. Furthermore, the mechanical conditions did not have an adverse impact on the biota.

Effects of warming

Autotrophic protists are relatively temperature insensitive as long as their photosynthesis is light-limited (Tilzer *et al.*, 1986). In contrast, heterotrophic MZP responds to temperature, and a relationship between an increase in production and an increase in temperature has often been observed (Weisse and Montagnes, 1998; Montagnes and Lessard, 1999; Rose and Caron, 2007). The different reactions of heterotrophs and autotrophs to warming are based on the basic difference in the former being temperature-dependent due to the biochemical processes of their metabolism and the latter being in large parts light-dependent due to photosynthesis (Bernacchi *et al.*, 2001). The response of autotrophs and heterotrophs to warming is therefore unbalanced and thus will create shifts in interactions (McGowan *et al.*, 2003; Smol *et al.*, 2005).

In our study, we found a reduced time-lag between the phytoplankton bloom and the MZP biomass maximum. High temperatures resulted in a significantly higher MZP growth rate and an earlier bloom followed by a subsequent decline, an observation supporting hypothesis (i) which is in line with findings from previous studies (Aberle *et al.*, 2007, 2012; O'Connor *et al.*, 2009). Additionally, phytoplankton cell size decreased with warming thus providing better food for ciliates (Sommer *et al.*, 2015), an effect also indicated by previous studies (Aberle *et al.*, 2015). Overall, only a weak indication for taxonomic shifts in phytoplankton was found during the present mesocosms study (Sommer *et al.*, 2015) while we observed a higher diversity for MZP communities in the warm treatments.

The reduced carrying capacity of phytoplankton (Table 1), in relation to warming observed in our experiment as well as in other Baltic Sea experiments (Lewandowska and Sommer, 2010; Sommer *et al.*, 2012; Suikkanen *et al.*, 2013) and in the North Atlantic (Rose *et al.*, 2009), led to an overall decrease in MZP biomass in the warm treatments, confirming hypothesis (i). In fact, Lewandowska *et al.* (2014) pointed out that a potential positive reaction of phytoplankton to warming is likely to occur, but would be masked by grazing pressure from MZP. This might have happened in our experiment as MZP followed the phytoplankton increase in the warm treatments almost instantaneously, pointing towards a strengthened coupling between phytoplankton and MZP based on warming, a finding which is in line with observations by Aberle *et al.* (2015).

A stronger top-down effect caused by warming has been reported in previous studies, which was explained by the temperature insensitivity of photosynthesis in combination with the temperature-stimulated

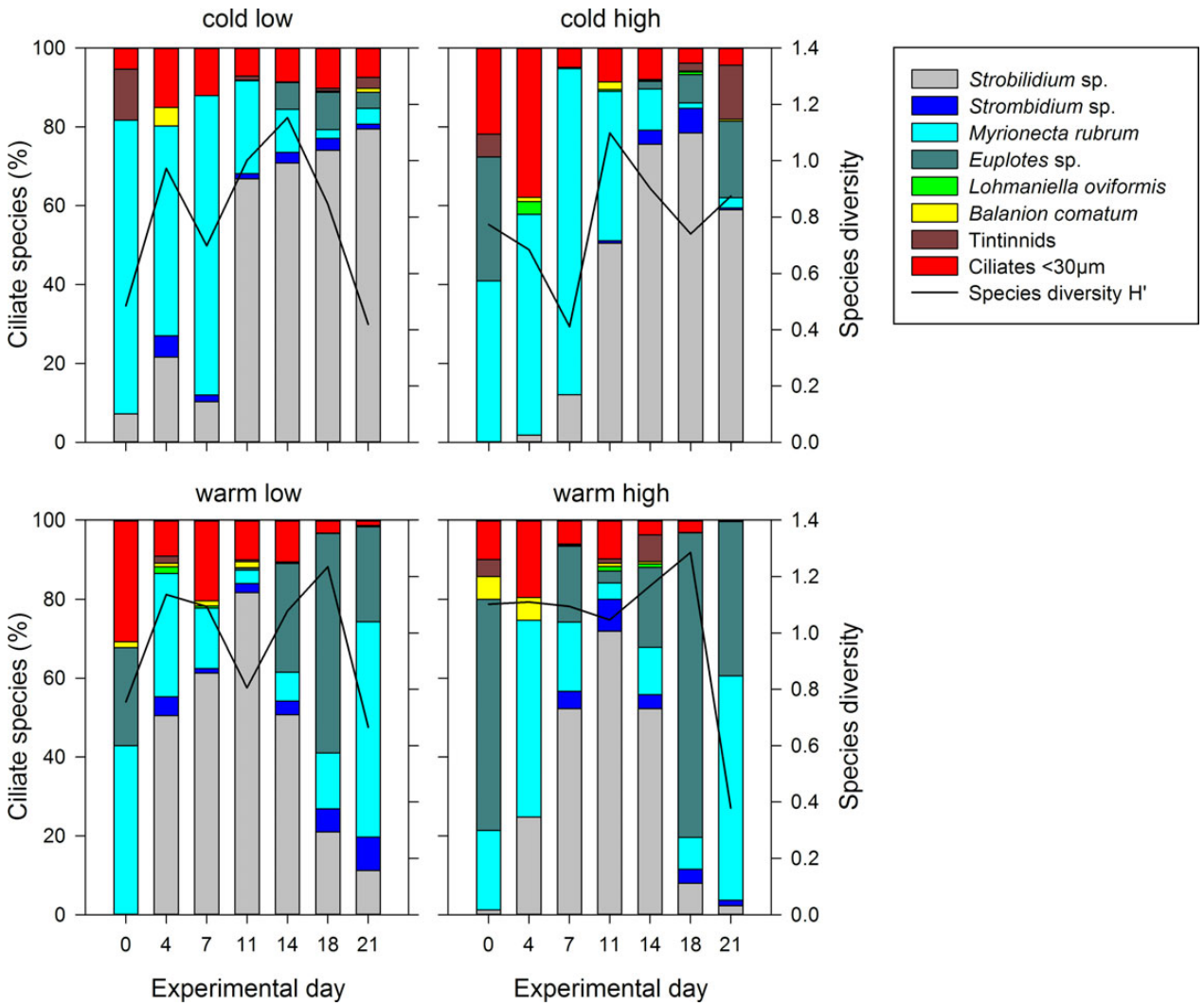

Figure 3. Relative ciliate species composition and species diversity index (*H'*; black lines) over the time of the experiment for the two temperature (warm and cold) and CO_2 treatments (low and high).

MZP biomass increase (O'Connor *et al.*, 2009; Sommer and Lewandowska, 2011). Similarly, it has been shown for North Sea plankton communities that intense grazing by zooplankton caused by warm autumn or winter temperatures could lead to a depression and delay of the spring bloom in the subsequent year (Wiltshire and Manly, 2004). The more intense grazing seems to be primarily caused by warming, not zooplankton densities (Wiltshire *et al.*, 2008). An intensified grazing by copepods on MZP caused by warming could be an explanation for the overall low MZP densities we found in our study. It seems likely that a high copepod predation in our mesocosms resulted in a strong suppression of ciliates as MZP is considered as a preferred food item for copepods (Löder *et al.*, 2011).

Effects of pCO_2

An increase in pCO_2 resulting in a decrease in pH could directly affect the physiology of both autotrophic and heterotrophic protists and lead to e.g. changes in intracellular pH, membrane potentials, and enzyme activities (Nielsen *et al.*, 2010). There are indications for a pH sensitivity of MZP from a variety of ecosystems like the Baltic Sea (Pedersen and Hansen, 2003) and the North Atlantic, Rhode Island, USA (Hinga, 1992). However, as Hinga (2002) pointed out, it largely depends on the inherent pH tolerance of a plankton species if it can grow at a broad or a narrow range of pH values. Unusually, high or low pH values often occurring in coastal systems can favour the selection towards the growth of species adapted to a wide range of pH values.

While there is evidence from other experimental studies showing that high pCO_2 negatively affected heterotrophic ciliates in terms of biomass and growth (Calbet *et al.*, 2014, western Norway) or even inhibited growth (Nielsen *et al.* 2010, Baltic Sea), we observed the opposite. In our experiment with its comparatively moderate CO_2 elevation of effectively 1040 ppm, we showed that the present coastal MZP community was tolerant against the effects of CO_2. This might be related to a high pH tolerance of the Baltic Sea coastal plankton community in the Kiel Fjord to habitat pCO_2 fluctuations (Melzner *et al.*, 2013). Generally, the Kiel Fjord is characterized by a low buffering capacity due to its low salinity (Rossoll *et al.*, 2013) and a stratification with a bottom layer of CO_2-rich water originating in the heterotrophic degradation of organic material (Melzner *et al.*, 2013). Upwelling of CO_2-rich deep water masses, especially during summer and autumn, leads to acidification of

the surface waters (Hansen *et al.*, 1999), an effect which is also found on the west coast of the United States and which is predicted to worsen in the future with additional anthropogenic CO_2 input (Feely *et al.*, 2008, 2010).

A similarly high tolerance was found in mesocosm studies using coastal plankton communities in the Arctic, Svalbard (Aberle *et al.*, 2013), off Bergen, Norway (Suffrian *et al.*, 2008) and another study from Kiel Fjord (Rossoll *et al.*, 2013). While food availability and phytoplankton composition were affected by the different pCO_2 treatments, the authors observed no or only very subtle indirect effects of OA on the MZP community composition and biomass maxima. While, in our study, indeed no direct effects on MZP species composition were found, there were also no indirect effects despite there being a changed phytoplankton community. Thus, hypothesis (ii) was not confirmed.

Furthermore, we hypothesized that an elevated pCO_2 might result in a higher carrying capacity of phytoplankton, thus leading to increases in MZP biomass (hypothesis iii). In the literature, there is some evidence that such indirect effects are induced by an increase in pCO_2, mainly due to changes in phytoplankton availability (Suffrian *et al.*, 2008; Rose *et al.*, 2009; Calbet *et al.*, 2014). Concerning phytoplankton, direct effects from an elevated pCO_2 concentration include an increased photosynthetic rate at high CO_2 levels due to an increased availability of CO_2 and HCO_3^- (Burkhardt *et al.*, 2001; Rost *et al.*, 2008), changes in stoichiometry affecting phytoplankton food quality (Burkhardt *et al.*, 1999; Schoo *et al.*, 2013), and inhibition of the development for calcifying algae (Riebesell *et al.*, 2000b; Orr *et al.*, 2005; Iglesias-Rodriguez *et al.*, 2008). In our study, an increased phytoplankton biomass at high pCO_2 was observed at high temperatures only (Sommer *et al.*, 2015). Consequently, a general increase in MZP biomass due to higher phytoplankton biomass at high pCO_2 could not be confirmed and hypothesis (iii) was rejected. Nonetheless, copepod densities were higher in the high pCO_2 treatment, thus the increased grazing pressure on MZP and, to a smaller part, on phytoplankton could have masked changes in the carrying capacity resulting from enhanced copepod predation.

Additionally, no change in elemental ratios of phytoplankton and only weak changes in species composition due to a high pCO_2 were found; all of which can be attributed to the high tolerance of the phytoplankton community to a high pCO_2 (Paul *et al.*, 2015; Sommer *et al.*, 2015). However, one effect reported from the present mesocosm study is an increased cell size of phytoplankton at high pCO_2, turning them into less preferred food items for ciliates (Sommer *et al.*, 2015).

In the close-to-natural high pCO_2 scenario, we chose for the experiment with a value of 1040 ppm we observed a strong tolerance of the Kiel Fjord MZP community. Nevertheless, with the already strong fluctuations of pCO_2 today, it could happen that the values in terms of acidification will be even higher than what is currently predicted as a worst case scenario (Caldeira and Wickett, 2003). In this case, a direct effect on MZP could be expected as some species do react to extreme pH values as shown by Pedersen and Hansen (2003). Furthermore, additional factors, such as light regime, hypoxia, and eutrophication, have been identified to affect plankton communities (Lewandowska and Sommer, 2010; Melzner *et al.*, 2013; Suikkanen *et al.*, 2013). However, whether these factors act antagonistically or synergistically remains still unclear. Also, long-term adaptations of organisms are a factor that needs further investigation as they can result in adaptation of previously OA-sensitive plankton species (Lohbeck *et al.*, 2012).

Combination of the effects of warming and pCO_2

While there is an increasing number of studies available addressing the impacts of either ocean warming or OA, multiple-stressor approaches are rare, despite the importance of finding synergistic or antagonistic effects of these two stressors (Pörtner, 2008; Rost *et al.*, 2008; Calbet *et al.*, 2014). So far, there are few multiple-stressor studies dealing with the effects of warming and high CO_2 in combination with, for example, a focus on copepods (Mayor *et al.*, 2012), bacterioplankton (Lindh *et al.*, 2013), phytoplankton (Hare *et al.*, 2007; Feng *et al.*, 2009; Kim *et al.*, 2011, 2013), and MZP (Rose *et al.*, 2009; Calbet *et al.*, 2014).

Calbet *et al.* (2014) found negative effects of OA on the ciliate biomass maximum indirectly caused by stoichiometric changes in phytoplankton quality in a near-natural, large-scale mesocosm experiment in a Norwegian fjord. In contrast, the authors found that warming and acidification in concert did not affect the MZP biomass maximum, but led to a shift towards a more autotrophic foodweb based on the ratio of autotrophic to heterotrophic biomass. For an oligotrophic plankton community from the Mediterranean Sea, no effects of a multiple-stressor treatment on heterotrophic prokaryotes were reported (Maugendre *et al.*, 2015). In contrast, Rose *et al.* (2009) observed a significantly higher MZP abundance in a multiple-stressor treatment during a spring bloom experiment in the oligotrophic North Atlantic, although overall, the temperature effect was stronger. The study by Rose *et al.* (2009) was conducted in an open sea situation; however, where the seawater pCO_2 is close to the atmospheric values. Generally, the aforementioned studies point towards the importance of indirect effects of elevated pCO_2 on MZP and showed that the effects differ depending on the marine province.

Our experiment did not result in any significant interaction effects of high pCO_2 and warming as far as MZP growth rate, total biomass, and D_{max} are concerned thus supporting hypothesis (iv). We observed no effects of high pCO_2 on MZP biomass or growth, not even in the cold treatments, where a masking of possible CO_2 effects on MZP biomass and growth due to the pronounced reaction to warming could be excluded. This also supports previous findings that indirect effects of high pCO_2 observed for simple "one phytoplankton species—one consumer species" treatments can be compensated at the ecosystem level by species richness and trophic interactions (Rossoll *et al.*, 2013). Furthermore, it emphasizes the importance of using a near-natural plankton community instead of single-species systems that cannot provide enough information about indirect effects of high CO_2 and warming between trophic levels (Riebesell *et al.*, 2008; Maugendre *et al.*, 2015).

Implications for the foodweb

While warming was found to lower the biomass, increase the growth rates, lead to an earlier bloom and a higher diversity of MZP, an elevated CO_2 level did not affect any of the measured parameters. Phytoplankton stoichiometry was also not affected by CO_2 while biomass decreased and growth rates increased with warming (Paul *et al.*, 2015). Additionally, phytoplankton cell size increased at high pCO_2 (Sommer *et al.*, 2015).

However, our study also included copepods as mesograzers. Ciliates are ideal food items for copepods due to their ideal size compared with phytoplankton cells which are often either too small or too large (Frost, 1972). They make up 30–50% of the copepods daily diet depending on the phytoplankton concentration (Calbet and Saiz, 2005; Löder *et al.*, 2011). In our case, total copepod biomass was at 29 $\mu g\ C\ l^{-1}$ initially and increasing in all treatments

during the experiment, most notably in the high temperature/high CO_2 treatment. In fact, copepod biomass was significantly higher in the high CO_2 mesocosms, which is in contrast to previous studies where no such effect was found (Rossoll *et al.*, 2012; Cripps *et al.*, 2014). Considering that copepod, MZP, and phytoplankton starting conditions were the same for all mesocosms and no increase in MZP or phytoplankton biomass in the high CO_2 treatments was observed, the question arises: what caused the increase in copepod biomass?

As mentioned before, an increase in MZP usually supports an increase in copepods. This numerical response of copepods to increasing ciliate densities is an effect also described by other authors (Stoecker and Capuzzo, 1990). Generally, the strong top-down control of MZP by copepods could be one of the factors explaining the comparatively low MZP biomass during the experiment. As pointed out by other studies, a high CO_2 level can lead to an increase in phytoplankton biomass (Rost *et al.*, 2008; Havenhand, 2012; Low-Decarie *et al.*, 2014), which in turn has the potential to cause an increase in MZP biomass. It seems plausible that, in our experiment, a positive effect of high CO_2 on phytoplankton and subsequently on MZP was masked by a high copepod grazing pressure on both phytoplankton and MZP. This is in line with observations by Lewandowska *et al.* (2014) in a single-stressor mesocosm experiment, showing comparable impacts of copepod abundance and thus grazing being enhanced by warming.

Our results indicate that high temperatures favour a top-down control of plankton communities, whereas a high CO_2 seems to promote bottom-up controlled mechanisms. However, the near-natural mesocosms we used were complex systems and did not allow us to prove these conclusions. MZP grazing experiments would have been a valuable addition to disentangle the effects of the multiple stressors on the different community levels, but unfortunately we were unable to conduct additional grazing experiments.

Conclusions

Overall, the present study shows that productive coastal ecosystems like the Kiel Fjord and especially MZP communities are not expected to be directly affected by a high pCO_2 in the future. This is most likely related to a high tolerance of MZP species to average pCO_2 levels of 700 ppm (Thomsen *et al.*, 2010). In fact, most ecologically important groups in the Baltic Sea foodweb seem to be rather tolerant to acidification (Havenhand, 2012). Additionally, there was no indication of changes in phytoplankton food quality in terms of stoichiometry due to high CO_2 [see Paul *et al.* (2015) for details] that could indirectly affect MZP or higher trophic levels during our short-term experiment. Indirect positive effects resulting from increases in phytoplankton biomass can be expected. However, it seems that such effects might be masked by increased grazing pressure from mesozooplankton. Finally, our results indicate that global warming affects MZP plankton communities in terms of higher total biomass, increased growth rates, and earlier autumn bloom timing. This could, in turn, lead to changes in trophic dynamics due to a tighter coupling of phytoplankton and MZP, in particular, the phytoplankton-ciliate link, which is likely to enhance energy transfer efficiency to higher trophic levels (Aberle *et al.*, 2015).

Acknowledgements

This study was part of the BMBF funded "Verbundprojekt" BIOACID phase II (Biological Impacts of Ocean ACIDification), consortium 1, WP 1.6 (03F0655B). We thank all members of the BIOACID indoor mesocosm group for their cooperation and their help with sampling. C. Paul is acknowledged for information about phytoplankton development. T. Hansen, C. Meyer, and B. Gardeler are additionally acknowledged for technical and analytical support. We also thank two anonymous reviewers for their helpful comments on improving the manuscript.

References

Aberle, N., Bauer, B., Lewandowska, A., Gaedke, U., and Sommer, U. 2012. Warming induces shifts in microzooplankton phenology and reduces time-lags between phytoplankton and protozoan production. Marine Biology, 159: 2441–2453.

Aberle, N., Lengfellner, K., and Sommer, U. 2007. Spring bloom succession, grazing impact and herbivore selectivity of ciliate communities in response to winter warming. Oecologia, 150: 668–681.

Aberle, N., Malzahn, A. M., Lewandowska, A. M., and Sommer, U. 2015. Some like it hot: the protozooplankton-copepod link in a warming ocean. Marine Ecology Progress Series, 519: 103–113.

Aberle, N., Schulz, K. G., Stuhr, A., Malzahn, A. M., Ludwig, A., and Riebesell, U. 2013. High tolerance of microzooplankton to ocean acidification in an Arctic coastal plankton community. Biogeosciences, 10: 1471–1481.

Bernacchi, C. J., Singsaas, E. L., Pimentel, C., Portis, A. R., and Long, S. P. 2001. Improved temperature response functions for models of Rubisco-limited photosynthesis. Plant Cell and Environment, 24: 253–259.

Boyce, D. G., Lewis, M. R., and Worm, B. 2010. Global phytoplankton decline over the past century. Nature, 466: 591–596.

Brock, T. D. 1981. Calculating solar-radiation for ecological-studies. Ecological Modelling, 14: 1–19.

Burkhardt, S., Amoroso, G., Riebesell, U., and Sultemeyer, D. 2001. CO_2 and HCO_3^- uptake in marine diatoms acclimated to different CO_2 concentrations. Limnology and Oceanography, 46: 1378–1391.

Burkhardt, S., Zondervan, I., and Riebesell, U. 1999. Effect of CO_2 concentration on C:N:P ratio in marine phytoplankton: a species comparison. Limnology and Oceanography, 44: 683–690.

Calbet, A., and Landry, M. R. 2004. Phytoplankton growth, microzooplankton grazing, and carbon cycling in marine systems. Limnology and Oceanography, 49: 51–57.

Calbet, A., and Saiz, E. 2005. The ciliate-copepod link in marine ecosystems. Aquatic Microbial Ecology, 38: 157–167.

Calbet, A., Sazhin, A. F., Nejstgaard, J. C., Berger, S. A., Tait, Z. S., Olmos, L., Sousoni, D., *et al.* 2014. Future climate scenarios for a coastal productive planktonic food web resulting in microplankton phenology changes and decreased trophic transfer efficiency. PLoS ONE, 9: e94388.

Calbet, A., Trepat, I., Almeda, R., Salo, V., Saiz, E., Movilla, J. I., Alcaraz, M., *et al.* 2008. Impact of micro- and nanograzers on phytoplankton assessed by standard and size-fractionated dilution grazing experiments. Aquatic Microbial Ecology, 50: 145–156.

Caldeira, K., and Wickett, M. E. 2003. Anthropogenic carbon and ocean pH. Nature, 425: 365.

Carey, P. G. 1992. Marine interstitial ciliates: An illustrated key. Chapman & Hall, London, New York.

Caron, D. A., and Hutchins, D. A. 2012. The effects of changing climate on microzooplankton grazing and community structure: Drivers, predictions and knowledge gaps. Journal of Plankton Research, 35: 235–252.

Ciais, P., Sabine, C., Bala, G., Bopp, L., Brovkin, V., Canadell, J., Chhabra, A., *et al.* 2013. Carbon and other biogeochemical cycles. In Climate Change 2013: The Physical Science Basis. Contribution of Working Group I to the Fifth Assessment Report of the Intergovernmental Panel on Climate Change. Ed. by T. F. Stocker, D. Qin, G.-K. Plattner, M. Tignor, S. K. Allen, J. Boschung, A. Nauels, Y. Xia, V. Bex, and P. M. Midgley. Cambridge University Press, New York, Cambridge, NY, UK, USA. 1552 pp.

Collins, M., Knutti, R., Arblaster, J., Dufresne, J.-L., Fichefet, T., Friedlingstein, P., Gao, X., *et al.* 2013. Long-term climate change: Projections, commitments and irreversibility. In Climate Change 2013: The Physical Science Basis. Contribution of Working Group I to the Fifth Assessment Report of the Intergovernmental Panel on Climate Change. Ed. by T. F. Stocker, D. Qin, G.-K. Plattner, M. Tignor, S. K. Allen, J. Boschung, A. Nauels, Y. Xia, V. Bex, and P. M. Midgley. Cambridge University Press, New York, Cambridge, NY, UK, USA. 1552 pp.

Cripps, G., Lindeque, P., and Flynn, K. J. 2014. Have we been underestimating the effects of ocean acidification in zooplankton? Global Change Biology, 20: 3377–3385.

Feely, R. A., Alin, S. R., Newton, J., Sabine, C. L., Warner, M., Devol, A., Krembs, C., *et al.* 2010. The combined effects of ocean acidification, mixing, and respiration on pH and carbonate saturation in an urbanized estuary. Estuarine Coastal and Shelf Science, 88: 442–449.

Feely, R. A., Sabine, C. L., Hernandez-Ayon, J. M., Ianson, D., and Hales, B. 2008. Evidence for upwelling of corrosive "acidified" water onto the continental shelf. Science, 320: 1490–1492.

Feng, Y. Y., Hare, C. E., Leblanc, K., Rose, J. M., Zhang, Y. H., DiTullio, G. R., Lee, P. A., *et al.* 2009. Effects of increased pCO(2) and temperature on the North Atlantic spring bloom. I. The phytoplankton community and biogeochemical response. Marine Ecology Progress Series, 388: 13–25.

Frost, B. W. 1972. Effects of size and concentration of food particles on feeding behavior of marine planktonic copepod Calanus pacificus. Limnology and Oceanography, 17: 805–815.

Garzke, J., Ismar, S. M. H., and Sommer, U. 2015. Climate change affects low trophic level marine consumers: Warming decreases copepod size and abundance. Oecologia, 177: 849–860.

Hansen, H. P., Giesenhagen, H. C., and Behrends, G. 1999. Seasonal and long-term control of bottom-water oxygen deficiency in a stratified shallow-water coastal system. ICES Journal of Marine Science, 56: 65–71.

Hare, C. E., Leblanc, K., DiTullio, G. R., Kudela, R. M., Zhang, Y., Lee, P. A., Riseman, S., *et al.* 2007. Consequences of increased temperature and CO_2 for phytoplankton community structure in the Bering Sea. Marine Ecology Progress Series, 352: 9–16.

Havenhand, J. N. 2012. How will ocean acidification affect Baltic Sea ecosystems? An assessment of plausible impacts on key functional groups. Ambio, 41: 637–644.

Hillebrand, H., Durselen, C. D., Kirschtel, D., Pollingher, U., and Zohary, T. 1999. Biovolume calculation for pelagic and benthic microalgae. Journal of Phycology, 35: 403–424.

Hinga, K. R. 1992. Co-occurrence of dinoflagellate blooms and high pH in marine enclosures. Marine Ecology Progress Series, 86: 181–187.

Hinga, K. R. 2002. Effects of pH on coastal marine phytoplankton. Marine Ecology Progress Series, 238: 281–300.

Hoegh-Guldberg, O., and Bruno, J. F. 2010. The impact of climate change on the World's Marine Ecosystems. Science, 328: 1523–1528.

Iglesias-Rodriguez, M. D., Halloran, P. R., Rickaby, R. E. M., Hall, I. R., Colmenero-Hidalgo, E., Gittins, J. R., Green, D. R. H., *et al.* 2008. Phytoplankton calcification in a high-CO_2 world. Science, 320: 336–340.

Javidpour, J., Molinero, J. C., Peschutter, J., and Sommer, U. 2009. Seasonal changes and population dynamics of the ctenophore *Mnemiopsis leidyi* after its first year of invasion in the Kiel Fjord, Western Baltic Sea. Biological Invasions, 11: 873–882.

Joint, I., Doney, S. C., and Karl, D. M. 2011. Will ocean acidification affect marine microbes? ISME Journal, 5: 1–7.

Kim, J. H., Kim, K. Y., Kang, E. J., Lee, K., Kim, J. M., Park, K. T., Shin, K., *et al.* 2013. Enhancement of photosynthetic carbon assimilation efficiency by phytoplankton in the future coastal ocean. Biogeosciences, 10: 7525–7535.

Kim, J. M., Lee, K., Shin, K., Kang, J. H., Lee, H. W., Kim, M., Jang, P. G., *et al.* 2006. The effect of seawater CO_2 concentration on growth of a natural phytoplankton assemblage in a controlled mesocosm experiment. Limnology and Oceanography, 51: 1629–1636.

Kim, J. M., Lee, K., Shin, K., Yang, E. J., Engel, A., Karl, D. M., and Kim, H. C. 2011. Shifts in biogenic carbon flow from particulate to dissolved forms under high carbon dioxide and warm ocean conditions. Geophysical Research Letters, 38: 5.

Kraberg, A. C., Baumann, M., and Dürselen, C-D. 2010. Coastal Phytoplankton: Photo Guide for Northern European Seas. Pfeil, Munich, Germany. 204 pp.

Kroeker, K. J., Kordas, R. L., Crim, R., Hendriks, I. E., Ramajo, L., Singh, G. S., Duarte, C. M., *et al.* 2013. Impacts of ocean acidification on marine organisms: Quantifying sensitivities and interaction with warming. Global Change Biology, 19: 1884–1896.

Le Quéré, C., Andres, R. J., Boden, T., Conway, T., Houghton, R. A., House, J. I., Marland, G., *et al.* 2013. The global carbon budget 1959–2011. Earth System Science Data, 5: 165–185.

Lengfellner, K. 2008. The Impact of Climate Warming on Plankton Spring Succession: A Mesocosm Study. Christian Albrecht University of Kiel, Kiel, Germany. p. 131.

Lewandowska, A., and Sommer, U. 2010. Climate change and the spring bloom: A mesocosm study on the influence of light and temperature on phytoplankton and mesozooplankton. Marine Ecology Progress Series, 405: 101–111.

Lewandowska, A. M., Boyce, D. G., Hofmann, M., Matthiessen, B., Sommer, U., and Worm, B. 2014. Effects of sea surface warming on marine plankton. Ecology Letters, 17: 614–623.

Lindh, M. V., Riemann, L., Baltar, F., Romero-Oliva, C., Salomon, P. S., Graneli, E., and Pinhassi, J. 2013. Consequences of increased temperature and acidification on bacterioplankton community composition during a mesocosm spring bloom in the Baltic Sea. Environmental Microbiology Reports, 5: 252–262.

Löder, M. G. J., Meunier, C., Wiltshire, K. H., Boersma, M., and Aberle, N. 2011. The role of ciliates, heterotrophic dinoflagellates and copepods in structuring spring plankton communities at Helgoland Roads, North Sea. Marine Biology, 158: 1551–1580.

Lohbeck, K. T., Riebesell, U., and Reusch, T. B. H. 2012. Adaptive evolution of a key phytoplankton species to ocean acidification. Nature Geoscience, 5: 346–351.

Low-Decarie, E., Fussmann, G. F., and Bell, G. 2014. Aquatic primary production in a high-CO_2 world. Trends in Ecology and Evolution, 29: 223–232.

Malzahn, A. M., Hantzsche, F., Schoo, K. L., Boersma, M., and Aberle, N. 2010. Differential effects of nutrient-limited primary production on primary, secondary or tertiary consumers. Oecologia, 162: 35–48.

Maugendre, L., Gattuso, J-P., Louis, J., de Kluijver, A., Marro, S., Soetaert, K., and Gazeau, F. 2015. Effect of ocean warming and acidification on a plankton community in the NW Mediterranean Sea. ICES Journal of Marine Science, 72: 1744–1755.

Mayor, D. J., Everett, N. R., and Cook, K. B. 2012. End of century ocean warming and acidification effects on reproductive success in a temperate marine copepod. Journal of Plankton Research, 34: 258–262.

Mayor, D. J., Matthews, C., Cook, K., Zuur, A. F., and Hay, S. 2007. CO_2-induced acidification affects hatching success in *Calanus finmarchicus*. Marine Ecology Progress Series, 350: 91–97.

McGowan, J. A., Bograd, S. J., Lynn, R. J., and Miller, A. J. 2003. The biological response to the 1977 regime shift in the California Current. Deep Sea Research Part II: Topical Studies in Oceanography, 50: 2567–2582.

Melzner, F., Thomsen, J., Koeve, W., Oschlies, A., Gutowska, M. A., Bange, H. W., Hansen, H. P., *et al.* 2013. Future ocean acidification will be amplified by hypoxia in coastal habitats. Marine Biology, 160: 1875–1888.

Montagnes, D. J. S., and Lessard, E. J. 1999. Population dynamics of the marine planktonic ciliate *Strombidinopsis multiauris*: Its potential to control phytoplankton blooms. Aquatic Microbial Ecology, 20: 167–181.

Montagnes, D. J. S., Strüder-Kype, M. C., Kype, M. R., Agatha, S., and Warwick, J. 2001. The Planktonic Ciliate Project: The user-friendly guide to coastal planktonic ciliates. http://www.zooplankton.cn/ciliate/intro.htm (last accessed 1 April 2014).

Nielsen, L. T., Jakobsen, H. H., and Hansen, P. J. 2010. High resilience of two coastal plankton communities to twenty-first century seawater acidification: Evidence from microcosm studies. Marine Biology Research, 6: 542–555.

O'Connor, M. I., Piehler, M. F., Leech, D. M., Anton, A., and Bruno, J. F. 2009. Warming and resource availability shift food web structure and metabolism. PLos Biology, 7: 6.

Orr, J. C., Fabry, V. J., Aumont, O., Bopp, L., Doney, S. C., Feely, R. A., Gnanadesikan, A., *et al.* 2005. Anthropogenic ocean acidification over the twenty-first century and its impact on calcifying organisms. Nature, 437: 681–686.

Paul, C., Matthiessen, B., and Sommer, U. 2015. Warming, but not enhanced CO_2 concentration, quantitatively and qualitatively affects phytoplankton biomass. Marine Ecology Progress Series, 528: 39–51.

Pedersen, M. F., and Hansen, P. J. 2003. Effects of high pH on a natural marine planktonic community. Marine Ecology Progress Series, 260: 19–31.

Pörtner, H. 2008. Ecosystem effects of ocean acidification in times of ocean warming: A physiologist's view. Marine Ecology Progress Series, 373: 203–217.

Putt, M., and Stoecker, D. K. 1989. An experimentally determined carbon–volume ratio for marine oligotrichous ciliates from estuarine and coastal waters. Limnology and Oceanography, 34: 1097–1103.

Riebesell, U., Bellerby, R. G. J., Grossart, H. P., and Thingstad, F. 2008. Mesocosm CO_2 perturbation studies: From organism to community level. Biogeosciences, 5: 1157–1164.

Riebesell, U., Revill, A. T., Holdsworth, D. G., and Volkman, J. K. 2000a. The effects of varying CO_2 concentration on lipid composition and carbon isotope fractionation in *Emiliania huxleyi*. Geochimica et Cosmochimica Acta, 64: 4179–4192.

Riebesell, U., Zondervan, I., Rost, B., Tortell, P. D., Zeebe, R. E., and Morel, F. M. M. 2000b. Reduced calcification of marine plankton in response to increased atmospheric CO_2. Nature, 407: 364–367.

Riegman, R., Kuipers, B. R., Noordeloos, A. A. M., and Witte, H. J. 1993. Size-differential control of phytoplankton and the structure of plankton communities. Netherlands Journal of Sea Research, 31: 255–265.

Rose, J. M., and Caron, D. A. 2007. Does low temperature constrain the growth rates of heterotrophic protists? Evidence and implications for algal blooms in cold waters. Limnology and Oceanography, 52: 886–895.

Rose, J. M., Feng, Y., Gobler, C. J., Gutierrez, R., Hare, C. E., Leblanc, K., and Hutchins, D. A. 2009. Effects of increased pCO_2 and temperature on the North Atlantic spring bloom. II. Microzooplankton abundance and grazing. Marine Ecology Progress Series, 388: 27–40.

Rossoll, D., Bermudez, R., Hauss, H., Schulz, K. G., Riebesell, U., Sommer, U., and Winder, M. 2012. Ocean acidification-induced food quality deterioration constrains trophic transfer. PLoS ONE, 7: e34737.

Rossoll, D., Sommer, U., and Winder, M. 2013. Community interactions dampen acidification effects in a coastal plankton system. Marine Ecology Progress Series, 486: 37–46.

Rost, B., Zondervan, I., and Wolf-Gladrow, D. 2008. Sensitivity of phytoplankton to future changes in ocean carbonate chemistry: Current knowledge, contradictions and research directions. Marine Ecology Progress Series, 373: 227–237.

Sabine, C. L., Feely, R. A., Gruber, N., Key, R. M., Lee, K., Bullister, J. L., Wanninkhof, R., *et al.* 2004. The oceanic sink for anthropogenic CO_2. Science, 305: 367–371.

Schoo, K. L., Malzahn, A. M., Krause, E., and Boersma, M. 2013. Increased carbon dioxide availability alters phytoplankton stoichiometry and affects carbon cycling and growth of a marine planktonic herbivore. Marine Biology, 160: 2145–2155.

Shannon, C., and Weaver, W. 1963. The Mathematical Theory of Communication. University of Illinois Press, Urbana. 117 pp.

Smol, J. P., Wolfe, A. P., Birks, H. J. B., Douglas, M. S. V., Jones, V. J., Korhola, A., Pienitz, R., *et al.* 2005. Climate-driven regime shifts in the biological communities of arctic lakes. Proceedings of the National Academy of Sciences of the United States of America, 102: 4397–4402.

Sommer, U., Aberle, N., Engel, A., Hansen, T., Lengfellner, K., Sandow, M., Wohlers, J., *et al.* 2007. An indoor mesocosm system to study the effect of climate change on the late winter and spring succession of Baltic Sea phyto- and zooplankton. Oecologia, 150: 655–667.

Sommer, U., Aberle, N., Lengfellner, K., and Lewandowska, A. 2012. The Baltic Sea spring phytoplankton bloom in a changing climate: An experimental approach. Marine Biology, 159: 2479–2490.

Sommer, U., and Lewandowska, A. 2011. Climate change and the phytoplankton spring bloom: Warming and overwintering zooplankton have similar effects on phytoplankton. Global Change Biology, 17: 154–162.

Sommer, U., Paul, C., and Moustaka-Gouni, M. 2015. Warming and ocean acidification effects on phytoplankton-from species shifts to size shifts within species in a mesocosm experiment. PLoS ONE, 10: e0125239.

Stoecker, D. K., and Capuzzo, J. M. 1990. Predation on protozoa: Its importance to zooplankton. Journal of Plankton Research, 12: 891–908.

Suffrian, K., Simonelli, P., Nejstgaard, J. C., Putzeys, S., Carotenuto, Y., and Antia, A. N. 2008. Microzooplankton grazing and phytoplankton growth in marine mesocosms with increased CO_2 levels. Biogeosciences, 5: 1145–1156.

Suikkanen, S., Pulina, S., Engstrom-Ost, J., Lehtiniemi, M., Lehtinen, S., and Brutemark, A. 2013. Climate change and eutrophication induced shifts in Northern summer plankton communities. PLoS ONE, 8: e66475.

Thomsen, J., Gutowska, M. A., Saphorster, J., Heinemann, A., Trubenbach, K., Fietzke, J., Hiebenthal, C., *et al.* 2010. Calcifying invertebrates succeed in a naturally CO_2-rich coastal habitat but are threatened by high levels of future acidification. Biogeosciences, 7: 3879–3891.

Tilzer, M. M., Elbrachter, M., Gieskes, W. W., and Beese, B. 1986. Light-temperature interactions in the control of photosynthesis in Antarctic phytoplankton. Polar Biology, 5: 105–111.

Utermöhl, H. 1958. Zur Vervollkommnung der quantitativen Phytoplankton-Methodik. Mitteilungen der Internationalen Vereinigung für Theoretische und Angewandte Limnologie, 9: 1–38.

Wasmund, N., Gobel, J., and Von Bodungen, B. 2008. 100-years-changes in the phytoplankton community of Kiel Bight (Baltic Sea). Journal of Marine Systems, 73: 300–322.

Weisse, T., and Montagnes, D. J. S. 1998. Effect of temperature on inter- and intraspecific isolates of Urotricha (Prostomatida, Ciliophora). Aquatic Microbial Ecology, 15: 285–291.

Wiltshire, K. H., Malzahn, A. M., Wirtz, K., Greve, W., Janisch, S., Mangelsdorf, P., Manly, B. F. J., *et al.* 2008. Resilience of North Sea phytoplankton spring bloom dynamics: An analysis of long-term data at Helgoland Roads. Limnology and Oceanography, 53: 1294–1302.

Wiltshire, K. H., and Manly, B. F. J. 2004. The warming trend at Helgoland Roads, North Sea: Phytoplankton response. Helgoland Marine Research, 58: 269–273.

Winder, M., Berger, S. A., Lewandowska, A., Aberle, N., Lengfellner, K., Sommer, U., and Diehl, S. 2012. Spring phenological responses of marine and freshwater plankton to changing temperature and light conditions. Marine Biology, 159: 2491–2501.

Handling editor: Stéphane Plourde

ICES Journal of Marine Science

ICES Journal of Marine Science (2016), 73(3), 783–790. doi:10.1093/icesjms/fsv171

Contribution to Special Issue: 'Towards a Broader Perspective on Ocean Acidification Research'

Original Article

Sperm motility and fertilisation success in an acidified and hypoxic environment

Helen Graham[1]*, Samuel P. S. Rastrick[2,3], Helen S. Findlay[4], Matthew G. Bentley[1‡], Stephen Widdicombe[4], Anthony S. Clare[1], and Gary S. Caldwell[1]

[1]*School of Marine Science and Technology, Newcastle University, Ridley Building, Claremont Road, Newcastle upon Tyne, Tyne and Wear NE1 7RU, UK*
[2]*Marine Biology and Ecology Research Centre, University of Plymouth, Davy 618, Drake Circus, Plymouth PL4 8AA, UK*
[3]*Institute of Marine Research, PO Box 1870 Nordness, 5870 Bergen, Norway*
[4]*Plymouth Marine Laboratory, Prospect Place, West Hoe, Plymouth PL1 3DH, UK*

**Corresponding author: Uni Research Environment, Postboks 7810, 5020 Bergen, Norway. e-mail: helen.graham@uni.no*

[‡]*Present Address: Faculty of Science & Technology, Bournemouth University, Talbot Campus, Poole, BH12 5BB.*

Graham, H., Rastrick, S. P. S., Findlay, H. S., Bentley, M. G., Widdicombe, S., Clare, A. S., and Caldwell, G. S. Sperm motility and fertilisation success in an acidified and hypoxic environment. – ICES Journal of Marine Science, 73: 783–790.

Received 14 March 2015; revised 12 August 2015; accepted 6 September 2015; advance access publication 13 October 2015.

The distribution and function of many marine species is largely determined by the effect of abiotic drivers on their reproduction and early development, including those drivers associated with elevated CO_2 and global climate change. A number of studies have therefore investigated the effects of elevated pCO_2 on a range of reproductive parameters, including sperm motility and fertilisation success. To date, most of these studies have not examined the possible synergistic effects of other abiotic drivers, such as the increased frequency of hypoxic events that are also associated with climate change. The present study is therefore novel in assessing the impact that an hypoxic event could have on reproduction in a future high CO_2 ocean. Specifically, this study assesses sperm motility and fertilisation success in the sea urchin *Paracentrotus lividus* exposed to elevated pCO_2 for 6 months. Gametes extracted from these pre-acclimated individuals were subjected to hypoxic conditions simulating an hypoxic event in a future high CO_2 ocean. Sperm swimming speed increased under elevated pCO_2 and decreased under hypoxic conditions resulting in the elevated pCO_2 and hypoxic treatment being approximately equivalent to the control. There was also a combined negative effect of increased pCO_2 and hypoxia on the percentage of motile sperm. There was a significant negative effect of elevated pCO_2 on fertilisation success, and when combined with a simulated hypoxic event there was an even greater effect. This could affect cohort recruitment and in turn reduce the density of this ecologically and economically important ecosystem engineer therefore potentially effecting biodiversity and ecosystem services.

Keywords: climate change, fertilisation success, hypoxia, ocean acidification, oxygen saturation, sperm motility.

Introduction

Global climate change, fuelled by enriched atmospheric carbon inventories, is altering the physicochemical status of the global ocean (Diaz and Rosenberg, 2008; Kroeker *et al.*, 2010; Byrne, 2012). The increasing partial pressure of seawater CO_2 (pCO_2) is driving a decline in seawater pH—a process termed ocean acidification (OA). Seawater pH is predicted to drop by 0.3–0.5 units by 2100 (based on pCO_2 concentrations of 730–1020 μatm, respectively (IPCC, 2013). The combination of rising pCO_2 and increasing sea surface temperature will place an additional burden on marine systems by reducing oxygen solubility (Hofmann and Schellnhuber, 2009). Increased frequencies of ocean hypoxic events, such as may occur via ocean upwelling, are predicted (Pörtner and Langenbuch, 2005; Oschlies *et al.*, 2008; Pörtner, 2008) making it necessary to understand the combined effects of OA and hypoxia on marine species and ecosystems (Reum *et al.*, 2016).

Reproductive processes and early ontogenetic stages of marine animals appear particularly vulnerable to changing seawater properties (Pörtner and Farrell, 2008; Byrne *et al.*, 2010a, b; Cooper *et al.*, 2012). Broadcast spawning, a reproductive strategy common in many marine animals, exposes gametes directly to the seawater environment (Crimaldi, 2012). Spawned gametes have therefore been used

extensively in attempts to describe the potential impacts of OA on reproductive processes (Havenhand and Schlegel, 2009; Byrne *et al.*, 2010a, b; Ericson *et al.*, 2010; Frommel *et al.*, 2010; Morita *et al.*, 2010; Cooper *et al.*, 2012). Hitherto, reductions in seawater pH have been shown in several studies to impact sperm swimming ability by causing changes in internal pH (pH_i) of sperm and affecting motility of the flagellum (Havenhand *et al.*, 2008; Fitzpatrick *et al.*, 2009; Morita *et al.*, 2010; Caldwell *et al.*, 2011). These changes in sperm pH_i affect fertilisation by slowing the fast block to polyspermy through interfering with the Na^+/H^+ exchange and preventing the fertilisation membrane being raised (Reuter *et al.*, 2011; Gonzalez-Bernat *et al.*, 2013). Despite variable results, the consensus is that OA, as a function of climate change, will negatively impact marine biodiversity and ecosystem function via disruption of reproductive processes (Dupont *et al.*, 2010; Byrne, 2012).

Over the past decade, the dissolved oxygen (DO) content of coastal waters has changed dramatically and this has led to widespread occurrences of hypoxia, especially in coastal areas, which have shown an exponential increase of hypoxic events of 5.54% $year^{-1}$ (Diaz and Rosenberg, 1995; Diaz, 2001; Vaquer-Sunyer and Duarte, 2008). Normal DO levels range between 5.0 and 8.0 mg O_2 l^{-1} in coastal waters, while hypoxic conditions are defined as occurring when levels fall $<$2.8 mg O_2 l^{-1} (30% oxygen saturation or less) (Diaz and Rosenberg, 1995). The duration of an hypoxic event can be long term/permanent or short term (incidental or episodic) as investigated in the present study (Middelburg and Levin, 2009). Hypoxia has been shown to negatively affect reproduction and development of marine invertebrates across a range of reproductive endpoints including gonad growth (Siikavuopio *et al.*, 2007), reproduction (Cheung *et al.*, 2008), egg production (Marcus *et al.*, 2004), reproductive output (Spicer and El-Gamal, 1990), and embryonic development (Chan *et al.*, 2008). A recent study by Shin *et al.* (2014) reported that hypoxia, as a single stressor, significantly reduced sperm motility in *Hydroides elegans*, which compromised fertilisation success. There was also a negative effect of hypoxia on embryonic development with an increase in the number of malformed embryos (Shin *et al.*, 2014). As elevated pCO_2 and hypoxia, when applied individually, are reported to have similar negative effects on reproduction, they may be expected to have synergistic or additive effects when applied together. Consequently, we examined the effects of long-term exposure (6 months) of adult sea urchins to elevated pCO_2 before spawning, followed by the exposure of spawned gametes to hypoxia and OA before and during fertilisation. This study was designed to represent the effect of an hypoxic event in a high pCO_2 ocean, and the effects that this may have on sperm motility and fertilisation success of the sea urchin *Paracentrotus lividus*; an ecologically and economically important marine grazing species. With the occurrence of hypoxic events set to rise, it is important to understand the potential impacts on animal reproduction in an already acidifying ocean and to consider possible effects on the future abundance and distribution of marine biodiversity.

Material and methods

Animal husbandry and culture history

To assess the effects of long-term parental exposure to elevated pCO_2 on sperm motility and fertilisation success, adult *P. lividus* (supplied by Dunmanus Seafoods Ltd, Durrus, Bantry, Co. Cork, Ireland) were exposed for 6 months to mean pCO_2 conditions predicted to occur by the end of this century (Caldeira and Wickett, 2003). Exposures were conducted in the Plymouth Marine Laboratory (Plymouth, UK) Intertidal Mesocosm Acidification System (PML-IMAS) previously described by Queiros *et al.* (2015) and Collard *et al.* (2016). In brief, the nominal treatments used in the present study were 380 and 750 μatm pCO_2. Within each of these nominal treatments, urchins were randomly assigned to one of four tanks per pCO_2 treatment (8 tanks total, tank volume 1 m^3). Within each of these separate tanks, urchins were further divided into three baskets (30 cm × 20 cm × 20 cm) with original stocking densities of six urchins per basket (18 per tank). The temperature of each tank was maintained independently using aquarium heaters (Aqua One, 150 W, Kong's (UK) Limited, Romsey, UK) and chillers (BOYU L-350). pCO_2 gas mixes were also supplied separately to each tank. Ambient pCO_2 treatments were maintained by bubbling untreated air through the water in each tank. Elevated pCO_2 treatments were maintained by enriching the air with CO_2 before bubbling (after Findlay *et al.*, 2008). pCO_2 levels (μatm) of both the untreated and CO_2-enriched air were monitored using a CO_2 Analyser (LI-820, Li-Cor, Lincoln, USA) . To prevent pCO_2 and temperature gradients forming within the tanks, the water was circulated using pumps (Aquael 1000 filter, Aquael, Warszawa, Poland). Natural seasonal variation in temperature and photoperiod is known to impact on gametogenesis and spawning condition. Consequently, these cycles were recreated in the laboratory by monthly adjustments in temperature appropriate to replicate the mean ambient monthly seasonal temperature of Plymouth Sound. Photoperiod was also adjusted monthly by changing the length of time the lighting was on each day using T8 triphosphor fluorescent tubes (which are designed to meet saltwater aquarium lighting requirements) to match natural seasonal changes in daylength. Each tank (1 m^3) received a one-third by volume water change every 3 weeks or if nitrate levels, which were monitored weekly using a nutrient autoanalyser (Branne and Luebbe Ltd. AAIII; Brewer and Riley, 1965), exceeded 25 mg l^{-1}. However, no particular tank needed to be changed more often than others. Urchins were fed *ad libitum* for 48 h once every week with fresh macroalgae (*Ulva lactuca* and *Laminaria* sp.; ~500 g per basket) collected from Plymouth Sound. Following feeding, the remaining macroalgae and any faecal pellets were removed to prevent nitrate build-up.

Simulated hypoxic events

After 6 months of acclimation to present ambient and future predicted pCO_2 levels in the PML-IMAS, 20 randomly selected adult *P. lividus* (7 from the 380 μatm treatment and 13 from the 750 μatm treatment) were induced to spawn by intra-coelomic injection of 0.5–1.0 ml 0.5 M KCl until gametes from 3 males and 3 females from each treatment had been collected for analysis for fertilisation success. Three males were used for sperm motility analysis and at least 200 sperm were tracked per time point per individual. Subsamples of the gametes collected from these individuals were then exposed to either normoxic or hypoxic conditions at their respective acclimatory pCO_2 level. Oxygen content was manipulated through input of nitrogen into sealed chambers. Normoxic conditions were set at $>$80% DO and hypoxic conditions were maintained at $<$30% DO. Normoxic or hypoxic air from these chambers was then mixed with CO_2 in a second sealed chamber to produce either 380 or 750 μatm pCO_2 and monitored using a CO_2 analyser (LI-820, Li-Cor, Lincoln, USA) before entering the experimental chambers where the well plates containing the sperm motility and fertilisation assay were placed. Oxygen content in these plates was determined using an OxySense® system

(OxySense® 5250i, Dallas, USA) for both normoxic and hypoxic conditions. pH was monitored continually using a micro pH probe (Micro-Inlab pH combination electrode, Metter Toledo, Leicester, UK) connected to a calibrated pH meter (Seven Easy pH meter, Metter Toledo, Leicester, UK). Temperature was maintained to match the monthly acclimation temperature of 15°C using a water bath (Grant Cambridge Ltd, Cambridge, UK) and was monitored using a K-type thermocouple in each chamber connected to a temperature logger (Omega, HH806AU, Manchester, UK). Specific water chemistry for gamete incubations is shown in Table 2.

Reproduction analysis

Following spawning (as described above), sperm were collected dry (i.e. undiluted) and stored on ice for no more than 1 h. Sperm were not pooled and males were treated as individuals. Female were allowed to express their eggs for 1 h, and the eggs kept separate for analysis. Egg densities were determined by counting 3 × 50 µl aliquots from each female. Sperm densities were determined by haemocytometer and adjusted to 10^7 sperm ml^{-1} using either hypoxic or normoxic filtered seawater at 380 or 750 µatm pCO_2 (FSW 0.22 µm filtered). Three subsamples (5 µL) of sperm from each individual, held at 15°C from each of the combined CO_2 and oxygen levels (380 µatm pCO_2 and 750 µatm pCO_2; 30% and >80% O_2 saturation; Table 2) were taken at 10 min intervals (from 1 to 61 min) and transferred immediately to a glass slide (18 samples per individual in total). Sperm motility, determined as percentage motility and swimming speed (curvilinear velocity, VCL), was measured by computer-assisted sperm analysis (CASA) at 15°C according to Caldwell *et al.* (2011). A minimum of 200 sperm were tracked per time point.

Fertilisation assays were conducted at combined CO_2 and oxygen levels (380 and 750 µatm; 30% and >80% O_2 saturation; Table 2) in 6-well multi-plates with gametes collected from 3 males and 3 females at densities of 2.5×10^5 ml^{-1} for sperm and 500 eggs per well, containing 10 ml FSW. Fertilisation success was determined after 2 h based on the occurrence of the first mitotic cleavage.

Carbonate chemistry

Seawater for the experimental system was collected from PML's long-term monitoring site, the Western Channel Observatory, station L4 (50° 15.00′N, 4° 13.02′W). The physicochemical parameters (temperature, salinity, pH, dissolved inorganic carbon (DIC), and total alkalinity (A_T)) of the seawater were measured three times a week for the duration of the experimental period using the methods of Findlay *et al.* (2013). Additional carbonate system parameters were calculated from temperature, salinity, A_T, and pH as described in Findlay *et al.* (2013). The long-term physicochemical data are presented in Findlay *et al.* (2013) and Collard *et al.* (2016). The water chemistry parameters after 6 months of incubation in the 380 and 750 µatm ambient temperature treatments used in the present study are presented in Table 1. The physicochemical parameters for gamete incubation were measured/calculated in the same way and are presented in Table 2.

Table 1. Water chemistry parameters for the ambient and future predicted OA scenarios (mean ± SD) (after Findlay *et al.*, 2013).

Nominal pCO_2 treatment (µatm)	380	750
TA (µmol kg^{-1})	2255.24 ± 133.1	2183.17 ± 101.6
pH	8.08 ± 0.03	7.93 ± 0.09
Temperature (°C)	15.04 ± 0.90	15.66 ± 0.65
Salinity	35.00 ± 0.1	34.90 ± 0.2
DIC (µmol kg^{-1})[a]	2073.90 ± 122.9	2062.90 ± 131.3
pCO_2 (µatm)[a]	483.00 ± 24.6	722.40 ± 198.2
Ω Cal[a]	3.18 ± 0.25	2.31 ± 0.32
Ω Arg[a]	2.04 ± 0.15	1.49 ± 0.21
L:D cycle	16 : 8	16 : 8
Nitrate (µmol l^{-1})	7.313 ± 12.97	7.93 ± 13.20

Parameters labelled with "a" were calculated using CO2Sys software. Seasonal light (L): dark (D) cycles are presented for the date of the experiment.

Table 2. Water chemistry parameters for the ambient and future predicted OA scenarios used in experimental chambers (mean ± SD).

Nominal oxygen and pCO_2 treatment (µatm)	380 normoxic	380 hypoxic	750 normoxic	750 hypoxic
Sperm motility				
TA (µmol kg^{-1})	2366.70 ± 68.3	2366.70 ± 68.3	2207.05 ± 222.5	2207.05 ± 222.5
pH	8.07 ± 0.01	8.07 ± 0.01	7.94 ± 0.01	7.94 ± 0.01
Temperature (°C)	15.2 ± 0.12	15.3 ± 0.07	15.3 ± 0.09	15.24 ± 0.08
Salinity	35.0 ± 0.1	35.0 ± 0.01	34.9 ± 0.2	34.9 ± 0.2
DIC (µmol kg^{-1})[a]	2123.90 ± 3.13	2036.72 ± 2.90	2125.73 ± 3.28	2036.31 ± 3.30
pCO_2 (µatm)[a]	376.36 ± 5.54	501.89 ± 8.89	382.29 ± 6.27	499.99 ± 11.97
Ω Cal[a]	4.17 ± 0.05	3.00 ± 0.004	4.14 ± 0.04	3.00 ± 0.05
Ω Arg*	2.68 ± 0.03	1.93 ± 0.03	2.66 ± 0.03	1.93 ± 0.03
Oxygen (µatm)	190.70 ± 4.4	54.08 ± 3.0	189.85 ± 4.2	52.96 ± 3.1
Fertilisation				
TA (µmol kg^{-1})	2366.70 ± 68.3	2366.70 ± 68.3	2207.05 ± 222.5	2207.05 ± 222.5
pH	8.08 ± 0.01	8.06 ± 0.02	7.94 ± 0.01	7.95 ± 0.02
Temperature (°C)	15.2 ± 0.16	15.3 ± 0.08	15.3 ± 0.17	15.3 ± 0.08
Salinity	35.0 ± 0.1	35.0 ± 0.1	34.9 ± 0.2	34.9 ± 0.2
DIC (µmol kg^{-1})[a]	2122.45 ± 5.90	2035.92 ± 4.58	2130.62 ± 9.42	2031.3 ± 10.16
pCO_2 (µatm)[a]	375.88 ± 11.37	498.14 ± 13.96	390.63 ± 18.75	486.41 ± 29.72
Ω Cal[a]	4.19 ± 0.09	3.01 ± 0.06	4.07 ± 0.09	3.07 ± 0.15
Ω Arg[a]	2.69 ± 0.06	1.94 ± 0.04	2.61 ± 0.09	1.98 ± 0.09
Oxygen (µatm)	190.96 ± 3.6	52.11 ± 4.8	190.81 ± 3.7	53.24 ± 4.4

Parameters labelled with "a" were calculated using CO2Sys software.

Data analysis

Motility data from sperm with a head area <5 and >35 μm^2 were discounted to eliminate false negatives attributable to sperm clumping or sperm misidentification by the CASA software (Caldwell *et al.*, 2011). A test for normality (Kolmogorov–Smirnov) was carried out and data transformed using a natural logarithm when not normally distributed. A two-way ANOVA was conducted on the log VCL data to determine significant factors and interactions using time as a co-factor. Percentage sperm motility and fertilisation success data were arcsine transformed before statistical analysis and a test for normality (Kolmogorov–Smirnov) was carried out. Two-way ANOVA was conducted for percentage sperm motility with time as a co-factor.

Results

Sperm motility

Neither time ($p = 0.141$) nor pCO_2 ($p = 0.370$) as single variables significantly affected percentage motility (Table 3a, Figure 1a). Percentage motility decreased under hypoxia at both 380 μatm pCO_2 ($p = 0.032$) and 750 μatm pCO_2 ($p < 0.005$; Table 3a) levels. Hypoxia at 750 μatm pCO_2 led to the lowest percentage motility, although this did not differ significantly from the percentage motility at the 380 μatm pCO_2 hypoxic level, and there was no significant interaction between pCO_2 and hypoxia (Table 3a; Figure 1a). Swimming speed (VCL) increased at 750 μatm pCO_2 under both normoxic and hypoxic conditions relative to 380 μatm pCO_2 treatments (Table 3b, Figure 1b). Both pCO_2 and hypoxia separately showed significant effects on VCL (both $p < 0.01$); however, there was no significant interaction (Table 3b). VCL was significantly reduced under 380 μatm pCO_2 hypoxic conditions ($p < 0.05$) compared with controls. Overall, there was a significant effect of time on VCL ($p < 0.01$) (Figure 2). This was driven by changes in the 380 μatm pCO_2 and 750 μatm pCO_2 normoxic treatments. In the 380 μatm, pCO_2 normoxic treatment VCL was highest at 1 min and significantly decreased after 50 min ($p < 0.05$) and 60 min ($p < 0.05$; Figure 2). In the 750 μatm, pCO_2 normoxic treatment VCL was highest at 10 min but had decreased significantly at 20 min ($p < 0.01$). Although this decrease did not remain significant at 30 min ($p = 0.115$) and 40 min ($p = 0.051$), it was significant at 50 min ($p < 0.01$) and 60 min ($p < 0.01$; Figure 2). There was no significant difference in VCL across track time in the 380 μatm pCO_2 ($p = 0.844$) and 750 μatm pCO_2 ($p = 0.719$) hypoxic treatments.

Table 3. ANOVA table for (a) percentage sperm motility, (b) sperm curvilinear velocity, and (c) fertilisation success at elevated pCO_2 (750 vs. 380 μatm) in combination with hypoxic and normoxic conditions.

	D.f.	Sum squared	Mean squared	*F*-value	*P*(>*f*)
(a)					
pCO_2	2	49.961	49.961	0.813	0.370
Oxygen	2	643.293	643.293	10.470	0.002
Time	7	135.788	135.788	2.210	0.141
pCO_2 × oxygen	4	1.023	1.023	0.017	0.898
Residuals	79	4853.940	61.442		
(b)					
pCO_2	2	3.253	3.253	9.105	0.003
Oxygen	2	3.445	3.445	9.642	0.003
Time	7	4.013	4.013	11.233	0.001
pCO_2 × oxygen	4	0.069	0.069	0.194	0.661
Residuals	79	28.223	0.357		
(c)					
pCO_2	1	1621.303	1621.303	62.735	<0.005
Oxygen	1	20 801.082	20 801.082	804.876	<0.005
pCO_2 × oxygen	1	521.013	521.013	20.160	<0.005
Residuals	32	827.002	25.844		

Sperm motility data corrected for time.

Fertilisation success

Fertilisation success was significantly reduced by both elevated pCO_2 and by reduced oxygen (Figure 3). Under normoxic conditions, the elevated pCO_2 caused a decrease of 7% ($p = <0.005$). Hypoxic conditions under normal pCO_2 levels, however, caused a further decrease by 63% ($p = <0.005$). The combined impact of high pCO_2 and low oxygen was most detrimental, with fertilisation success reduced to 3% ($p = <0.005$). There was, therefore, a significant interaction between hypoxia and elevated pCO_2 ($p = <0.005$).

Discussion

The results of the current study suggest that if an hypoxic event were to occur under future OA scenarios, there would be a significant decrease in the fertilisation success of *P. lividus*, although sperm motility would not be significantly affected by combined pCO_2 and hypoxic conditions. The results also highlight the need for further studies into the synergistic effects of abiotic factors, as OA is unlikely to occur in isolation from other climate-related stressors such as warming and hypoxia.

There was no significant effect of pCO_2 on the percentage of motile sperm, in agreement with a previous study (Havenhand and Schlegel, 2009), although sperm swimming speed, which remained high across all treatments, was significantly higher at elevated pCO_2. In contrast, the majority of previous studies (e.g. Havenhand and Schlegel, 2009; Frommel *et al.*, 2010; Morita *et al.*, 2010) concerned with sperm swimming speed reported a slowing under acidified conditions. However, the current study differs from much of the previous literature as sperm motility and swimming speed were tracked over a 1-h period; substantially longer than many previous studies which have used track times of a few seconds post activation (Morita *et al.*, 2010; Schlegel *et al.*, 2012). This longer tracking time was used, because fertilisation of broadcast spawners may not necessarily happen immediately, as gametes need to disperse. Tracking for 1 h allows a more realistic assessment of what may happen naturally. Consistent with this reasoning, the present study shows that changes in sperm swimming speed over the first hour of activation differed between treatments (Figure 2); a point which may have been missed previously due to shorter tracking times. An explanation for an increase in sperm swimming speed is offered in previous work (Caldwell *et al.*, 2011) by sperm activation pH. This is the mechanism whereby sperm are stored in an immotile state at pH 7.2, below the activation threshold of sperm dynein ATPase that powers the flagellum (Johnson *et al.*, 1983). When the sperm are released into the water column the pH of the sperm is increased to 7.6 and the flagellum is activated and mitochondrial respiration begins (Christen *et al.*, 1983). This indicates that there will be an increase in sperm swimming speed, perhaps modulated by sperm-activating peptides (SAPs), which are released by the egg jelly coat. These SAPs evolved 70 million years ago when atmospheric CO_2 was far higher than present day levels and oceans had a lower pH (pH 7.4–7.6) (Neill and Vacquier, 2004; Darszon *et al.*, 2008; Caldwell *et al.*, 2011).

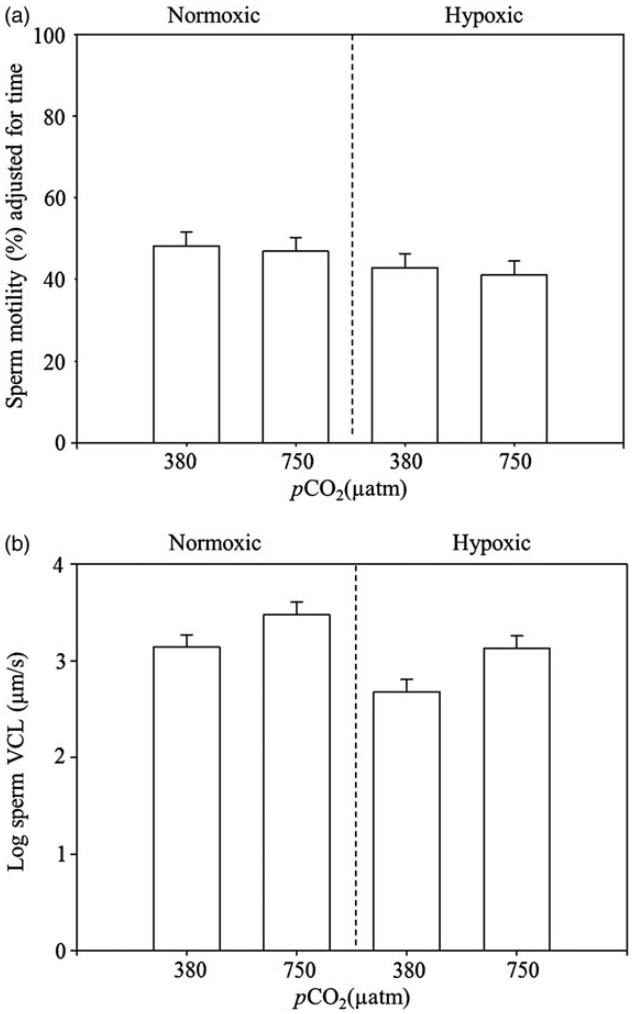

Figure 1. The effects of CO_2-induced acidification in combination with hypoxia on *P. lividus* sperm: (a) percentage sperm motility adjusted for time and (b) log VCL. Means ± standard error. Graph (b) adjusted for time at 30 min.

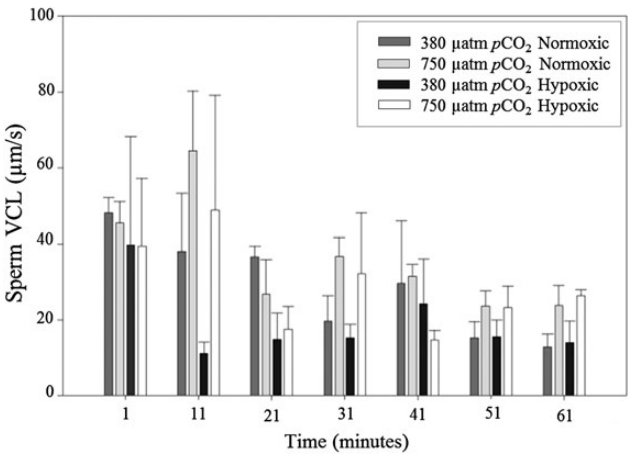

Figure 2. The effects of CO_2-induced acidification in combination with hypoxia on *P. lividus* sperm swimming speed (VCL) over time. Data are means ± 95% confidence intervals.

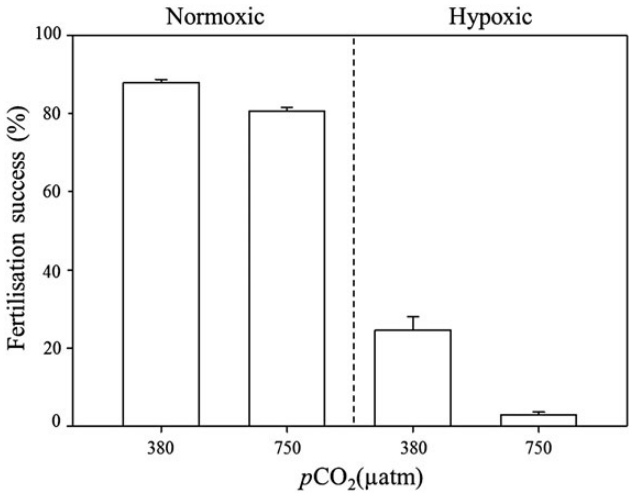

Figure 3. Effects of CO_2-induced acidification in combination with hypoxia on *Paracentrotus lividus* fertilisation success. Data are means ± standard error.

Hypoxia is also an important factor in relation to sperm motility. The current study shows that both sperm percentage motility and VCL were reduced under hypoxic conditions. Previous research into the effects of hypoxia on sperm swimming speed gave contrasting results, with the majority of studies seeing a reduction in sperm swimming speed when exposed to hypoxic conditions (Bencic *et al.*, 1999a, b; Wu *et al.*, 2003; Shin *et al.*, 2014), similar to the results described here. Sperm motility is an energetically demanding process requiring ATP, which is generated in mitochondria located in the mid piece of the sperm. In the absence of oxygen, ATP cannot be synthesized from ADP via oxidative phosphorylation, thereby limiting energy availability for flagellum activity. Therefore, under hypoxic conditions where oxygen availability is limited, sperm are unable to become active (Billard and Cosson, 1990; Fitzpatrick *et al.*, 2009). However, when increased pCO_2 and hypoxia are considered together, both percentage sperm motility and sperm VCL did not differ significantly from the control treatment. If the reduction in sperm motility through hypoxia is considered with the increase in sperm swimming speed due to increasing pCO_2, there is potential for a mediating effect of hypoxia on the impact of OA (Figure 1b).

In contrast to sperm motility, fertilisation success is reduced under both increased pCO_2 and hypoxic conditions. The effects of increased pCO_2 on fertilisation success have been widely studied and are believed to be attributable to developmental delay (Kurihara and Shirayama, 2004) or to the slowing of the fast block to polyspermy (Reuter *et al.*, 2011). Previous studies on the effects of OA on fertilisation success have obtained variable results but there was no significant effect on fertilisation success in the majority of studies on echinoderms (e.g. Byrne *et al.*, 2009, 2010a, b; Martin *et al.*, 2011). However, a few studies reported results similar to those of the current study. A reduction in fertilisation success under OA was noted for the sea urchins *Heliocidaris erythrogamma* (Havenhand *et al.*, 2008) and *P. lividus* from below pH 7.6 (Moulin *et al.*, 2011). *Paracentrotus lividus* naturally lives in a variable pH environment (Collard *et al.*, 2016) and consequently previous studies have shown that small short-term changes in pH above pH 7.8 show no significant effect on fertilisation success (Moulin *et al.*, 2011). The present study highlights that smaller but longer term (6 months)

chronic changes in pH during gonad development could affect fertilisation success. These intra- and interspecific differences have previously been attributed to variations in experimental design. In addition, none of these previous studies have pre-acclimated the adults from which the gametes were obtained, in contrast to the present study.

Here, hypoxia as a single factor caused a significant decrease in fertilisation success. In general, studies on effects of hypoxia on reproductive capacity show a significant negative effect on reproductive endpoints including fertilisation success. This significant reduction suggests that early embryonic development is reliant on aerobic respiration. A marked increase in respiratory rate of sea urchin eggs after fertilisation, as previously shown (Yasumasu *et al.*, 1996), would account for the reduction seen here under hypoxic conditions. After fertilisation, oxygen is required primarily for the oxygenation of glycogen, which is stored in the eggs and is an essential energy reserve for development. The oxygen used is attained through diffusion across the oocyte membrane and this diffusion is determined by the difference in oxygen partial pressure between the egg and the external environment. For broadcast spawners, the relevant conditions are those of the external marine environment (Herreid, 1980; Wang and Zhang, 1995). Hypoxic conditions may cause a decrease in this gradient, so that the eggs are less capable of acquiring adequate oxygen, which in turn may lead to the inhibition of embryonic development. Riveros *et al.* (1996) showed a significant reduction in fertilisation success (<40%) when the sea urchin *Arbacia spatuligera* was exposed to oxygen levels of 30% and below. Similarly, in the sea urchin, *Strongylocentrotus droebachiensis*, there was a significant negative effect of hypoxia on gonad growth (Siikavuopio *et al.*, 2007). Reductions in reproductive ability and output also occur in brine shrimp (Spicer and El-Gamal, 1990), copepods (Marcus *et al.*, 2004; Sedlaceck and Marcus, 2005; McAllen and Brennan, 2009), and gastropods (Cheung *et al.*, 2008). The results from previous studies also indicate a reduction in energy allocation for reproduction (Cheung *et al.*, 2008) as well as a reduction in developmental rate, indicating developmental delay (McAllen and Brennan, 2009).

The results of the present study suggest a synergistic effect between increased pCO_2 and hypoxia, as there was a significant reduction in fertilisation success under hypoxic conditions and this reduction was significantly greater when combined with acidified conditions. The diffusion of pCO_2 created during respiration is reliant on a diffusion gradient similar to that for oxygen. Under increased pCO2, however, the CO_2 molecules do not move as readily across the egg membrane, leading to reductions in fertilisation success. This synergistic effect may lead to severe negative effects on species recruitment and distribution. Recent studies (Gobler *et al.*, 2014) also found a negative synergistic effect of increasing OA and hypoxia in relation to larval development and survivorship. Reduced survivorship (by >50%) and inhibition of growth and metamorphosis (by >50%) occurred under low oxygen conditions in two calcifying bivalves: bay scallops, *Argopecten irradians*, and hard clams, *Mercenaria mercenaria*. However, in contrast to Gobler *et al.* (2014), Frieder *et al.* (2014) found that there was no significant effect of low pH or low O_2 on survivorship of the mytilid species, *Mytilus californianus* and *M. galloprovincialis*, and no effect of combined increased pCO_2 and low O_2 on their early development.

The present study is novel in assessing the impact that an hypoxic event would have on the reproductive parameters of sperm motility and fertilisation success in a future high CO_2 world. There is a significant effect of both pCO_2 and hypoxia on sperm swimming speed, with reduced speeds seen under hypoxic conditions and increased speeds observed under increased pCO_2 levels. In normoxic conditions, increased speed at elevated pCO_2 could possibly have negative effects on fertilisation success because sperm that swim faster use up their available energy faster (motility decreased after 20 min) leading to a possible trade-off between sperm swimming speed and longevity; however, further research is required. This suggests that sperm swimming speed is not necessarily the most important factor in fertilisation success. Broadcast spawning is affected by many factors, including water currents and chemistry, and as fertilisation may not happen immediately, sperm need to be motile for longer (Levitan, 2000). Sperm released in a future high pCO_2 ocean may use up their energy quicker, translating to a reduction in fertilisation success. However, as also shown in this study, if swimming speed decreases to lower levels, as associated with hypoxia under ambient pCO_2 levels, fertilisation success is reduced despite swimming activity remaining constant for longer (>1 h). In addition, when elevated pCO_2 and hypoxia are combined, their contrasting effects lead to sperm swimming speed similar to that observed in control treatments and swimming activity remaining constant for over an hour. Nevertheless, fertilisation success was lowest in this treatment. This suggests that, at least under the combination of hypoxia and elevated pCO_2, the direct synergistic effects of these stressors on fertilisation success are more important than indirect effects of sperm motility and longevity.

It appears that an hypoxic event will negatively affect fertilisation success regardless of oceanic pCO_2, but this effect will be intensified under near future pCO_2 conditions. This is in contrast to the results for sperm motility, which suggest an increase in sperm swimming speed under increased pCO_2 conditions will be mediated by an hypoxic event. If fertilisation success is negatively impacted, there will likely be knock-on effects such as reduced recruitment but also effects on the food chain, as *P. lividus* is not only an important grazing species but also an important source of prey for larger organisms. It is also an important commercial species and the impacts of climate change may negatively affect its aquaculture.

Acknowledgements

The original concept was developed by HG and SPSR. Experiments were carried out by HG and SPSR. Data analysis were carried out by HG. Animals and seawater parameters were maintained by staff at Plymouth Marine Laboratory under supervision of HSF, SPSR, and SW; particular thanks go to technicians Amanda Beesley, Joana Nunes, and Adam Cowles. The CO_2 system was designed by HSF who also analysed the seawater chemistry. All authors contributed to the final manuscript. The NERC Consortium Grant NE/H017127/1 "Impacts of ocean acidification on key benthic ecosystems, communities, habitats, species and life cycles" awarded to SW and HF funded the PML-IMAS and supported SPSR. HG was supported by NERC studentship NE/H525046/1 awarded to ASC, MGB, and GSC.

References

Bencic, D. C., Krisfalusi, M., Cloud, J. G., and Ingermann, R. L. 1999a. ATP levels of chinook salmon (*Oncorhynchus tshawytscha*) sperm following *in vitro* exposure to various oxygen tensions. Fish Physiology and Biochemistry, 20: 389–397.

Bencic, D. C., Krisfalusi, M., Cloud, J. G., and Ingermann, R. L. 1999b. Maintenance of steelhead trout (*Oncorhynchus mykiss*) sperm at different *in vitro* oxygen tensions alters ATP levels and cell functional characteristics. Fish Physiology and Biochemistry, 21: 193–200.

Billard, R., and Cosson, M. P. 1990. The energetics of fish sperm motility. *In* Controls of Sperm Motility: Biological and Clinical Aspects. Ed. by C. Gagnon. CRC Press Inc., Boca Raton, FL. pp. 153–157.

Brewer, P. G., and Riley, J. P. 1965. The automatic determination of nitrates in sea water. Deep Sea Research, 12: 765–772.

Byrne, M. 2012. Global change ecotoxicology: Identification of early life history bottlenecks in marine invertebrates, variable species responses and variable experimental approaches. Marine Environmental Research, 76: 3–15.

Byrne, M., Ho, M., Selvakumaraswamy, P., Nguyen, H. D., Dworjanyn, S. A., and Davis, A. R. 2009. Temperature, but not pH, compromises sea urchin fertilization and early development under near-future climate change scenarios. Proceedings of the Royal Society B: Biological Sciences, 276: 1883–1888.

Byrne, M., Soars, N., Dworjanyn, S. A., and Davis, A. R. 2010a. Sea urchin fertilization in a warm, acidified and high pCO_2 ocean across a range of sperm densities. Marine Environmental Research, 69: 234–239.

Byrne, M., Soars, N. A., Ho, M. A., Wong, E., McElroy, D., Selvakumaraswamy, P., Dworjanyn, S. A., *et al.* 2010b. Fertilisation in a suite of coastal marine invertebrates from SE Australia is robust to near-future ocean warming and acidification. Marine Biology, 157: 2061–2069.

Caldeira, K., and Wickett, M. E. 2003. Anthropogenic carbon and ocean pH. Nature, 425: 365.

Caldwell, G. S., Fitzer, S., Gillespie, C. S., Pickavance, G., Turnbull, E., and Bentley, M. G. 2011. Ocean acidification takes sperm back in time. Invertebrate Reproduction and Development, 55: 217–221.

Chan, H. Y., Xu, W. Z., Shin, P. K. S., and Cheung, S. G. 2008. Prolonged exposure to low dissolved oxygen affects early development and swimming behaviour in the gastropod *Nassarius festivus* (Nassariidae). Marine Biology, 153: 735–743.

Cheung, S. G., Chan, H. Y., Liu, C. C., and Shin, P. K. S. 2008. Effect of prolonged hypoxia on food consumption, respiration, growth and reproduction in marine scavenging gastropod *Nassarius festivus*. Marine Pollution Bulletin, 57: 280–286.

Christen, R., Schackmann, R. W., and Shapiro, B. M. 1983. Metabolism of sea urchin sperm. Interrelationships between intracellular pH, ATPase activity, and mitochondrial respiration. Journal of Biological Chemistry, 258: 5392–5399.

Collard, M., Rastrick, S. P. S., Calosi, P., Demolder, Y., Dillie, J., Findlay, H. S., Hall-Spencer, J. M., *et al.* 2016. The impact of ocean acidification and warming on the skeletal mechanical properties of the sea urchin *Paracentrotus lividus* from laboratory and field observations. ICES Journal of Marine Science, 73: 727–738.

Cooper, T. F., O'Leary, R. A., and Lough, J. M. 2012. Growth of Western Australian corals in the Anthropocene. Science, 335: 593–596.

Crimaldi, J. P. 2012. The role of structured stirring and mixing on gamete dispersal and aggregation in broadcast spawning. Journal of Experimental Biology, 215: 1031–1039.

Darszon, A., Guerrero, A., Galindo, B. E., Nishigaki, T., and Wood, C. D. 2008. Sperm-activating peptides in the regulation of ion fluxes, signal transduction and motility. International Journal of Developmental Biology, 52: 595–606.

Diaz, R. J. 2001. Overview of hypoxia around the world. Journal of Environmental Quality, 30: 275–281.

Diaz, R. J., and Rosenberg, R. 1995. Marine benthic hypoxia: a review of its ecological effects and the behavioural responses of benthic macrofauna. Oceanography and Marine Biology: An Annual Review, 33: 245–3.3.

Diaz, R. J., and Rosenberg, R. 2008. Spreading dead zones and consequences for marine ecosystems. Science, 321: 926–929.

Dupont, S., Dorey, N., and Thorndyke, M. 2010. What meta-analysis can tell us about vulnerability of marine biodiversity to ocean acidification? Estuarine, Coastal and Shelf Science, 89: 182–185.

Ericson, J. A., Lamare, M. D., Morley, S. A., and Barker, M. F. 2010. The response of two ecologically important Antarctic invertebrates (*Sterechinus neumayeri* and *Parborlasia corrugatus*) to reduced seawater pH: Effects on fertilisation and embryonic development. Marine Biology, 157: 2689–2702.

Findlay, H. S., Beesley, A., Dashfield, S., McNeill, C. L., Nunes, J., Queiros, A. M., and Woodward, E. M. S. 2013. UKOA Benthic Consortium, PML Intertidal Mesocosm Experimental Environment Dataset. British Oceanographic Data Centre—Natural Environment Research Council, UK.

Findlay, H. S., Kendall, M. A., Spicer, J. I., Turley, C., and Widdicombe, S. 2008. Novel microcosm system for investigating the effects of elevated carbon dioxide and temperature on intertidal organisms. Aquatic Biology, 3: 51–62.

Fitzpatrick, J. L., Craig, P. M., Bucking, C., Balshine, S., Wood, C. M., and McClelland, G. B. 2009. Sperm performance under hypoxic conditions in the intertidal fish *Porichthys notatus*. Canadian Journal of Zoology, 87: 464–469.

Frieder, C. A., Gonzalez, J. P., Bockmon, E. E., Navarro, M. O., and Levin, L. A. 2014. Can variable pH and low oxygen moderate ocean acidification outcomes for mussel larvae? Global Change Biology, 20: 754–764.

Frommel, A. Y., Stiebens, V., Clemmesen, C., and Havenhand, J. 2010. Effect of ocean acidification on marine fish sperm (Baltic cod: *Gadus morhua*). Biogeosciences, 7: 5859–5872.

Gobler, C. J., DePasquale, E. L., Griffith, A. W., and Baumann, H. 2014. Hypoxia and acidification have additive and synergistic negative effects on the growth, survival, and metamorphosis of early life stage bivalves. PLoS ONE, 9: e83648.

Gonzalex-Bernat, M. J., Lamare, M., and Barker, M. 2013. Effects of reduced seawater pH on the fertilisation, embryogenesis and larval development in the Antarctic sea star *Odontaster validus*. Polar Biology, 36: 235–247.

Havenhand, J. N., Buttler, F., Thorndyke, M. C., and Williamson, J. E. 2008. Near-future levels of ocean acidification reduce fertilisation success in a sea urchin. Current Biology, 18: R651–R652.

Havenhand, J. N., and Schlegel, P. 2009. Near-future levels of ocean acidification do not affect sperm motility and fertilization kinetics in the oyster *Crassostrea gigas*. Biogeosciences, 6: 3009–3015.

Herreid, C. F. 1980. Hypoxia in invertebrates. Comparative Biochemistry and Physiology, 67A: 311–320.

Hofmann, M., and Schellnhuber, H. J. 2009. Oceanic acidification affects marine carbon pump and triggers extended marine oxygen holes. Proceedings of the National Academy of Science, 106: 3017–3022.

IPCC, 2013. Climate Change 2013: The physical science basis. In Contribution of Working Group I to the Fifth Assessment Report of the Intergovernmental Panel on Climate Change. Ed. by T. F. Stocker, D. Qin, G. K. Plattner, M. Tignor, S. K. Allen, J. Boschung, A. Nauels, Y. Xia, V. Bex, and P. M. Midgley. Cambridge University Press, Cambridge, UK and New York, NY, USA.

Johnson, C. H., Clapper, D. L., Winkler, M. M., Lee, H. C., and Epel, D. 1983. A volatile inhibitor immobilizes sea urchin sperm in semen by depressing the intracellular pH. Developmental Biology, 98: 493–501.

Kroeker, K. J., Kordas, R. L., Crim, R. N., and Singh, G. G. 2010. Meta-analysis reveals negative yet variable effects of ocean acidification on marine organisms. Ecology Letters, 13: 1419–1434.

Kurihara, H., and Shirayama, Y. 2004. Effects of increased atmospheric CO_2 on sea urchin early development. Marine Ecology Progress Series, 274: 161–169.

Levitan, D. R. 2000. Sperm velocity and longevity trade off each other and influence fertilization in the sea urchin *Lytechinus variegatus*. Proceedings of the Royal Society of London, Series B, 267: 531–534.

Marcus, N. H., Richmond, C., Sedlacek, C., Miller, G. A., and Oppert, C. 2004. Impact of hypoxia on the survival, egg production and population dynamics of *Acartia tonsa* Dana. Journal of Experimental Marine Biology and Ecology, 301: 111–128.

Martin, S., Richier, S., Pedrotti, M. L., Dupont, S., Castejon, C., Gerakis, Y., Kerros, M. E., *et al.* 2011. Early development and molecular plasticity in the Mediterranean sea urchin *Paracentrotus lividus* exposed to CO_2-driven acidification. Journal of Experimental Biology, 214: 1357–1368.

McAllen, R., and Brennan, E. 2009. The effect of environmental variation on the reproductive development time and output of the high-shore rockpool copepod *Tigriopus brevicornis.* Journal of Experimental Marine Biology and Ecology, 368: 75–80.

Middelburg, J. J., and Levin, L. A. 2009. Coastal hypoxia and sediment biogeochemistry. Biogeosciences, 6: 1273–1293.

Morita, M., Suwa, R., Iguchi, A., Nakamura, M., Shimada, K., Sakai, K., and Suzuki, A. 2010. Ocean acidification reduces sperm flagellar motility in broadcast spawning reef invertebrates. Zygote, 18: 103–107.

Moulin, L., Catarino, A. I., Claessens, T., and Dubois, P. 2011. Effects of seawater acidification on early development of the intertidal sea urchin *Paracentrotus lividus* (Lamarck 1816). Marine Pollution Bulletin, 62: 48–54.

Neill, A. T., and Vacquier, V. D. 2004. Ligands and receptors mediating signal transduction in sea urchin spermatozoa. Reproduction, 127: 141–149.

Oschlies, A., Shulz, K. G., Riebesell, U., and Schmittner, A. 2008. Simulated 21st century's increase in oceanic suboxia by CO_2-enhanced biotic carbon export. Global Biogeochemical Cycles, 22: GB4008.

Pörtner, H. O. 2008. Ecosystem effects of ocean acidification in times of ocean warming: a physiologist's view. Marine Ecology Progress Series, 373: 203–217.

Pörtner, H. O., and Farrell, A. P. 2008. Physiology and climate change. Science, 322: 690–692.

Pörtner, H. O., and Langenbuch, M. 2005. Synergistic effects of temperature extremes, hypoxia, and increases in CO_2 on marine animals: From Earth history to global change. Journal of Geophysical Research, 110: C09S10.

Queirós, A. M., Fernandes, J. A., Faulwetter, S., Nunes, J., Rastrick, S. P. S., Mieszkowska, N., Artioli, Y., *et al.* 2015. Scaling-up experimental ocean acidification and warming research: from individuals to the ecosystem. Global Change Biology, 21: 130–143.

Reum, J. C. P., Alin, S. R., Harvey, C. J., Bednarsek, N., Evans, W., Feely, R. A., Hales, B., *et al.* 2016. Interpretation and design of ocean acidification experiments in upwelling systems in the context of carbonate chemistry co-variation with temperature and oxygen. ICES Journal of Marine Science, 73: 582–595.

Reuter, K. E., Lotterhos, K. E., Crim, R. N., Thompson, C. A., and Harley, C. D. G. 2011. Elevated *p*CO2 increases sperm limitation and risk of polyspermy in the red sea urchin *Strongylocentrotus franciscanus.* Global Change Biology, 17: 163–171.

Riveros, A., Zuniga, M., Larrain, A., and Becerra, J. 1996. Relationships between fertilization of the southeastern Pacific sea urchin *Arbacia spatuligera* and environmental variables in polluted coastal waters. Marine Ecology Progress Series, 134: 159–169.

Schlegel, P., Havenhand, J. N., Gillings, M. R., and Williamson, J. E. 2012. Individual variability in reproductive success determines winners and losers under ocean acidification: A case study with sea urchins. PLoS ONE, 7: e53118.

Sedlaceck, C., and Marcus, N. H. 2005. Egg production of the copepod *Acartia tonsa*: The influence of hypoxia and food concentration. Journal of Experimental Marine Biology and Ecology, 318: 183–190.

Shin, P. K. S., Leung, J. Y. S., Qiu, J. W., Ang, P. O., Chiu, J. M. Y., Thiyagarajan, V., and Cheung, S. G. 2014. Acute hypoxic exposure affects gamete quality and subsequent fertilization success and embryonic development in a serpulid polychaete. Marine Pollution Bulletin, 85: 439–445.

Siikavuopio, S. I., Dale, T., Mortensen, A., and Foss, A. 2007. Effects of hypoxia on feed intake and gonad growth in the green sea urchin, *Strongylocentrotus droebachiensis*. Aquaculture, 266: 112–116.

Spicer, J. I., and El-Gamal, M. M. 1990. Hypoxia accelerates respiratory regulation in brine shrimp but at a cost. Journal of Experimental Biology, 202: 3637–3646.

Vaquer-Sunyer, R., and Duarte, C. M. 2008. Thresholds of hypoxia for marine biodiversity. Proceedings of the National Academy of Science, 105: 15452–15457.

Wang, C., and Zhang, F. 1995. Effects of environmental oxygen deficiency on embryos and larvae of bay scallops *Ergopecten irradians irradians*. Chinese Journal of Oceanography and Limnology, 13: 362–369.

Wu, R. S. S., Zhou, B. S., Randall, D. J., Woo, N. Y. S., and Lam, P. K. S. 2003. Aquatic hypoxia is an endocrine disruptor and impairs fish reproduction. Environmental Science and Technology, 37: 1137–1141.

Yasumasu, I., Tazawa, E., Asami, K., and Fujiwara, A. 1996. Does the low respiratory rate in unfertilized eggs result mainly from depression of the redox reaction catalyzed by flavoproteins? Analysis of the respiratory system by light-induced release of CO-mediated inhibition. Developmental Growth and Differentiation, 38: 359–371.

Handling editor: C. Brock Woodson

ICES Journal of Marine Science

ICES Journal of Marine Science (2016), 73(3), 791–802. doi:10.1093/icesjms/fsv221

Contribution to Special Issue: 'Towards a Broader Perspective on Ocean Acidification Research'

Original Article

Combined effects of low pH and low oxygen on the early-life stages of the barnacle *Balanus amphitrite*

Camilla Campanati[1], Stella Yip[2], Ackley Lane[1], and Vengatesen Thiyagarajan[1]*

[1]*The Swire Institute of Marine Sciences and School of Biological Sciences, The University of Hong Kong, Pok Fu Lam, Hong Kong SAR*
[2]*Department of Biology, Dalhousie University, Halifax, NS, Canada B3H 4R2*

**Corresponding author: tel: +852 22990601; fax: +852 25176082; e-mail: rajan@hku.hk*

Campanati, C., Yip, S., Lane, A., and Thiyagarajan, V. Combined effects of low pH and low oxygen on the early-life stages of the barnacle *Balanus amphitrite*. – ICES Journal of Marine Science, 73: 791–802.

Received 4 May 2015; revised 30 September 2015; accepted 2 November 2015; advance access publication 13 December 2015.

Ocean acidification (OA) is anticipated to interact with the more frequently occurring hypoxic conditions in shallow coastal environments. These could exert extreme stress on the barnacle-dominated fouling communities. However, the interactive effect of these two emerging stressors on early-life stages of fouling organisms remains poorly studied. We investigated both the independent and interactive effect of low pH (7.6 vs. ambient 8.2) and low oxygen (LO; 3 mg l^{-1} vs. ambient 5 mg l^{-1}) from larval development through settlement (attachment and metamorphosis) and juvenile growth of the widespread fouling barnacle, *Balanus amphitrite*. In particular, we focused on the critical transition between planktonic and benthic phases to examine potential limiting factors (i.e. larval energy storage and the ability to perceive cues) that may restrain barnacle recruitment under the interactive stressors. LO significantly slowed naupliar development, while the interaction with low pH (LO – LP) seemed to alleviate the negative effect. However, 20 – 50% of the larvae became cyprid within 4 d post-hatching, regardless of treatment. Under the two stressors interaction (LO – LP), the barnacle larvae increased their feeding rate, which may explain why their energy reserves at competency were not different from any other treatment. In the absence of a settlement-inducing cue, a significantly lower percentage of cyprids (~15% lower) settled in LO and LO – LP. The presence of an inducing cue, however, elevated attachment up to 50 – 70% equally across all treatments. Post-metamorphic growth was not altered, although the condition index was different between LO and LO – LP treatments, potentially indicating that less and/or weaker calcified structures were developed when the two stressors were experienced simultaneously. LO was the major driver for the responses observed and its interaction with low pH should be considered in future studies to avoid underestimating the sensitivity of biofouling species to OA and associated climate change stressors.

Keywords: *Balanus amphitrite*, cyprid attachment, early-life stages, low oxygen, multiple stressors, naupliar larvae, ocean acidification.

Introduction

It is now clear that CO_2 emissions from human activities are lowering seawater pH and shifting the carbonate chemistry equilibrium through the process of ocean acidification (OA; Caldeira and Wickett, 2003; IPCC, 2014). Models estimate that over the next 100 years, the average pH of surface oceans will decrease by 0.3–0.4 units (IPCC, 2014). There are many consequences of increased CO_2 emissions (i.e. warming, freshening, OA, hypoxia, etc.) and it is unlikely that any will occur in isolation (Harley *et al.*, 2006; Brewer and Peltzer, 2009; Doney *et al.*, 2012). Concurrently with human population growth, increased nutrients and organic discharge in coastal seas are causing extended eutrophication and hypoxic events (Huang *et al.*, 2003; Diaz and Rosenberg, 2008; Doney, 2010). Increased bacterial respiration in the water column not only affects the oxygen concentration, but also releases CO_2, which may increase acidification rates in coastal waters (Gilbert *et al.*, 2010; Cai *et al.*, 2011; Howarth *et al.*, 2011; Melzner *et al.*, 2012) and potentially exacerbate the effects of OA on coastal marine organisms (Pörtner, 2010). The interaction between high CO_2 (low pH–LP) and seawater deoxygenation (low oxygen—LO) is still largely unexplored (Crain *et al.*, 2008; Gobler *et al.*, 2014) and in particular, its associated consequences on fouling organisms yet, remains poorly studied (Mukherjee *et al.*, 2013). Previous research has examined the effects of these two emerging

stressors individually (e.g. Desai and Prakash, 2009; McDonald *et al.*, 2009). Though to better anticipate how littoral species, which often experience deoxygenated environments (Davenport and Irwin, 2003), might respond to near future OA, it is critical to examine their responses to the interactive effects of low pH and LO, especially during the most sensitive periods of life, which are usually represented by the early-life stages (Levin *et al.*, 2009; Byrne, 2012). Most marine invertebrates are R-selected and produce many diverse offspring propagules, which could increase the dispersal ability and the chances of surviving under different environments (Pechenik, 1999). However, the preference of quantity over quality translates into larvae being more vulnerable than their parents, and leads to the description of early-life stages as a "bottleneck in a changing ocean" (Byrne, 2012).

The larvae of many marine species are sensitive to high CO_2/low pH, with increased mortality, abnormal development, and impaired metamorphosis (Hofmann *et al.*, 2010; Kroeker *et al.*, 2010). For example, high CO_2/low pH disrupted the ability to discriminate chemical cues for settlement in fish larvae (*Amphiprion percula*) (Munday *et al.*, 2009) and reduced lipid stores in bivalve larvae (Talmage and Gobler, 2010; Ko *et al.*, 2014) and the spider crab *Hyas araneus* (Walther *et al.*, 2010). Lipids represent the predominant form of energy reserves in the larval stage of many marine organisms (Holland, 1978), and may be a critical resource in the early phases if an additional environmental stress (i.e. high CO_2/low pH and/or LO) demands more energy for maintaining homeostasis. Shifts in energy allocation to compensate for stress responses have been observed in sea urchin larvae (e.g. Stumpp *et al.*, 2011). If not buffered, an increased energetic demand for maintenance under high CO_2/low pH may propagate and impair subsequent life stages (e.g. *Strongylocentrotus droebachiensis* in Dupont *et al.*, 2013).

This is particularly relevant in organisms with a complex life cycle in which the energy reserves acquired and stored during the planktonic stage support the processes of substrate selection, metamorphosis, and early-juvenile (post-metamorphosis) growth, as demonstrated in sea urchins and barnacles (Thiyagarajan *et al.*, 2002, 2003, 2007; Byrne *et al.*, 2008). Although heterogeneous responses to the upcoming environmental changes among different species and populations have been observed (e.g. Gray *et al.*, 2002; Kroeker *et al.*, 2010), noticeably the energy use and accumulation in the early-life phases appears critical to survival under stress. In barnacles, for example, the pelagic–benthic transition could be further constrained under environmental stressful conditions, due to the high amount of energy needed for larval metamorphosis (Lucas *et al.*, 1979; Thiyagarajan *et al.*, 2002; Chen *et al.*, 2014), as well as the required ability to perceive external cues for successful substrate selection (Thiyagarajan, 2010).

Crustaceans appear to be robust to high CO_2/low pH since their early stages, for example, they have a higher tolerance than mussels and echinoids (Kroeker *et al.*, 2010; Ishimatsu and Dissanayake, 2010; Whiteley, 2011). However, compared with other marine invertebrates, they seem more sensitive to LO levels (Gray *et al.*, 2002; Vaquer-Sunyer and Duarte, 2008; Levin *et al.*, 2009). Barnacles in particular seem to be rather tolerant to high CO_2/low pH, possibly due to their high plasticity and adaptations for variable environments (Hall-Spencer *et al.*, 2008; McDonald *et al.*, 2009; Wong *et al.*, 2011; Pansch *et al.*, 2013). In contrast, barnacle larvae are sensitive to hypoxia (e.g. ≥ 1 mg l^{-1}; Desai and Prakash, 2009) though with some evidence for possible adaptive strategies (e.g. Davenport and Irwin, 2003). The relatively opposite responses of barnacles to low pH and LO environments individually emphasize the importance of understanding their responses under both of these stressors simultaneously. Despite the importance of the two stressors' interaction, no studies have investigated the combined effects of high CO_2/low pH and LO upon the early development of barnacles. We hypothesize that barnacle larvae, when exposed simultaneously to LO and low pH, will perform worse than those exposed to only low pH, resulting in lower physiological quality and recruitment (attachment and early juvenile growth) success. To test this hypothesis, we examined the interactive effect of environmentally relevant pH and oxygen levels based on IPCC projections applied to local environments (EPOCA, 2010; i.e. low pH: 7.6 vs. ambient pH: 8.2 and LO: 3 mg l^{-1} vs. ambient oxygen: 5 mg l^{-1}) on various early developmental stages of the barnacle *B. amphitrite*, a biofouler distributed worldwide and a dominant settler in tropical coastal community assemblages (Bishop, 1950). Using multiple endpoints such as larval development, survivorship, settlement (i.e. attachment and metamorphosis), and juvenile growth, we examined the effect of low pH and LO on pre- and post-settlement stages. Moreover, possible limiting factors for the transition between planktonic and benthic phase (i.e. energy reserves and sensitivity to conspecific settlement cues) were also tested under high CO_2/low pH and/or LO.

Material and methods

Adult and larvae collection

Adult *Balanus amphitrite* were collected at low tide by scraping with putty knives from a pier in Pak Sha Wan, Hong Kong (22°21.45′N, 114°15.35′E) in October 2014. Specimens were transported in air to the Swire Institute of Marine Science laboratory and placed in 0.22-μm natural filtered seawater (FSW) at ambient temperature (25° C) and salinity (33 psu) within 2 h of collection, which induced the release of instar I nauplii (Thiyagarajan *et al.*, 2002). Nauplii quickly (2–3 h) became instar II nauplii and were collected by sieve and transferred into new 0.22 μm FSW by pipette. The number of larvae was estimated by counting 50 μl aliquots of larvae sieved and concentrated in a known volume of FSW and subsequently added to 24 treatment culture tanks (described below) to make a final larval concentrations of ~1 larva ml^{-1} in 5 l of seawater.

Environmental conditions in the adult barnacle habitat

The adult barnacle population used in this study naturally experience a broad range of environmental seawater conditions due to the seasonal monsoon climate (Hong Kong Observatory, HKO; Yin, 2002), which characterizes the region and causes high levels of fluctuation in the intertidal area over the year (Supplementary Figure S1). The Pak Sha Wan pier is located in a shallow bay in Port Shelter area with weak water circulation and occasional high chlorophyll *a* concentration (Yung *et al.*, 2001). At an observation point near the collection site (PM6 station; HKEPD, 2014), sea surface temperature and salinity for the last 27 years (1986–2013) ranged from ca.18 to 29°C and from ca. 19.9 to 35.6 psu, respectively. Throughout the same period, pH values ranged between 7.1 and 8.7 and DO levels ranged 3.8–10.7 (Supplementary Figure S1).

Experimental design

Considering the natural variability experienced by this barnacle population, we have tested the interactive effect of two levels of environmentally relevant seawater pH and dissolved oxygen (DO) on

pre- and post-settlement stages of the barnacle, *B. amphitrite*. The seawater in the barnacle site is expected to experience pH = 7.6 by the year 2100 due to global anthropogenic CO_2 emissions (scenario RCP 8.5, IPCC, 2014; Supplementary Figure S2). In this study, four treatments created by crossing two levels of pH (NBS scale): 8.2 (ambient or control) and 7.6 (low pH—"LP"), and two levels of DO: 5 mg l^{-1} (ambient or control) and 3 mg l^{-1} ("LO") were used. There were six biologically independent replicate culture tanks (5 l) per treatment. The control condition (CON) was achieved by bubbling natural filtered (pore size: 0.22 μm) seawater (FSW) with ambient air (~400 μatm CO_2). For the LP and the LO–LP treatments, the seawater pH was lowered and the carbonate chemistry was altered by bubbling CO_2-enriched air (~2000 μatm CO_2). Seawater oxygen levels in the LO and LO–LP treatments were reduced by replacing a portion of the air bubbled into the cultures with nitrogen (combined with additional CO_2 to account for the ambient CO_2 concentrations). For all treatment conditions, pH and DO levels were kept constant by regulating gas flow rates before entering the culture tanks (5 l), using high-resolution valves and gas flow rotameters (Cole-Parmer Inc.). Only the culture tank pH and DO levels were fixed constant—neither the air, nor the CO_2 and/or the N_2 concentrations. All cultures were maintained at the optimal temperature (28°C) and salinity (33 psu). Seawater temperature was maintained by placing the 24 culture tanks (4 treatments × 6 replicates) in a water bath containing water heaters and circulation pumps. In each culture, tank levels of pH and DO, as well as temperature and salinity, were measured daily. Seawater pH (NBS scale) and temperature were monitored using a Mettler-Toledo (SG2) probe, DO levels with a Thermos Scientific (Orion 5 star 080017; Singapore) probe and salinity with a refractometer (ATAGO, S/Mill-E; Japan). The pH probe was calibrated before the experiment using NIST buffers (pH = 4.01, 7.00, and 9.21; Mettler Toledo, Gmbh Analytical CH8603 Schwerzenbach, Switzerland). Daily measurements (i.e. pH, DO, and temperature) were first averaged within and among days per each culture tank. Hence, the treatment mean (± s.e.; Table 1) was computed, by averages of the replicate culture tanks within each treatment ($n = 6$).

Samples of seawater from each tank were collected every week, poisoned with 10 μl of a 250 mM mercuric chloride solution for later total alkalinity (TA) analysis. TA samples were measured using the Apollo Scitech titrator (AS-ALK2) and checked against seawater reference materials (Batch 106, A.G. Dickson, Scripps Institution of Oceanography). Total dissolved inorganic carbon (DIC μmol kg^{-1}), pCO_2 levels (μatm), bicarbonate and carbonate ions concentration ($[HCO_3^-]$, $[CO_3^-]$; μmol kg^{-1}], as well as calcite and aragonite saturation states (Ω_{cal}, Ω_{ara}) were calculated with the CO2SYS program (Pierrot *et al.*, 2006) from TA and pH (NBS) measurements, employing the dissociation constants of Mehrbach *et al.* (1973) as refitted by Dickson and Millero (1987; Table 1).

Larval development and feeding rate

Within 3 h of spawning, aliquots of barnacle nauplii (instar II) were randomly assigned to 1 of the 24 treatment culture tanks at the density of ~1 larva ml^{-1} and fed daily with 10^5 cells ml^{-1} of the diatom *Chaetoceros gracilis* (Thiyagarajan *et al.*, 2003). Every 2 d, cultured larvae were sieved, concentrated, and samples (i.e. 1 ml from each culture tank) were taken to quantify larval density, check for larval abnormalities, and assess larval development. The remaining larvae were then re-placed into culture tanks with fresh natural FSW pre-equilibrated to treatment conditions. Algal ingestion rate by barnacle nauplii from each replicate culture tank was measured on day 2 using 4 replicate 40 ml vials equilibrated to treatment conditions (i.e. 4 treatments × 6 replicates × 4 vials (3 with larvae, 1 blank) = 96 vials total) with 10^5 cells ml^{-1} *C. gracilis*. All vials were incubated in the dark for 12 h at 28°C. Water samples (1 ml) were taken after 12 h and fixed with 10% formalin. Algal concentration was determined by hemocytometer. The algal clearance rate by larvae was calculated with the equation from Coughlan (1969) following Thiyagarajan *et al.* (2007):

$$\mathrm{CR} = \left(\frac{V}{nt}\right) \ln\left(\frac{C_0}{C_t}\right),$$

where CR is the clearance rate (ml ind.$^{-1}$ h^{-1}), V the volume (ml) of the vial, n the number of larvae in the vial, t the time (h) between sample collection ($t_t - t_0$) and C_0 and C_t are the algal concentration at time t_0 and t_t respectively. Clearance rate was determined after 12 h, averaged among the three samples from each replicate tank and the background noise was detracted with the use of the blanks.

Table 1. Physicochemical parameters of the seawater in the experimental system.

Treatment/parameter	Control	Low oxygen	Low pH	Low oxygen – low pH
$[O_2]$ (mg l^{-1})	5.15 ± 0.01^A	3.38 ± 0.06^B	5.14 ± 0.01^A	3.43 ± 0.01^B
Salinity (psu)	33 ± 0.00^A	33 ± 0.00^A	33 ± 0.00^A	33 ± 0.00^A
Temperature (°C)	27.86 ± 0.03^A	27.83 ± 0.08^A	27.88 ± 0.02^A	27.85 ± 0.03 ^{A}
pH	8.20 ± 0.00^A	8.19 ± 0.01^A	7.61 ± 0.00^B	7.60 ± 0.00 ^{B}
TA (μequiv kg^{-1})	2 575.42 ± 14.09^A	2 575.01 ± 19.51^A	2 597.76 ± 34.44^A	2 588.98 ± 31.60^A
TCO_2 (μmol kg^{-1})^a	2 230.94 ± 14.02^A	2 274.92 ± 12.70^A	2 542.65 ± 33.15^B	2 537.42 ± 30.43^B
pCO_2 (μatm)^a	427.36 ± 5.24^A	540.75 ± 15.34^A	2 165.79 ± 50.05^B	2 202.95 ± 29.28^B
$[HCO_3^-]$ (μmol kg^{-1})^a	1 962.72 ± 16.15^A	2 033.43 ± 8.51^A	2 403.43 ± 31.15^B	2 398.87 ± 29.28^B
$[CO_3^{2-}]$ (μmol kg^{-1})^a	256.44 ± 6.19^A	226.66 ± 6.06^B	81.80 ± 1.93^C	79.95 ± 1.41^C
Ω^a_{cal}	6.31 ± 0.15^A	5.58 ± 0.15^B	2.01 ± 0.05^C	1.97 ± 0.03^C
Ω^a_{ara}	4.18 ± 0.11^A	3.69 ± 0.10^B	1.34 ± 0.03^C	1.30 ± 0.02^C

Data are means ± s.e. of the replicate culture tanks ($n = 6$) for the seawater parameters measured or calculated during the duration of the experiment: oxygen concentration (O_2; mg l^{-1}), salinity (psu), temperature (°C), pH (National Bureau of Standards scale), TA (μequiv kg^{-1}), total CO_2 (TCO_2; μmol kg^{-1}), carbon dioxide partial pressure (pCO_2; μatm), bicarbonate and carbonate ion concentration ($[HCO_3^-]$ and $[CO_3^{2-}]$; μmol kg^{-1}), and calcite and aragonite saturation states (Ω_{cal} and Ω_{ara}). Values were first averaged within and among days per each of the replicate culture tanks. Hence, the treatment mean was computed. Superscript capital letters indicate a significant difference among treatments as analysed by standard one-way ANOVA or Kruskal–Wallis test followed by the *post hoc* Tukey's test ($p < 0.05$).

[a]Parameters were calculated using the CO2SYS program (Pierrot *et al.*, 2006), employing the dissociation constants of Mehrbach *et al.* (1973) as refitted by Dickson and Millero (1987).

Larval physiological condition

Measurement of total lipids, as a proxy of energy reserves in the terminal phase of larval development, i.e. cyprid stage, was used to quantitatively evaluate the larval physiological condition before attachment (Thiyagarajan *et al.*, 2003, 2007). Total lipid content of cyprid larvae was quantified using a sulphuric acid charring technique following Mann and Gallager (1985). Fifty cyprids, in duplicate or triplicate samples per replicate culture tank, were frozen in Eppendorf tubes with Milli-Q water and stored in −20° C until analysis. Briefly, each sample was homogenized in 300 µl of deionized water by ultrasonication (BRANSON sonifier 150). Lipids were extracted first with a 1:2 and then a 2:1 chloroform ($CHCl_3$): methanol (CH_3OH) solution. Lipid content was measured spectrophotometrically (Spectra Max M2e) after saponification and derivatization with sulphuric acid and compared with a tripalmitin standard.

Larval settlement

When the *B. amphitrite* larvae reached the competent stage for attachment and metamorphosis (i.e. the cyprid stage) 4 d post-spawning, they were sieved out from all culture tanks. The cyprids' ability to settle on a substrate was assessed using two no-choice (closed dish) bioassays (reviewed in Thiyagarajan, 2010): one consisted of enclosing cyprid larvae in clean Petri dishes, in the absence of any settlement-inducing chemical (or biological) cue, the other used Petri dishes coated with a settlement-inducing cue (∼60 µg $dish^{-1}$) derived from conspecific adults, i.e. settlement factor (SF; see Rittschof *et al.*, 1984). From each culture tank ($n = 6$ in control and LP treatment; $n = 5$ in LO and LO–LP treatments), ∼150 cyprids were divided into six polystyrene dishes (Falcon #1006): three un-manipulated dishes (CLEAN), and three dishes coated with conspecific SF. The dishes were filled with FSW of the same water conditions in which the larvae developed, sealed, and returned in the culture tanks. The percentage of larval settlement was measured as the number of individuals that successfully attached and metamorphosed on the Petri dishes over those that remained as cyprid larvae after 12 h of incubation. After the assay period, the Petri dishes with metamorphosed juveniles (swimming cyprids removed) were kept open inside the culture tanks and used for measures of juvenile performance (see below).

Juvenile culture and post-metamorphic performance

Following the settlement assay, early juvenile barnacles (∼20 ind. $tank^{-1}$) were maintained in the Petri dishes in the same 5 l culture tanks with natural FSW (temperature = 28° C; salinity = 33 psu) in the same treatment conditions (CON, LO, LP, LO–LP) in which they developed as larvae. After settlement, performances in juveniles settled on clean or SF-coated dishes were pooled and averaged within each replicate culture tank. Every 2 d, the water in the culture tanks was replaced with new FSW equilibrated to the same pH, DO, temperature, and salinity and fed a diet of *C. gracilis* at the concentration of 10^5 cells ml^{-1}. On days 3, 9, and 11 post-settlement, every specimen in each Petri dish was photographed under a dissecting microscope (LEICA, MZ95) connected to a camera (CANON, EOS 700D). Photographs were examined through the image analysis software Image J (Schneider *et al.*, 2012) and measures of the basal shell diameter (RCD, rostro carinal diameter) were used to determine the growth rate (GR) of the juvenile barnacles (Pechenik *et al.*, 1993). Performances of individuals were averaged within the Petri dishes where the barnacles developed ($n = 3$ clean + 3 sf-coated dishes = 6), and then within the replicate culture tank ($n = 6$ in control and LP treatment; $n = 5$ in LO and LO–LP treatments). After the final shell growth measurement, individuals were sacrificed for weight measurements. Barnacles were removed from the Petri dishes, rinsed with Milli-Q water, and grouped by Petri dish in preweighed aluminum foil sachets. These were first dried at 80 °C for 24 h and weighed to determine the dry weight (DW). Subsequently, samples were burned in a furnace at 500°C and weighed to determine the ash weight (AW). All weights were measured to the nearest 0.001 mg with an electronic balance (Sartorius, R200D). Ash-free dry weight (AFDW) was calculated as AFDW = DW − AW and a condition index (CI) was also calculated as CI = AFDW/AW (Pansch *et al.*, 2013).

Statistical analysis

All data were checked through inspection of residuals, normality, and homogeneity of variances tests before the analyses of variances (ANOVA) test. Normality was checked using the Shapiro–Wilk's test and homogeneity of variances was checked using the Levene's test. When homoscedasticity was not met, data were log-transformed before using an analysis of variance. To test the independent and interactive effect of pH and DO, a two-way ANOVA was performed. A three-way ANOVA was used to test the effect of pH, DO, and SF on cyprid attachment. When a significant interaction was found, it followed a Tukey's test for multiple comparisons. Larval development was analysed though one-way Kruskal–Wallis test (treatment as factor) as even after transformations, some of the data did not meet the ANOVA requirements. It followed a multiple comparison test (kruskalmc{pgirmess} in R) when the treatment was found having a significant effect on the percentages of developmental stages. The regression coefficient of basal diameter over time for each replicate tank was used to represent post-settlement GR. The GR was not homoscedastic because of high variance in the LP treatment, so it was analysed using a one-way Kruskal–Wallis test. All statistical analyses were performed in the R environment for statistical computation (R Core Team, 2015) and the level applied for significance in each statistical analysis was 0.05. The values reported in the text and in the figures represent means ± standard error of the mean.

Results

Seawater chemistry

The experimental seawater conditions in the culture tanks remained relatively stable for the duration of the experiment with slight fluctuations of the physicochemical parameters in the seawater. Temperature (∼28°C) and TA (∼2600 µequiv kg^{-1}) did not vary significantly between treatments. Measured and calculated physicchemical parameters are reported in Table 1. None of the seawater treatment conditions used in this study were under-saturated with respect to the $CaCO_3$ minerals.

Larval development

During the experiment, one replicate of the six culture tanks in both the LO and LO–LP treatments were lost due to larval mass mortality, which is not unusual in barnacle culturing practices (McDonald *et al.*, 2009). In the remaining culture tanks, larval survival on days 2 and 4 of development (post-spawning) was not affected by low pH, LO, nor by their interaction (Table 2). There was no evidence of developmental abnormalities in larvae exposed to any treatment. Generally, on day 2 of development, the larval cultures in all

Table 2. Two-way analysis of variance testing the effect of low pH, LO, and their interaction on pre- and post-settlement stages of the barnacle, *B. amphitrite*: larval survival on days 2 and 4 post-hatching, larval clearance rate (ml h^{-1} $ind.^{-1}$), cyprid lipid content (μg $ind.^{-1}$), juvenile survival on days 3, 9, and 11 post-settlement, juvenile AFDW (mg), juvenile AW (mg), juvenile CI (mg organic × mg $inorganic^{-1}$).

	d.f.	*F*	*p*-value		d.f.	*F*	*p*-value
Larval survival				Juvenile survival			
Day 2				Day 3			
pH	1	0.112	0.741	**pH**	1	4.909	**0.040**
DO	1	1.295	0.268	DO	1	0.115	0.739
pH × DO	1	1.853	0.189	pH × DO	1	0.041	0.842
Residuals	20			Residuals	18		
Day 4				Day 9			
pH	1	0.903	0.355	**pH**	1	5.08	**0.037**
DO	1	0.106	0.749	DO	1	0.126	0.727
pH × DO	1	0.299	0.591	pH × DO	1	0.042	0.839
Residuals	17			Residuals	18		
Larval clearance rate				Day 11			
pH	1	8.242	**0.009**	pH	1	2.743	0.115
DO	1	26.549	**0.000**	DO	1	0.294	0.594
pH × DO	1	10.474	**0.004**	pH × DO	1	1.265	0.276
Residuals	20			Residuals	18		
Cyprid lipid content				Juvenile AFDW			
pH	1	1.811	0.195	pH	1	2.153	0.161
DO	1	0.018	0.895	DO	1	0.182	0.675
pH × DO	1	0.035	0.854	pH × DO	1	1.062	0.317
Residuals	18			Residuals	17		
Larval settlement				Juvenile AW			
pH	1	0.162	0.690	pH	1	2.149	0.161
DO	1	3.098	0.087	DO	1	0.002	0.967
SF	1	20.854	**0.000**	pH × DO	1	0.081	0.779
pH × DO	1	0.144	0.706	Residuals	17		
pH × SF	1	0.213	0.647				
DO × SF	1	4.793	**0.035**	Juvenile CI			
pH × DO × SF	1	1.206	0.280	pH	1	2.846	0.110
Residuals	36			DO	1	1.552	0.230
				pH × DO	1	6.078	**0.025**
				Residuals	17		

Three-way analysis of variance testing the effect of low pH, LO, SF, and their interaction on larval settlement (%). In the analysis of larval survival on day 4 post-hatching, $n = 5$ in CON, LO, and LOLP treatments; $n = 6$ in LP treatment. The measurements after day 4 (cyprid lipid content and juvenile responses), accounted for 22 culture tanks ($n = 5$ in LO and LO–LP treatments; $n = 6$ in CON and LP treatments). Values of $p < 0.05$ are highlighted in bold characters.

treatments were dominated by instar IV nauplii, and on day 4, larvae had developed to instar VI nauplii and cyprid larvae (Figure 1). However, on day 2, a significantly higher percentage of early larval stage (instar III nauplii) was found in LO-treatment compared with the LO–LP treatment (KW: $\chi^2 = 8.94$, d.f. = 3, $p = 0.03$). Likewise, a significantly lower percentage of nauplii developed to instar IV in the cultures exposed to LO, compared with those exposed to low pH (LP) and the combination of low pH–LO (LO–LP; Figure 1; KW: $\chi^2 = 12.25$, d.f. = 3, $p = 0.01$). On day 4 of development, the LO treatment had a significantly lower occurrence of cyprids compared with the LP treatment (Figure 1; KW: $\chi^2 = 8.61$, d.f. = 3, $p = 0.03$). In control conditions, the competent cyprid stage was reached by 31.54 ± 8.19% of the larvae, whereas in LP and LO–LP treatments, 44.22 ± 4.82 and 35.07 ± 8.47% of the larvae, respectively, reached competency. Notably, only 16.44 ± 4.8% of larvae become cyprids at LO (Figure 1).

Larval feeding rate

On day 2 of development (post-hatching), the larval feeding rate was significantly affected by pH, DO, and their interaction (Figure 2; Table 2; Supplementary Table S1). Particularly, *post hoc* analysis confirmed that the LO–LP treatment was significantly different from the other treatments, with algal clearance rate (0.088 ± 0.007 ml h^{-1} $ind.^{-1}$) almost twice that of the control, LO, and LP (Figure 2).

Larval physiological condition and settlement

The total lipid reserves in cyprids varied from ~0.5 to ~1.5 μg $ind.^{-1}$. There was no significant difference among treatments (Figure 3; Table 2).

The cyprids' ability to settle was measured within a given period of assay time (12 h) both in the absence and presence of a settlement-inducing cue, in clean Petri dishes ($n = 3$ per replicate culture tank) and in SF-coated Petri dishes ($n = 3$ per replicate culture tank, ~60 μg of proteins in each dish), respectively. The settlement percentage was significantly different between the clean dishes and those with SF, with higher settlement in SF-coated dishes compared with clean dishes (Figure 4; Table 2). A significant interaction between SF and DO was also found (Table 2, Supplementary Table S2). In the absence of the settlement-inducing cue (in clean dishes), settlement was significantly reduced in low-oxygen conditions. Compared with the SF-coated dishes, settlement was ~50 and 30% lower in LO and LO–LP, respectively, whereas in control and LP treatments, the settlement on clean dishes was

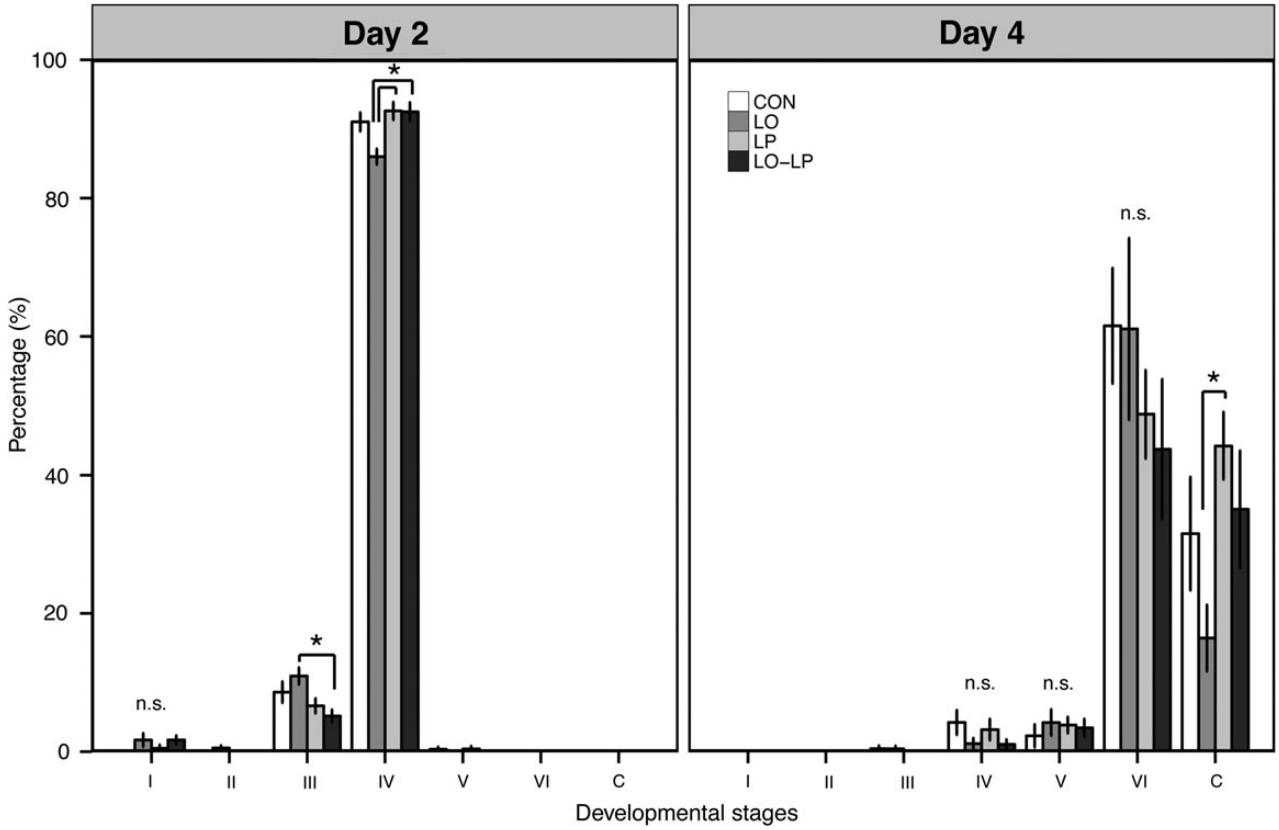

Figure 1. Percentages of developmental stages (i.e. Instar I – VI nauplii and cyprid larvae) in *B. amphitrite* reared under control (CON), low-oxygen (LO), low-pH (LP), and low-oxygen – low-pH (LO – LP) conditions. Data on day 2 (left panel) and day 4 (right panel) post-spawning are presented as mean ± s.e. (standard error) of replicate culture tanks. On day 2 post-spawning, all treatments had six replicate tanks, whereas on day 4, due to mass mortality in two replicates, both LO and LO – LP, treatments had only five replicates. Asterisks denote significant differences among treatments, detected with multiple comparison test following one-way KW test.

reduced by ~15 and 20%, respectively, compared with SF dishes. In the presence of SF, 50–70% of cyprids attached on the substrate regardless of treatment (Figure 4).

Juvenile growth

On days 3 and 9 post-settlement, the LP-treatment had significantly less mortality ($p < 0.05$) than the control and LO treatments, whereas on day 11, post-settlement juvenile survival was not different among treatments (Table 2). The best fitted curve for the growth of early-juveniles *B. amphitrite* was exponential in relation to the time (days) of development (Supplementary Table S3). There was no significant difference in GR among treatments (GR: $\chi^2 = 2.29$ d.f. = 3 and $p = 0.51$; Figure 5). At the end of the experimental exposure, juvenile barnacles measured 2.74 ± 0.09 mm in the control, 2.67 ± 0.19 mm in LO, 2.82 ± 0.35 mm in LP, and 2.5 ± 0.15 mm in LO–LP. AW (inorganic) and AFDW (organic) of juvenile barnacles did not differ among treatments (Figure 6a; Table 2). However, the interaction between low pH and LO affected the proportion of AFDW to AW (CI; Figure 6b; Table 2, Supplementary Table S4). *Post hoc* analysis highlighted that the difference in CI laid between LO and LO–LP treatments (Supplementary Table S4).

Discussion

In our study, barnacle larvae appeared to be tolerant to the low pH and DO levels tested, with larval survival showing no significant differences between any treatments. High mortality in *B. amphitrite* nauplii was observed when cultured at oxygen levels ≤ 1 mg l^{-1} (Desai and Prakash, 2009); however, sublethal effects associated with growth and reproduction at intermediate levels of oxygen demand greater attention (Marcus *et al.*, 2004). As an example, juvenile horseshoe crabs (*Tachypleus tridentatus*) were able to survive even at 2 mg O_2 l^{-1}; however, sublethal impairment in energy acquisition and utilization was observed at oxygen levels as high as 4 mg l^{-1} (Shin *et al.*, 2014). Sublethal effects were observed in this study as well, as low levels of oxygen significantly affected the larval developmental rate. By identifying the developmental stages of larvae in the cultures at days 2 and 4, we observed that LO slowed the developmental rate, whereas the addition of low pH in the seawater conditions seemingly alleviates the negative effect. Similarly, larval growth under LO was also reduced in bivalves (Gobler *et al.*, 2014) and gastropods (Chan *et al.*, 2008). However, when coupled with temperature stress, low pH resulted in delayed development in the larvae of the barnacle *Amphibalanus (Balanus) improvisus*, the spider crab *H. araneus*, and the northern shrimp *Pandalus borealis* (Walther *et al.*, 2010; Pansch *et al.*, 2012; Arnberg *et al.*, 2013). Early studies exposing *B. amphitrite* to low pH saw no differences in larval growth (McDonald *et al.*, 2009; Lane *et al.*, unpublished data); however, high heterogeneity in pH responses among different larval cohorts (Lane *et al.*, unpublished data) and replicates (McDonald *et al.*, 2009) probably prevented

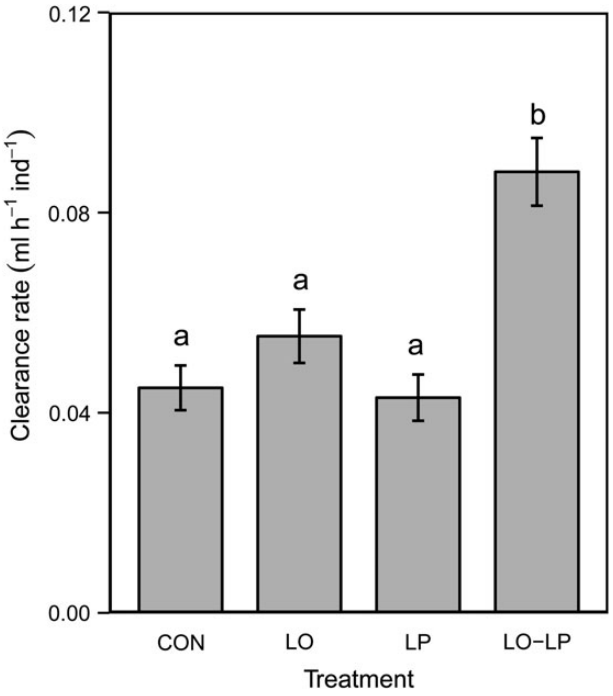

Figure 2. Larval clearance rate (ml h^{-1} ind.$^{-1}$) in *B. amphitrite* reared under control (CON), low-oxygen (LO), low-pH (LP), and low-oxygen – low-pH (LO – LP) conditions. Data on day 2 post-spawning are presented as mean ± s.e. of six replicate culture tanks. Different lower case letters illustrate significant differences ($p < 0.05$) among treatments found through multiple comparisons Tukey's test following a two-way ANOVA (Supplementary Table S1).

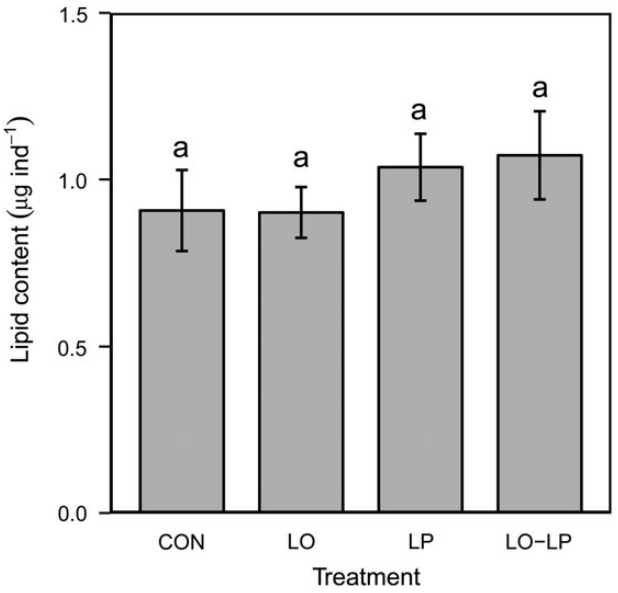

Figure 3. Lipid content (µg ind.$^{-1}$) of *B. amphitrite* cyprid larvae reared under control (CON), low-oxygen (LO), low-pH (LP), and low-oxygen – low-pH (LO – LP) conditions. Data presented are mean ± s.e. of six replicate culture tanks except for LO and LO – LP treatments, which data represent the mean ± s.e. from five replicate tanks. Lower case letters denote no difference found among treatments following a two-way ANOVA (Table 2).

observations of significant differences in larval development. Despite the heterogeneity, which is a common feature in studies of marine invertebrate larvae and is especially evident in barnacle

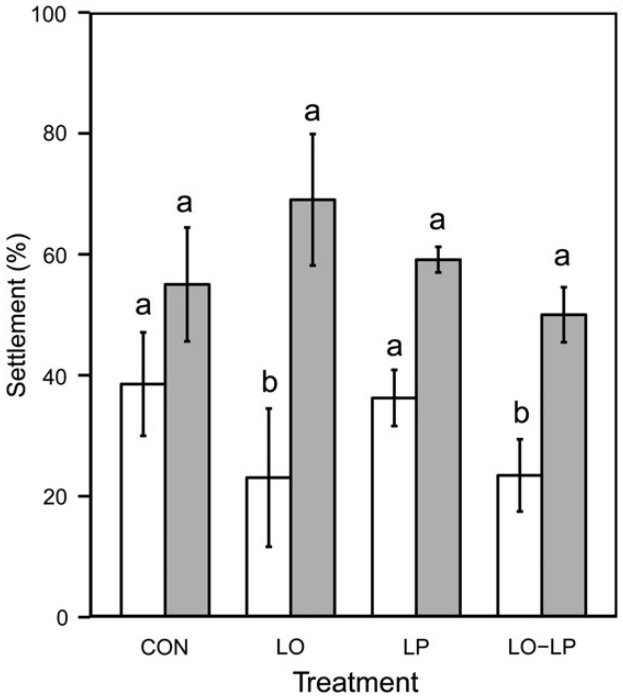

Figure 4. Settlement percentage in cyprid larvae of *B. amphitrite* reared under control (CON), LO, low-pH (LP), and low oxygen – low-pH (LO – LP) conditions in clean dishes (white bars) and dishes coated with SF (grey bars). CON and LP treatments had six replicate tanks, whereas the LO and LO – LP treatments had five replicates. Each replicate tank contained 6 bioassay Petri dishes with 25 cyprids each: 3 clean dishes and 3 coated with SF. The settlement (%) in each tank were averaged among the three Petri dishes and the data analysed and presented are means ± s.e. of the replicate culture tanks. Different lower case letters represent significant differences obtained from multiple comparisons Tukey's test following a three-way ANOVA (Supplementary Table S2).

studies (e.g. Holm *et al.*, 2000), our study was able to detect the negative effect of LO on larval developmental rates, which were then restored when the two stressors were experienced simultaneously.

Nonetheless, cyprid larvae were found on day 4 of development in the cultures of all treatments. In a pilot study conducted at 25°C (3°C lower than this study), we saw that pH 7.5 (0.1 units lower than this study) combined with LO delayed the time from nauplii to cyprids by 1 d. The slowed development due to this interaction was observed in the early larval stages, persisted into the competent cyprid stage and further to the benthic phase: larvae cultured at pH 7.5 and 3 mg O_2 l^{-1} ($T = 25$°C, salinity = 33) developed slower, stored almost half of the lipids [measured as index (%)] compared with control conditions and, although it did not translate into differential settlement rate, it significantly reduced the early juvenile growth and calcification (Campanati *et al.*, unpublished data). The differences between the developmental delays in the two experiments may have resulted from differences in temperature between the two experiments; optimal temperature benefits individual responses to stress (Pörtner and Farrell, 2008; Vaquer-Sunyer and Duarte, 2008) and temperature-dependent hypoxaemia has been reported for crustaceans (reviewed in Pörtner, 2010). However, further experiments with temperature as a factor are required to confirm the role of temperature and its interaction with pH and LO in the responses observed.

In the study presented here, larvae in the LO–LP treatment doubled their feeding rate, possibly indicating a higher metabolic

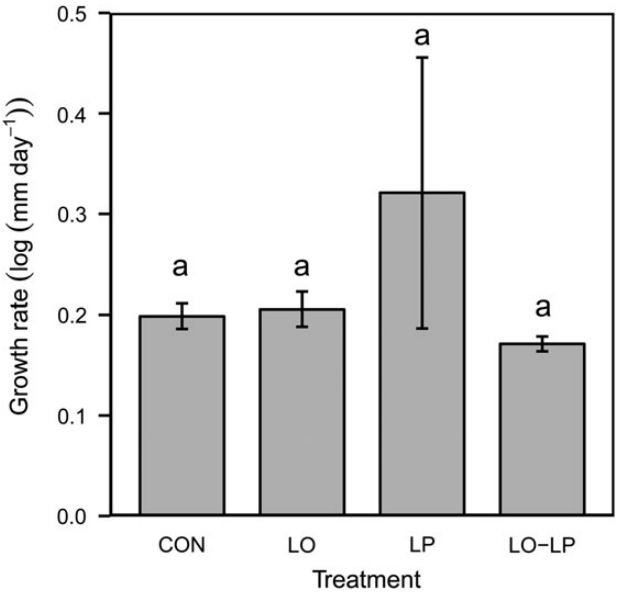

Figure 5. Post-settlement juvenile GRs [log (mm d^{-1})] of *B. amphitrite* reared under control (CON), low-oxygen (LO), low-pH (LP), and low-oxygen – low-pH (LO – LP) conditions. Juvenile GR was calculated as the regression coefficient of the exponential relationship between basal shell diameter (mm) and time (days post-settlement) for each replicate culture tank ($n = 5$ in LO and LOLP, whereas $n = 6$ in CON and LP) and averaged within treatment conditions. Lower case letters denote no difference found among treatments through one-way KW test.

need to compensate the external environmental stress in the early stages. This phenotypic buffering could have ensured that the larvae had sufficient energy stored for normal development and a successful pelagic–benthic transition. High food availability under low pH or LO has already been shown to increase an individual's resistance to these stressors (e.g. Desai and Prakash, 2009; Pansch *et al.*, 2014). Feeding rates were not affected at pH 7.6 in the larvae of the caridean shrimp *Pandalus borealis,* but increased significantly when low pH was coupled with higher temperatures (Arnberg *et al.*, 2013). On the other hand, exposure to LO decreased ingestion rates of juveniles of the horseshoe crab *Tachypleus tridentus* (Shin *et al.*, 2014) and adults of the mud snail *Nassarius festivus* (Cheung *et al.*, 2008) at O_2 levels of 4 and 3 mg l^{-1}, respectively. At DO levels lower than those in our study (1 and 0.5 vs. 3 mg O_2 l^{-1}), *B. amphitrite* nauplii lowered their metabolism by reducing their feeding rate and oxygen consumption while increasing the activity of antioxidant enzymes (Desai and Prakash, 2009). This suggests that the levels of pH and DO used here did not constitute critical levels for the barnacle nauplii to maintain the physiological function, but instead we found that increased ingestion was sufficient to acquire the energy storage necessary for the following life stages.

Cyprid energy reserves were not affected by the levels of pH and oxygen used in this study, indicating that the decreased settlement observed in LO treatments may not be due to the amounts of energy stored, as has been the case in previous studies regarding food levels, salinity, temperature, and cyprid age (reviewed in Thiyagarajan, 2010). Interestingly, by comparing the larval settlement in dishes with no biofilm and those with SF, we found a

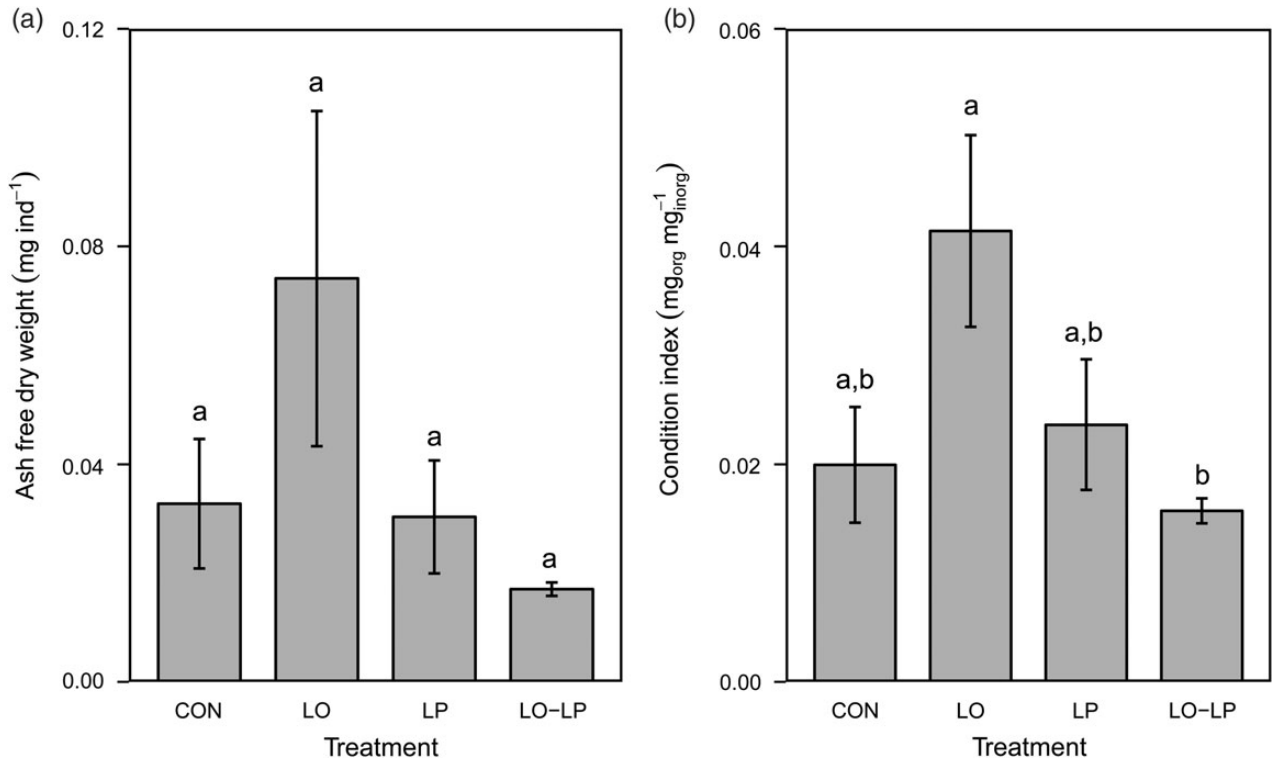

Figure 6. (a) Juvenile ash-free DW (mg ind.$^{-1}$) and (b) CI (mg $_{organic}$ × mg $^{-1}_{inorganic}$) of *B. amphitrite* on day 15 of development under control (CON), low-oxygen (LO), low-pH (LP), and low-oxygen – low-pH (LO – LP) conditions. Data are means ± s.e. of the replicate culture tanks ($n = 5$ in LO and LO – LP treatments, $n = 6$ in CON and LP). Different lower case letters illustrate significant differences ($p < 0.05$) among treatments found through multiple comparisons Tukey's test following a two-way ANOVA (Table 2; Supplementary Table S4).

significant interaction between LO and dish type. Conspecific SF contains the Settlement Inducing Protein Complex (SIPC; Matsumura *et al.*, 1998), within which arthropodin has been singled out as the "barnacle settlement pheromone" (reviewed in Hadfield, 2011). As a positive external cue for the recruitment of barnacle larvae on a substrate, it seemed to counteract the negative effects of LO, which otherwise inhibited the settlement process. Reduced larval settlement (i.e. attachment and metamorphosis) in LO conditions has been observed in many marine invertebrates such as the scallop *Argopecten irradians* and hard clam *Mercenaria mercenaria* (Gobler *et al.*, 2014), the mud snail *N. festivus* (Chan *et al.*, 2008), and the crab *Portunus trituberculatus* (Ariyama and Secor, 2010). Interestingly, the interaction of LO (2.8 mg l^{-1}) and low pH (7.6) had no effects on *Hydroides elegans*; however, the larvae altered their proteome and protein phosphorylation status (Mukherjee *et al.*, 2013). Similarly, proteome plasticity may have enabled *B. amphitrite* larvae to cope with low pH stress (pH 7.6; Wong *et al.*, 2011), in agreement with previous studies where no pH influence on larval settlement was detected on *B. amphitrite* (McDonald *et al.*, 2009; Lane *et al.*, unpublished data) and *A. improvisus* (Pansch *et al.*, 2012). The effect of LO, reducing the settlement by 23%, while pH made no significant difference, may indicate that barnacles are less adapted to LO than low pH conditions.

Our results suggest that LO neither reduced the energy available to the competent larvae for settlement nor did it impair their sensory capacity to perceive external cues, as indicated by their successful responses to the SF. It may be, then, that the low O_2 environments are indicative of poor habitats. Hence, rather than settle in a suboptimal location, the larvae could choose to continue searching for appropriate conditions. In support of this, adaptive avoidance behaviour such as a change in swimming pattern has been seen in gastropod larvae exposed to DO levels of 3–4 mg l^{-1} (Chan *et al.*, 2008; Liu *et al.*, 2011). Moreover, Hadfield (2011) showed that larvae in clean dishes, contrary to biofilmed dishes, do not touch the surfaces but instead swim in straight lines. If true, LO could pose a trade-off between the attractiveness of the substrate cues and those of the planktonic environment. Furthermore, during the settlement process, cyprids also respond to "foot prints", or the temporary adhesive, left by cyprids that have previously explored the substrate (Clare and Matsumura, 2000), and these footprints contain the same glycoprotein found in adult shells (Hadfield, 2011). It may be then that in the LO treatments, the "foot printing" was reduced and therefore the release of the glycoprotein was also reduced. It is known that *B. amphitrite* cyprid larvae, to successfully attach and metamorphose, utilize ~4–5 mJ ind.$^{-1}$ of their stored energy (Thiyagarajan *et al.*, 2003); however, the amount of energy invested in substrate selection remains unknown (Thiyagarajan, 2010). Behavioural observations coupled with settlement bioassay should be implemented to better understand the impaired attachment and metamorphosis. The selection of favourable sites on which to settle is essential for all sessile marine invertebrates to ensure successful survival and reproduction (Hadfield and Paul, 2001). Therefore, understanding the sensory ability of larvae to perceive and respond to cues under multiple stressors is essential to predict recruitment patterns in future climatic scenarios. We showed that LO levels more than low pH represent a threat in the settlement process for *B. amphitrite* larvae.

Finally, juvenile growth was not affected by any treatment, but the interaction between low pH and LO did influence the juvenile CI, which represents the proportion of organic weight to inorganic weight. In particular, different CI were found between LO and LO–LP treatments. Organic content (AFDW) was on average lower in LO–LP compared with LO treatment; however, the difference could not be detected due to high variance in the LO treatment. McDonald *et al.* (2009) found weaker lateral shearing force of juvenile *B. amphitrite* shells reared at pH 7.4, indicating differences in adherence strength, and possibly compromised calcification. None of the low pH treatments in our study were under-saturated in regard to calcite or aragonite, which may explain why we did not observe similar effects of pH on calcification in our study. Nonetheless, we found that the combination of low pH and LO significantly decreased *B. amphitrite* juvenile CI compared with the low-oxygen condition alone. This could arise from less or weaker calcified structures developed under the interaction of the two stressors, which would increase the barnacle susceptibility to predators (Connell, 1970; Grey *et al.*, 2007). Warming and elevated pCO_2 did not affect the GR in *Semibalanus balanoides*, but the survival and the shell's calcium content were lowered in this species when exposed to both of the stressors (Findlay *et al.*, 2009, 2010). On the other hand, in *Elminius modestus*, a reduction in growth was observed when the barnacles were exposed to low pH alone, but the survival and shell mineralogy were not impacted, also when low pH was combined with an increased temperature (Findlay *et al.*, 2010). In populations of *A. improvisus*, high CO_2/low pH did not affect the CI (Pansch *et al.*, 2014), whereas warming alone had an impact (Pansch *et al.*, 2013).

Low pH and LO, acting in synergy, have been predicted to be additive (Pörtner, 2005). LO was the major driver of the negative impacts observed on the early-life stages of *B. amphitrite* in this study and in some traits (i.e. larval development), low pH seemed to ameliorate the negative effects of LO.

LO in coastal waters is occurring more frequently (Huang *et al.*, 2003), potentially in conjunction with low pH, both simultaneously acting to affect benthic organisms as they spawn and settle (Levin *et al.*, 2009; Ekau *et al.*, 2010; Spicer, 2014). Therefore, in situations where food is not plentiful, future scenarios involving both pH and LO have the potential to affect the success of population recruitment (Shin *et al.*, 2014). However, as highlighted by Gobler *et al.* (2014), the co-occurring acidification of waters, following bacterial respiration in eutrophic basins (Cai *et al.*, 2011; Rabalais *et al.*, 2014), are not often considered in hypoxia studies. Likewise, very few others have examined the interaction between high CO_2/low pH and LO on early-life stages (e.g. Mukherjee *et al.*, 2013; Rosa *et al.*, 2013; Gobler *et al.*, 2014). We have tested the interactive effect of environmentally relevant seawater pH and DO levels on pre- and post-settlement stages of the barnacle, *B. amphitrite*. Our results emphasize the importance of evaluating the interactive effects of low pH and LO and avoiding underestimation of the sensitivity of organisms to OA and associated climate change stressors.

Supplementary data

Supplementary material is available at the *ICESJMS* online version of the manuscript.

Acknowledgements

The authors would like to thank Dr Dineshram Ramadoss for the valuable help in SF-protein quantification, Profs. Maria Byrne and Lisa Levin for useful comments, which improved the experimental design for this study. Thanks to P. Sriyutha Murthy (BARC, Kalpakkam India) for proofreading the manuscript. We are grateful

to two anonymous reviewers and the editor who offered several constructive comments and criticism on the previous version of this paper. This work is jointly supported by the Research Grants Committee of the Hong Kong Special Administration Region (HKSAR) via General Research Funding Scheme (Project No. 705511P; 705112P; and 17304914).

References

Ariyama, H., and Secor, D. H. 2010. Effect of environmental factors, especially hypoxia and typhoons, on recruitment of the gazami crab *Portunus trituberculatus* in Osaka Bay, Japan. Fisheries Science, 76: 315–324.

Arnberg, M., Calosi, P., Spicer, J. I., Tandberg, A. H. S., Nilsen, M., Westerlund, S., and Bechmann, R. K. 2013. Elevated temperature elicits greater effects than decreased ph on the development, feeding and metabolism of northern shrimp (*Pandalus borealis*) larvae. Marine Biology, 160: 2037–2048.

Bishop, M. W. H. 1950. Distribution of *Balanus amphitrite* Darwin var. denticulata Broch. Nature, 165: 409–410.

Brewer, P. G., and Peltzer, E. T. 2009. Limits to marine life. Science, 324: 347–348.

Byrne, M. 2012. Global change ecotoxicology: identification of early life history bottlenecks in marine invertebrates, variable species responses and variable experimental approaches. Marine Environmental Research, 76: 3–15.

Byrne, M., Prowse, T. A. A., Sewell, M. A., Dworjanyn, S., Williamson, J. E., and Vaïtilingon, D. 2008. Maternal provisioning for larvae and larval provisioning for juveniles in the toxopneustid sea urchin *Tripneustes gratilla*. Marine Biology, 155: 473–482.

Cai, W-J., Hu, X., Huang, W-J., Murrell, M. C., Lehrter, J. C., Lohrenz, S. E., Chou, W-C., *et al.* 2011. Acidification of subsurface coastal waters enhanced by eutrophication. Nature Geoscience, 4: 766–770.

Caldeira, K., and Wickett, M. E. 2003. Oceanography: anthropogenic carbon and ocean pH. Nature, 425: 365.

Chan, H. Y., Xu, W. Z., Shin, P. K. S., and Cheung, S. G. 2008. Prolonged exposure to low dissolved oxygen affects early development and swimming behaviour in the gastropod *Nassarius festivus* (Nassariidae). Marine Biology, 153: 735–743.

Chen, Z-F., Zhang, H., Wang, H., Matsumura, K., Wong, Y. H., Ravasi, T., and Qian, P-Y. 2014. Quantitative proteomics study of larval settlement in the barnacle *Balanus amphitrite*. PLoS ONE, 9: e88744.

Cheung, S. G., Chan, H. Y., Liu, C. C., and Shin, P. K. S. 2008. Effect of prolonged hypoxia on food consumption, respiration, growth and reproduction in marine scavenging gastropod *Nassarius festivus*. Marine Pollution Bulletin, 57: 280–286.

Clare, A. S., and Matsumura, K. 2000. Nature and perception of barnacle settlement pheromones. Biofouling, 15: 57–71.

Connell, J. H. 1970. A predator–prey system in the marine intertidal region. I. *Balanus glandula* and several predatory species of *Thais*. Ecological Monographs, 40: 49–78.

Coughlan, J. 1969. The estimation of filtering rate from the clearance of suspensions. Marine Biology, 2: 356–358.

Crain, C. M., Kroeker, K., and Halpern, B. S. H. 2008. Interactive and cumulative effects of multiple human stressors in marine systems. Ecology Letters, 11: 1304–1315.

Davenport, J., and Irwin, S. 2003. Hypoxic life of intertidal acorn barnacles. Marine Biology, 143: 555–563.

Desai, D. V., and Prakash, S. 2009. Physiological responses to hypoxia and anoxia in *Balanus amphitrite* (Cirripedia: Thoracica). Marine Ecology Progress Series, 390: 157–166.

Diaz, R. J., and Rosenberg, R. 2008. Spreading dead zones and consequences for marine ecosystems. Science, 321: 926–929.

Dickson, A. G., and Millero, F. J. 1987. A comparison of the equilibrium constants for the dissociation of carbonic acid in seawater media. Deep Sea Research, 34: 1733–1743.

Doney, S. C. 2010. The growing human footprint on coastal and open-ocean biogeochemistry. Science, 328: 1512–1516.

Doney, S. C., Ruckelshaus, M., Duffy, J. E., Barry, J. P., Chan, F., English, C. A., Galindo, H. M., *et al.* 2012. Climate change impacts on marine ecosystems. Annual Review of Marine Science, 4: 11–37.

Dupont, S., Dorey, N., Stumpp, M., Melzner, F., and Thorndyke, M. 2013. Long-term and trans-life-cycle effects of exposure to ocean acidification in the green sea urchin *Strongylocentrotus droebachiensis*. Marine Biology, 160: 1835–1843.

Ekau, W., Auel, H., Pörtner, H-O., and Gilbert, D. 2010. Impacts of hypoxia on the structure and processes in pelagic communities (zooplankton, Macro-Invertebrates and Fish). Biogeosciences, 7: 1669–1699.

EPOCA. 2010. Guide to Best Practices for Ocean Acidification Research and Data Reporting. Ed. by U. Riesbell, V. J. Fabry, L. Hansson, and J-P. Gattuso. Publication office of the European Union, Luxembourg. 260 pp.

Findlay, H. S., Kendall, M. A., Spicer, J. I., and Widdicombe, S. 2009. "Future high CO_2 in the intertidal may compromise adult barnacle *Semibalanus balanoides* survival and embryonic development rate. Marine Ecology Progress Series, 389: 193–202.

Findlay, H. S., Kendall, M. A., Spicer, J. I., and Widdicombe, S. 2010. Post-larval development of two intertidal barnacles at elevated CO_2 and temperature. Marine Biology, 157: 725–735.

Gilbert, D., Rabalais, N. N., Díaz, R. J., and Zhang, J. 2010. Evidence for greater oxygen decline rates in the coastal ocean than in the open ocean. Biogeosciences, 7: 2283–2296.

Gobler, C. J., DePasquale, E. L., Griffith, A. W., and Baumann, H. 2014. Hypoxia and acidification have additive and synergistic negative effects on the growth, survival, and metamorphosis of early life stage bivalves. PLoS ONE, 9: e83648.

Gray, J. S., Wu, R. S. S., and Or, Y. Y. 2002. Effects of hypoxia and organic enrichment on the coastal marine environment. Marine Ecology Progress Series, 238: 249–279.

Grey, M., Lelievre, P. G., and Boulding, E. G. 2007. Selection for prey shell thickness by the naticid gastropod *Euspira lewisii* (Naticidae) on the bivalve *Protothaca staminea* (Veneridae). Veliger, 48: 317–322.

Hadfield, M. G. 2011. Biofilms and marine invertebrate larvae: what bacteria produce that larvae use to choose settlement sites. Annual Review of Marine Science, 3: 453–470.

Hadfield, M. G., and Paul, V. J. 2001. Natural chemical cues for settlement and metamorphosis of marine invertebrate larvae. *In* Marine Chemical Ecology, pp. 431–461. Ed. by J. B. McClintock, and W. Baker. CRC Press, New York.

Hall-Spencer, J. M., Rodolfo-Metalpa, R., Martin, S., Ransome, E., Fine, M., Turner, S. M., Rowley, S. J., *et al.* 2008. Volcanic carbon dioxide vents show ecosystem effects of ocean acidification. Nature, 454: 96–99.

Harley, C. D. G., Hughes, A. R., Hultgren, K. M., Miner, B. G., Sorte, C. J. B., Thornber, C. S., Rodriguez, L. F., *et al.* 2006. The impacts of climate change in coastal marine systems. Ecology Letters, 9: 228–241.

HKEPD. 2014. Marine Water Quality in Hong Kong. Hong Kong Government Printer, Hong Kong. http://epic.epd.gov.hk/EPICRIVER/marine/?lang=en.

Hofmann, G. E., Barry, J. P., Edmunds, P. J., Gates, R. D., Hutchins, D. A., Klinger, T., and Sewell, M. A. 2010. The effect of ocean acidification on calcifying organisms in marine ecosystems: an organism-to-ecosystem perspective. Annual Review of Ecology, Evolution, and Systematics, 41: 127–147.

Holland, D. L. 1978. Lipid reserves and energy metabolism in the larvae of benthic marine invertebrates. Biochemical and Biophysical Perspectives in Marine Biology, 4: 85–123.

Holm, E. R., McClary, M., and Rittschof, D. 2000. Variation in attachment of the barnacle *Balanus amphitrite*: sensation or something else? Marine Ecology Progress Series, 202: 153–162.

Howarth, R., Chan, F., Conley, D. J., Garnier, J., Doney, S. C., Marino, R., and Billen, G. 2011. Coupled biogeochemical cycles: eutrophication and hypoxia in temperate estuaries and coastal marine ecosystems. Frontiers in Ecology and the Environment, 9: 18–26.

Huang, X. P., Huang, L. M., and Yue, W. Z. 2003. The characteristics of nutrients and eutrophication in the Pearl River Estuary, South China. Marine Pollution Bulletin, 47: 30–36.

IPCC. 2014. Climate Change 2014: Synthesis Report. Contribution of Working Groups I, II and III to the Fifth Assessment Report of the Intergovernmental Panel on Climate Change. Ed. by Core Writing Team, R. L. Pachauri, and L. A. Meyer. IPCC, Geneva, Switzerland. 151 pp.

Ishimatsu, A., and Dissanayake, A. 2010. Life threatened in acidic coastal waters. A. Ishimatsu, and H. J. Lie (eds) *In* Coastal Environmental and Ecosystem Issues of the East China Sea. TERRAPUB and Nagasaki University, Tokyo, pp. 283–303.

Ko, G. W. K., Dineshram, R., Campanati, C., Chan, B. S. V., Havenhand, J., and Thiyagarajan, V. 2014. Interactive effects of ocean acidification, elevated temperature and reduced salinity on early-life stages of the Pacific oyster. Environmental Science and Technology, 48: 10079–10088.

Kroeker, K. J., Kordas, R. L., Crim, R. N., and Singh, G. G. 2010. Meta-analysis reveals negative yet variable effects of ocean acidification on marine organisms: biological responses to ocean acidification. Ecology Letters, 13: 1419–1434.

Levin, L. A., Ekau, W., Gooday, A. J., Jorissen, F., Middelburg, J. J., Naqvi, S. W. A., Neira, C., *et al.* 2009. Effects of natural and human-induced hypoxia on coastal benthos. Biogeosciences, 6: 2063–2098.

Liu, C. C., Chiu, J. M. Y., Li, L, Shin, P. K. S., and Cheung, S. G. 2011. Respiration rate and swimming activity of larvae of two sub-tidal nassariid gastropods under reduced oxygen levels: implications for their distributions in Hong Kong waters. Marine Pollution Bulletin, 63: 230–236.

Lucas, M. I., Walker, G., Holland, D. L., and Crisp, D. J. 1979. An energy budget for the free-swimming and metamorphosing larvae of *Balanus balanoides* (Crustacea: Cirripedia). Marine Biology, 55: 221–229.

Mann, R., and Gallager, S. M. 1985. Physiological and biochemical energetics of larvae of *Teredo navalis* L. and *Bankia gouldi* (Bartsch) (Bivalvia: Teredinidae). Journal of Experimental Marine Biology and Ecology, 85: 211–228.

Marcus, N. H., Richmond, C., Sedlacek, C., Miller, G. A., and Oppert, C. 2004. Impact of hypoxia on the survival, egg production and population dynamics of *Acartia tonsa* dana. Journal of Experimental Marine Biology and Ecology, 301: 111–128.

Matsumura, K., Nagano, M., and Fusetani, N. 1998. Purification of a larval settlement-inducing protein complex (SIPC) of the barnacle, *Balanus amphitrite*. Journal of Experimental Zoology, 281: 12–20.

McDonald, M. R., McClintock, J. B., Amsler, C. D., Rittschof, D., Angus, R. A., Orihuela, B., and Lutostanski, K. 2009. Effects of ocean acidification over the life history of the barnacle *Amphibalanus amphitrite*. Marine Ecology Progress Series, 385: 179–187.

Mehrbach, C., Culberson, C. H., Hawley, J. E., and Pytkowicz, R. M. 1973. Measurement of the apparent dissociation constants of carbonic acid in seawater at atmospheric pressure. Limnology and Oceanography, 18: 897–907.

Melzner, F., Thomsen, J., Koeve, W., Oschlies, A., Gutowska, M. A., Bange, H. W., Hansen, H. P., *et al.* 2012. Future ocean acidification will be amplified by hypoxia in coastal habitats. Marine Biology, 160: 1875–1888.

Mukherjee, J., Wong, K. K. W., Chandramouli, K. H., Qian, P-Y., Leung, P. T. Y., Wu, R. S. S., and Thyiagarajan, V. 2013. Proteomic response of marine invertebrate larvae to ocean acidification and hypoxia during metamorphosis and calcification. Journal of Experimental Biology, 216: 4580–4589.

Munday, P. L., Dixson, D. L., Donelson, J. M., Jones, G. P., Pratchett, M. S., Devitsina, G. V., and Døving, K. B. 2009. Ocean acidification impairs olfactory discrimination and homing ability of a marine fish. Proceedings of the National Academy of Sciences of the United States of America, 106: 1848–1852.

Pansch, C., Nasrolahi, A., Appelhans, Y. S., and Wahl, M. 2012. Impacts of ocean warming and acidification on the larval development of the barnacle *Amphibalanus improvisus*. Journal of Experimental Marine Biology and Ecology, 420–421: 48–55.

Pansch, C., Nasrolahi, A., Appelhans, Y. S., and Wahl, M. 2013. Tolerance of juvenile barnacles (*Amphibalanus improvisus*) to warming and elevated pCO_2. Marine Biology, 160: 2023–2035.

Pansch, C., Schaub, I., Havenhand, J., and Wahl, M. 2014. Habitat traits and food availability determine the response of marine invertebrates to ocean acidification. Global Change Biology, 20: 765–777.

Pechenik, J. A. 1999. On the advantages and disadvantages of larval stages in benthic marine invertebrate life cycles. Marine Ecology Progress Series, 177: 269–297.

Pechenik, J. A., Rittschof, D., and Schmidt, A. R. 1993. Influence of delayed metamorphosis on survival and growth of juvenile barnacles *Balanus amphitrite*. Marine Biology, 115: 287–294.

Pierrot, D., Lewis, E., and Wallace, D. W. R. 2006. MS Excel Program Developed for CO2 System Calculations. ORNL/CDIAC-105a. Carbon Dioxide Information Analysis Center, Oak Ridge National Laboratory, US Department of Energy, Oak Ridge, TN.

Pörtner, H-O. 2005. Synergistic effects of temperature extremes, hypoxia, and increases in co_2 on marine animals: from earth history to global change. Journal of Geophysical Research, 110(C9): S10.

Pörtner, H-O. 2010. Oxygen- and capacity-limitation of thermal tolerance: a matrix for integrating climate-related stressor effects in marine ecosystems. Journal of Experimental Biology, 213: 881–893.

Pörtner, H-O., and Farrell, A. P. 2008. Physiology and climate change. Science, 322: 690–692.

R Core Team. 2015. R: a Language and Environment for Statistical Computing. R Foundation for Statistical Computing, Vienna, Austria. http://www.R-project.org/.

Rabalais, N. N., Cai, W-J., Carstensen, J., Conley, D. J., Fry, B., Hu, X., Quiñones-Rivera, Z., *et al.* 2014. Eutrophication-driven deoxygenation in the coastal ocean. Oceanography, 27: 172–183.

Rittschof, D., Branscomb, E. S., and Costlow, J. D. 1984. Settlement and behaviour in relation to flow and surface in larval barnacles, *Balanus amphitrite* Darwin. Journal of Experimental Marine Biology and Ecology, 82: 131–146.

Rosa, R., Trubenbach, K., Repolho, T., Pimentel, M., Faleiro, F., Boavida-Portugal, J., Baptista, M., *et al.* 2013. Lower hypoxia thresholds of cuttlefish early life stages living in a warm acidified ocean. Proceedings of the Royal Society B: Biological Sciences, 280: 20131695.

Schneider, C. A., Rasband, W. S., and Eliceiri, K. W. 2012. NIH Image to ImageJ: 25 years of image analysis. Nature Methods, 9: 671–675.

Shin, P. K. S., Chan, C. S. K., and Cheung, S. G. 2014. Physiological energetics of the fourth instar of Chinese horseshoe crabs (*Tachypleus tridentatus*) in response to hypoxic stress and re-oxygenation. Marine Pollution Bulletin, 85: 522–525.

Spicer, J. I. 2014. What can an ecophysiological approach tell us about the physiological responses of marine invertebrates to hypoxia? Journal of Experimental Biology, 217: 46–56.

Stumpp, M., Wren, J., Melzner, F., Thorndyke, M. C., and Dupont, S. 2011. CO_2 induced seawater acidification impacts sea urchin larval development I: elevated metabolic rates decrease scope for growth and induce developmental delay. Comparative Biochemistry and Physiology Part A: Molecular and Integrative Physiology, 160: 331–340.

Talmage, S. C., and Gobler, C. J. 2010. Effects of past, present, and future ocean carbon dioxide concentrations on the growth and survival of larval shellfish. Proceedings of the National Academy of Sciences of the United States of America, 107: 17246–17251.

Thiyagarajan, V. 2010. A review on the role of chemical cues in habitat selection by barnacles: new insights from larval proteomics. Journal of Experimental Marine Biology and Ecology, 392: 22–36.

Thiyagarajan, V., Harder, T., and Qian, P-Y. 2002. Relationship between cyprid energy reserves and metamorphosis in the barnacle *Balanus amphitrite* Darwin (Cirripedia; Thoracica). Journal of Experimental Marine Biology and Ecology, 280: 79–93.

Thiyagarajan, V., Harder, T., and Qian, P-Y. 2003. Combined effects of temperature and salinity on larval development and attachment of the subtidal barnacle *Balanus trigonus* Darwin. Journal of Experimental Marine Biology and Ecology, 287: 223–236.

Thiyagarajan, V., Pechenik, J. A., Gosselin, L. A., and Qian, P-Y. 2007. Juvenile growth in barnacles: combined effect of delayed metamorphosis and sub-lethal exposure of cyprids to low-salinity stress. Marine Ecology Progress Series, 344: 173–184.

Vaquer-Sunyer, R., and Duarte, C. M. 2008. Thresholds of hypoxia for marine biodiversity. Proceedings of the National Academy of Sciences of the United States of America, 105: 15452–15457.

Walther, K., Anger, K., and Pörtner, H-O. 2010. Effects of ocean acidification and warming on the larval development of the spider crab *Hyas araneus* from different latitudes (54° vs. 79°N). Marine Ecology Progress Series, 417: 159–170.

Whiteley, N. M. 2011. Physiological and ecological responses of crustaceans to ocean acidification. Marine Ecology Progress Series, 430: 257–271.

Wong, K. K. W., Lane, A. C., Leung, P. T. Y., and Thiyagarajan, V. 2011. Response of larval barnacle proteome to CO_2-driven seawater acidification. Comparative Biochemistry and Physiology Part D: Genomics and Proteomics, 6: 310–321.

Yin, K. 2002. Monsoonal influence on seasonal variations in nutrients and phytoplankton biomass in coastal waters of Hong Kong in the vicinity of the Pearl River estuary. Marine Ecology Progress Series, 245: 111–122.

Yung, Y-K., Wong, C. K., Yau, K., and Qian, P. Y. 2001. Long-term changes in water quality and phytoplankton characteristics in Port Shelter, Hong Kong, from 1988–1998. Marine Pollution Bulletin, 42: 981–992.

Handling editor: Stéphane Plourde

ICES Journal of Marine Science

ICES Journal of Marine Science (2016), 73(3), 803–813. doi:10.1093/icesjms/fsv213

Contribution to Special Issue: 'Towards a Broader Perspective on Ocean Acidification Research'

Original Article

Tropical crustose coralline algal individual and community responses to elevated pCO_2 under high and low irradiance

Elizabeth Dutra[1], Marguerite Koch[1]*, Katherine Peach[1], and Carrie Manfrino[2,3,4]

[1]*Department of Biological Sciences, Florida Atlantic University, 777 Glades Road, Boca Raton, FL 33431, USA*
[2]*Central Caribbean Marine Institute, (US) PO Box 1461, Princeton, NJ 08542, USA*
[3]*Little Cayman Research Centre, North Coast Road, PO Box 37, Little Cayman KY3-2501, Cayman Islands*
[4]*School of Environmental and Sustainability Sciences, Kean University, 1000 Morris Ave., Union, NJ 07083, USA*

Corresponding author: tel: +1 561-297-3325; e-mail: mkoch@fau.edu

Dutra, E., Koch, M., Peach, K., and Manfrino, C. Tropical crustose coralline algal individual and community responses to elevated pCO_2 under high and low irradiance. – ICES Journal of Marine Science, 73: 803–813.

Received 6 April 2015; revised 28 October 2015; accepted 28 October 2015; advance access publication 7 December 2015.

Crustose coralline algae (CCA) cement reefs and create important habitat and settling sites for reef organisms. The susceptibility of CCA to increasing ocean pCO_2 and declining pH or ocean acidification (OA) is a growing concern. Although CCA are autotrophs, there has been little focus on the interaction of elevated pCO_2 and irradiance. We examined elevated pCO_2 effects on individual CCA and macroalgal benthic communities at high and low irradiance (205–13 μmol photons m^{-2} s^{-1}) in an aquaria experiment (35 d, June–August 2014) on Little Cayman Island, Caribbean. A dominant Cayman reef wall CCA (*Peyssonnelia* sp.) in its adult lobed form and individual CCA recruits were used as experimental units. Changes in CCA, fleshy macroalgae (branching and turfs), and microalgae (including microbial biofilm) per cent cover and frequency were examined on macroalgal communities that settled onto plates from the reef. Reef diel cycles of pCO_2 and pH were simulated using seawater inflow from a back reef. Although CO_2 enrichment to year 2100 levels resulted in 1087 μatm pCO_2 in the elevated pCO_2 treatment, $CaCO_3$ saturation states remained high ($\Omega_{cal} \geq 2.7$). Under these conditions, elevated pCO_2 had no effect on *Peyssonnelia* sp. calcification rates or survival regardless of irradiance. Individual CCA surface area on the bottom of settling plates was lower under elevated pCO_2, but per cent cover or frequency within the community was unchanged. In contrast, there was a strong and consistent community assemblage response to irradiance. Microalgae increased at high irradiance and CCA increased under low irradiance with no significant pCO_2 interaction. Based on this short-term experiment, tropical macroalgal communities are unlikely to shift at pCO_2 levels predicted for year 2100 under high or low irradiance. Rather, irradiance and other factors that promote microalgae are likely to be strong drivers of tropical benthic algal community structure under climate change.

Keywords: CCA, coral reef, irradiance, Little Cayman Island, macroalgae, ocean acidification.

Introduction

Crustose coralline algae (CCA) are important components of reef structure because they encrust and bind together the framework of coral reefs with high magnesium calcite. CCA surfaces are also colonized by coral and other marine organisms allowing them to settle onto reefs (Littler and Littler, 1984; Adey, 1998). Because of their ecological importance, the susceptibility of this group to anthropogenic climate change and ocean acidification (OA) has been a growing concern over the last decade (Diaz-Pulido *et al.*, 2007; Kuffner *et al.*, 2008; Martin and Gattuso, 2009). Lower saturation states of $CaCO_3$ minerals can negatively influence calcification rates and growth in marine calcifiers (Hoegh-Guldberg *et al.*, 2007; Kuffner *et al.*, 2008; Diaz-Pulido *et al.*, 2012; Anthony *et al.*, 2013; Martin *et al.*, 2013; Comeau *et al.*, 2014a). Under a lower pH, the energetic requirements to remove H^+ generated by calcification across a steeper concentration gradient are likely to increase for calcifiers (Jokiel, 2011, 2013; Jokiel *et al.*, 2015). Regardless of the mechanism that limits calcification, there is evidence from CO_2 vent sites in the Mediterranean and Papua New Guinea that elevated pCO_2 promotes dominance by fleshy algae and seagrasses at the expense of calcifiers, including

CCA (Martin *et al.*, 2006; Hall-Spencer *et al.*, 2008; Fabricius *et al.*, 2011; Porzio *et al.*, 2011; reviewed in Koch *et al.*, 2013). The competitive superiority of fleshy macroalgae and seagrasses over calcifiers at CO_2 vents may be attributed to greater photosynthetic and growth responses to elevated pCO_2 and total DIC, or a reduction in growth of calcifiers under lower saturation states or higher energetic demands. Hall-Spencer *et al.* (2008) reported a 60% reduction in CCA and 60% increase in non-calcareous algal cover at natural volcanic CO_2 vents. Based on results from recent pCO_2 experiments and field CO_2 vent studies, fleshy macroalgae are predicted to become dominant at the expense of CCA under OA (Hall-Spencer *et al.*, 2008; Kuffner *et al.*, 2008; Martin and Gattuso, 2009; Koch *et al.*, 2013; Johnson *et al.*, 2014b; Short *et al.*, 2014; Fabricius *et al.*, 2015). A shift to fleshy algal dominance would have cascading consequences on carbonate sediment production and hard substrate availability for larval settlement, and potentially alter basic biogeochemical processes and foodweb dynamics as fleshy algal biomass increases over time.

Although the present paradigm suggests a loss of calcified algae under OA, CCA tolerance to elevated pCO_2 predicted for the year 2100 (~600–1000 μatm) is influenced by multiple factors, including the natural pH variance at collection sites, temperature, and irradiance (Martin *et al.*, 2013; Comeau *et al.*, 2014a; Johnson *et al.*, 2014a). High variance in pH and pCO_2 at vent sites contrasts modest natural variance in these parameters driven by metabolic activity, which has recently been shown to enhance OA tolerance by calcifiers (Martin *et al.*, 2013; Comeau *et al.*, 2014a; Johnson *et al.*, 2014a). CO_2 vents provide excellent field analogues to examine OA effects on benthic communities, but have limitations due to high variance (reviewed in Koch *et al.*, 2013). It is unclear if minimum pH values, at times dropping below 7.0, and high CO_2 levels (>6000 ppm), may partially account for observations of calcified algal decline at these sites. Under moderate oscillating pCO_2 from 400 to 600 μatm, CCA (*Porolithon onkodes*) calcification rates were reported by Johnson *et al.* (2014a) to be 42% higher than under constant elevated pCO_2.

Under elevated pCO_2 and temperature (30°C), high irradiance (500 μmol photons m^{-2} s^{-1}) enhanced calcification by 29% relative to low (150 μmol photons m^{-2} s^{-1}) irradiance in a tropical CCA, *Hydrolithon reinboldii* (Comeau *et al.*, 2014a). Calcification rates were maximal during high irradiance and summer temperatures in the CCA, *Lithophyllum cabiochae* (Martin *et al.*, 2013). Positive calcification responses of CCA to high summer seawater temperatures may be related to their ability to maintain elevated pH at sites of calcification via the uptake of CO_2 under high rates of photosynthesis, regardless of external pH (Hurd *et al.*, 2011; Hofmann and Bischof, 2014). This positive relationship between photosynthesis and calcification in calcifying macroalgae has been recognized for many decades (Borowitzka, 1981; Adey, 1998; Chisholm, 2000; de Beer and Larkum, 2001). If temperature or irradiance can stimulate photosynthesis, or induce proton pumps (Hofmann *et al.*, unpublished data), without becoming a stress (Diaz-Pulido *et al.*, 2012), the thalli surface microenvironment pH can be raised above bulk seawater pH and shift the carbonate equilibria to increase $[CO_3^{2-}]$ at the site of calcification (de Beer and Larkum, 2001; Hofmann and Bischof, 2014). This mechanism may sustain high net calcification rates in CCA under OA.

While irradiance can enhance CCA calcification, high irradiance also promotes fleshy algae over CCA at the community level. Many CCA species are low-irradiance-adapted and weak competitors for space during recruitment (Kuffner *et al.*, 2008). It is well established that fleshy algae can outcompete CCA on reefs (Mumby, 2009). Elevated pCO_2 and low pH also stimulate filamentous macroalgal turf dominance on coral reefs, increasing competition for space with calcifying species, including CCA (Kuffner *et al.*, 2008; Johnson *et al.*, 2014b; Short *et al.*, 2014). CCA are generally found covered by epiphytes and fleshy macroalgal canopies in shallow water habitats exposed to high irradiance (Steneck, 1986). Understanding irradiance effects on CCA tolerance to elevated pCO_2 at the individual and community level will be critical to provide predictions about CCA responses to OA.

We examined community and individual growth and calcification responses of CCA to elevated pCO_2 at high and low irradiance in an aquaria experiment (35 d) conducted on Little Cayman Island, Caribbean (June–August 2014). The experimental design incorporated natural reef pCO_2 and pH dynamics by using seawater from a fringing back reef and CO_2 added to the flow-through system to achieve year 2100 pCO_2 levels (~1000 μatm). Calcification responses to elevated pCO_2 were examined in adult individuals of the CCA *Peyssonnelia* sp. under high and low irradiance. *Peyssonnelia* sp. was chosen because of its dominance on reef walls of the Caribbean where it provides an important habitat for organisms living in cryptic, low-irradiance environments. Because *Peyssonnelia* sp. typically occupies a low irradiance niche on the reef under ledges, it was predicted to have higher tissue mortality and lower net calcification in elevated pCO_2 treatments at high irradiance. At the community level, changes in per cent cover and frequency of functional algal groups collected onto settling plates placed on an outer fore reef were determined in the aquaria experiment. Functional groups included CCA, fleshy macroalgae (branching and turfs), and microalgae (including microbial biofilm). Individual CCA surface area changes on settling plates were also determined. We hypothesized that elevated pCO_2 and high irradiance would promote fleshy turf macroalgae and microalgae dominance, while CCA would be restricted to low irradiance conditions and only represent a minor component of the community under elevated pCO_2.

Methods

Experimental units

At the individual level, calcified adult lobes of *Peyssonnelia* were the experimental units. At the community level, experimental units were settling plates (surface and bottom) onto which benthic algal communities from an outer fore reef were collected. Benthic algal communities were classified by functional group using a dissection microscope. Individual CCA adult lobes were classified to the genus level using scanning electron microscopy (SEM) and a dichotomous key (Littler and Littler, 2000). For identification of *Peyssonnelia* by SEM, CCA lobes were pre-fixed in 2% glutaraldehyde in 0.05 M sodium cacodylate-buffered seawater followed by post-fixation in 1% osmium tetroxide in buffer. Lobes were subsequently dehydrated through a series of graded ethanol concentrations (20–100%) ending in hexamethyldisilazane. Dehydrated samples were fractured to expose a cross section of the growing margin of the lobe and mounted on aluminium stubs. Stub-mounted samples were sputter coated with a platinum target and observed with a Zeiss Merlin VP Compact SEM (Max Planck Electron Microscopy Core Facility; Jupiter, FL, USA).

Field site and sample collection

Little Cayman Island (Figure 1) is a 17 km by 2 km, low-lying island 120 km northeast of Grand Cayman with expansive barrier, patch, and wall reefs in excellent condition (Manfrino *et al.*, 2013). Macroalgal communities were collected onto settling plates

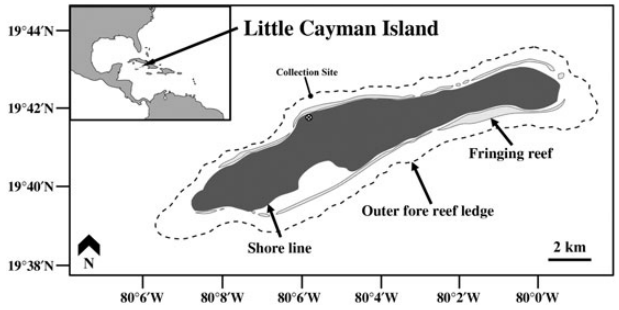

Figure 1. Location of the Little Cayman Research Center (LCRC) shown as encircled multi symbol on Little Cayman Island (LCI), located within the Caribbean Sea. The collection site shown on the map is where individual CCA lobes were collected and settling plates placed near the outer fore reef ledge of a spur and groove reef system located north of LCRC. Map design credit: Katherine Peach.

($n = 60$) deployed at an (~18 m) outer fore reef located north of the Little Cayman Research Center (LCRC) on Little Cayman Island (N19.42′01″, W80.03′34″; Figure 1). Settling plates were placed (March 2014) in a groove of a spur and groove reef, and were held above the benthos on an aluminium structure embedded in a cement block to allow for unimpeded water flow across the plates (Figure 2e). When the plates were collected for experiments (June 2014), they had calcifying (CCA) and non-calcifying (fleshy) macroalgal communities accreted on the plate surface and bottom. Because algae had settled on the surface and bottom of plates, they were fixed onto stands suspended ~4 cm above the bottom of aquaria (Figure 2b). Plates were allowed to acclimate (2–4 d) before being randomly assigned to pCO_2 and irradiance treatments.

CCA *Peyssonnelia* sp. lobes were harvested with hammer and chisel at ~18 m depth in proximity to where settling plates were deployed along the outer fore reef ledge (Figure 1). CCA lobes were gently cleaned of all visible epiphytes, photographed, and allowed to acclimate in aquaria (as above).

Experimental set-up, treatments, and monitoring

Seawater from the back reef ~250 m offshore of LCRC (Figure 1) was continuously pumped (~3000 l h^{-1}) to the experimental facility. The pump intake was positioned where the reef narrowed and seawater exchange was greatest between the fore and back reef. A 1 mm filter covered the intake and was cleaned of fouling organisms weekly. Seawater inflows were split and water flowed into two source tanks (600 l), a treatment and ambient control tank. The high CO_2 treatment tank was continuously bubbled with a mixture of air and CO_2 at a rate of 10 and 90 ml min^{-1}, respectively, with precise delivery regulated by mass flow controllers (Sierra Instruments Inc., Smart-Trak 100). The elevated pCO_2 treatment was based on the 2013 IPCC RCP 6.0 and 8.5 scenarios of a ~650–1000 μatm. All aquaria received 1.1 l seawater min^{-1} from the source tanks achieving a turnover rate of 6 times h^{-1}. The experimental system had a total of 20 aquaria each holding 11 l of seawater (Figure 2a). Half of the aquaria ($n = 10$) received ambient seawater, while the remaining half ($n = 10$) received ambient seawater enriched with CO_2. Because seawater from the reef was continuously flowing into the source tanks, the pCO_2 and pH fluctuated based on reef metabolism with elevated pCO_2 superimposed on reef metabolism in the high pCO_2 treatment.

The experiment was closely monitored daily at 8:00, 12:00, and 18:00 and four diel (24 h) sampling events (sampling every 2 h) were conducted during the experiment (data presented in Bedwell *et al.*, this issue). The pCO_2 concentrations in the ambient and CO_2-enriched source tanks were measured by infrared gas analyser (Qubit S151) within the headspace of an equilibrator. To facilitate semi-continuous monitoring of pCO_2, equilibrators were hung above each source tank and water from the tank was continuously cycled through the equilibrator with a small submersible pump. In addition to pCO_2, daily temperature and pH_{NST} (Orion Star AS11; Ross Ultra Triode Probe) measurements were made in each of the source tanks at 8:00, 12:00, and 18:00. Tests were conducted to compare water chemistry between source tanks and aquaria verifying that our turnover rate (6 h^{-1}) was fast enough to preclude any change in treatments from source tanks to aquaria and across all aquaria. Rapid turnover rates and water bath tables with flow-through seawater maintained aquaria temperatures within 0.1°C of ambient seawater from source tanks and among aquaria.

Oxygen concentrations were also measured weekly (Thermo Scientific Orion; RDO; 3 M) and total alkalinity (TA) determined at the beginning of the experiment by titration (Titrando® Metrohm USA, Inc.) in a jacketed beaker maintained at 25°C and certified with reference material (CRM) (Andrew Dickson Lab, Scripps Institute of Oceanography). DIC species and the saturation state of calcite (Ω_{cal}) were calculated with CO2SYS (Pierrot *et al.*, 2006), including measured conductivity (YSI 3100). Back reef TA samples were preserved in $HgCl_2$ (0.02% volume-saturated solution) and transported by air to the lab (FAU) for titrations. Although TA was only measured at the beginning of the experiment, a test of diurnal TA change (08:00, 12:00, 18:00) was conducted and the variance ($\pm$20–30 μmol kg^{-1}) was close to our level of detection $\pm$10 μmol kg^{-1} in this open water flow-through system. Therefore, reef metabolism was the major driver of pCO_2 dynamics and the calcification signal (TA change) on the open reef was not within our limits of detection. Further, recalculating calcite saturation states using our maximum variance ($\pm$30 μmol kg^{-1}) through CO2SYS only shifted saturation states by <0.1 which was within our sample variance (0.4–0.6, Table 1).

The irradiance treatment (high and low irradiance) was achieved by adding shade cloth around half of each aquarium (Figure 2a and b). The high irradiance corresponded to saturation of *Peyssonnelia* sp. photosynthesis (200–300 μmol photons m^{-2} s^{-1}) and the low irradiance treatment was ~10 μmol photons m^{-2} s^{-1} above the photosynthetic compensation point (I_c = ~50 μmol photons m^{-2} s^{-1}) for this species (MK, unpublished data). The irradiance where the plates were placed and lobes collected based on light extinction (566 μmol photons m^{-2} s^{-1}; $y = 1804e^{-0.058}$; $r^2 = 0.97$) was higher than *Peyssonnelia* sp. saturation. However, this species is primarily found under ledges at the site, and the CCA that colonized on our plates in the field was greatest on the underside in the shade. Therefore, the high irradiance treatment used for this experiment corresponded to *Peyssonnelia* sp. saturation, rather than irradiance on the sandy carbonate bottom at the collection site.

The irradiance reaching plates in the aquaria under high and low irradiance conditions was measured using a spherical 4-π sensor (LI-COR). As the larger 4-π sensor would not fit under plates, irradiance on the bottom of each plate was determined by calculating the extinction between the upper and lower plate with a small submersible 2-π sensor (Ocean Optics USB2000) and multiplying this fraction by the 4-π sensor surface readings. The irradiance readings were: (i) 205 $\pm$ 34 μmol photons m^{-2} s^{-1} on the surface of the plates in high irradiance treatment, (ii) 64 $\pm$ 8 μmol photons m^{-2} s^{-1} on the surface of the plates in low irradiance

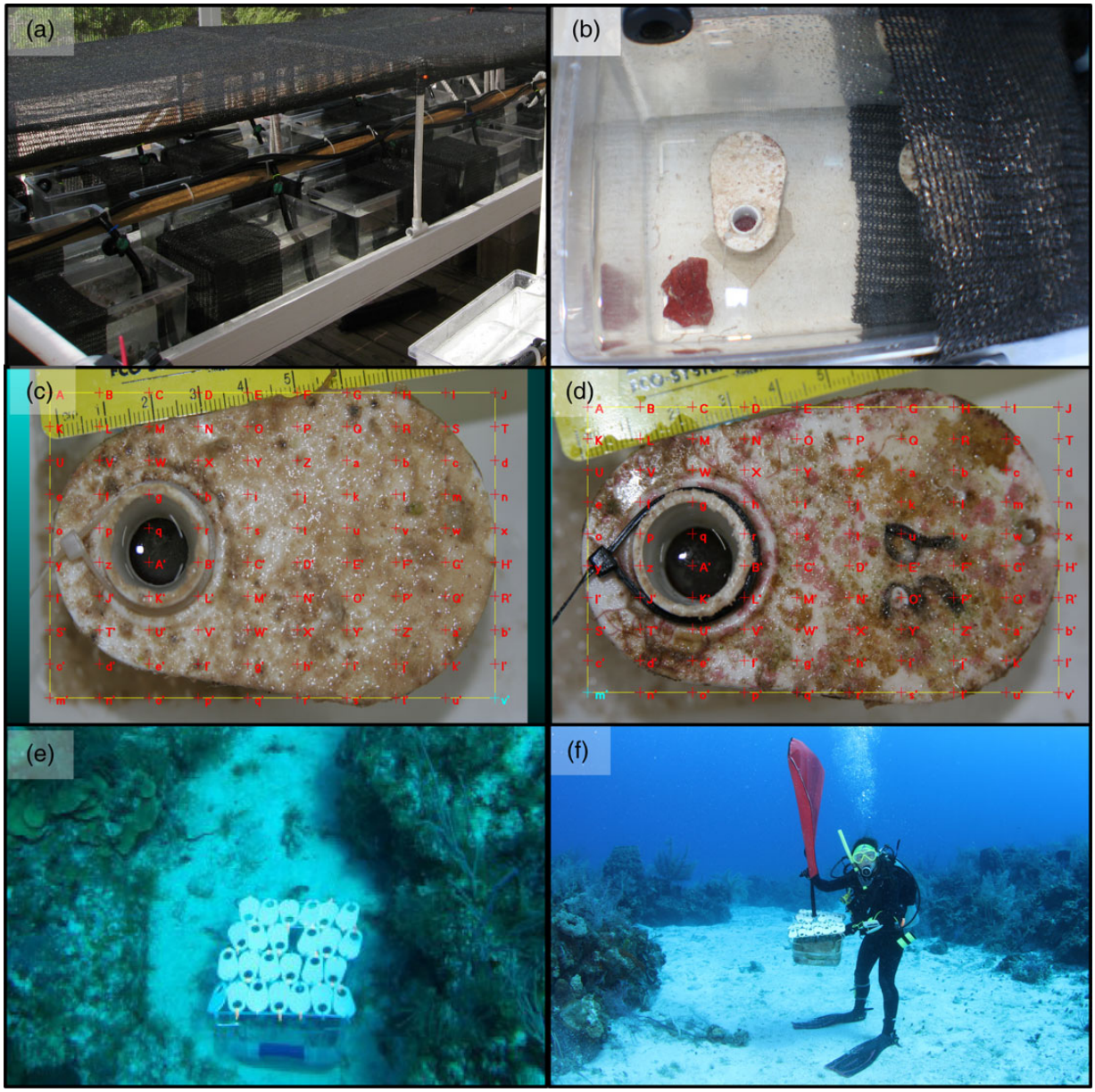

Figure 2. (a) Experimental design showing random placement of aquaria receiving elevated pCO_2 ($n = 10$) or ambient seawater ($n = 10$) under high and low irradiance. (b) High and low irradiance treatments were achieved by shading one half of each aquarium. (c) The surfaces of settling plates in the high irradiance treatment were dominated by microalgae, (d) while the bottoms of the plates had CCA that were individually tracked for changes in surface area in response to treatments. A total of 100 points was randomly distributed across images of plates (15 cm^2) and analysed with CPCe (see text). (e and f) Settling plates were deployed in March 2014 in a sandy groove of a spur and groove outer fore reef system and retrieved in June 2014.

treatment, (iii) 92 μmol photons m^{-2} s^{-1} on the bottom of the plates in the high irradiance treatment, and (iv) 13 μmol m^{-2} s^{-1} on the bottom of the plates in the low irradiance treatment. The irradiance levels were measured at mid-day on a clear day. Four irradiance measurements were taken in each aquarium, two in the low irradiance treatment (surface and bottom of plate) and two in the high irradiance treatment (surface and bottom of plate). There were significant differences in the high and low irradiance treatments and on the surface and bottom of the plates. Each of these average mid-day measurements were based on $n = 20$.

Biological response variables

Peyssonnelia lobe tissue and calcification analysis

Peyssonnelia sp. live tissue change in response to the treatments was analysed using Coral Point Count with Excel extensions (CPCe; Kohler and Gill, 2006). Surface area of live tissue for each individual was digitized at the beginning and end of the experiment. Per cent survival of the CCA lobes within each treatment was calculated. Additionally, *Peyssonnelia* sp. net calcification rates for individual lobes were determined by buoyant weighing according to Davies (1989) over a 7 d period (July 26–August 2) at the end of the 35 d experiment.

Table 1. Summary of measured and calculated treatment parameters determined three times daily during the 35 d experiment (28 June – 2 August 2014).

Measured				Calculated				
Time (24 h)	pCO_2 (μatm)	pH_{NBS}	Temp (°C)	CO_2 (μmol kg^{-1})	HCO_3^- (μmol kg^{-1})	CO_3^{2-} (μmol kg^{-1})	Ω_{cal} ($\bar{x} \pm$ s.d.)	Ω_{cal} (range)
Ambient CO_2								
8:00	658 ± 129	8.07 ± 0.07	29.1 ± 0.7	14 ± 2	1794 ± 70	195 ± 28	4.6 ± 0.4	4.0 – 5.4
12:00	439 ± 91	8.21 ± 0.06	30.2 ± 0.6	9 ± 2	1654 ± 61	252 ± 25	6.1 ± 0.6	4.8 – 7.1
18:00	363 ± 41	8.29 ± 0.03	30.8 ± 0.7	7 ± 1	1557 ± 45	291 ± 18	7.0 ± 0.4	3.6 – 7.8
Elevated CO_2								
8:00	1087 ± 213	7.88 ± 0.08	29.2 ± 0.6	23 ± 4	1940 ± 62	138 ± 25	3.2 ± 0.4	2.7 – 4.6
12:00	712 ± 155	8.03 ± 0.06	30.3 ± 0.5	15 ± 3	1822 ± 49	185 ± 20	4.5 ± 0.5	3.5 – 5.3
18:00	575 ± 70	8.12 ± 0.04	31.0 ± 0.7	12 ± 1	1739 ± 41	219 ± 17	5.3 ± 0.4	4.6 – 5.9

Temperature, pH (NBS scale), and pCO_2 were measured and used to calculate (CO2SYS, Pierrot *et al.*, 2006) the concentration of dissolved inorganic carbon species (CO_2, HCO_3^-, CO_3^{2-}) and calcite saturation state (Ω_{cal}). Reported values are means ± s.d. ($n = 24 – 31$ d); we also provide the range (min – max) for Ω_{cal}. Dissociation constants for carbonate determined by Mehrbach *et al.* (1973), refit by Dickson and Millero (1987). Most parameters were measured three times a day, but equipment malfunctions at times limited sampling for a few periods during the study.

Community analysis

To quantify algal community shifts in response to irradiance and pCO_2 treatments, the surface and bottom of each settling plate was digitally photographed with a high-resolution camera (Canon EOS 20D) at the beginning and end of the experiment. Resulting photos were analysed using CPCe. A total of 100 points was randomly distributed across images of plates (15 cm^2). Each point (8000 point total) was visually classified using a dissecting microscope into one of five algal categories: (i) branching macroalgae, (ii) brown turf (Ochrophyta), (iii) green turf (Chlorophyta), (iv) microalgae (including microbial biofilm), and (v) CCA. A code file was created from the CPCe data based on each category to establish initial and final per cent cover. Community change for each category was determined by the difference between initial and final per cent cover. Presence and absence frequencies of each category were also determined on ten replicate plates in each treatment combination.

Individual CCA analysis on settling plates

In addition to quantifying changes in community per cent cover, several CCA individuals were identified on the plates (e.g. Figure 2d) and their surface area was determined (CPCe as above) at the beginning and end of the experiment. Following individual CCA on the plates allowed us to ascertain potential loss of tissue surface area or growth in the different treatments. Owing to low presence of CCA on the surfaces of the plates (e.g. Figure 2c) at the termination of the experiment, only the bottoms of the settling plates were analysed for changes in CCA individual surface area (e.g. Figure 2d).

Statistical analysis

The experiment was conducted as a split-plot design with pCO_2 as the whole-plot factor, and irradiance as the subplot factor. Changes in per cent cover of each categorical group within the community on the surface and bottom of settling plates were analysed using two-way split-plot ANOVAs with random blocking to control for differences among aquaria (Proc GLM SAS 9.3). A two-way split-plot ANOVA was also used to test for differences in surface area changes of CCA individuals on plate bottoms. Calcification rates of CCA adult lobes were also analysed using a two-way split-plot ANOVA with pCO_2 and irradiance as fixed factors. Although some categorical data in the per cent cover analysis did not meet the assumption of normality (Shapiro–Wilk's test), all variances were homogeneous (Levene's test) and robust enough for ANOVA analysis (Zar, 2010). Factors in all analyses were considered significant at $p < 0.05$ and differences among treatments for main factors and significant interactions were determined using *post hoc* multiple comparisons (lsmeans statement/diff adjust = Tukey, SAS9.2).

Results

Seawater treatments

CO_2 was taken up during the day and released at night following a natural diel metabolic cycle on the back reef (Table 1). On average, the pCO_2 was approximately twofold higher in the morning at 8:00 than the end of the day at 18:00. The CO_2-enriched treatment had a 58–65% higher average pCO_2 (575–1087 μatm) than the ambient control (363–658 μatm), similar to the per cent increase (64–71%) in CO_2 concentration calculated using TA and pH in CO2SYS. Enrichment with CO_2 caused the pH to fall below 8.0 and maintain a lower average range (7.88–8.12) than ambient seawater, which fluctuated throughout diel cycles (8.07–8.29), but remained above 8.0 (Table 1). While CO_2 enrichment increased pCO_2 by ~65%, HCO_3^- increased ~10% and CO_3^{2-} declined by 25–29% relative to ambient seawater (Table 1). Although Ω_{cal} dropped 24–30% in the elevated pCO_2 treatment, the minimum early morning (8:00) and 24 h survey saturation states were 2.7 and 3.6 in the elevated pCO_2 treatment and ambient seawater, respectively. Therefore, although pCO_2 was simulated to year 2100 levels, Ω_{cal} in both treatments remained relatively high and did not approach under-saturation with respect to calcite. Temperatures were consistent between treatments (± 1°C) with a range (~29–31°C) corresponding to summer Caribbean coastal seawater temperatures. Average TA measurements in ambient and elevated pCO_2 treatments were 2275 ± 2 and 2278 ± 2 μmol kg^{-1}, respectively, and did not significantly change over time (see the Methods section).

CCA individuals

Adult lobes

Adult lobes of *Peyssonnelia* sp. showed no visible signs of bleaching in response to elevated pCO_2, and only slightly lighter pigmentation was observed in individuals under high (Figure 3a) compared with low (Figure 3b) irradiance. Based on digitization of the dark red pigmented tissue surface area, there was 100% survival of *Peyssonnelia* sp. across all pCO_2 and irradiance treatments (Figure 4). Further, *Peyssonnelia* sp. calcification rates did not differ between pCO_2 or irradiance treatments regardless of the

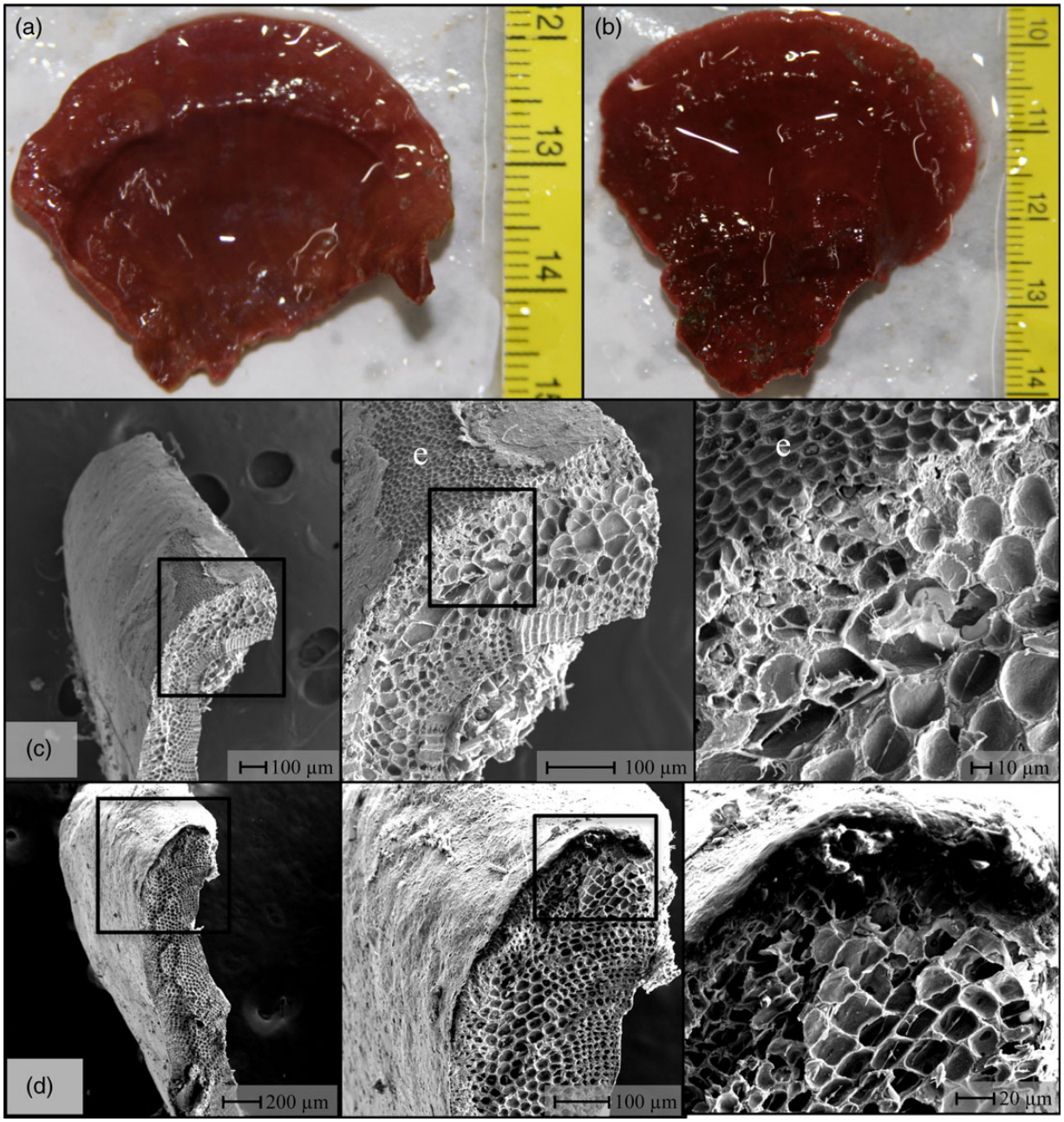

Figure 3. (a and b) Representative individual adult lobes of *Peyssonnelia* sp. used in the experiment illustrating the lack of bleaching in elevated pCO_2 treatments and slightly lower pigment content indicated by a lighter colour under the (a) high compared with (b) low irradiance treatment. SEM images of the growing margin of individual lobes after 35 d at elevated pCO_2 treatments under (c) high and (d) low irradiance with the lobes' leading margin expanded from 100× to 300× and 1000× (left to right) showing no clear indication of carbonate dissolution or cellular deformity. Note: Epithallial sloughing of cells resulting in un-epiphytized surface layer is shown in (c) denoted by the letter (e).

unit used to normalize rates (Table 2). Finally, SEM images of the leading edge of several lobes revealed no observable structural changes indicative of acute negative pCO_2 effects on the growing adult thalli (Figure 3c and d).

CCA surface area change: plate bottoms

The CCA community level response to elevated pCO_2 and irradiance was more complex than that of individual adult *Peyssonnelia* sp. thalli. Individual CCA surface area changes on settling plate bottoms declined ~70–85% in the high irradiance treatment (92 µmol photons m^{-2} s^{-1}) under elevated and ambient seawater pCO_2 levels (Figure 5). In the low irradiance treatment (13 µmol photons m^{-2} s^{-1}), the surface areas of CCA individuals on plate bottoms in ambient seawater nearly doubled at the end of the experiment (Figure 5). While there was considerable variance in the low irradiance treatment, plate bottoms exposed to elevated pCO_2 gained, on average, only 20% of the surface area compared with those in ambient seawater. Although the two-way split-plot ANOVA indicated a significant pCO_2 effect ($p < 0.05$) and a highly significant irradiance effect ($p < 0.01$), the community analysis results did not identify a significant pCO_2

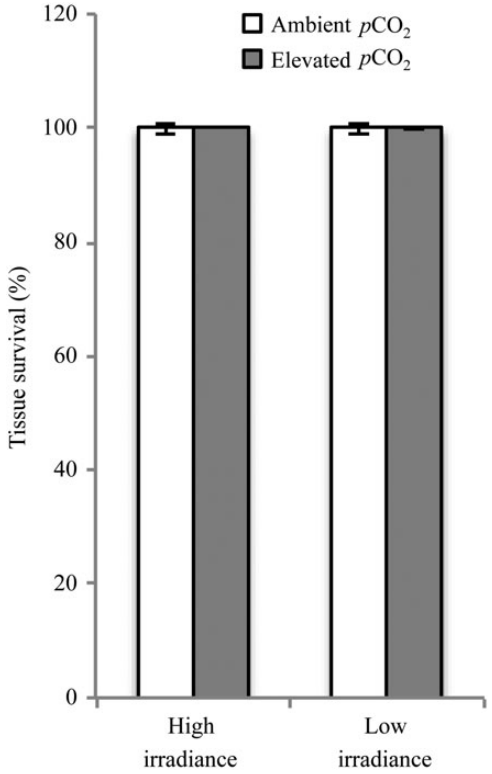

Figure 4. Per cent survival based on digitized surface area of live intact lobes of *Peyssonnelia* sp. exposed to elevated pCO_2 and high and low irradiance treatments for 35 d ($n = 10$; ± s.e.). There were no statistical differences among treatments based on per cent survival.

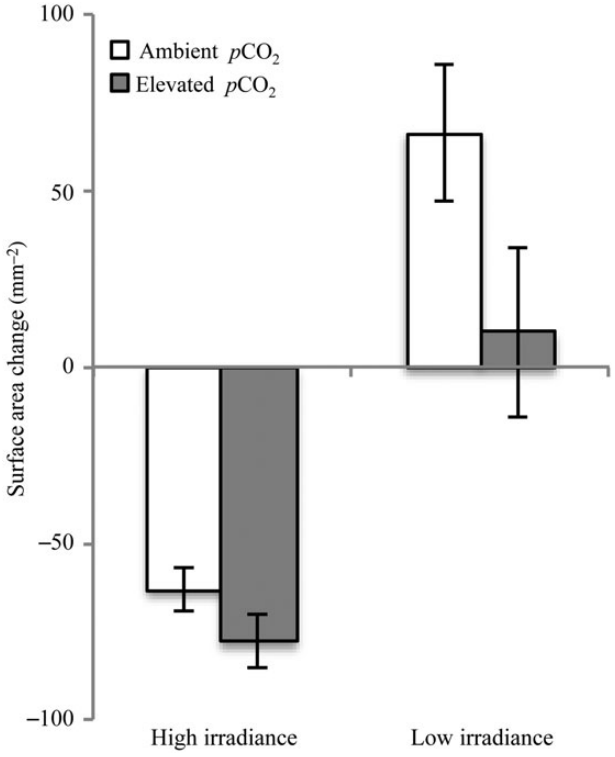

Figure 5. Changes in digitized surface area of CCA on settling plate bottoms after 35 d under elevated pCO_2 compared with ambient seawater controls and high and low irradiance treatments.

Table 2. Calcification rates of individual adult *Peyssonnelia* sp. lobes under elevated (HCO_2) compared with ambient (ACO_2) pCO_2 and high (H) and low (L) irradiance treatments during a 7-d period at the end of the experiment (26 July–2 August 2014).

	CCA calcification rates		
Treatment	**mg d^{-1}**	**mg cm^{-2} d^{-1}**	**mg g^{-1} d^{-1}**
HCO_2 × H	3.04 ± 1.04	0.29 ± 0.10	3.72 ± 0.99
HCO_2 × L	2.56 ± 0.73	0.22 ± 0.05	1.88 ± 0.51
ACO_2 × H	1.70 ± 0.55	0.26 ± 0.63	3.24 ± 0.86
ACO_2 × L	2.25 ± 0.50	0.30 ± 0.07	3.77 ± 1.14

Calcification rates are reported as non-normalized and normalized to lobe area (cm^{-2}) and buoyant weight (g^{-1}). There were no statistical differences among treatments regardless of the unit used to normalize rates.

effect on changes in CCA per cent cover or frequency on the bottom of plates; therefore, this result should be interpreted with caution (discussed below).

Macroalgal community response

The microalgae group showed the greatest increase in per cent cover across all community groups, particularly on plate surfaces in the high (60–74%) and low (46–55%) irradiance treatments (Figure 6). Microalgal coverage also significantly increased ($p < 0.05$) on plate bottoms under high irradiance (7–11%). Microalgal frequency on plates in the high irradiance treatment showed a similar pattern to per cent cover with 100% cover on the plate surfaces and only 20–30% cover on plate bottoms (Table 3). This was the case although the initial per cent cover of this group was low on both the surface (3–4%) and bottom (1–2%) of plates (Table 4). Microalgal coverage on plate bottoms was unaffected by pCO_2. Thus, irradiance on the plate surface was the primary factor that influenced change in community dominance of microalgae.

The responses of CCA to irradiance were opposite to those of microalgae. Per cent cover of CCA increased under low irradiance and decreased under high irradiance on both the surface and bottom of plates ($p < 0.01$; Figure 6). This is consistent with its absence on plate surfaces (0%) in the high irradiance treatment, moderate coverage on plate surfaces in low irradiance (50–60%) and on plate bottoms in high irradiance (20–40%), and 100% coverage on plate bottoms in low irradiance (Table 3). There was no significant pCO_2 effect on CCA per cent cover on the surface or bottom of plates, in contrast to the significant pCO_2 effect identified by changes in surface area of CCA individuals on plate bottoms. Thus, a pCO_2 effect on CCA at the community level is uncertain. This result is in contrast to the observed highly significant and consistent irradiance response.

Per cent cover of the fleshy macroalgal branching forms remained unchanged on settling plate surfaces and bottoms in low and high irradiance treatments (Figure 6). However, branching macroalgae had a twofold higher frequency on plate bottoms (70–80%) than the surface (20–30%; Table 3). This was likely confounded by the group's greater initial presence on the bottom of plates (Table 4). The fleshy green and brown turf algae had inverse changes in per cent cover on the bottom of plates. Brown turfs had a greater per cent cover change in the high irradiance treatments, while green turfs had a greater per cent change in low irradiance ($p < 0.05$; Figure 6). Both algal turf groups were more prevalent on the bottom (70–100%) than surface (10–50%) of plates (Table 3,

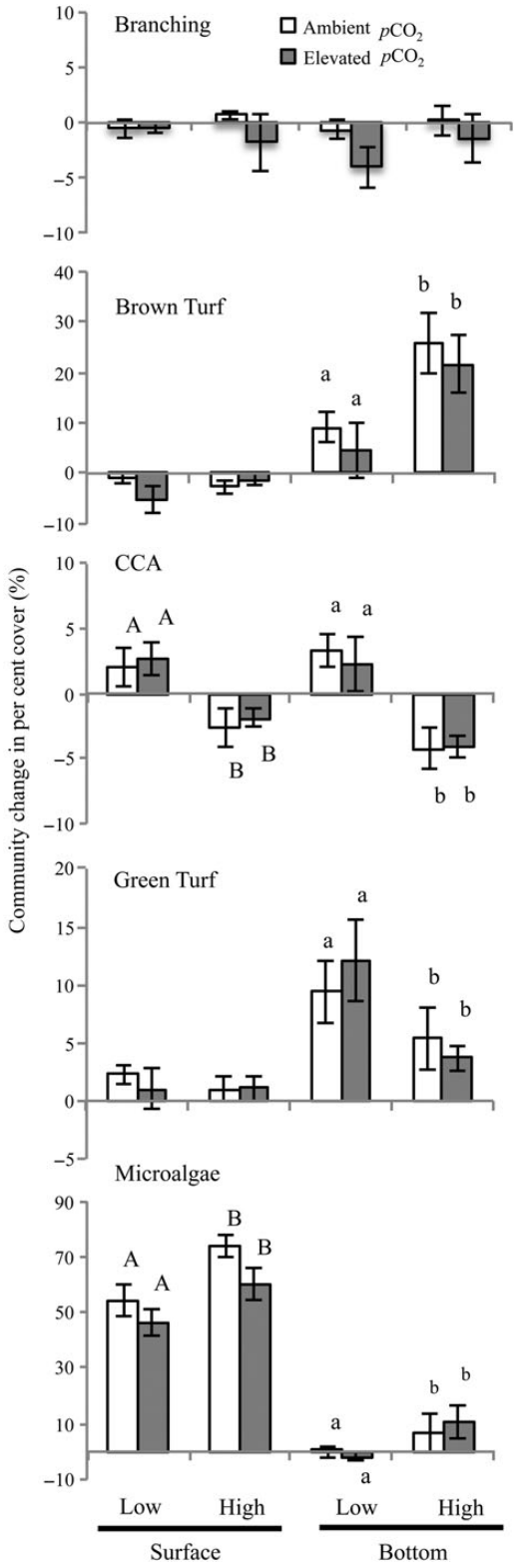

Figure 6. Community changes in per cent cover relative to initial cover on the surface and bottom of plates after 35 d under elevated pCO_2 compared with ambient seawater controls and high and low irradiance treatments. Upper and lower case letters represent significant differences in high and low irradiance treatments on the surface and bottom plates, respectively. Note different scales in per cent cover among groups in the community.

Table 3. Per cent of plates with communities classified as branching (BRA), brown turf (BRT), CCA, green turf (GRT), and microalgae (MIC) on the surface (S) and bottom (B) of plates and under high (H) and low (L) irradiance with elevated (H) and ambient (A) pCO_2.

	Categories						
S/B	Irradiance	CO_2	BR	BT	CCA	GT	Micro
S	L	A	20	10	60	50	50
S	L	H	20	20	50	30	100
S	H	A	30	20	0	10	100
S	H	H	30	40	0	10	100
B	L	A	80	100	100	70	10
B	L	H	70	100	100	90	20
B	H	A	70	100	40	70	20
B	H	H	80	100	20	70	30

Frequencies based on presence/absence data ($n = 10$).

Figure 6). The dominance of fleshy macroalgae on the bottom of plates may have been partially influenced by its initial presence, but it is notable that the turf groups did not increase in cover on the surface of plates where microalgae dominated (Figure 6).

Algal group changes in cover, area, and frequency of occurrence on settling plates in response to pCO_2 treatment were inconsistent, while irradiance was a significant and consistent parameter driving macroalgal community change. As a whole, macroalgal community changes highlight the complex interrelationships between irradiance and competition among algal groups that appear a stronger driver than year 2100 pCO_2 levels.

Discussion

Although several OA experiments demonstrate that growth and recruitment of CCA can be reduced by elevated pCO_2 (Diaz-Pulido *et al.*, 2007; Jokiel *et al.*, 2008; Kuffner *et al.*, 2008; Comeau *et al.*, 2013), our relatively short-term (35 d) study in the Caribbean indicated a high level of tolerance to elevated pCO_2 with regard to survival, calcification, and changes in per cent cover. Elevated pCO_2 under natural diel CO_2 cycles of a fringing reef did not significantly affect CCA per cent cover or surface area, based on a community analysis. Calcification rates and tissue survival of individual adult lobes of a dominant Cayman Island reef CCA species, *Peyssonnelia* sp., were also unchanged by elevated pCO_2. *Peyssonnelia* sp. calcification rates were modestly higher than other tropical species recorded, calcifying at rates threefold higher (0.22–0.30 mg $CaCO_3$ cm^{-2} d^{-1}) than the tropical fast-growing coralline *Neogoniolithon conicum* (0.08 mg $CaCO_3$ cm^{-2} d^{-1}; Chisholm, 2000) and CCA (0.13 mg cm^{-2} d^{-1}) from the Florida Keys (Kuffner *et al.*, 2013). Ries (2011) also found a twofold increase in *Neogoniolithon* sp. calcification at intermediate pCO_2 levels (~605–903 µatm) that corresponded to our year 2100 pCO_2 treatment. Studies with short-term incubations suggest that fast calcifiers may be more sensitive to OA (Comeau *et al.*, 2014b). However, although we measured high calcification rates for adult lobes of *Peyssonnelia* sp., we found no significant response to elevated pCO_2 or irradiance. Several factors likely contributed to the observed lack of response to pCO_2 treatments in this study: higher seawater temperature associated with the Caribbean summer, exposure to high saturation states or low $[H^+]$ during the day due to natural diel variability in pCO_2, and/or the ability of adult CCA to slough epithallial cells making them more resistant to microalgal overgrowth.

Our calcification rates were in the upper end of the range reported in the literature for CCA, likely due to the summer season. Average

Table 4. Per cent cover of each community group (BRT, brown turf; CCA, crustose coralline algae; MIC, microalgae; BRA, branching; GRT, green turf) at the initiation (INIT) and end (FIN) of the experiment and difference (DIF) after 35 d from elevated (H) and ambient (A) pCO_2 and high (H) and low (L) irradiance treatments.

COM	CO_2	Irradiance	INIT	FIN	DIF
Community per cent cover (surface plate)					
BRT	H	H	4.3 ± 1.5	3.1 ± 1.8	−1.2 ± 1.1
BRT	H	L	5.6 ± 2.6	0.4 ± 0.3	−5.2 ± 2.6
BRT	A	H	3.5 ± 1.2	0.8 ± 0.6	−2.7 ± 1.3
BRT	A	L	2.0 ± 0.6	1.0 ± 1.0	1.2 ± 1.2
CCA	H	H	1.9 ± 0.7	0.0 ± 0.0	−1.9 ± 0.7
CCA	H	L	0.5 ± 0.4	3.2 ± 1.3	2.7 ± 1.3
CCA	A	H	2.6 ± 1.5	0.0 ± 0.0	−2.6 ± 1.5
CCA	A	L	2.0 ± 0.7	4.0 ± 1.5	2.0 ± 1.5
MIC	H	H	3.4 ± 1.1	63.6 ± 5.1	60.2 ± 5.6
MIC	H	L	3.6 ± 1.4	50.0 ± 4.5	46.4 ± 4.6
MIC	A	H	4.3 ± 1.4	78.0 ± 3.7	73.7 ± 3.9
MIC	A	L	4.2 ± 1.5	58.7 ± 5.1	54.5 ± 5.7
BRA	H	H	3.8 ± 2.2	2.1 ± 1.4	−1.7 ± 2.6
BRA	H	L	1.1 ± 0.6	0.7 ± 0.5	−0.4 ± 0.5
BRA	A	H	0.0 ± 0.0	0.7 ± 0.4	0.7 ± 0.4
BRA	A	L	1.9 ± 0.9	1.3 ± 0.9	−0.6 ± 0.8
GRT	H	H	0.0 ± 0.0	1.1 ± 1.1	1.1 ± 1.1
GRT	H	L	1.3 ± 1.3	2.3 ± 1.4	1.0 ± 1.7
GRT	A	H	0.0 ± 0.0	1.0 ± 1.0	1.0 ± 1.0
GRT	A	L	0.0 ± 0.0	2.3 ± 0.8	2.3 ± 0.8
Community per cent cover (bottom plate)					
BRT	H	H	26.0 ± 3.4	47.7 ± 6.1	21.7 ± 5.7
BRT	H	L	26.5 ± 5.8	31.1 ± 5.0	4.6 ± 5.7
BRT	A	H	26.5 ± 3.6	52.4 ± 6.0	25.9 ± 6.2
BRT	A	L	27.5 ± 4.7	36.7 ± 4.3	9.2 ± 3.0
CCA	H	H	4.5 ± 0.9	0.4 ± 0.3	−4.1 ± 0.9
CCA	H	L	6.2 ± 1.2	8.5 ± 1.5	2.3 ± 2.1
CCA	A	H	5.6 ± 1.4	1.4 ± 0.7	−4.2 ± 1.7
CCA	A	L	6.8 ± 1.2	10.2 ± 0.9	3.4 ± 1.3
MIC	H	H	2.4 ± 1.6	13.0 ± 7.0	10.6 ± 6.0
MIC	H	L	5.3 ± 2.4	3.4 ± 2.7	−1.9 ± 1.6
MIC	A	H	0.6 ± 0.6	7.3 ± 6.7	6.7 ± 6.8
MIC	A	L	2.3 ± 1.2	2.3 ± 2.3	0.0 ± 2.2
BRA	H	H	8.0 ± 2.5	6.7 ± 1.8	−1.3 ± 2.2
BRA	H	L	6.7 ± 2.0	2.7 ± 0.8	−4.0 ± 1.9
BRA	A	H	3.6 ± 1.6	3.8 ± 1.5	0.2 ± 1.3
BRA	A	L	4.4 ± 1.4	3.8 ± 1.3	−0.6 ± 0.8
GRT	H	H	2.1 ± 0.9	5.8 ± 1.8	3.7 ± 1.1
GRT	H	L	2.8 ± 1.3	14.9 ± 4.3	12.1 ± 3.5
GRT	A	H	3.7 ± 1.7	9.1 ± 3.8	5.4 ± 2.7
GRT	A	L	1.3 ± 1.0	10.7 ± 3.2	9.4 ± 2.7

$n = 10$, average ± s.e.

seawater temperatures in our study were typical of Caribbean summers, averaging 29–31°C over diel periods and peaking at 32°C during the day. Elevated temperature is recognized to promote $CaCO_3$ precipitation (Langdon *et al.*, 2000; Ries, 2010; Anthony *et al.*, 2013) as observed in a temperate coralline alga (*L. cabiochae*) which had four to eight times higher calcification rates in summer compared with winter (Martin *et al.*, 2013). Increasing temperatures can elevate the saturation state (Ω) of carbonate minerals (Gattuso *et al.*, 1999a). Although our pH was lowered to levels predicted for the year 2100 (7.88), saturation states were still high ($\Omega_{cal} \geq 2.7$, Table 1) perhaps limiting night-time dissolution. Previous studies suggest that the combination of elevated temperature and pCO_2 may exacerbate (e.g. Reynaud *et al.*, 2003) or enhance (e.g. Anthony *et al.*, 2008) calcification. While tropical organisms are living at their thermal limits (Hoegh-Guldberg *et al.*, 2007; Koch *et al.*, 2013), high temperature in this study did not appear to limit calcification.

Natural diel variability of reef pCO_2 and pH may have also contributed to the lack of a CCA response to elevated pCO_2 treatments. At the end of the day, pCO_2 was low in treatment, 575 μatm, and controls, 363 μatm, influenced by photosynthetic CO_2 drawdown. During the night, pCO_2 peaked at 1087 and 658 μatm in the CO_2-enriched and control treatments, respectively, as respiration and the efflux of CO_2 dominated. Treatment pH at dusk was 8.12 in CO_2-enriched treatments compared with 8.29 in controls, while at night, treatment pH dropped as low as 7.88 compared with 8.07 in the controls. This diel signal of pCO_2 and pH may have allowed CCA to increase calcification rates during the day when saturation states of $CaCO_3$ were high and $[H^+]$ low. Gradual declines in pH have been shown to result in increased net calcification in CCA (Kamenos *et al.*, 2013). Reef communities can alter carbon chemistry daily with diel ranges exceeding those of seawater pCO_2 changes predicted under climate change (Gattuso *et al.*, 1999b; Kleypas *et al.*, 2011). Further, CCA collected from highly variable pH environments have shown greater tolerance to elevated pCO_2 oscillations (Johnson *et al.*, 2014a) compared with experiments using stable pCO_2 levels (e.g. Kuffner *et al.*, 2008, Diaz-Pulido *et al.*, 2012, Short *et al.*, 2014). This suggests that the response of CCA to variable pCO_2 is dependent on the conditions of the habitat where CCA is collected (Johnson *et al.*, 2014a). CCA within our experiment were expected to be exposed to natural pCO_2 fluctuations as Cayman Island reefs are primarily shallow with high metabolic rates (Table 1) or are positioned at the interface of very deep walls associated with the Cayman Trench. These wall-associated reefs are likely exposed to upwelling of deep CO_2-enriched waters, but these chemical dynamics need further examination. As our study and others are beginning to show, incorporating metabolic reef dynamics in OA experiments may clarify our understanding of future impacts and potential tolerance to OA in marine ecosystems (Hofmann *et al.*, 2011; Kline *et al.*, 2012; Cornwall *et al.*, 2013; Comeau *et al.*, 2014b). As these are benthic ecosystems strongly competing for space and irradiance, it is also important to consider how OA affects community dynamics under various irradiance conditions.

At the community level, our results indicate no consistent pCO_2 effects or interactions with irradiance on macroalgal group per cent cover. Rather, we found high irradiance increased rapid colonization of benthic microalgae on settling plates in the aquaria experiment. Conversely, high irradiance reduced CCA recruitment onto uncolonized plate surfaces. CCA are known to be poor competitors for space, recruitment, and growth (Littler and Littler, 1980; Underwood, 1980; Sebens, 1986; Steneck and Dethier, 1994) and filamentous algal overgrowth of CCA is high during warm summer conditions (Martin and Gattuso, 2009). Short *et al.* (2014) reported CCA overgrowth by epiphytic turf algae (>20%) under elevated pCO_2 compared with ambient seawater, but we found little evidence for this elevated pCO_2 effect. Although no macroalgal group consistently responded to elevated pCO_2, our results indicate that microalgae positively responded to high irradiance, potentially outcompeting CCA and other macroalgal groups.

The community level effects of irradiance and potential competitive interactions were in stark contrast to *Peyssonnelia* sp. individuals that remained epiphyte-free and unresponsive to high irradiance or pCO_2 throughout the 35 d experiment. Several species of CCA demonstrate the capacity to shed epithallial cells as a way to remove epiphytes (Keats *et al.*, 1997; Bôas and Figueiredo, 2004; Harrington *et al.*, 2004). Epithallial sloughing is an important survival strategy for CCA, making it a better competitor against microalgae and

microbes (Sebens, 1986). Thus, various life stages of CCA may have different responses to OA. Adult lobes of *Peyssonnelia* sp. demonstrated plasticity to elevated pCO_2 and irradiance, while new recruits (spp. unknown) on settling plates were replaced by microalgae under high irradiance. It was interesting that CCA on the plate surface succumbed to microalgal dominance by the end of the experiment, while the sides of the aquaria in all treatments were covered with small (<1 cm) CCA recruits (ED, pers. obs.). These data and observations suggest that direct OA effects may not be the most important driver of community compositional changes on reefs, but rather how microalgae with rapid growth rates may respond and interfere with CCA recruitment and early development. This may be observed in areas where space is limiting and rapid fleshy algal growth is advantageous, as on tropical coral reefs (Gao *et al.*, 1999; Kranz *et al.*, 2009), and in environments undergoing coastal nutrient enrichment which promotes growth of microalgal assemblages (Doney *et al.*, 2009). Once CCA reach adult stages, particularly those characterized by rapid epithallial sloughing, they may compete more successfully with microalgae. Shaded microhabitats can provide refuge for CCA lacking the ability to resist competition from microalgae. More research is needed on competitive interactions in response to OA under various conditions of irradiance, nutrients, and with top-down herbivory controls. Our data suggest that macroalgal communities are unlikely to shift under pCO_2 levels predicted for the year 2100 in tropical carbonate environments under high and low irradiance, but this supposition should be corroborated in long-term experiments and field studies.

Acknowledgements

This project was made possible in part by funding from the NFWF to the LCRC and an FAU Climate Change Initiative Grant. Laboratory experiments benefited from an NSF FSML Grant (#1227093) to enhance LCRC's capacity for coral reef stress and climate change research. We appreciate the Cayman Island Marine Conservation Board and Department of Environment for permitting our research. We also acknowledge field support of the LCRC staff.

References

Adey, W. H. 1998. Coral reefs: algal structured and mediated ecosystems in shallow, turbulent, alkaline waters. Journal of Phycology, 34: 393–406.

Anthony, K. R. N., Diaz-Pulido, G., Verlinden, N., Tilbrook, B., and Andersson, A. J. 2013. Benthic buffers and boosters of ocean acidification on coral reefs. Biogeosciences, 10: 4897–4909.

Anthony, K. R. N., Kline, D. I., Diaz-Pulido, G., and Hoegh-Guldberg, O. 2008. Ocean acidification causes bleaching and productivity loss in coral reef builders. Proceedings of National Academy of Sciences of the United States of America, 105: 17442–17446.

Bôas, A. B. V., and Figueiredo, M. A. O. 2004. Are anti-fouling effects in coralline algae species specific? Brazilian Journal of Oceanography, 52: 11–18.

Borowitzka, M. A. 1981. Photosynthesis and calcification in the articulated coralline red algae *Amphiroa anceps* and *A.* foliacea. Marine Biology, 62: 17–23.

Chisholm, J. R. M. 2000. Calcification by crustose coralline algae on the northern Great Barrier Reef, Australia. Limnology and Oceanography, 45: 1476–1484.

Comeau, S., Carpenter, R. C., and Edmunds, P. J. 2014a. Effects of irradiance on the response of the coral *Acropora pulchra* and the calcifying alga *Hydrolithon reinboldii* to temperature elevation and ocean acidification. Journal of Experimental Marine Biology and Ecology, 453: 28–35.

Comeau, S., Edmunds, P. J., Spindel, N. B., and Carpenter, R. C. 2013. The response of eight coral reef calcifiers to increasing partial pressure of CO_2 do not exhibit a tipping point. Limnology and Oceanography, 58: 388–398.

Comeau, S., Edmunds, P. J., Spindel, N. B., and Carpenter, R. C. 2014b. Fast coral reef calcifiers are more sensitive to ocean acidification in short-term laboratory incubations. Limnology and Oceanography, 59: 1081–1091.

Cornwall, C. E., Hepburn, C. D., McGraw, C. M., Currie, K. I., Pilditch, C. A., Hunter, K. A., Boyd, P. W., *et al.* 2013. Diurnal fluctuations in seawater pH influence the response of a calcifying macroalga to ocean acidification. Proceedings of the Royal Society B, 280: 20132201.

Davies, P. S. 1989. Short-term growth measurements of corals using an accurate buoyant weighing technique. Marine Biology, 101: 389–395.

de Beer, D., and Larkum, A. W. D. 2001. Photosynthesis and calcification in the calcifying algae *Halimeda discoidea* studied with microsensors. Plant, Cell and Environment, 24: 1209–1217.

Diaz-Pulido, G., Gouezo, M., Tilbrook, B., Dove, S., and Anthony, K. R.N. 2012. High CO_2 enhances the competitive strength of seaweeds over corals. Ecology, 14: 156–162.

Diaz-Pulido, G., McCook, L. J., Larkum, A. W. D., Lotze, H. K., Raven, J. A., Swchaffelke, B., Smith, J. E., *et al.* 2007. Vulnerability of macroalgae of the Great Barrier Reef to climate change. *In* Climate Change and the Great Barrier Reef, pp. 153–192. Ed. by J. E. E. Johnson, and P. A. Marshall. Great Barrier Reef Marine Park Authority & Australian Greenhouse Office, Townsville, QLD, Australia.

Dickson, A. G., and Millero, F. J. 1987. A comparison of the equilibrium constants for the dissociation of carbonic acid in seawater media. Deep Sea Research, 34: 1733–1743.

Doney, S. C., Fabry, V. J., Feely, R. A., and Kleypas, J. A. 2009. Ocean acidification: the other CO_2 problem. Annual Review of Marine Science, 1: 169–192.

Fabricius, K. E., Kluibenschedl, A., Harrington, L., Noonan, S., and De' ath, G. 2015. In situ changes of tropical crustose coralline algae along carbon dioxide gradients. Nature Scientific Reports, 5. doi:10.1038/srep09537.

Fabricius, K. E., Langdon, C., Uthicke, S., Humphrey, C., Noonan, S., De' ath, G., Okazaki, R., *et al.* 2011. Losers and winners in coral reefs acclimatized to elevated carbon dioxide concentrations. Nature Climate Change, 1: 165–169.

Gao, K., Ji, Y., and Aruga, Y. 1999. Relationship of CO_2 concentrations to photosynthesis of intertidal macroalgae during emersion. Hydrobiologia, 398/399: 355–359.

Gattuso, J. -P., Allemand, D., and Frankignoulle, M. 1999a. Photosynthesis and calcification at cellular, organismal and community levels in coral reefs: a review on interactions and control by carbonate chemistry. American Zoology, 39: 160–183.

Gattuso, J-P., Frankignoulle, M., and Smith, S. V. 1999b. Measurement of community metabolism and significance in coral reef CO_2 source-sink debate. Proceedings of the National Academy of Sciences of the United States of America, 96: 13017–13022.

Hall-Spencer, J. M., Rodolfo-Metalpa, R., Martin, S., Ransome, E., Fine, M. E., Turner, S. M., Rowley, S. J., *et al.* 2008. Volcanic carbon dioxide vents show ecosystem effects of ocean acidification. Nature, 454: 96–99.

Harrington, L., Fabricius, K., De' ath, G., and Negri, A. 2004. Recognition and selection of settlement substrata determine post-settlement survival in corals. Ecology, 85: 3428–3437.

Hoegh-Guldberg, O., Mumby, P. J., and Hooten, A. J. 2007. Coral reefs under rapid climate change and ocean acidification. Science, 318: 1737–1742.

Hofmann, G. E., Smith, J. E., Johnson, K. S., Send, U., Levin, L. A., Micheli, F., Paytan, A., *et al.* 2011. High-frequency dynamics of ocean pH: a multi-ecosystem approach. PLoS ONE, 6: e28983.

Hofmann, L., and Bischof, K. 2014. Review: Ocean acidification effects on calcifying macroalgae. Aquatic Biology, 22: 261–279.

Hurd, C. L., Cornwall, K., Hepburn, C. D., McGraw, C. M., and Hunter, K. A. 2011. Metabolically induced pH fluctuations by some coastal calcifiers exceed projected 22nd century ocean acidification: a mechanism for differential susceptibility? Global Change Biology, 17: 3254–3262.

IPCC. 2013. Climate Change 2013. The Physical Science Basis. Contribution of Working Group I to the Fifth Assessment Report of the Intergovernmental Panel on Climate Change. Ed. by T. F. Stocker, D. Qin, G-K. Plattner, M. Tignor, S. K. Allen, J. Boschung, A. Nauels, *et al.* Cambridge University Press, Cambridge, UKandNew York, NY, USA. 1535 pp.

Johnson, M. D., Moriarty, V. W., and Carpenter, R. C. 2014a. Acclimatization of the crustose coralline alga *Porolithon onkodes* to variable pCO_2. PLoS ONE, 9: e87678.

Johnson, M. D., Price, N. N., and Smith, J. E. 2014b. Contrasting effects of ocean acidification on tropical fleshy and calcareous algae. Peer J, 2: e411.

Jokiel, P. L. 2011. Ocean acidification and control of reef coral calcification by boundary layer limitation of proton flux. Bulletin of Marine Science, 87: 639–657.

Jokiel, P. L. 2013. Coral reef calcification: carbonate, bicarbonate and proton flux under conditions of increasing ocean acidification. Proceedings of the Royal Society B, http://dx.doi.org/10.1098/rspb.2013.0031.

Jokiel, P. L., Rodgers, K. S., Brown, E. K., Kenyon, J. C., Aeby, G., Smith, W. R., and Farrell, F. 2015. Comparison of methods used to estimate coral cover in the Hawaiian Islands. Peer J, 3: e954. https://dx.doi.org/10.7717/peerj.954.

Jokiel, P. L., Rodgers, K. S., Kuffner, I. B., Andersson, A. J., Cox, E. F., and Mackenzie, F. F. 2008. Ocean acidification and calcifying reef organisms: a mesocosm investigation. Coral Reefs, 27: 473–483.

Kamenos, N. A., Burdett, H. L., Aloisio, E., Findlay, H. S., Martin, S., Longbone, C., Dunn, J., *et al.* 2013. Coralline algal structure is more sensitive to rate, rather than magnitude, of ocean acidification. Global Change Biology, 19: 3621–3628.

Keats, D. W., Knight, M. A., and Pueschel, C. M. 1997. Antifouling effects of epithallial shedding in three crustose coralline algae (Rhodophyta, Corallinales) on a coral reef. Journal of Experimental Marine Biology and Ecology, 213: 281–293.

Kleypas, J. A., Anthony, K. R. N., and Gattuso, J-P. 2011. Coral reefs modify their seawater carbon chemistry—case study from a barrier reef (Moorea, Frech Polynesia). Global Change Biology, 17: 3667–3678.

Kline, D., Teneva, L., Schneider, K., Miard, T., Chai, A., Marker, M., Headley, K., *et al.* 2012. A short-term *in situ* CO_2 enrichment experiment on Heron Island (GBR). Scientific Reports, 2: 413.

Koch, M. S., Bowes, G., Ross, C., and Zhang, X. 2013. Climate change and ocean acidification effects on seagrasses and marine macroalgae. Global Change Biology, 19: 103–132.

Kohler, K. E., and Gill, S. M. 2006. Coral Point Count with Excel extensions (CPCe): a Visual Basic program for the determination of coral and substrate coverage using random point count methodology. Computers and Geosciences, 32: 1259–1269.

Kranz, S. A., Sültemeyer, D., Richter, K. U., and Rost, B. 2009. Carbon acquisition in *Trichodesmium*: the effect of *p*CO2 and diurnal changes. Limnology and Oceanography, 54: 548–559.

Kuffner, I. B., Andersson, A. J., Jokiel, P. L., Rodgers, K. S., and Mackenzie, F. 2008. Decreased abundance of crustose coralline algae due to ocean acidification. Nature Geosciences, 1: 114–117.

Kuffner, I. B., Hickey, T. D., and Morrison, J. M. 2013. Calcification rates of the massive coral *Siderastrea siderea* and crustose coralline algae along the Florida Keys (USA) outer-reef tract. Coral Reefs, 32: 987–997.

Langdon, C., Takahashi, T., Sweeney, C., Chipman, D., Goddard, J., Marubini, F., and Atkinson, M. J. 2000. Effect of calcium carbonate saturation state on the calcification rate of an experimental coral reef. Global Biogeochemical Cycles, 14: 639–654.

Littler, M. M., and Littler, D. S. 1980. The evolution of thallus form and survival strategies in benthic marine macroalgae: field and laboratory test of a functional form model. The American Naturalist, 116: 25–44.

Littler, M. M., and Littler, D. S. 1984. Relationships between macroalgal functional form groups and bubstrata stability in a subtropical rock-intertidal system. Journal of Experimental Marine Biology and Ecology, 74: 13–34.

Littler, M. M., and Littler, D. S. 2000. Caribbean Reef Plants. Offshore Graphics, Inc., Washington, DC, USA.

Manfrino, C., Jacoby, C. A., Camp, E., and Frazer, T. K. 2013. A positive trajectory for corals at Little Cayman Island. PLoS ONE, 8: e75432.

Martin, S., Castets, M., and Clavier, J. 2006. Primary production, respiration and calcification of the temperate free-living coralline alga *Lithothamnion corallioides.* Aquatic Botany, 85: 121–128.

Martin, S., Cohu, S., Vignot, C., Zimmerman, G., and Gattuso, J. -P. 2013. One-year experiment on the physiological response of the Mediterranean crustose coralline alga, *Lithophyllum cabiochae*, to elevated pCO_2 and temperature. Ecology and Evolution, 3: 676–693.

Martin, S., and Gattuso, J-P. 2009. Response of Mediterranean coralline algae to ocean acidification and elevated temperature. Global Change Biology, 15: 2089–2100.

Mehrbach, C., Culberson, C. H., Hawley, J. E., and Pytkowics, R. M. 1973. Measurement of the apparent dissociation constants of carbonic acid in seawater at atmospheric pressure. Limnology and Oceanography, 18: 897–907.

Mumby, P. 2009. Phase shifts and the stability of macroalgal communities on Caribbean coral reefs. Coral Reefs, 28: 761–773.

Pierrot, D., Lewis, E., and Wallace, D. W. R. 2006. MS Excel program developed for CO_2 system calculations: ORNL/CDIAC-105a. Carbon Dioxide Information Analysis Center Oak Ridge National Laboratory, US Department of Energy, Oak Ridge, TN.

Porzio, L., Buia, M. C., and Hall-Spencer, J. M. 2011. Effects of ocean acidification on macroalgal communities. Journal of Experimental Marine Biology and Ecology, 400: 278–287.

Reynaud, S., Leclercq, N., Romaine-Lioud, S., Ferrier-Pages, C., Jaubert, J., and Gattuso, J-P. 2003. Interacting effects of CO_2 partial pressure and temperature on photosynthesis and calcification in a scleractinian coral. Global Change Biology, 9: 1660–1668.

Ries, J. B. 2010. Review: geological and experimental evidence for secular variation in seawater Mg/Ca (calcite-aragonite seas) and its effects on marine biological calcification. Biogeosciences, 7: 2795–2849.

Ries, J. B. 2011. Skeletal mineralogy in a high-CO_2 world. Journal of Experimental Biology and Ecology, 403: 54–64.

Sebens, K. P. 1986. Spatial relationships among encrusting marine organisms in the New England subtidal zone. Ecological Monographs, 56: 73–96.

Short, J., Kendrick, G. A., Falter, J., and McCulloch, M. T. 2014. Interactions between filamentous turf algae and coralline algae modified under ocean acidification. Journal of Experimental Biology and Ecology, 456: 70–77.

Steneck, R. 1986. The ecology of coralline algal crusts: convergent patterns and adaptative strategies. Annual Review of Ecology and Systematics, 17: 273–303.

Steneck, R., and Dethier, M. N. 1994. A functional group approach to the structure of algal dominated communities. Oikos, 69: 476–498.

Underwood, A. 1980. The effects of grazing by gastropods and physical factors on the upper limits of distribution of intertidal macroalgae. Oecologia, 46: 201–213.

Zar, J. H. 2010. Biostatistical Analysis. Person Prentice Hall, Inc., Upper Saddle River, NJ.

Handling editor: Howard Browman

ICES Journal of Marine Science

ICES Journal of Marine Science (2016), 73(3), 814–824. doi:10.1093/icesjms/fsv208

Contribution to Special Issue: 'Towards a Broader Perspective on Ocean Acidification Research'

Original Article

Physiological responses and scope for growth in a marine scavenging gastropod, *Nassarius festivus* (Powys, 1835), are affected by salinity and temperature but not by ocean acidification

Haoyu Zhang[1], Paul K. S. Shin[1,2], and Siu Gin Cheung[1,2]*

[1]*Department of Biology and Chemistry, City University of Hong Kong, Hong Kong, China*
[2]*State Key Laboratory in Marine Pollution, City University of Hong Kong, Tat Chee Avenue, Kowloon, Hong Kong, China*

**Corresponding author: tel: + 852 34427749; fax: + 852 34420522; e-mail: bhsgche@cityu.edu.hk*

Zhang, H., Shin, P. K. S., and Cheung, S. G. Physiological responses and scope for growth in a marine scavenging gastropod, *Nassarius festivus* (Powys, 1835), are affected by salinity and temperature but not by ocean acidification. – ICES Journal of Marine Science, 73: 814–824.

Received 4 June 2015; revised 17 September 2015; accepted 19 October 2015; advance access publication 11 November 2015.

In the past few years, there has been a dramatic increase in the number of studies revealing negative or positive effects of ocean acidification on marine organisms including corals, echinoderms, copepods, molluscs, and fish. However, scavenging gastropods have received little attention despite being major players in energy flow, removing carrion, and recycling materials in marine benthic communities. The present study investigated the physiological responses (ingestion, absorption rate and efficiency, respiration, and excretion) and scope for growth (SfG) of an intertidal scavenging gastropod, *Nassarius festivus*, to the combined effects of ocean acidification (pCO_2 levels: 380, 950, and 1250 μatm), salinity (10 and 30 psu), and temperature (15 and 30°C) for 31 d. Low salinity (10 psu) reduced ingestion, absorption rate, respiration, excretion, and SfG of *N. festivus* throughout the exposure period. Low temperature (15°C) had a similar effect on these parameters, except for SfG at the end of the exposure period (31 d). However, elevated pCO_2 levels had no effects in isolation on all physiological parameters and only weak interactions with temperature and/or salinity for excretion and SfG. In conclusion, elevated pCO_2 will not affect the energy budget of adult *N. festivus* at the pCO_2 level predicted to occur by the Intergovernmental Panel on Climate Change (IPCC) in the year 2300.

Keywords: *Nassarius festivus*, ocean acidification, physiological energetics, salinity, scope for growth, temperature.

Introduction

For over 800 000 years, carbon dioxide has been relatively stable in the atmosphere at 172–300 μatm by volume concentration (Luthi *et al.*, 2008). The level reached in 2000 (395 μatm) is predicted to rise to 1000 μatm by 2100 (Collins *et al.*, 2013). During the period 2000–2008, approximately one quarter of anthropogenic carbon dioxide was dissolved in the ocean (Le Quéré *et al.*, 2009), and increasing CO_2 availability is causing a global decrease in pH of seawater, a phenomenon known as ocean acidification.

Effects of ocean acidification have been extensively reported among marine organisms including bacteria, plants, and animals [reviewed by Caldeira and Wickett (2003)]. The unsaturated state of calcium carbonate caused by excess H^+ and lower Ca^{2+} availability in acidifying seawater makes calcifying invertebrates potential victims of changes to ocean chemistry. Among such organisms, corals are considered to be one of the most vulnerable groups (Bramanti *et al.*, 2013; Reyes-Nivia *et al.*, 2013). For molluscs, Abduraji and Danilo (2015) found that the pH-driven survival rate of *Haliotis asinina* was reduced from 86.3 to 47.2% at pH 7.99, and 18.3% at pH 7.62 and 7.42, respectively, after 20 d of exposure. Acidified seawater also restrained pteropods from maintaining shells made up of aragonite (Honjo *et al.*, 2000). Dissolution of the shell at the growing edge of the aperture was observed in the pteropod *Clio pyramidata* within 48 h of exposure to 788 μatm pCO_2 (Orr *et al.*, 2005).

Physiological responses of ocean acidification are species-specific with differential responses being observed in closely related species. For example, the Mediterranean mussel *Mytilus galloprovincialis* showed a reduced metabolic rate and slower growth when exposed to pH 7.3 for 3 months (Michaelidis *et al.*, 2005). In contrast, no

physiological disturbance was observed in the blue mussel *Mytilus edulis* at pH 7.14 for 60 d (Thomsen and Melzner, 2010). Some species are robust or show positive responses to ocean acidification [reviewed by Andersson *et al.* (2011)]. The brittlestar *Amphiura filiformis* showed an increase in metabolism and calcification with a substantial cost (muscle wastage) upon exposure to acidified seawater (pH 7.7) for 40 d (Wood *et al.*, 2008). Neutral responses in metabolic rates have been observed in three echinoderms, *Asterias rubens*, *Ophiothrix fragilis*, and *A. filiformis* after 1 week of exposure to pH 7.5 (Carey *et al.*, 2014). High metabolic rates commonly found in crustaceans facilitate the control of extracellular pH through active ion transport (Whiteley, 2011), hence reducing the impact of ocean acidification. For instance, after 10 d of incubation, there were no net changes in survival or overall development of larvae of the barnacle *Amphibalanus improvisus* raised at pH 7.6 compared with the control pH of 8.0 (Pansch *et al.*, 2013). This may be partly due to the absence of calcified structures in barnacle larvae that are developed only when they settle and metamorphose into the juvenile stage.

Shifts in energy allocation upon exposure to ocean acidification may reduce fitness and produce low functional capacities, hence increasing sensitivity to environmental stressors such as temperature, food supply, and salinity (Zittier *et al.*, 2013; Carey *et al.*, 2014). According to Pörtner (2008), ocean acidification enhances sensitivity to thermal stress, resulting in a narrowing of the thermal tolerance window and aerobic capacity. For example, the brown crab *Cancer pagurus* reduced its upper thermal limit of aerobic scope by 5°C under hypercapnia (pH 7.06) exposure for 16 h (Metzger *et al.*, 2007). The scope for performance of the Arctic spider crab *Hyas araneus* was reduced at the limits of thermal tolerance (4°C) and exacerbated by an elevated CO_2 level of 3000 μatm (Zittier *et al.*, 2013). Synergistic effects have also been observed between ocean acidification and low salinity. Combined exposure to hypercapnia and low salinity negatively affected mortality, tissue growth, energy storage, and mechanical properties of shells of juvenile oysters *Crassostrea virginica* (Dickinson *et al.*, 2012). In addition, the larval mortality of a subtidal scavenging gastropod *Nassarius conoidalis* was enhanced by high pCO_2 level (1250 μatm) at low salinity (10 psu) but not at normal salinity (30 psu; Zhang *et al.*, 2014).

Acclimation occurs when organisms adjust physiologically to changes in the environment, allowing them to maintain performance relatively independently of the changes. Such adjustment occurs over a short period and depends on lifespan (Barry *et al.*, 2011). Acclimation to temperature and salinity is commonly found in marine animals. For instance, intertidal barnacles *Elminus modestus* and *Balanus balanoides* can tolerate salinities as low as 14–17 psu following experimental or natural acclimation (Foster, 1970). A range of homeostatic responses which serve to offset the passive effects of reduced temperature have been shown to allow teleost fish to adapt to lower temperatures (Johnston and Dunn, 1987). In the cold-water coral *Lophelia pertusa*, short-term (1 week) exposure to pH 7.77 resulted in the dissolution of calcium carbonate, but acclimation was observed after 6 months and resulted in an enhancement of calcification (Form and Riebesell, 2012). Physiological responses of the subtidal scavenging gastropod, *N. conoidalis*, were sensitive to ocean acidification under acute exposure for 3 d, but complete acclimation was observed after incubation for 1 month (Zhang *et al.*, 2015).

Scope for growth (SfG) is an integrated index reflecting energy allocation strategies in living organisms and has been shown to be a useful indicator of physiological stress (Bayne and Newell, 1983; Liu *et al.*, 2011). For instance, a reduced SfG has been observed in juveniles of the sea star *Asterias rubens* upon exposure to 1120 μatm pCO_2 for 39 weeks with no acclimation observed (Appelhans *et al.*, 2014). In addition, SfG measurements of the sea urchin *Strongylocentrotus purpuratus* raised under high pCO_2 (129 Pa, 1271 μatm) indicate that an average of 39–45% of the available energy was spent in somatic growth, while control larvae could allocate between 78 and 80% of the available energy to growth processes.

As one of the most dominant and competitive scavengers on sandy shores in Hong Kong, *Nassarius festivus* plays an important role in matter cycling and energy flow, and serves as an important cleaner in removing carrion (Briton and Morton, 1992). Previous studies on physiological energetics have shown that this species is tolerant of environmental stresses, including low salinity and hypoxia (Cheung and Lam, 1995; Chan *et al.*, 2008). The interactive effects of ocean acidification, high temperature, and low salinity increased the mortality of the veliger larvae (Zhang *et al.*, 2014). The maintenance cost, as shown by the respiration rate, also increased with temperature and pCO_2 level. In the present study, *N. festivus* adults were exposed to the combined effect of ocean acidification, temperature, and salinity for 31 d. The acute responses to the combined stresses and physiological adjustments, if any, following prolonged exposure to the stresses were investigated. To understand if there are any life-stage differences in sensitivities to multiple stressors that could create a bottleneck in population performance, results were compared with those obtained for the larvae in a previous study (Zhang *et al.*, 2014). Reduction in population performance could eventually lessen the role of *N. festivus* in removing carrion on sandy shores, hence resulting in a deterioration of environmental quality.

Based on climate models in the IPCC Fifth Assessment Report (AR5), The Hong Kong Observatory has predicted the temperature and rainfall changes in Hong Kong in the 21st century (http://www.hko.gov.hk/climate_change/proj_hk_rainfall_e.htm). Under the high greenhouse gas concentration scenario (RCP8.5) proposed in this report, temperature is expected to rise by 1.5–3 and 3–6°C in the mid-21st century (2051–2060) and late 21st century (2091–2100), respectively, when compared with the 1986–2005 average of 23.3°C. The number of extremely wet years is expected to increase from 3 in 1885–2005 to about 12 in 2006–2100. The annual rainfall in the late 21st century is expected to rise by ~180 mm when compared with the 1986–2005 average. Such predictions indicate that Hong Kong is facing an increase in temperature and rainfall due to climate change and by inference, salinity, and temperature stresses on coastal marine organisms would be both more frequent and more abrupt. The results of this study can thus aid in predicting the performance of an important beach cleaner under the combined effects of ocean acidification temperature change and salinity stresses.

Methods

Study organisms

Nassarius festivus (shell length: 13 ± 2 mm) were collected from Starfish Bay, a sandy beach located in the northeast of Hong Kong (22.48130°N, 114.24411°E). As the experiment lasted for a month and all the replicates could not be completed at the same time due to logistical problems, individuals from each replicate were collected from the field before each experiment and were acclimated to laboratory conditions (24°C, 30 psu, 12 h light–12 h dark) for 2 weeks before experimentation. The experiment was conducted with three replicates in two periods (August 2012 and April 2013). The

experimental period were chosen to avoid the reproductive season (between November and February) as this could affect the physiology of the experimental animals. A preliminary experiment was conducted to compare physiological responses of individuals collected in August and April and no significant differences were observed. Individuals were fed with the short-necked clam *Ruditapes philippinarum* (a predominant food source of *N. festivus* at the collection site) for 2 h to satiation once every 3–4 d, a feeding frequency similar to that observed in their natural environment (Chan *et al.*, 2008). Seawater was changed immediately after feeding to avoid the accumulation of unconsumed food and metabolic wastes.

Experimental set-up

Combined effects of pCO_2, temperature, and salinity on the physiological responses of *N. festivus* were investigated using a full-factorial experimental design with three pCO_2 levels (380, 950, and 1250 μatm), two temperatures (15 and 30°C), and two salinities (10 and 30 psu). The pCO_2 concentration of 380 μatm (LC) was the estimated current global level, whereas 950 μatm (MC) and 1250 μatm (HC) were the predicted levels in the years 2100 and 2300, respectively, according to the IPCC (Intergovernmental Panel on Climate Change, PCR8.5 scenario, Collins *et al.*, 2013). The average winter and summer temperatures in Hong Kong are 15 ± 0.4°C (LT) and 30 ± 0.3°C (HT), respectively (http://epic.epd.gov.hk/EPICRIVER/marine/history/result/). A water bath at 15°C was maintained by a chiller and another water bath at 30°C by a thermostatically controlled heater. A salinity of 10 psu represents the lowest salinity *N. festivus* experiences in summer during heavy rainfall at the study site, while 30 psu is the normal salinity in Hong Kong waters (Morton and Morton, 1983). In this experiment, the lowest pH level *N. festivus* were exposed to was 7.25, which was beyond the range experienced in the field. According to the Hong Kong Environmental Protection Department (2015), the pH of the sampling site varied between 7.75 and 9.00, and pH values below 7.50 were recorded only three times during the last 17 years (1986–2013). Various CO_2 partial pressures were prepared by mixing air and industrial CO_2 gas (purity of 99.5%, Hong Kong Oxygen and Acetylene Co., Ltd). The flow rate of gases was regulated by digital flowmeters (GCR-B9SA-BA15, Vogtlin, Sweden), and air and CO_2 were mixed in sealed bottles containing water, then dried in conical flasks with silica gel balls. The gas mixture was then delivered to individual experimental chambers using plastic tubing and valves (Zhang *et al.*, 2015). The control group was supplied only with ambient air. As *N. festivus* specimens were collected at an ambient temperature of 24°C and transferred to experimental temperatures of either 15 or 30°C, a control group (24°C, 30 psu) was set up to investigate changes in physiological responses, if any, after they were transferred to a new temperature. A carbon dioxide online analyser (LI-260, Li-Cor Company, Switzerland) was used to monitor the real-time pCO_2 levels. Temperature, pH (NBS scale), pCO_2, and salinity were recorded daily using a thermometer, pH meter (HI9124, Hanna, USA), carbon dioxide online analyser (LI-260, Li-Cor Company), and a refractometer (HI-211ATC, HT, China), respectively. The software CO2SYS was used to calculate the saturation state of calcite (ΩCa) and aragonite (ΩAr), total alkalinity (At), and the relationship between these factors. Total alkalinity was also checked weekly using an alkalinity titrator (HANNA, HI 84431, Germany); the variation between the calculated and measured total alkalinity was between 2.5 and 5%. Environmental parameters of the 12 treatments are summarized in Table 1.

In each replicate, 20 individuals were maintained in each glass bottle containing 1000 ml of 0.45 μm filtered natural seawater collected from a pier 9 km away from the study site; five replicates were prepared for each treatment. Replicates of 20 individuals were used because *N. festivus* is small, and the amount of food consumed and faeces produced by an individual could not be accurately determined. This inevitably would sacrifice individual variability. Seawater was changed daily to minimize the effect of microbial activity and to avoid the metabolism of the experimental animals adversely affecting seawater chemistry. In our preliminary experiment, pH was measured at the beginning and after 24 h in the experimental containers; the change in pH was only 0.02–0.03 NBS unit. This practice was continued in the main experiment. The exposure period was 31 d. All physiological parameters were measured once between Days 1 and 3 and between Days 29 and 31 to investigate the acute (first 3 d of exposure) and short-term responses and physiological adjustments, if any, to the combined stresses.

Ingestion rate

Ingestion rate (I) was measured on Days 1 and 29. The tissue wet weight of the clam *R. philippinarum* was measured to the nearest 0.0001 g. Individuals in each replicate were fed with excess clam tissue for 2 h to ensure that they were satiated as a previous study had shown that *N. festivus* required less than an hour to complete a meal (Cheung, 1994). Dry weight of clam tissue, W_{dry}, was calculated using linear regression equations established in preliminary

Table 1. Environmental parameters of the 12 treatments (mean ± SD).

	Temperature (°C)	Salinity (psu)	pCO_2 (μatm)	pH	At (mg l^{-1})	ΩCa	ΩAr
LT–LC–LS	15.2 ± 0.2	10.1 ± 0.4	392 ± 46	7.80 ± 0.18	90.3 ± 15.4	0.58	0.33
LT–LC–HS	15.1 ± 0.3	30.0 ± 0.7	392 ± 46	8.05 ± 0.09	199.3 ± 11.9	4.62	2.93
LT–MC–LS	15.4 ± 0.1	10.1 ± 0.3	934 ± 83	7.50 ± 0.07	97.7 ± 0.6	0.33	0.19
LT–MC–HS	15.2 ± 0.2	30.3 ± 0.2	934 ± 83	7.75 ± 0.02	201.1 ± 19.4	2.14	1.36
LT–HC–LS	15.3 ± 0.1	10.3 ± 0.4	1260 ± 76	7.34 ± 0.09	97.3 ± 5.5	0.21	0.12
LT–HC–HS	15.5 ± 0.3	29.8 ± 0.4	1260 ± 76	7.52 ± 0.04	197.9 ± 6.1	0.98	0.62
HT–LC–LS	29.1 ± 0.7	10.7 ± 0.8	392 ± 46	7.84 ± 0.10	87.3 ± 17.2	1.20	0.71
HT–LC–HS	29.4 ± 0.4	31.0 ± 0.7	392 ± 46	8.18 ± 0.08	199.0 ± 10.8	7.73	5.11
HT–MC–LS	29.2 ± 0.6	10.8 ± 0.5	934 ± 83	7.56 ± 0.05	102.8 ± 4.2	0.75	0.44
HT–MC–HS	29.4 ± 0.3	30.3 ± 0.6	934 ± 83	7.70 ± 0.07	198.1 ± 8.8	3.18	2.10
HT–HC–LS	29.3 ± 0.4	11.0 ± 0.4	1260 ± 76	7.37 ± 0.06	96.9 ± 2.1	0.41	0.24
HT–HC–HS	29.2 ± 0.6	30.5 ± 0.5	1260 ± 76	7.60 ± 0.06	216.4 ± 22.0	2.30	1.52

L, low; M, medium; H, high; T, temperature; C, pCO_2 levels; S, salinity.

experiments at two different salinities:

$$W_{\text{dry}-30\text{psu}} = 0.2288 \times W_{\text{fresh}} - 0.1369(\text{g})$$
$$(n = 35,\ r^2 = 0.9528,\ p < 0.01),$$
$$W_{\text{dry}-10\text{psu}} = 0.2243 \times W_{\text{fresh}} - 0.0730(\text{g})$$
$$(n = 35,\ r^2 = 0.9591,\ p < 0.01),$$

where $W_{\text{dry-30psu}}$ and $W_{\text{dry-10psu}}$ are the tissue dry weight at a salinity of 30 and 10 psu, respectively, and W_{fresh} is the tissue wet weight.

After feeding, the unconsumed tissue was oven-dried at 105°C for 24 h to constant weight then weighed. Dry weight of tissue consumed was the difference between initial tissue dry weight and unconsumed tissue dry weight.

The calorific value of the dry body tissue of *R. philippinarum* was 20.46 ± 0.36 (1 SD) kJ g^{-1} (Cheung, 1994). Ingestion rate (I, J h^{-1} ind^{-1}) was calculated by multiplying tissue dry weight consumed by the energy value of *R. philippinarum*.

$$I = 20.46 \times 1000 \times \frac{W_{\text{dry}}}{3.5 \times 24 \times 20}.$$

Absorption efficiency

The absorption efficiency (A) was determined using the following equation:

$$A = \frac{F - E}{[(1 - E) \times F]} \times 100\%,$$

where F is the ash-free dry weight : dry weight ratio of clam tissue and E the ash-free dry weight : dry weight ratio of faeces (Conover, 1966). F was determined by drying the tissue of 30 clams separately at 105°C to obtain dry tissue weight. Dry tissue was then ashed at 500°C for 3 h to obtain the ash-free dry weight. F was estimated at 89.4%. To determine E, faeces were collected on Days 2 and 30 by filtering the seawater through a dry preweighed glass filter paper of 0.45 μm (Whatman GF/C 47 mm). Filter papers were rinsed with isotonic ammonium formate (3%) to remove salts and dried to constant weight at 105°C for 24 h to obtain the dry weight, then ashed at 500°C for 3 h to get the ash-free dry weight.

Absorption rate

Absorption rate (Ab, J h^{-1} ind^{-1}) was calculated using I (J h^{-1} ind^{-1}) and A as follows:

$$\text{Ab} = I \times \frac{A}{100}.$$

Energy expended on respiration

Energy expended on respiration (R) was determined on Days 3 and 31. As the individuals were small, 20 individuals in each replicate were divided into four groups with five individuals each and respiration rate was determined for each group of five individuals by incubating them for 1 h in a sealed syringe containing 50 ml of seawater from the corresponding treatment. The respiration rate obtained was divided by five to obtain the rate per individual. The mean respiration rate was obtained for each replicate by averaging the values obtained from the four groups. Precautions were taken to prevent air bubbles being trapped in the syringe. One syringe without gastropods served as the control for each treatment. The initial and final dissolved oxygen (DO) levels in each syringe were monitored by a DO meter (TauTheta SOO-100) and respiration rate estimated by the software (TTI O2 1.08). The initial DO levels were ca. 6.0 mg l^{-1} (21 kPa), and the final DO levels were not less than 3.0 mg l^{-1} to prevent reduction in the metabolic rate due to low DO content. The respiration rate (mg h^{-1} ind^{-1}) was converted to energy expended (J h^{-1} ind^{-1}) using a conversion factor of 14.14 J mg^{-1} O_2 (Elliott and Davison, 1975). The mean values and SDs obtained from the five replicates were used in subsequent statistical analyses.

Energy expended on ammonia excretion

Energy expended on ammonia excretion rate (U) was determined immediately after respiration rate measurement. For each replicate, five gastropods were assigned to each group and four groups were prepared for each replicate. Each group was incubated for 1 h in a well-sealed syringe with 50 ml of seawater from the corresponding treatment. One syringe without gastropods was prepared for each treatment and served as a control. Ammonia content in the samples and blanks was determined using a Flow Injection Analyser (Lachat QuikChem 8500).

The ammonia excretion rate was converted into an energy equivalent using a conversion factor of 0.025 J μg^{-1} NH_4-N (Elliott and Davison, 1975). For each replicate, a mean value was calculated by averaging the values obtained from the four groups. The mean values and SDs obtained from the five replicates were used in subsequent statistical analyses.

Scope for growth

SfG (J h^{-1} ind^{-1}) was calculated using the following equation (Winberg, 1960):

$$\text{SfG} = \text{Ab} - (R + U),$$

where Ab was the absorption rate, R the energy expended on respiration, and U the energy expended on ammonia excretion. SfG was calculated on Days 3 and 31 using data collected on Day 1, Day 2 and Day 29, Day 30, respectively.

Mortality

Cumulative mortality was recorded daily throughout the experiment. Individuals were defined as dead if they retracted their siphon and could not extend their body out of the shell in ambient seawater after 10 min in addition to the smell of decomposing soft tissue.

Data analysis

As the amount of food consumed and amount of faeces produced by each gastropod were very small, ingestion rate, absorption rate and efficiency, and SfG were determined for each replicate by incubating 20 individuals in the same experimental chamber. The data were analysed by three-way ANOVA. When there was an interaction among the three factors, the effects of temperature, salinity, and pCO_2 were analysed separately at each level of the other factors by one-way ANOVA followed by multiple comparison Tukey test. As the gastropods were maintained at 24°C before the experiment and transferred to either 15 or 30°C, a control group at 24°C, and 380 μatm pCO_2 was set up. Physiological responses of the control group were compared by one-way ANOVA with the groups exposed to either 15°C and 380 μatm pCO_2 or 30°C and

380 μatm. Normality and equal variance of the data were checked by the Shapiro–Wilk test and Levene's test, respectively. All the analyses were performed using SPSS 20.0.

Results

Mortality

Most individuals (≥80%) survived the 31 d of exposure for all the treatment groups. No mortality was observed for the control group and some high salinity groups (i.e. LT–MC–HS and HT–LC–HS). However, significantly higher cumulative mortality was found under low salinity (d.f. = 1, $F = 36.37$, $p < 0.001$). On the other hand, pCO_2 and temperature did not have any effect on cumulative mortality (Figure 1).

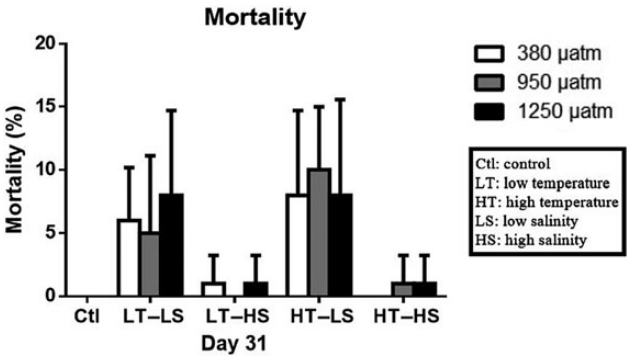

Figure 1. Cumulative mortality of *N. festivus* upon exposure to different combinations of temperature, salinity, and pCO_2 level for 31 d.

Ingestion rate

Ingestion rate was reduced following exposure to low salinity (Day 1: d.f. = 1, $F = 181.71$, $p < 0.001$; Day 29: d.f. = 1, $F = 10.22$, $p < 0.005$) or low temperature (Day 1: d.f. = 1, $F = 5.20$, $p < 0.05$; Day 29: d.f. = 1, $F = 33.61$, $p < 0.001$; Figure 2). Interaction between temperature and pCO_2 was observed on Day 1 as analysed by three-way ANOVA (d.f. = 2, $F = 4.20$, $p < 0.05$). However, when the effect of temperature was compared at each pCO_2 level and the effect of pCO_2 at each temperature, no significant differences were found. Ingestion rates at 15 and 30°C were not significantly different from the control at 24°C, but the rate at 15°C was significantly lower than at 30°C (d.f. = 1, $F = 4.62$, $p < 0.05$).

Absorption efficiency

Absorption efficiency (A) varied between 71 and 96% and was not affected significantly by temperature (d.f. = 1, $F = 0.298$, $p = 0.588$), salinity (d.f. = 1, $F = 3.47$, $p = 0.068$), pCO_2 (d.f. = 2, $F = 0.06$, $p = 0.939$), or the interactions between these factors on Day 2 (temperature × pCO_2: d.f. = 2, $F = 0.06$, $p = 0.940$; temperature × salinity: d.f. = 1, $F = 1.57$, $p = 0.217$; pCO_2 × salinity: d.f. = 2, $F = 0.13$, $p = 0.876$; temperature × pCO_2 × salinity: d.f. = 2, $F = 0.03$, $p = 0.975$). On Day 30, salinity reduced A significantly (d.f. = 1, $F = 9.08$, $p < 0.005$) (Figure 3). One-way ANOVA showed that A values at 15, 24, and 30°C were not significantly different (Day 2: d.f. = 1, $F = 0.38$, $p = 0.694$; Day 30: d.f. = 1, $F = 2.49$, $p = 0.133$).

Absorption rate

Absorption rate (Ab) was reduced substantially (Figure 4) under low salinity on Day 2 (d.f. = 1, $F = 163.37$, $p < 0.001$) and the effect was

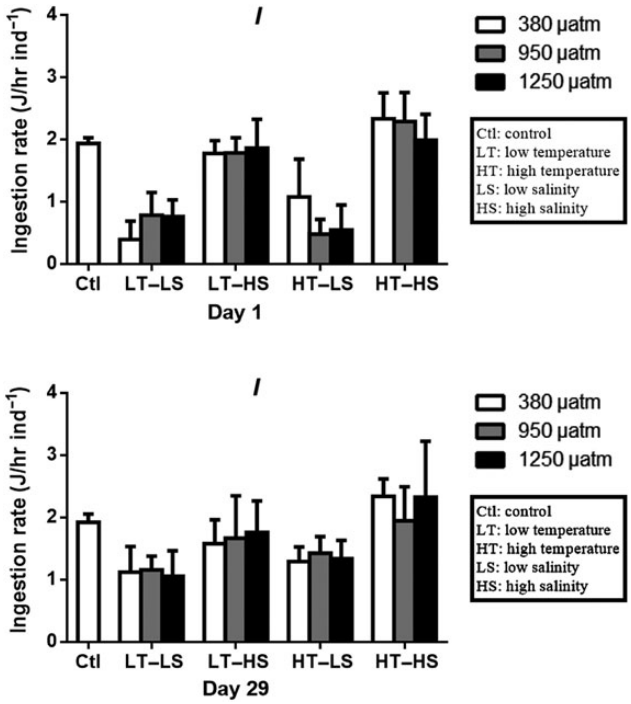

Figure 2. Combined effect of temperature, salinity, and pCO_2 on the ingestion rate (I) of *N. festivus* on Days 1 and 29.

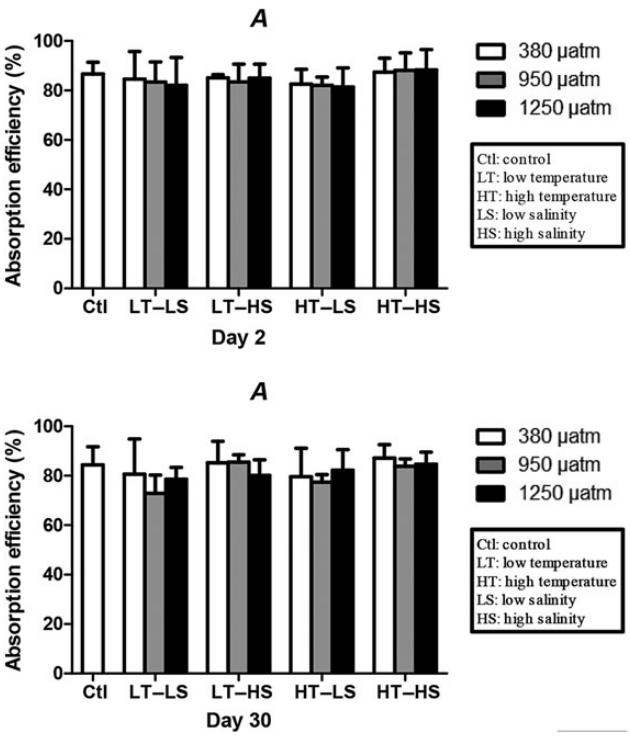

Figure 3. Combined effect of temperature, salinity, and pCO_2 on the absorption efficiency (A) of *N. festivus* on Days 2 and 30.

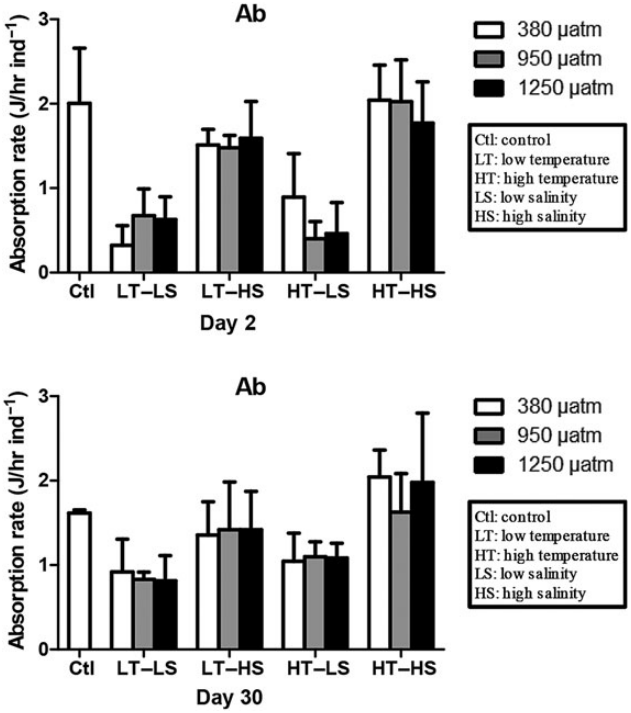

Figure 4. Combined effect of temperature, salinity, and pCO_2 on the absorption rate (Ab) of *N. festivus* on Days 2 and 30.

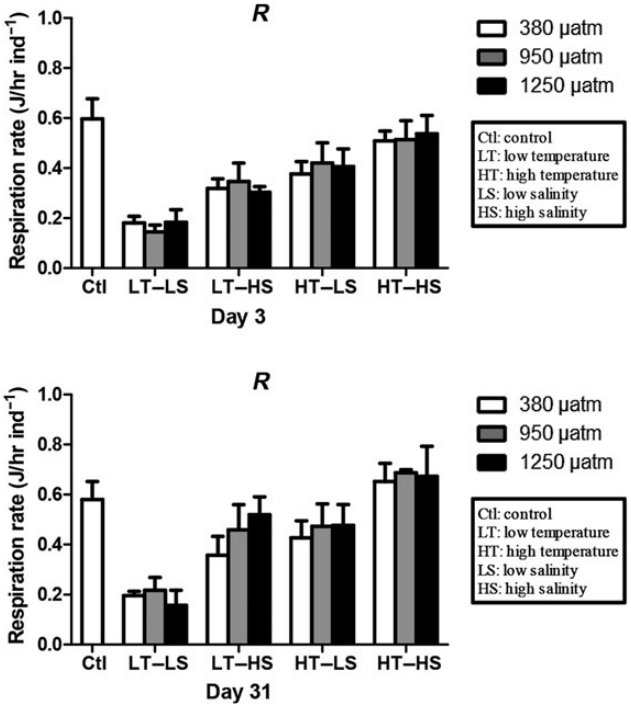

Figure 5. Combined effect of temperature, salinity, and pCO_2 on the respiration rate (*R*) of *N. festivus* on Days 3 and 31.

also seen at the end of the experiment on Day 30 (d.f. = 1, $F = 6.84$, $p < 0.001$). Reduction in Ab was also observed at the lower temperature on both Day 2 (d.f. = 1, $F = 6.65$, $p < 0.05$) and Day 30 (d.f. = 1, $F = 10.71$, $p < 0.005$). The effect of pCO_2, however, was statistically indistinguishable (d.f. = 2, $F = 0.26$, $p = 0.771$). No interaction between the three factors was observed throughout the experiment (Day 2: temperature × pCO_2: d.f. = 2, $F = 3.08$, $p = 0.055$; temperature × salinity: d.f. = 1, $F = 3.87$, $p = 0.055$; pCO_2 × salinity: d.f. = 2, $F = 0.10$, $p = 0.904$; temperature × salinity × pCO_2: d.f. = 2, $F = 1.62$, $p = 0.208$; Day 30: temperature × pCO_2: d.f. = 2, $F = 0.29$, $p = 0.750$; temperature × salinity: d.f. = 1, $F = 1.50$, $p = 0.227$; pCO_2 × salinity: d.f. = 2, $F = 0.31$, $p = 0.738$; temperature × salinity × pCO_2: d.f. = 2, $F = 0.70$, $p = 0.501$).

Energy expended on respiration

Energy expended on respiration (*R*) did not change under elevated pCO_2 levels (d.f. = 2, $F = 0.24$, $p = 0.791$), but increased significantly at elevated temperatures (d.f. = 1, $F = 216.56$, $p < 0.001$) or salinities (d.f. = 1, $F = 86.88$, $p < 0.001$) and the effects persisted until the end of the experiment (Figure 5). No interaction between the three factors was observed throughout the experiment (Day 2: temperature × pCO_2: d.f. = 2, $F = 0.55$, $p = 0.579$; temperature × salinity: d.f. = 1, $F = 1.34$, $p = 0.253$; pCO_2 × salinity: d.f. = 2, $F = 0.21$, $p = 0.808$; temperature × salinity × pCO_2: d.f. = 2, $F = 1.62$, $p = 0.208$; Day 30: temperature × pCO_2: d.f. = 2, $F = 0.16$, $p = 0.85$; temperature × salinity: d.f. = 1, $F = 1.24$, $p = 0.270$; pCO_2 × salinity: d.f. = 2, $F = 1.68$, $p = 0.198$; temperature × salinity × pCO_2: d.f. = 2, $F = 3.02$, $p = 0.058$). At 380 µatm pCO_2, *R* at 24°C was not significantly different from that at 30°C (Day 3: $p = 0.087$; Day 31, $p = 0.410$), but was significantly higher than that at 15°C on both days (Day 3: $p < 0.001$; Day 31, $p < 0.005$).

Energy expended on ammonia excretion

Ammonia excretion (*U*) was reduced significantly at low salinity or temperature on both Days 3 and 31 (Figure 6). On Day 3, the interaction between temperature and pCO_2 was significant (d.f. = 2, $F = 3.36$, $p < 0.05$). No statistical difference in *U* was found between three pCO_2 levels at both 15 and 30°C, but the rate was significantly higher at 30°C than at 15°C for all the pCO_2 levels (Table 2). Significant interaction between the three factors was also found on Day 31 (d.f. = 2, $F = 3.95$, $p < 0.05$; Table 3). The effect of temperature was significant at all combinations of pCO_2 and salinity. The effect of salinity, however, was only significant at 380 and 1250 µatm pCO_2 at 15°C, and 950 and 1250 µatm pCO_2 at 30°C. Differences in *U* among the three pCO_2 levels were significant at 10 psu and 30°C only. *U* at 15°C were not statistically different from that at 24°C on both days (Day 3: $p = 0.367$; Day 31: $p = 0.163$), whereas *U* at 30°C was significantly higher on Day 3 ($p < 0.050$) but not on Day 31 ($p = 0.804$).

Scope for growth

SfG was reduced significantly at low salinity on Day 3 (d.f. = 1, $F = 121.94$, $p < 0.001$) and Day 31 (d.f. = 1, $F = 16.52$, $p < 0.001$; Figure 7). The interactive effect between temperature and pCO_2 (d.f. = 2, $F = 3.33$, $p < 0.05$) and that between temperature and salinity (d.f. = 1, $F = 4.49$, $p = 0.05$) were significant on Day 3. Multiple comparison tests showed that SfG reduced at low salinity for both temperatures (Table 4). SfG at 24°C was not significantly different from that at 15 and 30°C on Day 3 (d.f. = 1, $F = 0.70$, $p = 0.520$) and Day 31 (d.f. = 1, $F = 2.12$, $p = 0.171$).

Discussion

The physiological responses of *N. festivus* were positively correlated with temperature and salinity. In contrast, the effect of pCO_2 was

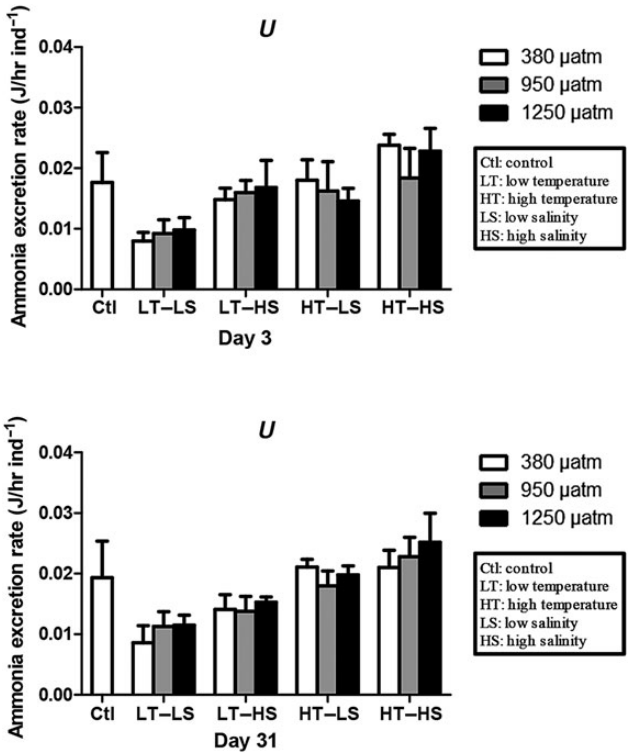

Figure 6. Combined effect of temperature, salinity, and pCO_2 on the excretion rate (U) of *N. festivus* on Days 3 and 31.

insignificant and its combined effects with temperature and/or salinity were also weak and only occurred in the early phase of the experiment.

Responses to future ocean acidification have been extensively studied in the past few years with negative effects observed in the most species tested, including molluscs (Kroeker *et al.*, 2010; Parker *et al.*, 2013), and neutral or positive effects appearing to differ among species and life stages (Dupont *et al.*, 2013). For instance, the sea urchin *Echinometra* sp. showed no significant differences in somatic and gonadal growth under pCO_2 1433 µatm after 11 months exposure (Hazan *et al.*, 2014). *Sterechinus neumayeri* also showed acclimation after 8 months exposure to low pH (−0.5 U; Suckling, *et al.*, 2015). Cross *et al.* (2015) reported no ocean acidification effects on shell growth and repair in the New Zealand brachiopod *Calloria inconspicua* after exposure to pH 7.62 for 12 weeks. Nevertheless, increased rates of calcification in low pH waters have been observed for a few taxa including crustaceans (Ries *et al.*, 2009; Kroeker *et al.*, 2010), ophiuroids (Wood *et al.*, 2008), and pisces (Melzner *et al.*, 2009a; Hurst *et al.*, 2013). The sea star, *Asterias rubens*, and the brittlestars, *O. fragilis* and *A. filiformis*, showed neutral responses in metabolic rate after being exposed to warming (20°C) and ocean acidification (pH 7.5) for 1 week (Carey *et al.*, 2014).

In the present study, *N. festivus* showed high resilience to ocean acidification as no physiological effects were observed. Generally, intertidal organisms are more tolerant of variations in environmental variables, such as pH, temperature, and salinity, as they naturally exist in a fluctuating environment (Maderira *et al.*, 2014). This phenomenon has been observed for the larvae of the sea urchin

Table 2. One-way ANOVA and the multiple comparison Tukey test for the temperature effect at each pCO_2 level and the effect of pCO_2 at each temperature on energy expended on excretion on Day 3.

	d.f.	MS	*F*	*p*	Tukey test		
15°C	2	$9.233^{E-0.006}$	0.488	0.619	380 µatm	950 µatm	1250 µatm
30°C	2	$3.293^{E-0.005}$	1.515	0.238	380 µatm^{a}	950 µatm	1250 µatm
380 µatm	1	0.000	28.875	**0.000**	15°C^{a}	30°C^{b}	
950 µatm	1	0.000	5.608	**0.029**	15°C^{a}	30°C^{b}	
1250 µatm	1	0.000	5.678	**0.028**	15°C^{a}	30°C^{b}	

Values in bold are statistically significant. Values in the same row with different letter designations indicate that they are statistically different.

Table 3. One-way ANOVA and the multiple comparison Tukey test of energy expended on excretion on Day 31.

	d.f.	MS	*F*	*p*	Tukey test		
10 psu-15°C	2	$1.047^{E-0.005}$	1.880	0.195	380 µatm	950 µatm	1250 µatm
10 psu-30°C	2	$1.287^{E-0.005}$	3.899	**0.050**	380 µatm^{a}	950 µatm^{b}	1250 µatm^{ab}
30 psu-15°C	2	$3.467^{E-0.006}$	0.819	0.464	380 µatm	950 µatm	1250 µatm
30 psu-30°C	2	$2.427^{E-0.005}$	1.742	0.217	380 µatm	950 µatm	1250 µatm
15°C-380 µatm	1	$7.290^{E-0.005}$	9.785	**0.014**	10 psu^{a}	30 psu^{b}	
15°C-950 µatm	1	$1.690^{E-0.005}$	2.965	0.123	10 psu	30 psu	
15°C-1250 µatm	1	$4.000^{E-0.005}$	25.806	**0.001**	10 psu^{a}	30 psu^{b}	
30°C-380 µatm	1	$1.000^{E-0.007}$	0.020	0.892	10 psu	30 psu	
30°C-950 µatm	1	$6.250^{E-0.005}$	7.812	**0.023**	10 psu^{a}	30 psu^{b}	
30°C-1250 µatm	1	$7.840^{E-0.005}$	6.149	**0.038**	10 psu^{a}	30 psu^{b}	
10 psu-380 µatm	1	0.000	73.923	**0.000**	15°C^{a}	30°C^{b}	
10 psu-950 µatm	1	0.000	19.761	**0.002**	15°C^{a}	30°C^{b}	
10 psu-1250 µatm	1	0.000	78.400	**0.000**	15°C^{a}	30°C^{b}	
30 psu-380 µatm	1	0.000	15.728	**0.004**	15°C^{a}	30°C^{b}	
30 psu-950 µatm	1	0.000	26.955	**0.001**	15°C^{a}	30°C^{b}	
30 psu-1250 µatm	1	0.000	20.747	**0.002**	15°C^{a}	30°C^{b}	

Values in bold indicate the differences were statistically significant. Values in the same row with different letter designations indicate that they are statistically different.

Paracentrotus lividus living in contrasting environments, with intertidal populations being more tolerant of a decrease in pH than subtidal populations (Moulin *et al.*, 2011). Tolerance of an organism to elevated pCO_2 may be due to its ability to compensate for CO_2-induced changes in extracellular pH (Wittmann and Pörtner, 2013). Our previous study on the subtidal gastropod *N. conoidalis*, a congeneric counterpart of the intertidal *N. festivus*, demonstrated metabolic depression when exposed to ocean acidification (Zhang *et al.*, 2015). This is a common phenomenon of uncompensated changes in extracellular pH and intracellular pH, but was not observed for *N. festivus* (Zhang *et al.*, 2015).

Extracellular acid–base regulation during short-term hypercapnia has been shown in the Dungeness crab, *Cancer magister*, which inhabits fluctuating shallow waters, but was absent in the relatively stable habitat of the deep-sea Tanner crab *Chionoecetes tanneri* (Pane and Barry, 2007). Compensation for hypercapnic acidosis in body fluids and calcification compartments during exposure to ocean acidification involves pH and ion regulation across the epithelia of gills, gut, and kidneys and is driven by energy-consuming ion pumps (Wittmann and Pörtner, 2013). The associated energetic costs may shift the energy budget of the organism (Pörtner, 2008). Although ocean acidification did not affect physiological responses and SfG in *N. festivus*, an increase in the cost of acid–base regulation, if any, may alter the energy allocation strategy (e.g. reduction in reproductive output), and this deserves further investigations.

A weak interactive effect between temperature and pCO_2 on physiological responses (ingestion, excretion and SfG) in *N. festivus* was recorded in the early phase of the present experiment (Days 1–3). Enhancement of temperature effects under low pH has been shown in various marine species. For example, production of the heat shock protein HSP70 in the crab *Pachygrapsus marmoratus* was significantly reduced by the combined effects of temperature and pH, but not by thermal stress alone (Maderira *et al.*, 2014). Spine development in the sea urchin *Heliocidaris erythrogramma* was negatively affected by an increase in temperature (+2 to 4°C) and extreme acidification (pH 7.4), with a complex interaction between the stressors (Wolfe *et al.*, 2013). In our previous study, reduction in physiological responses (ingestion, absorption, respiration, and excretion) upon exposure to pCO_2 was enhanced at high temperature (30°C) in the benthic gastropod *N. conoidalis* (Zhang *et al.*, 2015). Most organisms have an optimal temperature range within which physiological performance is maximized (Pörtner *et al.*, 2005). However, acidification may intensify the sensitivity of the organisms to temperature change, resulting in a synergistic effect of elevated temperature and CO_2-induced ocean acidification on energy metabolism that narrows the thermal tolerance window of marine ectotherms (Pörtner and Farrell, 2008).

Reduced animal performance upon exposure to salinity outside of their natural range, regardless of hyper- or hyposalinity, is widely recognized (Newell, 1976; Chaparro *et al.*, 2014). Hyposalinity may cause hypo-osmotic stress-induced physiological and ion-osmoregulatory responses in marine animals (Sinha *et al.*, 2015) and enhances the effect of ocean acidification on acid–base regulation (Zhang *et al.*, 2014). For instance, when both pH and salinity were reduced simultaneously (pH 7.6, salinity 26.2 psu), the interaction between the two stresses affected the predatory gastropod *Limacina retroversa* negatively both in terms of survival rate and an ability to swim upwards (Manno *et al.*, 2012). Low salinity reduced growth, elevated mortality, and impaired shell maintenance in juveniles of the hard-shell clam, *Mercenaria mercenaria*,

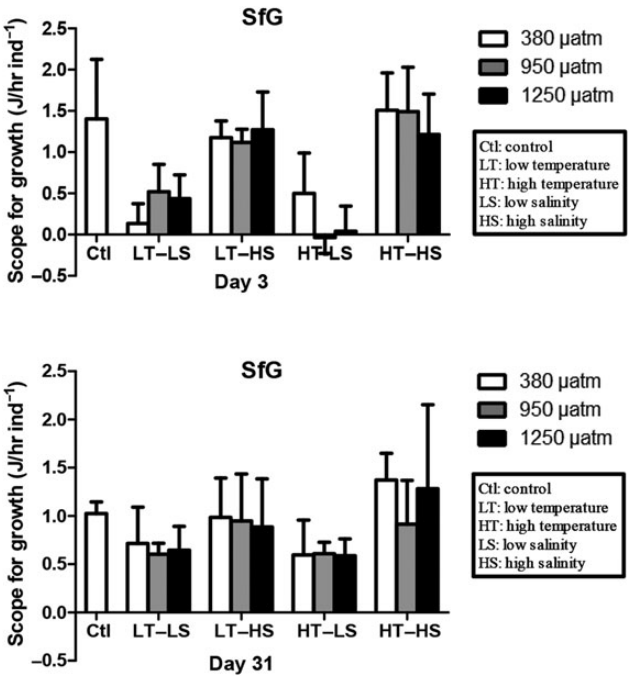

Figure 7. Combined effect of temperature, salinity, and pCO_2 on the SfG of *N. festivus* on Days 3 and 31.

Table 4. One-way ANOVA and the multiple comparison Tukey test for the (a) temperature effect at each pCO_2 level and pCO_2 effect at each temperature and (b) temperature effect at each salinity and salinity effect at each temperature on SfG on Day 3.

	d.f.	MS	*F*	*p*	Tukey test		
(a) Temperature effect at each pCO_2 level and pCO_2 effect at each temperature							
15°C	2	0.104	0.378	0.689	380 µatm	950 µatm	1250 µatm
30°C	2	0.380	0.633	0.539	380 µatm	950 µatm	1250 µatm
380 µatm	1	0.605	1.463	0.242	15°C	30°C	
950 µatm	1	0.025	0.053	0.821	15°C	30°C	
1250 µatm	1	0.256	0.601	0.448	15°C	30°C	
(b) Temperature effect at each salinity and salinity effect at each temperature							
15°C	1	5.270	62.804	**0.000**	10 psu[a]	30 psu[b]	
30°C	1	11.463	58.079	**0.000**	10 psu[a]	30 psu[b]	
10 psu	1	0.248	1.986	0.170	15°C	30°C	
30 psu	1	0.350	2.241	0.146	15°C	30°C	

Values in the same row with different letter designations indicate that they are statistically significant ($p < 0.05$).

owing to strongly elevated basal energy demand. Low salinity also modulated responses to elevated pCO_2 through negatively affecting the mechanical properties of the shell (Dickinson *et al.*, 2013).

Low salinity had a major effect on the survival and physiological energetics of *N. festivus* in the present study. Unlike *M. mercenaria*, both energy intake and expenditure in *N. festivus* was reduced at low salinity, possibly owing to the experimental salinity approaching the lethal limit as the lowest salinity for *N. festivus* to survive indefinitely has been estimated at 11.5 psu (Morton, 1990). This may also help explain the absence of interactive effects between salinity and pCO_2, as the effect of low salinity possibly overshadowed that of pCO_2.

pCO_2 levels enhanced the effects of temperature/salinity on physiological responses only in the first few days of the present experiment, but the pCO_2 effect was absent after 1 month. This may indicate rapid adjustment of physiological responses to pCO_2, possibly through regulation of extra- and/or intracellular pH. In the cold-water coral *L. pertusa*, short-term (1 week) high CO_2 exposure under pH 7.77 resulted in a decline of calcification by 26–29% and a net dissolution of calcium carbonate. Acclimation to acidified conditions, however, has been observed following long-term (6 months) experiments, leading to even slightly enhanced rates of calcification (Form and Riebesell, 2012). Although a short-term exposure (1 month) to ocean acidification had no effect on the physiological responses in *N. festivus*, reduction in physiological performance may eventually lead to a gradual deterioration of body conditions and result in negative effects on growth and reproduction. For example, reduction in female fecundity has been observed in the sea urchin *Strongylocentrotus droebachiensis* following exposure to pCO_2 for 4 months (Dupont *et al.*, 2013). Movilla *et al.* (2014) found that the calcification rate of the coral *Desmophyllum dianthus* was not reduced by pH 7.81 after 49 d of exposure, but the rate was significantly reduced when the exposure period was extended to 314 d. An experiment for an extended period of several months could clarify whether the neutral effects of ocean acidification on the physiological responses of *N. festivus* observed in the present study were results of complete acclimation.

Physiological energetics reveals the energy allocation strategy of individuals. However, many studies have shown that effects of ocean acidification can be cumulative and carryover to successive life stages as well as across generations (transgenerational effect). Significant transgenerational responses are expected when environmental changes such as ocean acidification persist (Sunday *et al.*, 2011). For example, adult sea urchins pre-exposed for 4 months to 1200 μatm pCO_2 had a direct negative impact on subsequent larval settlement success, with five to nine times fewer offspring reaching the juvenile stage (Dupont *et al.*, 2013). After the calanoid copepod *Pseudocalanus acuspes* was grown for two generations under 1550 μatm pCO_2, there was an apparent alleviation of effects on fecundity and metabolic stress as a result of transgenerational factors (Thor and Dupont, 2015).

Carryover effects of ocean acidification have also been reported in the Olympia oyster (*Ostrea lurida*), where juveniles reared as larvae under reduced pH exhibited a 41% decrease in shell growth rate. This effect was persistent regardless of the pH level the oysters experienced as juveniles, indicating a strong carryover effect from the larval phase (Hettinger *et al.* 2012). In addition, the carryover effect of larvae may reduce adult fitness, including brain development (Trokovic *et al.*, 2011) and reproduction (Araki and Blouin, 2009). Our previous study on early life stages of *N. festivus* has demonstrated that larvae hatched under an elevated high pCO_2 level (1250 μatm) were smaller and the juveniles grew slower (unpublished data). Smaller newly hatched larvae may experience a slower growth and take a longer time to metamorphose into juveniles which, themselves, may be smaller. This highlights the importance of tests for transgenerational and carryover effects in future research programmes.

Under the combined effect of temperature, salinity, and ocean acidification, mortality and the maintenance cost of the larvae of *N. festivus* increased (Zhang *et al.*, 2014). Larvae hatched under an elevated pCO_2 were smaller and the juveniles grew slower (unpublished data). Younger life stages, therefore, are more sensitive to these stresses than adults. An extensive review of studies on sea urchins has shown that larvae and juveniles are much more sensitive to ocean acidification than adults and gametes (Dupont and Thorndyke, 2013). Similar observations have been reported for marine molluscs (Parker *et al.*, 2013), possibly due to shell structure, which is composed of more soluble forms of calcium carbonate, i.e. amorphous calcium carbonate and aragonite (Wicks and Roberts, 2012) and the lack of the ability to maintain acid–base status (Melzner *et al.*, 2009b). Although neutral effects have been observed for the energy budget of *N. festivus* adults upon exposure to multiple stressors, population performance may be impacted through observed effects on younger life stages.

Acknowledgements

We thank two anonymous reviewers for their constructive comments on the manuscript and Bruce Richardson for improving the English. Our work was fully supported by a strategic research grant (grant no. 7004027) of the City University of Hong Kong.

References

Abduraji, T. S., and Danilo, D. T. 2015. Effects of reduced pH on the growth and survival of postlarvae of the donkey's ear abalone, *Haliotis asinina* (L.). Aquaculture International, 23: 141–153.

Andersson, A. J., Mackenzie, F. T., and Gattuso, J-P. 2011. Effects of ocean acidification on benthic processes, organisms, and ecosystems. *In* Ocean Acidification, pp. 122–153. Ed. by J-P. Gattuso, and L. Hansson. Oxford University Press, Oxford.

Appelhans, Y. S., Thomsen, J., Opitz, S., Pansch, C., and Melzner, F. 2014. Juvenile sea stars exposed to acidification decrease feeding and growth with no acclimation potential. Marine Ecology Progress Series, 509: 227–239.

Araki, H., and Blouin, M. S. 2009. Carry-over effect of captive breeding reduces reproductive fitness of wild-born descendants in the wild. Biology Letters, 5: 621–624.

Barry, J. P., Widdicombe, S., and Hall-Spencer, J. M. 2011. Effect of ocean acidification on marine biodiversity and ecosystem function. *In* Ocean Acidification, pp. 192–209. Ed. by J-P. Gattuso, and L. Hansson. Oxford University Press, Oxford.

Bayne, B. L., and Newell, R. C. 1983. Physiological energetics of marine molluscs. *In* The Mollusca, Vol. 4, Physiology, Part 1, pp. 407–515. Ed. by K. M. Wilbur, and A. S. M. Salenddin. Academic Press, London.

Bramanti, L., Movilla, J., Guron, M., Calvo, E., Gori, A., Dominguez-Carrió, C., Grinyó, J., *et al.* 2013. Detrimental effects of ocean acidification on the economically important Mediterranean red coral (*Corallium rubrum*). Global Change Biology, 19: 1897–1908.

Briton, J. C., and Morton, B. 1992. The ecology and feeding behaviour of *Nassarius festivus* (Prosobranchia: Nassariidae) from two Hong Kong bays. In The Marine Flora and Fauna of Hong Kong and southern China III. Proceedings of the Fourth International Marine Biological Workshop: The Marine Flora and Fauna of Hong Kong and Southern China, Hong Kong, pp. 395–416. Ed. by B. Morton. Hong Kong University Press, Hong Kong.

Caldeira, K., and Wickett, M. E. 2003. Anthropogenic carbon and ocean pH. Nature, 425: 365.

Carey, N., Dupont, S., Lundve, B., and Sigwart, J. D. 2014. One size fits all: Stability of metabolic scaling under warming and ocean acidification in echinoderms. Marine Biology, 161: 2131–2142.

Chan, H. Y., Xu, W. Z., Shin, P. K. S., and Cheung, S. G. 2008. Prolonged exposure to low dissolved oxygen affects early development and swimming behavior in the gastropod *Nassarius festivus* (Nassariidae). Marine Biology, 153: 735–743.

Chaparro, O. R., Segura, C. J., Osores, S. J. A., Pechenik, J. A., Pardo, L. M., and Cubillos, V. M. 2014. Consequences of maternal isolation from salinity stress for brooded embryos and future juveniles in the estuarine direct-developing gastropod *Crepipatella dilatata*. Marine Biology, 161: 619–629.

Cheung, S. G. 1994. Feeding behavior and activity of the scavenging gastropod *Nassarius festivus* (Powys). *In* Proceedings of the Third International Workshop on the Malacofauna of Hong Kong and Southern China, pp. 557–574. Ed. by B. Morton. Hong Kong University Press, Hong Kong.

Cheung, S. G., and Lam, S. W. 1995. Effect of salinity, temperature and acclimation on oxygen consumption of *Nassarius festivus* (Powys, 1835) (Gastropoda: Nassariidae). Comparative Biochemistry and Physiology, 111(A): 625–631.

Collins, M., Knutti, R., Arblaster, J., Dufresne, JL., Fichefet, T., Friedlingstein, P., Gao, X., *et al.* 2013. Long-term climate change: Projections, commitments and irreversibility. *In* Climate Change 2013: The Physical Science Basis. Contribution of Working Group I to the Fifth Assessment Report of the Intergovernmental Panel on Climate Change, pp. 1029–1136. Ed. by T. F. Stocker, D. Qin, G-K. Plattner, M. Tignor, S. K. Allen, J. Boschung, A. Nauels, Y. Xia, V. Bex, and P. M. Midgley. Cambridge University Press, Cambridge, UK.

Conover, R. J. 1966. Assimilation of organic matter by zooplankton. Limnology and Oceanography, 11: 338–354.

Cross, E. L., Peck, L. S., and Harper, E. M. 2015. Ocean acidification does not impact shell growth or repair of the Antarctic brachiopod *Liothyrella uva* (Broderip, 1833). Journal of Experimental Marine Biology and Ecology, 462: 29–35.

Dickinson, G. H., Ivanina, A. V., Matoo, O. B., Pörtner, H-O., Lannig, G., Bock, C., Beniash, E., *et al.* 2012. Interactive effects of salinity and elevated CO_2 levels on juvenile eastern oysters, *Crassostrea virginica*. Journal of Experimental Biology, 215: 29–43.

Dickinson, G. H., Matoo, O. B., Tourek, R. T., Sokolova, I. M., and Beniash, E. 2013. Environmental salinity modulates the effects of elevated CO_2 levels on juvenile hard-shell clams, *Mercenaria mercenaria*. Journal of Experimental Biology, 216: 2607–2618.

Dupont, S., Dorey, N., Stumpp, M., Melzner, F., and Thorndyke, M. 2013. Long-term and trans-life cycle effects of exposure to ocean acidification in the green sea urchin *Strongylocentrotus*. Marine Biology, 160: 1835–1843.

Dupont, S. T., and Thorndyke, M. S. 2013. Direct impacts on near-future ocean acidification on sea urchins. *In* Climate Change Perspectives from the Atlantic: Past, Present and Future, pp. 461–485. Ed. by J. M. Fernandez-Palacios, L. de Nascimento, J. C. Hernandez, S. Clemente, A. Gonzalez, and J. P. Diaz-Gonzalez. Servicio de Publicaciones, Universidad de La Laguna, La Laguna, Spain.

Elliott, J. M., and Davison, W. 1975. Energy equivalents of oxygen consumption in animals energetics. Oecologia, 19: 195–201.

Environmental Protection Department. 2015. Marine Water Quality Monitoring. Environmental Protection Department, Hong Kong SAR Government. http://wqrc.epd.gov.hk/en/water-quality/marine-1.aspx (last accessed 3 November 2015).

Form, A. U., and Riebesell, U. 2012. Acclimation to ocean acidification during long-term CO_2 exposure in the cold-water coral *Lophelia pertusa*. Global Change Biology, 18: 843–853.

Foster, B. A. 1970. Response and acclimation to salinity in the adults of some balanomorph barnacles. Philosophical Transactions of the Royal Society of London, B256: 377–400.

Hazan, Y., Wangensteen, O. S., and Fine, M. 2014. Tough as a rock-boring urchin: Adult *Echinometra* sp. EE from the Red Sea show high resistance to ocean acidification over long-term exposures. Marine Biology, 161: 2531–2545.

Hettinger, A., Sanford, E., Hill, T. M., Russell, A. D., Sato, K. N., Hoey, J., Forsch, M., *et al.* 2012. Persistent carry-over effects of planktonic exposure to ocean acidification in the Olympia oyster. Ecology, 93: 2758–2768.

Honjo, S., Francois, R., Manganini, S., Dymond, J., and Collier, R. 2000. Particle fluxes to the interior of the Southern Ocean in the Western Pacific sector along 170°W. Deep Sea Research Part II: Topical Studies in Oceanography, 47: 3521–3548.

Hurst, T. P., Fernandez, E. R., and Mathis, J. T. 2013. Effects of ocean acidification on hatch size and larval growth of walleye pollock (*Theragra chalcogramma*). ICES Journal of Marine Science, 70: 812–822.

Johnston, I. A., and Dunn, J. 1987. Temperature acclimation and metabolism in ectotherms with particular reference to teleost fish. Symposia of the Society for Experimental Biology, 41: 67–93.

Kroeker, K. J., Kordas, R. L., Crim, R. N., and Singh, G. G. 2010. Meta-analysis reveals negative yet variable effects of ocean acidification on marine organisms. Ecology Letters, 13: 1419–1434.

Le Quéré, C., Raupach, M. R., Canadell, J. G., Marland, G., Bopp, L., Ciais, P., Conway, T. J., *et al.* 2009. Trends in the sources and sinks of carbon dioxide. Nature Geoscience, 2: 831–836.

Liu, C. C., Chiu, J. M. Y., Li, L., Shin, P. K. S., and Cheung, S. G. 2011. Physiological responses of two sublittoral nassariid gastropods to hypoxia. Marine Ecology Progress Series, 429: 75–85.

Luthi, D., Le Floch, M., and Bereiter, B. 2008. High-resolution carbon dioxide concentration record 650,000–800,000 years before present. Nature, 453: 379–382.

Maderira, D., Narciso, L., Diniz, M. S., and Vinagre, C. 2014. Synergy of environmental variables alters the thermal window and heat shock response: An experimental test with the crab *Pachygrapsus marmoratus*. Marine Environmental Research, 98: 21–28.

Manno, C., Morata, N., and Primicerio, R. 2012. *Limacina retroversa*'s response to combined effects of ocean acidification and seawater freshening. Estuarine, Coastal and Shelf Science, 113: 163–171.

Melzner, F., Göbel, S., Langenbuch, M., Gutowska, M., Pörtner, H-O., and Lucassen, M. 2009a. Swimming performance in Atlanatic Cod (*Gadus morhua*) following long-term (4–12 months) acclimation to elevated seawater pCO_2. Aquatic Toxicology, 92: 30–37.

Melzner, F., Gutowska, M. A., Langenbuch, M., Dupont, S., Lucassen, M., Thorndyke, M. C., Bleich, M., *et al.* 2009b. Physiological basis for high CO_2 tolerance in marine ectothermic animals: Pre-adaptation through lifestyle and ontogeny? Biogeosciences, 6: 2313–2331.

Metzger, R., Sartoris, F. J., Langenbuch, M., and Pörtner, H-O. 2007. Influence of elevated CO_2 concentrations on thermal tolerance of the edible crab *Cancer pagurus*. Journal of Thermal Biology, 32: 144–151.

Michaelidis, B., Ouzounis, C., Paleras, A., and Portner, H-O. 2005. Effect of long-term moderate hypercapnia on acid-base balance and growth rate in marine mussels *Mytilus galloprovincialis*. Marine Ecology Progress Series, 293: 109–118.

Morton, B. 1990. The physiology and feeding behaviour of two marine scavenging gastropods in Hong Kong: The subtidal *Babylonia lutosa* (Lamarck) and the intertidal *Nassarius festivus* (Powys). Journal of Molluscan Studies, 56: 275–288.

Morton, B., and Morton, J. 1983. The Sea Shore Ecology of Hong Kong. Hong Kong University Press, Hong Kong.

Moulin, L., Catarino, A. I., Claessens, T., and Dubois, P. 2011. Effects of seawater acidification on early development of the intertidal sea urchin *Paracentrotus lividus* (Lamarck 1816). Marine Pollution Bulletin, 62: 48–54.

Movilla, J., Orejas, C., Calvo, E., Gori, A., Lopez-Sanz, A., Grinyo, J., Dominguez-Carrio, C., *et al.* 2014. Differential response of two Mediterranean cold-water coral species to ocean acidification. Coral Reefs, 33: 675–686.

Newell, R. C. 1976. Adaptation to intertidal life. *In* Adaptation to Environment, Essays on the Physiology of Marine Animals, pp. 1–82. Ed. by R. C. Newell. Butterworths, Boston.

Orr, J. C., Fabry, V. J., Aumont, O., Bopp, L., Doney, S. C., Feely, R. A., Gnanadesikan, A., *et al.* 2005. Anthropogenic ocean acidification over the twenty-first century and its impact on calcifying organisms. Nature, 437: 681–686.

Pane, E. F., and Barry, J. P. 2007. Extracellular acid–base regulation during short-term hypercapnia is effective in a shallow-water crab, but ineffective in a deep-sea crab. Marine Ecology Progress Series, 334: 1–9.

Pansch, C., Schlegel, P., and Havenhand, J. 2013. Larval development of the barnacle *Amphibalanus improvisus* responds variably but robustly to near-future ocean acidification. ICES Journal of Marine Science, 70: 805–811.

Parker, L. M., Ross, P. M., O'Connor, W. A., Pörtner, H-O., Scanes, E., and Wright, J. M. 2013. Predicting the response of molluscs to the impact of ocean acidification. Biology, 2: 651–692.

Pörtner, H-O. 2008. Ecosystem effects of ocean acidification in times of ocean warming: A physiologist's view. Marine Ecology Progress Series, 373: 203–217.

Pörtner, H-O., and Farrell, A. P. 2008. Physiology and climate change. Science, 322: 690–692.

Pörtner, H-O., Langenbuch, M., and Michaelidis, B. 2005. Synergistic effects of temperature extremes, hypoxia and increases in CO_2 on marine animals: From earth history to global change. Journal of Geophysical Research, 110: C09S10.

Reyes-Nivia, C., Diaz-Pulido, G., Kline, D., Gulderg, O., and Dove, S. 2013. Ocean acidification and warming scenarios increase microbioerosion of coral skeletons. Global Change Biology, 19: 1919–1929.

Ries, J. B., Cohen, A. L., and McCorkle, D. C. 2009. Marine calcifiers exhibit mixed responses to CO_2-induced ocean acidification. Geology, 37: 1131–1134.

Sinha, A. K., Dasan, A. F., Rasoloniriana, R., Pipralia, N., and Blust, R. 2015. Hypo-osmotic stress-induced physiological and ion-osmoregulatory responses in European sea bass (*Dicentrarchus labrax*) are modulated differentially by nutritional status. Comparative Biochemistry and Physiology, Part A: Molecular and Integrative Physiology, 181: 87–99.

Suckling, C. C., Clark, M. S., Richard, J., Morley, S. A., Thorne, M. A. S., Harper, E. M., and Peck, L. S. 2015. Adult acclimation to combined temperature and pH stressors significantly enhances reproductive outcomes compared to short-term exposures. Journal of Animal Ecology, 84: 773–784.

Sunday, J. M., Crim, R. N., Harley, C. D. G., and Hart, M. W. 2011. Quantifying rates of evolutionary adaptation in response to ocean acidification. PLoS ONE, 6: e22881.

Thomsen, J., and Melzner, F. 2010. Moderate seawater acidification does not elicit long-term metabolic depression in the blue mussel *Mytilus edulits*. Marine Biology, 157: 2667–2676.

Thor, P., and Dupont, S. 2015. Transgenerational effects alleviate severe fecundity loss during ocean acidification in a ubiquitous planktonic copepod. Global Change Biology, 21: 2261–2271.

Trokovic, N., Gonda, A., Herczeg, G., Laurila, A., and Merila, J. 2011. Brain plasticity over the metamorphic boundary: Carry-over effect of larval environment on froglet brain development. Journal of Evolutionary Biology, 24: 1380–1385.

Whiteley, N. M. 2011. Physiological and ecological responses of crustaceans to ocean acidification. Marine Ecology Progress Series, 430: 257–271.

Wicks, L. C., and Roberts, M. 2012. Benthic invertebrates in a high-CO_2 world. Oceanography and Marine Biology Annual Review, 50: 127–188.

Winberg, G. G. 1960. Rate of metabolism and food requirements of fishes. Journal of Fisheries Research Board of Canada, 194: 1–239.

Wittmann, A. C., and Pörtner, P. -O. 2013. Sensitivities of extant animal taxa to ocean acidification. Nature Climate Change, 3: 995–1001.

Wolfe, K., Dworjanyn, S. A., and Byrne, M. 2013. Effects of ocean warming and acidification on survival, growth and skeletal development in the early benthic juvenile sea urchin (*Heliocidaris erythrogramma*). Global Change Biology, 19: 2698–2707.

Wood, H. L., Spicer, J. I., and Widdicombe, S. 2008. Ocean acidification may increase calcification rates, but at a cost. Proceedings of the Royal Society B: Biological Sciences, 275: 1767–1773.

Zhang, H. Y., Cheung, S. G., and Shin, P. K. S. 2014. The larvae of congeneric gastropods showed differential responses to the combined effects of ocean acidification, temperature and salinity. Marine Pollution Bulletin, 79: 39–46.

Zhang, H. Y., Shin, P. K. S., and Cheung, S. G. 2015. Physiological responses and scope for growth upon medium-term exposure to the combined effects of ocean acidification and temperature in a subtidal scavenger *Nassarius conoidalis*. Marine Environmental Research, 106: 51–60.

Zittier, Z. M. C., Hirse, T., and Pörtner, H-O. 2013. The synergistic effects of increasing temperature and CO_2 levels on activity capacity and acid-base balance in the spider crab, *Hyas araneus*. Marine Biology, 160: 2049–2062.

Handling editor: C. Brock Woodson

ICES Journal of Marine Science

ICES Journal of Marine Science (2016), 73(3), 825–835. doi:10.1093/icesjms/fsv201

Contribution to Special Issue: 'Towards a Broader Perspective on Ocean Acidification Research'

Original Article

Effects of high pCO_2 on Tanner crab reproduction and early life history—Part I: long-term exposure reduces hatching success and female calcification, and alters embryonic development

Katherine M. Swiney*, William Christopher Long, and Robert J. Foy

Kodiak Laboratory, Alaska Fisheries Science Center, National Marine Fisheries Service, National Oceanic and Atmospheric Administration, 301 Research Court, Kodiak, AK 99615, USA

**Corresponding author: tel: + 1 907 481 1733; fax: + 1 907 481 1701; e-mail: katherine.swiney@noaa.gov*

Swiney, K. M., Long, W. C., and Foy, R. J. Effects of high pCO_2 on Tanner crab reproduction and early life history—Part I: long-term exposure reduces hatching success and female calcification, and alters embryonic development. – ICES Journal of Marine Science, 73: 825–835.

Received 17 February 2015; revised 24 September 2015; accepted 12 October 2015; advance access publication 27 November 2015.

Ocean acidification, a decrease in ocean pH due to absorption of anthropogenic atmospheric CO_2, has variable effects on different species. To examine the effects of long-term exposure on Tanner crab (*Chionoecetes bairdi*) embryonic development, hatching success, and calcification, ovigerous females were reared in one of three treatments: ambient pH (~8.1), pH 7.8, and pH 7.5 for 2 years. Embryos and larvae in year 1 were from oocytes developed in the field and appear resilient to high pCO_2. Embryos and larvae in year 2 were from oocytes developed under high pCO_2 conditions. Oocyte development appears sensitive to high pCO_2, effects carryover and altered embryonic development, and reduced hatching success with on average 71% fewer viable larvae hatched in the pH 7.5 treatment than in the other treatments. Per cent calcium was reduced among females exposed to pH 7.5 waters, and their carapaces were noticeably more pliable than those in the other treatments. Softer carapaces may result in reduced defences against predators, and a reduction in the ability to feed on prey with hard parts such as shells. The results from this long-term study suggest that projected ocean pH levels within the next two centuries will likely have a pronounced impact on Tanner crab populations unless the crab are able to acclimatize or adapt to changing conditions.

Keywords: calcification, *Chionoecetes bairdi*, embryonic development, hatching success, ocean acidification, Tanner crab.

Introduction

Carbon dioxide (CO_2) is released into the atmosphere with the burning of fossil fuels, during cement production, and by other human activities (The Royal Society, 2005). Absorption of this anthropogenic CO_2 by the world's oceans has reduced global mean surface water 0.1 pH units below pre-industrial levels, an increase in pH of ~26% (Caldeira and Wickett, 2003; Intergovernmental Panel on Climate Change, 2014). This reduction in ocean's pH due to anthropogenic CO_2 is referred to as ocean acidification. In addition to reducing oceanic pH, surface waters that are currently supersaturated ($\Omega > 1$) with respect to calcium carbonate (both calcite and aragonite forms), which is needed to build and maintain calcified structures, such as shells for marine organisms, are expected to become undersaturated ($\Omega < 1$; Orr *et al.*, 2005).

High latitude waters are particularly vulnerable to ocean acidification because of a loss of sea ice, high rates of primary productivity, increased oceanic uptake of anthropogenic CO_2, and carbonate ion concentrations are naturally low in these waters compared with mid and low latitudes (Fabry *et al.*, 2009). High latitude waters are predicted to be the first to be persistently undersaturated with respect to calcium carbonate, which could occur within decades, not centuries as previously suggested (Orr *et al.*, 2005; Fabry *et al.*, 2009; Mathis *et al.*, 2011).

Ocean acidification has a variety of effects on different life stages of decapods including decreased survival (Kurihara *et al.*, 2008; Long *et al.*, 2013b), decreased growth (Kurihara *et al.*, 2008; Long *et al.*, 2013b), decreased egg production (Kurihara *et al.*, 2008), decreased calcification (Arnold *et al.*, 2009; Long *et al.*, 2013b),

increased deformities (Agnalt *et al.*, 2013), increased calcification (Long *et al.*, 2013a), increased hatch duration (Long *et al.*, 2013a), and altered haematology physiology and function (Meseck *et al.*, 2015). Carryover effects "occur when an individual's previous history and experience explains their current performance in a given situation" (O'Connor *et al.*, 2014). Carryover effects of ocean acidification between life stages can occur such as was observed in the crab *Hyas araneus*; larvae hatched and reared in acidified waters from embryos that developed in acidified waters had greater mortality and developmental delays than when just larvae were reared in acidified waters (embryos developed in ambient waters; Schiffer *et al.*, 2014).

Tanner crab (*Chionoecetes bairdi*) occur in the Pacific Ocean from Oregon to Alaska, in the Bering Sea, Aleutian Islands, and the Sea of Okhotsk (Jadamec *et al.*, 1999), and have historically supported valuable commercial fisheries in Alaskan waters. In recent years, reduced stock sizes have resulted in many fishery closures (North Pacific Fishery Management Council, 2013; Spalinger, 2013). Tanner crab are found at depths ranging from subtidal to ~440 m with mature male and female Tanner crab migrating to the deeper waters where they remain (Stevens *et al.*, 1993; Jadamec *et al.*, 1999). The depths that Tanner crab are found in are within the range of depths where the highest dissolution rates of calcium carbonate are in the North Pacific, Gulf of Alaska, and eastern Bering Sea (Fabry *et al.*, 2009; Feely *et al.*, 2012; Mathis *et al.*, 2014). Mating occurs after a female undergoes her molt to maturity, which is terminal (final), and in subsequent years she can mate while hard shelled or use stored sperm to fertilize egg clutches (Paul, 1984; Paul and Adams, 1984). Extrusion of a fertilized egg clutch occurs within 48 h of mating, brooding duration is ~12–16 months and larval hatching typically occurs in April and May (Donaldson and Adams, 1989; Swiney, 2008).

It is critical to examine the potential effects of ocean acidification, including carryover effects, on different life stages of Tanner crab. In this study, we exposed ovigerous Tanner crab to ambient pH, pH 7.8, and pH 7.5 treatments for 2 years which allowed us to observe direct and/or carryover effects of high pCO_2 during the entire reproductive cycle (oogenesis through larval hatching). The first year of the study examined effects of high pCO_2 on embryos and larvae from oocytes developed in the field under ambient conditions, whereas the second year of the study examined effects of high pCO_2 on embryos and larvae from oocytes developed under high pCO_2 conditions (during year 1). We specifically studied the effects of high pCO_2 on Tanner crab embryonic development, the mean number of viable larvae hatched, hatching success, mean hatch duration, mean brooding duration, and calcification rates of adults.

Methods

Sample collection and laboratory study

Ethical approval for this research was not required by any federal, state, or international laws because the study was conducted on invertebrates which are not covered under these laws.

The experiment was divided into 2 years based on reproductive cycles. Year 1 began 21 June 2011 when ovigerous females brooding newly extruded eggs were placed in the treatments and ended when larval hatching occurred in May 2012. Year 2 began in May 2012 after the females extruded a new clutch of eggs and ended 15 July 2013 after larval hatching occurred. Multiparous female Tanner crab were collected using crab pots and a 3-m beam trawl from Chiniak Bay, Kodiak, Alaska (57°43.25′N, 152°17.5′W) May and June 2011, and brought to the Alaska Fisheries Science Center's Kodiak Laboratory seawater facility in Kodiak, Alaska. Only females that appeared healthy, were brooding at least a three-fourth full clutch of newly extruded eggs, had at least one claw, and not missing more than three legs total were used in the experiment. At the beginning of year 1, 42 of the experimental females extruded their egg clutch in the field. An additional six females that hatched larvae in the laboratory for a related high pCO_2 experiment (Swiney *et al.*, 2016) were mated with mature males that were collected with the females in May and June 2011 and included in this study to increase the sample size to 48 females.

At the beginning of the experiment (year 1), 48 females were randomly assigned to one of three acidification treatments based on projected future changes to ocean pH: (i) ambient pH (~8.1), (ii) pH 7.8 (ca. ~2100), and (iii) pH 7.5 (ca. ~2200; Caldeira and Wickett, 2003; Intergovernmental Panel on Climate Change, 2014) for a total of 16 females per treatment. Mean female size at the beginning of year 1 was 98.7 (standard deviation, SD = 4.8) mm carapace width and female size did not vary with treatment (ANOVA, $F_{2,45} = 1.115$, $p = 0.337$). Crab died throughout the experiment, and at the end of year 1 there were 12 females in the ambient treatment, 11 females in the pH 7.8 treatment, and 12 females in the pH 7.5 treatment. After these females extruded a new clutch, they were used in year 2 of the experiment. Females are receptive to mating after larval hatching is complete (Paul, 1984) so at the end of year 1 (spring 2012) a mature male was placed in a female's tub to mate after her larvae hatched. Males were collected in the field March 2012 and held in ambient waters until they were placed with females. The females were checked daily and the day that a new clutch was extruded was recorded. It is not known if individual females mated or used stored sperm to extrude a new clutch, but all females extruded a viable clutch. Mean female size at the beginning of year 2 was 98.2 (SD = 5.2) mm carapace width and female size did not vary with treatment (ANOVA, $F_{2,32} = 2.593$, $p = 0.09$). Brooding duration for each female was defined as beginning the day of egg extrusion in 2012 (beginning of year 2) and ended when larval hatching began in 2013. At the end of year 2, there were 10 females in the ambient treatment, 6 females in the pH 7.8 treatment, and 7 females in the pH 7.5 treatment.

Each female was reared in an individual 68-l experimental tub with the treatment water flowing at 1 l min^{-1}. Water was chilled when needed and allowed to fluctuate seasonally to ensure appropriate temperatures. The mean daily temperature was 5.0 (SD = 1.5)°C for both years of the experiment, varied seasonally from a low of ~1°C in January 2012 to a high of ~9°C in August 2011, and did not vary among treatments (Kruskal–Wallis, $H = 0.761$, $p = 0.684$; Figure 1 and Table 1). Crab were fed twice weekly a diet of fish and squid in excess except they were not fed during larval hatching. Females were examined daily to ensure they were alive and pH and temperature were recorded daily for each tub (see below for more detail).

Once a month, ~20 eggs were randomly sampled from each female. The embryonic developmental stage was determined using methods described by Swiney (2008) for Tanner crab which was based on Moriyasu and Lanteigne (1998) methods for staging snow crab, *Chionoecetes opilio*, embryonic development. Un-eyed eggs were stained for 5 min with Bouin's solution to facilitate observation of the external morphology of the embryos; eyed eggs were not stained. The embryonic stages were determined under a compound microscope at ×50 magnification (Table 2). Additionally, digital images of 10 fresh eggs from each female were taken with a

digital camera attached to a compound microscope at a total magnification of ×63. Using image analysis software (Image Pro Plus Versions 6.00.260 and 7.0.1.658, Media Cybernetics, Inc., Rockville, MD, USA), egg area and diameters (maximum, minimum, and average) were measured. Once embryos were discernible, embryo areas and yolk areas and diameters (maximum, minimum, and average) were also measured. Finally, when embryos become eyed, eyespot area and diameters (maximum, minimum, and average) were measured (Figure 2).

Larval hatching occurred at the end of years 1 and 2; hatching duration and the number of viable larvae hatched was estimated for each female each year. Hatching duration was defined as the first day 50 or more larvae were hatched and ended when females began to strip their pleopods clean to remove empty egg cases and unhatched eggs (Donaldson and Adams, 1989). Hatching duration was not determined for the females that did not strip their pleopods clean. Before larval hatching, nets were placed on the outflow of each tub to retain all the larvae from each female and newly hatched larvae were collected and dried daily at 60°C until a constant weight was achieved. Average weight per larva for each female each year was calculated from 3 to 6 replicates (number varied with female) of 50 dried larvae. The average weight per larva for each female was used to calculate how many larvae each female hatched daily. If less than ~200 larvae hatched, then all the larvae were counted. On days when live larvae were needed for experiments, they could not be dried [for larval experiment details, see Swiney *et al.* (2016)], so the number of viable larvae hatched was estimated by counting the number of larvae in three to four subsamples of known volume and calculating the total number hatched for the day. For each female, total number of viable larvae hatched was estimated by adding together the number of larvae hatched daily. The number of viable larvae hatched is a little less than what the true number of larvae hatched would have been since we sampled eggs monthly for the embryonic development portion of the project; however, given that the smallest females typically release >100,000 larvae and fecundity increases with female size, the ~240 eggs removed from each crab is negligible.

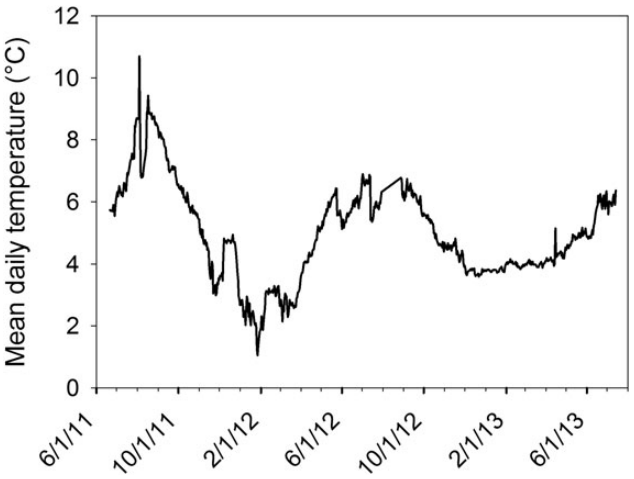

Figure 1. Mean daily temperature (°C) for the duration of the experiment.

Hatching success was defined as the per cent of viable larvae hatched divided by the calculated total number of larvae that could have hatched (number of viable larvae hatched + number of non-viable larvae hatched + number of eggs that did not hatch). The percentage of non-viable larvae hatched and the percentage of eggs that did not hatch were also calculated. Non-viable larvae that hatched were larvae that did not molt past the pre-zoea stage to the first zoeal stage. For each female, the debris from pleopod cleaning was collected, examined microscopically, and all viable larvae, non-viable larvae, and dead eggs counted in a volumetric subsample. At the end of year 2, 10% of females in the ambient treatment (1 of 10), 33% of females in the pH 7.8 treatment (2 of 6), and 86% of females in the pH 7.5 treatment (6 of 7) did not hatch their entire brood or clean their pleopods. Microscopic examination of these clutches confirmed that they were carrying dead eggs. At the end of the experiment when the females were sacrificed, the abdominal flap with dead eggs attached was removed from these females, frozen, and later processed to estimate the number of dead eggs.

At the end of the experiment (July 2013), calcium and magnesium content was analysed for 9 ambient, 5 pH 7.8 and 5 pH 7.5 treatment females from the same portion of their carapace (approximately a square centimetre of the posterior margin region) by an analytical laboratory.

Seawater acidification

Sand filtered seawater was pumped into the laboratory from 15 and 26 m depth intakes in Trident Basin, which is ~30 m from the laboratory. Only one intake line is in use at any given time and typically lines are switched when maintenance is needed on a line. Seawater was acidified using the same methods described in Long *et al.* (2013a). In short, a 170-l tank of pH 5.5 seawater was established by bubbling CO_2 into ambient seawater. This pH 5.5

Table 1. The mean and SD of water chemistry parameters in the three treatments during years 1 and 2 of the experiments.

Treatment	Temperature (°C)	Salinity (PSU)	pH_F	pCO_2 (μatm)	HCO_3^- (mmol/kg)	CO_3^{-2} (mmol/kg)	DIC (mmol/kg)	Alkalinity (mmol/kg)	$\Omega_{Aragonite}$	$\Omega_{Calcite}$
Year 1										
Ambient	5.03 (2.07)	31.26 (0.28)	8.06 (0.06)	418.6 (52.2)	1.90 (0.05)	0.09 (0.01)	2.00 (0.04)	2.12 (0.03)	1.32 (0.16)	2.11 (0.25)
pH 7.8	4.97 (2.07)	31.27 (0.030)	7.80 (0.04)	773.7 (29.2)	1.97 (0.04)	0.05 (0.00)	2.06 (0.04)	2.10 (0.03)	0.76 (0.05)	1.22 (0.08)
pH 7.5	4.93 (2.07)	31.25 (0.28)	7.50 (0.03)	1595.5 (78.9)	2.03 (0.04)	0.03 (0.00)	2.14 (0.04)	2.09 (0.02)	0.39 (0.03)	0.63 (0.05)
Year 2										
Ambient	4.97 (0.95)	31.16 (0.36)	8.10 (0.08)	373.9 (67.9)	1.89 (0.04)	0.10 (0.02)	2.01 (0.03)	2.15 (0.02)	1.52 (0.27)	2.43 (0.43)
pH 7.8	4.93 (0.95)	31.19 (0.34)	7.80 (0.02)	786.2 (31.6)	2.00 (0.03)	0.05 (0.00)	2.09 (0.03)	2.13 (0.03)	0.78 (0.04)	1.25 (0.06)
pH 7.5	4.92 (0.92)	31.14 (0.35)	7.50 (0.03)	1598.2 (50.7)	2.06 (0.03)	0.03 (0.00)	2.17 (0.03)	2.12 (0.03)	0.41 (0.02)	0.65 (0.03)

pH (free scale) and temperature were measured daily (year 1 $n = 316$ and year 2 $n = 412$ per treatment); DIC, salinity, and alkalinity were measured weekly (year 1 $n = 40–41$ and year 2 $n = 61–63$ per treatment); and all other parameters were calculated.

Table 2. Embryonic developmental stages modified from Moriyasu and Lanteigne (1998) descriptions for *Chionoecetes opilio*. See Moriyasu and Lanteigne (1998) for detailed descriptions.

Stage no.	Embryonic developmental stage	Stage description
1	Prefuniculus formation	The egg is filled with yolk until stage 6. The funiculus is not formed.
2	Funiculus formation	The funiculus is formed.
3	Cleave and blastula	Yolk segmentation goes from two cells to the blastula.
4	Gastrula	The blastophore appears as a disc-shaped structure on the surface of the gastrula.
5	Lateral ectodermal band	The germinal disc with three rudiments appears as a U-shaped structure.
6	Prenauplius	The percentage of yolk diminishes steadily until stage 12. The rudiments of larval structures appear. A clear area representing the developing embryo is visible.
7	Nauplius	The antennae are biramous and the antennae and antenules are rod-shaped and separated from the centre. The segments forming the upper region are fused.
8	Maxilliped formation	The rudiments of the first and second maxillipeds appear. Crescent-shaped carapace rudiments are present in the anterior part of the thoracic abdomen.
9	Metanauplius	The rudiments of the first and second maxillae and the third maxillipeds appear. The labrum is triangular. The telson is forked.
10	Late metanauplius	The rudiments of the dorsal spine are a disc-shaped structure in the middle of the yolk. The optic lobes are well developed and a thin pigmented crescent of the compound eye is visible.
11	Eye-pigment formation	Eye pigments spread. All the larval appendages have formed. The rudiments of the dorsal spine separate the yolk into two parts.
12	Chromotophore formation	Dot-like chromatophores appear on the maxillipeds. The lateral spines elongate and separate the yolk into four parts. The eye pigment spreads and become teardrop-shaped.
13	Reduced yolk	Almost no yolk is visible. The rudiments of the dorsal and lateral spines become wider. The thoracic abdomen forms six segments including the telson.
14	Prehatching	The eyes are completely pigmented and no yolk is visible.

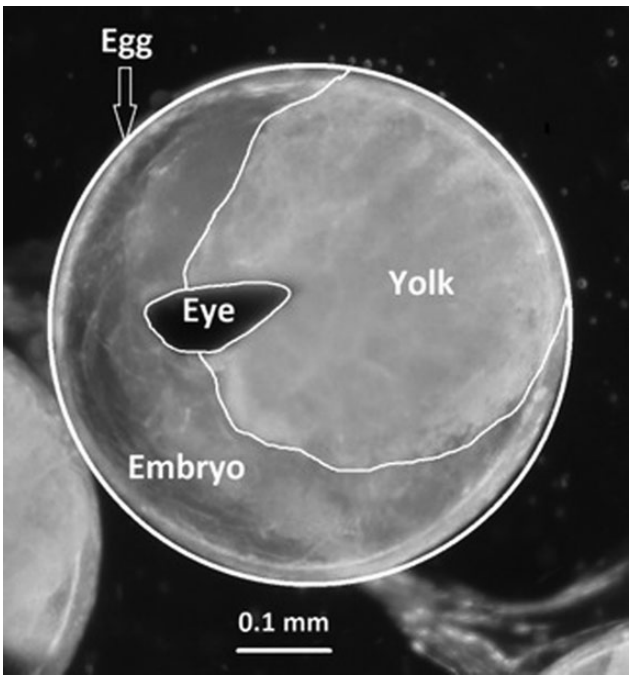

Figure 2. Tanner crab egg, embryo, yolk, and eye sections measured for embryonic morphometric analysis.

seawater was mixed with ambient seawater in the 170-l treatment head tanks via peristaltic pumps controlled by Honeywell controllers and Durafet III pH probes. The ambient head tank did not receive any pH 5.5 water. Waters from the pH 7.8 and pH 7.5 treatment head tanks were then supplied to the individual tubs containing females. pH_F (free scale) and temperature were measured daily in each experimental tub using a Durafet III pH probe calibrated using a TRIS buffer solution and when the pH deviated from the target pH by more than ± 0.02 pH units, the Honeywell controller set points were adjusted to bring the pH back to the target value. Weekly water samples from each treatment were taken, poisoned with mercuric chloride, and sent to one of the two analytic laboratories for dissolved inorganic carbon (DIC) and total alkalinity (TA) analysis. The two laboratories used similar, but slightly different instruments. At the first laboratory, DIC was determined using a CM5014 Coulometer with a CM5130 Acidification Module (UIC Inc., Joliet, IL, USA) using Certified Reference Material from the Dickson Laboratory (Scripps Institute, San Diego, CA, USA; Dickson *et al.*, 2007). TA was measured via open cell titration according to the procedure in Dickson *et al.* (2007). At the second laboratory, DIC and TA were determined using a VINDTA 3C (Marianda, Kiel, Germany) coupled with a 5012 Coulometer (UIC Inc.) using Certified Reference Material from the Dickson Laboratory (Scripps Institute) and the procedures in DOE (1994). Target pHs were achieved throughout the experiment (Table 1). Alkalinity decreased with decreasing pH, and DIC increased with decreasing pH (Table 1). Aragonite was supersaturated in the ambient treatment, but undersaturated in the pH 7.8 and pH 7.5 treatments. Calcite was supersaturated in the ambient and pH 7.8 treatments, and undersaturated in the pH 7.5 treatment (Table 1).

Statistical analysis

The effects of seawater pH on the development of embryos were analysed using principal component analysis (PCA) in Primer 6.1.15 (Primer-E Ltd, Lutton, UK); each year was analysed separately. Embryo measurements were normalized before analysis. We retained all PCs that were necessary to explain at least 90% of the variation in the data each year. Each retained PC was analysed with an ANOVA with pH treatment fully crossed with month and female nested in treatment crossed with month as factors. The second PC in the second year failed to meet the assumption of homogeneity of variance, so we analysed the average PC2 score for each female on each date (which met the assumption) using an

ANOVA with pH treatment fully crossed with month and female nested in treatment as factors.

The effects of different seawater pH on the mean number of viable larvae hatched, hatching success, mean hatch duration (2012 only), mean brooding duration, and calcification were examined using one-way ANOVAs or Kruskal–Wallis tests with pH as the factor. The 2013 mean hatch duration was examined with a two-sample *t*-test because hatching duration could only be estimated for one female in the pH 7.5 treatment, so this treatment was not included in the analysis. Anderson–Darling test for normality and Levene's test for homogeneity of variance were used to determine if data meet the assumptions of ANOVA and when data failed these test, the non-parametric Kruskal–Wallis test was used. When significant differences were detected with ANOVAs, Tukey's HSD *post hoc* multiple comparisons tests were used to examine the differences between pH treatments. When significant differences were detected with Kruskal–Wallis tests, Conover–Inman tests for all pairwise comparisons were used to examine the differences between pH treatments. Statistical analyses were conducted in SYSTAT 10.00.05 (Systat Software, Inc., Chicago, IL, USA).

We modelled female mortality using a binomial distribution of errors assuming a constant mortality rate such that $N_t = N_0 e^{-rt}$, where N_t is the number surviving at time t (in days), N_0 is the initial number, and r is the mortality rate. We fit the survival data to three models using maximum likelihood in R (V2.14.0, Vienna, Austria), one in which the mortality rate did not differ among treatments, one in which it differed among all treatments, and one in which the rate in the Ambient treatment differed from the two experimental treatments. We selected the best model using the Akaike's information criterion corrected for small sample size (AIC_c). Models whose AIC_c differed by <2 were considered to explain the data equally well (Burnham and Anderson, 2002).

Results

Mean embryo stage by date did not differ among pH treatments in either year 1 or 2 of the experiment (Figure 3). In year 1, stage 14, which is the prehatching stage (Table 2), was not observed during the monthly sampling because after the April 2012 sampling females were either hatching their larvae or they had finished hatching and extruded a new clutch.

Embryonic morphometrics were significantly different among pH treatments in both years, and PCA results were qualitatively similar between the years. In both years, the first two PCs explained >90% of the variance and were the only two retained (Tables 3 and 4). The first PCs were negatively associated with egg, embryo, and eye size, and positively associated with yolk size, and are interpreted as embryo maturity, with more mature embryos having smaller PC1 scores. The second PCs were positively associated with egg and yolk size. In both years, there was a significant interaction between month and treatment on the PC1 scores (Tables 3 and 4, and Figure 4); early in development, there were no differences among the treatments, but there began to be significant differences starting in December in the first year and in November the second year. These differences persisted through hatching (Tables 3 and 4, and Figure 4); the lack of a difference in May in the second year was because this sampling took place during the hatching period, and 70% of the ambient females and 40% of the pH 7.8 females had completed hatching (none of the pH 7.5 females had completed hatching) and the remaining embryos were at the prehatching stage (Table 2). In general, embryos in the ambient and pH 7.8 treatments differed from those in the pH 7.5 treatment, but not from each other.

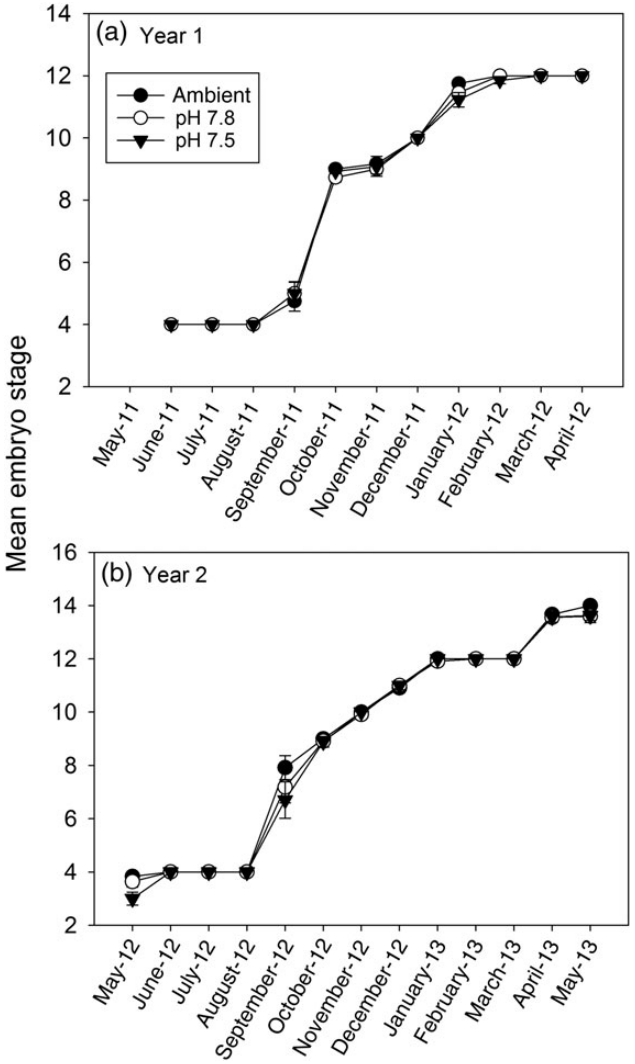

Figure 3. Comparison of Tanner crab mean embryo stage by pH treatment for (a) year 1 and (b) 2 of the experiment. See Table 2 for embryo stage descriptions. Values are means and vertical bars represent standard errors.

PC2 showed similar trends. In the first year, there were significant differences among the pH treatments with the ambient and pH 7.8 treatments differing from the pH 7.5 treatment, but not from each other whereas in the second year this was the case in most, but not all, months leading to a significant interactive effect (Tables 3 and 4, and Figure 4). In both years, the pH 7.5 embryos had larger yolks and smaller eyes and embryos. Although there were statistically significant differences among the treatments, the effect size in year 1 was slight; the average difference in the measurements between the ambient and pH 7.5 embryos was only 3.6% in April 2012, with a maximum difference in any one measurement of 7.1%. In the second year, effect sizes were larger; embryos in the pH 7.5 treatment had 10.1% larger yolks and 6.3% smaller embryos than those in the ambient treatment.

The mean number of viable larvae hatched in year 1 of the experiment did not differ with pH treatment (Kruskal–Wallis, $H = 2.253$, $p = 0.324$; Figure 5a). Furthermore, there was not a significant difference in the mean number of viable larvae hatched in year 2 among the ambient and pH 7.8 treatments, however, on average,

Table 3. PCA of Tanner crab embryo morphometrics in year 1.

PC	Eigenvalues	Percentage variation	Cumulative percentage variation
1	10.8	82.8	82.8
2	1.32	10.2	92.9
	Eigenvectors		
Variable	**PC1**	**PC2**	
Egg area	−0.273	0.377	
Egg maximum diameter	−0.231	0.45	
Egg minimum diameter	−0.269	0.275	
Egg average diameter	−0.272	0.378	
Yolk area	0.276	0.334	
Yolk maximum diameter	0.256	0.365	
Yolk minimum diameter	0.268	0.282	
Yolk average diameter	0.277	0.327	
Embryo area	−0.301	−0.06	
Eye area	−0.291	0.025	
Eye maximum diameter	−0.29	−0.039	
Eye minimum diameter	−0.297	−0.01	
Eye average diameter	−0.297	−0.024	
ANOVA			
Variable	**Factor**	***F***	***p***
PC1	Treatment	77.291	<0.0005
	Month	21,702.58	<0.0005
	T * M	10.025	<0.0005
	Crab(T * M)	9.027	<0.0005
PC2	Treatment	12.355	<0.0005
	Month	28.304	<0.0005
	T * M	0.931	0.548
	Crab(T)	10.286	<0.0005

The first two PCs, representing 93% of the cumulative variation, are retained. ANOVA analysis with treatment (T) fully crossed with month (M), and crab (nested) was performed for the first two eigenvectors.

Table 4. PCA of Tanner crab embryo morphometrics in year 2.

PC	Eigenvalues	Percentage variation	Cumulative percentage variation
1	10.5	80.6	80.6
2	1.73	13.3	93.9
	Eigenvectors		
Variable	**PC1**	**PC2**	
Egg area	−0.261	0.398	
Egg maximum diameter	−0.231	0.429	
Egg minimum diameter	−0.256	0.331	
Egg average diameter	−0.259	0.405	
Yolk area	0.284	0.271	
Yolk maximum diameter	0.249	0.367	
Yolk minimum diameter	0.282	0.254	
Yolk average diameter	0.275	0.313	
Embryo area	−0.305	−0.084	
Eye area	−0.299	−0.050	
Eye maximum diameter	−0.291	−0.013	
Eye minimum diameter	−0.302	−0.045	
Eye average diameter	−0.300	−0.030	
ANOVA			
Variable	**Factor**	***F***	***p***
PC1	Treatment	104.60	<0.0005
	Month	16,523.18	<0.0005
	T * M	5.318	<0.0005
	Crab(T * M)	13.807	<0.0005
PC2	Treatment	121.16	<0.0005
	Month	297.588	<0.0005
	T * M	5.607	<0.0005
	Crab(T * M)	11.576	<0.0005

The first two PCs, representing 94% of the cumulative variation, are retained. ANOVA analysis with treatment (T) fully crossed with month (M), and crab (nested within treatment crossed with month) was performed for the first four eigenvectors.

71% less viable larvae hatched from the pH 7.5 treatment in year 2 (ANOVA, $F_{2,\ 27} = 5.796$, $p = 0.008$; Figure 5b). For all three treatments, less viable larvae hatched in year 2 than in year 1. In the ambient pH treatment, on average, 47% less viable larvae hatched in year 2 than in year 1, in the pH 7.8 treatment 54% less viable larvae hatched in year 2, and in the pH 7.5 treatment 83% less viable larvae hatched in year 2 than in year 1 (Figure 5).

Hatching success, measured as the per cent of viable larvae hatched, did not differ in year 1 among pH treatments and averaged 99% (Kruskal–Wallis, $H = 0.265$, $p = 0.876$; Figure 6). In year 2, hatching success in the pH 7.5 treatment was, on average, 46% and significantly lower than the average 87% hatching success observed in the ambient treatment; the ambient and pH 7.8 treatments did not differ statistically (Kruskal–Wallis, $H = 7.988$, $p = 0.018$; Figure 6). Overall fewer viable larvae were hatched in year 2 than in year 1 as 99% hatching success was observed in year 1 and in year 2 hatching success averaged 46–87% depending on the pH treatment (Figure 6). More non-viable larvae hatched in year 2, averaging 3–15% depending on pH treatment (Figure 6), compared with <1% observed in year 1. Likewise, on average, more eggs did not hatch in year 2, 10–39% depending on pH treatment (Figure 6), compared with <1% observed in year 1.

In year 1, mean larval hatching duration did not differ with pH treatment (Kruskal–Wallis, $H = 3.783$, $p = 0.151$) nor did it differ in year 2 (t-test, $t = 0.515$, $p = 0.616$). In year 1, average larval hatching duration was 6 (SE = 0.182) days and ranged from 4 to 8 days. In year 2, average larval hatching duration was longer and more variable averaging 16 (SE = 3.537) days, and ranged from 6 to 59 days with only one female from treatment pH 7.5 completing hatching. Mean brood duration, which was only estimated for year 2 of the experiment, did not differ with pH treatment (Kruskal–Wallis, $H = 0.800$, $p = 0.670$) and averaged 356 (SE = 1.150) days.

In the best fit model, the mortality rate of adult females throughout the 2 years of the experiment differed among all treatments and increased under high pCO_2 conditions (Figure 7 and Table 5). At the end of the experiment, adult females from the ambient pH treatment had the highest survival rate (63%) followed by females in the 7.5 pH treatment (44%), and survival was lowest in the 7.8 pH treatment (38%); however, the difference in survival between the 7.8 and 7.5 pH treatments was only one crab (Figure 7). The per cent dry weight of calcium in the females' carapace at the end of the experiment was significantly less in the pH 7.5 treatment than in either the ambient or pH 7.8 treatments which did not differ (Kruskal–Wallis, $H = 11.041$, $p = 0.004$; Figure 8a). The per cent dry weight of magnesium contained in the carapace did not differ with pH treatment (ANOVA, $F_{2,16} = 0.929$, $p = 0.415$; Figure 8b). The ratio of magnesium and calcium differed between the ambient and 7.5 pH treatments, but did not differ among the other pH treatments (ANOVA, $F_{2,16} = 5.108$, $p = 0.019$; Figure 8c). The carapaces of females held in the pH 7.5 treatment were noticeably more pliable than the females reared in the other pH treatments.

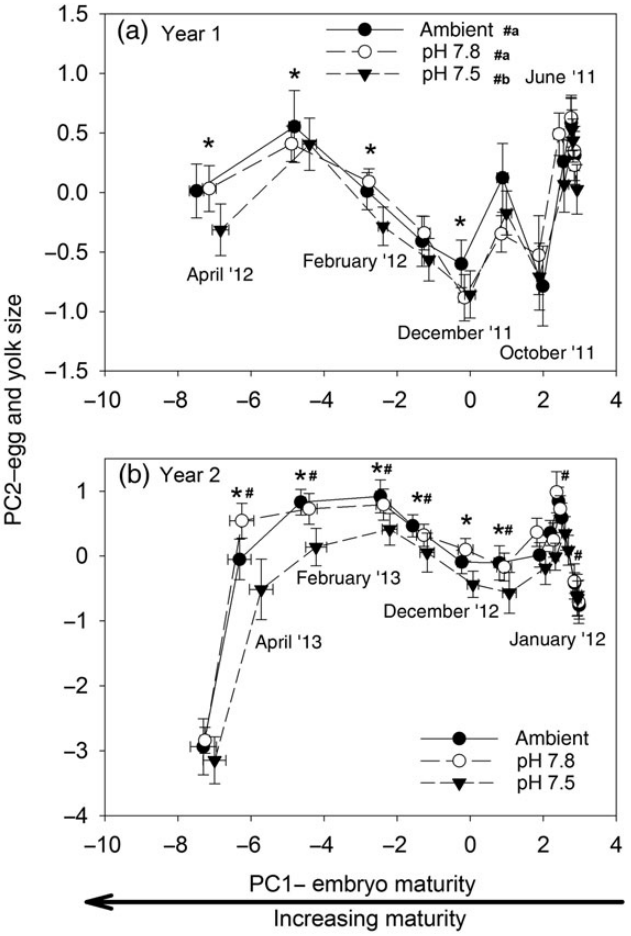

Figure 4. Average principal component (PC) 1 and 2 scores ± standard errors for Tanner crab embryos measured monthly during (a) year 1 and (b) year 2. The scores were averaged among females within each treatment, so sample size varied with the number of females surviving each month and varied from 16 at the beginning of the experiment to as low as 6 in the pH 7.8 treatment at the end. PC1 is associated with embryo maturity and PC2 is associated with egg and embryo size. Every other month is labelled. When there were significant differences among treatments within a month, it is indicated with asterisks for PC1 and an hash for PC2. When there were differences among the treatments in all months, it is indicated in the figure legend using the same symbols; treatments with the different letters next to them are significantly different.

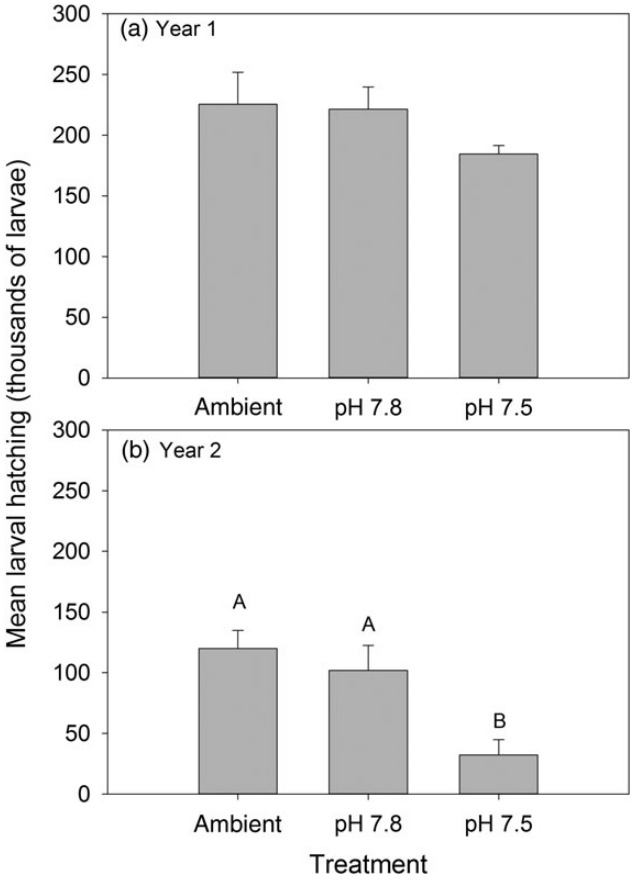

Figure 5. Comparison of the mean number of viable Tanner crab larvae hatched by pH treatment in (a) year 1 and (b) year 2. Bars are mean with standard error. Bars with different letters above them differ significantly.

Discussion

Decreased pH had a slight effect on Tanner crab embryonic development and no effect on larval hatching in year 1 of this study, suggesting that Tanner crab embryonic development and larval hatching are not sensitive to high pCO_2 if oocytes are developed under ambient (not high pCO_2) conditions. Under high pCO_2 conditions, significant effects were detected in embryonic development, the number of viable larvae hatched, and hatching success in year 2 of this study, which suggests that Tanner crab reproductive success is most susceptible to the effects of high pCO_2 during oocyte development and that these effects carryover into embryonic development and larval hatching. Variability in the sensitivity of different life stages and carryover effects between stages to acidified waters has been found for other crab species. For the great spider crab *H. araneus*, larval mortality was significantly higher and developmental delays observed under acidified conditions when larvae were hatched from embryos developed in acidified waters compared with larvae exposed to acidified conditions, but embryos that did not develop under acidified conditions (Schiffer *et al.*, 2014). For the porcelain crab *Petrolisthes cinctipes*, the embryo stage is more sensitive to acidified waters than the larval and juveniles stages (Carter *et al.*, 2013). Acidified waters did not affect embryonic development rate, heart rate, or oxygen consumption of the Norway lobster *Nephrops norvegicus* after 4 months of exposure (Styf *et al.*, 2013). Embryonic development for red king crab, *Paralithodes camtschaticus*, is sensitive to acidified waters, even with only short-term exposure (2 months; Long *et al.*, 2013a). These studies highlight the need for ocean acidification research to examine the potential effects of acidification on all stages and for different species (Kurihara, 2008).

Tanner crab embryos that developed in pH 7.5 waters had larger yolks and smaller embryos than embryos reared in pH 7.8 and ambient waters, suggesting that development was delayed for embryos reared in the lowest pH treatment. Hatching success was low among pH 7.5 embryos in year 2 of the study and differences in embryo development may be due to these embryos not developing normally and ultimately not hatching. Regardless, the developmental differences were not large enough to cause a difference in the mean monthly embryo stages among the treatments or brood

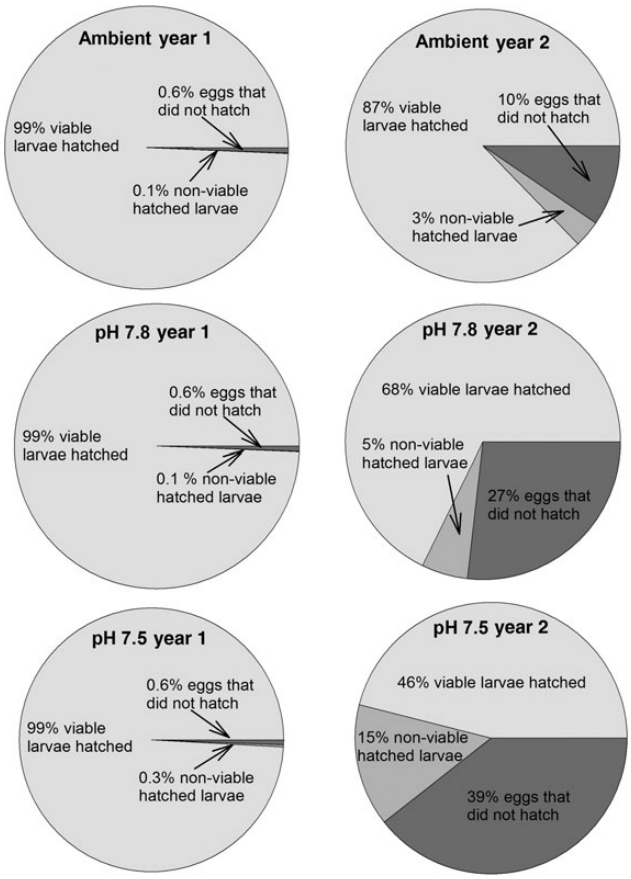

Figure 6. Comparison of the mean per cent viable Tanner crab larvae hatched, non-viable larvae hatched, and eggs that did not hatch in year 1 and year 2 among ambient, pH 7.8, and pH 7.5 treatments.

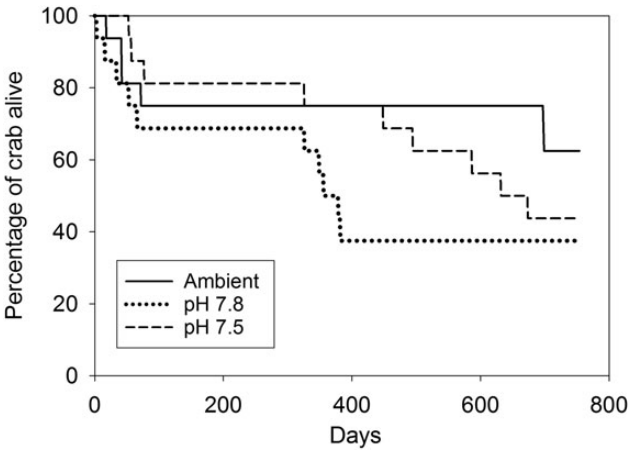

Figure 7. Daily percentage survival of female Tanner crab by treatment for the 2-year experiment.

duration among females that had a successful hatch. Similarly, exposure of porcelain crab embryos to acidified waters (pH 7.6) resulted in lower metabolism and dry mass which may cause delayed development (Carter *et al.*, 2013). In contrast, red king crab embryos that developed in acidified waters (pH 7.7) had larger embryos and smaller yolks, suggesting an increase in the development rate under acidified conditions (Long *et al.*, 2013a).

Table 5. Ranking of models of adult female Tanner crab mortality using AIC_c.

Model	*K*	AIC_c	ΔAIC_c	Likelihood	AIC_c weight
m(T)	3	7993.72	0.00	1.00	1.00
m(T2)	2	8773.83	780.11	0.00	0.00
m	1	9497.13	1503.42	0.00	0.00

Model indicates how the mortality rate, *r*, was modelled. T indicates the rate varied among all treatments and T2 indicates the rate differed between the ambient and experimental treatments (see text for full model description). *K* is the number of parameters in each model.

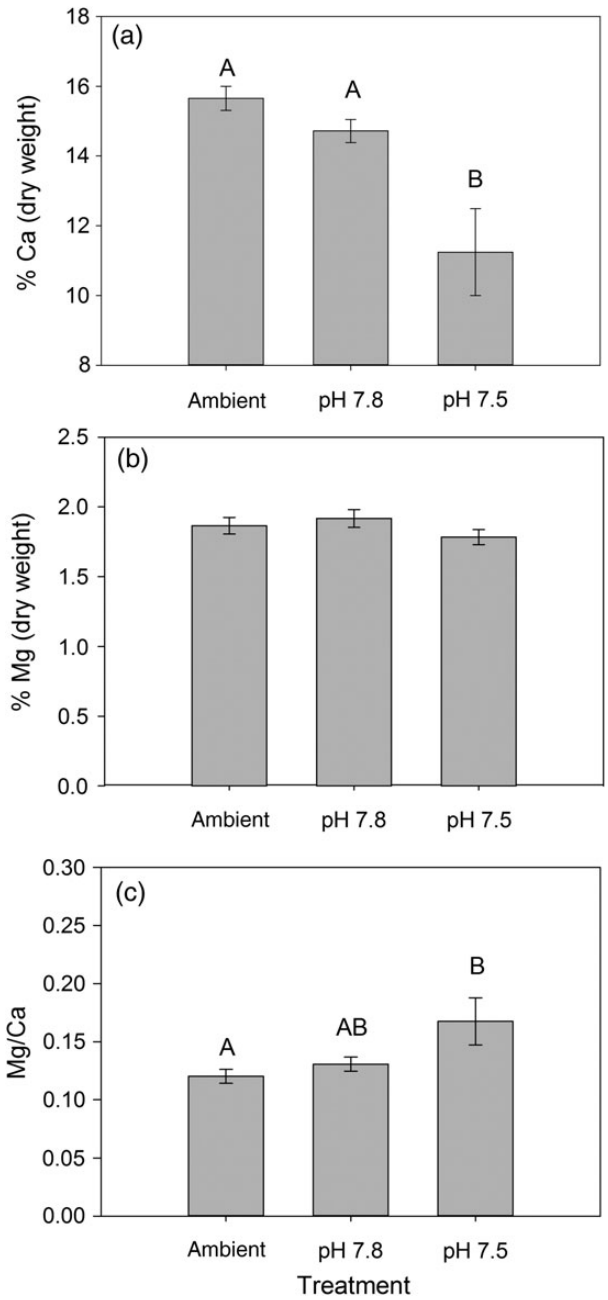

Figure 8. Comparison of the mean (a) per cent dry weight calcium, (b) per cent dry weight magnesium, and (c) magnesium calcium ratio from carapaces of female Tanner crab reared in ambient, 7.8 pH and 7.5 pH treatments for 2 years. Bars are mean with standard error. Bars with different letters above them differ significantly.

High pCO_2 waters had a pronounced effect on the reproductive output in year 2 of this study; females reared in pH 7.5 waters hatched on average 71% fewer viable larvae than the other two treatments, and hatching success in the pH 7.5 treatment was 40% less than in the ambient treatment. The significant reduction in the reproductive output of females reared in the pH 7.5 waters will likely have a substantial impact on Tanner crab population size and fisheries under these conditions. Likewise, acidified waters (pH 7.89) reduce the reproductive output of the marine shrimp *Palaemon pacificus* by reducing the number of clutches individual females' brood (Kurihara *et al.*, 2008).

For all the treatments, fewer viable larvae hatched and hatching success were lower in year 2 than in year 1 of the study. This may have occurred due to senescence and/or laboratory affects. The closely related snow crab, *C. opilio*, is thought to have a maximum post-terminal molt lifespan of 6–7 years in the eastern Bering Sea (Ernst *et al.*, 2005), and become senescent with age (Kon *et al.*, 2010). Longevity information on Tanner crab is lacking (North Pacific Fishery Management Council, 2013), but if Tanner crab are similar to snow crab, the reduction in viable larvae hatched and hatching success in year 2 of the experiment may have been due to senescence. The females used in this study were multiparous in year 1, so they were at a minimum of 3 years post-terminal molt during year 2 of the study. Regardless of the reason for reduced numbers of viable larvae hatched and hatching success in year 2, we are confident that the significant reduction in reproductive output in the pH 7.5 treatment is real since all the crab were randomly assigned to treatments, and in the laboratory for the same amount of time so laboratory effects should be the same for all treatments.

High pCO_2 water did not affect Tanner crab larval hatching duration in either year of the study, suggesting that this process is not sensitive to high pCO_2 conditions for this species. These results support the notion that hatching duration is innate, heritable, and not easily altered by most environmental parameters (Morgan, 1995). It has been hypothesized that Tanner crab hatching is controlled by an endogenous biological clock, and that hatching corresponds to the period of greatest tidal exchange to optimize larval transport (Stevens, 2003). Hatching was longer and more variable for all treatments in year 2 of the study, which may have been the result of senescence or laboratory effects. With the crab being in the laboratory for 2 years, their biological clocks may have been affected by the crab not having direct environmental influences, such as tidal fluctuations, which appear important cues for hatching. In contrast, red king crab hatching duration was 33% longer in acidified waters (pH 7.7; Long *et al.*, 2013a). King crab have a longer hatching duration than Tanner crab (~22 days), and it is thought that the longer hatching duration is an evolutionary response to conditions that were highly variable and unpredictable. A longer hatching duration increases that chance that some larvae will be released during a time of high food availability which will improve larval survival (Stevens, 2006). For red king crab, acidified waters may be perceived as increased environmental variability resulting in the longer hatching duration observed (Long *et al.*, 2013a).

Based on the few adult decapod species examined, acidified waters have either a positive or no effect on calcification (Ries *et al.*, 2009; Landes and Zimmer, 2012; Long *et al.*, 2013a). In this study, the reduced calcification (per cent dry weight of calcium) in the 7.5 pH treatment is unprecedented. The difference between our results and other studies may simply be that, in our experiment, the crab were reared in high pCO_2 water for 2 years, whereas the previous studies were shorter (maximum of 5 months) in duration and effects may not be seen due to the shorter duration of the studies. Long-term ocean acidification studies are needed to see if other decapod species experience reduced calcification or if this response is unique to Tanner crab. Alternately, Tanner crab physiological responses to acidification may differ from other decapod species, regardless of exposure duration, as was observed in a long-term study (nearly 200 days) comparing the responses of juvenile Tanner and red king crab with ocean acidification (Long *et al.*, 2013b). Juvenile Tanner crab had decreased calcium content and an unaffected condition index (dry body mass divided by carapace width or length cubed), whereas juvenile red king crab calcium content was unaffected, but the condition index was reduced (Long *et al.*, 2013b). Ries *et al.* (2009) suggest that organisms, such as crustaceans, expend energy to physiologically elevate pH at the site of calcification and depending on the efficiency of their specific proton-regulating mechanism end up with similar conditions at the site of calcification as they currently experience. It is unclear why Tanner crab have reduced calcium content under high pCO_2 conditions, but they may not be as efficient at increasing pH at the site of calcification as other decapods. Alternatively, the calcium carbonate in the carapace may be dissolved internally in an attempt to buffer internal pH.

Among crustaceans, typically when calcium content is altered under acidified conditions, magnesium content is also altered (Arnold *et al.*, 2009; Long *et al.*, 2013a), but that was not the case with adult Tanner crab in this study or juvenile Tanner crab (Long *et al.*, 2013b). Adult and juvenile Tanner crab had reduced calcium content under high pCO_2 conditions, but magnesium did not vary, and thus, the Mg/Ca ratio was higher under high pCO_2 conditions. Because the strength of calcite is proportional to the Mg/Ca ratio (Magdans and Gies, 2004), the increase in the Mg/Ca ratio may be an adaptive response to reduced calcification in that it may reduce the overall loss of carapace strength although the mechanism is unclear. In this study, we observed more pliable shells under high pCO_2 conditions, so although the shell may be stronger than they would have been if calcium and magnesium were reduced in the same proportion, the amount of calcium content lost under high pCO_2 conditions was high enough to result in adults with more pliable shells in the pH 7.5 treatment. Additional research is needed to better understand the effects of ocean acidification on Tanner crab calcification, including both calcium and magnesium content and their effects on shells strength.

Projected ocean pH levels within the next two centuries will likely have a pronounced negative effect on Tanner crab populations unless the crab are able to adapt as conditions change. Tanner crab appear resilient to medium term (1 year) exposure to high pCO_2 waters. However, the distressing effects of high pCO_2 on Tanner crab populations exposed to acidified water for the entire reproductive cycle (from oocyte development to hatching) are apparent by the relatively small number of viable larvae hatched among females reared in the pH 7.5 treatment year 2 of this study. Furthermore, calcification was reduced among females reared in the pH 7.5 treatment and their carapaces were noticeably more pliable than females reared in the other treatments. Softer carapaces may result in reduced defences against predators, and a reduction in the ability to feed on prey with shells such as bivalves. The components of an organism's energy budget are linked together with stressed organisms requiring additional energy for somatic maintenance, thus reducing or eliminating the amount of energy available for activities such as growth and reproduction (Sokolova

et al., 2012; Sara *et al.*, 2014). The decreased hatching success and calcification observed in this study were likely the result of high pCO_2 altering the crab's energy budgets. In fact, crab in the pH 7.5 treatment were stressed to the point that they appear to not have had enough energy to maintain the integrity of their carapaces. Results from this study highlight the need for long-term ocean acidification research that encompasses many life stages, so potential carryover effects can be observed.

Acknowledgements

This project was funded by the North Pacific Research Board (NPRB publication no. 536) and the National Marine Fisheries Service (NMFS). We thank NMFS biologists and laboratory technicians for their assistance who made this project possible. Previous versions of this paper were improved by comments from J. Napp and C. Ryer and two anonymous reviewers. The findings and conclusions in the paper are those of the authors and do not necessarily represent the views of the National Marine Fisheries Service, NOAA. Reference to trade names does not imply endorsement by the National Marine Fisheries Service, NOAA.

References

Agnalt, A. L., Grefsrud, E. S., Farestveit, E., Larsen, M., and Keulder, F. 2013. Deformities in larvae and juvenile European lobster (*Homarus gammarus*) exposed to lower pH at two different temperatures. Biogeosciences, 10: 7883–7895.

Arnold, K. E., Findlay, H. S., Spicer, J. I., Daniels, C. L., and Boothroyd, D. 2009. Effect of CO_2-related acidification on aspects of the larval development of the European lobster, *Homarus gammarus* (L.). Biogeosciences, 6: 1747–1754.

Burnham, K. P., and Anderson, D. R. 2002. Model Selection and Multimodel Inference—A Practical Information—Theoretic Approach. Springer, New York. 499 p.

Caldeira, K., and Wickett, M. E. 2003. Anthropogenic carbon and ocean pH. Nature, 425: 1.

Carter, H. A., Ceballos-Osuna, L., Miller, N. A., and Stillman, J. H. 2013. Impact of ocean acidification on metabolism and energetics during early life stages of the intertidal porcelain crab *Petrolisthes cinctipes*. The Journal of Experimental Biology, 216: 1412–1422.

Dickson, A. G., Sabine, C. L., and Christian, J. R. 2007. Guide to Best Practices for Ocean CO_2 Measurements. PICES Special Publication 3, Sidney, British Columbia. 176 p.

DOE. 1994. Handbook of Methods for the Analysis of the Various Parameters of the Carbon Dioxide System in Seawater. Version 2. Rep. ORNL/CDIAC-74. 197 p.

Donaldson, W. E., and Adams, A. E. 1989. Ethogram of behavior with emphasis on mating for the Tanner crab *Chionoecetes bairdi* Rathbun. Journal of Crustacean Biology, 9: 37–53.

Ernst, B., Orensanz, J. M., and Armstrong, D. A. 2005. Spatial dynamics of female snow crab (*Chionoecetes opilio*) in the eastern Bering Sea. Canadian Journal of Fisheries and Aquatic Sciences, 62: 250–268.

Fabry, V. J., McClintock, J. B., Mathis, J. T., and Grebmeier, J. M. 2009. Ocean acidification at high latitudes: The bellweather. Oceanography, 22: 160–171.

Feely, R. A., Sabine, C. L., Byrne, R. H., Millero, F. J., Dickson, A. G., Wanninkhof, R., Murata, A., *et al.* 2012. Decadal changes in the aragonite and calcite saturation state of the Pacific Ocean. Global Biogeochemical Cycles, 26: 15.

Intergovernmental Panel on Climate Change. 2014. Climate Change 2014 Fifth Assessment Synthesis Report. Intergovernmental Panel on Climate Change. 132 pp.

Jadamec, L. S., Donaldson, W. E., and Cullenberg, P. 1999. Biological Field Techniques for *Chionoecetes* Crabs. University of Alaska Sea Grant College Program, Rep. AK-SG-00–02, Fairbanks. 80 pp.

Kon, T., Ono, M., and Honma, Y. 2010. Histological studies on the spent ovaries of aged snow crabs *Chionoecetes opilio* caught in the Sea of Japan. Fisheries Science, 76: 227–233.

Kurihara, H. 2008. Effects of CO_2-driven ocean acidification on the early developmental stages of invertebrates. Marine Ecology Progress Series, 373: 275–284.

Kurihara, H., Matsui, M., Furukawa, H., Hayashi, M., and Ishimatsu, A. 2008. Long-term effects of predicted future seawater CO_2 conditions on the survival and growth of the marine shrimp *Palaemon pacificus*. Journal of Experimental Marine Biology and Ecology, 367: 41–46.

Landes, A., and Zimmer, M. 2012. Acidification and warming affect both a calcifying predator and prey, but not their interaction. Marine Ecology Progress Series, 450: 1–10.

Long, W. C., Swiney, K. M., and Foy, R. J. 2013a. Effects of ocean acidification on the embryos and larvae of red king crab, *Paralithodes camtschaticus*. Marine Pollution Bulletin, 69: 38–47.

Long, W. C., Swiney, K. M., Harris, C., Page, H. N., and Foy, R. J. 2013b. Effects of ocean acidification on juvenile red king crab (*Paralithodes camtschaticus*) and Tanner crab (*Chionoecetes bairdi*) growth, condition, calcification, and survival. PLos ONE, 8 (4): e60959.

Magdans, U., and Gies, H. 2004. Single crystal structure analysis of sea urchin spine calcites: Systematic investigations of the Ca/Mg distribution as a function of habitat of the sea urchin and the sample location in the spine. European Journal of Mineralogy, 16: 261–268.

Mathis, J. T., Cross, J. N., and Bates, N. R. 2011. The role of ocean acidification in systemic carbonate mineral suppression in the Bering Sea. Geophysical Research Letters, 38: L19602.

Mathis, J. T., Cross, J. N., Monacci, N., Feeley, R. A., and Stabeno, P. 2014. Evidence of prolonged aragonite undersaturations in the bottom waters of the southern Bering Sea shelf from autonomous sensors. Deep Sea Research Part II, 109: 125–133.

Meseck, S. L., Alix, J. H., Swiney, K. M., Long, W. C., Wikfors, G. H., and Foy, R. J. 2015. Ocean acidification affects hemocyte physiology in the Tanner crab (*Chionoecetes bairdi*). PLos ONE, in press.

Morgan, S. G. 1995. The timing of larval release. *In* Ecology of Marine Invertebrate Larvae, pp. 157–191. Ed. by L. McEdward. CRC Press, Boca Raton.

Moriyasu, M., and Lanteigne, C. 1998. Embryo development and reproductive cycle in the snow crab, *Chionoecetes opilio* (Crustacea: Majidae), in the southern Gulf of St. Lawrence, Canada. Canadian Journal of Zoology, 76: 2040–2048.

North Pacific Fishery Management Council. 2013. Stock Assessment and Fishery Evaluation Report for the King and Tanner Crab Fisheries of the Bering Sea and Aleutian Islands Regions. Anchorage, AK: North Pacific Fishery Management Council, 828 pp.

O'Connor, C. M., Norris, D. R., Crossin, G. T., and Cooke, S. J. 2014. Biological carryover effects: Linking common concepts and mechanisms in ecology and evolution. Ecosphere, 5: 1–11.

Orr, J. C., Fabry, V. J., Aumont, O., Bopp, L., Doney, S. C., Feely, R. A., Gnanadesikan, A., *et al.* 2005. Anthropogenic ocean acidification over the twenty-first century and its impact on calcifying organisms. Nature, 437: 681–686.

Paul, A. J. 1984. Mating frequency and viability of stored sperm in the Tanner crab *Chionoecetes bairdi* (Decapoda, Majidae). Journal of Crustacean Biology, 4: 375–381.

Paul, A. J., and Adams, A. E. 1984. Breeding and fertile period for female *Chionoecetes bairdi* (Decapoda, Majidae). Journal of Crustacean Biology, 4: 589–594.

Ries, J. B., Cohen, A. L., and McCorkle, D. C. 2009. Marine calcifiers exhibit mixed responses to CO_2-induced ocean acidification. Geology, 37: 1131–1134.

Sara, G., Rinaldi, A., and Montalto, V. 2014. Thinking beyond organism energy use: A trait-based bioenergetic mechanistic approach for predictions of life history traits in marine organisms. Marine Ecology, 35: 506–515.

Schiffer, M., Harms, L., Poertner, H. O., Mark, F. C., and Storch, D. 2014. Pre-hatching seawater pCO_2 affects development and survival of

zoea stages of Arctic spider crab *Hyas araneus*. Marine Ecology Progress Series, 501: 127–139.

Sokolova, I. M., Frederich, M., Bagwe, R., Lannig, G., and Sukhotin, A. A. 2012. Energy homeostasis as an integrative tool for assessing limits of environmental stress tolerance in aquatic invertebrates. Marine Environmental Research, 79: 1–15.

Spalinger, K. 2013. Bottom trawl Survey of Crab and Groundfish: Kodiak, Chignik, South Peninsula, and Eastern Aleutian Management Districts, 2012. Alaska Department of Fish and Game, Fishery Management Report No. 13–27, 127 pp.

Stevens, B. G. 2003. Timing of aggregation and larval release by Tanner crabs, *Chionoecetes bairdi*, in relation to tidal current patterns. Fisheries Research, 65: 201–216.

Stevens, B. G. 2006. Timing and duration of larval hatching for blue king crab *Paralithodes platypus* Brandt, 1850 held in the laboratory. Journal of Crustacean Biology, 26: 495–502.

Stevens, B. G., Donaldson, W. E., Haaga, J. A., and Munk, J. E. 1993. Morphometry and maturity of paired Tanner crabs, *Chionoecetes bairdi*, from shallow- and deepwater environments. Canadian Journal of Fisheries and Aquatic Sciences, 50: 1504–1516.

Styf, H. K., Skold, H. N., and Eriksson, S. P. 2013. Embryonic response to long-term exposure of the marine crustacean *Nephrops norvegicus* to ocean acidification and elevated temperature. Ecology and Evolution, 3: 5055–5065.

Swiney, K. M. 2008. Egg extrusion, embryo development, timing and duration of eclosion, and incubation period of primiparous and multiparous tanner crabs (*Chionoecetes bairdi*). Journal of Crustacean Biology, 28: 334–341.

Swiney, K. M., Long, W. C., and Foy, R. J. 2016. Effects of high pCO_2 on Tanner crab reproduction and early life history, Part II: carryover effects on larvae from oogenesis and embryogenesis are stronger than direct effects. ICES Journal of Marine Science, 73: 825–835.

The Royal Society. 2005. Ocean Acidification Due to Increasing Atmospheric Carbon Dioxide. The Royal Society, Policy doc. 12/05. 57 pp.

Handling editor: C. Brock Woodson

ICES Journal of Marine Science

ICES Journal of Marine Science (2016), 73(3), 836–848. doi:10.1093/icesjms/fsv251

Contribution to Special Issue: 'Towards a Broader Perspective on Ocean Acidification Research'

Original Article

Effects of high pCO_2 on Tanner crab reproduction and early life history, Part II: carryover effects on larvae from oogenesis and embryogenesis are stronger than direct effects

W. Christopher Long*, Katherine M. Swiney, and Robert J. Foy

NOAA, National Marine Fisheries Service, Alaska Fisheries Science Center, Resource Assessment and Conservation Engineering Division, Kodiak Laboratory, 301 Research Ct, Kodiak, AK 99615, USA

**Corresponding author: tel: +1 907 481 1715; fax: +1 907 481 1701; e-mail: chris.long@noaa.gov.*

Long, W. C., Swiney, K. M., and Foy, R. J. Effects of high pCO_2 on Tanner crab reproduction and early life history, Part II: carryover effects on larvae from oogenesis and embryogenesis are stronger than direct effects. – ICES Journal of Marine Science, 73: 836–848.

Received 17 February 2015; revised 19 November 2015; accepted 30 November 2015; advance access publication 10 January 2016.

Anthropogenic CO_2 release is increasing the pCO_2 in the atmosphere and oceans and causing a decrease in the pH of the oceans. This decrease in pH, known as ocean acidification, can have substantial negative effects on marine life. In this study, we use wild-brooded larvae and larvae from females held in treatment pH for two brooding cycles over 2 years to detect carryover effects from oogenesis and embryogenesis. Ovigerous females were held at three pHs: ~8.1 (Ambient), 7.8, and 7.5. Exposure to acidified conditions at the larval stage alone had minimal effects on the larvae, possibly because larvae may be adapted to living in an environment with large pH swings. Exposure of Tanner crab larvae to low pH during the embryo phase had a more substantial effect on morphology, size, Ca/Mg content, and metabolic rate than exposure during the larval phase, and maternal exposure during the oogenesis phase increased the carryover effect. Although the larval phase itself is resilient to low pH, carryover effects are likely to have a negative effect on larvae in the wild. These results, combined with negative effects of high pCO_2 at other life history stages, indicate that high pCO_2 may have a negative effect on the Tanner crab populations and fisheries soon.

Keywords: crabs, early life history, hypercapnia, larvae, mortality, ocean acidification, Tanner crabs, transgenerational.

Introduction

Anthropogenic activities are increasing the concentration of CO_2 in the atmosphere and ocean and are predicted to reduce ocean pH of ~0.3 units by 2100 and 0.5 units by 2200 (Caldeira and Wickett, 2003). High-latitude areas are expected to be affected sooner than other areas. For example, in North Pacific waters, a number of factors interact to affect the severity of ocean acidification. CO_2 is more soluble in the colder water that exists at high-latitude waters, and thus uptake from the atmosphere is more rapid at the surface, while upwelling (particularly in the Gulf of Alaska) brings up CO_2-rich waters from the deep (Fabry *et al.*, 2009). Ice melt from sea ice and glaciers, exacerbated by increased temperatures, can reduce the saturation state of calcium carbonate minerals, particularly in surface waters (Evans *et al.*, 2014; Mathis *et al.*, 2014). These factors, combined with stratified waters and seasonal, high rates of carbon export from the surface layers during periods of high productivity, can lead to pCO_2 in bottom waters exceeding 1600 ppm in the late summer and early fall (Mathis *et al.*, 2014). Surface waters are predicted to become, on average, undersaturated with respect to aragonite by 2070 in Bering Sea (Mathis *et al.*, 2015).

Ocean acidification is expected to have a physiological effect on many marine animals, particularly on those with calcium carbonate shells or exoskeletons (Fabry *et al.*, 2008). Although crustaceans are among the many calcifying marine organisms, their response to ocean acidification is mixed (Wittmann and Pörtner, 2013). Even at early life history stages, such as the embryo and larval stages, a wide response is seen, although these developmental stages are thought to be more sensitive to stressors. The larvae of some crustacean species have reduced survival (Walther *et al.*, 2010; Long *et al.*, 2013b) and growth (Keppel *et al.*, 2012; Schiffer *et al.*, 2014) or

exhibit deformities (Agnalt *et al.*, 2013) under acidified conditions, although other species are resilient to such changes (Styf *et al.*, 2013; Small *et al.*, 2015).

Because the larval stage is typically only a small fraction of the life history of most crustaceans and other marine invertebrates, exposure to ocean acidification during this stage is relatively brief. However, carryover effects from previous stages may be important. Carryover effects occur when exposure to a stressor at one life history stage affects performance in a subsequent stage. For example, juvenile Olympia oysters, *Ostrea lurida*, suffer reduced growth after settlement if exposed to low pH during the larval phase regardless of the pH juveniles are exposed to (Hettinger *et al.*, 2012, 2013). The larval phase of both the spider crab, *Hyas araneus*, and red king crab, *Paralithodes camtschaticus*, suffers greater mortality following exposure to acidified water as embryos (Long *et al.*, 2013a; Schiffer *et al.*, 2014). Thus, understanding carryover effects is critical for our understanding of how ocean acidification will affect a particular species.

The Tanner crab, *Chionoecetes bairdi*, is a commercially important crab species in Alaskan waters (NPFMC, 2011). Primiparous (first egg clutch) Tanner crab females molt to maturity, mate, and extrude a batch of eggs in the late winter (Paul and Adams, 1984), whereas multiparous, brooding a second or subsequent clutch, release their larvae typically in April to May and then mate, and extrude new eggs right thereafter (Munk *et al.*, 1996). Eggs are brooded for about a year before larval hatching (Swiney, 2008); during that year, oogenesis in the female ovaries is preparing oocytes for the next year's clutch. Larvae spend ~3 months in the plankton as they pass through a prezoeal stage which lasts only a few hours (Haynes, 1973), followed by two zoeal and a megalops stage which each last about a month, before settling into the benthic environment, and molting to the first crab stage (Incze *et al.*, 1982).

The waters at the high latitudes where Tanner crabs live are expected to acidify more rapidly than elsewhere (Fabry *et al.*, 2009). Seasonal variability in the pH of bottom water in Bering Sea results in pH levels that are physiologically stressful (pH < 7.8) to juvenile Tanner crabs for at least part of the year (Cross *et al.*, 2013). Juvenile Tanner crabs exhibit decreased growth, survival, and calcification under near-future levels of CO_2 (Long *et al.*, 2013b); adults suffer increased haemocyte mortality and a decreased intracellular pH in semi-granular and granular haemocytes (Meseck *et al.*, 2015). Given the sensitivity of this species to high pCO_2, it is imperative to understand its effects at all life history stages; different life history stages may differ in their response (e.g. Hettinger *et al.*, 2012). In addition, because of the year-long duration of both oogenesis and embryogenesis, it is critical to understand potential carryover effects because direct effects alone may substantially underestimate the cumulative effects of high pCO_2 exposure (Hettinger *et al.*, 2012, 2013; Schiffer *et al.*, 2014).

To determine how high pCO_2 is likely to affect the Tanner crab stocks, we performed a series of experiments examining a wide range of life history stages and responses. In an initial study, we determined how high pCO_2 affected juvenile Tanner crab growth, survival, calcification, and condition (Long *et al.*, 2013b). This paper is the second in a two-part series that examines the effects of high pCO_2 on reproduction and early life history stages. In the first paper, we determine the effects of high pCO_2 on embryogenesis, larval hatching success, and ovigerous Tanner crabs (Swiney *et al.*, 2016). In this paper, we examine the effects of high pCO_2 on the starvation-survival, carbon and nitrogen content, and calcium/magnesium content of larval Tanner crabs. By using larvae from embryos reared in the first experiment, we examine carryover effects to the larval stage from exposure during oogenesis and embryogenesis. Understanding how both the direct and carryover effects of high pCO_2 affect larval fitness is critical for understanding how these stocks may respond to ocean acidification.

Methods

Overview

To determine the effects of high pCO_2 on larval Tanner crabs, we performed three sets of experiments over 3 years, 2011–2013 (overall experimental design is depicted in Supplementary material S1). In 2011, we used wild-brooded larvae to determine the effects on the larval stage only. We then held females with newly extruded embryos in the laboratory at three pH treatments, ambient and two experimental pH levels (pH 7.8 and pH 7.5), until the larvae hatched and, in 2012, we used these larvae to determine carryover effects of exposure at the embryo stage on larvae using a fully crossed design between embryo and larval treatments. Finally, we held the females for another year in their pH treatments. So, in 2013, the larvae that hatched out came from oocytes that developed in the females while they were in treatment water and embryos that had developed in treatment water. These larvae allowed us to determine carryover effects of exposure during both oogenesis and embryogenesis on larvae, again via a fully crossed experimental design. All larval experiments were performed on the first zoeal stage and no molting was observed during any of the experiments.

Water acidification

Water was acidified using CO_2 as described in Long *et al.* (2013a) and Swiney *et al.* (2016) to produce water with pHs of 7.8 and 7.5 (expected pHs in ~2100 and 2200). pH and temperature in experimental units were measured daily using a Durafet II or III pH probe during all experiments. Water samples to monitor experimental conditions were taken once a week, from the head tanks (2011), or from the larval experimental tanks (2012 and 2013; see details on set-up below) poisoned with mercuric chloride, and sent to the NOAA's Auke Bay Laboratories (2011 and 2012) or to the University of Alaska Fairbanks (2013) for analysis of salinity, dissolved inorganic carbon (DIC), and total alkalinity (TA) as described in Swiney *et al.* (2016). Samples sizes (total) were 6 in 2011, 16 in 2012, and 13 in 2013. The seacarb package in R (V2.14.0, Vienna, Austria) was used to calculate the pCO_2, carbonate, and bicarbonate concentrations, and the saturation state of calcite and aragonite (Lavigne and Gattuse, 2012).

The pH in the larval experiments stayed well within the nominal range in all 3 years (Table 1). Temperatures were slightly (~0.4°C) lower in 2012 than in 2013, and ~2°C lower in 2011 than 2012 reflecting differences in the ambient incoming seawater. pCO_2 increased with decreasing pH. Ambient water pH and pCO_2 differed slightly among the years and was always above saturation for both aragonite and calcite, pH 7.8 water was undersaturated with respect to aragonite, and pH 7.5 water was undersaturated with respect to both aragonite and calcite. Full water chemistry parameters in the female/embryo treatments, presented elsewhere (Swiney *et al.*, 2016), were similar to the conditions in these larval experiments with pHs ± 1 standard deviation (s.d.) of 8.09 ± 0.07, 7.80 ± 0.03, and 7.50 ± 0.03 in the Ambient, pH 7.8, and pH 7.5 treatments.

Table 1. Average water chemistry parameters in experimental units (± 1 standard deviation) during experiments on larval Tanner crabs for each of the 3 years.

Treatment	Temperature (°C)	pH_F	pCO_2 (µatm)	HCO_3^- (mmol kg^{-1})	CO_3^{-2} (mmol kg^{-1})	DIC (mmol kg^{-1})	Alkalinity (mmol kg^{-1})	$\Omega_{Aragonite}$	$\Omega_{Calcite}$
2011									
Ambient	4.66 ± 0.19	8.21 ± 0.04	269.42 ± 20.45	1.81 ± 0.01	0.12 ± 0.01	1.95 ± 0.00	2.13 ± 0.01	1.88 ± 0.09	3.00 ± 0.14
pH 7.8	4.61 ± 0.13	7.79 ± 0.02	810.33 ± 22.89	1.97 ± 0.00	0.05 ± 0.00	2.06 ± 0.00	2.10 ± 0.01	0.76 ± 0.03	1.21 ± 0.05
pH 7.5	4.63 ± 0.17	7.49 ± 0.02	1665.48 ± 161.70	2.02 ± 0.02	0.03 ± 0.00	2.14 ± 0.01	2.09 ± 0.02	0.39 ± 0.03	0.62 ± 0.05
2012									
Ambient	6.85 ± 0.66	8.16 ± 0.04	345.66 ± 34.66	1.87 ± 0.01	0.11 ± 0.01	2.00 ± 0.01	2.16 ± 0.06	1.70 ± 0.13	2.71 ± 0.21
pH 7.8	6.58 ± 0.43	7.81 ± 0.02	787.30 ± 21.50	2.02 ± 0.02	0.06 ± 0.00	2.11 ± 0.02	2.17 ± 0.05	0.85 ± 0.03	1.36 ± 0.04
pH 7.5	6.69 ± 0.50	7.50 ± 0.02	1643.71 ± 91.51	2.03 ± 0.04	0.03 ± 0.00	2.14 ± 0.05	2.23 ± 0.14	0.42 ± 0.02	0.66 ± 0.04
2013									
Ambient	7.01 ± 0.55	8.16 ± 0.03	326.53 ± 33.75	1.85 ± 0.01	0.12 ± 0.01	1.98 ± 0.01	2.12 ± 0.01	1.76 ± 0.16	2.81 ± 0.25
pH 7.8	7.12 ± 0.59	7.79 ± 0.01	811.36 ± 38.31	1.99 ± 0.02	0.05 ± 0.00	2.09 ± 0.02	2.09 ± 0.02	0.81 ± 0.04	1.29 ± 0.07
pH 7.5	7.06 ± 0.54	7.50 ± 0.02	1619.80 ± 59.85	2.05 ± 0.02	0.03 ± 0.00	2.15 ± 0.02	2.13 ± 0.01	0.43 ± 0.02	0.69 ± 0.03

Temperature and pH (free scale) were measured daily, DIC (all years) and alkalinity (2012 and 2013 only) were measured weekly, and all other parameters were calculated from pH and DIC.

2011 wild-brooded larvae

Ethical approval for this research was not required by any federal, state, or international laws because the study was conducted on invertebrates not covered under these laws. Healthy, multiparous, ovigerous female Tanner crabs were captured in Chiniak Bay, Kodiak, Alaska, in the spring of 2011 in crab pots and a 3 m beam trawl. Four healthy females with clutches of eyed eggs, average carapace width (CW) ± s.d. of 93.3 ± 3.1 mm were held in individual 68 l tubs with flow-through ambient water without food for 5 d, after which larvae for the experiments were collected in a single day in water baths and pooled. The larvae were held at ambient pH and temperature for 24 h before beginning the experiments, and only healthy, actively swimming larvae were used. Experiments were performed in PVC inserts with mesh bottoms placed inside beakers, with the tops of beakers covered with a piece of plastic bubble wrap to reduce gas exchange with the atmosphere as described in Long *et al.* (2013a). The same three pH treatments as above were used (Ambient, pH 7.8, and pH 7.5). The beakers were kept in a cold room at 5°C, which was ambient temperature of incoming seawater at the time, and water was changed once a day by moving each insert from its old beaker to a beaker of new treatment water. The pH and temperature were measured in each insert each day. Two experiments were performed to determine the effects of high pCO_2 on larval (i) morphology and (ii) survival under starvation conditions. For each experiment, there were five replicates of each treatment.

Larval morphology experiments were performed in 2 l PVC inserts/beakers. Approximately 200 larvae were placed in each beaker. Seven larvae were measured initially, before the experiment. Larvae were held for 10 d when three larvae from each beaker were measured (15 per treatment). As the larvae did not molt during the experiment and larvae morphology does not change within a molt stage under normal conditions, we were looking to see if any degradation of the exoskeleton was occurring such as observed by Kurihara *et al.* (2008). Larvae were photographed under a stereomicroscope and Image-Pro Plus v. 6.00.260 (Media Cybernetics, Inc., Bethesda, MD, USA) was used to measure the carapace width (including spines), lateral spine length, dorsal spine length, rostro-dorsal length, rostral spine length, and protopodite length (Supplementary material S2) as per Webb *et al.* (2006). Larval morphometrics were analysed using an analysis of similarity (ANOSIM) performed on a Bray–Curtis similarity matrix with pH treatment as the factor in Primer 6.1.13 (Primer, UK).

Larval starvation-survival experiments were performed in 1 l PVC inserts/beakers. Each beaker was stocked with ~20 larvae. Larvae were checked daily and any larvae that failed to move within a 15 s observation period (based on previous experience with larvae (Long *et al.*, 2013a) and initial observations) were considered dead and discarded. The experiment continued until all larvae were dead. The survival data were fit to a logistic regression model assuming a binomial distribution of data: $P_m = 1/[1+(t/t_{50})^s]$, where P_m is the probability of mortality, t the time in days, t_{50} the time of 50% mortality (sometimes called the LT_{50}) also in days, and s a slope parameter. The t_{50} parameter indicates how long on average a larvae survives. The slope parameter is proportional to the slope of the curve at t_{50} (Long, 2016), larger absolute values of s indicate that most of the individual mortality events occurred close to t_{50}, smaller absolute values indicate a greater spread in individual survival times around t_{50}. In this paper, the t_{50} parameter is the parameter of interest as we want to know if and how the pH treatment affects the survival time; s is necessary for the model but is not interpreted directly. We constructed a series of *a priori* models in which t_{50} or s was allowed to vary among the pH treatments and fit them to the data in R 2.14.0 (Vienna, Austria). *Post hoc*, we noticed that pH 7.8 and Ambient had similar t_{50} values, so we included models in which those two treatments differed from the pH 7.5 treatment. We selected the best model using the Akaike's information criterion corrected for small sample size (AIC_c). Models whose AIC_c differed by <2 were considered to explain the data equally well (Burnham and Anderson, 2002).

2012 and 2013 laboratory-reared larvae

Healthy, multiparous, ovigerous female Tanner crabs, CW 98.7 ± 4.8 mm (s.d.), were captured as described above. Their embryos were either newly extruded (uneyed) or about to hatch (eyed); females which hatched larvae in the lab were allowed to mate and extrude a clutch of eggs in ambient seawater before being placed in the experiment (this occurred within 13 d of capture). Each female was held in an individual container with flow-through seawater. A total of 48 females were used and each was randomly assigned to one of the three pH treatments, for a total of 16 replicates per treatment. Details of the female holding conditions and the

effects of high pCO_2 on embryo development and Tanner crab fecundity and hatching success are published separately (Swiney *et al.*, 2016). In short, the females were placed in treatment water on 21 June 2011, and held during brooding for the first year. At hatching in May 2012, larvae were collected and used for the 2012 larval experiments. Because the females reach peak hatching at different times, larvae from 2 (Ambient) to 3 (pH 7.8 and 7.5) females within each treatment that were at peak hatching were collected on the same day and used for the experiments. The larvae were pooled and a similar number of larvae were used from each female within each treatment. After hatching, a male crab was placed in with each of the females to allow for mating, and all female extruded a new batch of eggs. Mortality during the first year resulted in 12 females in the Ambient and pH 7.5 treatments and 11 in the pH 7.8 treatment at the beginning of the second brooding year. Females were held in their treatment water until the embryos hatched out in April–June 2013 and were used for the 2013 larval experiments. Larvae from two females from each treatment that were at peak hatching were collected, pooled, and used in the experiments.

In 2012 and 2013, experiments were performed in the same-sized 1 and 2 l PVC inserts as in 2011. These were placed in a tank (one per treatment) with flow-through seawater at the appropriate treatment pH and ambient temperature. The water within the tank was recirculated into each of the inserts. This set-up allowed for better control over the pH, reduced the amount of manipulation the larvae received (no changing of water), and allowed for better water quality (flow-through vs. static conditions). We performed four experiments to determine the effects of high pCO_2 on: (i) larval survival, (ii) larval carbon and nitrogen content (CN), (iii) larval calcium and magnesium content, and (iv) larval mass all under starvation conditions to allow interpretation of the survival data in the light of the changing organic and mineral content of the larvae. In 2011, we had planned to run all of these experiments, but the total mass of larvae in each replicate beaker at the end of the experiment was insufficient for the measurement of some of the parameters, so the data could not be collected; this is also why we increased the density of larvae in the experiments and decreased the exposure time from 10 to 7 d. Each of the experiments was fully crossed between embryo treatment and larval treatment, allowing us to examine carryover effects between the stages (Long *et al.*, 2013a), and five replicates were performed for each experiment for each embryo–larval treatment combination. In 2013, however, so few larvae hatched from females in the pH 7.5 treatment (Swiney *et al.*, 2016) that we were only able to perform the starvation survival experiments on these larvae. Before the beginning of the experiments, five samples for CN, calcium/magnesium content, and average larval mass analyses were taken from the starting pool of larvae as described below. In addition, because we did not observe any change in larval morphology after rearing larvae in acidified water in 2011 (see the Results section), we did not examine larval morphology after exposure to acidified waters in 2012 or 2013; instead, we examined if exposure to acidified conditions for a year as embryos affected larval morphology by measuring 15 newly hatched larvae from each treatment as above. Differences in larval morphometrics were analysed using an ANOSIM performed on a Bray–Curtis similarity matrix with embryo treatment as the factor.

Starvation survival experiments were performed in 1 l sized PVC inserts as above until all larvae had died. The data were fit to a series of logistic regressions as above, where the t_{50} or s parameters were allowed to vary linearly with the embryo and larval treatments. The AIC_c was calculated for each model and the best model selected. For CN, calcium/magnesium content, and larval mass experiments, ~300 larvae were stocked in 2 l PVC inserts, held at their treatment pH for 7 d, dried to a constant mass, and then sent to analytical laboratories to be analysed for CN, calcium, and magnesium contents. The CN analysis was performed at the University of California Santa Barbara using the Dumas combustion method and an automated organic elemental analyser (Gnaiger and Bitterlich, 1984). In 2012, calcium/magnesium contents were analysed at the NOAA Auke Bay Laboratory using a Dionex Ion Chromatography system. In 2013, calcium/magnesium contents were analysed at Gel Laboratories via inductively coupled plasma-atomic emission spectrometry. To determine the average mass, subset of 50 larvae was counted, dried, and massed from each replicate PVC insert in both the CN and calcium/magnesium content experiments in 2012 (sample size of 10 per treatment combination), and from each replicate PVC insert in the calcium/magnesium experiments only in 2013 (5 per treatment combination). The average mass of each larva was calculated and the sample was recombined with the remaining larvae from each replicate before CN or calcium/magnesium analysis. The per cent dry mass of carbon, nitrogen, calcium, magnesium, the C:N and Ca:Mg ratios, and the average mass of a larvae were analysed with fully crossed two-way analysis of variance with embryo and larval treatments as factors. Always, the assumption of homogeneity of variance was checked with Levene's test and the data were transformed to meet the assumption, when necessary. When there were significant effects, Tukey's *post hoc* test was used to detect differences among treatments.

Results

2011 wild-brooded larvae

Larval morphometrics did not vary with treatment (ANOSIM, Global $R = 0.009$, $p = 0.364$) and did not change between the beginning and end of the experiment (Figure 1). pH treatment had little to no effect on starvation survival times. Two models fit the survival data equally well: in the first, only the slope parameter varied among the treatments, and in the second, the slope parameter varied among the treatments and the t_{50} for Ambient and pH 7.8 larvae differed from the pH 7.5 larvae (Table 2). However, the differences among the treatment were slight, with the t_{50} parameter varying by only 0.18 d, and likely not biologically relevant (Table 2, Figure 2).

2012 and 2013 laboratory-reared larvae

In 2012, there was a statistically significant effect of embryo treatment on larval morphometrics (Global $R = 0.074$, $p = 0.02$). Pairwise comparisons showed that the only difference was between pH 7.8 and pH 7.5, and ordination showed that, on average, pH 7.5 embryos were slightly larger than pH 7.8; however, there was significant overlap and the effect size was small; a 2% difference in the rostro-dorsal length, for example (Figure 3), is unlikely to have any discernible effect on larval survival or performance. Additionally, the low Global R value also indicates that the differences were not biologically relevant (Clarke and Warwick, 2001). In 2013, larval morphometrics differed among embryo pH treatments (Global $R = 0.383$, $p < 0.0001$), with pH 7.8 and Ambient larvae being larger than pH 7.5 larvae (Figure 3); the effect sizes were larger than in 2012, with pH 7.5 larvae having 10% smaller carapace width than Ambient and pH 7.8 larvae, for example (Figure 3).

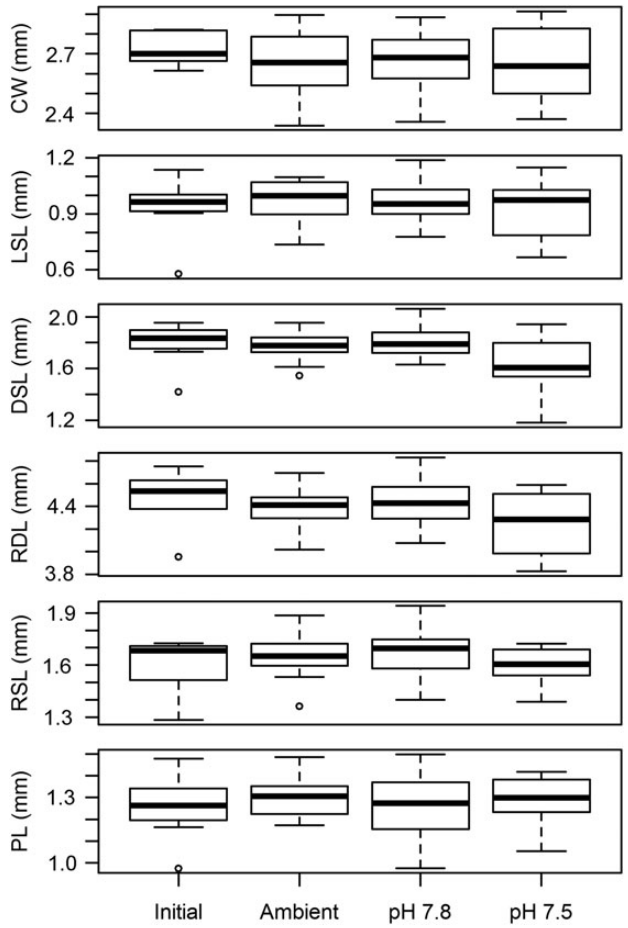

Figure 1. Box-plots of measurements made on larvae in the 2011 experiment. Initial represents larvae measured the day after hatching. Ambient, pH 7.8, and pH 7.5 represent larvae that had been held in ambient and acidified water for 10 d. Measurements included CW—carapace width, LSL—lateral spine length, DSL—dorsal spine length, RDL—rostro-dorsal length, RSL—rostral spine length, and PL—protopodite length.

In 2012 and 2013, the t_{50} and s parameters varied among treatments at both the embryo and larval stages as well as in their interaction in the best fit models of larval survival (Supplementary material S3). In 2012, the full model contained a number of parameters whose 95% confidence intervals, as indicated by the standard error of the parameter estimates, substantially overlapped 0. We thus created a *post hoc* model in which these parameters were eliminated, thus increasing the parsimony of the best model substantially (Supplementary material S3). In both years, the effect of treatment at the embryo stage was larger than treatment at the larval stage; larvae from embryos that developed in pH 7.5 water died 3.01 d later in 2012 and 3.32 d later in 2013 (when averaged across the larval treatments) than those that developed in Ambient water (Figure 4, Table 3). In 2012, larvae from embryos that had developed in pH 7.8 water were similar to Ambient larvae, whereas in 2013, they were intermediate between the Ambient and pH 7.5 larvae. The effect of treatment at the larval stage and the interactive effects were much smaller and no clear pattern in the data is apparent (Figure 4, Table 3).

The C and N content of larvae varied with the larval and embryo treatments in both years (Figure 5, Supplementary material S4). In general, exposure to acidified water at the embryo and larval stages increased the C and N content of the larvae, with the effect of the embryo treatment being larger (Figure 5). Larvae exposed to pH 7.8 as embryos did not differ from the Ambient larvae in 2012, but did in 2013. In addition, there was always a drop in the C and N content between the initial measurement made right after hatching and after 7 d of larval starvation. Although there was a significant effect of treatment on the C:N ratio in 2013 (though not in 2012), the effect was small and no pattern is discernible (Figure 5, Supplementary material S4).

Larval Ca and Mg content varied with larval and embryo treatments in both years (Figure 6, Supplementary material S4). Exposure to acidified water at the embryo stage reduced the Ca content in both years and the Mg content in 2012 (the lack of a difference in 2013 is probably because we were unable to run this experiment with pH 7.5 larvae). Ca content was highest in larval reared at pH 7.8 and was lowest in those reared at pH 7.5, with those reared at the Ambient in between. Larvae also generally increased their Ca and Mg contents during their first 7 d as larvae

Table 2. Ranking of models of Tanner crab larvae mortality in 2011 using AIC_c and the parameter estimates ± standard error for the best fit models.

Model	*K*	AIC_c	ΔAIC_c	Likelihood	AIC_c weight
t_{50}, s	2	923.39	4.01	0.13	0.05
$t_{50}(T)$, s	4	924.39	5.01	0.08	0.03
$t_{50}(T2)$, s	3	922.85	3.47	0.18	0.07
t_{50}, $s(T)$	4	919.38	0.00	1.00	0.40
$t_{50}(T)s(T)$	6	921.79	2.41	0.30	0.12
$t_{50}(T2)s(T)$	5	919.84	0.46	0.80	0.32

	Parameter estimates	
Parameter	t_{50}, $s(T)$	$t_{50}(T)$,$s(T2)$
t_{50}	9.47 ± 0.07	–
t_{50}(*A*, pH 7.8)	–	9.54 ± 0.09
t_{50} (pH 7.5)	–	9.36 ± 0.11
s(*A*)	−6.18 ± 0.32	−6.22 ± 0.33
s(pH 7.8)	−7.12 ± 0.37	−7.16 ± 0.38
s(pH 7.5)	−7.6 ± 0.41	−7.53 ± 0.41

Model indicates the parameters used and how they were modelled (see text for details). Where factors are included parenthetically, the parameter is modelled as a linear function of those parameters. *T* indicates that the parameter varies among all treatments and *T2* indicates the *post hoc* models in which the parameter was the same for the Ambient (A) and pH 7.8 treatments which differed from the pH 7.5 treatment. *K* is the number of parameters for each model. To show the greatest difference among the treatments supported by the data, the more complex $t_{50}(T2)s(T)$ model is presented in Figure 2. The t_{50} parameters have units of days and the s parameters are unitless.

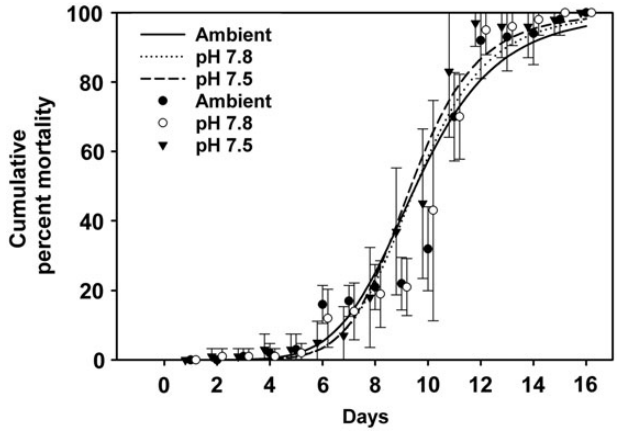

Figure 2. Mortality of Tanner crab larvae during starvation in 2011 at three pH treatments over time. Points are the average per cent mortality ± 1 standard deviation at each treatment and lines are one of the best fit logistic regression model for each [the $t_{50}(T2)s(T)$ model is presented, see Table 2 for parameter estimates]. The points for pH 7.8 and pH 7.5 are offset by 0.2 and −0.2 d, respectively, to avoid overlapping error bars.

(Figure 6). In 2012, the Mg content of larvae exposed to pH 7.5 water at the embryo stage was lower than the other two treatments. The Ca:Mg ratio also decreased in acidified water at the embryo stage, and was highest in larvae reared at pH 7.8 during the larval phase (Figure 6). To meet the assumption of homogeneity of variance, the Ca:Mg ratio in 2012 was square-root-transformed, and the 2013 Mg content was log-transformed before analysis.

In 2012, the average larval mass varied among the larval treatments, with those reared in pH 7.8 being highest, pH 7.5 being intermediate, and Ambient being lowest (Figure 7, Supplementary material S4). In 2013, exposure to ambient water at both the embryo and larval stages was associated with higher larval mass (Figure 7).

All data and metadata associated with this project have been archived at the NPRB website (http://project.nprb.org/view.jsp?id=ab9b22fc-3409-4bf9-8d5e-454e28371d7b). Metadata is currently available and data will be publically available after a 2-year embargo period or upon request.

Discussion

Exposure to acidified water had a significant effect on the Tanner crab larvae, and there were substantial carryover effects from

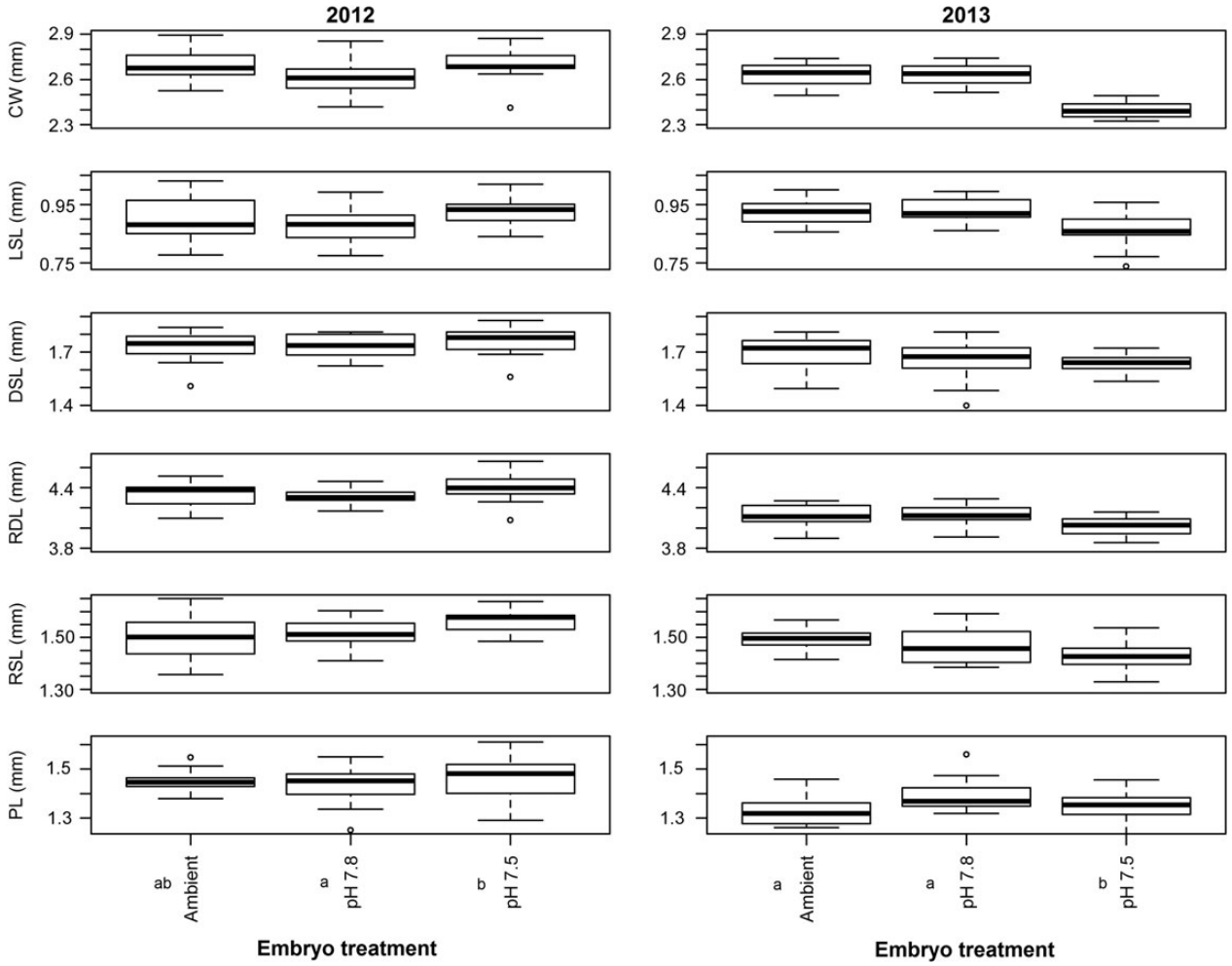

Figure 3. Box-plots of measurements made on larvae in the 2012 and 2013 experiment. Ambient, pH 7.8, and pH 7.5 represent the treatment embryos were reared at. Measurements included CW—carapace width, LSL—lateral spine length, DSL—dorsal spine length, RDL—rostro-dorsal length, RSL—rostral spine length, and PL—protopodite length. Statistical differences within each year are indicated with different letters next to the treatments.

exposure of the females during oogenesis and embryogenesis. Starvation-survival time and morphology of wild-brooded larvae were not affected by low pH water, indicating that they were generally tolerant of the range of pHs in this experiment. However, exposure to low pH water during embryogenesis increased survival time (indicative of decreased metabolism), decreased the calcium content and mass, and changed the morphology of the larvae. Effects were mostly apparent at pH 7.5, indicating that Tanner crab larvae are moderately sensitive to high pCO_2. However, given the presence of carryover effects and the effects high pCO_2 have on other life history stages (Long *et al.*, 2013b; Swiney *et al.*, 2016), high pCO_2 may have a substantial effect on Tanner crab populations, and fisheries, within the next 80 years (Punt *et al.*, 2016).

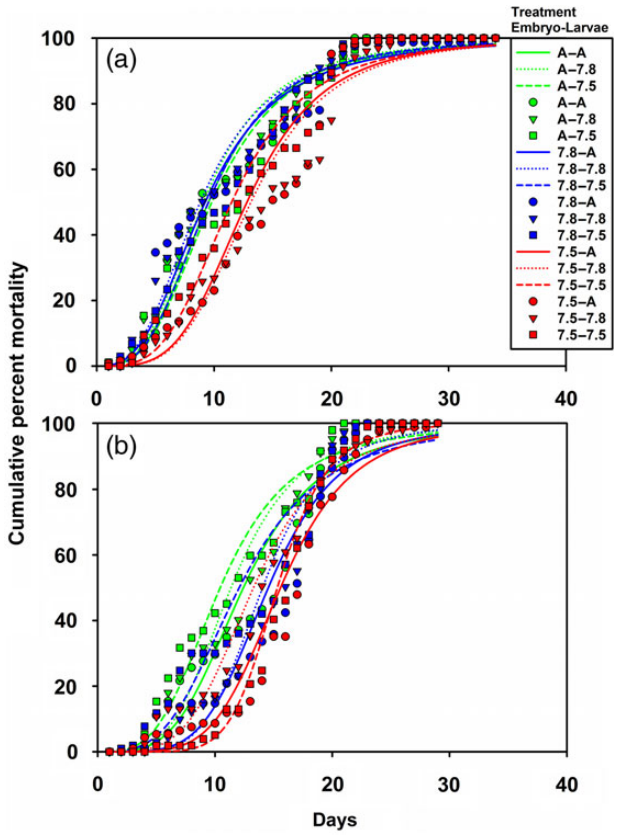

Figure 4. Mortality of Tanner crab larvae during starvation at three pH treatments first as embryos and then as larvae in (a) 2012 and (b) 2013. Points are the average per cent mortality and lines are the best fit logistic regression model for each (see Table 3 for parameter estimates). The treatments are A—Ambient, 7.8—pH 7.8, and 7.5—pH 7.5. For example, A – 7.8 denotes the mortality of larval crab in pH 7.8 water who spent their embryonic stages in Ambient pH water.

Exposure to acidified water at the larval phase had little effect on larvae. We saw no biologically significant differences among larval treatments for the wild-brooded larvae, and only slight (if any) differences in carbon and nitrogen content, calcium or magnesium content, or starvation survival in the lab-brooded larvae. Effect sizes were either small or zero in 2012 and were greater in 2013. The biggest difference was lower calcium content followed by higher per cent carbon and nitrogen contents of pH 7.5 larvae. The higher C and N content may be because in 2013, the pH 7.5 larvae also had a smaller average mass than the other two treatments, indicating that total carbon and nitrogen content per larvae were similar among treatments. Similarly, the mass of embryo porcelain crab, *Petrolisthes cinctipes*, reared under low pH was lower; the per cent carbon was higher leading to almost identical carbon content per embryo (Carter *et al.*, 2013). Of the Tanner crab life history stages tested, including the embryos (Swiney *et al.*, 2016) and juveniles (Long *et al.*, 2013b) both of which exhibited increases in the mortality rate, the larval phase seems the least affected by direct exposure to high pCO_2. Stage-specific sensitivities to ocean acidification are common in crustacean. In *Pe. cinctipes*, acidified water does not affect larval survival, but does decrease juvenile survival (Ceballos-Osuna *et al.*, 2013). The barnacle, *Semibalanus balanoides*, does not show increased mortality at the embryo (Findlay *et al.*, 2009) or the post-larval (Findlay *et al.*, 2010b) stages under acidified conditions, but does at the larval (Findlay *et al.*, 2010a) and adult stages (Findlay *et al.*, 2009). Even different larval phases can differ in sensitivity; *H. araneus* and *Homarus gammarus* larvae are only sensitive at the megalopa stage (Walther *et al.*, 2010; Small *et al.*, 2015). Therefore, insensitivity to acidification at one stage does not imply a general insensitivity throughout an organism's ontogeny. Later larval stages of larval development in Tanner crabs may be more sensitive than the first stage tested here.

Tanner crab larvae may be better adapted to changes in pH than other life history stages because of their natural environment; many species of crustaceans have larvae that are tolerant of low pH (Arnold *et al.*, 2009; Arnberg *et al.*, 2013; Schiffer *et al.*, 2013). The larval phase occurs in the water column during the spring bloom when diel fluctuations in the water pH often high; short-term pH variability is higher during periods of high biological activity (Hofmann *et al.*, 2011, 2015), whereas deeper benthic habitat has less short-term variability (Matson *et al.*, 2014). Many crustacean larvae, including Tanner crab larvae (Wolotira *et al.*, 1990), exhibit diel vertical migration, and there is a large difference in the carbonate chemistry between surface waters and those below the

Table 3. Parameter estimates for logistic regressions on larval survival experiments in 2012 and 2013 graphed in Figure 4.

Embryo	A	A	A	7.8	7.8	7.8	7.5	7.5	7.5
Larvae	A	7.8	7.5	A	7.8	7.5	A	7.8	7.5
2012									
t_{50}	9.52	9.09	9.80	9.24	8.81	9.52	12.80	13.14	11.50
s	−3.13	−3.13	−3.13	−2.86	−2.86	−3.18	−3.93	−3.93	−3.54
2013									
t_{50}	12.42	11.36	10.44	14.54	14.05	12.06	15.58	13.28	15.31
s	−3.81	−4.01	−3.44	−4.86	−5.31	−3.39	−5.10	−4.25	−7.25

Embryo and Larvae indicates the treatments at the embryo and larval stages and include A—Ambient, 7.8—pH 7.8, and 7.5—pH 7.5. The t_{50} parameters have units of days and the s parameters are unitless.

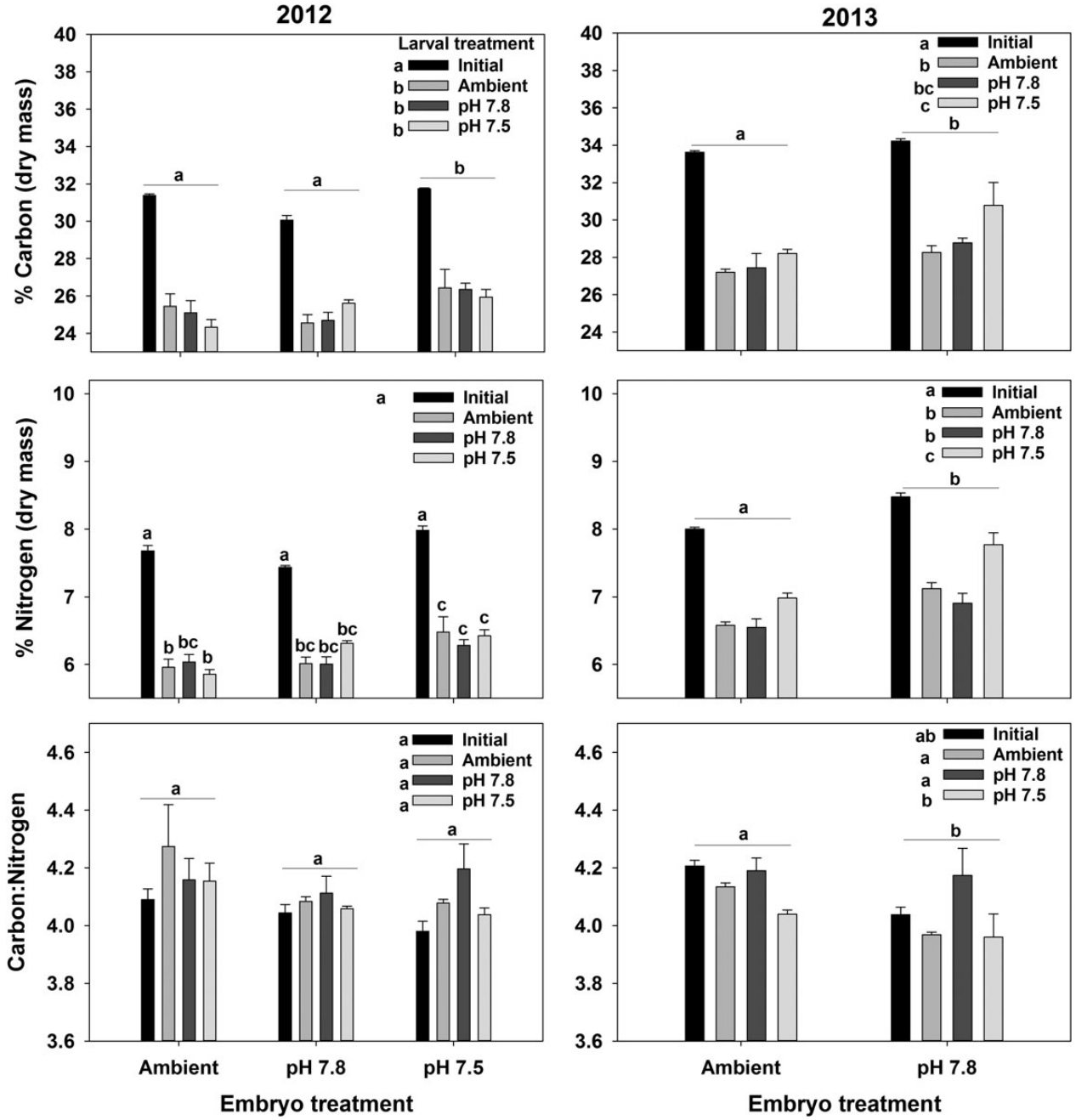

Figure 5. Effects of exposure to acidified water at the embryo and larval stages on carbon (C) and nitrogen (N) content and the C:N ratio in Tanner crab larvae. Bars are the mean + 1 standard error. For the larval treatments, Initial represents C, N, or C:N of the larvae immediately after hatching and Ambient, pH 7.8, and pH 7.5 represent the treatment larvae we held in for 7 d. Statistically significant differences (Tukey's test) among embryo treatments are indicated with letters over groups of bars; differences among Larval treatments are indicated with letters next to the legend. Where there was an interactive effect, difference is indicated with letters over each bar. Results for the 2012 experiments are in the left-side plots and those for the 2013 experiments are on the right-side plots.

mixed layer in the Bering Sea when Tanner larvae are present (Cross *et al.*, 2013). Larval Tanner crabs may therefore be exposed to much higher short-term variability in pH than later benthic phases, and may therefore be better adapted to such pH variability than other stages. Similarly, Styf *et al.* (2013) argued that the insensitivity of *Nephrops norvegicus* embryos to low pH water was an adaptation to the naturally low pH environment in burrows in which the embryos are incubated in the wild.

Carryover effects (sometimes called transgenerational effects) from exposure to low pH during the embryo phase had larger effect sizes on Tanner crab larvae than effects from direct exposure, and carryover effects from maternal exposure during the oogenesis phase increased the effect sizes. Larval morphometry did not differ among larval treatments for wild-brooded larvae; differed statistically, but not biologically, among embryo treatment in 2012; and differed both statistically and biologically among embryo treatment

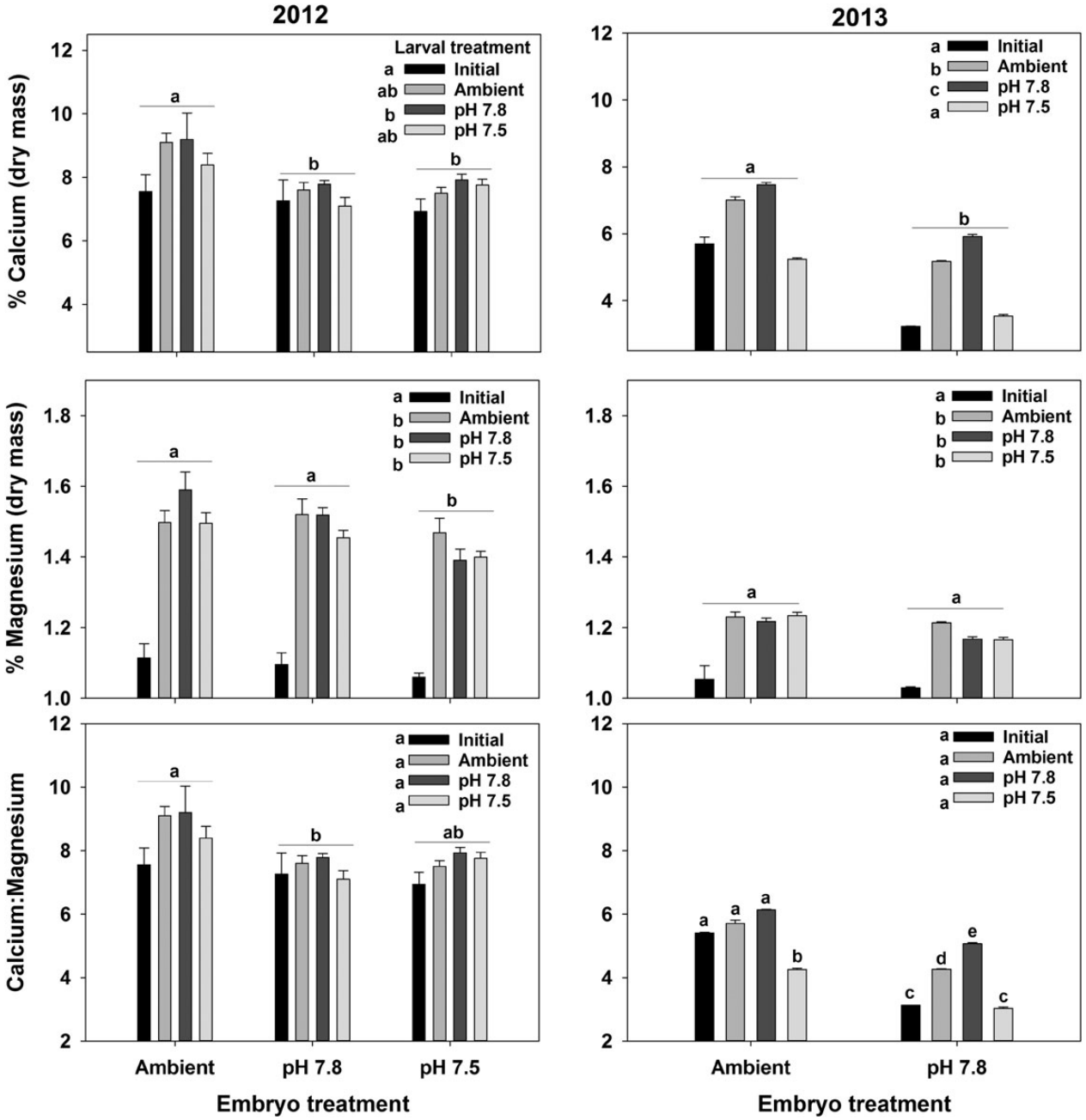

Figure 6. Effects of exposure to acidified water at the embryo and larval stages on calcium and magnesium content and the Ca:Mg ratio in Tanner crab larvae. Bars are the mean + 1 standard error. For the larval treatments, Initial represents the larvae immediately after hatching and Ambient, pH 7.8, and pH 7.5 represent the treatment larvae we held in for 7 d. Statistically significant differences (Tukey's test) among embryo treatments are indicated with letters over groups of bars; differences among Larval treatments are indicated with letters next to the legend. Where there was an interactive effect, difference is indicated with letters over each bar. Results for the 2012 experiments are in the left-side plots and those for the 2013 experiments are on the right-side plots.

in 2013. The direct effects of acidification on Tanner crab embryos were similar (Swiney *et al.*, 2016); differences among pH treatments on embryo development were not biologically significant until 2013. Similarly, the reduction in calcium and magnesium content and the increase in starvation survival time between the Ambient and pH 7.8 embryo treatments were greater in 2013 than in 2012. Because of high mortality at the embryo and pre-zoea stages for the pH 7.5 embryo treatment (Swiney *et al.*, 2016), we cannot explicitly compare these parameters between the years for the pH 7.5 embryo treatment; however, the greater mortality rate of the first larval stage is a clear indication of substantial carryover effects, despite the lack of data on non-lethal effects. Although the larval exposure experiments were of a short duration and a longer exposure time might change the relative importance of direct vs. carryover effect, this does not lessen the import of carryover effects.

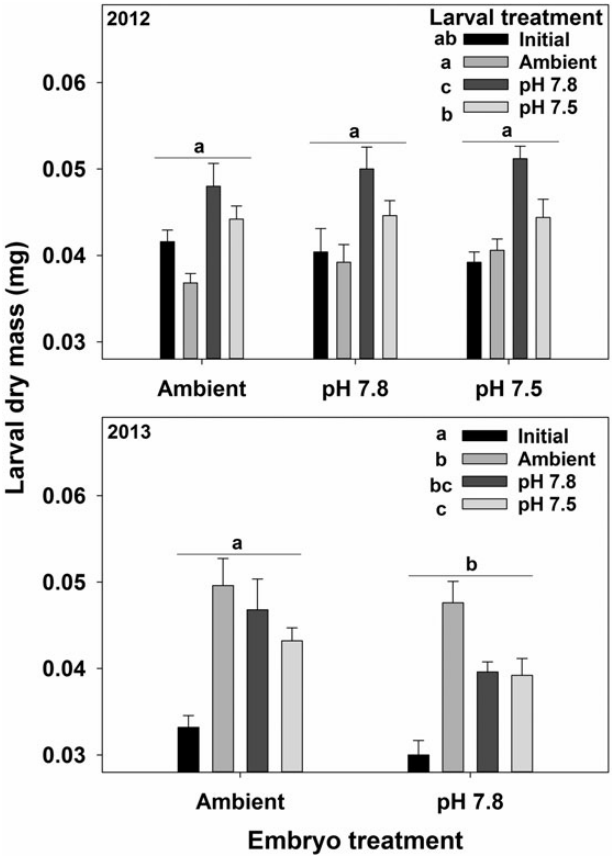

Figure 7. Effects of exposure to acidified water at the embryo and larval stages on the mass of Tanner crab larvae in 2012 and 2013 experiments. Bars are the mean + 1 standard error. For the larval treatments, Initial represents the larvae immediately after hatching and Ambient, pH 7.8, and pH 7.5 represent the treatment larvae we held in for 7 d. Statistically significant differences (Tukey's test) among embryo treatments are indicated with letters over groups of bars; differences among Larval treatments are indicated with letters next to the legend.

These results highlight the cumulative importance of carryover effects throughout the entire life history in determining the overall effects of high pCO_2. In Tanner crabs, larvae experienced negative effects due to exposure at earlier stages. Similarly, Olympic oysters (*O. lurida*) juveniles experience decreased growth as juveniles if exposed to low pH water as larvae (Hettinger *et al.*, 2012) and *H. araneus* larvae had reduced survival following exposure at the embryo stage (Schiffer *et al.*, 2014). In these cases, energetic costs incurred at earlier stages may have reduced later performance. In contrast, in other species, carryover effects ameliorate the effects of ocean acidification. Sydney rock oyster, *Saccostrea glomerata*, larvae have lower survival and growth in acidified water unless their parents are exposed before spawning (Parker *et al.*, 2012); these positive effects extend into adulthood (Parker *et al.*, 2015). Effects may also be mixed and depend on life history stage; maternal exposure to high pCO_2 eliminates negative effects of larval exposure in *Strongylocentrotus droedachiensis*, but larval exposure reduces juvenile survival (Dupont *et al.*, 2013). Ameliorative effects may be a product of physiological plasticity (Dupont *et al.*, 2013; Thor and Dupont, 2015) or increased maternal investment in each offspring (Parker *et al.*, 2012). There is no evidence of positive carryover effects on Tanner crabs in this study though. Many studies fail to account for carryover effects and thus likely underestimate (or overestimate) the cumulative effects of ocean acidification (Hettinger *et al.*, 2013).

Reduced calcium and magnesium content and Ca:Mg ratio at pH 7.5 could affect larval behaviour and survival and is consistent with effects on mature females (Swiney *et al.*, 2016), and juveniles (Long *et al.*, 2013b), and with effects on larvae of other species, such as the European lobster, *Ho. gammarus* (Arnold *et al.*, 2009; Small *et al.*, 2015) and spider crab, *H. araneus* (Walther *et al.*, 2011). Where effect size differs among larval stages, the megalopa stage, which is typically more calcified than earlier stages (Anger, 2001), is the most likely to show effects (Arnold *et al.*, 2009; Walther *et al.*, 2011; Small *et al.*, 2015). Tanner crab larvae from embryos reared at pH 7.8 and 7.5 hatched with lower calcium contents than those reared at Ambient pH and larvae held at pH 7.5 did not accumulate any additional calcium over the first 7 d, whereas larvae at pH 7.8 and Ambient pH did accumulate calcium. Lower calcium content in larvae likely decreases the hardness of their cuticle. This could lead to increased vulnerability to predators (Amaral *et al.*, 2012); a small change in prey vulnerability (Long *et al.*, 2008) can substantially increase predation (Long and Seitz, 2008) and decrease population size (Long *et al.*, 2014). Reduced hardness in the cuticle could lead also to a decreased capacity to masticate food, which could reduce larval survival. Although a lower Ca:Mg ratio is associated with stronger calcite (Magdans and Gies, 2004), any increase in hardness from this is unlikely to compensate for the reduction in the overall Ca and Mg content. Also, although later larval stages might be able to "catch-up" to ambient larvae in terms of calcium content (Walther *et al.*, 2011), there would still be a period of increase vulnerability from low calcium levels. The effects at pH 7.8 are interesting. Exposure at the larval stage increased calcium content (trend in 2012, statistically in 2013), while exposure at the embryo stage decreased calcium content. At pH 7.8, red king crab larvae also exhibited increased calcium content (Long *et al.*, 2013a). Although such dome-shaped response, with highest calcification levels at intermediate pHs, occurs in other taxa (Ries *et al.*, 2009), this is the first time, to our knowledge, that it has been observed in a crustacean.

The carbon and nitrogen contents and larval size indicate that ocean acidification has a complex effect on larval development and energetics. At hatching, larvae exposed to low pH as embryos had a smaller size but a higher per cent carbon and nitrogen content. Similarly, just before hatching, embryos held in low pH were smaller, but had larger yolks (Swiney *et al.*, 2016). Embryos might have developed more slowly at low pH, similar to barnacle embryos (Findlay *et al.*, 2009), and this might affect the hatching size and elemental composition of the larvae. A larger hatch size could have a positive effect; larger *Chasmagnathus granulate* larvae had a shorter developmental time than smaller ones (Giménez *et al.*, 2004). One aspect of carbon and nitrogen metabolism that we did not observe was an increase in protein metabolism under reduced pH. Larval *Ho. gammarus* (Small *et al.*, 2015), *H. araneus* (Walther *et al.*, 2010), and *Pe. cinctipes* (Carter *et al.*, 2013) all increased protein metabolism as evidenced by increased C:N ratios under acidified conditions. However, this is not a universal response; larval red king crab, *P. camtschaticus*, do not increase protein metabolism at reduced pH (Long *et al.*, 2013a).

The starvation survival time increased with decreasing pH. Larval starvation survival times are primarily a function of the energetic reserves at hatching and the metabolic rate after hatching (Hunter, 1981). At hatching, the total (not per cent) carbon and

nitrogen content of the larvae were similar among embryo treatments, indicating similar lipid and protein reserves (Anger and Harms, 1990). After 7 d of starvation, Ambient larvae had a larger decrease in both carbon and nitrogen content than larvae held in low pH water in 2013. Under starvation conditions, crustacean larvae typically use lipid reserves (carbon) for energy first and then protein (nitrogen) (Anger, 2001). This suggests that larvae held under acidified conditions have a lower metabolic rate than those under Ambient conditions, and that after 7 d, Ambient larvae had depleted their lipid reserves and were metabolizing proteins. Lower metabolism in larvae held in acidified conditions would lead to an increase in their survival time. Metabolic depression is a common response to ocean acidification among many taxa, including crustacean, likely because it reduces hemolymph and intracellular acidity by reducing CO_2 production from respiration (Small *et al.*, 2010; Carter *et al.*, 2013; Schiffer *et al.*, 2014). Although it does, as in this case, increase survival time under starvation conditions, it can have negative consequences for growth (Carter *et al.*, 2013) and therefore (in mature animals) reproduction (Swiney *et al.*, 2012). This increase in starvation survival time and decrease in metabolism contrasts with the response of other crustaceans. Larval *Ho. gammarus* (Small *et al.*, 2015) and (during molting) *H. araneus* (Schiffer *et al.*, 2013) both increase metabolism in acidified water. Larval *P. camtschaticus* under acidified conditions had a decreased starvation survival time and a faster depletion of carbon reserves, indicating a higher metabolism (Long *et al.*, 2013a).

These results, when combined with those on other life history stages, suggest that the effects of ocean acidification on the Tanner crab population and fishery are likely to be felt within 80 years. Although the direct effects on larvae were relatively slight, effects on embryos, juveniles, and adults are larger (Long *et al.*, 2013b; Swiney *et al.*, 2016). Further, strong carryover effects on the larval stage from earlier stages suggest carryover effects occur at later stages (juvenile and adult) and may be magnified by increased exposure time. Mortality at the juvenile, and to a lesser extent, the embryo stages was significantly higher at pH 7.8, and even higher at pH 7.5, compared with Ambient pH. This is predicted to cause a decrease in the Tanner crab population and fishery before the end of the century (Punt *et al.*, 2016).

A number of questions on the effects of ocean acidification on Tanner crabs remain unanswered. The gradual change in pH over decades may allow evolutionary adaptation. Even at the lowest pH tested, pH 7.5, some larvae, embryos, and juveniles survived and grew, indicating variability in the individual tolerances for low pH (Long *et al.*, 2013a, b; Meseck *et al.*, 2015; Swiney *et al.*, 2016) and the potential for natural selection to allow adaptation to acidified conditions (Reusch, 2014). Indirect effects, such as changes in predation on Tanner crabs or in their ability to feed, may alter the net effect of ocean acidification. Other stressors, such as increasing temperatures, may interact with ocean acidification (Breitburg *et al.*, 2015). Further research is necessary to inform policy-makers of the likely effects that ocean acidification will have on this commercial species and the best management steps to protect this resource.

Supplementary data

Supplementary material is available at the *ICESJMS* online version of the manuscript.

Acknowledgements

This project was funded by the North Pacific Research Board (NPRB publication no. 537) and the National Marine Fisheries Service (NMFS). We thank NMFS biologists and laboratory technicians for their assistance which made this project possible. Previous versions of this paper were improved by comments from J. Napp, C. Ryer, J. Long, and four anonymous reviewers. The findings and conclusions in the paper are those of the authors and do not necessarily represent the views of the National Marine Fisheries Service, NOAA. Reference to trade names does not imply endorsement by the National Marine Fisheries Service, NOAA.

References

Agnalt, A. L., Grefsrud, E. S., Farestveit, E., Larsen, M., and Keulder, F. 2013. Deformities in larvae and juvenile European lobster (*Homarus gammarus*) exposed to lower pH at two different temperatures. Biogeosciences, 10: 7883–7895.

Amaral, V., Cabral, H. N., and Bishop, M. J. 2012. Effects of estuarine acidification on predator–prey interactions. Marine Ecology Progress Series, 445: 117–127.

Anger, K. 2001. The Biology of Decapod Crustacean Larvae. A.A. Balkema Publishers, Lisse.

Anger, K., and Harms, J. 1990. Elemental (CHN) and proximate biochemical composition and decapod crustacean larvae. Comparative Biochemistry and Physiology B: Comparative Biochemistry, 97: 69–80.

Arnberg, M., Calosi, P., Spicer, J. I., Tandberg, A. H. S., Nilsen, M., Westerlund, S., and Bechmann, R. K. 2013. Elevated temperature elicits greater effects than decreased pH on the development, feeding and metabolism of northern shrimp (*Pandalus borealis*) larvae. Marine Biology, 160: 2037–2048.

Arnold, K. E., Findlay, H. S., Spicer, J. I., Daniels, C. L., and Boothroyd, D. 2009. Effect of CO_2-related acidification on aspects of the larval development of the European lobster, *Homarus gammarus* (L.). Biogeosciences, 6: 1747–1754.

Breitburg, D. L., Salisbury, J., Bernhard, J. M., Cai, W-J., Dupont, S., Doney, S. C., Kroeker, K. J., *et al.* 2015. And on top of all that... coping with ocean acidification in the midst of many stressors. Oceanography, 28: 48–61.

Burnham, K. P., and Anderson, D. R. 2002. Model Selection and Multimodel Inference: a Practical Information-Theoretic Approach. Springer Science + Business Media, New York.

Caldeira, K., and Wickett, M. E. 2003. Anthropogenic carbon and ocean pH. Nature, 425: 365.

Carter, H. A., Ceballos-Osuna, L., Miller, N. A., and Stillman, J. H. 2013. Impact of ocean acidification on metabolism and energetics during early life stages of the intertidal porcelain crab *Petrolisthes cinctipes*. The Journal of Experimental Biology, 216: 1412–1422.

Ceballos-Osuna, L., Carter, H. A., Miller, N. A., and Stillman, J. H. 2013. Effects of ocean acidification on early life-history stages of the intertidal porcelain crab *Petrolisthes cinctipes*. The Journal of Experimental Biology, 216: 1405–1411.

Clarke, K. R., and Warwick, R. M. 2001. Change in Marine Communities: an Approach to Statistical Analysis and Interpretation, 2nd edn. Plymouth Marine Laboratory, PRIMER-E, Plymouth, UK.

Cross, J. N., Mathis, J. T., Bates, N. R., and Byrne, R. H. 2013. Conservative and non-conservative variations of total alkalinity on the southeastern Bering Sea shelf. Marine Chemistry, 154: 100–112.

Dupont, S., Dorey, N., Stumpp, M., Melzner, F., and Thorndyke, M. 2013. Long-term and trans-life-cycle effects of exposure to ocean acidification in the green sea urchin *Strongylocentrotus droebachiensis*. Marine Biology, 160: 1835–1843.

Evans, W., Mathis, J. T., and Cross, J. N. 2014. Calcium carbonate corrosivity in an Alaskan inland sea. Biogeosciences, 11: 365–379.

Fabry, V. J., McClintock, J. B., Mathis, J. T., and Grebmeier, J. M. 2009. Ocean acidification at high latitudes: the bellweather. Oceanography, 22: 160–171.

Fabry, V. J., Seibel, B. A., Feely, R. A., and Orr, J. C. 2008. Impacts of ocean acidification on marine fauna and ecosystem processes. ICES Journal of Marine Science, 65: 414–432.

Findlay, H. S., Burrows, M. T., Kendall, M. A., Spicer, J. I., and Widdicombe, S. 2010a. Can ocean acidification affect population dynamics of the barnacle *Semibalanus balanoides* at its southern range edge? Ecology, 91: 2931–2940.

Findlay, H. S., Kendall, M. A., Spicer, J. I., and Widdicombe, S. 2009. Future high CO_2 in the intertidal may compromise adult barnacle *Semibalanus balanoides* survival and embryonic development rate. Marine Ecology Progress Series, 389: 193–202.

Findlay, H. S., Kendall, M. A., Spicer, J. I., and Widdicombe, S. 2010b. Relative influences of ocean acidification and temperature on intertidal barnacle post-larvae at the northern edge of their geographic distribution. Estuarine Coastal and Shelf Science, 86: 675–682.

Giménez, L., Anger, K., and Torres, G. 2004. Linking life history traits in successive phases of a complex life cycle: effects of larval biomass on early juvenile development in an estuarine crab, *Chasmagnathus granulata*. Oikos, 104: 570–580.

Gnaiger, E., and Bitterlich, G. 1984. Proximate biochemical composition and caloric content calculated from elemental CHN analysis: a stoichiometric concept. Oecologia, 62: 289–298.

Haynes, E. 1973. Descriptions of prezoeae and stage I zoeae of *Chionoecetes bairdi* and *C. opilio* (Oxyrhyncha, Oregoniinae). Fishery Bulletin, 71: 769–775.

Hettinger, A., Sanford, E., Hill, T. M., Lenz, E. A., Russell, A. D., and Gaylord, B. 2013. Larval carry-over effects from ocean acidification persist in the natural environment. Global Change Biology, 19: 3317–3326.

Hettinger, A., Sanford, E., Hill, T. M., Russell, A. D., Sato, K. N. S., Hoey, J., Forsch, M., *et al.* 2012. Persistent carry-over effects of planktonic exposure to ocean acidification in the Olympia oyster. Ecology, 93: 2758–2768.

Hofmann, G., Kelley, A. L., Shaw, E. C., Martz, T. R., and Hofmann, G. E. 2015. Near-shore Antarctic pH variability has implications for the design of ocean acidification experiments. Scientific Reports, 5: 9.

Hofmann, G. E., Smith, J. E., Johnson, K. S., Send, U., Levin, L. A., Micheli, F., Paytan, A., *et al.* 2011. High-frequency dynamics of ocean pH: a multi-ecosystem comparison. PloS ONE, 6: e28983.

Hunter, J. R. 1981. Feeding ecology and predation of marine fish larvae. *In* Marine Fish Larvae: Morphology, Ecology, and Relation to Fisheries, pp. 33–77. Ed. by R. Lasker. University of Washington, Seattle, WA.

Incze, L. S., Armstrong, D. A., and Wencker, D. L. 1982. Rates of development and growth of larvae of *Chionoecetes bairdi* and *C. opilio* in the southeastern Bering Sea. *In* Proceedings of the International Symposium on the Genus *Chionoecetes*, 3rd edn, pp. 191–218. Ed. by A. J. Paul, F. Gaffney, D. Haapa, J. Reeves, R. Baglin, and S. K. Davis. Alaska Sea Grant College Program, University of Alaska Fairbanks, Anchorage, AK.

Keppel, E. A., Scrosati, R. A., and Courtenay, S. C. 2012. Ocean acidification decreases growth and development in American lobster (*Homarus americanus*) larvae. Journal of Northwest Atlantic Fishery Science, 44: 61–66.

Kurihara, H., Matsui, M., Furukawa, H., Hayashi, M., and Ishimatsu, A. 2008. Long-term effects of predicted future seawater CO_2 conditions on the survival and growth of the marine shrimp *Palaemon pacificus*. Journal of Experimental Marine Biology and Ecology, 367: 41–46.

Lavigne, H., and Gattuse, J. 2012. Seacarb: Seawater Carbonate Chemistry with R. R package version 2.4.6 edn. http://CRAN.R-project.org/package=seacarb.

Long, W. C. 2016. A new quantitative model of multiple transitions between discrete stages, applied to the development of crustacean larvae. Fishery Bulletin, 114: 58–66.

Long, W. C., Brylawski, B. J., and Seitz, R. D. 2008. Behavioral effects of low dissolved oxygen on the bivalve *Macoma balthica*. Journal of Experimental Marine Biology and Ecology, 359: 34–39.

Long, W. C., and Seitz, R. D. 2008. Trophic interactions under stress: hypoxia enhances foraging in an estuarine food web. Marine Ecology Progress Series, 362: 59–68.

Long, W. C., Seitz, R. D., Brylawski, B. J., and Lipcius, R. N. 2014. Individual, population, and ecosystem effects of hypoxia on a dominant benthic bivalve in Chesapeake Bay. Ecological Monographs, 84: 303–327.

Long, W. C., Swiney, K. M., and Foy, R. J. 2013a. Effects of ocean acidification on the embryos and larvae of red king crab, *Paralithodes camtschaticus*. Marine Pollution Bulletin, 69: 38–47.

Long, W. C., Swiney, K. M., Harris, C., Page, H. N., and Foy, R. J. 2013b. Effects of ocean acidification on juvenile red king crab (*Paralithodes camtschaticus*) and Tanner crab (*Chionoecetes bairdi*) growth, condition, calcification, and survival. PLoS ONE, 8: e60959.

Magdans, U., and Gies, H. 2004. Single crystal structure analysis of sea urchin spine calcites: systematic investigations of the Ca/Mg distribution as a function of habitat of the sea urchin and the sample location in the spine. European Journal of Mineralogy, 16: 261.

Mathis, J. T., Cross, J. N., Evans, W., and Doney, S. C. 2015. Ocean acidification in the surface waters of the Pacific–Arctic boundary regions. Oceanography, 28: 122–135.

Mathis, J. T., Cross, J. N., Monacci, N., Feely, R. A., and Stabeno, P. 2014. Evidence of prolonged aragonite undersaturations in the bottom waters of the southern Bering Sea shelf from autonomous sensors. Deep Sea Research II: Topical Studies in Oceanography, 109: 125–133.

Matson, P. G., Washburn, L., Martz, T. R., and Hofmann, G. E. 2014. Abiotic versus biotic drivers of ocean pH variation under fast sea ice in McMurdo Sound, Antarctica. PLoS ONE, 9: 12.

Meseck, S. L., Alix, J. H., Swiney, K. M., Long, W. C., Wikfors, G. H., and Foy, R. J. 2015. Ocean acidification affects hemocyte physiology in the Tanner crab (Chionoecetes bairdi). PLoS ONE, in press.

Munk, J. E., Payne, S. A., and Stevens, B. G. 1996. Timing and duration of the mating and molting season for shallow water tanner crab (*Chionoecetes bairdi*). *In* High Latitude Crabs: Biology, Management and Economics, 13th edn, p. 341. Ed. by B. Baxter, W. E. Donaldson, A. J. Paul, R. S. Otto, and D. B. Witherell. Alaska Sea Grant College Program, University of Alaska Fairbanks, Anchorage, AK.

NPFMC. 2011. Stock assessment and fishery evaluation report for the king and Tanner crab fisheries of the Bering Sea and Aleutian Islands regions. 677 pp.

Parker, L. M., O'Connor, W. A., Raftos, D. A., Pörtner, H-O., and Ross, P. M. 2015. Persistence of positive carryover effects in the oyster, *Saccostrea glomerata*, following transgenerational exposure to ocean acidification. PLoS ONE, 10: e0132276.

Parker, L. M., Ross, P. M., O'Connor, W. A., Borysko, L., Raftos, D. A., and Pörtner, H. O. 2012. Adult exposure influences offspring response to ocean acidification in oysters. Global Change Biology, 18: 82–92.

Paul, A. J., and Adams, A. E. 1984. Breeding and fertile period for female *Chionoecetes bairdi* (Decapoda, Majidae). Journal of Crustacean Biology, 4: 589–594.

Punt, A. E., Foy, R. J., Dalton, M. G., Long, W. C., and Swiney, K. M. 2016. Effects of long term exposure to ocean acidification on future southern Tanner crab (Chionoecetes bairdi) fisheries management. ICES Journal of Marine Science, 73: 849–864.

Reusch, T. B. H. 2014. Climate change in the oceans: evolutionary versus phenotypically plastic responses of marine animals and plants. Evolutionary Applications, 7: 104–122.

Ries, J. B., Cohen, A. L., and McCorkle, D. C. 2009. Marine calcifiers exhibit mixed responses to CO_2-induced ocean acidification. Geology, 37: 1131–1134.

Schiffer, M., Harms, L., Portner, H., Lucassen, M., Mark, F. C., and Storch, D. 2013. Tolerance of *Hyas araneus* zoea I larvae to elevated seawater PCO_2 despite elevated metabolic costs. Marine Biology, 160: 1943–1953.

Schiffer, M., Harms, L., Pörtner, H., Mark, F., and Storch, D. 2014. Pre-hatching seawater pCO_2 affects development and survival of

zoea stages of Arctic spider crab *Hyas araneus*. Marine Ecology Progress Series, 501: 127–139.

Small, D., Calosi, P., White, D., Spicer, J. I., and Widdicombe, S. 2010. Impact of medium-term exposure to CO_2 enriched seawater on the physiological functions of the velvet swimming crab *Necora puber*. Aquatic Biology, 10: 11–21.

Small, D. P., Calosi, P., Boothroyd, D., Widdicombe, S., and Spicer, J. I. 2015. Stage-specific changes in physiological and life-history responses to elevated temperature and Pco_2 during the larval development of the European lobster *Homarus gammarus* (L.). Physiological and Biochemical Zoology, 88: 494–507.

Styf, H. K., Skold, H. N., and Eriksson, S. P. 2013. Embryonic response to long-term exposure of the marine crustacean *Nephrops norvegicus* to ocean acidification and elevated temperature. Ecology and Evolution, 3: 5055–5065.

Swiney, K. M. 2008. Egg extrusion, embryo development, timing and duration of eclosion, and incubation period of primiparous and multiparous tanner crabs (*Chionoecetes bairdi*). Journal of Crustacean Biology, 28: 334–341.

Swiney, K. M., Long, W. C., Eckert, G. L., and Kruse, G. H. 2012. Red king crab, *Paralithodes camtschaticus*, size–fecundity relationship, and inter-annual and seasonal variability in fecundity. Journal of Shellfish Research, 31: 925–933.

Swiney, K. M., Long, W. C., and Foy, R. J. 2016. Effects of high pCO_2 on Tanner crab reproduction and early life history, Part I: long-term exposure reduces hatching success and female calcification, and alters embryonic development. ICES Journal of Marine Science, 73: 825–835.

Thor, P., and Dupont, S. 2015. Transgenerational effects alleviate severe fecundity loss during ocean acidification in a ubiquitous planktonic copepod. Global Change Biology, 21: 2261–2271.

Walther, K., Anger, K., and Portner, H. O. 2010. Effects of ocean acidification and warming on the larval development of the spider crab *Hyas araneus* from different latitudes (54 degrees vs. 79 degrees N). Marine Ecology Progress Series, 417: 159–170.

Walther, K., Sartoris, F. J., and Portner, H. 2011. Impacts of temperature and acidification on larval calcium incorporation of the spider crab *Hyas araneus* from different latitudes (54 degrees vs. 79 degrees N). Marine Biology, 158: 2043–2053.

Webb, J. B., Eckert, G. L., Shirley, T. C., and Tamone, S. L. 2006. Changes in zoeae of the snow crab, *Chionoecetes opilio*, with variation in incubation temperature. Journal of Experimental Marine Biology and Ecology, 339: 96–103.

Wittmann, A. C., and Pörtner, H. O. 2013. Sensitivities of extant animal taxa to ocean acidification. Nature Climate Change, 3: 995–1001.

Wolotira, R. J., Bowerman, J. H., and Munk, E. 1990. Distribution and abundance of decapod larvae of the Kodiak shelf. Outer Continental Shelf Environmental Assessment Program: Final Reports of Principal Investigators, 67: 463.

Handling editor: C. Brock Woodson

ICES Journal of Marine Science

ICES Journal of Marine Science (2016), 73(3), 849–864. doi:10.1093/icesjms/fsv205

Contribution to Special Issue: 'Towards a Broader Perspective on Ocean Acidification Research'

Original Article

Effects of long-term exposure to ocean acidification conditions on future southern Tanner crab (*Chionoecetes bairdi*) fisheries management

André E. Punt[1]*, Robert J. Foy[2], Michael G. Dalton[2], W. Christopher Long[2], and Katherine M. Swiney[2]

[1]*School of Aquatic and Fishery Sciences, University of Washington, PO Box 355020, Seattle, WA 98195, USA*
[2]*Alaska Fisheries Science Center, National Marine Fisheries Service, NOAA, 7600 Sand Way Point Way, NE, Seattle, WA 98115, USA*

**Corresponding author: tel: +1 206 2216319; fax: +1 206 6857471; e-mail: aepunt@uw.edu*

Punt, A. E., Foy, R. J., Dalton, M. G., Long, W. C., and Swiney, K. M. Effects of long-term exposure to ocean acidification conditions on future southern Tanner crab (*Chionoecetes bairdi*) fisheries management. – ICES Journal of Marine Science, 73: 849–864.

Received 18 June 2015; revised 16 October 2015; accepted 17 October 2015; advance access publication 6 November 2015.

Demographic models of pre- and post-recruitment population dynamics were developed to account for the effects of ocean acidification on biological parameters that affect southern Tanner crab (*Chionoecetes bairdi*) larval hatching success and larval and juvenile survival. Projections of stock biomass based on these linked models were used to calculate biological and economic reference points on which fisheries management advice is based and thus provide fisheries managers with strategic advice on the likely long-term consequences of ocean acidification. The models utilized information for southern Tanner crab in the eastern Bering Sea. This information included the monitoring data on which conventional size-structured stock assessments are based, as well as the functional relationships that determine survival based on experiments that evaluated the consequences of ocean acidification over the next 100–200 years on crab larval hatching success, larval survival, and the survival of juvenile crab. The results highlighted that juvenile survival had the largest effect (~20% decrease over 75 years) on biological and economic reference points, while hatching success, particularly if density dependence occurs after hatching, and larval survival have smaller effects (<10% decrease). Catch and profits would be expected to decrease by >50% in 20 years if natural mortality is affected by ocean acidification. Additional laboratory data on oocyte and embryo development leads to large changes in biological reference points depending on the timing of ocean acidification effects relative to natural mortality. The results highlight the need for experiments to evaluate the longer term physiological effects of ocean acidification on multiple life history stages and to measure indices that directly inform population dynamics models to evaluate future management scenarios.

Keywords: *Chionoecetes bairdi*, North Pacific, ocean acidification, southern Tanner crab, stock assessment.

Introduction

Ocean acidification is the change in seawater chemistry due to increases in dissolved anthropogenic CO_2 that has already reduced the mean global ocean surface water pH by 26% (0.1 pH units) below preindustrial levels (Caldeira and Wickett, 2003; Orr *et al.*, 2005). The reduction in pH leads to a decrease in the depth below which calcium carbonate will dissolve. The increased difficulty in precipitating calcium carbonate may negatively affect the formation of shells and support structures by some calcifying organisms such as crustaceans (Caldeira and Wickett, 2003; Feely *et al.*, 2004; Orr *et al.*, 2005), in addition to affecting their physiology and acid–base balance (e.g. Spicer *et al.*, 2007; Small *et al.*, 2010). Southern Tanner crab, *Chionoecetes bairdi*, are ecologically and commercially important crustaceans that inhabit the North Pacific shelf where the saturation depth of calcium carbonate is already relatively shallow without the added effects of ocean acidification (Doney *et al.*, 2009). Laboratory studies found that the condition, shell calcification, and in particular, survival of southern Tanner crab were negatively affected by average global levels of ocean acidification conditions expected by the year 2200 (Long *et al.*, 2013, This volume; Swiney *et al.*, This volume). In particular, these studies found that incorporating long-term exposure to

increased pCO_2 (and subsequent decreased pH) during oocyte development compounded the effects of ocean acidification in later stages. The population level effects of decreased individual survival on the biological reference points used to manage crab stocks in Alaska, and the sensitivity of those reference points to short- vs. long-term experimental results are, however, unknown.

Ocean acidification may have significant effects on the development of marine invertebrate embryos (Kurihara *et al.*, 2004a, b; Findlay *et al.*, 2009; Parker *et al.*, 2009) and larvae (Kurihara *et al.*, 2007; Dupont *et al.*, 2008; Talmage and Gobler, 2009). Southern Tanner crab larvae (known as zoea) hatch at depth after an ~12-month brooding period and live pelagically in surface waters before settling to the benthos during the megalopa stage and molting to the juvenile stage. In the Gulf of Alaska, juvenile female southern Tanner crab are found in shallow water (<13 m) before their molt to maturity (Stevens *et al.*, 1993), and adult females aggregate in deeper water (~150 m) (Stevens *et al.*, 1993). Adult southern Tanner crab in the eastern Bering Sea are found at depths from 18 to 440 m. As such, the different life stages of southern Tanner crab are exposed to variable ocean acidification conditions, ranging from surface waters exposed to anthropogenic-driven changes in ocean pH to waters undersaturated in $CaCO_3$ at depth.

The effects of decreased ocean pH on southern Tanner crab were assessed during short- and long-term laboratory experiments conducted from 2011 to 2013 where developing oocytes, embryos, and larvae were reared in one of three pH treatments to simulate current and expected average global conditions in approximately 2100 and 2200 (Swiney *et al.*, this volume; Long *et al.*, this volume). Three experiments were conducted where (i) oocyte and embryo development occurred *in situ* while larvae were in treatments, (ii) oocytes developed *in situ* but embryos and larvae developed in laboratory treatment conditions, and (iii) oocytes, embryos, and larvae were developed in laboratory treatment conditions. Larvae were exposed to the same three pH treatments in a fully crossed experimental design to examine starvation survival, morphology, condition, and calcium/magnesium content. Embryo development in ambient and pH 7.8 treatments differed from the pH 7.5 treatment in both years. Hatching success was much lower for embryos that were exposed during both oogenesis and embryogenesis. At the larval stage, effects were also substantially greater for larvae exposed to more acidified conditions during oogenesis and embryogenesis. Larval crab differed morphometrically, were smaller, and had lower calcium and magnesium contents (Swiney *et al.*, This volume; Long *et al.*, This volume).

Crab, including southern Tanner crab, contributes substantially to the revenue generated by the fisheries off Alaska, USA. Alaska crab stocks are jointly managed by the North Pacific Fishery Management Council (NPFMC) and the Alaska Department of Fish and Game (ADFG). The NPFMC makes recommendations for the overfishing level (OFL) and the acceptable biological catch (ABC) for each crab stock, while the State of Alaska makes decisions on total allowable catches (TACs), which have to be less than the ABCs. The OFLs are set using a tier system that includes five tiers depending on data availability, and the ability to estimate key stock assessment parameters (NPFMC, 2008). The scientific basis for setting of OFLs, ABCs, and TACs derive from quantitative stocks assessments. For the more data-rich crab stocks, including southern Tanner crab in the eastern Bering Sea, these assessments are based on fitting sex- and size-structured population dynamics models to monitoring data from the fishery and surveys (e.g. NPFMC, 2014). These assessments provide estimates of key biological reference points such as the fishing mortality rate at which mature male-per-recruit is reduced to 35% of its unfished level, $F_{35\%}$, and the proxy for the biomass at which MSY is achieved, B_{MSY} (NPFMC, 2008). These biological reference points are then used in the control rules for calculating the OFL.

Increasingly, management bodies are using economic information to make decisions regarding management practices and reference points (e.g. Kompas *et al.*, 2010; Punt *et al.*, 2012, 2014a). While reference points and OFLs for Alaska crab stocks are still currently based on biological considerations only, the selection of the buffer between the OFL and ABC for these stocks takes economic as well as biological information into account (Punt *et al.*, 2012). The changes in population dynamics due to ocean acidification conditions will likely have biological and economic consequences.

The overall goal of this study was to incorporate laboratory results on crab mortality associated with decreased ocean pH into existing stock assessment models to evaluate how ocean acidification conditions can affect the survival of juvenile crab and hence the yield and revenue from the fishery (c.f. Punt *et al.*, 2014b). In contrast, to the earlier modelling work, this study examined the effects of ocean acidification conditions on several life stages and developed models that can represent these effects. In addition, the models were used to examine the sensitivity of quantities of management interest to the increased information on crab mortality gained by conducting long- vs. short-term laboratory experiments (Long *et al.*, This volume; Swiney *et al.*, This volume). Specific objectives included (i) developing a pre-recruitment model for southern Tanner crab, (ii) developing a post-recruitment model for southern Tanner crab, and (iii) informing the pre- and post-recruitment models using laboratory data on crab survival in acidified conditions to predict biological and economic reference points.

Methods

Crab collection and experimental design

Data from short- and long-term experimental results from early life stages (pre-juvenile) exposed to ocean acidification conditions were used to inform the pre-recruitment model. Detailed laboratory experimental design and results can be found in Swiney *et al.* (this volume) and Long *et al.* (this volume). Two collections of mature female Tanner crab were made in May and June 2011 from Chiniak Bay, Kodiak Island, in the Gulf of Alaska and held at the Alaska Fisheries Science Center's (AFSC) Kodiak Laboratory. In the first collection, ovigerous females were collected and larvae hatched immediately. Larvae were randomly assigned to a control or treatment that simulated current (ambient) and predicted future (about 2100 and 2200) ocean pH levels: (i) ambient pH (~8.1), (ii) pH 7.8, and (iii) pH 7.5 (Caldeira and Wickett, 2003). In the second collection, 48 mature female Tanner crab were collected and randomly assigned to the same control and treatments as above. These females were held for 2 years where they were mated with mature males, extruded a new clutch in spring of 2011 and 2012, and each clutch was brooded for ~1 year. Larvae hatched and were collected in spring of 2012 and 2013. Therefore, reproductive development did not occur in treatments for larvae hatched immediately in 2011, only embryo development occurred in treatments for 2012 larvae, and both oocytes and embryo development occurred in acidified treatments for larvae hatched in 2013. Embryological assessment included embryo development, hatching success, and hatch duration. Larval experiments were conducted by isolating five replicates of 20 larvae in containers from a

pool of larvae from multiple adult females within each pH treatment for a fully crossed design between embryo and larval treatments. Larvae were not fed during this starvation experiment and larval response variables included morphology, condition, calcification, and starvation survival.

Data from experimental results from juvenile crab exposed to decreased ocean pH (Long *et al.*, 2013) were used to inform the pre- and post-recruitment models for southern Tanner crab. This experiment was separate from that used to obtain the embryo and larval data. Ninety newly settled juvenile southern Tanner crab (carapace width 2.8–5.2 mm) were collected from Chiniak Bay, Alaska in May 2010 and held at the AFSC's Kodiak Laboratory. Each juvenile crab was randomly assigned to the same pH treatments as described for the pre-juvenile experiments above. During the 199 day experiment, calcification, growth, and survival decreased, while the condition did not change with exposure to lower pH (Long *et al.*, 2013).

Informing pre- and post-recruitment models with experimental results

The pre-recruitment (recruitment is to the range 25–64 mm carapace width (CW), the smallest size included in the post-recruitment model.) model considered 11 pre-recruitment stages: two pelagic larval (zoeal) stages (Z1–Z2), one megalopa settling stage (ME), and eight juvenile benthic instars (C1–C8) (Table 1). Based on laboratory experimental results, ocean acidification conditions were assumed to change the mortality rates for all pre-recruitment stages, except the megalopa stage for which no experimental data were available. The following experimental results were used to inform the pre-recruitment model: hatching success, larval survival during each stage, and juvenile survival during each stage. In contrast, Punt *et al.* (2014b) only considered ocean acidification effects on juvenile survival.

Hatching success was defined as the proportion of embryos that hatch with viable larvae standardized by the total number of larvae hatched under experimental conditions for the treatment groups relative to this proportion for the control group (pH = 8.1).The hatching success for the control group is confounded with average recruitment and density-independent mortality in the model. The model consequently sets hatching success for the control group and density-independent survival to 1, and selects the average recruitment to match the monitoring data. The hatching success for the two treatment levels of pH (7.8 and 7.5) were 0.917 and 0.688 (Swiney *et al.*, This volume). Interpolation of hatching success to other levels of pH was achieved using the simplest equation that has a shape that allows interpolation between pHs of 7.5 and 8.1:

$$H = \left(1 - \alpha_1 \left[\frac{8.1 - \text{pH}}{8.1}\right]^{\alpha_2}\right), \tag{1}$$

where α_1 and α_2 were selected so that the predictions from Equation (1) match the observed hatching successes at pHs of 7.8 and 7.5.

Survival over t days during larval stages (Z1–Z2) was modelled using the equation:

$$S_t = 1 - (1 + \exp(-\beta(t - t_{50})))^{-1}, \tag{2a}$$

where t_{50} is the number of days until half of the larvae die, which is itself a function of pH, i.e.:

$$t_{50} = \gamma_1 \left(1 - \gamma_2 \left[\frac{8.1 - \text{pH}}{8.1}\right]^{\gamma_3}\right), \tag{2b}$$

where γ_1, γ_2, and γ_3 are parameters determining the relationship between t_{50} and pH, and β determines the slope in the logistic curve in Equation (2a). The values for the parameters of Equations (2a) and (2b) were estimated by fitting this model to data from the larval experiments (Figure 5 in Long *et al.*, this volume). This involves maximizing the following likelihood, i.e.:

$$\prod_p \prod_i \left((S_{p,t_{\max}})^{N_{p,i,t_{\max}}} \prod_{t<t_{\max}} (M_{p,t})^{N_{p,i,t}} \right), \tag{3}$$

where $M_{p,t}$ is the probability of a larva dying during day t:

$$M_{p,t} = \begin{cases} 1 - S_{p,1} & \text{if } t = 1 \\ S_{p,t-1} - S_{p,t} & \text{otherwise} \end{cases}, \tag{4}$$

where $S_{p,t}$ is the survival rate over t days during the larval stages when pH is p, and $N_{p,i,t}$ is the observed number of mortalities in container i on day t ($N_{p,t,t_{\max}}$ is the number of animals that were still alive on the last day of the experiment) when pH is p. To test the effects of crab development in acidified treatments and on short- vs. long-term experimentation, four variants of the analysis for the larval data were conducted: (i) 2013 data, basing the analysis on crab that developed entirely in ambient conditions; (ii) 2013 data, basing the analysis on crab that developed in pH 7.8 or 7.5 treatments through oocyte, embryo, and larval development; (iii) same as for (i) except using 2012 data where oocyte development occurred *in situ* (i.e. not in treatment); and (iv) same as for (ii) except using 2012 data.

The data on juvenile survival were analysed using an equation of the form:

$$S_t = \tilde{S}^t, \tag{5a}$$

where $\tilde{S}$ is the daily survival rate, related to pH according to the equation:

$$\tilde{S} = \delta_1 \left(1 - \delta_2 \left[\frac{8.1 - \text{pH}}{8.1}\right]^{\delta_3}\right), \tag{5b}$$

where δ_1, δ_2, and δ_3 are parameters determining the relationship between $\tilde{S}$ and pH. The values for the parameters of Equations

Table 1. Stage durations for southern Tanner crab.

Stage	Duration (Average) (days)	Source
Z1	30	Haynes (1973, 1981), Incze *et al.* (1982)
Z2	30	Haynes (1981), Incze *et al.* (1982)
ME	30 – 180[a]	Jewett and Haight (1977), Incze *et al.* (1982)
C1	21	Donaldson *et al.* (1981)
C2	30	Donaldson *et al.* (1981)
C3	42	Donaldson *et al.* (1981)
C4	51	Donaldson *et al.* (1981)
C5	69	Donaldson *et al.* (1981)
C6	90	Donaldson *et al.* (1981)
C7	120	Donaldson *et al.* (1981)
C8	156	Donaldson *et al.* (1981)

[a]Taken to 105 days for the purposes of this paper.

(5a) and (5b) were estimated by fitting this model to data from juvenile experiments (Figure 3 in Long *et al.*, 2013). The likelihood function maximized to estimate the parameters of Equation (5b) followed Equation (3), except that there was only one container.

Southern Tanner crab pre-recruitment model

As in Punt *et al.* (2014b), a stage-structured population model was used to forecast the changes over time in recruitment to the first size class in the post-recruitment model (25–64 mm CW):

$$\underline{N}_{T+t+1} = G_T \Omega_T \underline{N}_{T+t}, \tag{6}$$

where $\underline{N}_{T+t}$ is the vector of numbers-at-stage at time $T+t$ (all embryos enter the first stage when they are spawned), G_T is the growth transition matrix (i.e. the matrix of probabilities of growing from one stage to each other stage for embryos spawned at time T; consistent with assessments for most crustaceans, the matrix G_T was assumed to be lower triangular, reflecting the assumption that very few animals shrink following moulting), and Ω_T is the survival matrix for embryos spawned at time T. The survival and growth rates for animals spawned at time T until they reach 25–64 mm CW were set to those calculated for time T. This was an adequate approximation given the slow change over time in pH relative to the time between spawning and reaching 25 mm CW (Punt *et al.*, 2014b). The last stage in this model was the first size class in the post-recruitment model. Several crab assessment models allow recruits to enter the model over a range of size classes. However, the size classes selected for the post-recruitment model were chosen to be sufficiently large that all the recruitment occurs to one size class.

The stage with the shortest duration, C1, lasts on average 21 days (Table 1). The time-step for the model (6 days) was set so that the time-step is able to match the lengths of each stage relatively closely (the mortality by stage was allocated equally across the time-steps that constitute a stage, so that the fact that some stages durations were not exact multiples of 6 days is inconsequential). Following Punt *et al.* (2014b), it was assumed that all individuals within a stage were subject to the same survival probability and stage duration, and that individuals must stay in a stage for a defined minimum amount of time before progressing to the next stage. This was achieved by dividing each of the 11 stages into sub-stages where the number of sub-stages was one plus the number of time-steps that an animal needs to remain in a stage.

The matrix $G_T\Omega_T$ determines the combined effects of growth and mortality. This matrix can be written as:

$$G_T\Omega_T = \begin{array}{c} \begin{matrix} \quad & \quad & \quad & \quad & \quad & \quad \end{matrix} \\ \begin{pmatrix} 0 & 0 & 0 & 0 & 0 & \dots \\ S_{1,T} & S_{1,T}(1-P_{1,T}) & 0 & 0 & 0 & \dots \\ 0 & S_{1,T}P_{1,T} & 0 & 0 & 0 & \dots \\ 0 & 0 & S_{2,T} & 0 & 0 & \dots \\ 0 & 0 & 0 & S_{2,T} & S_{2,T}(1-P_{2,T}) & \dots \\ 0 & 0 & 0 & 0 & S_{2,T}P_{2,T} & \dots \\ 0 & 0 & 0 & 0 & 0 & \dots \\ \dots & \dots & \dots & \dots & \dots & \dots \end{pmatrix} \end{array} \tag{7}$$

(−From−) (−From−) (From)
(−Z1−) (−Z2−) (Stages 3 +)

for the case in which animals must stay at least one time-step in Z1 and two time-steps in Z2. The variable $S_{i,T}$ is the probability of survival for stage i for animals spawned at time T, and $P_{i,T}$ is the probability of growing out of stage i for animals spawned at time T.

The values for $S_{i,T}$ and $P_{i,T}$ were solved to match values for expected survival predicted from the functions fitted to the experimental data ($\tilde{S}_{i,T}$) for stage i for embryos spawned at time T and the expected stage duration ($\tilde{d}_i$), which was not affected by ocean acidification. The predicted values for $\tilde{S}_{i,T}$ and $\tilde{d}_i$ for a stage with n sub-stages were (see Appendix A of Punt *et al.*, 2014b):

$$\tilde{S}_{i,T} = \frac{S_{i,T}^{n} P_{i,T}}{1 - S_{i,T}(1 - P_{i,T})}; \quad \tilde{d}_i = \frac{\sum_{y=T}^{T+tt} (y+1) x_{i,y} S_{i,T} P_{i,T}}{\sum_{y=T}^{T+tt} x_{i,y} S_{i,T} P_{i,T}}, \tag{8}$$

where $x_{i,y}$ is the number of animals leaving stage i at time-step y [for stage 1, this would be the numbers entering class 2 in Equation (7)], and tt is the total number of time-steps ($tt \sim 1100$). The values for $\tilde{S}_{i,T}$ were determined from Equations (2a) and (5b) [larvae and juveniles, respectively (The survival rate for megalopa was assumed to be constant, independent of ocean pH, in the absence of data to parameterize a model such as Equation (4).)]. Table 1 lists the values for the stage durations.

Southern Tanner crab post-recruitment model

The dynamics of animals of 25 mm CW and larger (and hence the impacts of the fishery) were modelled using a population dynamics model with an annual time-step, which was a simplification of the current stock assessment model for southern Tanner crab in the eastern Bering Sea (Stockhausen, 2014) in which only males were modelled, fewer size classes were used, and no consideration was taken of shell condition and maturity stage. These simplifications facilitated quicker computations, but do not affect the results markedly as the fishery is only allowed to retain males. Mature male biomass (MMB) at the time of mating (taken to be 15 February) was used as a proxy for fertilized egg production in this model, consistent with how management advice is provided for Bering Sea and Aleutian Islands crab fisheries (NPFMC, 2008). The basic dynamics of the population in the model were:

$$\underline{N}_{y+1} = X S_y \underline{N}_y + \underline{R}_{y+1}, \tag{9}$$

where $\underline{N}_y$ is the vector of numbers-at-stage (males only) at the start of year y, $\mathbf{X}$ is the growth transition matrix (assumed as before to be lower triangular), $\mathbf{S}_y$ is the survival matrix for year y, and $\underline{R}_y$ is the vector of recruits for year y. The matrix $\mathbf{S}_y$ was diagonal with elements:

$$S_{y,i,i} = \mathrm{e}^{-M_y} \prod_{k=1}^{3} (1 - J_{i,k}^{B} F_{y,k}^{B})(1 - J_i^{D} F_y^{D}), \tag{10}$$

where M_y is the instantaneous rate of natural mortality for year y, $J_{i,k}^{B}$ is selectivity due to the kth fleet which takes southern Tanner crab as bycatch on animals in size class i (the fleets are the pot fisheries that target snow crab, *Chionoecetes opilio*, and red king crab, *Paralithodes camtschaticus*, and the pot and trawl fisheries that target groundfish), $F_{y,k}^{B}$ is the proportionate exploitation rate due to kth fleet that takes southern Tanner crab as bycatch during year y, J_i^{D} is selectivity for the directed fishery on animals in size class i, and F_y^{D} is the exploitation rate due to the directed fishery during year y. In model projections, $F_{y,k}^{B}$ in Equation (10) was set to the average exploitation rate over 2008–2012. Future values for F_y^{D} were determined by the scenario under consideration (see below). The products in Equation (10) were constrained to be 1 or less in the projections.

Owing to a minimum size limit, some crabs caught during the directed fishery are discarded. The retained and discarded catch (in mass) by the directed fishery during year y, $\tilde{C}_y^D$, and $\bar{C}_y^D$, were:

$$\tilde{C}_y^D = \sum_i Q_i w_i J_i^D F_y^D N_{y,i} e^{-0.5M_y} = \sum_i w_i \tilde{C}_{y,i}^D, \quad (11a)$$

$$\bar{C}_y^D = \sum_i (1 - Q_i) w_i J_i^D F_y^D N_{y,i} e^{-0.5M_y} = \sum_i w_i \bar{C}_{y,i}^D, \quad (11b)$$

where Q_i is the proportion of crab in size class i that is retained, w_i is the average mass of a male crab in size class i, $N_{y,i}$ is the number of animals in size class i at the start of year y, and the fishery is assumed to take place half way through the model year, which starts on 1 July.

The discard by the fleets that take southern Tanner crab as bycatch was computed under the assumption that the directed and the other fisheries are sequential (the directed fishery has historically occurred over a very short interval whereas the trawl fishery, one of those that takes Tanner crab as bycatch in the Bering sea, occurs essentially throughout the year):

$$\bar{C}_{y,k}^B = \sum_i w_i J_{i,k}^B F_{y,k}^B N_{y,i} e^{-0.5M_y} (1 - J_i^D F_y^D) \prod_{l=1}^{k-1} (1 - J_{i,l}^B F_{y,l}^B) = \sum_i w_i \bar{C}_{y,i}^B. \quad (12)$$

In principle, the trawl fishery could be modelled as occurring over the entire year rather than as a pulse in the middle of the year. However, the catch by the trawl fishery is negligible compared with that by the directed fishery so this complication was ignored here.

Under the assumption that only the directed fishery occurs before mating, and that mating occurs on 15 February of year $y+1$, the mature male biomass for year y, MMB_y, is computed using the equation:

$$MMB_y = \sum_i N_{y,i} f_i e^{-0.75M_y} (1 - J_i^D F_y^D), \quad (13)$$

where f_i is the fecundity of a crab in size class i. Density-dependence was assumed to affect the survival rate of embryos [see Equation (16)] and was modelled based on the mature male biomass at the time of mating for consistency with how management advice is provided and projections conducted for crab stocks in Bering Sea (NPFMC, 2008). Consequently, high values for mature male biomass led to lower survival rates for embryos all other things being equal.

Recruitment only occurred to the first size class in the model (25–64 mm CW). Recruitment during future year y was calculated as the sum of the numbers recruiting during year y based on spawning during years y', where the spawning year ranges from 1 to 10 years before year y.

$$R_y = \phi \sum_{y'=y-10}^{y-1} \kappa_{y'} f(\omega_{y'} MMB_{y'}) G(y', y), \quad (14)$$

where $G(y', y)$ is the fraction of animals that were spawned during year y' that recruit during year y, κ_y is the effect of ocean acidification on the hatching rate that occurs after density-dependent embryo mortality and ω_y is the effect of ocean acidification on the hatching rate that occurs before density-dependence. The matrix **G** is the link between the pre- and post-recruitment models. The entries in this matrix were computed by projecting the pre-recruitment model forward for embryos produced during year y', and recording the fraction of these embryos that survived to the stage corresponding to the first size class in the post-recruitment model in each future year. The entries of the matrix **G** depended on ocean acidification because of ocean acidification-affected survival in the pre-recruitment model. The symbol ϕ in Equation (14) was a constant, computed so that the population remained at its equilibrium unfished level in the absence of ocean acidification and exploitation ($F_y^D = F_{y,k}^B = 0$). To find the value of ϕ, R_y was set to 1, the resulting MMB was found, and $G(y', y)$ was set based on the pre-recruitment model with no ocean acidification effect, i.e.:

$$\phi = \frac{1}{\sum_{y'=y-10}^{y-1} f(MMB_{y'}) G(y', y)}. \quad (15)$$

The number of animals entering the first stage of the pre-recruitment model was governed by a Beverton–Holt relationship, i.e.:

$$f(MMB_{y'}) = \frac{4hR_0 MMB_{y'}/MMB_0}{(1-h) + (5h-1) MMB_{y'}/MMB_0}, \quad (16)$$

where MMB_y can be a historical or projected value. The variables R_0 and MMB_0 were the recruitment and mature male biomass, respectively, in an unfished state and h is the "steepness" of Equation (16) (the expected numbers entering the first stage of the pre-recruitment model when $MMB = 0.2MMB_0$, expressed as a proportion of R_0; Francis, 1992).

Computing fishery profits and maximum economic yield

The profit to the boats (excluding fixed costs that do not affect maximum economic yield, MEY) in the directed crab fishery during year y was given by

$$\pi_y = (p\tilde{C}_y^D - V_y), \quad (17)$$

where p is price of crab per kilogram (assumed to be time-invariant), and V_y is the summation of variable costs associated with fuel, food, and bait during year y:

$$V_y = E_y c_F + E_y c_G + P_y^D c_b, \quad (18)$$

where E_y is the sum of days fishing (E_y^F) and days traveling (E_y^T), and c_F, c_G, and c_b are, respectively, the average daily costs of fuel, food, and bait, and P_y^D is the number of potlifts during year y (Table 2). The number of potlifts in the directed fishery during year y, P_y^D, was a linear function of days fishing, $P_y^D = 64.25E_y^F$, while days fishing was a linear function of F_y^D, $E_y^F = 29\,759.5F_y^D$, and days

Table 2. The values for economic parameters (USD; M. Dalton, unpublished data).

Price per kilogram	\$4.82
Fuel cost per day	\$1248.19
Food cost per day	\$176.18
Bait cost per pot lift	\$5.95

traveling was a linear function of days fishing, $E_y^T = 0.4049E_y^F$ (see Punt *et al.*, 2014b for how these relationships were derived).

Projection model parameterization

Ocean acidification trends

A simple approximation to a standard ocean acidification scenario with changes over time in ocean pH was calculated using the straight line that joins the predictions of average global pH levels in the oceans between 2000 and 2200; $pH_{2000} = 8.1$, $pH_{2200} = 7.4$ (Caldeira and Wickett, 2003). The expected stage survivals ($\tilde{S}_i$) in the absence of ocean acidification effects were calculated so the population remains stable in the absence of exploitation (i.e. no other climate change variables affect juvenile crab survival).

Post-recruitment model

The parameters of the post-recruitment model that were estimated by fitting it to the data collected from the fishery and assessment surveys during 1968–2013 were: (i) natural mortality (M), (ii) the fully selected fishing mortality for each year for the directed fishery and the fisheries that took southern Tanner crab as bycatch when the catch was non-zero (e.g. when the directed fishery was not closed) (F_y^D and $F_{y,k}^B$), (iii) the parameters that defined the growth transition matrix ($X_{i,i+1}$), (iv) selectivity-at-length for each fishery (J_i^D and $J_{i,k}^B$), (v) catchability and selectivity-at-length for male crab in the surveys conducted by the NMFS (separately before and after 1982), (vi) the probability of being landed and retained given being caught in the directed pot fishery (Q_i), (vii) the initial size-structure of the population ($N_{1965,i}$), (viii) the mean recruitment ($\bar{R}$), and (ix) the deviations in recruitment about mean recruitment (ε_y, i.e. $R_y = \bar{R}e^{\varepsilon_y}$). Appendix B of Punt *et al.* (2014b) outlines the likelihood function that was maximized to obtain the values for the parameters of the post-recruitment model. The values for fecundity- and weight-at-length were set based on the outcomes of auxiliary studies (Table 3).

The values for h and R_0 were chosen so that $F_{MSY} = F_{35\%}$ and $B_{MSY} = B_{35\%}$, where the recruitment at $B_{35\%}$ was set to an average recruitment (from 1995 to present) selected by the Scientific and Statistical Committee of the NPFMC (NPFMC, 2008; Punt *et al.*, 2012). The assumption that $F_{MSY} = F_{35\%}$ and $B_{MSY} = B_{35\%}$ are commonly made when conducting projections for North Pacific crab and groundfish stocks (e.g. Punt *et al.*, 2012). Punt *et al.* (2014c) showed that the assumption $F_{MSY} = F_{35\%}$ was supported for several North Pacific crab stocks.

Economic model

The average price per kilogram for Tanner crab from 2006 to 2013 was calculated from State of Alaska fish ticket data as the ratio of total ex-vessel revenues (current dollars corrected for inflation summed over 2006–2013) to total landings (crab weight in pounds summed over 2006–2020 and converted to kilograms). The average costs for fuel, food, and bait were calculated from values in the Bering Sea and Aleutian Islands Crab Rationalization Program Economic Data Reports (EDRs) for the years 2006–2013 (Garber-Yonts and Lee, 2013). Fuel and food cost per day were calculated as the ratio of total fuel and food costs for 2006–2013 to the sum of days fishing and days traveling, which were reported in the EDRs in 2006–2011, but then were discontinued. For 2012–2013, days fishing and days traveling were derived from the confidential interview form of the State of Alaska shellfish observer programme. Bait cost per pot lift was calculated as the ratio of total bait costs for 2006–2013 to the total number of potlifts, where the number of potlifts was taken from fish ticket data.

Table 3. Weight- and fecundity-at-age (kg) for southern Tanner crab.

Size class	25–64 mm	65–84 mm	85–109 mm	110–134 mm	135–159 mm	160 mm+
Weight	0.033	0.125	0.281	0.566	0.980	1.498
Fecundity	0.001	0.028	0.177	0.494	0.952	1.476

Projection model scenarios

Model projections were made for a range of values for effort, with effort and hence fishing mortality assumed to be constant into the future. The parameters determining growth, costs, and prices were set to the estimates for the last year of the assessment period (2012).

The model scenarios explored the implications of various assumptions regarding which biological processes were affected by ocean acidification. The base model included all the effects on which data were available: (i) hatching success, (ii) mortality for the Z1 and Z2 larval stages, and (iii) mortality on juvenile stages C1–C8. It based the level of larval mortality on the 2013 hatched larvae (long-term experiments with treatments during oocyte and embryo development) in which pH was that expected in future years (linear decrease from 8.1 to 7.4 in 2200), assuming that ocean acidification effects on hatching success occurred before density-dependent effects on embryo survival and assuming that the level of natural morality for animals of stage C8+ equalled that for the last juvenile stage. Results were shown for the alternative models:

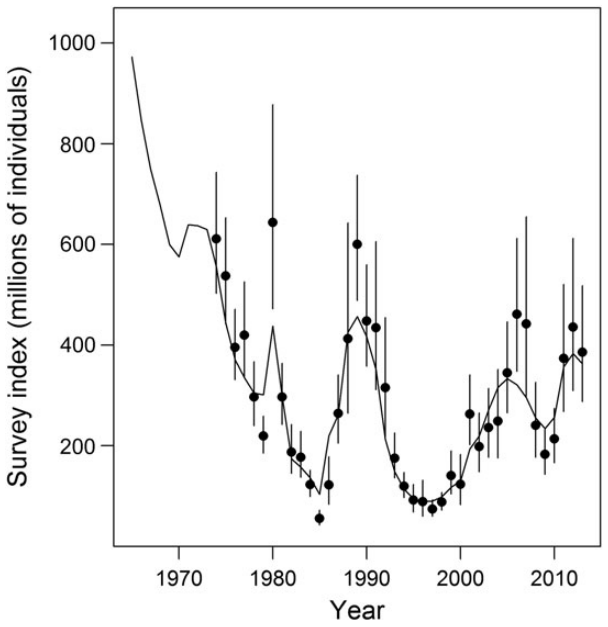

Figure 1. Time-trajectory of area-swept survey indices of male biomass (1974–2013; dots) and the post-recruitment model fit (line). The vertical bars indicate 95% confidence intervals for the data.

(i) Ocean acidification only affects hatching success based on the 2013 hatched larvae data.

(ii) Ocean acidification only affects larval mortality based on the 2013 hatched larvae data.

(iii) Ocean acidification only affects the mortality of juvenile stages C1–C8.

(iv) The level of larval mortality is based on analyses in which oocytes developed *in situ* and treatments occurred during embryo and larval development (larvae hatched in 2012; short-term experimental results).

(v) The level of larval mortality is based on analyses in which oocytes and embryos developed *in situ* and treatments occurred during larval development (larvae hatched in 2011; short-term experimental results).

(vi) The ocean acidification effects on hatching success occurred after, rather than before, density-dependent effects on embryo survival based on the 2013 hatched larvae data.

Cases (A)—(C) explored the consequences of only having experimental information on the effects of ocean acidification on one biological process. The analyses conducted by Punt *et al.* (2014b) were effectively Case C because that study based its projections on ocean acidification affecting the mortality rate of juvenile stage animals. Case D explored ignoring the effect of oocyte development occurring in acidified treatments, but considered the effects of ocean acidification on hatching success, larval mortality, and juvenile mortality. Case E explored the implications of conducting experiments in which the oocytes and embryos are not developed in water with the same acidification as the waters in which the larvae develop. Case F explored the consequences of when the effects on hatching success occur. Results are shown for Cases A–F for the assumption that natural mortality for stages C8+ is equal to that under non-ocean acidification-affected conditions ($0.25\ yr^{-1}$) and that natural mortality for such animals is equal to that for stage C8 crab. This should bound the range for this unknown process.

Results

Parameterization of the models

The post-recruitment population dynamics model was fitted to a variety of data sources. However, the ability to mimic the trends

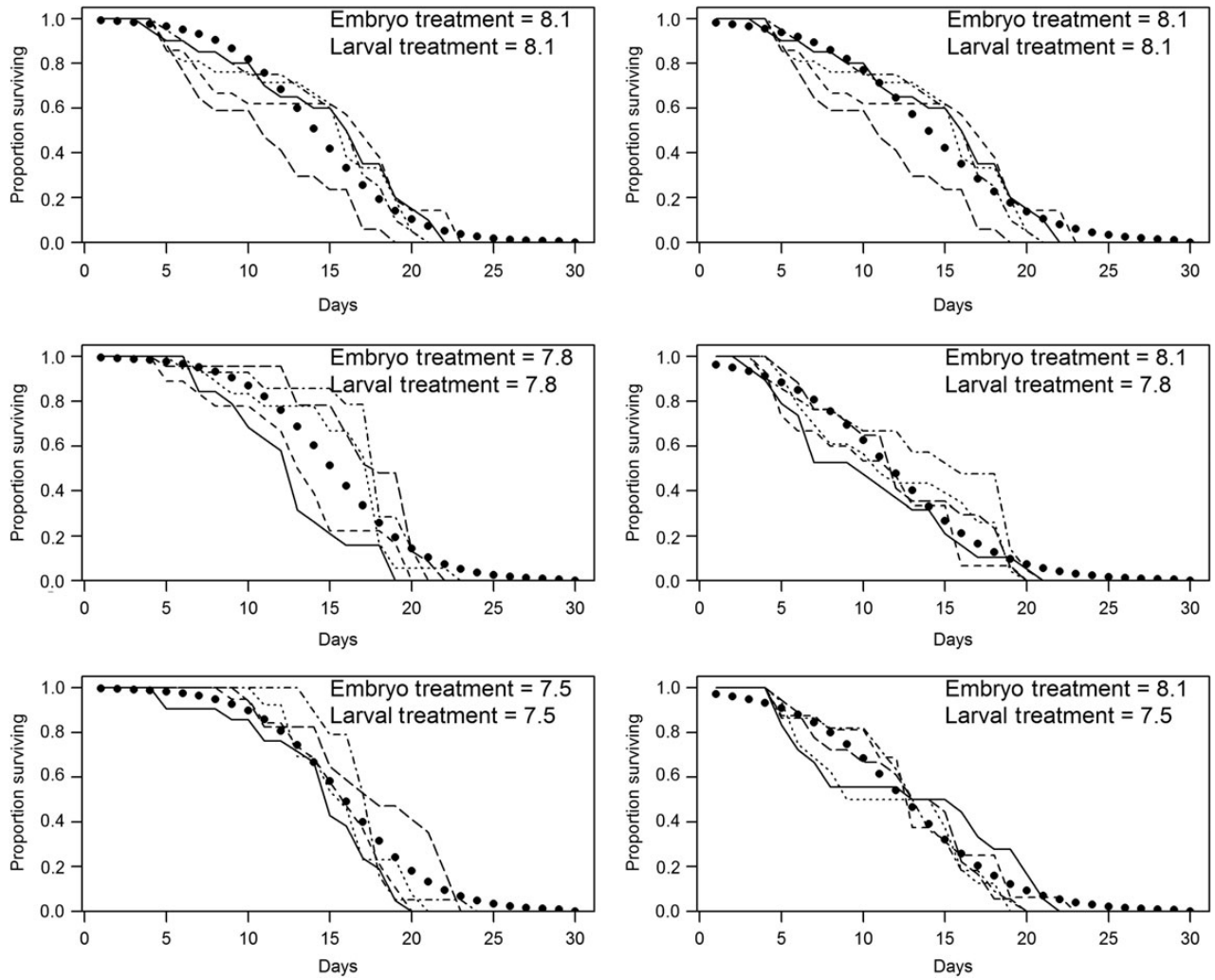

Figure 2. Observed (light lines) and model-predicted (dots) 2013 larval survival from long-term experiments. Each light line indicates a different container. Results are shown for experiments in which all animals were hatched at the same pH as they were developed (left panels) and under control conditions (right panels).

in abundance inferred from surveys is the most important in terms of the consequences for being able to adequately conduct long-term projections such as those on which this paper is based. Figure 1 therefore plots observed and model-predicted survey indices of male abundance. The observed indices were computed using area-swept analysis methods based on surveys conducted by the National Marine Fisheries Service. The post-recruitment model was able to mimic the marked fluctuations in abundance adequately, although it was unable to capture some of the outlying survey estimates, including the high 2006 and 2007 abundance estimates.

Figure 2 shows the base model fits to the data from 2013 larval survival experiment. There was a fairly large amount of between-container variation (light lines in Figure 2). However, given the small sample sizes, a random effects structure is not supported for these data. In addition, a model in which the parameter β [Equation (2a)] depends on pH was not supported by AICc. The model predictions for the two upper panels of Figure 2 are not identical because the predictions are based on fitting to the entire dataset and not each experiment individually. The model captures the data adequately. However, it tends to predict that more larvae should have survived beyond the end of the experiment than was observed. The model predicts little difference in survival rate over 30 days among treatments.

Figure 3 shows the fits of the constant survival rate model to the data from the experiment to determine the survival of juvenile stage southern Tanner crab. The model fits the data for pH = 7.5 very well, but the fits to the data for pH = 8.1 and 7.8 are poorer, with some evidence of increasing mortality rates with age or for increased mortality during periods of moulting. The poor fit for pH = 7.8 is similar to the fit obtained by Punt *et al.* (2014b) to similar data

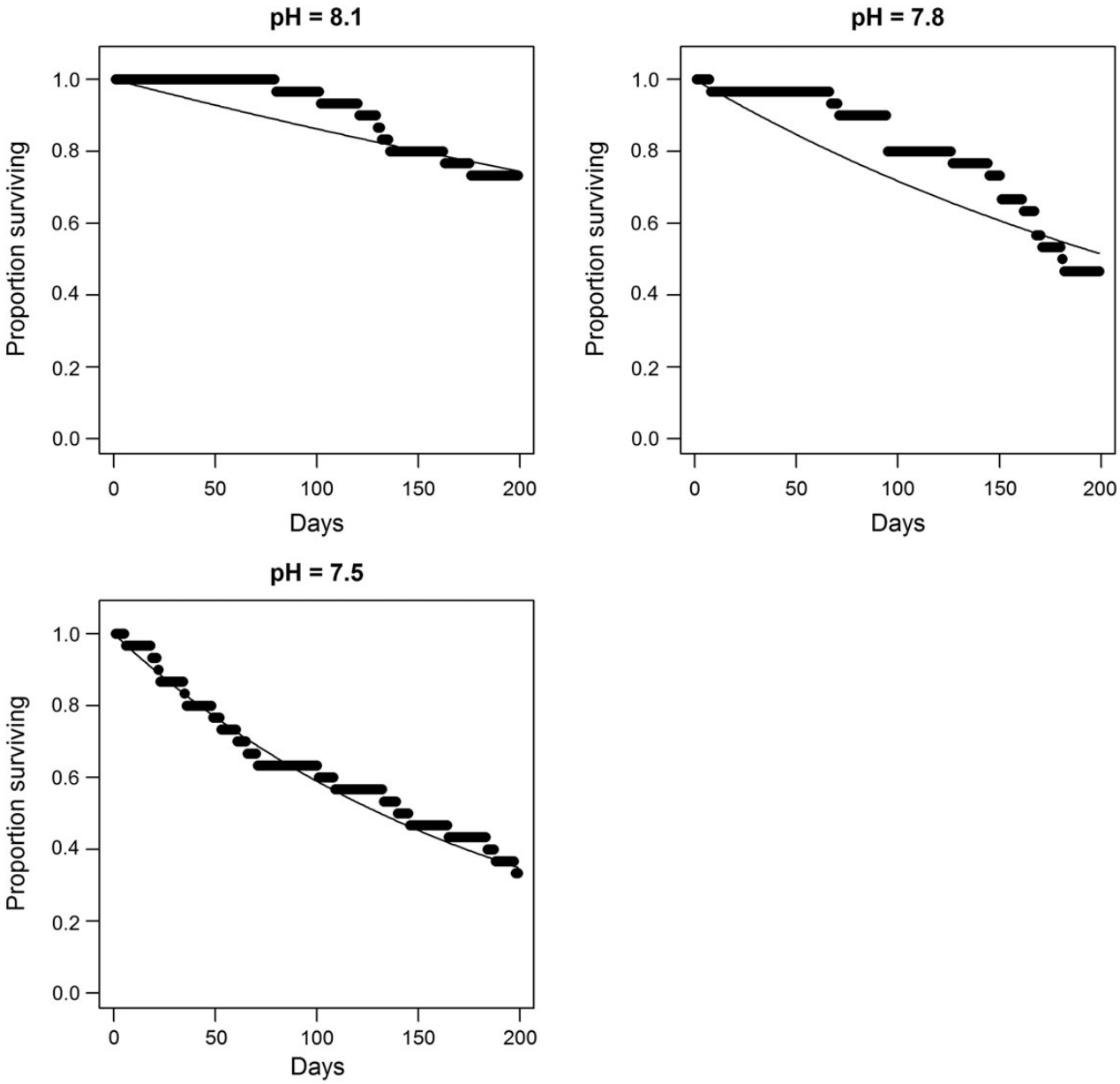

Figure 3. Observed (solid dots) and model-predicted (lines) survival for juvenile stage southern Tanner crab.

for red king crab. An alternative model in which survival is a logistic function of age was not supported over the constant survival model. In principle, a model in which the relationship between survival and age or moulting event changes with pH would fit the data in Figure 3 best, but it would not be straightforward to infer the relationship between survival and age (or moulting) for different levels of pH.

Application of the pre-recruitment model

Figure 4 shows various parameters of the pre-recruitment model for the base-case set of specifications (which include that the survival rate of larvae is best represented by experiments in which animals are spawned at the same pH at which they develop). The effects of ocean acidification on hatching success were fairly small even over a 100-year period. In contrast, the survival rate of juvenile stage animals could decline substantially over the next 100 years while the survival rate of larvae could increase. The effect of ocean acidification was greater for the later stages (Figure 4b) because the duration of these stages is longer (Table 1). Survival for 25 mm+ CW crab could be substantially reduced under the somewhat pessimistic assumption that the daily survival rate for >25 mm CW crab equals that for stage C8 crab (Figure 4c). Combining the effect of ocean acidification on the survival rates of larvae and juvenile stages (glaucothoe stage animals being assumed not to be affected by ocean acidification) suggests that the proportion of hatchlings that survive to stage C8 (the first stage of the post-recruitment model) could decline by up to 25% over next 100 years.

Yield and profit curves

Figure 5 shows yield curves in the absence of ocean acidification as a reference against which the ocean acidification-affected scenarios can be compared. The equilibrium catch is maximized at a full-selection exploitation rate of 0.567 (Figure 5a) which is, by construction, equal to $F_{35\%}$ given that stock–recruitment steepness was set (to 0.860) with the intent that $F_{MSY} = F_{35\%}$. MSY is estimated to be 14.3 kt, which is substantially larger than recent catches. The yield curve in Figure 5a does not hit the abscissa because some of the animals in the first post-recruitment stage are mature and because steepness is fairly high.

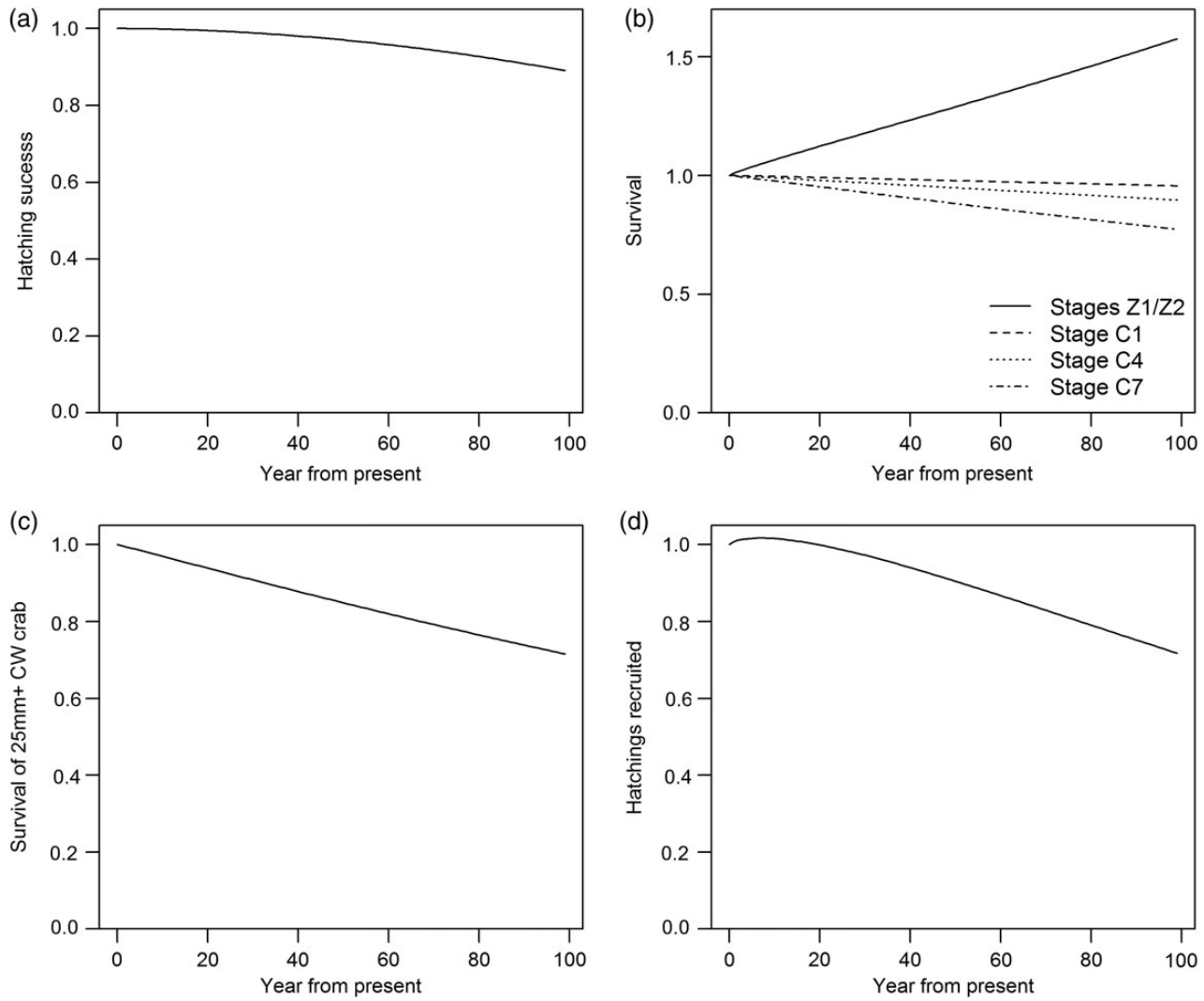

Figure 4. Temporal effects of ocean acidification for the base-case set of specifications: (a) proportion of embryos that hatch, (b) survival of a subset of the larval and juvenile stages, and (c) survival of stage C8+ crab. (d) The proportion of hatchlings that survive to recruit to 25 mm CW as a function of the year of spawning.

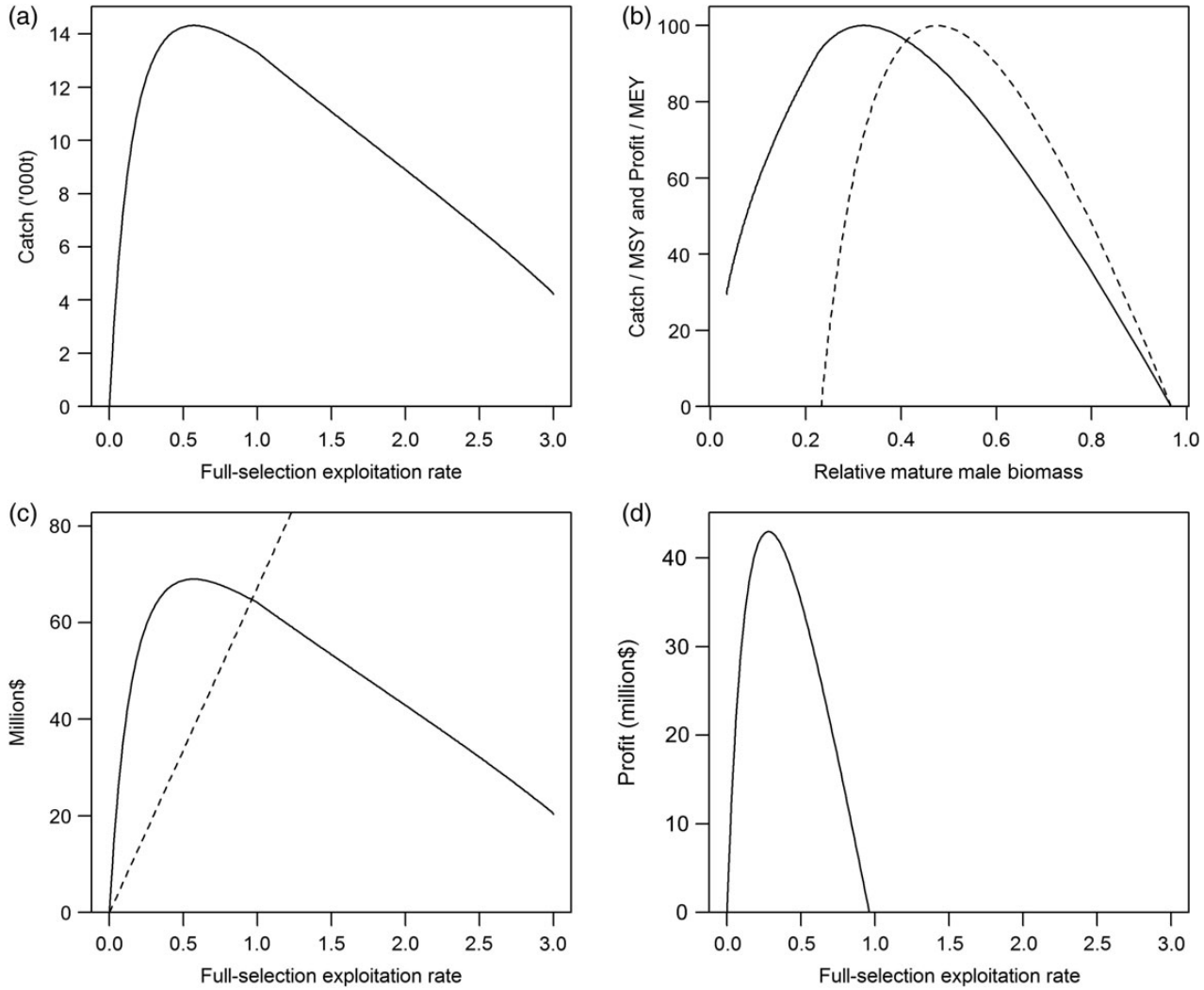

Figure 5. Equilibrium model behaviour in the absence of ocean acidification effects. (a) Equilibrium yield vs. full-selection exploitation rate, (b) catch relative to MSY (solid curve) and profit relative to MEY (dashed curve) vs. equilibrium mature male biomass expressed relative to the unfished mature male biomass, revenue (solid curve) and cost (dashed line) as a function of full-selection exploitation rate, and (d) profit as a function of full-selection exploitation rate.

In contrast to yield, profit, which is the difference between revenue and cost (Figure 5c), is maximized at a much lower full-selection exploitation rate (0.280) than the full-selection exploitation rate at which catch (and revenue) are maximized (Figure 5a and d). One consequence of this is that selecting a full-selection exploitation rate to maximize profit will stabilize the mature male biomass at a much higher level than selecting a full-selection exploitation rate to maximize catch (Figure 5b).

Figure 6 shows the sensitivity of the relationship between equilibrium catch and full-selection exploitation rate and that between equilibrium profit and full-selection exploitation rate at present and in 20, 40, 60, and 80 years into the future. Results are shown for the case in which natural mortality for 25 mm+ CW crab was affected by ocean acidification and the case in which this is not the case because this factor has the largest effect on the yield curve (and hence biological and economic reference points). In addition, there is no direct evidence that ocean acidification will reduce the survival rate for adult southern Tanner crab, let alone to the extent to which this is predicted for stage C8 crab.

As expected, ocean acidification reduced both MSY and F_{MSY} (Figure 6a and c), with the extent of change in these quantities depending markedly on whether ocean acidification affects natural mortality for animals of 25 mm+ CW crab. Ocean acidification also affected the relationship between profit and full-selection exploitation rate, except that the effect is much larger than for yield (Figure 6b and d). For example, MSY and F_{MSY} are zero after 60 years while MEY and the corresponding fishing mortality rate, F_{MSY}, are zero even after 40 years if ocean acidification affects natural mortality of 25 mm+ CW crab. In contrast, MSY and MEY are both non-zero if this natural mortality rate is not affected by ocean acidification (Figure 6b and d).

Figure 7 extends Figure 6 by providing the relationships between $F_{35\%}$, F_{MSY}, MSY, B_{MSY}, F_{MEY}, MEY, B_{MEY}, and years from the present. As expected from Figure 6, the values for all the reference points decline over time in the presence of ocean acidification, and do so faster when ocean acidification affects natural mortality for 25 mm+ CW crab (solid line). There is a perhaps somewhat surprising initial increase in F_{MSY} with time when ocean acidification

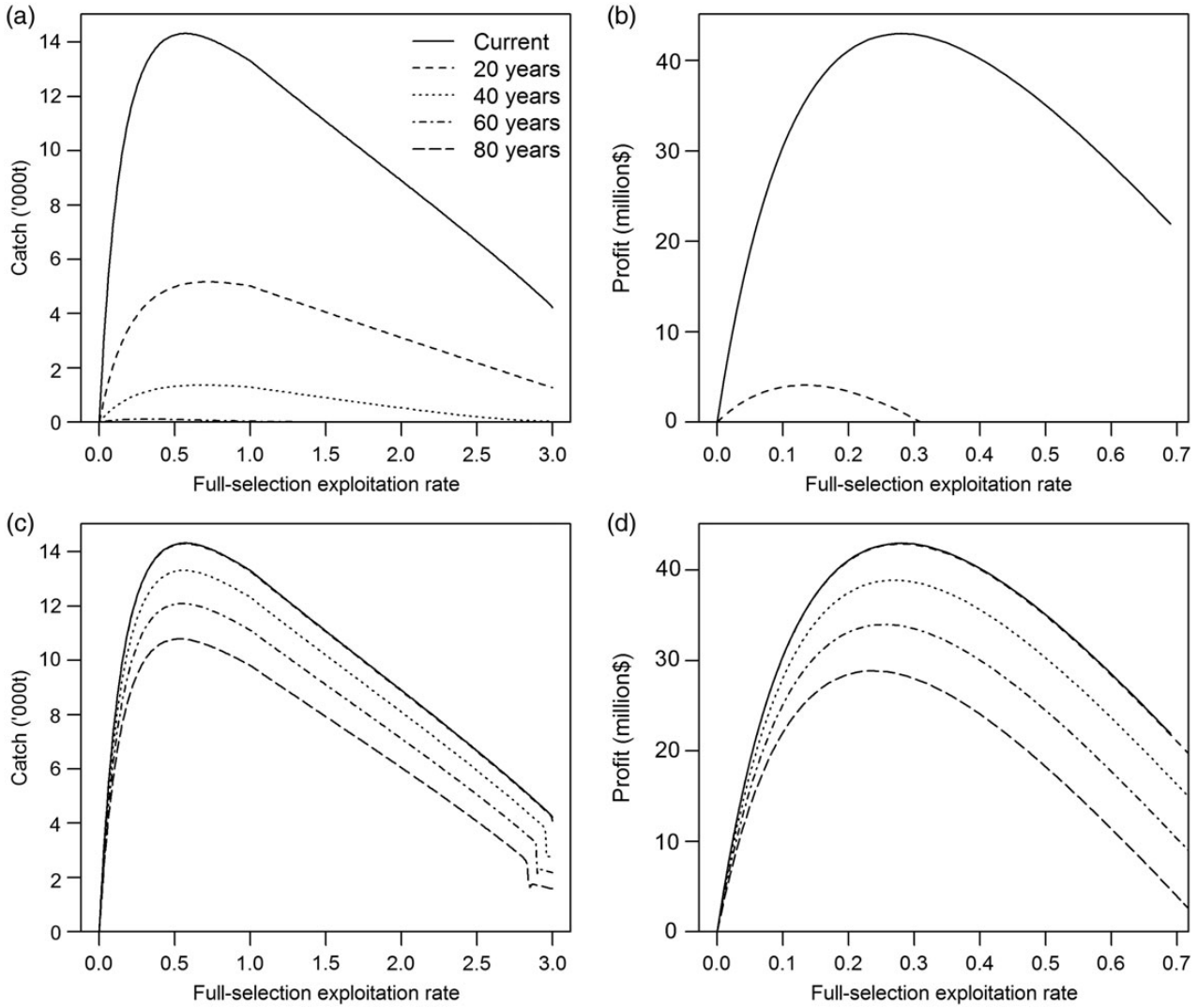

Figure 6. Equilibrium yield (a) and (c) and equilibrium profit (b) and (d) vs. full-selection exploitation rate by year. Results are shown when natural mortality for 25 mm+ CW crab is affected by ocean acidification and when this is not the case (upper and lower panels, respectively). [Note the difference in *x*-axis range between the left and right sets of panels].

impacts 25 mm+ CW crab (Figure 7a). This arises because F_{MSY} tends to be higher when natural mortality is higher. However, this tendency becomes swamped over time as the effect of ocean acidification increases because recruitment is reduced so fishing mortality must be reduced to prevent a collapse of recruitment.

The variable $F_{35\%}$ equals F_{MSY} in the absence of ocean acidification effects (Figure 5a). However, the rate at which $F_{35\%}$ (which does not depend on the form of the stock–recruitment relationship) changes over time differs from that of F_{MSY} (Figure 7a and g). This is because the biomass at which *MSY* is achieved drops over time (Figure 7e and f), but there is no requirement that it needs to stay above the level corresponding to $F_{35\%}$.

Effects on biological reference points

Figures 8 and 9 summarize the effect of ocean acidification on the biological reference points $F_{35\%}$, F_{MSY}, and F_{MEY}, 10, 25, and 50 years into the future for each of the cases. Results are shown when ocean acidification affects natural mortality for 25 mm+ crab (Figure 8) and when this is not the case (Figure 9). The values of the reference points are expressed relative to their value in the absence of ocean acidification. The results for the cases in which juvenile stage crab are not affected by ocean acidification, but animals 25 mm and larger are affected are presented but that case seems unrealistic.

As expected from Figures 6 and 7, the results are very sensitive to whether natural mortality for 25 cm+ CW crab is affected by ocean acidification. Also, and expected from Figure 7, $F_{35\%}$ changes more over time than F_{MSY} and F_{MEY}. The upper right panel of Figure 8 is blank because $F_{35\%}$ is zero within 50 years for all the cases when natural mortality for 25 cm+ CW crab is affected by ocean acidification.

Basing the analyses on ocean acidification only affecting larval survival (case B) would lead to the conclusion that the effects of ocean acidification are less negative than the base-case analysis (in fact they may be positive rather than negative if ocean acidification does not affect natural mortality of 25 mm+ crab), but only if the

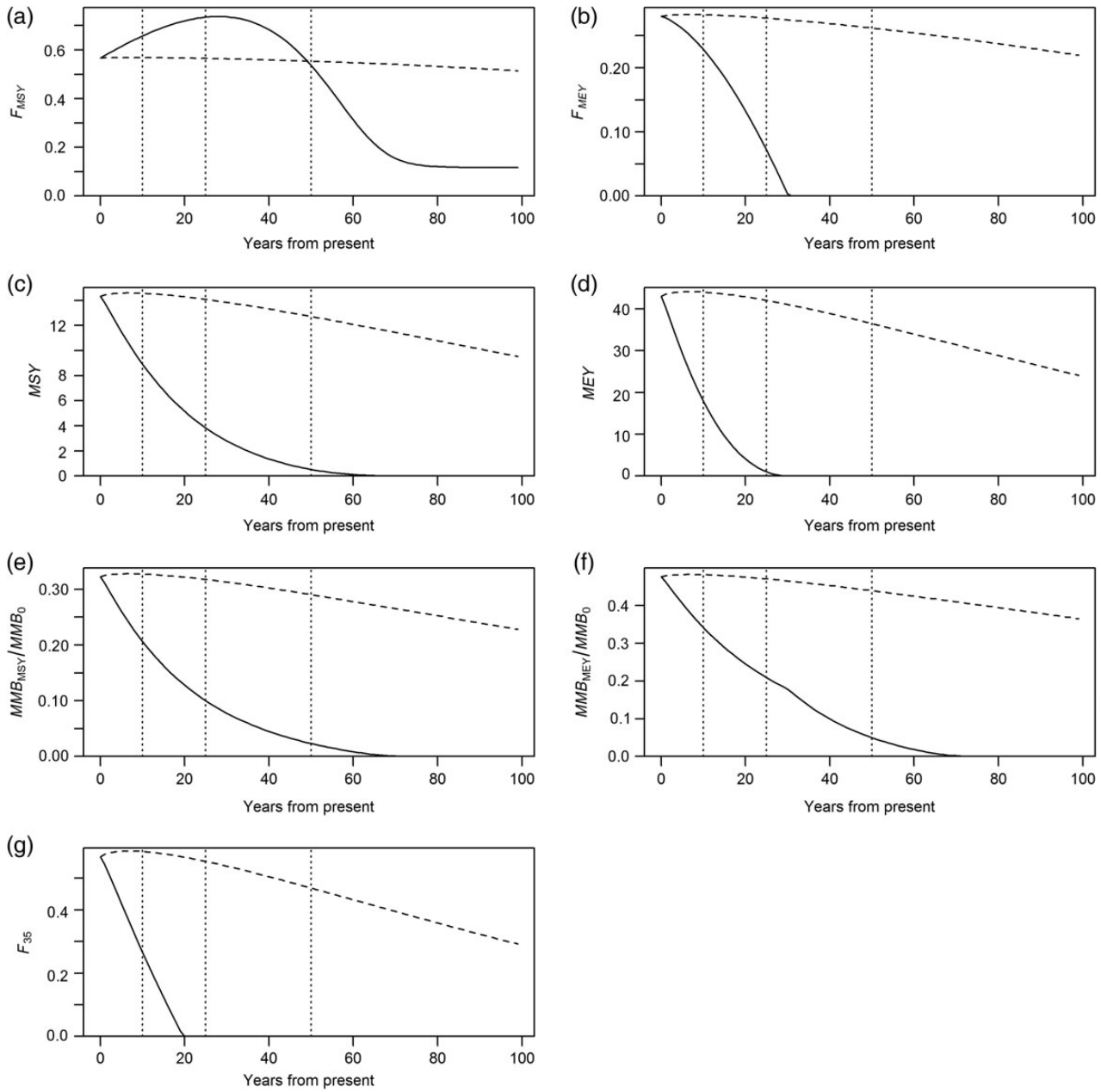

Figure 7. Effect of ocean acidification on biological reference points related to catch (a, c and e) and profit (b, d and f). The lower left panel (g) shows the relationship between $F_{35\%}$ and time. The results are shown when ocean acidification affects post-recruitment natural mortality (solid curves) and when this is not the case (dashed curves). The vertical lines indicate the years for which results are shown in Figures 8 and 9.

larval survival was based on the experiments with treatments during oocyte, embryo, and juvenile development. In contrast, the results of projections for cases using the outcomes of the 2012 experiments and when ocean acidification is assumed to affect only during larval development (cases C and D) are markedly more pessimistic than the base-case analysis. Ignoring the effect of ocean acidification on hatching success leads to overestimates of F_{MSY} after 50 years compared with the base-case results (Figures 8f and 9f), but the effect is small. Assuming that the effect of ocean acidification on hatching success occurs after rather than before density-dependent effects on survival leads to larger effects than those for the base-case analysis (results not shown), but the effects remain small even over a 50-year projection period.

Discussion

A framework within which the effects of ocean acidification can be integrated into how fisheries management advice is developed under the types of fisheries laws implemented within the USA. The current application to southern Tanner crab in the eastern Bering Sea accounts for ocean acidification effects on hatching success, survival rate of larvae, and survival of juveniles. It could be extended to allow other parameters to change with pH such as growth rates (both pre- and post-recruitment), fecundity (but that would likely require explicit modelling of females), and the extent of density-dependence. Growth rates of southern Tanner crab juveniles, for instance, were reduced in acidified treatments (Long *et al.*, 2013). Inclusion of additional effects would require

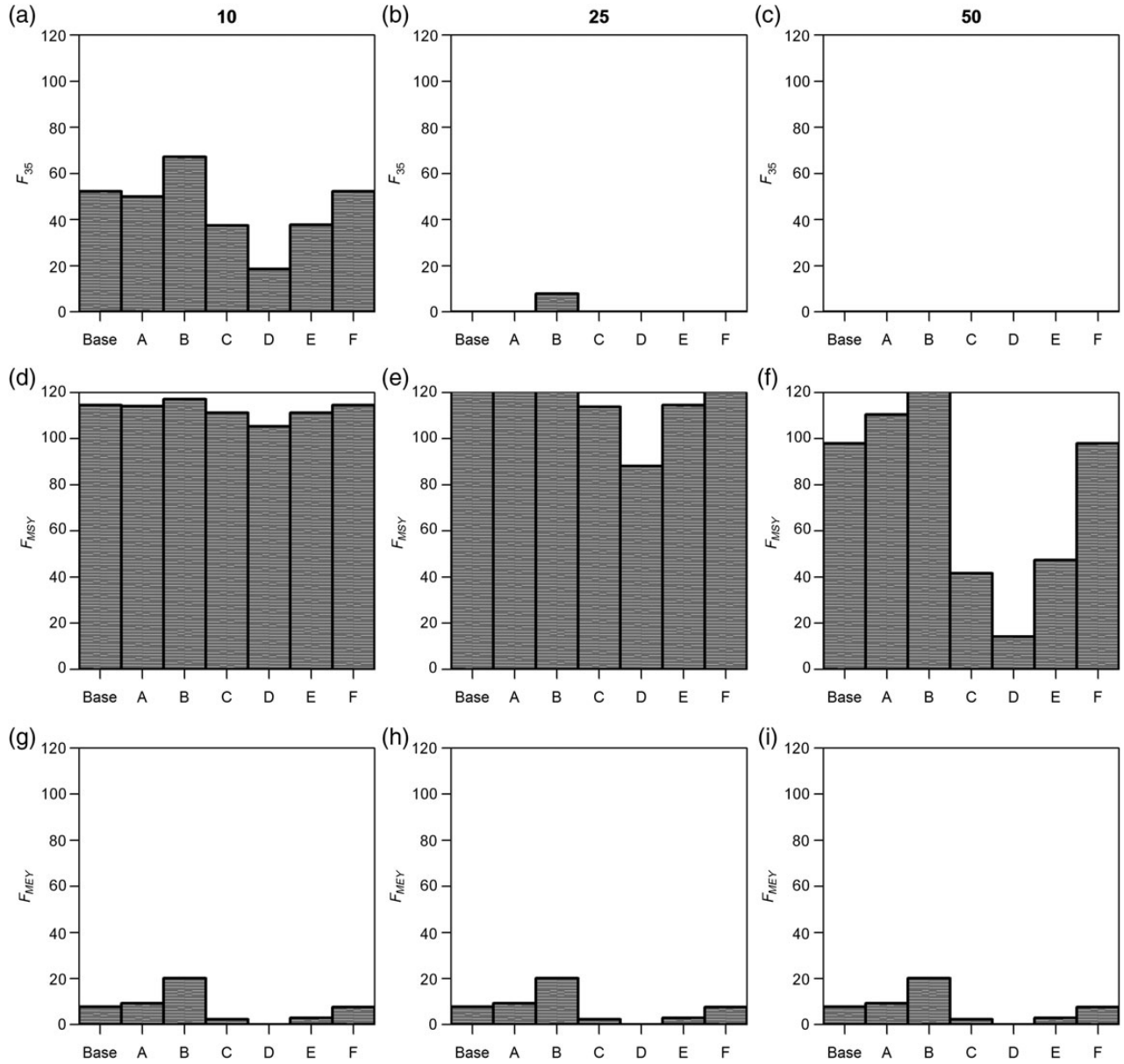

Figure 8. Values for three biological reference points ($F_{35\%}$, F_{MSY}, and F_{MEY}) relative to their values in the absence of ocean acidification by case (A – F) for 10, 25, and 50 years into the future. The results in this panel assume that ocean acidification affects natural mortality for 25 mm+ CW crab.

that appropriate experiments be conducted to parameterize the size of effects.

Results confirm expectations from demographic models that effects on the longer life stages have the largest consequences for population productivity. In the context of this paper, effects of ocean acidification on the rate of natural mortality for 25 mm+ CW and juvenile stage crab had by far the largest consequences for biological and economic reference points. In contrast, the consequences of ocean acidification effects on hatching success and larval survival were substantially smaller. As expected, if the effects on hatching success occur before density-dependence, the consequences of reduction in hatching success on biological and economic reference points are reduced. This was confirmed by the results of projections in which the only process affected by ocean acidification was hatching success and those effects occurred after density-dependence (results not shown). The lack of sensitivity to hatching success is expected from Figure 4a and b, which show that the reduction in hatching success over 50 years is small as is true for larval survival. The consequences of ocean acidification on larval survival differ depending on how the experiments designed to estimate the effects are conducted, with the results when ocean acidification effects occur only during larval development being markedly more optimistic than when such effects occur throughout oocyte and embryo development.

The results of this study complement those of Punt *et al.* (2014b) who used a similar approach to explore the implications of ocean acidification for red king crab in Bristol Bay, Alaska. Unlike this study, Punt *et al.* (2014b) only allowed for ocean acidification effects on juvenile stage crab. They therefore ignored effects on

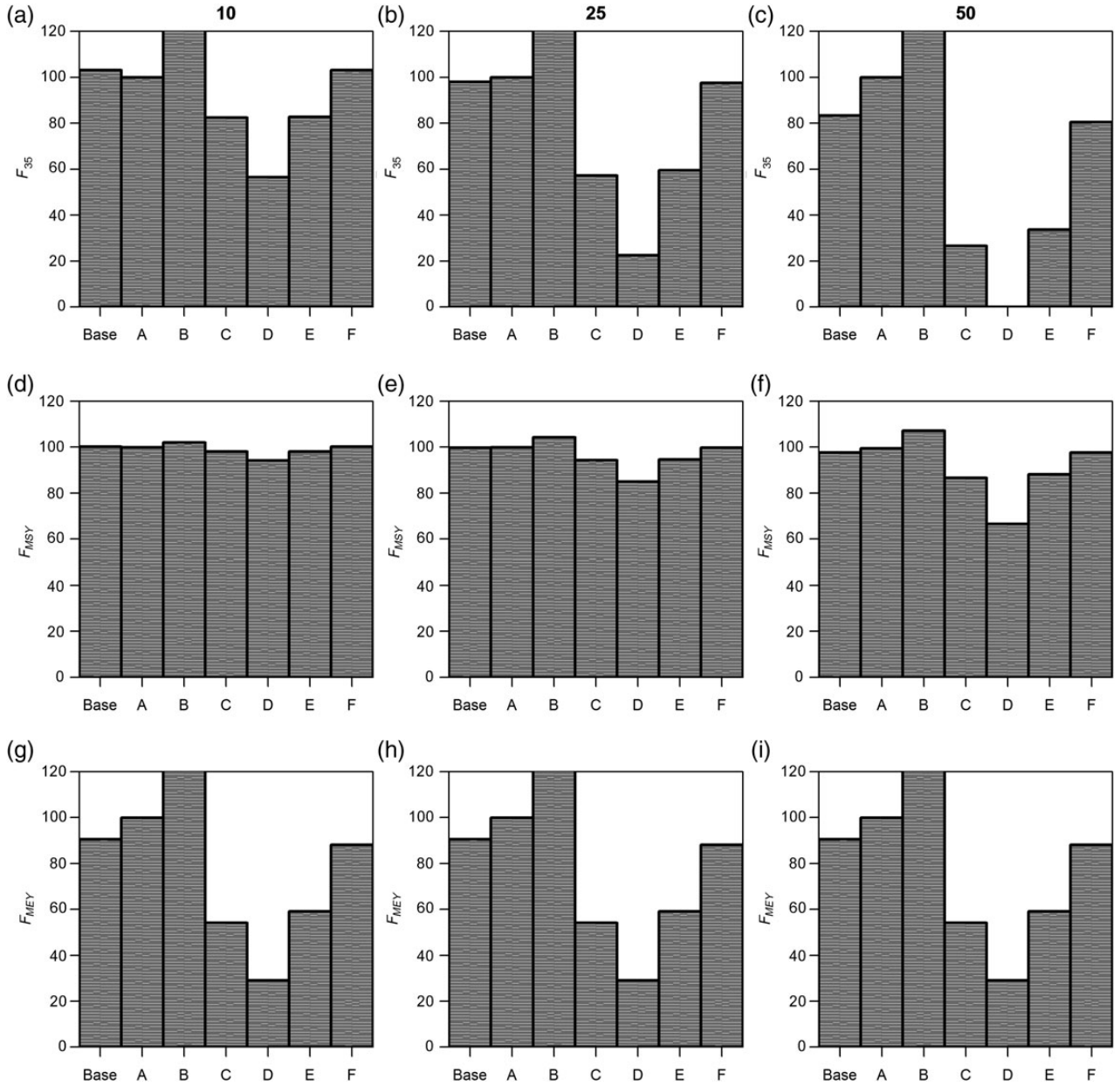

Figure 9. Values for three biological reference points ($F_{35\%}$, F_{MSY}, and F_{MEY}) relative to their values in the absence of ocean acidification by case (A – F) for 10, 25, and 50 years into the future. The results in this panel assume that ocean acidification does not affect natural mortality for 25 mm + CW crab.

hatching success and larval survival as well as effects on adult crab (although Punt *et al.* (2014b) considered a broader range of instars as juvenile crab so the effect of increased mortality on juvenile crab was higher). The results of this paper suggest that Punt *et al.* (2014b) considered the life history stage that has the largest effect on biological and economic reference points. However, by ignoring the possibility that ocean acidification affects all adult crab, Punt *et al.* (2014b) may have underestimated the consequences of ocean acidification on future stock status and fishery catches.

The results of this study emphasize the need to consider multiple life stages in research on the physiological effects of ocean acidification conditions. Although the consequences of ocean acidification on hatching success was found to be relatively small, at least over a 50-year period (Figures 8 and 9), this could not have been anticipated *a priori*. The fact that juvenile and adult natural mortality had the largest effect on biological and economic reference points has implications for research priorities. In contrast to the experiments to estimate effects on hatching success and larval survival (30 days in duration), examination of ocean acidification effects on juvenile stage and adult crab requires a large research and infrastructure investment.

We did not quantify the uncertainty associated with the effects of ocean acidification on hatching success and survival and propagate this uncertainty through to values for the biological and economic reference points. Punt *et al.* (2014b) quantified uncertainty associated with ocean acidification effects on juvenile stage crab using a Monte Carlo approach, and combined this uncertainty with the variation in recruitment about the estimated stock–recruitment

relationship. They concluded that the effects of ocean acidification would not be detectable for 20–40 years. Similar results would have been obtained in this study. The model has not explored all possible scenarios. For example, the assumption that density-dependence occurs early in life is common in assessment models, but is not the only possible assumption. For example, density-dependence could occur throughout most of the pre-recruitment stages and in particular during settlement. Although the qualitative results are robust to the timing of density-dependence, quantitatively, the effects of ocean acidification will be reduced if density-dependence occurs after some of the effects of ocean acidification on survival, as is evident from the analyses that explored whether the effect on hatching occurs before or after density-dependence.

The results of this study would be sensitive to some of the assumptions which that could not be explored. In particular, the quantitative, but not qualitative, results would be sensitive to violation of the assumption that the stock–recruitment relationship is of the Beverton–Holt form and that $F_{MSY} = F_{35\%}$ in the absence of ocean acidification. In addition, the relative mortality of larvae among treatments was based on starvation experiments under the assumption that the pattern of mortality for healthy larvae would be similar. This may explain the model's overestimate of larval survival relative to the experimental data and may suggest that the increase in larval survival rate (Figure 4b) is incorrect. Finally, we assumed that ocean acidification would be the only environmental change as a result of climate change in the North Pacific. As such, we ignored the potential effects of other physical variables (e.g. temperature and water column structure) and biological variables (e.g. primary production and increased acidity due to respiration) and the overall effects these variables would have on crab production, movement, and predator/prey interactions. Future research should attempt to incorporate a more holistic view of the role of expected environmental changes on the biological forcing specific to commercial crab stocks in the North Pacific.

Relative little effort has been directed towards understanding the fishery-related consequences of ocean acidification (Griffith *et al.*, 2011; Malakoff, 2012), particularly for Alaska. Exceptions to this include Kaplan *et al.* (2010) who explored the consequences of ocean acidification for the US West Coast groundfish fishery using the implementation of the ecosystem model Atlantis for the US West Coast (Brand *et al.*, 2007; Kaplan and Levin, 2009), although that analysis was based on catch scenarios rather than actual harvest regimes applied for fisheries management. Mathis *et al.* (2015) applied a risk assessment framework to the impacts of ocean acidification on Alaskan fisheries broadly, by identifying the vulnerability and susceptibility of a range of fisheries across a range of Alaskan regions to the effects of ocean acidification. However, unlike this study (and that of Punt *et al.*, 2014), Mathis *et al.* (2015) did not base their analyses on the population dynamics models developed for the impacted species and fisheries. However, their analysis provides information related to broad policy development. In contrast, while this study does not include the breath of species and fisheries examined by Mathis *et al.* (2015), it provides results in terms of the quantities (fishing mortality rates, biomass expressed relative to reference points, catches, and revenue) used by fisheries decision makers.

The research strategy follows the plan in Sigler *et al.* (2008) to start with theoretical principles of population biology and use experiments to estimate effects of ocean acidification conditions on early life history parameters as the most effective way to forecast effects of ocean acidification on the abundance of Alaska crab stocks. This strategy combines biological and economic theory to extrapolate from results obtained in a tightly controlled laboratory setting to conditions that young crab in the Bering Sea may someday experience. Furthermore, the population projections for crab stocks presented in this paper are based on coarse assumptions about future ocean conditions that are necessary in applications that involve scenarios for future carbon emissions to begin to predict effects of ocean acidification on marine ecosystems. The coarsest assumptions can be tested and improved, and striving for a forecasting methodology is a useful objective that can be shared across scientific disciplines. For example, multispecies bioeconomic models are feasible. Bycatch in the fisheries for Alaska red king crab and snow crab appear as independent sources of fishing mortality in the bioeconomic model for Tanner crab presented in this paper. It could be useful and interesting to link population dynamics models for these crab stocks. Inevitably, questions about ecosystem effects arise and addressing those will be difficult.

Acknowledgements

This work was partially funded by the Joint Institute for the NOAA Ocean Acidification Program through the Joint Institute of the Study of the Atmosphere and Ocean (JISAO) under NOAA Cooperative agreement No. NA10OAR4320148, Contribution No. 2476. The biological experiments on crab were funded by the North Pacific Research Board (NPRB Project #1010). We thank the NOAA biologists and laboratory technicians responsible for the collection of the biological data at the Kodiak Laboratory. Martin Dorn (NOAA, AFSC), Gordon Kruse (UAF), and an anonymous reviewer are thanked for comments on an earlier version of the manuscript. OMB disclaimer: The findings and conclusions in the paper are those of the authors and do not necessarily represent the views of the National Marine Fisheries Service, NOAA.

References

Brand, E. J., Kaplan, I. C., Harvey, C. J., Levin, P. S., Fulton, E. A., Hermann, A. J., and Field, J. C. 2007. A spatially explicit ecosystem model of the California Current's food web and oceanography. US Departmet ofCommerce. NOAA Technical Memorandum. NMFSNWFSC-84. www.nwfsc.noaa.gov/publications/index.cfm (last accessed 2 October 2015).

Caldeira, K., and Wickett, M. E. 2003. Anthropogenic carbon and ocean pH. Nature, 425: 365–365.

Donaldson, W. E., Cooney, R. T., and Hilsinger, J. R. 1981. Growth, age and size at maturity of Tanner crab, *Chionoecetes bairdi* M.J. Rathbun, in the northern Gulf of Alaska (Decapoda, Brachyura). Crustaceana, 4: 286–302.

Doney, S. C., Fabry, V. J., Feely, R. A., and Kleypas, J. A. 2009. Ocean acidification: the other CO_2 problem. Annual Review of Marine Science, 1: 169–192.

Dupont, S., Havenhand, J., Thorndyke, W., Peck, L., and Thorndyke, M. 2008. Near-future level of CO_2-driven ocean acidification radically affects larval survival and development in the brittlestar *Ophiothrix fragilis*. Marine Ecology Progress Series, 373: 285–294.

Feely, R. A., Sabine, C. L., Lee, K., Berelson, W., Kleypas, J., Fabry, V. J., and Millero, F. J. 2004. Impact of anthropogenic CO_2 on the $CaCO_3$ system in the oceans. Science, 305: 362–366.

Findlay, H. S., Kendall, M. A., Spicer, J. I., and Widdicombe, S. 2009. Future high CO_2 in the intertidal may compromise adult barnacle *Semibalanus balanoides* survival and embryonic development rate. Marine Ecology Progress Series, 389: 193–202.

Francis, R. I. C. C. 1992. Use of risk analysis to assess fishery management strategies: a case study using orange roughy (*Hoplostethus atlanticus*) on the Chatham Rise, New Zealand. Canadian Journal of Fishery and Aquatic Sciences, 49: 922–930.

Garber-Yonts, B., and Lee, J. 2013. Stock assessment and fishery evaluation report for king and Tanner crab fisheries of the Bering Sea and Aleutian Islands regions: economic status of the BSAI crab fisheries, 2013. North Pacific Fishery Management Council, 605 W., 4th Avenue, Anchorage, AK 99501.

Griffith, G. P., Fulton, E. A., and Richardson, A. J. 2011. Effects of fishing and acidification-related benthic mortality on the southeast Australian marine ecosystem. Global Change Biology, 17: 3058–3074.

Haynes, E. 1973. Descriptions of prezoeae and stage I zoeae of *Chionoecetes bairdi* and *C. opilio* (Oxyrhyncha, Oregoniinae). Fishery Bulletin, 71: 769–775.

Haynes, E. 1981. Descriptions of stage II zoeae of snow crab, *Chionoecetes bairdi*, (Oxyrhyncha, Majidae). Fishery Bulletin, 79: 17–182.

Incze, L. S., Armstrong, D. L., and Wencker, D. L., 1982. Rates of development and growth of larvae of *Chionoecetes bairdi* and *C. opilio* in the southeastern Bering Sea. *In* Proceedings of the international symposium on the genus *Chionoecetes*, pp. 191–218. Fairbanks, Alaska. Alaska Sea Grant Report No. 82-10.

Jewett, S., and Haight, R. E. 1977. Description of megalopa of snow crab, *Chionoecetes bairdi* (Majidae, subfamily Oregoniinae). Fishery Bulletin, 75: 459–463.

Kaplan, I. C., and Levin, P. S. 2009. Ecosystem based management of what? An emerging approach for balancing conflicting objectives in marine resource management. *In* The future of fisheries. In North America, pp. 77–95. Ed. by R.J. Beamish, and B.J. Rothschild. Springer, New York, N.Y

Kaplan, I. C., Levin, P. S., Burden, M., and Fulton, E. A. 2010. Fishing catch shares in the face of global change: a framework for integrating cumulative impacts and single species management. Canadian Journal of Aquatic and Fishery Sciences, 67: 1968–1982.

Kompas, T., Dichmont, C. M., Punt, A. E., Deng, A., Che, T. N., Bishop, J., Gooday, P., *et al.* 2010. Maximizing profits and conserving stocks in the Australian northern prawn fishery. Australian Journal of Agricultural Resource Economics, 54: 281–299.

Kurihara, H., Kato, S., and Ishimatsu, A. 2007. Effects of increased seawater pCO_2 on early development of the oyster *Crassostrea gigas*. Aquatic Biology, 1: 91–98.

Kurihara, H., Shimode, S., and Shirayama, Y. 2004a. Effects of raised CO2 concentration on the egg production rate and early development of two marine copepods (*Acartia steueri* and *Acartia erythraea*). Marine Pollution Bulletin, 49: 721–727.

Kurihara, H., Shimode, S., and Shirayama, Y. 2004b. Sub-lethal effects of elevated concentration of CO2 on planktonic copepods and sea urchins. Journal of Oceanography, 60: 743–750.

Long, W. C., Swiney, K. M., and Foy, R. J. 2016. Effects of high pCO_2 on Tanner crab reproduction and early life history, Part II: carryover effects on larvae from oogenesis and embryogenesis are stronger than direct effects. ICES Journal of Marine Science, 73: 836–848.

Long, W. C., Swiney, K. M., Harris, C., Page, H. N., and Foy, R. J. 2013. Effects of ocean acidification on juvenile red king crab (*Paralithodes camtschaticus*) and Tanner crab (*Chionoecetes bairdi*) growth, condition, calcification, and survival. PLoS ONE, 8: e60959.

Malakoff, D. 2012. Researchers struggle to assess responses to ocean acidification. Nature, 338: 27–28.

Mathis, J. T., Cooley, S. R., Lucey, N., Colt, S., Ekstrom, J., Hurst, T., Hauri, C., *et al.* 2015. Ocean acidification risk assessment for Alaska's fishery sector. Marine Policy, 136: 71–91.

North Pacific Fishery Management Council (NPFMC). 2008. Amendment 24. Final Environmental Assessment for amendment 24 to the Fishery Management Plan for Bering Sea/Aleutian Islands King and Tanner Crabs to Revise Overfishing Definitions. North Pacific Fishery Management Council, 605 West, 4th Avenue, Anchorage, AK 99501.

North Pacific Fishery Management Council (NPFMC). 2014. Stock Assessment and Fishery Evaluation Report for the king and Tanner crab fisheries of the Bering Sea and Aleutian Islands Regions. North Pacific Fishery Management Council, 605 W., 4th Avenue, #306, Anchorage, AK 99501.

Orr, J. C., Fabry, V. J., Aumont, O., Bopp, L., Doney, S. C., Feely, R. A., Gnanadesikan, A., *et al.* 2005. Anthropogenic ocean acidification over the twenty-first century and its impact on calcifying organisms. Nature, 437: 681–686.

Parker, L. M., Ross, P. M., and O'Connor, W. A. 2009. The effect of ocean acidification and temperature on the fertilization and embryonic development of the Sydney rock oyster *Saccostrea glomerata* (Gould 1850). Global Change Biology, 15: 2123–2136.

Punt, A. E., Poljak, D., Dalton, M. G., and Foy, R. J. 2014b. Evaluating the impact of ocean acidification on fishery yields and profits: The example of red king crab in Bristol Bay. Ecological Modelling, 285: 30–53.

Punt, A. E., Siddeek, M. S. M., Garber-Yonts, B., Dalton, M., Rugolo, L., Stram, D., Turnock, B. J., *et al.* 2012. Evaluating the impact of buffers to account for scientific uncertainty when setting TACs: application to red king crab in Bristol Bay. Alaska. ICES Journal of Marine Science, 69: 624–634.

Punt, A. E., Smith, A. D. M., Smith, D. C., Tuck, G. N., and Klaer, N. L. 2014a. Selecting relative abundance proxies for B_{MSY} and B_{MEY}. ICES Journal of Marine Science, 71: 469–483.

Punt, A. E., Szuwalski, C. S., and Stockhausen, W. 2014c. An evaluation of stock–recruitment proxies and environmental change points for implementing the US Sustainable Fisheries Act. Fisheries Research, 157: 28–40.

Sigler, M. F., Foy, R. J., Short, J. W., Dalton, M., Eisner, L. B., Hurst, T. P., Morado, J. F., *et al.* 2008. Forecast fish, shellfish and coral population responses to ocean acidification in the North Pacific Ocean and Bering Sea: An ocean acidification research plan for the Alaska Fisheries Science Center. AFSC Processed Rep. 2008–07, 35 p. Alaska Fish. Sci. Cent., NOAA, Natl. Mar. Fish. Serv., 17109 Point Lena Loop Road, Juneau AK 99801.

Small, D., Calosi, P., White, D., Spicer, J. I., and Widdicombe, S. 2010. Impact of medium-term exposure to CO_2 enriched seawater on the physiological functions of the velvet swimming crab *Necora puber*. Aquatic Biology, 10: 11–21.

Spicer, J. I., Raffo, A., and Widdicombe, S. 2007. Influence of CO_2-related seawater acidification on extracellular acid-base balance in the velvet swimming crab *Necora puber*. Marine Biology, 151: 1117–1125.

Stevens, B. G., Donaldson, W. E., Haaga, J. A., and Munk, J. E. 1993. Morphometry and maturity of paired Tanner crabs, *Chionoecetes bairdi*, from shallow- and deepwater environments. Canadian Journal of Fisheries and Aquatic Sciences, 50: 1504–1516.

Stockhausen, W. T. 2014. 2014 Stock Assessment and Fishery Evaluation Report for the Tanner Crab Fisheries of the Bering Sea and Aleutian Islands Regions. Pages 324–545 in Stock Assessment and Fishery Evaluation Report for the king and Tanner crab fisheries of the Bering Sea and Aleutian Islands Regions. North Pacific Fishery Management Council, 605 W., 4th Avenue, #306, Anchorage, AK 99501.

Swiney, K. M., Long, W. C., and Foy, R. J. 2016. Effects of high pCO_2 on Tanner crab reproduction and early life history—Part I: long-term exposure reduces hatching success and female calcification, and alters embryonic development. ICES Journal of Marine Science, 73: 825–835.

Talmage, S. C., and Gobler, C. J. 2009. The effects of elevated carbon dioxide concentrations on the metamorphosis, size, and survival of larval hard clams (*Mercenaria mercenaria*), bay scallops (*Argopecten irradians*), and Eastern oysters (*Crassostrea virginica*). Limnology and Oceanography, 54: 2072–2080.

Handling editor: Steven Cadrin

ICES Journal of Marine Science

ICES Journal of Marine Science (2016), 73(3), 865–875. doi:10.1093/icesjms/fsv187

Contribution to Special Issue: 'Towards a Broader Perspective on Ocean Acidification Research'

Original Article

Bacterioplankton community resilience to ocean acidification: evidence from microbial network analysis

Yu Wang[1‡], Rui Zhang[1‡], Qiang Zheng[1], Ye Deng[2], Joy D. Van Nostrand[3], Jizhong Zhou[3,4,5*], and Nianzhi Jiao[1*]

[1]*State Key Laboratory of Marine Environmental Science, Institute of Marine Microbes and Ecospheres, Xiamen University, Xiamen, Fujian 361005, People's Republic of China*

[2]*CAS Key Laboratory of Environmental Biotechnology, Research Center for Eco-Environmental Sciences, Chinese Academy of Sciences, Beijing 100085, People's Republic of China*

[3]*Institute for Environmental Genomics and Department of Microbiology and Plant Biology, University of Oklahoma, Norman, OK 73019, USA*

[4]*State Key Joint Laboratory of Environment Simulation and Pollution Control, School of Environment, Tsinghua University, Beijing 100084, China*

[5]*Earth Sciences Division, Lawrence Berkeley National Laboratory, Berkeley, CA 94720, USA*

**Corresponding author: e-mail: jiao@xmu.edu.cn (N.J.); jzhou@ou.edu (J.Z.)*

[‡]*Equal contribution.*

Wang, Y., Zhang, R., Zheng, Q., Deng, Y., Van Nostrand, J. D., Zhou, J., and Jiao, N. Bacterioplankton community resilience to ocean acidification: evidence from microbial network analysis. – ICES Journal of Marine Science, 73: 865–875.

Received 7 April 2015; revised 22 August 2015; accepted 28 September 2015; advance access publication 20 November 2015.

Ocean acidification (OA), caused by seawater CO_2 uptake, has significant impacts on marine calcifying organisms and phototrophs. However, the response of bacterial communities, who play a crucial role in marine biogeochemical cycling, to OA is still not well understood. Previous studies have shown that the diversity and structure of microbial communities change undeterminably with elevated pCO_2. Here, novel phylogenetic molecular ecological networks (pMENs) were employed to investigate the interactions of native bacterial communities in response to OA in the Arctic Ocean through a mesocosm experiment. The pMENs results were in line with the null hypothesis that elevated pCO_2/pH does not affect biogeochemistry processes. The number of nodes within the pMENs and the connectivity of the bacterial communities were similar, despite increased pCO_2 concentrations. Our results indicate that elevated pCO_2 did not significantly affect microbial community structure and succession in the Arctic Ocean, suggesting bacterioplankton community resilience to elevated pCO_2. The competitive interactions among the native bacterioplankton, as well as the modular community structure, may contribute to this resilience. This pMENs-based investigation of the interactions among microbial community members at different pCO_2 concentrations provides a new insight into our understanding of how OA affects the microbial community.

Keywords: Arctic Ocean, community structure, mesocosm experiment, molecular ecological network, ocean acidification.

Introduction

Since the industrial revolution, the impact of human activity on the global climate has increased greatly as a result of increasing carbon dioxide (CO_2) emissions from anthropogenic sources. The uptake of anthropogenic carbon dioxide by the ocean has caused a decrease of pH 0.1 units (ocean acidification, OA; IPCC, 2015). Previous studies have demonstrated that some phototrophic communities, like sea grass (Zimmerman *et al.*, 1997; Jiang *et al.*, 2010), diatoms (Riebesell *et al.*, 1993; Baragi *et al.*, 2015; Taucher *et al.*, 2015), and coccolithophorids (Hiwatari *et al.*, 1995; Lv *et al.*, 2015), have higher photosynthesis rates under a higher partial pressure of carbon dioxide (pCO_2). However, the response of marine bacterioplankton, a crucial player in marine biogeochemical cycling (Azam, 1998; Jiao *et al.*, 2010), to OA is not well understood at present. Joint *et al.* (2011) proposed that "marine microbes possess the flexibility to accommodate pH change". Indeed, several mesocosm studies have found that elevated pCO_2 has little effect on bacterial communities in the Arctic Ocean (Allgaier *et al.*, 2008; Tanaka *et al.*, 2008;

Oliver *et al.*, 2014). The abundance and activity of bacteria in these communities did not differ statistically under three different pCO_2 treatments (350, 700, and 1085 μatm; Allgaier *et al.*, 2008). Furthermore, phylogenetic diversity analysis revealed no clear effect of elevated pCO_2 on a bacterioplankton assemblage in the high Arctic Ocean (Monier *et al.*, 2014). In contrast, a few studies have demonstrated that elevated pCO_2 has some influence on microbial community composition (Krause *et al.*, 2012; Bowen *et al.*, 2013). Other studies have also shown that the production and growth rates of bacterial isolates were strongly affected by high pCO_2 and low pH (Takeuchi *et al.*, 1997; Labare *et al.*, 2010; Teira *et al.*, 2012). For example, *Vibrio alginolyticus* growth was suppressed under low pCO_2 levels (Michael *et al.*, 2010). In contrast, high pCO_2 stimulated the growth efficiency of one *Flavobacteria* strain (Teira *et al.*, 2012). Moreover, the rate of microbial ammonia oxidation is inhibited by reduced pH in both surface and deep seawater (Huesemann *et al.*, 2002). Conflicting results from the population/ecosystem and species levels indicate that community may play a crucial role in determining the response of microbes to OA. In addition to community structure and the number of species, micro-organism interaction is an important component of diversity (Olesen *et al.*, 2007). For example, ecological networks among different species bridge ecosystem complexity and stability (Montoya *et al.*, 2006). The interaction between plants and pollination enhances the relative resistance of plants to environmental disturbance (Sole and Montoya, 2001; Memmott *et al.*, 2004). Compared with network investigations among macro-organisms (Elton, 1927; Paine, 1980; Bascompte *et al.*, 2003), microbial interactions and ecological networks are understudied and have only been investigated recently with advances in molecular technology (Sherr and Sherr, 2008; Chaffron *et al.*, 2010; Steele *et al.*, 2011). Several microbial network investigations have been conducted on temporal variation in microbial communities and the interactions among bacteria, phage, and protists at the San Pedro Ocean Time-series (SPOT) station off southern California (Chow *et al.*, 2013, 2014). Bacterial interaction has also been proposed as a determinant of phytoplankton bloom dynamics (Tan *et al.*, 2015). Currently, only a few investigations have been performed to illustrate the interaction of microbial communities in response to climate change in soil environments (Zhou *et al.*, 2010; Tu *et al.*, 2015), but no studies have addressed interactions among micro-organisms under elevated pCO_2 in the marine environment.

A large-scale mesocosm experiment, European Project on OCean Acidification (EPOCA), was set up in the pelagic coastal area of the Arctic Ocean to assess the impact of OA on the marine ecosystem. Previous EPOCA studies have demonstrated that the phytoplankton community was more susceptible to elevated pCO_2 than the bacterioplankton community, where pico-phytoplankton and diatoms were stimulated by nutrient addition and elevated pCO_2, resulting in increased primary production (Riebesell *et al.*, 2013b). Bacterial activity was subsequently spurred by stimulated primary production and elevated pCO_2, leading to a decrease in net production (Engel *et al.*, 2013; Motegi *et al.*, 2013). However, bacterial production and respiration were generally similar among the pCO_2 mesocosms during the incubation period (Motegi *et al.*, 2013). Nonetheless, bacterioplankton activity was closely related to phytoplankton under both ambient and elevated pCO_2, and limited by both nutrient availability and elevated pCO_2 (Riebesell *et al.*, 2013b). The general diversity and composition of microbial communities has been evaluated by Automated Ribosomal Spacer Analysis (Sperling *et al.*, 2013), T-RFLP, clone libraries (Zhang *et al.*, 2013), and next-generation sequencing (Roy *et al.*, 2013), all of which indicated that increased pCO_2 did not significantly impact the communities. However, because of limited sample numbers and sequencing depth, the above dataset cannot be used to explore the interactions among bacterial groups under elevated pCO_2. Thus, we examined the structure and diversity of microbial communities at this site using Illumina sequencing and performed phylogenetic molecular ecological network (pMEN) analysis using the Molecular Ecological Network Analysis Pipeline (MENAP; Deng *et al.*, 2012) for samples collected from nine mesocosms, each having a different pCO_2 level (175–1085 μatm), which simulated different acidification scenarios. We tested the null hypothesis that elevated pCO_2 would have an insignificant or indirect impact on bacterial assemblages as proposed by Joint *et al.* (2011), with a focus on the interactions among bacterioplankton under different pCO_2 concentrations. Our results indicated an insignificant effect of elevated pCO_2 on microbial assemblage interactions and connectivity and provide a deep insight into our understanding of bacterioplankton assemblage resistance to climate change.

Material and methods

Experimental set-up and sampling

A large-scale mesocosm experiment, supported by EPOCA, was conducted in the Arctic Ocean at Kongsfjorden, Svalbard, Norway (78°56.2′N, 11°54.6′E), from June to July 2010. Experimental set-up details have been described previously (Riebesell *et al.*, 2013a). Briefly, nine mesocosms (45 m^3 volume), each simulating a different pCO_2 concentration (~175, ~180, ~250, ~340, ~450, ~600, ~675, ~860, and ~1085 μatm) by bubbled CO_2, were deployed into the Arctic Ocean. On day 13, nutrients were added to induce phytoplankton bloom development (Schulz *et al.*, 2013).

Sample collection was carried out according to Zhang *et al.* (2013). Briefly, seawater (2 l) collected from nine mesocosms was filtered onto a 0.22 μm pore filter (GTTP, Millipore) to collect microbial cells. The filters were stored at −80°C until DNA extraction. In total, we obtained 165 environmental DNA samples from the nine mesocosms over 19 sampling points (not all treatments contain all time points; Supplementary Table S1). Geochemistry and biological parameters were downloaded from the EPOCA website (http://www.epoca-project.eu; Nisumaa *et al.*, 2010). The geochemistry parameters included temperature, salinity, pH, oxygen, particle organic carbon (POC), particle organic nitrogen, particle organic phosphorus, NO_3, Si, PO_4, and NH_4; the biological parameters included bacterial production, chlorophyll *a* concentration, bacterial abundance, bacterial respiration, bacterial biomass production, viral abundance, and pico-phytoplankton abundance.

DNA extraction, Illumina high-throughput sequencing, and analysis

DNA was extracted by a freeze-grinding method as described previously (Zhang *et al.*, 2013). The forward (515F, 5′-GTGCCAGCMGCCGCGG-3′) and reverse (806R, 5′-GGACTACHVGGGTWTCTAAT-3′) primers were used to target the bacterial 16S rDNA gene V4 hyper-variable region (Caporaso *et al.*, 2012). PCR amplification was performed as described by Caporaso *et al.* (2010). The amplicons were then paired-end sequenced using the Illumina MiSeq platform (Illumina, Inc., San Diego, CA, USA) and the reads were then analysed through an in-house sequence analysis pipeline (IEG sequence analysis pipeline, http://zhoulab5.rccc.ou.edu). Briefly, the sequence length was trimmed (minimum length, 100 bp), Btrim was used to remove sequencing adaptors and low quality regions, and sequences with quality scores <20 were then removed

(Kong, 2011). Thereafter, UCHIME was employed to remove the chimeric sequences (Edgar *et al.*, 2011). The number of sequences from each sample was resampled randomly to 35 000. The sequences were then clustered using the CD-HIT algorithm (Li and Godzik, 2006). The taxonomic assignment was determined using the RDP (Ribosome Database Project) classifier against the RDP 16S rRNA database based on BLAST (Wang *et al.*, 2007).

pMEN construction and network analysis

Sequence alignment was carried out by the PyNAST alignment method against pre-aligned reference 16S rRNA sequences (Caporaso *et al.*, 2009), followed by approximately maximum-likelihood tree construction using the FastTree method with default settings (Price *et al.*, 2009; Morgan *et al.*, 2010). Comparison of microbial community diversity was performed using the Unifrac method in a phylogenetic context (Lozupone and Knight, 2005, 2007; Lozupone *et al.*, 2006) followed by principal coordinates analysis (PCoA). pMENs analysis was performed based on the relative abundance of all samples through the molecular ecological networks analysis pipeline (http://ieg2.ou.edu/MENA; Zhou *et al.*, 2010,2011; Deng *et al.*, 2012). The whole process and details are given in a previous MENA study (Deng *et al.*, 2012); we briefly introduced the major process in the present study. OTUs that appeared in 13 or fewer samples were removed. The relative abundance of OTUs was log-transformed and missing values were filled with a very small number (0.01) if paired valid values were available. This step ensured a more statistically reliable correlation coefficient between two OTUs. Following data preparation, the relative abundance of each OTU in each sample was used to generate the similarity matrix as the foundation for subsequent steps. Similarity matrices (adjacency matrix) were created for each network based on the pairwise Pearson correlation coefficient across the time-series (one time points lag). To obtain a confident network construction, the threshold of pairwise Pearson correlation coefficient values between OTUs was identified by an RMT-based approach that observed a transition point of nearest-neighbour spacing distribution of eigenvalues from Gaussian to Poisson distribution (Zhou *et al.*, 2010). To compare networks, an identification cut-off of 0.84 (0.85 for 175 and 860 μatm treatments) was used to construct the microbial community networks. Additionally, ecological networks predicted by R^2 ($R^2 > 0.8$) generated based on the random matrix theory (RMT) should be scale-free (Zhou *et al.*, 2010). An identification cut-off of 0.84 for 175 and 860 μatm treatments did not obtain an $R^2 > 0.8$, where 0.85 could. To evaluate whether or not the constructed networks were random, we employed a permutation-based null model analysis with 100 permutations and kept the number of nodes and links constant. A Student's *t*-test was performed to evaluate significance differences between random and experimental networks. Once the pMEN was determined, the topological indices were calculated based on the adjacency matrix. Module detection of each network was based on fast greedy modularity optimization (Newman, 2006a). Identification of key module members was based on within-module connectivity (Z_i) and among-module connectivity (P_i) of each node (Olesen *et al.*, 2007). Eigen-gene, which is a linear combination of genes and eigenvalues (Deng *et al.*, 2012), was detected by singular value decomposition analysis (Alter *et al.*, 2000). Thereafter, trait-based gene significance (GS), which is the correlation of relative abundance of each OTU to a sample trait (e.g. pCO_2, temperature), was calculated. Networks were visualized with the NetworkAnalyzer plugin of the Cytoscape 3.1.1 (Assenov *et al.*, 2008). Mantel tests were performed to identify relationships between pMENs and biological and chemical variables (Zhou *et al.*, 2010).

Nucleotide sequence accession number

Sequences obtained in this study were uploaded to the MG-RAST database under the ID number 4626065.3.

Results

A previous study sequenced samples from this same experimental site, collected across nine time-points, using the Illumina HiSeq2000 platform (Roy *et al.*, 2013); however, network analysis studies and our preliminary tests suggested that this sampling frequency does not result in accurate and reliable network analysis. Therefore, we expanded this sample set to include 19 time-points for each of nine pCO_2 treatments, nine more time-points than Roy *et al.* (2013; Supplementary Table S1). These DNA samples were also used to investigate the bacterioplankton community by T-RFLP in a previous study (Zhang *et al.*, 2013). Results from different sequencing platforms or different runs on the same platform can affect the estimation of microbial diversity (Zhou *et al.*, 2013), so all samples were sequenced together on the Illumina MiSeq platform. The microbial community structure revealed in our study (discussed below) did not show obvious differences from those of Roy *et al.* (2013). In total, ~8 900 000 paired-end reads were generated after quality control in this study, with an average length of ~250 bp (Supplementary Table S1). To increase the reliability of comparison among samples, the sequences were resampled with a threshold of 35 000.

Bacterial community composition and diversity

Similar bacterial community composition and structure were observed in the nine pCO_2 treatments during the entire incubation period (Table 1, Figure 1, and Supplementary Figure S2), which is consistent with previous results (Roy *et al.*, 2013; Sperling *et al.*, 2013; Zhang *et al.*, 2013). The *Proteobacteria*, *Bacteroidetes*, *Actinobacteria*, and *Cyanobacteria*/chloroplast were predominant in all nine mesocosms. The relative abundance of these microorganisms varied over the incubation period. For example, the *Proteobacteria* dominated at the beginning of the incubation period and then decreased in relative abundance; while the *Bacteroidetes* exhibited a relatively high abundance at the end of the incubation, which could be a response to the phytoplankton bloom (Figure 1). Meanwhile, the rarefaction curves for all samples revealed variations in richness and diversity among samples (Supplementary Figure S1). The bacterioplankton community diversity, including Chao index and PD, as well as richness, decreased during the incubation period in all pCO_2 treatments (Supplementary Figures S2 and S3). The weighted PCoA results revealed that the bacterial community structures were altered by nutrient addition, although there was no clear pattern among different pCO_2 treatments (Supplementary Figure S4).

Microbial community interactions

The increased number of sequences obtained by high-throughput sequencing technology afforded us the unprecedented opportunity to investigate the interaction and connectivity within these microbial communities using network analysis. pMEN analysis is a novel RMT-based framework for studying microbial interaction, which has been used in long-term CO_2 experiments (Zhou *et al.*, 2010, 2011; Tu *et al.*, 2015). In the pMEN analysis, a node in pMEN indicates an OTU, while a link indicates a correlation between two connected nodes. The connectivity, also called node degree, indicates the connection strength of a node; therefore,

Table 1. Percentage of major phylum and class bacterioplankton community OTUs in nine pCO_2 mesocosms.

Mesocosm	M3		M7		M2		M4		M8		M1		M6		M5		M9					
pCO_2	175		180		250		340		425		600		675		860		1085		Ambient[a]		Elevated	
Phylum	Percen[b]	s.d.	Percen	s.d.	Percen	s.d.	Percen	s.d.	Percen	s.d.	Percen	s.d.	Percen	s.d.	Percen	s.d.	Percen	s.d.	Percen	s.d.	Percen	s.d.
Proteobacteria	52.46[b]	8.02	56.45	9.13	53.05	7.84	49.88	6.87	49.09	5.05	52.99	9.35	52.20	8.18	52.26	8.54	52.19	7.81	54.46	8.58	51.67	1.38
Alphaproteobacteria (class)	71.36[c]	14.10	71.62	12.46	68.83	13.70	68.06	9.54	71.33	11.32	68.84	8.89	71.88	7.97	71.54	9.56	75.32	9.18	52.36	13.12	42.83	10.15
Betaproteobacteria (class)	6.09	3.88	4.99	2.41	6.18	4.24	5.74	2.48	6.31	3.87	7.88	3.36	5.04	2.53	7.69	3.70	5.66	3.26	4.99	3.23	4.98	3.46
Gammaproteobacteria (class)	21.79	10.12	22.55	10.80	24.20	10.33	25.32	8.40	21.71	8.29	22.47	6.68	22.52	6.84	19.86	7.22	18.55	6.47	18.16	10.32	15.57	7.93
Bacteroidetes	32.99	12.30	25.14	12.85	30.28	13.07	32.53	10.99	31.61	14.39	30.69	13.35	29.06	11.08	30.00	12.25	29.44	10.67	29.06	12.57	30.52	1.41
Flavobacteria (class)	90.30	5.49	90.31	6.44	84.44	10.24	90.85	4.96	89.59	4.91	90.85	3.36	87.26	7.75	86.24	9.88	86.17	11.86	90.30	5.90	87.92	8.28
Sphingobacteria (class)	1.18	0.66	2.40	3.23	2.08	2.21	1.68	1.59	2.07	2.96	1.85	1.78	2.25	2.34	2.87	5.93	1.47	0.80	1.79	2.38	2.04	2.93
Actinobacteria	5.12	3.09	7.03	4.27	6.86	6.13	6.40	3.98	5.91	3.47	6.28	3.18	7.17	4.73	7.03	4.42	6.62	5.25	6.08	3.68	6.61	1.03
Firmicutes	0.33	0.33	0.44	0.40	0.38	0.38	0.24	0.19	0.47	0.35	0.30	0.31	0.40	0.51	0.67	0.84	0.41	0.30	0.38	0.36	0.41	0.21
Cyanobacteria/chloroplast	7.68	11.27	5.79	9.15	4.57	6.17	7.10	10.09	7.39	11.19	6.01	8.34	7.92	11.02	5.45	5.60	8.26	10.90	6.73	10.21	6.67	2.37
Others	2.43	1.55	6.20	5.81	6.40	5.19	6.35	10.01	6.83	4.73	6.02	6.40	4.64	6.51	7.54	4.36	4.64	4.31	4.45	5.89	0.88	

[a]Ambient indicates ambient pCO_2 cosmosms contained M3 and M7, while elevated indicates the other 7 mecosoms.
[b]Average phylum OTU percentage of total OTUs with standard deviation.
[c]Average class OTU percentage of total phylum OTUs with standard deviation.

higher average connectivity means a more complex network. Geodesic distance means the shortest path between two nodes, while a smaller average geodesic distance means the nodes in a network are closer. The average clustering coefficient means the extent of a module in a network, where the clustering coefficient describes how well a node is connected with its neighbours. The network can be separated into communities or modules (Newman, 2006b). The modularity value indicates how well a network can be divided into modules. In our study, elevated pCO_2 generally had no consistent influence on the connectivity of micro-organisms observed via pMENs analysis (Table 1). For example, the size (number of total nodes) of pMENs under 175 and 180 μatm pCO_2 were smaller than for higher-level treatments (250, 425, 600, and 675 μatm), while they were similar to those from the 860 and 1085 μatm mesocosms. Additionally, the total number of links and average connectivity were similar among the nine pCO_2 treatments. Average geodesic distance and average clustering coefficients revealed a discrepancy change along the pCO_2 gradient. The modularity of nine pMENs, which contained at least four modules each, suggested that the bacterial communities in these mesocosms were highly complex (Olesen *et al.*, 2007). Strong negative correlations were observed in all nine pMENs, while positive correlations primarily occurred in submodules (Figure 2). These results suggested potential competition among bacterial lineages in these ecosystems.

Connectivity analysis among or within the modules showed that different microbial clades played different roles in the pMENs (Figure 3). From an ecological perspective, the peripherals may represent specialists, whereas module hubs and connectors may be more generalists and network hubs may be super-generalists (Olesen *et al.*, 2007; Deng *et al.*, 2012). The relatively higher abundance of *Alphaproteobacteria* and *Flavobacteria* suggest that they play crucial roles in the pMENs. The number of connectors was greater under 250, 600, and 1085 μatm pCO_2, which suggested a greater complexity in these microbial communities (Supplementary Figure S5). Larger numbers of OTUs belonging to *Alphaproteobacteria* and *Flavobacteria* were observed under 250 and 600 pCO_2. Network module hubs are another important factor in network topology. Compared with connectors, there were fewer module hubs, but they were dominated by *Gammaproteobacteria* (Supplementary Table S4). Unexpectedly, no network connectors or module hubs were detected under 175 and 860 μatm. Consistent with previous studies, no network hub was detected in any pMEN (Zhou *et al.*, 2010, 2011; Deng *et al.*, 2012). These results indicated that *Alphaproteobacteria*, *Gammaproteobacteria*, and *Flavobacteria* play an important role in maintaining the stability of microbial ecosystems in these mesocosms.

The Mantel test was performed to investigate the correlation between environmental variables and micro-organism interactions. The OTU significance (*GS*) in the pMENs were calculated, which were defined as the square of the Pearson correlation coefficient (r^2) of OTU abundance profile with environmental traits (Deng *et al.*, 2012), and did not significantly correlate with either biological or chemical parameters in almost all of the pMENs, except for the 860 μatm treatment (Supplementary Table S2). Furthermore, rare individual variables were significantly correlated with the network topological properties. However, the 250 and 340 μatm pMENs were significantly correlated with particle organic phosphorus and NO_2 concentration, respectively. The 675 and 860 μatm pMENs were significantly correlated with incubation day and pH, and bacterial abundance, viral abundance, and particle organic nitrogen, respectively. These significant correlations indicated connectivity

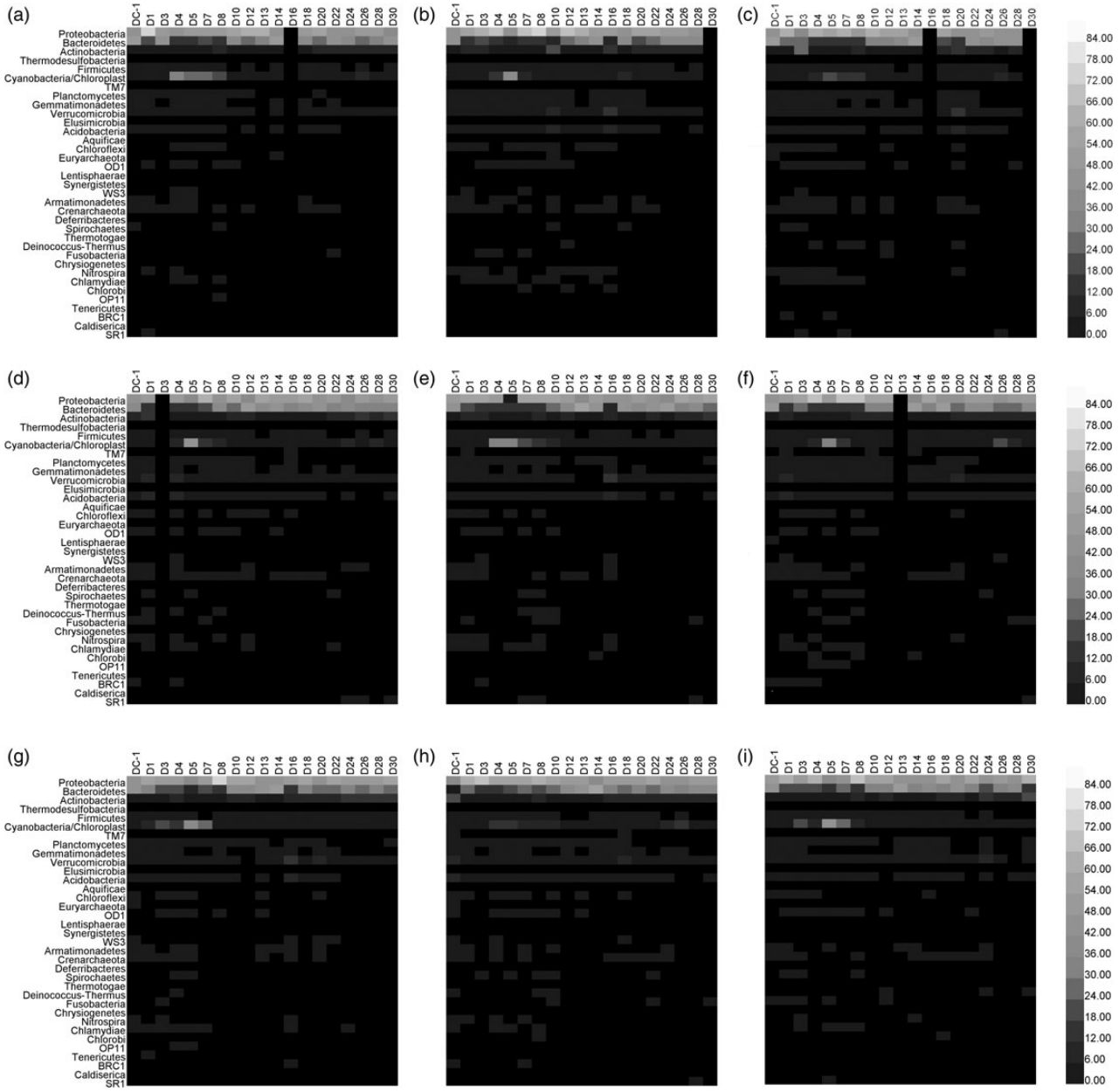

Figure 1. Heatmap of sample compositions based on the proportion of each classes. Black represents the non-detected class; colour from dark to light indicates the proportion from low to high. The pCO_2 concentrations (μatm) from A to I are 175, 180, 250, 340, 425, 600, 675, 860, and 1085. *x*-axis (D and a number) indicate the incubation day from −1 (DC-1) to day 30.

among these micro-organisms under 860 μatm pCO_2 because both were significantly associated with changes in biological and geochemical variables. However, there was no clear trend in these correlations between topology properties and environmental variables along the pCO_2 gradient, which suggested that elevated pCO_2 had little effect on the global interaction properties. Mantel analysis was also used to investigate the correlation between environmental variables and pMEN microbial composition. Similarly, the Mantel test results between pMEN topology and environmental variables revealed that few OTUs were significantly correlated with environmental variables (Supplementary Table S3). *Cyanobacteria*/chloroplast were significantly correlated with environmental properties under the 180 and 1085 μatm pCO_2 treatments. *Betaproteobacteria* and *Gammaoproteobacteria* were significant in the 675 μatm pCO_2 pMEN. These results indicated that *Proteobacteria* were more sensitive to changes in marine variables, especially under high pCO_2. They also indicated that no specific bacteria was significantly correlated with changes in either environmental variables or pCO_2 concentrations.

Discussion

Understanding the response of bacterioplankton communities to elevated pCO_2 is important for evaluating climate change effects on the ocean ecosystem. However, how the marine bacteria respond to elevated pCO_2 and decreased pH is not well understood and remains controversial (Liu *et al.*, 2010; Joint *et al.*, 2011). The EPOCA mesocosm experiments have provided a great opportunity to answer this critical question at the community-level (Riebesell *et al.*, 2013b). The present study surveyed bacterioplankton communities by MiSeq

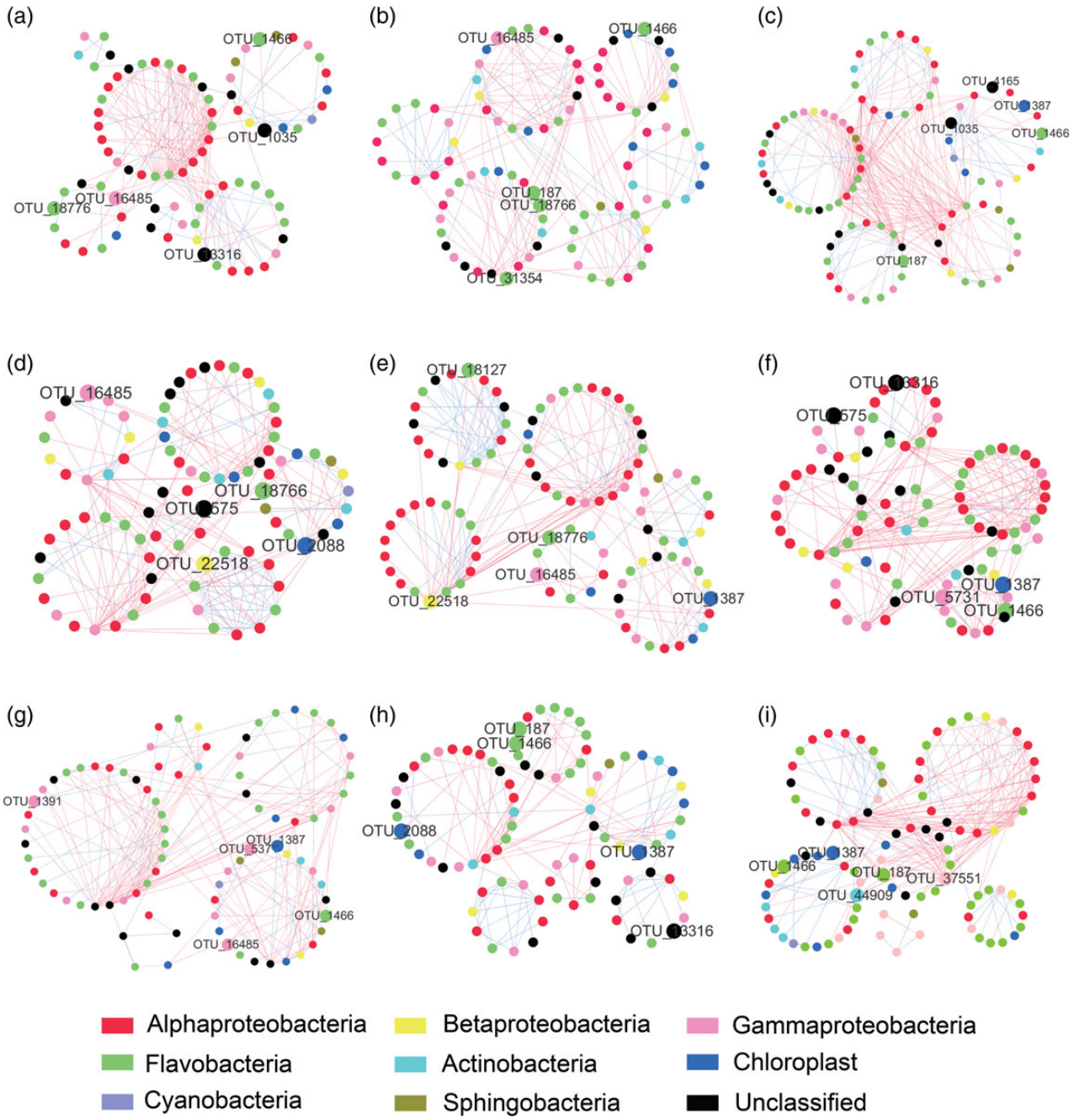

Figure 2. Bacterioplankton network interactions under 175 (a), 180 (b), 250 (c), 340 (d), 425 (e), 600 (f), 675 (g), 860 (h), and 1085 (i) µatm pCO_2. Five to seven modules were formed under different pCO_2 concentrations. Each node represents an out, which signified a species. Node colours indicate different phyla. Each line connects two OTUs. A blue line indicates a positive interaction between two individual nodes suggesting a mutualism or cooperation, while a red line indicates a negative interaction suggesting predation or competition. Top five highest-abundance OTUs are indicated by bigger dots and marked with OTU identification numbers. The cycle composed of several nodes is a module in the pMEN, which is more correlated in a module than between other modules. Only the module containing more than five OTUs are displayed.

sequencing of 16S rRNA gene amplicons and RMT-based ecological network analysis. Previous studies have demonstrated that phytoplankton respond significantly to elevated pCO_2 (Riebesell *et al.*, 2013a, b; Schulz *et al.*, 2013). Moreover, primary production and bacterial protein production are simultaneously stimulated by elevated pCO_2 (Engel *et al.*, 2013; Motegi *et al.*, 2013; Piontek *et al.*, 2013), which generally results in net production decreases by the end of incubation experiments (Engel *et al.*, 2013). Our results indicated that the phylogenetic diversity and structure of bacterioplankton communities were generally similar among different pCO_2 treatments, which is consistent with previous EPOCA bacterial community investigations (Roy *et al.*, 2013; Sperling *et al.*, 2013). Furthermore, the pMEN analysis suggested that the bacterioplankton community did not respond significantly to elevated pCO_2 at the community level, which means that our study agreed with the null hypothesis that changes in pCO_2 concentration have little

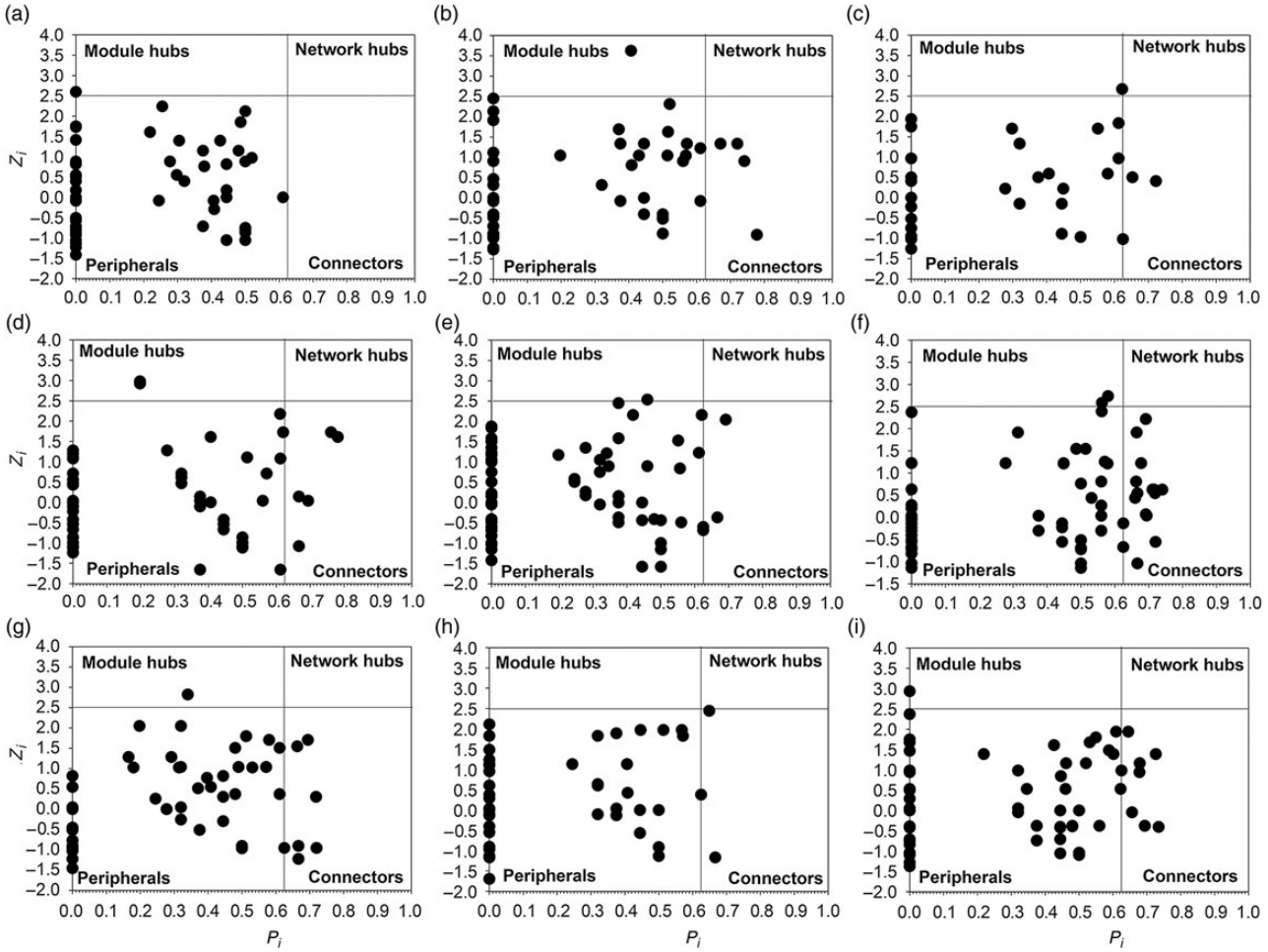

Figure 3. pMEN submodules under nine different pCO_2 treatments. Each dot represents an OTU from nine different pCO_2 treatments (a – i indicate pCO_2 concentration from 175 to 1085 μatm). The $Z-P$ plot showing OTU distribution based on their module-based topological role according to within-module (Z) and among-module (P) connectivity. The nodes of $Z_i > 2.5$ and $P_i < 0.625$ are indicated as the module hubs that were more closely connected within the module, while the nodes of $Z_i < 2.5$ and $P_i > 0.625$ are the connectors that were more closely connected to nodes in other modules. Peripherals of $Z_i < 2.5$ and $P_i < 0.625$ are considered specialists in each module, while the network hubs of $Z_i > 2.5$ and $P_i > 0.625$ are super-generalists.

influence on the affected microbial communities (Joint *et al.*, 2011) and the bacterioplankton community had a certain resilience to the pCO_2 perturbations. The present study provides novel insights into how bacterioplankton communities respond to ongoing pCO_2 increases.

Generally, high diversity is thought to allow bacterial communities to resist disturbance, this is known as the "insurance effect" (Boles *et al.*, 2004). Joint *et al.* (2011) suggested that high diversity is one of the mechanisms employed by bacterioplankton resist to elevated pCO_2 and decreased pH. Besides, micro-organisms do not live in isolation but form complex ecological interaction webs, which are also closely related to community stability (Faust and Raes, 2012). Changes global interactions (e.g. connectivity and modularity) among bacterioplankton communities along the pCO_2 gradient were unclear in the present study (Table 2 and Figure 2). These results suggested that the community interaction webs were relatively stable, despite the pCO_2 changes. In an ecological network, a negative correlation suggests a competitive relationship between species (Faust and Raes, 2012). The competition between species should yield less variation in total abundance or biomass, known as compensatory dynamics (Gonzalez and Loreau, 2009). A community with more competitors would be more stable under environmental fluctuations through maintaining relatively low covariations in community densities (Ives and Hughes, 2002). Klug *et al.* (2000) conducted a microcosm experiment and suggested strong compensatory dynamics when plankton were directly affected by pH perturbations. Furthermore, the competition might increase both the amplitude and asynchrony of population fluctuations generated by the asynchrony in species responses to the environment, which is the basis for functional compensation between species and potentially stabilizes aggregate community or ecosystem properties (Loreau, 2010). Ecosystem modelling indicates that asynchrony in species intrinsic rates of natural increase could stabilize the community (Fowler *et al.*, 2012). Therefore, the dominant competitive relationships observed in our study (Figure 2) might sustain population diversity and enhance ecosystem resilience to perturbations.

Additionally, the high modularity observed in our study (Table 2) might result in a more complex ecosystem that would be more stable than dispersal ecosystems. Because of the tighter

Table 2. Topological properties of the microbial communities' phylogenic molecular networks under nine pCO_2 concentrations and their rewired random networks.

	Experimental networks								Random networks		
pCO_2 (μatm)	Cut-off	Total nodes	Total links	R^2 of power-law	Avg. connectivity	Avg. geodesic distance	Avg. clustering coefficient	Modularity	Avg. geodesic distance	Avg. clustering coefficient	Avg. modularity
175	0.85	86	187	0.843	4.349	4.088[a]	0.224[a]	0.452[a]	2.941 ± 0.136	0.133 ± 0.021	0.384 ± 0.010
180	0.84	99	185	0.878	3.737	3.572[a]	0.177[a]	0.558[a]	3.153 ± 0.178	0.076 ± 0.018	0.454 ± 0.011
250	0.84	108	315	0.836	5.833	2.281[a]	0.218[a]	0.330[a]	2.629 ± 0.146	0.180 ± 0.017	0.303 ± 0.008
340	0.84	92	186	0.850	4.043	3.062[a]	0.213[a]	0.561[a]	3.642 ± 0.153	0.157 ± 0.023	0.442 ± 0.011
425	0.84	116	226	0.850	3.897	2.773[a]	0.243[a]	0.592[a]	3.164 ± 0.189	0.068 ± 0.014	0.451 ± 0.010
600	0.84	113	219	0.887	3.876	2.488[a]	0.079[a]	0.453[a]	2.909 ± 0.227	0.068 ± 0.013	0.442 ± 0.009
675	0.84	100	215	0.801	4.300	2.692[a]	0.178[a]	0.465[a]	2.974 ± 0.167	0.082 ± 0.017	0.411 ± 0.010
860	0.85	95	154	0.870	3.242	3.435[a]	0.148[a]	0.638[a]	3.275 ± 0.256	0.047 ± 0.015	0.513 ± 0.015
1085	0.84	99	245	0.831	4.949	2.965[a]	0.293[a]	0.461[a]	2.838 ± 0.114	0.141 ± 0.019	0.357 ± 0.010

[a]Significant difference between experimental network and random network by the *t*-test ($p < 0.001$).

interactions between nodes within the modules, the disturbances that influenced these nodes were unlikely to spread to other modules. For example, the OTU_1466 in the 175 μatm pMEN only connected with nodes within that module, hence the abundance variation of OTU_1466 must affect more than two nodes to spread this variation to other modules (Figure 2). The extinction of a module hub might cause the module to fragment, having little or no cascading impact on other modules. In contrast, the extinction of connectors might cause the network to fragment but with minor impacts on the interactions within the isolated modules (Olesen *et al.*, 2007). Therefore, compared with a non-modular structure, a modular structure should dampen the rapid spread of disturbance in a community (Olesen *et al.*, 2007). Since each module in a pMEN indicates an ecological niche (Chaffron *et al.*, 2010), our observation that negative relationships dominated between rather than within the modules suggested that the variations within a niche did not affect community stability. Therefore, competitive relationships and the modular structure of bacterioplankton communities provided resistance to variations in pCO_2 in the present mesocosm experiment. However, previous studies have shown that interactions among soil bacterial communities are influenced by elevated atmospheric CO_2 over a longer time-scale (i.e. annually; Zhou *et al.*, 2010, 2011; Tu *et al.*, 2015). Whether or not marine bacterioplankton also respond to long-term pCO_2 changes is worthy of investigation.

In an ecological network, the module hubs and connecters are considered keystone species, which have a crucial role in sustaining community stability (Paine, 1969). We found a relatively larger proportion of *Gammaproteobacteria* and *Flavobacteria* in pMEN module hubs and connectors in our study (Supplementary Figure S5 and Table S4). The relative abundance of *Gammaproteobacteria* and *Flavobacteria* did not change significantly among the pCO_2 treatments (Roy *et al.*, 2013; Supplementary Figure S6) and they were not significantly correlated with geochemical variables under elevated pCO_2. Therefore, these stable keystone species likely provided stability to the entire bacterial community. Monier *et al.* (2014) found the relative abundance of two groups of *Gammaproteobacteria* (*Alteromonadales* and *Oceanospirillales*) responded significantly to variations in pCO_2 in the north Arctic Ocean, but they did not respond significantly to decreased pH in terms of general phylogenetic structure. In our experiment, these potentially sensitive groups were not the major components and only a few OTUs belonging to these two *Gammaproteobacteria* groups were found in nine pMENs. Furthermore, we did not observe a clear trend in the interaction between the *Gammaproteobacteria* and their closest neighbours with elevated pCO_2 (Supplementary Figures S7 and S8).

Despite their general structure, bacterioplankton communities were insensitive to elevated pCO_2 in the EPOCA experiments, the low abundance species had the potential to respond to elevated pCO_2. Roy *et al.* (2013) found that some rare species, like *Methylotenera*, *Fluviicola* and *Colwellia*, were significantly correlated with changes in pCO_2. However, only a few of these bacterioplankton appeared within the nine pMENs in our analysis. For example, *Colwellia* appeared in the high pCO_2 treatment at the end of the incubation period, but was almost non-existent before that (Roy *et al.*, 2013; Supplementary Figure S9). Because variations in keystone species have a greater impact on ecosystem stability and resilience than rare species (Paine, 1969), we used the major components of the bacterioplankton community to construct the networks.

Elevated pCO_2 had increased the POC and dissolved organic carbon (DOC) production by the end of the incubation period; therefore, bacterial protein activity and production were also stimulated (Motegi *et al.*, 2013; Piontek *et al.*, 2013). However, bacterial production, respiration, and growth efficiency were similar over the incubation period among the different pCO_2 treatments, which suggested that elevated pCO_2 had little impact on bacterial metabolism at the community level (Motegi *et al.*, 2013). Previous meta-analyses have found no evidence that bacterial community growth efficiency is stimulated by elevated pCO_2 (Liu *et al.*, 2010; Motegi *et al.*, 2013). We did not find any significant correlation between network topology and bacterial production (except for the 675 μatm treatment) and picophytoplankton abundance change. These results suggested that primary production stimulation had little influence on these keystone components. In fact, the variations in DOC and POC production during the incubation were greater those among the different pCO_2 levels (Engel *et al.*, 2013). This is perhaps partially explained by the insignificant network response to pCO_2 among different mesocosms. However, another possible reason is different bacterial assemblage living strategies, i.e. free-living vs. particle-attached. Allgaier *et al.* (2008) reported that the free-living fraction of a bacterioplankton community was significantly correlated with elevated pCO_2 in a temperate fjord in Norway. However, the dynamics of the bacterioplankton community particle-attached fraction, compared with the free-

living fraction, had a strong relationship with phytoplankton bloom, and exhibited a higher richness at the end of the incubation period in the EPOCA experiments (Sperling *et al.*, 2013). The richness of the free-living fraction, however, decreased at the same time (Sperling *et al.*, 2013). Thus, we would expect that the networks based upon entire bacterioplankton communities in the present study could not reflect the response of particle-attached bacteria to pCO_2 changes. Additionally, the lower bacterial abundance during this period combined with increased viral lysis in the higher pCO_2 mesocosm suggested top-down control on bacterial production (Brussaard *et al.*, 2013), which might also not have reflected pMENs and suggested the importance of top-down control during this experiment. Therefore, the network analysis involved in both bacterioplankton and virioplankton, even zooplankton, would provide a more comprehensive explanation of the future effect of elevated pCO_2 in the ocean.

A few studies have found that decreased pH significantly influences specific bacterial groups in various oceans (Krause *et al.*, 2012; Maas *et al.*, 2013). However, their results were not consistent with ours; this might have been because of the difference between pH manipulations by HCl and CO_2. Manipulation with HCl, which modifies the total alkalinity (TA) and pH with constant dissolved inorganic carbon (DIC), is not the most accurate approach to mimic future carbonate chemistry (Hurd *et al.*, 2009; Krause *et al.*, 2012). In contrast, CO_2 addition induces a pH decrease and DIC increase when TA is constant (Hurd *et al.*, 2009). Even the carbonate chemistry parameters were similar between both manipulation methods when pCO_2 $<$700 ppm (Hurd *et al.*, 2009). However, when pH was modified to 7.5 by HCl, the [HCO_3^-] value was 22% lower compared with the pH value obtained by pCO_2 manipulation (Hurd *et al.*, 2009). The previous study has demonstrated that this difference in DIC affects some algal groups, e.g. those lacking a carbon-concentrating mechanism exhibited lower growth rate in pH 7.5 by HCl manipulation compared with pCO_2 manipulation (Hurd *et al.*, 2009). Yet, the impact of this difference on the bacterioplankton is still unclear. Because mixotrophic micro-organisms are widespread carbon in the world's oceans (Hugler and Sievert, 2010), methodological differences may have affected the response of bacteria to changes in pH. Thus, pCO_2 manipulation is the most appropriate method available to mimic future changes in oceanic carbonate chemistry.

Conclusion

The hypothesis that "marine microbes possess the flexibility to accommodate pH change" is primarily based on the observation that microbial populations confront large variations in pH, both short-term and seasonally, in marine environments (Joint *et al.*, 2011). This hypothesis is supported by recent studies at the microbial community level (Allgaier *et al.*, 2008; Newbold *et al.*, 2012; Roy *et al.*, 2013; Sperling *et al.*, 2013; Zhang *et al.*, 2013). In combination with the present study, these data suggest that a larger population size and higher diversity within a microbial community contribute to the resistance of communities to high pCO_2. Additionally, our network analysis provides further evidence that complex interactions (e.g. interspecies competition and modularity) among individual microbial species in a natural population help microbes resist and recover from pH and pCO_2 disturbances. This could explain the contradictory observations between OA effects on single species (e.g. pure culture) and natural marine microbe populations.

Supplementary data

Supplementary material is available at the *ICESJMS* online version of the manuscript.

Acknowledgements

This work is a contribution to the European Project on Ocean Acidification (EPOCA), which is funded by the European Community's Seventh Framework Programme (FP7/2007–2013) under grant agreement no. 211384. We gratefully acknowledge Greenpeace International for assistance with the transport of the mesocosm facility from Kiel to Ny-Ålesund and back. We also thank the captains and crews of M/V ESPERANZA (Greenpeace) and RV Viking Explorer [University Centre in Svalbard (UNIS)] for assistance during mesocosm transport, deployment, and recovery in Kongsfjord. We thank Liyou Wu, Chongqing Wen, Lanlan Cai, and Kanagarajan Umapathy for their assistance during this study. This work was supported by the NSFC (41522603), the SOA Project (GASI-03-01-02-05) and the 973 project (2013CB955700). RZ was partially supported by GCMAC1408 and IC201504.

References

Allgaier, M., Riebesell, U., Vogt, M., Thyrhaug, R., and Grossart, H. P. 2008. Coupling of heterotrophic bacteria to phytoplankton bloom development at different pCO_2 levels: a mesocosm study. Biogeosciences, 5: 1007–1022.

Alter, O., Brown, P. O., and Botstein, D. 2000. Singular value decomposition for genome-wide expression data processing and modeling. Proceedings of the National Academy of Sciences of the United States of America, 97: 10101–10106.

Assenov, Y., Ramírez, F., Schelhorn, S-E. E., Lengauer, T., and Albrecht, M. 2008. Computing topological parameters of biological networks. Bioinformatics, 24: 282–284.

Azam, F. 1998. Microbial control of oceanic carbon flux: the plot thickens. Science, 280: 694–696.

Baragi, L., Khandeparker, L., and Anil, A. 2015. Influence of elevated temperature and pCO_2 on the marine periphytic diatom *Navicula distans* and its associated organisms in culture. Hydrobiologia, 1–16.

Bascompte, J., Jordano, P., Melián, C. J., and Olesen, J. M. 2003. The nested assembly of plant-animal mutualistic networks. Proceedings of the National Academy of Sciences of the United States of America, 100: 9383–9387.

Boles, B. R., Thoendel, M., and Singh, P. K. 2004. Self-generated diversity produces "insurance effects" in biofilm communities. Proceedings of the National Academy of Sciences of the United States of America, 101: 16630–16635.

Bowen, J. L., Kearns, P. J., Holcomb, M., and Ward, B. B. 2013. Acidification alters the composition of ammonia-oxidizing microbial assemblages in marine mesocosms. Marine Ecology Progress Series, 492: 1–8.

Brussaard, C. P. D., Noordeloos, A. A. M., Witte, H., Collenteur, M. C. J., Schulz, K. G., Ludwig, A., and Riebesell, U. 2013. Arctic microbial community dynamics influenced by elevated CO_2 levels. Biogeosciences, 10: 719–731.

Caporaso, J. G., Bittinger, K., Bushman, F. D., DeSantis, T. Z., Andersen, G. L., and Knight, R. 2009. PyNAST: a flexible tool for aligning sequences to a template alignment. Bioinformatics, 26: 266–267.

Caporaso, J. G., Lauber, C. L., Walters, W. A., Berg-Lyons, D., Huntley, J., Fierer, N., Owens, S. M., *et al.* 2012. Ultra-high-throughput microbial community analysis on the Illumina HiSeq and MiSeq platforms. The ISME Journal, 6: 1621–1624.

Caporaso, J. G., Lauber, C. L., Walters, W. A., Berg-Lyons, D., Lozupone, C. A., Turnbaugh, P. J., Fierer, N., *et al.* 2010. Global patterns of 16S rRNA diversity at a depth of millions of sequences per sample.

Proceedings of the National Academy of Sciences of the United States of America, 108(Suppl. 1): 4516–4522.

Chaffron, S., Rehrauer, H., Pernthaler, J., and von Mering, C. 2010. A global network of coexisting microbes from environmental and whole-genome sequence data. Genome Research, 20: 947–959.

Chow, C. E., Kim, D. Y., Sachdeva, R., Caron, D. A., and Fuhrman, J. A. 2014. Top-down controls on bacterial community structure: microbial network analysis of bacteria, T4-like viruses and protists. The ISME Journal, 8: 816–829.

Chow, C-E. T. E., Sachdeva, R., Cram, J. A., Steele, J. A., Needham, D. M., Patel, A., Parada, A. E., *et al.* 2013. Temporal variability and coherence of euphotic zone bacterial communities over a decade in the Southern California Bight. The ISME Journal, 7: 2259–2273.

Deng, Y., Jiang, Y-H., Yang, Y., He, Z., Luo, F., and Zhou, J. 2012. Molecular ecological network analyses. BMC Bioinformatics, 13: 113.

Edgar, R. C., Haas, B. J., Clemente, J. C., Quince, C., and Knight, R. 2011. UCHIME improves sensitivity and speed of chimera detection. Bioinformatics, 27: 2194–2200.

Elton, C. S. 1927. Animal Ecology. Macmillan Co., New York.

Engel, A., Borchard, C., Piontek, J., Schulz, K. G., Riebesell, U., and Bellerby, R. 2013. CO_2 increases ^{14}C primary production in an Arctic plankton community. Biogeosciences, 10: 1291–1308.

Faust, K., and Raes, J. 2012. Microbial interactions: from networks to models. Nature Reviews Microbiology, 10: 538–550.

Fowler, M. S., Laakso, J., Kaitala, V., Ruokolainen, L., Ranta, E., and Post, D. 2012. Species dynamics alter community diversity–biomass stability relationships. Ecology Letters, 15: 1387–1396.

Gonzalez, A., and Loreau, M. 2009. The causes and consequences of compensatory dynamics in ecological communities. Annual Review of Ecology, Evolution, and Systematics, 40: 393–414.

Hiwatari, T., Yuzawa, A., Okazaki, M., Yamamoto, M., Akano, T., and Kiyohara, M. 1995. Effects of CO_2 concentrations on growth in the coccolithophorids (haptophyta). Energy Conversion and Management, 36: 779–782.

Huesemann, M. H., Skillman, A. D., and Crecelius, E. A. 2002. The inhibition of marine nitrification by ocean disposal of carbon dioxide. Marine Pollution Bulletin, 44: 142–148.

Hugler, M., and Sievert, S. M. 2010. Beyond the Calvin cycle: autotrophic carbon fixation in the ocean. Annual Review of Marine Science, 3: 261–289.

Hurd, C. L., Hepburn, C. D., Currie, K. I., Raven, J. A., and Hunter, K. A. 2009. Testing the effects of ocean acidification on algal metabolism: considerations for experimental designs. Journal of Phycology, 45: 1236–1251.

IPCC. 2015. IPCC, 2014: Climate Change 2014: Synthesis Report. Contribution of Working Groups I, II and III to the Fifth Assessment Report of the Intergovernmental Panel on Climate Change. IPCC, Geneva, Switzerland. 151 pp.

Ives, A. R., and Hughes, J. B. 2002. General relationships between species diversity and stability in competitive systems. The American Naturalist, 159: 388–395.

Jiang, Z. J., Huang, X. P., and Zhang, J. P. 2010. Effects of CO_2 enrichment on photosynthesis, growth, and biochemical composition of seagrass *Thalassia hemprichii* (Ehrenb.) Aschers. Journal of Integrative Plant Biology, 52: 904–913.

Jiao, N., Herndl, G. J., Hansell, D. A., Benner, R., Kattner, G., Wilhelm, S. W., Kirchman, D. L., *et al.* 2010. Microbial production of recalcitrant dissolved organic matter: long-term carbon storage in the global ocean. Nature Reviews Microbiology, 8: 593–599.

Joint, I., Doney, S. C., and Karl, D. M. 2011. Will ocean acidification affect marine microbes? The ISME Journal, 5: 1–7.

Klug, J. L., Fischer, J. M., Ives, A. R., and Dennis, B. 2000. Compensatory dynamics in planktonic community responses to pH perturbations. Ecology, 81: 387–398.

Kong, Y. 2011. Btrim: a fast, lightweight adapter and quality trimming program for next-generation sequencing technologies. Genomics, 98: 152–153.

Krause, E., Wichels, A., Giménez, L., Lunau, M., Schilhabel, M. B., and Gerdts, G. 2012. Small changes in pH have direct effects on marine bacterial community composition: a microcosm approach. PLoS One, 7: e47035.

Labare, M. P., Bays, J. T., Butkus, M. A., Snyder-Leiby, T., Smith, A., Goldstein, A., Schwartz, J. D., *et al.* 2010. The effects of elevated carbon dioxide levels on a Vibrio sp. isolated from the deep-sea. Environonmental Science and Pollution Research International, 17: 1009–1015.

Li, W., and Godzik, A. 2006. CD-HIT: a fast program for clustering and comparing large sets of protein or nucleotide sequences. Bioinformatics, 22: 1658–1659.

Liu, J. W., Weinbauer, M. G., Maier, C., Dai, M. H., and Gattuso, J. P. 2010. Effect of ocean acidification on microbial diversity and on microbe-driven biogeochemistry and ecosystem functioning. Aquatic Microbial Ecology, 61: 291–305.

Loreau, M. 2010. From Populations to Ecosystems: Theoretical Foundations for a New Ecological Synthesis. Princeton University Press, Princeton.

Lozupone, C., Hamady, M., and Knight, R. 2006. UniFrac—an online tool for comparing microbial community diversity in a phylogenetic context. BMC Bioinformatics, 7: 371.

Lozupone, C., and Knight, R. 2005. UniFrac: a new phylogenetic method for comparing microbial communities. Applied and Environmental Microbiology, 71: 8228–8235.

Lozupone, C., and Knight, R. 2007. Global patterns in bacterial diversity. Proceedings of the National Academy of Sciences of the United States of America, 104: 11436–11440.

Lv, J., Kuang, Y., Zhao, H., and Andersson, A. 2015. Patterns of coccolithophore pigment change under global acidification conditions based on in-situ observations at BATS site between July 1990–Dec 2008. Frontiers of Earth Science, doi: 10.1007/s11707-015-0503-x.

Maas, E. W., Law, C. S., Hall, J. A., Pickmere, S., Currie, K. I., Chang, F. H., Voyles, K. M., *et al.* 2013. Effect of ocean acidification on bacterial abundance, activity and diversity in the Ross Sea, Antarctica. Aquatic Microbial Ecology, 70: 1–15.

Memmott, J., Waser, N. M., and Price, M. V. 2004. Tolerance of pollination networks to species extinctions. Proceedings of the Royal Society B: Biological Sciences, 271: 2605–2611.

Michael, P. L., Bays, J. T., Michael, A. B., Teresa, S-L., Alicia, S., Amanda, G., Jenna, D. S., *et al.* 2010. The effects of elevated carbon dioxide levels on a Vibrio sp. isolated from the deep-sea. Environmental Science and Pollution Research, 17: 1009–1015.

Monier, A., Findlay, H. S., Charvet, S., and Lovejoy, C. 2014. Late winter under ice pelagic microbial communities in the high Arctic Ocean and the impact of short-term exposure to elevated CO_2 levels. Frontiers in Microbiology, 5: 490.

Montoya, J. M., Pimm, S. L., and Solé, R. V. 2006. Ecological networks and their fragility. Nature, 442: 259–264.

Morgan, N. P., Paramvir, S. D., and Adam, P. A. 2010. FastTree 2—approximately maximum-likelihood trees for large alignments. PLoS One, 5: e9490.

Motegi, C., Tanaka, T., Piontek, J., Brussaard, C. P. D., Gattuso, J. P., and Weinbauer, M. G. 2013. Effect of CO_2 enrichment on bacterial metabolism in an Arctic fjord. Biogeosciences, 10: 3285–3296.

Newbold, L. K., Oliver, A. E., Booth, T., Tiwari, B., Desantis, T., Maguire, M., Andersen, G., *et al.* 2012. The response of marine picoplankton to ocean acidification. Environmental Microbiology, 14: 2293–2307.

Newman, M. E. J. 2006a. Finding community structure in networks using the eigenvectors of matrices. Physical Review E, 74: 036104-1–036104-19.

Newman, M. E. J. 2006b. Modularity and community structure in networks. Proceedings of the National Academy of Sciences of the United States of America, 103: 8577–8582.

Nisumaa, A. M., Pesant, S., Bellerby, R. G. J., Delille, B., Middelburg, J. J., Orr, J. C., Riebesell, U., *et al.* 2010. EPOCA/EUR-OCEANS data compilation on the biological and biogeochemical responses to ocean acidification. Earth System Science Data, 2: 167–175.

Olesen, J. M., Bascompte, J., Dupont, Y. L., and Jordano, P. 2007. The modularity of pollination networks. Proceedings of the National Academy of Sciences of the United States of America, 104: 19891–19896.

Oliver, A. E., Newbold, L. K., Whiteley, A. S., and van der Gast, C. J. 2014. Marine bacterial communities are resistant to elevated carbon dioxide levels. Environmental Microbiology Reports, 6: 574–582.

Paine, R. T. 1969. A note on trophic complexity and community stability. The American Naturalist, 103: 91.

Paine, R. T. 1980. Food webs—linkage, interaction strength and community infrastructure—the 3rd Tansley Lecture. Journal of Animal Ecology, 49: 667–685.

Piontek, J., Borchard, C., Sperling, M., Schulz, K. G., Riebesell, U., and Engel, A. 2013. Response of bacterioplankton activity in an Arctic fjord system to elevated pCO_2: results from a mesocosm perturbation study. Biogeosciences, 10: 297–314.

Price, M. N., Dehal, P. S., and Arkin, A. P. 2009. FastTree: computing large minimum evolution trees with profiles instead of a distance matrix. Molecular Biology and Evolution, 26: 1641–1650.

Riebesell, U., Czerny, J., Bröckel, K. V., Boxhammer, T., Büdenbender, J., Deckelnick, M., Fischer, M., *et al.* 2013a. Technical note: a mobile sea-going mesocosm system—new opportunities for ocean change research. Biogeosciences, 10: 1835–1847.

Riebesell, U., Gattuso, J. P., Thingstad, T. F., and Middelburg, J. J. 2013b. Preface "Arctic ocean acidification: pelagic ecosystem and biogeochemical responses during a mesocosm study". Biogeosciences, 10: 5619–5626.

Riebesell, U., Wolf-Gladrow, D. A., and Smetacek, V. 1993. Carbon dioxide limitation of marine phytoplankton growth rates. Nature, 361: 249–251.

Roy, A. S., Gibbons, S. M., Schunck, H., Owens, S., Caporaso, J. G., Sperling, M., Nissimov, J. I., *et al.* 2013. Ocean acidification shows negligible impacts on high-latitude bacterial community structure in coastal pelagic mesocosms. Biogeosciences, 10: 555–566.

Schulz, K. G., Bellerby, R. G. J., Brussaard, C. P. D., Budenbender, J., Czerny, J., Engel, A., Fischer, M., *et al.* 2013. Temporal biomass dynamics of an Arctic plankton bloom in response to increasing levels of atmospheric carbon dioxide. Biogeosciences, 10: 161–180.

Sherr, E., and Sherr, B. 2008. Understanding roles of microbes in marine pelagic food webs: a brief history. *In* Microbial Ecology of the Oceans, pp. 27–44. Ed. by D. L. Kirchman. John Wiley & Sons, Inc., Hoboken, New Jersey.

Sole, R. V., and Montoya, J. M. 2001. Complexity and fragility in ecological networks. Proceedings of the Royal Society B: Biological Sciences, 268: 2039–2045.

Sperling, M., Piontek, J., Gerdts, G., Wichels, A., Schunck, H., Roy, A. S., Roche, J. L., *et al.* 2013. Effect of elevated CO_2 on the dynamics of particle-attached and free-living bacterioplankton communities in an Arctic fjord. Biogeosciences, 10: 181–191.

Steele, J. A., Countway, P. D., Xia, L., Vigil, P. D., Beman, J. M., Kim, D. Y., Chow, C-E. T. E., *et al.* 2011. Marine bacterial, archaeal and protistan association networks reveal ecological linkages. The ISME Journal, 5: 1414–1425.

Takeuchi, K., Fujioka, Y., Kawasaki, Y., and Shirayama, Y. 1997. Impacts of high concentration of CO_2 on marine organisms; a modification of CO_2 ocean sequestration. Energy Conversion and Management, 38: S337–S341.

Tan, S., Zhou, J., Zhu, X., Yu, S., Zhan, W., Wang, B., Cai, Z., *et al.* 2015. An association network analysis among microeukaryotes and bacterioplankton reveals algal bloom dynamics. Journal of Phycology, 51: 120–132.

Tanaka, T., Thingstad, T. F., Løvdal, T., Grossart, H. P., Larsen, A., Allgaier, M., Meyerhöfer, M., *et al.* 2008. Availability of phosphate for phytoplankton and bacteria and of glucose for bacteria at different pCO_2 levels in a mesocosm study. Biogeosciences, 5: 669–678.

Taucher, J., Jones, J., James, A., Brzezinski, M. A., Carlson, C. A., Riebesell, U., and Passow, U. 2015. Combined effects of CO_2 and temperature on carbon uptake and partitioning by the marine diatoms *Thalassiosira weissflogii* and *Dactyliosolen fragilissimus*. Limnology and Oceanography, 60: 901–919.

Teira, E., Fernández, A., Álvarez-Salgado, X. A., García-Martín, E. E., Serret, P., and Sobrino, C. 2012. Response of two marine bacterial isolates to high CO_2 concentration. Marine Ecology Progress Series, 453: 27–36.

Tu, Q., Yuan, M., He, Z., Deng, Y., Xue, K., Wu, L., Hobbie, S. E., *et al.* 2015. Fungal communities respond to long-term CO_2 elevation by community reassembly. Applied and Environmental Microbiology, 81: 2445–2454.

Wang, Q., Garrity, G. M., Tiedje, J. M., and Cole, J. R. 2007. Naive Bayesian classifier for rapid assignment of rRNA sequences into the new bacterial taxonomy. Applied and Environmental Microbiology, 73: 5261–5267.

Zhang, R., Xia, X., Lau, S. C. K., Motegi, C., Weinbauer, M. G., and Jiao, N. 2013. Response of bacterioplankton community structure to an artificial gradient of pCO_2 in the Arctic Ocean. Biogeosciences, 10: 3679–3689.

Zhou, J., Deng, Y., Luo, F., He, Z., Tu, Q., and Zhi, X. 2010. Functional molecular ecological networks. MBio, 1: e00169-10.

Zhou, J., Deng, Y., Luo, F., He, Z., and Yang, Y. 2011. Phylogenetic molecular ecological network of soil microbial communities in response to elevated CO_2. MBio, 2: e00122-11.

Zhou, J., Jiang, Y. H., Deng, Y., Shi, Z., Zhou, B. Y., Xue, K., Wu, L., *et al.* 2013. Random sampling process leads to overestimation of beta-diversity of microbial communities. MBio, 4: e00324-13.

Zimmerman, R. C., Kohrs, D. G., Steller, D. L., and Alberte, R. S. 1997. Impacts of CO_2 enrichment on productivity and light requirements of eelgrass. Plant Physiology, 115: 599–607.

Handling editor: Rubao Ji

ICES Journal of Marine Science

ICES Journal of Marine Science (2016), 73(3), 876–886. doi:10.1093/icesjms/fsv157

Contribution to Special Issue: 'Towards a Broader Perspective on Ocean Acidification Research'

Original Article

The effects of long-term *in situ* CO_2 enrichment on tropical seagrass communities at volcanic vents

M. Takahashi[1,2], S. H. C. Noonan[1], K. E. Fabricius[1], and C. J. Collier[2,3]*

[1]*Australian Institute of Marine Science, PMB 3, Townsville, QLD 4810, Australia*
[2]*College of Marine and Environmental Sciences, James Cook University, Townsville, QLD 4811, Australia*
[3]*Centre for Tropical Water and Aquatic Ecosystem Research, James Cook University, Cairns, QLD 4870, Australia*

**Corresponding author: tel: +61 7 4232 1855; fax: +61 7 4781 5589; e-mail: catherine.collier@jcu.edu.au*

Takahashi, M., Noonan, S. H. C., Fabricius, K. E., and Collier, C. J. The effects of long-term *in situ* CO_2 enrichment on tropical seagrass communities at volcanic vents. – ICES Journal of Marine Science, 73: 876–886.

Received 27 April 2015; revised 24 July 2015; accepted 14 August 2015; advance access publication 7 September 2015.

The effects of long-term exposure to elevated levels of carbon dioxide (CO_2) on seagrass communities are still poorly understood. This study investigates the tropical subtidal seagrass communities at three shallow volcanic CO_2 vents in Papua New Guinea. Seagrass cover and biomass increased threefold and fivefold, respectively, from control to medium and high pCO_2 sites (average pH = 7.9, 7.7, and 7.5, respectively). The seagrass community composition differed significantly between the pCO_2 sites: *Cymodocea serrulata*, *Cymodocea rotundata*, and *Halodule uninervis* were more abundant at high pCO_2 sites, whereas *Halophila ovalis*, *Thalassia hemprichii*, and *Syringodium isoetifolium* occurred only at low and mid pCO_2 sites. *Cymodocea rotundata* was the only species common among all pCO_2 sites and locations. The $\delta^{13}C$ in its leaves significantly declined with increasing pCO_2, indicating that additional CO_2 influenced seagrass carbon uptake, and specifically, that there was discrimination against the heavier isotope (^{13}C) when carbon was more abundant. Size-specific leaf growth rates (i.e. leaf turnover) also significantly declined with increasing pCO_2; however, leaf growth rates showed no consistent difference in response to elevated pCO_2 in two of four surveys. Our study suggests that progressive ocean acidification may lead to higher cover and above- and below-ground biomass, but lower size-specific growth and altered species composition in tropical seagrass communities. The effects of co-limiting factors, such as light and nutrient availability, on early-responding parameters, such as growth rates, require further attention to improve projections.

Keywords: biomass, Cymodocea, growth, ocean acidification, seagrass.

Introduction

Rising atmospheric carbon dioxide (CO_2) concentrations have reduced average sea surface pH from 8.2 to 8.1 units since the Industrial Revolution (Raven *et al.*, 2005). It is projected that accelerating carbon emissions by anthropogenic activity will reduce ocean surface pH by 0.3 units by 2100 (IPCC, 2014), and up to 0.77 units by 2300 (Caldeira and Wickett, 2003). Evidence is strengthening that ocean acidification (OA) will exert significant and at times unexpected effects on marine ecosystems; for instance, the performance of calcareous organisms, such as corals and echinoderms, are expected to be negatively impacted, whereas photosynthetic organisms, such as seagrass and algae, may benefit from the increasing pCO_2 which is an essential resource for their photosynthesis and survival (Fabricius *et al.*, 2011; Koch *et al.*, 2013; Russell *et al.*, 2013).

Seagrass meadows are one of the most important ecosystems in the coastal zone, providing food and habitat to many species (Bostrom and Mattila, 1999). Seagrasses also play a significant role in the global oceans' carbon budget (Costanza *et al.*, 1997; Duarte *et al.*, 2013). It is estimated that seagrass captures ~27.4 Tg C $year^{-1}$ (Fourqurean *et al.*, 2012) and global meadows account for 15% of the World's "blue carbon" (the carbon sequestered and stored by marine biota; Duarte and Chiscano, 1999). Globally, seagrass meadows have been declining at an accelerating rate and are now being lost at a rate of 7% $year^{-1}$ primarily because of coastal development and subsequent declines in water quality (Waycott *et al.*, 2009). Due to the rapid, significant global loss of such an ecologically important ecosystem and the increasing certainty of OA projections, there is an urgent need to better understand the effects of OA on seagrasses.

Laboratory studies have shown increases in biomass (Palacios and Zimmerman, 2007), photosynthesis, and leaf growth rates in seagrass when exposed to CO_2-enriched water (elevated partial pressure—pCO_2; Zimmerman *et al.*, 1995, 1997; Invers *et al.*, 2001; Jiang *et al.*, 2010). Seagrasses grown in water with elevated pCO_2 also contained more carbon, as non-structural carbohydrates in their leaves and below-ground biomass (Zimmerman *et al.*, 1997; Jiang *et al.*, 2010; Campbell and Fourqurean, 2013b), which are important energy reserves to sustain growth and improve survival during prolonged unfavourable conditions, such as low light (Ralph *et al.*, 2007; Collier *et al.*, 2009). These results suggest that seagrasses in the current environment can be carbon limited (Beer and Koch, 1996; Invers *et al.*, 2001) and that increases in oceanic pCO_2 under OA may prove beneficial for some seagrass populations.

The results of CO_2 enrichment experiments may not always be extrapolated to predict the *in situ* long-term responses of seagrass to OA. For example, 40% higher growth rates of seagrasses were measured after 14–21 d of acclimation in CO_2-enriched water (Jiang *et al.*, 2010), whereas no significant changes were observed after medium-term enrichment (6 months; Campbell and Fourqurean, 2013b; 1 year; Palacios and Zimmerman, 2007). Conversely, the 6 months *in situ* experiment conducted by Campbell and Fourqurean (2013b) did not detect changes in seagrass shoot density, while shoot densities were two to four times higher around volcanic CO_2 vents, where seagrass have been exposed to elevated pCO_2 for decades or centuries (Hall-Spencer *et al.*, 2008; Fabricius *et al.*, 2011; Russell *et al.*, 2013). These contradicting results emphasize the importance of studying the future chronic effects of OA on seagrasses in settings that facilitate long-term pCO_2 exposure.

At three volcanic CO_2 vents in Milne Bay Province, Papua New Guinea (PNG), streams of gas bubbles emerge from the seabed into the water column. The gas consists of ~99% carbon dioxide, increasing dissolved inorganic carbon (DIC) and reducing the pH in the surrounding water column without affecting water temperatures (Fabricius *et al.*, 2011). The existence of these seeps is confirmed for at least eight decades (unpublished data), yet they may have been active at this location for much longer. We aimed to investigate whether seagrass growing near vents had characteristics consistent with those previously reported for exposure to high CO_2. Specifically, our objectives were to: (i) examine percentage cover, biomass, and species composition of seagrass communities; and (ii) investigate changes in leaf growth rates and morphology, and isotope and carbohydrate concentrations in the common seagrass species, *Cymodocea rotundata*, along three independent CO_2 gradients.

Material and methods

Study site

The study was conducted at three shallow volcanic seep locations (Dobu, Esa'Ala, and Upa-Upasina) in Milne Bay Province, PNG (see maps in Fabricius *et al.*, 2011). Volcanic activities result in the seeping of ~99% CO_2 gas from the seabed, locally increasing the acidity and concentrations of CO_2 and DIC in the seawater surrounding the seep sites (Fabricius *et al.*, 2011, 2014; Uthicke *et al.*, 2013).

Sampling was conducted during two expeditions: most measures were taken in January 2013, with some additional measures at Upa-Upasina undertaken in May 2013 (cruise schedules prohibited repeat sampling at the other sites). Plots were set up at 1.0 m depth, at three pCO_2 sites at each of the three seep locations: low (i.e. ambient), mid, and high pCO_2. The three pCO_2 sites were selected at each location in the relation to the vicinity to the vents along the natural pH gradients. Low pCO_2 sites (control with ambient pCO_2) were positioned just far enough away from the seeps as not to be influenced by vent CO_2. Mid pCO_2 sites had daily pH levels between 7.6 and 7.8, reflecting the predicted acidification scenario with very high greenhouse gas emissions (representative concentration pathways 8.5) for 2100 (IPCC, 2014). High pCO_2 sites were placed at the most active seeping areas to investigate the capacity of seagrass to cope with extremely high pCO_2 conditions. At Esa'Ala, the pH level was not significantly reduced even at the most active seep sites during our visit, possibly due to rough weather stirring up the water column. However, long-term CO_2 enrichment at Esa'Ala has been shown by biological indicators, such as abundance and species compositions of corals and other invertebrates (Fabricius *et al.*, 2011; Uthicke *et al.*, 2013). At Esa'Ala, pCO_2 sites were selected based on proximity to visible streams of gas, while other sites were chosen based on measured differences in pH. The meadows were mixed-species communities, but all three sites contained *C. rotundata* (Supplementary Figure S1). Substrates consist of soft sediment at Esa'Ala and Dobu, and soft sediment interspersed with terrestrial stones of up to ~15 cm diameter at Upa-Upasina.

Seabird CTD data loggers with auxiliary pH sensors (SBE 16 plus and SBE 18, Washington, USA) were deployed for one 24 h period at each pCO_2 site at Dobu and Upa-Upasina in January to record temperature, pH, water depth, and salinity (Supplementary Table S1). The loggers were not available at Esa'Ala and Upa-Upasina in May. Photosynthetic photon flux density (PPFD) was recorded every 10 min using Odyssey photosynthetic active radiation loggers which were deployed at the height of the canopies in the seagrass meadows at each pCO_2 site at Upa-Upasina during both sampling periods (2 d in January and 3 d in May 2013). The loggers were not available at Dobu and Esa'Ala. Seagrass leaves around the loggers were removed to avoid shading. The light values between 9 a.m. and 3 p.m. were used to calculate the average PPFD of each day, which covers the time of saturating irradiance for most tropical seagrass species (Beer *et al.*, 2006; Lee *et al.*, 2007; Supplementary Table S2).

Seawater chemistry

Water samples were collected in triplicates in 250 ml polycarbonate bottles three times a day (6:00, 12:00, 18:00) over a cycle of 12 h (9 samples in total), ~10 cm above the seagrass meadows. Water temperature was measured to the nearest 0.1°C soon after the samples were collected. The samples were fixed with 125 µl saturated (>7 g l^{-1}) mercuric chloride to analyse DIC and total alkalinity (TA), using a VINDTA Marianda 3C titrator (Marianda, Kiel, Germany). Other carbonate parameters (pH_{TOTAL}, pCO_2, HCO_3^-, and aragonite saturation state) were calculated from DIC, TA, and temperature using the program CO_2Sys (Pierrot and Wallace, 2006). Gas at the central vent at Upa-Upasina was collected into a glass septa-sealed bottle for carbon isotopic composition. For analysis, CO_2 was extracted from the glass bottle, and was cryogenically purified and transferred into a 5.9 ml septa sealed exetainer vial. Using helium as a carrier, the CO_2 was analysed on a SERCON 20–20 continuous flow isotope ratio mass spectrometer. CO_2 samples are calibrated against reference CO_2 and multiple in-house and IAEA-certified carbonate standards.

Cover, species composition, biomass

Seagrass per cent cover and species composition were visually determined using a 25 × 25 cm quadrat, placed haphazardly three times at each of the three pCO_2 sites at each of the three locations. Per cent species composition within the quadrat was recorded, and multiplied by per cent cover to obtain the standardized per cent cover for each species. Above-ground biomass (leaves and sheaths) of all seagrasses within the quadrat was collected separately to below-ground biomass (roots and rhizomes), which were collected to a depth of 10 cm using a trowel. After the 25 × 25 × 10 cm block of sediment was removed, only minute amounts of very fine roots and no rhizomes remained in the sediment deeper than 10 cm, believed to be <1% of total below-ground biomass (MT, pers. obs.). Sediment, epiphytes, and sheaths were removed from the above-ground and below-ground biomass samples, and the samples were sun-dried on site. In the laboratory, they were dried in an oven at 60°C for 2 d, and weighed to the nearest 0.001 g.

Leaf growth and morphology

Leaf growth rates of *C. rotundata* were examined at each of the pCO_2 sites using the leaf hole punch technique (Zimmerman *et al.*, 1996). Growth was measured on days with <30% cloud cover to achieve light-saturation. Sampling was conducted twice at Upa-Upasina (January and May 2013), and once at Dobu and Esa'Ala (January 2013). Five markers were placed at each site, which were spaced at least 2 m apart to reduce the likelihood of sampling the same individuals. At each site, five replicate groups of 20–30 shoots around the markers were marked using a hypodermic needle. Between 6 and 19 shoots from each replicate group were recovered after 2–3 d; however, only three groups were recovered from the mid pCO_2 site at Esa'Ala as two markers were lost.

Growth of each marked shoot was measured with calipers to the nearest 0.1 mm. All new growth within a shoot was summed to estimate the total growth rate of each shoot. The length and width of the longest leaf within a shoot were also measured to the nearest 0.1 mm, and the number of leaves per shoot was counted. In January, newly emerge leaves that had not been marked (because they had not yet emerged from the sheath at the time of marking) were assumed to be new growth, thus the distances from the bottom hole to the tip of these leaves were recorded and added to the total growth. In May, newly emerged leaves were accidentally not measured as part of growth (only fully emerged leaves, which were still extending were included in the growth measure), preventing a seasonal comparison of growth rates. The May data are nevertheless included here, as they provide additional information on differences in growth rates and leaf morphologies between the pCO_2 sites.

Size-specific growth rates (G_{SS}) (%) were calculated as:

$$G_{SS} = \frac{G_A}{L_T} \times 100,$$

where G_A is the absolute leaf growth rates (mm d^{-1}) and L_T the total length of leaves per shoot (mm),

$$L_T = L_L \times (N_L - 0.5),$$

where L_L is the length of the longest leaf within a shoot (mm), and N_L the number of leaves per shoot. It was assumed that the length of the youngest leaf was half of L_L, and the rest of the leaves are the same length as L_L to estimate L_T.

Above- and below-ground biochemistry

Above-ground (leaves) and below-ground (roots and rhizomes) tissues of *C. rotundata* ($n = 5$) were collected at each pCO_2 site, cleaned to remove epiphytes, sundried, further dried in an oven at 60°C for 2 d and ground to a fine powder. Ground above-ground samples were examined for per cent C and N, and for the stable isotopic ratios $\delta^{13}C$ and $\delta^{15}N$, using a PDZ Europa ANCA-GSL elemental analyser interfaced to a PDZ Europa 20–20 isotope ratio mass spectrometer (Sercon Ltd, Cheshire, UK). Laboratory standards, which were calibrated against NIST Standard Reference Materials (IAEA-N1, IAEA-N2, IAEA-N3, USGS-40, and USGS-41) and were compositionally similar to the leaf samples, were selected and interspersed among the samples. The results were corrected according to the known values of the included standards.

Total soluble sugars and total non-structural carbohydrates (TNSC, or starch) were examined from the below-ground samples according to Collier *et al.* (2012).

Statistical analyses

Generalized additive mixed effects models (GAMM) with a log-link function and quasipoisson distribution were used to analyse the differences between pCO_2 sites and locations in the following response variables: seawater chemistry (pH_{TOTAL}, DIC), seagrass cover, above-ground biomass, below-ground biomass, total biomass, below- to above-ground biomass ratio, leaf growth rates, leaf length, number of leaves per shoot, above-ground biochemistry (per cent C, per cent N, $\delta^{13}C$, $\delta^{15}N$, C:N ratio), and below-ground biochemistry (total soluble sugars and TNSC). Locations (Dobu, Esa'Ala, and Upa-Upasina) and pCO_2 sites (high pCO_2, mid pCO_2, and control) were treated as random and fixed factors, respectively. Month was added as additional term to the analysis of leaf growth rates and size-specific leaf growth rates, due to differences in sampling protocols between January and May. Comparisons of responses across sites within individual locations were done with generalized linear models with log link function and quasipoisson distribution. Species compositions, standardized by seagrass cover, were examined using redundancy analysis with the locations and pCO_2 as factors. The software R (v.3.0.2) was used for all statistical analyses (R Development Core Team, 2014).

Results

Seawater chemistry

Average seawater pH_{TOTAL} significantly decreased with proximity to the seeps at Dobu and Upa-Upasina; the mean pH values were lowest at the high pCO_2 sites (7.65 ± 0.06, 7.29 ± 0.16, and 7.32 ± 0.02 at Dobu, Upa-Upasina in January, and Upa-Upasina in May, respectively) and highest at the control sites (7.98 ± 0.02, 7.91 ± 0.03, and 7.94 ± 0.02 at Dobu, Upa-Upasina in January, and Upa-Upasina in May, respectively; Tables 1 and 2). At Esa'Ala, pH was similar across sites during the observation period, ranging from 7.92 ± 0.02 s.e. to 7.97 ± 0.01, probably due to wave mixing (Table 1).

The average DIC significantly increased from the low to high pCO_2 sites, in a pattern inversely correlated with pH (Table 2). The average DIC at the control sites ranged between 1967 and 1984 μmol kg^{-1}, and values increased to 2093–2175 μmol kg^{-1} at the mid pCO_2 sites at Dobu and Upa-Upasina (Table 1). DIC values rose further at the high pCO_2 sites at Upa-Upasina (2439 ± 114 and 2354 ± 15 μmol kg^{-1} in January and May, respectively), whereas the average DIC at Esa'Ala did not vary across the pCO_2 sites (Table 1).

Table 1. Average water temperature and carbonate parameters at the control, mid, and high pCO_2 sites at three volcanic seep seagrass locations in PNG.

	pCO_2 site	Temperature (°C)	pH	TA (μmol kg^{-1})	DIC (μmol kg^{-1})	pCO_2 (μatm)	HCO_3^- (μmol kg^{-1})	Ωar
Dobu	Control	29.3 (0.40)	7.98 (0.02)	2264 (8.0)	1967 (22)	475 (36)	1744 (31)	3.4 (0.16)
	Mid	29.7 (0.43)	7.75 (0.04)	2310 (3.9)	2122 (23)	918 (104)	1952 (32)	2.4 (0.21)
	High	29.5 (0.42)	7.65 (0.06)	2265 (4.1)	2127 (28)	1252 (193)	1978 (36)	1.9 (0.21)
Esa'Ala	Control	28.5 (0.25)	7.97 (0.01)	2268 (2.8)	1984 (7.8)	481 (13)	1768 (11)	3.3 (0.06)
	Mid	28.7 (0.26)	7.93 (0.01)	2269 (8.8)	2006 (5.4)	543 (20)	1803 (9.3)	3.1 (0.11)
	High	29.1 (0.24)	7.92 (0.02)	2245 (6.8)	1984 (18)	548 (32)	1782 (25)	3.0 (0.14)
Upa Jan	Control	29.5 (0.24)	7.91 (0.03)	2228 (3.5)	1973 (19)	574 (45)	1775 (28)	3.0 (0.16)
	Mid	29.7 (0.26)	7.57 (0.06)	2285 (14)	2175 (38)	1550 (232)	2032 (46)	1.7 (0.23)
	High	29.8 (0.27)	7.29 (0.16)	2420 (44)	2439 (114)	5098 (1870)	2236 (86)	1.2 (0.28)
Upa May	Control	29.0 (0.07)	7.94 (0.02)	2221 (6.5)	1954 (18)	519 (36)	1749 (25)	3.1 (0.12)
	Mid	28.8 (0.15)	7.74 (0.06)	2267 (8.4)	2093 (34)	966 (141)	1931 (46)	2.2 (0.25)
	High	29.1 (0.08)	7.32 (0.02)	2367 (17)	2354 (15)	2754 (128)	2225 (14)	0.94 (0.05)

Measured values of temperature, total alkalinity (TA), and DIC were used to calculate the carbonate system parameters (pH_{TOTAL}, pCO_2, HCO_3^-, and aragonite saturation state; nine samples per treatment). Standard errors are shown in parentheses.

Table 2. The results of mixed model effect analyses, showing the significance of differences between pCO_2 levels for the dependent variables.

	Control vs. mid pCO_2			Control vs. high pCO_2			Mid vs. high pCO_2		
	Est. dif.	*t*	*p*-value	Est. dif.	*t*	*p*-value	Est. dif.	*t*	*p*-value
pH	−0.026	−4.37	<0.001	−0.052	−8.70	<0.001	−0.026	−4.30	<0.001
DIC	0.062	3.383	<0.01	0.098	5.319	<0.001	0.036	1.971	0.0524
% cover	0.568	4.96	<0.001	0.966	9.19	<0.001	0.398	4.41	<0.001
B-gr biomass	0.419	1.70	0.104	1.58	7.68	<0.001	1.16	6.38	<0.001
A-gr biomass	0.708	2.95	<0.01	1.42	6.58	<0.001	0.709	4.13	<0.001
B-gr/A-gr ratio	0.530	1.90	0.0705	−0.184	−0.569	0.575	−0.714	−2.41	<0.05
Total biomass	0.523	2.17	<0.05	1.54	7.47	<0.001	1.02	5.97	<0.001
G_A January 2013	0.0347	0.359	0.721	0.0178	0.190	0.850	−0.0169	−0.178	0.859
G_A May 2013	0.0569	0.501	0.626	0.355	3.33	<0.01	0.298	2.85	<0.05
G_{ss} January 2013	−0.358	−5.69	<0.001	−0.433	−7.02	<0.001	−0.075	−1.09	0.281
G_{ss} May 2013	−0.060	−0.692	0.502	−0.635	−6.16	<0.001	−0.574	−5.52	<0.001
No. of leaves	0.108	2.91	<0.01	0.156	4.36	<0.001	0.0478	1.35	0.182
Leaf length	0.260	2.67	<0.05	0.398	4.27	<0.001	0.139	1.62	0.11
Leaf width	0.00238	0.095	0.925	−0.0233	−0.948	0.347	−0.0257	−1.06	0.294
$\delta^{13}C$	−3.55	−6.56	<0.001	−6.05	−11.8	<0.001	−2.50	−4.53	<0.001
$\delta^{15}N$	0.142	0.789	0.435	−0.684	−4.00	<0.001	−0.826	−4.50	<0.001
% C	0.0118	0.01	0.992	−1.47	−1.26	0.214	−1.48	−1.20	0.237
% N	−0.0232	−0.208	0.836	−0.237	−2.22	<0.05	−0.214	−1.89	0.0661
C/N ratio	0.270	0.391	0.698	1.68	2.53	<0.05	1.41	2.01	0.0518
Carbohydrates	−5.69	−1.67	0.103	−4.72	−1.36	0.183	0.977	0.281	0.78
Starch	0.472	1.11	0.273	0.725	1.68	0.101	0.253	0.584	0.562

Estimated difference (Est. dif.) shows the differences of the mean values of the second pCO_2 level from the first pCO_2 levels. The analyses on leaf growth rates (G_A) and size-specific leaf growth rate (G_{SS}) were conducted separately for January and May to accommodate the difference in the sampling technique used.

Calculated pCO_2 increased with the proximity to the seeps (Table 1). The variation was smaller at the control sites (475 ± 36 to 574 ± 45) than those at the high pCO_2 sites (548 ± 32, 1252 ± 193, 5098 ± 1870, 2754 ± 128 at Esa'Ala, Dobu, Upa-Upasina in January, and Upa-Upasina in May, respectively). Calculated HCO_3^- at the control sites ranged between 1744 ± 31 to 1775 ± 28, and the values increased at the high pCO_2 sites except at Esa'Ala (1782 ± 25, 1978 ± 36, 2236 ± 86, and 2225 ± 14 at Esa'Ala, Dobu, Upa-Upasina in January, and Upa-Upasina in May, respectively; Table 1).

Seagrass per cent cover, and above- and below-ground biomass

Seagrass cover averaged 33 ± 1.7–38 ± 8.3% across the locations at the control sites, and 91 ± 1.7–94 ± 2.3% at high pCO_2 sites (Figure 1, Table 2). At the mid pCO_2 sites, cover was highly variable between locations, ranging from 40 ± 0.0% at Upa-Upasina to 83 ± 1.7% at Dobu (Figure 1). The average total biomass increased by 4.6-fold from the control (137 ± 14 g DW m^{-2}) to the high pCO_2 sites (634 ± 68 g DW m^{-2}), and the differences were significant (Table 2). Above-ground biomass significantly increased from the control to high pCO_2 sites, yet the rates of increase were highly variable among locations (521, 188, and 501% at Dobu, Esa'Ala, and Upa-Upasina, respectively; Figure 2, Table 2). The average below-ground biomass at the control sites ranged between 84.8 ± 19.4and 116.9 ± 17.4 g DW m^{-2}. There were no significant differences in the below-ground biomass between the control and mid pCO_2 sites, but values increased 4- to 5.6-fold at the high pCO_2 sites (477 ± 107, 455 ± 87, and 464 ± 101 g DW m^{-2} at Dobu, Esa'Ala, and Upa-Upasina, respectively; Figure 2, Table 2). The

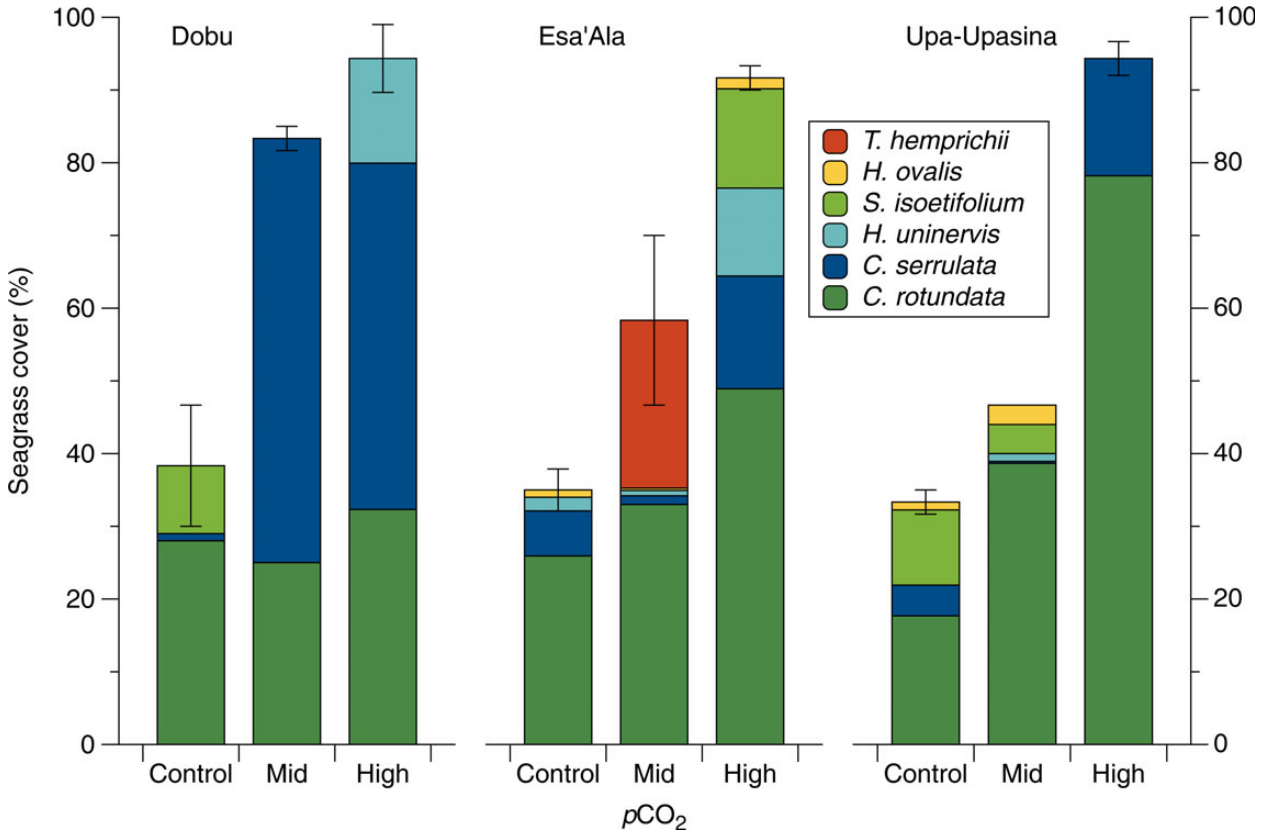

Figure 1. Average seagrass cover (%) and the species composition at three pCO_2 sites from the three locations. The error bars represent standard error of total seagrass covers ($n = 3$).

below- to above-ground biomass ratios did not vary significantly with pCO_2 at Dobu and Upa-Upasina (ranging between 0.8 ± 0.3 and 1.7 ± 0.1, and 3.0 ± 0.9 and 3.5 ± 0.5, respectively; $p > 0.05$); however, the ratio increased threefold (from 2.2 ± 0.2 to 6.3 ± 1.0) from the control to high pCO_2 sites at Esa'Ala.

Species composition

Seagrass community composition was significantly different among the three pCO_2 sites [permutation test, $F_{(2,21)} = 3.91$, $p = 0.01$] and also among the locations [$F_{(2,21)} = 2.76$, $p = 0.02$; Figure 3]. Of the total variation in community composition, 30.5 and 26.1% were explained by the first two RDA axes, respectively. *Cymodocea rotundata* was the most common species at all locations, making up 20–80% of the seagrass communities (Figure 1). *Cymodocea serrulata* was the second dominant species across the three locations, but particularly abundant at the high and mid pCO_2 sites of Dobu with the average per cent composition of 50 and 70%, respectively (Figure 1). *Thalassia hemprichii* was only found at the mid pCO_2 sites at Esa'Ala where it was dominant, which resulted in the sites and the species clustering away from others in the RDA. *Halodule uninervis* was also mostly found at the high pCO_2 sites, whereas *Halophila ovalis* occurred at lower pCO_2. The latter was found at low and mid pCO_2 sites and at Upa-Upasina and Esa'Ala, but it was not abundant anywhere.

Leaf morphology

In *C. rotundata*, the mean number of leaves per shoot ranged between 2.2 ± 0.1 and 2.4 ± 0.1 at the control sites, and was significantly higher at the high pCO_2 sites (ranging from 2.5 ± 0.2 to 3.0 ± 0.1; Figure 4, Table 2). The length of the longest leaf within a shoot was twofold greater at high pCO_2 compared with control sites at Dobu and at Upa-Upasina in May ($t = 6.50$, $p < 0.001$, and $t = 6.07$, $p < 0.001$, respectively). At Esa'Ala, leaves at the high pCO_2 site were slightly shorter than at mid and control sites ($t = -3.31$, $p = 0.011$, and $t = -3.53$, $p = 0.008$, respectively), and leaf lengths were similar at all Upa-Upasina sites in January, although the length at the high pCO_2 site was slightly greater than from the mid pCO_2 site ($t = 2.64$, $p = 0.023$; Figure 4). There was no difference in the leaf width (ranging between 3.8 ± 0.1 and 4.9 ± 0.1 mm) among pCO_2 sites at all three locations (Table 2).

Leaf growth rates

Average leaf growth rates of *C. rotundata* significantly increased with pCO_2 at Dobu [from 10.5 ± 0.78 mm d^{-1} at low pCO_2 to 16.9 ± 1.18 mm d^{-1} at high pCO_2: $F_{(2,12)} = 12.352$, $p = 0.001$] and also at Upa-Upasina in May [from 6.9 ± 0.43 to 9.9 ± 0.97 mm d^{-1}, $F_{(2,12)} = 6.686$, $p = 0.011$], with high pCO_2 sites having significantly higher growth than control sites ($t = 4.878$, $p < 0.001$, and $t = 3.33$, $p = 0.006$, respectively; Figure 4). At Upa-Upasina in January, the growth rates ranged between 6.7 ± 0.56 and 7.8 ± 0.35 mm d^{-1}, and did not differ between the different pCO_2 levels. Patterns were more complex at Esa'Ala, where growth averaged 11.7 ± 0.27 mm d^{-1} at the control site, being similar to the highly variable mid pCO_2 site (10.0 ± 1.91 mm d^{-1}; $t = -1.43$, $p = 0.182$) but significantly higher than that at the high pCO_2 site (6.8 ± 0.21 mm d^{-1}; $t = -5.13$, $p < 0.001$). The average size-specific leaf growth rates

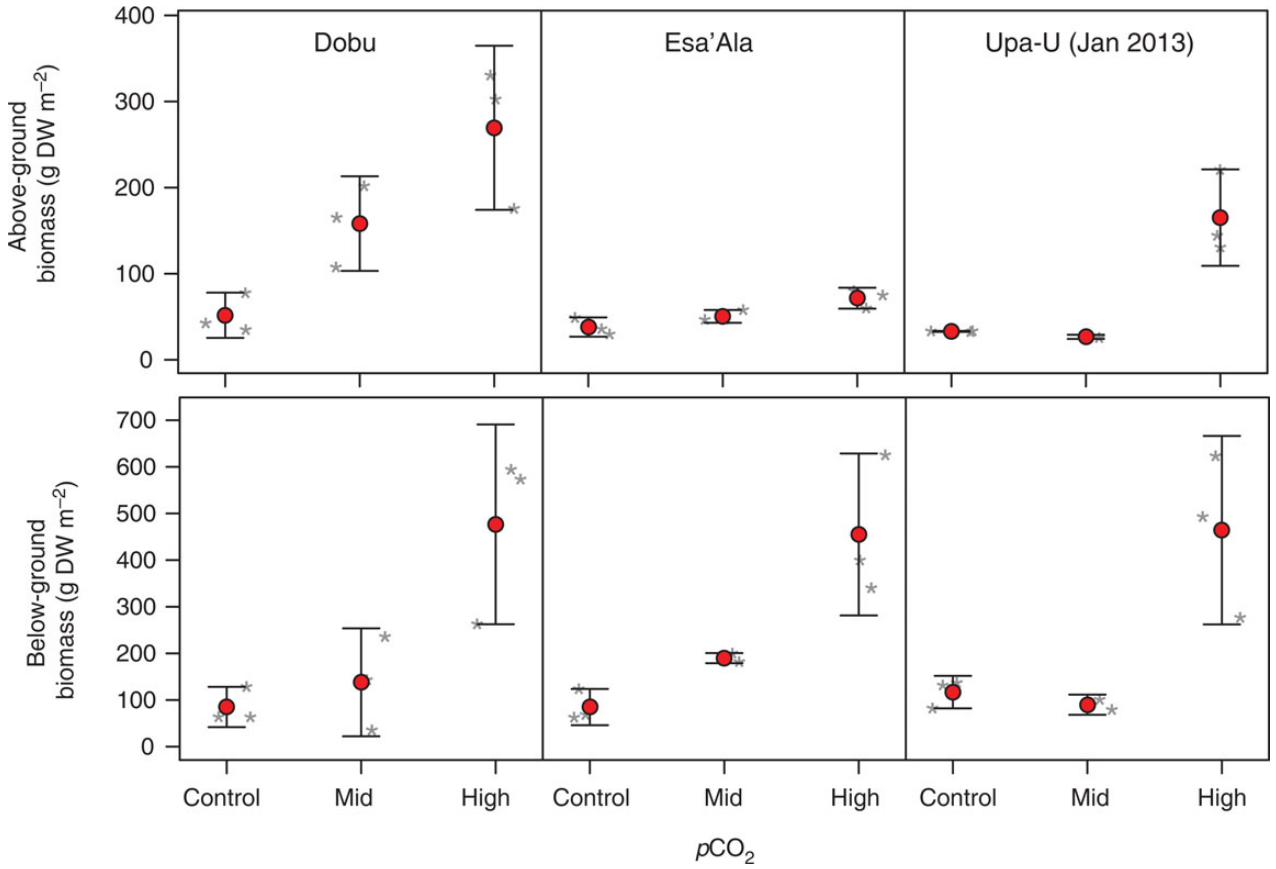

Figure 2. Average above- (top) and below-ground (bottom) biomass at three pCO_2 sites from three locations. The error bars, circles, and asterisks represent 95% confidence intervals, overall median, and means of individual samples ($n = 9$), respectively. Asterisks are jittered horizontally to avoid overlaps and improve clarity. Asterisks represent individual plots ($n = 3$).

decreased with proximity to the seeps at all locations (Table 2). The values ranged between 1.6 ± 0.1 and 2.4 ± 0.1% across the locations at the high pCO_2 sites, 2.1 ± 0.1 and 2.9 ± 0.1% at mid pCO_2 sites, and 3.1 ± 0.1 and 3.3 ± 0.1% at the control sites (Figure 4).

Above- and below-ground biochemistry

Between 33.3 ± 1.4 and 39.5 ± 0.7% of the above-ground dry biomass of *C. rotundata* consisted of carbon (Supplementary Table S3), and concentrations were not significantly different between the pCO_2 sites (Table 2). There was a significant increase in the average $\delta^{13}C$ in leaves from the high pCO_2 to control sites (Table 2, Figure 5). The largest change was observed at Dobu where $\delta^{13}C$ increased twofold from −17.3 ± 0.4 to −8.5 ± 0.1‰ from the high pCO_2 to the control site (Figure 5, Supplementary Table S3). In contrast, the $\delta^{13}C$ signature of gases venting at the high pCO_2 site at Upa-Upasina was −2.48 ± 0.08‰.

The average N content of leaves varied from 1.7 ± 0.1 to 2.3 ± 0.04% (Supplementary Table S3), with significant declines from the control to the high pCO_2 sites (Table 2). $\delta^{15}N$ was reduced at the high pCO_2 sites at all three locations (Supplementary Table S3), and the difference from high pCO_2 to mid pCO_2 and control sites was significant (Table 2). The mean C/N ratio was also significantly higher at the high pCO_2 sites than at the control sites (Table 2). The ratio ranged from 17.3 ± 0.6 to 20.7 ± 0.3 at Dobu, and 16.4 ± 0.2 to 21.0 ± 0.5 at Esa'Ala with the highest values observed at the high pCO_2 sites, whereas it did not vary between the pCO_2 sites at Upa-Upasina, ranging between 18.1 ± 0.9 and 19.4 ± 1.0 (Supplementary Table S3).

The contents of soluble carbohydrates in the below-ground biomass of *C. rotundata* ranged from 22.4 ± 3.6 to 46.2 ± 2.6% of dry weight, and starch content ranged from 1.0 ± 0.1 to 3.1 ± 0.7% of dry weight (Supplementary Table S3). Both of these carbohydrate concentrations were not significantly different between the pCO_2 sites (Table 2).

Discussion

The volcanic vents in PNG have had elevated pCO_2 for many decades (perhaps millennia), providing insights into the likely effects of OA on seagrass communities. Our study documented changes in seagrass physiology, morphology, abundance, and composition within the vicinity of CO_2 vents. However, other measures, namely leaf growth and carbohydrate content, did not respond to carbon enrichment at our sites, which contradicts with the response previously observed following experimental increase in pCO_2 (Zimmerman *et al.*, 1995, 1997; Jiang *et al.*, 2010). These discrepancies highlight the importance of field studies to elucidate future seagrass responses to OA in their natural environment.

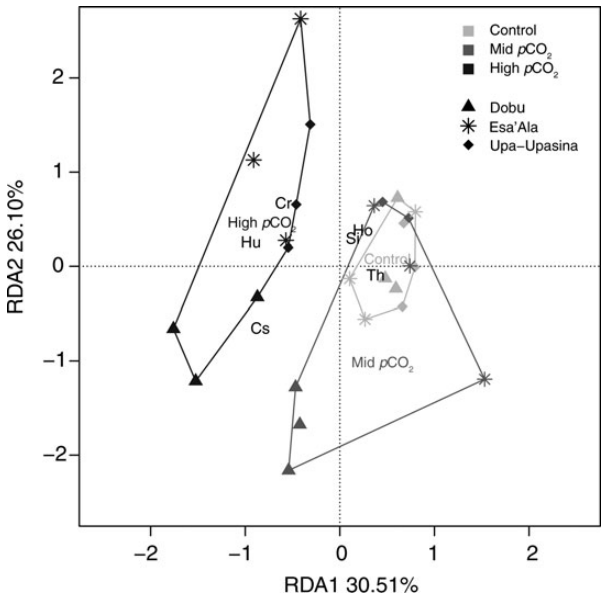

Figure 3. Redundancy analysis of seagrass species composition at three different pCO_2 sites at each of three locations, Dobu, Esa'Ala, and Upa-Upasina. Cs, *Cymodocea serrulata*; Cr, *Cymodocea rotundata*; Th, *Thalassia hemprichii*; Hu, *Halodule uninervis*; Ho, *Halophila ovalis*; Si, *Syringodium isoetifolium*.

Distinct differences in carbon isotopic signatures, with $\delta^{13}C$ in seagrass leaves steeply declining from the control to high pCO_2 sites at all three locations, suggest that photosynthetic carbon uptake was influenced by the seep carbon supply. Our finding of reduced $\delta^{13}C$ in the leaves does not necessarily imply that photosynthetic rates of seagrasses had increased (as this was not measured in our study); however, increased photosynthetic production in seagrass was documented in water enriched with CO_2 at the same seeps at Esa'Ala in previous work (Russell *et al.*, 2013). $\delta^{13}C$ depletion in seagrass at volcanic vents was also observed in previous studies (Vizzini *et al.*, 2010; Campbell and Fourqurean, 2011; Apostolaki *et al.*, 2014). The $\delta^{13}C$ values of seagrass leaves at the seeps (between −12.4 and −17.8‰) were below those previously observed for *C. rotundata* (−9.6 to −7.4‰; McMillan *et al.*, 1980; Fry *et al.*, 1983) and far below those in gases seeping from the vents (−2.5). The $\delta^{13}C$ of seep gas was similar to that reported at other hydrothermal vents (−3 to −3.5‰) and is slightly lower than in other marine waters (∼0‰; Vizzini *et al.*, 2010). Therefore, the depletion of $\delta^{13}C$ in leaves at high pCO_2 sites may have been somewhat influenced by the depleted signature of the carbon source, but is mostly explained by a biological discrimination against ^{13}C, where more ^{12}C is incorporated than the heavier and energetically more expensive ^{13}C (Raven *et al.*, 2002). Therefore, C supply is increased more relative to demand nearest to seeps, enabling discrimination against ^{13}C.

We documented a threefold increase in tropical seagrass cover and a fivefold increase in biomass from the low to high pCO_2 sites. Our finding is consistent with the results from a study on the temperate Mediterranean species, *Posidonia oceanica,* at the volcanic CO_2 vent in Italy (Hall-Spencer *et al.*, 2008), where similar increases in shoot density occurred (threefold increase from control to pH 7.6). Other environmental factors, such as light and nutrients, which were not measured in this study, may also have been influential. However, the comparable findings from the two separate CO_2 vents in PNG and Italy confirm that seagrass communities are likely to increase their abundance in a future with elevated CO_2 conditions (Fabricius *et al.*, 2011), as long as other environmental factors, such as water turbidity and dissolved nutrient levels, do not limit their development. The approach to testing long-term effects of increasing pCO_2 using volcanic CO_2 vents as natural laboratories is inherently limited, and one of these limitations is the high variability in pCO_2 exposure. Despite this, given that the vents have been seeping CO_2 gas for at least eight decades (Fabricius *et al.*, 2011), the treatments represent current (control), future 2100 (mid), and beyond (high) pCO_2 enabling us to assess the likely long-term *in situ* effects of increasing pCO_2. Laboratory and mesocosm experiments are subject to other limitations, e.g. natural levels of waves, flow, light, nutrient levels, and interactions with grazers, epiphytes and space competitors cannot be easily replicated, yet co-determine seagrass performances. The multi-decadal pCO_2 exposure at the vents and the environmentally relevant settings therefore complement controlled laboratory experiments, and in combination may help to predict the effects of future chronic OA on marine ecosystems.

Along with the cover of seagrass, there was an increase in below-ground biomass (up to 5.6-fold) when comparing the control and high pCO_2 sites. There are strong natural species-specific differences in seagrass biomass per unit area. The most abundant species at the study sites in Milne Bay, *C. rotundata* and *C. serrulata*, are typically relatively low in below-ground biomass compared with other species (37.9–62.5 g DW m^{-2}; Duarte and Chiscano, 1999). At our control sites, the mean below-ground biomass was slightly above this typical range, while at the high pCO_2 sites, it was significantly higher (465 g DW m^{-2}) than the average for this genus. It was even higher than global mean values for seagrass meadows (237 g DW m^{-2}), which includes other high biomass species, such as *Phyllospadix* and *Posidonia* sp. (Duarte and Chiscano, 1999). Today, seagrass meadows, together with the organic-rich sediments that they stabilize, are one of the largest carbon sinks in the world, an attribute of coastal ecosystems that has become valued for its "blue-carbon" storage potential (Costanza *et al.*, 1997; Fourqurean *et al.*, 2012; Pendleton *et al.*, 2012; Duarte *et al.*, 2013; Lavery *et al.*, 2013). The significantly higher below-ground biomass at the high pCO_2 sites indicates the potential for rising pCO_2 to increase investment of carbon into below-ground tissues, although this projection also depends on other factors, such as water quality.

The below- to above-ground biomass ratio did not differ from control to high pCO_2 sites at Dobu and Upa-Upasina, due to the consistent rates of increase (approximately fivefold) in both along the pCO_2 gradient. In contrast, the ratio increased threefold from control to high pCO_2 at Esa'Ala, due to the smaller increase in above-ground relative to below-ground biomass (188 vs. 536%). Above-ground biomass is mainly influenced by shoot density, but can also vary depending on leaf morphology and losses from grazing (Cebrian and Duarte, 1998). Arnold *et al.* (2012) identified that seagrass at CO_2 seeps contained significantly lower concentrations of phenolic substances than at the control sites, which enabled higher levels of grazing. However, fish exposed to elevated CO_2 can also have impaired learning, and neurotransmitter function, making them more vulnerable to predation, which in turn may affect population size and recruitment (Chivers *et al.*, 2014). Ecological interactions, including herbivorous grazing pressure, are priority future research directions for investigating the effects

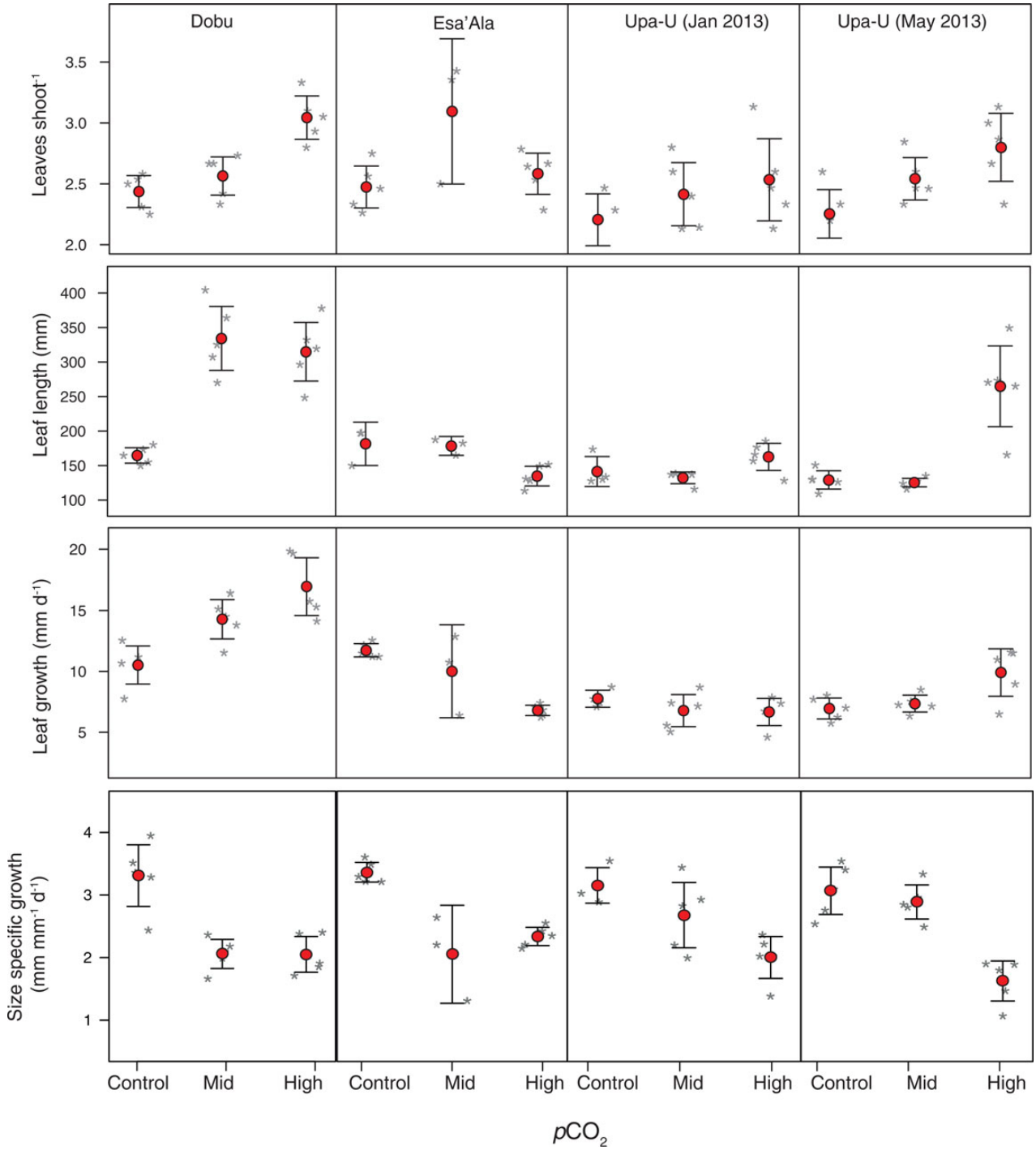

Figure 4. Average number of leaves per shoot, leaf length, leaf growth rate, and size-specific growth rate of *C. rotundata* at three pCO_2 sites. Asterisks represent the means of 6–19 shoots within each of the replicate groups ($n = 3–5$).

of CO_2 enrichment on seagrass meadows. Leaf morphology changes with exposure to CO_2 were location-specific: leaf length and the number of leaves per shoot of *C. rotundata* both increased with pCO_2 at Dobu and Upa-Upasina, whereas at Esa'Ala, there was no difference in the number of leaves per shoot, and leaf lengths were shortest at the high pCO_2 site. For now, the effects of grazing on this morphological variability among sites cannot be established. However, we can conclude that the morphological differences likely dampened the increases in above-ground biomass along the pCO_2 gradient at Esa'Ala.

Vicinity to the vents was associated with differences in species composition, potentially indicating future shifts in competitive strengths between seagrass species with increasing OA. Most notably, the canopy-forming species *C. rotundata*, *C. serrulata*, and *H. uninervis* with blade-like leaves increased in dominance at high pCO_2 sites. In contrast, *H. ovalis*, often considered as an early-

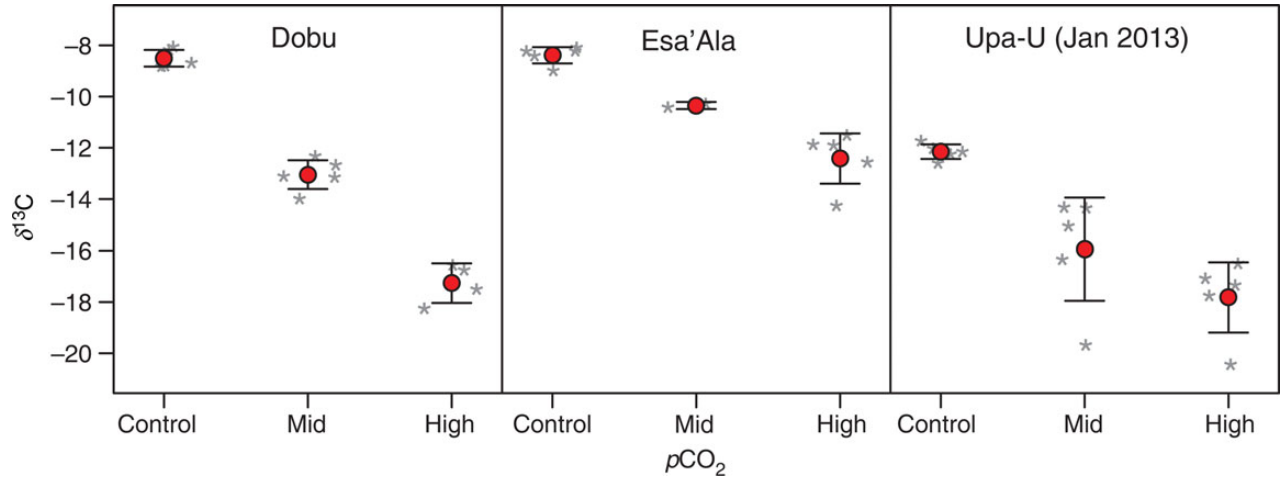

Figure 5. $\delta^{13}C$ within leaves of *C. rotundata* at different pCO_2 sites at three locations in PNG. Asterisks represent the means of replicate samples ($n = 2–5$).

successional species, has small, oval-shaped leaves, and was found only at low pCO_2 sites. The low and sparse morphology of *H. ovalis* restricts this species from reaching sufficient light in the dense canopies formed by the taller blade-like seagrass species, which may have led to their lesser abundance at increased pCO_2. Species-specific physiology, such as different ability to utilize HCO_3^- (Campbell and Fourqurean, 2013a), may also be influential. However, it was beyond the scope of this field study to elucidate the specific ecological or physiological drivers for species-specific differences in response to pCO_2 enrichment.

We observed inconsistent differences in growth rates, and no differences in storage carbohydrates (soluble carbohydrates and starch) and per cent carbon content in above- and below-ground tissues among the pCO_2 sites. This contradicts results of laboratory studies, where short-term pCO_2 enrichment (weeks or months) and other environmental conditions were controlled (Zimmerman *et al.*, 1997; Jiang *et al.*, 2010). Several transient environmental factors, such as light and nutrient availability, can affect short-term plant responses measured here, potentially masking the effects of elevated pCO_2. The exposure to CO_2 at the seeps also varies over time, depending on mixing and flushing rates by wind, waves, and tides (Fabricius *et al.*, 2014). This variability presents a difficulty when examining *in situ* the effects of pCO_2 enrichment on fast responding parameters, such as growth rates and carbon contents (Collier *et al.*, 2012), as other factors can temporarily fluctuate during the experiments. Repeated measurements, which capture variation in environmental parameters, are required to verify whether these findings reflect long-term responses.

Leaf growth rates varied significantly with carbon availability only in two of the four sets of measurements. Size-specific growth rates significantly decreased from the control to high pCO_2 sites, despite the inconsistent patterns in the leaf extension rates. This was attributable to the longer leaves and more leaves per shoot at the seeps. Size-specific growth rates are the reciprocal of leaf turnover time, with leaves being replaced more slowly at high pCO_2 sites. Previous studies at volcanic vents identified the significant decline in calcified epiphytes on seagrass leaves with the proximity to the seeps (Hall-Spencer *et al.*, 2008; Fabricius *et al.*, 2011). Reduced pressure from epiphyte accumulations may enable the leaves to turnover more slowly.

We also observed a small decline in per cent nitrogen and a small but significant decline in $\delta^{15}N$ values of the above-ground tissues at elevated pCO_2, which were associated with slightly higher C/N. These observations are consistent with previous CO_2 enrichment studies in seagrass (Jiang *et al.*, 2010) and terrestrial plants (Weerakoon *et al.*, 1999). Per cent N and $\delta^{15}N$ values are often related, and values can decline at higher carbon uptake (e.g. from increasing production or carbon storage) that dilute the N resources (Collier *et al.*, 2010). Multi-factorial studies on seagrasses that manipulate CO_2, nutrients, and light are required to better understand the main drivers of plant biochemistry and energetics, including growth rates.

In conclusion, the present study provided insight into the effects of multi-decadal exposure to vents enriched with CO_2 on tropical seagrass communities. Previous studies have shown that CO_2 enrichment can affect photosynthetic rates, growth, and biomass in some seagrasses. We are unable to determine whether changes in photosynthetic rates or other ecological or environmental factors were the driver of the physiological and morphological differences across the gradient in CO_2 exposure. However, our findings highlight that long-term CO_2 exposure can increase seagrass biomass, and can convey a competitive advantage for canopy-forming species with elongated leaves over shorter species, potentially suggesting profound changes in seagrass ecosystems in a future high CO_2 world.

Supplementary data

Supplementary material is available at the *ICESJMS* online version of the manuscript.

Acknowledgements

We thank the families of the Dobu Island, Esa'Ala, and Illi Illi Bwa Bwa (Koruwea/Upa-Upasina) for allowing us to study their seagrass meadows. Many thanks also to the National Research Institute of Papua New Guinea, the crew of the MV Chertan, and QantasLink, for ongoing logistic support. Thank you to S. Fallon from the Australian National University for measurement of $\delta^{13}C$ in seep gas. The study was funded by the Great Barrier Reef Foundation's "Resilient Coral Reefs Successfully Adapting to Climate Change" research and development programme in collaboration with the Australian Government, and the Australian Institute of Marine Science.

References

Apostolaki, E. T., Vizzini, S., Hendriks, I. E., and Olsen, Y. S. 2014. Seagrass ecosystem response to long-term high CO_2 in a Mediterranean volcanic vent. Marine Environmental Research, 99: 9–15.

Arnold, T., Mealey, C., Leahey, H., Miller, A. W., Hall-Spencer, J. M., Milazzo, M., and Maers, K. 2012. Ocean acidification and the loss of phenolic substances in marine plants. PLoS ONE, 7: 1–10.

Beer, S., and Koch, E. 1996. Photosynthesis of marine macroalgae and seagrasses in globally changing CO_2 environments. Marine Ecology Progress Series, 141: 199–204.

Beer, S., Mtolera, M., Lyimo, T., and Björk, M. 2006. The photosynthetic performance of the tropical seagrass *Halophila ovalis* in the upper intertidal. Aquatic Botany, 84: 367–371.

Bostrom, C., and Mattila, J. 1999. The relative importance of food and shelter for seagrass-associated invertebrates: a latitudinal comparison of habitat choice by isopod grazers. Oecologia, 120: 162–170.

Caldeira, K., and Wickett, M. E. 2003. Anthropogenic carbon and ocean pH. Nature, 425: 365–365.

Campbell, J. E., and Fourqurean, J. W. 2011. Novel methodology for in situ carbon dioxide enrichment of benthic ecosystems. Limnology and Oceanography: Methods, 9: 97–109.

Campbell, J. E., and Fourqurean, J. W. 2013a. Mechanisms of bicarbonate use influence the photosynthetic carbon dioxide sensitivity of tropical seagrasses. Limnology and Oceanography, 58: 839–848.

Campbell, J. E., and Fourqurean, J. W. 2013b. Effects of in situ CO_2 enrichment on the structural and chemical characteristics of the seagrass *Thalassia testudinum*. Marine Biology, 160: 1465–1475.

Cebrian, J., and Duarte, C. M. 1998. Patterns in leaf herbivory on seagrasses. Aquatic Botany, 60: 67–82.

Chivers, D. P., Mccormick, M. I., Nilsson, G. E., Munday, P. L., Watson, S. A., Meekan, M. G., Mitchell, M. D., *et al.* 2014. Impaired learning of predators and lower prey survival under elevated CO_2: a consequence of neurotransmitter interference. Global Change Biology, 20: 515–522.

Collier, C. J., Lavery, P. S., Ralph, P. J., and Masini, R. J. 2009. Shade-induced response and recovery of the seagrass *Posidonia sinuosa*. Journal of Experimental Marine Biology and Ecology, 370: 89–103.

Collier, C. J., Prado, P., and Lavery, P. S. 2010. Carbon and nitrogen translocation in response to shading of the seagrass *Posidonia sinuosa*. Aquatic Botany, 93: 47–54.

Collier, C. J., Waycott, M., and Ospina, A. G. 2012. Responses of four Indo-West Pacific seagrass species to shading. Marine Pollution Bulletin, 65: 342–354.

Costanza, R., D'Arge, R., De-Groot, R., Farber, S., Grasso, M., Hannon, B., Limburg, K., *et al.* 1997. The value of the world's ecosystem services and natural capital. Nature, 387: 253–260.

Duarte, C. M., and Chiscano, C. L. 1999. Seagrass biomass and production: a reassessment. Aquatic Botany, 65: 159–174.

Duarte, C. M., Kennedy, H., Marbà, N., and Hendriks, I. 2013. Assessing the capacity of seagrass meadows for carbon burial: current limitations and future strategies. Ocean and Coastal Management, 83: 32–38.

Fabricius, K. E., Langdon, C., Uthicke, S., Humphrey, C., Noonan, S., De, G., Okazaki, R., *et al.* 2011. Losers and winners in coral reefs acclimatized to elevated carbon dioxide concentrations. Nature Climate Change, 1: 165–169.

Fabricius, K. E., Noonan, S., and Uthicke, S. 2014. Ecological effects of ocean acidification and habitat complexity on reef-associated macroinvertebrate communities. Proceedings of the Royal Society B: Biological Sciences, 281: 20132479.

Fourqurean, J. W., Duarte, C. M., Kennedy, H., Marbà, N., Holmer, M., Mateo, M. A., Apostolaki, E. T., *et al.* 2012. Seagrass ecosystems as a globally significant carbon stock. Nature Geoscience, 5: 505–509.

Fry, B., Scalanb, R. S., and Parkerb, P. L. 1983. $^{13}C/^{12}C$ ratios in marine food webs of the Torres Strait, Queensland. Marine and Freshwater Research, 34: 707–715.

Hall-Spencer, J. M., Rodolfo-Metalpa, R., Martin, S., Ransome, E., Fine, M., Turner, S. M., Rowley, S. J., *et al.* 2008. Volcanic carbon dioxide vents show ecosystem effects of ocean acidification. Nature, 454: 96–99.

Invers, O., Zimmerman, R. C., Alberte, R. S., Perez, M., and Romero, J. 2001. Inorganic carbon sources for seagrass photosynthesis: an experimental evaluation of bicarbonate use in species inhabiting temperate waters. Journal of Experimental Marine Biology and Ecology, 265: 203–217.

IPCC. 2014. Climate Change 2014: Synthesis Report. Cambridge University Press, NY, USA.

Jiang, Z. J., Huang, X-P., and Zhang, J-P. 2010. Effects of CO_2 enrichment on photosynthesis, growth, and biochemical composition of seagrass *Thalassia hemprichii* (Ehrenb.) Aschers. Journal of Integrative Plant Biology, 52: 904–913.

Koch, M., Bowes, G., Ross, C., and Zhang, X. H. 2013. Climate change and ocean acidification effects on seagrasses and marine macroalgae. Global Change Biology, 19: 103–132.

Lavery, P. S., Mateo, M. A., Serrano, O., and Rozaimi, M. 2013. Variability in the carbon storage of seagrass habitats and its implications for global estimates of blue carbon ecosystem service. PLoS ONE, 8: e73748.

Lee, K. S., Park, S. R., and Kim, Y. K. 2007. Effects of irradiance, temperature, and nutrients on growth dynamics of seagrasses: a review. Journal of Experimental Marine Biology and Ecology, 350: 144–175.

McMillan, C., Parker, P. L., and Fry, B. 1980. $^{13}C/^{12}C$ ratio in seagrasses. Aquatic Botany, 9: 237–249.

Palacios, S. L., and Zimmerman, R. C. 2007. Response of eelgrass *Zostera marina* to CO_2 enrichment: possible impacts of climate change and potential for remediation of coastal habitats. Marine Ecology Progress Series, 344: 1–13.

Pendleton, L., Donato, D. C., Murray, B. C., Crooks, S., Jenkins, W. A., Sifleet, S., Craft, C., *et al.* 2012. Estimating global "blue carbon" emissions from conversion and degradation of vegetated coastal ecosystems. PLoS ONE, 7: e43542.

Pierrot, D. E. L., and Wallace, D. W. R. 2006. MS Excel Program Developed for CO_2 System Calculations. ORNL/CDIAC-105a. Carbon Dioxide Information Analysis Center, Oak Ridge National Laboratory, US Department of Energy, Oak Ridge, TN. doi:10.3334/CDIAC/otg.CO2SYS_XLS_CDIAC105a.

R Development Core Team. 2014. A Language and Environment for Statistical Computing. R Foundation for Statistical Computing, Vienna, Austria. ISBN 3-900051-07-0, http://www.R-project.org.

Ralph, P. J., Durako, M. J., Enríquez, S., Collier, C. J., and Doblin, M. A. 2007. Impact of light limitation on seagrasses. Journal of Experimental Marine Biology and Ecology, 350: 176–193.

Raven, J. A., Johnston, A. M., Kubler, J. E., Korb, R., McInroy, S. G., Handley, L. L., Scrimgeour, C. M., *et al.* 2002. Mechanistic interpretation of carbon isotope discrimination by marine macroalgae and seagrasses. Functional Plant Biology, 29: 355–378.

Raven, J., Calderia, K., Elderfield, H., Hoegh-Guldberg, O., Liss, P., Riebesell, U., Shepherd, J., *et al.* 2005. Ocean acidification due to increasing atmospheric carbon dioxide. The Royal Society.

Russell, B. D., Connell, S. D., Uthicke, S., Muehllehner, N., Fabricius, K. E., and Hall-Spencer, J. M. 2013. Future seagrass beds: can increased productivity lead to increased carbon storage? Marine Pollution Bulletin, 73: 463–469.

Uthicke, S., Momigliano, P., and Fabricius, K. E. 2013. High risk of extinction of benthic foraminifera in this century due to ocean acidification. Scientific Reports, 3: 1–5.

Vizzini, S., Tomasello, A., Maida, G. D., Pirrotta, M., Mazzola, A., and Calvo, S. 2010. Effect of explosive shallow hydrothermal vents on

$\delta^{13}C$ and growth performance in the seagrass *Posidonia oceanica*. Journal of Ecology, 98: 1284–1291.

Waycott, M., Duarte, C. M., Carruthers, T. J. B., Orth, R. J., Dennison, W. C., Olyarnik, S., Calladine, A., *et al.* 2009. Accelerating loss of seagrasses across the globe threatens coastal ecosystems. Proceedings of the National Academy of Sciences of the United States of America, 106: 12377–12381.

Weerakoon, W. M., Olszyk, D. M., and Moss, D. N. 1999. Effects of nitrogen nutrition on responses of rice seedlings to carbon dioxide. Agriculture, Ecosystems and Environment, 72: 1–8.

Zimmerman, R. C., Kohrs, D. G., and Alberte, R. S. 1996. Top-down impact through a bottom-up mechanism: the effect of limpet grazing on growth, productivity and carbon allocation of *Zostra marina* L. (eelgrass). Oecologia, 107: 560–567.

Zimmerman, R. C., Kohrs, D. G., Steller, D. L., and Alberte, R. S. 1995. Carbon partitioning in eelgrass: regulation by photosynthesis and the response to daily light-dark cycles. Plant Physiology, 108: 1665–1671.

Zimmerman, R. C., Kohrs, D. G., Steller, D. L., and Alberte, R. S. 1997. Impacts of CO_2 enrichment on productivity and light requirements of eelgrass. Plant Physiology, 115: 599–607.

Handling editor: Joanna Norkko

ICES Journal of Marine Science

ICES Journal of Marine Science (2016), 73(3), 887–896. doi:10.1093/icesjms/fsv081

Contribution to Special Issue: 'Towards a Broader Perspective on Ocean Acidification Research'

Original Article

Two intertidal, non-calcifying macroalgae (*Palmaria palmata* and *Saccharina latissima*) show complex and variable responses to short-term CO_2 acidification

Joana Nunes[1]*, Sophie J. McCoy[1], Helen S. Findlay[1], Frances E. Hopkins[1], Vassilis Kitidis[1], Ana M. Queirós[1], Lucy Rayner[2], and Stephen Widdicombe[1]

[1]*Plymouth Marine Laboratory, Prospect Place, West Hoe, Plymouth PL1 3DH, UK*
[2]*Marine Biology and Ecology Research Centre, Plymouth University, Drake Circus, Plymouth PL4 8AA, UK*

**Corresponding author: tel: +44 1752 633 407; e-mail: jonu@pml.ac.uk*

Nunes, J., McCoy, S. J., Findlay, H. S., Hopkins, F. E., Kitidis, V., Queirós, Ana M., Rayner, L., and Widdicombe, S. Two intertidal, non-calcifying macroalgae (*Palmaria palmata* and *Saccharina latissima*) show complex and variable responses to short-term CO_2 acidification. – ICES Journal of Marine Science, 73: 887–896.

Received 11 December 2014; revised 10 March 2015; accepted 14 April 2015; advance access publication 11 May 2015.

Ocean acidification, the result of increased dissolution of carbon dioxide (CO_2) in seawater, is a leading subject of current research. The effects of acidification on non-calcifying macroalgae are, however, still unclear. The current study reports two 1-month studies using two different macroalgae, the red alga *Palmaria palmata* (Rhodophyta) and the kelp *Saccharina latissima* (Phaeophyta), exposed to control ($pH_{NBS} = \sim 8.04$) and increased ($pH_{NBS} = \sim 7.82$) levels of CO_2-induced seawater acidification. The impacts of both increased acidification and time of exposure on net primary production (NPP), respiration (*R*), dimethylsulphoniopropionate (DMSP) concentrations, and algal growth have been assessed. In *P. palmata*, although NPP significantly increased during the testing period, it significantly decreased with acidification, whereas *R* showed a significant decrease with acidification only. *S. latissima* significantly increased NPP with acidification but not with time, and significantly increased *R* with both acidification and time, suggesting a concomitant increase in gross primary production. The DMSP concentrations of both species remained unchanged by either acidification or through time during the experimental period. In contrast, algal growth differed markedly between the two experiments, in that *P. palmata* showed very little growth throughout the experiment, while *S. latissima* showed substantial growth during the course of the study, with the latter showing a significant difference between the acidified and control treatments. These two experiments suggest that the study species used here were resistant to a short-term exposure to ocean acidification, with some of the differences seen between species possibly linked to different nutrient concentrations between the experiments.

Keywords: DMSP, growth, macroalgae, net primary production, ocean acidification, *Palmaria palmata*, respiration, *Saccharina latissima*.

Introduction

It has been >10 years since the projections of Caldeira and Wickett (2003) that, by the end of the century, average surface ocean pH might decrease by 0.3–0.4 pH units from pre-industrial levels. In that time, the process of ocean acidification, which also affects seawater carbonate chemistry, has been an increasingly investigated subject (Riebesell and Gattuso, 2015). Many organismal responses to CO_2-induced acidification have now been documented, with particular focus on calcifying algae and invertebrates, those expected to depend the most on seawater carbonate processes (Kroeker *et al.*, 2010, 2013). However, substantially less information is available on non-calcifying macroalgae.

In calcifying organisms, the lower carbonate saturation states which result from increased seawater CO_2 concentrations will significantly reduce an organism's ability to support this energetically expensive physiological process (Wood *et al.*, 2008). The energetic cost of maintaining calcification has a further impact on other key processes such as growth and reproduction (Findlay *et al.*, 2011; Burdett *et al.*, 2012; Ragazzola *et al.*, 2012; McCoy and Ragazzola, 2014). Ultimately, the impacts of ocean acidification on an

organism's health and performance can lead to significant changes in population viability and distribution, and consequently in species interactions and community structure (Findlay *et al.*, 2010; McCoy and Pfister, 2014; Queirós *et al.*, 2014).

More recently, there has been a growing interest in how ocean acidification might also affect non-calcifying species, especially organisms that contribute significantly to processes or activities that humans benefit from, i.e. ecosystem services (Beaumont *et al.*, 2008). One such group of organisms are non-calcifying macroalgae, which provide ecosystem services such as habitat structure and complexity, primary productivity, and biodiversity (Dayton, 1985), as well as commercial benefits such as the provision of industrial products, fertilizer, and food (Mabeau and Fleurence, 1993; Wei *et al.*, 2013). For example, kelp forests are one of the most productive habitats on Earth (Schaal *et al.*, 2010; Brodie *et al.*, 2014; Smale *et al.*, 2014) and their three-dimensional structure provides shelter, feeding, and nursery areas for many species (Steneck *et al.*, 2003; Christie *et al.*, 2009). Kelps are also an important carbon sink, which is becoming progressively more significant in light of rising levels of atmospheric CO_2 (Alonso *et al.*, 2012).

Many fleshy algae are expected to benefit from acidification, as an increase in CO_2 can potentially lead to increased productivity (Koch *et al.*, 2013) and growth (Hepburn *et al.*, 2011; Roleda *et al.*, 2012). Some macroalgal species can use both CO_2 and HCO_3^- through the application of CO_2 carbon concentrating mechanisms (CCMs). These algae can then preferentially use HCO_3^- over CO_2, which obligate CO_2 users cannot do. The use of HCO_3^- by CCM species is, however, more energetically costly than using CO_2 (Koch *et al.*, 2013). Changes in carbonate and CO_2 concentrations as a result of acidification will, therefore, affect the strategies used by CCM species and impact upon the competitive interactions between those species with and those without CCMs (Hepburn *et al.*, 2011; Cornwall *et al.*, 2012; Koch *et al.*, 2013).

If algae are indeed able to increase photosynthetic rates under higher CO_2 conditions, the energy available for somatic growth could consequently increase (Gutow *et al.*, 2014). At high CO_2, CCM species may be able to switch to use CO_2 (less energetically demanding than HCO_3^-) and allocate this additional energy to tissue growth (Zou and Gao, 2009). In addition, increased levels of CO_2 may also enhance the growth of turf-forming algae, which might prevent recruitment of other macroalgae, such as kelps (Connell and Russell, 2010). Differential responses between algal species to ocean acidification could thus critically alter the species composition of many marine habitats.

Environmental stressors, such as acidification, can impact more than just an alga's ability to photosynthesise and grow. Marine algae produce a variety of secondary metabolites that play a number of important cellular roles (Van Alstyne *et al.*, 2001; Krumhansl and Scheibling, 2012). The production of such compounds is influenced by environmental conditions and cellular fitness, such that stressors including desiccation (Renaud *et al.*, 1990), salinity (Pedersen, 1984), and elevated CO_2 (Swanson and Fox, 2007; Arnold *et al.*, 2012; Burdett *et al.*, 2012; Kerrison *et al.*, 2012) may alter the synthesis of these compounds. One such metabolite is dimethylsulphoniopropionate (DMSP) which is a tertiary sulphonium compound, with several roles, such as cryoprotectant, antioxidant, and precursor to anti-herbivore activated defences (Van Alstyne *et al.*, 2001; Van Alstyne, 2008). DMSP breaks down to produce dimethyl sulphide (DMS), a trace gas that constitutes the greatest biogenic source of reduced sulphur to the marine atmosphere. The atmospheric oxidation products of DMS participate in secondary aerosol formation in the marine boundary layer, and thus play a key role in climate-related processes (Rap *et al.*, 2013). The worldwide distribution of dense macroalgal growth in coastal-zones may result in a significant flux of DMS to the atmosphere in these regions (Burdett *et al.*, 2012; Kerrison *et al.*, 2012). To date, there are very few studies on the effects of increased CO_2 on macroalgal DMSP production. DMSP production in the red coralline alga *Lithothamnion glaciale* has been shown to remain unmodified under continuous high CO_2 conditions; however, with an acute increase in CO_2, both intracellular and water column DMSP concentrations were seen to increase, thought to be a result of damage to the algal cell walls (Burdett *et al.*, 2012). In non-calcifying macroalgae, the effects of CO_2 on DMSP concentration have been investigated in the green alga *Ulva*, where *U. lactuca* showed a significant increase in the production of extracellular total DMSP in high CO_2 treatments (Kerrison *et al.*, 2012).

The current study reports on two separate experiments which have both studied the physiological responses to CO_2-induced seawater acidification in two ecologically important macroalgae from the Northeast Atlantic. The red alga *Palmaria palmata* and the kelp *Saccharina latissima*, which both possess CCMs, are common perennial macroalgae found primarily in the low intertidal zone of rocky shores. *Palmaria palmata* is an understory alga often found under the canopy-forming kelps, among other algae such as *Fucus serratus* and *Chondrus crispus* (Schaal *et al.*, 2010). The responses of *P. palmata* and *S. latissima* will inform our understanding of how ocean acidification will affect the function of these important nearshore ecosystems.

Methods

Sample collection and experimental set up

The two macroalgal species, *P. palmata* and *S. latissima*, were studied in separate experiments. Sixty *P. palmata* (Linnaeus) individuals (length of ~20 cm) were collected at low tide from Mount Batten (N 50° 21.371, W 4° 7.673), Plymouth, UK in October 2013 and the experimental exposures to CO_2-induced seawater acidification ran from October to November. Thirty-six *S. latissima* (Linnaeus) individuals (length of ~40 cm) were collected at low tide from the same location in February 2013 and the experimental exposures ran from March to April.

Both experiments used the same exposure set-up. Algae were kept in clear acrylic tanks (*S. latissima*: 12 tanks −60 cm long × 30 cm wide × 38 cm high, 3 individuals per tank; *P. palmata*: 30 tanks−20 cm long × 20 cm wide × 40 cm high, two individuals per tank) supplied with recirculating seawater. The tanks were lit by four evenly spaced LED strip lights (Betta 120 cm, 15 K, 22 W) on 12-h light−dark cycles, positioned at a distance of 40 cm from the water surface. Irradiance (Photosynthetic Active Radiation: PAR) was ~ 40 μmol photons m^{-2} s^{-1}. During this initial settling phase, which lasted 1 week in the *P. palmata* experiment and four weeks in the *S. latissima* experiment, tanks were continuously bubbled with ambient air and algae were kept under ambient conditions (pH_{NBS} = ~8.04).

In each experiment, half the experimental tanks were randomly allocated to the acidification treatment (OA: pH_{NBS} =~ 7.82), representative of an IPCC year 2100 OA scenario (IPCC, 2007), while the other half were allocated to ambient conditions (control: pH_{NBS} =~ 8.04). The pH in the acidification treatment is below the seasonal pH range (pH_{NBS}: 8.00–8.44) reported for coastal waters near the sampling sites (Kitidis *et al.*, 2012). Acidification

was initiated once the settling phase was completed, and applied gradually by reducing the pH by ~ 0.02 unit each day. For logistical reasons *S. latissima* had an acclimatization to acidification period of 2 weeks and *P. palmata* had an acclimatization to acidification period of 1 week. In both cases, the first set of measurements were taken after the acclimatization period, as soon as the target treatment level was reached. These measurements are referred to as T_0 hereafter. For both experiments, the actual time of pH exposure (post acclimatization period) was the same and lasted 4 weeks. The second set of measurements were taken at the end of the pH exposure (4 weeks after T_0), i.e. in April for *S. latissima* and in November for *P. palmata*, and will be collectively referred to as T_4 hereafter. Acidification was achieved by continuously bubbling the experimental tanks with pre-mixed air and CO_2 following the method by Findlay *et al.* (2008). The pre-mixed high-[CO_2] air passed through a Licor CO_2 analyser (LI-6262) and the atmospheric [CO_2] was recorded daily. pH (NBS scale, Metrohm pH meter), temperature, and salinity (WTW LF197 combination temperature and salinity probe) were recorded three times a week. Total alkalinity (TA) samples were collected weekly from each tank in 250 ml amber glass bottles and poisoned with 100 µl of a saturated mercuric chloride in deionised water solution. TA was measured using an open-cell potentiometric titration method with an automated titrator (Apollo SciTech Alkalinity Titrator Model AS-ALK2) following standard methods (Dickson *et al.*, 2007) and using certified reference materials (CO_2 CRM_s (Batch 127), Dickson Laboratory, University of California). To determine dissolved inorganic nutrient concentrations, 50 ml of seawater was collected weekly from each tank. The water was filtered (Acrodisc syringe filter with 0.8/0.2 µm Supor Membrane) into acid-cleaned, aged, 60 ml Nalgene bottles. The samples were frozen (−20°C) until ready for analysis. Analysis was carried out using a Bran and Luebbe AAIII segmented flow autoanalyser for the colorimetric determination of inorganic nutrients: combined nitrate + nitrite (Brewer and Riley, 1965), nitrite (Grasshoff, 1976), phosphate (Zhang and Chi, 2002), and silicate (Kirkwood, 1989). Nitrate concentrations were calculated by subtracting the nitrite from the combined nitrate + nitrite concentration. pCO_2, bicarbonate and carbonate concentrations were calculated using CO2SYS (Lewis and Wallace, 1998; Pierrot *et al.*, 2006) with dissociation constants from Mehrbach *et al.* (1973) refit by Dickson and Millero (1987) and KSO_4 using Dickson (1990).

Determination of net primary production and respiration

Net primary production (hereafter referred to as NPP) and respiration (hereafter referred to as R) were assessed as changes in dissolved oxygen concentrations during light (mean PAR = 34 mmol photons m^{-2} s^{-1}) and dark incubation periods, respectively. One whole alga per tank was incubated in one light and in one dark incubation at T_0 and again 4 weeks later (T_4). Each incubation lasted for one and a half hours for *S. latissima* and for 2 h for *P. palmata*. Incubation times were determined by preliminary trials. Incubation chambers consisted of 5.3 l air tight acrylic tanks. A magnetic stirrer was placed at the bottom of each tank to homogenize oxygen concentration in the incubation water and chambers were placed in a water bath, on top of a large Variomag stirring plate. In addition to the algal incubations, blank incubations (seawater of each treatment only) were done in 0.9 l incubation chambers to correct for the contribution of planktonic and microbial activity. All individual algae were acclimatized to incubation conditions for 20–30 min, during which water flow into the chambers was maintained. At the end of this period, each chamber was sealed and incubations initiated.

In the *S. latissima* experiment, dissolved oxygen concentrations were determined using the Winkler titration method (Carritt and Carpenter, 1966) on water samples taken at the beginning and at the end of each incubation. Acid washed, gravimetrically calibrated, 120 ml borosilicate glass bottles were carefully filled with incubation seawater using silicon tubing. For each incubated alga, triplicate samples were collected at: (a) Start (fixed immediately, see below), (b) Light (incubated under light before fixing), and (c) Dark (incubated in the dark before fixing). The concentration of oxygen (O_2) in each bottle was determined by automated Winkler titration (Carritt and Carpenter, 1966) with photometric endpoint detection. Briefly, O_2 is precipitated with alkaline iodide (NaOH + NaI) and $MnSO_4$ and the samples stored in a water bath at room temperature until analysis (24–48 h). The precipitate is dissolved by addition of H_2SO_4 and titrated against thiosulfate (transmission endpoint detection). The thiosulfate was calibrated every 3 days against 0.1 mol l^{-1} KIO_3 standards (Sigma-Aldrich, product number: 34273). O_2 saturation with respect to atmospheric equilibrium was calculated from the solubility of O_2 at *in situ* temperature, salinity, and pressure (Benson and Krause, 1984; Garcia and Gordon, 1992).

In the *P. palmata* experiment, oxygen measurements were taken using a non-invasive optical O_2 analyser (5250i, OxySense, Dallas, USA) as detailed in Rastrick and Whiteley (2011) and Calosi *et al.* (2013). The OxySense fibre optic pen measures the fluorescence characteristics of an O_2 sensitive dot which was previously placed inside the incubation chambers. Before the first incubations, the oxygen optode was calibrated against the O_2 sensitive dots. Oxygen measurements were taken at the beginning and at 20 min intervals over a period of 2 h.

For both experiments, NPP was calculated as the O_2 concentration difference between 'Light' and 'Start' treated samples and R was calculated as the O_2 concentration difference between 'Dark' and 'Start'.

At the end of T_4 incubations, the biomass of each alga was estimated as ash-free dry weight ($AFDW$ = dry weight − ash weight). Algal dry weights were obtained after drying the algae at 60°C for 48 h and algal ash weights were obtained after combusting the dried algae at 350°C for 62 h. Each alga's R and NPP were corrected for biomass ($AFDW$) and the contribution of plankton and bacteria following the equation:

$$R_{algae} = \frac{R_{incubation} - R_{blank}}{AFDW(g)}$$

DMSP sampling and analysis

Samples for DMSP analysis were collected at T_0 and T_4 from all individuals. Vegetative algal tissue samples were collected using a holeborer size 10 (1.5 cm in diameter). To test for differences in DMSP production along the frond, half the algae were sampled at the base of the frond (just above the stipe) and the other half were sampled at the tip of the frond. The exact fresh weight of samples was recorded.

In the *S. latissima* experiment, algal samples were dried at 60°C for 48 h and dry weight recorded. Each sample was placed in a 20-ml serum vial containing 10 ml of Milli-Q water and one NaOH pellet, and the vial was quickly crimp sealed. In the *P. palmata* experiment, only fresh tissue samples were used (no drying) in smaller 8 mL serum vials containing 6 ml of 500 µM sodium hydroxide. This was due to very low concentrations of DMSP in this species.

All samples were refrigerated in the dark until the time of analysis and analysed in the same way. Before analysis, samples were placed in a water bath overnight at 30°C to equilibrate DMS in the water and gas phases. One hundred to 250 µl of the supernatant was transferred to a glass purge tower using a Hamilton syringe for quantification of DMS. Samples were purged with helium at 60 ml min^{-1} for 5 min while cryogenically trapping the DMS (Archer *et al.*, 2013). DMS concentrations were determined using a Varian 3800 gas chromatograph equipped with a pulsed flame photometric detector. DMS standards for calibration were prepared from DMSP (>98% purity; Centrum voor Analyse, Spectroscopie and Synthese, Rijksuniversiteit Groningen) following base hydrolysis in a 1.0 mol l^{-1} NaOH solution. A five-point calibration was carried out at regular intervals throughout the sample analysis period, with an r^2 for the resulting linear regression of nanogram sulphur vs. square root of the peak area of typically >0.995.

Algal growth

Perforation areas at T_0 were the 1.5 cm diameter circular perforations done for DMSP analysis. At T_4 the perforations had become ellipses in some individuals. In *S. latissima* growth was assessed based on perforation area at T_4 (perforation area = $\Pi \times (1.5/2) \times$ (perforation major axis/2)) and by perforation migration (calculated as the distance the perforation punched at T_0 had migrated by the time of the T_4 sampling point; Pfister, 1992).

Because *P. palmata* has smaller fronds than the kelp *S. latissima*, and because this experiment was run in autumn when algae were not actively growing, perforation area at T_4 was considered a better method to estimate algal growth in *P. palmata*.

Statistical analysis

The effects of acidification treatment (control cf. OA) and time (T_0 cf. T_4) on all measured parameters (NPP, R, DMSP concentration; perforation area at T_4 and perforation migration, i.e. algal growth, were only assessed for the effect of acidification) were individually investigated using generalized least-squares (GLS) analysis (Zuur *et al.*, 2009) given that data exhibited strong heteroskedasticity, therefore violating linear model assumptions. Linear model assumptions were verified by investigation of normal quantile–quantile (qq) plots and visual inspection of residual dispersion against treatments. Model structures investigated included acidification and time of exposure, and first-order interaction as fixed effects. To model heteroskedascity various possible variance structures as a function of the predictor structure were compared. Models of increasingly higher complexity were then compared with simpler models hierarchically, using Akaike's information criterion (AIC) for each model, and estimation of likelihood-ratio statistics for evaluation of the improvement of fits. The best and most parsimonious fit for each response variable was selected. The effect of variance structures on model fit was investigated using restricted maximum likelihood estimates, while the effect of the predictor structure was investigated using maximum likelihood estimates (Pinheiro and Bates, 2000; Pinheiro *et al.*, 2007). The data from the two experiments were analysed separately.

Results

Palmaria palmata

Table 1 summarizes the seawater chemistry details during the T_0 and T_4 periods for the *P. palmata* experiment. The carbonate chemistry remained significantly different between control and acidified treatments (two-group *t*-test for pH, $p < 0.01$, two-group *t*-test for TA, $p = 0.75$) throughout the duration of this experiment (two-group *t*-test for pH, $p = 0.46$, two-group *t*-test for TA, $p = 0.81$).

Nitrate and phosphate concentrations varied throughout the experimental period (Table 3). In the *P. palmata* experiment, a

Table 1. Seawater chemistry (mean ± SD) during the *Palmaria palmata* experiment.

	T_0		T_4	
Parameter	**Control**	**OA**	**Control**	**OA**
Temperature (°C)	15.8 ± 0.2	15.9 ± 0.1	15.8 ± 0.1	15.9 ± 0.1
Salinity	35.1 ± 2.4	35.0 ± 2.5	36.1 ± 2.0	36.0 ± 2.0
pH_{NBS}	8.02 ± 0.02	7.90 ± 0.04	8.01 ± 0.01	7.85 ± 0.05
TA (µmol kg^{-1})	2718.7 ± 167.4	2738.7 ± 129.8	2735.0 ± 90.6	2745.5 ± 89.2
pCO_2 (µatm)	689.70 ± 43.73	960.27 ± 123.10	699.78 ± 34.55	1066.92 ± 157.28
Bicarbonate (µmol kg^{-1})	2362.98 ± 127.36	2461.22 ± 118.80	2376.07 ± 70.31	2484.87 ± 82.25
Carbonate (µmol kg^{-1})	147.60 ± 18.81	115.28 ± 10.98	149.00 ± 8.70	108.23 ± 12.12

Temperature, salinity, pH, and TA were measured. pCO_2, bicarbonate, and carbonate concentrations were calculated using CO2SYS (Lewis and Wallace, 1998; Pierrot *et al.*, 2006) with dissociation constants from Mehrbach *et al.* (1973) refit by Dickson and Millero (1987) and KSO_4 using Dickson (1990).

Table 2. Seawater chemistry (mean ± SD) during *S. latissima* experiment.

	T_0		T_4	
Parameter	**Control**	**OA**	**Control**	**OA**
Temperature (°C)	12.4 ± 0.7	12.2 ± 0.5	13.1 ± 2.5	13.7 ± 2.0
Salinity	36.6 ± 0.2	36.6 ± 0.3	35.7 ± 1.2	35.8 ± 1.2
pH_{NBS}	8.09 ± 0.05	7.75 ± 0.04	8.06 ± 0.05	7.77 ± 0.04
TA (µmol kg^{-1})	2850.2 ± 91.3	2908.9 ± 200.7	2878.1 ± 165.4	2831.3 ± 114.3
pCO_2 (µatm)	580.91 ± 74.80	1392.12 ± 150.62	645.15 ± 78.22	1329.14 ± 145.68
Bicarbonate (µmol kg^{-1})	2448.21 ± 81.77	2708.09 ± 187.81	2495.17 ± 132.16	2622.84 ± 115.97
Carbonate (µmol kg^{-1})	167.27 ± 22.18	83.75 ± 9.91	160.21 ± 37.73	86.83 ± 6.69

Temperature, salinity, pH, and TA were measured. pCO_2, bicarbonate, and carbonate concentrations were calculated using CO2SYS (Lewis and Wallace, 1998; Pierrot *et al.*, 2006) with dissociation constants from Mehrbach *et al.* (1973) refit by Dickson and Millero (1987) and KSO_4 using Dickson (1990).

significant decrease in both nutrients was observed over time in both acidified and control treatments (nitrate: nitrate–time, AIC = 28.2603, logLik = − 10.1301, d.f. = 4, p-value < 0.01; phosphate: phosphate–time, AIC = 35.8434, logLik = − 13.9217, d.f. = 4, p-value < 0.01).

In *P. palmata*, both acidification and time had a significant effect on NPP (NPP ~ OA + time; Table 4; Figure 1). In this experiment, *R* significantly decreased (i.e. higher O_2 concentration) in the acidified treatments, and this did not relate to time (R–OA; Table 4; Figure 2).

DMSP concentrations did not differ at different frond locations in *P. palmata* (mean base DMSP: 0.67 ± 0.80 μg g^{-1}, mean tip DMSP: 0.61 ± 0.79 μg g^{-1}; AIC = 282.1255, logLik = − 137.0627, d.f. = 4, and p-value = 0.65; Figure 3). For this reason, in the *P. palmata* experiment, all samples were used in the DMSP analysis. DMSP concentrations did not differ significantly with either time or with acidification levels in this species (Table 5).

Palmaria palmata showed uniform growth along the frond, with no difference in growth between the base and the tip of the frond (AIC = − 72.5359, logLik = 39.2679, d.f. = 3, p-value = 0.32; Figure 4). For this reason, data from all individuals were used to test the effect of acidification on growth, which showed that exposure to acidified seawater had no significant impact on growth in *P. palmata* (Table 5). In fact, the *P. palmata* experiment did not show substantial algal growth from the initial perforation size of 1.77 cm^2, with bottom perforations averaging at 2.16 cm^2 (Figure 4).

Saccharina latissima

Table 2 summarizes the seawater chemistry details during the T_0 and T_4 periods for the *S. latissima* experiment. The carbonate chemistry remained significantly different between control and acidified treatments (two-group t-test for pH, $p < 0.01$, two-group t-test for TA, $p = 0.89$) throughout the duration of this experiment (two-group t-test for pH, $p = 0.88$, two-group t-test for TA, $p = 0.56$).

Nitrate and phosphate concentrations varied throughout the experimental period (Table 3). During the *S. latissima* experiment, both nitrate and phosphate significantly increased towards the end of the testing period (nitrate: nitrate–time, AIC = − 32.5912, logLik = 20.2956, d.f. = 4, p-value < 0.01; phosphate: phosphate–t, AIC = − 23.4771, logLik = 15.7385, d.f. = 4, p-value < 0.01).

In *S. latissima*, acidification had a significant effect on NPP, but time did not cause change (NPP–OA; Table 4; Figure 1). In *S. latissima*, *R* significantly increased in the acidified treatment and with time (R–OA + time; Table 4; Figure 2).

In *S. latissima*, DMSP concentrations varied between the base (mean base DMSP: 12.40 ± 7.18 μg g^{-1}) and the tip of the frond (mean tip DMSP: 1.83 ± 0.96 μg g^{-1}; Figure 3). This difference was highly significant (AIC = 349.0890, logLik = − 170.5445, d.f. = 4, p-value < 0.01). For this reason, in the *S. latissima* experiment DMSP analysis was focused on samples taken from the base of the frond only. DMSP concentrations did not differ significantly with either time of exposure or with acidification levels in *S. latissima* (Table 5).

Based on T_4 perforation area, *S. latissima* growth was observed at the base of the frond, rather than at its tip (AIC = 51.5082, logLik = − 21.7541, d.f. = 4, p-value < 0.01; Figure 4). Therefore, subsequent analysis focused only on those samples taken at the base of the frond. During the 4-week exposure experiment there was no significant difference in growth between *S. latissima* grown in control conditions and those exposed to acidified seawater (Table 5). In *S. latissima* bottom perforations averaged at 5.43 cm^2 at T_4 (Figure 4), showing substantial growth during the 4-week experiment.

Based on perforation migration, and on bottom perforations only, acidification did have a significant effect on growth in *S. latissima* (growth by perforation migration–OA, AIC = 56.0671, logLik = − 24.0335, d.f. = 4, p-value = 0.02, Figure 5).

Table 3. Nitrate and phosphate concentrations (mean ± SD) during oxygen incubations.

Species	Sampling time	Acidification treatment	Nitrate (μmol l^{-1})	Phosphate (μmol l^{-1})
Palmaria palmata	T_0	Control	3.47 ± 2.65	1.06 ± 0.93
		OA	2.57 ± 2.53	1.29 ± 0.73
	T_4	Control	0.24 ± 0.10	0.44 ± 0.34
		OA	0.26 ± 0.17	0.55 ± 0.29
Saccharina latissima	T_0	Control	0.02 ± 0.01	0.14 ± 0.03
		OA	0.02 ± 0.01	0.12 ± 0.07
	T_4	Control	0.04 ± 0.04	0.41 ± 0.20
		OA	0.19 ± 0.29	0.34 ± 0.25

Discussion

The current study describes two separate experiments which used the same experimental set-up to examine the impacts of CO_2-induced acidification on key physiological functions in two species of

Table 4. Results from GLS models for the effect of sampling time (time) and acidification treatment (OA) on NPP and *R* for *P. palmata* and *S. latissima*.

		NPP				*R*			
Species	**Source of variation**	**AIC**	**logLik**	**d.f.**	***p***	**AIC**	**logLik**	**d.f.**	***p***
Palmaria palmata	Time × OA	−77.5536	44.7768	6	0.44	−110.1263	61.0632	6	0.74
	Time + OA	**−78.9664**	**44.4832**	**5**	**<0.01, <0.01**	−112.0128	61.0064	5	<0.01, 0.08
	Time	−71.8358	39.9179	4	<0.01	−96.5592	52.2796	4	0.64
	OA	−70.8763	39.4382	4	<0.01	**−110.9779**	**59.4890**	**4**	**<0.01**
	~1	−63.0992	34.5496	3	na	−98.3418	52.1709	3	na
Saccharina latisssima	Time × OA	−31.9217	21.9609	6	0.31	−63.7202	37.8601	6	0.51
	Time + OA	−32.8842	21.4421	5	<0.01, 0.07	**−65.2886**	**37.6443**	**5**	**<0.01, 0.02**
	Time	−15.0206	11.5103	4	0.06	−58.9119	33.4560	4	0.05
	OA	**−31.5179**	**19.7589**	**4**	**<0.01**	−61.7799	34.8900	4	0.01
	~1	−13.5983	9.7992	3	na	−57.1323	31.5662	3	Na

AIC, Akaike information criterion; logLik, log-likelihood; d.f., degrees of freedom; p, level of confidence ($\alpha = 0.05$). The values in bold represent the selected model.

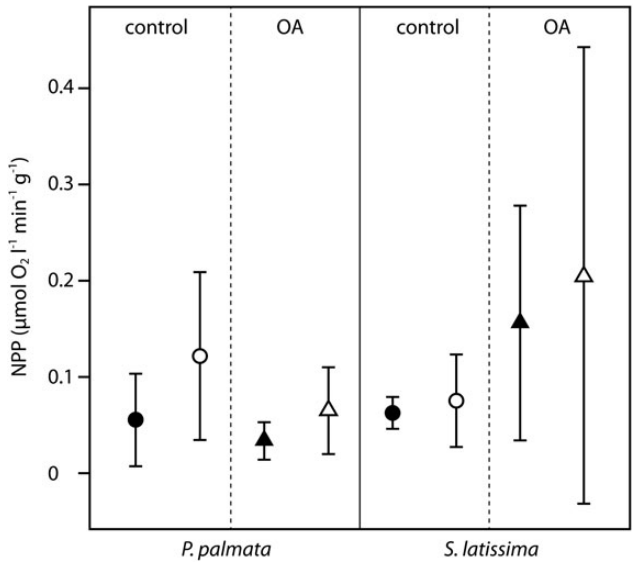

Figure 1. Mean ± SD Net Primary Production, NPP, of *P. palmata* and *S. latissima* under control and acidified (OA) treatments. Black symbols represent T_0, white symbols represent T_4.

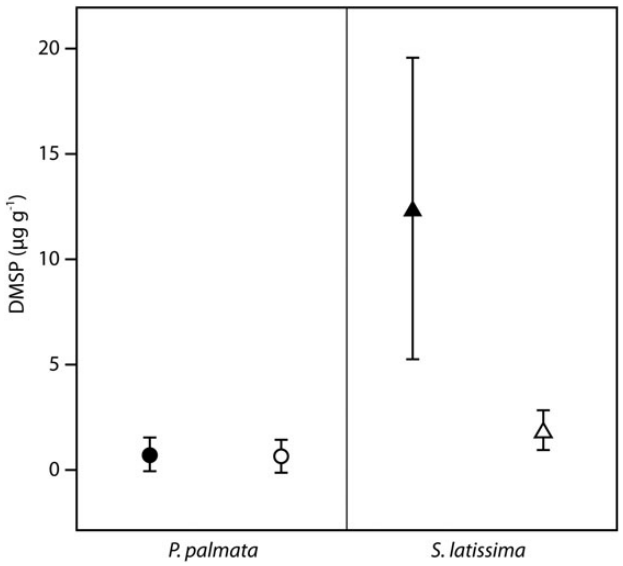

Figure 3. DMSP concentration (mean ± SD) of *P. palmata* and *S. latissima* at the base (black symbols) and tip (white symbols) of the frond.

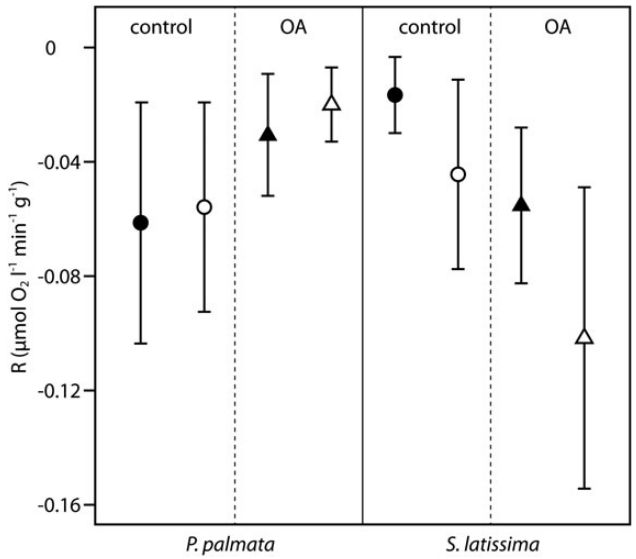

Figure 2. Mean ± SD Respiration, R, of *P. palmata* and *S. latissima* under control and acidified (OA) treatments. Black symbols represent T_0, white symbols represent T_4.

intertidal fleshy algae. While the data from the two experiments cannot be directly compared in formal statistical analysis, the general responses and results do provide an insight into the variety of responses that can be seen across the macroalgal group, contributing towards an increased understanding of algal responses to ocean acidification.

A key factor in driving algal response over time could be nutrient supply. In the current studies, the statistical analysis showed that both nitrate and phosphate concentrations decreased significantly over the course of the *P. palmata* experiment, while the concentrations of these nutrients increased significantly over the course of the *S. latissima* experiment. Despite the statistically significant increase in nutrient concentrations observed in the *S. latissima* experiment, which opposes that observed in the *P. palmata* experiment, the actual nutrient levels during the *S. latissima* experiment can be considered as extremely low and remained close to or even below the detection limit of the analytical techniques (0.02 µmol l^{-1} detection limit for nitrate). This, together with the fact, that *P. palmata* was tested in autumn, while *S. latissima* was tested in spring, might explain some of the contrasting responses reported here and the interspecies variability seen in some cases.

The observed responses of R to acidified conditions contrasted between the two species studied: *P. palmata* showed a significant decrease in *R*, whereas *S. latissima* exhibited a significant increase in *R*, in response to CO_2-induced acidification. For *P. palmata*, both NPP and *R* decreased significantly under higher acidification levels, and no increase in growth was observed. Given that CO_2 is a resource for photosynthesis and might be expected to stimulate growth and function in non-calcifying algae, it is somewhat surprising that this alga appears down-regulating its photosynthesis and metabolism under high CO_2, and therefore limiting growth. However, this reduction in metabolic activity and lack of increased growth may not be caused by changes in acidification but may actually be a result of other important environmental factors. For example, daylength and net heat-flux, which would normally act as a cue to trigger growth, were held constant throughout the course of these experiments. The current results may, again, be confounded by the timing of the experiments. *P. palmata* specimens were collected in October when they may have already down-regulated their metabolism in response to environmental cues for the onset of winter. The suppressed growth of *P. palmata* in early autumn, a consequence of the low light and temperature typical of this time of year, has been previously reported (Martínez and Rico, 2002). Yet, despite the absence of growth, nutrients were depleted between T_0 and T_4 in the *P. palmata* experiment. Perhaps the algae took up the nutrients and stored these for future use.

Table 5. Results from GLS models for the effect of sampling time (time) and acidification treatment (OA) on DMSP concentration and growth for *P. palmata* and *S. latissima*.

		DMSP				Growth (perforation area)			
Species	**Source of variation**	**AIC**	**logLik**	**d.f.**	***p***	**AIC**	**logLik**	**d.f.**	***p***
Palmaria palmata	Time + OA	280.7390	−135.3695	5	0.41, 0.20	na	na		na
	Time	279.4138	−135.7069	4	0.09	na	na		na
	OA	280.3574	−136.1787	4	0.16	−71.5484	38.7742	3	0.90
	∼1	**280.3360**	**−137.1680**	**3**	**na**	**−73.5315**	**38.7658**	**2**	**na**
Saccharina latisssima	Time + OA	250.5462	−121.2731	4	0.60, 0.58	na	na	na	na
	Time	248.8167	−121.4084	3	0.58	na	na	na	na
	OA	248.8581	−121.4291	3	0.60	84.7740	−39.3870	3	0.29
	∼1	**247.1264**	**−121.5632**	**2**	**na**	**83.8798**	**−39.9399**	**2**	**na**

AIC, Akaike information criterion; logLik, log-likelihood; d.f., degrees of freedom; *p*, level of confidence ($\alpha = 0.05$). The values in bold represent the selected model.

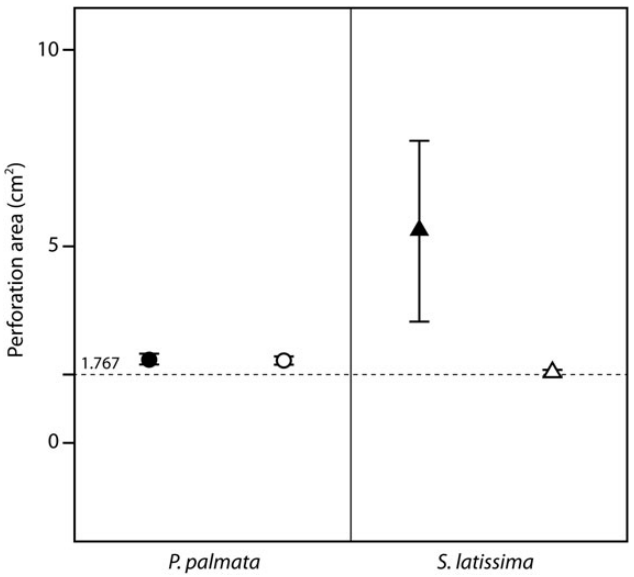

Figure 4. Mean ± SD T_4 perforation area of *P. palmata* and *S. latissima* at the base (black symbols) and tip (white symbols) of the frond; the dotted line indicates the perforation area at T_0.

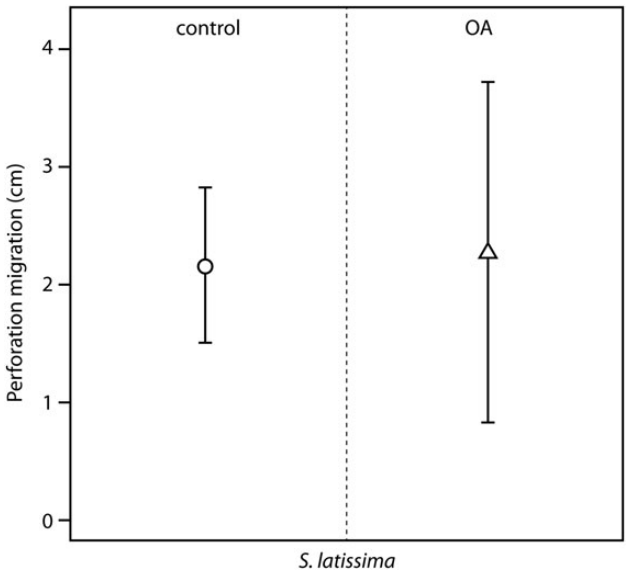

Figure 5. Mean ± SD T_4 perforation migration of *S. latissima* at the base of the frond at control and acidified (OA) treatments.

Saccharina latissima showed an overall upregulation of both NPP and *R* when exposed to the acidified treatment, suggesting that these individuals are taking advantage of an increased availability of carbon. While the average level of NPP significantly increased in acidified seawater, it should be noted that the variability of this parameter also increased the longer the algae were under laboratory conditions (exposure time) as well as with increased acidification (Figure 1). Increased variability may suggest that algal "fitness" was more variable as time progressed and at high CO_2 levels, meaning that some individuals were able to withstand laboratory conditions and an acidified environment, while others were not. It is not clear if this increase in variability reflects differences in individual fitness at the genetic level, or differences in other factors, e.g. stored nutrients. It is unlikely that the small increase in nitrate and phosphate availability in the *S. latissima* experiment would have been sufficient to produce a significant algal response. These algae may therefore have experienced nutrient limitation from the beginning of the experiment, which could also partially explain the observed variability in responses. Perhaps nutrient limitation may have been exacerbated through the duration of the four week experiment and under acidification, manifesting itself as high variability in NPP and R. Though this interpretation is somewhat speculative, it further highlights the possibility of synergistic effects of different stressors (Russell *et al.*, 2009) and individual variability (Pistevos *et al.*, 2011). *Saccharina latissima* exhibited an increase in *R* at T_4 in both control and acidified treatments, possibly caused by poor acclimation to the experimental conditions, which would explain why these differences between T_0 and T_4 were also seen in the control treatment. Again, the variability in NPP and *R* response is especially evident at T_4 in acidified treatments, indicating that responses to acidification might have been exacerbated by the end of the experiment. Regardless of the mechanism, this variable response between individuals of the same species is a key element for future acclimation or potential adaption to changing environmental conditions.

Algal growth, in terms of perforation area, of both *P. palmata* and *S. latissima* remained unaffected by increased levels of CO_2 after 1 month of exposure. The fact that the effects of time and acidification on the NPP of *P. palmata* and *S. latissima*, respectively, were only

marginally significant, might suggest that not much extra energy was available to be allocated to somatic growth and support the perforation area results obtained here. In fact, *P. palmata* did not grow considerably, in either acidification or control treatments. However, in *S. latissima*, when estimating growth by comparing basal perforation migration between the control and the acidification treatment, it was apparent that perforations travelled (i.e. algae grew) more under acidified conditions than under control treatments. So in contrast to the perforation area results, it would appear that when growth is measured using the perforation migration method, there is some evidence that elevated CO_2 could have a stimulatory impact on *S. latissima* growth. The response of perforation migration to acidification is in accordance with the observed overall up-regulation of NPP and *R*, and suggests that a greater supply of CO_2 might indeed have slightly enhanced the performance of *S. latissima*. This highlights the need to consider CO_2 as both an important resource for non-calcifying macroalgae as well as a potential stressor. In addition, these growth results also demonstrate the importance of choosing the most appropriate method to assess particular biological responses.

In the kelp *Laminaria hyperborea*, an increase in growth rate has been previously linked to an increase in primary production in conjunction with stored nitrogen use (Abdullah and Fredriksen, 2004). Again, at least in the *S. latissima* experiment, nitrogen availability in the seawater was limited, which possibly further restricted the ability of the algae to grow. Furthermore, acidification did not affect algal growth during the stage of their life cycle studied here (mature sporophytes). It is worth considering that this may not be valid at other life-stages (e.g. juveniles or during reproduction). At the same time, it is likely that in these species algal growth is not prioritized when additional carbon is available. Macroalgae may instead preferably enhance reproduction or defences.

In the experiments here, there were no significant changes in DMSP concentration between acidified and control treatments in either *P. palmata* or *S. latissima*. This might be because both species produce relatively small quantities of this compound. Macroalgae reported to contain the highest concentrations of DMSP are Chlorophyta and Rhodophyta in the genus *Polysiphonia* (Van Alstyne *et al.*, 2001; Van Alstyne, 2008). In green algae of the genus *Ulva*, concentrations of DMSP are typically 320–1600 mg g^{-1} fresh weight (Van Alstyne and Puglisi, 2007). In contrast, and comparable to the current results, Lyons *et al.* (2007) found non-detectable levels of DMSP in *Laminaria digitata* and *Saccharina longicruris*, kelps from the Northwestern Atlantic coast, and also in *P. palmata*. It is thus possible that the species used in the current studies preferably invest in producing secondary metabolites other than DMSP when faced with a stressor, therefore maintaining their DMSP production unaltered between control and acidified treatments. Furthermore, the time of sampling of these experiments might have not been ideal, as seasonal variations in DMSP concentrations have been documented in *Codium fragile* ssp. *tomentosoides* (Chlorophyta) in Nova Scotia and shown to peak in winter then decrease through to autumn (Lyons *et al.*, 2007). This seasonality might be related to an increased demand for the cryoprotectant properties of DMSP in winter. Additionally, DMSP occurs in high amounts in the genera *Enteromorpha*, *Ulva* and *Polysiphonia*, which are opportunistic macroalgae that can endure high salinity and desiccation (Van Alstyne *et al.*, 2001). In the current experiments, the algae used were collected from the low intertidal and were typically aerially exposed for no longer than a couple of hours on an extreme low tide, unlike *Enteromorpha*, *Ulva*, and *Polysiphonia* which are found at higher tidal elevations that become exposed during daily low tides for several hours.

The fact that *S. latissima* had significantly higher levels of DMSP at the base, rather than at the tip, of the frond, where tissues were also shown to be growing the most, suggests that this compound is mainly allocated to younger tissues. One hypothesis to explain the strategy of associating DMSP with younger tissues is that an alga should protect new growth, where resources have recently been allocated, in favour of old tissue at the frond tips that is most susceptible to physical damage. *Palmaria palmata* on the other hand, showed no differences in DMSP concentration or growth between base and tip of the frond. The lack of a difference in DMSP concentration between tissue locations might be supported by the fact that this species grows by dichotomous branching, as opposed to the elongated strap-shaped growth of a single frond in the kelp *S. latissima* (Bunker *et al.* 2010).

Finally, there are other compounds macroalgae produce to deal with changes in the environment. For instance, *S. latissima* in Canada has been found to invest in phlorotannin production when exposed to increased CO_2 levels (Swanson and Fox, 2007). However, this response was identified during a 55-day experiment. It is therefore also possible that the duration of the current experiments (4 weeks) was insufficient to identify detectable responses to CO_2 enrichment. Indeed, the distinct effects of short- and long-term exposures to climate stressors on marine organisms (Form and Riebesell, 2012; Godbold and Solan, 2013), have indicated that realistic climate change impact assessments may require far longer exposure times.

Conclusions

North Atlantic macroalgal community structure and ecosystem functioning are expected to change in the future, as a consequence of the combined effects of acidification and warming (Brodie *et al.*, 2014). However, in the present experiments few changes in the NPP, R, DMSP concentrations and algal growth of individual macroalgae exposed to CO_2-induced seawater acidification were observed after 4 weeks. Specific elements of these experiments might have limited the study's ability to identify significant responses to ocean acidification, and it is recommended that future investigations of fleshy macroalgae consider seasonal variability in combination with longer exposure times. Nevertheless, the current studies have demonstrated that *P. palmata* and *S. latissima* possess a certain degree of resistance to ocean acidification. In light of these results, it is suggested that further experiments focus on the several parameters that might indicate macroalgal well-being, such as growth or grazing defences. Doing so in a multi-response approach, will help to disentangle possible trade-offs taking place in response to climate stressors. In addition, this study has highlighted the danger of extrapolating data from a single experiment to describe a generic acidification response for any particular species or group. Only by exploring the way in which underlying, seasonally variable, factors (such as organism condition, exposure history, reproductive/growth state, nutritional condition, or additional stressors or pressures) modify an organism's response to acidification, can a generic species-wide assessment be made. This will require multiple additional experiments to be conducted on species which may have already been studied. The effects of ocean acidification on habitat-forming non-calcifying macrophytes are likely to greatly modify present ecosystems, justifying the investment in such future research efforts for this group.

Acknowledgements

The authors are grateful to Laure Noël and Fanny Noisette from Station Biologique Roscoff, France, who provided guidance to JN on running macroalgal experiments and measuring photosynthesis (exchange visits funded by Marinexus and the NERC funded UKOA program project "Impacts of ocean acidification on key benthic ecosystems, communities, habitats, species and life cycles" (NE/H01747X/1)). We thank John Stephens and Michael Steinke for advice on DMSP analysis, John Jury for IT support, Dawn Ashby for graphical assistance, and both Carolyn Harris and Malcolm Woodward for help with the nutrient analysis.

References

Abdullah, M. I., and Fredriksen, S. 2004. Production, respiration and exudation of dissolved organic matter by the kelp *Laminaria hyperborea* along the west coast of Norway. Journal of the Marine Biological Association of the United Kingdom, 84: 887–894.

Alonso, I., Weston, K., Gregg, R., and Morecroft, M. 2012. Carbon storage by habitat -Review of the evidence of the impacts of management decisions and condition on carbon stores and sources. Natural England Research Reports, Number NERR043.

Archer, S. D., Kimmance, S. A., Stephens, J. A., Hopkins, F. E., Bellerby, R. G. J., Schulz, K. G., Piontek, J., *et al.* 2013. Contrasting response of DMS and DMSP to ocean acidification in Arctic waters. Biogeosciences, 10: 1893–1908.

Arnold, T., Mealey, C., Leahey, H., Miller, A. W., Hall-Spencer, J. M., Milazzo, M., and Maers, K. 2012. Ocean acidification and the loss of phenolic substances in marine plants. PLoS ONE, 7: e35107.

Beaumont, N. J., Austen, M. C., Mangi, S. C., and Townsend, M. 2008. Economic valuation for the conservation of marine biodiversity. Marine Pollution Bulletin, 56: 386–396.

Benson, B. B., and Krause, D. 1984. The concentration and isotopic fractionation of oxygen dissolved in fresh-water and seawater in equilibrium with the atmosphere. Limnology and Oceanography, 29: 620–632.

Brewer, P. G., and Riley, J. P. 1965. The automatic determination of nitrate in sea water. Deep-Sea Research, 12: 765–772.

Brodie, J., Williamson, C. J., Smale, D. A., Kamenos, N. A., Mieszkowska, N., Santos, R., Cunliffe, M., *et al.* 2014. The future of the northeast Atlantic benthic flora in a high CO_2 world. Ecology and Evolution, 4: 2787–2798.

Bunker, F., Stp, D., Maggs, C. A., Brodie, J. A., and Bunker, A. R. 2010. Seaweeds of Britain and Ireland. Wild Nature Press, Plymouth, UK. 158 pp.

Burdett, H. L., Aloisio, E., Calosi, P., Findlay, H. S., Widdicombe, S., Hatton, A. D., and Kamenos, N. A. 2012. The effect of chronic and acute low pH on the intracellular DMSP production and epithelial cell morphology of red coralline algae. Marine Biology Research, 8: 756–763.

Caldeira, K., and Wickett, M. E. 2003. Anthropogenic carbon and ocean pH. Nature, 425: 365.

Calosi, P., Rastick, S. P. S., Lombardi, C., de Guzman, H. J., Davidson, L., Jahnke, M., Giangrande, A., *et al.* 2013. Adaptation and acclimatization to ocean acidification in marine ectotherms: an *in situ* transplant experiment with polychaetes at a shallow CO_2 vent system. Philosophical Transactions of the Royal Society B, 368: 20120444.

Carritt, D. E., and Carpenter, J. H. 1966. Comparison and evaluation of currently employed modifications of the Winkler method for determining dissolved oxygen in seawater; a NASCO Report. Journal of Marine Research, 24: 286–319.

Christie, H., Norderhaug, K. M., and Fredriksen, S. 2009. Macrophytes as habitat for fauna. Marine Ecology Progress Series, 396: 221–233.

Connell, S. D., and Russell, B. D. 2010. The direct effects of increasing CO_2 and temperature on non-calcifying organisms: increasing the potential for phase shifts in kelp forests. Proceedings of the Royal Society of London B: Biological Sciences, 277: 1409–1415.

Cornwall, C. E., Hepburn, C. D., Pritchard, D., Currie, K. I., McGraw, C. M., Hunter, K. A., and Hurd, C. L. 2012. Carbon-use strategies in macroalgae: differential responses to lowered pH and implications for ocean acidification. Journal of Phycology, 48: 137–144.

Dayton, P. K. 1985. Ecology of kelp communities. Annual Review of Ecological Systems, 16: 215–245.

Dickson, A. G. 1990. Standard potential of the reaction: $AgCl(s) + 1/2H_2(g) = Ag(s) + HCl(aq)$, and the standard acidity constant of the ion HSO_4^- in synthetic sea water from 273.15 to 318.15 K. The Journal of Chemical Thermodynamics, 22: 113–127.

Dickson, A. G., and Millero, F. J. 1987. A comparison of the equilibrium constants for the dissociation of carbonic acid in seawater media. Deep Sea Research Part A Oceanographic Research Papers, 34: 1733–1743.

Dickson, A. G., Sabine, C. L., and Christian, J. R. (Ed.) 2007. Guide to best practices for ocean CO_2 measurements. PICES Special Publication 3.

Findlay, H. S., Burrows, M. T., Kendall, M. A., Spicer, J. I., and Widdicombe, S. 2010. Can ocean acidification affect population dynamics of the barnacle *Semibalanus balanoides* at its southern range edge? Ecology, 91: 2931–2940.

Findlay, H. S., Kendall, M. A., Spicer, J. I., Turley, C., and Widdicombe, S. 2008. Novel microcosm system for investigating the effects of elevated carbon dioxide and temperature on intertidal organisms. Aquatic Biology, 3: 51–62.

Findlay, H. S., Wood, H. L., Kendall, M. A., Spicer, J. I., Twitchett, J., and Widdicombe, S. 2011. Comparing the impact of high CO_2 on calcium carbonate structures in different marine organisms. Marine Biology Research, 7: 565–575.

Form, A. U., and Riebesell, U. 2012. Acclimation to ocean acidification during long-term CO_2 exposure in the cold-water coral *Lophelia pertusa*. Global Change Biology, 18: 843–853.

Garcia, H. E., and Gordon, L. I. 1992. Oxygen solubility in seawater – better fitting equations. Limnology and Oceanography, 37: 1307–1312.

Godbold, J. A., and Solan, M. 2013. Long-term effects of warming and ocean acidification are modified by seasonal variation in species responses and environmental conditions. Philosophical Transactions of the Royal Society B, 368: 20130186.

Grasshoff, K. 1976. Methods of seawater analysis. *In* Verlag Chemie. Ed. by Weinheim. pp. 317.

Gutow, L., Rahman, M. M., Bartl, K., Saborowski, R., Bartsch, I., and Wiencke, C. 2014. Ocean acidification affects growth but not nutritional quality of the seaweed *Fucus vesiculosus* (Phaeophyceae, Fucales). Journal of Experimental Marine Biology and Ecology, 453: 84–90.

Hepburn, C. D., Pritchard, D. W., Cornwall, C. E., McLeod, R. J., Beardalls, J., Raven, J. A., and Hurd, C. L. 2011. Diversity of carbon use strategies in a kelp forest community: implications for a high CO_2 ocean. Global Change Biology, 17: 2488–2497.

IPCC. 2007. Summary for policymakers. *In* Climate Change 2007: The Physical Science Basis. Contribution of Working Group I to the Fourth Assessment Report of the Intergovernmental Panel on Climate Change. Ed. by S. Solomon, D. Qin, M. Manning, Z. Chen, M. Marquis, K. B. Averyt, M. Tignor, *et al.* editors. Cambridge University Press, Cambridge, UK. http://www.ipcc.ch/publications_and_data/ar4/wg1/en/spm.html (last accessed 21 November 2014).

Kerrison, P., Suggett, D. J., Hepburn, L. J., and Steinke, M. 2012. Effect of elevated pCO_2 on the production of dimethylsulphoniopropionate (DMSP) and dimethylsulphide (DMS) in two species of *Ulva* (Chlorophyceae). Biogeochemistry, 110: 5–16.

Kirkwood, D. S. 1989. Simultaneous determination of selected nutrients in sea water. International Council for the Exploration of the Sea, CM/C:29.

Kitidis, V., Hardman-Mountford, N. J., Litt, E., Brown, I., Cummings, D., Hartman, S., Hydes, D., *et al.* 2012. Seasonal dynamics of the

carbonate system in the Western English Channel. Continental Shelf Research, 42: 30–40.

Koch, M., Bowes, G., Ross, C., and Zhang, X. 2013. Climate change and ocean acidification effects on seagrasses and marine macroalgae. Global Change Biology, 19: 103–132.

Kroeker, K. J., Kordas, R. L., Crim, R. N., Hendriks, I. E., Ramajo, L., Singh, G. S., Duarte, C. M., *et al.* 2013. Impacts of ocean acidification on marine organisms: quantifying sensitivities and interaction with warming. Global Change Biology, 19: 1884–1896.

Kroeker, K. J., Kordas, R. L., Crim, R. N., and Singh, G. G. 2010. Meta-analysis reveals negative yet variable effects of ocean acidification on marine organisms. Ecology Letters, 13: 1419–1434.

Krumhansl, K. A., and Scheibling, R. E. 2012. Detrital subsidy from subtidal kelp beds is altered by the invasive green alga *Codium fragile* ssp. *fragile*. Marine Ecology Progress Series, 456: 73–85.

Lewis, E., and Wallace, D. W. R. 1998. Program Developed for CO_2 System Calculations, ORNL/CDIAC-105. Carbon Dioxide Information Analysis Center, Oak Ridge National Laboratory, U.S. Department of Energy, Oak Ridge, Tennessee.

Lyons, D. A., Van Alstyne, K. L., and Scheibling, R. E. 2007. Anti-grazing activity and seasonal variation of dimethylsulfoniopropionate-associated compounds in the invasive alga *Codium fragile* ssp. *tomentosoides*. Marine Biology, 153: 179–188.

Mabeau, S., and Fleurence, J. 1993. Seaweed in food products: biochemical and nutritional aspects. Trends in Food Science and Technology, 4: 103–107.

Martínez, B., and Rico, J. M. 2002. Seasonal variation of P content and major N pools in *Palmaria palmata* (Rhodophyta). Journal of Phychology, 38: 1082–1089.

McCoy, S. J., and Pfister, C. A. 2014. Historical comparisons reveal altered competitive interactions in a guild of crustose coralline algae. Ecology Letters, 17: 475–483.

McCoy, S. J., and Ragazzola, F. 2014. Skeletal trade-offs in coralline algae in response to ocean acidification. Nature Climate Change, 4: 719–723.

Mehrbach, C., Culberson, C. H., Hawley, J. E., and Pytkowicz, R. M. 1973. Measurement of the apparent dissociation constants of carbonic acid in seawater at atmospheric pressure. Limnology and Oceanography, 18: 897–907.

Pedersen, A. 1984. Studies on phenol content and heavy-metal uptake in fucoids. Hydrobiologia, 116: 498–504.

Pfister, C. A. 1992. Costs of reproduction in an intertidal kelp—patterns of allocation and life history consequences. Ecology, 73: 1586–1596.

Pierrot, D., Lewis, E., and Wallace, D. W. R. 2006. CO2SYS DOS Program developed for CO_2 system calculations. ORNL/CDIAC-105. Carbon Dioxide Information Analysis Center, Oak Ridge National Laboratory, U.S. Department of Energy, Oak Ridge, Tennessee.

Pinheiro, J. C., and Bates, D. M. 2000. Mixed-effects models in S and S-PLUS. Springer-Verlag, New York.

Pinheiro, J. C., Bates, D. M., DebRoy, S., and Sarkar, D. 2007. Linear and nonlinear mixed effects models. R package version 3, 57. http://cran.r-project.org/package=nlme (last accessed 9 March 2015).

Pistevos, J. C. A., Calosi, P., Widdicombe, S., and Bishop, J. D. D. 2011. Will variation among genetic individuals influence species responses to global climate change? Oikos, 120: 675–689.

Queirós, A. M., Fernandes, J. A., Faulwetter, S., Nunes, J., Rastrick, S. P. S., Mieszkowska, N., Artioli, Y., *et al.* 2014. Scaling up experimental ocean acidification and warming research: from individuals to the ecosystem. Global Change Biology. doi: 10.1111/gcb.12675.

Ragazzola, F., Foster, L. C., Form, A., Anderson, P. S. L., Hansteen, T. H., and Fietzke, J. 2012. Ocean acidification weakens the structural integrity of coralline algae. Global Change Biology, 18: 2804–2812.

Rap, A., Scott, C. E., Spracklen, D. V., Bellouin, N., Forster, P. M., Carslaw, K. C., Schmidt, A., *et al.* 2013. Natural aerosol direct and indirect radiative effects. Geophysical Research Letters, 40: 3297–3301.

Rastrick, S. P. S., and Whiteley, N. M. 2011. Congeneric amphipods show differing abilities to maintain metabolic rates with latitude. Physiological and Biochemical Zoology, 84: 154–165.

Renaud, P. E., Hay, M. E., and Schmitt, T. M. 1990. Interactions of plant stress and herbivory—intraspecific variation in the susceptibility of a palatable versus and an unpalatable seaweed to sea urchin grazing. Oecologia, 82: 217–226.

Riebesell, U., and Gattuso, J -P. 2015. Lessons learned from ocean acidification research. Nature Climate Change, 5: 12–14.

Roleda, M. Y., Morris, J. N., McGraw, C. M., and Hurd, C. L. 2012. Ocean acidification and seaweed reproduction: increased CO_2 ameliorates the negative effect of lowered pH on meiospore germination in the giant kelp *Macrocystis pyrifera* (Laminariales, Phaeophyceae). Global Change Biology, 18: 854–864.

Russell, B. D., Thompson, J. A. I., Falkenberg, L. J., and Connell, S. D. 2009. Synergistic effects of climate change and local stressors: CO_2 and nutrient-driven change in subtidal rocky habitats. Global Change Biology, 15: 2153–2162.

Schaal, G., Riera, P., and Leroux, C. 2010. Trophic ecology in a Northern Brittany (Batz Island, France) kelp (*Laminaria digitata*) forest, as investigated through stable isotopes and chemical assays. Journal of Sea Research, 63: 24–35.

Smale, D. A., Wernberg, T., Yunnie, A. L. E., and Vance, T. 2014. The rise of *Laminaria ochroleuca* in the Western English Channel (UK) and comparisons with its competitor and assemblage dominant *Laminaria hyperborea*. Marine Ecology. doi: 10.1111/maec.12199.

Steneck, R. S., Graham, M. H., Bourque, B. J., Corbett, D., Erlandson, J. M., Estes, J. A., and Tegner, M. J. 2003. Kelp forest ecosystems: biodiversity, stability, resilience and future. Environmental Conservation, 29: 436–459.

Swanson, A. K., and Fox, C. H. 2007. Altered kelp (Laminariales) phlorotannins and growth under elevated carbon dioxide and ultraviolet-B treatments can influence associated intertidal food webs. Global Change Biology, 13: 1696–1709.

Van Alstyne, K. L. 2008. The distribution of DMSP in green macroalgae from northern New Zealand, eastern Australia and southern Tasmania. Journal of the Marine Biological Association of the United Kingdom, 88: 799–805.

Van Alstyne, K. L., and Puglisi, M. P. 2007. DMSP in marine macroalgae and macroinvertebrates: distribution, function, and ecological impacts. Aquatic Science, 69: 394–402.

Van Alstyne, K. L., Wolfe, G. V., Freidenburg, T. L., Neill, A., and Hicken, C. 2001. Activated defense systems in marine macroalgae: evidence for an ecological role for DMSP cleavage. Marine Ecology Progress Series, 213: 53–65.

Wei, N., Quarterman, J., and Jin, Y. S. 2013. Marine macroalgae: an untapped resource for producing fuels and chemicals. Trends in Biotechnology, 31: 70–77.

Wood, H. L., Spicer, J. I., and Widdicombe, S. 2008. Ocean acidification may increase calcification rates, but at a cost. Proceedings of the Royal Society of London, Series B: Biological Sciences. doi:10.1098/rspb.2008.0343.

Zhang, J., and Chi, J. 2002. Automated analysis of nanomolar concentrations of phosphate in natural waters with liquid waveguide. Environmental Science and Technology, 36: 1048–1053.

Zou, D., and Gao, K. 2009. Effects of elevated CO_2 on the red seaweed Gracilaria lemaneiformis (Gigartinales, Rhodophyta) grown at different irradiance levels. Phycologia, 48: 510–517.

Zuur, A. F., Ieno, E. N., Walker, N. J., Saveliev, A. A., and Smith, G. M. 2009. Mixed Effects Models and Extensions in Ecology with R. Springer Science+Business Media, New York, USA. 74–90 pp.

Handling editor: C. Brock Woodson

ICES Journal of Marine Science

ICES Journal of Marine Science (2016), 73(3), 897–909. doi:10.1093/icesjms/fsv194

Contribution to Special Issue: 'Towards a Broader Perspective on Ocean Acidification Research'

Original Article

Biochemical responses to ocean acidification contrast between tropical corals with high and low abundances at volcanic carbon dioxide seeps

J. Strahl[1]*, D. S. Francis[2], J. Doyle[1], C. Humphrey[1], and K. E. Fabricius[1]

[1]*Australian Institute of Marine Science, PMB 3, Townsville, MC, QLD 4810, Australia*
[2]*School of Life and Environmental Sciences, Centre for Chemistry and Biotechnology (Warrnambool Campus), Deakin University, Sherwood Park, PO Box 423, Warrnambool, VIC 3280, Australia*

**Corresponding author: tel: +61 7475 34312; fax +61 7475 35852; e-mail: j.strahl@aims.gov.au*

Strahl, J., Francis, D. S., Doyle, J., Humphrey, C., and Fabricius, K. E. Biochemical responses to ocean acidification contrast between tropical corals with high and low abundances at volcanic carbon dioxide seeps. – ICES Journal of Marine Science, 73: 897–909.

Received 27 April 2015; revised 29 September 2015; accepted 2 October 2015; advance access publication 2 November 2015.

At two natural volcanic seeps in Papua New Guinea, the partial pressure of carbon dioxide (pCO_2) in the seawater is consistent with projections for 2100. Here, the cover of massive scleractinian corals *Porites* spp. is twice as high at elevated compared with ambient pCO_2, while that of branching corals such as *Acropora millepora* is greater than twofold reduced. To assess the underlying mechanisms for such community shifts under long-term exposure to elevated pCO_2, biochemical parameters related to tissue biomass, energy storage, pigmentation, cell protection, and cell damage were compared between *Porites* spp. and *A. millepora* from control (mean $pH_{total} = 8.1$, $pCO_2 = 323$ μatm) and CO_2 seep sites (mean $pH_{total} = 7.8$, $pCO_2 = 803$ μatm) each at two reefs. In *Porites* spp., only one of the biochemical parameters investigated (the ratio of photoprotective to light-harvesting pigments) responded to pCO_2, while tissue biomass, total lipids, total proteins, and some pigments differed between the two reefs, possibly reflecting differences in food availability. Furthermore, some fatty acids showed pCO_2 – reef interactions. In *A. millepora*, most pigments investigated were reduced at elevated pCO_2, while other parameters (e.g. tissue biomass, total proteins, total lipids, protein carbonyls, some fatty acids and pigments) differed between reefs or showed pCO_2 – reef interactions. Tissue biomass, total lipids, and cell-protective capacities were distinctly higher in *Porites* spp. than in *A. millepora*, indicating higher resistance to environmental stress in massive *Porites*. However, our data suggest that important biochemical measures remain relatively unaffected in these two coral species in response to elevated pCO_2 up to 800 μatm, with most responses being smaller than differences between species and locations, and also when compared with responses to other environmental stressors such as ocean warming.

Keywords: energy storage, fatty acids, lipid classes, ocean acidification, oxidative stress, pigments, scleractinia, volcanic carbon dioxide seeps.

Introduction

Anthropogenic carbon dioxide (CO_2) emissions and rising partial pressures of carbon dioxide (pCO_2) in seawater are a major threat to highly productive and diverse coral reef ecosystems (Dove *et al.*, 2013). The oceans' uptake of atmospheric CO_2 leads to modifications of its seawater carbonate chemistry, including reductions in pH and carbonate ion concentration, in a process termed ocean acidification (OA). Most recently published literature shows that calcification decreases and decalcification processes increase in corals and coral reef ecosystems under OA (Erez *et al.*, 2011; Dove *et al.*, 2013).

At natural volcanic CO_2 seeps in Japan, Italy, and Papua New Guinea (PNG), pCO_2 conditions are consistent with projections for 2100 (RCP 6.0; IPCC, 2014). These seeps are unique places, where organisms are exposed to enhanced pCO_2 and changing seawater carbonate chemistry throughout their post-settlement life, while most experimental OA studies are short term (days–months, reviewed in Erez *et al.*, 2011). At the seeps, the densities of sensitive species and the diversity of benthic invertebrates are significantly reduced in the low compared with ambient pH zones (Fabricius *et al.*, 2011, 2014; Kroeker *et al.*, 2011). Consequently,

seep sites are dominated by generalists, robust enough to withstand acidified conditions (Kroeker *et al.*, 2011; Inoue *et al.*, 2013), such as massive scleractinian corals *Porites* spp. at the CO_2 seeps in PNG (Fabricius *et al.*, 2011; Strahl *et al.*, 2015).

Physiological studies conducted *in situ* at the seep sites may help to understand the processes that lead to the observed community shifts under high pCO_2. Two recent studies report that differences in the physiological responses of soft and hard coral species matched the observed differences in abundances at the high vs. ambient pCO_2 sites in Japan and PNG (Inoue *et al.*, 2013; Strahl *et al.*, 2015). The soft coral *Sarcophyton elegans*, which dominates medium pCO_2 zones of 830 μatm at the seeps in Japan, benefited from elevated pCO_2 (390–850 μatm) via enhanced photosynthesis, while net calcification remained stable (Inoue *et al.*, 2013). Similarly, at the Upa-Upasina seep site in PNG, dark and net calcification rates remained stable in the highly abundant massive *Porites* spp., but significantly declined in branching *Acropora millepora* and *Seriatopora hystrix* which both show considerably reduced abundances (−60 and −80%) at high compared with ambient pCO_2 (Strahl *et al.*, 2015).

To date, studies on the impact of OA on corals have focused mainly on calcification and photosynthesis (Erez *et al.*, 2011; Inoue *et al.*, 2013; Comeau *et al.*, 2014). They show that many species have declining calcification rates in response to high pCO_2, while other species show stimulation, hence estimates of changes in rates of calcification at twofold ambient atmospheric pCO_2 range from +23 to −78% (reviewed in Erez *et al.*, 2011). Similarly, rates and efficiency of photosynthesis can either increase or remain unaffected by pCO_2 (Schneider and Erez, 2006; Crawley *et al.*, 2010; Inoue *et al.*, 2013; Strahl *et al.*, 2015).

However, other physiological processes related to energy storage, cell protection, and cell damage are equally important as they influence organism health and indirectly affect biogenic calcium carbonate deposition (Pörtner, 2008; Kaniewska *et al.*, 2012). Assessing the effects of high pCO_2 on these processes may help to explain currently observed discrepancies in calcification and photosynthesis, and in the heterogeneity of responses and susceptibility of different coral species to OA. Two recent studies indicate that elevated pCO_2 may lead to higher levels of oxidative stress in corals and bivalves. In the coral *A. millepora*, genes involved in cellular antioxidant protection and in programmed cell death (apopotosis) were up-regulated after 28 d of exposure to 1010 μatm pCO_2 (Kaniewska *et al.*, 2012). Similarly, the oyster *Crassostrea virginica* up-regulated the expression of proteins associated with oxidative stress in response to >2000 μatm pCO_2 (e.g. superoxide dismutase, peroxiredoxins; Tomanek *et al.*, 2011). The mechanisms causing oxidative stress under hypercapnia and reduced oxygen conditions are not well understood, but for corals, it has been suggested that hypercapnia impairs the photosynthetic apparatus of the symbiotic *Symbiodinium* spp. and/or the mitochondria of the coral host tissue, leading to higher production rates of reactive oxygen species (Kaniewska *et al.*, 2012).

Oxidative stress can cause apoptosis, autophagy or necrosis, and the expulsion of photosynthetic *Symbiodinium* spp. from the coral host, a process called coral bleaching (Lesser, 2011). Richier *et al.* (2008) reported a loss of pigments and/or expulsion of *Symbiodinium* spp. as the first step of cellular defence against environmental stress (in this case, irradiance), while both chlorophyll *a* concentration and endosymbiont density declined in two coral species after 24 d of exposure to 600 μatm pCO_2 (Schoepf *et al.*, 2013). A loss of pigments and/or *Symbiodinium* spp. may lead to a decline in phototrophic energy generation in stressed corals, and subsequently, to depleted energy reserves such as lipids or proteins and/or to changing ratios of structural to storage lipids and changing fatty acid compositions (Bachok *et al.*, 2006; Imbs and Yakovleva, 2012). For example, lipid and fatty acid contents in corals declined 1.5- to 3-fold following bleaching events in Hawaii and Okinawa, while the proportion of structural lipids increased at the expenses of storage lipids (Grottoli *et al.*, 2004; Yamashiro *et al.*, 2005; Bachok *et al.*, 2006).

Energetic costs for corals may rise in the coming decades under projected pCO_2, e.g. due to an increasing need for active, ATP consuming ion regulation at the site of calcification (McCulloch *et al.*, 2012). In a recent study, an up-regulation of triglyceride lipase and Acyl-CoA dehydrogenase point to an increase in the breakdown of lipids for energy use in *A. millepora* under high pCO_2 (Kaniewska *et al.*, 2012). Conversely, energy reserves including lipids, proteins, and carbohydrates were largely maintained in four tropical and one Mediterranean hard coral species under a decreased pH of 7.8–7.9 (Bramanti *et al.*, 2013; Schoepf *et al.*, 2013).

The physiological effects of hypercapnia on cellular metabolic pathways in corals including energy storage, cellular protection, and production of reactive oxygen species are largely understudied and at present, data on corals exposed to high pCO_2 *in situ* (e.g. at volcanic CO_2 seeps) are lacking. A better understanding of these processes might explain the observed heterogeneity of responses and susceptibility/resilience of corals to OA, and might re-evaluate predictions of community shifts in tropical coral reefs in a future of projected pCO_2 (RCP 6.0; IPCC, 2014).

In the present study, two coral taxa were investigated after long-term exposure to OA at natural CO_2 seeps in PNG: (i) massive *Porites* spp., which have established dominance at the seep sites with a cover twice as high as under ambient pCO_2, and (ii) branching *A. millepora*, which are greater than twofold reduced at high pCO_2 (Fabricius *et al.*, 2011; Strahl *et al.*, 2015). Tissue biomass, contents of lipids and proteins, pigment concentrations, and oxidative stress parameters were compared in corals growing at two control and two CO_2 seep sites.

Material and methods

Site description and sampling of corals

The "seep" sites at Upa-Upasina Reef (S 9° 49.446′, E 150° 49.055′) and at Dobu Island (S 9° 44.199′, E 150° 52.060′) in Milne Bay Province, PNG, were near areas of CO_2 venting and had low pH and high pCO_2. Bubble streams consist of 99% CO_2 and 1% of O_2, N_2, and CH_4 (Fabricius *et al.*, 2011). The control sites with ambient pH and pCO_2 were located 0.5 and 2.5 km from the seep sites at Upa-Upasina Reef (S 9° 49.693′, E 150° 49.231′) and Dobu Island (S 9° 45.125′, E 150° 51.248′), respectively. Seawater samples were collected at the two control and two seep sites and analysed for temperature and carbonate chemistry parameters by Vogel *et al.* (2015). Water was repeatedly collected on several days in April/May 2012 and May/June 2013 incorporating diurnal fluctuations, with a total number of seawater samples of 36 (Vogel *et al.*, 2015). The seawater temperature was 29.5 ± 0.6°C. For Dobu and Upa-Upasina Reef, the pH_{Total} was 8.14 ± 0.03 (mean ± s.d.) at the control and 7.84 ± 0.11 at the seep sites. The concentration of dissolved inorganic carbon was 1914 ± 28 μmol kg^{-1} SW at the control and 2107 ± 52 μmol kg^{-1} SW at the seep sites. The pCO_2 and Ω_{AR} were 323 ± 31 μatm and 4.25 ± 0.32 at the control sites and 803 ± 252 μatm and 2.72 ± 0.54 at the seep sites (carbonate

chemistry data re-calculated from Vogel *et al.*, 2015, detailed description of all sites in Fabricius *et al.*, 2011).

Massive *Porites* spp. and *A. millepora* colonies were sampled by scuba diving in April 2012 from each of the two seep and two control sites at 4–5 m depth. For each species, six colonies were sampled that were >10 m apart, and duplicate samples were obtained from each colony (massive *Porites* spp.: fragments of 3–4 cm diameter, *A. millepora:* branchlets of ~4 cm length and 1 cm diameter). The samples were immediately snap-frozen in liquid nitrogen, and transported to the Australian Institute of Marine Science for biochemical analyses.

Sample preparation

To determine pigment content and tissue biomass, the two coral taxa had to be treated differently because the tissue of *Porites* spp. penetrates up to 5 mm deep into the tissue (Lough and Barnes, 1997) and is therefore not suitable for the air gun technique, while that of *A. millepora* is <1 mm thick. For *Porites* spp., one fragment per colony was crushed with a French press (Civilab, Australia), constantly cooled down with liquid nitrogen. Before crushing, the surface area of frozen *Porites* spp. was determined using the aluminium foil technique (Marsh, 1970). For *A. millepora,* the tissue was removed from the skeleton with an air gun in 10 ml of ultra-filtered (0.05 mm) seawater, and the coral homogenate was separated into host and *Symbiodinium* spp. fraction by centrifugation (3 min, 1500*g*, 4°C). Skeletons of *A. millepora* were dried overnight in the oven at 60°C and their surface area was determined using the single wax dipping technique (Veal *et al.*, 2010).

To determine all remaining biochemical parameters, the second fragment/branchlet of each *Porites* spp./*A. millepora* colony was crushed with a French press (Civilab, Australia), constantly cooled down with liquid nitrogen. Sixty per cent of this crushed material was freeze dried for 24 h (FD12 Freeze Dryer, Dynavac, USA) for determination of ash-free dry weight (AFDW), contents of total lipids, lipid classes, fatty acids, and total proteins. The remaining crushed material was stored at −80°C to analyse total antioxidant capacity (TAC) and protein carbonyls (i.e. proteins damaged by reactive oxygen species).

Biochemical investigations

Tissue biomass and total protein content

Protein content (host and *Symbiodinium* spp. fraction of first fragment/branchlet of each colony) per unit surface area was determined as an index of tissue biomass, while the total protein content (host and *Symbiodinium* spp. fraction of second fragment/branchlet) related to AFDW provided information on energy storage capacity. 0.1 g of freeze-dried crushed sample or 200 µl of coral homogenate was dissolved in 1 M NaOH 1:10 (w/v) or 1:1 (v/v) for protein quantification following Dove *et al.* (2006). The coral samples were homogenized, incubated for 1 h at 90°C and centrifuged for 10 min at 1500*g* and room temperature. The protein content of the supernatant (for determination of tissue biomass/total protein content) was determined spectrophotometrically (BioTek Powerwave microplate spectrophotometer, USA) using the DC protein assay kit (Bio-Rad Laboratories, Australia) with bovine serum albumin standards (Leuzinger *et al.*, 2003).

Total lipid content

Total lipid content was extracted from 1 to 2 g of freeze-dried sample in 4 ml of the solvent dichloromethane:methanol (CH_2Cl_2:CH_3OH) (2:1) according to Folch *et al.* (1957) and following the modifications of Conlan *et al.* (2014). The samples were sonicated (Ultrasonic processor XL heat systems, John Morris Scientific Pty, Australia) for 10 min and filtered into a scintillation vial. This process was repeated two times. The combined filtrates (~12 ml) were then washed with 6.5 ml of KCl (0.44%) in H_2O/CH_3OH (3:1). After 12 h incubation in the dark at room temperature, the bottom layer containing the extracted lipid was recovered and the solvent was evaporated under nitrogen. The lipid was then weighed and standardized to AFDW.

Tissue energy content (calories g^{-1} AFDW) was then calculated from enthalpies of combustion based on values by Gnaiger and Bitterlich (1984): lipid (39.5 kJ g^{-1}) and protein (23.9 kJ g^{-1}).

Lipid classes

A 250 µl subsample of the re-dissolved total lipid fraction was taken and analysed for lipid class composition using an Iatroscan MK 6 s thin layer chromatography—flame ionization detector (Mitsubishi Chemical Medience, Japan) according to Nichols *et al.* (2001) and following the modifications of Conlan *et al.* (2014). Briefly, each sample was spotted on silica gel S4-chromarods (5 µm particle size). Lipid separation followed a two-step elution sequence. First, elution of lyso-phosphatidylcholine (L-PC), phosphatidylcholine (PC), phosphatidylserine and phosphatidylinositol (PS-PI), and phosphatidylethanolamine (PE) was achieved in a dichloromethane:methanol:water (50:20:2, by volume) solvent. Second, elution of wax esters (WE), triacylglycerol (TG), free fatty acid (FFA) 1,3-diacylglycerol (1,3-DG), sterol (ST), and 1,2-diacylglycerol (1,2-DG) was achieved in a hexane:diethyl ether:formic acid (60:15:1.5, by volume) solvent. Individual lipid classes were collectively calculated as the ratio of storage (L-PC, PC, PS-PI, PE, ST) to structural (WE, TG, FFA, 1,3-DG, 1,2-DG) lipids.

Fatty acids

Fatty acids were esterified into methyl esters using the acid-catalyzed methylation method (Christie, 2003) following the protocol of Conlan *et al.* (2014). The purified hexane supernatant of the coral samples was placed in a gas chromatography (GC) vial for GC injection. Fatty acid methyl esters were isolated and identified using an Agilent Technologies 7890B GC System (Agilent Technologies, USA) equipped with a BPX70 capillary column (120 m × 0.25 mm internal diameter, 0.25 µm film thickness, SGE Analytical Science, Australia), a flame ionization detector (FID), an Agilent Technologies 7693 auto sampler, and a splitless injection system. The injection volumes, temperature sequences, and flow rates followed the protocol of Conlan *et al.* (2014). The carrier gas was hydrogen. The individual fatty acids were identified relative to known external standards (a series of mixed and individual standards from Sigma-Aldrich, Inc., St Louis, USA and Nu-Chek Prep Inc., USA), using the software GC ChemStation (Rev B.04.03, Agilent Technologies). The resulting peaks were corrected by theoretical relative FID response factors (Ackman, 2002) and quantified relative to the internal standard C23:0 (0.75 mg mg^{-1}, Sigma-Aldrich, Inc., USA).

Ash-free dry weight

Approximately 0.5 g of freeze dried and preweighed coral material was transferred into a preweighted aluminium container and burned for 5 h in the muffle furnace at 480°C. The AFDW of the sample was standardized to dry weight.

Total antioxidant capacity

TAC was measured with the OxiSelect™ Total Antioxidant Capacity Assay Kit (Cell Biolabs, USA) according to the

manufacturer's protocol. Samples of crushed corals were homogenized in phosphate-buffered saline (PBS, pH 7.4) at 1:3 (w/v), sonicated on ice for 40 s and centrifuged for 10 min at 10 000*g* and 4°C. Uric acid standards were prepared (0.0, 0.05, 0.1, 0.35, 0.6, and 1.0 mM) and 10 μl of the coral supernatant/standards was pipetted into wells of a 96-well microtitre plate. Initial and final absorbance

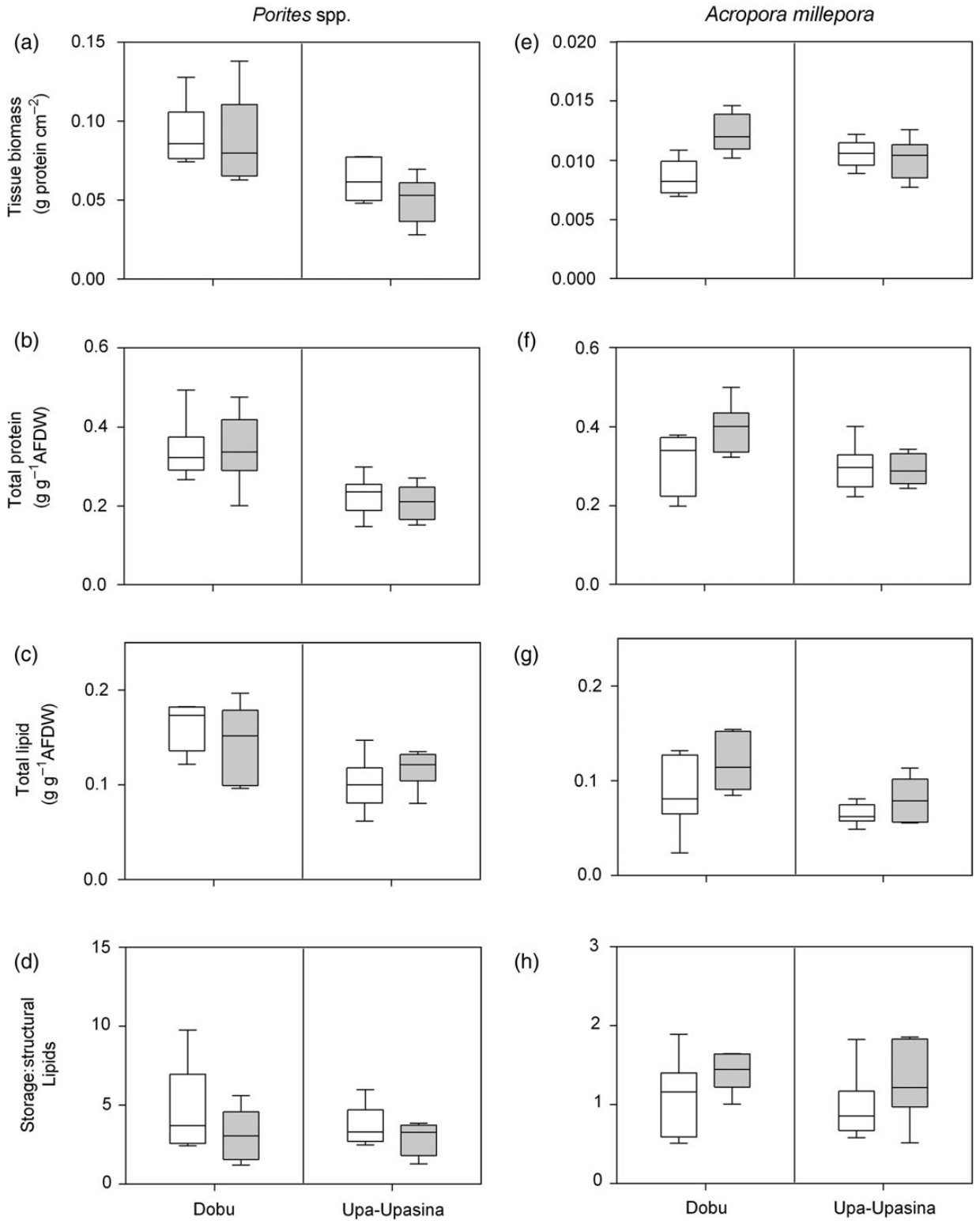

Figure 1. Tissue biomass (a and e) and contents of total protein (b and f) and lipid (c and g) and lipid classes (d and h) in massive *Porites* spp. and *A. millepora* at the control (ambient pCO_2, white boxes) and seep sites (high pCO_2, grey boxes) at the two reefs, $n = 6$ per species, reef/pCO_2 site, and parameter.

readings of samples/standards were conducted at 490 nm with the Synergy H4 microplate reader (BioTek, USA). The TAC was calculated in copper reducing equivalents standardized to the protein content of the sample.

Protein carbonyl content

The protein carbonyl content was assessed in corals by using an OxiSelect protein carbonyl enzyme-linked immunosorbent assay (ELISA) kit (Cell Biolabs, USA) according to the manufacturer's protocol. Briefly, crushed coral samples were resuspended in chilled 1× PBS (pH 7.4) at 1:13 (w/v) and homogenized in a Mini Beadbeater (Biospec Products, USA) for 2 min. The homogenate was then centrifuged for 10 min at 10 000*g* and 4°C, and the protein content of the supernatant was determined. The supernatant was diluted to 10 μg ml^{-1} protein in 1× PBS, and protein carbonyl-bovine serum albumin standards were prepared (0, 0.75, 3, 6 nmol protein carbonyl mg^{-1} protein). To a well of a 96-well protein binding plate, 100 μl of sample/standard was added and incubated overnight at 4°C. Subsequently, the wells were incubated for 45 min in 2,4-dinitrophenylhydrazine working solution and for 1 h in blocking solution. Immunodetection was performed using 2,4-dinitrophenol and horseradish peroxidase-conjugated antibodies provided by the manufacturer. Wells were incubated for 2 min in substrate solution before reading the absorbance at 450 nm with a Synergy H4 microplate reader (BioTek, USA). The protein carbonyl content of the samples was standardized to the protein content of the sample.

Symbiodinium spp. pigment content

Pigments from the complete *Symbiodinium* spp. pellet of *A. millepora* obtained during tissue stripping and from 0.5 g crushed fragment material of *Porites* spp. were sonicated and extracted on ice in the dark in two consecutive 1 h extractions in 2.5 ml of chilled (4°C) buffered methanol [98% MeOH/2% 0.5 M tetrabutylammonium acetate (TBAA) pH 6.5]. Filtered (0.2 μm) extracts were diluted 1:1 with 28 mM TBAA (pH 6.5), and injected into an ultra-performance liquid chromatography (UPLC) system (Acquity UPLC, Waters, USA). Injection volumes and flow rates, as well as gradient conditions and the reference pigments followed Uthicke *et al.* (2012). Pigment content of coral samples was quantified using calibration curves based on the run time and spectral signatures of reference pigments under the same running conditions, and related to surface area.

Statistical analysis

Statistical analyses were conducted with Graph Pad Prism (version 6, GraphPad Software, USA). Data were tested for normality (Kolmogorov–Smirnov test) and homogeneity of variances (Bartlett's test). Outliers of all datasets were identified and removed by ROUT outlier test. A two-way ANOVA was used to evaluate the effect of pCO_2 (ambient vs. high) and reef (Dobu vs. Upa-Upasina) on all physiological measures for each species. Tukey's HSD was used for *post hoc* examinations of significant interaction terms (pCO_2 × reef). Lipid class data were arcsine transformed and PP/LH and Dtx/(Dtx + Ddx) ratios were *log*-transformed before statistical analysis. The ratios of the mean values of the biochemical parameters in *Porites* spp. to *A. millepora* were *log*-transformed before testing the null hypothesis (=no species difference) with *t*-tests.

Results

Tissue biomass, total protein and lipid content, lipid classes, and fatty acids

In massive *Porites* spp., tissue biomass (protein content per unit surface area), total protein content (protein content related to AFDW), and total lipid content remained unaffected by pCO_2, but were higher (37, 36, and 29%) at Dobu compared with Upa-Upasina (Figure 1a–c, Table 1). Similarly, tissue energy content (=calculated from the total protein and lipid contents) was not affected by pCO_2, but was 33% higher at Dobu (3.38 ± 0.48 calories g^{-1} AFDW) than at Upa-Upasina (2.25 ± 0.35 calories g^{-1} AFDW, Table 1). The lipid classes were not significantly affected by pCO_2 or reef (Figure 1d). On average, the fractions of storage lipids were three times higher than structural lipids in *Porites* spp. (75 vs. 25% of total lipids). Saturated, polyunsaturated, and *n*-3 long-chain polyunsaturated fatty acids displayed a significant interaction between pCO_2 and reef (Tables 2 and 3). At ambient pCO_2, they were 42–51% higher at Dobu compared with Upa-Upasina (Tukey $p < 0.005$), whereas

Table 1. ANOVA results comparing biochemical parameters in *Porites* spp. and *A. millepora* at the control (ambient pCO_2) and seep site (high pCO_2) at Dobu and Upa-Upasina Reef.

	***Porites* spp.**			***Acropora millepora***		
	d.f.	***F***	***p*-value**	**d.f.**	***F***	***p*-value**
Tissue biomass						
pCO_2	1	1.112	0.305	1	7.185	**0.015**
Reef	1	15.100	**0.001**	1	0.021	0.887
pCO_2:reef	1	0.196	0.663	1	11.190	**0.003**
Residuals	19	–	–	19	–	–
Total protein						
pCO_2	1	0.061	0.808	1	2.651	0.119
Reef	1	18.160	**0.001**	1	5.535	**0.029**
pCO_2:reef	1	0.172	0.683	1	3.308	0.084
Residuals	19	–	–	20	–	–
Total lipid						
pCO_2	1	0.004	0.955	1	4.366	0.050
Reef	1	13.500	**0.002**	1	7.092	**0.015**
pCO_2:reef	1	1.911	0.182	1	0.572	0.459
Residuals	20	–	–	19	–	–
Tissue energy content						
pCO_2	1	0.065	0.802	1	9.046	**0.007**
Reef	1	39.510	**<0.001**	1	15.030	**0.001**
pCO_2:reef	1	0.246	0.626	1	5.601	**0.028**
Residuals	20	–	–	20	–	–
Storage:structural lipid						
pCO_2	1	2.432	0.135	1	3.191	0.090
Reef	1	0.700	0.413	1	0.013	0.911
pCO_2:reef	1	0.267	0.611	1	0.182	0.675
Residuals	20	–	–	20	–	–
Total antioxidant capacity						
pCO_2	1	0.122	0.731	1	0.228	0.639
Reef	1	0.041	0.842	1	0.243	0.627
pCO_2:reef	1	2.683	0.117	1	0.080	0.780
Residuals	20	–	–	20	–	–
Protein carbonyls						
pCO_2	1	0.498	0.489	1	0.288	0.598
Reef	1	0.097	0.759	1	5.193	0.034
pCO_2:reef	1	0.944	0.344	1	1.619	0.219
Residuals	19	–	–	19	–	–

Significant differences ($p < 0.05$) are highlighted in bold. d.f., degrees of freedom.

Table 2. Contents of fatty acids in mg g^{-1} AFDW in massive *Porites* spp. and *A. millepora* at the control (ambient pCO_2) and seep sites (high pCO_2) at the two reefs.

	Porites spp.				*Acropora millepora*			
	Dobu, control	Dobu, seep	Upa-Upasina, control	Upa-Upasina, seep	Dobu, control	Dobu, seep	Upa-Upasina, control	Upa-Upasina, seep
Saturates	66.6 ± 12.4	50.2 ± 13.1	37.3 ± 11.2	45.7 ± 8.0	29.9 ± 9.6	50.9 ± 21.4	36.1 ± 26.8	28.5 ± 14.0
Monounsaturates	15.7 ± 2.3	14.2 ± 3.9	8.8 ± 2.6	9.1 ± 2.2	3.0 ± 1.0	4.2 ± 1.6	2.4 ± 0.7	2.6 ± 0.9
Polyunsaturates	24.0 ± 2.6	21.6 ± 3.2	13.6 ± 2.6	16.8 ± 2.6	17.3 ± 6.1	21.7 ± 5.6	17.2 ± 8.8	15.2 ± 4.8
n-6 polyunsaturates	14.1 ± 1.7	13.0 ± 1.3	8.3 ± 2.1	10.0 ± 1.8	7.4 ± 2.6	9.9 ± 2.3	5.9 ± 2.1	6.5 ± 2.0
n-3 polyunsaturates	9.9 ± 1.7	8.7 ± 2.1	5.2 ± 1.7	6.8 ± 1.2	9.9 ± 3.9	11.8 ± 3.4	9.7 ± 4.6	8.7 ± 2.9
n-6 long chain	9.3 ± 1.3	9.4 ± 0.9	5.9 ± 1.7	6.6 ± 1.2	4.2 ± 1.7	4.7 ± 1.1	4.0 ± 1.6	3.9 ± 1.1
n-3 long chain	8.5 ± 0.6	6.5 ± 2.0	4.2 ± 1.7	5.1 ± 0.4	7.9 ± 3.1	9.5 ± 2.7	8.0 ± 3.8	7.0 ± 2.3

Displayed are means ± s.d., $n = 6$ per species and reef/pCO_2 site. *n*-6 long chain, *n*-6 long-chain polyunsaturated fatty acids; *n*-3 long chain, *n*-3 long-chain polyunsaturated fatty acids.

differences were not statistically significant between reefs at high pCO_2. Monounsaturated, *n*-6 polyunsaturated, *n*-3 polyunsaturated, and *n*-6 long-chain polyunsaturated fatty acids were significantly (32–40%) higher at Dobu compared with Upa-Upasina (Table 3).

In *A. millepora*, tissue biomass displayed a significant interaction between pCO_2 and reef. At Dobu, it was 44% higher at elevated compared with ambient pCO_2 (Tukey $p < 0.05$), whereas at Upa-Upasina, values were unaffected by pCO_2 (Figure 1e, Table 1). Total protein and lipid contents remained unaffected by pCO_2, but were significantly higher at Dobu compared with Upa-Upasina Reef (Figure 1f and g, Table 1). The tissue energy content displayed a significant interaction between pCO_2 and reef (Table 1). At Dobu, it was 28% higher at elevated (3.58 ± 0.59 calories g^{-1} AFDW) compared with ambient pCO_2 (2.56 ± 0.59 calories g^{-1} AFDW; Tukey $p < 0.005$), whereas at Upa-Upasina, values were unaffected by pCO_2 (2.34 ± 0.28 calories g^{-1} AFDW). Contents of lipid classes and fatty acids were not significantly affected by pCO_2 (Figure 1h, Tables 1–3). On average, the total lipid consisted 58% of storage and 42% of structural lipids. Monounsaturated and *n*-6 polyunsaturated fatty acids were 20–39% higher at Dobu compared with Upa-Upasina, while contents of all other fatty acids did not differ significantly between the two reefs (Tables 2 and 3).

TAC and protein carbonyls

In massive *Porites* spp., the TAC and the content of protein carbonyls were not affected by pCO_2 and reef (Figure 2a and b, Table 1).

In *A. millepora*, the TAC remained unaffected by pCO_2 and reef, while protein carbonyls were twice as high at Upa-Upasina compared with Dobu (Figure 2c and d, Table 1).

Symbiodinium spp. pigment content

In massive *Porites* spp., most *Symbiodinium* spp. pigment concentrations were not significantly affected by pCO_2 (Figure 3). However, the ratio of photo-protective (PP: Ddx, Dnx, diatoxanthin and β-carotene) to light harvesting (LH: chlorophyll *a*, chlorophyll *c2*, and peridinin) pigments increased significantly at elevated pCO_2 (Dobu: +8%, Upa-Upasina: +17%, Figure 3h, Table 4). Pigment concentrations significantly differed between the two reefs: chlorophyll *c2*, peridinin, and the combination of diadinoxanthin (Ddx) and dinoxanthin (Dnx) were 20–26% higher, and β-carotene concentrations were 56% lower at Dobu compared with Upa-Upasina, respectively (Table 4). Meanwhile, concentrations of chlorophyll *a*, diatoxanthin (Dtx), and the Dtx/(Dtx + Ddx) ratio (as an indicator of the xanthophyll cycle) were similar at all sites.

Table 3. ANOVA results comparing fatty acid groups in *Porites* spp. and *A. millepora* at the control (ambient pCO_2) and seep site (high pCO_2) at Dobu and Upa-Upasina Reef.

	Porites spp.			*Acropora millepora*		
	d.f.	*F*	*p*-value	d.f.	*F*	*p*-value
Saturates						
pCO_2	1	0.704	0.412	1	0.680	0.420
Reef	1	13.020	**0.002**	1	0.994	0.331
pCO_2:reef	1	6.956	**0.016**	1	3.110	0.094
Residuals	19	–	–	19	–	–
Monosaturates						
pCO_2	1	0.228	0.639	1	1.901	0.185
Reef	1	26.370	**<0.001**	1	5.219	**0.035**
pCO_2:reef	1	0.595	0.450	1	0.940	0.345
Residuals	19	–	–	18	–	–
Polyunsaturates						
pCO_2	1	0.103	0.752	1	1.488	0.238
Reef	1	35.150	**<0.001**	1	1.348	0.260
pCO_2:reef	1	4.708	**0.043**	1	0.197	0.663
Residuals	19	–	–	19	–	–
n-6 polyunsaturates						
pCO_2	1	0.146	0.707	1	2.584	0.125
Reef	1	35.530	**<0.001**	1	6.379	**0.021**
pCO_2:reef	1	3.691	0.070	1	0.934	0.347
Residuals	19	–	–	18	–	–
n-3 polyunsaturates						
pCO_2	1	0.035	0.854	1	0.083	0.776
Reef	1	21.110	**0.001**	1	1.130	0.301
pCO_2:reef	1	3.815	0.066	1	0.888	0.358
Residuals	19	–	–	19	–	–
n-6 long chain						
pCO_2	1	0.638	0.435	1	0.153	0.700
Reef	1	31.170	**<0.001**	1	0.727	0.404
pCO_2:reef	1	0.350	0.561	1	0.309	0.585
Residuals	19	–	–	19	–	–
n-3 long chain						
pCO_2	1	0.911	0.353	1	0.068	0.797
Reef	1	24.470	**0.001**	1	0.889	0.357
pCO_2:reef	1	5.942	0.026	1	1.003	0.329
Residuals	17	–	–	19	–	–

Significant differences ($p < 0.05$) are highlighted in bold; d.f., degrees of freedom. *n*-6 long chain, *n*-6 long-chain polyunsaturated fatty acids; *n*-3 long chain, *n*-3 long-chain polyunsaturated fatty acids.

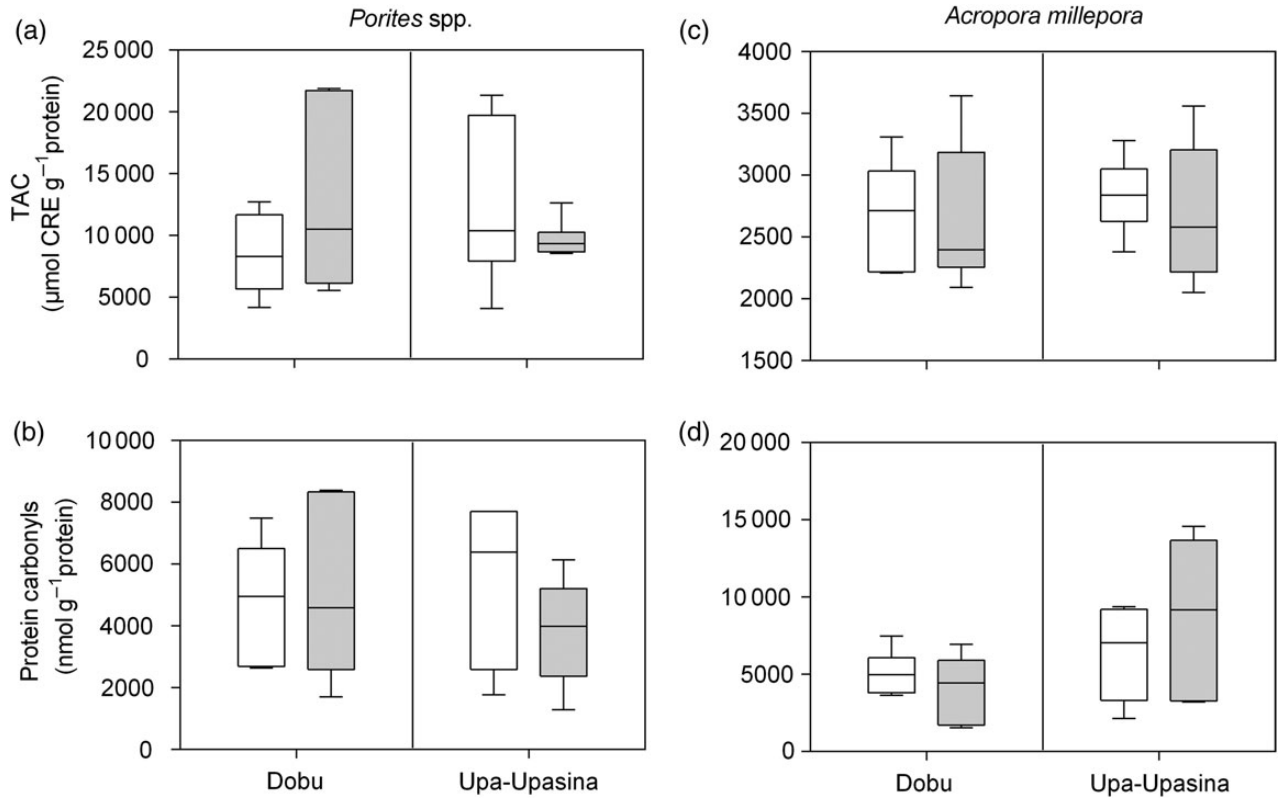

Figure 2. Total antioxidant capacity (TAC) (a and c) and content of protein carbonyls (b and d) in massive *Porites* spp. and *A. millepora* at the control (ambient pCO_2, white boxes) and seep sites (high pCO_2, grey boxes) at the two reefs, $n = 6$ per species, reef/pCO_2 site, and parameter.

In *A. millepora*, the concentrations of chlorophyll *a* and *c2*, peridinin, and the combination of Ddx and Dnx declined significantly by 22–31% at elevated pCO_2 at Dobu and Upa-Upasina (Figure 4a, c, and f), while β-carotene at elevated pCO_2 was reduced by 51% at Dobu and 88% at Upa-Upasina (Figure 4d, Table 4). Between sites, the concentrations of β-carotene and diatoxanthin were 73% and 31% lower at Upa-Upasina compared with Dobu (Figure 4d and e). Furthermore, the ratio of PP:LH and Dtx/(Dtx + Ddx) were 19% lower at Upa-Upasina compared with Dobu, respectively, while pCO_2 had no significant effect (Figure 4g and h, Table 4).

Comparison of massive *Porites* spp. and *A. millepora*

At ambient and elevated pCO_2, many of the energy-related and cell-protective parameters were significantly higher in *Porites* spp. than in *A. millepora* (Table 5). Tissue biomass was 5–11 times, total lipid content 1–2 times, TAC 3–5 times, and contents of LH and PP pigments 13–24 times higher in *Porites* spp. than in *A. millepora* at Dobu and Upa-Upasina Reef, while contents of total protein and protein carbonyls were similar in both corals (Table 5).

Discussion

We investigated *in situ* the effects of high pCO_2 on biochemical parameters in the apparently CO_2-resistant massive *Porites* spp., and the more CO_2-sensitive branching *A. millepora*. Our data support the conclusion of high tolerance of massive *Porites* spp. to elevated pCO_2. Tissue biomass, lipid, protein and tissue energy content, fatty acid content, pigment content, and oxidative stress parameters remained unaffected by pCO_2 up to ~800 µatm. Corals will experience such pCO_2 concentrations at the end of this century, should CO_2 emissions follow the representative concentration pathway 6.0 (IPCC, 2014). *Porites* spp. also shows unaltered net calcification rates after lifelong exposure to elevated pCO_2 at Upa-Upasina seeps (Fabricius *et al.*, 2011; Strahl *et al.*, 2015) and after experimental exposure to up to 1000 µatm pCO_2 for 2–4 weeks (Edmunds, 2011; Comeau *et al.*, 2014). In accordance, Edmunds (2011) reported that massive *Porites* maintained biomass and *Symbiodinium* spp. content at 400–800 µatm pCO_2, and McCulloch *et al.* (2012) identified *Porites* spp. as one of the most OA tolerant coral taxa due to their ability to maintain higher internal pH values at the site of calcification than many other species, as shown by boron isotope analysis. In contrast, *Acropora* spp. were classified as among the most sensitive coral species. Tissue biomass, total lipid content, and cell-protective capacities (e.g. TAC, photoprotective pigments) were much higher in *Porites* spp. compared with *A. millepora* at control and seep sites, which suggest increased resilience of the former to environmental stressors such as increased temperature or ultraviolet radiation.

Nevertheless, the physiological performance of *A. millepora* at the seep sites in PNG was unexpectedly strong, despite their greater than twofold lesser abundances and net calcification rates that were up to 50% reduced at the Upa-Upasina seep site in PNG (Fabricius *et al.*, 2011; Strahl *et al.*, 2015) and under experimentally increased pCO_2 (Schneider and Erez, 2006; Anthony *et al.*, 2008; Schoepf *et al.*, 2013). *Acropora millepora* was chosen for the study because, unlike for many other species of *Acropora*, enough colonies of this species existed at the seep sites to conduct the study. This may suggest that the CO_2 tolerance of this particular species may be higher than in other species of the genus *Acropora*. Most parameters investigated in *A. millepora* showed little negative responses to lifelong exposure to high pCO_2. Contents of protein and lipid as well as

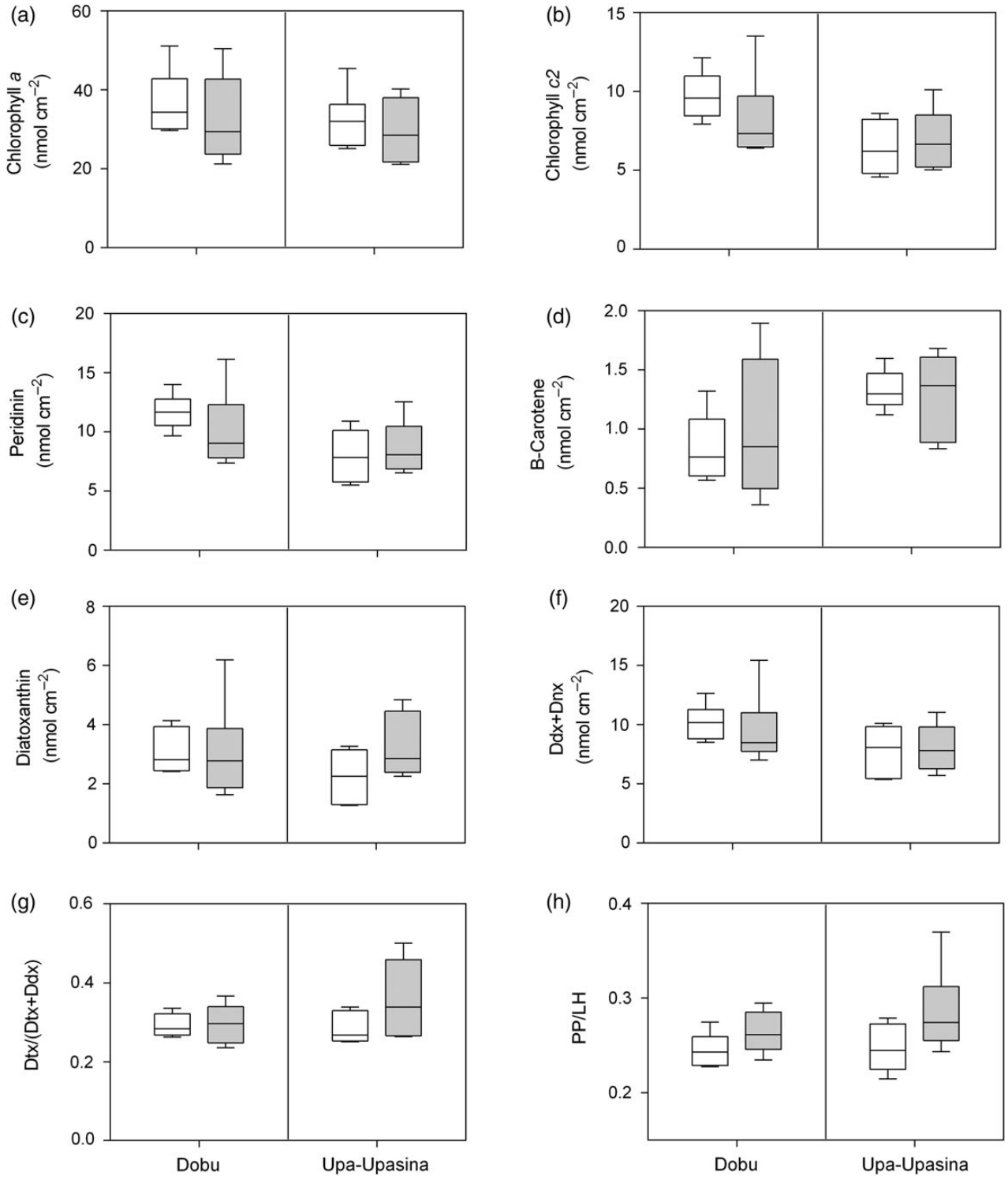

Figure 3. *Symbiodinium* spp. pigment content in massive *Porites* spp. at the control (ambient pCO_2, white boxes) and seep sites (high pCO_2, grey boxes) at the two reefs, $n = 6$ per reef/pCO_2 site and parameter. Dtx, diatoxanthin; Ddx, diadinoxanthin; Dnx, dinoxanthin; PP, photoprotective pigments; LH, light-harvesting pigments.

fatty acids, TAC, and protein carbonyls remained stable under acidified conditions, while tissue biomass and energy content at Dobu slightly increased at high pCO_2. A distinct pCO_2 impact was a significant reduction in many of the *Symbiodinium* spp. pigments in *A. millepora* at the seep sites.

Tissue biomass, proteins, and lipids

While calcification rates are traditionally investigated as a proxy of coral response to environmental stressors (reviewed in Erez *et al.*, 2011), biomass and energy reserves are often ignored as sensitive indicators for coral health. Corals with high biomass level and

Table 4. ANOVA results comparing pigment concentrations and pigment ratios in *Porites* spp. and *A. millepora* at the control (ambient pCO_2) and seep site (high pCO_2) at Dobu and Upa-Upasina reef.

	***Porites* spp.**			***Acropora millepora***		
	d.f.	***F***	***p*-value**	**d.f.**	***F***	***p*-value**
Chlorophyll *a*						
pCO_2	1	0.926	0.347	1	8.317	**0.009**
Reef	1	1.037	0.321	1	0.059	0.811
pCO_2:reef	1	0.036	0.851	1	0.130	0.722
Residuals	20	–	–	20	–	–
Chlorophyll *c2*						
pCO_2	1	0.362	0.554	1	6.964	**0.016**
Reef	1	8.042	**0.010**	1	0.096	0.760
pCO_2:reef	1	1.528	0.231	1	0.046	0.831
Residuals	20	–	–	20	–	–
Peridinin						
pCO_2	1	0.218	0.646	1	9.538	**0.006**
Reef	1	7.103	**0.015**	1	0.449	0.511
pCO_2:reef	1	1.418	0.248	1	0.011	0.919
Residuals	20	–	–	20	–	–
β-Carotene						
pCO_2	1	0.105	0.749	1	7.770	**0.012**
Reef	1	6.811	**0.017**	1	13.560	**0.002**
pCO_2:reef	1	1.273	0.273	1	0.442	0.514
Residuals	20	–	–	19	–	–
Diatoxanthin						
pCO_2	1	1.159	0.294	1	2.432	0.135
Reef	1	0.486	0.494	1	9.001	**0.007**
pCO_2:reef	1	1.229	0.281	1	0.294	0.594
Residuals	20	–	–	20	–	–
Ddx + Dnx						
pCO_2	1	0.073	0.790	1	7.769	**0.011**
Reef	1	4.559	**0.045**	1	1.408	0.249
pCO_2:reef	1	0.278	0.604	1	0.090	0.768
Residuals	20	–	–	20	–	–
Dtx/(Dtx + Ddx)						
pCO_2	1	2.666	0.118	1	0.045	0.835
Reef	1	1.275	0.272	1	7.755	**0.011**
pCO_2:reef	1	2.102	0.163	1	0.630	0.437
Residuals	20	–	–	20	–	–
PP/LH						
pCO_2	1	5.859	**0.025**	1	0.006	0.937
Reef	1	0.966	0.337	1	16.760	**0.001**
pCO_2:reef	1	0.704	0.411	1	0.010	0.923
Residuals	20	–	–	20	–	–

Significant differences ($p < 0.05$) are highlighted in bold. d.f., degrees of freedom; Dtx, diatoxanthin; Ddx, diadinoxanthin; Dnx, dinoxanthin; PP, photoprotective pigments (Ddx, Dnx, diatoxanthin, β-carotene); LH, light-harvesting pigments (chlorophyll *a* and *c2*, peridinin).

energy storages are more resilient and show higher rates of survival and recovery from bleaching than starved corals and corals with low biomass (Rodrigues and Grottoli, 2007; Thornhill *et al.*, 2011). This difference will become more critical with predicted increasing frequencies in bleaching events in the coming decades (Donner, 2009). On average, tissue biomass was 7-fold higher and lipid content 1.5-fold higher in massive *Porites* compared with *A. millepora* at the four sites in PNG, which will make the latter generally more susceptible to environmental stressors.

However, the reduced abundance of *A. millepora* at the seep compared with the control sites in PNG (Fabricius *et al.*, 2011; Strahl *et al.*, 2015) cannot be explained by these parameters. Tissue biomass, total protein and lipid content (as a proportion of AFDW), and tissue energy content in both *Porites* spp. and *A. millepora* were not impacted by high pCO_2. A coral that does not up-regulate energy expenditure towards skeletal growth under acidified conditions can instead maintain energy investment into tissue biomass. Strahl *et al.* (2015) showed that photosynthetic rates increased under elevated supply of CO_2 in *A. millepora* at the Upa-Upasina seep site, but both dark and net calcification significantly decreased (−117 and −44%; Strahl *et al.*, 2015), while soft-tissue-related parameters remained unaffected or increased (this study) at high pCO_2. Similarly, total lipid/protein content and tissue biomass were fully maintained or increased by 18–60% in *A. millepora* and *Stylophora pistillata* after exposure to enhanced pCO_2 (740 and >1900 μatm), while calcification rates decreased by 18–53% (Krief *et al.*, 2010; Schoepf *et al.*, 2013). The Mediterranean red octocoral *Corallium rubrum* responded to increased pCO_2 (800 μatm) for >10 months by decreasing calcification rates (−59%), while no changes were found in total lipid and protein content between control and acidified treatment (Bramanti *et al.*, 2013). In the present study, total carbohydrate content was not determined, but similar to total lipid and protein content, total carbohydrate content remained constant or increased in *A. millepora* and *C. rubrum* at experimentally elevated pCO_2s of 740–800 μatm (Bramanti *et al.*, 2013; Schoepf *et al.*, 2013).

In massive *Porites*, energy demands for tissue and skeletal growth seemed to be met at both high and low pCO_2. Neither tissue biomass, contents of total protein, lipid and tissue energy (this study), nor net calcification (Strahl *et al.*, 2015) showed any pCO_2 effect, but some of these measures contrasted between the reefs. Thus, despite the assumption that the energetic costs of calcification increase at high pCO_2 (Cohen *et al.*, 2009; Erez *et al.*, 2011), evidence is increasing that many species of scleractinian corals do not deplete their energy reserves to sustain calcification under acidified conditions (this study; Krief *et al.*, 2010; Bramanti *et al.*, 2013; Schoepf *et al.*, 2013). Instead, some species grow more slowly but maintain their energy reserves (e.g. *A. millepora*), possibly aided by higher photosynthetic carbon gain at elevated concentrations of dissolved inorganic carbon (this study; Strahl *et al.*, 2015). Further, high rates of heterotrophic feeding may prevent reductions in rates of calcification at high pCO_2 in some corals (Towle *et al.*, 2015). For example, the Caribbean coral *Acropora cervicornis* maintained growth rates at both elevated temperature and elevated CO_2 when fed, while unfed corals experienced significant decreases in growth (Towle *et al.*, 2015).

Lipid classes and fatty acids

The examination of lipid classes and fatty acids provides insights into how corals utilize their energy resources under different environmental conditions. Neither the lipid class composition nor total fatty acid content/proportions in *Porites* spp. and *A. millepora* were impacted by long-term exposure (up to 70 years, present study) to high pCO_2, which is in agreement with findings in *C. rubrum* after >10 months of exposure to enhanced pCO_2 (Bramanti *et al.*, 2013). In contrast, lower levels of key storage lipids, TG, and WE had been detected in *Porites* spp. and *Montipora verrucosa* after bleaching/warm-water events off the coasts of Hawaii and the Republic of Kiribati (Grottoli *et al.*, 2004; Carilli *et al.*, 2012). Similarly, both structural and storage lipids declined by 60–70% in stony corals (*Acropora intermedia, Montipora digitata*) and soft corals during a short-term heat stress experiment (33°C for 10–48 h; Imbs and Yakovleva, 2012). And after a heat stress and bleaching event in Japan in 2003, corals contained significantly lower total fatty acids as well as lower amounts of polyunsaturated fatty acids

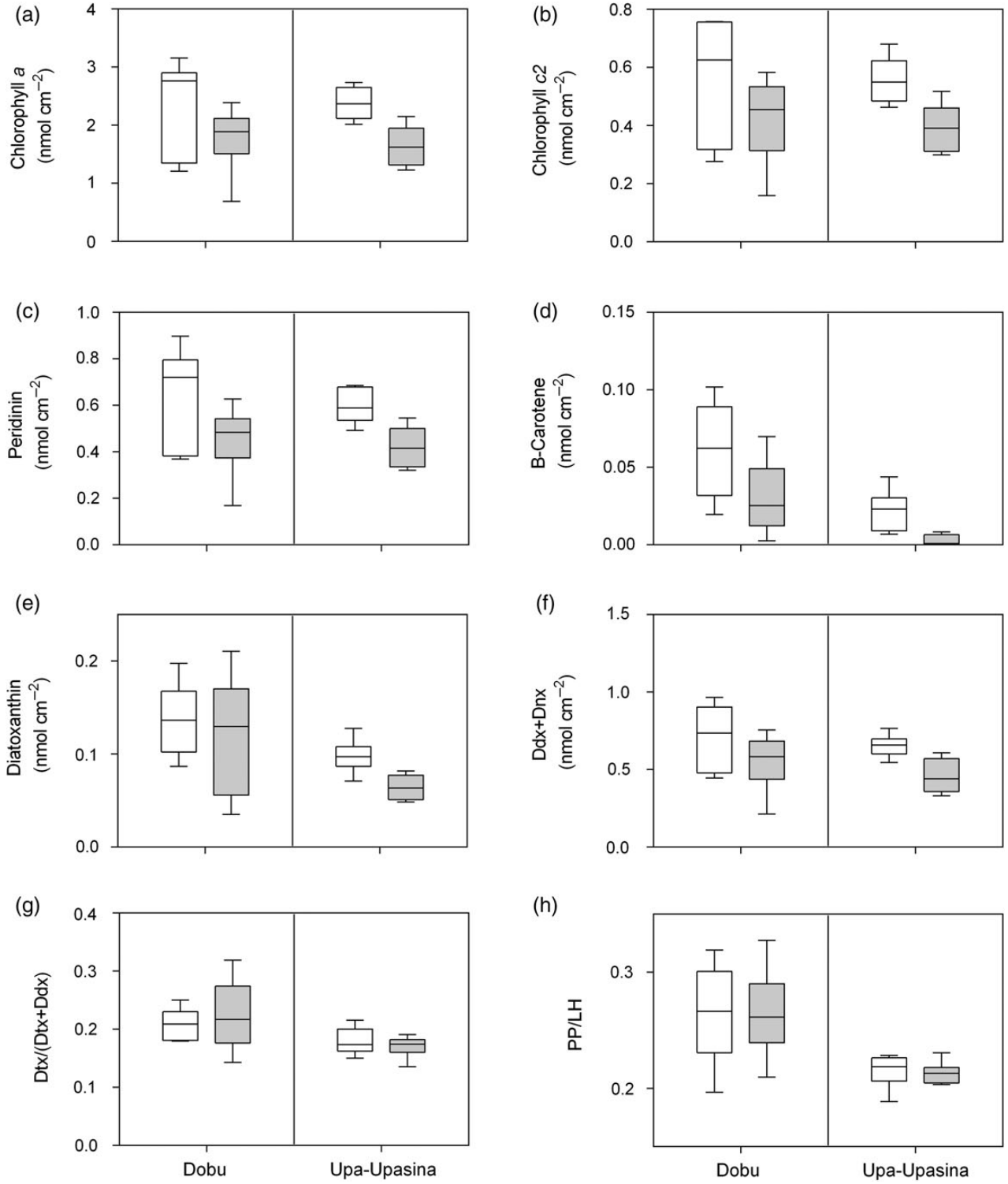

Figure 4. *Symbiodinium* spp. pigment content in *A. millepora* at the control (ambient pCO_2, white boxes) and seep sites (high pCO_2, grey boxes) at the two reefs, $n = 6$ per reef/pCO_2 site and parameter. Dtx, diatoxanthin; Ddx, diadinoxanthin; Dnx, dinoxanthin; PP, photoprotective pigments; LH, light-harvesting pigments.

and higher relative amounts of saturated and monounsaturated fatty acids (Bachok *et al.*, 2006). These studies and our data in combination suggest that increasing seawater temperatures and bleaching events are more stressful and energetically more costly for corals than elevated pCO_2 levels of up to 800 μatm.

Oxidative stress parameters

Total antioxidant capacities were on average 4-times higher, and photoprotective capacities 17-times higher in *Porites* spp. than in *A. millepora*, which will increase the resilience of massive *Porites* to increasing production rates of reactive oxygen species induced

Table 5. Ratios of the mean values of the biochemical parameters of *Porites* spp. to *A. millepora* at the control (ambient pCO_2) and seep sites (high pCO_2) at the two reefs, and their significance (*t*-test).

	Average, all sites	Dobu, control	Dobu, seep	Upa-Upasina, control	Upa-Upasina, seep	*t*-value	d.f.	*p*-value
Tissue biomass	7.2	10.7	7.0	6.0	5.0	11.69	3	**0.001**
Total protein content	0.9	1.1	0.9	0.8	0.7	1.54	3	0.222
Total lipid content	1.5	1.9	1.2	1.6	1.5	4.52	3	**0.020**
Light-harvesting pigments	18.5	15.6	19.3	15.1	24.0	26.81	3	**<0.001**
Photoprotective pigments	16.8	16.3	19.2	13.2	18.4	33.83	3	**<0.001**
Total antioxidant capacity	4.0	3.2	4.8	4.4	3.6	14.47	3	**<0.001**
Protein carbonyls	0.8	0.9	1.0	0.9	0.5	1.43	3	0.248

Tabled are ratios of tissue biomass (g protein cm^{-2}), total protein and lipid content (g g^{-1} AFDW), photoprotective and light-harvesting pigments (nmol cm^{-2}), total antioxidant capacity (μmol CRE g^{-1} protein), and protein carbonyls (nmol g^{-1} protein). Significant differences ($p < 0.05$) are highlighted in bold; d.f., degrees of freedom.

by environmental stressors (e.g. increasing seawater temperatures, solar ultraviolet radiation), which are known to directly induce photo-oxidative stress in corals (Lesser, 1996; Downs *et al.*, 2013).

However, oxidative stress parameters in massive *Porites* spp. and *A. millepora* were highly variable between colonies and were not considerably impacted by increased pCO_2. The activity of cellular protective antioxidants (e.g. TAC), which can be stimulated by enhanced production rates of harmful reactive oxygen species (Halliwell, 2006) in coral host tissues and photosynthetic active *Symbiodinium* spp., remained similarly high in corals at control and seep sites in the present study. In accordance, the contents of protein carbonyls remained unaffected by pCO_2 in both *Porites* spp. and *A. millepora*. Our findings do not support the hypothesis that mild hypercapnia might impair the photosynthetic apparatus of *Symbiodinium* spp. and/or the mitochondria of the coral host tissue, leading to higher production rates of reactive oxygen species (Kaniewska *et al.*, 2012).

Pigments

In the present study, light harvesting and photoprotective pigments decreased significantly (by 22–31% and 30–88%, respectively) in *A. millepora* at the seep compared with the control sites, but remained unaffected by pCO_2 in massive *Porites*. A decline of *Symbiodinium* spp./pigments in corals at high pCO_2 can be a sign of stress, indicating a breakdown in the symbiotic relationship due to changes in carbon concentrating mechanisms, photorespiration, and/or direct impacts of acidosis (Anthony *et al.*, 2008; Kaniewska *et al.*, 2012). Similar to our findings, Anthony *et al.* (2008) observed a stronger decline in pigmentation in *Acropora intermedia* (20% bleaching) than in *Porites lobata* (10% bleaching) exposed to pCO_2 and temperature conditions similar to the present study (pH 7.85 vs. 7.87, temperature 28–29°C vs. 29 °C). Muehllehner (2013) reported significantly reduced symbiont to host cell ratios in *A. millepora* (−54%) at the seep (~850 μatm pCO_2) compared with the control site of Upa-Upasina Reef *in situ* in August 2010, which supports the results of the present study. Similarly, the content of *Symbiodinium* spp. declined by 50% in *A. millepora* after 24–28 d of exposure to up to 1350 μatm pCO_2 (Kaniewska *et al.*, 2012; Schoepf *et al.*, 2013). Our pigment data support earlier studies stating that *Porites* spp. will be more resilient than *Acropora* spp. in a future of increasing pCO_2 (Fabricius *et al.*, 2011; McCulloch *et al.*, 2012; Comeau *et al.*, 2014; Strahl *et al.*, 2015).

Furthermore, the ratio of photoprotective to light-harvesting pigments (PP:LH) increased in massive *Porites* at the two seep sites, providing the coral with a higher level of photo protection as a response to the elevated photosynthetic activity. Strahl *et al.* (2015) reported a benefical effect of elevated pCO_2 on the photosynthetic rates in massive *Porites* (+43%) and *A. millepora* (24%) at Upa-Upasina Reef (corals at Dobu were not investigated in the study). The production rate of harmful reactive oxygen species potentially increases when rates of photosynthesis are high (Lesser, 1996). Photoprotective mechanisms in *Symbiodinium* spp. have been reported widely in the form of xanthophyll cycling and in their capacity to generate more photoprotective diatoxanthin pigments in response to environmental stressors (e.g. solar radiation; Ambarsari *et al.*, 1997; Brown *et al.*, 2002). Thus, an elevated ratio of PP:LH at high pCO_2 in *Porites* spp.—but not in *A. millepora*—will counteract oxidative damage accumulation and lead to a higher resistance of massive *Porites* to increasing reactive oxygen species concentrations.

Reef-related differences in biochemical parameters (Dobu vs. Upa-Upasina)

The observed differences in the physiological performance of corals between the two reefs may be related to potential differences in oceanographic conditions (e.g. currents, wave exposure, turbidity) and food availability, also demonstrating the difficulty to compare the effects of high pCO_2 between regions. Tissue biomass and contents of total lipid, protein, fatty acids, and pigments were significantly higher at Dobu compared with Upa-Upasina in *Porites* spp. and/or *A. millepora*, suggesting more effective heterotrophic feeding at Dobu. Similarly, photosynthesizing foraminifera species dominate Upa-Upasina sites, while heterotrophic species are more abundant at the Dobu sites (Uthicke *et al.*, 2013), which indicates a higher food supply/nutrient content at the latter reef. For example, concentrations of dissolved inorganic nutrients in seawater were twofold higher at the Dobu compared with Upa-Upasina sites in April 2012 and May 2013 (N. Vogel and S. Uthicke, pers. comm.), potentially fuelling organic enrichment of particulate matter at Dobu as one possible food source for corals. Previous studies report that some symbiotic corals show strong biochemical responses to heterotrophic feeding, e.g. lipid contents were two to fourfold higher in *A. millepora, Acropora valida*, and *Turbinaria mesenterina* at turbid, inshore reefs compared with offshore reefs (Anthony, 2006; Bay *et al.*, 2009). In accordance, fed *A. cervicornis* maintained ambient growth rates and showed highest lipid contents at elevated temperature and pCO_2 in an 8-week aquarium experiment, while unfed corals experienced significant decreases in growth and lipid content (Towle *et al.*, 2015). Well-fed corals also maintained photosynthetic efficiency and cell division rates of *Symbiodinium* spp. under temperature stress, while both parameters progressively declined in experimentally

starved corals (reviewed in Fabricius *et al.*, 2013). Thus, further investigation of corals in PNG under long-term OA (e.g. feeding experiments and measurements of photosynthesis, respiration, and calcification rates in corals at Dobu) and a more detailed biochemical and oceanographic characterization of ambient and high pCO_2 sites at Dobu and Upa-Upasina are required to more explicitly explain the observed reef-related differences in biochemical parameters.

Conclusion

Most of the biochemical parameters investigated in *Porites* spp. and *A. millepora* were less impacted than expected under lifelong exposure to predicted future pCO_2 (RCP6.0; IPCC, 2014) and can therefore not explain the observed community shift in coral reefs at the seep sites in PNG. Coral calcification more than other physiological parameters related to coral health (e.g. tissue biomass, energy storage capacity, cell damage) seem to be predominantly affected in pCO_2-sensitive corals such as *A. millepora* under lifelong exposure to high pCO_2 (this study; Strahl *et al.*, 2015). However, our study could not investigate any of the coral species most negatively affected by acidified conditions, because they were too rare at the seep sites to be included in this study. This suggests that the CO_2 tolerance of *A. millepora* may be higher than in those other species of the genus *Acropora* that were rare or absent at elevated pCO_2.

Our study and recent publications (Grottoli *et al.*, 2004; Carilli *et al.*, 2012; Imbs and Yakovleva, 2012) in combination show that other environmental stressors such as increasing seawater temperature and bleaching are energetically more costly for corals than OA alone. Key physiological and biochemical features in generalists such as massive *Porites* underpin their resilience to combined stressors (e.g. high pCO_2 and increasing sea surface temperature/bleaching) and support their recovery from stress events, while more sensitive coral species such as *A. millepora* have lower tolerance thresholds. This might lead to changes in species composition and reduced diversity in tropical coral reefs (Fabricius *et al.*, 2011; Inoue *et al.*, 2013; Strahl *et al.*, 2015) under projected pCO_2 and ocean warming. However, a better understanding of physiological mechanisms and responses in different coral taxa to OA, and especially to combined stressors such as lifelong increased pCO_2 and ocean warming is needed to predict the future of coral reef ecosystems.

Acknowledgements

We thank the communities at Upa-Upasina and Dobu for their permission to study the corals on their reef. Many thanks to S. Noonan, N. Vogel, S. Uthicke, and the crew of the M.V. Chertan for their support during the fieldwork, and to H. Martinez, S. Hinz, C. Assaille, K. Berry, and P. Buerger for their assistance in the laboratory. We thank P. Davern and M. Donaldson for their help with the logistics and shipment of the equipment, and QantasLink for continued support. This project was funded by the Australian Government's Super Science Initiative (Grant FS110200034), the Australian Government's National Environmental Research Programme, and the Australian Institute of Marine Science.

References

Ackman, R. G. 2002. The gas chromatograph in practical analyses of common and uncommon fatty acids for the 21st century. Analytica Chimica Acta, 465: 175–192.

Ambarsari, I., Brown, B. E., Barlow, R. G., Britton, G., and Cummings, D. 1997. Fluctuations in algal chlorophyll and carotenoid pigments during solar bleaching in the coral *Goniastrea aspera* at Phuket, Thailand. Marine Ecology Progress Series, 159: 303–307.

Anthony, K. R. N. 2006. Enhanced energy status of corals on coastal, high-turbidity reefs. Marine Ecology Progress Series, 319: 111–116.

Anthony, K. R. N., Kline, D. I., Diaz-Pulido, G., Dove, S., and Hoegh-Guldberg, O. 2008. Ocean acidification causes bleaching and productivity loss in coral reef builders. Proceedings of the National Academy of Sciences of the United States of America, 105: 17442–17446.

Bachok, Z., Mfilinge, P., and Tsuchiya, M. 2006. Characterization of fatty acid composition in healthy and bleached corals from Okinawa, Japan. Coral Reefs, 25: 545–554.

Bay, L., Ulstrup, K. E., Nielsen, H. B., Jarmer, H., Goffard, N., Willis, B. L., Miller, D. J., *et al.* 2009. Microarray analysis reveals transcriptional plasticity in the reef building coral *Acropora millepora*. Molecular Ecology, 18: 3062–3075.

Bramanti, L., Movilla, J., Guron, M., Calvo, E., Gori, A., Dominguez-Carrió, C., Grinyó, A., *et al.* 2013. Detrimental effects of ocean acidification on the economically important Mediterranean red coral (*Corallium rubrum*). Global Change Biology, 19: 1897–1908.

Brown, B., Dunne, R., Goodson, M., and Douglas, A. 2002. Experience shapes the susceptibility of a reef coral to bleaching. Coral Reefs, 21: 119–126.

Carilli, J., Donner, S. D., and Hartmann, A. C. 2012. Historical temperature variability affects coral response to heat stress. PloS ONE, 7: e34418.

Christie, W. W. 2003. Lipid Analysis, Isolation, Separation, Identification and Structural Analysis of Lipids, 3rd edn. The Oily Press, Bridgewater, UK.

Cohen, A. L., McCorkle, D. C., de Putron, S., Gaetani, G. A., and Rose, K. A. 2009. Morphological and compositional changes in the skeletons of new coral recruits reared in acidified seawater: insights into the biomineralization response to ocean acidification. Geochemistry, Geophysics, Geosystems, 10: Q07005.

Comeau, S., Carpenter, R. C., Nojiri, Y., Putnam, H. M., Sakai, K., and Edmunds, P. J. 2014. Pacific-wide contrast highlights resistance of reef calcifiers to ocean acidification. Proceedings of the Royal Society of London Series B: Biological Science, 281: 20141339.

Conlan, J. A., Jones, P. L., Turchini, G. M., Hall, M. R., and Francis, D. S. 2014. Changes in the nutritional composition of captive early-mid stage *Panulirus ornatus* phyllosoma over ecdysis and larval development. Aquaculture, 434: 159–170.

Crawley, A., Kline, D., Dunn, S., Anthony, K. R. N., and Dove, S. 2010. The effect of ocean acidification on symbiont photorespiration and productivity in *Acropora formosa*. Global Change Biology, 16: 851–863.

Donner, S. D. 2009. Coping with commitment: projected thermal stress on coral reefs under different future scenarios. PloS ONE, 4: e5712.

Dove, S., Klinea, D. I., Pantosa, O., Anglyd, F. E., Tysond, G. W., and Hoegh-Guldberga, O. 2013. Future reef decalcification under a business-as-usual CO_2 emission scenario. Proceedings of the National Academy of Science of the United States of America, 110: 15342–15347.

Dove, S., Ortiz, J. C., Enriquez, S., Fine, M., Fisher, P., Iglesias-Prieto, R., Thornhill, D., *et al.* 2006. Response of holosymbiont pigments from the scleractinian coral *Montopora monasteriata* to short-term heat stress. Limnology and Oceanography, 51: 1149–1158.

Downs, C. A., McDougall, K. E., Woodley, C. M., Fauth, J. E., Richmond, R. H., Kushmaro, A., Gibb, S. W., *et al.* 2013. Heat-stress and light-stress induce different cellular pathologies in the symbiotic dinoflagellate during coral bleaching. PloS ONE, 8: e77173.

Edmunds, P. J. 2011. Zooplanktivory ameliorates the effects of ocean acidification on the reef coral *Porites* spp. Limnology and Oceanography, 56: 2402–2410.

Erez, J., Reynaud, S., Silverman, J., Schneider, K., and Allemand, D. 2011. Coral calcification under ocean acidification and global change. *In* Coral Reefs: an Ecosystem in Transition, pp. 151–176. Ed. by S. Dubinsky, and N. Stambler. Springer, New York.

Fabricius, K. E., Cséke, S., Humphrey, C., and De'ath, G. 2013. Does trophic status enhance or reduce the thermal tolerance of scleractinian corals? A review, experiment and conceptual framework. PloS ONE, 8: e54399.

Fabricius, K. E., De'ath, G., Noonan, S., and Uthicke, S. 2014. Ecological effects of ocean acidification and habitat complexity on reef-associated macroinvertebrate communities. Proceedings of the Royal Society of London Series B: Biological Science, 281: 20132479.

Fabricius, K. E., Langdon, C., Uthicke, S., Humphrey, C., Noonan, S., De'ath, G., Okazaki, R., *et al.* 2011. Losers and winners in coral reefs acclimatized to elevated carbon dioxide concentrations. Nature Climate Change, 1: 165–169.

Folch, J. M., Less, M., and Sloane-Stanley, G. H. 1957. A simple method for the isolation and purification of total lipides from animal tissues. The Journal of Biological Chemistry, 226: 497–509.

Gnaiger, E., and Bitterlich, G. 1984. Proximate biochemical composition and caloric content calculated from elemental CHN analysis: a stoichiometric concept. Oecologia, 62: 289–298.

Grottoli, A. G., Rodrigues, L. J., and Juarez, C. 2004. Lipids and stable carbon isotopes in two species of Hawaiian corals, *Porites compressa* and *Montipora verrucosa*, following a bleaching event. Marine Biology, 145: 621–631.

Halliwell, B. 2006. Reactive species and antioxidants. Redox biology is a fundamental theme of aerobic life. Plant Physiology, 141: 312–322.

Imbs, A. B., and Yakovleva, I. M. 2012. Dynamics of lipid and fatty acid composition of shallow-water corals under thermal stress: an experimental approach. Coral Reefs, 2012: 41–53.

Inoue, S., Kayanne, H., Yamamoto, S., and Kurihara, H. 2013. Spatial community shift from hard to soft corals in acidified water. Nature Climate Change, 3: 683–687.

IPCC. 2014. Climate Change 2014: impacts, adaptation, and vulnerability. *In* Contribution of Working Group II to the Fifth Assessment Report of the Intergovernmental Panel on Climate Change. Ed. by C. B. Field, V. R. Barros, D. J. Dokken, K. J. Mach, M. D. Mastrandrea, T. E. Bilir, M. Chatterjee, *et al.* Cambridge University Press, Cambridge, UK and New York, NY, USA.

Kaniewska, P., Campbell, P. R., Kline, D. I., Rodriguez-Lanetty, M., Miller, D. J., Dove, S., and Hoegh-Guldberg, O. 2012. Major cellular and physiological impacts of ocean acidification on a reef building coral. PloS ONE, 7: e34659.

Krief, S., Hendy, E. J., Fine, M., Yamd, R., Meibom, A., Foster, G. L., and Shemesh, A. 2010. Physiological and isotopic responses of scleractinian corals to ocean acidification. Geochimica and Cosmochima Acta, 74: 4988–5001.

Kroeker, K. J., Michelia, F., Gambib, M. C., and Martz, T. R. 2011. Divergent ecosystem responses within a benthic marine community to ocean acidification. Proceedings of the National Academy of Science of the United States of America, 108: 14515–14520.

Lesser, M. P. 1996. Elevated temperatures and ultraviolet radiation cause oxidative stress and inhibit photosynthesis in symbiotic dinoflagellates. Limnology and Oceanography, 41: 271–283.

Lesser, M. P. 2011. Coral bleaching: causes and mechanisms. *In* Coral Reefs: an Ecosystem in Transition, pp. 405–419. Ed. by S. Dubinsky, and N. Stambler. Springer, New York.

Leuzinger, S., Anthony, K. R. N., and Willis, B. L. 2003. Reproductive energy investment in corals: scaling with module size. Oecologia, 136: 524–531.

Lough, J. M., and Barnes, D. J. 1997. Several centuries of variation in skeletal extension, density and calcification in massive *Porites* colonies from the Great Barrier Reef: a proxy for seawater temperature and a background of variability against which to identify unnatural change. Journal of Experimental Marine Biology and Ecology, 211: 29–67.

Marsh, J. A. 1970. Primary productivity of reef-building calcareous red algae. Ecology, 51: 255–263.

McCulloch, M., Falter, J., Trotter, J., and Montagna, P. 2012. Coral resilience to ocean acidification and global warming through pH up-regulation. Nature Climate Change, 2: 623–627.

Muehllehner, N. 2013. The relationship between carbonate chemistry and calcification on the Florida Reef Tract, and in the symbiotic reef coral, *Acropora cervicornis*. Dissertation, University of Miami. http://scholarlyrepository.miami.edu/oa_dissertations.

Nichols, P. D., Mooney, B. D., and Elliot, N. 2001. Unusually high levels of non-saponifiable lipids in the fishes escolar and rudderfish: identification by gas and thin-layer chromatography. Journal of Chromatography A, 936: 183–191.

Pörtner, H.-O. 2008. Ecosystem effects of ocean acidification in times of ocean warming: a physiologist's view. Marine Ecology Progress Series, 373: 203–217.

Richier, S., Cottalorda, J. M., Guillaume, M. M., Fernandez, C., Allemand, D., and Furla, P. 2008. Depth-dependant response to light of the reef building coral, *Pocillopora verrucosa*: Implication of oxidative stress. Journal of Marine Biology and Ecology, 357: 48–56.

Rodrigues, L. J., and Grottoli, A. G. 2007. Energy reserves and metabolism as indicators of coral recovery from bleaching. Limnology and Oceanography, 52: 1874–1882.

Schneider, K., and Erez, J. 2006. The effect of carbonate chemistry on calcification and photosynthesis in the hermatypic coral *Acropora eurystoma*. Limnology and Oceanography, 51: 1284–1293.

Schoepf, V., Grottoli, A. G., Warner, M. E., Cai, W-J., Melman, T. F., Hoadley, K. D., Pettay, D. T., *et al.* 2013. Coral energy reserves and calcification in a high-CO_2 world at two temperatures. PloS ONE, 8: 1–11.

Strahl, J., Stolz, I., Uthicke, S., Vogel, N., Noonan, S., and Fabricius, K. E. 2015. Physiological and ecological performance differs in four coral taxa at a volcanic carbon dioxide seep. Comparative Biochemistry and Physiology, Part A, 184: 179–186.

Thornhill, D. J., Rotjan, R. D., Todd, B. D., Chilcoat, G. C., Iglesias-Prieto, R., Kemp, D. W., LaJeunesse, T. C., *et al.* 2011. A connection between colony biomass and death in Caribbean reef-building corals. PloS ONE, 6: e29535.

Tomanek, L., Zuzow, M. J., Ivanina, A. V., Beniash, E., and Sokolova, I. M. 2011. Proteomic response to elevated pCO_2 level in eastern oysters, *Crassostrea virginica*: evidence for oxidative stress. The Journal of Biology, 214: 1836–1844.

Towle, E. K., Enochs, I. C., and Langdon, C. 2015. Threatened Caribbean coral is able to mitigate the adverse effects of ocean acidification on calcification by increasing feeding rate. PloS ONE, 10: e0123394.

Uthicke, S., Momigliano, P., and Fabricius, K. E. 2013. High risk of extinction of benthic foraminifera in this century due to ocean acidification. Scientific Reports, 3: 1769–1774.

Uthicke, S., Vogel, N., Doyle, J., Schmidt, C., and Humphrey, C. 2012. Interactive effects of climate change and eutrophication on the dinoflagellate-bearing benthic foraminifera *Marginopora vertebralis*. Coral Reefs, 31: 401–414.

Veal, C. J., Carmi, M., Fine, M., and Hoegh-Goudberg, O. 2010. Increasing the accuracy of surface area estimation using single wax dipping of coral fragments. Coral Reefs, 29: 893–897.

Vogel, N., Fabricius, K. E., Strahl, J., Noonan, S. H. C., Wild, C., and Uthicke, S. 2015. Calcareous green alga *Halimeda* tolerates ocean acidification conditions at tropical carbon dioxide seeps. Limnology and Oceanography, 60: 263–275.

Yamashiro, H., Oku, H., and Onaga, K. 2005. Effect of bleaching on lipid content and composition of Okinawan corals. Fisheries Science, 71: 448–453.

Handling editor: Howard Browman

ICES Journal of Marine Science

ICES Journal of Marine Science (2016), 73(3), 910–919. doi:10.1093/icesjms/fsv159

Contribution to Special Issue: 'Towards a Broader Perspective on Ocean Acidification Research'

Original Article

Micro-CT analysis of the Caribbean octocoral *Eunicea flexuosa* subjected to elevated pCO_2

I. C. Enochs[1,2]*, D. P. Manzello[2], H. H. Wirshing[3], R. Carlton[1,2], and J. Serafy[4]

[1]*Cooperative Institute for Marine and Atmospheric Studies, Rosenstiel School of Marine and Atmospheric Science, University of Miami, 4600 Rickenbacker Cswy, Miami, FL 33149, USA*
[2]*Atlantic Oceanographic and Meteorological Laboratory, NOAA, 4301 Rickenbacker Cswy, Miami, FL 33149, USA*
[3]*Smithsonian Institution, National Museum of Natural History, PO Box 37012, MRC 163, Washington, DC 20013-7012, USA*
[4]*Southeast Fisheries Science Center, NOAA, 75 Virginia Beach Dr, Miami, FL 33149, USA*

**Corresponding author: tel: +1 305 361 4399; fax: +1 305 361 4447; e-mail: ienochs@rsmas.miami.edu*

Enochs, I. C., Manzello, D. P., Wirshing, H. H., Carlton, R., and Serafy, J. Micro-CT analysis of the Caribbean octocoral *Eunicea flexuosa* subjected to elevated pCO_2. – ICES Journal of Marine Science, 73: 910–919.

Received 17 March 2015; revised 8 July 2015; accepted 19 August 2015; advance access publication 12 September 2015.

Rising anthropogenic carbon dioxide has resulted in a drop in ocean pH, a phenomenon known as ocean acidification (OA). These acidified waters have many ramifications for diverse marine biota, especially those species which precipitate calcium carbonate skeletons. The permanence of coral reef ecosystems is therefore closely related to OA stress as habitat-forming corals will exhibit reduced calcification and growth. Relatively little is known concerning the fate of other constituent taxa which may either suffer concomitant declines or be competitively favoured in acidified waters. Here, we experimentally (49 d) test the effects of next century predictions for OA (pH = 7.75, pCO_2 = 1081 μatm) vs. near-present-day conditions (pH = 8.01, pCO_2 = 498 μatm) on the common Caribbean octocoral *Eunicea flexuosa*. We measure linear extension of this octocoral and use a novel technique, high-resolution micro-computed tomography, to measure potential differences in the morphology of calcified internal skeletal structures (sclerites) in a 2 mm apical section of each branch. Despite the use of highly accurate procedures, we found no significant differences between treatments in either the growth of *E. flexuosa* branches or the structure of their sclerites. Our results suggest a degree of resilience to OA stress and provide evidence that this octocoral species may persist on Caribbean coral reefs, despite global change.

Keywords: calcification, micro-CT, ocean acidification, octocoral, sclerite.

Introduction

Anthropogenic carbon dioxide has resulted in a 0.11°C increase in sea surface temperature (SST) since the 1970s, and current estimates predict a further 0.6–2.0°C rise by the end of the century (Collins *et al.*, 2013; Rhein *et al.*, 2013). Rising atmospheric carbon dioxide has been accompanied by an increase in the partial pressure of CO_2 (pCO_2) in ocean water. This phenomenon, known as ocean acidification (OA), is responsible for a decline of 0.1 pH units since the preindustrial era and an estimated drop of another 0.14–0.35 pH units by the end of the century (IPCC, 2007; Rhein *et al.*, 2013).

The resulting warmer and more-acidic seas associated with global change will have widespread impacts on marine ecosystems, perhaps most notably coral reefs, which are hotspots of biodiversity (Reaka-Kudla, 1997; Kleypas *et al.*, 1999; Hoegh-Guldberg *et al.*, 2007). Reef-building or hermatypic scleractinian corals within the cnidarian subclass Hexacorallia are currently distributed close to their maximum thermal tolerance, making them especially sensitive to rising temperatures associated with global change. Protracted periods above this threshold can result in expulsion of symbiotic zooxanthellae (dinoflagellates in the genus *Symbiodinium*), leading to coral mortality and reef degradation if stress is not quickly ameliorated (Baker *et al.*, 2008). OA will also negatively influence reef health via many mechanisms directly impacting the corals themselves, including reduced calcification (Langdon and Atkinson, 2005) and recruitment (Albright *et al.*, 2010). OA may also affect many other taxa (Kuffner *et al.*, 2007; Johnson *et al.*, 2012; Bignami *et al.*, 2013; Enochs *et al.*, 2015), disrupt competitive

hierarchies (Diaz-Pulido *et al.*, 2011; Kroeker *et al.*, 2012), and favour communities dominated by taxa other than hermatypic corals. For some species, however, short-term experimental studies and real-world systems have revealed no significant adverse effects of OA and low carbonate saturation states (Ω), providing nuance to the concept of OA as a universal stressor (Kroeker *et al.*, 2010; Cryonak *et al.*, 2016; Jokiel, 2016).

Regardless, the influence of OA and other anthropogenic stressors is already apparent in the Caribbean. In the last 30 years, average coral cover on reefs in this region has dropped by roughly 80% (Gardner *et al.*, 2003). The resulting lower calcification and high rates of erosion have contributed to a drop in structural complexity (Alvarez-Filip *et al.*, 2009) that likely has influenced associated fish and invertebrate populations (Graham and Nash, 2013). Currently, it is believed that as reefs degrade in structural complexity and coral cover, they will be replaced with larger proportions of macroalgae, potentially shifting into a less desirable alternative stable state (Hoegh-Guldberg *et al.*, 2007). Evidence from a volcanic CO_2 vent off Japan, however, revealed healthy octocoral communities in low pH water, suggesting a shift from hexacorals to octocorals under OA conditions (Inoue *et al.*, 2013).

Relative to hermatypic hexacorals, octocorals are poorly studied. This is unfortunate considering their high abundances (Lasker and Coffroth, 1983; Yoshioka and Yoshioka, 1989; Ruzicka *et al.*, 2013) and diversity (Alcolado *et al.*, 2003; Guzmán, 2003) among coral reef and hard bottom habitats throughout the Florida Keys and Caribbean. In these and other environments, octocorals fulfil a number of important ecological roles, including trophic and habitat functions, by consolidating and forming carbonate substrates as well as providing shelter to invertebrates and fish (Goh *et al.*, 1999; Glynn and Enochs, 2011; Jeng *et al.*, 2011).

Current data on the effects of OA on octocorals are mixed. Bramanti *et al.* (2013) found that the non-reef-dwelling red coral *Corallium rubrum*, collected from deep temperate waters in the Mediterranean, exhibited significantly reduced skeletal growth, abnormally shaped sclerites, and increased total organic matter at a pH of 7.81. In contrast, Gabay *et al.* (2013) found no significant differences in three species of octocoral from Eilat, even after prolonged exposure (up to 5 months) under pH conditions as low as 7.6 and 7.3. At these extremely reduced pHs, however, sclerites free of living tissues were found to degrade, but those that were maintained inside of living specimens were intact, suggesting a degree of protection to OA stress conferred by the living coral (Gabay *et al.*, 2014). Inoue *et al.* (2013), working with *Sarcophyton elegans* from reefs off Japan, found that elevated pCO_2 enhanced photosynthesis and significantly increased night-time decalcification, but did not significantly impact daytime calcification. Finally, the only study to date on the influence of OA on a Caribbean octocoral was conducted by Gómez *et al.* (2014). Working with *Eunicea fusca*, they found that a reduction in pH consistent with IPCC projections for the end of the century (7.8) resulted in a slight increase in growth and calcification. However, over the full spectrum of OA treatments that Gómez *et al.* (2014) applied (down to 7.1), there was a significant negative relationship between OA and all measured growth metrics, including buoyant weight, linear extension, and per cent incorporation of calcein stain into sclerites.

Perhaps, the lack of a consistency in the response of previously studied octocorals to OA is due to the great diversity of both colony and skeletal morphologies present among these taxa. Further work is therefore needed to more clearly understand the response of these taxa to OA. To this end, we experimentally tested the effects of elevated pCO_2 on the growth of sclerites and branch tips of the Caribbean octocoral *Eunicea flexuosa*. We employed high-resolution micro-computed tomography (micro-CT), for *in situ* quantification of growth and skeletal metrics. While micro-CT technology has previously been applied to octocorals in a methods paper to identify and map internal canal networks (Morales Pinzón *et al.*, 2014), our study is the first to quantify calcified structures within an octocoral and use these data to statistically compare treatment groups.

Methods

Experimental manipulations

Four colonies of *E. flexuosa* were collected from ∼7 m depth at Cheeca Rocks, Florida Keys. Colonies were transported to laboratory facilities at the University of Miami (Key Biscayne, FL, USA) where they were fragmented into seven to eight individual branches (∼10 cm length) and affixed to labelled PVC tiles using underwater epoxy (All-Fix). The resulting replicates were divided among eight experimental tanks (15 in high CO_2, 14 in low CO_2) for 49 d. An additional apical branch tip from each of the parent colonies was removed at the time of collection and immediately preserved in EtOH for subsequent scanning of initial branch characteristics.

Each of the eight independent experimental systems consisted of two connected ∼75-l tanks, the top of which contained the *E. flexuosa* replicates and a circulation pump (Figure 1). Temperature and carbonate chemistry were manipulated in the lower of the two tanks. Temperature was maintained at 25°C through the use of a chilled water bath and aquarium heaters. Treatment gas was introduced into each tank using a venturi pump at a constant flow rate regulated with a valved variable area flowmeter (Cole Parmer). A target OA treatment level of 1000 μatm was set based on IPCC predictions for roughly 100 years from now, assuming the continued reliance on fossil fuel-based energy technologies (IPCC, 2007, model A1F1). The concentration of the enriched CO_2 treatment gas was precisely regulated using mass flow controllers (Sierra Mass-Trak 810C), compressed air, and pure CO_2. Fresh seawater was dripped into each system at a rate so that the entire volume of the system was refreshed multiple times per day. The experiment was performed in a blacked-out room with artificial light (two 216 W T5 fixtures) illuminating on a 12 h cycle.

The temperature, salinity, and pH of each tank were measured three times per week using a hand-held YSI Professional Plus multiprobe unit. Seawater xCO_2 was measured five times per week from 11 February to 7 March using a non-dispersive infrared CO_2 gas analyser (LI-COR, LI-810), connected to air–gas equilibrator (General Oceanics). Discrete water samples were collected from each tank one to two times weekly for analysis of dissolved inorganic carbon (DIC) and total alkalinity (TA). Both parameters were measured using ApolloSciTech instruments (AS-C3 and AS-ALK2, DIC and TA, respectively). Temperature, salinity, DIC, and TA were used to calculated pCO_2 using the CO2SYS software package (Lewis and Wallace, 1998) and the dissociation constants of Mehrbach *et al.* (1973), as refit by Dickson and Millero (1987) and Dickson (1990) for boric acid.

To minimize tank effects, every 2 weeks, replicates of *E. flexuosa* were randomly reassigned to different tanks within the same treatment (high vs. low CO_2). The height of each *E. flexuosa* branch was measured at the beginning and end of the experiment using Vernier calipers to determine linear extension. The tips of each branch were removed following the experiment, preserved in 70% EtOH, and reserved for analysis using micro-CT.

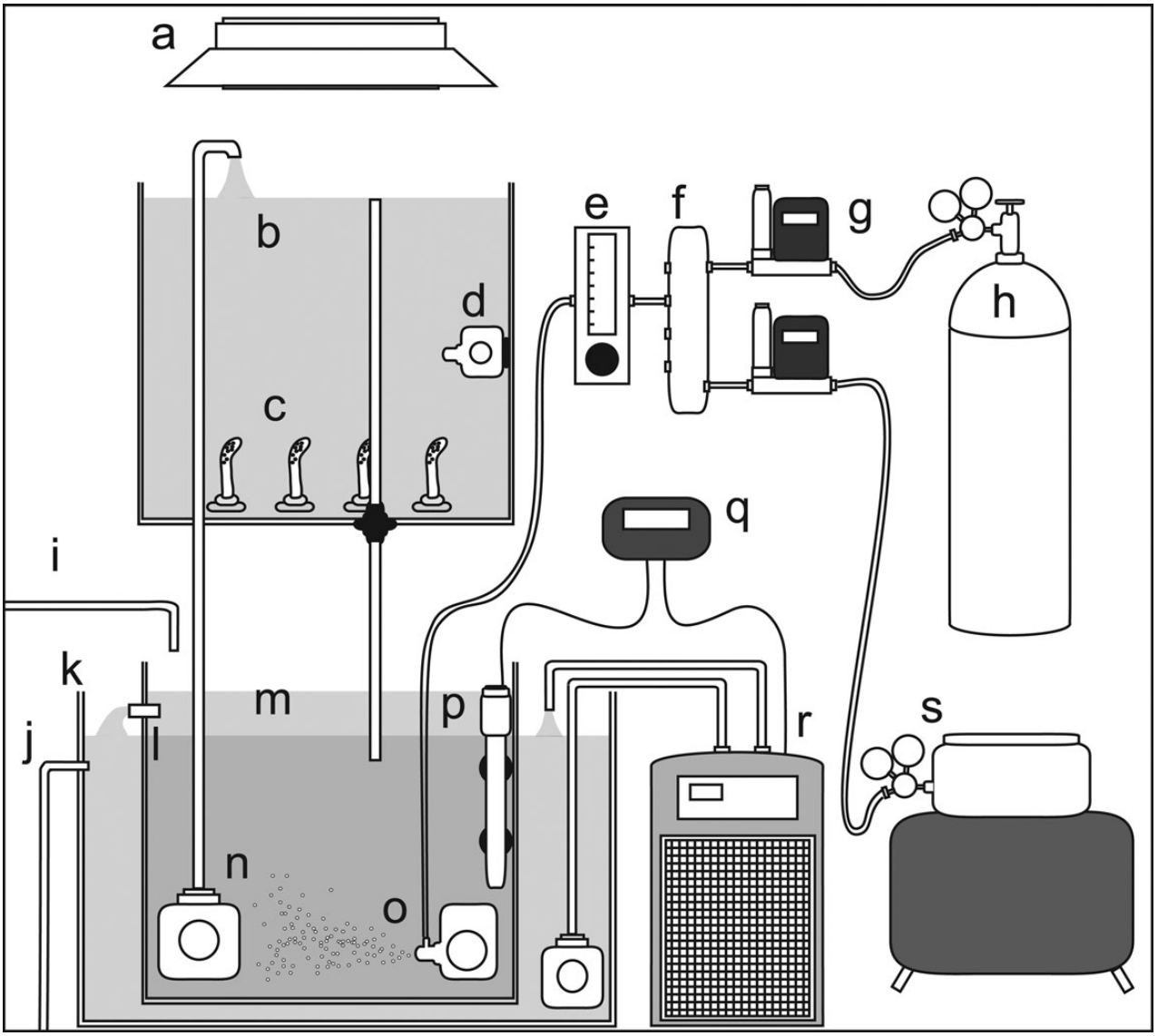

Figure 1. Experimental aquarium setup used to treat *E. flexuosa* with present-day and future carbonate chemistry conditions for 49 d. a, light; b, aquarium; c, octocorals; d, circulation pump; e, valved flowmeter; f, gas mixing chamber; g, mass flow controller; h, compressed CO_2 cylinder; i, fresh seawater input; j, seawater outflow; k, water bath; l, overflow; m, sump aquarium; n, water return pump; o, venturi pump; p, aquarium heater; q, microcontroller; r, chiller; s, air compressor.

Scanning procedure

Octocoral branch tips were scanned using a Skyscan 1174 micro-CT (Bruker) with a 50 kV, 800 μA X-ray source. Samples were secured to the stage using parafilm and a 0.25 mm aluminium filter was used to block lower energy X-rays. Samples were scanned at a pixel resolution of 6.97 μm using a 4400 ms exposure. X-ray images were collected every 0.7° over 180° of rotation. Flat images of X-ray transmittance, taken around the vertical axis, were reconstructed into a stack of transverse images using the NRecon software package (Figure 2). A 20% beam hardening correction factor, a ring artefact correction of four, and a dynamic range of 0.0–0.24 were consistently employed during reconstruction and were selected based on visual inspection and iterative optimization of multiple scans.

Analysis of micro-CT image stacks was conducted using CTAn. Regions of interest (ROI) were manually defined around the outer surface of the first 2 mm of each apical branch tip. Growth rates of wild *E. flexuosa* reported from Puerto Rico range from 1.77 to 2.15 cm $year^{-1}$ (Yoshioka and Yoshioka, 1991), and the mean extension rates for individuals subjected to a transplant experiment were 1.55 cm $year^{-1}$ (Prada *et al.*, 2008). The 2 mm used for analysis was therefore chosen as an estimate of new growth exclusively during experimental conditions (49 d). Calcification and sclerite formation likely also occurred outside of this apical region, though this area was excluded due to the difficulty of separating growth under experimental conditions from that which occurred prior. Volume, surface area, and mean attenuation coefficient of this region were recorded. Each of the 8-bit greyscale slices within the ROI was thresholded to create a binary image containing only high-density sclerites (Figure 2). The mean attenuation coefficient was recorded from this region and an ROI "shrink-wrapping"

function was applied to measure the volume and number of high-density sclerites. Per cent volume of sclerites was calculated by dividing the volume of the thresholded high-density regions by the total volume of the 2 mm branch tip.

Statistical analysis

Statistical analysis was performed using SPSS software (IBM, 2013). Variation in branch and sclerite parameters was investigated using general linear models (GLMs) with parent colony, pCO_2 treatment, and their interaction as factors. Upon finding the interaction effects non-significant ($p > 0.05$), they were removed and the analyses was re-run with main effects only.

Results

The mean temperature and salinity, as well as carbonate chemistry parameters (DIC, TA, calculated pCO_2, xCO_2), are shown for each tank and CO_2 treatment in Table 1. During the seventh week of the experiment, equipment malfunction resulted in an absence of DIC data, and consequently, calculated pCO_2 values are not available for this week. However, tank and treatment averages for both TA and xCO_2 include data during this period. During week 4, TA was measured to be anomalously low in tanks 1–6 (2332.1 ± 1.0, mean ± s.e.m.), resulting in elevated calculated pCO_2.

Micro-CT was successful at resolving both octocoral branch morphology and internal high-density sclerites (Figure 3). Large middle cortex sclerites and smaller outer cortex sclerites were clearly visible in the reconstructed micro-CT scans, and were subsequently detected using thresholding of the higher-density materials (Figure 2a). No significant differences due to CO_2 treatments were detected among any of the branch (Figure 4, Tables 2 and 3) or sclerite (Figure 5, Tables 3 and 4) metrics. Significant parent colony effects were detected for branch extension and sclerite volume (Table 3).

Discussion

The absence of significant effects in *E. flexuosa* branch and sclerite morphology from CO_2 conditions projected to occur near the end

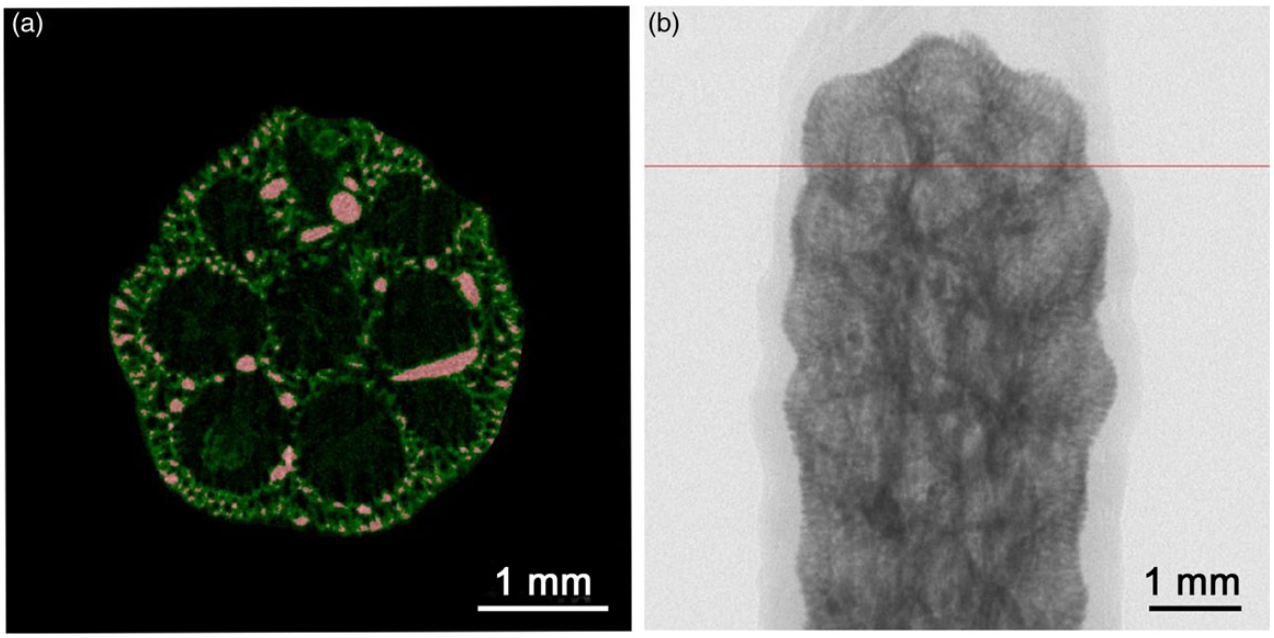

Figure 2. Two-dimensional micro-CT images of *E. flexuosa*. (a) Transverse section showing high-density sclerites thresholded in red and lower density structures in green; (b) coronal view X-ray transmittance. Red line in (b) denotes location of section in (a).

Table 1. Mean seawater parameters for each experimental tank as well as overall treatment means.

Tank	Temp. (°C)	Salinity (psu)	xCO_2 (ppm)	TA (μmol kg^{-1})	DIC (μmol kg^{-1})	pH (Total)	pCO_2 (μatm)	$\Omega_{Aragonite}$
Tank 1	24.8 (0.04)	36.6 (0.11)	446.5 (8.8)	2516.5 (27.36)	2216.7 (19.74)	7.99 (0.031)	516.5 (50.28)	3.45 (0.187)
Tank 2	24.7 (0.09)	36.5 (0.1)	443.8 (9.46)	2513.4 (26)	2204.3 (18.23)	8.01 (0.031)	493.1 (49.35)	3.55 (0.188)
Tank 3	24.3 (0.17)	36.5 (0.1)	429.4 (8.53)	2518 (26.49)	2213 (19.12)	8.01 (0.035)	493.1 (55.83)	3.5 (0.205)
Tank 4	24.5 (0.18)	36.5 (0.09)	437.1 (7.57)	2519.9 (27.93)	2211.9 (18.46)	8.01 (0.034)	487.9 (50.35)	3.54 (0.202)
Tank 5	24.8 (0.07)	36.6 (0.06)	1013.4 (64.99)	2516.7 (25.7)	2361 (28.7)	7.71 (0.063)	1196.1 (206.87)	2.09 (0.235)
Tank 6	24.6 (0.1)	36.6 (0.07)	998.1 (78.29)	2515.5 (25.29)	2344.2 (28.75)	7.75 (0.062)	1094.2 (229.3)	2.23 (0.223)
Tank 7	24.4 (0.21)	36.5 (0.08)	859.2 (53.01)	2520.4 (27.91)	2332.9 (28.18)	7.79 (0.055)	953 (165.85)	2.37 (0.222)
Tank 8	24.8 (0.13)	36.6 (0.08)	873 (47.27)	2537.1 (34.02)	2363.7 (33.5)	7.75 (0.059)	1079.3 (181.67)	2.25 (0.23)
L-CO_2	24.6 (0.07)	36.5 (0.05)	439.2 (4.29)	2517 (12.95)	2211.5 (9.11)	8.01 (0.016)	497.7 (24.81)	3.51 (0.094)
H-CO_2	24.6 (0.07)	36.5 (0.04)	934.9 (31.37)	2522.4 (13.73)	2350.5 (14.48)	7.75 (0.029)	1080.6 (95.84)	2.23 (0.111)

Parameter periodicity as reported in the Methods section. xCO_2 values measured with an infrared gas analyser and equilibrator. pH, pCO_2, Ω calculated from TA and DIC. Standard error in parentheses.

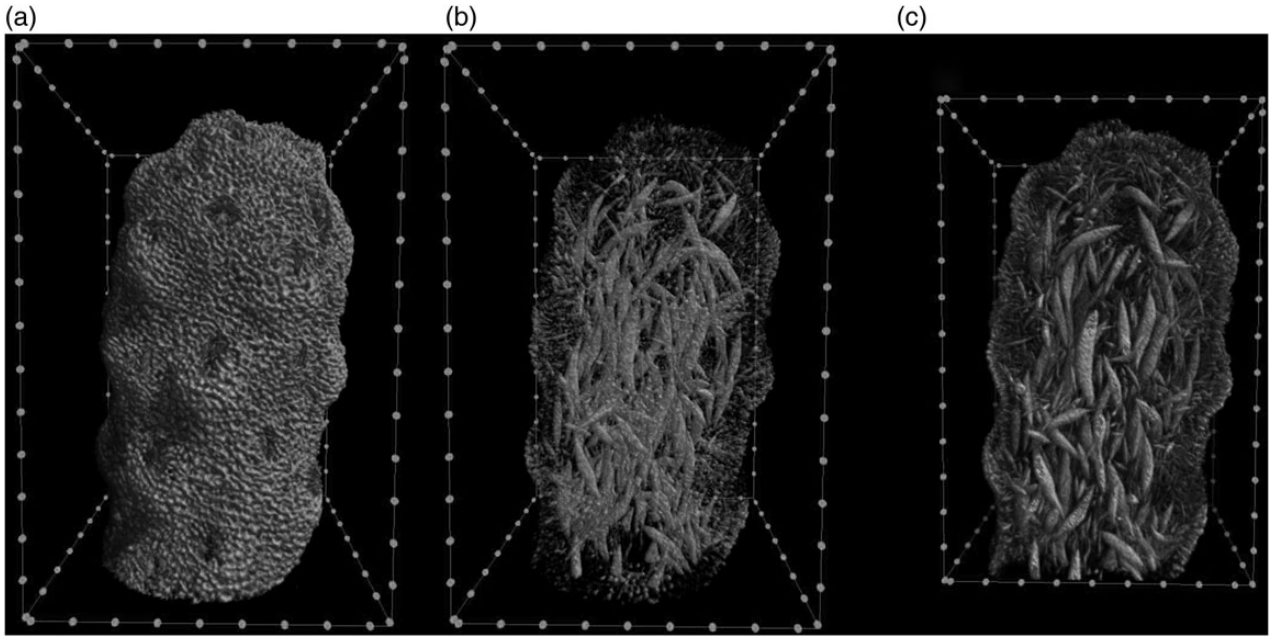

Figure 3. Micro-CT scans of *E. flexuosa*. (a) Surface of branch tip; (b) increased transparency showing high-density sclerites within branch tip; (c) digitally sectioned scan showing internal structure of branch tip. Spheres along margins of bounding boxes are 500 μm apart.

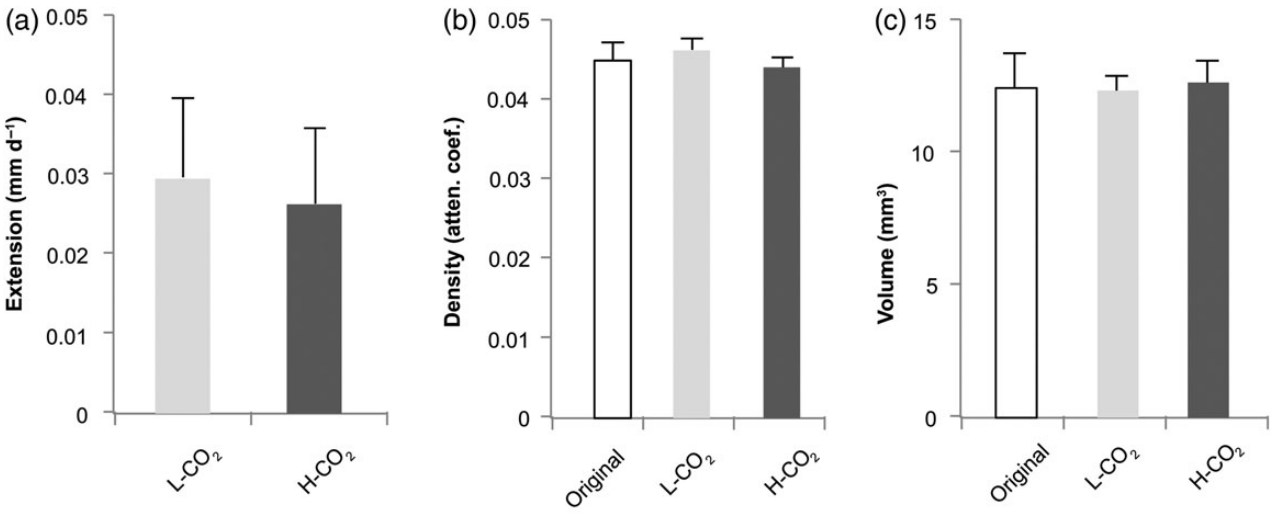

Figure 4. The response of *E. flexuosa* branches to low (L-CO_2, $n = 14$) and high CO_2 (H-CO_2, $n = 15$) conditions, as well as original branch characteristics. (a) Linear extension; (b) density of top 2 mm of branch tip; (c) volume of top 2 mm of branch tip. Error bars are standard error. No significant differences detected among L-CO_2 and H-CO_2 treatment means.

of the century are consistent with the findings of Gabay *et al.* (2013), who found no significant differences in the response of three species of octocorals, subjected to pCO_2 treatments more extreme (up to 3898 μatm) than those tested here (1081 μatm). While linear extension, branch morphology, and sclerite morphology were not directly measured in that study, they found no significant differences in protein and chlorophyll concentration, polyp and sclerite weight, zooxanthellae density, or polyp pulsation rate. Similarly and also consistent with our study, Gabay *et al.* (2014) used s.e.m. to visualize sclerite morphology and found no significant evidence of degradation within living colonies of *Ovabunda manrospiculata*. In apparent contrast to the work of Gabay *et al.* (2014), Gómez *et al.* (2014) found significant negative correlation between pCO_2 and weight, linear extension, and the uptake of calcein stain into sclerites of *E. fusca*. *Eunicea fusca* is a congeneric of the *E. flexuosa*, used in this study, and while a significant relationship between pCO_2 and growth was observed in their study, extreme pCO_2 treatments (4568 μatm) were much greater than treatments utilized herein. Similar to our findings, however, when samples were subjected to CO_2 values predicted by the end of the century, differences

Table 2. Treatment and colony averages for *E. flexuosa* branch characteristics.

	Branch dens. (atten. coef.)	Branch vol. (mm^3)	Branch SA (mm^2)	Branch extension ($mm\ d^{-1}$)
L-CO_2	0.046 (0.0013)	12.31 (0.498)	35.33 (0.987)	0.03 (0.01)
Colony 1	0.049 (0.0022)	12.70 (0.509)	34.91 (0.895)	0.03 (0.014)
Colony 2	0.041 (0.0020)	11.88 (0.254)	34.87 (1.21)	0.00 (0.013)
Colony 3	0.047 (0.0023)	11.34 (0.808)	34.26 (1.316)	0.06 (0.027)
Colony 4	0.046 (0.0034)	13.51 (2.021)	37.79 (4.357)	0.02 (0.013)
H-CO_2	0.044 (0.0011)	12.61 (0.725)	36.46 (1.543)	0.03 (0.010)
Colony 1	0.047 (0.0009)	14.36 (2.466)	39.59 (5.048)	0.02 (0.013)
Colony 2	0.042 (0.0010)	10.99 (1.479)	33.97 (3.708)	0.02 (0.017)
Colony 3	0.044 (0.0033)	11.27 (0.883)	33.97 (2.295)	0.06 (0.025)
Colony 4	0.044 (0.0022)	14.27 (0.178)	39.1 (1.013)	0.00 (0.000)
Total	0.045 (0.0009)	12.47 (0.438)	35.92 (0.920)	0.03 (0.007)
Initial	0.045 (0.0021)	12.41 (1.379)	35.18 (2.762)	n.a.

Initial values calculated as the mean of each parent colony sampled in advance of the experiment. Standard error in parentheses.

Table 3. Results of GLM analysis of branch and sclerite characteristics.

	Dependent variable	Source	d.f.	MS	*F*	*p*-value
Branch characteristics	Density	CO_2	1	1.95E−05	1.078	0.309
		Colony	3	5.19E−05	2.864	0.058
		Error	24	1.81E−05	–	–
	Volume	CO_2	1	0.858	0.18	0.675
		Colony	3	13.615	2.853	0.058
		Error	24	4.771	–	–
	Surface area	CO_2	1	9.366	0.388	0.539
		Colony	3	32.718	1.356	0.28
		Error	24	24.137	–	–
	Extension	CO_2	1	5.47E−06	0.005	0.944
		Colony	3	0.004	3.714	0.025
		Error	24	0.001	–	–
Sclerite characteristics	Density	CO_2	1	2.77E−08	1.707	0.204
		Colony	3	7.55E−09	0.465	0.71
		Error	24	1.62E−08	–	–
	Volume	CO_2	1	0.1	0.32	0.577
		Colony	3	1.394	4.446	0.013
		Error	24	0.314	–	–
	Surface area	CO_2	1	543.521	0.281	0.601
		Colony	3	4207.539	2.178	0.117
		Error	24	1931.403		
	Per cent volume	CO_2	1	19.205	1.61	0.217
		Colony	3	29.552	2.477	0.086
		Error	24	11.93		
	Count	CO_2	1	1 310 904	0.021	0.887
		Colony	3	237 055 402.7	3.763	0.024
		Error	24	62 997 773.5		

Note that all initial models included Colony × CO_2 treatment interaction terms; however, as these all emerged as non-significant, only main effects model results are shown.

Table 4. Treatment and colony averages for *E. flexuosa* sclerites characteristics.

	Sclerite dens. (atten. coef.)	Sclerite vol. (mm^3)	Sclerite SA (mm^2)	Per cent sclerite vol.	Count
L-CO_2	0.24 (0.0000)	2.69 (0.154)	232.92 (9.93)	21.9 (1.09)	20 344.6 (1879.94)
Colony 1	0.24 (0.0000)	3.07 (0.184)	248.3 (14.971)	24.3 (1.71)	21 540.8 (2550.90)
Colony 2	0.24 (0.0000)	2.10 (0.176)	204.38 (13.573)	17.8 (1.87)	14 383.3 (1546.91)
Colony 3	0.24 (0.0001)	2.61 (0.396)	231.94 (28.516)	22.7 (1.86)	19 350.5 (5235.76)
Colony 4	0.24 (0.0002)	2.85 (0.140)	242.28 (11.091)	21.9 (2.68)	26 036.7 (1178.43)
H-CO_2	0.24 (0.0000)	2.50 (0.188)	220.31 (13.978)	19.9 (0.87)	20 483.3 (2742.86)
Colony 1	0.24 (0.0000)	3.26 (0.640)	270.36 (55.734)	22.5 (0.54)	27 778.0 (11587.82)
Colony 2	0.24 (0.0000)	2.08 (0.287)	190.99 (26.536)	18.9 (0.88)	13 853.5 (2894.35)
Colony 3	0.24 (0.0000)	2.24 (0.208)	212.83 (8.881)	20.3 (2.46)	15 387.5 (1276.07)
Colony 4	0.24 (0.0000)	2.64 (0.232)	219.55 (12.296)	18.6 (1.88)	26 737.8 (2205.40)
Total	0.24 (0.0000)	2.59 (0.121)	226.4 (8.605)	20.9 (0.71)	20 416.3 (1654.69)
Initial	0.24 (0.0000)	2.57 (0.315)	206.86 (27.247)	20.79 (1.45)	22 318.3 (5737.50)

Initial values calculated as the mean of each parent colony sampled in advance of the experiment. Standard error in parentheses.

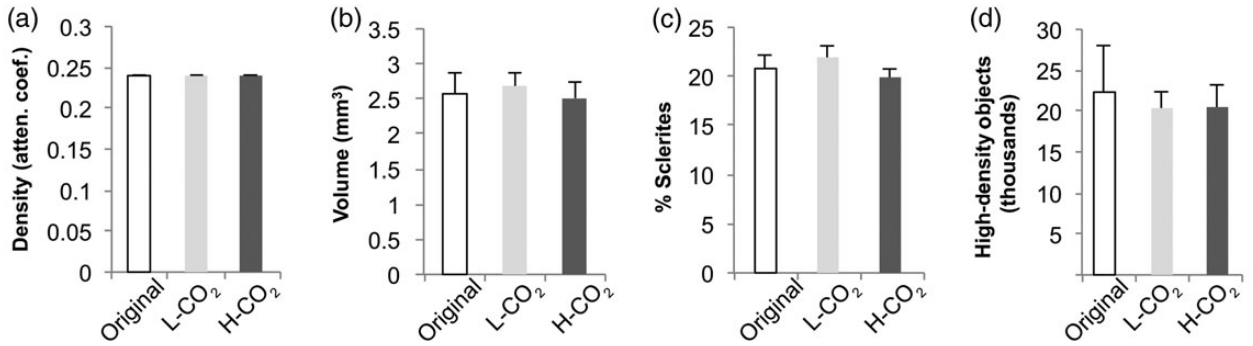

Figure 5. The response of sclerites in the top 2 mm tip of *E. flexuosa* branches to low (L-CO_2) and high CO_2 (H-CO_2) conditions, as well as original sclerites characteristics at the time of collection. (a) Total sclerite volume; (b) density of sclerites; (c) per cent volume of sclerites in the upper 2 mm of the branch tip; (d) number of high-density sclerites in upper 2 mm of branch tip as determined by thresholding micro-CT scans. Error bars are standard error. No significant differences detected among L-CO_2 and H-CO_2 treatment means.

in growth and calcification were not as apparent. In their study, as pCO_2 increased from 285 to 709 μatm, calcification was actually observed to increase.

Field-based evidence of the resilience of octocorals to OA and corroboration of the findings reported herein can be found in Inoue *et al.* (2013). Naturally occurring high CO_2 vents at Iwotorishima, Japan, mimic OA conditions projected for the end of the century. While nearby and unaffected ecosystems are dominated by scleractinian corals, those experiencing 831 μatm pCO_2 are dominated by *S. elegans*, and those experiencing 524 μatm pCO_2 have high densities of *Sinularia* spp. The presence of these soft coral species in elevated CO_2, presumably for durations greatly more than experimental studies, underscores the resilience of these taxa to OA stress. It is worth noting, however, that in closer proximity to the vent where CO_2 conditions reached 1465 μatm, few octocorals were found. It is therefore possible that this reflects a threshold that limits the distribution of these taxa, although this is in apparent contrast to shorter experimental studies.

We cannot completely eliminate the potential that OA does indeed significantly affect *E. flexuosa*, yet we were unable to detect the subtle differences utilizing our methodologies. Given our novel high-precision technique and our analysis of actively calcifying branch tips, coupled with the agreement of our results with similar species in the literature, we find this unlikely. This is especially true under realistic OA scenarios and considering levels of response that are physiologically and ecologically relevant. We do not dispute, therefore, that under extreme levels of OA outside that predicted for the next 100 years, octocoral growth and calcification may be influenced by CO_2 (Gómez *et al.*, 2014).

Among the more-sensitive scleractinian hexacorals, considerable evidence has pointed to differential susceptibility of various species and genera to OA stress (Fabricius *et al.*, 2011; McCulloch *et al.*, 2012; Takahashi and Kurihara, 2012). Persistence of the calcification process despite reduced pH may be related to tissue separating the site of calcification from low pH water (Rodolfo-Metalpa *et al.*, 2011). For example, Gabay *et al.* (2014) observed that sclerites removed from living octocoral tissue experienced degradation and dissolution at extremely low pH's, while those within protective layers of live tissue were unaffected.

Shirur *et al.* (2014) have measured especially high calcified sclerite mass relative to organic tissues within *E. flexuosa* (81% dry tissue), indicating a high degree of calcification occurs within this species. Octocoral calcification is complicated, poorly understood, and very different from that of hexacorals. Sclerite formation is initiated in the vacuole of scleroblasts contained in the mesoglea (Kingsley and Watabe, 1982). This vacuole contains a proteinaceous organic matrix or framework on which the sclerites are formed, and has been shown to be closely involved in regulating the structure and calcification of these sclerites (Rahman *et al.*, 2007; Rahman and Oomori, 2008). The vacuole increases in size as the sclerite calcifies, until the vacuole and cell membrane fuse and the sclerite transitions into the intercellular space (Kingsley and Watabe, 1982). This intracellular sclerite calcification is fundamentally different from the extracellular and extraorganismal skeletogenesis of scleractinian hexacorals (Cohen and McConnaughey, 2003). Indeed, this difference may be responsible for the relative stability of octocoral calcification, despite altered carbonate chemistry.

In addition to sclerite structures found within the mesoglea, holaxonian gorgonians have an axial skeleton made of gorgonin, a collagen and protein matrix that surrounds hollow canals. Internal cavities or loculi within this skeleton often contain calcified material, especially within the base and branches of colonies (Bond *et al.*, 2005). In some species (e.g. *Plexaurella dichotoma*), the spherulitic crystalline structure of these deposits indicates rapid formation via biological means (Bond *et al.*, 2005). However, in *E. flexuosa*, crystal shapes indicative of non-biogenic calcium carbonate precipitation have been observed (Lewis *et al.*, 1992), suggesting an internal environment highly conducive to calcification. X-ray diffraction of these crystals conducted by Lewis *et al.* (1992) revealed an unidentified diffraction pattern and an indeterminate crystal structure, though Lowenstam (1964) had previously sampled aragonite from within *E. flexuosa*. It remains to be seen if these structures respond differently to OA conditions than sclerites, though evidence indicates that they exist in a controlled internal environment, favourable for calcification.

Octocorals have highly diverse colony morphologies, both internally and externally. Colony shapes can be whip-like, fan-like, arborescent, or laminar and can vary with respect to their density and tissue thickness. Internally, they have many shapes and types of sclerites that differ in their distance from colony surfaces (Lewis and Von Wallis, 1991). These differences should be considered when evaluating the influence of OA on additional octocoral species and, as pointed out by Gabay *et al.* (2014), likely explain the apparent incongruities among previously published literature. For example, significant effects of OA have been measured in the relatively thin-tissued genus

Corallium, but not in the more fleshy genus *Sarcophyton* (Bramanti *et al.*, 2013; Gabay *et al.*, 2013).

While previous studies have referenced the high-magnesian calcite structure of sclerites (>4 mol%), we caution that this does not necessarily translate into high solubility and greater OA susceptibility. The relationship between magnesium content and solubility is poorly understood and somewhat contentious (Morse and Mackenzie, 1990). Concentrations of $MgCO_3$ vary greatly among octocoral species, but range from roughly 6 to 11 mol% (Velimirov and Böhm, 1976; Weinbauer and Velimirov, 1995). While older studies calculate higher solubility (e.g. Plummer and Mackenzie, 1974), in Morse and Mackenzie's (1990, Table 3.7) biogenic "best fit" curve, mole percentages of $MgCO_3$ <10 are not that different from aragonite with respect to solubility. In contrast, present-day $MgCO_3$ mole percentages for crustose coralline algae may be 18% (Ries, 2006), translating to a much higher solubility (Morse and Mackenzie, 1990), and resulting in a strong sensitivity to OA (Kuffner *et al.*, 2007). The only reported decline in calcification reported for an octocoral under conditions predicted for the end of the century has been for *C. rubrum* (Bramanti *et al.*, 2013). Microprobe investigation of the Mg content of their skeletons reveals values lower than what can be considered high-magnesian calcite, though subsequent X-ray analysis reveals much higher concentrations of 11.6 mol% (reviewed in Long *et al.*, 2014). Further research is needed to examine the relationship between magnesium concentration and solubility, especially with respect to the molecular composition of octocoral sclerites and their ability to withstand OA.

In addition to OA stress, coral reefs are impacted by climate change through increased SSTs, potentially leading to coral bleaching and mortality (Hoegh-Guldberg *et al.*, 2007). While octocorals are also known to bleach due to thermal stress, the long-term impact on their survivability may not be as severe as for hermatypic corals. In fact, relative to hexacorals, there are few documented cases in the scientific literature of Caribbean octocorals bleaching (Lasker *et al.*, 1984; Harvell *et al.*, 2001; Prada *et al.*, 2009). Prada *et al.* (2009) documented a high temperature event in Puerto Rico in 2005, resulting in 18% of octocorals bleaching, including colonies of *E. flexuosa*. Although individuals in the genus *Muricea* suffered mortality as a result of the event, most species and colonies recovered, and the overall mortality was low. While bleaching may occur cryptically in some octocoral species (with little change in colour), extreme 1983 ENSO-related warming resulted in no appreciable change in zooxanthellae densities in the octocoral *Plexaura kuna*, despite extensive bleaching and mortality of nearby scleractinian corals (Lasker, 2003).

The resistance to bleaching and OA stress demonstrated by several species of octocorals potentially indicates a degree of resilience to global change, especially with respect to structure, rigidity, and growth, of which sclerites play an important role (Lewis and Von Wallis, 1991). In the absence of other stressors (e.g. sedimentation, eutrophication, and overfishing), these data suggest that octocorals may become increasingly more prominent members of Caribbean reef ecosystems. Indeed, while scleractinian corals have steadily declined throughout the Caribbean (Gardner *et al.*, 2003), octocoral populations in the Florida Keys have generally increased since the mid-1990s, especially in shallow forereef habitats (Ruzicka *et al.*, 2013). Similarly, in St John, US Virgin Islands, octocoral abundances have remained relatively stable, while scleractinian coral populations have experienced dramatic declines (Colvard and Edmunds, 2011; Edmunds, 2013). While octocorals do provide habitat to associated invertebrates and fish, they lack the permanence and structural complexity of scleractinian corals. Consequently, a shift from hermatypic scleractinians to octocorals may nevertheless correspond to a loss in reef ecosystem function.

Acknowledgements

We gratefully acknowledge funding from NOAA's CRCP and OAP.

References

Albright, R., Mason, B., Miller, M., and Langdon, C. 2010. Ocean acidification compromises recruitment success of the threatened Caribbean coral *Acropora palmata*. Proceedings of the National Acadamy of Sciences of the United States of America, 107: 20400–20404.

Alcolado, P. M., Claro-Madruga, R., Menéndez-Macias, G., García-Parrado, P., Marti?nez-Daranas, B., and Sosa, M. 2003. The Cuban coral reefs. *In* Latin American Coral Reefs, pp. 53–75. Ed. by J. Cortés. Elsevier, Amsterdam. 497 pp.

Alvarez-Filip, L., Dulvy, N. K., Gill, J. A., Cote, I. M., and Watkinson, A. R. 2009. Flattening of Caribbean coral reefs: region-wide declines in architectural complexity. Proceedings of the Royal Society B, 276: 3019–3025.

Baker, A. C., Glynn, P. W., and Riegl, B. 2008. Climate change and coral reef bleaching: an ecological assessment of long-term impacts, recovery trends and future outlook. Estuarine, Coastal and Shelf Science, 80: 435–471.

Bignami, S., Enochs, I. C., Manzello, D. P., Sponaugle, S., and Cowen, R. K. 2013. Ocean acidification alters the otoliths of a pantropical fish species with implications for sensory function. Proceedings of the National Acadamy of Sciences of the United States of America, 110: 7366–7370.

Bond, Z. A., Cohen, A. L., Smith, S. R., and Jenkins, W. J. 2005. Growth and composition of high-Mg calcite in the skeleton of a Bermudian gorgonian (*Plexaurella dichotoma*): potential for paleothermometry. Geochemistry, Geophysics, Geosystems, 6: 1–10.

Bramanti, L., Movilla, J., Guron, M., Calvo, E., Gori, A., Dominguez-Carrió, C., Grinyó, J., *et al.* 2013. Detrimental effects of ocean acidification on the economically important Mediterranean red coral (*Corallium rubrum*). Global Change Biology, 19: 1897–1908.

Cohen, A. L., and McConnaughey, T. A. 2003. Geochemical perspectives on coral mineralization. Reviews in Mineralogy and Geochemistry, 54: 151–187.

Collins, M., Knutti, R., Arblaster, J., Dufresne, J-L., Fichefet, T., Friedlingstein, P., Gao, X., *et al.* 2013. Long-term climate change: projections, commitments and irreversibility. *In* Climate Change 2013: the Physical Science Basis. Contribution of Working Group I to the Fifth Assessment Report of the Intergovernmental Panel on Climate Change. Ed. by T. F. Stocker, D. Qin, G-K. Plattner, M. Tignor, S. K. Allen, J. Boschung, A. Nauels, *et al.* Cambridge University Press, Cambridge, UK and New York, NY.

Colvard, N. B., and Edmunds, P. J. 2011. Decadal-scale changes in abundance of non-scleractinian invertebrates on a Caribbean coral reef. Journal of Experimental Marine Biology and Ecology, 397: 153–160.

Cryonak, T., Schulz, K. G., and Joliel, P. L. 2016. The Omega myth: what really drives lower calcification rates in an acidifying ocean. ICES Journal of Marine Science, 73: 558–562.

Diaz-Pulido, G., Gouezo, M., Tilbrook, B., Dove, S., and Anthony, K. R. 2011. High CO_2 enhances the competitive strength of seaweeds over corals. Ecology Letters, 14: 156–162.

Dickson, A. G. 1990. Thermodynamics of the dissociation of boric acid in synthetic seawater from 273.15 to 318.15 K. Deep Sea Research, 37: 755–766.

Dickson, A. G., and Millero, F. J. 1987. A comparison of the equilibrium constants for the dissociation of carbonic acid in seawater media. Deep Sea Research, 34: 1733–1743.

Edmunds, P. J. 2013. Decadal-scale changes in the community structure of coral reefs of St. John, US Virgin Islands. Marine Ecology Progress Series, 489: 107–123.

Enochs, I. C., Manzello, D. P., Carlton, R. D., Graham, D. M., Ruzicka, R., and Colella, M. A. 2015. Ocean acidification enhances the bioerosion of a common coral reef sponge: implications for the persistence of the Florida Reef Tract. Bulletin of Marine Science, 91: 271–290.

Fabricius, K. E., Langdon, C., Uthicke, S., Humphrey, C., Noonan, S., De'ath, G., Okazaki, R., *et al.* 2011. Losers and winners in coral reefs acclimatized to elevated carbon dioxide concentrations. Nature Climate Change, 1: 165–169.

Gabay, Y., Benayahu, Y., and Fine, M. 2013. Does elevated pCO_2 affect reef octocorals? Ecology and Evolution, 3: 465–473.

Gabay, Y., Fine, M., Barkay, Z., and Benayahu, Y. 2014. Octocoral tissue provides protection from declining oceanic pH. PLoS One, 9: e91553.

Gardner, T. A., Cote, I. M., Gill, J. A., Grant, A., and Watkinson, A. R. 2003. Long-term region-wide declines in Caribbean corals. Science, 301: 958–960.

Glynn, P. W., and Enochs, I. C. 2011. Invertebrates and their roles in coral reef ecosystems. *In* Coral Reefs: an Ecosystem in Transition, pp. 273–325. Ed. by Z. Dubinsky, and N. Stambler. Springer, New York. 552 pp.

Goh, N. K. C., Ng, P. K. L., and Chou, L. M. 1999. Notes on the shallow water gorgonian-associated fauna on coral reefs in Singapore. Bulletin of Marine Science, 65: 259–282.

Gómez, C. E., Paul, V. J., Ritson-Williams, R., Muehllehner, N., Langdon, C., and Sánchez, J. A. 2014. Responses of the tropical gorgonian coral *Eunicea fusca* to ocean acidification conditions. Coral Reefs, 34: 451–460.

Graham, N. A. J., and Nash, K. L. 2013. The importance of structural complexity in coral reef ecosystems. Coral Reefs, 32: 315–326.

Guzmán, H. M. 2003. Caribbean coral reefs of Panamá: present status and future perspectives. *In* Latin American Coral Reefs, pp. 241–274. Ed. by J. Cortés. Elsevier, Amsterdam. 497 pp.

Harvell, D., Kim, K., Quirolo, C., Weir, J., and Smith, G. 2001. Coral bleaching and disease: contributors to 1998 mass mortality in *Briareum asbestinum* (Octocorallia, Gorgonacea). Hydrobiologia, 460: 97–104.

Hoegh-Guldberg, O., Mumby, P. J., Hooten, A. J., Steneck, R. S., Greenfield, P., Gomez, E., Harvell, C. D., *et al.* 2007. Coral reefs under rapid climate change and ocean acidification. Science, 318: 1737–1742.

IBM. 2013. IBM SPSS Statistics for Windows. Armonk, NY.

Inoue, S., Kayanne, H., Yamamoto, S., and Kurihara, H. 2013. Spatial community shift from hard to soft corals in acidified water. Nature Climate Change, 3: 683–687.

IPCC. 2007. Climate change 2007: the physical science basis. *In* Contribution of Working Group I to the Fourth Assessment Report of the Intergovernmental Panel on Climate Change. Ed. by S. Solomon, D. Qin, M. Manning, Z. Chen, M. Marquis, K. B. Averyt, M. Tignor, *et al.* Cambridge University Press, Cambridge, UK and New York, NY.

Jeng, M. S., Huang, H. D., Dai, C. F., Hsiao, Y. C., and Benayahu, Y. 2011. Sclerite calcification and reef-building in the fleshy octocoral genus *Sinularia* (Octocorallia: Alcyonacea). Coral Reefs, 30: 925–933.

Johnson, V. R., Russell, B. D., Fabricius, K. E., Brownlee, C., and Hall-Spencer, J. M. 2012. Temperate and tropical brown macroalgae thrive, despite decalcification, along natural CO_2 gradients. Global Change Biology, 18: 2792–2803.

Jokiel, P. L. 2016. Predicting the impact of ocean acidification on coral reefs: evaluating the assumptions involved. ICES Journal of Marine Science, 73: 550–557.

Kingsley, R. J., and Watabe, N. 1982. Ultrastructural investigation of spicule formation in the gorgonian *Leptogorgia virgulata* (Lamarck) (Coelenterata: Gorgonacea). Cell and Tissue Research, 223: 325–334.

Kleypas, J. A., Buddemeier, R. W., Archer, D., Gattuso, J. P., Langdon, C., and Opdyke, B. N. 1999. Geochemical consequences of increased atmospheric carbon dioxide on coral reefs. Science, 284: 118–120.

Kroeker, K. J., Kordas, R. L., Crim, R. N., and Singh, G. G. 2010. Meta-analysis reveals negative yet variable effects of ocean acidification on marine organisms. Ecology Letters, 13: 1419–1434.

Kroeker, K. J., Micheli, F., and Gambi, M. C. 2012. Ocean acidification causes ecosystem shifts via altered competitive interactions. Nature Climate Change, 3: 156–159.

Kuffner, I. B., Andersson, A. J., Jokiel, P. L., Rodgers, K. u. S., and Mackenzie, F. T. 2007. Decreased abundance of crustose coralline algae due to ocean acidification. Nature Geoscience, 1: 114–117.

Langdon, C., and Atkinson, M. 2005. Effect of elevated pCO_2on photosynthesis and calcification of corals and interactions with seasonal change in temperature/irradiance and nutrient enrichment. Journal of Geophysical Research, 110: C09S07.

Lasker, H. R. 2003. Zooxanthella densities within a Caribbean octocoral during bleaching and non-bleaching years. Coral Reefs, 22: 23–26.

Lasker, H. R., and Coffroth, M. A. 1983. Octocoral distributions at Carrie Bow Cay, Belize. Marine Ecology Progress Series, 13: 21–28.

Lasker, H. R., Peters, E. C., and Coffroth, M. A. 1984. Bleaching of reef coelenterates in the San-Blas Islands, Panama. Coral Reefs, 3: 183–190.

Lewis, E., and Wallace, D. 1998. Program Developed for CO_2 System Calculations. ORNL/CDIAC, Oak Ridge, TN.

Lewis, J. C., and Von Wallis, E. 1991. The function of surface sclerites in gorgonians (Coelenterata, Octocorallia). The Biological Bulletin, 181: 275–288.

Lewis, J. C., Barnowski, T. F., and Telesnicki, G. J. 1992. Characteristics of carbonates of gorgonian axes (Coelenterata, Octocorallia). The Biological Bulletin, 183: 278–296.

Long, X., Ma, Y., and Qi, L. 2014. Biogenic and synthetic high magnesium calcite—a review. Journal of Structural Biology, 185: 1–14.

Lowenstam, H. A. 1964. Coexisting calcites and aragonites from skeletal carbonates of marine organisms and their strontium and magnesium contents. *In* Recent Researches in the Fields of Hydrosphere, Atmosphere and Nuclear Geochemistry, pp. 373–404. Ed. by Y. Miyake, and T. Koyama. Maruzeu Co., Ltd, Tokyo.

McCulloch, M., Falter, J., Trotter, J., and Montagna, P. 2012. Coral resilience to ocean acidification and global warming through pH up-regulation. Nature Climate Change, 2: 623–627.

Mehrbach, C., Culberson, C. H., Hawley, J. E., and Pytkowicz, R. M. 1973. Measurement of the apparent dissociation constants of carbonic acid in seawater at atmospheric pressure. Limnology and Oceanography, 18: 897–907.

Morales Pinzón, A., Orkisz, M., Rodríguez Useche, C. M., Torres González, J. S., Teillaud, S., Armando Sánchez, J., and Hernández Hoyos, M. 2014. A semi-automatic method to extract canal pathways in 3D micro-CT images of octocorals. PLoS ONE, 9: e85557.

Morse, J. W., and Mackenzie, F. T. 1990. Geochemistry of Sedimentary Carbonates. Elsevier, New York. 707 pp.

Plummer, L. N., and Mackenzie, F. T. 1974. Predicting mineral solubility from rate data: application to the dissolution of magnesian calcites. American Journal of Science, 274: 61–83.

Prada, C., Schizas, N. V., and Yoshioka, P. M. 2008. Phenotypic plasticity or speciation? A case from a clonal marine organism. BMC Evolutionary Biology, 8: 47.

Prada, C., Weil, E., and Yoshioka, P. M. 2009. Octocoral bleaching during unusual thermal stress. Coral Reefs, 29: 41–45.

Rahman, M. A., and Oomori, T. 2008. Structure, crystallization and mineral composition of sclerites in the alcyonarian coral. Journal of Crystal Growth, 310: 3528–3534.

Rahman, M. A., Oomori, T., and Uehara, T. 2007. Carbonic anhydrase in calcified endoskeleton: novel activity in biocalficiation in alcyonarian. Marine Biotechnology, 10: 31–38.

Reaka-Kudla, M. L. 1997. The global biodiversity of coral reefs: a comparison with rain forests. *In* Biodiversity II, pp. 83–108. Ed. by M. W.

Reaka-Kudla, D. E. Wilson, and E. O. Wilson. Joseph Henry Press, Washington, DC.

Rhein, M., Rintoul, S. R., Aoki, S., Campos, E., Chambers, D., Feely, R. A., Gulev, S., *et al.* 2013. Observation: Ocean. *In* Climate Change 2013: the Physical Science Basis. Contribution of Working Group I to the Fifth Assessment Report of the Intergovernmental Panel on Climate Change. Ed. by T. F. Stocker, D. Qin, G-K. Plattner, M. Tignor, S. K. Allen, J. Boschung, A. Nauels, *et al.* Cambridge University Press, Cambridge, UK and New York, NY.

Ries, J. B. 2006. Mg fractionation in crustose coralline algae: geochemical, biological, and sedimentological implications of secular variation in the Mg/Ca ratio of seawater. Geochimica et Cosmochimica Acta, 70: 891–900.

Rodolfo-Metalpa, R., Houlbrèque, F., Tambutté, É., Boisson, F., Baggini, C., Patti, F. P., Jeffree, R., *et al.* 2011. Coral and mollusc resistance to ocean acidification adversely affected by warming. Nature Climate Change, 1: 308–312.

Ruzicka, R. R., Colella, M. A., Porter, J. W., Morrison, J. M., Kidney, J. A., Brinkhuis, V., Lunz, K. S., *et al.* 2013. Temporal changes in benthic assemblages on Florida Keys reefs 11 years after the 1997/1998 El Niño. Marine Ecology Progress Series, 489: 125–141.

Shirur, K. P., Ramsby, B. D., Iglesias-Prieto, R. I., and Goulet, T. L. 2014. Biochemical composition of Caribbean gorgonians: implications for gorgonian—*Symbiodinium* symbiosis and ecology. Journal of Experimental Marine Biology and Ecology, 461: 275–285.

Takahashi, A., and Kurihara, H. 2012. Ocean acidification does not affect the physiology of the tropical coral *Acropora digitifera* during a 5-week experiment. Coral Reefs, 32: 305–314.

Velimirov, B., and Böhm, E. L. 1976. Calcium and magnesium carbonate concentrations in different growth regions of gorgonians. Marine Biology, 35: 269–275.

Weinbauer, M. G., and Velimirov, B. 1995. Calcium, magnesium and strontium concentrations in the calcite sclerites of Mediterranean gorgonians (Coelenterata: Octocorallia). Estuarine, Coastal and Shelf Science, 40: 87–104.

Yoshioka, P. M., and Yoshioka, B. B. 1989. Multispecies, multiscale analysis of spatial pattern and its application to a shallow-water gorgonian community. Marine Ecology Progress Series, 54: 257–264.

Yoshioka, P. M., and Yoshioka, B. B. 1991. A comparison of the survivorship and growth of shallow-water gorgonian species of Puerto Rico. Marine Ecology Progress Series, 69: 253–260.

Handling editor: Joanna Norkko

ICES Journal of Marine Science

ICES Journal of Marine Science (2016), 73(3), 920–926. doi:10.1093/icesjms/fsv031

Contribution to Special Issue: 'Towards a Broader Perspective on Ocean Acidification Research'

Original Article

No ocean acidification effects on shell growth and repair in the New Zealand brachiopod *Calloria inconspicua* (Sowerby, 1846)

Emma L. Cross[1,2]*, Lloyd S. Peck[1], Miles D. Lamare[3], and Elizabeth M. Harper[2]

[1]*British Antarctic Survey, Natural Environment Research Council, High Cross, Madingley Road, Cambridge CB3 0ET, UK*
[2]*Department of Earth Sciences, University of Cambridge, Downing Street, Cambridge CB2 3EQ, UK*
[3]*Department of Marine Science, University of Otago, 310 Castle Street, Dunedin 9016, New Zealand*

**Corresponding author: tel: +44 1223333493; e-mail: emmoss@bas.ac.uk*

Cross, E. L., Peck, L. S., Lamare, M. D., and Harper, E. M. No ocean acidification effects on shell growth and repair in the New Zealand brachiopod *Calloria inconspicua* (Sowerby, 1846). – ICES Journal of Marine Science, 73: 920–926.

Received 24 October 2014; revised 23 January 2015; accepted 7 February 2015; advance access publication 4 March 2015.

Surface seawaters are becoming more acidic due to the absorption of rising anthropogenic CO_2. Marine calcifiers are considered to be the most vulnerable organisms to ocean acidification due to the reduction in the availability of carbonate ions for shell or skeletal production. Rhychonelliform brachiopods are potentially one of the most calcium carbonate-dependent groups of marine organisms because of their large skeletal content. Little is known, however, about the effects of lowered pH on these taxa. A CO_2 perturbation experiment was performed on the New Zealand terebratulide brachiopod *Calloria inconspicua* to investigate the effects of pH conditions predicted for 2050 and 2100 on the growth rate and ability to repair shell. Three treatments were used: an ambient pH control (pH 8.16), a mid-century scenario (pH 7.79), and an end-century scenario (pH 7.62). The ability to repair shell was not affected by acidified conditions with >80% of all damaged individuals at the start of the experiment completing shell repair after 12 weeks. Growth rates in undamaged individuals >3 mm in length were also not affected by lowered pH conditions, whereas undamaged individuals <3 mm grew faster at pH 7.62 than the control. The capability of *C. inconspicua* to continue shell production and repair under acidified conditions suggests that this species has a robust control over the calcification process, where suitable conditions at the site of calcification can be generated across a range of pH conditions.

Keywords: calcification, carbonate saturation, climate change, CO_2, pH.

Introduction

Rising levels of anthropogenic CO_2 are affecting the carbonate chemistry of surface seawaters and causing our oceans to acidify (Caldeira and Wickett, 2003, 2005; Orr *et al.*, 2005; Gattuso and Hansson, 2011; IPCC, 2013). Excess atmospheric CO_2 since the industrial revolution has already caused a 0.1 pH unit decline and the rate of this change is predicted to increase considerably with a further decrease of 0.3–0.5 pH units by 2100 (Caldeira and Wickett, 2005; Orr *et al.*, 2005). Marine calcifying organisms such as corals, coccolithophores, molluscs, and brachiopods are considered to be the most susceptible to ocean acidification due to the predicted reduction in the availability of carbonate ions that is required for shell or skeletal production (Doney *et al.*, 2009; Byrne, 2011; Watson *et al.*, 2012; Byrne and Przeslawski, 2013; Kroeker *et al.*, 2013). Consequently, shell production and maintenance will likely become more difficult and more energetically expensive. Studies have shown variable responses of calcifying organisms to future predicted pH conditions with an increasing number of studies demonstrating tolerant species (Havenhand and Schlegel, 2009; Ries *et al.*, 2009; Parker *et al.*, 2012; Suckling *et al.*, 2014; Cross *et al.*, 2015).

Rhychonelliform brachiopods inhabit all the world's oceans from the intertidal to hadal depths (James *et al.*, 1992; Peck, 2001a). They are important organisms in shallow water communities as they provide a habitat for a broad range of epifauna, including other brachiopods, sponges, bryozoans, and algae, and may act as a significant carbon sink (Barnes and Peck, 1996; Rodland *et al.*, 2004). They have also been characterised as one of the most

calcium carbonate-dependent groups of marine organisms due to the very large proportion of their dry mass (>90%) accounted for by their calcareous skeleton and support structures (Peck, 1993, 2008). Most brachiopod research has focused on extinct taxa as they are one of the few phyla to be represented as fossils extensively throughout the last 500 million years (Richardson, 1986; James *et al.*, 1992; Pennington and Stricker, 2001). Despite a relatively recent increase in the literature on the distribution, ecology, and biology of extant brachiopods (Peck *et al.*, 1997, 2005; Peck, 2005; Harper *et al.*, 2009; Lee *et al.*, 2010; Peck and Harper, 2010), only two studies have investigated ocean acidification impacts (McClintock *et al.*, 2009; Cross *et al.*, 2015), both of which used the Antarctic brachiopod, *Liothyrella uva*, as their study species. McClintock *et al.* (2009) found significant shell dissolution after only 14 d in pH 7.4 conditions. Only empty valves, however, were used; so, the ability of *L. uva* to compensate any acidification impacts on their shells was not investigated. Cross *et al.* (2015) extended this research further by investigating future pH conditions on shell growth and repair in living *L. uva* and found no impact on calcification. The target taxon in the current research is the New Zealand brachiopod *Calloria inconspicua* (Sowerby, 1846), which is in the same order (Terebratulida) as *L. uva*, therefore providing a temperate comparison to the Antarctic species studied by Cross *et al.* (2015).

Calloria inconspicua is a small (maximum length reported is 28 mm; Stewart, 1981), epifaunal, sessile, suspension-feeding terebratellid brachiopod endemic to New Zealand (Doherty, 1979). It has a widespread distribution throughout New Zealand and is highly abundant in the intertidal and shallow subtidal regions, with reported densities of over 1000 ind. m^{-2} (Doherty, 1979). This species also has a broad temperature tolerance of 8–18°C (Lee, 1991). *Calloria inconspicua* is usually found individually or in conspecific clumps attached to hard substrata such as rock, other brachiopods, bivalves, bryozoans, gastropods, and corals (Lee, 1991). An early study reported slow growth in this species which is unevenly distributed throughout life; fastest during the first 4 years (up to 10 mm in length) and decreases after reproduction commences (Rickwood, 1977).

Growth is an indicator of an animal's well being in a particular environment as it represents the collective responses of physiological, cellular, and biochemical processes within the organism (Riisgård and Randløv, 1981). Another essential process to the existence of the vast majority of marine, shelled organisms is shell repair. Brachiopods become damaged in their natural environment due to impacts from a variety of causes including impacts from saltating clasts and predator attack (Harper *et al.*, 2009). Such damage requires quick shell repair to prevent the loss of body fluids, protect against predators, and prevent encounters with harmful substances (Harper *et al.*, 2012). Shell repair frequencies in *C. inconspicua* are variable between different localities with a maximum recorded frequency of 0.355 (number of damaged individuals/total number of individuals; E. M. Harper and L. S. Peck, unpublished data). Given the importance of maintaining shell production and repair, in addition to the limited research on ocean acidification effects on brachiopods, the aims of this study were to establish how shell growth and the ability to repair shell in *C. inconspicua* were affected by forecasted future pH conditions and to compare results for this temperate species with those for the Antarctic *L. uva* (Cross *et al.*, 2015). Growth rates and the frequency of shell repair following damage were measured in control conditions and predicted mid- and end-century pH levels.

Material and methods

Sample collection

Specimens of *C. inconspicua* were hand collected at low tide from under rocks in Portobello Bay, Otago Harbour, New Zealand (45° 82.000′S, 170° 70.00′E) in January 2013. Samples remained in their conspecific clumps and, to minimise disturbance, were only collected if they were attached to removable substratum to ensure that no pedicles were cut. Environmental conditions in Otago Harbour are surface seawater temperatures of 6.4–16.0°C (Roper and Jillett, 1981; Greig *et al.*, 1988), pH range of 8.10–8.21 (K. Currie, pers. comm.), and salinity is 32.5–34.8 (Roper and Jillett, 1981). Brachiopods were kept in seawater during the short transportation from the sampling site to Portobello Marine Laboratory, Otago Peninsula. Specimens were then immediately placed in the experimental system.

Experimental design

This study was conducted in a flow-through CO_2 perturbation system where seawater pumped from the harbour passed through sand filters (50 μm) and a finer cartridge filter (5–10 μm) before entering the system. Three treatments were used; a control at the average local current pH_{NIST} (8.1), the predicted oceanic pH by 2050 (pH 7.8), and the predicted pH by 2100 (pH 7.6) according to the IPCC "business-as-usual" scenario of the forecasted reduction of 0.3–0.5 pH units (IPCC, 2013) with three replicate 10 l tanks for each treatment. The pH of the acidified treatments was lowered in header tanks by intermittently bubbling CO_2 gas through a ceramic diffuser to maintain the pH at predetermined pH levels via a solenoid valve connected to a TUNZE 7070/2pH-controlled computer and electrode system. The experimental pH control system had an identical set up except that it lacked CO_2 injection. A circulating pump in each mixing header tank ensured a constant pH. This set up was shown to provide stable pH conditions over >200 d (Cunningham *et al.*, 2015). Seawater was gravity fed from each header tank at a rate of 1.05 ± 0.05 l min^{-1} into the experimental tanks.

Seawater temperature was not manipulated and was ambient for Otago Harbour. It was measured up to three times a day (°C, Digital Testo 106) with only small differences (<0.5°C) between treatments (Table 1) and no variation between replicate tanks in each treatment. Flow rate was also checked three times per day as was the computer-controlled pH. pH_{NIST} was measured in each treatment tank accurately twice weekly with a EUTECH instruments pH 5–10 pH/mV/°C meter and calibrated with pH buffers of pH 4.0, 7.0,

Table 1. Mean (± s.d.) seawater parameters in all three treatments during the 12-week experiment which follow the format recommended by Barry *et al.* (2010).

Seawater parameter	pH control	pH 7.8	pH 7.6
pH_{NIST}	8.16 ± 0.03	7.79 ± 0.06	7.62 ± 0.05
DIC (μmol kg^{-1})	2082.8 ± 22.0	2211.4 ± 8.3	2252.4 ± 25.3
Alkalinity (μmol kg^{-1})	2278.5 ± 18.8	2269.7 ± 9.2	2271.9 ± 6.5
pCO_2 (μatm)	464.8 ± 82.8	1130.2 ± 11.8	1535.6 ± 234.8
Ω calcite	3.5 ± 0.5	1.6 ± 0.0	1.3 ± 0.2
Ω aragonite	2.2 ± 0.3	1.0 ± 0.0	0.8 ± 0.1
Temperature (°C)	16.5 ± 1.7	16.9 ± 1.7	16.6 ± 1.7
Salinity	33.9 ± 0.2	33.9 ± 0.2	33.9 ± 0.2

Values for pCO_2, Ω calcite, and Ω aragonite were calculated using CO_2calc (Robbins *et al.*, 2010) with refitted constants (Mehrbach *et al.*, 1973; Dickson and Millero, 1987) as recommended by Wanninkhof *et al.* (1999).

and 9.2 (Pro-analys, Biolab, New Zealand). Salinity was measured once a week using a YSI data logger. A water sample from each treatment was fixed with saturated mercuric chloride ($HgCl_2$) at the beginning, middle, and end of the experiment. Dissolved inorganic carbon and total alkalinity were later determined by a Single Operator Multi-parameter Metabolic Analyser (SOMMA) and closed-cell potentiometric titration, respectively (Dickson *et al.*, 2007). Other carbonate system parameters, including the partial pressure of CO_2 (pCO_2) and the saturation values for calcite (Ω_C) and aragonite (Ω_A), were calculated using CO_2calc (Robbins *et al.*, 2010). Seawater properties were determined using CO_2 equilibrium constants from Mehrbach *et al.* (1973) refitted by Dickson and Millero (1987) as recommended by Wanninkhof *et al.* (1999).

Brachiopods were fed three times a week with microalgal concentrate of $\sim 397 \times 10^4$ cells mL^{-1} of *Tetraselmis* spp., which is within the natural range of phytoplankton cell abundance in Otago Harbour. Faeces and other debris were removed twice weekly by siphon.

Growth rates

One hundred and twenty-three specimens of *C. inconspicua* between 0.71 and 14.47 mm length (maximum shell dimension) were used in this experiment. At the start of the experiment, shell lengths of each individual >3 mm in length were measured to the nearest 0.01 mm using Vernier calipers. For individuals <3 mm, shell lengths were measured on a graticule eyepiece in a field microscope. The conspecific clumps of specimens were then divided evenly across all tanks ensuring a similar size range of specimens in each treatment. After 6 weeks and at the end of the 12-week experiment, the length of each individual was measured again and the shell edge photographed. Growth rates were calculated from the increase in length (presented as $\mu m\ d^{-1}$).

Shell repair frequencies

The largest (>14 mm in length) 10 or 11 individuals in each treatment were damaged by creating a 1–2 mm deep notch at the valve edge using a metal file. This style of injury replicated very similar damage seen in natural populations of rhychonelliform brachiopods and interpreted as indicative of either predator attacks or abiotic stresses (Harper *et al.*, 2009). Notches of similar size and extent were made and care was taken not to break shells or cause other damage. After 6 and 12 weeks, the damaged section of each shell edge was photographed.

Statistical analyses

All data were analysed using Minitab (Statistical Software™ Version 15). Growth rate data for each treatment were all significantly different from normal (Anderson–Darling test; $p < 0.009$). These data were still not normally distributed after square root, logarithmic, and double logarithmic transformations because of the presence of zeros in the dataset. Non-parametric Kruskal–Wallis tests were thus used to determine whether treatment affected growth. When significant differences were found in the different datasets, further Kruskal–Wallis multiple comparison tests were used to identify which treatments were different from each other. A χ^2 test was used to establish any treatment effect on the percentage of undamaged individuals that did not grow throughout the experiment. χ^2 tests were also used to determine if treatment affected the percentage of damaged individuals that had completed shell repair at the different time periods.

Results

All seawater parameters in the control were within the ranges reported for shallow surface seawater (Table 1; Barry *et al.*, 2010), although seawater temperature was unusually high for Otago Harbour in January–April 2013 (MDL, pers. obs.) and slightly above the reported range of 6.4–16.0°C (Roper and Jillett, 1981; Greig *et al.*, 1988). Saturation states with respect to calcite and aragonite in both acidified treatments were just below the reported shallow surface seawater values ($\Omega < 1.9$ and <1.2, respectively); however, calcite was supersaturated ($\Omega > 1$) in both treatments and aragonite was supersaturated in pH 7.8 but undersaturated ($\Omega < 1$) in the pH 7.6 treatment. No mortality occurred throughout the 12-week experiment in any treatment. In addition, throughout the experiment, no individual demonstrated any signs of stress such as slow snapping responses, remaining closed for extended periods or wide gaping when open, and all specimens responded rapidly to physical stimulation when disturbed (Peck, 2001b; Cross *et al.*, 2015).

Shell repair frequencies

After 6 weeks, all damaged individuals had started to repair their notch and >36% of specimens had completed shell repair across all treatments (Table 2). Treatment had no effect on shell repair frequencies ($\chi^2 = 1.714$, $p = 0.424$). After 12 weeks, >80% of individuals had fully repaired their notch in every treatment (Table 2; Figure 1) with only three individuals (one specimen in pH 7.8 and two specimens in the pH 7.6 treatments) not completing shell repair. Treatment did not affect overall shell repair frequencies ($\chi^2 = 1.173$, $p = 0.556$). Although the majority of the damaged individuals managed to fully repair their shell, none of the large, notched individuals continued to produce new shell once the repair was complete.

Growth rates

The majority of individuals grew with growth rates ranging to values over 15 $\mu m\ d^{-1}$ in the pH control and the pH 7.6 treatment and up to 10.70 $\mu m\ d^{-1}$ in the pH 7.8 treatment (Figure 2). The only apparent ontogenetic trend was a slight decrease in growth rates for individuals >10 mm in length. Growth rates of undamaged individuals >3 mm in both acidified conditions were not significantly different from that of the pH control (Kruskal–Wallis, $H = 4.04$, $p = 0.133$).

Table 2. Shell repair frequencies after 6 weeks and after 12 weeks in the stated conditions.

Treatment	Number of individuals damaged at the start of the experiment	Length range of damaged individuals (mm)	Percentage of individuals that had completed repair	
			After 6 weeks	After 12 weeks
pH control	11	14.18–17.79 (mean = 15.59)	36% ($n = 4$)	100% ($n = 11$)
pH 7.8	10	14.14–17.62 (mean = 15.80)	40% ($n = 4$)	90% ($n = 9$)
pH 7.6	10	14.05–17.52 (mean = 15.31)	50% ($n = 5$)	80% ($n = 8$)

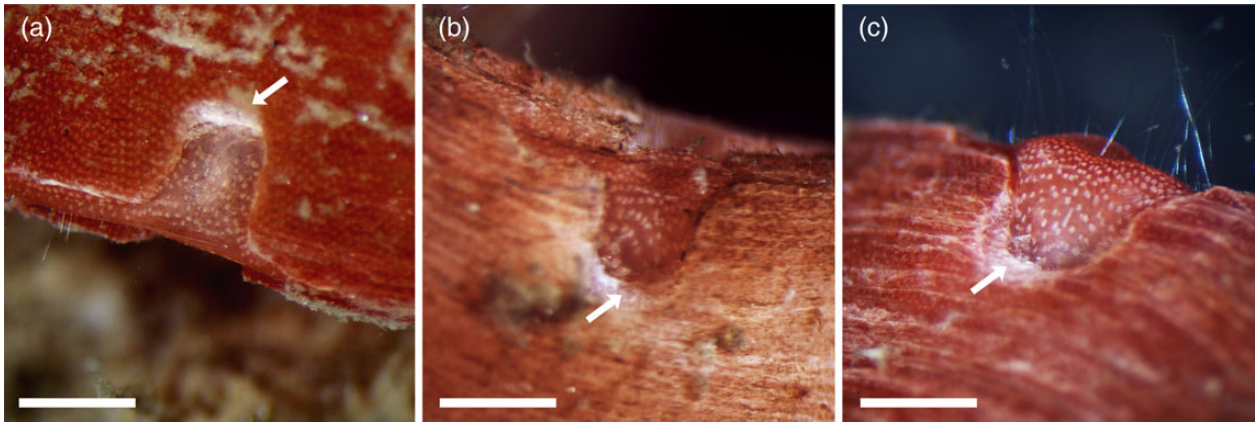

Figure 1. Examples of completed shell repair in damaged individuals after 12 weeks in the (a) pH control, (b) pH 7.8, and (c) pH 7.6 treatment. The arrow indicates the notch created at the start of the experiment. Scale bar = 100 μm.

Whereas growth rates were different among treatments in undamaged individuals <3 mm ($H = 6.23$, $p = 0.044$) and also when all undamaged individuals across the total size range were pooled ($H = 7.90$, $p = 0.019$). A further Kruskal–Wallis multiple comparison test on undamaged individuals <3 mm indicated that growth rates were higher in the most acidified treatment (pH 7.6; $Z = 2.488$, $p = 0.013$) compared with the moderately acidified treatment (pH 7.8) but not compared with the pH control ($Z = 0.826$, $p = 0.409$). Growth rates of undamaged individuals <3 mm in the moderately acidified treatment were not significantly different from the pH control ($Z = 0.746$, $p = 0.456$). A further Kruskal–Wallis Multiple Comparison test on all undamaged individuals indicated that in the most acidified treatment, growth rates were higher than in the pH control ($Z = 2.762$, $p = 0.006$) but not compared with the moderately acidified treatment ($Z = 1.918$, $p = 0.055$). Growth rates of all undamaged individuals in the moderately acidified treatment were also not significantly different from the pH control ($Z = 0.980$, $p = 0.327$). There was also no treatment effect on the proportion of undamaged individuals that did not grow throughout the experiment ($\chi^2 = 1.500$, $p = 0.472$).

Discussion

There were no signs of stress and no mortalities throughout the 12-week experiment, indicating that *C. inconspicua* are able to tolerate predicted mid- and end-century pH conditions. Similarly, mortality rates in other equivalent ocean acidification studies with brachiopods (*L. uva*; Cross *et al.*, 2015) and molluscs (*Arctica islandica*; Hiebenthal *et al.*, 2012) were low (3.9 and 3.3%, respectively). *Calloria inconspicua* will also be able to repair shell damage in the natural environment in the next 100 years as suggested by the ability of damaged individuals to continue shell repair under acidified conditions with >80% of injured specimens in all treatments completing shell repair after 12 weeks. Shell repair in the gastropod *Subninella undulata* was also unaffected by ocean acidification; however, the gastropod *Austrocochlea porcata* had a decreased shell repair rate, suggesting a species-specific response of marine shelled organisms in the ability to repair shell (Coleman *et al.*, 2014). Although the majority of the damaged individuals managed to repair their shell fully, none of them continued to produce new shell once the repair was complete. All damaged individuals of *C. inconspicua* in this study were, however, the largest in their treatment, all being above 14 mm. This size coincides with the reported 14–16 mm size of sexual maturity in *C. inconspicua* (Doherty, 1976; Lee and Wilson, 1979) indicating that growth rates were already low in these individuals due to a transfer of energy and resources from somatic growth to reproduction. Therefore, once the critical process of repair was complete, these individuals were much less likely to grow than the smaller juveniles. It remains unknown how smaller individuals will respond to the additional stress of shell repair in future oceans. Furthermore, shell production in *C. inconspicua* should be unaffected by changing pH levels in the natural environment up to the year 2100, as growth rates in undamaged individuals were either not affected (>3 mm in length) or positively affected (<3 mm in length) by acidified conditions. Shell growth studies in lowered pH conditions on molluscs have shown varied responses (Michaelidis *et al.*, 2005; Berge *et al.*, 2006; Nienhuis *et al.*, 2010; Thomsen *et al.*, 2010; Hiebenthal *et al.*, 2012), which could be due to the short- to medium-term duration (44 d) of some studies or the individual tolerance of different species (Ries *et al.*, 2009). The ability of *C. inconspicua* to continue shell production in low pH conditions suggests that this species has a strong control over their calcification process, similar to molluscs, by being able to generate suitable conditions at the site of calcification against a stronger concentration gradient (Ries, 2011; Gazeau *et al.*, 2013; Wittmann and Pörtner, 2013). Apart from the capability of marine calcifiers to elevate pH in calcifying compartments to facilitate precipitation of calcium carbonate, the mechanisms are poorly known, particularly in less-studied brachiopods.

This resilience to predicted future pH levels is also apparent in the Antarctic brachiopod, *L. uva* (Cross *et al.*, 2015). Similar large proportions (>90%) of identically damaged *L. uva* fully repaired their notch in the only other ocean acidification study to involve brachiopods (Cross *et al.*, 2015). The Antarctic study was conducted over 7 months, whereas the current work was a 12-week experiment, suggesting repair mechanisms may be faster in temperate brachiopods than Antarctic species as has been reported for growth (Peck *et al.*, 1997; Baird *et al.*, 2013). The high success rates of shell repair in lowered pH conditions in both a temperate and polar brachiopod suggest these species can maintain the rate of shell repair and regeneration in challenging chemical environments just as had previously been seen in the ophiuroid *Amphiura filiformis* (Wood *et al.*, 2008). Over 63% of all injured specimens in *L. uva* made new shell after repairing their notch (Cross *et al.*, 2015) further demonstrating the tolerance of this species. A wide size

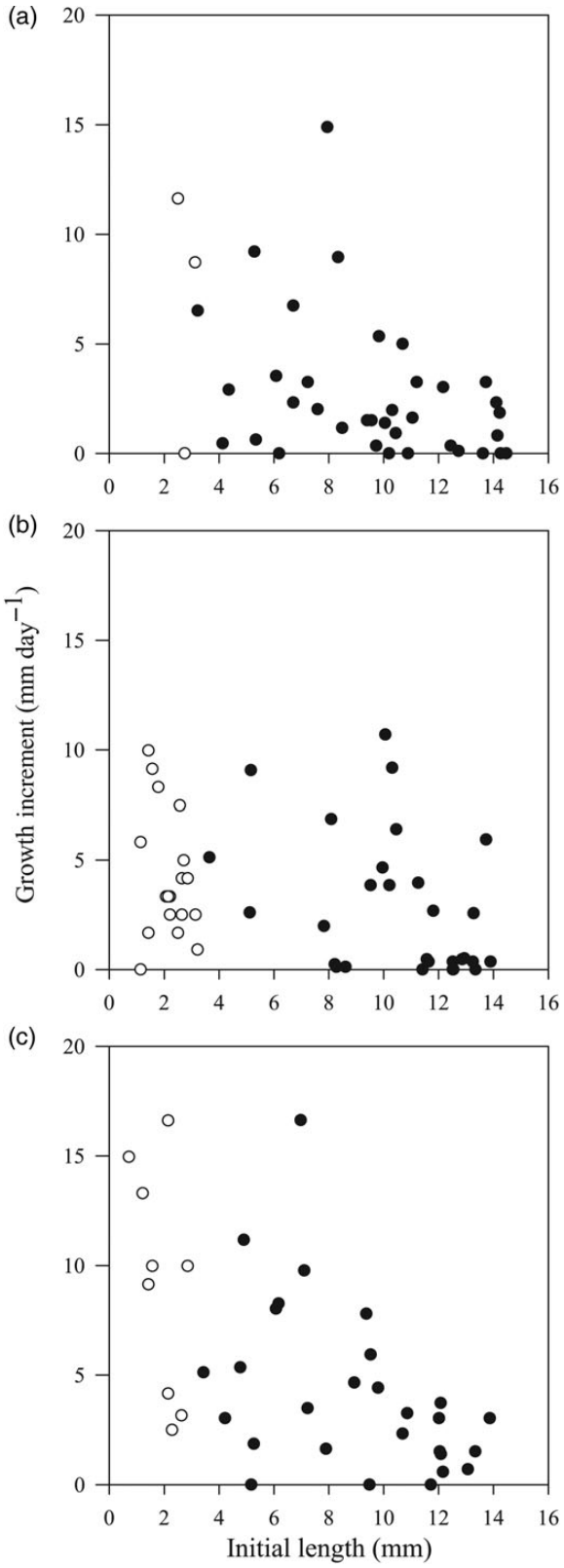

Figure 2. Growth rates of individuals <3 mm (open circle) and >3 mm (filled circle) that were left undamaged at the start of the experiment after 12 weeks in (a) the pH control (pH 8.16 ± 0.03), (b) pH 7.8 (pH 7.79 ± 0.06), and (c) pH 7.6 (pH 7.62 ± 0.05) treatments. Different symbols have been used for individuals above and below 3 mm for the two different methods used.

range (5.0–37.0 mm in length) of individuals had been damaged at the start of the Antarctic experiment, though compared with the limited size range used in the current experiment, specimens of all ages were included and therefore more were likely to continue shell deposition after repair. As here, shell growth rates of undamaged individuals of *L. uva* were not affected by acidified conditions. A 2°C increase in temperature, however, positively affected shell growth in *L. uva*.

Multiple stressors are becoming more widely used in ocean acidification studies where parameters such as temperature, food availability, and hypoxia have been shown to have a greater effect on marine organisms than lowered pH (Hiebenthal *et al.*, 2012; Thomsen *et al.*, 2013; Wolfe *et al.*, 2013; Hardy and Byrne, 2014; Hyun *et al.*, 2014; Noisette *et al.*, 2014; Cross *et al.*, 2015; Queiros *et al.*, 2015), although some studies demonstrate an interactive effect (Ericson *et al.*, 2012; Reymond *et al.*, 2013; Gobler *et al.*, 2014; Ko *et al.*, 2014). Research on the mollusc *Mytilus edulis* revealed that acidified conditions did not affect growth rate but rising temperature increased growth up to 20°C, which then sharply declined at 25°C, indicating that 25°C is above this species temperature tolerance limit (Pörtner, 2008; Hiebenthal *et al.*, 2012). Another study on the same species found that an abundant food supply outweighed the effects of ocean acidification on growth and calcification (Thomsen *et al.*, 2013). Oxygen availability, along with temperature but not pCO_2, were also found to be the dominating factors determining metabolic rate reductions in the squid *Dosidicus gigas* (Rosa and Seibel, 2008).

Overall, studies showing tolerance of marine species to ocean acidification are increasing, especially with the wider use of longer term experiments (Hazan *et al.*, 2014; Suckling *et al.*, 2014; Cross *et al.*, 2015; Queiros *et al.*, 2015). After 3 months, it was apparent that *C. inconspicua* is resilient to lowered pH in terms of shell growth and repair, highlighting the need for longer term ocean acidification studies to allow for acclimation and adaptation to better understand different species capabilities to respond to changing pH conditions. However, perhaps other biological processes could have been impacted by increasing acidity as seen in the ophiuroid *A. filiformis* where muscle wastage was reported in lowered pH treatments (Wood *et al.*, 2008). Further investigation is needed to determine such effects in *C. inconspicua.* Therefore, more environmentally relevant research, including several variables over long-term durations, is crucial to fully understand and predict how organisms will respond to near future changing environmental conditions.

Acknowledgements

The authors would like to thank the science support staff at the Portobello Marine Laboratory, University of Otago, for their help in the set up and maintenance of the ocean acidification experimental system. Thanks also to Kim Currie at National Institute of Water and Atmospheric Research for the DIC and total alkalinity measurements. ELC is supported by the NERC PhD Studentship (NE/T/A/2011).

References

Baird, M. J., Lee, D. E., and Lamare, M. D. 2013. Reproduction and growth of the terebratulid brachiopod *Liothyrella neozelanica* Thomson, 1918 from Doubtful Sound, New Zealand. The Biological Bulletin, 225: 125–136.

Barnes, D. K. A., and Peck, L. S. 1996. Epibiota and attachment substrata of deep-water brachiopods from Antarctica and New Zealand.

Philosophical Transactions of the Royal Society of London Series B: Biological Sciences, 351: 677–687.

Barry, J. P., Tyrell, T., Hansson, L., Plattner, G. K., and Gattuso, J. P. 2010. Atmospheric CO_2 targets for ocean acidification perturbation experiments. *In* Guide to Best Practices for Ocean Acidification Research and Data Reporting, pp. 53–66. Ed. by U. Riebesell, V. F. Fabry, L. Hansson, and J. P. Gattuso. Publications Office of the European Union.

Berge, J. A., Bjerkeng, B., Pettersen, O., Schaanning, M. T., and Oxnevad, S. 2006. Effects of increased sea water concentrations of CO_2 on growth of the bivalve *Mytilus edulis* L. Chemosphere, 62: 681–687.

Byrne, M. 2011. Impact of ocean warming and ocean acidification on marine invertebrate life history stages: vulnerabilities and potential for persistence in a changing ocean. Oceanography and Marine Biology: An Annual Review, 49: 1–42.

Byrne, M., and Przeslawski, R. 2013. Multistressor impacts of warming and acidification of the ocean on marine invertebrates' life histories. Integrative and Comparitive Biology, 53: 582–596.

Caldeira, K., and Wickett, M. E. 2003. Anthropogenic carbon and ocean pH. Nature, 425: 365.

Caldeira, K., and Wickett, M. E. 2005. Ocean model predictions of chemistry changes from carbon dioxide emissions to the atmosphere and ocean. Journal of Geophysical Research, 110: C09S04.

Coleman, D. W., Byrne, M., and Davis, A. R. 2014. Molluscs on acid: gastropod shell repair and strength in acidifying oceans. Marine Ecology Progress Series, 509: 203–211.

Cross, E. L., Peck, L. S., and Harper, E. M. 2015. Ocean acidification does not impact shell growth or repair of the Antarctic brachiopod *Liothyrella uva* (Broderip, 1833). Journal of Experimental Marine Biology and Ecology, 462: 29–35.

Cunningham, S. C., Smith, A. M., and Lamare, M. D. 2015. The effects of elevated pCO_2 on growth, shell production and metabolism of cultured juvenile abalone, *Haliotis iris*. Aquaculture Research, doi:10.1111/are.12684.

Dickson, A. G., and Millero, F. J. 1987. A comparison of the equilibrium-constants for the dissociation of carbonic-acid in seawater media. Deep Sea Research A: Oceanographic Research Papers, 34: 1733–1743.

Dickson, A. G., Sabine, C. L., and Christian, J. R. 2007. Guide to Best Practices for Ocean CO_2 Measurements. IOCCP Report No. 8.

Doherty, P. J. 1976. Aspects of the feeding ecology of the sub-tidal brachiopod *Terebratella inconspicua* (Sowerby, 1846). Unpublished PhD thesis, Zoology Department, University of Auckland.

Doherty, P. J. 1979. A demographic study of a subtidal population of the New Zealand articulate brachiopod *Terebratella inconspicua*. Marine Biology, 52: 331–342.

Doney, S. C., Fabry, V. J., Feely, R. A., and Kleypas, J. A. 2009. Ocean acidification: the other CO_2 problem. Annual Review of Marine Science, 1: 169–192.

Ericson, J. A., Ho, M. A., Miskelly, A., King, C. K., Virtue, P., Tilbrook, B., and Byrne, M. 2012. Combined effects of two ocean change stressors, warming and acidification, on fertilization and early development of the Antarctic echinoid *Sterechinus neumayeri*. Polar Biology, 35: 1027–1034.

Gattuso, J. P., and Hansson, L. 2011. Ocean Acidification. Oxford University Press, Oxford.

Gazeau, F., Parker, L. M., Comeau, S., Gattuso, J-P., O'Connor, W. A., Martin, S., Pörtner, H-O., *et al.* 2013. Impacts of ocean acidification on marine shelled molluscs. Marine Biology, 160: 2207–2245.

Gobler, C., DePasquale, E. L., Griffith, A. W., and Baumann, H. 2014. Hypoxia and acidification have additive and synergistic negative effects on the growth, survival, and metamorphosis of early life stage bivalves. PLoS ONE, 9: e83648.

Greig, M. J., Ridgway, N. M., and Shakespeare, B. S. 1988. Sea surface temperature variations at coastal sites around New Zealand. New Zealand Journal of Marine and Freshwater Research, 22: 391–400.

Hardy, N. A., and Byrne, M. 2014. Early development of congeneric sea urchins (*Heliocidaris*) with contrasting life history modes in a warming and high CO_2 ocean. Marine Environmental Research, 102: 78–87.

Harper, E. M., Clark, M. S., Hoffman, J. I., Philipp, E. E., Peck, L. S., and Morley, S. A. 2012. Iceberg scour and shell damage in the Antarctic bivalve *Laternula elliptica*. PLoS ONE, 7: e46341.

Harper, E. M., Peck, L. S., and Hendry, K. R. 2009. Patterns of shell repair in articulate brachiopods indicate size constitutes a refuge from predation. Marine Biology, 156: 1993–2000.

Havenhand, J. N., and Schlegel, P. 2009. Near-future levels of ocean acidification do not affect sperm motility and fertilisation kinetics in the oyster *Crassostrea gigas*. Biogeosciences, 6: 3009–3015.

Hazan, Y., Wangensteen, O. S., and Fine, M. 2014. Tough as a rock-boring urchin: adult *Echinometra* sp. EE from the Red Sea show high resistance to ocean acidification over long-term exposures. Marine Biology, 161: 2531–2545.

Hiebenthal, C., Philipp, E. E. R., Eisenhauer, A., and Wahl, M. 2012. Effects of seawater pCO_2 and temperature on shell growth, shell stability, condition and cellular stress of Western Baltic Sea *Mytilus edulis* (L.) and *Arctica islandica* (L.). Marine Biology, 160: 2073–2087.

Hyun, B., Choi, K-H., Jang, P-G., Jang, M-C., Lee, W-J., Moon, C-H., and Shin, K. 2014. Effects of increased CO_2 and temperature on the growth of four diatom species (*Chaetoceros debilis*, *Chaetoceros didymus*, *Skeletonema costatum* and *Thalassiosira nordenskioeldii*) in laboratory experiments. Journal of Environmental Science International, 23: 1003–1012.

IPCC. 2013. Climate change 2013: the physical science basis. *In* Working Group I Contribution to the Fifth Assessment Report of the Intergovernmental Panel on Climate Change, p. 1552. Ed. by T. F. Stocker, D. Qin, G-K. Plattner, M. Tignor, S. K. Allen, J. Boschung, A. Nauels, *et al.* Cambridge, UK and New York, NY, USA.

James, M. A., Ansell, A. D., Collins, M. J., Curry, G. B., Peck, L. S., and Rhodes, M. C. 1992. Biology of living brachiopods. Advances in Marine Biology, 28: 175–387.

Ko, G. W., Dineshram, R., Campanati, C., Chan, V. B., Havenhand, J., and Thiyagarajan, V. 2014. Interactive effects of ocean acidification, elevated temperature, and reduced salinity on early-life stages of the pacific oyster. Environmental Science and Technology, 48: 10079–10088.

Kroeker, K. J., Kordas, R. L., Crim, R., Hendriks, I. E., Ramajo, L., Singh, G. S., Duarte, C. M., *et al.* 2013. Impacts of ocean acidification on marine organisms: quantifying sensitivities and interaction with warming. Global Change Biology, 19: 1884–1896.

Lee, D. E. 1991. Aspects of the ecology and distribution of the living Brachiopoda of New Zealand. *In* Brachiopods Through Time, pp. 273–279. Ed. by D. I. MacKinnon, D. E. Lee, and J. D. Campbell. A.A Balkema Publishers, Rotterdam, The Netherlands.

Lee, D. E., Robinson, J. H., Witman, J. D., Copeland, S. E., Harper, E. M., Smith, F., and Lamare, M. D. 2010. Observations on recruitment, growth and ecology in a diverse living brachiopod community, Doubtful Sound, Fiordland, New Zealand. Special Papers in Palaeontology, 84: 177–191.

Lee, D. E., and Wilson, J. B. 1979. Cenozoic and recent rhynchonellide brachiopods of New Zealand: Systematics and variation in the genus Notosaria. Journal of the Royal Society of New Zealand, 9: 437–463.

McClintock, J. B., Angus, R. A., McDonald, M. R., Amsler, C. D., Catledge, S. A., and Vohra, Y. K. 2009. Rapid dissolution of shells of weakly calcified Antarctic benthic macroorganisms indicates high vulnerability to ocean acidification. Antarctic Science, 21: 449.

Mehrbach, C., Culberson, C. H., Hawley, J. E., and Pytkowicxz, R. M. 1973. Measurement of apparent dissociation constants of carbonic acid in seawater at atmospheric pressure. Limnology and Oceanography, 18: 897–907.

Michaelidis, B., Ouzounis, C., Paleras, A., and Portner, H. O. 2005. Effects of long-term moderate hypercapnia on acid-base balance and growth rate in marine mussels *Mytilus galloprovincialis*. Marine Ecology Progress Series, 293: 109–118.

Nienhuis, S., Palmer, A. R., and Harley, C. D. 2010. Elevated CO_2 affects shell dissolution rate but not calcification rate in a marine snail. Proceedings of the Royal Society of London Series B: Biological Sciences, 277: 2553–2558.

Noisette, F., Richard, J., Le Fur, I., Peck, L. S., Davoult, D., and Martin, S. 2014. Metabolic responses to temperature stress under elevated pCO_2 in *Crepidula fornicata*. Journal of Molluscan Studies, doi:10.1093/mollus/eyu084.

Orr, J. C., Fabry, V. J., Aumont, O., Bopp, L., Doney, S. C., Feely, R. A., Gnanadesikan, A., *et al.* 2005. Anthropogenic ocean acidification over the twenty-first century and its impact on calcifying organisms. Nature, 437: 681–686.

Parker, L. M., Ross, P. M., O'Connor, W. A., Borysko, L., Raftos, D. A., and Pörtner, H. 2012. Adult exposure influences offspring response to ocean acidification in oysters. Global Change Biology, 18: 82–92.

Peck, L. S. 1993. The tissues of articulate brachiopods and their value to predators. Philosophical Transactions of the Royal Society of London Series B: Biological Sciences, 339: 17–32.

Peck, L. S. 2001a. Ecology. *In* Brachiopods Ancient and Modern: a Tribute to G. Arthur Cooper. The Paleontology Society Papers, pp. 171–183. Ed. by S. Carlson, and M. Sandy. Yale University, New Haven, CT.

Peck, L. S. 2001b. Physiology. *In* Brachiopods Ancient and Modern: a Tribute to G. Arthur Cooper. The Paleontology Society Papers, pp. 89–104. Ed. by S. Carlson, and M. Sandy. Yale University, New Haven, CT.

Peck, L. S. 2005. Prospects for survival in the Southern Ocean: vulnerability of benthic species to temperature change. Antarctic Science, 17: 497.

Peck, L. S. 2008. Brachiopods and climate change. Earth and Environmental Science Transactions of the Royal Society of Edinburgh, 98: 451–456.

Peck, L. S., Barnes, D. K. A., and Willmott, J. 2005. Responses to extreme seasonality in food supply: diet plasticity in Antarctic brachiopods. Marine Biology, 147: 453–463.

Peck, L. S., Brockington, S., and Brey, T. 1997. Growth and metabolism in the Antarctic brachiopod *Liothyrella uva*. Philosophical Transactions of the Royal Society of London Series B: Biological Sciences, 352: 851–858.

Peck, L. S., and Harper, E. M. 2010. Variation in size of living articulated brachiopods with latitude and depth. Marine Biology, 157: 2205–2213.

Pennington, J. T., and Stricker, S. A. 2001. Phylum Brachiopoda. *In* Atlas of Marine Invertebrate Larval Forms, pp. 441–461. Ed. by C. M. Young. Academic Press, New York.

Pörtner, H. 2008. Ecosystem effects of ocean acidification in times of ocean warming: a physiologist's view. Marine Ecology Progress Series, 373: 203–217.

Queiros, A. M., Fernandes, J. A., Faulwetter, S., Nunes, J., Rastrick, S. P., Mieszkowska, N., Artioli, Y., *et al.* 2015. Scaling up experimental ocean acidification and warming research: from individuals to the ecosystem. Global Change Biology, 21: 130–143.

Reymond, C. E., Lloyd, A., Kline, D. I., Dove, S. G., and Pandolfi, J. M. 2013. Decline in growth of foraminifer Marginopora rossi under eutrophication and ocean acidification scenarios. Global Change Biology, 19: 291–302.

Richardson, J. R. 1986. Brachiopods. Scientific American, 255: 100–106.

Rickwood, A. E. 1977. Age, growth and shape of the intertidal brachiopod *Waltonia inconspicua* Sowerby, from New Zealand. American Zoologist, 17: 63–73.

Ries, J. B. 2011. A physicochemical framework for interpreting the biological calcification response to CO_2-induced ocean acidification. Geochimica et Cosmochimica Acta, 75: 4053–4064.

Ries, J. B., Cohen, A. L., and McCorkle, D. C. 2009. Marine calcifiers exhibit mixed responses to CO_2-induced ocean acidification. Geology, 37: 1131–1134.

Riisgård, H. U., and Randløv, A. 1981. Energy budgets, growth and filtration rates in *Mytilus edulis* at different algal concentrations. Marine Biology, 61: 227–234.

Robbins, L. L., Hansen, M. E., Kleypas, J. A., and Meylan, S. C. 2010. CO_2calc: a User-friendly Carbon Calculator for Windows, Mac OS X, and iOS (iPhone).

Rodland, D. L., Kowalewski, M., Carroll, M., and Simões, M. G. 2004. Colonization of a "Lost World": encrustation patterns in modern subtropical brachiopod assemblages. Palaios, 19: 381–395.

Roper, D. S., and Jillett, J. B. 1981. Seasonal occurrence and distribution of flatfish (Pisces: Pleuronectiformes) in inlets and shallow water along the Otago coast. New Zealand Journal of Marine and Freshwater Research, 15: 1–13.

Rosa, R., and Seibel, B. A. 2008. Synergistic effects of climate-related variables suggest future physiological impairment in a top oceanic predator. Proceedings of the National Academy of Sciences of the United States of America, 105: 20776–20780.

Stewart, I. R. 1981. Population structure of articulate brachiopod species from soft and hard substrates. New Zealand Journal of Zoology, 8: 197–207.

Suckling, C. C., Clark, M. S., Richard, J., Morley, S. A., Thorne, M. A. S., Harper, E. M., and Peck, L. S. 2014. Adult acclimation to combined temperature and pH stressors significantly enhances reproductive outcomes compared to short-term exposures. Journal of Animal Ecology, doi:10.1111/1365-2656.12316.

Thomsen, J., Casties, I., Pansch, C., Kortzinger, A., and Melzner, F. 2013. Food availability outweighs ocean acidification effects in juvenile *Mytilus edulis*: laboratory and field experiments. Global Change Biology, 19: 1017–1027.

Thomsen, J., Gutowska, M. A., Saphörster, J., Heinemann, A., Trübenbach, K., Fietzke, J., Hiebenthal, C., *et al.* 2010. Calcifying invertebrates succeed in a naturally CO_2-rich coastal habitat but are threatened by high levels of future acidification. Biogeosciences, 7: 3879–3891.

Wanninkhof, R., Lewis, E., Feely, R. A., and Millero, F. J. 1999. The optimal carbonate dissociation constants for determining surface water pCO_2 from alkalinity and total inorganic carbon. Marine Chemist, 65: 291–301.

Watson, S-A., Peck, L. S., Tyler, P. A., Southgate, P. C., Tan, K. S., Day, R. W., and Morley, S. A. 2012. Marine invertebrate skeleton size varies with latitude, temperature and carbonate saturation: implications for global change and ocean acidification. Global Change Biology, 18: 3026–3038.

Wittmann, A. C., and Pörtner, H. 2013. Sensitivities of extant animal taxa to ocean acidification. Nature Climate Change, 3: 995–1001.

Wolfe, K., Dworjanyn, S. A., and Byrne, M. 2013. Effects of ocean warming and acidification on survival, growth and skeletal development in the early benthic juvenile sea urchin (*Heliocidaris erythrogramma*). Global Change Biology, 19: 2698–2707.

Wood, H. L., Spicer, J. I., and Widdicombe, S. 2008. Ocean acidification may increase calcification rates, but at a cost. Proceedings of the Royal Society of London, Series B: Biological Sciences, 275: 1767–1773.

Handling editor: C. Brock Woodson

ICES Journal of Marine Science

ICES Journal of Marine Science (2016), 73(3), 927–936. doi:10.1093/icesjms/fsv226

Contribution to Special Issue: 'Towards a Broader Perspective on Ocean Acidification Research'

Original Article

Ocean acidification does not alter grazing in the calanoid copepods *Calanus finmarchicus* and *Calanus glacialis*

Nicole Hildebrandt[1]*, Franz J. Sartoris[1], Kai G. Schulz[2,3], Ulf Riebesell[2], and Barbara Niehoff[1]

[1]*Alfred Wegener Institute, Helmholtz Centre for Polar and Marine Research, Am Handelshafen 12, Bremerhaven 27570, Germany*
[2]*GEOMAR Helmholtz Centre for Ocean Research Kiel, Düsternbrooker Weg 20, Kiel 24105, Germany*
[3]*Centre for Coastal Biogeochemistry, School of Environmental Science and Management, Southern Cross University, PO Box 157, Lismore, NSW 2480, Australia*

*Corresponding author: tel: +49 471 4831 1810; fax: +49 471 4831 1149; e-mail: nicole.hildebrandt@awi.de

Hildebrandt, N., Sartoris, F. J., Schulz, K. G., Riebesell, U., and Niehoff, B. Ocean acidification does not alter grazing in the calanoid copepods *Calanus finmarchicus* and *Calanus glacialis*. – ICES Journal of Marine Science, 73: 927–936.

Received 30 June 2015; revised 4 November 2015; accepted 5 November 2015; advance access publication 13 December 2015.

It is currently under debate whether organisms that regulate their acid–base status under environmental hypercapnia demand additional energy. This could impair animal fitness, but might be compensated for via increased ingestion rates when food is available. No data are yet available for dominant *Calanus* spp. from boreal and Arctic waters. To fill this gap, we incubated *Calanus glacialis* at 390, 1120, and 3000 µatm for 16 d with *Thalassiosira weissflogii* (diatom) as food source on-board RV *Polarstern* in Fram Strait in 2012. Every 4 d copepods were subsampled from all CO_2 treatments and clearance and ingestion rates were determined. During the SOPRAN mesocosm experiment in Bergen, Norway, 2011, we weekly collected *Calanus finmarchicus* from mesocosms initially adjusted to 390 and 3000 µatm CO_2 and measured grazing at low and high pCO_2. In addition, copepods were deep frozen for body mass analyses. Elevated pCO_2 did not directly affect grazing activities and body mass, suggesting that the copepods did not have additional energy demands for coping with acidification, neither during long-term exposure nor after immediate changes in pCO_2. Shifts in seawater pH thus do not seem to challenge these copepod species.

Keywords: *Calanus*, clearance rate, CO_2, food uptake, ingestion rate.

Introduction

Anthropogenic CO_2 emissions, which recently amounted to ~34 billion tons year^{-1} (Friedlingstein *et al.*, 2010), have increased the atmospheric CO_2 concentration since pre-industrial times from 280 to ~400 µatm (Tans, 2014). About 30% of the emitted CO_2 is absorbed by the world's oceans (Solomon *et al.*, 2007), making them the second largest sink for human-made CO_2. The CO_2 uptake changes seawater chemistry, resulting in decreasing seawater pH and carbonate ion concentrations (Raven *et al.*, 2005). Model calculations based on the IPCC emissions scenario IS92a (Alcamo *et al.*, 1995) projected that CO_2 concentrations might increase to ~750 µatm by 2100 and to almost 2000 µatm by the year 2300 (Caldeira and Wickett, 2003), with a corresponding decline in surface ocean pH by ~0.4 units until the end of the century and by a maximum of 0.77 units until 2300, a process usually referred to as "ocean acidification" (OA).

OA has the potential to severely affect the performance of marine organisms. Metabolic rates can be depressed at elevated CO_2 concentrations (Reipschläger and Pörtner, 1996; Rosa and Seibel, 2008; Seibel *et al.*, 2012), possibly triggered by a lack of or incomplete compensation for increasing pCO_2 in extracellular fluids due to environmental hypercapnia (Reipschläger and Pörtner, 1996; Pörtner *et al.*, 1998). Food uptake and growth may then be impaired and mortality may increase (Michaelidis *et al.*, 2005; Miles *et al.*, 2007; Appelhans *et al.*, 2012; Vargas *et al.*, 2013). For species that are able to actively regulate their internal acid–base balance, such as crustaceans (Widdicombe and Spicer, 2008), it is discussed that additional energy has to be allocated to maintaining the acid–base status, and therefore fitness is lowered at elevated seawater pCO_2 (Wood *et al.*, 2008; Thomsen and Melzner, 2010; Melzner *et al.*, 2011; Appelhans *et al.*, 2012, Saba *et al.*, 2012). Therefore, negative effects seem to be particularly distinct when food is

limited (Melzner *et al.*, 2011; Appelhans *et al.*, 2012), while, when food supply is sufficient, feeding rates may increase to meet the additional energy demands, as suggested for krill (Saba *et al.*, 2012) and the calanoid copepod *Centropages tenuiremis* (Li and Gao, 2012).

Calanoid copepods are key players in pelagic marine environments and often dominate zooplankton communities (Longhurst, 1985). Studies on the sensitivity of copepods to future OA show mixed responses. Levels of OA that are predicted to occur until 2300 were detrimental in four species. Dupont and Thorndyke (2008) reported that generation times in *Acartia tonsa* increased under elevated pCO_2. Cripps *et al.* (2014) showed for the same species that hatching success and nauplii survival are also sensitive to OA. In *A. spinicauda* and *C. tenuiremis*, survival of females as well as egg hatching rates was negatively affected (Zhang *et al.*, 2011), and in *Pseudocalanus acuspes*, egg production rates significantly decreased (Thor and Dupont, 2015). In all other species studied so far, parameters such as growth, egg production, hatching success and survival of nauplii, copepodites and adults were only affected at CO_2 concentrations $\geq$5000 μatm, if at all (e.g. Kurihara *et al.*, 2004; Zhang *et al.*, 2011; Mayor *et al.*, 2012; McConville *et al.*, 2013; Pedersen *et al.*, 2013; Isari *et al.*, 2015). Under controlled laboratory conditions, food uptake of calanoid copepods in response to elevated pCO_2 has only been studied in two species so far. In *C. tenuiremis*, grazing rates decreased at elevated pCO_2 (1000 μatm) during the 1 d of exposure; however, no significant effects were found thereafter (Li and Gao, 2012). In *P. acuspes*, effects of OA (~800 and 1400 μatm CO_2) on ingestion rates were non-linear, and also dependent on the geographical region and food concentration (Thor and Oliva, 2015).

In our study, we focus on two *Calanus* species, i.e. *C. finmarchicus* (Gunnerus, 1770) and *Calanus glacialis* Jaschnov (1955). Both are important components of the lipid-based foodweb of the Arctic (Falk-Petersen *et al.*, 2007 and references therein). *Calanus finmarchicus* is a North Atlantic species and is transported into the Arctic Ocean via the West Spitsbergen Current, into the Barents Sea with the North Cape Current and into Davis Strait with the West Greenland Current (e.g. Jaschnov, 1970; Conover, 1988). *Calanus glacialis* has its origin in the Arctic shelf regions and penetrates southward into Fram Strait with the East Greenland Current (Jaschnov, 1970; Conover, 1988). In areas where the warm Atlantic water submerges under the cold Arctic water, both species co-occur (Conover, 1988). During spring and summer, they inhabit surface waters where they feed on phytoplankton and accumulate large lipid stores (e.g. Marshall and Orr, 1955; Lee, 1974; Pasternak *et al.*, 2001). In late summer, they descend to deeper waters and enter a diapause to sustain the food scarce period in winter (e.g. Tande *et al.*, 1985; Hirche, 1998). The natural seawater pH the copepods experience during their seasonal migrations ranges from ~8.2 in surface waters (Charalampopoulou *et al.*, 2008) to ~7.9 in deep waters (Jutterström *et al.*, 2010).

Previous studies on the effects of OA on mortality, body mass, metabolic rates, and reproductive output of *C. finmarchicus* and *C. glacialis* indicate that copepodites V (CV) and females are robust to CO_2 levels predicted for the next centuries (Mayor *et al.*, 2007; Weydmann *et al.*, 2012; Hildebrandt *et al.*, 2014). Feeding has not been studied under controlled laboratory conditions yet; however, Pedersen *et al.* (2013) published a study on *C. finmarchicus* that were raised from eggs to adults at CO_2 concentrations of 3300–9700 μatm and showed that fat contents in CV grown at control and elevated pCO_2 were similar. We may thus hypothesize that the food uptake was not lowered by high CO_2 concentrations. It remains open, however, whether *C. finmarchicus* compensated for additional energy demands due to OA stress with an increase in grazing rates (Saba *et al.*, 2012). At more realistic surface seawater CO_2 concentrations ($\leq$1420 μatm), de Kluijver *et al.* (2013) examined trophic interactions during a 30-day mesocosm study in an Arctic fjord, using ^{13}C as a tracer. Their study found reduced rates of ^{13}C incorporation in *Calanus* spp. in high pCO_2 mesocosms, indicating that grazing rates decrease with increasing pCO_2. However, as the food quality, i.e. the algal community composition in the mesocosms, changed with the CO_2 concentration (Brussaard *et al.*, 2013; Schulz *et al.*, 2013), the decrease in grazing could reflect indirect effects of OA.

To elucidate whether *Calanus* spp. ingest more food to compensate for additional energy demands or whether ingestion rates decrease when exposed to OA, we performed controlled laboratory experiments at different pCO_2, feeding the copepods with monoalgal food (*Thalassiosira weissflogii*). Part of our study was conducted within the SOPRAN 2011 mesocosm experiment in Bergen, Norway. Here, we weekly sampled *C. finmarchicus* from mesocosms initially adjusted to 390 and 3000 μatm CO_2 and exposed the copepods of each group to both, high and low pCO_2 conditions to study immediate responses to changing pCO_2 as well as long-term effects of exposure to high pCO_2. In addition, we incubated *C. glacialis* at 390, 1120, and 3000 μatm CO_2 for 16 d in the cold-rooms on-board RV *Polarstern* and repeatedly conducted grazing experiments.

Methods

Experiments during the SOPRAN mesocosm study 2011

Sampling

In May and June 2011, experiments were conducted within the framework of the SOPRAN mesocosm experiment at Espegrend, the Marine Biological Station of the University of Bergen, Norway. Nine KOSMOS (Kiel Offshore Mesocosms for Future Ocean Simulations) mesocosms of 25 m length and 2 m diameter were deployed in the Raunefjord at N 60° 15.87′, E 005° 12.33′ for 6 weeks. For technical details on the mesocosms and their deployment, see Riebesell *et al.* (2013). Briefly, each mesocosm enclosed ~75 m^3 of fjord water containing natural plankton <3 mm. Larger mesozooplanktonic and nektonic organisms were excluded by a mesh (3 mm mesh size) that covered the openings of the mesocosm bags during deployment, as these organisms occur only in low numbers and are patchily distributed. On the lower end of each mesocosm, a sediment trap was installed to collect settling material. Ambient fjord water was aerated with pure CO_2 and added to seven of the mesocosms in five steps over 5 d to adjust the pH to ~390, ~560, ~840, ~1120, ~1400, ~2000, and ~3000 μatm CO_2, while two mesocosms were kept at *in situ* pCO_2 (~280 μatm). For our experiments, only copepods from the mesocosms with 390 (control) and 3000 μatm CO_2 (high pCO_2) were used. The pH (reported on the total scale) in the control mesocosm ranged between 8.0 and 8.1 throughout the experiment. In the high CO_2 mesocosm, the initial pH after CO_2 manipulation was ~7.2. However, due to outgassing and biological activities, it increased over time, especially in the upper water column. At the end of the experiment, the pH was 7.8 at the surface and 7.4 at depth. On Day 14, nutrients (~5 μmol l^{-1} NO_3, ~0.16 μmol l^{-1} PO_4) were added to the mesocosms to induce a phytoplankton bloom.

Once a week zooplankton was sampled with an Apstein net (mesh size 55 μm). Sampling was performed in the fjord on Day 0 and thereafter in the nine mesocosms. Sampling depth was

limited to 23 m in order not to resuspend material from the sediment traps. Within 1 h, the plankton samples were brought to a cold room adjusted to 10°C, which was the approximate *in situ* temperature at that time.

Preparation of experimental water and food algae

Filtered seawater was adjusted to target values of 390 (control) and 3000 µatm CO_2 (high CO_2) by mixing with filtered CO_2 saturated fjord water. The pH was monitored with a pH electrode (Mettler Toledo InLab Routine Pt1000, connected to a pH meter WTW pH 3310), which was calibrated with NIST buffers (pH 6.865 and 9.180). Then the pH was converted to total scale (pH_T) using TRIS-based reference material (Batch no. 4, A. Dickson, Scripps Institution of Oceanography). Dissolved inorganic carbon (DIC) in the experimental water was measured with a Technicon Analyzer TrAAcs 800 (Seal Analytical GmbH, Germany). pH_T and DIC were then used to calculate DIC using the programme CO2SYS (Lewis and Wallace, 1998). Mean pH values of control and high CO_2 treatments were 7.9 (592 ± 42 µatm pCO_2) and 7.2 (3202 ± 521 µatm pCO_2), respectively (Table 1). Temperature and salinity were determined with a conductivity meter WTW Cond340i (Table 1). Monocultures of the diatom *T. weissflogii* were grown in f/2 medium (Guillard, 1975) at 10 °C under constant light as food for the copepods.

Determination of grazing rates

About 60 *C. finmarchicus* copepodites V (CV) were sorted from the control and high CO_2 mesocosm sample, respectively. To eliminate the effect of possibly different feeding conditions in the mesocosms on grazing rates during the experiments, the copepods were pre-incubated for 1 d at 10°C in filtered seawater adjusted to the respective CO_2 concentration and containing *T. weissflogii* in excess.

For the determination of grazing rates, high and control CO_2 water was inoculated with *T. weissflogii* at a concentration of 4000 cells ml^{-1}. Thirty copepods each from pre-incubation at control and pre-incubation at high pCO_2 were transferred to 1 l bottles (10 copepods $bottle^{-1}$) containing seawater of the respective pCO_2. To test whether immediate changes in CO_2 concentration affect the food uptake, 30 copepods from pre-incubation at control seawater pH were placed in three 1 l bottles containing high CO_2 water, and 30 copepods from the pre-incubation at high pCO_2 were transferred to 1 l bottles with control seawater. Three additional bottles for each CO_2 concentration were prepared that contained seawater with algae but no copepods. These bottles were run as a blank to correct the grazing rates of the copepods for algal growth. After transfer of algal suspensions and copepods, all bottles were immediately sealed airtight and mounted to a plankton wheel for 17.5 to 22 h in the dark. After the experiment, the copepods were sorted from all bottles, rinsed in distilled water and stored in groups of two to six in tin caps at −20°C to measure C and N content. Subsamples of 3 × 100 ml of the experimental water for each CO_2 treatment were filtered on GF/F filters and frozen to determine the chlorophyll *a* (chl *a*) concentration before and at the end of the experiments.

Prosome length of *C. finmarchicus* was measured under a stereomicroscope with an ocular micrometre (error ± 5 µm) in 36 individuals sampled from the fjord at the beginning of the study.

On-board incubation experiment

Copepod sampling and incubation

The experiment with *C. glacialis* was conducted in July 2012 during a cruise with RV *Polarstern* to Fram Strait (ARK-XXVII/1 and 2). Copepods were sampled with vertical bongo net hauls (200 and 300 µm mesh size, 0–250 m) at approximately N 79° 40.3′, W 011° 59.3′ (PS 80/91) and immediately brought to a cooling container adjusted to 0°C. About 1350 *C. glacialis* CV were sorted from the samples and acclimated to laboratory conditions in filtered seawater enriched with *T. weissflogii* for 2 d.

Preparation of incubation water and food algae

Filtered seawater was adjusted to 1120 (intermediate) and 3000 µatm (high) CO_2 by bubbling with gas mixtures from a gas cylinder (purchased from Air Liquide Deutschland GmbH, Düsseldorf). Untreated filtered seawater was used as a control (390 µatm). The resulting pH values (Table 1) differed at least by 0.3 units between control and intermediate and between intermediate and high CO_2 treatments. There was no possibility to measure DIC samples onboard, and as storage of such samples for a period of several months, until the return of RV *Polarstern* to Bremerhaven, is not recommended, we did not measure parameters other than pH. However, preliminary tests have shown that bubbling with the used air/CO_2 mixes yield the desired seawater pCO_2. *T. weissflogii* was cultured according to the experiment in 2011, but at temperatures of 10 and 18°C. Before it was fed to the copepods, the algal suspension was adjusted to the incubation temperature.

CO_2 incubation

The copepods were transferred to 6 l glass bottles and incubated at control, intermediate and high CO_2 for 16 d. Three bottles, each containing 150 *C. glacialis*, were set up for each CO_2 treatment. The copepods were fed daily with *T. weissflogii* at a concentration of 8000 cells ml^1 to prevent food limitation as these large bottles could not be mounted on a plankton wheel and therefore part of the algae sank to the bottom. Every 4 d, the incubation water was completely changed and pH, salinity, and temperature were measured. pH values increased on average by 0.19, 0.13, and 0.06

Table 1. Water parameters during the determination of grazing rates (a) and during the CO_2 incubations on RV *Polarstern* in 2012 (b).

	Species	CO_2 treatment (µatm)	Temp. (°C)	Salinity (psu)	pH (total scale)	*N*
(a)	*C. finmarchicus*	390	10.0 ± 0.3	32.4 ± 0.2	7.86 ± 0.03	4
	C. finmarchicus	3000	9.9 ± 0.2	32.4 ± 0.4	7.16 ± 0.07	4
	C. glacialis	390	1.1 ± 0.7	32.4 ± 1.2	7.97 ± 0.06	5
	C. glacialis	1120	1.0 ± 0.7	32.9 ± 0.5	7.62 ± 0.04	5
	C. glacialis	3000	1.0 ± 0.7	32.7 ± 0.7	7.21 ± 0.05	5
(b)	*C. glacialis*	390	1.4 ± 0.3	33.2 ± 0.4	7.86 ± 0.13	24
	C. glacialis	1120	1.3 ± 0.4	33.1 ± 0.4	7.54 ± 0.09	24
	C. glacialis	3000	1.3 ± 0.4	33.3 ± 0.4	7.21 ± 0.07	24

Values are presented as mean ± SD. Temp., temperature; *N*, number of measurements throughout the experiments/incubations.

units in between water exchanges at 390, 1120, and 3000 μatm CO_2, respectively. When the water was changed, 10 copepods from each bottle were removed to determine grazing rates. Thus, the number of copepods in the bottles decreased over time. At start and at the end of the CO_2 incubation, 36–66 copepods from each CO_2 treatment were measured under a stereomicroscope with an ocular micrometre (prosome length) then deep-frozen individually for C and N measurements.

Determination of grazing rates

Thirty copepods from each of the three different CO_2 treatments were transferred to three 1 l bottles (10 copepods bottle^{-1}) with seawater of the respective pCO_2. *T. weissflogii* was added at a concentration of 2000 cells ml^{-1}. Along with three blanks for each CO_2 concentration (see above), the bottles were mounted to a plankton wheel for 21.5–25 h. Subsamples for chl *a* measurements as well as copepod C and N samples were taken as described above.

Sample analysis

To determine the chl *a* concentration in the incubation bottles and blank bottles at the start and the end of the grazing experiments, the algal cells on the GF/F filters were first disrupted in 90% acetone using ultrasound (Branson Sonifier 250, Heinemann, Schwäbisch Gmünd, Germany). Then, the chl *a* was extracted from the algal cells for 2 h in the dark at 5°C. After centrifugation at 4500 rpm for 15 min at 0°C, the chl *a* fluorescence in the supernatant was determined with a Turner fluorometer (TD-700, Turner Designs, Sunnyvale, CA, USA) at 665 nm before and after adding two drops of 1 N HCl. Clearance rates (CRs) and ingestion rates (IRs) of the copepods were then calculated after Frost (1972).

On some days, initial chl *a* concentrations were significantly different among CO_2 treatments (*C. finmarchicus*: Day 8; *C. glacialis*: Days 1 and 8). In order not to bias the results of the grazing experiments, we excluded the grazing rates that were measured on these days from our analyses.

To determine carbon and nitrogen content, the copepods in the tin caps were dried at 60°C for 48 h then combusted with subsequent gas chromatographic separation by an elemental analyser (Euro EA, HEKAtech GmbH, Wegberg, Germany). Acetanilide was used as a standard.

Statistics

Statistical analyses were performed with SigmaStat 3.5 (Systat Software, Inc.). A *t*-test or a one-way ANOVA followed by a *post hoc* Holm-Sidak test was performed to identify differences in grazing and body mass between copepods from different CO_2 treatments at each experimental day. A Spearman rank-order correlation was used to identify changes in body carbon and nitrogen during the experiments, and to test for correlation between CR/IR and the initial chl *a* content in the incubation water to determine whether our food concentrations limited grazing rates. Data were considered significantly different at a $p < 0.05$. Results are presented as mean ± standard deviation.

Results

Mean initial chl *a* concentrations ranged between 7.8 and 9.6 μg l^{-1} in the grazing experiments with *C. finmarchicus* CV from Bergen and between 3.9 and 6.2 μg l^{-1} in the experiments on-board RV *Polarstern* with *C. glacialis* CV (Table 2). The concentrations were significantly different among days but not among the pCO_2 treatments at a specific day. At the end of the grazing experiment, chl *a* concentrations were still high at 5.6–9.5 (*C. finmarchicus*) and 1.4–4.3 μg l^{-1} (*C. glacialis*).

In *C. finmarchicus* collected from the Raunefjord on Day 0 of the mesocosm experiment, clearance and ingestion rates at control pCO_2 were 2.2 ± 0.7 ml copepod^{-1} h^{-1} and 0.018 ± 0.005 μg chl *a* copepod^{-1} h^{-1}, respectively (Figure 1). On Days 15, 22, and 28, *C. finmarchicus* were collected from the control (390 μatm) and high pCO_2 mesocosm (initially 3000 μatm), and grazing rates were determined at the respective CO_2 concentrations. Mean CR (Figure 1a) and IR (Figure 1b) were similar to the control values measured at Day 0. The pCO_2 generally did not affect the grazing rates. Only during the experiment on Day 28, CR and IR were significantly lower in copepods from the control than from the high pCO_2 mesocosm (Table 3). Neither CR nor IR correlated with the initial

Table 2. Chlorophyll *a* concentration (mean ± SD, $n = 3$) in the experimental water at the start and at the end of grazing experiments with *Calanus* spp. as well as in blank bottles.

			Chlorophyll *a* (μg l^{-1})		
Species	**Day**	**CO_2 treatment**	**Start**	**End**	**Blank (end)**
C. finmarchicus	0	390	9.6 ± 0.3	9.5 ± 0.9	12.0 ± 3.6
	15	390	7.9 ± 0.1	5.6 ± 0.6	8.5 ± 1.4
	15	3000	7.8 ± 0.1	6.0 ± 0.4	8.8 ± 0.4
	22	390	9.0	5.8 ± 0.7	8.6 ± 2.5
	22	3000	8.7	6.6 ± 1.1	9.8 ± 0.7
	28	390	9.3	9.5 ± 0.4	11.0 ± 0.6
	28	3000	9.4	9.0 ± 1.5	12.0 ± 0.5
C. glacialis	4	390	3.9 ± 0.3	1.4 ± 0.3	3.6 ± 0.3
	4	1120	4.1 ± 0.2	1.7 ± 0.3	3.9 ± 0.1
	4	3000	3.9 ± 0.2	1.6 ± 0.4	3.7 ± 0.3
	12	390	4.7 ± 0.2	3.1 ± 0.4	5.2 ± 0.3
	12	1120	5.1 ± 0.3	3.7 ± 0.5	5.6 ± 0.4
	12	3000	4.7 ± 0.2	4.0 ± 0.6	5.2 ± 0.2
	16	390	6.0 ± 0.2	3.7 ± 0.7	5.9 ± 0.7
	16	1120	6.2 ± 0.5	4.3 ± 0.1	6.2 ± 0.1
	16	3000	5.4 ± 0.6	3.1 ± 0.5	5.9 ± 0.4

On Days 22 and 28 (*C. finmarchicus*), there was only one start measurement for chlorophyll *a*.

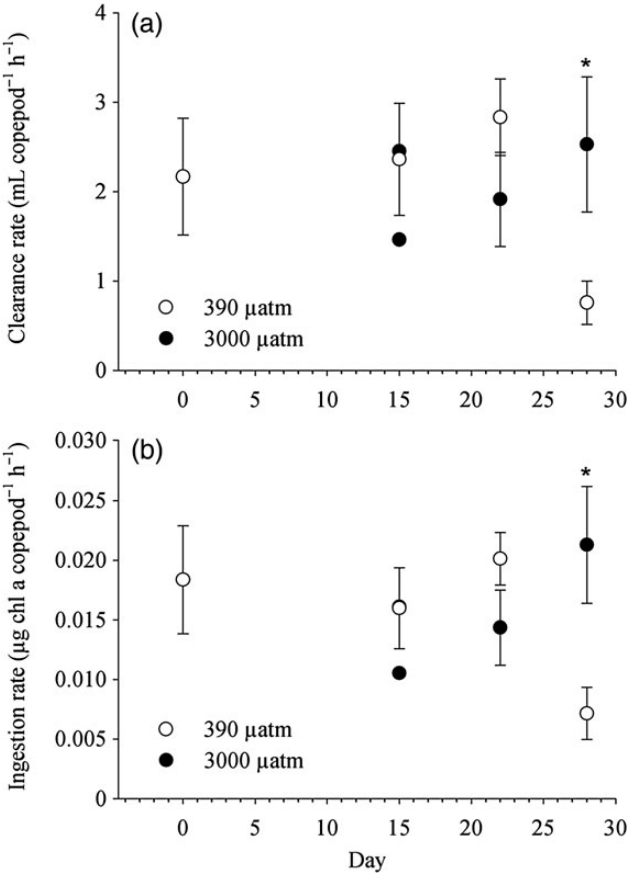

Figure 1. Long-term response of *C. finmarchicus* CV to OA: clearance rate (a) and ingestion rate (b) at control (white circles) and high pCO_2 (black circles). Data on Day 0 present only control measurements at low pCO_2, conducted before the adjustment of the pH in the mesocosms. Data are presented as mean ± standard deviation. Asterisk marks significant differences between CO_2 treatments.

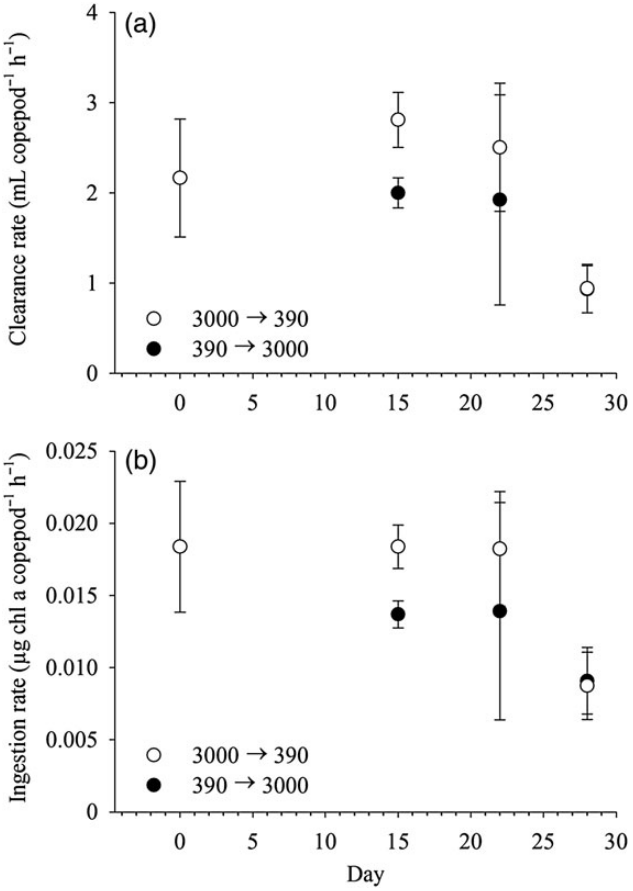

Figure 2. Immediate response of *C. finmarchicus* CV to OA: clearance rate (a) and ingestion rate (b) of copepods originating in the high CO_2 mesocosm that were incubated at control pCO_2 (white circles) and of copepods originating in the control mesocosm that were incubated at high pCO_2 (black circles). The data on Day 0 present only control measurements at low pCO_2, conducted before the adjustment of the pH in the mesocosms. Data are presented as mean ± standard deviation, except for Day 15, where only two data points were available for the high pCO_2 treatment. Here, both data points are shown separately.

Table 3. Results of the one-way ANOVAs to test for differences in grazing rates of *C. finmarchicus* and *C. glacialis* among different CO_2 treatments.

Species	Parameter	Day	d.f.	*F*	*p*	Power
C. finmarchicus	CR	15	3	1.985	0.205	0.172
		22	3	1.064	0.417	0.057
		28	**3**	**10.701**	**0.004**	**0.955**
	IR	15	3	2.342	0.160	0.222
		22	3	1.254	0.353	0.080
		28	**3**	**12.954**	**0.002**	**0.983**
C. glacialis	CR	4	2	0.212	0.815	0.050
		12	2	2.244	0.187	0.178
		16	2	3.626	0.093	0.335
	IR	4	2	2.134	0.200	0.166
		12	2	2.435	0.168	0.200
		16	2	2.586	0.155	0.217

Values presented in bold indicate significant differences in grazing rates among CO_2 treatments. CR, clearance rates; IR, ingestion rates. In *C. finmarchicus*, the analysis compares data from both long-term and immediate response groups.

chl *a* content in the incubation water ($p > 0.05$), indicating that food concentrations did not limit grazing.

Also sudden changes in pCO_2 did not affect the grazing activity (Figure 2, Table 3). In copepods transferred from control to high CO_2 and *vice versa*, CR and IR at Days 15 and 22 were again similar to the rate measured on Day 0, whereas lower rates (CR: 0.9 ml copepod^{-1} h^{-1}, IR: 0.009 µg chl *a* copepod^{-1} h^{-1}) were measured on Day 28. Again, no correlation was found between CR or IR and the initial chl *a* content ($p > 0.05$).

The mean C and N contents of *C. finmarchicus* CV (2.4 ± 0.1 mm prosome length) from the control mesocosms were 161 and 19 µg, respectively (Table 4), and did not change significantly over time (Table 5). In copepods from the high CO_2 mesocosm, the C and N contents were significantly lower when compared with copepods from the control mesocosm on Days 8 and 15 (*t*-test, $0.001 \leq p \leq 0.008$). On the last two sampling days, however, C and N had increased, and no differences in body mass were found between copepods from high and control mesocosms (Tables 4 and 5).

In *C. glacialis* CV from the Fram Strait (Figure 3), mean clearance rates were 1.4–4.7 ml copepod^{-1} h^{-1}, and ingestion rates varied from 0.006 to 0.013 µg chl *a* copepod^{-1} h^{-1} independent from CO_2 conditions (Table 3). There was no correlation between IR and the initial chl *a* concentration, while for copepods incubated

Table 4. Carbon and nitrogen contents of *C. finmarchicus* CV sampled from control and high CO_2 mesocosms.

	Control CO_2			High CO_2		
Day	C (µg)	N (µg)	*n*	C (µg)	N (µg)	*n*
0	151 ± 34	19 ± 2	19	151 ± 34	19 ± 2	19
8	167 ± 26	19 ± 2	11	134 ± 17	17 ± 1	8
15	167 ± 26	19 ± 2	12	123 ± 23	16 ± 2	12
22	162 ± 12	19 ± 1	12	158 ± 12	18 ± 1	12
28	164 ± 25	18 ± 2	12	169 ± 26	19 ± 2	12

Values are presented as mean ± standard deviation. C, carbon content; N, nitrogen content; *n*, number of samples. For each sample, 2–6 copepods (usually 5) were pooled. In the control CO_2 group, all copepods initially sampled from the control mesocosm are included (i.e. also copepods from the immediate response group which were transferred to high pCO_2 during the grazing experiments). Likewise, in the high CO_2 group, all copepods initially sampled from the high CO_2 mesocosm are represented.

Table 5. Spearman rank-order correlation analyses between carbon and nitrogen content in *C. finmarchicus* CV and time during 28 d of the SOPRAN mesocosm experiment 2011.

[CO_2] (µatm)	Parameter	Correlation coefficient	*p*
390	C	0.167	0.180
3000	C	0.256	**0.043**
390	N	0.019	0.881
3000	N	0.139	0.275

Values presented in bold indicate significant correlations between C and N content and time.
[CO_2], CO_2 concentration; C, carbon content; N, nitrogen content.

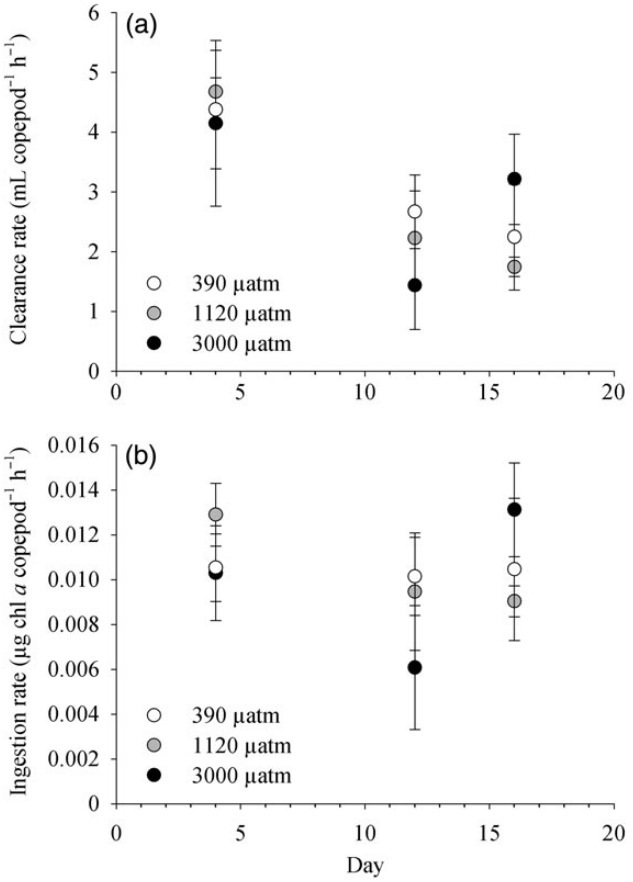

Figure 3. Response of *C. glacialis* CV to OA: clearance rate (a) and ingestion rate (b) at control (white circles), intermediate (grey circles), and high pCO_2 (black circles). Data are presented as mean ± standard deviation.

at 390 and 1120 µatm CO_2, a negative correlation between CR and chl *a* was found ($p = 0.009$). This indicates that food uptake was not limited during the grazing experiments but copepods at 390 and 1120 µatm CO_2 had to filter more water to ingest the same amount of algae compared with copepods from 3000 µatm.

The C and N contents of *C. glacialis* (3.5 ± 0.1 mm prosome length) at the start of the incubation were 646 and 56 µg, respectively (Table 6). Over time, the N content increased significantly by 30–40% at all CO_2 concentrations. Also the carbon content increased, however, significantly only in copepods kept at 1120 and 3000 µatm CO_2 (Table 7). The pCO_2 did not have significant effects on body mass, with two exceptions. On Day 15, the C content in copepods from 390 µatm was significantly lower when compared with the other CO_2 treatments (Holm-Sidak test, $p \leq 0.004$), whereas on Day 16 copepods from 1120 µatm had significantly more body carbon than those from 3000 µatm CO_2 ($p = 0.011$).

Discussion

Ocean acidification (OA) has been shown to influence feeding rates of marine organisms. In the common sea star *Asterias rubens*, for example, which does not compensate for elevated extracellular pCO_2 under environmental hypercapnia, feeding rates are lower when exposed to OA than under normocapnic conditions (Appelhans *et al.*, 2012). Also in larval sea urchins, i.e. *Strongylocentrotus droebachiensis* and *Dendraster excentricus*, and in larvae of the gastropod *Concholepas concholepas*, food uptake was significantly impaired by elevated seawater pCO_2 (Dupont and Thorndyke, 2008; Chan *et al.*, 2011; Vargas *et al.*, 2013). Other species regulate the extracellular pH, such as the shore crab *Carcinus maenas*. Feeding in this species was reduced at high when compared with low pCO_2 during a 10-week incubation experiment, but not in short-term feeding assays (Appelhans *et al.*, 2012). The authors suggested that during long-term exposure additional energy had to be allocated to acid–base regulation, which affected energy demanding processes related to feeding such as digestion or prey handling (Appelhans *et al.*, 2012). In contrast, the Antarctic krill *Euphausia superba* ingested more food at elevated pCO_2 (Saba *et al.*, 2012), and this study discussed that the increase in feeding compensated for elevated energetic needs due to acid–base regulation. Li and Gao (2012) came to a similar conclusion in their study on the copepod *Centropages tenuiremis*, although the differences in grazing rates were not significant. In *Pseudocalanus acuspes* from the Svalbard area, elevated CO_2 concentrations led to increased ingestion rates at intermediate and high food concentrations; however, respiration rates were not significantly affected by pCO_2 (Thor and Oliva, 2015).

Calanus glacialis was incubated at relatively stable CO_2 concentrations throughout our experiments, simulating a realistic scenario that is projected to occur in about the year 2100 (1120 µatm) and an extreme scenario (3000 µatm) that is not realistic for surface waters (Caldeira and Wickett, 2003). *Calanus finmarchicus* were sampled from large-scale mesocosms which were initially adjusted to 390 and 3000 µatm CO_2. In the high CO_2 mesocosm, the pH increased by 0.2–0.6 units over time, depending on the water depth, and thus, *C. finmarchicus* in this mesocosm was not kept at a stable pCO_2.

Table 6. Prosome length, carbon, and nitrogen contents of *C. glacialis* CV incubated at different CO_2 concentrations.

	390 µatm CO_2			1120 µatm CO_2			3000 µatm CO_2		
Day	**C (µg)**	**N (µg)**	***n***	**C (µg)**	**N (µg)**	***n***	**C (µg)**	**N (µg)**	***n***
0	646 ± 168	56 ± 12	36	646 ± 168	56 ± 12	36	646 ± 168	56 ± 12	36
1	789 ± 124	69 ± 9	**9**	674 ± 105	63 ± 7	**9**	687 ± 55	63 ± 4	**10**
4	704 ± 137	64 ± 9	**6**	743 ± 134	71 ± 11	**6**	629 ± 94	61 ± 8	**9**
8	713 ± 74	70 ± 5	**8**	736 ± 63	71 ± 6	**6**	702 ± 108	62 ± 22	**9**
12	719 ± 93	72 ± 9	**9**	747 ± 60	66 ± 22	**9**	672 ± 104	65 ± 8	**8**
15	693 ± 159	71 ± 18	44	788 ± 140	77 ± 17	41	783 ± 132	76 ± 16	43
16	725 ± 85	73 ± 7	**9**	778 ± 58	78 ± 7	**9**	685 ± 67	72 ± 8	**9**

Values are presented as mean ± standard deviation.
C, carbon content; N, nitrogen content; *N*, number of samples; usually 3–4 copepods were pooled for analyses (*n* highlighted in bold); single copepods measurements are indicated by regular numbers.

Table 7. Spearman rank-order correlation analyses between carbon and nitrogen content in *C. glacialis* CV and time during 16 d of incubation on-board RV *Polarstern* in 2012.

[CO_2] (µatm)	**Parameter**	**Correlation coefficient**	***p***
390	C	0.117	0.200
1120	C	0.391	**<0.001**
3000	C	0.299	**<0.001**
390	N	0.471	**<0.001**
1120	N	0.625	**<0.001**
3000	N	0.596	**<0.001**

[CO_2], CO_2 concentration; C, carbon content; N, nitrogen content. Values presented in bold indicate significant correlations between C and N content and time.

There were, however, marked differences in pH between control and high CO_2 mesocosms throughout the study, which allowed for detecting possible changes in feeding activity due to OA.

Ingestion rates are generally sigmoidally related to the food concentration (e.g. Kiørboe *et al.*, 1982; Urban-Rich *et al.*, 2004). Thus, a compensation for elevated energy demands via increased feeding rates is likely only detected under non-limiting food concentrations, as was the case during our study. The final chl *a* content in the incubation bottles at the end of the grazing experiments with *C. finmarchicus* ranged between 5.6 and 9.5 µg l^{-1} (Table 2), which is higher than typically found during spring phytoplankton blooms in western Norwegian coastal areas and the Norwegian Sea (Meyer-Harms *et al.*, 1999; Larsen *et al.*, 2004; Husa *et al.*, 2014) and also above the peak of the artificially induced phytoplankton bloom in the mesocosms which ranged between 3 and 5 µg l^{-1} chl *a*. During the shipboard experiments with *C. glacialis*, final chl *a* concentrations were between 1.4 and 4.3 µg l^{-1} (Table 2), which is similar to bloom conditions in Arctic waters (Wu *et al.*, 2007; Cherkasheva *et al.*, 2014). Furthermore, in both species, IR were not significantly correlated with the chl *a* content, while correlations between CR and chl *a* were either negative or not significant. This also indicates that algae were provided in excess and the copepods were not food limited throughout the grazing experiments. In the 6 l CO_2 incubation bottles on-board RV *Polarstern*, we did not monitor chl *a*. However, we provided algal concentrations which were ~4 times higher than during the incubation for measuring grazing rates while the copepod densities were at maximum only 2.5 times higher when compared with the grazing experiments. In addition, C and N contents of *C. glacialis* increased and we therefore believe that the copepods were not food limited during the long-term incubation.

High food concentrations, on the other hand, might bear the risk that grazing rates of the copepods are already at or close to the maximum physiological feeding capacity. This would hinder the copepods to increase their feeding rates as a response to OA stress. However, Urban-Rich *et al.* (2004) found ingestion rates of up to 0.04 µg chl *a* copepod^{-1} h^{-1} for *C. finmarchicus* CIV and CV while the rates during our experiment did not exceed 0.027 µg chl *a* copepod^{-1} h^{-1}. Also for *C. glacialis*, higher CR and IR than measured in our study were reported (Tande and Båmstedt, 1985). We thus believe that, despite high food supply, the copepods would have been able to increase their grazing rates if environmental hypercapnia had led to additional energy demands.

Our data, however, indicate that elevated seawater pCO_2 did not affect the grazing activity of *C. finmarchicus* and *C. glacialis*, neither after sudden changes in pCO_2 nor after 2–4 weeks of exposure. We found significant differences in grazing between copepods from control and high pCO_2 treatments only on one occasion and there was no consistent trend, neither to higher nor lower grazing activity under OA scenarios. All copepods from control and high pCO_2 treatments were fed with diatoms, i.e. *Thalassiosira weissflogii*, which were grown at control conditions. The copepods thus received food organisms of the same quality. De Kluijver *et al.* (2013) inferred from a calculation of the amount of incorporated ^{13}C during a mesocosm study in an Arctic fjord that the food uptake of *Calanus* spp. decreased at elevated CO_2 concentrations. Their approach, however, addressed both direct and indirect effects of OA, as CO_2 affected the algal community composition in the mesocosms (Brussaard *et al.*, 2013; Leu *et al.*, 2013; Schulz *et al.*, 2013) and therefore the food quality for the copepods.

When ingestion rates are similar, differences in body weight may serve as another indicator for changes in energy demands due to elevated pCO_2, i.e. the copepod body mass may increase to a lesser extent or even decrease if coping with OA stress is energetically costly. In our laboratory experiments, however, the body mass of *C. glacialis* kept at low, medium, and high CO_2 levels was not significantly different and, thus, there was no indication for additional energy demands. Only during the mesocosm experiments, we found significantly lower body mass in *C. finmarchicus* CV from the high pCO_2 mesocosm on 2 d (Days 8 and 15). This may be attributed to lower food quality in high pCO_2 mesocosms as the phytoplankton community changed with pCO_2 (J. R. Bermúdez Monsalve (GEOMAR), pers. comm.). At day 14, nutrients were added, which induced a phytoplankton bloom (KGS and UR, unpublished data). The food availability thus improved in all mesocosms and this could explain why there were no differences in body mass at later sampling dates.

In conclusion, we did not find direct effects of elevated pCO_2 on the copepods grazing rates and body mass, neither in *C. finmarchicus* nor in *C. glacialis*, suggesting that the energy demand of these two *Calanus* species does not increase when exposed to future OA. The mechanisms responsible for the tolerance to OA in *C. finmarchicus* and *C. glacialis*, as was also reported in other studies (Mayor *et al.*, 2007; Weydmann *et al.*, 2012; Niehoff *et al.*, 2013; Hildebrandt *et al.*, 2014), remain unknown. Just recently, a seasonal study on *C. glacialis* has shown that this species strongly regulates its extracellular acid–base status, exhibiting extracellular pH (pH_e) values as low as 5.5 during winter (i.e. during diapause) and high pH_e (7.9) during summer (Freese *et al.*, 2015). Similar mechanisms were also reported from two diapausing Antarctic copepod species (Sartoris *et al.*, 2010; Schründer *et al.*, 2013). Compensating for comparably small shifts in seawater pH due to environmental hypercapnia might therefore not be a challenge for these copepods.

Acknowledgements

We thank J. Büdenbender, D. Freese, and all scientists on site for their help in copepod sampling and sorting during the SOPRAN mesocosm study. Furthermore, we acknowledge the support of S. Koch Klavsen and A. Ludwig in chlorophyll *a* measurements during the mesocosm study and of M. Bullwinkel who measured DIC. N. Knüppel and the officers and crew of RV *Polarstern* are thanked for their help in copepod sampling in Fram Strait. E. Allhusen kindly provided algae cultures. Two anonymous reviewers are thanked for their valuable comments which have improved our manuscript.

Funding

Financial support was provided by the Federal Ministry of Education and Research (BMBF) through the projects SOPRAN (FKZ 03F0611A) and BIOACID (FKZ 03F0608).

References

Alcamo, J., Bouwman, A., Edmonds, J., Grübler, A., Morita, T., and Sugandhy, A. 1995. An evaluation of the IPCC IS92 emission scenarios. In Climate Change 1994, pp. 247–304. Ed. by J. T. Houghton, L. G. Meira Filho, J. Bruce, H. Lee, B. A. Callander, E. Haites, N. Harris, *et al.* Cambridge University Press, Cambridge, New York, Melbourne. 339 pp.

Appelhans, Y. S., Thomsen, J., Pansch, C., Melzner, F., and Wahl, M. 2012. Sour times: seawater acidification effects on growth, feeding behaviour and acid-base status of *Asterias rubens* and *Carcinus maenas*. Marine Ecology Progress Series, 459: 85–97.

Brussaard, C. P. D., Noordeloos, A. A. M., Witte, H., Collenteur, M. C. J., Schulz, K., Ludwig, A., and Riebesell, U. 2013. Arctic microbial community dynamics influenced by elevated CO_2 levels. Biogeosciences, 10: 719–731.

Caldeira, K., and Wickett, M. E. 2003. Anthropogenic carbon and ocean pH. Nature, 425: 365.

Chan, K. Y. K., Grünbaum, D., and O'Donnell, M. J. 2011. Effects of ocean-acidification-induced morphological changes on larval swimming and feeding. The Journal of Experimental Biology, 214: 3857–3867.

Charalampopoulou, A., Poulton, A. J., Tyrrell, T., and Lucas, M. 2008. Surface seawater carbonate chemistry, nutrients and phytoplankton community composition on a transect between North Sea and Arctic Ocean. doi:10.1594/PANGAEA.763990.

Cherkasheva, A., Bracher, A., Melsheimer, C., Köberle, C., Gerdes, R., Nöthig, E.-M., Bauerfeind, E., *et al.* 2014. Influence of the physical environment on polar phytoplankton blooms: a case study in the Fram Strait. Journal of Marine Systems, 132: 196–207.

Conover, R. J. 1988. Comparative life histories in the genera *Calanus* and *Neocalanus* in high latitudes of the northern hemisphere. Hydrobiologia, 167/168: 127–142.

Cripps, G., Lindeque, P., and Flynn, K. J. 2014. Have we been underestimating the effects of ocean acidification in zooplankton? Global Change Biology, 20: 3377–3385.

De Kluijver, A., Soetaert, K., Czerny, J., Schulz, K. G., Boxhammer, T., Riebesell, U., and Middelburg, J. J. 2013. A ^{13}C labeling study on carbon fluxes in Arctic plankton communities under elevated CO_2 levels. Biogeosciences, 10: 1425–1440.

Dupont, S., and Thorndyke, M. C. 2008. Ocean acidification and its impact on the early life-history stages of marine animals. CIESM Workshop Monographs, 36: 89–97.

Falk-Petersen, S., Pavlov, V., Timofeev, S., and Sargent, J. R. 2007. Climate variability and possible effects on arctic food chains: The role of *Calanus*. In Arctic Alpine Ecosystems and People in a Changing Environment, pp. 147–166. Ed. by J. B. Ørbæk, R. Kallenborn, I. Tombre, E. N. Hegseth, S. Falk-Petersen, and A. H. Hoel. Springer, Berlin, Heidelberg. 434 pp.

Freese, D., Niehoff, B., Søreide, J. E., and Sartoris, F. J. 2015. Seasonal patterns in extracellular ion concentrations and pH of the Arctic copepod *Calanus glacialis*. Limnology and Oceanography, 60: 2121–2129.

Friedlingstein, P., Houghton, R. A., Marland, G., Hackler, J., Boden, T. A., Conway, T. J., Canadell, J. G., *et al.* 2010. Update on CO_2 emissions. Nature Geoscience, 3: 811–812.

Frost, B. W. 1972. Effects of size and concentration of food particles on the feeding behavior of the marine planktonic copepod *Calanus pacificus*. Limnology and Oceanography, 17: 805–815.

Guillard, R. R. L. 1975. Culture of phytoplankton for feeding marine invertebrates. In Culture of Marine Invertebrate Animals, pp. 26–60. Ed. by W. L. Smith, and M. H. Chanley. Plenum Press, New York. 338 pp.

Hildebrandt, N., Niehoff, B., and Sartoris, F. J. 2014. Long-term effects of elevated CO_2 and temperature on the Arctic calanoid copepods *Calanus glacialis* and *C. hyperboreus*. Marine Pollution Bulletin, 80: 59–70.

Hirche, H.-J. 1998. Dormancy in three *Calanus* species (*C. finmarchicus*, *C. glacialis* and *C. hyperboreus*) from the North Atlantic. Archiv fur Hydrobiologie Special Issues Advances in Limnology, 52: 359–369.

Husa, V., Kutti, T., Ervik, A., Sjøtun, K., Hansen, P. K., and Aure, J. 2014. Regional impact from fin-fish farming in an intensive production area (Hardangerfjord, Norway). Marine Biology Research, 10: 241–252.

Isari, S., Zervoudaki, S., Saiz, E., Pelejero, C., and Peters, J. 2015. Copepod vital rates under CO_2-induced acidification: a calanoid species and a cyclopoid species under short-term exposures. Journal of Plankton Research, 37: 912–922.

Jaschnov, W. A. 1970. Distribution of *Calanus* species in the seas of the northern hemisphere. Internationale Revue der Gesamten Hydrobiologie und Hydrographie, 55: 197–212.

Jutterström, S., Anderson, L. G., Bates, N. R., Bellerby, R., Johannessen, T., Jones, E. P., Key, R. M., *et al.* 2010. Arctic Ocean data in CARINA. Earth System Science Data, 2: 71–78.

Kiørboe, T., Møhlenberg, F., and Nicolajsen, H. 1982. Ingestion rate and gut clearance in the planktonic copepod *Centropages hamatus* (Lilljeborg) in relation to food concentration and temperature. Ophelia, 21: 181–194.

Kurihara, H., Shimode, S., and Shirayama, Y. 2004. Effects of raised CO_2 concentration on the egg production rate and early development of two marine copepods (*Acartia steueri* and *Acartia erythraea*). Marine Pollution Bulletin, 49: 721–727.

Larsen, A., Fonnes Flaten, G. A., Sandaa, R.-A., Castberg, T., Thyrhaug, R., Erga, S. R., Jacquet, S., *et al.* 2004. Spring phytoplankton bloom dynamics in Norwegian coastal waters: microbial community succession and diversity. Limnology and Oceanography, 49: 180–190.

Lee, R. F. 1974. Lipid composition of the copepod *Calanus hyperboreas* from the Arctic ocean. Changes with depth and season. Marine Biology, 26: 313–318.

Leu, E., Daase, M., Schulz, K. G., Stuhr, A., and Riebesell, U. 2013. Effect of ocean acidification on the fatty acid composition of a natural plankton community. Biogeosciences, 10: 1143–1153.

Lewis, E., and Wallace, D. W. R. 1998. CO2SYS – program developed for the CO_2 system calculations. Report ORNL/CDIAC-105. Carbon Dioxide Information Analysis Center, Oak Ridge National Laboratory, Oak Ridge, TN, USA. 21 pp.

Li, W., and Gao, K. 2012. A marine secondary producer respires and feeds more in a high CO_2 ocean. Marine Pollution Bulletin, 64: 699–703.

Longhurst, A. R. 1985. The structure and evolution of plankton communities. Progress in Oceanography, 15: 1–35.

Marshall, S. M., and Orr, A. P. 1955. On the biology of *Calanus finmarchicus* VIII. Food uptake, assimilation and excretion in adult and stage V *Calanus*. Journal of the Marine Biological Association of the United Kingdom, 34: 495–529.

Mayor, D. J., Everett, N. R., and Cook, K. B. 2012. End of century ocean warming and acidification effects on reproductive success in a temperate marine copepod. Journal of Plankton Research, 34: 258–262.

Mayor, D. J., Matthews, C., Cook, K., Zuur, A. F., and Hay, S. 2007. CO_2-induced acidification affects hatching success in *Calanus finmarchicus*. Marine Ecology Progress Series, 350: 91–97.

McConville, K., Halsband, C., Fileman, E. S., Somerfield, P. J., and Findlay, H. S. 2013. Effects of elevated CO_2 on the reproduction of two calanoid copepods. Marine Pollution Bulletin, 73: 428–434.

Melzner, F., Stange, P., Trübenbach, K., Thomsen, J., Casties, I., Panknin, U., Gorb, S. N., *et al.* 2011. Food supply and seawater pCO_2 impact calcification and internal shell dissolution in the blue mussel *Mytilus edulis*. PLoS ONE, 6: e24223.

Meyer-Harms, B., Irigoien, X., Head, R., and Harris, R. 1999. Selective feeding on natural phytoplankton by *C. finmarchicus* before, during, and after the 1997 spring bloom in the Norwegian Sea. Limnology and Oceanography, 44: 154–165.

Michaelidis, B., Ouzounis, C., Paleras, A., and Pörtner, H. O. 2005. Effects of long-term moderate hypercapnia on acid-base balance and growth rate in marine mussels *Mytilus galloprovincialis*. Marine Ecology Progress Series, 293: 109–118.

Miles, H., Widdicombe, S., Spicer, J. I., and Hall-Spencer, J. 2007. Effects of anthropogenic seawater acidification on acid-base balance in the sea urchin *Psammechinus miliaris*. Marine Pollution Bulletin, 54: 89–96.

Niehoff, B., Schmithüsen, T., Knüppel, N., Daase, M., Czerny, J., and Boxhammer, T. 2013. Mesozooplankton community development at elevated CO_2 concentrations: results from a mesocosm experiment in an Arctic fjord. Biogeosciences, 10: 1391–1406.

Pasternak, A., Arashkevich, E., Tande, K., and Falkenhaug, T. 2001. Seasonal changes in feeding, gonad development and lipid stores in *Calanus finmarchicus* and *C. hyperboreus* from Malangen, northern Norway. Marine Biology, 138: 1141–1152.

Pedersen, S. A., Hansen, B. H., Altin, D., and Olsen, A. J. 2013. Medium-term exposure of the North Atlantic copepod *Calanus finmarchicus* (Gunnerus, 1770) to CO_2-acidified seawater: effects on survival and development. Biogeosciences, 10: 7481–7491.

Pörtner, H. O., Reipschläger, A., and Heisler, N. 1998. Acid-base regulation, metabolism and energetics in *Sipunculus nudus* as a function of ambient carbon dioxide level. Journal of Experimental Biology, 201: 43–55.

Raven, J., Caldeira, K., Elderfield, H., Hoegh-Guldberg, O., Liss, P., Riebesell, U., Shepherd, J., *et al.* 2005. Ocean acidification due to increasing atmospheric carbon dioxide. Policy document 12/05, The Royal Society, London, UK. 60 pp.

Reipschläger, A., and Pörtner, H. O. 1996. Metabolic depression during environmental stress: the role of extracellular versus intracellular pH in *Sipunculus nudus*. The Journal of Experimental Biology, 199: 1801–1807.

Riebesell, U., Czerny, J., von Bröckel, K., Boxhammer, T., Büdenbender, J., Deckelnick, M., Fischer, M., *et al.* 2013. Technical note: a mobile sea-going mesocosm system – new opportunities for ocean change research. Biogeosciences, 10: 1835–1847.

Rosa, R., and Seibel, B. A. 2008. Synergistic effects of climate-related variables suggest future physiological impairment in a top oceanic predator. Proceedings of the National Academy of Sciences of the United States of America, 105: 20776–20780.

Saba, G. K., Schofield, O., Torres, J. J., Ombres, E. H., and Steinberg, D. K. 2012. Increased feeding and nutrient excretion of adult Antarctic krill, *Euphausia superba*, exposed to enhanced carbon dioxide (CO_2). PLoS ONE, 7: e52224.

Sartoris, F. J., Thomas, D. N., Cornils, A., and Schnack-Schiel, S. B. 2010. Buoyancy and diapause in Antarctic copepods: the role of ammonium accumulation. Limnology and Oceanography, 55: 1860–1864.

Schründer, S., Schnack-Schiel, S. B., Auel, H., and Sartoris, F. J. 2013. Control of diapause by acidic pH and ammonium accumulation in the hemolymph of Antarctic copepods. PLoS ONE, 8: e77498.

Schulz, K. G., Bellerby, R. G. J., Brussaard, C. P. D., Büdenbender, J., Czerny, J., Engel, A., Fischer, M., *et al.* 2013. Temporal biomass dynamics of an Arctic plankton bloom in response to increasing levels of atmospheric carbon dioxide. Biogeosciences, 10: 161–180.

Seibel, B. A., Maas, A. E., and Dierssen, H. M. 2012. Energetic plasticity underlies a variable response to ocean acidification in the pteropod, *Limacina helicina antarctica*. PLoS ONE, 7: e30464.

Solomon, S., Quin, D., Manning, M., Alley, R. B., Berntsen, T., Bindoff, N. L., Chen, Z., *et al.* 2007. Technical summary. In Climate Change 2007: The Physical Science Basis. Contribution of Working Group I to the Fourth Assessment Report of the Intergovernmental Panel on Climate Change, pp. 20–91. Ed. by S. Solomon, D. Quin, M. Manning, Z. Chen, M. Marquis, K. B. Averyt, M. Tignor, *et al.* Cambridge University Press, Cambridge and New York. 996 pp.

Tande, K. S., and Båmstedt, U. 1985. Grazing rates of the copepods *Calanus glacialis* and *C. finmarchicus* in arctic waters of the Barents Sea. Marine Biology, 87: 251–258.

Tande, K. S., Hassel, A., and Slagstad, D. 1985. Gonad maturation and possible life cycle strategies in *Calanus finmarchicus* and *Calanus glacialis* in the northwestern part of the Barents Sea. In Marine Biology of the Polar Regions and Effects of Stress on Marine Organisms, pp. 141–155. Ed. by J. S. Gray, and M. E. Christiansen. John Wiley & Sons Ltd, New York. 660 pp.

Tans, P. 2014. Trends in Atmospheric Carbon Dioxide. NOAA/ESRL, Boulder, CO, USA. http://www.esrl.noaa.gov/gmd/ccgg/trends/ (last accessed 23 November 2015).

Thomsen, J., and Melzner, F. 2010. Moderate seawater acidification does not elicit long-term metabolic depression in the blue mussel *Mytilus edulis*. Marine Biology, 157: 2667–2676.

Thor, P., and Dupont, S. 2015. Transgenerational effects alleviate severe fecundity loss during ocean acidification in a ubiquitous planktonic copepod. Global Change Biology, 21: 2261–2271.

Thor, P., and Oliva, E. O. 2015. Ocean acidification elicits different energetic responses in an Arctic and a boreal population of the copepod *Pseudocalanus acuspes*. Marine Biology, 162: 799–807.

Urban-Rich, J., McCarty, J. T., and Shailer, M. 2004. Effects of food concentration and diet on chromophoric dissolved organic matter accumulation and fluorescent composition during grazing experiments with the copepod *C.* finmarchicus. ICES Journal of Marine Sciences, 61: 542–551.

Vargas, C. A., de la Hoz, M., Aguilera, V., San Martin, V., Manríquez, P. H., Navarro, J. M., Torres, R., *et al.* 2013. CO_2-driven ocean acidification reduces larval feeding efficiency and change food selectivity in the mollusc *Concholepas concholepas*. Journal of Plankton Research, 35: 1059–1068.

Weydmann, A., Søreide, J. E., Kwasniewski, S., and Widdicombe, S. 2012. Influence of CO2-induced acidification on the reproduction

of a key Arctic copepod *Calanus glacialis*. Journal of Experimental Marine Biology and Ecology, 428: 39–42.

Widdicombe, S., and Spicer, J. I. 2008. Predicting the impact of ocean acidification on benthic biodiversity: What can animal physiology tell us? Journal of Experimental Marine Biology and Ecology, 366: 187–197.

Wood, H. L., Spicer, J. I., and Widdicombe, S. 2008. Ocean acidification may increase calcification rates, but at a cost. Proceedings of the Royal Society B, 275: 1767–1773.

Wu, Y., Peterson, I. K., Tang, C. C. L., Platt, T., Sathyendranath, S., and Fuentes-Yaco, C. 2007. The impact of the sea ice on the initiation of the spring bloom in the Newfoundland and Labrador Shelves. Journal of Plankton Research, 29: 509–514.

Zhang, D., Li, S., Wang, G., and Guo, D. 2011. Impacts of CO_2-driven seawater acidification on survival, egg production rate and hatching success of four marine copepods. Acta Oceanologica Sinica, 30: 86–94.

Handling editor: Stéphane Plourde

ICES Journal of Marine Science

ICES Journal of Marine Science (2016), 73(3), 937–950. doi:10.1093/icesjms/fsv258

Contribution to Special Issue: 'Towards a Broader Perspective on Ocean Acidification Research'

Original Article

End of the century CO_2 concentrations do not have a negative effect on vital rates of *Calanus finmarchicus*, an ecologically critical planktonic species in North Atlantic ecosystems

Jeffrey A. Runge[1]*, David M. Fields[2], Cameron R. S. Thompson[2], Steven D. Shema[3], Reidun M. Bjelland[3], Caroline M. F. Durif[3], Anne Berit Skiftesvik[3], and Howard I. Browman[3]

[1]*School of Marine Sciences, University of Maine and Gulf of Maine Research Institute, 350 Commercial Street, Portland, ME 04103, USA*
[2]*Bigelow Laboratory for Ocean Sciences, East Boothbay, ME 04544, USA*
[3]*Institute of Marine Research, Austevoll Research Station, Storebø 5392, Norway*

**Corresponding author: tel: +1 207 228 1652; fax: +1 207 773 8672; e-mail: jeffrey.runge@maine.edu*

Runge, J. A., Fields, D. M., Thompson, C. R. S., Shema, S. D., Bjelland, R. M., Durif, C. M. F., Skiftesvik, A. B., and Browman, H. I. End of the century CO_2 concentrations do not have a negative effect on vital rates of *Calanus finmarchicus*, an ecologically critical planktonic species in North Atlantic ecosystems. – ICES Journal of Marine Science, 73: 937–950.

Received 1 July 2015; revised 4 December 2015; accepted 7 December 2015; advance access publication 10 January 2016.

The Subarctic copepod, *Calanus finmarchicus*, is an ecologically critical foundation species throughout the North Atlantic Ocean. Any change in the abundance and distribution of *C. finmarchicus* would have profound effects on North Atlantic pelagic ecosystems and the services that they support, particularly on the coastal shelves located at the southern margins of the species' range. We tested the hypothesis that the physiological rates and processes of *C. finmarchicus*, determining its vital rates, are unaffected by increases in CO_2 concentration predicted to occur in the surface waters of the ocean during the next 100 years. We reared *C. finmarchicus* from eggs to adults at a control (580 μatm, the ambient concentration at the laboratory's seawater intake) and at predicted mid-range (1200 μatm) and high (1900 μatm) pCO_2. There was no significant effect of pCO_2 on development times, lipid accumulation, feeding rate, or metabolic rate. Small but significant treatment effects were found in body length and mass (in terms of dry, carbon and nitrogen mass), notably a somewhat larger body size at the mid-pCO_2 treatment; that is, a putatively beneficial effect. Based on these results, and a review of other studies of *Calanus*, we conclude that the present parameterizations of vital rates in models of *C. finmarchicus* population dynamics, used to generate scenarios of abundance and distribution of this species under future conditions, do not require an "ocean acidification effect" adjustment. A review of research on planktonic copepods indicates that, with only a few exceptions, impacts of increased CO_2 are small at the levels predicted to occur during the next century.

Keywords: climate change, copepods, grazing rate, growth and development rate, negative result, non-effect, Ocean acidification, respiration rate.

Introduction

Predictions of long-term change in pCO_2 and pH in the ocean, and consequences for marine life, has driven intense research activity into the effects of these drivers on marine organisms (e.g. Caldeira and Wickett, 2003; Fabry *et al.*, 2008; Dupont and Pörtner, 2013). Meta-analyses indicate variable responses to pCO_2 among taxa, species within taxa, populations within species, and individuals in any given experiment (e.g. Kroeker *et al.*, 2010; Whiteley, 2011; Garrard *et al.*, 2013; Wittmann and Portner, 2013). While this rapidly growing field of research indicates that some components of marine foodwebs may be vulnerable to ocean acidification, these differences in sensitivity make it difficult to predict the extent to which future change will disrupt ecosystems (e.g. Dupont *et al.*, 2010; Gaylord *et al.*, 2011).

In pelagic ecosystems of the northern North Atlantic Ocean, the Subarctic planktonic copepod, *Calanus finmarchicus*, is an ecologically critical foundation species (Melle *et al.*, 2014; Runge *et al.*, 2015). The lipid-rich stages serve as a primary source of energy to consumers such as herring (*Clupea harengus*), mackerel (*Scomber scombrus*), capelin (*Mallotus villosus*), and sand lance (*Ammodytes*

spp.) that are in turn prey for top predators, including groundfish, tuna (*Thunnus thynnus*), marine mammals, and many seabirds (e.g. Skjoldal, 2004; Baumgartner *et al.*, 2007; Johnson *et al.*, 2011; Trenkel *et al.*, 2014). Since *C. finmarchicus* plays such a crucial role, any impacts of increased pCO_2 would likely have important consequences for coastal and shelf ecosystems of the northern North Atlantic.

Approaches developed to understand and predict population responses of *C. finmarchicus* and other zooplankton species to environmental change involve life cycle modelling (e.g. Carlotti *et al.*, 2000; Maps *et al.*, 2012). Over the past several decades, advances in modelling have made it possible to couple these life cycle models with physical models that simulate water temperature and advective transport, allowing analysis of both the biological and physical processes determining the species' population dynamics (e.g. Speirs *et al.*, 2006; Maps *et al.*, 2011; Hjollo *et al.*, 2012; Curchitser *et al.*, 2013). Decades of research have provided quantitative knowledge of the *C. finmarchicus* physiological rates that are needed to parameterize life cycle models (Melle *et al.*, 2014). These models would have to be re-parameterized if there are significant impacts of increased oceanic pCO_2 on these rates.

In this study, we investigated growth, development, feeding, and respiration rates of *C. finmarchicus* in response to increased dissolved CO_2. We synthesized these findings with results from other studies on *Calanus* spp. to assess the impact of increased pCO_2 levels (predicted by realistic global change scenarios) on the physiological rates and processes in *C. finmarchicus* that determine its vital rates. We also compared the responses of *C. finmarchicus* with reported responses of other species in the genus, and across the Copepoda, in an effort to identify general patterns and mechanisms underlying their responses to future increases in pCO_2.

Material and methods

Experimental design

Eggs were collected from wild-caught females and reared through all life stages in three replicate tanks for each of a control and two pCO_2 treatment levels. Two of the replicate tanks were monitored frequently, as described below, to measure developmental rates, body size, carbon, nitrogen and dry mass of each stage, and lipid accumulation at stage C5, as well as respiration and feeding rates at selected stages. The third replicate tank for each treatment was held under the same experimental conditions and served as a reserve if the two other replicates did not provide a sufficient quantity of samples as the experiment progressed.

Facilities and analysis of carbonate chemistry variables

Experiments were conducted at the Austevoll Research Station, Institute of Marine Research, Norway (60.086 N, 5.262 E). Ambient seawater (serving as the control) was pumped from the Bjørn afjord at a depth of 160 m to the laboratory facilities, where it was first sand filtered then passed through a 20 μm Arcal disc filter before entering the experimental system. The ambient pH ($_{NBS}$) of seawater at the intake depth is ∼7.95, corresponding to a pCO_2 of ∼580 μatm. A depth of 160 m represents the lower end of vertical range of *C. finmarchicus* stages C1–C4 in spring in the Northeast Atlantic and is shallower than overwintering depths of stage C5 (e.g. Williams and Conway, 1988). Water temperature flowing into the preparation room next to the experimental facilities was about 12°C, rising slowly during the experimental period. In the preparation room, a high pCO_2 stock seawater solution was maintained at a pH of ∼5.8. The stock solution was mixed into holding tanks (100 l) to create seawater at treatment pCO_2 levels (ambient control, 1200 and 1900 μatm: Table 1). The pH in each tank was maintained at pre-set pH levels by adding stock solution to the tank using dosage pumps (IWAKI) controlled by feedback from pH electrodes/controllers (Endress and Hauser, Liquiline CM 442). The pCO_2 treatment water in the holding tanks was then pumped to three header tanks in the temperature-controlled (12°C) experiment room and distributed by gravity to the experimental tanks. The water level in the holding tanks was maintained by flotation valves. To maintain stable temperature and pH, water flow into the header tanks was much higher than the flow from header tanks to the experimental tanks. The 40 l experimental tanks, identical for all treatments, were 44 cm in diameter and made of high-density polyethylene (HDPE). The inlet tube into each experimental tank was fitted with a 60 μm mesh nitex screen, cleaned periodically to prevent contamination of the tank by microplankton from the plumbing system. The flow rate of water into the experimental tanks varied between 5 and 12 l h^{-1}. Water in the experimental tanks drained through a screen (70 μm) placed over a perforated 35 mm diameter plastic standpipe running the height of the tank. This setup ensured very low exit flow rates at any point along the tube. As the copepods grew during the experiment, the size of the exit screen was increased to 150 μm. Early life stage copepods in close vicinity of the exit pipe could easily swim away from the suction and were not drawn back in, with no indication of stress or abnormal behavior. This system provided a sufficiently gentle environment for rearing copepod life stages while maintaining high water replacement within the tanks and stable pCO_2 treatment levels.

Routine measurement of tank conditions and analysis of carbonate chemistry were conducted to assess consistency of conditions during the experiment. Temperature and salinity in the tanks were measured daily with a hand-held multimeter (Cond 340i conductivity meter: WTW, Germany). The pH level in each exposure tank was measured daily in a 100 ml sample using a Mettler-Toledo pH meter equipped with a Mettler-Toledo InLab® ExpertPro pH-probe, calibrated with 4.00, 7.00, and 9.00 buffers (Certipur® buffer solutions, Merck KGaA, 64271 Darmstadt, Germany, traceable to standard reference material from NIST (NBS) (Andersen *et al.*, 2013). The daily electrode pH (mV) was corrected to the spectrophotometrically determined pH (pH_{tot}; see below) by plotting the mV from the pH electrode as a function of the (pH_{spec}). Over the course of the experiment electrode voltage was highly correlated with pH_{spec} measurements ($r^2 = 0.985$; Pearson Coeff. $= -0.992$; $p << 0.001$; $n = 15$).

The $pH_{(tot)}$ was measured spectrophotometrically twice per week (Hitachi U-2900 dual-beam) using the pH sensitive indicator dye m-cresol purple (Sigma-Aldrich) following SOP (standard operating procedure 6b: Dickson, 2007). Samples of seawater were collected in 20 ml glass scintillation vials (leaving no head space) from all experimental vessels and held in a dark, 12°C water bath for temperature equilibration. Preliminary experiments confirmed no deterioration in measured pH values during the first 8 h after sampling, and pH was always measured within 3–5 h of sample collection. To make each pH measurement, 12 ml of each sample was slowly pipetted into two quartz cuvettes with a 5 cm path length (a modification of the 10 cm path length in SOP 6b). The cuvettes were sealed with a Teflon cover, and held at 12°C in the temperature-controlled chamber of the spectrophotometer. M-cresol purple (10 μl) was added to the sample cuvette, while the second cuvette

Table 1. Mean carbonate chemistry during the 5 weeks incubation.

Treatment (pCO_2)	A_T (µmol kg^{-1})	N (µmol kg^{-1})	P (µmol kg^{-1})	Si (µmol kg^{-1})	C_T (µmol kg^{-1})	HCO_3^- (µmol kg^{-1})	CO_3^{2-} (µmol kg^{-1})	CO_2 (µmol kg^{-1})	pCO_2-calculated (µatm)	$pH_{(Tot)}$ calculated	Ω_{Ar}	Ω_{Ca}
Control	2316.74 (10.26)	11.20 (0.74)	2.25 (0.96)	6.98 (1.06)	1745.55 (733.73)	2033.33 (11.68)	113.05 (8.56)	23.51 (2.87)	584.3 (71.5)	7.90 (0.04)	1.72 (0.13)	2.69 (0.20)
Mid	2317.31 (7.49)	9.84 (0.23)	1.31 (0.39)	6.26 (0.59)	2272.17 (23.08)	2159.86 (28.12)	62.82 (13.37)	49.49 (8.62)	1232.3 (216.3)	7.61 (0.09)	0.96 (0.20)	1.50 (0.32)
High	2315.43 (6.90)	9.90 (1.98)	1.42 (0.67)	6.28 (0.74)	2330.60 (6.06)	2213.10 (3.64)	40.56 (3.04)	79.95 (7.03)	1912.8 (173.9)	7.42 (0.04)	0.62 (0.05)	0.97 (0.07)

Total alkalinity (A_T), total inorganic carbon (C_T), phosphate and silicate concentrations were collected from one of the replicate tanks every 7–10 d ($n = 3$) and at the beginning and end of the experiment in the other two replicate tanks. Inorganic carbon species, pCO_2, $pH_{(Tot)}$ and the saturation state of aragonite (Ω_{ar}) and calcite (Ω_{ca}) were calculated using CO2sys v2.1. Numbers in parentheses are *SD*.

served as a reference. Absorbance was measured at 578 nm (A1), 434 nm (A2), and 730 nm (background). The sample cuvette was inverted three times and the absorbance was re-measured at the three wavelengths. We used equations in section 8.3 of SOP 6b to correct A1/A2 for the addition of dye. The pK2 and final pH value was determined from Liu *et al.* (2011, equation 18).

Carbonate chemistry was determined from total dissolved inorganic carbon (C_T), total alkalinity (A_T), temperature, salinity, and nutrients (phosphate, silicate, and nitrate). Water was taken from all replicate tanks during the first and third weeks and at the end of the experiment and stored in a 1 l borosilicate flask with a ground glass stopper. The samples were poisoned with a saturated mercuric chloride solution (Riebesell *et al.*, 2010) and stored in the dark at 8°C until analysis. Dissolved inorganic carbon (C_T) was analysed by coulometric titration (Dickson, 2007) using a CM5015 coulometer (UIC Inc., USA) connected to a VINDTA 043 (Marianda, Germany) after acidification with 8.5% phosphoric acid. A_T was analysed by potentiometric titration (Dickson, 2007) in an open cell with 0.1 M HCl using a VINDTA 042 (Marianda, Germany). Certified reference material provided by Andrew Dickson (Scripps Institution of Oceanography, San Diego, USA) was used to calibrate C_T and A_T measurements. An additional sample (20 ml) was collected, passed through a sterile 0.2 µm cellulous acetate syringe membrane filter (VWR-USA), and stored in HDPE bottles with HDPE caps with 50 µl of chloroform added. These samples were analysed for silica, phosphorus, and nitrogen. Carbonate chemistry parameters including $pH_{(T)}$ were calculated using CO2SYS2.1 (Lewis *et al.*, 1998) with the standard set of carbonate system equations and constants of Mehrbach *et al.* (1973) after applying the refit of Dickson and Millero (1987).

Phytoplankton culture and food distribution

The copepods were fed an algal mixture consisting of the cryptophyte, *Rhodomonas baltica* (6–8 µm equivalent spherical diameter, ESD), the prymnesiophyte, *Isochrysis galbana* (4–5 µm ESD), and the diatoms, *Skeletonema costatum* (6–7 µm ESD) and *Chaetoceros mulleri* (4–6 µm ESD). The algae were cultured at 22°C in the phytoplankton culture facility at the Austevoll Research Station. Unialgal batch cultures were incubated in Superba^{TM} NPK 14-4-21 in 100 l cylindrical plastic bags bubbled with CO_2-mixed air under a 24 h light cycle at average light intensities of 100 µE m^{-2} s^{-1}. The batch cultures were harvested in the exponential growth phase. Daily subsamples from the batch cultures were counted and sized using a Z2 Beckman Coulter Counter. Carbon content per cell (*R. baltica*: 18.1 pg cell^{-1}; *I. galbana*: 8.9 pg cell^{-1}; *S. costatum*: 7.9 pg cell^{-1}; *C. mulleri*: 8.1 pg cell^{-1}) was determined from existing carbon volume conversion equations (Strathmann, 1967; Menden-Deuer and Lessard, 2000). The volume of stock culture of each species needed to provide a 50:20:15:15 carbon ratio of *R. baltica*, *I. galbana*, *S. costatum*, and *C. mulleri*, respectively, to the control and treatment tanks was determined periodically. The food mixture was distributed from a 5 l reservoir to each tank using a peristaltic pump to maintain a nominal concentration of 600 µg C l^{-1}, taking into account the average water exchange rate of 10 l h^{-1}. Typical hourly dosage volumes (50–120 ml) of phytoplankton stock solution, with lower pCO_2, were less than 1% of tank volume and did not alter treatment or control levels. Phytoplankton cell concentrations in each tank were monitored daily by counting subsamples using a Coulter Counter, following the methods described in Kim and Menden-Deuer (2013).

Initiation of the experiment

Calanus finmarchicus adult females used to inoculate the control and treatment tanks with eggs were collected in Bjørn afjord using either a light trap or plankton net. A light trap (500 μm mesh BellaMare) was deployed for ~10 h at night from the dock at the research station (water depth: 40 m) at a depth of 20–30 m. Alternatively, copepods were collected using a 0.5 m diameter plankton net towed obliquely at low speed from ~300 m to the surface in the adjacent fjord (water depth: 500 m). The animals were transported to a cold room (12°C) in the laboratory where females were sorted. Females were maintained in large egg separators in 15 l of ambient control seawater and fed the stock algal culture at a concentration sufficient to support maximum feeding rates (i.e. >600 μg C l^{-1}). The containers were routinely monitored for egg production rate and hatching success until the start of the experiment.

The experiment was designed to ensure that all the tanks received eggs from the same population of females and had staggered start dates to allow the team of 2–4 people sufficient time to sample and analyse each tank over the duration of the experiment. Females were evenly divided among four egg separators and immersed in an experimental tank. The egg separators (6 l) were constructed from 25 cm diameter PVC cylinders with a 500 μm nitex mesh bottom that retained females but allowed eggs to pass through. The females were fed using the food distribution system described above. After the females had released eggs for 24–26 h, the cylinders were transferred to the next experimental tank. Tanks were transitioned to the appropriate pCO_2 treatment source immediately after inoculation. The total number of eggs in each tank varied between 13 000 and 55 000 (Table 2). Inoculations of replicate treatment tanks were staggered in a semi-random order. The A and B replicates were used for routine sampling of copepods for the measurements described below. One of the treatment replicates (High A: Table 2) was short lived and had to be restarted (High A, restart). A third replicate (Tank C) was also initiated as a backup for each treatment. Because of the late restart of High A, which did not complete the full developmental cycle by the termination of the experiment, samples of females were taken from High C to supplement measurements of mass for this treatment.

Biological measurements

Individual *C. finmarchicus* (average number: 37) were sampled daily from each tank to assess developmental progress. Age zero for each tank was set at 13 h, the midpoint after the start of inoculation with

Table 2. Daily measurements and tank inoculations.

pH treatment Replicate tank	Inoculation start date *N* (d)	Female number Duration (h)	Egg number EPR	Food (μgC $^{-1}$)	Temp (°C)	Salinity (PSU)	pH (NBS)
Control	1 May 2013	523	13 000	675	12.65	35.11	7.94
A	28	26	24	± 97	± 0.04	± 0.01	± 0.006
Control	8 May 2013	847	43 000	479	12.75	35.12	7.93
B	27	26	47	± 62	± 0.04	± 0.01	± 0.005
Control	4 May 2013	523	31 000	397	12.74	35.13	7.94
C	31	42	34	± 51	± 0.04	± 0.01	± 0.003
Mid	3 May 2013	523	17 000	685	12.73	35.11	7.63
A	33	26	31	± 94	± 0.04	± 0.01	± 0.004
Mid	6 May 2013	847	37 000	443	12.77	35.13	7.62
B	30	26	41	± 52	± 0.04	± 0.01	± 0.004
Mid	9 May 2013	820	44 000	506	12.79	35.13	7.62
C	28	26	50	± 70	± 0.04	± 0.01	± 0.005
High	2 May 2013	523	16 000	573	12.49	35.1	7.49
A	8	26	27	± 155	± 0.04	± 0.00	± 0.015
High	7 May 2013	847	40 000	658	12.8	35.14	7.5
B	22	26	44	± 126	± 0.03	± 0.02	± 0.007
High	11 May 2013	810	48 000	493	12.73	35.13	7.49
C	29	26	55	± 61	± 0.03	± 0.01	± 0.004
High	15 May 2013	800	55 000	782	12.75	35.13	7.51
A, restart	26	26	64	± 136	± 0.03	± 0.01	± 0.005

Treatment (pCO_2)	Replicate	pH (NBS) Electrode	pH (Tot) Spec
Control	1	7.94 (0.03)	7.918 (0.012)
	2	7.94 (0.03)	7.925 (0.055)
	3	7.95 (0.02)	7.918 (0.012)
Mid	1	7.63 (0.03)	7.618 (0.012)
	2	7.64 (0.06)	7.611 (0.011)
	3	7.63 (0.03)	7.621 (0.015)
High	1	7.50 (0.04)	7.530 (0.067)
	2	7.51 (0.08)	7.507 (0.073)
	3	7.50 (0.03)	7.503 (0.038)

Experimental tank inoculations were staggered in a random order. Number of eggs starting in each tank estimated from the number of females, the inoculation duration and the estimated egg production rate (EPR: eggs female^{-1} d^{-1}) from measurements made near the start, middle, and end of the inoculation period. The daily sampling data begins on the third day after inoculation and continues to the conclusion of that tank (*N*: total duration of sampling period). Temperature, salinity, pH (calibrated electrode readings), and cell counts were measured daily. Food concentration was determined by multiplying cell counts and pg C per algal cell. Mean and standard errors are provided.

Temperature (mean ± SD; $n = 43$), salinity (mean ± SD; $n = 43$), and pH (calibrated electrode; mean ± SD; $n = 43$) values for each treatment during the 5-week incubation. pH (mean ± SD; $n = 10$) was also measured spectrophotometrically twice a week.

females which lasted for 26 h. Animals were subsampled with a large bore pipette immersed in different locations in the tank to obtain a random sample. Each sample was examined (staged and photographed) under a Leica MS5 dissecting scope fitted with a Planapo ×1.0 magnifier and an Olympus DP70 digital camera. The photographs were analysed for body length (nauplius stages) and prosome length (copepodid stages) using ImageJ software (NIH, USA). The area of the lipid oil sac in stage C1–C5 was measured using ImageJ software, and the lipid (wax ester) weight calculated directly from the oil sac area using the perimeter line method (Vogedes *et al.*, 2010).

Additional specimens of the developing life stages were removed from the experimental tanks every 1–3 d (over a 7- week period) to measure dry weight and C and N mass, using methods similar to those reported in Campbell *et al.* (2001). Dry weights of eggs and stages N1–C4 were measured by pipetting a known number of single stage animals onto a pre-combusted 25 mm diameter glass fibre filter mounted on a filter holder and connected to a vacuum pump used to gently suction off seawater. The filter was rinsed with a standard amount of distilled water (3 ml). Controls were routinely run to account for loss in filter weight by this process, presumably from loose fibres that were suctioned off with the water. The preweighed filters were dried in an oven at 60°C for 24–48 h, reweighed to the nearest 1 μg on a Mettler-Toledo UMX2 microbalance, then folded into tin boats for C:H:N analysis. Some of the stage C4, and all the stage C5 and adult animals, were rinsed then placed individually into preweighed tin boats, which were then dried in the oven and re-weighed. The samples were taken back to the Darling Marine Center (Walpole, ME, USA) for measurement of C and N content. Those samples were combusted with a Perkin Elmer 2400 Series II CHNS/O analyser equipped with a thermal conductivity detector using ultra high purity helium as a carrier gas. While the dry weight and carbon mass of individual C5 and early adult stages were well above instrument levels of sensitivity, the N mass of individual C5 and early-stage adults was near the limit of sensitivity of the C:H:N analyser. Individual N masses that were <1 SD above the N blank were discarded as unreliable, resulting in the loss of 32 observations.

Ingestion rate experiments were performed using C5 stage *C. finmarchicus* reared in the experimental tanks. The experiments were run for 24 h in the dark at 13°C, with the animals feeding on the cryptophyte, *Rhodomonas baltica* (Equivalent Spherical Diameter: 6.0 μm) with a measured concentration of 2×10^4 cells ml^{-1} (760 μg C l^{-1}). Copepods from the three pCO_2 treatment levels were handpicked and placed into 2 l flasks at a concentration of four copepods per l. Algal concentrations at the start of the experiment were measured in triplicate using a Beckman Z2 Coulter Counter which required a total of 3 ml of sample (0.15% of total volume). Removed fluid was replaced with the same quantity of fluid at approximately the same algal concentration to ensure that no air bubbles were present in the feeding container. The combination of jar size and the number of copepods used was chosen such that changes in phytoplankton cell numbers due to grazing would be detectable (>5% decrease) yet would not deplete cell concentrations by >25%. Three control flasks (containing algae but no copepods) and three experimental replicates were used for each treatment. All experimental and control flasks were gently turned on a plankton wheel at 0.5 rpm to maintain algae in suspension. After 24 h, each jar was removed from the plankton wheel, and a 1 ml subsample (in triplicate) was withdrawn with a pipette for immediate cell counts. Initial and final cell concentrations were measured in each flask, such that each replicate provided an independent estimate of grazing or phytoplankton growth rate. Contents were then poured through a 100 μm Nitex screen to recover the animals. Copepods were counted and their number, stage, and viability verified. Only live animals were used in the grazing rate calculations. Ingestion rates were calculated based on the equations in Frost (1972).

Oxygen consumption rates (*OCR*s) were measured using animals collected from each replicate tank and sorted for stage and sex (adult) under a binocular microscope. The animals were transferred to the experimental chambers (4.8 ml) filled with seawater (containing no air spaces) from their individual tanks. Experimental chambers were sealed with a ground glass top equipped with a small hole (0.4 mm) to accommodate the oxygen sensitive microelectrode. Between 10 and 30 individuals were used to measure the respiration rates of stages N3 and N6 and 1–5 individuals for adults. Dissolved oxygen concentrations were measured with a Clark-type oxygen microelectrode (Unisense; Aarhus, Denmark). The linear response of each electrode was calibrated with 0.2 μm filtered seawater bubbled for a minimum of 1 h to set the 100% dissolved oxygen calibration point. The anoxic calibration point was determined by placing seawater into a silicone tube that was immersed in a solution of 0.1 M sodium ascorbate and 0.1 M sodium hydroxide for over 4 h. All oxygen measurements were made at 13°C ($\pm$0.01°C) in a ThermoScientific water bath (Model A10B with thermostat SC100). Oxygen concentrations within the chambers, measured every 2 s for up to 1.5 h, never decreased by >20% below saturation. Control chambers without animals were used to monitor oxygen changes due to microbial/algal respiration. Oxygen consumption was computed as the difference between the beginning and end of the incubation, corrected for changes in the control bottles. Data were normalized per unit dry weight obtained from both direct measurements and compared with literature data (Cohen and Lough, 1981).

Data analysis

ANOVA was used to test for differences in experimental conditions among the tanks, and to test for differences among the control and two pCO_2 treatments in the biological variables. When the assumption of normality was not met, non-parametric tests were applied, as specified below. Except where noted, MATLAB statistical software was used to conduct the analyses.

To estimate instantaneous growth rate (g), we applied an exponential growth model ($W_t = W_0e^{gt}$), where W is mass (in terms of dry weight, carbon, or nitrogen), g is growth rate (d^{-1}) and t is age (d). Since the same females were used to inoculate each set of replicate tanks, and egg mass is assumed to be invariant (Runge, 1984), we used a common initial mass for stage N3 (W_0), using values for egg dry weight, C and N mass from Campbell *et al.* (2001) and assuming no weight loss between during the non-feeding stages N1 and N2. Before fitting the data to the model, measurements of individual copepods were averaged according to stage, sampling day, treatment and replicate tank. The mean measurements were more consistent across stages since observations of younger stages were based on up to 100 animals. Exponential growth between stage N3 and early-stage females was assumed. After 32 d, the mass of females is assumed to be constant as energy in females is shunted to egg production (Myers and Runge, 1983). Growth equations were fit to data using the MATLAB fit function.

The effect of pCO_2 treatment on growth rate (stages N6 to early adult) was investigated using ANCOVA, after preliminary exploration to detect outliers and heterogeneity of variance (Zuur *et al.*, 2009). Mass was ln-transformed since it increases exponentially with age and ANCOVA assumes linear relationships. Age was set as the continuous explanatory variable and pCO_2 treatment as the co-factor. Residual plots for the model were inspected and revealed no violation of homoscedasticity. This analysis was conducted in the "R" statistical and programming environment.

Results

Conditions in the control and experimental tanks are summarized in Tables 1 and 2. Calculated CO_2 values were 584 (71.5 SD) μatm, 1232 (216.3) μatm, and 1912 (173.9) μatm for ambient mid and high pCO_2 treatments. Spectrophotometrically measured $pH_{(T)}$ values were 7.920(0.004 SD), 7.617 (0.005 SD), and 7.513 (0.014 SD) for the ambient, mid and high pCO2 treatments, respectively. These values agreed well with the calculated (CO2SYS2.1) pH values for the ambient and mid treatments. For the highest pCO_2 treatment, calculated values underestimated measured $pH_{(T)}$ by 0.09 pH units. The pH within individual tanks remained stable over time and was consistent between replicate tanks. There were no significant differences in daily $pH_{(NBS)}$ among replicates within each treatment (one-way ANOVA, Control: d.f. = 85, $F = 2.45$, $p = 0.09$; Mid: d.f. = 90, $F = 0.3$, $p = 0.74$; High: d.f. = 84, $F = 1.93$, $p = 0.13$). Daily $pH_{(NBS)}$ values (SE < 0.01) were 7.94; 7.62 and 7.50 for ambient, mid and high pCO_2 treatments, respectively (Table 2). The seawater temperature in control and treatment tanks increased throughout the experiment, likely reflecting warming of ambient seawater at the intake, resulting in a net 0.5°C increase across the experiment. The short-lived treatment tank (High A: Table 2) had the lowest mean temperature (12.49°C). Excluding this tank, the overall mean temperature was 12.7°C, with no significant differences among tanks (one-way ANOVA: d.f. = 253, $F = 1.17$, $p = 0.32$). There was no observable change in salinity (overall mean: 35.12) over the course of the experiment.

The overall mean food concentration for the treatment tanks was 564 μg C l^{-1} (Table 2). However, the variance of food concentration in each tank was higher in the first set of replicates (Bartlett test of equal variance; $T = 48.9$; d.f. = 9; $p < 0.001$) which was a consequence of refinements to improve food distribution as the experiment progressed. Food levels were above the critical concentration for *Calanus* species (Frost, 1972; Runge, 1985; Hirche *et al.*, 1997).

Overview of biological measurements

We were able to successfully rear *C. finmarchicus* adults from eggs spawned by wild females at the control (584 μatm), mid-level (1232 μatm), and high-level (1912 μatm) pCO_2 concentrations. In all treatments, the nauplius and copepodid stages appeared healthy and exhibited normal swimming behaviours and evasion responses to our pipettes during sorting.

While we did not quantitatively measure survival rates, we noted large numbers of developing stages in all nine treatment tanks. The one high pCO_2 replicate (High A: Table 2) that suffered high mortality between stage N3–C1 was re-inoculated and had developed successfully to C1 at the time when the entire experiment was terminated. The reason for the crash of this one tank is not known, but there is no evidence that it was due to the pCO_2 treatment. Data from the samples collected from this tank are included in the figures and analyses below.

Development time

Copepod stages were enumerated and summed across replicate tanks on each age day for which there were samples. Development times at control and treatment levels were similar whether calculated as cumulative percentage (Campbell *et al.*, 2001) or weighted stage value (Figures 1 and 2). There was an initial delay of 1–2 d in transition from stages C4 to C5 in the high pCO_2 treatment. However, development at the high pCO_2 treatment returned to the same trajectory as the other treatments within several days and moulting to the adult stage occurred at the same time in all tanks. A Wilcoxon rank-sum test confirmed that there were no significant differences in development time among pCO_2 levels (Control vs. High: $Z = 0.07$, $p = 0.95$; Control vs. Mid: $Z = 0.38$, $p = 0.70$; Mid vs. High: $Z = 0.48$, $p = 0.63$).

Prosome length

There was a small but discernible pCO_2 treatment-related difference in prosome length with respect to age across all stages (ANCOVA: d.f. = 3398, $F = 29$; $p < 0.005$; nauplius $n = 1421$, copepodid stages $n = 1899$, adult females $n = 84$), although there was no consistent trend (Figure 3). The mid-pCO_2 treatment had the largest adjusted (age effect removed) overall mean prosome length 1.035 mm, significantly greater, by ~5%, than the adjusted mean prosome length of both the control (0.989 mm) and high pCO_2 (0.974 mm) treatments, which were not statistically different. Removal of females and nauplii from the analysis did not change this result; the mid pCO_2 adjusted mean prosome length (1.480 mm) was still significantly larger (ANCOVA, d.f. = 2652, $F = 48$, $p < 0.005$) than the control (1.442 mm) and high treatment lengths (1.388 mm). However, the mean prosome length of females in the ambient control (2.568 mm) is significantly larger (ANCOVA, d.f. = 80, $F = 11.1$, $p < 0.005$), by ~6 and 9%, respectively, than the mid (2.431 mm) and high treatment females (2.354 mm). Over the entire dataset, an analysis of covariance attributes <0.2% of the variance to treatment, with the rest of the non-residual variance attributed to age.

Growth rates: dry, carbon, and nitrogen mass

Across all treatments, the dry weight, nitrogen, and carbon mass of *C. finmarchicus* increased exponentially throughout development (Figure 4). Growth rates are more accurately estimated from mass and age in days, regardless of the stage structure on any given day (Figure 5). Fitted growth estimates (to mass and age in days, Figure 5) across the control and elevated pCO_2 treatments ranged between 0.23 and 0.24 d^{-1} in terms of dry weight and C mass, and between 0.21 and 0.22 d^{-1} in terms of N mass (Table 3). ANCOVA analysis showed a significant effect of treatment on overall dry weight, C and N mass (small differences in intercept, notably for the mid pCO_2 treatment) but the interaction term was not significant when related to age. In other words, the rate at which mass increased over time (i.e. growth) was not significantly different between control and treatments (Table 4).

The C:N ratio increased from an overall mean of 4.0 at Stage C1 to 7.9 at Stage C5, reflecting accumulation of lipid mass during copepodid growth. There was no consistent difference in C:N ratio across stages and treatments.

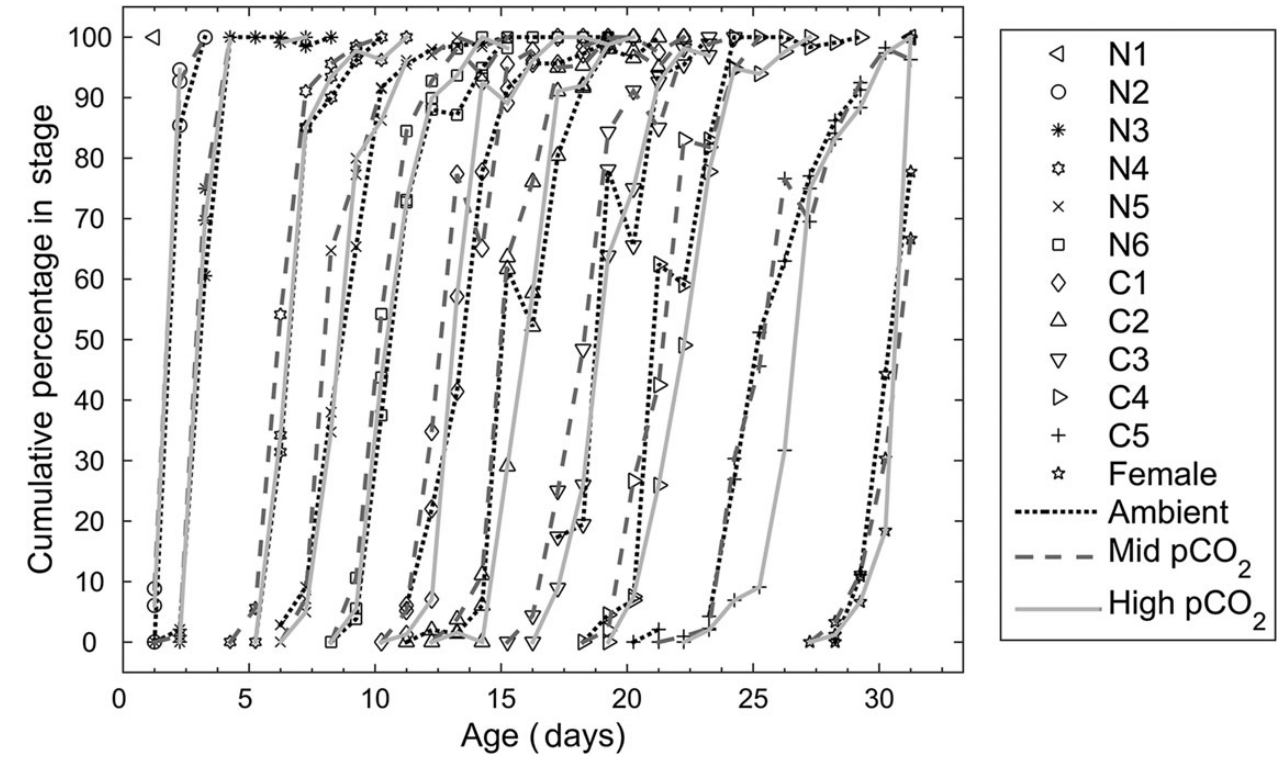

Figure 1. *Calanus finmarchicus*. Stage progression showing development time. Cumulative percentage of copepods (the percentage greater than or equal to a given stage at each sample time) for both replicates of each treatment (ambient mid CO_2 and high CO_2) as shown.

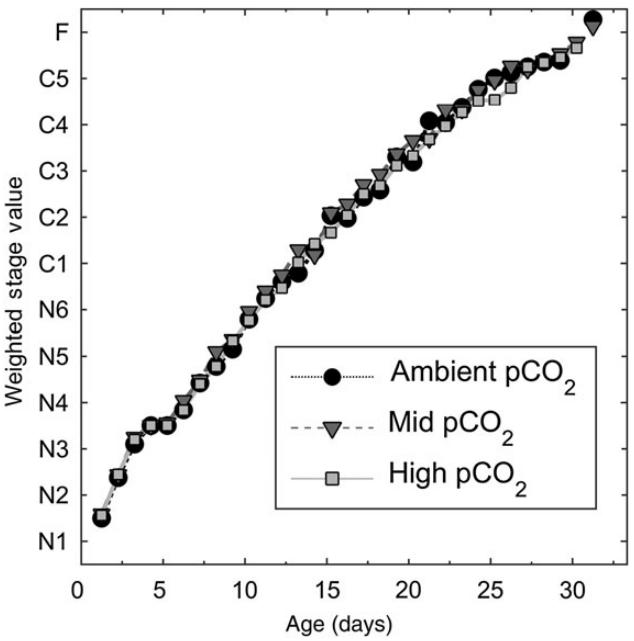

Figure 2. *Calanus finmarchicus* Stage progression in each OA treatment shown by weighted stage value. The weighted stage value determined at each sampling date is equal to the sum of each stage fraction multiplied by its weight (N1 = 1, N2 = 2, N3 = 3 . . . C1 = 7, C2 = 8, C3 = 9 . . . C6 = 12).

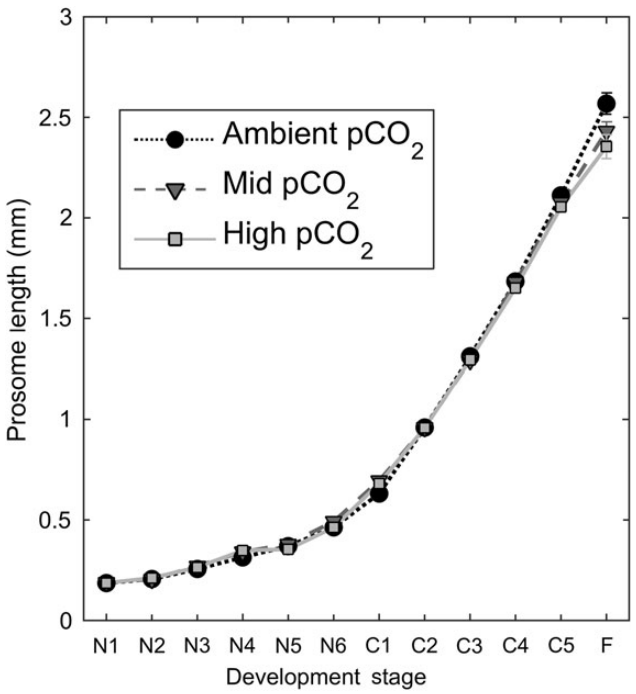

Figure 3. *Calanus finmarchicus* mean prosome length and 95% confidence intervals at each stage in each treatment.

Lipid accumulation

Lipid mass was estimated in 107 mature stage C5 copepods (within 3 d of moulting to adult) from control and higher pCO_2 tanks. The mean lipid/dry mass ratio varied between 26 and 31% and was not significantly different (one-way ANOVA (F (2, 104) = 1.2, $p = 0.305$) among treatments (Figure 6).

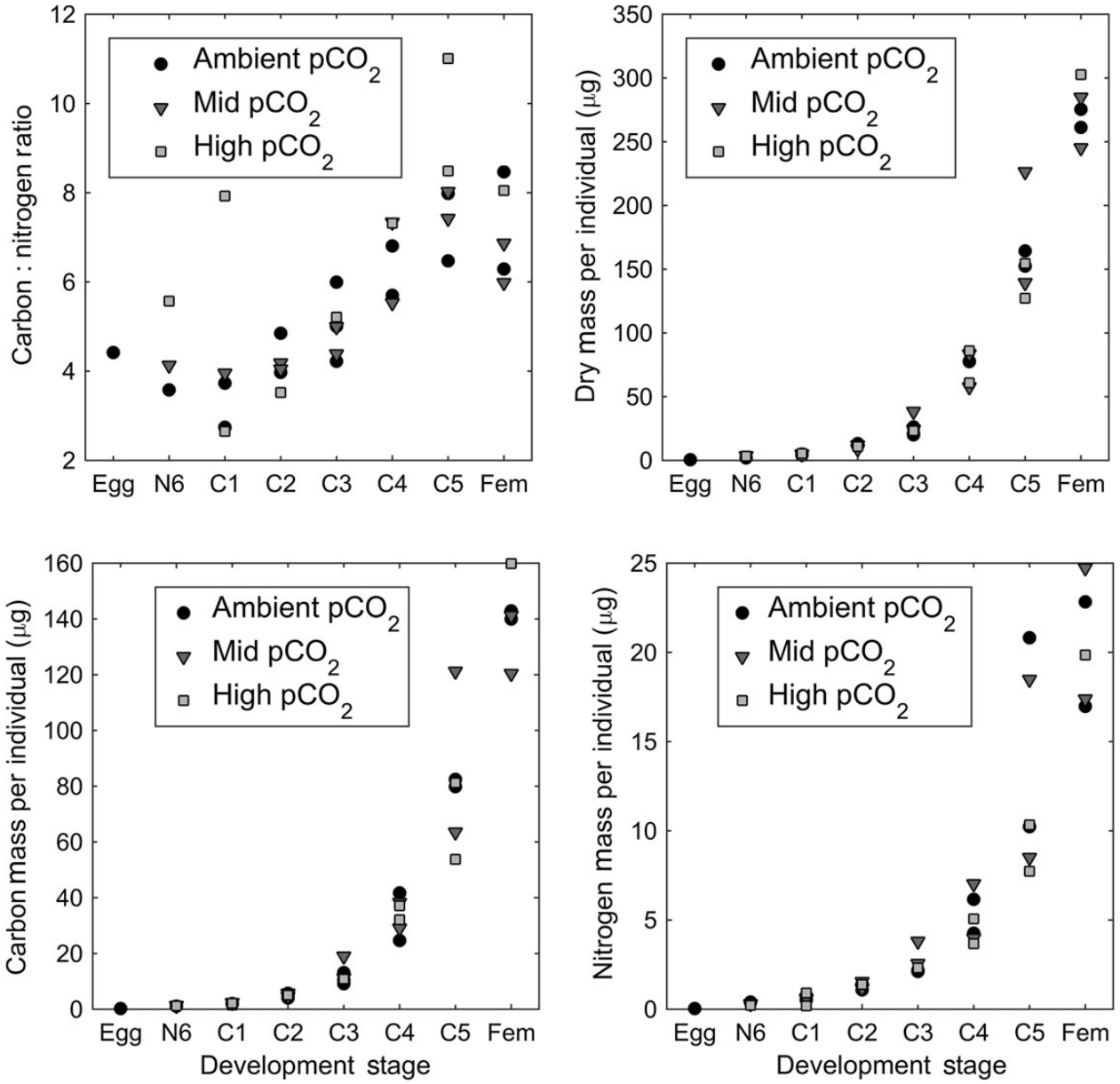

Figure 4. *Calanus finmarchicus*. Dry, carbon, and nitrogen mass (μg) as well as carbon to nitrogen ratio at each stage and treatment: ambient control (circles), mid CO_2 (triangles), and high CO_2 (squares). All replicates are shown. Mass of adult females was measured in only 1 replicate tank for the high CO_2 treatment; the experiment was terminated before individuals from the other high treatment tanks attained adult stage.

Ingestion rates

There were no significant differences in the ingestion rates of *C. finmarchicus* stage C5 reared at different pCO_2 levels (Figure 7: one-way ANOVA; (F (2, 26) = 0.51; p = 0.61). Animals consumed on average 2.2 × 10^5 cells copepod^{-1} d^{-1} (8.37 μg C d^{-1}) with average clearance rates of ~11.0 ml copepod^{-1} d^{-1} at cell concentrations of 2.0 × 10^4 cells ml^{-1}. Total daily ingestion rates were ~10.0% of the average body carbon (Figure 4) for stage C5. This is consistent with the maximum reported rate for adult females of this species (Mauchline, 1998).

Oxygen consumption rates

OCR increased as a function of copepod stage in all pCO_2 treatments. There was no significant difference in *OCR* between the pCO_2 treatments (ANOVA: $p > 0.5$ for N3, N6, C5, Adults). The average *OCR* for adult females at 13°C was 44 nmol O_2 ind^{-1} h^{-1}. The data were fit to a modified exponential curve as a function of stage, $OCR = \exp(6.55(S - -0.69))$, where S = the numerical equivalent for each stage of the copepod (d.f. = 13, F = 221.3, $p < 0.0001$: Figure 8). As a function of dry wt. (DW), *OCR* increased linearly, as $OCR = 0.10 + 0.15 \times DW$, $F(2,13) = 259.4$, $p = <0.001$: Figure 9). When normalized to the copepod's dry weight, the *OCR* decreased linearly with stage, indicating that N6 stage animals consumed 400% more oxygen per unit dry weight than adult females (Figure 9).

Discussion

Effect of pCO_2 on *Calanus finmarchicus* vital rates

Oceanic pCO_2 concentrations predicted to occur during the next century did not directly affect *C. finmarchicus* development rate, growth rate, respiration rates, and feeding rates. Further, our

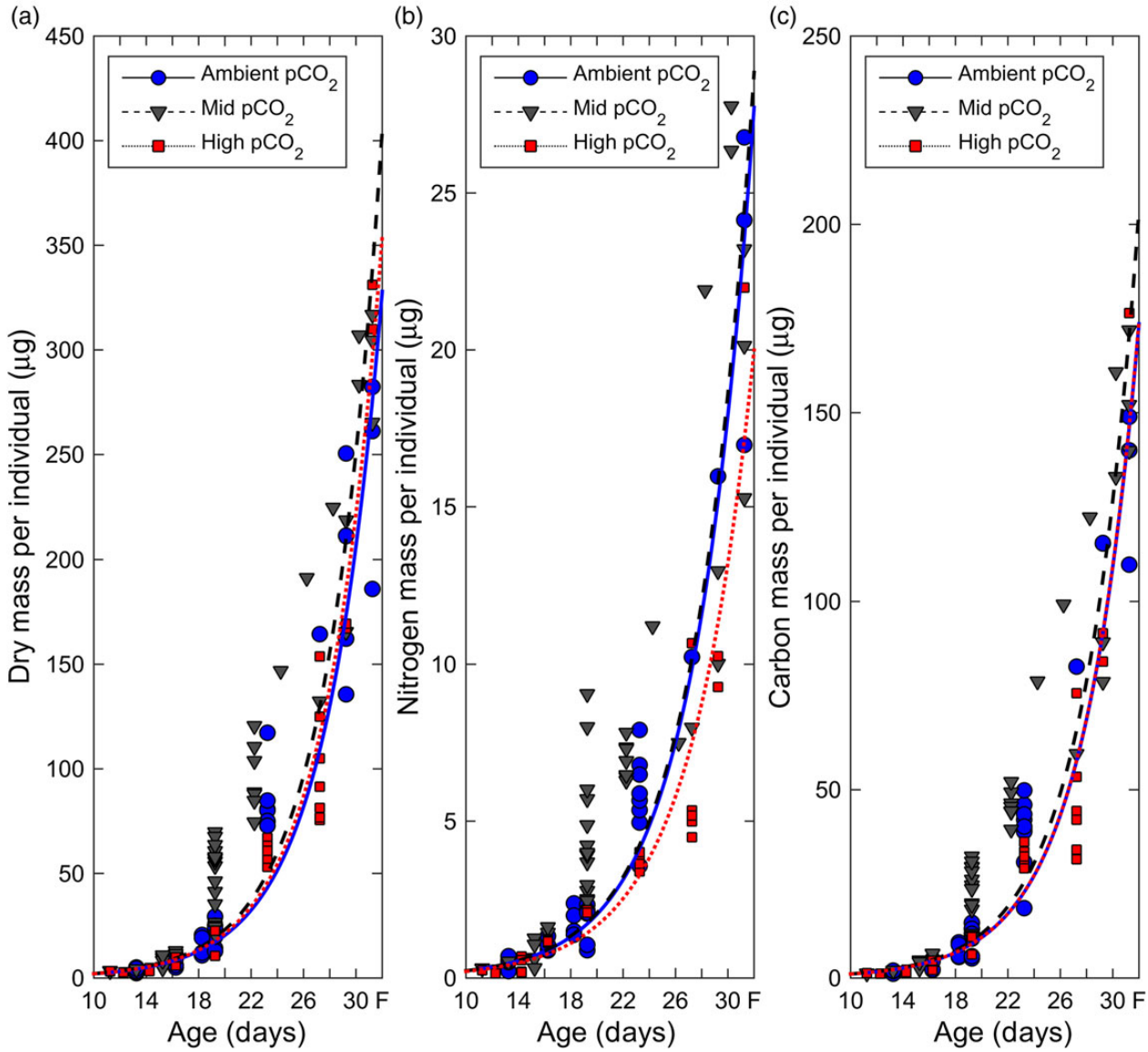

Figure 5. *Calanus finmarchicus*. Increase in mass as a function of time (days) at the ambient control and two treatment levels. (a) Dry weight; (b) nitrogen mass, and (c) carbon mass. Females older than 32 d were considered mature, ages for those observations are set to day 32 in the plots and model fit. Curves represent best overall fit to the growth model ($W_t = W_0 e^{gt}$). Growth rates (g) for the model are indicated. R^2: dry weights, 0.85; nitrogen, 0.79; carbon, 0.86.

qualitative observations did not reveal any indication of differences in survivorship or behaviour. Our analysis did detect a small but significant treatment difference in prosome length and body mass, notably a somewhat *larger* body size in the mid-pCO_2 treatment (i.e. a putatively beneficial effect). This was driven mainly by the higher mass and length of stages C3–C5 in replicate tank Mid A (Table 2). A more precise method for estimating mass at age, perhaps by measuring mass at the time of moult, might resolve whether there is indeed a small and perhaps beneficial treatment effect on body size at age.

Calanus finmarchicus is tolerant of elevated pCO_2

The evidence in support of tolerance of *C. finmarchicus* for predicted future pCO_2 levels is extensive and consistent (Table 5). Experiments have been conducted on all life stages originating from both wild (this study) and cultured females (Pedersen *et al.*, 2014a), including possible carry over effects from an F_1 generation through to the hatching success of eggs from F_2 females (Pedersen *et al.*, 2014a). These studies suggest that parental history (i.e. wild vs. cultured) is not an influential factor and they allay concerns about misrepresenting pCO_2 effects when extrapolating from one life stage (or sex) to another (Cripps *et al.*, 2014). While we did not measure them in this study, previous research is consistent in finding no effect of increased pCO_2 concentrations (<2000 µatm) on egg production rate, fertilization, or egg hatching success (Mayor *et al.*, 2007; Preziosi, 2012; Pedersen *et al.*, 2014a, b). Pedersen *et al.* (2014a) reported a significant decrease in body length and dry weight (by 5–25%), as well as a significant increase (by up to 40%) in respiration rate in stage C5, as treatment pCO_2 increased from ambient to 3482 µatm. However, this interpretation is based on linear regressions across all pCO2 treatment levels. Inspection of these data (Pedersen *et al.*, 2014a: Figure 2) indicates

Table 3. Estimate of instantaneous growth rate, g (d^{-1}), in terms of dry weight (μg), nitrogen mass (μgN), and carbon mass (μgC) at each pCO_2 treatment, assuming exponential growth between egg and early female stages.

	g	CI	*N*	r^2
Dry weight				
Ambient	0.231	0.004	37	0.85
Mid CO2	0.239	0.004	44	0.81
High CO_2	0.234	0.002	34	0.96
Nitrogen				
Ambient	0.218	0.003	34	0.93
Mid CO_2	0.219	0.005	44	0.70
High CO_2	0.207	0.004	30	0.88
Carbon				
Ambient	0.232	0.003	34	0.90
Mid CO_2	0.237	0.004	44	0.83
High CO_2	0.232	0.004	31	0.90

The starting stage N3 mass (W_0) is assumed to be identical in control and treatments. Individual mass measurements of stages C4 and C5 were averaged at each age (d). Model fitted in MATLAB. CI: 95% confidence interval, *N*: number of data points, and r^2 of model fits.

Table 4. Summary of the ANCOVA carried out on copepod mass (DW, dry weight; N, nitrogen; C, carbon) raised under three different pCO_2 treatments.

	D.F.	SS	MS	*F*-value	*p* value
Response variable: ln (DW)					
Age	1	222.82	222.82	1344.55	<0.0001
Treatment	2	8.88	4.441	26.80	<0.0001
Age:treatment	2	0.36	0.181	1.09	0.339
Residuals	109	18.06	0.166		
Response variable: ln (N)					
Age	1	151.19	151.187	749.8287	<0.0001
Treatment	2	10.22	5.111	25.3479	<0.0001
Age:treatment	2	0.29	0.143	0.7085	0.495
Residuals	102	20.57	0.202		
Response variable: ln (C)					
Age	1	209.67	209.67	1141.74	<0.0001
Treatment	2	9.25	4.63	25.19	<0.0001
Age:treatment	2	0.63	0.31	1.71	0.187
Residuals	103	18.91	0.18		

Age is days from inoculation. Multiple R^2: 0.93 (DW); 0.89 (N); 0.92 (C). D.F., degrees of freedom; SS, sum of squares; MS, mean square.

no change in any of these variables at pCO_2 concentrations up to the medium treatment level of 2020 μatm; always, the linear regression is driven by lower values at the highest concentration of 3482 μatm. Therefore, based on the evidence from our experiments and from other studies, we conclude that parameterization of physiological rates and processes determining *C. finmarchicus* vital rates in models of population dynamics of this species do not have to be adjusted to account for direct effects of ocean acidification at pCO_2 concentrations <2000 μatm.

Possible threshold response of *Calanus finmarchicus* to elevated pCO_2

Some studies on the effect of pCO_2 on *C. finmarchicus* indicate that there may be a response at concentrations >2000 μatm. For example, Pedersen *et al.* (2014a) observed significant differences in the egg production rates of females at their highest pCO_2 treatment (3482 μatm), although Mayor *et al.* (2007) found no effect on food-limited egg production rates at 8000 μatm. Both Mayor *et al.* (2007) and Pedersen *et al.* (2013) reported substantial egg mortality at 8000 μatm. Cumulative development time at stage C5 of the parental generation was delayed by 2.5 and 3.8 d at pCO_2 concentrations of 2200 and 3500 μatm, respectively, but only at 3500 μatm in the F_1 generation (Pedersen *et al.*, 2014a). Based upon these results, we suggest that pCO_2 impacts on *C. finmarchicus* vital rates would be best modelled as a step function, with effects occurring only above a threshold of ~3000 μatm, corresponding to pH values <7.2. Importantly, however, these values are far beyond predictions of oceanic pH levels over the next several hundred years. Moreover, this threshold concept does not take into account the possibility for adaptation by the organism that would potentially mitigate the effects of even these high pCO_2 levels.

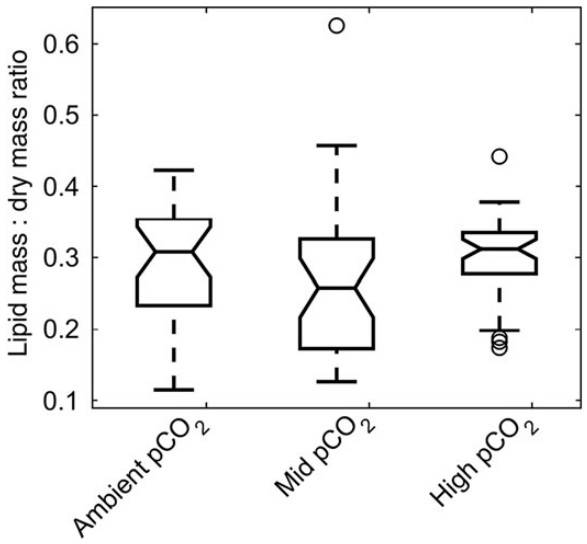

Figure 6. *Calanus finmarchicus*. Lipid mass to dry mass ratio, stage C5. One-way ANOVA: $p = 0.305$; $n = 29, 34, 44$, for ambient, mid, and high CO_2 treatments, respectively.

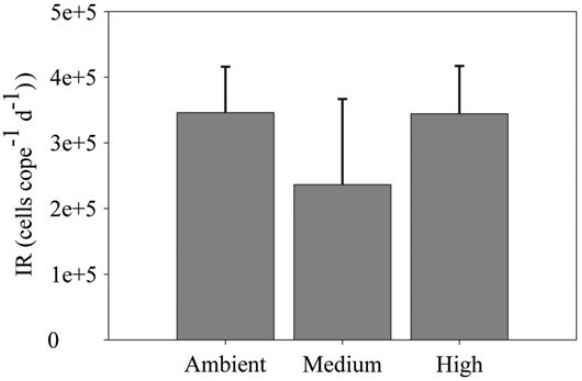

Figure 7. *Calanus finmarchicus*. Ingestion rates of adult females reared in different pCO_2 conditions. One-way ANOVA: $p = 0.095$; $n = 6, 10, 15$, for ambient, mid, and high CO_2 treatments, respectively.

Possible indirect and multiple stressor effects of pCO_2 on *Calanus finmarchicus*

The possibility of indirect effects of pCO_2 on copepods (*sensu* Reum *et al.*, 2015) have received little attention. The type and quality of the food available for *C. finmarchicus* to graze might be altered by pCO_2

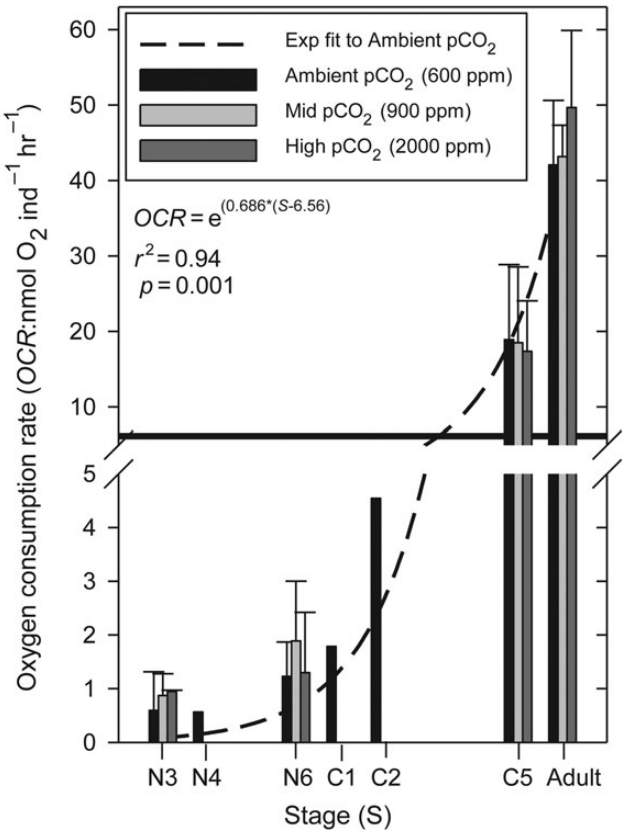

Figure 8. *Calanus finmarchicus*. *OCRs* of adult females reared in different pCO_2 conditions. Measurements at N3, N6, C5, and adult stages were made for all CO_2 treatments. ANOVA at each stage found no significant difference between treatments. *OCR* for N4, C1, and C2 stages were measured only at ambient CO_2 levels. Curve was fit to the pooled data from all measurements.

(Rossoll *et al.*, 2012), affecting the copepod's ability to accumulate or synthesize key proteins, carbohydrates, or fatty acids. While our experiments were conducted at non-limiting food concentrations, food limitation might prevent individuals from obtaining sufficient energy to cover the possible added energetic costs of maintaining intracellular pH levels (Whiteley, 2011). However, two studies (Mayor *et al.*, 2007; Pedersen *et al.*, 2014a) found that egg production rates in food-limited animals were not affected by pCO_2 levels <2020 μatm. Moreover, food was limiting in the growth experiments conducted by Pedersen *et al.* (2014a). Thus, the evidence indicates that, even when food is limiting, growth and development are not affected by pCO_2.

The timing of entry and exit from diapause, and its success, are critical to the modelling of *C. finmarchicus* population dynamics (e.g. Maps *et al.*, 2012). Because pCO_2 concentrations at the depths at which diapause occurs (500–2000 m: Heath *et al.*, 2008) are already at 800–1500 μatm (Hoffman *et al.*, 2013), present adaptation to elevated pCO_2 levels would be expected (Lewis *et al.*, 2013). However, successful diapause at depth is hypothesized to be dependent on fatty acid composition of the wax esters (Pond *et al.*, 2012), and effects of increased surface layer pCO_2 concentrations on fatty acid composition have not been studied.

There is also the possibility of multiple stressor interactions affecting physiological rates of *C. finmarchicus*. For example, an interaction between elevated surface layer temperature and pCO_2 concentrations would have ecological relevance for understanding shifts in distribution at the southern margins of the species' range. However, Preziosi (2012) did not find an effect of elevated temperature (15°C) on hatching success at pH levels >7.4, suggesting that the threshold for a pCO_2 effect may be lower, but still not of concern in the context of predicted increases in either temperature or pCO_2. Nevertheless, further investigation of the possible combined effects of increasing temperature and pCO_2 concentration in surface waters on *C. finmarchicus* growth and development may be useful in the context of modelling the population dynamics under future scenarios at the southern margins of the species distribution.

The response of other copepods to elevated pCO_2

Calanus finmarchicus is currently the most studied species among the Copepoda with respect to the effects of pCO_2. It is, therefore, reasonable to assess how well it represents the responses of other species of *Calanus*, and other copepod species generally. Whiteley (2011) concludes that there is considerable variability in the response of crustaceans to pCO_2, but suggests that species exposed to a broad range of environmental conditions should be better equipped physiologically to tolerate increased pCO_2 and lower pH. As vertical migrators, older life stages of *C. finmarchicus* experience daily change between the ambient pCO_2 levels at the surface and higher pCO_2 levels at depth (up to 250 m: Plourde *et al.*, 2001) and, in addition, stage C5 *C. finmarchicus* overwinter for months in deep water, as noted above. Other *Calanus* species have similar daily and ontogenetic migration behaviours and may, therefore, be more tolerant than smaller copepod species that always reside in surface waters (Lewis *et al.*, 2013). Studies of responses of Arctic species *C. glacialis* and *C. hyperboreus*, as well as the more temperate *C. helgolandicus* (Supplementary Table S1), generally report no effects at pCO_2 concentrations up to 3000 μatm. However, Lewis *et al.* (2013) reported lower survival of nauplius stages believed to be a mixture of *C. glacialis* and *C. hyperboreus* at pCO_2 concentrations as low as 700 μatm. If borne out, this suggests that even among *Calanus* spp. there is species and possibly population specificity in response.

We reviewed what is currently known about the effects of increased pCO_2 across the Copepoda (Supplementary Table S1). Not all life stages or life history characteristics have been investigated within any one species. Nevertheless, significant effects of pCO_2 concentrations <2000 μatm have been reported in only three studies. Effects on egg hatching success and nauplius survival of the estuarine and coastal copepod, *Acartia tonsa*, have been reported at pCO_2 concentrations of 1000 μatm (Cripps *et al.*, 2014). Survival of adults and nauplii of the small but common cyclopoid copepod, *Oithona similis*, as well as the nauplius stages of *C. glacialis* (and possibly, *C. hyberboreus*, discussed above) were negatively affected at pCO_2 concentrations as low as 700 μatm (Lewis *et al.*, 2013). Finally, body size and nauplius survival at low pCO_2 concentrations (400–600 μatm) have been reported for the harpacticoid copepod, *Tisbe battagliai* (Fitzer *et al.*, 2012). All these species are either broadly distributed geographically and/or are exposed to a very wide range of environmental conditions. The life stages of *Oithona* and *Tisbe*, and the nauplius stages of *C. glacialis* and *C. hyperboreus*, are relatively small, consistent with the argument that smaller copepods are more sensitive than larger ones. However, many of the other species listed in Supplementary Table S1 are also small, and we have discussed above that no effect of pCO_2 concentrations <2000 μatm have been observed in the

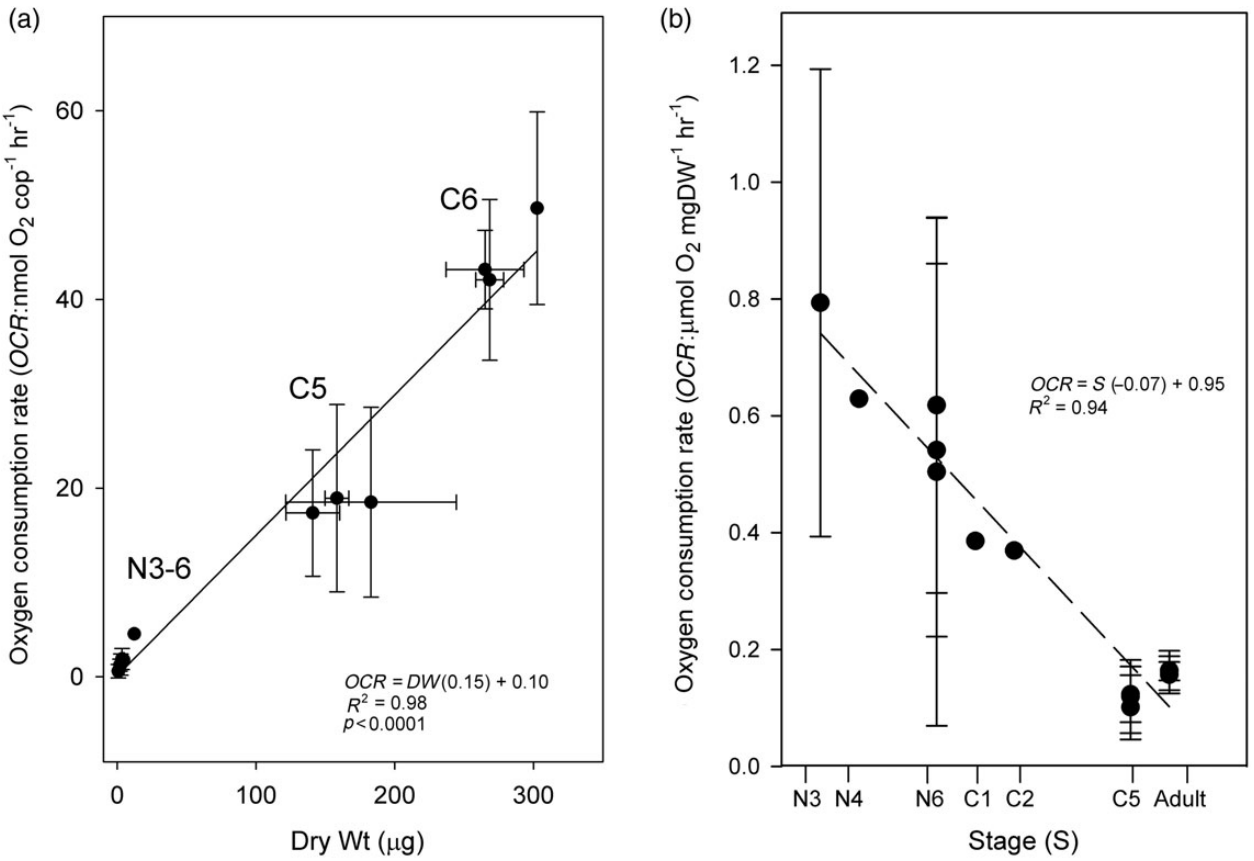

Figure 9. *Calanus finmarchicus*. *OCR*s of individual stages reared in different CO_2 conditions. Measurements at N3, N6, CV, and adult stages were made for all CO_2 treatments. *OCR* for N4, C1, and C2 stages were measured only at ambient CO_2 levels. Dry wts were taken from bulk measurements shown in Fig 4. (a) Relationships between dry weight and *OCR*. (b) *OCR* normalized dry weight as a function of developmental stage.

Table 5. Summary of experimental results investigating CO_2 treatment effects on life history traits of *C. finmarchicus*.

Life history trait	Impact of CO_2 < 1900 µatm	Highest CO_2 level (µatm) at which no effect	Comments
Egg production rate	No[1,4]	8000[1]/2020[4]	No effect on food limited F_0 females[1]; Food limited EPR of F_1 females reduced by 70% at 3500 µatm[4]
Egg hatching success	No[1,3,5]	3500[3]	90% decline observed at 8000 µatm[1] 41% decline observed at 8800 µatm, although not significant[3]
Survival, nauplius stages	No[1,2]	4600[3]	Survival to N2/N3 reduced by 75% at 8800 µatm[3]
Survival, copepodid stages	No[2]	3300[2]	Survival to stage C5 reduced by 49% at 7300 µatm; no survival at 9700 µatm[2]
Development rate, nauplius	No[3,4,6]	4600[3]	Development of nauplius stages N1 – N3 reduced at 8800 µatm
Development rate, copepodid	No[3,4,6]	1912[6]	Development to C5 of F_0 delayed by 7% at 2307 µatm Development to C4 of F_1 delayed by 32% at 3482 µatm
Prosome length	No[4,6]	1912[6]/2020[4]	Prosome length of F_1 decreased by ~5% at 3482 µatm[4] (see text)
Stage CV dry mass	No[6]/possible[4]	1912[6]	F_1 Stage C5 dry mass reduced by 20% at 2020 µatm (but see text) and by 36% at 3482 µatm[4]; no change in stage C5 dry mass at 1912 µatm[6]
Stage CV C mass	No[6]	1912[6]	No data for effects on C5 C mass at CO_2 levels >1912 µatm[6]
Stage CV N mass	No[6]	1912[6]	No data for effects on C5 C mass at CO_2 levels >1912 µatm[6]
Lipid accumulation	No[4,6]	1912[6]/2020[4]	Oil sac volume reduced by 42% at 3482 µatm[4]
Feeding rate	No[4,6]	3500[4]	No change in F_1 stage C5 feeding rate at 3482 µatm[4]
Respiration rate	No[6]/possible[4]	1912[6]	F_1 stage C% respiration rates 15% higher at 2020 µatm (but see text) and 30% higher at 3482 µatm[4]
Predator evasion	No[6]	1912[6]	Qualitative observations[6]

References: [1]Mayor *et al.* (2007), [2]Pedersen *et al.* (2013), [3]Pedersen *et al.* (2014a), [4]Pedersen *et al.* (2014b), [5]Preziosi (2012), and [6]this study.

relatively small early life stages of *C. finmarchicus*. Interestingly, two of the three studies that report an effect of pCO_2 were conducted using animals that had been maintained in culture for many generations. Further research is needed to understand the extent to which some species may or may not be affected by relatively low pCO_2 concentrations and why, as well as their capacity to adapt (physiologically, epigenetically, and genetically) to changing conditions.

The tolerance of modern populations of *C. finmarchicus* to increased pCO_2 appears challenged somewhere ~3000 μatm (pH of ~7.3). This appears true for other species of copepods as well. This threshold may be lower if individuals are simultaneously challenged by other environmental stressors. Whiteley (2011) reviews the mechanisms used by crustaceans to buffer the pH of their internal fluids using haemolymph proteins and bicarbonate ions (HCO_3^-). If the same mechanisms are used by copepods, perhaps there is a threshold buffering capacity that is exceeded at very high pCO_2 concentrations. Comparison of the physiology and epigenetic/genetic control of intracellular buffering capacity of *C. finmarchicus* with that of a copepod species exhibiting low tolerance to elevated pCO_2 would provide insight into the basis for this physiological limit.

Supplementary data

Supplementary material is available at the *ICESJMS* online version of the manuscript.

Acknowledgements

We gratefully acknowledge R. Campbell for guidance on culturing methods, R. Jones for technical assistance during early phases of the study, K. Thornton for assistance with analysis of copepod carbon and nitrogen mass, and I. Altman for comments on growth rate analysis.

Funding

This research was supported by projects from the Institute of Marine Research, Norway (Project #83192-01) and the Fram Centre (Project #13717-06) to HIB. JAR and CRST were additionally supported by the National Science Foundation award OCE-1041081. DMF also received support from NSF award OCE-1220068.

References

Andersen, S., Grefsrud, E. S., and Harboe, T. 2013. Effect of increased pCO_2 level on early shell development in great scallop (*Pecten maximus* Lamarck) larvae. Biogeosciences, 10: 6161–6184.

Baumgartner, M. F., Mayo, C. A., and Kenney, R. D. 2007. Enormous carnivores, microscopic food and a restaurant that's hard to find. *In* The Urban Whale: North Atlantic Right Whales at the Crossroads, pp. 138–171. Ed. by S. D. Kraus, and R. M. Rolland. Harvard University Press, Cambridge, MA.

Caldeira, K., and Wickett, M. E. 2003. Anthropogenic carbon and ocean pH. Nature, 425: 365.

Campbell, R. G., Wagner, M. M., Teegarden, G. J., Boudreau, C. A., and Durbin, E. G. 2001. Growth and development rates of the copepod *Calanus finmarchicus* reared in the laboratory. Marine Ecology Progress Series, 221: 161–183.

Carlotti, F., Giske, J., and Werner, F. 2000. Modeling zooplankton dynamics. *In* ICES Zooplankton Methodology Manual. Ed. by R. P. Harris, P. Wiebe, J. Lenz, M. Huntley, and H. R. Skjoldal. Academic Press, New York.

Cohen, R. E., and Lough, R. G. 1981. Length-weight relationships for several copepods dominant in the Georges Bank-Gulf of Marine area. Journal of Northwest Atlantic Fishery Science, 2: 47–52.

Cripps, G., Lindeque, P., and Flynn, K. J. 2014. Have we been underestimating the effects of ocean acidification in zooplankton? Global Change Biology, 20: 3377–3385.

Curchitser, E. N., Batchelder, H. P., Haidvogel, D. B., Fiechter, J., and Runge, J. 2013. Advances in physical, biological, and coupled ocean models during the US GLOBEC program. Oceanography, 26: 52–67.

Dickson, A. G. 2007. SOP7 Determination of the pH of sea water using the indicator dye m-cresol purple. *In* Guide to Best Practice for Ocean CO2 Measurements. PICES Special Publication. 191 pp.

Dickson, A. G., and Millero, F. J. 1987. A comparison of the equilibrium constants for the dissociation of carbonic-acid in seawater media. Deep-Sea Research Part A-Oceanographic Research Papers, 34: 1733–1743.

Dupont, S., and Pörtner, H.-O. 2013. A snapshot of ocean acidification research. Marine Biology, 160: 1765–1771.

Dupont, S., Dorey, N., and Thorndyke, M. 2010. What can meta-analysis tell us about vulnerability of marine biodiversity to ocean acidification? Estuarine, Coastal and Shelf Science, 89: 182–185.

Fabry, V. J., Seibel, B. A., Feely, R. A., and Orr, J. C. 2008. Impacts of ocean acidification on marine fauna and ecosystem processes. ICES Journal of Marine Science, 65: 414–432.

Fitzer, S. C., Caldwell, G. S., Close, A. J., Clare, A. S., Upstill-Goddard, R. C., and Bentley, M. G. 2012. Ocean acidification induces multigenerational decline in copepod naupliar production with possible conflict for reproductive resource allocation. Journal of Experimental Marine Biology and Ecology, 418: 30–36.

Frost, B. W. 1972. Effects of size and concentration of food particles on the feeding behavior of the marine planktonic copepod *Calanus pacificus*. Limnology and Oceanography, 17: 805–815.

Garrard, S. L., Hunter, R. C., Frommel, A. Y., Lane, A. C., Phillips, J. C., Cooper, R., Dineshram, R., *et al.* 2013. Biological impacts of ocean acidification: a postgraduate perspective on research priorities. Marine Biology, 160: 1789–1805.

Gaylord, B., Hill, T. M., Sanford, E., Lenz, E. A., Jacobs, L. A., Sato, K. N., Russell, A. D., *et al.* 2011. Functional impacts of ocean acidification in an ecologically critical foundation species. Journal of Experimental Biology, 214: 2586–2594.

Heath, M. R., Rasmussen, J., Ahmed, Y., Allen, J., Anderson, C. I. H., Brierley, A. S., Brown, L., *et al.* 2008. Spatial demography of *Calanus finmarchicus* in the Irminger Sea. Progress in Oceanography, 7: 39–88.

Hirche, H-J., Meyer, U., and Niehoff, B. 1997. Egg production of *Calanus finmarchicus*: effect of temperature, food and season. Marine Biology, 127: 609–620.

Hjollo, S. S., Huse, G., Skogen, M. D., and Melle, W. 2012. Modelling secondary production in the Norwegian Sea with a fully coupled physical/primary production/individual-based Calanus finmarchicus model system. Marine Biology Research, 8: 508–526.

Hoffman, A. F., Peltzer, E. T., and Brewer, P. G. 2013. Kinetic bottlenecks to chemical exchange rates for deep-sea animals – Part 2: carbon dioxide. Biogeosciences, 10: 2409–2425.

Johnson, C. L., Runge, J. A., Curtis, K. A., Durbin, E. G., Hare, J. A., Incze, L. S., Link, J. S., *et al.* 2011. Biodiversity and ecosystem function in the Gulf of Maine: pattern and role of Zooplankton and Pelagic Nekton. PLoS ONE, 6: 1–18.

Kim, H., and Menden-Deuer, S. 2013. Reliability of rapid, semi-automated assessment of plankton abundance, biomass, and growth rate estimates: Coulter Counter versus light microscope measurements. Limnology Oceanography Methods, 11: 382–393.

Kroeker, K. J., Kordas, R. L., Crim, R. N., and Singh, G. G. 2010. Meta-analysis reveals negative yet variable effects of ocean acidification on marine organisms. Ecology Letters, 13: 1419–1434.

Lewis, C. N., Brown, K. A., Edwards, L. A., Cooper, G., and Findlay, H. S. 2013. Sensitivity to ocean acidification parallels natural pCO_2 gradients experienced by Arctic copepods under winter sea ice.

Proceedings of the National Academy of Sciences of the United States of America, 110: E4960–E4967.

Lewis, E., Wallace, D., and Allison, L. J. 1998. CO2SYS – program developed for CO_2 system calculations. Carbon Dioxide Information Analysis Center, Oak Ridge National Laboratory, Oak Ridge, Tennessee.

Liu, X., Patsavas, M. C., and Byrne, R. H. 2011. Purification and characterization of meta-Cresol purple for spectrophotometric seawater pH measurements. Environmental Science & Technology, 45: 4862–4868.

Maps, F., Runge, J. A., Leising, A., Pershing, A. J., Record, N. R., Plourde, S., and Pierson, J. J. 2012. Modelling the timing and duration of dormancy in populations of *Calanus finmarchicus* from the Northwest Atlantic shelf. Journal of Plankton Research, 34: 36–54.

Maps, F., Zakardjian, B., Plourde, S., and Saucier, F. J. 2011. Modeling the interactions between the seasonal and diel migration behaviors of Calanus finmarchicus and the circulation in the Gulf of St. Lawrence (Canada). Journal of Marine Systems, 88: 183–202.

Mauchline, J. 1998. The Biology of Calanoid Copepods. Academic Press, San Diego. 710 pp.

Mayor, D. J., Matthews, C., Cook, K., Zuur, A. F., and Hay, S. 2007. CO_2-induced acidification affects hatching success in *Calanus finmarchicus*. Marine Ecology-Progress Series, 350: 91–97.

Mehrbach, C., Culberson, C. H., Hawley, J. E., and Pytkowic, R. M. 1973. Measurement of apparent dissociation constants of carbonic acid in seawater at atmospheric pressure. Limnology and Oceanography, 18: 897–907.

Melle, W., Runge, J., Head, E., Plourde, S., Castellani, C., Licandro, P., Pierson, J., *et al.* 2014. The North Atlantic Ocean as habitat for *Calanus finmarchicus*: Environmental factors and life history traits. Progress in Oceanography, 129: 244–284.

Menden-Deuer, S., and Lessard, E. J. 2000. Carbon to volume relationships for dinoflagellates, diatoms, and other protist plankton. Limnology and Oceanography, 45: 569–579.

Myers, R. A., and Runge, J. A. 1983. Predictions of seasonal natural mortality rates in a copepod population using life-history theory. Marine Ecology Progress Series, 11: 189–194.

Pedersen, S. A., Hakedal, O. J., Salaberria, I., Tagliati, A., Gustavson, L. M., Jenssen, B. M., Olsen, A. J., *et al.* 2014a. Multigenerational exposure to ocean acidification during food limitation reveals consequences for copepod scope for growth and vital rates. Environmental Science & Technology, 48: 12275–12284.

Pedersen, S. A., Hansen, B. H., Altin, D., and Olsen, A. J. 2013. Medium-term exposure of the North Atlantic copepod *Calanus finmarchicus* (Gunnerus, 1770) to CO_2-acidified seawater: effects on survival and development. Biogeosciences, 10: 7481–7491.

Pedersen, S. A., Vage, V. T., Olsen, A. J., Hammer, K. M., and Altin, D. 2014b. Effects of elevated carbon dioxide (CO_2) concentrations on early developmental Stages of the marine copepod *Calanus finmarchicus Gunnerus* (Copepoda: Calanoidae). Journal of Toxicology and Environmental Health-Part A-Current Issues, 77: 535–549.

Plourde, S., Joly, P., Runge, J. A., Zakardjian, B., and Dodson, J. 2001. Life cycle of *Calanus finmarchicus* in the lower St. Lawrence Estuary: the imprint of circulation and late timing of the spring phytoplankton bloom. Canadian Journal of Fisheries and Aquatic Sciences, 58: 647–658.

Pond, D. W., Tarling, G. A., Ward, P., and Mayor, D. J. 2012. Wax ester composition influences the diapause patterns in the copepod *Calanoides acutus*. Deep-Sea Research Part II-Topical Studies in Oceanography, 59: 93–104.

Preziosi, B. 2012. The effects of ocean acidification and climate change on the reproductive processes of the marine copepod, *Calanus finmarchicus*. MSc thesis, University of Maine, Orono. 41 pp.

Reum, J. C. P., Ferris, B. E., McDonald, P. S., Farrell, D. M., Harvey, C. J., Klinger, T., and Levin, P. S. 2015. Evaluating community impacts of ocean acidification using qualitative network models. Marine Ecology Progress Series, 536: 11–24.

Riebesell, U., Fabry, V. J., Hansson, L., and Gattuso, J.-P. 2010. Guide to best practices for ocean acidification research and data reporting. Office for Official Publications of the European Union, Luxembourg.

Rossoll, D., Bermudez, R., Hauss, H., Schulz, K. G., Sommer, U., and Winder, M. 2012. Ocean acidification-induced food quality deterioriation constrains trophic transfer. PLoS ONE, 7: e34737.

Runge, J. A. 1984. Egg production of *Calanus pacificus* Brodsky: laboratory observations. Journal of Experimental Marine Biology and Ecology, 74: 53–66.

Runge, J. A. 1985. Relationship of egg production of *Calanus pacificus* Brodsky to seasonal changes in phytoplankton availability in Puget Sound, Washington. Limnology and Oceanography, 30: 382–396.

Runge, J. A., Ji, R., Thompson, C. R. S., Record, N. R., Chen, C., Vandemark, D. C., Salisbury, J. E., *et al.* 2015. Persistence of Calanus finmarchicus in the western Gulf of Maine during recent extreme warming. Journal of Plankton Research, 37: 221–232.

Skjoldal, H. R. 2004. The Norwegian Sea Ecosystem. Tapir, Trondheim.

Speirs, D. C., Gurney, W. S. C., Heath, M. R., Horbelt, W., Wood, S. N., and de Cuevas, B. A. 2006. Ocean-scale modelling of the distribution, abundance, and seasonal dynamics of the copepod *Calanus finmarchicus*. Marine Ecology Progress Series, 313: 173–192.

Strathmann, R. 1967. Estimating the organic carbon content of phytoplankton from cell volume or plasma volume. Limnology and Oceanography, 12: 411–418.

Trenkel, V. M., Huse, G., MacKenzie, B. R., Alvarez, P., Arrizabalaga, H., Castonguay, M., Gani, N., *et al.* 2014. Comparative ecology of widely distributed pelagic fish species in the North Atlantic: implications for modelling climate and fisheries impacts. Progress in Oceanography, 129: 219–243.

Vogedes, D., Varpe, O., Soreide, J. E., Graeve, M., Berge, J., and Falk-Petersen, S. 2010. Lipid sac area as a proxy for individual lipid content of arctic calanoid copepods. Journal of Plankton Research, 32: 1471–1477.

Whiteley, N. M. 2011. Physiological and ecological responses of crustaceans to ocean acidification. Marine Ecology Progress Series, 430: 257–271.

Williams, R., and Conway, D. V. P. 1988. Vertical distribution and seasonal numerical abundance of the Calanidae in oceanic waters to the south-west of the British Isles. Hydrobiologia, 167/168: 259–266.

Wittmann, A. C., and Poertner, H-O. 2013. Sensitivities of extant animal taxa to ocean acidification. Nature Climate Change, 3: 995–1001.

Zuur, A. F., Ieno, E. N., and Elphick, C. S. 2009. A protocol for data exploration to avoid common statistical problems. Methods in Ecology and Evolution, 1: 314.

Handling editor: C. Brock Woodson

ICES Journal of Marine Science

ICES Journal of Marine Science (2016), 73(3), 951–961. doi:10.1093/icesjms/fsv073

Contribution to Special Issue: 'Towards a Broader Perspective on Ocean Acidification Research'

Original Article

Impacts of ocean acidification on survival, growth, and swimming behaviours differ between larval urchins and brittlestars

Kit Yu Karen Chan[1,2]*, Daniel Grünbaum[2], Maj Arnberg[3], and Sam Dupont[4]

[1]*Division of Life Science, Hong Kong University of Science and Technology, Clear Water Bay, Hong Kong*
[2]*School of Oceanography, University of Washington, Seattle, WA, USA*
[3]*IRIS-International Research Institute of Stavanger, Stavanger, Norway*
[4]*Department of Biological and Environmental Sciences, University of Gothenburg, The Sven Lovén Centre for Marine Sciences - Kristineberg, Fiskebäckskil, Sweden*

**Corresponding author: tel: +852 2358 7998; fax: +852 2358 1599; e-mail: karenchan@ust.hk*

Chan, K.Y.K., Grünbaum, D., Arnberg, M., and Dupont, S. Impacts of ocean acidification on survival, growth, and swimming behaviours differ between larval urchins and brittlestars. – ICES Journal of Marine Science, 73: 951–961.

Received 21 August 2014; revised 17 March 2015; accepted 6 April 2015; advance access publication 7 May 2015.

Ocean acidification (OA) is widely recognized as an increasing threat to marine ecosystems. Many marine invertebrates have dual-phase life cycles in which planktonic larvae connect and sustain otherwise disconnected benthic adult populations. Many planktonic larvae are particularly sensitive to environmental stresses including OA. Here, we compared the developmental dynamics, survivorship, and swimming behaviours of plutei of two ecologically important echinoderm species that naturally experience variability in ambient pH: the purple urchin *Strongylocentrotus purpuratus* and the infaunal brittlestar *Amphiura filiformis*. Sensitivity to decreased pH differed between these two species and between maternal lineages. Larvae of both species experienced increased mortality and reduced growth rate under low pH conditions. However, larval brittlestars appeared more sensitive and experienced over 80% mortality after 7-d exposure to pH 7.7. Larval urchins from one maternal lineage underwent highly synchronized budding (release of blastula-like particles) at low pH. Observed budding temporarily increased numerical density and reduced individual size, leading to differences in growth and mortality rates between the two half-sibling groups and another population. Swimming speeds of larval brittlestars were reduced in decreased pH. In contrast, acidification had either no effect or positive effect on swimming speeds of larval urchins. The observed differences between species may be a reflection of pre-exposure in their natural habitats: larval brittlestars experience a relatively stable *in situ* pH environment, whereas larval urchins are occasionally exposed to low pH in upwelling regions. Urchins may therefore exhibit short-term compensatory responses such as budding and increased swimming speed. Natural selection could act upon the significant variations we observed between maternal lineages, resulting in more resilient populations confronting chronic exposure to OA.

Keywords: *Amphiura filiformis*, echinopluteus, global climate change, *Strongylocentrotus purpuratus*, video motion analysis.

Introduction

Dissolution of anthropogenic carbon dioxide (CO_2) from the atmosphere into the ocean has altered its carbonate chemistry and led to reduced pH, a process known as ocean acidification (OA). The average surface ocean pCO_2 level is predicted to rise to 1000 μatm by 2100, causing pH to drop from 8.1 to 7.7 units (Caldeira and Wickett, 2003; Zeebe, 2012). A growing body of evidence suggests that these changes can significantly affect survival, growth, behaviour, and physiology of diverse marine organisms (Dupont and Thorndyke, 2013; Dupont and Pörtner, 2013).

For benthic organisms, the planktonic larval stage is generally considered the most vulnerable part of the dual-phase life history (Kurihara, 2008; Byrne, 2011; Aze *et al.*, 2014). However, vulnerability differs between species. Larvae of some species are sensitive to OA and experience high mortality (e.g. Dupont *et al.*, 2008), whereas others experience sublethal effects (see Dupont *et al.*, 2010a, for review) or even positive effects (e.g. Dupont *et al.*, 2010b; Kroeker *et al.*, 2013). These impacts include increased metabolic costs (e.g. Stumpp *et al.*, 2011b, 2012; Matson *et al.*, 2012), altered feeding physiology (e.g. Stumpp *et al.*, 2013; Challener *et al.*, 2014), delays

in growth and development (e.g. Brennand *et al.*, 2010; Martin *et al.*, 2011; Dorey *et al.*, 2013), and changes in gene expression patterns (e.g. O'Donnell *et al.*, 2009; Stumpp *et al.*, 2011a; Evans and Watson-Wynn, 2014). It is assumed that failure to perform key physiological functions (feeding, growth, acid-base regulation, calcification, etc.) can translate into reduced fitness. For example, a delay in development can translate into significant mortality due to predation during a prolonged planktonic period (Morgan, 1995; Dorey *et al.*, 2013). Aside from physiological vulnerability to environmental stresses, another critical aspect of larval ecology is their key role as vehicles for dispersal and genetic exchange. This dispersive role is significantly affected by larval swimming behaviours: individual movements affect their vertical distribution, and hence, the environmental conditions encountered (Metaxas and Saunders, 2009). The impact of OA on larval swimming and dispersal potential has received surprisingly little attention (but see Chan *et al.*, 2011). However, swimming and other OA impacts on larval stages are likely to affect both evolutionary and demographic dynamics of vulnerable species.

Echinoderms play important roles in coastal ecosystems and are ideal candidates for studying ecologically significant elements of organismal performance, such as swimming, under acidification stress. Plutei larvae of echinoderms have long ciliated projections (arms) attached to a pyramid-shaped larval body. Larvae add pairs of arms throughout larval growth and development. These arms are supported by calcified structures and are used for both feeding and swimming (Strathmann, 1975). Modelling and experimental studies have shown that slight changes in larval morphology significantly impact larval feeding and swimming and suggest trade-offs between the two functions (Grünbaum and Strathmann, 2003; Strathmann and Grunbaum, 2006; Clay and Grünbaum, 2011). When reared under reduced pH conditions, the larval sand dollar, *Dendraster excentricus*, showed morphological changes, including reduced stomach size, but showed no reduction in swimming speeds (Chan *et al.*, 2011). This observation suggests that OA could alter trade-offs in larval morphology between swimming and feeding.

Many echinoderms inhabit coastal areas where they naturally experience exposure to reduced pH, e.g. intertidal habitats, upwelling zones, and sediments (Cai and Reimers, 1993; Dai *et al.*, 2009; Yu *et al.*, 2011; Hu *et al.*, 2014). These echinoderms are good models to investigate possible adaptations to cope with reduced pH (Hoffmann and Sgrò, 2011; Kelly *et al.*, 2013; Pespeni *et al.*, 2013; Sunday *et al.*, 2014). In this study, we compared two echinoderm species that naturally experience low pH conditions as adults, the purple urchin *Strongylocentrotus purpuratus* and the infaunal brittlestar *Amphiura filiformis*.

Strongylocentrotus purpuratus is an abundant, long-lived species and key component of the intertidal and subtidal zone of the Eastern Pacific coast, with a distribution range from Mexico to Alaska (Biermann *et al.*, 2003). Its distribution includes upwelling areas in which both adult and larval stages can experience low pH levels (Yu *et al.*, 2011). Larval *S. purpuratus* were the focus of several previous OA studies (see Dupont and Thorndyke, 2013, for review). When reared under low pH conditions, no differences were observed in the first cell division (Place and Smith, 2012). Larval survivorship was not reduced by low pH (Matson *et al.*, 2012); however, larvae exposed to reduced pH had smaller size (Stumpp *et al.*, 2011b; Yu *et al.*, 2011) and slower growth rate (Stumpp *et al.*, 2011b; Dorey *et al.*, 2013). Larval respiration rates increased at low pH, whereas feeding rate remained unaffected (Stumpp *et al.*, 2013), suggesting a shift in energy budget with less energy available for somatic growth (Stumpp *et al.*, 2011b; Matson *et al.*, 2012). With a fully sequenced genome, the purple urchin was one of the first species investigated using genomics tools. Impacts of OA on embryos and larval transcriptomics were assessed using both microarrays (Todgham and Hofmann, 2009) and qPCR (Stumpp *et al.*, 2011a; Hammond and Hofmann, 2012). However, only subtle differences in gene expression were observed. *Strongylocentrotus purpuratus* presented apparently high adaptation potential to OA, with differential changes in allele frequencies in larvae grown under pH 7.0, suggesting allele-specific survival (Pespeni *et al.*, 2013).

Amphiura filiformis is an important species in many polar and temperate marine benthic habitats, with densities reaching 3500 ind. m^{-2} (Rosenberg *et al.*, 1997). It lives in semi-permanent sediment burrows. Within these burrows, adults often experience hypoxic and reduced pH conditions (Hu *et al.*, 2014). However, spawning occurs in summer when the pH level is relatively high and larval stages never experience *in situ* pH lower than pH 7.9 (Dorey *et al.*, 2013). When exposed to OA scenarios, adult brittlestars experienced only sublethal effects, e.g. muscle wastage (Wood *et al.*, 2008; Hu *et al.*, 2014). No information is available on the impacts of OA on the larval stages of *A. filiformis*. However, a study on another brittlestar found in similar habitats, *Ophiothrix fragilis*, observed extreme larval sensitivity of larvae to OA: larvae suffered 100% mortality within a few days of exposure to low pH (Dupont *et al.*, 2008).

Here, we focus on the vulnerable larval life-history stage to investigate the impacts of the reduced pH level on survival, growth, and swimming behaviours of these two echinoderms. Due to differences in their reproductive timing, larval purple urchins, *S. purpuratus*, experience variable pH but larval brittlestars, *A. filiformis*, develop in a relatively stable pH environment. Interspecific differences in responses between these echinoderms to stresses like OA could be interpreted as indicators of potentially altered ecological interactions that may promote shifts in abundance or range relative to other species comprising their marine communities. Intraspecific differences in stress responses could be interpreted as variability subject to natural selection, and hence as indicators of potential for rapid adaptation to changing environmental conditions. Comparative studies of ecologically significant organismal performance are therefore essential for understanding future population and community dynamics.

Material and methods

Animal collection and spawning

Adults of the sea urchin *S. purpuratus* were collected from 25 to 30-m depth in San Diego Bay, CA, USA, and transferred to the Sven Lovén Centre for Marine Sciences—Kristineberg (Fiskebäckskil, Sweden) in June 2011. They were maintained in a flow-through system at 11°C, salinity 32, pH_T 8.0, and fed *ad libitum* on a diet of *Ulva lactuca*. Spawning was induced by injecting 0.5–1 ml of 0.5 M KCl into the coelomic cavity (Strathmann, 1987). Eggs from females were collected in filtered seawater (FSW, 0.45 μm) at 11°C, salinity 32, pH_T 8.0, and sperm were collected dry and kept on ice until use. Sperm stock solution in FSW was added to the egg suspension to a final concentration of ~1000 sperm ml^{-1}. After 15 min and confirmation that there was >95% fertilization success, fertilized eggs were rinsed with FSW.

Adults of the brittlestar *A. filiformis* were collected at 25–40-m depth using a Petersen mud grab in the Gullmarsfjord near the

Sven Lovén Centre for Marine Sciences—Kristineberg (Fiskebäckskil, Sweden) between July and August 2011. Individuals were immediately sampled from the sediment cores by gentle rinsing then maintained in natural flowing seawater at 11°C, salinity 32, and pH_T 8.0. Individuals with ripe gonads (white for testes and orange for ovaries) which were clearly visible through the extended wall of bursae were used for fertilization. Three males and 15 females were heat-shocked at 26°C for 15 min then kept in 1 l of FSW in the dark at 11°C until the release of sperm that induces the female to spawn (Dupont *et al.*, 2009). Fertilized eggs were rinsed in FSW after confirming fertilization success.

Larval rearing and carbonate chemistry

Two-cell stage embryos of both species were transferred at the density of ~5 ind. ml^{-1} to aerated 5 l culturing vessels containing FSW. Three experiments were started: experiment one with *A. filiformis* from mixed gametes from 3 males and 15 females, experiment two with *S. purpuratus* gametes from two different females fertilized with the same male (maternal half-siblings, hereafter females 1 and 2), and experiment three with a common garden culture with gametes two male and two females of *S. purpuratus* (hereafter mixed population). Duplicate or triplicate cultures were set up for each pH treatment. Larvae were reared at 14°C and salinity 32 in a 12:12 light–dark cycle and were fed *Rhodomonas* sp. at 150 $\mu gC\ l^{-1}$ (~4000–5000 cells ml^{-1}) starting from 5 d post-fertilization. The carbon content of the algae was estimated using biovolume measurements, quantified as equivalent spherical diameter with an electronic particle analyser (Elzone 5380, Micrometrics, Aachen, Germany; Mullin, 1966). Complete water changes were performed every 3 d.

pH in each culturing vessel was maintained using a computerized feedback system (AquaMedic) that regulated pH by addition of pure gaseous CO_2 directly into the seawater (± 0.02 pH units). *Strongylocentrotus purpuratus* larvae were reared at three nominal pH levels: 8.0, 7.7, and 7.3. Based on a pilot study, *A. filiformis* larvae were reared only in pH 8.1 and 7.7, due to high larval mortality under more acidified conditions (Dupont *et al.*, pers. obs.) Our experimental scenarios correspond to (i) average pH experienced today (pH 8.0); (ii) average pH in 2100 and extreme of present natural variability (pH 7.7); and (iii) extreme pH in 2100 outside of present natural variability (pH 7.3; Dorey *et al.*, 2013). pH was measured every second day with a Metrohm 827 pH lab electrode adjusted for pH measurements on the total scale (pH_T) using TRIS (Tris–HCl) and AMP (2-aminopyridine/HCl) buffer solutions with a salinity of 32 (provided by Unité d'Océanographie Chimique, Université de Liège, Belgium). Alkalinity was measured weekly following Sarazin *et al.* (1999). Carbonate system speciation (pCO_2, Ω_{Ca}, and Ω_{Ar}) was calculated from pH_T and alkalinity using CO2SYS (Pierrot *et al.*, 2006) with dissociation constants from Mehrbach *et al.* (1973) refitted by Dickson and Millero (1987).

Mortality, budding, and growth

Larval density (ind. ml^{-1}) was monitored daily for the duration of the experiments (14–26 d for *S. purpuratus*, 7 d for *A. filiformis*) by taking duplicate 10 ml subsamples from the culturing vessels. Individuals were immediately fixed with a drop of paraformaldehyde solution (4% PFA in FSW, buffered at pH 8.3), counted, and stored in 4% PFA solution at 4°C until further measurements. Visual evidence of budding—release of blastula-like particles (Chan *et al.*, 2013)—was recorded. Larval densities were normalized relative to initial densities, then compared between pH treatments using ANCOVA with age as a covariate.

To measure larval growth, photographs of ten larvae per replicate at several time points and body length (TL, in μm) were measured with ImageJ (Figure 1, Abràmoff *et al.*, 2004). The larval growth rate [ln(μm) d^{-1}] was calculated as the coefficient of the significant logarithmic regressions between TL and time (Stumpp *et al.*, 2011b). The effect of pH on TL was tested using ANCOVA with age as a covariate following a logarithmic transformation.

Video motion analysis

Larval behaviours were quantified using the video motion analysis methods detailed in Chan and Grünbaum (2010) and Chan *et al.* (2011). Briefly, ~100 individuals were randomly selected and gently injected into a 2.5 × 2.5 × 30-cm plexiglas chamber containing FSW equilibrated to the respective pH levels. Six chambers were submerged in a water bath maintained at 11°C. Two-minute long video clips were collected at 15 frames s^{-1} with two modified webcams (Logitech webcam Pro9000) equipped with 7.5 mm CCTV lens (Rainbow Tech. Inc., AL, USA). Cameras were mounted on a computer-controlled platform to capture video from two fields of view, 0–13 and 13–25 cm. Video clips were collected every 6 min for a total of 36 min. Two more sets of observations were made on the same group of larvae after gently mixing the chambers to redistribute individuals. Video clips were analysed with a customized version of Avidemux2.4 software to subtract background, to threshold for size and brightness, and to extract pixel coordinates. An in-house Matlab program, Tracker3D, was used to calibrate and to assemble individual tracks over time.

Using smoothing splines with different knot spacing, frame rate noise was removed to generate smoothed track and the overall direction of travel (axis) was differentiated from the oscillatory (helical) components of each individual trajectory. Weighted means of six swimming metrics were computed by sampling at 5 s time intervals and averaging across tracks intersecting each time point (see Chan and Grünbaum, 2010, for details). Three key swimming metrics presented here: gross speed (the averaged magnitude of the time derivative of the smoothed track), and net horizontal and vertical velocities (the displacement between the starting and ending point of the track divided by observation duration).

Effects of pH treatments were tested using ANCOVA with larval age or calculated TL as covariate. TL at a given day was calculated using the logarithmic regression for growth described above to test if changes in the growth rate measured by size alone could account for the differences in swimming behaviours. Larval swimming did not vary within the 36 min of observation or between repeated observations (data not shown); therefore, these factors were not included as random factors in the statistical analysis. *Post hoc* analyses with Bonferroni corrections were conducted.

All data were checked for distribution and homoscedasticity. All statistical analyses were conducted using PASW Statistics 13 (IBM).

Results

Seawater chemistry

Mean ± SD for seawater carbonate chemistry parameters measured and calculated for all species, treatments, and replicates are reported in Table 1. The pH treatment had a significant effect on all carbonate chemistry parameters (ANOVA 3, model: $F_{15,\ 106} > 30$, $p < 0.0001$, parameter: $p < 0.0001$), except on alkalinity, where there was no difference between species ($p > 0.05$), replicates ($p > 0.05$), or their interactions ($p > 0.05$). Mean pH_T were 8.04 ± 0.02, 7.69 ± 0.02, and 7.27 ± 0.03 for nominal pH 8.0, 7.7, and 7.3, respectively.

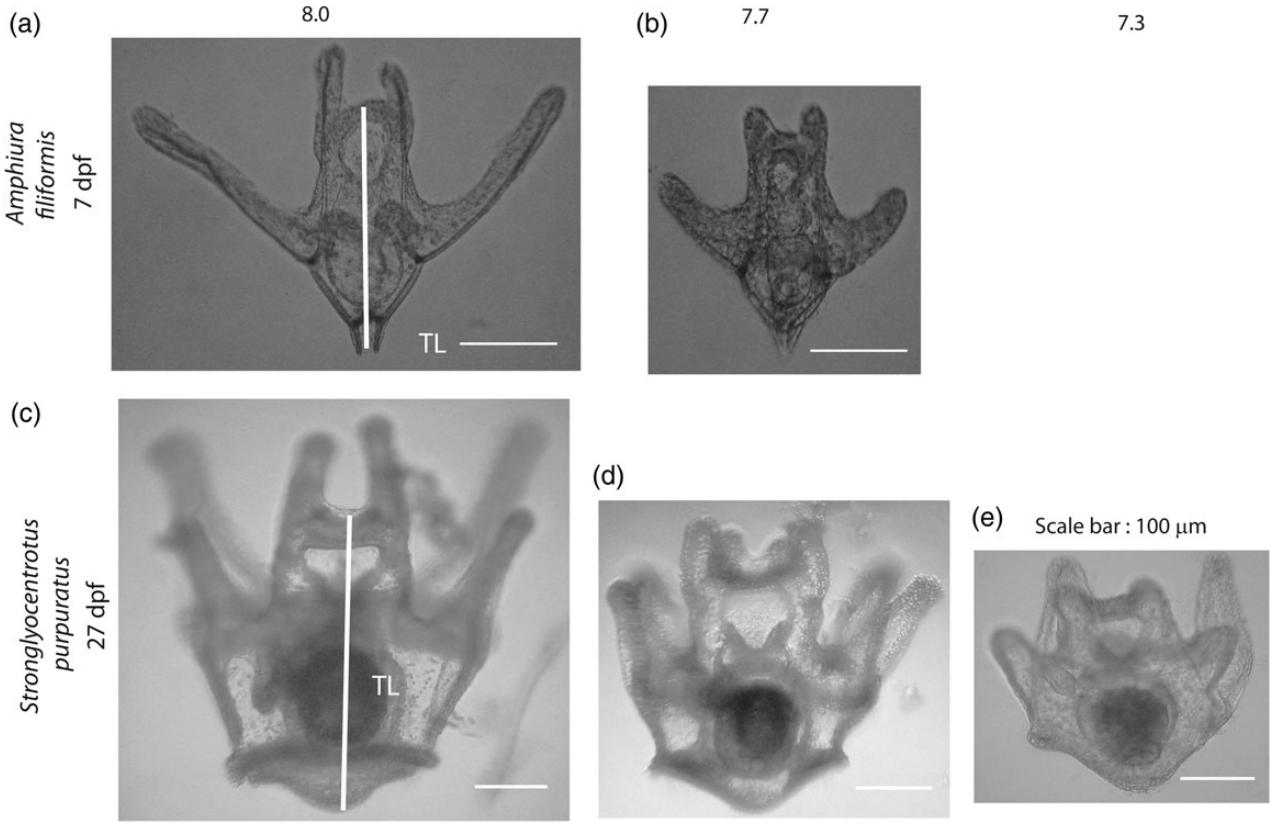

Figure 1. Micrographs of representative of 13 d post-fertilization (dpf) larvae of *A. filiformis* reared under pH 8.0 (a) and pH 7.7 (b); and 27 dpf larvae of *S. purpuratus* reared under pH 8.0 (c), pH 7.7 (d), and pH 7.3 (e). White bar corresponds to the measured total body length (TL). All scale bars are 100 µm.

Seawater was under-saturated regarding both calcite and aragonite in the lowest pH treatment.

Effects of decreased pH on growth

The larval growth rate [$\ln(\mu m)\ d^{-1}$] was computed as the coefficient of logarithmic regression between total body length (µm) and larval age (d). All regressions for both *A. filiformis* and *S. purpuratus* were statistically significant ($p < 0.0001$, Supplementary Table S1).

For larval *A. filiformis*, both age and pH treatment had significant effect on growth rates, with larvae in decreased pH growing significantly slower (ANCOVA, age: $F_{1,\ 309} = 275.276$, $p < 0.0001$, pH: $F_{1,\ 309} = 36.254$, $p < 0.001$, Figure 2a).

Larval *S. purpuratus* from both maternal lineages (females 1 and 2) showed similar responses. Larvae reared under decreased pH had significantly slower growth (ANCOVA, female 1, age: $F_{1,\ 229} = 407.106$, $p < 0.001$; pH: $F_{2,\ 229} = 104.771$, $p < 0.001$; female 2, age: $F_{1,\ 226} = 312.531$, $p < 0.001$, pH: $F_{2,\ 226} = 134.317$, $p < 0.001$). *Post hoc* tests showed that observed growth rates in the three pH treatments were significantly different from each other (Figure 2b and c). Significant differences in growth rates were observed between the two females (ANCOVA, $F_{1,\ 456} = 8.156$, $p = 0.004$) but there were no significant female × pH interactions ($F_{2,\ 456} = 0.771$, $p = 0.463$). Larval growth rates were compared within each pH treatment. Larvae from female 1 had significantly higher growth rate at pH 7.7 compared with female 2 (ANCOVA, $F_{1,\ 147} = 11.564$, $p = 0.001$) but there were no significant differences between females in the other two tested pH treatments (ANCOVA, pH 8.1: $F_{1,\ 146} = 1.590$, $p = 0.209$; pH 7.3: $F_{1,\ 161} = 0.734$, $p = 0.393$).

Effects of decreased pH on mortality

Relative larval mortality rates (RMR) were calculated as the coefficient of the significant relationship between relative larval densities and either age (d^{-1}) or calculated total body length (using regressions in Supplementary Table S1; in μm^{-1}). All regressions for both species were statistically significant (Supplementary Table S2).

Larvae of *A. filiformis* raised in decreased pH experienced significantly greater mortality rate both expressed per age (RMR in d^{-1}, ANCOVA, age: $F_{1,34} = 54.375$, $p < 0.0001$, pH: $F_{1,34} = 12.93$, $p = 0.001$) and per total body length (RMR in μm^{-1}, ANCOVA, body length: $F_{1,\ 34} = 30.629$, $p < 0.0001$, pH: $F_{1,\ 34} = 20.428$, $p < 0.0001$).

pH treatment had significant effects on relative mortality rates of larval *S. purpuratus* of both female 1 (RMR in d^{-1}, ANCOVA, age: $F_{1,\ 135} = 70.071$, $p < 0.0001$, pH: $F_{2,\ 135} = 10.121$, $p < 0.0001$; RMR in μm^{-1}, ANCOVA, age: $F_{1,\ 135} = 41.259$, $p < 0.0001$, pH: $F_{2,\ 135} = 17.439$, $p < 0.0001$) and female 2 (RMR in d^{-1}, ANCOVA, age: $F_{1,\ 141} = 185.028$, $p < 0.0001$, pH: $F_{2,\ 141} = 19.354$, $p < 0.0001$; RMR in μm^{-1}, ANCOVA, age: $F_{1,\ 141} = 167.582$, $p < 0.0001$, pH: $F_{2,\ 141} = 63.121$, $p < 0.0001$). *Post hoc* tests showed two different patterns for the two females. For female 1, RMR of individuals reared under pH 7.7 was significantly higher than the two other treatments. For female 2, RMR of individuals reared at pH 7.3 was significantly higher than those reared at pH 8.0 (*Post hoc* Tukey's test, $p < 0.05$). When comparing the two females using an ANCOVA with pH as the fixed factor and age or size as the covariate, both female and the interactions between female and pH had significant effects on RMR (RMR in d^{-1}, ANCOVA, age: $F_{1,\ 277} = 196.82$, $p < 0.0001$, pH: $F_{2,\ 277} = 13.579$, $p < 0.0001$,

Table 1. Seawater carbonate chemistry parameters presented as the mean ± SD.

				Calculated			
Species	**rep**	**Nominal pH**	**MeasuredpH_T**	**Temp (°C)**	**pCO_2 (μatm)**	**Ωca**	**Ωar**
Amphiura filiformis							
	1	8.0	8.06 ± 0.02	11.20 ± 0.04	414 ± 17	3.39 ± 0.10	2.15 ± 0.06
		7.7	7.71 ± 0.06	11.14 ± 0.04	1044 ± 138	1.74 ± 0.24	1.10 ± 0.15
	2	8.0	8.04 ± 0.02	11.19 ± 0.03	435 ± 19	3.27 ± 0.12	2.07 ± 0.08
		7.7	7.64 ± 0.03	11.13 ± 0.04	1208 ± 91	1.43 ± 0.10	0.90 ± 0.06
	Mean	*8.0*	*8.05 ± 0.01*	*11.19 ± 0.02*	*425 ± 13*	*3.32 ± 0.08*	*2.11 ± 0.05*
		7.7	*7.67 ± 0.03*	*11.14 ± 0.03*	*1126 ± 83*	*1.58 ± 0.13*	*1.00 ± 0.08*
Strongylocentrotus purpuratus							
Female 1	1	8.0	8.05 ± 0.02	11.06 ± 0.28	418 ± 24	3.37 ± 0.15	2.14 ± 0.09
		7.7	7.72 ± 0.05	11.08 ± 0.20	1011 ± 108	1.76 ± 0.23	1.12 ± 0.14
		7.3	7.23 ± 0.06	10.95 ± 0.32	3309 ± 471	0.59 ± 0.08	0.37 ± 0.05
	2	8.0	8.02 ± 0.03	11.00 ± 0.23	464 ± 38	3.15 ± 0.19	2.00 ± .12
		7.7	7.71 ± 0.03	12.63 ± 0.09	1005 ± 82	1.76 ± 0.13	1.12 ± 0.08
		7.3	7.36 ± 0.04	10.68 ± 0.12	2339 ± 197	0.77 ± 0.08	0.48 ± 0.05
	Mean	*8.0*	*8.04 ± 0.02*	*11.03 ± 0.20*	*441 ± 22*	*3.26 ± 0.12*	*2.07 ± 0.08*
		7.7	*7.72 ± 0.04*	*11.59 ± 0.26*	*1009 ± 75*	*1.76 ± 0.15*	*1.12 ± 0.10*
		7.3	*7.29 ± 0.04*	*10.83 ± 0.18*	*2868 ± 301*	*0.67 ± 0.06*	*0.42 ± 0.04*
Female 2	1	8.0	8.06 ± 0.02	10.80 ± 0.28	415 ± 22	3.36 ± 0.15	2.12 ± 0.09
		7.7	7.72 ± 0.11	11.80 ± 0.61	1059 ± 248	1.92 ± 0.55	1.22 ± 0.35
		7.3	7.20 ± 0.04	12.07 ± 0.40	3466 ± 362	0.58 ± 0.05	0.36 ± 0.03
	2	8.0	7.98 ± 0.08	10.94 ± 0.25	589 ± 171	3.04 ± 0.32	1.93 ± 0.20
		7.7	7.67 ± 0.03	11.33 ± 0.41	1114 ± 70	1.53 ± 0.09	0.97 ± 0.06
		7.3	7.31 ± 0.07	11.10 ± 0.26	2751 ± 301	0.77 ± 0.18	0.49 ± 0.12
	Mean	*8.0*	*8.02 ± 0.04*	*10.87 ± 0.18*	*502 ± 86*	*3.20 ± 0.17*	*2.02 ± 0.11*
		7.7	*7.69 ± 0.05*	*11.52 ± 0.33*	*1092 ± 100*	*1.68 ± 0.22*	*1.07 ± 0.14*
		7.3	*7.26 ± 0.04*	*11.55 ± 0.25*	*3085 ± 245*	*0.68 ± 0.10*	*0.43 ± 0.06*
Overall		*8.0*	*8.03 ± 0.02*	*11.02 ± 0.09*	*458 ± 32*	*3.26 ± 0.08*	*2.06 ± 0.05*
		7.7	*7.69 ± 0.02*	*11.39 ± 0.13*	*1078 ± 48*	*1.67 ± 0.09*	*1.06 ± 0.06*
		7.3	*7.27 ± 0.03*	*11.25 ± 0.18*	*2993 ± 188*	*0.68 ± 0.04*	*0.43 ± 0.04*

Seawater pH on the total scale (pH_T), temperature (*T*; °C), salinity of 32, and total alkalinity of 2386 μmol kg^{-1} were used to calculate CO_2 partial pressure (pCO_2) and saturation of carbonate species (Ωca and Ωar).

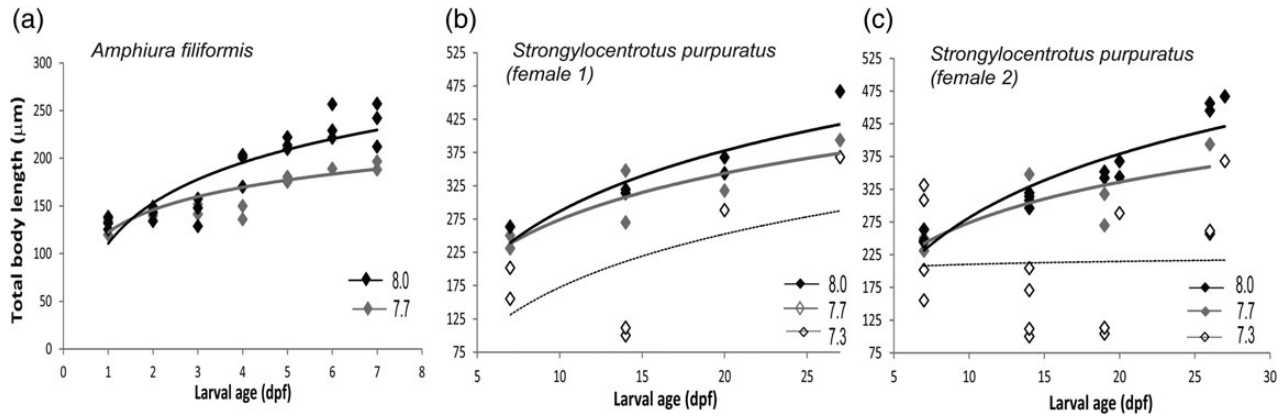

Figure 2. Increase in total body length (TL in μm) over time (day post-fertilization, dpf) and significant logarithmic relationships per pH treatments in (a) *A. filiformis* (1–7 dpf), (b and c) *S. purpuratus* (females 1 and 2, 7–27 dpf).

female: $F_{1,\ 277} = 16.786$, $p < 0.0001$, pH × female: $F_{2,\ 277} = 11.654$, $p < 0.0001$; RMR in μm^{-1}, ANCOVA, age: $F_{1,\ 277} = 138.3362$, $p < 0.0001$, pH: $F_{2,\ 277} = 45.07$, $p < 0.0001$, female: $F_{1,\ 277} = 16.683$, $p < 0.0001$, pH × female: $F_{2,\ 277} = 9.874$, $p < 0.0001$). When comparing within treatments, there was no significant difference in RMR between the two females in the control condition (*t*-test, $p = 0.458$). Larvae of female 1 reared at pH 7.7 had significantly higher RMR than those of female 2 (*t*-test, $F_{1,\ 83} = 12.509$, $p = 0.001$). Larvae of female 2 reared at pH 7.3 had a significantly higher RMR than those of female 1 (*t*-test, $F_{1,\ 92} = 4.107$, $p = 0.046$).

Effects of decreased pH on larval swimming

In larval *A. filiformis*, larval age had significant effects on gross swimming speed, and net vertical and horizontal velocities, with

Table 2. Statistical output from ANCOVA for swimming metrics of larval *A. filiformis* and *S. purpuratus* with age as a covariate.

Source	Parameter	d.f.	MS	*F*-value	*p*-value
Amphiura filiformis					
Age	Gross speed	1	88 472.82	31.80	<0.0001
	Horizontal velocity	1	158.63	0.09	0.76
	Vertical velocity	1	78 144.16	19.29	<0.0001
pH	Gross speed	1	2474.67	0.89	0.35
	Horizontal velocity	1	20 987.63	11.96	<0.0001
	Vertical velocity	1	5611.11	1.39	0.24
Error	Gross speed	153	2782.31		
	Horizontal velocity	153	1755.25		
	Vertical velocity	153	4051.27		
Strongylocentrotus purpuratus (Female 1)					
Age	Gross speed	1	137 227.27	37.69	0.00
	Horizontal velocity	1	454 551.54	181.88	0.00
	Vertical velocity	1	1141.75	0.21	0.64
pH	Gross speed	2	3613.94	0.99	0.37
	Horizontal velocity	2	6960.75	2.79	0.06
	Vertical velocity	2	1814.82	0.34	0.71
Error	Gross speed	293	3641.34		
	Horizontal velocity	293	2499.13		
	Vertical velocity	293	5367.72		
Strongylocentrotus purpuratus (Female 2)					
Age	Gross speed	1	77 559.97	20.59	0.00
	Horizontal velocity	1	159 490.34	57.80	0.00
	Vertical velocity	1	702.12	0.14	0.71
pH	Gross speed	2	13 806.01	3.66	0.03
	Horizontal velocity	2	4362.54	1.58	0.21
	Vertical velocity	2	19 023.00	3.78	0.02
Error	Gross speed	203	3767.35		
	Horizontal velocity	203	2759.43		
	Vertical velocity	203	5039.12		

Table 3. Statistical output from ANCOVA for swimming metrics of larval *A. filiformis* and *S. purpuratus* with calculated total body length (TBL) as a covariate.

Source	Parameter	d.f.	MS	*F*-value	*p*-value
Amphiura filiformis					
TBL	Gross speed	1	94 782.19	34.58	<0.0001
	Horizontal velocity	1	1468.88	0.84	0.36
	Vertical velocity	1	92 886.80	23.49	<0.0001
pH	Gross speed	1	50 077.19	18.27	<0.0001
	Horizontal velocity	1	6908.54	3.96	0.05
	Vertical velocity	1	58 387.91	14.76	<0.0001
Error	Gross speed	153	2741.07		
	Horizontal velocity	153	1746.68		
	Vertical velocity	153	3954.92		
Strongylocentrotus purpuratus (Female 1)					
TBL	Gross speed	1	128 918.22	35.13	0.00
	Horizontal velocity	1	402 301.46	150.26	0.00
	Vertical velocity	1	486.59	0.09	0.76
pH	Gross speed	2	50 948.92	13.88	0.00
	Horizontal velocity	2	96 019.15	35.86	0.00
	Vertical velocity	2	1579.61	0.29	0.75
Error	Gross speed	293	3669.70		
	Horizontal velocity	293	2677.46		
	Vertical velocity	293	5369.96		
Strongylocentrotus purpuratus (Female 2)					
TBL	Gross speed	1	79 813.78	21.25	0.00
	Horizontal velocity	1	163 234.04	59.55	0.00
	Vertical velocity	1	946.91	0.19	0.67
pH	Gross speed	2	51 350.28	13.67	0.00
	Horizontal velocity	2	39 836.87	14.53	0.00
	Vertical velocity	2	10 301.34	2.04	0.13
Error	Gross speed	203	3756.25		
	Horizontal velocity	203	2740.99		
	Vertical velocity	203	5037.91		

swimming speeds generally decreasing as larvae aged (Table 2, Figure 4). However, pH treatment did not have significant effects on gross swimming speed nor net vertical velocities (ANCOVA, $F_{1,\ 153} = 0.89$ and 1.39, $p = 0.35$ and 0.24, respectively). Horizontal velocity was significantly higher among larvae reared under pH 8.0 ($F_{1,\ 153} = 11.96$, $p < 0.0001$). When controlling for differences in the growth rate between larvae growth under different conditions by using total body length as a covariate, pH treatment had significant impacts on all three swimming metrics observed: at a given size, larvae reared under pH 8.0 had significantly higher swimming speeds (gross, horizontal, and vertical) than those under pH 7.7 (ANCOVA, $F_{1,\ 153} \geq 3.96$, $p \leq 0.05$, Table 3).

In larval *S. purpuratus*, age had significant effects on gross swimming speed and horizontal swimming speed ($F \geq 0.21, p \leq 0.0001$) but not vertical velocities ($F \leq 0.21$, $p > 0.6$, Table 2) in larvae from both maternal lineages (females 1 and 2). Swimming of larval urchins was more horizontally directed as they aged such that gross speed increased without a corresponding increase in vertical velocity (Table 2, Figure 4). Using age as a covariate, the pH level affected the swimming speeds of larvae from the two maternal lineages differently. In female 1, pH had no significant effect on any of the three swimming metrics ($F_{2,\ 203} \leq 3.79$, $p > 0.34$). In female 2, larvae reared under decreased pH conditions had higher gross swimming speeds and vertical velocity ($F_{2,\ 203} \geq 3.66$, $p < 0.03$). However, pH treatments had no significant effect on horizontal velocity ($p = 0.21$). These differences in how larval swimming speeds respond to pH treatments between the two maternal lineages was removed when total body length was used as a covariate (Table 3). In larval urchins from both females 1 and 2, total larval body length had significant effects on gross speed and horizontal velocity ($F \geq 25.25$, $p < 0.001$). The pH level significantly affected gross swimming speed and horizontal velocity ($F \geq 13.67, p < 0.0001$); however, vertical velocity was not affected ($F \leq 2.04, p > 0.13$).

Discussion

We compared larval sensitivity to reduced pH of two echinoderm species that naturally experience low pH as adults but different pH environments as larvae. Both echinoderm species experienced elevated mortality and reduced growth rates when exposed to decreased pH. However, the effects of decreased pH differed between these two species, and even between familial groups of *S. purpuratus*. The presence of both inter- and intraspecific variations in responses of two important echinoderm species to reduced pH has significant implications for adaptive potential and ecosystem responses to global climate change.

Interspecific variability: larval brittlestars are highly sensitivity to reduced pH

Larval *A. filiformis* experienced a greater mortality rate at decreased pH when compared with *S. purpuratus*, with an average of 20% survivorship after 6 d compared with 25% after 27 d for *S. purpuratus*. Such high larval mortality over short durations suggests that numbers of successful recruits may be significantly reduced under

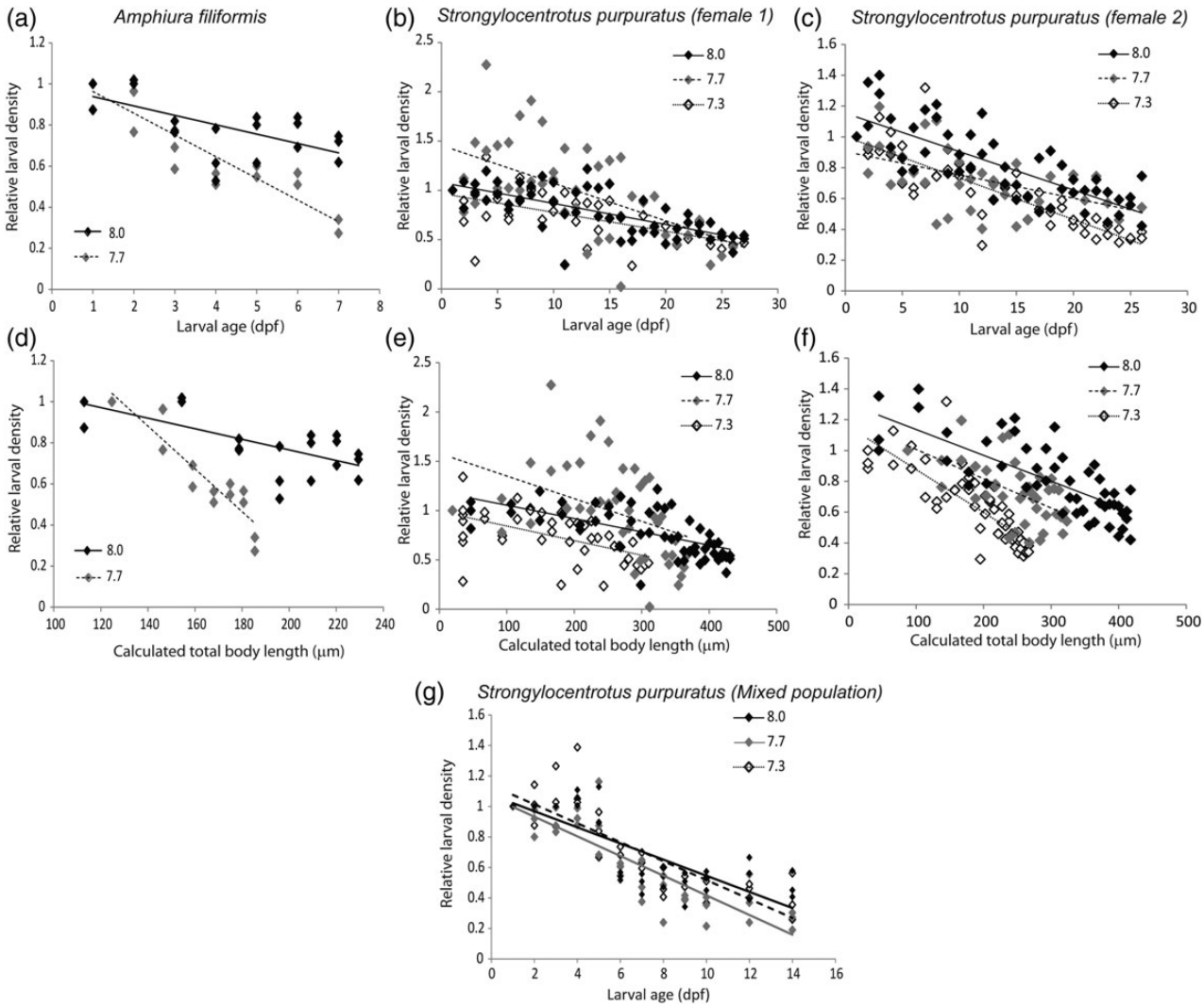

Figure 3. Changes in relative larval densities, calculated based on duplicate 10 ml subsamples, over time (day post-fertilization, dpf) for (a) larval *A. filiformis* and (b and c) *S. purpuratus* (females 1 and 2). The RMR was computed as the coefficient of significant linear regression. To correct for the difference in the growth rate, changes in relative larval densities were also plotted against total body length calculated using regression equations shown in Figure 2.

prolonged exposure. Decreased pH reduced the larval growth rate of both species in our study. This observation is consistent with previous studies on other echinoderm larvae (Stumpp *et al.*, 2011b; Dorey *et al.*, 2013; Dupont and Thorndyke, 2013). However, the magnitudes of pH effects on larval growth differed between species. A 100% decrease in the growth rate between pH 8.0 and 7.7 was observed for *A. filiformis*, whereas less than a 40% decrease between the three tested pH levels (8.0, 7.7, and 7.3) was observed for *S. purpuratus* (Figure 3, Supplementary Table S2). *Amphiura filiformis* is highly abundant in the muddy substratum of the North Sea, playing important roles in bioturbation and hence in biogeochemical cycling I. It is also an important food source for various flat fish and crabs (O'Connor *et al.*, 1983). If the growth rate and survivorship observed in the laboratory under low pH are indicative of natural *A. filiformis* population under future OA conditions, negative responses of this key ecosystem engineer could lead to significant impacts on energy transfer and other aspects of benthic community structure.

Given larval swimming is tightly coupled to the biomechanical limitations imposed by larval morphologies (Chan, 2012), we considered the differences in sizes between pH treatments when assessing their impacts on swimming (Figure 4, Table 3). When corrected for size, pH had significant effects on all swimming metrics, such that larval brittlestars in low pH swam significantly slower (gross speed and horizontal and vertical velocity). In contrast, reduced pH had significant positive effect on size-corrected swimming of larval *S. purpuratus*, such that individuals reared under decreased pH had higher gross and horizontal speeds. One possible interpretation is that the two species employ different behavioural responses to similar pH levels, i.e. reduced swimming for larval brittlestars but increased swimming for larval urchins. Alternatively, this interspecific difference could imply larval urchins have a wider range of behavioural plasticity when challenged by reduced pH to maintain swimming. This could be a consequence of adaptation to different pH envelopes, in which *A. filiformis* is naturally exposed to a narrower range of pH when compared with *S. purpuratus*.

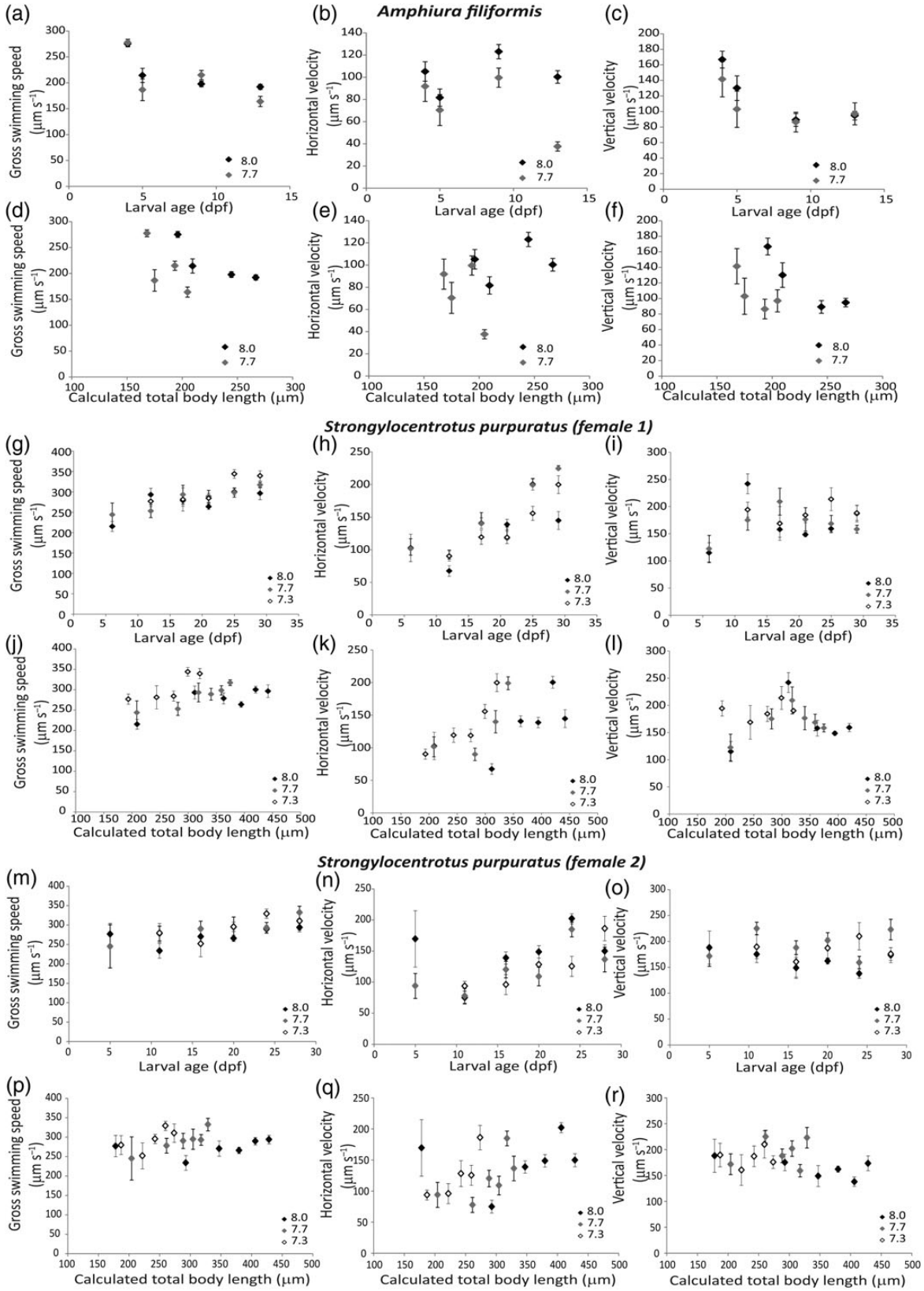

Figure 4. Swimming metrics, gross swimming speed and horizontal and vertical velocities (mean ± standard error) of larval *A. filiformis* (a – f) and *S. purpuratus* [female 1 (g – l) and female 2 (m – r)] plotted against larval age and calculated total body length.

Differences in sensitivity between the two tested species may reflect adaptation to different pH environment experienced during the larval stages (stable for *A. filiformis*, variable for *S. purpuratus*) rather than the pH environment experienced by adults (variable for both species). Beyond differences in larval exposure to low pH, further comparative studies are needed to better understand the roles of evolutionary history (e.g. ophiuroids vs. echinoids), maternal investment [e.g. egg size of *A. filiformis* is ~60 μm and *S. purpuratus* is ~80 μm (Bowner, 1982; Levitan, 1993)], and timing of life-history events [e.g. spawning in late summer of *A. filiformis* and spring for *S. purpruatus* (Bowner, 1982; Cochran and Engelmann, 1975)] in shaping an organism's ability to cope with pH stress. Such studies are essential for building a mechanistic understanding to predict community responses to OA.

Intraspecific variability: maternal lineage affects larval urchins' sensitivity

Effects of reduced pH on growth and swimming performance differed between the two maternal lineages of larval urchins studied. These differences could be explained by the difference in the mortality rate between larvae from females 1 and 2. Highly synchronized budding was observed in a large fraction of larval urchins of female 1 reared under pH 7.7, but not in female 2. Most released buds did not grow into functional individuals. The transitory increases of larval density due to the release of buds led to a higher estimate of the larval mortality rate, which is the slope of a significant linear regression of all the density count over time. Similar maternal differences in timing and frequencies of larval cloning have also been reported in larval sand dollars exposed to fish mucus (Vaughn, 2009, 2010).

Age-specific swimming metrics of larval *S. purpuratus* were affected by pH differently in the two maternal lineages: no significant effects on larvae from female 1, but significantly higher gross speeds and vertical velocities in larvae from female 2 (Table 3, Figure 4). These differences are likely due to the different growth pattern caused by the size reduction during budding, because these differences disappeared when developmental delays were taken into account. When corrected for size, larval urchins from both lineages had significantly higher gross speeds and horizontal velocities but not vertical velocities when reared under decreased pH. This effect of pH on size-corrected larval swimming also highlights the multifaceted potential impacts of pH, both directly through changes in behavioural choices and indirectly through altered morphologies that in turn alter swimming biomechanics.

Larval urchins demonstrate plasticity during acute exposure

Our observations were limited to short-term exposure to reduction in pH in the laboratory. Hence, generalization of our results to how larval urchins might response to chronic exposure to OA conditions under future field conditions should be approached cautiously. The observed plasticity in larval urchin response in growth and swimming appeared to be strategies to cope with stressful conditions during short-term exposure, but are not necessarily beneficial to surviving prolonged exposure. Nonetheless, our observations suggest hypotheses about the natural selection of responses to low pH by an important urchin species.

The budding we observed did not lead to numerical increases in viable larval population under laboratory conditions, because the buds released did not survive and develop into functional larvae. If budding has a selective value as an OA response, it may lead to numerical increases under different acidification conditions. An alternative hypothesis is that budding may act as a mechanism for size reduction. Size reduction could be beneficial to larvae in the short term, e.g. by reducing respiratory demands, but are likely to have legacy effects on later larval and juvenile stages that are at least partly deleterious (Chan *et al.*, 2013). Observed changes in larval urchin gross swimming speed did not translate into changes in vertical velocity. Maintenance of vertical velocity under reduced pH conditions could help larvae retain capacity to regulate their vertical positions in the water column. Larvae are known to use vertical swimming to regulate exposure to food, predators, stresses, such as UV and other environmental variations (Pennington and Emlet, 1986), and to influence lateral transport due to advection in ambient currents (Metaxas and Saunders, 2009; Miller and Morgan, 2013). Because some depth strata with unfavourable pH may nonetheless have favourable ambient currents and turbulence levels, larvae may confront trade-offs between reducing transport losses in a short term. However, chronic low pH exposure could slow development; assuming larvae are transported by the same current, they may reach their settlement sites prematurely at a small size or miss suitable habitat due to the increase in dispersal distance with longer pelagic larval duration.

In summary, exposure to reduced pH had overall negative impacts on larval echinoderms but sensitivity varied greatly between species. Interspecific variations suggest that ecological interactions between species and community structure could be altered due to the differential responses. For some species, large variation such as that observed between lineages of *S. purpuratus* could be a basis for future selective evolution, conferring resilience under future climate conditions.

Supplementary data

Supplementary material is available at the *ICESJMS* online version of the manuscript.

Acknowledgements

We thank the editor and two reviewers for helpful suggests which greatly improved the manuscript; R. Strathmann, E. Tobin, O. Coyle, M. Schatz for helpful comments, staff, and research scientists at the Sven Lovén Centre for Marine Sciences for logistical support and insightful discussions. KYKC is currently funded by the Croucher Foundation. KYKC was funded by a Boeing International Fellowship, the Postdoctoral Scholar Programme at the Woods Hole Oceanographic Institution (WHOI), with funding provided by the Coastal Ocean Institute, the Croucher Foundation, and the Royal Swedish Academy of Sciences. DG and KYKC were supported by Washington Sea Grant (NA10OAR4170057). SD was financially supported by the Linnaeus Centre for Marine Evolutionary Biology at the University of Gothenburg (http://www.cemeb.science.gu.se/) and a Linnaeus grant from the Swedish Research Councils VR and Formas. Additional funding was provided from the European Seventh Framework Programme under grant agreement 265847.

References

Abràmoff, M. D., Magalhães, P. J., and Ram, S. J. 2004. Image processing with ImageJ. Biophotonics International, 11: 36–43.

Aze, T., Barry, J., Bellerby, R. G., Brander, L., Byrne, M., Dupont, S., Gattuso, J. -P., *et al.* 2014. An Updated Synthesis of the Impacts of Ocean Acidification on Marine Biodiversity (CBD Technical Series; 75). Secretariat of the Convention on Biological Diversity.

Biermann, C. H., Kessing, B. D., and Palumbi, S. R. 2003. Phylogeny and development of marine model species: strongylocentrotid sea urchins. Evolution and Development, 5: 360–371.

Bowner, T. 1982. Reproduction in *Amphiura filiformis* (Echinodermata: Ophiuroidea): seasonality in gonad development. Marine Biology, 69: 281–290.

Brennand, H. S., Soars, N., Dworjanyn, S. A., Davis, A. R., and Byrne, M. 2010. Impact of ocean warming and ocean acidification on larval development and calcification in the sea urchin Tripneustes gratilla. PLoS ONE, 5: e11372.

Byrne, M. 2011. Impact of ocean warming and ocean acidification on marine invertebrate life history stages: vulnerabilities and potential for persistence in a changing ocean. Oceanography and Marine Biology: an Annual Review, 49: 1–42.

Cai, W-J., and Reimers, C. E. 1993. The development of pH and pCO_2 microelectrodes for studying the carbonate chemistry of pore waters near the sediment-water interface. Limnology and Oceanography, 38: 1762–1773.

Caldeira, K., and Wickett, M. E. 2003. Anthropogenic carbon and ocean pH. Nature, 425: 365–365.

Challener, R. C., Watts, S. A., and McClintock, J. B. 2014. Effects of hypercapnia on aspects of feeding, nutrition, and growth in the edible sea urchin Lytechinus variegatus held in culture. Marine and Freshwater Behaviour and Physiology, 47: 41–62.

Chan, K. Y. K. 2012. Biomechanics of larval morphology affect swimming: insights from the sand dollars Dendraster excentricus. Integrative and Comparative Biology, 52: 458–469.

Chan, K., and Grünbaum, D. 2010. Temperature and diet modified swimming behaviors of larval sand dollar. Marine Ecology Progress Series, 415: 49–59.

Chan, K., Grünbaum, D., Arnberg, M., Thorndyke, M., and Dupont, S. 2013. Ocean acidification induces budding in larval sea urchins. Marine Biology, 160: 2129–2135.

Chan, K. Y. K., Grünbaum, D., and O'Donnell, M. J. 2011. Effects of ocean-acidification-induced morphological changes on larval swimming and feeding. Journal of Experimental Biology, 214: 3857–3867.

Clay, T. W., and Grünbaum, D. 2011. Swimming performance as contraint on larval morphology in plutei. Marine Ecology Progress Series, 423: 185–196.

Cochran, R. C., and Engelmann, F. 1975. Environmental regulation of the annual reproductive season of *Strongylocentrotus purpuratus* (Stimpson). Biological Bulletin, 148: 393–401.

Dai, M., Lu, Z., Zhai, W., Chen, B., Cao, Z., Zhou, K., Cai, W. J., *et al.* 2009. Diurnal variations of surface seawater pCO_2 in contrasting coastal environments. Limnology and Oceanography, 54: 735–745.

Dickson, A., and Millero, F. 1987. A comparison of the equilibrium constants for the dissociation of carbonic acid in seawater media. Deep Sea Research I: Oceanographic Research Papers, 34: 1733–1743.

Dorey, N., Lançon, P., Thorndyke, M., and Dupont, S. 2013. Assessing physiological tipping point of sea urchin larvae exposed to a broad range of pH. Global Change Biology, 19: 3355–3367.

Dupont, S., Dorey, N., and Thorndyke, M. 2010a. What meta-analysis can tell us about vulnerability of marine biodiversity to ocean acidification? Estuarine, Coastal and Shelf Science, 89: 182–185.

Dupont, S., Havenhand, J., Thorndyke, W., Peck, L., and Thorndyke, M. 2008. Near-future level of CO_2-driven ocean acidification radically affects larval survival and development in the brittlestar *Ophiothrix fragilis*. Marine Ecology Progress Series, 373: 285–294.

Dupont, S., Lundve, B., and Thorndyke, M. 2010b. Near future ocean acidification increases growth rate of the lecithotrophic larvae and juveniles of the sea star *Crossaster papposus*. Journal of Experimental Zoology, Part B: Molecular and Developmental Evolution, 314: 382–389.

Dupont, S., and Pörtner, H. 2013. Marine science: get ready for ocean acidification. Nature, 498: 429–429.

Dupont, S., and Thorndyke, M. 2013. Direct impacts of near-future ocean acidification on sea urchins. In Climate Change Perspective from the Atlantic: Past, Present and Future, pp. 461–485. Ed. by J. Fernández-Palacios, L. Nascimento, J. Hernández, S. Clemente, A. González, and J. Díaz-González. Universidad de La Laguna.

Dupont, S., Thorndyke, W., Thorndyke, M. C., and Burke, R. D. 2009. Neural development of the brittlestar *Amphiura filiformis*. Development Genes and Evolution, 219: 159–166.

Evans, T. G., and Watson-Wynn, P. 2014. Effects of Seawater Acidification on Gene Expression: Resolving Broader-Scale Trends in Sea Urchins. Biological Bulletin, 226: 237–254.

Grünbaum, D., and Strathmann, R. R. 2003. Form, performance and trade-offs in swimming and stability of armed larvae. Journal of Marine Research, 61: 659–691.

Hammond, L. M., and Hofmann, G. E. 2012. Early developmental gene regulation in *Strongylocentrotus purpuratus* embryos in response to elevated CO_2 seawater conditions. Journal of Experimental Biology, 215: 2445–2454.

Hoffmann, A. A., and Sgrò, C. M. 2011. Climate change and evolutionary adaptation. Nature, 470: 479–485.

Hu, M. Y., Casties, I., Stumpp, M., Ortega-Martinez, O., and Dupont, S. T. 2014. Energy metabolism and regeneration impaired by seawater acidification in the infaunal brittlestar, *Amphiura filiformis*. Journal of Experimental Biology. doi:10.1242/jeb.100024.

Kelly, M. W., Padilla-Gamiño, J. L., and Hofmann, G. E. 2013. Natural variation, and the capacity to adapt to ocean acidification in the keystone sea urchin *Strongylocentrotus purpuratus*. Global Change Biology, 19:2536–2546.

Kroeker, K. J., Kordas, R. L., Crim, R., Hendriks, I. E., Ramajo, L., Singh, G. S., Duarte, C. M., *et al.* 2013. Impacts of ocean acidification on marine organisms: quantifying sensitivities and interaction with warming. Global Change Biology, 19: 1884–1896.

Kurihara, H. 2008. Effects of CO_2-driven ocean acidification on the early developmental stages of invertebrates. Marine Ecology Progress Series, 373: 275–284.

Levitan, D. R. 1993. The importance of sperm limitation to the evolution of egg size in marine invertebrates. American Naturalist, 141: 517–536.

Martin, S., Richier, S., Pedrotti, M. -L., Dupont, S., Castejon, C., Gerakis, Y., Kerros, M. -E., *et al.* 2011. Early development and molecular plasticity in the Mediterranean sea urchin Paracentrotus lividus exposed to CO2-driven acidification. Journal of Experimental Biology, 214: 1357–1368.

Matson, P. G., Pauline, C. Y., Sewell, M. A., and Hofmann, G. E. 2012. Development under elevated pCO2 conditions does not affect lipid utilization and protein content in early life-history stages of the purple sea urchin, Strongylocentrotus purpuratus. Biological Bulletin, 223: 312–327.

Mehrbach, C., Culberson, C., Hawley, J., and Pytkowicz, R. 1973. Measurement of the apparent dissociation constants of carbonic acid in seawater at atmospheric pressure. Limnology and Oceanography, 18: 897–907.

Metaxas, A., and Saunders, M. 2009. Quantifying the "bio-" components in biophysical models of larval transport in marine benthic invertebrates: advances and pitfalls. Biological Bulletin, 216: 257–272.

Miller, S. H., and Morgan, S. G. 2013. Interspecific differences in depth preference: regulation of larval transport in an upwelling system. Marine Ecology Progress Series, 476: 301–306.

Morgan, S. 1995. Life and death in the plankton: larval mortality and adaptation. In Ecology of marine invertebrate larvae, pp. 279–321.

Mullin, M. 1966. Relationship between carbon content, cell volume and area in phytoplankton. Limnology Oceanography, 11: 307–311.

O'Connor, B., Bowmer, T., and Grehan, A. 1983. Long-term assessment of the population dynamics of *Amphiura filiformis* (Echinodermata: Ophiuroidea) in Galway Bay (west coast of Ireland). Marine Biology, 75: 279–286.

O'Donnell, M. J., Todgham, A. E., Sewell, M. A., Hammond, L., Ruggiero, K., Fangue, N. A., Zippay, M. L., *et al.* 2009. Ocean acidification alters skeletogenesis and gene expression in larval sea urchins. Marine Ecology Progress Series, 398: 157.

Pennington, J. T., and Emlet, R. B. 1986. Ontogenetic and diel vertical migration of a planktonic echinoid larva, Dendraster excentricus (Eschscholtz): occurrence, causes, and probable consequences. Journal of Experimental Marine Biology and Ecology, 104: 69–95.

Pespeni, M. H., Sanford, E., Gaylord, B., Hill, T. M., Hosfelt, J. D., Jaris, H. K., LaVigne, M., *et al.* 2013. Evolutionary change during experimental ocean acidification. Proceedings of the National Academy of Sciences of the USA, 110: 6937–6942.

Pierrot, D., Lewis, E., and Wallace, D. 2006. CO2SYS MS Excel Program developed for CO_2 system calculations. ORNL/CDIAC-105. Carbon Dioxide Information Analysis Center, Oak Ridge National Laboratory, US Department of Energy, Oak Ridge, TN.

Place, S. P., and Smith, B. W. 2012. Effects of seawater acidification on cell cycle control mechanisms in *Strongylocentrotus purpuratus* embryos. PLoS One, 7: e34068.

Rosenberg, R., Nilsson, H. C., Hollertz, K., and Hellman, B. 1997. Density-dependent migration in an *Amphiura filiformis* (Amphiuridae, Echinodermata) infaunal population. Marine Ecology Progress Series, 159: 121–131.

Sarazin, G., Michard, G., and Prevot, F. 1999. A rapid and accurate spectroscopic method for alkalinity measurements in sea water samples. Water Research, 33: 290–294.

Strathmann, R. R. 1975. Larval feeding in echinoderms. American Zoologist, 15: 717–730.

Strathmann, R. R., and Grunbaum, D. 2006. Good eaters, poor swimmers: compromises in larval form. Integrative and Comparative Biology, 46: 312–322.

Strathmann, M. F. 1987. Reproduction and development of marine invertebrates of the northern Pacific coast: data and methods for the study of eggs, embryos, and larvae. University of Washington Press.

Stumpp, M., Dupont, S., Thorndyke, M., and Melzner, F. 2011a. CO_2 induced acidification impacts sea urchin larval development II: Ggene expression patterns in pluteus larvae. Comparative Biochemistry and Physiology, Part A: Molecular and Integrative Physiology, 160: 320–330.

Stumpp, M., Hu, M., Casties, I., Saborowski, R., Bleich, M., Melzner, F., and Dupont, S. 2013. Digestion in sea urchin larvae impaired under ocean acidification. Nature Climate Change, 3: 1044–1049.

Stumpp, M., Hu, M. Y., Melzner, F., Gutowska, M. A., Dorey, N., Himmerkus, N., Holtmann, W. C., *et al.* 2012. Acidified seawater impacts sea urchin larvae pH regulatory systems relevant for calcification. Proceedings of the National Academy of Sciences of the USA, 109: 18192–18197.

Stumpp, M., Wren, J., Melzner, F., Thorndyke, M., and Dupont, S. 2011b. CO_2 induced seawater acidification impacts sea urchin larval development I: elevated metabolic rates decrease scope for growth and induce developmental delay. Comparative Biochemistry and Physiology, Part A: Molecular and Integrative Physiology, 160: 331–340.

Sunday, J. M., Calosi, P., Dupont, S., Munday, P. L., Stillman, J. H., and Reusch, T. B. H. 2014. Evolution in an acidifying ocean. Trends in Ecology and Evolution, 29: 117–125.

Todgham, A. E., and Hofmann, G. E. 2009. Transcriptomic response of sea urchin larvae *Strongylocentrotus purpuratus* to CO_2-driven seawater acidification. Journal of Experimental Biology, 212: 2579–2594.

Vaughn, D. 2009. Predator-induced larval cloning in the sand dollar *Dendraster excentricus*: might mothers matter? Biological Bulletin, 217: 103–114.

Vaughn, D. 2010. Why run and hide when you can divide? Evidence for larval cloning and reduced larval size as an adaptive inducible defense. Marine Biology, 157: 1301–1312.

Wood, H. L., Spicer, J. I., and Widdicombe, S. 2008. Ocean acidification may increase calcification rates, but at a cost. Proceedings of the Royal Society of London, Series B: Biological Sciences, 275: 1767–1773.

Yu, P. C., Matson, P. G., Martz, T. R., and Hofmann, G. E. 2011. The ocean acidification seascape and its relationship to the performance of calcifying marine invertebrates: laboratory experiments on the development of urchin larvae framed by environmentally-relevant pCO2/pH. Journal of Experimental Marine Biology and Ecology, 400: 288–295.

Zeebe, R. E. 2012. History of seawater carbonate chemistry, atmospheric CO_2, and ocean acidification. Annual Review of Earth and Planetary Sciences, 40: 141–165.

Handling editor: C. Brock Woodson

ICES Journal of Marine Science

ICES Journal of Marine Science (2016), 73(3), 962–969. doi:10.1093/icesjms/fsv184

Contribution to Special Issue: 'Towards a Broader Perspective on Ocean Acidification Research'

Original Article

High pCO_2 affects body size, but not gene expression in larvae of the California mussel (*Mytilus californianus*)

Morgan W. Kelly[1]*, Jacqueline L. Padilla-Gamiño[2], and Gretchen E. Hofmann[3]

[1]*Department of Biological Science, Louisiana State University, Baton Rouge, LA 70803, USA*
[2]*Department of Biology, California State University, Dominguez Hills, Carson, CA, USA*
[3]*Ecology, Evolution, and Marine Biology, University of California, Santa Barbara, Santa Barbara, CA, USA*

**Corresponding author: tel: + 1 225 578 0224; fax: + 1 225 578 2597; e-mail: morgankelly@lsu.edu*

Kelly, M. W., Padilla-Gamiño, J. L., and Hofmann, G. E. High pCO_2 affects body size, but not gene expression in larvae of the California mussel (*Mytilus californianus*). – ICES Journal of Marine Science, 73: 962–969.

Received 25 June 2015; revised 20 September 2015; accepted 23 September 2015; advance access publication 21 October 2015.

Many studies have reported reductions in body size and calcification rates for marine larvae exposed to ocean acidification conditions. However, the physiological mechanisms driving these effects, and mechanisms underlying body size variation in general, are poorly understood. Here, we combine transcriptome sequencing with bulked segregant analysis to assess the physiological response to acidification in larvae of the California mussel, *Mytilus californianus*, and to explore physiological basis of variation in larval size. We reared three families of *M. californianus* larvae under ambient (~350 µatm, pH_{total} 8.1) and high (~1300 µatm, pH_{total} 7.6) pCO_2 conditions, then passed larvae through a mesh filter, separating each family × pCO_2 treatment into fractions of larvae with large vs. small body sizes. We sequenced larval mRNA for each family × treatment × body size combination, and assembled a *de novo* transcriptome. We then mapped reads from each library to this assembly to identify effects of high pCO_2 on gene expression, and to identify transcriptomic differences between small vs. large larvae of the same age class. Although larvae reared under elevated pCO_2 were smaller, we observed no consistent effect of elevated pCO_2 on gene expression. Nevertheless, 1225 transcripts, primarily related to metabolism, were differentially expressed between large vs. small larvae, regardless of CO_2 treatment. We conclude that the observed reduction in larval body size under high CO_2 may be driven by a direct effect of the environment on phenotype, unmediated by changes in gene expression. Because *M. californianus* has evolved in the context of seasonal upwelling, exposure to 1300 µatm, pCO_2 may not produce the large stress-mediated effects on gene expression that might be expected for an organism exposed to conditions far outside those of its typical environment.

Keywords: bivalve, gene expression, global change biology, ocean acidification, physiology, RNA-seq, transcriptomics.

Introduction

Ocean acidification (OA) occurs through the absorption of atmospheric carbon dioxide, and reduces both ocean pH and the availability of free carbonate ions (CO_3^{2-}) used by many marine invertebrates for calcification (Hofmann *et al.*, 2010). Laboratory experiments across a variety of taxa have demonstrated negative effects of OA conditions, ranging from reductions in size and fecundity to increased mortality (Kroeker *et al.*, 2010). However, relatively little is known about the underlying physiological mechanisms for these effects.

One of the most widespread consequences of exposure to high pCO_2 is a reduction in the size of developing larvae. This has been observed in taxa ranging from brittle stars (Dupont *et al.*, 2008) to sea urchins (Kelly *et al.*, 2013) and mussels (Gaylord *et al.*, 2011), and may carry over into later life stages, long after exposure to high pCO_2 has ended (Hettinger *et al.*, 2012). CO_2-driven reductions in larval size may be due to lower overall growth rates stemming from metabolic depression (Lannig *et al.*, 2010; Seibel *et al.*, 2012). Alternately, reductions in size may stem more specifically from reduced calcification (and, hence, reduced skeletal growth), driven by lower availability of carbonate ions and increased energetic cost of calcification (Watson *et al.*, 2012; Waldbusser *et al.*, 2013). One way to address competing hypotheses regarding the physiological effects of OA conditions is with gene expression data, which provide a global view of physiological responses (Evans and Hofmann, 2012; Whitehead, 2012), identifying which stressors

(salinity, pH, temperature, etc.) have the biggest effects on physiology (Chapman *et al.*, 2011), and which physiological processes are most affected. For example in sea urchins, exposure to high pCO_2 led to down-regulation of spicule matrix 30 alpha protein, a major component of the larval skeleton, but not to metabolic depression (Padilla-Gamiño *et al.*, 2013). This suggests that the observed reductions in growth rates were a specific consequence of reduced calcification rather than generalized metabolic depression. However, despite their utility in providing a comprehensive view of physiological responses, transcriptomic data in the context of OA conditions are available for a relatively small number of taxa (Moya *et al.*, 2012; Evans *et al.*, 2013; Harms *et al.*, 2014; Vidal-Dupiol *et al.*, 2014).

In this study, we sought to use whole transcriptome sequencing to identify physiological effects of OA conditions in larvae of the California mussel, *M. californianus*, and the molecular mechanisms underlying variation in larval size. The California mussel is a foundation species in the rocky intertidal zone of the eastern Pacific, creating the physical habitat used by a diverse assemblage of species (Suchanek, 1992). Previous work has shown that exposure to high pCO_2 conditions produces *M. californianus* larvae with smaller, thinner shells that are more vulnerable to breakage (Gaylord *et al.*, 2011), suggesting that the effect of low pH on the growth of larval shells may be a key bottleneck in the response of this species to future acidification.

Because of the taxonomically widespread effects of OA on larval size, we were also interested in mechanisms underlying body size variation in general, and whether the same mechanisms (e.g. reduced metabolism) underlie body size variation under ambient and high pCO_2 conditions. To identify gene expression differences responsible for phenotypic variation in size among *Mytilus* larvae under ambient and high pCO_2, we combined transcriptome sequencing with bulked segregant analysis (BSA). In BSA, DNA (or in this case mRNA) is pooled among individuals sharing a particular trait value (e.g. large body size), and compared against a pool of individuals sharing an opposing trait value (e.g. small body size), with the expectation that on average, allele frequencies (or in this case gene expression) will differ only for loci or transcripts linked to the focal trait (Michelmore *et al.*, 1991).

We chose larval body size as the focal trait for this study, because declines in body size have been observed for *M. californianus* larvae and many other taxa in experiments simulating OA conditions (Kroeker *et al.*, 2010; Gaylord *et al.*, 2011). Larval size in marine invertebrates is tied to fitness through feeding rate and risk of predation (Allen, 2008), and reductions in body size have been an emergent response to climate change across multiple systems and stressors (Sheridan and Bickford, 2011). We also focused on size because effective use of BSA requires the accurate phenotyping of a large number of individuals, and so body size lends itself well to this type of study.

Here, we report the results of the first study to combine high throughput sequencing with BSA in the context of physiological responses to OA. We reared *M. californianus* under ambient and high pCO_2 conditions in laboratory cultures, used filters to separate larvae into pools of different body sizes, and then sequenced pools of mRNA for each treatment × body size combination to identify effects of high pCO_2 on gene expression, and gene expression differences between large and small larvae of the same age class. While we observed substantial gene expression differences between large and small larvae, we were unable to detect any consistent effect of high pCO_2 on gene expression.

Methods

Field collection and larval culture

We collected adult mussels from Campus Point, Goleta, CA (34.40°N; 119.84°W), and brought them back to the laboratory where they were maintained in flowing seawater at 15°C before spawning. To induce spawning, we scraped the mussels clean, and following Trevelyan and Chang (1983), immersed them in filtered seawater (FSW) with 30 mmol hydrogen peroxide buffered with 17 mmol TRIS for 1.5 h with periodic agitation. After 1.5 h, we rinsed mussels in FSW, then moved them to individual cups to monitor them for the release of gametes. We moved eggs from single females to clean 1 l beakers of FSW, where they were fertilized with 1 ml of dilute sperm suspension from a single male. We split the embryos from each family (the offspring of one male and one female) into high and low pCO_2 rearing conditions. We stocked larval culture buckets with 200 000 embryos each, at a density of 10 larvae ml^{-1}. Due to cost limitations imposed by next-generation sequencing efforts, we were not able to perform culture replicates (multiple buckets per family within a CO_2 treatment). However, previous work with this culturing set-up has shown it to be robust to container effects (Yu *et al.*, 2011).

We cultured larvae in a flow-through CO_2-mixing system described by Fangue *et al.* (2010). pCO_2 exposure levels were based on predictions for the California Current Large Marine Ecosystem, where anthropogenic inputs of CO_2 are expected to drive surface pH down to 7.6 during upwelling in only a few decades (Gruber *et al.*, 2012). Temperatures in seawater tables were held at 15°C using a Delta Star heat pump and a Nema 4x digital temperature controller (AquaLogic, San Diego, CA, USA). We measured temperature, salinity, and pH daily for each culture according to best-practice procedures outlined by Dickson *et al.* (2007), and described in detail in Fangue *et al.* (2010). Temperature was measured using a wire thermocouple (Themolyne PM 207000/Series 1218), and salinity was measured using a conductivity meter (YSI 3100). pH was measured on a total scale, following the standard operating procedure (SOP) 6b (Dickson *et al.*, 2007) using a spectrophotometer (Bio Spec-1601, Shimadzu) and dye *m*-cresol purple (Sigma-Aldrich) as the indicator. Total alkalinity (TA) was measured every 3 d following the SOP 3b (Dickson *et al.*, 2007). Both pH and alkalinity were assessed for accuracy using certified reference materials from Dickson (Scripps Institution of Oceanography), Batch 8 (pH 8.0923 + 0.0004) and Batch 103 (TA = 2232.94 + 0.79 mmol kg^{-1}) for pH and alkalinity, respectively. Parameters of pCO_2, Ω_{ara}, and Ω_{cal} were estimated using CO_2calc (Robbins *et al.*, 2010), with the carbonic acid dissociation constants of Mehrbach *et al.* (1973).

Temperature, salinity, and carbonate parameters of seawater used in experimental treatments are shown in Supplementary Table S1. While we did not explicitly measure survival, we did not observe evidence of mortality differences (e.g. visibly dead larvae or noticeable declines in density) between treatments. We measured the effects of high pCO_2 on growth in six families, and used larvae from three of these families for subsequent RNA-seq analyses. While we had intended from the start of the experiment to sequence the transcriptomes of only three families, we reared six families under each pCO_2 treatment in case of any failed cultures, to ensure that we would have adequate samples for subsequent transcriptomic analyses. The three families used for transcriptomic analyses were chosen haphazardly from the original six.

At 63 h post-fertilization (swimming veliger stage), we concentrated larvae using reverse filtration, then passed all the larvae for

a single culture through a 64-μm mesh sieve, separating each culture into fractions of larvae with diameters less than and greater than 64 μm, respectively. We used this combination of larval age and filter mesh size, because pilot experiments indicated that this was the combination that most reliably produced size-fractionated pools of larvae with substantial numbers of larvae in each pool. The size fraction containing smaller larvae also typically had fewer larvae, but still included a minimum of ~30 000 individuals. The size-fractioned samples were then concentrated to remove excess seawater, and immediately flash frozen.

Morphometrics

We preserved a sample of larvae from each bucket before size fractionation, and a sample from each size-fractionated sample in buffered formalin for subsequent morphometric analysis. We measured shell length (maximum axis parallel with the hinge) for 360 larvae ($n = 30$ per cross per treatment). Body size has been shown to decrease under high pCO_2 in this and other species (Gaylord *et al.*, 2011; Yu *et al.*, 2011) and is an important component of larval fitness (Allen, 2008). We made morphometric measurements on photographs of D-hinge larvae (63 h after fertilization) under ×20 compound magnification (Olympus, BX50, Lumenera, Infinity Lite). We tested for an effect of pCO_2 treatment on larval shell length in a paired *t*-test, with families as replicates ($N = 6$).

Library construction and RNA sequencing

We created cDNA libraries for sequencing from three families of *M. californianus*, each reared under high and low pCO_2 treatments, with each family × pCO_2 treatment separated into fractions of large (>64 μm diameter) vs. small (<64 μm diameter) larvae (12 libraries total). We extracted total RNA from all (30 000–150 000) larvae in each sample using guanidine isothiocyanate (Chomczynski and Sacchi, 1987). Following extraction, we processed RNA to remove tRNA and degraded fragments using an RNeasy Mini Kit according to manufacturer's instructions (Cat. no. 74104, Qiagen, Valencia, CA, USA). RNA yield and purity were assessed by measuring A_{260} and A_{260}/A_{280} ratio, respectively, with a NanoDrop spectrophotometer (NanoDrop Technologies, Wilmington, DE, USA), then using a Bioanalyzer (Agilent, Santa Clara, CA). We constructed cDNA libraries using the Illumina TruSeq RNA sample prep kit (Illumina, San Diego, CA, USA), following the manufacturer's instructions. Each library was given an individual barcode adapter, then all 12 libraries were pooled and sequenced using paired end, 100 base reads in an Illumina HiSeq 2500 (Illumina) at the UC Davis Genome Center Core Facility.

We assessed raw sequence quality using FastQC (v 0.10.1, www.bioinformatics.bbsrc.ac.uk/projects/fastqc.), then trimmed low-quality and adapter sequences using trimgalore (v. 3.23, http://www.bioinformatics.babraham.ac.uk/projects/trim_galore), a wrapper script around Cutadapt (v.1.2; Martin, 2011) and FastQC, under the default settings. Initial QC assessment indicated substantial mitochondrial sequence contamination in our samples, mostly from the mitochondrial 16s rRNA gene. The polyA selection used by the Illumina TruSeq kit should remove the majority of ribosomal RNA in most organisms; however, ribosomal RNA may be polyadenylated post-transcription. In particular, mitochondrial RNA may be internally adenylated at specific loci (Shepard *et al.*, 2011), consistent with our finding of over-represented sequences from specific internal positions of the mitochondrial 16s rRNA gene. To remove mitochondrial rRNA sequence contamination from our dataset, we used bowtie 2–2.1.0 (Langmead *et al.*, 2009) to filter out all sequences that aligned to either the maternal (JX486124.1) or paternal (JX486123.1) mitochondrial genomes. Filtering for quality, adapter contamination and mitochondrial rRNA, resulted in 80 million clean read pairs.

Transcriptome assembly

We assembled the transcriptome using Trinity v. 2013-8-25 (Grabherr *et al.*, 2011) with default parameter settings. Reads from all 12 libraries were combined into a single assembly. To reduce transcript redundancy, we used CD-HIT (Fu *et al.*, 2012) to collapse the assembly to contigs with <98% similarity. To remove additional mistakes and rare variants, we also filtered all contigs that did not have expression support that averaged at least one transcript per million per library. We BLASTed all contigs in the final transcriptome assembly against the NCBI non-redundant nucleotide database, with an *e*-value cutoff of 10^{-4}, using standalone blast tools, v. 2.2.28 (Altschul *et al.*, 1990).

Gene expression analysis

To measure gene expression, reads from each sample were mapped to the final transcriptome assembly using the default settings of RSEM v. 1.2.7 (Li and Dewey, 2011). We investigated patterns of gene expression using the R Bioconductor package, limma (Law *et al.*, 2014; Ritchie *et al.*, 2015). Limma employs an empirical Bayes method to estimate log-fold changes in expression, and has recently been shown to be more robust to false positives than methods that rely heavily on fitting a negative binomial distribution to the data (Rocke *et al.*, 2015). In limma, we fit a series of nested generalized linear models to the data, testing for an effect of family, larval size (nested within family), and CO_2 treatment (nested within size and family) on gene expression. To identify genes differentially expressed between treatments, we set the threshold for false discovery to FDR <0.05 (Benjamini and Hochberg, 1995).

We assessed our power to detect differential gene expression, given the number of reads per library and given the observed dispersion among samples within the same treatment using the software *Scotty* (Busby *et al.*, 2013). We assigned functional annotations and tested for enrichment in GO terms in differentially expressed genes using BLAST2GO (Conesa and Götz, 2008), and assessed significance using Fisher's exact test after correcting for multiple comparisons (FDR; Benjamini and Hochberg, 1995).

Results

Morphometrics

Rearing at elevated (1310 μatm) pCO_2 resulted in 63-h-old D-hinge stage larvae that were 4% smaller than those reared under ambient (345 μatm) pCO_2 conditions (paired *t*-test, $p = 0.004$, $N = 6$ families; Figure 1 and Table 1). We did not observe any differences between treatments in larval developmental stage, nor did we observe substantial numbers of deformed or abnormal larvae in any of our treatments.

Transcriptome

We assembled 80 million pairs of 100 bp reads. This assembly, collapsed to all contigs <98% similarity, contained 52 173 contigs, with an N_{50} of 1620 bp and a GC content of 33.05%. To remove additional mistakes and rare variants, we also filtered contigs that did not have an average expression support of at least one read per million per library. The final assembly contained 34 073 unique contigs. We blasted this assembly to the nr. database, and obtained

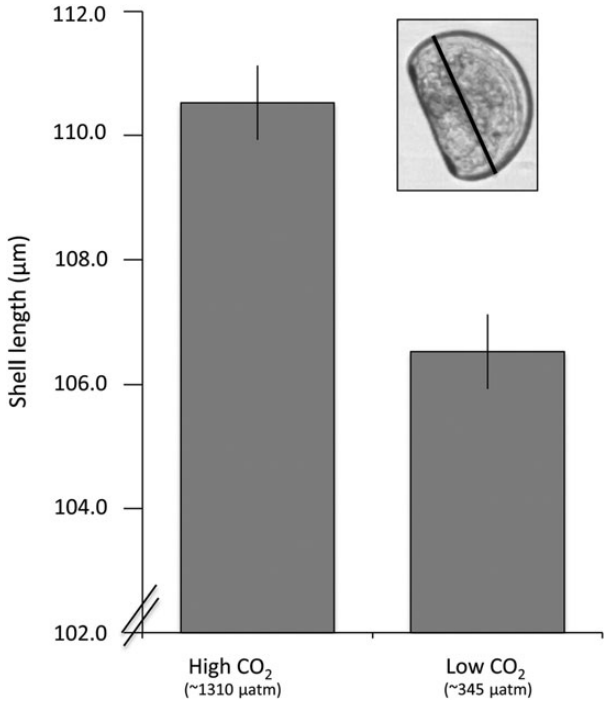

Figure 1. Shell length of 63-h-old larvae of *M. californianus* reared under elevated and ambient pCO_2 conditions. Thirty larvae were measured for each of six families (a single male – female cross) split into high and low pCO_2, respectively. Larvae reared under high CO_2 were 4% smaller on average ($p = 0.004$, paired *t*-test, $N = 6$ families).

Table 1. Shell length ± SE of 63-h old larvae of *M. californianus* reared under elevated and ambient pCO_2 conditions.

Family	Size under low pCO_2 (µm) ± SE	Size under high pCO_2 (µm) ± SE
1	114.7 ± 0.4	113.0 ± 0.4
2	109.9 ± 1.1	106.2 ± 0.4
3	104.1 ± 3.7	101.6 ± 2.9
4	111.9 ± 2.9	104.7 ± 3.2
5	111.0 ± 1.9	105.8 ± 0.6
6	111.5 ± 0.5	107.9 ± 0.5

Thirty larvae were measured for each of six families (a single male – female cross) split into high and low pCO_2, respectively.

significant blast hits for 40.5% of contigs, with 81.0% of top blast hits going to other mollusc sequences.

Gene expression

Overall patterns of gene expression differed among families (343 differentially expressed transcripts, FDR = 0.05), between large and small larvae within families (1225 differentially transcripts, FDR = 0.05), but not among pCO_2 treatments, within families (0 differentially expressed transcripts, FDR = 0.05), or among pCO_2 treatments within size classes (0 differentially expressed transcripts, FDR = 0.05). The lack of observed differences in gene expression persisted, regardless of the stringency of our FDR cutoff. There were still no differentially expressed genes even at an FDR cutoff of 0.5, and the top 10 genes with the greatest probability of differential expression between pCO_2 treatments all had adjusted *p*-values >0.95.

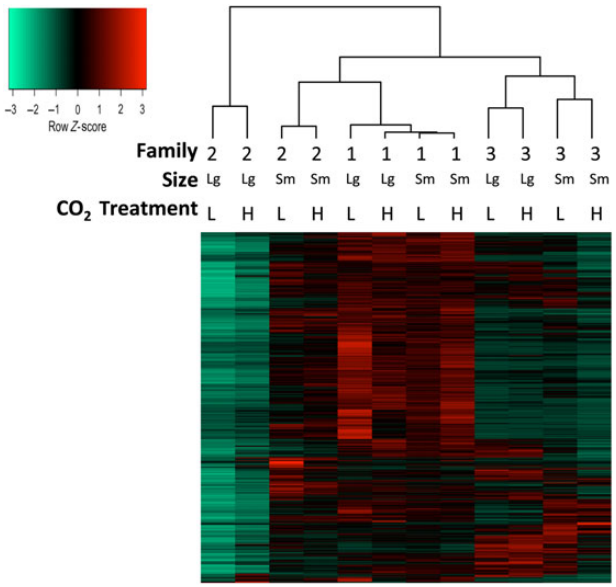

Figure 2. Hierarchical clustering analysis of the transcripts and samples for *M. californianus* larvae exposed to elevated and ambient pCO_2 conditions. Colour key represents normalized fragment counts per kilobase per million transcripts, with red indicating high expression, black indicating intermediate expression, and green indicating low expression. Columns are clustered according to Spearman correlation among treatments; rows are clustered according to Pearson correlations among transcripts. Clustering of samples clearly indicates the strongest correlation among expression patterns of larvae from the same family, regardless of treatment, followed by clustering of expression patterns between larvae of the same size, within families. There was no tendency for expression patterns from the same pCO_2 treatment to cluster with each other.

A hierarchical clustering analysis of gene expression patterns revealed clustering by family, then by size class, but no clustering by pCO_2 treatment (Figure 2), nor was there any significant correlation among overall patterns of gene expression within pCO_2 treatments (Supplementary Figure S1). Many of the 1225 transcripts whose expression pattern differed between large and small larvae were classified as metabolic genes, but this set of genes was not enriched for any specific functional categories (Figure 3, Fisher's exact test, $p > 0.05$).

Given the observed dispersion among replicates, our estimated our statistical power to detect a twofold difference in expression between pCO_2 treatments at $p < 0.05$ was 50%, whereas our power to detect a fourfold change in expression was 80%. Our powers to detect two- and fourfold differences in expression between size classes were 60 and 90%, respectively.

Discussion

We found that *Mytilus* larvae reared under elevated pCO_2 were smaller, but we found no evidence that these differences in size were driven by an effect of high pCO_2 on gene expression. The lack of any observed effect of high pCO_2 on gene expression is surprising, given that we observed phenotypic effects (smaller body size) under high pCO_2, and given that studies in other taxa have documented substantial effects of OA conditions on gene expression, especially for genes related to metabolism and biomineralization pathways (Kurihara *et al.*, 2012; Moya *et al.*, 2012; Benner *et al.*,

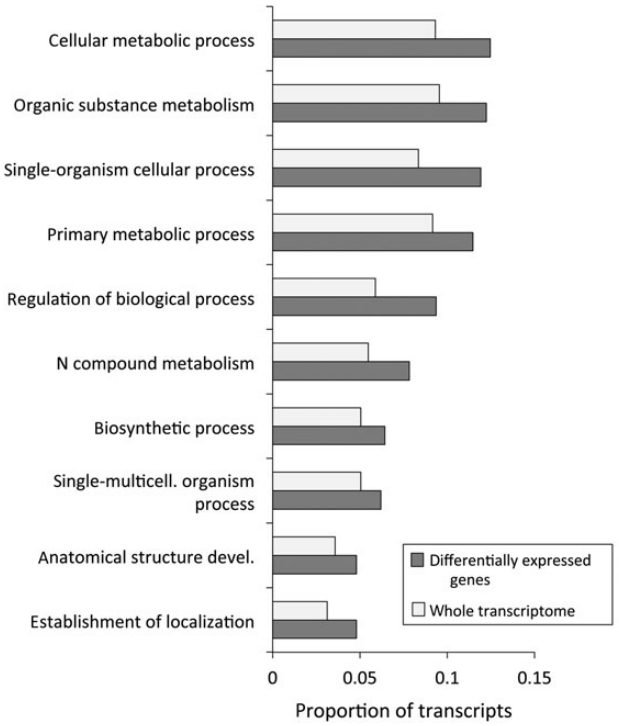

Figure 3. Top ten biological processes represented among ontologies for transcripts that differed in expression between large and small larvae from the same family of the California mussel *M. californianus*.

2013; Padilla-Gamiño *et al.*, 2013; Lohbeck *et al.*, 2014). However, at least one other study failed to document strong effects of high pCO_2 on gene expression in marine larvae: Evans *et al.* (2013) exposed sea urchin larvae to elevated pCO_2 (pH 7.6, as in this study) and detected little effect on gene expression at two different stages of development. Importantly, despite a lack of change in gene expression, *Strongylocentrotus purpuratus* larvae exhibited an even greater reduction in size at pH 7.6 (9.6%, Kelly *et al.*, 2013) than the one we observe here (4%) in *M. californianus.* The lack of concordance between genotypic and phenotypic data highlights the importance of integrating both types of information when seeking to understand and predict the biological consequences of OA.

The lack of observed differences in gene expression between pCO_2 treatments could have been driven partly by the lack of power. After adapter trimming and removal of sequence contamination, we mapped an average of 6.7 million reads per sample to the reference transcriptome. In contrast, Moya *et al.* (2012) obtained 28 million reads per sample in a study of the coral *Acropora millepora*, and found CO_2-driven changes in gene expression in 19% of genes. Nevertheless, our power analysis suggests that if high pCO_2 produces changes in gene expression in *M. californianus* larvae, these changes must be relatively small. Given the observed level of dispersion among samples, we should have been able to detect 50% of genes with a twofold difference in expression, and 80% of genes with a fourfold expression change under elevated pCO_2.

The contrast between expression responses of *Mytilus* and a species like *Acropora* to high CO_2 may also be driven by differences in natural CO_2 fluctuations experienced by each species. In the eastern Pacific habitat of *M. californianus*, seasonal wind-driven upwelling produces large fluctuations in surface water pH (Yu *et al.*, 2011; Booth *et al.*, 2012) with transient pH values as low as 7.8 in nearshore habitats (Evans *et al.*, 2013). Although coral reef habitats also experience daily fluctuations driven by the effects of respiration and photosynthesis, these are shorter in duration that those produced by seasonal upwelling (Kline *et al.*, 2015; Rivest and Gouhier, 2015). Because *Mytilus* has evolved in the context of seasonal upwelling, beginning in the Northeast Pacific some 15–12 million years ago (Vermeij, 1989), exposure to pH 7.6 may not produce the generalized stress response in *M. californianus* larvae that might be expected for a species exposed to conditions far outside those of its typical environment. Upwelling is less strong in southern California (where samples were collected for this study) than further to the north, but populations of *M. californianus* are relatively panmictic (Levinton and Suchanek, 1978), so that southern populations likely receive substantial gene flow from northern populations that experience frequent upwelling. Given that *M. californianus* has evolved in the context of fluctuating CO_2, we might expect larvae to exhibit an adaptive plastic response to low pH, such as increased energy devoted to calcification to compensate for the lower availability of carbonate. However, it also seems possible that *Mytilus* larvae are always calcifying at the maximum rate possible given available energy reserves, and thus do not devote any additional resources to calcification when faced with lower carbonate availability. It is also possible that *Mytilus*, in general, are relatively tolerant of high pCO_2. Recent work with congeners, *M. edulis* and *M. galloprovincialis*, showed limited impacts of high pCO_2 on growth and mortality (even at levels >3000 μatm), and much greater effects of factors like food availability and temperature (Thomsen *et al.*, 2013; Gazeau *et al.*, 2014). This is despite the fact that *M. galloprovincialis*, unlike *M. californianus*, does not originate in a high upwelling region.

Two other studies taking proteomic approaches have demonstrated broad-scale down-regulation of proteins in Pacific oysters (*Crassostrea gigas*) subjected to OA conditions (Dineshram *et al.*, 2012; Timmins-Schiffmann *et al.*, 2014). Differences between these results and those in the present study might relate to more extreme pH conditions used in those studies (pH 7.6 in the present study, vs. pH 7.5 and 7.3, respectively) or a lower tolerance of oysters, relative to mussels, to OA conditions. However, a third, intriguing possibility is that proteomics might have greater sensitivity to changes in organismal physiology than transcriptomics, highlighting the need, wherever possible, to integrate the two approaches.

Some have argued that reductions in the size of marine larvae under high pCO_2 are driven by metabolic depression and changes in the rate of development (Pörtner, 2008; Stumpp *et al.*, 2011). We found strong evidence of a general relationship between metabolism and larval size: there were substantial gene expression differences between large and small larvae, and these differentially expressed transcripts were predominantly related to metabolic function. However, we found no evidence of a specific effect of high pCO_2 on expression of metabolic genes (or any other genes) in *M. californianus* larvae. Our results are consistent with recent findings of Waldbusser *et al.* (2015), who observed reductions in shell growth rate in *Mytilus* larvae driven by reductions in aragonite saturation state, but not changes in pCO_2 or pH, and observed effects of OA conditions on metabolism only at very low pH values (~7.4). Given these findings, it is probably unsurprising that we did not find any gene expression changes related to metabolic depression or any other global physiological changes in *M. californianus* larvae exposed to pH 7.6.

An important consideration when interpreting our results, or those of similar studies, is that they are essentially acute toxicity

challenges. Compared with the time-scale of our experiment and others like it, OA will occur slowly, over the next 10–20 decades. As a result, observed responses (or in our case, the lack of a response) should be interpreted with caution. Responses to OA that may occur on multi-generational time-scales include parental effects, acclimatization, and genetic adaptation, all of which will be missed by short-term studies (Kelly and Hofmann, 2013).

Transcriptomic data are useful in studies of organismal responses to climate change stressors in that they provide a global view of the physiological response (or in this case, lack of a response) to that stressor (Stillman and Armstrong, 2015). As we continue to try to understand biological responses to OA, it will be important to document which organisms are responding to OA conditions, and along which physiological axes. In this context, negative results (especially when published with their associated estimates of statistical power) will be as important as positive ones. *Mytilus californianus* larvae exposed to OA conditions exhibit a reduction in growth rate, but no associated changes in gene expression. The lack of transcriptomic response does not necessarily mean that *M. californianus* larvae will not be affected by OA conditions, merely that we cannot detect any evidence that they are compensating for these effects through changes in gene expression. More studies that integrate transcriptomic data with other phenotypic measurements, and that span multiple life stages, will be needed before we can fully appreciate the sensitivity, or potential resilience of this species to future ocean change.

Data accessibility

Illumina RNA-Seq data have been submitted to the NCBI Sequence Read Archive (SRA; accession numbers SRX1309994). Differential expression data/results, R-scripts and larval size measurements are available upon request.

Supplementary material

Supplementary material is available at the *ICESJMS* online version of the manuscript.

Acknowledgements

We thank B. Gaylord, M. Debiasse, and two anonymous reviewers for helpful comments on earlier versions of this manuscript. S. Bachuber and C. Sugano assisted with morphological measurements of larval mussels. This project was supported by US National Science Foundation (NSF) awards OCE-1040960 and IOS-1021536 to GEH, and by a University of California multi-campus research programme, Ocean acidification: A Training and Research Consortium (http://oceanacidification.msi.ucsb.edu/) to GEH.

References

Allen, J. D. 2008. Size-specific predation on marine invertebrate larvae. The Biological Bulletin, 214: 42–49.

Altschul, S. F., Gish, W., Miller, W., Myers, E. W., and Lipman, D. J. 1990. Basic local alignment search tool. Journal of Molecular Biology, 215: 403–410.

Benjamini, Y., and Hochberg, Y. 1995. Controlling the false discovery rate: A practical and powerful approach to multiple testing. Journal of the Royal Statistical Society; Series B, 57: 289–300.

Benner, I., Diner, R. E., Lefebvre, S. C., Li, D., Komada, T., Carpenter, E. J., and Stillman, J. H. 2013. *Emiliania huxleyi* increases calcification but not expression of calcification-related genes in long-term exposure to elevated temperature and pCO_2. Philosophical Transactions of the Royal Society of London: Series B, Biological Sciences, 368: 20130049.

Booth, J. A. T., McPhee-Shaw, E. E., Chua, P., Kingsley, E., Denny, M., Phillips, R., Bograd, S. J., *et al.* 2012. Natural intrusions of hypoxic, low pH water into nearshore marine environments on the California coast. Continental Shelf Research, 45: 108–115.

Busby, M. A., Stewart, C., Miller, C. A., Grzeda, K. R., and Marth, G. T. 2013. Scotty: A web tool for designing RNA-Seq experiments to measure differential gene expression. Bioinformatics (Oxford, England), 29: 656–657.

Chapman, R. W., Mancia, A., Beal, M., Veloso, A., Rathburn, C., Blair, A., Holland, A. F., *et al.* 2011. The transcriptomic responses of the eastern oyster, *Crassostrea virginica*, to environmental conditions. Molecular Ecology, 20: 1431–1449.

Chomczynski, P., and Sacchi, N. 1987. Single-step method of RNA isolation by acid guanidinium thiocyanate-phenol-chloroform extraction. Analytical Biochemistry, 162: 156–159.

Conesa, A., and Götz, S. 2008. Blast2GO: A comprehensive suite for functional analysis in plant genomics. International Journal of Plant Genomics, 2008: 12 p.

Dickson, A. G., Sabine, C. L., and Christian, J. R. 2007. Guide to Best Practices for Ocean CO_2 Measurements. 191 pp. http://aquacomm.fcla.edu/1443/ (last accessed 6 October 2015).

Dineshram, R., Wong, K. K. W., Xiao, S., Yu, Z., Qian, P. Y., and Thiyagarajan, V. 2012. Analysis of Pacific oyster larval proteome and its response to high-CO_2. Marine Pollution Bulletin, 64: 2160–2167.

Dupont, S., Havenhand, J., Thorndyke, W., Peck, L., and Thorndyke, M. 2008. Near-future level of CO_2-driven ocean acidification radically affects larval survival and development in the brittlestar *Ophiothrix fragilis*. Marine Ecology Progress Series, 373: 285–294.

Evans, T. G., Chan, F., Menge, B. A., and Hofmann, G. E. 2013. Transcriptomic responses to ocean acidification in larval sea urchins from a naturally variable pH environment. Molecular Ecology, 22: 1609–1625.

Evans, T. G., and Hofmann, G. E. 2012. Defining the limits of physiological plasticity: How gene expression can assess and predict the consequences of ocean change. Philosophical Transactions of the Royal Society of London: Series B, Biological Sciences, 367: 1733–1745.

Fangue, N. A., O'Donnell, M. J., Sewell, M. A., Matson, P. G., MacPherson, A. C., and Hofmann, G. E. 2010. A laboratory-based, experimental system for the study of ocean acidification effects on marine invertebrate larvae. Limnology and Oceanography: Methods, 8: 441–452.

Fu, L., Niu, B., Zhu, Z., Wu, S., and Li, W. 2012. CD-HIT: Accelerated for clustering the next generation sequencing data. Bioinformatics (Oxford, England), 28: 3150–3152.

Gaylord, B., Hill, T. M., Sanford, E., Lenz, E. A., Jacobs, L. A., Sato, K. N., Russell, A. D., *et al.* 2011. Functional impacts of ocean acidification in an ecologically critical foundation species. The Journal of Experimental Biology, 214: 2586–2594.

Gazeau, F., Alliouane, S., Bock, C., Bramanti, L., López Correa, M., Gentile, M., Hirse, T., *et al.* 2014. Impact of ocean acidification and warming on the Mediterranean mussel (*Mytilus galloprovincialis*). Frontiers in Marine Science, 1: 1–12.

Grabherr, M. G., Haas, B. J., Yassour, M., Levin, J. Z., Thompson, D. A., Amit, I., Adiconis, X., *et al.* 2011. Full-length transcriptome assembly from RNA-Seq data without a reference genome. Nature Biotechnology, 29: 644–652.

Gruber, N., Hauri, C., Lachkar, Z., Loher, D., Frölicher, T. L., and Plattner, G-K. 2012. Rapid progression of ocean acidification in the California current system. Science (New York, NY), 337: 220–223.

Harms, L., Frickenhaus, S., Schiffer, M., Mark, F. C., Storch, D., Held, C., Pörtner, H-O., *et al.* 2014. Gene expression profiling in gills of the great spider crab *Hyas araneus* in response to ocean acidification and warming. BMC Genomics, 15: 789.

Hettinger, A., Sanford, E., Hill, T. M., Russell, A. D., Sato, K. N. S., Hoey, J., Forsch, M., *et al.* 2012. Persistent carry-over effects of planktonic exposure to ocean acidification in the Olympia oyster. Ecology, 93: 2758–2768.

Hofmann, G. E., Barry, J. P., Edmunds, P. J., Gates, R. D., Hutchins, D. A., Klinger, T., and Sewell, M. A. 2010. The effect of ocean acidification on calcifying organisms in marine ecosystems: An organism-to-ecosystem perspective. Annual Review of Ecology, Evolution, and Systematics, 41: 127–147.

Kelly, M. W., and Hofmann, G. E. 2013. Adaptation and the physiology of ocean acidification. Functional Ecology, 27: 980–990.

Kelly, M. W., Padilla-Gamiño, J. L., and Hofmann, G. E. 2013. Natural variation and the capacity to adapt to ocean acidification in the keystone sea urchin *Strongylocentrotus purpuratus*. Global Change Biology, 19: 2536–2546.

Kline, D. I., Teneva, L., Hauri, C., Schneider, K., Miard, T., Chai, A., Marker, M., *et al.* 2015. Six month *in situ* high-resolution carbonate chemistry and temperature study on a coral reef flat reveals asynchronous pH and temperature anomalies. PLoS ONE, 10: e0127648.

Kroeker, K. J., Kordas, R. L., Crim, R. N., and Singh, G. G. 2010. Meta-analysis reveals negative yet variable effects of ocean acidification on marine organisms. Ecology Letters, 13: 1419–1434.

Kurihara, H., Takano, Y., Kurokawa, D., and Akasaka, K. 2012. Ocean acidification reduces biomineralization-related gene expression in the sea urchin, *Hemicentrotus pulcherrimus*. Marine Biology, 159: 2819–2826.

Langmead, B., Trapnell, C., Pop, M., and Salzberg, S. L. 2009. Ultrafast and memory-efficient alignment of short DNA sequences to the human genome. Genome Biology, 10: R25.

Lannig, G., Eilers, S., Pörtner, H. O., Sokolova, I. M., and Bock, C. 2010. Impact of ocean acidification on energy metabolism of oyster, *Crassostrea gigas*—Changes in metabolic pathways and thermal response. Marine Drugs, 8: 2318–2339.

Law, C. W., Chen, Y., Shi, W., and Smyth, G. K. 2014. Voom: Precision weights unlock linear model analysis tools for RNA-seq read counts. Genome Biology, 15: R29.

Levinton, J. S., and Suchanek, T. H. 1978. Geographic variation, niche breadth and genetic differentiation at different geographic scales in the mussels *Mytilus californianus* and *M. edulis*. Marine Biology, 49: 363–375.

Li, B., and Dewey, C. N. 2011. RSEM: Accurate transcript quantification from RNA-Seq data with or without a reference genome. BMC Bioinformatics, 12: 323.

Lohbeck, K. T., Riebesell, U., and Reusch, T. B. H. 2014. Gene expression changes in the coccolithophore *Emiliania huxleyi* after 500 generations of selection to ocean acidification. Proceedings of Biological Sciences/The Royal Society, 281: 20140003.

Martin, M. 2011. Cutadapt removes adapter sequences from high-throughput sequencing reads. http://journal.embnet.org/index.php/embnetjournal/article/view/200/479 (last accessed 6 October 2015).

Mehrbach, C., Culberson, C. H., Hawley, J. E., and Pytkowicx, R. M. 1973. Measurement of the apparent dissociation constants of carbonic acid in seawater at atmospheric pressure. Limnology and Oceanography, 18: 897–907.

Michelmore, R. W., Paran, I., and Kesseli, R. V. 1991. Identification of markers linked to disease-resistance genes by bulked segregant analysis: A rapid method to detect markers in specific genomic regions by using segregating populations. Proceedings of the National Academy of Sciences of the United States of America, 88: 9828–9832.

Moya, A., Huisman, L., Ball, E. E., Hayward, D. C., Grasso, L. C., Chua, C. M., Woo, H. N., *et al.* 2012. Whole transcriptome analysis of the coral *Acropora millepora* reveals complex responses to CO?-driven acidification during the initiation of calcification. Molecular Ecology, 21: 2440–2454.

Padilla-Gamiño, J. L., Kelly, M. W., Evans, T. G., and Hofmann, G. E. 2013. Temperature and CO_2 additively regulate physiology, morphology and genomic responses of larval sea urchins, *Strongylocentrotus purpuratus*. Proceedings of the Royal Society B Biological Sciences, 280: 20130155.

Pörtner, H. O. 2008. Ecosystem effects of ocean acidification in times of ocean warming: A physiologist's view. Marine Ecology Progress Series, 373: 203–217.

Ritchie, M. E., Phipson, B., Wu, D., Hu, Y., Law, C. W., Shi, W., and Smyth, G. K. 2015. Limma powers differential expression analyses for RNA-sequencing and microarray studies. Nucleic Acids Research, 43: e47.

Rivest, E. B., and Gouhier, T. C. 2015. Complex environmental forcing across the biogeographical range of coral populations. PLoS ONE, 10: e0121742.

Robbins, L. L., Hansen, M. E., Kleypas, J. A., and Meylan, S. C. 2010. CO2calc—A User-friendly Seawater Carbon Calculator for Windows, Max OS X, and iOS (iPhone). US Geological Survey Open-File Report 2010–1280, 17 pp.

Rocke, D. M., Ruan, L., Zhang, Y., Gossett, J. J., Durbin, B., and Aviran, S. 2015. Excess false positive rates in methods for differential gene expression analysis using RNA-Seq data. bioRxiv, doi: http://dx.doi.org/10.1101/020784.

Seibel, B. A., Maas, A. E., and Dierssen, H. M. 2012. Energetic plasticity underlies a variable response to ocean acidification in the pteropod, *Limacina helicina* antarctica. PLoS ONE, 7: e30464.

Shepard, P. J., Choi, E-A., Lu, J., Flanagan, L. A., Hertel, K. J., and Shi, Y. 2011. Complex and dynamic landscape of RNA polyadenylation revealed by PAS-Seq. RNA (New York, N.Y.), 17: 761–772.

Sheridan, J. A., and Bickford, D. 2011. Shrinking body size as an ecological response to climate change. Nature Climate Change, 1: 401–406.

Stillman, J. H., and Armstrong, E. 2015. Genomics are transforming our understanding of responses to climate change. Bioscience, 65: 1–10.

Stumpp, M., Dupont, S., Thorndyke, M. C., and Melzner, F. 2011. CO_2 induced seawater acidification impacts sea urchin larval development II: Gene expression patterns in pluteus larvae. Comparative Biochemistry and Physiology: A Molecular and Integrative Physiology, 160: 320–330.

Suchanek, T. H. 1992. Extreme biodiversity in the marine environment: Mussel bed communities of *Mytilus californianus*. Northwest Environmental Journal, 8: 150–152.

Thomsen, J., Casties, I., Pansch, C., Körtzinger, A., and Melzner, F. 2013. Food availability outweighs ocean acidification effects in juvenile *Mytilus edulis*: Laboratory and field experiments. Global Change Biology, 19: 1017–1027.

Timmins-Schiffmann, E., Coffey, W. D., Hua, W., Nunn, B. L., Dickinson, G. H., and Roberts, S. B. 2014. Shotgun proteomics reveals physiological response to ocean acidification in *Crassostrea gigas*. PeerJ, 2: 1–59.

Trevelyan, G. A., and Chang, E. S. 1983. Experiments on larval rearing of the California Mussel (*Mytilus californianus*). Journal of the World Mariculture Society, 14: 137–148.

Vermeij, G. J. 1989. Geographical restriction as a guide to the causes of extinction: The case of the cold northern oceans during the Neogene. Paleobiology, 15: 335–356.

Vidal-Dupiol, J., Dheilly, N. M., Rondon, R., Grunau, C., Cosseau, C., Smith, K. M., Freitag, M., *et al.* 2014. Thermal stress triggers broad *Pocillopora damicornis* transcriptomic remodeling, while *Vibrio coralliilyticus* infection induces a more targeted immuno-suppression response. PLoS ONE, 9: e107672.

Waldbusser, G. G., Brunner, E. L., Haley, B. A., Hales, B., Langdon, C. J., and Prahl, F. G. 2013. A developmental and energetic basis linking larval oyster shell formation to acidification sensitivity. Geophysical Research Letters, 40: 2171–2176.

Waldbusser, G. G., Hales, B., Langdon, C. J., Haley, B. A., Schrader, P., Brunner, E. L., Gray, M. W., *et al.* 2015. Ocean acidification has multiple modes of action on bivalve larvae. PLos ONE, 10: e0128376.

Watson, S. A., Peck, L. S., Tyler, P. A., Southgate, P. C., Tan, K. S., Day, R. W., and Morley, S. A. 2012. Marine invertebrate skeleton size varies with latitude, temperature and carbonate saturation: Implications

for global change and ocean acidification. Global Change Biology, 18: 3026–3038.

Whitehead, A. 2012. Comparative genomics in ecological physiology: Toward a more nuanced understanding of acclimation and adaptation. The Journal of Experimental Biology, 215: 884–891.

Yu, P. C., Matson, P. G., Martz, T. R., and Hofmann, G. E. 2011. The ocean acidification seascape and its relationship to the performance of calcifying marine invertebrates: Laboratory experiments on the development of urchin larvae framed by environmentally-relevant pCO_2/pH. Journal of Experimental Marine Biology and Ecology, 400: 288–295.

Handling editor: Howard Browman

ICES Journal of Marine Science

ICES Journal of Marine Science (2016), 73(3), 970–980. doi:10.1093/icesjms/fsv188

Contribution to Special Issue: 'Towards a Broader Perspective on Ocean Acidification Research'

Original Article

Elevated pCO_2 drives lower growth and yet increased calcification in the early life history of the cuttlefish *Sepia officinalis* (Mollusca: Cephalopoda)

Julia D. Sigwart[1,2]*, Gillian Lyons[1,2], Artur Fink[3], Magdalena A. Gutowska[4], Darren Murray[2], Frank Melzner[4], Jonathan D. R. Houghton[1,2,5], and Marian Yong-an Hu[6]

[1]*Marine Laboratory, Queen's University Belfast, 12-13 The Strand, Portaferry BT22 1PF, Northern Ireland*
[2]*School of Biological Sciences, Queen's University Belfast, 97 Lisburn Road, Belfast BT9 7BL, Northern Ireland*
[3]*Max Planck Institute for Marine Microbiology, Bremen 28359, Germany*
[4]*Helmholtz Centre for Ocean Research Kiel, GEOMAR, Kiel 24105, Germany*
[5]*Institute of Global Food Security, Queen's University Belfast, 18-30 Malone Road, Belfast BT9 5BN, Northern Ireland*
[6]*Institute of Physiology, University of Kiel, Kiel 24098, Germany*

*Corresponding author: e-mail: j.sigwart@qub.ac.uk

Sigwart, J. D., Lyons, G., Fink, A., Gutowska, M. A., Murray, D., Melzner, F., Houghton, J. D. R., and Hu, M. Y. Elevated pCO_2 drives lower growth and yet increased calcification in the early life history of the cuttlefish *Sepia officinalis* (Mollusca: Cephalopoda). – ICES Journal of Marine Science, 73: 970–980.

Received 29 April 2015; revised 22 September 2015; accepted 28 September 2015; advance access publication 29 October 2015.

Ocean acidification is an escalating environmental issue and associated changes in the ocean carbonate system have implications for many calcifying organisms. The present study followed the growth of *Sepia officinalis* from early-stage embryos, through hatching, to 7-week-old juveniles. Responses of cuttlefish to elevated pCO_2 (hypercapnia) were investigated to test the impacts of near-future and extreme ocean acidification conditions on growth, developmental time, oxygen consumption, and yolk utilization as proxies for individual fitness. We further examined gross morphological characteristics of the internal calcareous cuttlebone to determine whether embryonically secreted shell lamellae are impacted by environmental hypercapnia. Embryonic growth was reduced and hatching delayed under elevated pCO_2, both at environmentally relevant levels (0.14 kPa pCO_2 similar to predicted ocean conditions in 2100) and extreme conditions (0.40 kPa pCO_2). Comparing various metrics from control and intermediate treatments generally showed no significant difference in experimental measurements. Yet, results from the high pCO_2 treatment showed significant changes compared with controls and revealed a consistent general trend across the three treatment levels. The proportion of animal mass contributed by the cuttlebone increased in both elevated pCO_2 treatments. Gross cuttlebone morphology was affected under such conditions and cuttlebones of hypercapnic individuals were proportionally shorter. Embryonic shell morphology was maintained consistently in all treatments, despite compounding hypercapnia in the perivitelline fluid; however, post-hatching, hypercapnic animals developed denser cuttlebone laminae in shorter cuttlebones. Juvenile cuttlefish in acidified environments thus experience lower growth and yet increased calcification of their internal shell. The results of this study support recent findings that early cuttlefish life stages are more vulnerable towards hypercapnia than juveniles and adults, which may have negative repercussions on the biological fitness of cuttlefish hatchlings in future oceans.

Keywords: development, growth, metabolism, morphometrics, ocean acidification.

Introduction

An increase in open ocean pCO_2 from present levels of ~0.04 kPa to 0.07–0.10 kPa pCO_2 in open ocean habitats is expected to occur by 2100 (IPCC, 2007; Doney *et al.*, 2009). Particularly in many coastal habitats, much higher pCO_2 values of >0.2–0.4 kPa can be expected in the next century. This is due to additional CO_2 production through respiratory processes (Melzner *et al.*, 2013; Wallace *et al.*, 2014). Changes in future ocean chemistry may eventually

cross thresholds in carbonate system speciation that constrain biogenic calcification, especially in species whose carbonate structures are directly exposed to seawater and not covered by protective organic layers (Reis *et al.*, 2009; Tunnicliffe *et al.*, 2009). Elevated seawater pCO_2 causes an acidosis in body fluids of all water-breathing organisms. This acidosis can be countered by some taxa, e.g. fish (Heisler, 1984; Claiborne and Edwards, 2002), crustaceans (Wheatly and Henry, 1992; Spicer *et al.*, 2007), and cephalopods (Gutowska *et al.*, 2010a) via increasing blood bicarbonate concentrations and secretion of protons. These changes in body fluid acid–base chemistry have been shown to induce behavioural pathologies in fish (Munday *et al.*, 2009) and seem to be causally related to hypermineralization in fish and cephalopods (Checkley *et al.*, 2009; Gutowska *et al.*, 2010a).

In some oviparous marine taxa, including fish, crustaceans, and cephalopod molluscs, the final phase of embryogenesis is characterized by challenging abiotic conditions (i.e. naturally high pCO_2) inside the protecting egg capsule. To maintain a sufficient O_2 flux into, and a CO_2 flux output of the perivitelline space, the eggs of many aquatic organisms undergo a swelling process that leads to reduced egg wall thickness and increases gas conductance as well as increased effective surface area available for diffusion (e.g. Cronin and Seymour, 2000; Walther *et al.*, 2010; Tseng *et al.*, 2013). In addition, pO_2 and pCO_2 in the perivitelline fluid (PVF) are modulated to enhance diffusive flux of respiratory gases: this leads to low PVF pO_2 values of <6 kPa and high PVF pCO_2 values of $>0.2–0.4$ kPa and pH values as low as 7.2 (Gutowska and Melzner, 2009; Dorey *et al.*, 2013). Elevated environmental pCO_2 leads to proportional increases in PVF pCO_2, as excretory CO_2 flux depends on a stable pCO_2 gradient between PVF and seawater (Hu *et al.*, 2011b; Dorey *et al.*, 2013). The fact that cephalopod embryos are naturally confronted with strong hypercapnia has led to the evolution of a capable embryonic acid–base regulatory machinery (Hu *et al.*, 2011a).

Members of the cephalopod order Sepiida, the cuttlefish, are direct-developers with a long (ca. 2 months) developmental period *in ovo*, and form an internal shell composed of delicate layers of calcium carbonate (aragonite) and organic matrices. The shell is initially formed in the embryo before hatching. The cuttlebone is formed of overlaid sheets of calcium carbonate, vertically separated to form chambers that function in buoyancy control for the animal (Denton and Gilpin-Brown, 1961). As the animal grows, new lamellae are laid down ventrally and the cuttlebone grows anteriorly in proportion to the rest of the body. Contrary to studies on many calcifying invertebrates (e.g. Wood *et al.*, 2008; Kroeker *et al.*, 2010; Wittmann and Pörtner, 2013), juveniles of the common cuttlefish *Sepia officinalis* actually mineralize more $CaCO_3$ in their cuttlebones during exposure to elevated seawater pCO_2, while maintaining growth and metabolism (Gutowska *et al.*, 2008, 2010b; Dorey *et al.*, 2013).

Questions remain as to how *S. officinalis* responds to ocean acidification in terms of physiology, development, and growth. To ascertain the effects of realistic near-future ocean acidification, we examined embryonic and juvenile cuttlefish incubated *in ovo*, hatched, and subsequently raised under different pCO_2 treatments. Given that the embryos of this species are naturally capable of secreting a shell under hypercapnic conditions within the PVF, we hypothesized that embryonic calcification is less sensitive to acid–base disturbances compared with post-hatching juveniles. Our experiments were designed to test whether embryonic development of *S. officinalis* under acidified conditions leads to juveniles with reduced fitness. Growth rates of juvenile *S. officinalis* are reportedly not impacted by elevated pCO_2 (Gutowska *et al.*, 2008), for animals that had not been exposed to elevated seawater pCO_2 as embryos. Recent studies on other marine invertebrate species have found significant negative carry-over effects from one ontogenetic stage to the next in response to simulated ocean acidification, both in molluscs and echinoderms (Dupont *et al.*, 2008; Hettinger *et al.*, 2013). We reared *S. officinalis* embryos under simulated ocean acidification conditions to then assess juvenile growth performance. This study provided an opportunity to examine whether development under OA conditions increases stress at a vulnerable life stage, or alternatively provides an opportunity for early-ontogeny plasticity to cope with altered conditions.

Material and methods

Experimental animals and treatments

Eggs of *S. officinalis* were obtained from captive breeding at the Biological station in Luc-sur-Mer, Université de Caen (Normandy, France) and transported to Germany as very early-stage embryos (Stage 5–7 *sensu* Lemaire, 1970). Experiments were conducted at the facilities on the island Sylt at the Wadden Sea Station of the Alfred Wegener Institute for Polar and Marine Research (AWI), Germany, from May to August 2011.

To avoid bacterial infections, seawater was passed over a 15 W UV sterilizer (HW-Aquaristik, Germany). To avoid alterations of the seawater carbonate system by biological activity of experimental animals and micro-organisms, a flow through system using North Sea water (mean salinity 31.5) was maintained in a 16°C climate chamber with flow rates of seawater adjusted to a minimum twofold water exchange per tank per day (Table 1). All experimental tanks were maintained under a constant 12 h dark:12 h light cycle with water quality parameters monitored weekly to keep concentrations of nitrate below 0.2 mg l^{-1}. Eggs at embryonic stage 10 (after Lemaire, 1970; $n = 525$) were separated and randomly distributed to treatment groups, and each placed individually on the bottom of its assigned tank. Eggs were incubated for ~8 weeks before hatching. Post-hatching, temperature was increased to 18°C to improve growth (the range of 16–18°C is well within the optimum range of the species), and animals were fed twice-daily *ad libitum*, initially on a diet of mysids (*Neomysis integer*) and progressively transitioned to fresh brown shrimp (*Crangon crangon*).

CO_2 treatments

Three pCO_2 treatments were selected to facilitate comparison with other published studies (Gutowska *et al.*, 2008, 2010b; Hu *et al.*, 2011b; Dorey *et al.*, 2013): control, 0.05 kPa pCO_2; intermediate, 0.14 kPa pCO_2; and high, 0.37 kPa pCO_2 (Table 1). These were controlled by equilibrating experimental aquaria with an air/CO_2 gas mixture generated by a central automatic gas mixing-facility (Linde Gas, HTK Hamburg, Germany). The gas mixture was introduced into the experimental aquaria using diffuser stones (Dohse, Grafschaft-Gelsdorf, Germany). Fresh and sterilized (hw UV sterilizer 500, Krefeld, Germany) seawater ($S = 28–31.5$) was adjusted to a salinity of 32.2 (Instant Ocean, Aquarium Systems, Sarrebourg, France) and pre-equilibrated with the respective air/CO_2 mixtures in 150 l reservoirs. Daily exchange with pre-equilibrated seawater (40–80% of the tank volume) ensured NH_4^+ concentration below 0.2 mg l^{-1}. Temperature, salinity, and pH were checked daily. Seawater samples (0.5 l) for determination of total dissolved inorganic carbon (DIC) were collected weekly and poisoned with

Table 1. Seawater physiochemical parameters in for the control (0.05 kPa CO_2) and hypercapnic treatments (intermediate, ~0.14 kPa CO_2; and high, 0.37 kPa CO_2).

	Control ~0.05 kPa	pCO_2 ~ 0.14 kPa	pCO_2 ~ 0.37 kPa
Salinity	32.2 ± 0.2	32.2 ± 0.2	32.2 ± 0.2
Flow rate (ml min^{-1})	48.9 ± 7.6	46.4 ± 6.0	46.6 ± 5.0
pH_{NBS}	8.02 ± 0.04	7.76 ± 0.05	7.27 ± 0.03
pH_{NBS} min	7.84	7.45	7.10
pH_{NBS} max	8.07	7.95	7.35
DIC	2333 ± 88	2484 ± 120	2667 ± 140
TA	2567 ± 80	2557 ± 116	2595 ± 132
pCO_2	0.052 ± 0.008	0.135 ± 0.020	0.368 ± 0.039
$\Omega_{aragonite}$	2.85 ± 0.32	1.33 ± 0.17	0.55 ± 0.05
Day 19—*n* specimens	19	16	16
Day 34—*n* specimens	32	32	32
Day 47—*n* specimens	28	28	28

Measurements presented are the mean among all replicate aquariums over all daily measurements during the full experimental duration. Flow rate and pH_{NBS} (pH NBS scale) were measured daily in each tank, with a mean calculated for each aquarium and each treatment over the experimental period. Flow rate (flow, ml seawater min^{-1}) is the rate with which fresh seawater entered each aquarium. NBS, National Bureau of Standards; DIC, total dissolved inorganic carbon; TA, total alkalinity; $\Omega_{aragonite}$, saturation state of aragonite; pCO_2, CO_2 partial pressure. pH_{NBS} is the mean of daily measurements. Minimal (min) and maximal (max) values present minimal and maximal values in pH_{NBS} observed in any aquarium and are given as a measure for fluctuation.

100 µl of an $HgCl_2$ saturated solution. DIC was determined using an AIRICA analyzer (Marianda, Kiel, Germany). DICKSON seawater standard was used as reference (Dickson *et al.*, 2003). Seawater specifications were calculated from pH_{TOTAL} (recalibrated with seawater buffers) and DIC with the open source program CO2SYS (Lewis and Wallace, 1998) using the dissociation constants by Mehrbach *et al.* (1973) as refitted by Dickson and Millero (1987). Seawater pH and temperature (Table 1) were measured daily with a pH meter (WTW 340i pH-analyzer, WTW SenTix 81-measuring chain, precision 0.01 units) that was calibrated with Radiometer IUPAC precision pH buffers 7.00 and 10.00 (S11M44, S11 M007).

Oxygen consumption

Oxygen consumption of stage 29–30 embryos and hatchlings was determined via closed-chamber respirometry. Animals were gently placed into 44 ml (individual eggs, stage 29–30 embryos) or 130 ml (hatchlings, age 1–3 d) glass vessels filled with 0.2 µm-filtered seawater from an incubation tank with the respective pCO_2 level. Respiration chambers containing eggs were closed air-free with glass slides and placed into a temperature controlled water bath at 16.00 ± 0.02°C (Lauda Proline RP855, Lauda-Königshofen, Germany). After an equilibration time of 15 min (for embryos) and 30 min (for hatchlings), chambers were slowly inverted (2–5×) without disturbing the animal to ensure equal oxygen distribution. Chambers were carefully opened, and pO_2 at the beginning and after 2–3 h were determined by inserting a needle-type fibreoptic oxygen sensor (optodes, PreSens GmbH, Regensburg, Germany) connected to a fibreoptic oxygen meter (Oxy-4 Micro, PreSens GmbH). Oxygen never decreased below a critical value of 70% air saturation. Three chambers without animals served as controls. Due to epibiota on the egg capsule surface (Cronin and Seymour, 2000), oxygen consumption by the capsule after removal of the animal was measured separately in the same manner as described above, and embryonic MO_2 was determined as the difference between whole egg and capsule respiration (i.e. subtracting oxygen consumption attributable to epibiota). Measurements were recorded on a personal computer using software provided by the manufacturer (OXY 4 v2.11 Micro) and stable values were obtained after 2–3 min after probe insertion for initial and final values. Calibration of the oxygen sensors was performed at 16°C using water vapour-saturated air (100% oxygen saturation) and a 1% w/v Na_2SO_3 solution (0% oxygen saturation) at the respective ambient air pressure.

After respiration measurements, eggs were dried on paper tissues and egg wet mass was determined using a precision balance (Sartorius BA110S, Göttingen, Germany). Eggs were dissected, and embryos were checked for vitality. Measurements were omitted when ink was observed in the PVF, indicating a stress response during handling especially in late stage (stage 29–30) embryos. Yolk and animal were carefully wiped on tissue paper and wet masses were determined. Contractions of the mantle removed water from the mantle cavity. Total egg mass and yolk mass could be accurately determined to the nearest 0.01 g, but embryos were recorded to a precision of the nearest 0.05 g due to variation of measured wet masses.

Morphometrics

A subset of animals from each aquarium were retained post-hatching to examine growth of the cuttlebone (3 pCO_2 levels, 4 aquaria per pCO_2 level, 20 cuttlefish in each aquarium, 240 animals in total). After hatching, cuttlefish remained under the same experimental conditions and subsamples of each group were sacrificed at age 19 d ($n = 16$, in each elevated pCO_2 treatment; $n = 19$ in control conditions) and age 34 d ($n = 32$ in each treatment) with all remaining cuttlefish sacrificed at age 47 d ($n = 28$ in each treatment).

Upon termination, the wet mass (g) of each individual was recorded before the cuttlebone being removed by dissection. Care was taken to remove the cuttlebones in their entirety and all further measurements of cuttlebone dry mass (g), length, width, and height (mm) were performed on dried cuttlebones. Cuttlebone dry mass was quantified on a precision balance (AE ADAM, PW 124, Max 120 g, precision 0.0001 g). Length, width, and height of the cuttlebones were measured with digital vernier calipers.

The microstructure of ten cuttlebones each from control and CO_2 treatments was visualized by semi-thin sections of cuttlebones from specimens sacrificed at 47 d. These cuttlebones were selected from the total set based on length to ensure any differences found in internal morphometrics were not confounded by gross size

differences (overall mean length among three groups 26.74 ± 1.53 mm; $F_{2,45} = 0.697$, $p = 0.50$). To rehydrate the dried cuttlebones in preparation for embedding, we adapted protocols used for dry osteological samples. All stages were performed using degassed dH_2O and in a vacuum chamber. Specimens were serially rehydrated in ethanol and then decalcified in 1.5% EDTA. Decalcification was determined by visual inspection, then specimens were dehydrated in ethanol series (30, 50, 70, 90% ×2, 95% ×2, absolute ×2) and cleared in HistoClear (2 h × 2) Specimens were then immediately immersed in a mixture of HistoClear and hot wax (1:3 at 60°C). After 24 h, samples were embedded and allowed to set before sectioning (at 8 μm) using a rotary microtome (Thermo scientific Finesse E+). Each block was first cut in the saggital (longitudinal) midline, and semi-thin sections were taken from the central part of the cuttlebone, capturing several sections from each half of each block. These were stained with Coomassie blue (4 min), rinsed with dH_2O; coverslips were affixed using DPX (Di-*N*-butyle phthalate in xylene) before imaging. Digital images of individual sections were examined for microstructural morphometrics (Figure 1) using the freeware program Image J (Rasband, 2012).

The larval shell layers (i.e. the first eight lamellae deposited before hatching) are visually separate in the shell cross section from the "adult" or post-hatching lamellae (Figure 1). This allowed us to directly measure the size of the larval shell compared with total size at point of death, and the size of the interspace in both the early-stage and post-hatching lamellae. Lamellae are separated by minor, primarily proteinaceous (chitin) laminae which are also visible in stained sections and could therefore be counted.

Analyses

Statistical analyses were conducted using IBM SPSS 13 or SigmaPlot 10 (Systat Software Inc.). The d'Agostino omnibus test for normality was applied to datasets for each treatment group. One-way analysis of covariance (ANCOVA) was conducted to test for differences in embryonic wet mass, egg wet mass, and yolk wet mass; incubation time and embryo wet mass served as covariates. Measured values were transformed to obtain linear regressions between the dependent variables and the covariates. Before testing, linear regressions were tested for homogeneity of slopes. A one-way ANOVA was performed for comparison on oxygen consumption rates in different pCO_2 treatments. MO_2 and specific MO_2 of hatchlings were related to hatchling wet mass of 0.25 g using the mass exponents of the respective power equation regressions.

A two-factor ANOVA was used to test for the interactive effects of pCO_2 treatment and sampling time point on animal size. Because morphometric measurements of cuttlebones were not normally distributed, Kruskal–Wallis tests and Mann–Whitney *U*-tests for *post hoc* comparisons were used to test for (i) further differences in animal wet mass and cuttlebone dry mass at age 19 and 47 d among the three pCO_2 treatments, and (ii) differences among the three treatments at 47 d age for cuttlebone length, width, height, lamellar spacing, and number of minor laminae. A discriminant analysis was applied on the un-standardized measurements for cuttlebone width (mm), cuttlebone length (mm), cuttlebone mass (g), and animal wet mass (g), to investigate separation between the three pCO_2 treatment groups by morphometry. Relationships among these variables were also visualized using *z*-standardized data (using the transform $z = (x - \dot{x})/\sigma$, for each value *x* for a variable with mean $\dot{x}$ and standard deviation σ), to allow comparisons despite differing units.

Results

Growth, development, and hatching

There were two post-hatching mortalities over the course of the treatments; one animal from the high pCO_2 group at age 25 d, and one animal from the control group at age 26 d. There were no mortalities at age 27 d or later. Daily observation revealed no notable behavioural differences observed either between treatment groups or aquarium groups; however, this was not quantified during the course of this study.

Under control conditions, 50% of animals hatched after 65–69 d of incubation, while hatching was slightly delayed in the intermediate pCO_2 treatment (67–70 d) and further delayed under high pCO_2 (69–72 d). The mean dates were significantly different (Kruskal–Wallis $H_{2,N=531} = 144.46$, $p < 0.001$), with significant separation between both the control and intermediate compared with the high pCO_2 hatching date (Dunn's multiple comparison: $p < 10^{-6}$).

Overall, yolk wet mass was ~0.15 g at 30 d of incubation and exponentially decreased over time with higher values in embryos treated in high pCO_2 (Figure 2a). An ANCOVA revealed a significant effect of treatment on the relationship between yolk wet mass and incubation time ($F_{2,115} = 12.11$, $p < 0.0001$). Yolk mass remained larger in the high pCO_2 group. Pairwise comparisons with Tukey's HSD showed a significant influence of treatment on yolk mass decrease between the control and intermediate pCO_2 group ($p < 0.0001$), and also the intermediate and high pCO_2 groups ($p < 0.001$). The exponential decrease in yolk wet mass with increasing embryo wet mass was not significantly different between treatments (Figure 2b; ANCOVA, $F_{2,116} = 1.38$, $p > 0.25$). An ANCOVA comparing log-transformed egg wet masses with embryo wet mass as covariate revealed significant effects of treatment ($F_{2,117} = 7.31$, $p < 0.01$; Figure 2c).

Hatchling wet mass was significantly different among treatments, demonstrating a decreased body mass in high pCO_2-treated animals (Figure 3). An additional one-way ANOVA indicated that exposure to elevated pCO_2 stunted overall animal wet mass at age 19 d post-hatching (Kruskal–Wallis $\chi^2 = 16.43$, d.f. = 2, $p = 0.0003$); *post hoc* analyses showed no significant difference between control and intermediate treatment specimens (*Z*-score = 0.78, $p = 0.44$). At age 19 d, the mean animal wet mass remained depressed in the high pCO_2 group compared with the control treatment (mean mass ± SD = 0.5507 ± 0.14 g, compared with 0.8054 ± 0.20 g in the control group; $p < 0.001$). This difference becomes more pronounced with age (Figure 3a). To facilitate statistical comparisons, net mass measurements were log-transformed, the resulting slopes of mass over time showed growth rates were significantly lower in high pCO_2 groups ($F_{2,224} = 57.6$, $p < 0.0001$).

The mass of the hatchling cuttlebone was not in equal proportion to animal mass in all three groups and this ratio changed over early post-hatching ontogeny (Figures 3b). At the earliest time point sampled (19 d post-hatching), there was a significant difference between groups for the ratio of the dry (cuttlebone) mass to animal wet mass (Kruskal–Wallis $\chi^2 = 12.20$, d.f. = 2, $p = 0.0022$), but no significant difference separated control and intermediate treatments (*Z*-score = − 1.44, $p = 0.15$). At later time points, the mean dry-shell contribution to animal mass was significantly larger in the intermediate group and significantly larger again in the high pCO_2 group (age 34 d: KW $\chi^2 = 43.05$, $p < 0.001$; day 47: KW $\chi^2 = 48.60$, $p < 0.001$; *post hoc*, $p < 0.01$ for all comparisons; Figure 3b). Animals from the high pCO_2 group were on average 48% lighter than control animals by wet mass but in contrast

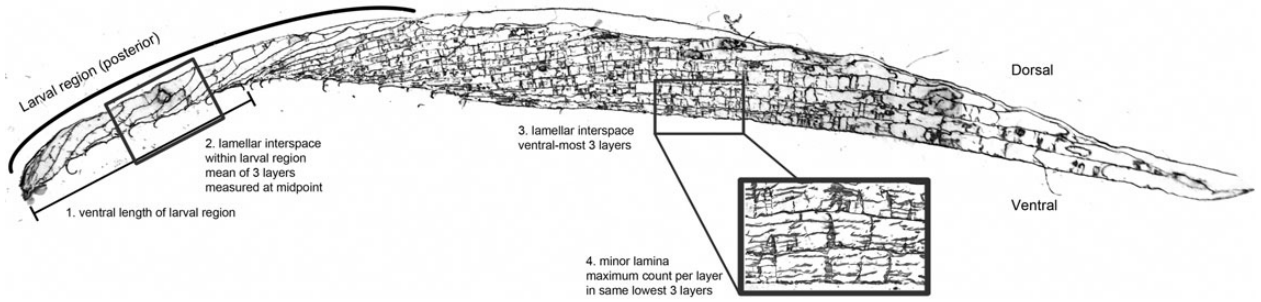

Figure 1. Example semi-thin sagittal section of the cuttlebone, indicating specific areas for microscopic measurements. Inset, higher magnification image of the lamellar structure in the most recent (ventral) part of the cuttlebone, showing minor laminae. The illustrated specimen was reared in an intermediate acidified treatment, 1120 ppm pCO_2 (pH 7.7) and sacrificed at age 47 d.

their cuttlebones were only 18% lighter on average. Shell mass as a percentage of body mass increased with increasing pCO_2 and this became more pronounced over early growth.

Oxygen consumption during development

Embryonic oxygen consumption increased in an exponential fashion over time and approximately tripled during the period of measurement. Compared with control and intermediate pCO_2 embryos, regression curves indicate ~20% lower oxygen consumption in high pCO_2-treated embryos at late stage incubation (day 62). Metabolic rates normalized to wet mass of hatchlings were around three times higher compared with those of late embryonic stages (Figure 4b). Mean MO_2 did not differ between treatment groups (μmol $O_2\ h^{-1}\ g^{-1}$; $F_{2,23} = 0.06$, $p > 0.95$). Corrected rates of MO_2 (μmol $O_2\ h^{-1}\ g^{-1}$) per gram fresh wet mass decreased with rising embryo wet mass as expected, but early-stage measurements were highly variable (Figure 4a). There was a greater range of mass-specific oxygen consumption rates in the control group (Figure 4a), but the overall average of all individuals resulted in no significant differences observed for oxygen consumption rates of embryos and hatchlings exposed to the tree pCO_2 treatments (Figure 4b).

Cuttlebone morphometrics

The gross biometrics (animal wet mass, cuttlebone dry mass, cuttlebone length, width, and height) generally followed the same pattern, and at each sampled time point, there was a significant difference between treatment groups overall, but no significant difference between control and intermediate-pCO_2 treatment groups. A canonical discriminant analysis (Figure 5a) of the same data (z-transformed normalized data illustrated in Figure 5b) determined that 96.8% of variance among the specimens is explained by the first (of two possible) discriminant function separating treatment groups (Figure 5a). This effectively demonstrates that morphometry is significantly different among the different cohorts. The distribution frequencies of the discriminant scores illustrate that morphometry is largely equivalent at age 19 d, but separates pCO_2 treatments at age 34 d—the high pCO_2 treatment is clearly different from the control but both overlap the intermediate treatment—and by age 47 d, the total shape is distinctly different between all three groups.

The shape and ontogeny of the adult cuttlebone can be gauged by the correlation of the dimensional metrics obtained after a standardization transformation (Figure 5b). The length–width ratio of the total cuttlebone provides a proxy for shape. Cuttlebones in extreme high pCO_2 were slightly but significantly shorter relative to their width, than those in animals grown in control conditions; overall, the aspect ratio (length/width) was significantly different between treatments (Kruskal–Wallis $\chi^2 = 10.71$, d.f. = 2, $p = 0.0047$), but there was no significant difference between control and intermediate pCO_2 treatment (Z-score = −0.86, $p = 0.39$).

While specimens in high pCO_2 treatment were smaller and with shorter cuttlebones, the specimens selected for sectioning were deliberately chosen to represent animals of similar size. No significant differences in overall cuttlebone length were found across specimens (age 47 d) selected for sectioning (KW $\chi^2 = 1.31$, d.f. = 2, $p = 0.52$), though the dry mass varied among the three treatment groups (KW $\chi^2 = 6.80$, $p = 0.033$).

Differential influences of the OA treatments were also reflected in the ventral (post-hatching) lamellae at age 47 d; the control group mean interspace was 0.2378 mm, intermediate and high-pCO_2 treatments were increasingly more compact 0.1786 and 0.1748 mm, respectively, which represented a significant difference (KW $\chi^2 = 12.20$, d.f. = 2, $p = 0.0074$). The number of minor (proteinaceous) laminae occurring in the interspace between calcified lamellae on the most recent (ventral) three layers (Figure 1) was also counted. The number of minor laminae ranged from four to six and was not significantly different between treatments ($\chi^2 = 15.31$, d.f. = 18, $p = 0.64$). Cuttlebones became more compact at increased pCO_2.

The embryonic shell is preserved as the posterior-most portion of the cuttlebone and is structurally distinct from the rest of the post-hatching cuttlebone (Figure 1). Embryonic shell size was not significantly different among treatments (KW $\chi^2 = 5.80$, d.f. = 2, $p = 0.055$) and the larval lamellar interspace did not differ between the three treatments (KW $\chi^2 = 1.26$, d.f. = 2, $p = 0.53$). The larval shell did not differ under varying embryonic exposure to elevated exterior pCO_2.

Discussion

In this study, we aimed to take a comprehensive approach to the impact of hypercapnia on *S. officinalis* and to synthesize the body of work on this species (Figure 6). Cuttlefish embryos are exposed to extreme natural hypercapnia *in ovo* which may be increased further under environmental ocean acidification. The developing animals under our near-future and extremely elevated pCO_2 treatments hatched at a slightly delayed tempo and at significantly smaller size. Yet, despite these conditions, the animals maintain an identical embryonic cuttlebone, and proceed to grow a relatively larger cuttlebone per unit wet mass after they have hatched.

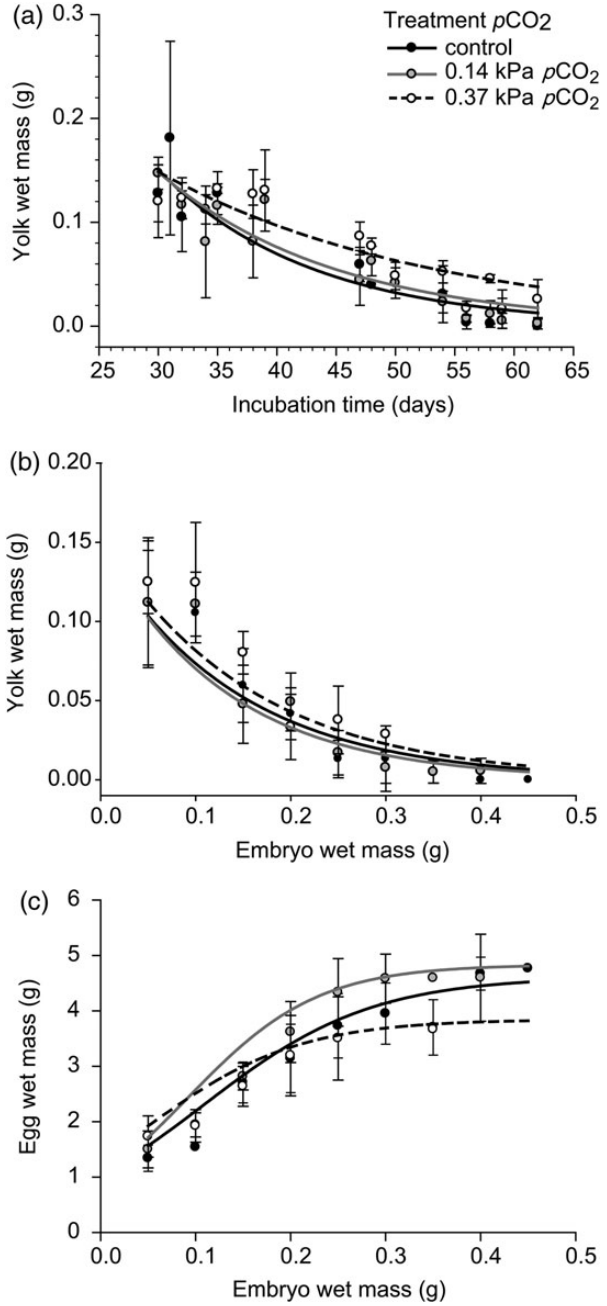

Figure 2. Yolk and egg biometric parameters as a function of time or body mass throughout development of *S. officinalis* in control and elevated CO_2 treatments. Circles and error bars represent mean measurements ± SD. (a) Change in outer yolk wet mass (OYM) over incubation time in days (t). Lines represent exponential regressions of raw data for control [$OYM = 1.51 \times \exp^{(0.077 \times t)}$, $R^2 = 0.77$], intermediate pCO_2 [$OYM = 1.10 \times \exp^{(0.067 \times t)}$, $R^2 = 0.74$], and the high pCO_2 group [$OYM = 0.54 \times \exp^{(0.043 \times t)}$, $R^2 = 0.67$]. (b) Change in outer yolk wet mass with embryo body mass. Lines represent exponential regressions of raw data for the control group [$OYM = 0.15 \times \exp^{(6.86 \times it)}$, $R^2 = 0.73$], intermediate group [$OYM = 0.15 \times \exp^{(7.54 \times it)}$, $R^2 = 0.71$], and high pCO_2 [$OYM = 0.15 \times \exp^{(6.42 \times it)}$, $R^2 = 0.73$]. (c) Total egg wet mass (EggM) as a function of embryo body mass (EmM). Lines represent sigmoid regressions of raw data for the control group [$EggM = 4.61/(1 + \exp^{(-(EmM - 0.11)/0.088))}$, $R^2 = 0.90$], the 0.14 kPa CO_2 group [$EggM = 4.83/(1 + \exp^{(-(EmM - 0.091)/0.069))}$, $R^2 = 0.92$], and the 0.37 kPa CO_2 group [$EggM = 3.84/(1 + \exp^{(-(EmM - 0.050)/0.080))}$, $R^2 = 0.6924$].

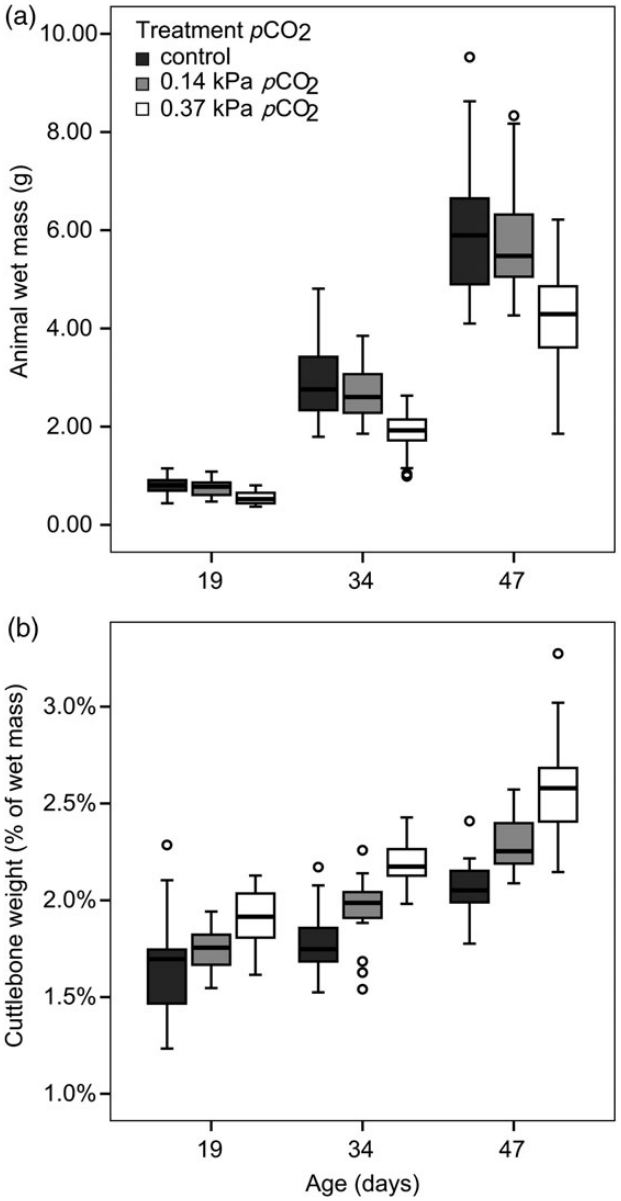

Figure 3. Boxplots illustrating median, upper and lower quartile, and inter-quartile range of size in cuttlefish in three pCO_2 treatments over three time sampling points over juvenile growth (circles indicate individual outliers outside the inter-quartile range). (a) Animal wet mass increases with age but is relatively stunted in elevated pCO_2. (b) The contribution of the cuttlebone as a percentage of total mass increases slightly with growth and is significantly greater in high pCO_2 treatment.

There is evidence that cuttlefish embryonic stages are more sensitive in terms of development and metabolism towards environmental hypercapnia than juveniles and adults (Gutowska *et al.*, 2008). Earlier work on juvenile cuttlefish growth under strongly acidified conditions (ca. 0.4 and 0.6 kPa) showed no change in somatic rates in post-hatching juveniles (Gutowska *et al.*, 2008, 2010b). Similarly, juveniles exposed to moderate hypercapnia (near-future pH) also apparently maintained somatic growth (Dorey *et al.*, 2013). Yet late embryos and hatchlings reared under 0.37 kPa CO_2 (our high pCO_2 treatment) had wet masses reduced

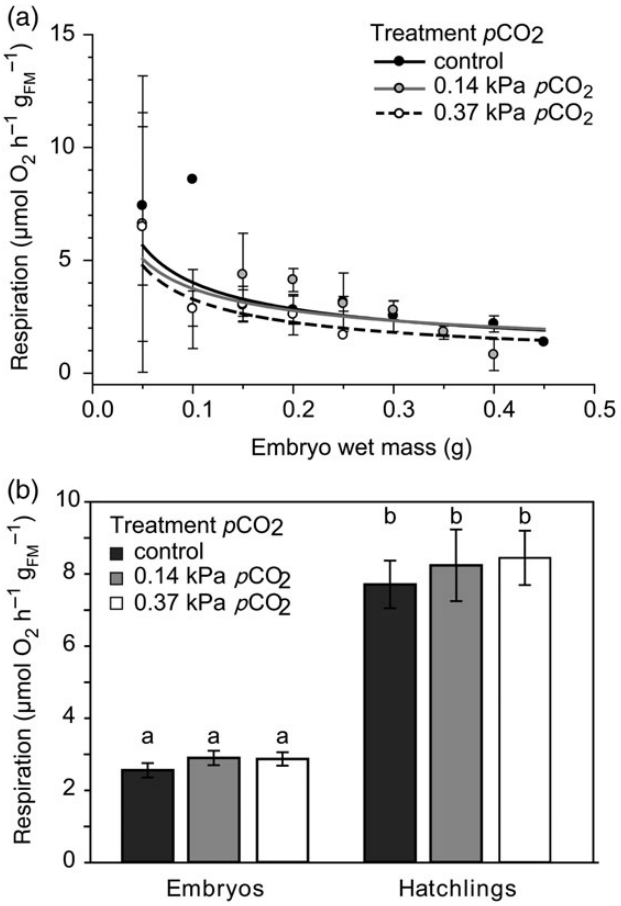

Figure 4. Oxygen consumption rates for embryos of *S. officinalis* (a) as a function of embryo individual wet mass, and (b) mean standard metabolic rates for embryos and hatchlings reared under different pCO_2 concentrations. Oxygen consumption rates were corrected by fresh mass (FM) and presented as mean ± SD.

by up to 30% in the final phase of embryonic development (Hu *et al.*, 2011b). Contradictory results concerning the greater sensitivity of embryonic growth rates during exposure to near-future acidification, compared with hatchling growth, have been reported (Lacoue-Labarthe *et al.*, 2009; Dorey *et al.*, 2013). The present results clarify this pattern: although there is no statistically significant suppression of growth in our near-future (intermediate) experimental condition, comparison with our extreme (high) pH condition reveal a distinctive pattern of deleterious growth effect (Figure 3a). Indeed in this study, there are limited observable differences between the control group (0.05 kPa pCO_2) and our intermediate elevated pCO_2 treatment (0.14 kPa), yet the significant changes in growth, morphometry, and laminar density at extreme pCO_2 (0.37 kPa) illuminate overall trends in the ways that ocean acidification affects the study organisms.

There is substantial controversy around experimental design and setting threshold pCO_2 levels for studying ocean acidification and this example underlines the empirical value of comparing a range of treatment conditions. To understand OA in the context of natural conditions, special attention should be dedicated to naturally acidified/hypercapnic microhabitats (sediment burrows, shells, egg capsules) in which an organisms lives or develops. For example, within the egg, embryonic cuttlefish are exposed to a naturally increasingly hypercapnic environment in the PVF (Gutowska and Melzner, 2009). Conditions *in ovo* are further exacerbated in acidified environmental seawater because of the egg capsule acting as a diffusion barrier for metabolic CO_2 generated by the embryo. Increases in external environmental hypercapnia are additive to the already high PVF pCO_2 levels (0.25 kPa), resulting in a PVF and pCO_2 of 0.78 kPa (pH 7.0) in the conditions we used as our high pCO_2 treatment (Hu *et al.*, 2011a). To minimize oxygen limitation, cuttlefish eggs swell in the course of development, which leads to a reduced capsule wall thickness and a higher diffusive area to support the rising oxygen demands and CO_2 excretion rates of the embryo (De Leersnyder and Lemaire, 1972; Cronin and Seymour, 2000; Gutowska and Melzner, 2009). Although the mechanisms of the egg swelling process are not well characterized, it was suggested that osmotically active organic compounds from the environment accumulate inside egg, or that the embryo itself maintains the osmotic gradient (De Leersnyder and Lemaire, 1972; Boyle, 1986). Our results showed that egg mass per volume is potentially slightly increased in embryos exposed to 0.14 kPa CO_2, but potentially decreased in 0.37 kPa-treated embryos (Figure 2c); this corresponds to observations of *S. officinalis* egg masses exposed to moderate pCO_2 levels of 0.09–0.14 kPa (Lacoue-Labarthe *et al.*, 2009). The increased swelling may be a consequence of physiological responses of embryos to CO_2 within the capsule. Alternatively, cuttlefish embryos may be capable of actively regulating PVF osmolarity, and thus, diffusion properties (i.e. effective surface area and diffusion distance) of the egg capsule to improve CO_2 excretion during environmental hypercapnia. Though the process is unknown, simulated ocean acidification has been demonstrated to additionally challenge the embryonic acid–base regulatory machinery of cephalopods to protect from a CO_2-induced acidosis (Hu *et al.*, 2013).

In adult cephalopods, the acid–base regulatory machinery of gill epithelia provides competent pH_e control and the resulting protection of the pH-sensitive respiratory pigment haemocyanin (Pörtner, 1990; Hu *et al.*, 2011a, b, 2015). Embryonic stages exhibit a potentially less efficient acid–base regulating machinery; before gill epithelia are functionally developed, cephalopod embryos possess epidermal ionocytes scattered on yolk and skin epithelia, that are capable of secreting proton equivalents (e.g. H^+ or NH_4^+; Hu *et al.* 2011a, 2013). The acid–base regulating capacities of the embryos may be limiting in high PVF pCO_2; the consequence would be uncompensated extracellular acidosis that may negatively influence oxygen transport capacities and metabolic processes of the embryo (Decleir *et al.*, 1971; Pörtner *et al.*, 1991). It has been suggested that an uncompensated acidosis as well as limited oxygen supply to the developing embryo directly translates into reduced growth and/developmental rates (Reipschläger and Pörtner, 1996; Pörtner *et al.*, 1998).

Hypercapnia-induced reductions in larval and embryonic growth associated with altered metabolic rates have been observed in many marine invertebrates (Kurihara and Shirayama, 2004; Kurihara *et al.*, 2004, 2007; Dupont *et al.*, 2008, 2010; Dupont and Thorndyke, 2009). The oxygen consumption of control and intermediate pCO_2 group embryos at stage 28–29 were similar to those values reported for *S. officinalis* stage 29 embryos (Wolf *et al.*, 1985). During development, cuttlefish embryos reared under high pCO_2 exhibited no overall change in aerobic metabolism when compared with control and intermediate pCO_2 animals. Standard metabolic rate in older *S. officinalis* acclimated to even higher seawater pCO_2

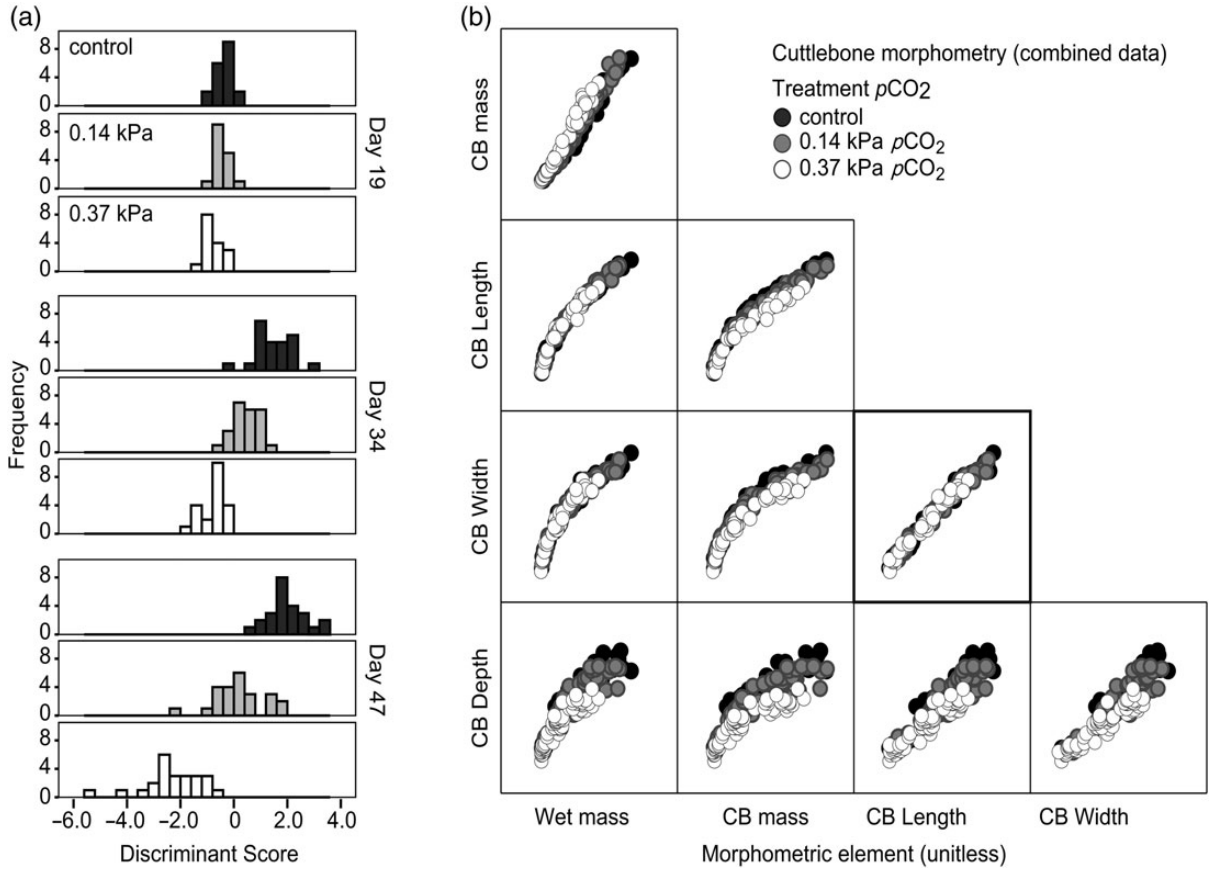

Figure 5. Morphometric discrimination of cuttlebones from animals reared in different ocean chemistry. (a) Stacked histogram of scores from first discriminant function of treatment, i.e. pCO_2, based on morphometry of the total dataset (measurements illustrated in Figure 1), $sep(D) = 1.057$, $D = 6.03$(wet mass) $-$ 5.83(cuttlebone mass) $-$ 0.75(CB height) $-$ 0.85(CB width) $+$ 1.61(CB depth). The distribution of individual scores from the first discriminant function illustrates increasing separation of total shape and size between treatment groups during growth over three progressive time points. (b) Matrix scatterplot of *z*-standardized (i.e. unitless) gross morphometric data for animal wet mass and cuttlebone (CB) dimensions, combining all sampling points (age 19, 34, and 47 d) over early life ontogeny.

(0.6 kPa) also did not differ from that of control animals (Gutowska *et al.*, 2008).

Exposure to low pH during the larval phase is known to adversely effect development in a range of species (reviewed in Byrne, 2011). Pecl *et al.* (2004) hypothesized that smaller cephalopod hatchlings would need more time to escape from the "window of vulnerability" and thus, elevated pCO_2 may negatively influence their survival with respect to predation. There may also be different responses in acclimated adult organisms compared with those that experience a modified environment during embryonic development. Importantly, exposure to high pCO_2 during development here did not prevent stunted growth in early life after hatching and in fact exacerbated size differences between groups in early life.

The present data build on previous work (Gutowska *et al.*, 2008, 2010b; Dorey *et al.*, 2013), by demonstrating that the increased calcification in *S. officinalis* occurs not only at extreme levels of pCO_2 tested in previous studies, but here at a level considered realistic for the oceans within the next 100–200 years as our intermediate treatment (0.14 kPa pCO_2) is similar to predicted ocean conditions in 2100 (IPCC, 2007). The shell of cuttlefish is fully internalized and the organism's ability to maintain calcification rates are directly dependent on its physiology and not on extrinsic dissolution from the surrounding medium. Other cephalopods are unable to maintain internal calcified structures under experimental OA (Kaplan *et al.*, 2013). The strong acid–base regulatory abilities, which protect extracellular pH homeostasis by increasing blood HCO_3^- may alter the precipitation kinetics of $CaCO_3^-$ and could explain higher calcification rates induced after hatching. This hypothesis is supported by the fact that the phenomenon of hypercalcification has only been observed in strong-acid–base regulators, including fish (Checkley *et al.*, 2009) crustaceans (Reis *et al.*, 2009), and cephalopods (Gutowska *et al.*, 2010b) that are capable of accumulating significant amounts of HCO_3^- in body fluids to buffer CO_2-induced acid–base disturbances.

Although animals hatched in the elevated pCO_2 treatments were smaller, including having shorter mantle length and lower wet mass, their calcareous cuttlebones were maintained at a similar size and thus proportionally greater in mass increasing in statistically significant increments between each treatment from 1.8% of wet mass (control) to 2.0% (intermediate) and 2.2% (high pCO_2; Figure 3b). The absolute cuttlebone mass is directly dependent on the animal mass and treatment conditions, including ocean chemistry but perhaps other factors as well. Cuttlebone dry mass is an effective proxy for calcium content (Gutowska *et al.*, 2010b). Increased calcification of the cuttlebone was observed at both a high pCO_2 and to a lesser degree an intermediate treatment

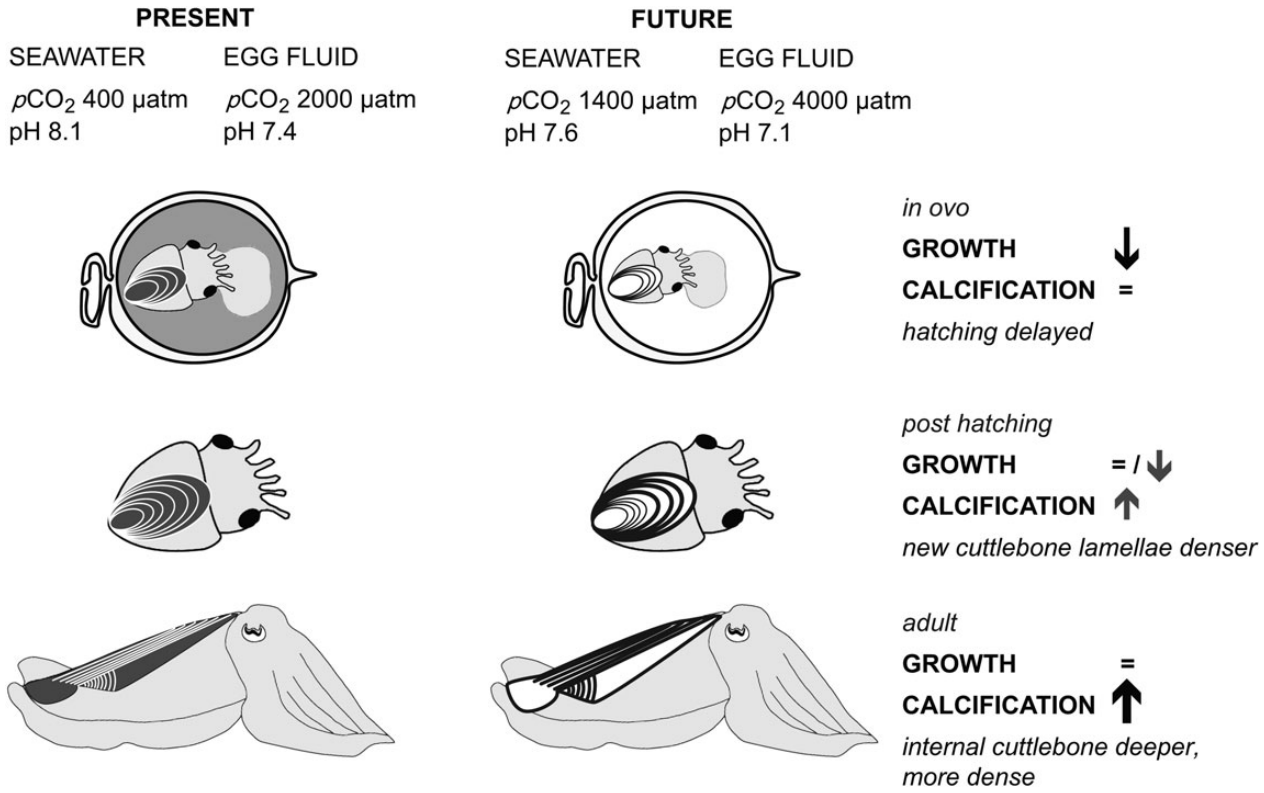

Figure 6. Schematic summary of the influence of ocean acidification on growth rate and cuttlebone calcification in *S. officinalis* embryos and hatchlings. Decreased growth rates observed during embryonic development do not carry over to hatchling growth performance. Cuttlebone hypercalcification does not take place *in ovo* but begins immediately on hatching and can be observed in hatchlings and later growth stages under exposure to elevated seawater pCO_2. An hypothesis is presented that attributes the high growth rates and cuttlebone hypercalcification in hatchlings to their strong acid–base regulatory capacities; the converse is concluded for embryonic life stages.

simulating ecologically relevant, pCO_2. Although there was no evidence of any difference in the embryonic shells (embryonic shells have the same size and same lamellar spacing in all treatments), previous work demonstrated a slight increase in calcium incorporation in embryonic cuttlebones in contrast to post-hatching hypercalcification (Dorey *et al.*, 2013). The cuttlebones in our high pCO_2 were proportionally heavier at age 19 d and with significant differences between all three groups by age 34 d post-hatching. This indicated that the observed influence of pH on ontogeny causes them to become morphologically more separated over time (Figure 5a).

This shift in morphometry was preliminarily described from juveniles, in that individuals exposed to extreme high pCO_2 had slightly shallower cuttlebones with more tightly packed lamellae than control individuals creating a denser cuttlebone (Gutowska *et al.*, 2010b). Such hypercalcification could be detrimental because the cuttlebone acts as a "low cost" or "passive" mechanism for buoyancy regulation, meaning that cuttlefish are able to maintain a position of choice in the water column without expending much energy to do so (Denton and Gilpin-Brown, 1961), by adjusting the gas:fluid ratio within this chambered shell.

Subtle changes in cuttlebone mass can markedly impact cuttlefish buoyancy (Denton and Gilpin-Brown, 1961), making cuttlefish potentially sensitive to over-mineralization through acidification. In the long run, these structural effects may increase and impact upon key currencies related to fitness (i.e. behavioural time budgets and energy costs; Lemon, 1991; Lyons *et al.*, 2012) with consequences for survivorship and reproductive success. Increased density of the cuttlebone has been found in deeper-water species and may increase strength at higher pressure (Ward and Von Boletzky, 1984; Sherrard, 2000). But the ability of the individual animal to regulate its buoyancy may speculatively be compromised if the total gas volume is reduced, which is correlated with increased cuttlebone density. In this context, malformations of the statoliths were found in the squid *Doryteuthis pealeii* exposed to acidified (0.22 kPa pCO_2; pH 7.3) conditions (Kaplan *et al.*, 2013) and also in *Loligo vulgaris* cultured even at less extreme acdification (pH 7.85 and 7.60: Lacoue-Labarthe *et al.*, 2011). Internal aragonitic statoliths function as balance and acceleration receptors and allow the detection of the particle motion component of a sound pressure wave stimuli in cephalopods (Budelmann, 1988). Quantitative determinations of energy allocations between processes like pH regulation, sensory responses and predation, buoyancy control, and growth will help provide a better understanding regarding the resilience of cuttlefish early life stages in future oceans. That cuttlebones are measurably denser in animals born into a realistic, near-future acidification scenario is a relevant potential threat to cuttlefish as an exploited species.

Acknowledgements

We are very grateful to J.P. Robin who helped to obtain the cuttlefish eggs. Ragnhild Asmus and her staff provided laboratory, cold room and office facilities and general support to GL at the Wadden Sea Station Sylt (Alfred Wegener Institute for Polar and Marine Research); Michael Schroedl (Zoologische Staattsammlung,

Munich, Gemany) provided valuable advice on embedding preparation; Alexandra Aitken (QUB) assisted with staining of sectioned samples. Contributions to this project were funded by the Department of Employment and Learning, NI (PhD scholarship awarded to GL). This is a contribution to the German Ministry of Education and Research (BMBF) funded project "Biological Impacts of Ocean ACIDification" (BIOACID) subproject 3.1.3 awarded to FM.

References

Boyle, P. R. 1986. Encapsulation of cephalopod embryos: a search for functional correlations. American Malacological Bulletin, 4: 217–227.

Budelmann, B. U. 1988. Morphological diversity of equilibrium receptor systems in aquatic invertebrates. *In* Sensory Biology of Aquatic Animals, pp. 757–782. Ed. by J. Atema, R. R. Fay, A. N. Popper, and W. N. Tavolga. Springer, New York. 945 pp.

Byrne, M. 2011. Impact of ocean warming and ocean acidification on marine invertebrate life history stages: vulnerabilities and potential for persistence in a changing ocean. Annual Reviews: Oceanography and Marine Biology, 49: 1–42.

Checkley, J., David, M., Dickson, A. G., Takahashi, M., Radich, J. A., Eisenkolb, N., and Asch, R. 2009. Elevated CO_2 enhances otolith growth in young fish. Science, 324: 1683.

Claiborne, J. B., and Edwards, S. L. 2002. Acid–base regulation in fishes: cellular and molecular mechanisms. Journal of Experimental Zoology, 293: 302–319.

Cronin, E. R., and Seymour, R. S. 2000. Respiration of the eggs of the giant cuttlefish *Sepia apama*. Marine Biology, 136: 863–870.

De Leersnyder, M., and Lemaire, J. 1972. Sur la composition minerale du liquide dembryonaire de loeuf de *Sepia officinalis* L. Cahiers de Biologie Marine, 13: 429–431.

Decleir, W., Lemaire, J., and Richard, A. 1971. The differentiation of blood proteins during ontogeny in *Sepia officinalis* L. Comparative Biochemistry and Physiology B, 40: 923–928.

Dickson, A. G., Afghan, J. D., and Anderson, G. C. 2003. Reference materials for oceanic CO_2 analysis: a method for the certification of total alkalinity. Marine Chemistry, 80: 185–197.

Dickson, A. G., and Millero, F. 1987. A comparison of the equilibrium constants for the dissociation of carbonic acid in seawater media. Deep Sea Research I, 34: 1733–1743.

Denton, E. J., and Gilpin-Brown, J. B. 1961. The buoyancy of the cuttlefish, *Sepia officinalis* (L.). Journal of the Marine Biology Association of the UK, 41: 319–342.

Doney, S., Balch, W., Fabry, V., and Feely, R. 2009. Ocean acidification: a critical emerging problem for the ocean sciences. Oceanography, 22: 16–25.

Dorey, N., Melzner, F., Martin, S., Oberhänsli, F., Teyssié, J-L., Bustamant, P., Gattuso, J-P., *et al.* 2013. Ocean acidification and temperature rise: effects on calcification during early development of the cuttlefish *Sepia officinalis*. Marine Biology, 160: 2007–2022.

Dupont, S., Havenhand, J., Thorndyke, W., Peck, L., and Thorndyke, M. C. 2008. CO_2-driven ocean acidification radically affect larval survival and development in the brittlestar *Ophiothrix fragilis*. Marine Ecology Progress Series, 373: 285–294.

Dupont, S., Ortega-Martinez, O., and Thorndyke, M. C. 2010. Impact of near-future ocean acidification on echinoderms. Ecotoxycology, 19: 449–462.

Dupont, S. T., and Thorndyke, M. C. 2009. Impact of CO_2-driven ocean acidification on invertebrates' early life-history—what we know, what we need to know, and what we can do? Biogeosci Discussions, 6: 3109–3131.

Gutowska, M. A., and Melzner, F. 2009. Abiotic conditions in cephalopod (*Sepia officinalis*) eggs: embryonic development at low pH and high pCO_2. Marine Biology, 156: 515–519.

Gutowska, M. A., Melzner, F., Langenbuch, M., Bock, C., Claireaux, G., and Pörtner, H. O. 2010a. Acid–base regulatory ability of the cephalopod (*Sepia officinalis*) in response to environmental hypercapnia. Journal of Comparative Physiology B, 180: 323–335.

Gutowska, M. A., Melzner, F., Pörtner, H. O., and Meier, S. 2010b. Cuttlebone calcification increases during exposure to elevated seawater pCO_2 in the cephalopod *Sepia officinalis*. Marine Biology, 157: 1653–1663.

Gutowska, M. A., Pörtner, H. O., and Melzner, F. 2008. Growth and calcification in the cephalopod *Sepia officinalis* under elevated seawater pCO_2. Marine Ecology Progress Series, 373: 303–309.

Heisler, N. 1984. Acid–Base Regulation in Fishes. Academic Press, New York.

Hettinger, A., Sanford, E., Hill, T. M., Lenz, E. A., Russell, A. D., and Gaylord, B. 2013. Larval carry-over effects from ocean acidification persist in the natural environment. Global Change Biology, 19: 3317–3326.

Hu, M. Y., Hwang, P-P., and Tseng, Y-C. 2015. Recent advances in understanding trans-epithelial acid-base regulation and excretion mechanisms in cephalopods. Tissue Barriers, 3: 4.

Hu, M. Y., Lee, J-R., Lin, L-Y., Shih, T-H., Stumpp, M., Lee, M-F., Hwang, P-P., *et al.* 2013. Development in a naturally acidified environment: Na^+/H^+-exchanger 3-based proton secretion leads to CO_2 tolerance in cephalopod embryos. Frontiers in Zoology, 10: 51.

Hu, M. Y., Tseng, Y-C., Lin, L-Y., Chen, P-Y., Charmantier-Daures, M., Hwang, P. P., and Melzner, F. 2011a. New insights into ion regulation of cephalopod molluscs: a role of epidermal ionocytes in acid–base regulation during embryogenesis. American Journal of Physiology: Regulatory, Integrative and Comparative Physiology, 301: 1700–1709.

Hu, M. Y., Tseng, Y-C., Stumpp, M., Gutowska, M. A., Kiko, R., Lucassen, M., and Melzner, F. 2011b. Elevated seawater pCO_2 differentially affects branchial acid–base transporters over the course of development in the cephalopod *Sepia officinalis*. American Journal of Physiology: Regulatory, Integrative and Comparative Physiology, 300: R1100–R1114.

IPCC. 2007. Climate Change 2007: an Assessment of the Intergovernmental Panel on Climate Change, pp. 1–52.

Kaplan, M. B., Mooney, T. A., McCorkle, D. C., and Cohen, A. 2013. Adverse effects of ocean acidification on early development of squid (*Doryteuthis pealeii*). PLoS ONE, 8: e63714.

Kroeker, K. J., Kordas, R. L., Crim, R. N., and Singh, G. G. 2010. Review and synthesis: meta-analysis reveals negative yet variable effects of ocean acidification on marine organisms. Ecology Letters, 13: 275–284.

Kurihara, H., Kato, S., and Ishimatsu, A. 2007. Effects of increased seawater pCO_2 on early development of the oyster Crassostrea gigas. Aquatic Biology, 1: 91–98.

Kurihara, H., Shimode, S., and Shirayama, Y. 2004. Effects of raised CO_2 concentration on the egg production rate and early development of two marine copepods (Acartia steueri and Acartia erythraea). Marine Pollution Bulletin, 49: 721–727.

Kurihara, H., and Shirayama, Y. 2004. Effects of increased atmospheric CO_2 on sea urchin early development. Marine Ecology Progress Series, 274: 161–169.

Lacoue-Labarthe, T., Martin, S., Oberhaensli, F., Teyssié, J-L., Markich, S., Jeffree, R., and Bustamante, P. 2009. Effects of increased pCO_2 and temperature on trace element (Ag, Cd and Zn) bioaccumulation in the eggs of the common cuttlefish, *Sepia officinalis*. Biogeoscience, 6: 2561–2573.

Lacoue-Labarthe, T., Réveillac, É., Oberhänsli, F., Teyssié, J. L., Jeffree, R., and Gattuso, J. P. 2011. Effects of ocean acidificaiton on trace element accumulation in the early-life stages of squid *Loligo vulgaris*. Aquatic Toxicology, 105: 166–176.

Lemaire, J. 1970. Table de developpement ebryonnaire de *Sepia officinalis* L. (Molluscque: Cephalopode). Bulletin de la Société zoologique de France, 95: 773–782.

Lemon, W. C. 1991. Fitness consequences of foraging behavior in the zebra finch. Nature, 352: 153–155.

Lewis, E., and Wallace, D. W. R. 1998. Program developed for CO_2 system calculations. Oak Ridge National Laboratory ORNL/CDIAC-105, Oak Ridge.

Lyons, G. N., Pope, E. C., Kostka, B., Wilson, R. P., Dobrajc, Z., and Houghton, J. D. R. 2012. Tri-axial accelerometers tease apart discrete behaviours in the common cuttlefish *Sepia officinalis*. Journal of the Marine Biology Association of the UK, 93: 1389–1392.

Mehrbach, C., Culberso, C., Hawley, J., and Pytkowic, R. 1973. Measurement of apparent dissociation constants of carbonic acid in seawater at atmospheric pressure. Limnology and Oceanography, 18: 897–907.

Melzner, F., Thomsen, J., Koeve, W., Oschlies, A., Gutowska, M. A., Bange, H. W., Hansen, H. P., *et al.* 2013. Future ocean acidification will be amplified by hypoxia in coastal habitats. Marine Biology, 160: 1875–1888

Munday, P. L., Dixson, D. L., Donelson, J. M., Jones, G. P., Pratchett, M. S., Devitsina, K. P., and Doving, K. B. 2009. Ocean acidification impairs olfactory discrimination and homing ability of a marine fish. Proceedings of the National Academy of Sciences of the United States of America, 106: 1848–1852.

Pecl, G. T., Steer, M. A., and Hodgson, K. E. 2004. The role of hatchling size in generating the intrinsic size-at-age variability of cephalopods: extending the Forsythe hypothesis. Marine and Freshwater Research, 55: 387–394.

Pörtner, H-O. 1990. An analysis of the effects of pH on oxygen binding by squid (*Illex illecebrosus, Loligo pealei*) haemocyanin. Journal of Experimental Biology, 150: 407–424.

Pörtner, H-O., Reipschläger, A., and Heisler, N. 1998. Acid-base regulation, metabolism and energetics in Sipunculus nudus as a function of ambient carbon dioxide level. Journal of Experimental Biology, 201: 43–55.

Pörtner, H. O., Webber, D. M., Boutilier, R. G., and O'Dor, R. K. 1991. Acid–base regulation in exercising squid (*Illex illecebrosus*, *Loligo pealei*). American Journal of Physiology: Regulatory, Integrative and Comparative Physiology, 261: R239–R246.

Rasband, W. S. 2012. ImageJ. 1997–2014. US National Institutes of Health, Bethesda, MD, USA. http://imagej.nih.gov/ij/.

Reipschläger, A., and Pörtner, H-O. 1996. Metabolic depression during environmental stress: the role of extra- versus intracellular pH in Sipunculus nududs. Journal of Experimental Biology, 199: 1801–1807.

Reis, J. B., Cohen, A. L., and McCorkle, D. C. 2009. Marine calcifiers exhibit mixed responses to CO_2-induced ocean acidification. Geology, 37: 1131–1134.

Sherrard, K. M. 2000. Cuttlebone morphology limits habitat depth in eleven species of *Sepia* (Cephalopoda: Sepiidae). Biological Bulletin, 198: 404–414.

Spicer, J. I., Raffo, A., and Widdicombe, S. 2007. Influence of CO_2-related seawater acidification on extracellular acid–base balance in the velvet swimming crab *Necora puber*. Marine Biology, 151: 1117–1125.

Tseng, Y-C., Hu, M. Y., Lin, L-Y., Melzner, F., and Hwang, P. P. 2013. CO_2-driven seawater acidification differentially affects development and molecular plasticity along life history of fish (*Oryzias latipes*). Comparative Biochemistry and Physiology A, 165: 119–130.

Tunnicliffe, V., Davies, K. T. A., Butterfield, D. A., Embley, R. W., Rose, J. M., and Chadwick, W. W., Jr 2009. Survival of mussels in extremely acidic waters on a submarine volcano. Nature Geoscience, 2: 344–348.

Wallace, R. B., Baumann, H., Grear, J. S., Aller, R. C., and Gobler, C. J. 2014. Coastal ocean acidification: the other eutrophication problem. Coastal, Estuarine, and Shelf Science, 148: 1–13.

Walther, K., Anger, K., and Pörtner, H. O. 2010. Effects of ocean acidification and warming on the larval development of the spider crab *Hyas araneus* from different latitudes (54° vs. 79°N). Marine Ecology Progress Series, 417: 159–170.

Ward, P. D., and Von Boletzky, S. 1984. Shell implosion depth and implosion morphologies in three species of *Sepia* (Cephalopoda) from the Mediterranean Sea. Journal of the Marine Biology Association of the UK, 64: 955–966.

Wheatly, M. G., and Henry, R. P. 1992. Extracellular and intracellular acid–base regulation in crustaceans. Journal of Experimental Zoology, 263: 127–142.

Wittmann, A. C., and Pörtner, H. O. 2013. Sensitivities of extant animal taxa to ocean acidification. Nature Climate Change, 3: 995–1001.

Wolf, G., Verheyen, E., Vlaeminck, A., Lemaire, J., and Decleir, W. 1985. Respiration of *Sepia officinalis* during embryonic and early juvenile life. Marine Biology, 90: 35–39.

Wood, H. L., Spicer, J. I., and Widdicombe, S. 2008. Ocean acidification may increase calcification rates, but at a cost. Proceedings of the Royal Society B, 275: 1767–1773.

Handling editor: C. Brock Woodson

ICES Journal of Marine Science

ICES Journal of Marine Science (2016), 73(3), 981–990. doi:10.1093/icesjms/fsv050

Contribution to Special Issue: 'Towards a Broader Perspective on Ocean Acidification Research'

Original Article

Effects of elevated CO_2 levels on eggs and larvae of a North Pacific flatfish

Thomas P. Hurst[1]*, Benjamin J. Laurel[1], Jeremy T. Mathis[2], and Lauren R. Tobosa[3]

[1]*Fisheries Behavioral Ecology Program, Resource Assessment and Conservation Engineering Division, Alaska Fisheries Science Center, National Marine Fisheries Service, National Oceanic and Atmospheric Administration, Hatfield Marine Science Center, Newport, OR 97365, USA*
[2]*Pacific Marine Environmental Laboratory, National Oceanic and Atmospheric Administration, Seattle, WA 98115, USA*
[3]*Hatfield Marine Science Center, Oregon State University, Newport, OR 97365, USA*

**Corresponding author: tel: +1 541 867 0222; fax: +1 541 867 0136; e-mail: thomas.hurst@noaa.gov*

Hurst, T. P., Laurel, B. J., Mathis, J. T., and Tobosa, L. R. Effects of elevated CO_2 levels on eggs and larvae of a North Pacific flatfish. – ICES Journal of Marine Science, 73: 981–990.

Received 29 December 2014; revised 5 March 2015; accepted 6 March 2015; advance access publication 6 April 2015.

The Bering Sea and Gulf of Alaska support a number of commercially important flatfish fisheries. These high latitude ecosystems are predicted to be most immediately impacted by ongoing ocean acidification, but the range of responses by commercial fishery species has yet to be fully explored. In this study, we examined the growth responses of northern rock sole (*Lepidopsetta polyxystra*) eggs and larvae across a range of CO_2 levels (ambient to 1500 μatm) to evaluate the potential sensitivity to ocean acidification. Laboratory-spawned eggs and larvae were reared at 8°C in a flow-through culture system in which CO_2 levels were maintained via computer-controlled injection of CO_2 into a seawater conditioning tank. Overall, we observed only minor effects of elevated CO_2 level on sizes of northern rock sole larvae. Size at hatch differed among offspring from four different females, but there was no significant effect of CO_2 level on egg survival or size at hatch. In three separate larval growth trials, there was little effect of CO_2 level on growth rates through the first 28 d post-hatch (DPH). However, in the one trial extended to 60 DPH, fish reared at the highest CO_2 level had lower condition factors after 28 DPH, suggesting that larvae undergoing metamorphosis may be more sensitive to environmental hypercapnia than earlier pre-flexion stages. These results suggest that while early life stages of northern rock sole are less sensitive to ocean acidification than previously examined flatfish, they may be more sensitive to elevated CO_2 levels than a previously studied gadid with a similar geographic range.

Keywords: climate change, early life history, flatfish, growth rate, hypercapnia, ocean acidification.

Introduction

Ocean acidification occurs as anthropogenically released CO_2 dissolves from the atmosphere into surface waters of the world's oceans (e.g. Feely *et al.*, 2004; Sabine *et al.*, 2004; Gattuso and Hansson, 2011), reducing the pH of seawater and the availability of carbonate ions. Significant concern has arisen that ocean acidification will disrupt the functioning of marine ecosystems and reduce the productivity of important fishery resources (Cooley and Doney, 2009; Denman *et al.*, 2011). The high-latitude seas of the North Pacific Ocean are of particular concern because they are predicted to be acutely affected by both acidification and continued warming (Fabry *et al.*, 2009; Mathis *et al.*, 2011a, 2014). Ocean acidification in the Arctic Ocean and Bering Sea is expected to be exacerbated by natural processes such as sea ice melt, river run-off, and the respiration of organic matter over the shallow continental shelves (Mathis, 2011b; Mathis and Questel, 2013). The most recent estimates from the coupled climate-ocean model NCAR CESM1-BGC (Lindsay *et al.*, 2014) with atmospheric CO_2 emissions from the IPCC RCP 8.5 scenario (van Vuuren *et al.*, 2011) are that pH of Gulf of Alaska and Bering Sea surface waters have already decreased by 0.10 units and will decrease an additional 0.35 units by the end of the century (see Mathis *et al.*, 2014 for additional details).

Experimental studies on marine organisms have demonstrated a range of effects from elevated CO_2 ("environmental hypercapnia") and reduced pH (Fabry *et al.*, 2008; Kroeker *et al.*, 2010). In general, fish are expected to be more resilient to the direct physiological effects of ocean acidification than invertebrates with carbonate exoskeletons (Pörtner *et al.*, 2004; Melzner *et al.*, 2009a). Although recent

studies have found that elevated CO_2 may disrupt the behavioral and sensory biology of juvenile fish (Leduc *et al.*, 2013), growth and condition of juvenile and adult stage fish appear generally resilient to the effects of ocean acidification (Ishimatsu *et al.*, 2008; Melzner *et al.*, 2009b; Hurst *et al.*, 2012). Egg and larval stages, however, are expected to be more sensitive to decreased pH because of their high surface to volume ratio and lack of specialized mechanisms for acid–base regulation (Kikkawa *et al.*, 2003; Ishimatsu *et al.*, 2008). Whereas several studies have found negative effects of elevated CO_2 on development or survival of larval fish (Baumann *et al.*, 2012; Frommel *et al.*, 2012; Pimentel *et al.*, 2014), a number of others have found negligible effects (Munday *et al.*, 2011; Bignami *et al.*, 2013; Hurst *et al.*, 2013). Additional experiments on a range of species are still required as there is currently little understanding of which taxonomic groups or life history types might be most sensitive.

A recent analysis evaluated the vulnerability of Alaskan communities to potential ocean acidification-induced declines in fishery productivity based on predicted regional degree of acidification, reliance on different fishery resources for commercial and subsistence harvests, and degree of community resilience (Mathis *et al.*, 2014). Sensitivity of major resource groups (shellfish, salmon, other marine fish) was ranked based on the likelihood of direct and indirect (via the foodweb) impacts of ocean acidification on population productivity. The greater sensitivity of Alaskan crabs is supported by experimental observations of negative effects on several species (Long *et al.*, 2013a,b). However, the assumption in that study that marine fish would be generally robust to the effects of ocean acidification was based primarily on theoretical responses of fish species as direct empirical observations on ocean acidification responses exist for only one of Alaska's harvested fish species (walleye pollock *Gadus chalcogrammus*; Hurst *et al.*, 2012, 2013). Experimental studies on a broad range of species with differing life histories are clearly required to refine such analyses of the ecosystem and socio-economic impacts of ocean acidification.

In this study, we examined the potential sensitivity of northern rock sole (*Lepidopsetta polyxystra*) to the direct effects of ocean acidification in a series of laboratory experiments rearing eggs and larvae under ambient and elevated CO_2 levels. Northern rock sole are commercially harvested in the Bering Sea and Gulf of Alaska groundfish fisheries. Through the 1990s, annual harvests (combined with southern rock sole *Lepidopsetta bilineata*) averaged 27 000 mt, but have increased to an average of 58 000 mt since 2008 in response to a strong market for the roe. In addition to their commercial importance, northern rock sole were selected for study because they differ from the previously studied walleye pollock in several reproductive and early life history traits. Northern rock sole mature around 7 years of age and spawn over the continental shelf in winter and spring (Stark and Somerton, 2002). Females produce a single batch of demersal eggs which are semi-adhesive during the early stages of development (Laurel and Blood, 2011). Larvae are found in the upper 30 m of the water column (Lanksbury *et al.*, 2007), undergo transformation, and settle into inner coastal nursery areas at a size of ~15 mm (Cooper *et al.*, 2014; Laurel *et al.*, 2014). Previous work has indicated that regional environmental and climatic conditions during the larval period influence recruitment rates and juvenile growth trajectories (Doyle *et al.*, 2009; Hurst *et al.*, 2010).

Because vital rates of early life history stages can dramatically influence population productivity, the experiments presented here focus on determining the effects of elevated CO_2 levels on size-at-hatch and larval growth rates. To facilitate direct comparison of species responses, we applied the same methodologies used in a recent study of walleye pollock (Hurst *et al.*, 2013). In multiple independent experiments, northern rock sole eggs and larvae were reared across a range of CO_2 levels to determine stage-specific sensitivity to environmental hypercapnia. Treatments were designed to reflect changes from ambient conditions predicted to occur in the North Pacific over the next century. The medium CO_2 addition treatments targeted an increase of ~ 400 μatm CO_2 (~0.35 pH decrease; IPCC, 2014; Mathis *et al.*, 2014), with low CO_2 addition treatments reflecting a nearer-term increase of ~150 μatm CO_2 (~0.10 pH decrease). High CO_2 treatments (to 1500 μatm) were included to better understand the overall physiological sensitivity of northern rock sole to CO_2 level (Riebesell *et al.*, 2010).

Methods

Rearing system

Eggs and larvae were incubated in a flow-through rearing system under controlled temperature and pH conditions (additional details and schematic in Hurst *et al.*, 2012). Ambient temperature and chilled seawater were mixed to achieve 8°C in two conditioning tanks. Injection of CO_2 into one of these conditioning tanks was regulated with a pH probe (Ag/AgCl electrode, Aqua Medic) to achieve the high CO_2 treatment (pH ~7.5). The second tank was maintained at the ambient CO_2 level (pH~8.10). Water from these conditioning tanks was pumped to two header tanks for the "high" and "ambient" CO_2 treatments, respectively. Two additional header tanks received a continuous supply of both ambient and high CO_2 seawater in fixed ratios to establish two treatments with intermediate levels of elevated CO_2 ("low" and "medium" CO_2 treatments). Each header tank gravity-fed 1000 ml egg incubation beakers or 100 l rearing tanks at 50 and 500 ml min^{-1}, respectively. Benchtop meters (VWR Symphony meter SB80PD) recorded the pH of outflow from one rearing tank in each treatment at 30 min intervals to monitor general functioning of the system. Carbonate conditions during experiments were described by chemical analysis of water samples drawn from each treatment header tank 2–3 times per week. Water samples were poisoned with $HgCl_2$ and shipped to the Ocean Acidification Research Center at the University of Alaska at Fairbanks. Samples were analysed for dissolved inorganic carbon (DIC) and total alkalinity (TA) using a VINDTA 3C (Versatile Instrument for the Determination of dissolved inorganic carbon and Total Alkalinity) coupled to a UIC 5014 coulometer. These data were used to calculate the pH, pCO_2, and carbonate mineral saturation states (Ω) of the water using the program developed by Lewis and Wallace (1998; Table 1). During part of the first egg batch incubation and part of the third larval trial, water samples were not available; during these periods, pH and CO_2 levels were based on observed relationships between benchtop meter readings of pH and calculations of pH and CO_2 based on DIC and TA measurements during adjacent periods (all model $r > 0.75$).

Parental broodstock

Eggs for these experiments were produced by a captive broodstock of northern rock sole at the Alaska Fisheries Science Center laboratory in Newport, Oregon. Fish for the broodstock were collected as adults (32–40 cm total length) from coastal waters of Kodiak Island, Alaska (57°46′N 152°21′W), and reared in the laboratory (see Laurel and Blood, 2011, for additional details). Unique-identifier passive-integrated transponder tags were injected into the dorsal

Table 1. Conditions during experimental exposures of northern rock sole (*L. polyxystra*) eggs and larvae to projected ocean acidification.

Experiment—treatment	Temp. (°C)	DIC (μmol kg^{-1})	TA (μmol kg^{-1})	pH (seawater scale)	pCO_2 (μatm)
Eggs[a,b]					
Ambient	7.7 ± 0.5	2036.3 ± 25.2	2140.7 ± 38.9	8.15 ± 0.07	296 ± 56
Low CO_2	7.8 ± 0.5	2068.1 ± 34.7	2163.5 ± 45.3	8.02 ± 0.11	423 ± 126
Medium CO_2	7.8 ± 0.5	2105.0 ± 28.2	2170.3 ± 55.8	7.83 ± 0.13	698 ± 243
High CO_2	7.7 ± 0.6	2165.4 ± 20.8	2189.1 ± 46.3	7.57 ± 0.18	1281 ± 320
Larvae—trial 1					
Ambient	8.3 ± 0.4	1979.0 ± 36.2	2155.0 ± 61.8	8.14 ± 0.09	300 ± 76
Low CO_2	8.3 ± 0.5	2007.4 ± 45.3	2144.3 ± 51.3	8.03 ± 0.14	403 ± 138
Medium CO_2	8.1 ± 0.04	2060.3 ± 40.1	2140.3 ± 71.9	7.86 ± 0.19	656 ± 337
High CO_2	8.3 ± 0.4	2147.8 ± 28.8	2151.8 ± 58.3	7.59 ± 0.17	1219 ± 477
Larvae—trial 2					
Ambient	8.0 ± 0.5	1975.1 ± 46.4	2178.0 ± 46.3	8.20 ± 0.07	255 ± 42
Low CO_2	8.0 ± 0.03	2045.0 ± 36.3	2199.1 ± 59.3	8.07 ± 0.06	351 ± 44
Medium CO_2	7.9 ± 0.4	2086.7 ± 34.5	2177.1 ± 53.8	7.92 ± 0.09	518 ± 105
High CO_2	8.1 ± 0.3	2144.7 ± 20.9	2158.5 ± 27.0	7.63 ± 0.03	1054 ± 76
Larvae—trial 3[b]					
Ambient	8.2 ± 0.8	2086.7 ± 84.6	2218.8 ± 67.1	8.01 ± 0.17	549 ± 211
Low CO_2	8.1 ± 0.8	2125.8 ± 87.8	2217.1 ± 84.8	7.90 ± 0.019	697 ± 284
Medium CO_2	8.2 ± 0.8	2175.5 ± 75.9	2212.5 ± 84.0	7.75 ± 0.19	978 ± 361
High CO_2	8.1 ± 0.8	2239.8 ± 87.7	2218.1 ± 80.0	7.54 ± 0.16	1541 ± 493

[a]Conditions are the averages of the mean and standard deviation in conditions observed during each of the four egg incubation trials. Response metrics are plotted against batch-specific CO_2 levels in Figure 2.
[b]Water samples during parts of egg incubation 1 and larval trial 3 were not available. During these periods, pH and CO_2 levels were based on observed relationships between benchtop meter readings of pH and calculations of pH and CO_2 based on DIC and TA measurements from adjacent periods. Carbonate system parameters (DIC, dissolved inorganic carbon; TA, total alkalinity; temperature; and salinity) were measured 2–3 times per week and used to calculate pH and pCO_2.

musculature of each fish. The fish were held in a 6 m tank under a seasonally varying temperature and photoperiod. Temperatures in the spawner tank were maintained at 7–10°C during summer and reduced to 4–5°C during winter; light was provided on a seasonal cycle varying from 14.5 h light during summer to a minimum of 9.5 h before the spawning season. During the 2013 spawning season, water samples were collected from the broodstock tank once per week and analysed to determine CO_2 (305 ± 69 μatm s.d.) and pH (8.13 ± 0.09) conditions as described above. Although we did not monitor pH or CO_2 levels in the adult broodstock tanks regularly outside the spawning season, measurements of ambient seawater during experiments in Hurst *et al.* (2012) demonstrate strong seasonal variation. During summer, when coastal upwelling brings CO_2-rich water to the surface (Gruber *et al.*, 2012), ambient CO_2 levels can reach more than 700 μatm during prolonged upwelling events.

Male and female fish were allowed to ripen naturally without the use of hormonal injection. When females showed external signs of egg ripening (distended abdomen), they were captured from the tank and checked for spawning condition by gently squeezing the abdomen. If eggs did not flow freely, the fish was returned to the tank and re-checked at 3–4 d intervals. When eggs flowed freely, they were collected in a clean, dry container and fertilized with milt from three male fish randomly selected from the broodstock (total of nine males used across all maternal egg batches). Gametes were mixed for 1 min and repeatedly rinsed with ambient pH seawater to remove excess milt and disperse egg clumps. In total, egg batches were collected from five different females with offspring used in egg incubation trials ($n = 4$) and/or larval growth trials ($n = 3$; Table 2).

Table 2. Northern rock sole (*L. polyxystra*) egg batches used for experimental rearing of eggs and larvae at ambient and elevated CO_2 levels.

Egg batch	Spawn date	DPF sampling hatchers	DPH larval growth
1	26 March 2012	18	–
2	7 February 2013	–	3–33
3	25 February 2013	21	–
4	4 March 2013	21	3–17
5	22 March 2013	21	3–60

Eggs from each female were fertilized with the milt from three males. Eggs from batches 1, 3, 4, and 5 were incubated at multiple CO_2 levels and sampled at 18 or 21 d post-fertilization (DPF) for determination of hatch success and size at hatch. Independently, eggs from batches 2, 4, and 5 were incubated at ambient CO_2 levels until 3 DPH then reared at ambient and elevated CO_2 levels for 14–57 d.

Egg incubation experiments

From each egg batch used for incubation experiments, three replicate samples of 0.5 ml of eggs (~450 eggs) were incubated in each of the four CO_2 treatments. Temperatures were maintained at 8°C during the incubation period. Each egg sample was incubated in a 1000 ml beaker with 220 μm mesh bottom suspended in a temperature- and pH-regulated tank which served as a water bath. A constant flow of 50 ml min^{-1} of pH-regulated water from the header tank was passed through a 10 μm particle filter into each incubation beaker to maintain pH at the targeted treatment level. The mesh bottoms of the beakers allowed the water to flow over the eggs and out of the incubation beakers into the water bath. The eggs were introduced into the incubation beakers at ambient pH within 10 min of fertilization, after which the flow of pH-controlled water from the header tanks was initiated and pH was adjusted to the treatment pH over a period of ~30 min.

The eggs were left undisturbed in the incubation beakers and allowed to hatch. Hatching occurred between 13 and 18 d after fertilization, consistent with previous observations at similar temperatures (Laurel and Blood, 2011). On day 21 (day 18 for egg batch 1),

all beakers were sampled to determine the number and size of hatched larvae in each replicate. All surviving larvae were counted and scanned for malformation (curved or twisted shape; Laurel and Blood, 2011). Because dead eggs were difficult to distinguish from the shed chorion of hatched larvae, estimates of hatching success were based on the number of hatched larvae counted during sampling and the estimated number of eggs introduced into the incubation beakers. A subsample of 15 larvae was randomly selected from each replicate for size measurements. These fish were digitally photographed under a dissecting microscope. An image analysis system was used to measure standard length (SL), myotome height at the anus (MH), and yolk area (YA) from the photographs. After photographing, subsampled larvae were pooled into groups of five larvae ($n = 3$/replicate) and dried for >24 h at 50°C for determination of dry weight (DW). In trial 1, dry weights were measured on groups of ten larvae independently sampled from all hatched larvae (i.e. the same fish were not used for length and weight measures). Because of the variation in amount of residual yolk at hatch, condition factors of newly hatched larvae were based on MH rather than DW (Hurst *et al.*, 2013). Larval condition index was calculated as the fractional deviation of each fish from a linear relationship between MH and SL (MH_{dev}). The mean value of each metric in each replicate incubation beaker was used as the level of observation in these analyses. Because the CO_2 levels in specific treatments varied across egg batches, ANCOVA with CO_2 level as the covariate and egg batch as a random main effect was used to examine variation in hatch success, fraction of curved larvae, and size-at-hatch metrics (SL, DW, MH_{dev}, and YA).

Larval growth experiments

Three independent larval rearing experiments were conducted with offspring from different egg batches (Table 2). Rearing techniques generally followed those used by Laurel *et al.* (2014) describing thermal effects on growth of northern rock sole larvae and by Hurst *et al.* (2013) in ocean acidification experiments on larval walleye pollock. After fertilization, all the eggs to be used in a larval growth trial were incubated together at ambient CO_2 levels (~300 μatm) in a single layer in a 175 l tank maintained at 6°C. Three days after the estimated midpoint of hatching, yolk sac larvae were gently scooped from the surface water of the egg incubation tank in batches of 200–300 larvae, warmed to 8°C over a 1 h period and introduced to larval rearing tanks. All tanks in each trial were stocked with the same estimated number of larvae, but the stocking density varied across trials due to differences in the cumulative number of larvae available for the experiment (range 1200–2500 fish per tank, Table 2). These stocking densities are similar to those used by Laurel *et al.* (2014) and below levels expected to induce density-dependent effects on growth rates (Baskerville-Bridges and Kling, 2000). Larvae were reared in black, 100 l tanks with weak upwelling circulation maintained by light aeration and positioning the in-flow (500 ml min^{-1}) at the bottom centre of the tank. Light was provided by overhead fluorescent bulbs on a 12:12 h light:dark photoperiod at a level of 6.7 μE m^{-2} s at the water surface. Prey was introduced 1 d after stocking. Larvae were reared on rotifers (*Brachionus plicatilis*) enriched with Algamac 3050 (Aquafauna, Hawthorne, CA, USA) which were supplied at densities of 5 prey ml^{-1} twice daily. After 4 weeks of rearing in trial 3, rotifers were supplemented with microparticulate dry food (Otohime A, Marubeni Nisshin Feed Co., Tokyo) 2–3 times per day.

Trial 1 was ended after 4 weeks of rearing (33 d post-hatch, DPH) and all remaining larvae were counted to estimate survival rates. Owing to lower initial numbers and lower overall survival rates in trial 2, this trial was ended and all surviving fish counted after only 2 weeks of experimental rearing (at 17 DPH). However, the larger numbers of larvae used in trial 3 (and rearing system availability) allowed us to extend two of the three replicates in each treatment through later stages of larval development (to 60 DPH). After 4 weeks of rearing (at 32 DPH), all tanks ($n = 12$) were sampled to determine fish length and weight. The number of larvae surviving to 32 DPH in each tank was estimated by averaging independent visual counts made by two observers (see Laurel *et al.*, 2014, for additional details). An estimated instantaneous daily mortality rate for each tank in all trials was determined from the initial stocking density, the number of fish removed during sampling, and number of survivors after 4 weeks of rearing (2 weeks in trial 2). Because estimated mortality rates were highly variable across tanks and trials and not normally distributed, analysis was performed on ranked values. The estimated mortality rates were ranked within each experimental trial (1 lowest, 12 highest) and compared with treatment CO_2 level across experiments using Spearman rank correlation ($n = 36$ tanks).

During the first 4 weeks of each trial, samples of 15–20 larvae were drawn from each replicate tank at weekly intervals. Additional sampling was conducted in the two extended duration replicates in each treatment of trial 3 at 47 and 60 DPH. Sampled larvae were digitally photographed under a dissecting microscope and measurements were made of SL and MH. After photographing, subsampled larvae were pooled into groups of five larvae ($n = 3$ per replicate) and dried for 24 h at 50°C for determination of dry weight (DW). Because DW was not measured separately for each fish, DW condition factors (DW_{dev}) were estimated for each tank on each sampling date as the per cent deviation from the observed relationship between mean SL and mean DW. The underlying relationship was described by fitting a negative exponential smoothing function to the SL-DW data as ontogenetic patterns in growth and development of the larvae resulted systematic departures from simple exponential, power, or polynomial functions (based on patterns in residuals). The mean size of fish in each replicate tank was used as the level of observation in statistical analyses. Within each experiment, fish size (SL and DW) and condition (DW_{dev}) were analysed with two-way ANOVA with CO_2 level and sampling date as main effects. *Post hoc* least significant difference (LSD) tests were used to indicate differences among treatments on specific sampling dates.

Results

Egg incubation experiments

Hatching success was high among incubation beakers, with estimated hatch rates averaging 91%. Estimated hatch rates did not differ significantly among egg batches (ANCOVA, $F_{3,42} = 1.45$, $p = 0.241$) and were not affected by incubation CO_2 level ($F_{1,42} = 0.11$, $p = 0.747$). The incidence of deformed ("curled") larvae in the first egg batch was estimated to be <2% but was not scored for individual hatching containers. Among the three later batches, incidence of deformed larvae was not affected by incubation CO_2 level ($F_{1,32} = 0.03$, $p = 0.859$), but did differ among egg batches ($F_{2,32} = 12.55$, $p < 0.01$; highest in batch 4 at 2.8%). There were no significant interactions between batch and CO_2 level on hatch rate or incidence of deformity ($p > 0.50$).

There was no consistent effect of incubation CO_2 level on any of the size-at-hatch metrics across the four egg batches (Figure 1). There was no significant main effect of CO_2 level on any of the

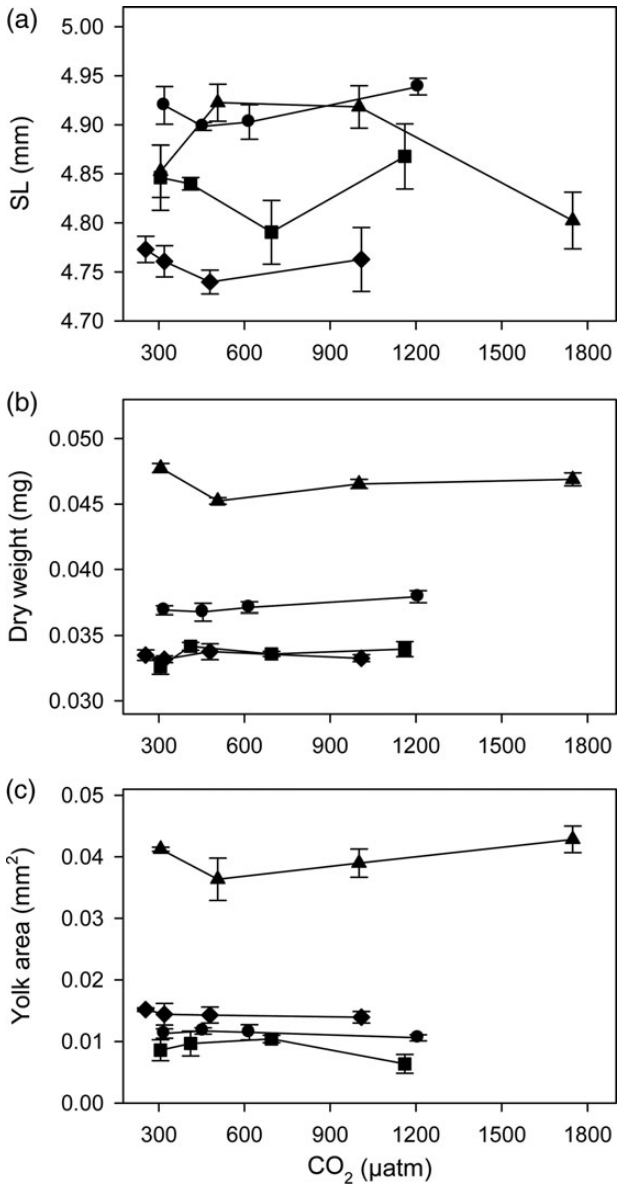

Figure 1. Size at hatch metrics of northern rock sole (*L. polyxystra*) larvae as a function of incubation CO_2 level. Points are the mean values (± s.e.) of three replicate incubation beakers in each CO_2 treatment. Symbols represent batches collected from different females from a laboratory broodstock: batch 1, filled triangle; batch 3, filled circle; batch 4, filled square; batch 5, filled diamond. The higher dry weights and yolk areas in egg batch 1 were due to earlier sampling (18 DPH) than in subsequent batches (21 DPH).

metrics (all $p > 0.1$, Table 3) but all differed significantly among egg batches ($p < 0.01$). Most clearly, larvae from egg batch 1 were significantly heavier and had much larger yolk areas than fish from the other egg batches because they were sampled at 18 rather than 21 d after fertilization.

Larval growth experiments

Larval mortality rates were based on estimated initial densities and direct counts of larvae surviving after 4 weeks (2 weeks in trial 2). Estimated mortality rates were highly variable across the experiment.

Table 3. Analysis of covariance of hatching metrics of four batches of northern rock sole (*L. polyxystra*) eggs incubated across a range of CO_2 levels.

Measure	Factor	d.f.	*F*	*p*-value
Standard length				
	CO_2 level	1	0.87	0.357
	Egg batch	3	25.09	<0.01
	Error	43	–	–
Dry weight				
	CO_2 level	1	2.64	0.112
	Egg batch	3	492.36	<0.01
	Error	42	–	–
Condition (MH_{dev})				
	CO_2 level	1	0.39	0.149
	Egg batch	3	23.88	<0.01
	Error	43	–	–
Yolk area				
	CO_2 level	1	6.81	0.768
	Egg batch	3	285.79	<0.01
	Error	43	–	–

Egg batch is treated as a random main effect. Response variables are the mean value measured in three replicate incubation beakers for each batch × CO_2 treatment.

Because estimated mortality rates were significantly higher in trial 2 than in trials 1 and 3 (Kruskal–Wallis ANOVA $H = 24.35$, $p < 0.01$), there was no overall effect of CO_2 level on estimated mortality rates (Figure 2a; Spearman rank correlation, $p < 0.50$). However, when tank mortality rates were ranked within each trial, there was a trend towards greater mortality rates in treatments with higher CO_2 levels, although this trend was not statistically significant (Figure 2b; Spearman $R = 0.322$, $p = 0.056$).

Despite the differences in stocking density and observed mortality rates, growth rates were generally similar across the three larval trials. There were no significant differences between trials in SL or DW after 2 weeks of growth (both $F_{2,30} < 1.0$, $p > 0.40$); after 4 weeks of growth, fish in trial 3 were slightly heavier than the fish in trial 1 ($F_{1,19} = 5.12$, $p = 0.036$), but there was no significant difference in length ($F_{1,19} = 1.62$, $p = 0.389$).

Throughout the three experimental trials, there were only minor differences in growth rates of northern rock sole larvae across CO_2 treatments (Figure 3). In trials 1 and 2, there was no significant main effect of CO_2 level or interaction with age on SL or DW (Table 4). In trial 3, which was extended to 60 DPH, there was a significant effect of CO_2 level with fish in the low CO_2 treatment being significantly longer than fish in the elevated CO_2 treatments, especially after 25 DPH (significant *post hoc* LSD tests among treatments at 25, 32, and 60 DPH). There was also a significant effect of CO_2 and significant interaction with age on DW in trial 3. Again, these responses were driven by the heaviest fish being in the low CO_2 treatment, especially after 25 DPH (significant differences among treatments at 47 and 60 DPH). The interaction was caused by fish in the ambient treatment which tended to be large through the first month of the experiment, were small on days 32 and 47, and large on the final sample at 60 DPH.

Dry weight condition factors were based on deviations of the relationship between tank mean SL and DW from samples pooled across the three experiments. Statistical patterns varied across the three trials (Table 4), but lower condition factors were generally observed in treatments with elevated CO_2 levels. In trial 1, there was a significant interaction between age and CO_2 level on condition factor, with the lowest condition factors observed in either the

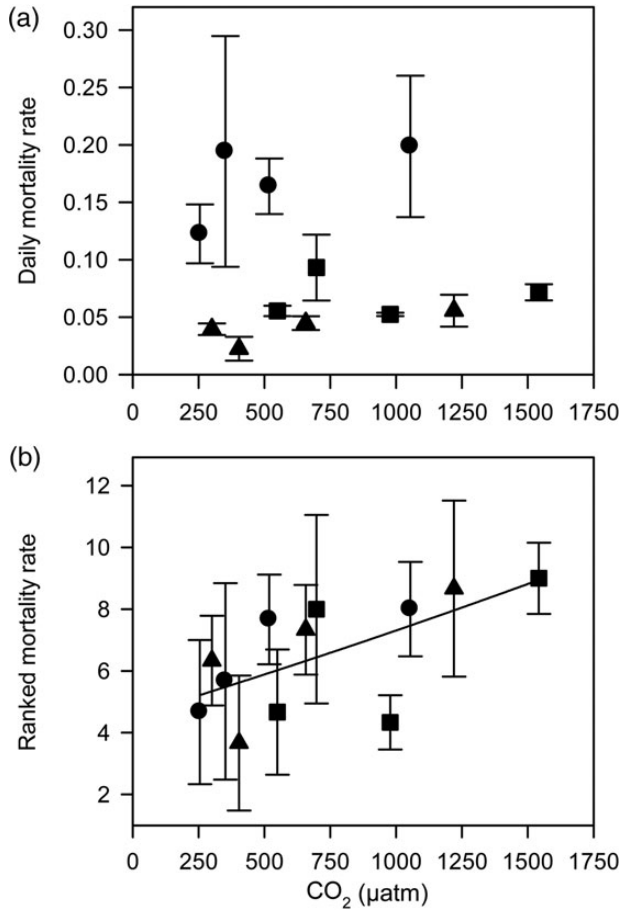

Figure 2. Mortality rates of northern rock sole (*L. polyxystra*) larvae as a function of CO_2 level. Values are mean ($\pm$ s.d.) of estimated mortality rates (a) and ranked mortality rates (1 – 12) within each experimental trial (b). Symbols represent trial 1, filled triangle; trial 2, filled circle; trial 3, filled square, reared from egg batches 2, 4, and 5, respectively.

medium or high CO_2 treatment at each sampling date (significant differences among treatments at 12, 19, and 26 DPH, but not 33 DPH; Figure 3). In trial 2, there were no significant effects of age or CO_2 level on condition factor. The differences among treatments were most dramatic during the extended trial 3 when there was a significant main effect of CO_2 treatment on condition factor; lowest values were observed in the high CO_2 treatment (Table 4) diverging markedly after 30 DPH (Figure 3). *Post hoc* LSD tests indicated that condition factor in the high CO_2 treatment was lower than the ambient and low CO_2 treatments at 47 DPH and lower than all other treatments at 60 DPH.

Discussion

Experimental work has demonstrated a wide range of biological effects stemming from exposure to elevated environmental CO_2 levels associated with ongoing ocean acidification. The nature and magnitude of these effects have been shown to vary widely among species groups (Fabry *et al.*, 2008; Wittmann and Pörtner, 2013). While fish as a group appear less sensitive to some of the direct effects of high CO_2 than calcifying invertebrates, negative effects on the early life stages and disruptions of behavioral and sensory biology have been demonstrated in a diverse group of species (Leduc *et al.*, 2013). Results of the experiments presented here suggest that during the first few weeks of life, northern rock sole are not negatively impacted by CO_2 levels that would be encountered in Alaskan surface waters over the next few decades (Mathis *et al.*, 2014). These results are generally similar to those observed for early life stages of walleye pollock, the only other commercially important North Pacific fish species examined to date (Hurst *et al.*, 2012, 2013). However, two observations suggested that northern rock sole larvae may be less resilient to high CO_2 levels than larval walleye pollock, despite having been tested across a narrower range of CO_2 levels. When reared for longer periods (trial 3), northern rock sole larvae in the highest CO_2 treatments were significantly smaller and in poorer condition than fish in the lower CO_2 treatments. In addition, although it was not statistically significant, we observed a trend of larvae in higher CO_2 treatment tanks generally having higher estimated mortality rates than fish at lower CO_2 levels, a pattern not observed in similarly conducted walleye pollock experiments (Hurst *et al.*, 2013). As these experiments addressed only the direct effects of high CO_2 on growth and survival northern rock sole larvae, a more comprehensive evaluation of the impacts of ocean acidification on the productivity of this resource species requires consideration of interactions with other environmental stressors and the behavioral and sensory deficits observed in other species (Leduc *et al.*, 2013; Gräns *et al.*, 2014). Below, we discuss these results in the context of other temperate and boreal marine fish species and the considerations of applying laboratory exposure studies to ocean acidification effects on natural populations.

Acidification effects in flatfish

Understanding the mechanisms responsible for species-specific differences in sensitivity to ocean acidification of fish early life stages will be critical to predicting ecosystem impacts. Unfortunately, there remain too few studies across the range of phylogenetic groups and life history guilds to draw firm conclusions about the factors that may influence species-specific sensitivity to the elevated CO_2 levels associated with ocean acidification. Flatfish (Pleuronectiformes) are a monophyletic group with a worldwide distribution in boreal, temperate, and tropical seas (Munroe, 2005). Flatfish's unique life history includes a metamorphosis more dramatic than that of most other fish. This complex development may make this species group vulnerable to environmental stressors and a potentially useful model group to explore the effects of ocean acidification in marine fish. In addition, due to interest in aquaculture of these species for commercial and conservation purposes, rearing and culture techniques are being established for an increasing number of flatfish species, facilitating laboratory experimentation and cross-species comparisons.

To date, there have been only two published reports of the effects of high CO_2 on the eggs and larvae of marine flatfish (Chambers *et al.*, 2014; Pimentel *et al.*, 2014). Among the three studied species, northern rock sole may be the least sensitive to elevated CO_2 levels as the effects were limited to a non-significant trend towards increased larval mortality rate and reduced growth and condition in post-flexion larvae. Conversely, Senegalese sole (*Solea senagalensis*) appear to be most sensitive to elevated CO_2 levels, exhibiting significantly reduced growth and survival of larvae at elevated CO_2 levels ($\sim$1600 µatm; Pimentel *et al.*, 2014). Responses in summer flounder (*Paralichthys dentatus*) were less severe than observed in Senegal sole but potentially more severe than those observed in northern rock sole as exposure to elevated CO_2 levels ($\sim$1800 and 4714 µatm) resulted in reduced hatching success and increased abnormalities in the livers and trunk musculature, but these were not associated with reductions in growth rate (Chambers *et al.*, 2014).

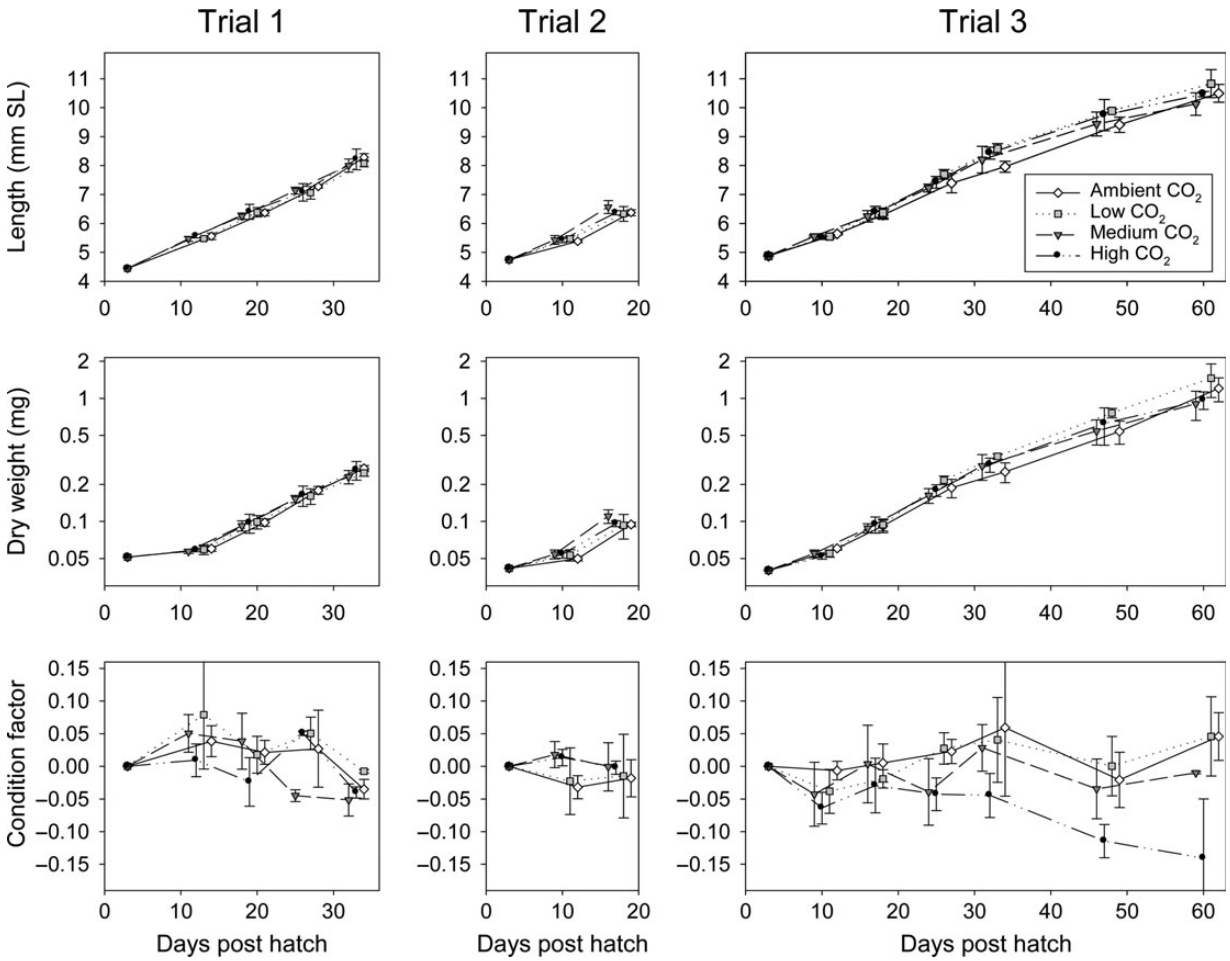

Figure 3. Growth and condition of northern rock sole (*L. polyxystra*) larvae reared at ambient and elevated CO_2 levels in three independent trials. Points represent mean (± s.d.) of replicate tanks within each treatment. Note: all tanks sampled on the same days in each trial, points offset horizontally for clarity.

Table 4. Analysis of variance of size and dry weight-condition factor of northern rock sole (*L. polyxystra*) larvae reared across a range of CO_2 levels.

		Standard length		Dry weight		Condition (DW_{dev})	
Factor	**d.f.**	***F***	***p*-value**	***F***	***p*-value**	***F***	***p*-value**
Trial 1							
CO_2 level	3	1.83	0.161	2.03	0.129	3.08	0.041
Day	3	475.18	<0.001	246.04	<0.001	11.14	<0.001
CO_2 × day	9	0.45	0.899	0.52	0.849	2.39	0.034
Error	32	–	–	–	–	–	–
Trial 2							
CO_2 level	3	0.79	0.157	1.305	0.307	1.42	0.273
Day	1	264.45	<0.001	133.35	<0.001	0.05	0.830
CO_2 × day	9	0.94	0.445	0.85	0.485	0.32	0.808
Error	32	–	–	–	–	–	–
Trial 3							
CO_2 level	3	6.32	0.001	5.68	0.002	12.07	<0.001
Day	5	592.99	<0.001	136.49	<0.001	2.68	0.035
CO_2 × day	15	1.01	0.461	2.01	0.040	1.06	0.416
Error	40	–	–	–	–	–	–

Response variables are the tank mean value measured on each sampling date in each of three replicate rearing tanks in each experiment.

The differences observed across flatfish species suggest that caution needs to be applied when making broad generalizations about the physiological sensitivity of fish guilds, but suggest a pattern in species sensitivity which has not been previously examined. The differences observed among flatfish species in magnitude of effects from high CO_2 may be related to thermal regimes and intrinsic development rates: Senegal sole is a subtropical species with rapid development rates. Perhaps the more slowly developing temperate and boreal species such as summer flounder and northern rock sole are less sensitive to the detrimental effects of hypercapnia. As indicated in extended rearing with northern rock sole, it is also possible that the negative effects of elevated CO_2 may take longer to manifest or that it is the later metamorphic-stages that are more sensitive to high CO_2 stress (Pope *et al.*, 2014). We suggest that comparisons across widely distributed taxonomic groups could be especially informative in identifying general patterns of sensitivity to ocean acidification and that comparisons consider the role of thermal guild as well as taxonomic classification.

Experimental considerations

A number of factors should be considered when inferring or modelling population and community level responses to ocean acidification based on experimental exposures to environmental

hypercapnia. These studies represent acute exposures to rapidly altered conditions and do not allow the opportunity for acclimation or adaptation to more gradual, long-term environmental change. In addition, no individual study is sufficiently comprehensive to evaluate the effects of elevated CO_2 across the full range of life history stages and physiological and behavioural responses. This can lead to over- or underestimation of overall species sensitivity as observed sensitivity (or resiliency) in one life stage or trait may not predict a similar degree of sensitivity in other stages or traits (Maneja *et al.*, 2012; Cripps *et al.*, 2014).

In particular, we suggest that experimental evaluations of sensitivity of marine fish larvae should be extended to encompass later developmental stages which may be more sensitive (Pope *et al.*, 2014). In early studies, Kikkawa *et al.* (2003) found that the median lethal CO_2 levels were higher in early stage "pre-flexion" larvae than later stage "post-flexion" larvae in both red sea bream (*Pagrus major*) and Japanese whiting (*Sillago japonica*). More recent studies with ocean acidification-relevant CO_2 levels have identified negative effects in later stages that were not evident in the first few weeks of life (Frommel *et al.*, 2012; but see Maneja *et al.*, 2012). This extended rearing will be especially important in studies of cold-water species with slow development rates.

The evolutionary and environmental history of the source population should also be considered in evaluating species-specific sensitivity to projected ocean acidification. Several studies have found differential responses among tested populations (e.g. Atlantic herring *Clupea harengus*; Franke and Clemmesen, 2011; Frommel *et al.*, 2014) and parental conditioning has been shown to mitigate some of the detrimental effects of high CO_2 in early life stages (Miller, *et al.*, 2012; Murray, *et al.*, 2014; but see Schade, *et al.*, 2014). In a previous study, Hurst *et al.* (2013) cautioned that the resilience of larval walleye pollock to elevated CO_2 levels may be greater in the examined Puget Sound population than would be observed in the more northerly harvested populations. The parental broodstock of northern rock sole used in this study were collected from the central Gulf of Alaska, in the middle of the commercial range of the species. Therefore, we do not believe that population differences would limit the applicability of these results to the harvested populations in Alaskan waters.

With regard to the potential effects of parental conditioning on the responses of northern rock sole offspring to elevated CO_2, the conditions experienced by fish in our laboratory culture are not unlike those that wild fish would experience in Alaskan waters. Recent observations from the Bering Sea shelf (Mathis *et al.*, 2013) found that while surface waters in spring (experienced by larvae) had CO_2 concentrations <300 μatm, CO_2 concentrations in the bottom waters (experienced by adults) over 1000 μatm were observed for extended periods (>3 months). Therefore, while exposure to seasonally elevated CO_2 levels experienced by the parental broodstock (outside the spawning season) may have conferred some acclimation to the offspring examined in this study, this would appear to be a natural aspect of the species life history that would influence sensitivity to future increases in environmental CO_2 levels (Murray *et al.*, 2014).

Conclusions

Prediction of the ecosystem and socio-economic effects of ocean acidification depends on identifying the nature and magnitude of high CO_2 effects across a range of ecosystem components and valuable resource species (Cooley and Doney, 2009; Mathis *et al.*, 2014). Species-specific sensitivity to ocean acidification is likely to be a function of both taxonomic and life history considerations. Experiments on the eggs and larvae of northern rock sole indicated a trend towards higher larval mortality rates and lower condition factors at elevated CO_2 levels, but only at CO_2 levels above those predicted for Alaskan waters in the next 100 years. While less severe than the effects observed in some other species (e.g. Frommel *et al.*, 2014; Pimentel *et al.*, 2014), these effects were observed in northern rock sole at CO_2 levels that did not induce any negative effects in walleye pollock, another commercially important fishery species in the Gulf of Alaska and Bering Sea (Hurst *et al.*, 2012, 2013). Comparing the results observed here for northern rock sole with those of other flatfish species, we suggest that thermal guild and developmental rate may be critically relevant traits determining the degree of sensitivity among species. Finally, we caution that these experiments have addressed only one aspect of the potential effects of ocean acidification on this species. Future work should focus on high-CO_2 interactions with other environmental factors and the potential for sensory and behavioural deficits (Leduc *et al.*, 2013; Gräns *et al.*, 2014) which may be the primary pathways of action of ocean acidification in some fish species.

Acknowledgements

Scott Haines, Mara Spencer, Eric Hanneman, Michele Ottmar, and Paul Iseri assisted with fish culture. Chris Magel assisted with maintenance of pH regulation and monitoring throughout the experiments. M. Hawkyard, J. Andrade, C. Ryer, and three anonymous reviewers provided valuable comments on this manuscript. Reference to trade names does not imply endorsement by the National Marine Fisheries Service. The findings and conclusions in this paper are those of the authors and do not necessarily represent the views of the National Marine Fisheries Service. This project was funded by grants to TPH and JTM from NOAA's Ocean Acidification Research Programme. LRT was supported by a Research Experience for Undergraduates internship co-funded by the Department of Defense ASSURE Programme and the National Science Foundation under award OCE-1263349 to the Oregon State University's Hatfield Marine Science Center.

References

Baskerville-Bridges, B., and Kling, L. J. 2000. Larval culture of Atlantic cod (*Gadus morhua*) at high stocking densities. Aquaculture, 181: 61–69.

Baumann, H., Talmage, S. C., and Gobler, C. J. 2012. Reduced early life growth and survival in a fish in direct response to increased carbon dioxide. Nature Climate Change, 2: 38–41.

Bignami, S., Sponaugle, S., and Cowen, R. K. 2013. Response to ocean acidification in larvae of a large tropical marine fish, *Rachycentron canadum*. Global Change Biology, 19: 996–1006.

Chambers, R. C., Candelmo, A. C., Habeck, E. A., Poach, M. E., Wieczorek, D., Cooper, K. R., Greenfield, C. E., *et al.* 2014. Effects of elevated CO_2 in the early life stages of summer flounder, *Paralichthys dentatus*, and potential consequences of ocean acidification. Biogeosciences, 11: 1613–1626.

Cooley, S. R., and Doney, S. C. 2009. Anticipating ocean acidification's economic consequences for commercial fisheries. Environmental Research Letters, 4: 1–8.

Cooper, D. W., Duffy-Anderson, J. T., Norcross, B. L., Holladay, B. A., and Stabeno, P. J. 2014. Northern rock sole (*Lepidopsetta polyxystra*) juvenile nursery areas in the eastern Bering Sea in relation to hydrography and thermal regimes. ICES Journal of Marine Science, 71: 1683–1695.

Cripps, G., Lindeque, P., and Flynn, K. J. 2014. Have we been underestimating the effects of ocean acidification in zooplankton? Global Change Biology, 20: 3377–3385.

Denman, K., Christian, J. R., Steiner, N., Pörtner, H. O., and Nojiri, Y. 2011. Potential impacts of future ocean acidification on marine ecosystems and fisheries: current knowledge and recommendations for future research. ICES Journal of Marine Science, 68: 1019–1029.

Doyle, M. J., Picquelle, S. J., Mier, K. L., Spillane, M. C., and Bond, N. A. 2009. Larval fish abundance and physical forcing in the Gulf of Alaska, 1981–2003. Progress in Oceanography, 80: 163–187.

Fabry, V. J., McClintock, J. B., Mathis, J. T., and Grebmeier, J. M. 2009. Ocean acidification at high latitudes: the bellweather. Oceanography, 22: 160–171.

Fabry, V. J., Seibel, B. A., Feely, R. A., and Orr, J. C. 2008. Impacts of ocean acidification on marine fauna and ecosystem processes. ICES Journal of Marine Science, 65: 414–432.

Feely, R. A., Sabine, C. L., Lee, K., Berelson, W., Kleypas, J., Fabry, V. J., and Millero, F. J. 2004. Impact of anthropogenic CO_2 on the $CaCO_3$ system in the oceans. Science, 305: 362–366.

Franke, A., and Clemmesen, C. 2011. Effect of ocean acidification on early life stages of Atlantic herring (*Clupea harengus* L.). Biogeosciences, 8: 3697–3707.

Frommel, A. Y., Maneja, R., Lowe, D., Malzahn, A. M., Geffen, A. J., Folkvord, A., Piatkowski, U., *et al.* 2012. Severe tissue damage in Atlantic cod larvae under increasing ocean acidification. Nature Climate Change, 2: 42–46.

Frommel, A. Y., Maneja, R., Lowe, D., Pascoe, C. K., Geffen, A. J., Folkvord, A., Piatkowski, U., *et al.* 2014. Organ damage in Atlantic herring larvae as a result of ocean acidification. Ecological Applications, 24: 1131–1143.

Gattuso, J-P., and Hansson, H. 2011. Ocean Acidification. Oxford University Press, Oxford.

Gräns, A., Jutfelt, F., Sandblom, E., Jonsson, E., Wiklander, K., Seth, H., Olsson, C., *et al.* 2014. Aerobic scope fails to explain the detrimental effects on growth resulting from warming and elevated CO_2 in Atlantic halibut. Journal of Experimental Biology, 217: 711–717.

Gruber, N., Hauri, C., Lachkar, Z., Loher, D., Frolicher, T. L., and Plattner, G. K. 2012. Rapid progression of ocean acidification in the California Current system. Science, 337: 220–223.

Hurst, T. P., Abookire, A. A., and Knoth, B. 2010. Quantifying thermal effects on contemporary growth variability to predict responses to climate change in northern rock sole (*Lepidopsetta polyxystra*). Canadian Journal of Fisheries and Aquatic Sciences, 67: 97–107.

Hurst, T. P., Fernandez, E. R., and Mathis, J. T. 2013. Effects of ocean acidification on hatch size and larval growth of walleye pollock (*Theragra chalcogramma*). ICES Journal of Marine Science, 70: 812–822.

Hurst, T. P., Fernandez, E. R., Mathis, J. T., Miller, J. A., Stinson, C. S., and Ahgeak, E. F. 2012. Resiliency of juvenile walleye pollock to projected levels of ocean acidification. Aquatic Biology, 17: 247–259.

IPCC. 2014. Climate Change 2014: Synthesis Report of the Fifth Assessment of the Intergovernmental Panel on Climate Change. 132 pp.

Ishimatsu, A., Hayashi, M., and Kikkawa, T. 2008. Fishes in high-CO_2, acidified oceans. Marine Ecology Progress Series, 373: 295–302.

Kikkawa, T., Ishimatsu, A., and Kita, J. 2003. Acute CO_2 tolerance during the early developmental stages of four marine teleosts. Environmental Toxicology, 18: 375–382.

Kroeker, K. J., Kordas, R. L., Crim, R. N., and Singh, G. G. 2010. Meta-analysis reveals negative yet variable effects of ocean acidification on marine organisms. Ecology Letters, 13: 1419–1434.

Lanksbury, J. A., Duffy-Anderson, J. T., Mier, K. L., Busby, M. S., and Stabeno, P. J. 2007. Distribution and transport patterns of northern rock sole, *Lepidopsetta polyxystra*, larvae in the southeastern Bering Sea. Progress in Oceanography, 72: 39–62.

Laurel, B. J., and Blood, D. M. 2011. The effects of temperature on hatching and survival of northern rock sole larvae (*Lepidopsetta polyxystra*). Fishery Bulletin, 109: 282–291.

Laurel, B. J., Haines, S. A., and Danley, C. 2014. The effects of temperature on growth, development and settlement of northern rock sole larvae (*Lepidopsetta polyxystra*). Fisheries Oceanography, 23: 495–505.

Leduc, A. O. H. C., Munday, P. L., Brown, G. E., and Ferrari, M. C. O. 2013. Effects of acidification on olfactory-mediated behaviour in freshwater and marine ecosystems: a synthesis. Philosophical Transactions of the Royal Society B—Biological Sciences, 368: 20120447.

Lewis, E., and Wallace, D. W. R. 1998. Program developed for CO_2 system calculations: ORNL/CDIAC-105.

Lindsay, K., Bonan, G. B., Doney, S. C., Hoffman, F. M., Lawrence, D. M., Long, M. C., Mahowald, N. M., *et al.* 2014. Preindustrial control and 20th century carbon cycle experiments with the earth system model CESM1(BGC). Journal of Climate, 27: 8981–9005.

Long, W. C., Swiney, K. M., and Foy, R. J. 2013a. Effects of ocean acidification on the embryos and larvae of red king crab, *Paralithodes camtschaticus*. Marine Pollution Bulletin, 69: 38–47.

Long, W. C., Swiney, K. M., Harris, C., Page, H. N., and Foy, R. J. 2013b. Effects of ocean acidification on juvenile red king crab (*Paralithodes camtschaticus*) and Tanner crab (*Chionoecetes bairdi*) growth, condition, calcification, and survival. Plos One, 8: e60959.

Maneja, R., Frommel, A. Y., Browman, H. I., Clemmensen, C., Geffen, A. J., Folkvord, A., Piatkowski, U., *et al.* 2012. The swimming kinematics of larval Atlantic cod, *Gadus morhua L.* are resilient to elevated pCO_2. Marine Biology, 160: 1963–1972.

Mathis, J. T., Cooley, S. R., Lucey, N., Hauri, C., Ekstrom, J., Hurst, T. P., Colt, S., *et al.* 2014. Ocean acidification risk assessment for Alaska's fishery sector. Progress in Oceanography, in press.

Mathis, J. T., Cross, J. N., and Bates, N. R. 2011a. The role of ocean acidification in systemic carbonate mineral suppression in the Bering Sea. Geophysical Research Letters, 38: GL048884.

Mathis, J. T., Cross, J. N., and Bates, N. R. 2011b. Coupling primary production and terrestrial runoff to ocean acidification and carbonate mineral suppression in the Eastern Bering Sea. Journal of Geophysical Research, 116: C02030.

Mathis, J. T., Cross, J. N., Monacci, N., Feely, R. A., and Stabeno, P. J. 2013. Evidence of prolonged undersaturations in the bottom waters of the southeastern Bering Sea shelf from autonomous sensors. Deep Sea Research II, 109: 125–133.

Mathis, J. T., and Questel, J. M. 2013. Assessing seasonal changes in carbonate parameters across small spatial gradients in the Northeastern Chukchi Sea. Continental Shelf Research, 67: 42–51.

Melzner, F., Gobel, S., Langenbuch, M., Gutowska, M. A., Pörtner, H-O., and Lucassen, M. 2009a. Swimming performance in Atlantic Cod (*Gadus morhua*) following long-term (4–12 months) acclimation to elevated seawater P(CO2). Aquatic Toxicology, 92: 30–37.

Melzner, F., Gutowska, M. A., Langenbuch, M., Dupont, S., Lucassen, M., Thorndyke, M. C., Bleich, M., *et al.* 2009b. Physiological basis for high CO_2 tolerance in marine ectothermic animals: pre-adaptation through lifestyle and ontogeny? Biogeosciences, 6: 2313–2331.

Miller, G. M., Watson, S-A., Donelson, J. M., McCormick, M. I., and Munday, P. L. 2012. Parental environment mediates impacts of increased carbon dioxide on a coral reef fish. Nature Climate Change, 12: 858–861.

Munday, P. L., Gagliano, M., Donelson, J. M., Dixson, D. L., and Thorrold, S. R. 2011. Ocean acidification does not affect the early life history development of a tropical marine fish. Marine Ecology Progress Series, 423: 211–221.

Munroe, T. A. 2005. Systematic diversity of the Pleuronectiformes. *In* Flatfishes: Biology and Exploitation, pp. 10–41. Ed. by R. N. Gibson. Blackwell, Oxford.

Murray, C. S., Malvezzi, A., Gobler, C. J., and Baumann, H. 2014. Offspring sensitivity to ocean acidification changes seasonally in a coastal marine fish. Marine Ecology Progress Series, 504: 1–11.

Pimentel, M. S., Faleiro, F., Dionisio, G., Repolho, T., Pousao-Ferreira, P., Machado, J., and Rosa, R. 2014. Defective skeletogenesis and oversized otoliths in fish early stages in a changing ocean. Journal of Experimental Biology, 217: 2062–2070.

Pope, E. C., Ellis, R. P., Scolamacchia, M., Scolding, J. W. S., Keay, A., Chingombe, P., Shields, R. J., *et al.* 2014. European sea bass, *Dicentrarchus labrax*, in a changing ocean. Biogeosciences, 11: 2519–2530.

Pörtner, H. O., Langenbuch, M., and Reipschlager, A. 2004. Biological impact of elevated ocean CO_2 concentrations: lessons from animal physiology and earth history. Journal of Oceanography, 60: 705–718.

Riebesell, U., Fabry, V. J., Hansson, L., and Gattuso, J-P. 2010. Guide to best practices for ocean acidification research and data reporting, p. 260. Publications Office of the European Union, Luxembourg.

Sabine, C. L., Feely, R. A., Gruber, N., Key, R. M., Lee, K., Bullister, J. L., Wanninkhof, R., *et al.* 2004. The oceanic sink for anthropogenic CO_2. Science, 305: 367–371.

Schade, F. M., Clemmesen, C., and Wegner, K. M. 2014. Within- and transgenerational effects of ocean acidification on life history of marine three-spined stickleback (*Gasterosteus aculeatus*). Marine Biology, 161: 1667–1676.

Stark, J. W., and Somerton, D. A. 2002. Maturation, spawning and growth of rock soles off Kodiak Island in the Gulf of Alaska. Journal of Fish Biology, 61: 417–431.

van Vuuren, D. P., Edmonds, J., Kainuma, M., Riahi, K., Thomson, A., Hibbard, K., Hurtt, G. C., *et al.* 2011. The representative concentration pathways: an overview. Climate Change, 109: 5–31.

Wittmann, A. C., and Pörtner, H-O. 2013. Sensitivities of extant animal taxa to ocean acidification. Nature Climate Change, 3: 995–1001.

Handling editor: Howard Browman